BEILSTEIN JOURNAL OF ORGANIC CHEMISTRY

Concept-driven strategies in target-oriented synthesis

Edited by David Yu-Kai Chen, Chao Li and Yefeng Tang

Imprint

Beilstein Journal of Organic Chemistry
www.bjoc.org
ISSN 1860-5397
Email: journals-support@beilstein-institut.de

The *Beilstein Journal of Organic Chemistry* is published by the Beilstein-Institut zur Förderung der Chemischen Wissenschaften.

Beilstein-Institut zur Förderung der Chemischen Wissenschaften
Trakehner Straße 7–9
60487 Frankfurt am Main
Germany
www.beilstein-institut.de

BEILSTEIN JOURNAL OF ORGANIC CHEMISTRY

Total synthesis of (±)-simonsol C using dearomatization as key reaction under acidic conditions

Xiao-Yang Bi, Xiao-Shuai Yang, Shan-Shan Chen, Jia-Jun Sui, Zhao-Nan Cai, Yong-Ming Chuan and Hong-Bo Qin*

Full Research Paper

Open Access

Address:
School of Chemistry and Environment, Yunnan Minzu University, Kunming 650000, China

Email:
Hong-Bo Qin* - qinhb@ymu.edu.cn

* Corresponding author

Keywords:
acidic dearomazation; benzofuran; (±)-simonsol C; total synthesis

Beilstein J. Org. Chem. **2025,** *21,* 601–606.
https://doi.org/10.3762/bjoc.21.47

Received: 18 January 2025
Accepted: 07 March 2025
Published: 17 March 2025

This article is part of the thematic issue "Concept-driven strategies in target-oriented synthesis".

Guest Editor: C. Li

Abstract

The total synthesis of (±)-simonsol C was accomplished using a dearomatization under acidic conditions as key step to construct an aryl-containing quaternary center. The 6/5/6 benzofuran unit was formed through reductive elimination with Zn/AcOH and a spontaneous oxy-Michael addition. This synthesis consists of 8 steps and achieves an overall yield of 13%, making it the shortest known route.

Introduction

Star anise, derived from *Illicium* species cultivated in southeastern China [1] possesses significant economic, culinary, and medicinal value [2]. Particularly noteworthy are its medicinal properties, including insecticidal, antibacterial, anti-inflammatory, analgesic, and neurotrophic activities [3]. In 2013, Wang's group isolated (±)-simonsol C from star anise, which features a unique 6/5/6 tricyclic benzofuran structure [4]. They found that it exhibits biological activity that promotes neuronal synapse growth and inhibits acetylcholinesterase.

(±)-Simonsol C (Figure 1) has received considerable attention due to the presence of an aryl- and allyl-containing quaternary carbon center, which is common in natural products such as galanthamine and morphine. To construct the quaternary carbon in simonsol C, two reports have utilized alkaline dearomatization strategies and another report used an intramolecular Heck reaction as the key reaction [5-7]. However, there have been no reports or studies utilizing acidic dearomatization, which is also effective, to synthesize an arylated quaternary carbon center.

In the first report on the total synthesis of simonsol C (Scheme 1), in 2016 Banwell's group employed an intramolecular Heck reaction as key step to furnish the aryl-containing quaternary center and simultaneously construct the benzofuran

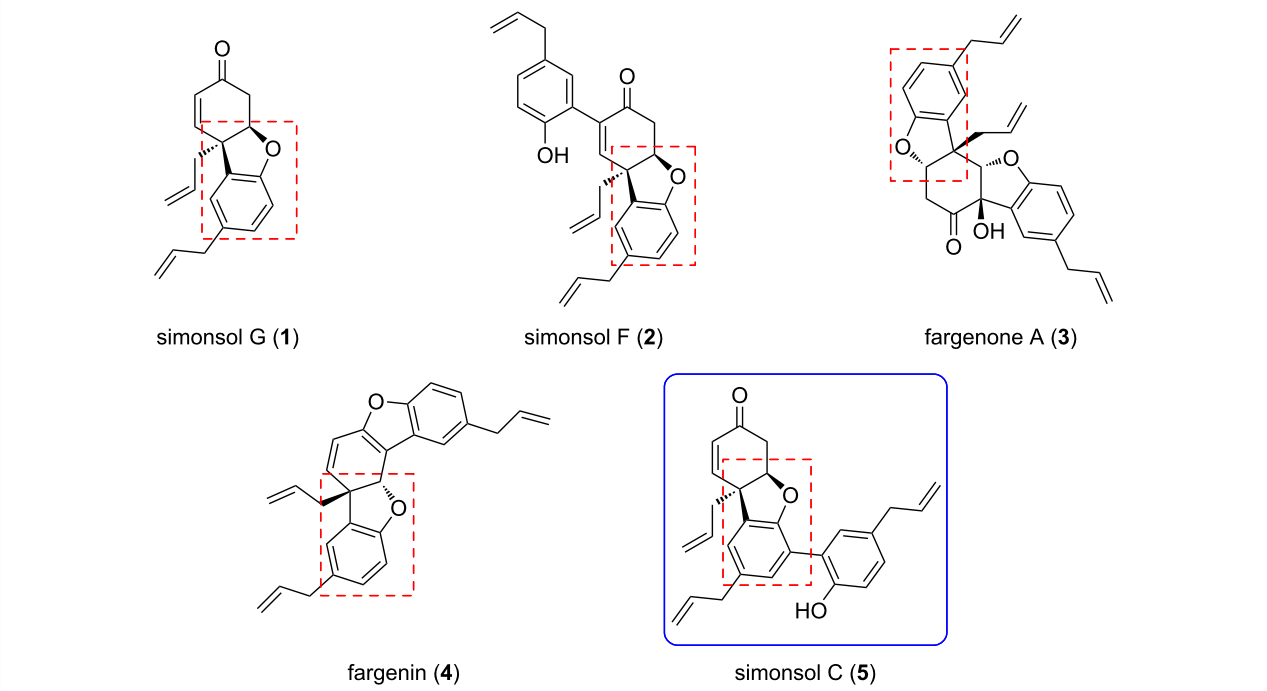

Figure 1: Representative sesquineolignan compounds.

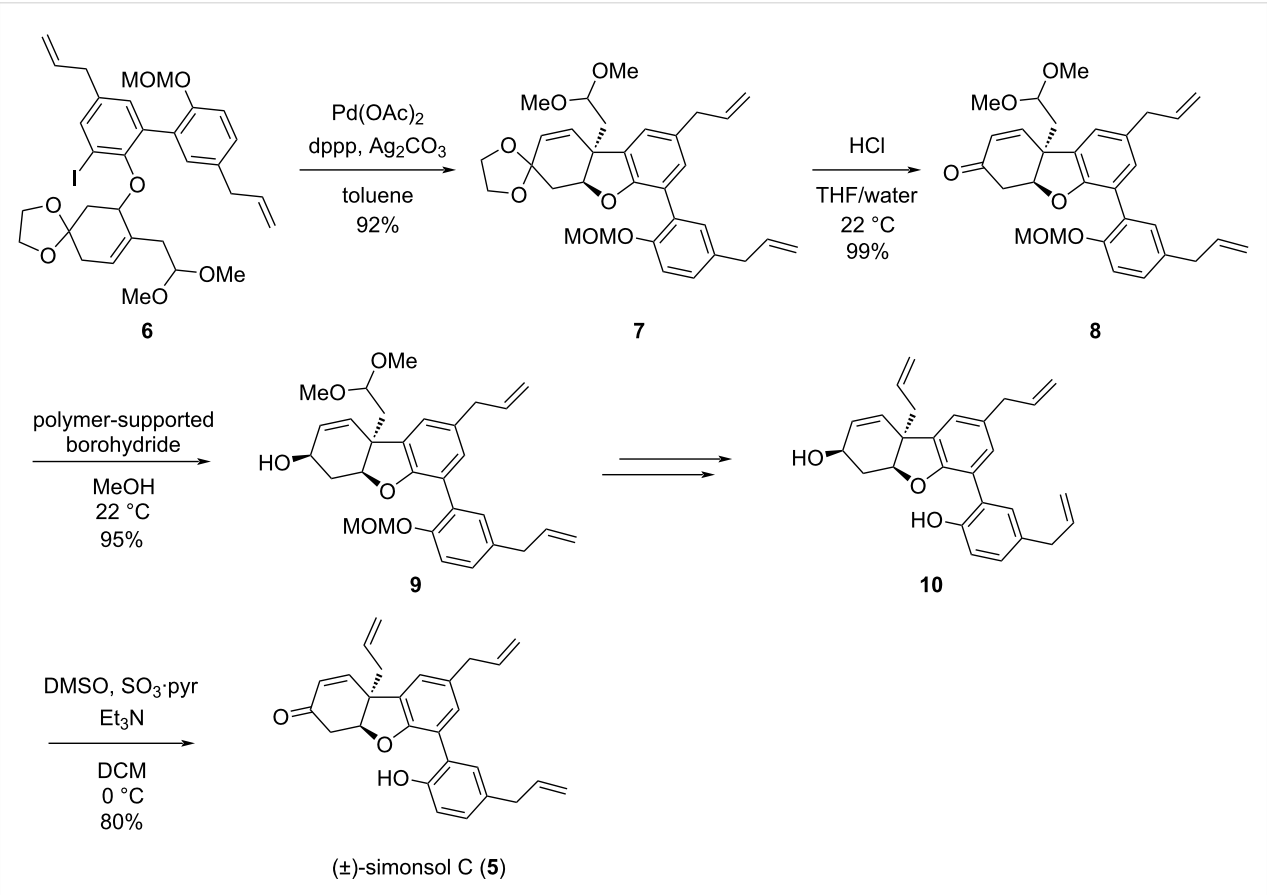

Scheme 1: The first total synthesis of (±)-simonsol C by Banwell's group.

skeleton [7]. This synthesis involved a total of 12 steps and achieved 12% overall yield.

In May 2024, the Qin group reported the second total synthesis of (±)-simonsol C (Scheme 2) [5]. An effective strategy to form the 6/5/6 benzofuran scaffold was developed which specifically involved a basic dearomatization and reductive elimination with Zn/AcOH to construct the aryl and allyl-containing quaternary center, and a simultaneous phenol-initiated oxy-Michael addition to afford the benzofuran unit. This synthesis took 9 steps and achieved an overall yield of 13%. Also in 2024, the Denton group reported another efficient way to access the 6/5/6 benzofuran scaffold of simonsol C, utilizing an alkaline dearomatization as the key reaction, followed by a functional-group-selective Wittig reaction and concurrent oxy-Michael addition [6]. A bromophenol acetal was used in the intramolecular alkylative dearomatization, which was first reported by Magnus et al. [8] and has been used in syntheses of natural products containing aryl quaternary carbon centers [9,10].

Unlike the intramolecular alkylation strategy of a phenol derivative, which can only be applied in basic dearomatization reactions, our approach using an α-iodophenol ether as precursor of the dearomatization offers considerable versatility. Not only can it be employed under basic dearomatization conditions, but it is also effective under Lewis acid conditions. Combined with a reductive elimination using Zn/AcOH, the benzofuran skeleton can be easily synthesized. This dual applicability of the new approach will be demonstrated next in the synthesis of simonsol C.

Results and Discussion

Based on extensive literature investigations, the retrosynthetic analysis strategy for our synthesis of (±)-simonsol C is as

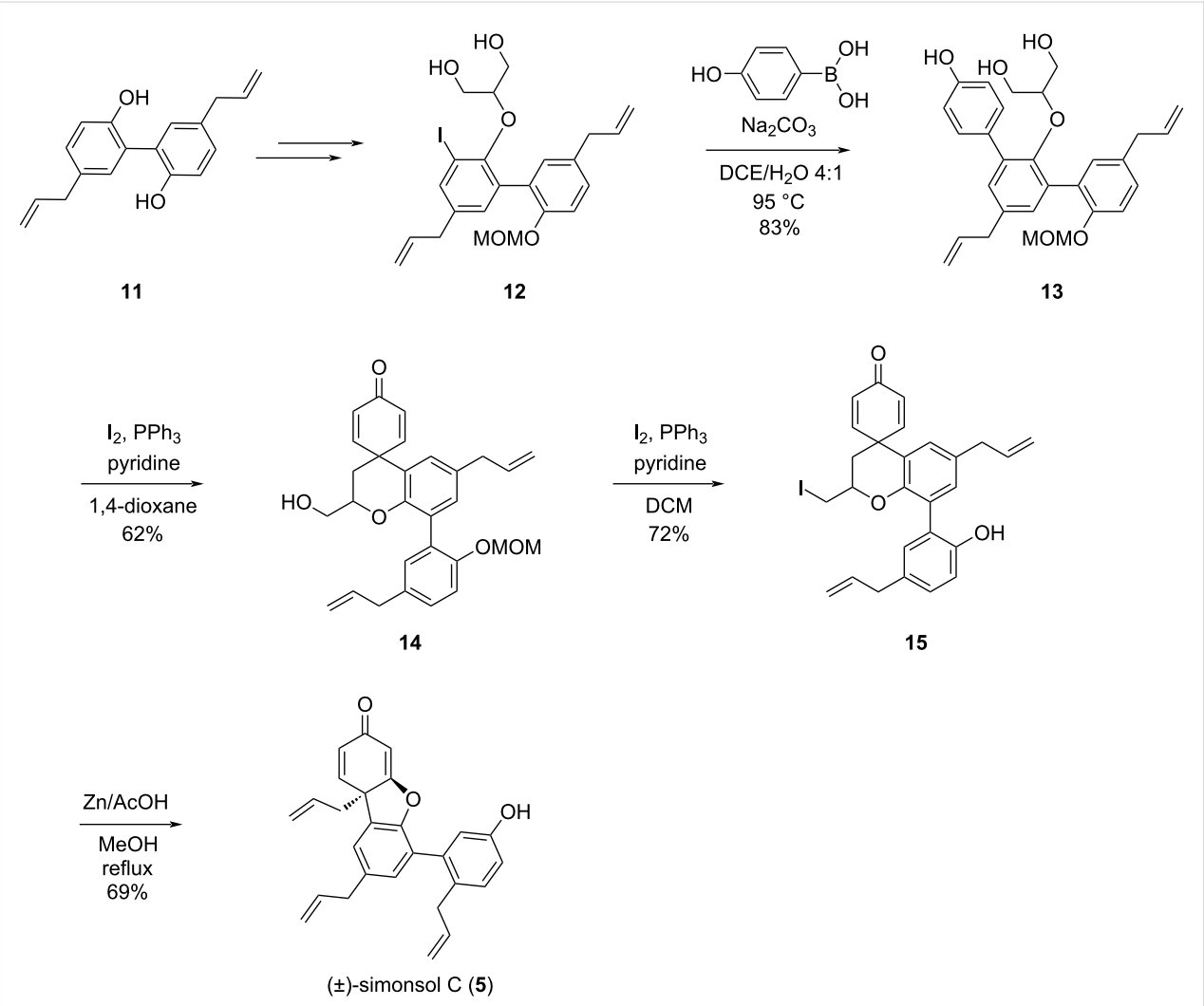

Scheme 2: The second total synthesis of (±)-simonsol C developed by the Qin group.

follows (Figure 2): The 6/5/6 benzofuran skeleton of (±)-simonsol C can be accessed via an oxy-Michael addition from dienone **15**. The 6/6/6 tricyclic structure in **15** can be constructed through dearomatization of compound **16**, which in turn can be readily synthesized through consecutive alkylation steps starting from magnolol (**11**). Additionally, using magnolol as the starting material brings two allyl groups into the product, thus avoiding the challenges associated with allyl formation reactions.

The chosen synthetic route towards (±)-simonsol C is shown in Scheme 3. Starting with magnolol (**11**), one of the phenol groups was selectively protected by controlling the equivalents of MOMCl and DIPEA, affording compound **17** with an 89% yield [11].

For the following alkylation step with *tert*-butyl bromoacetate, three bases were tested: potassium carbonate, cesium carbonate, and sodium hydride. Considering the targeted alkylation of a phenolic hydroxy group and the pK_a requirements of this reaction, weaker bases like potassium carbonate and cesium carbonate should theoretically suffice. However, the reaction outcomes with these two bases did not meet the desired expectations, as some starting material remained after 5 hours of reaction. Extending the reaction time did not lead to full consumption of the starting material. Subsequently, when the base was

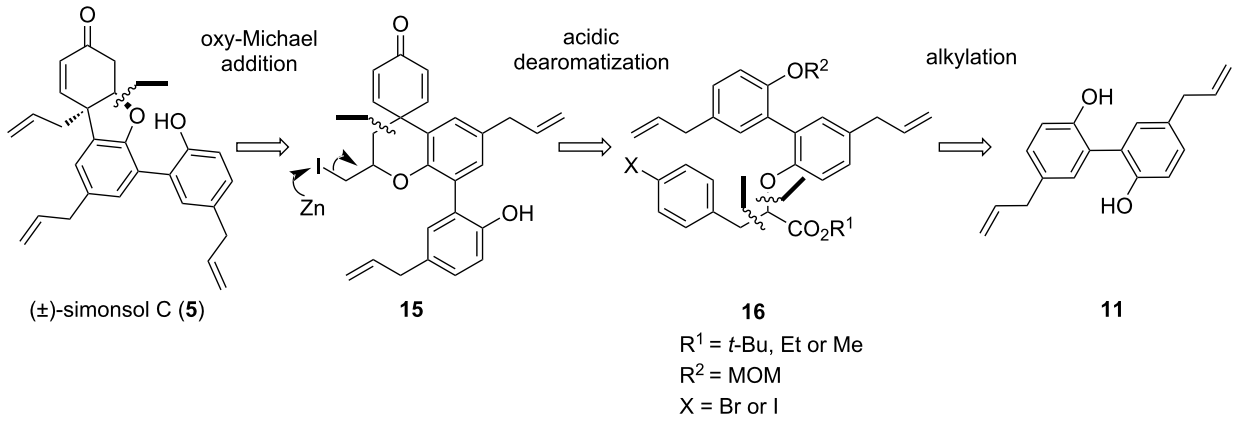

Figure 2: Retrosynthetic analysis of (±)-simonsol C.

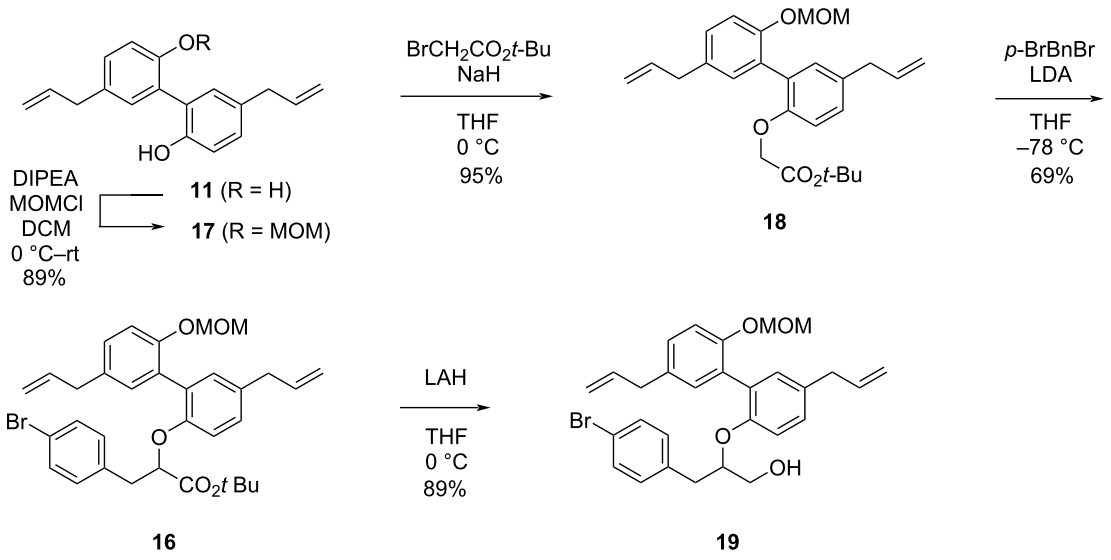

Scheme 3: Rapid access of the basic skeleton of (±)- simonsol C.

changed to the stronger base sodium hydride [12], the reaction proceeded much better. Within 2 hours, the starting material was completely converted, yielding compound **18** with 95% isolated yield.

Proton abstraction of the hydrogen in the α-position to the carbonyl group in **18** was achieved by using LDA, followed by the addition of 4-bromobenzyl bromide for alkylation, giving compound **16** with 69% isolated yield. Compound **16** was then reduced to alcohol **19** with 2 equiv LAH at 0 °C. The reaction was completed within 10 minutes and the desired alcohol **19** was isolated in 89% yield.

The copper-catalyzed replacement of the bromine substituent in **19** with a hydroxy group was achieved in the presence of a catalytic amount of oxalamide ligand **I** [13]. This transformation is critical for enabling further functionalization and the reaction conditions were optimized to achieve product **20** with 85% yield, minimizing potential side reactions. The subsequent dearomatization step is crucial for the construction of the cyclohexadienone unit. Oxidation of compound **20** with PIDA in trifluoroethanol, the original phenol was converted into a quinone moiety, successfully forming the aryl-containing quaternary center. However, in this step, the reaction was too rapid to control. After optimizing the reaction time and temperature, the reaction was carried out at −30 °C for 15 minutes and product **14** was isolated in a yield as high as 58% [14]. Iodination of compound **14** was performed next and the desired iodide was isolated and, to our delight, the cleavage of the MOM group occurred concomitantly, affording compound **15** in 75% yield. This reaction is likely triggered by the in situ-generated acid. As in our previously reported synthesis, a Zn/AcOH reductive elimination was utilized to liberate the allyl group and to simultaneously construct the 6/5/6 tricyclic skeleton via an oxy-Michael addition affording (±)-simonsol C in 70% yield (Scheme 4). The spectral data were in agreement with the reported ones [4,15,16] and the *cis* relation between the protons at C5 and C7 in simonsol C was confirmed by ^{1}H-^{1}H ROESY spectroscopy.

Conclusion

The total synthesis of (±)-simonsol C was accomplished using a dearomatization reaction under acidic conditions as key step to construct the aryl-containing quaternary center. The 6/5/6

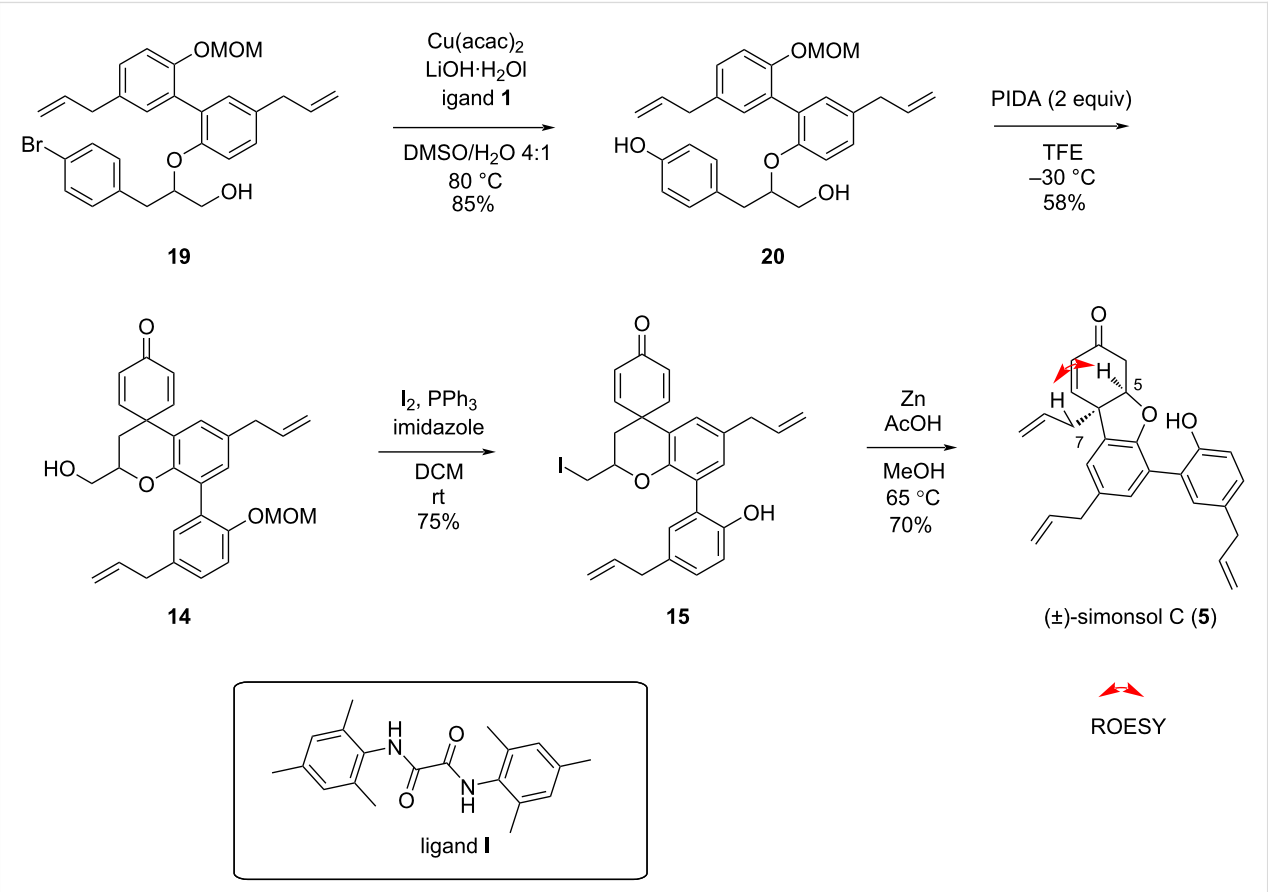

Scheme 4: Synthetic details to (±)-simonsol C.

benzofuran unit was formed through reductive elimination with Zn/AcOH and spontaneous oxy-Michael addition. This route largely enhances the synthetic efficiency and shortens the number of synthetic steps. The whole synthesis route involves 8 steps and affords the final product in a total yield of 13%, which could be the shortest synthesis route to date.

The structural motif of an all-carbon quaternary center containing an aryl group is common in many natural products, such as galanthamine and morphine. Our current strategy provides an alternative approach for the synthesis of aryl-containing quaternary carbon centers, which could be valuable for the synthesis of related natural products and their derivatives.

Supporting Information

Supporting Information File 1

Experimental procedures and characterization data of new compounds.
[https://www.beilstein-journals.org/bjoc/content/supplementary/1860-5397-21-47-S1.pdf]

Funding

This work was financially supported by start-up package of Yunnan Minzu University.

ORCID® iDs

Yong-Ming Chuan - https://orcid.org/0000-0003-3394-8618
Hong-Bo Qin - https://orcid.org/0000-0003-2603-9520

Data Availability Statement

All data that supports the findings of this study is available in the published article and/or the supporting information of this article.

Preprint

A non-peer-reviewed version of this article has been previously published as a preprint: https://doi.org/10.3762/bxiv.2025.3.v1

References

1. Zhang, X.; Meng, X.; Wu, J.; Huang, L.; Chen, S. *Chin. Med. (London, U. K.)* **2018,** *13,* 31. doi:10.1186/s13020-018-0186-9
2. Zou, Q.; Huang, Y.; Zhang, W.; Lu, C.; Yuan, J. *Molecules* **2023,** *28,* 7378. doi:10.3390/molecules28217378
3. Assiry, A. A.; Karobari, M. I.; Bhavikatti, S. K.; Marya, A. *BioMed Res. Int.* **2021,** 5510174. doi:10.1155/2021/5510174
4. Dong, C.; Liu, L.; Li, X.; Guan, Z.; Luo, H.; Wang, Y. *Planta Med.* **2013,** *79,* 338–347. doi:10.1055/s-0032-1328287
5. Sui, J.-J.; Wang, K.; Luo, S.-J.; Guo, K.; Yuan, M.-W.; Qin, H.-B. *J. Org. Chem.* **2024,** *89,* 7821–7827. doi:10.1021/acs.joc.4c00518
6. Arnold, R. E.; Saska, J.; Mesquita-Ribeiro, R.; Dajas-Bailador, F.; Taylor, L.; Lewis, W.; Argent, S.; Shao, H.; Houk, K. N.; Denton, R. M. *Chem. Sci.* **2024,** *15,* 11783–11793. doi:10.1039/d4sc03232b
7. Nugent, J.; Banwell, M. G.; Schwartz, B. D. *Org. Lett.* **2016,** *18,* 3798–3801. doi:10.1021/acs.orglett.6b01799
8. Magnus, P.; Sane, N.; Fauber, B. P.; Lynch, V. *J. Am. Chem. Soc.* **2009,** *131,* 16045–16047. doi:10.1021/ja9085534
9. Magnus, P.; Seipp, C. *Org. Lett.* **2013,** *15,* 4870–4871. doi:10.1021/ol402302k
10. Li, Q.; Zhang, H. *Chem. – Eur. J.* **2015,** *21,* 16379–16382. doi:10.1002/chem.201503594
11. Luo, G.; Li, X.; Zhang, G.; Wu, C.; Tang, Z.; Liu, L.; You, Q.; Xiang, H. *Eur. J. Med. Chem.* **2017,** *140,* 252–273. doi:10.1016/j.ejmech.2017.09.015
12. Nam, S.; Ware, D. C.; Brothers, P. J. *Org. Biomol. Chem.* **2018,** *16,* 6460–6469. doi:10.1039/c8ob00957k
13. Zhou, W.; Fan, M.; Yin, J.; Jiang, Y.; Ma, D. *J. Am. Chem. Soc.* **2015,** *137,* 11942–11945. doi:10.1021/jacs.5b08411
14. Roche, S. P.; Porco, J. A., Jr. *Angew. Chem., Int. Ed.* **2011,** *50,* 4068–4093. doi:10.1002/anie.201006017
15. Hu, J.; Bian, M.; Ding, H. *Tetrahedron Lett.* **2016,** *57,* 5519–5539. doi:10.1016/j.tetlet.2016.11.007
16. Küenburg, B.; Czollner, L.; Fröhlich, J.; Jordis, U. *Org. Process Res. Dev.* **1999,** *3,* 425–431. doi:10.1021/op990019q

License and Terms

BEILSTEIN JOURNAL OF ORGANIC CHEMISTRY

Recent advances in controllable/divergent synthesis

Jilei Cao[1], Leiyang Bai[*1] and Xuefeng Jiang[*1,2,3]

Review

Open Access

Address:
[1]Hainan Institute of East China Normal University, State Key Laboratory of Petroleum Molecular & Process Engineering, Shanghai Key Laboratory of Green Chemistry and Chemical Process, School of Chemistry and Molecular Engineering, East China Normal University, 3663 North Zhongshan Road, Shanghai 200062, PR China, [2]School of Chemistry and Chemical Engineering, Henan Normal University, Xinxiang, Henan 453007, PR China and [3]State Key Laboratory of Organometallic Chemistry, Shanghai Institute of Organic Chemistry, Chinese Academy of Sciences, 345 Lingling Road, Shanghai 200032, PR China

Email:
Leiyang Bai[*] - lybai@chem.ecnu.edu.cn; Xuefeng Jiang[*] - xfjiang@chem.ecnu.edu.cn

* Corresponding author

Keywords:
controllable; divergent; diverse products; switchable synthesis

Beilstein J. Org. Chem. **2025,** *21,* 890–914.
https://doi.org/10.3762/bjoc.21.73

Received: 10 February 2025
Accepted: 22 April 2025
Published: 07 May 2025

This article is part of the thematic issue "Concept-driven strategies in target-oriented synthesis".

Guest Editor: C. Li

Abstract

The development of streamlined methodologies for the expeditious assembly of structurally diverse organic architectures represents a paramount objective in contemporary synthetic chemistry, with far-reaching implications across pharmaceutical development, advanced materials innovation, and fundamental molecular science research. In recent years, controllable/divergent synthetic strategies for organic functional molecules using common starting materials have garnered significant attention due to their high efficiency. This review categorizes recent literatures focusing on key regulatory factors for product divergent formation, in which controlling chemical selectivity primarily relies on ligands, metal catalysts, solvents, time, temperature, acids/bases, and subtle modifications of substrates. To gain a deeper understanding of the mechanisms underlying reaction activity and selectivity differentiation, the review provides a systematic analysis of the mechanisms of critical steps through specific case studies. It is hoped that the controllable/divergent synthesis concept will spark the interest of practitioners and aficionados to delve deeper into the discipline and pursue novel advancements in the realm of chemical synthesis.

Introduction

In the era of synthetic organic chemistry, divergence can produce stereodivergence (including diastereodivergence and enantiodivergence) [1-4] and regiodivergence [5,6]. In both cases, starting from the same substrate, different stereoisomers (diastereomers and enantiomers) or regioisomers can be obtained under different reaction conditions. Over the past two decades, researchers have found that by changing reaction conditions and modifying the substrate, two structurally distinct

products that are neither stereoisomers nor regioisomers can be obtained from the same starting material (using the same reagents, if necessary), and significant progress has been made in recent years. Controllable/divergent synthetic strategies have increasingly attracted attention [5,7-14], for example, in 2024, Rana [15] and co-workers reported advances in solvent-controlled stereodivergent catalysis. Surprisingly, to our knowledge, there is currently no comprehensive review of studies on controllable/divergent synthesis. This review systematically examines, how these multidimensional control elements (including ligands, metal catalysts, solvents, time, temperature, acids/bases, and subtle modifications of substrates) synergize to achieve predictable product diversification. In addition, mechanistic insights are discussed providing illustrative examples across reaction classes, and emerging strategies for programming synthetic outcomes. The integration of these approaches promises to accelerate drug discovery and materials development through sustainable, atom-economic synthesis of complex molecular libraries.

Review

Ligand control

The precise regulation of product selectivity represents a fundamental challenge in transition-metal-catalyzed organic transformations, with significant implications for complex molecule synthesis. In this context, ligand-modulated divergent catalysis has emerged as a paradigm-shifting strategy, enabling programmable access to structurally distinct molecular architectures from identical substrate precursors through precise manipulation of metal coordination [16-18]. This sophisticated approach capitalizes on the stereoelectronic tunability of ancillary ligands to dictate reaction pathways, thereby offering unprecedented control over chemo-, regio-, and stereoselectivity parameters in catalytic manifolds. In 2015, the Jiang group developed a palladium-catalyzed regioselective three-component C1 insertion reaction (Scheme 1) [19]. In this reaction, an *o*-iodoaniline **1**, phenylacetylene, and carbon monoxide were used as starting materials, and two natural product frameworks of phenanthridone and acridone alkaloids could be selectively obtained by controlling ligands. The reaction of *o*-iodoaniline with in situ-generated arynes under CO atmosphere under ligand-free conditions selectively afforded phenanthridinones. Intriguingly, switching to the electron-rich bidentate ligand bis(diphenylphosphino)methane (dppm) redirected the pathway to yield acridones. Time-dependent NMR studies revealed that the selectivity hinges on the aryne release kinetics from its precursor. Employing CsF, tetrabutylammonium iodide (TBAI), and water significantly accelerated aryne generation, thereby increasing its local concentration. This favored aryne coordination to the palladium center, followed by CO insertion and reductive elimination to furnish phenanthridinones. In contrast, when dppm was introduced, oxidative addition of the C–I bond to palladium formed the four-membered aryl–palladium complex **Int-5**. Steric hindrance from the bulky dppm ligand, combined with slower aryne release (using KF as the fluoride source), attenuated aryne coordination. Under these electron-deficient conditions, CO preferentially occupied the palladium coordination site. Sequential insertion of CO and aryne, followed by reductive elimination, culminated in acridone formation. This ligand-dependent mechanistic dichotomy underscores the critical interplay between aryne availability, steric modulation, and electronic effects in steering catalytic selectivity.

In 2016, the Jiang group achieved regioselective control in the gold-catalyzed intramolecular hydroarylation of alkynes by modulating the electronic and steric effects of ligands (Scheme 2) [20]. Mechanistically, the electron-deficient phosphite ligand **L1** and the weakly coordinating OTf^- anion synergistically enhanced the electrophilicity of the gold center, enabling coordination with the amide group to form a three-coordinate Au(I)–π-alkyne intermediate **Int-12**. The umbrella-shaped steric shielding provided by the ligand-stabilized intermediate **Int-9**, followed by Friedel–Crafts-type addition and protonation to complete *ortho*-position cyclization. In contrast, *para*-position cyclization was exclusively achieved through π–π interactions between the electron-rich X-phos ligand and the substrate, compensating for the electron-deficient nature of the aromatic system and ensuring high regioselectivity.

In 2018, the Jiang group developed a regiodivergent synthetic method for indolo[3,2-*c*]coumarins **10** and benzofuro[3,2-*c*]quinolinones **9** via controllable palladium(II)-catalyzed carbonylative cyclization (Scheme 3) [21]. When ligand **L3** coordinates with the palladium center, the enhanced electrophilicity of palladium facilitates preferential coordination with the amino group and activates the alkyne to form the intermediate **Int-14** instead of **Int-14'**. Subsequent nucleophilic cyclization generates intermediate **Int-15**. Following CO insertion, complex **Int-16** is formed, and reductive elimination yields the benzofuro[3,2-*c*]quinolinone product **9** along with a Pd(0) species, which is reoxidized to Pd(II) by BQ (benzoquinone). When the ligand is switched to the sterically bulky and electron-rich dppm, the chemoselectivity is reversed: the palladium center now preferentially coordinates with the hydroxy group to form complex **Int-17** and the amino group undergoes nucleophilic attack to generate **Int-18**. After CO insertion complex **Int-19** is produced and reductive elimination ultimately affords the indolo[3,2-*c*]coumarin product **10**.

In 2023, the Garg group achieved the first example of utilizing in situ-generated π-allylpalladium complexes to capture strained

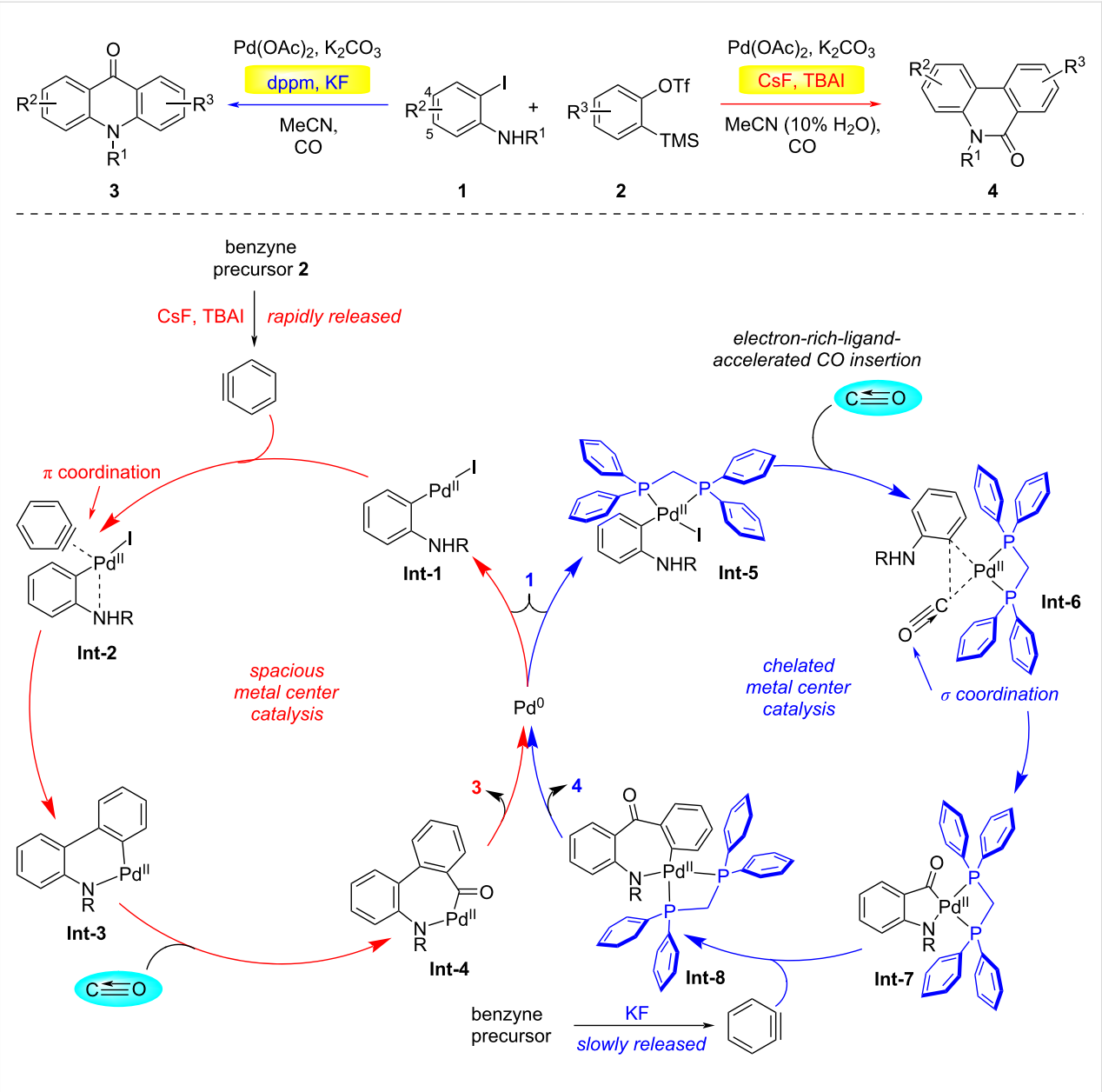

Scheme 1: Ligand-controlled regiodivergent C1 insertion into arynes [19].

cyclic allene intermediates (Scheme 4) [22]. By modulating the ligands in the reaction system, two distinct polycyclic scaffolds, **13** or **14**, could be synthesized with high selectivity. Mechanistically, the Pd(0) catalyst coordinates to substrate **11**, followed by oxidative addition and release of carbon dioxide to form the zwitterionic π-allylpalladium intermediate **Int-21**. Under the reaction conditions, silyl triflate **12** undergoes a fluoride-mediated 1,2-elimination to generate the cyclic allene intermediate **Int-22**. Through a ligand-controlled regioselective migratory insertion process, reaction of **Int-21** and **Int-22** leads to the formation of π-allylpalladium intermediates **Int-23** or **Int-24**, depending on the ligand employed. Finally, cyclization of **Int-23** or **Int-24** yields the tricyclic product **13** or the tetracyclic product **14**, respectively.

In 2024, the Song group achieved a ligand-controlled regiodivergent and enantioselective ring expansion of benzosilacyclobutenes with internal naphthylalkynes by strategically modulating the ligand steric profiles (Scheme 5) [23]. Employing cavity-engineered phosphoramidite ligands, the reaction pathway bifurcated based on the steric demands of Si–C-bond activation. The methyl-substituted ligand (*S*)-8*H*-binaphthyl phosphoramidite **L4**, featuring a spacious cavity, favored sterically encumbered Si–C(sp^3)-bond activation, selectively delivering

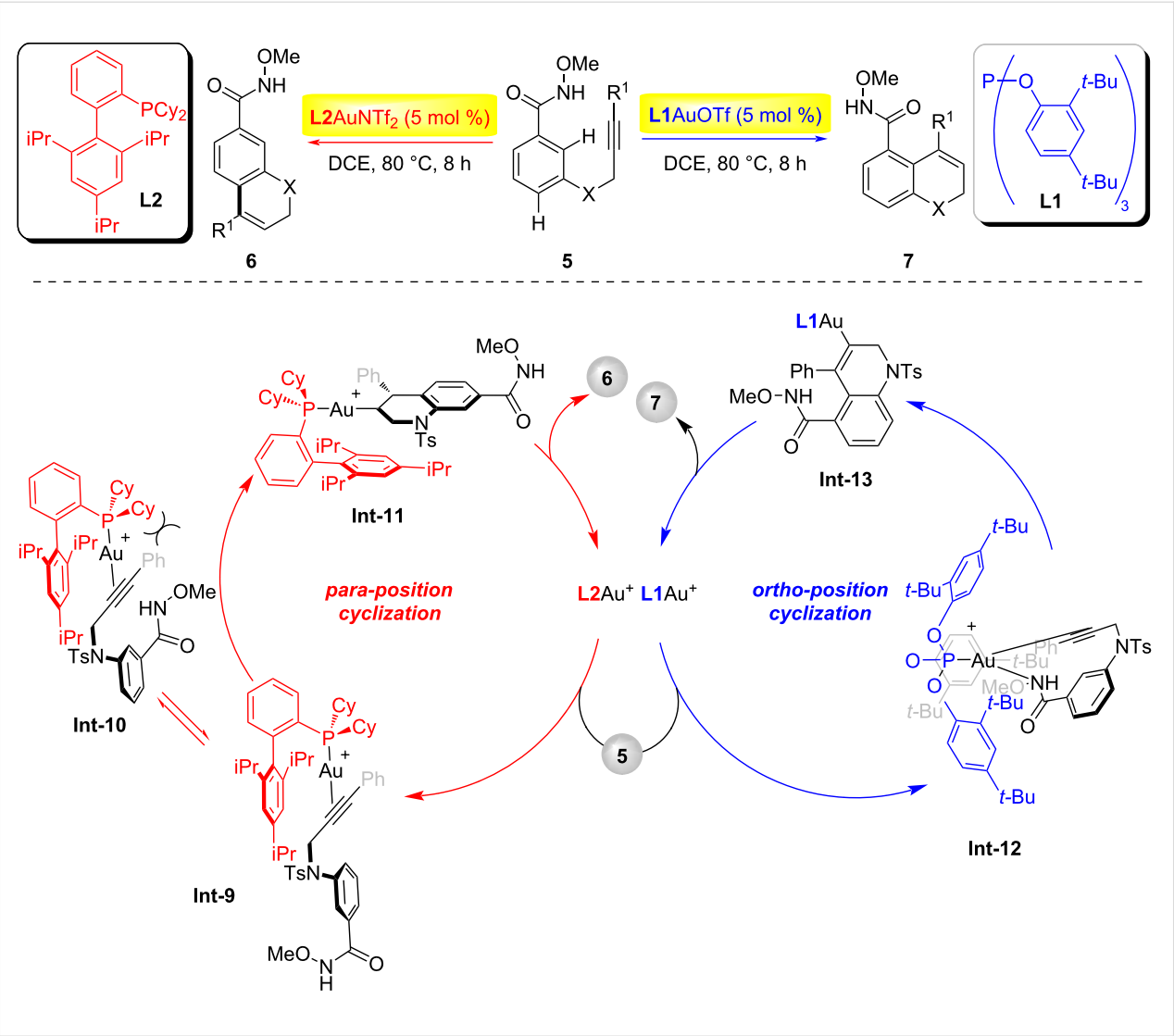

Scheme 2: Ligand effect in homogenous gold catalysis enabling regiodivergent π-bond-activated cyclization [20].

axially chiral (*S*)-1-silacyclohexenyl arenes **17** with high enantiocontrol. Conversely, the bulky *tert*-butyl-decorated (*R*)-spirophosphoramidite **L5** imposed a confined cavity, steering selectivity toward Si–C(sp^2)-bond activation and predominantly afforded the regioisomeric (*S*)-2-silacyclohexenylarenes **18**.

In 2025, Gong and co-workers reported a visible-light-mediated hydrogen atom transfer (HAT)/chiral copper dual catalytic system that achieved regiodivergent and enantioselective C(sp^3)–C(sp^3) and C(sp^3)–N oxidative cross-couplings between *N*-arylglycine ester/amide derivatives and abundant hydrocarbon C(sp^3)–H feedstocks (Scheme 6) [24]. This methodology also represents a highly challenging direct C(sp^3)–H asymmetric amination. Mechanistic insights: When using a bulky, electron-rich chiral bisphosphine ligand **L6**, the glycine ester substrate coordinates with the copper catalyst to form a key intermediate complex **Int-26**. The sterically hindered and electron-rich environment around the copper center disfavors a direct interaction with nucleophilic alkyl radicals. Instead, the reaction proceeds via an outer-sphere mechanism, where the alkyl radical reacts with the copper-activated C=N unsaturated bond, enabling stereocontrolled C(sp^3)–C(sp^3) coupling. In contrast, with the anionic cyano-substituted bisoxazoline ligand **L7**, the glycine ester and copper catalyst form a distinct intermediate complex **Int-28**. The ligand's reduced steric bulk and altered electronic properties facilitate direct interaction with alkyl radicals, forming a high-valent Cu(III) intermediate **Int-29**. This intermediate undergoes reductive elimination via an inner-sphere mechanism to generate the C(sp^3)–N-coupled chiral product **22**. Notably, benzoic acid acts as a critical additive, likely by stabilizing key intermediates and modulating the steric/electronic environment for enhanced enantiocontrol.

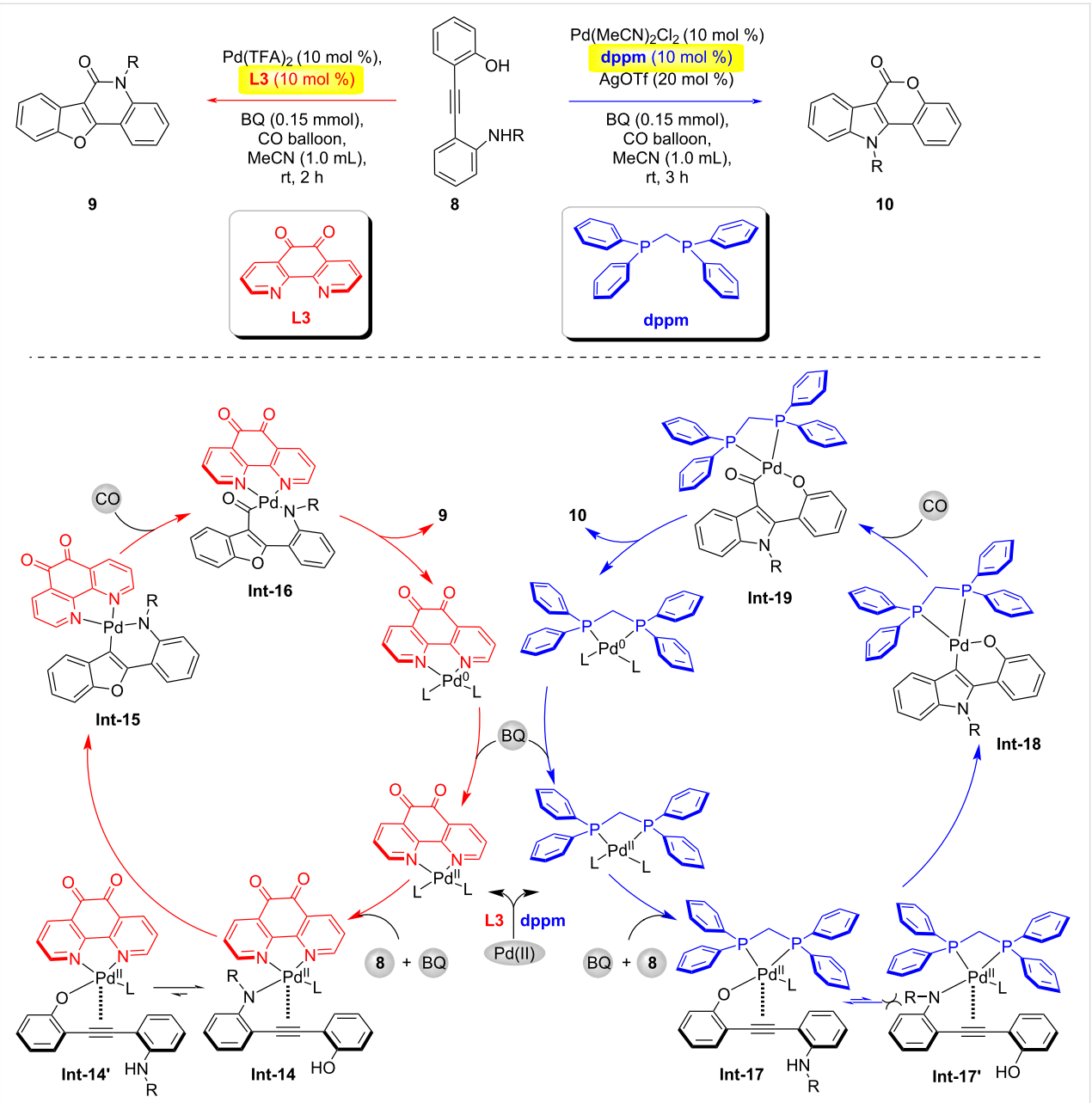

Scheme 3: Ligand-controlled palladium(II)-catalyzed regiodivergent carbonylation of alkynes [21].

Metal control

Over the past decade, the relentless pursuit of precision in natural products and pharmaceutical synthesis has driven remarkable advances in catalytic methodologies, particularly in the realm of catalyst-controlled chemoselective transformations [11,25-29]. In 2023, the Shu group developed a catalyst-controlled regioselective and enantioselective hydroamination reaction of electron-deficient alkenes (Scheme 7) [30]. By efficiently regulating the regioselectivity and enantioselectivity of alkene **23** hydrometallation through catalytic systems, they overcame the influence of steric and electronic effects during the hydrometallation process, simultaneously achieving the synthesis of chiral α-quaternary carbon amino acid derivatives **26** and α-chiral β-amino acid derivatives **27**. Using a copper catalyst, the chiral α-quaternary carbon amino acid derivatives **26** were obtained with exclusive regioselectivity and excellent enantioselectivity. Employing a nickel catalyst, α-chiral β-amino acid derivatives **27** were synthesized with single regioselectivity and outstanding enantioselectivity.

In the same year, Rong and co-workers reported a highly efficient catalyst-controlled regio- and enantioselective hydroalkyl-

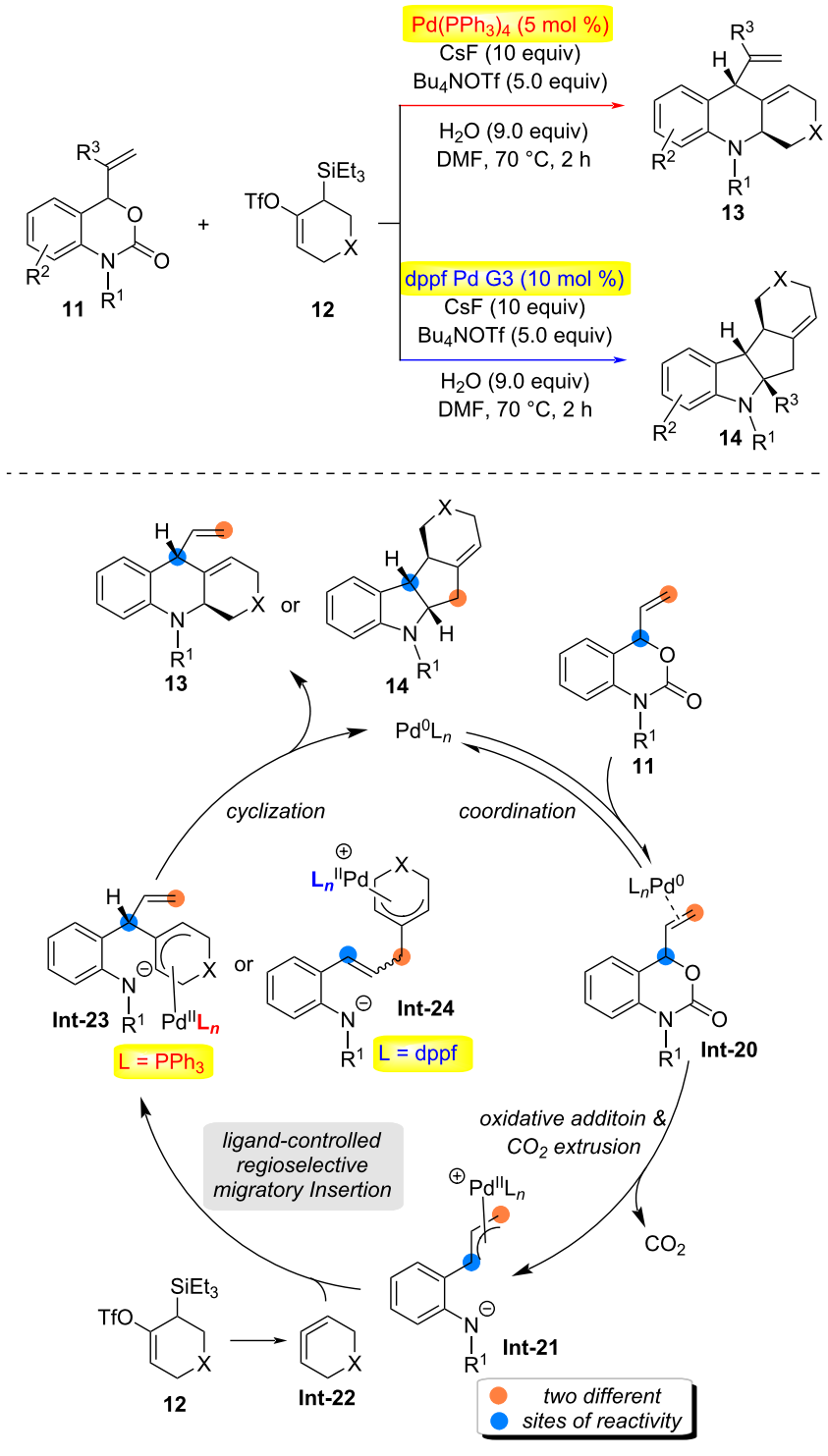

Scheme 4: Catalyst-controlled annulations of strained cyclic allenes with π-allyl palladium complexes and proposed mechanism [22].

ation reaction, enabling the divergent synthesis of chiral C2- and C3-alkylated pyrrolidines through desymmetrization of readily available 3-pyrrolines (Scheme 8) [31]. The cobalt catalytic system ($CoBr_2$ with modified bisoxazoline ligands) achieved asymmetric $C(sp^3)$–$C(sp^3)$ coupling via distal stereocontrol, efficiently producing C3-alkylated pyrrolidines, while the nickel catalytic system afforded C2-alkylated pyrrolidines through a tandem alkene isomerization/hydroalkylation process.

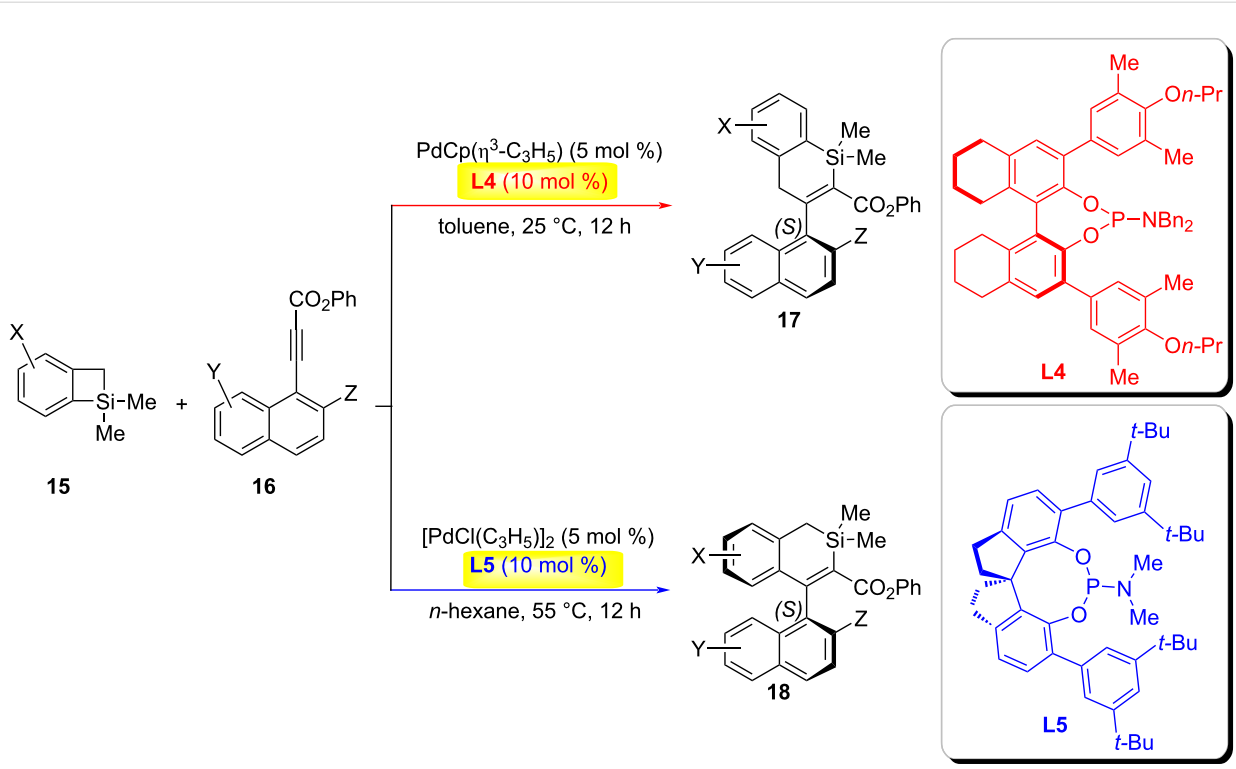

Scheme 5: Ring expansion of benzosilacyclobutenes with alkynes [23].

This method utilized readily accessible catalysts, chiral BOX ligands **L9**, and reagents, delivering enantioenriched 2-/3-alkyl-substituted pyrrolidines with excellent regio- and enantioselectivity (up to 97% enantiomeric excess). Radical-clock experiments and deuterium-labeled silane studies revealed that cobalt catalysis proceeded via irreversible Co–H migratory insertion to achieve C3 selectivity, whereas nickel catalysis involved alkene isomerization to generate a (2,3-dihydropyrrolyl) intermediate **Int-35**, followed by C2-selective coupling.

In 2024, the Zheng group reported a catalyst-controlled cyclization reaction of bicyclo[1.1.0]butanes (BCBs) **32** with α-alkenylazides **33**, achieving divergent synthesis of 2- and 3-azabicyclo[3.1.1]heptenes (aza-BCHepes) **35** or **36** (Scheme 9) [32]. This study developed a practical method for constructing novel 2- and 3-aza[3.1.1]heptene architectures from readily available α-alkenylazides and BCBs through catalyst-controlled (3 + 3) and (3 + 2) cyclization strategies. Two distinct pathways were established: (1) The titanium-catalyzed ring opening of bicyclobutane (BCB) **32** generates a γ-carbonyl radical intermediate **Int-42**, which undergoes trapping by vinylazide **33**. Subsequent dinitrogen extrusion produces an iminyl radical species **Int-44**. This reactive intermediate then engages with a Ti(IV)-enolate complex through radical recombination, ultimately delivering 2-aza-bicyclo[3.1.1]heptene (BCHepe) while regenerating the Ti(III) catalyst to complete the catalytic cycle. (2) Scandium-catalyzed pathway: Activation of the donor–acceptor BCB via $Sc(OTf)_3$ coordination to its carbonyl group facilitates nucleophilic attack by vinylazide **33**, forming an iminodiazonium intermediate **Int-40** accompanied by a δ-carbanion. Transannular cyclization of this species affords 2-azidobicyclo[3.1.1]hexane (2-azidoBCHs). Subsequent thermal activation induces selective migration of the less sterically hindered secondary carbon center with concomitant dinitrogen elimination, yielding 3-aza-BCHepe as the final product.

Solvent control

The solvent microenvironment emerged as a critical determinant in governing stereochemical outcomes, exerting profound influence through multifaceted solute–solvent interactions [5]. Solvent polarity, hydrogen-bonding propensity, and dielectric characteristics collectively orchestrate stereodivergent pathways through dynamic coordination effects and differential stabilization of transition states. Notably, these solvent-mediated electronic and steric modulations frequently dictate reaction stereoselectivity, with even subtle solvent permutations potentially inducing complete stereochemical inversion in sensitive systems [33-38]. In 2023, He and Sessler disclosed a versatile one-pot synthesis of structurally diverse macrocycles through the dynamic self-assembly of α,α'-linked oligopyrrolic

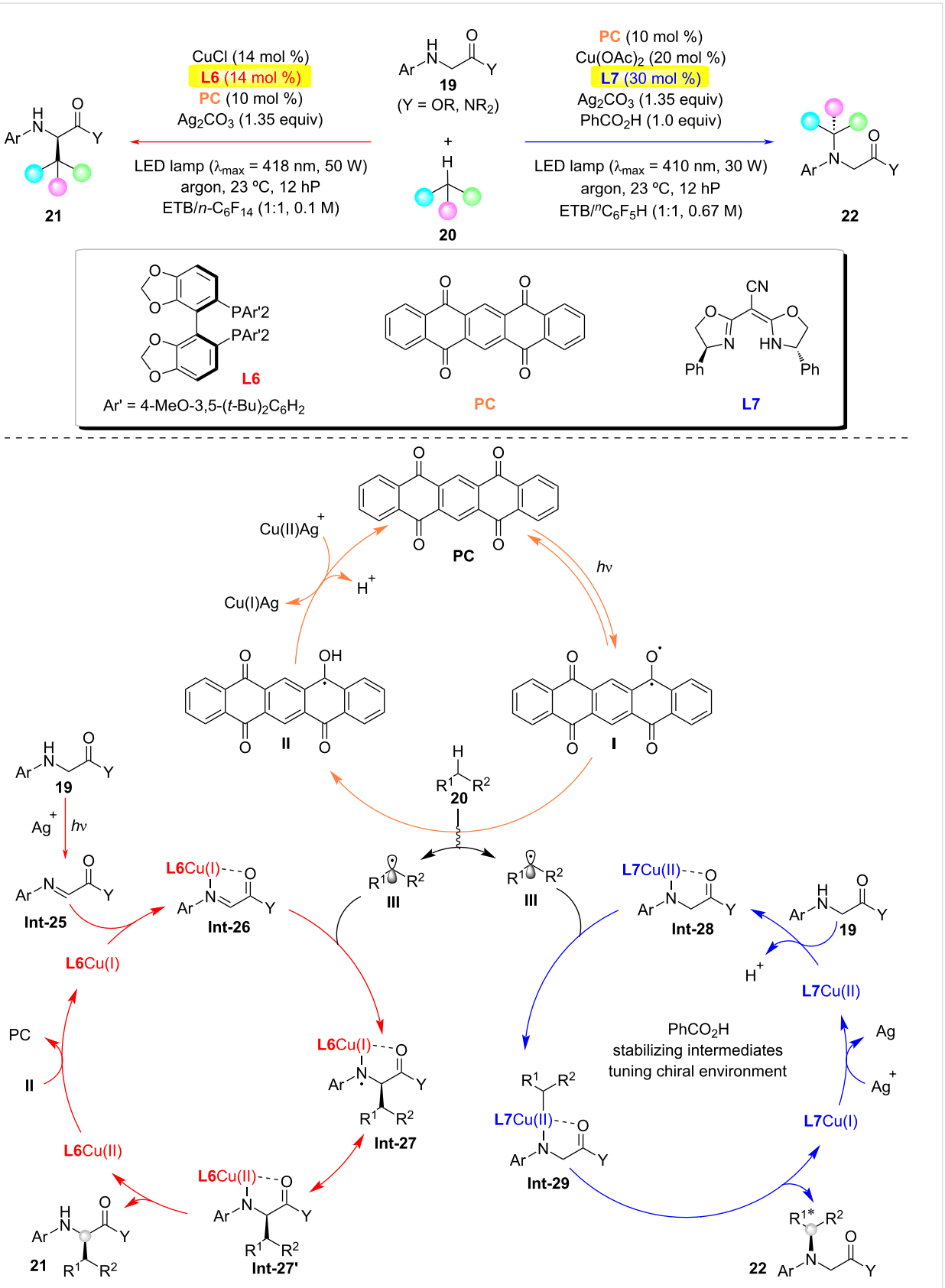

Scheme 6: Photoinduced regiodivergent and enantioselective cross-coupling [24].

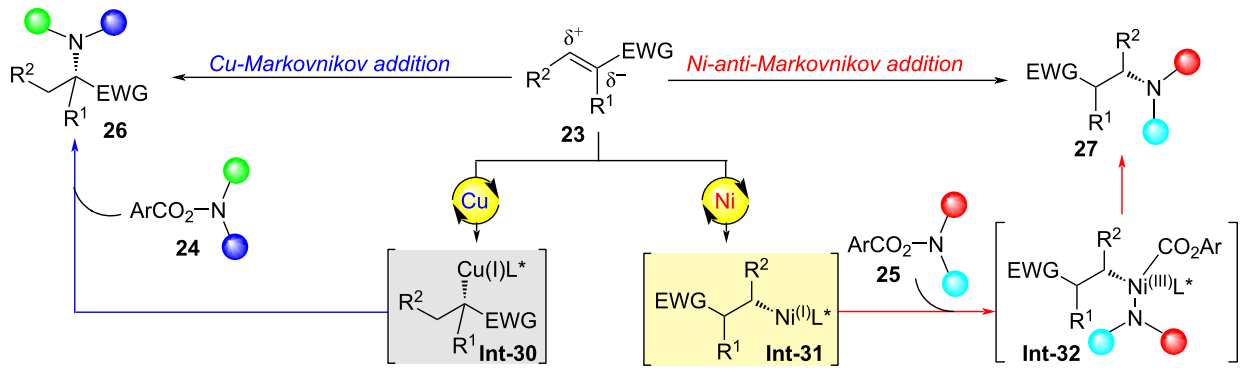

Scheme 7: Catalyst-controlled regiodivergent and enantioselective formal hydroamination of *N*,*N*-disubstituted acrylamides [30].

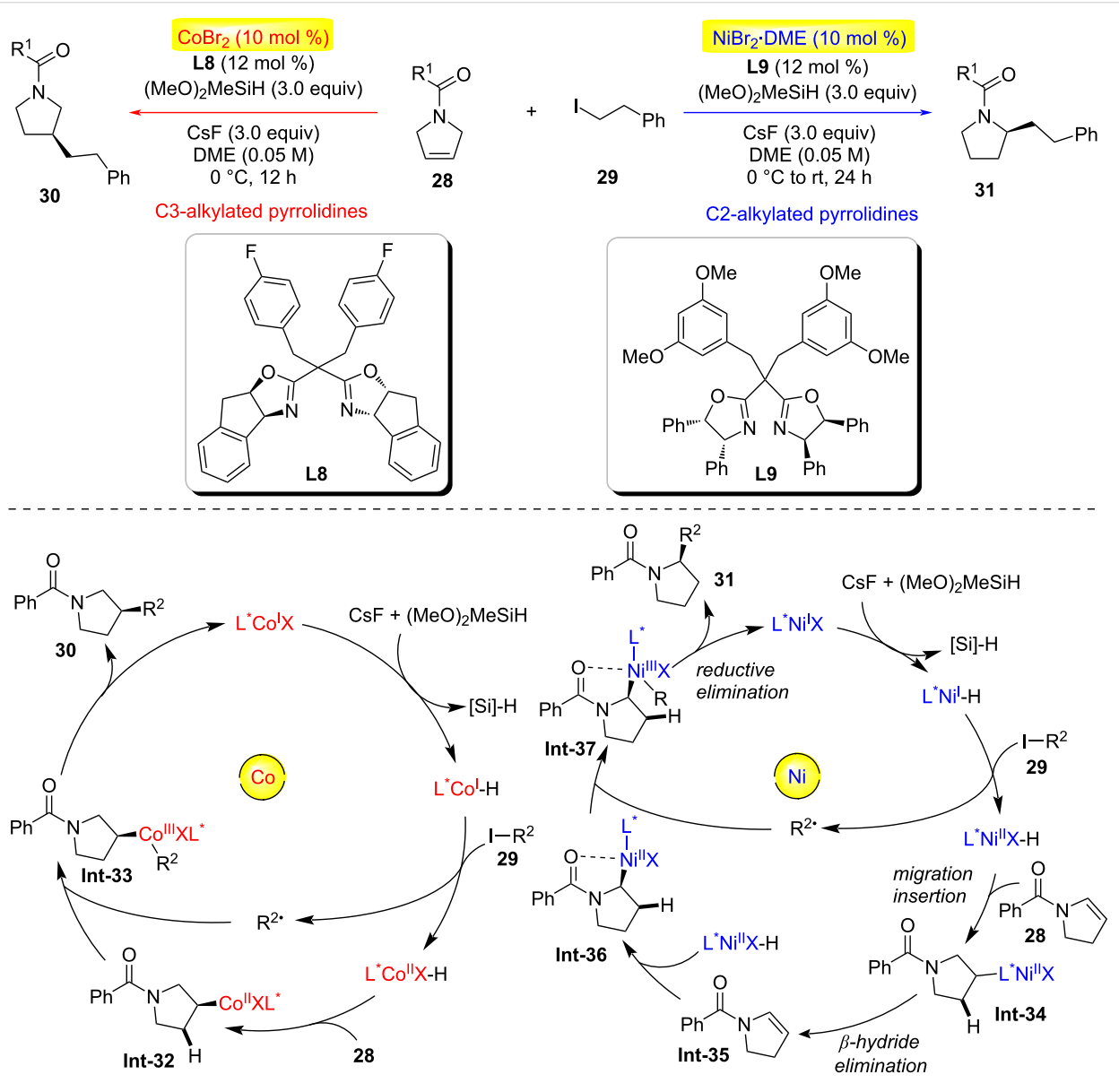

Scheme 8: Catalyst-tuned regio- and enantioselective C(sp^3)–C(sp^3) coupling [31].

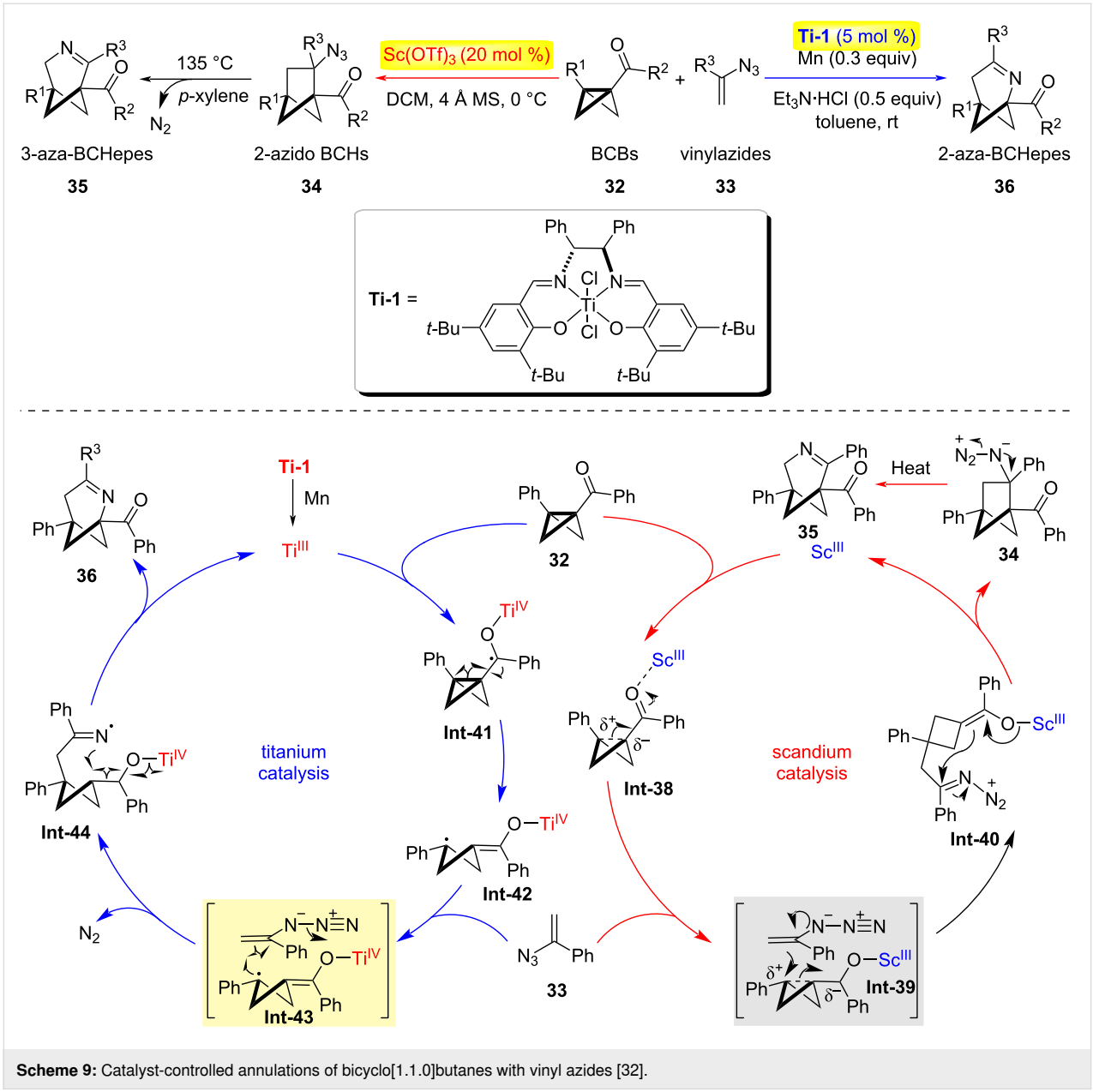

Scheme 9: Catalyst-controlled annulations of bicyclo[1.1.0]butanes with vinyl azides [32].

dialdehydes and alkyldiamines (Scheme 10) [39]. Their investigation revealed distinct solvent-mediated selectivity in product formation. Condensation of the pyridine-bridged oligopyrrolic dialdehyde **37** with simple alkyldiamines proceeded with solvent-independent regioselectivity, exclusively furnished [2 + 2] macrocyclic adducts. Strikingly, when **37** was combined with 2,2'-oxybis(ethylamine) (**38**), the reaction pathway exhibited pronounced solvent dependency. Reactions in methanol, ethanol, or chloroform selectively generated the [1 + 1] macrocycle **39** as the sole product. In contrast, polar aprotic solvents such as dimethyl sulfoxide (DMSO), *N*,*N*-dimethylformamide (DMF), or acetonitrile (MeCN) favored precipitation of the [2 + 2] macrocycle **40**. Notably, the macrocycle **40** underwent spontaneous structural reorganization in chloroform or dichloromethane (DCM), converting entirely into the thermodynamically stable [1 + 1] isomer **39**. This work demonstrates a solvent-driven approach for dynamically interconverting macrocycle sizes, governed by thermodynamic stability and solubility differences.

In the same year, Chauhan, Koenigs, and co-workers demonstrated solvent-controlled bifurcation in the light-driven reactivity of cyclic diazo imides **41** with thiols **42**, unveiling two mechanistically distinct pathways (Scheme 11) [40]. In dichloromethane (DCM), the reaction proceeds via a carbene intermediate, enabling cascade C(sp^2)–H functionalization/thio-

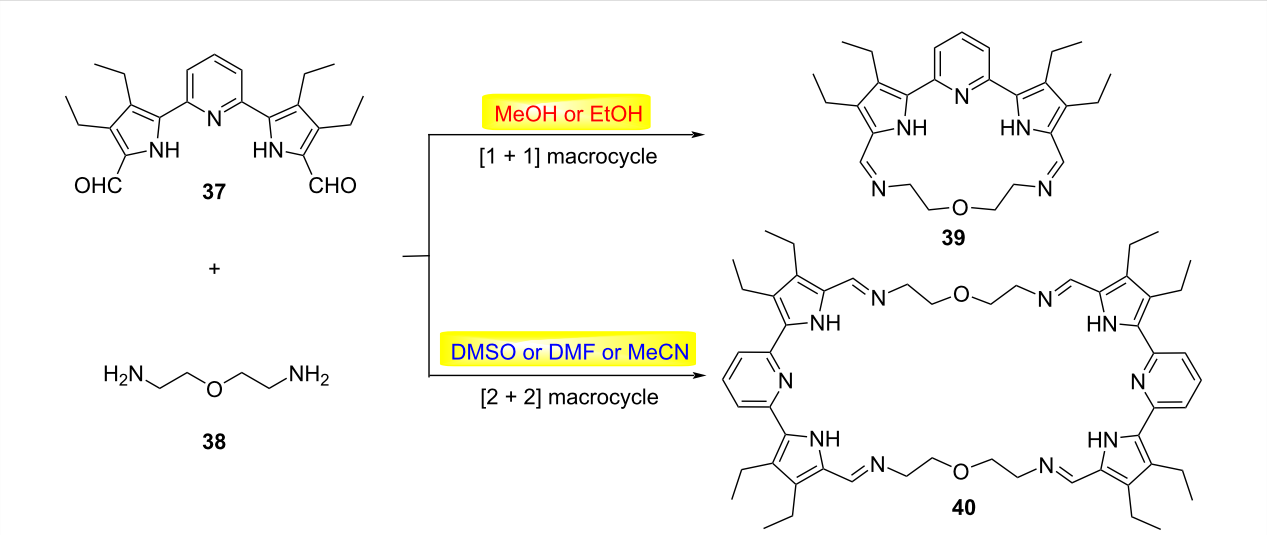

Scheme 10: Solvent-driven reversible macrocycle-to-macrocycle interconversion [39].

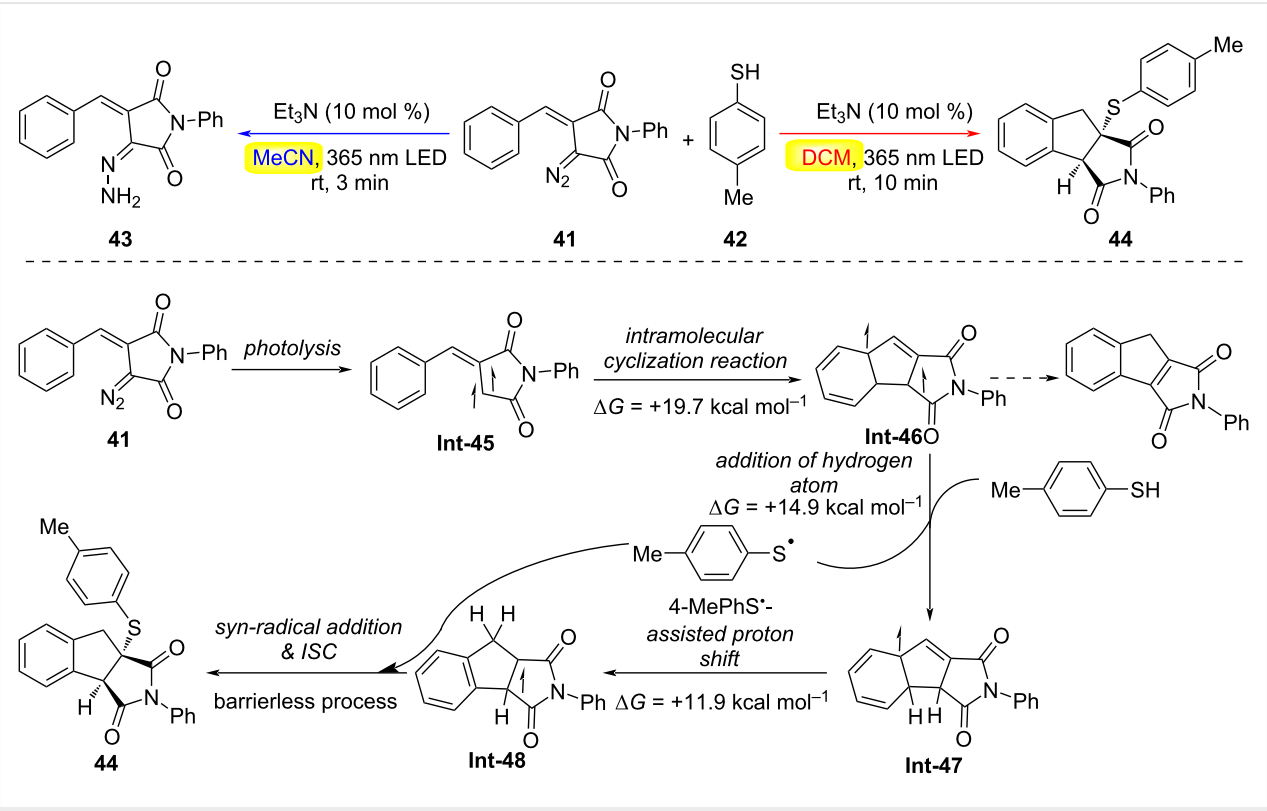

Scheme 11: Unexpected solvent-dependent reactivity of cyclic diazo imides and mechanism [40].

lation to deliver indane-fused pyrrolidines **43** in excellent yields (up to 92%). Strikingly, switching the solvent to acetonitrile completely suppresses carbene formation under identical conditions, redirecting the pathway toward an unconventional diazo reduction wherein aryl thiols act as stoichiometric reductants. Mechanistic insights, elucidated through control experiments and DFT calculations, revealed that photoexcitation of diazo imide **41** triggers nitrogen extrusion ($\Delta G^{\ddagger}$ = +10.0 kcal·mol^{-1}), generating the triplet carbene intermediate **Int-45**. In DCM, this species undergoes intramolecular cyclization into a proximal C(sp^2)–H bond ($\Delta G^{\ddagger}$ = +19.7 kcal·mol^{-1}) to form **Int-46**, which reacts with 4-MePhSH ($\Delta G^{\ddagger}$ = +14.9 kcal·mol^{-1}) to yield

radical intermediate **Int-47** and a thiyl radical (4-MePhS˙). Sequential thiol-assisted hydrogen shifts produce **Int-48**, followed by barrierless thiyl radical addition and intersystem crossing (ISC) to furnish the final product. In contrast, acetonitrile's polar aprotic environment destabilizes the carbene pathway, favoring direct reduction of the diazo moiety via electron transfer from the thiol. This solvent-gated selectivity underscores the critical role of reaction medium polarity in modulating reactive intermediates, offering a strategic lever to toggle between C–H functionalization and reductive manifolds in photochemical transformations.

In 2024, the Cheng group developed a palladium/chiral norbornene (NBE)-catalyzed cyclization reaction between aryl iodides **45** and phosphoramides **46** under varying solvent conditions of toluene (PhMe) and acetonitrile (MeCN), based on their studies of the Catellani reaction (Scheme 12) [41]. This method exhibited a broad substrate scope for both aryl iodides and phosphoramides, and enabled enantioselective access to both enantiomers of chiral P(V) molecules **47** or **48** using a single chiral NBE catalyst.

Time control

Time control of chemical reactivity offers an inherent strategy to program synthetic pathways through kinetic discrimination of transient intermediates. Diverging from additive-dependent or stimulus-responsive approaches, this paradigm capitalizes on the chronoselective evolution of reactive species to unlock sequence-controlled transformations. In 2020, the You group reported a reaction-time-dependent enantiodivergent synthesis method. Under the same chiral catalytic system, they achieved selective synthesis of either enantiomer of a target product by controlling the reaction duration (Scheme 13) [42]. When performing the asymmetric intermolecular allylic amination of 6-hydroxyisoquinoline (**49**) with *tert*-butyl(1-phenylallyl)carbonate ((*rac*)-**50**) using an Ir catalyst derived from $[Ir(cod)Cl]_2$ and the Carreira chiral phosphoramidite ligand (*S*)-**L10**, along with the addition of 3,5-dichlorobenzoic acid as an additive in MeOH at room temperature, the reaction proceeded smoothly for 10 hours to yield the aminated product **51**. Interestingly, when the reaction was quenched after 6 minutes in the absence of a Brønsted acid additive, the opposite enantiomer **52** was obtained. Mechanistically, an initial kinetic resolution (KR) of (*rac*)-**50** occurs via an Ir-catalyzed asymmetric allylic amination. Due to the higher reactivity of (*S*)-**50**, it reacts with 6-hydroxyisoquinoline within 6 minutes to generate **52**, while (*R*)-**50** remains largely unreacted during this period ($k_1^R << k_1^S$). However, as the reaction progresses, **52** undergoes further reaction with MeOH under the catalytic system to form **52'**. Meanwhile, the less reactive (*R*)-**50** gradually reacts with 6-hydroxyisoquinoline, leading to the accumulation of **51**. Since **51** is highly stable and resistant to reaction with MeOH ($k_2^R << k_2^S \approx k_1^R$), it can be obtained with high optical purity after an extended reaction time (10 hours)

In 2023, Yang and Liang jointly reported a tetrasilane (ODCS)-based method for time-controlled, palladium-catalyzed C–H activation in the divergent synthesis of silacyclic compounds

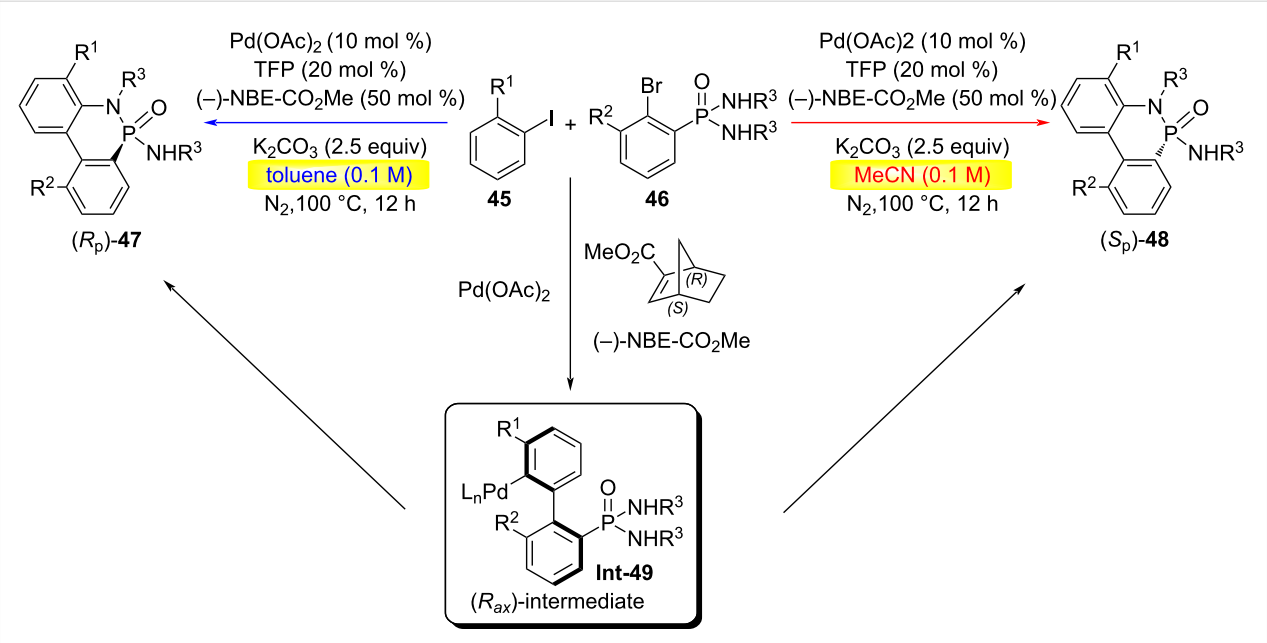

Scheme 12: Palladium-catalyzed annulation of prochiral *N*-arylphosphonamides with aromatic iodides [41].

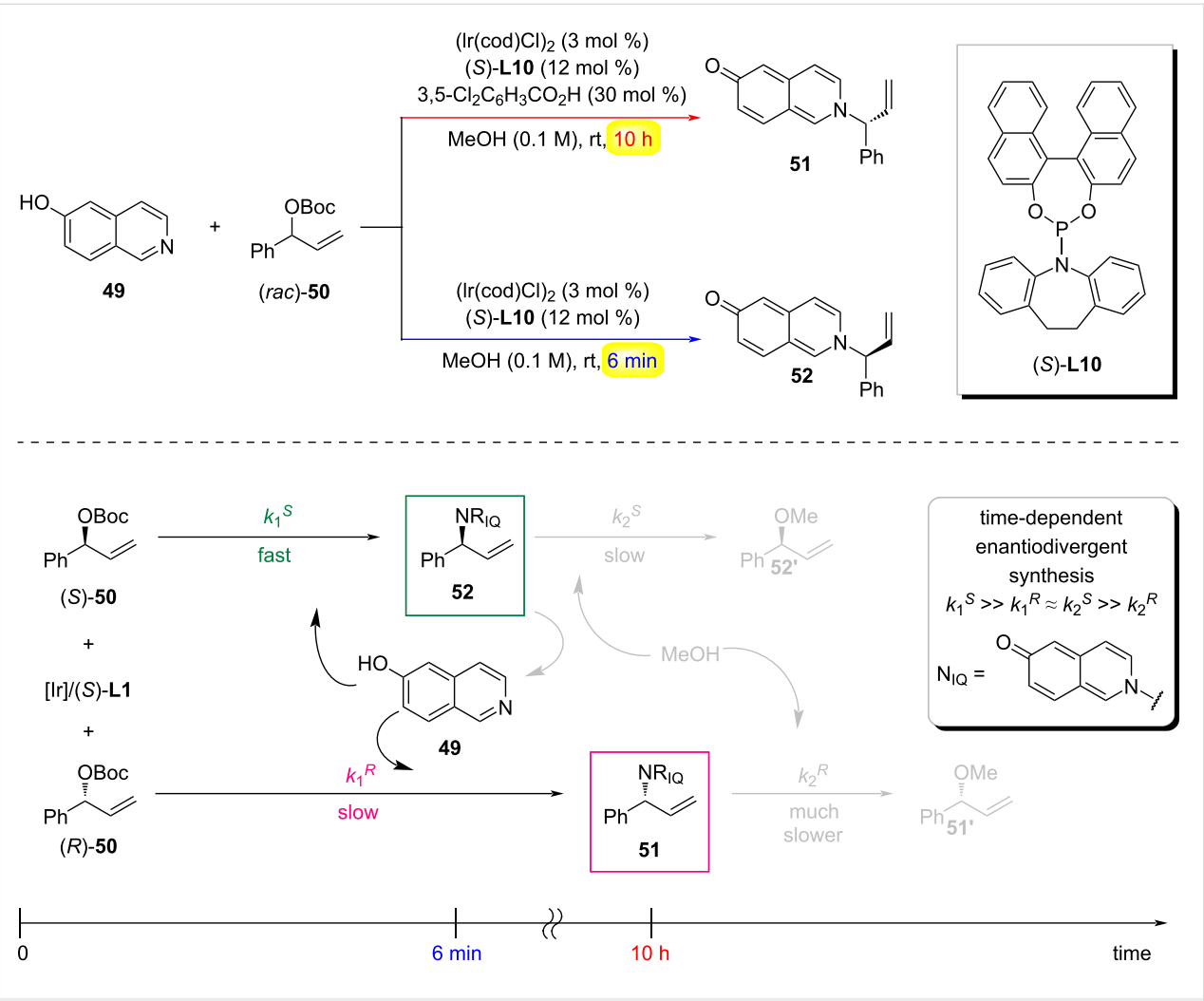

Scheme 13: Time-dependent enantiodivergent synthesis [42].

(Scheme 14) [43]. This reaction employs the ODCS reagent to capture a five-membered C,C-palladacycle species, using reaction time as a control switch to enable transformations of three distinct substrates – acrylamides, 2-halo-*N*-methylacryloylbenzamides, and 2-iodobiphenyls – thereby selectively synthesizing silacyclic compounds with varying ring sizes, including ten-membered, seven-membered, and five-membered rings. Mechanism (Scheme 15): Substrate **53** undergoes oxidative addition with Pd(0), followed by intramolecular carbopalladation to form the σ-alkylpalladium intermediate **Int-50**. The intermediate **Int-50** undergoes C–H activation to generate the spiro-palladacycle **Int-51**, which proceeds via two possible pathways: 1) Path a: oxidative addition/reductive elimination or 2) path b: transmetalation/reductive elimination giving rise to intermediates **Int-53** or **Int-53'**. Reductive elimination of **Int-53** or **Int-53'** regenerates Pd(0) and produces intermediate **55**. With the assistance of the base K_2CO_3, the ten-membered silacycle **55** undergoes rapid ring contraction via cleavage of two Si–O bonds and formation of one Si–O bond, leading to **56** and **Int-55**. Concurrently, **Int-55** dimerizes to form **54**, which is further transformed into cyclosiloxanes under K_2CO_3 and DMA conditions. Intermediate **56** undergoes additional ring contraction through cleavage of Si–O/Si–C bonds and formation of a Si–C bond, yielding **57** and **Int-56**, with **Int-56** polymerizing to generate cyclosiloxanes. An alternative pathway involving cleavage of another Si–O bond during the conversion from **55** to **56** and subsequently to **57** cannot be excluded.

Temperature control

Temperature, as a readily adjustable physical parameter in organic synthesis, offers a simple and versatile approach to control regioselectivity. It profoundly influences reaction kinetics, stability of intermediates, and reaction equilibria. Through precise temperature modulation, chemists can effectively steer the formation of regioisomers, often achieving desired selectivity with minimal alterations to other reaction

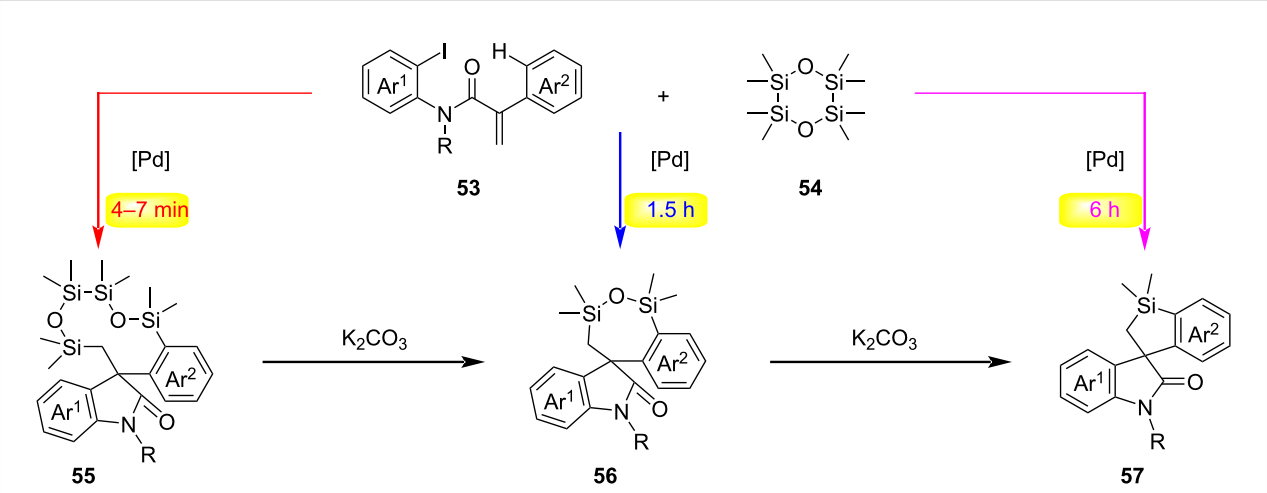

Scheme 14: Time-controlled palladium-catalyzed divergent synthesis of silacycles via C–H activation [43].

components. For instance, Rana and colleagues developed a temperature-dependent regiodivergent strategy to access functionalized maleimides and itaconimides [44]. This thermochemical strategy provides a robust platform for controlling reaction pathways while maintaining synthetic simplicity. In 2022, García-García and Fernández-Rodríguez reported on the practicality of metal-free BCl_3-catalyzed borylation cyclization reactions in synthesis (Scheme 16) [45]. Biphenyl-embedded 1,3,5-trienes-7-yne compounds **58** react with BCl_3 under catalyst-free and additive-free conditions to form novel polycyclic boronated structural units. By adjusting the temperature of the reaction medium, it is possible to precisely control the reaction pathway, thereby obtaining two different boronated frameworks from the same starting material: boronated phenanthrene derivatives **59** at 60 °C and phenanthrene-fused boronated cyclobutane **60** at 0 °C.

In the same year, Lu's research group reported a temperature-controlled site-selective olefin hydroalkylation reaction (Scheme 17) [46]. By adjusting only the reaction temperature, different skeletal structures of nitrogen α- and β-alkylated products could be obtained from the same olefin substrates **61**. At 10 °C, the catalytic system consisting of $NiBr_2$(diglyme), oxazoline ligand, $(EtO)_3SiH$, and $K_3PO_4(H_2O)$ achieved β-selective hydroalkylation. When the temperature was raised to 100 °C, the reaction selectively produced α-branched products. DFT calculations showed that at low temperatures, the six-membered nickel ring captures radicals and undergoes reductive elimination to form β-products (kinetic control); at high temperatures, the formation of a five-membered nickel ring leads to α-products (thermodynamic control). Therefore, the formation of the more stable nickel ring drives migration, while the thermodynamic and kinetic properties of different reductive elimination intermediates jointly determine the switchable site selectivity.

Acid–base control

The strategic modulation of acid–base interactions has emerged as a powerful paradigm in organic synthesis, enabling precise control over reaction pathways, selectivity, and catalytic efficiency. By exploiting dynamic acid–base equilibria or stimuli-responsive systems, chemists can manipulate substrate activation, stabilize reactive intermediates, and orchestrate complex multistep transformations under mild conditions [47]. In 2016, Lu's team designed a new class of acetylene carbonate reagents and successfully applied them to copper-catalyzed decarboxylative amination/hydroamination sequences (Scheme 18) [48]. By controlling acidic and basic reaction conditions, the authors achieved the controllable synthesis of two types of functionalized indoles. When treated with acid ($BF_3{\cdot}E_2O$), the intermediate 2-methylene-3-aminoindoline **69** undergoes an aza-Cope rearrangement to form 2-benzylindole **70**; when treated with a base (Cs_2CO_3), this intermediate undergoes a 1,3-proton migration process to convert back to 3-aminoindole **71**. The possible mechanism for the formation of the key intermediate **69** is outlined in Scheme 19: first, substrate **67**, under the action of a copper catalyst and diisopropylethylamine, undergoes a decarboxylation process to generate the allylidenecopper intermediate **Int-63** and its resonance form **Int-64**. Subsequently, these intermediates undergo a propargylation process (**Int-63**, **Int-64** to **Int-65**) followed by a proton elimination process to generate **Int-66** (**Int-5** to **Int-66**). Then, **Int-66** undergoes an intramolecular amination through copper-catalyzed activation to form **Int-68**, and finally, 2-methylene-3-aminoindoline **69** is generated via a proton transfer promoted by diisopropylethylamine.

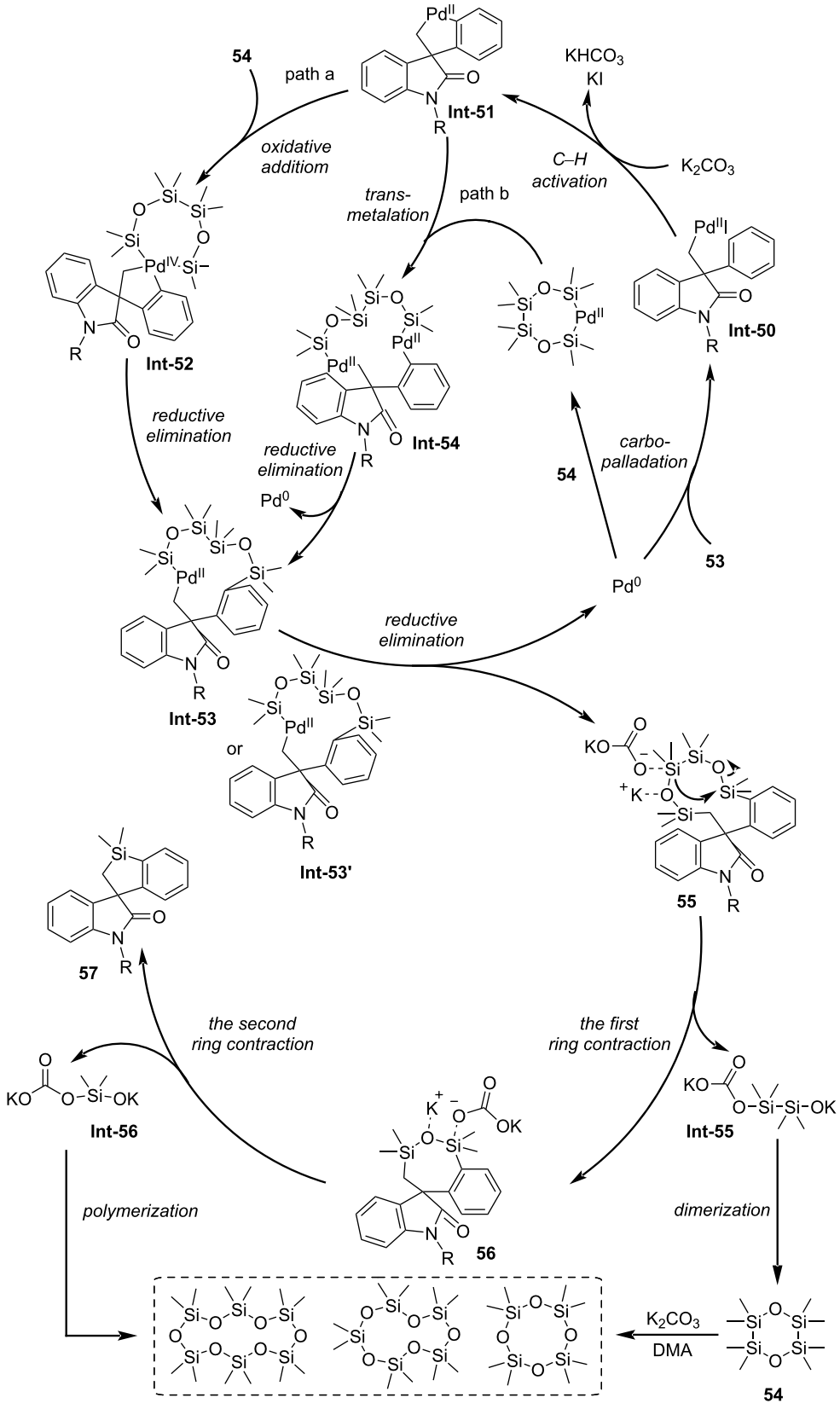

Scheme 15: Proposed mechanism for the time-controlled palladium-catalyzed divergent synthesis of silacycles [43].

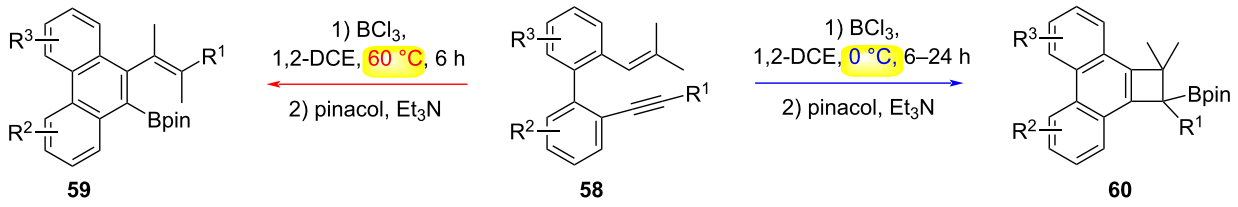

Scheme 16: Metal-free temperature-controlled regiodivergent borylative cyclizations of enynes [45].

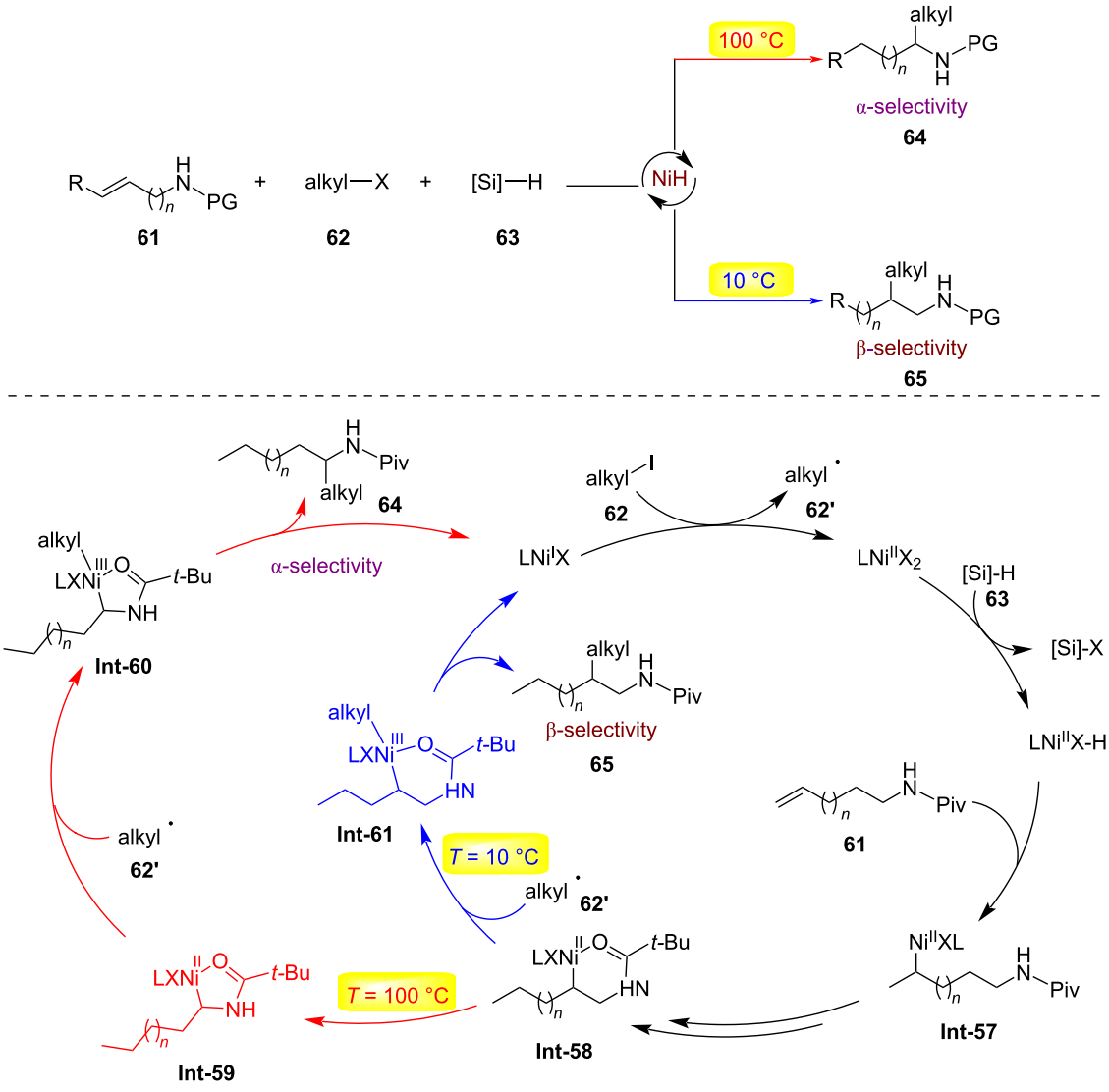

Scheme 17: Nickel-catalyzed switchable site-selective alkene hydroalkylation by temperature regulation [46].

In 2023, the Jiang research group achieved a chemically divergent photocatalytic asymmetric synthesis using a dual catalytic system consisting of a chiral phosphoric acid and dicyanopyrazine (DPZ) as the photosensitizer (Scheme 20) [49]. By regulating the chemical selectivity of a three-component radical cascade reaction involving α-brominated aryl ketones **72**, olefins **73**, and 1-methylquinoxalin-2(1*H*)-one (**74**) with an inorganic base, they were able to obtain two important types of products with high yield and enantioselectivity. Through mechanistic experiments and DFT calculations, the authors proposed

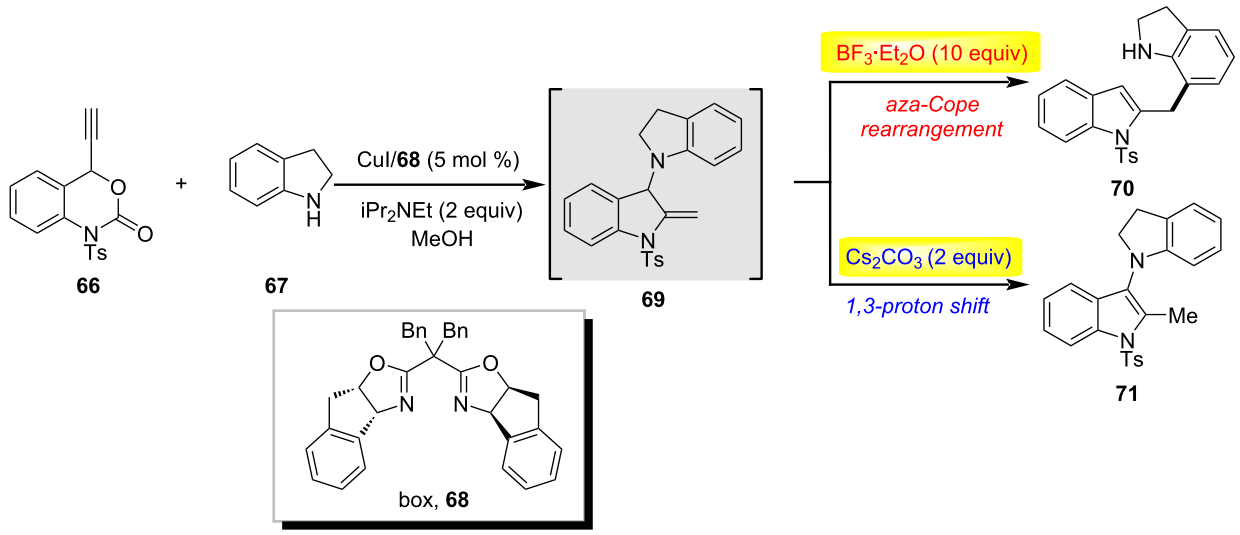

Scheme 18: Copper-catalyzed decarboxylative amination/hydroamination sequence [48].

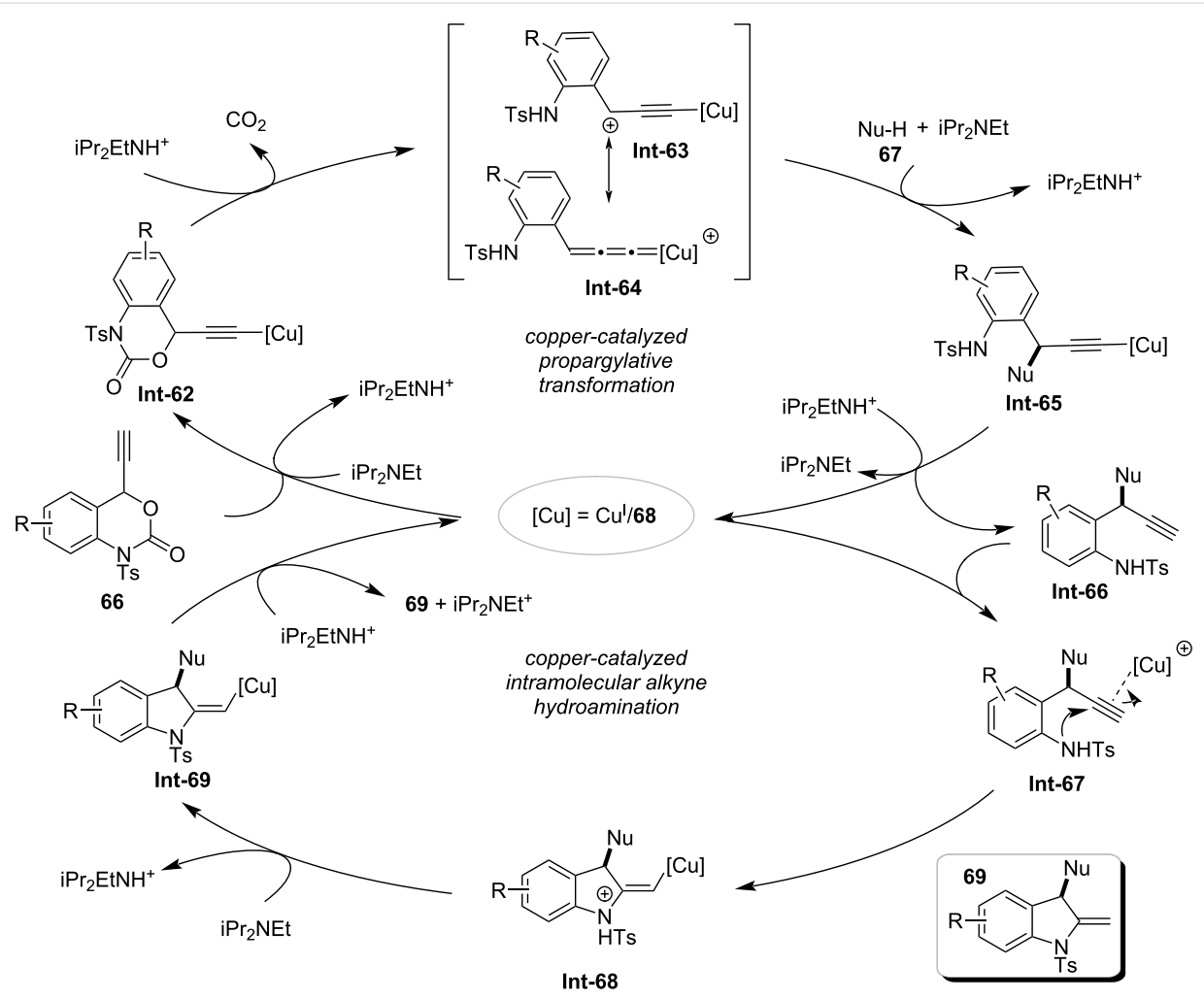

Scheme 19: Proposed mechanism of copper-catalyzed decarboxylative amination/hydroamination sequence [48].

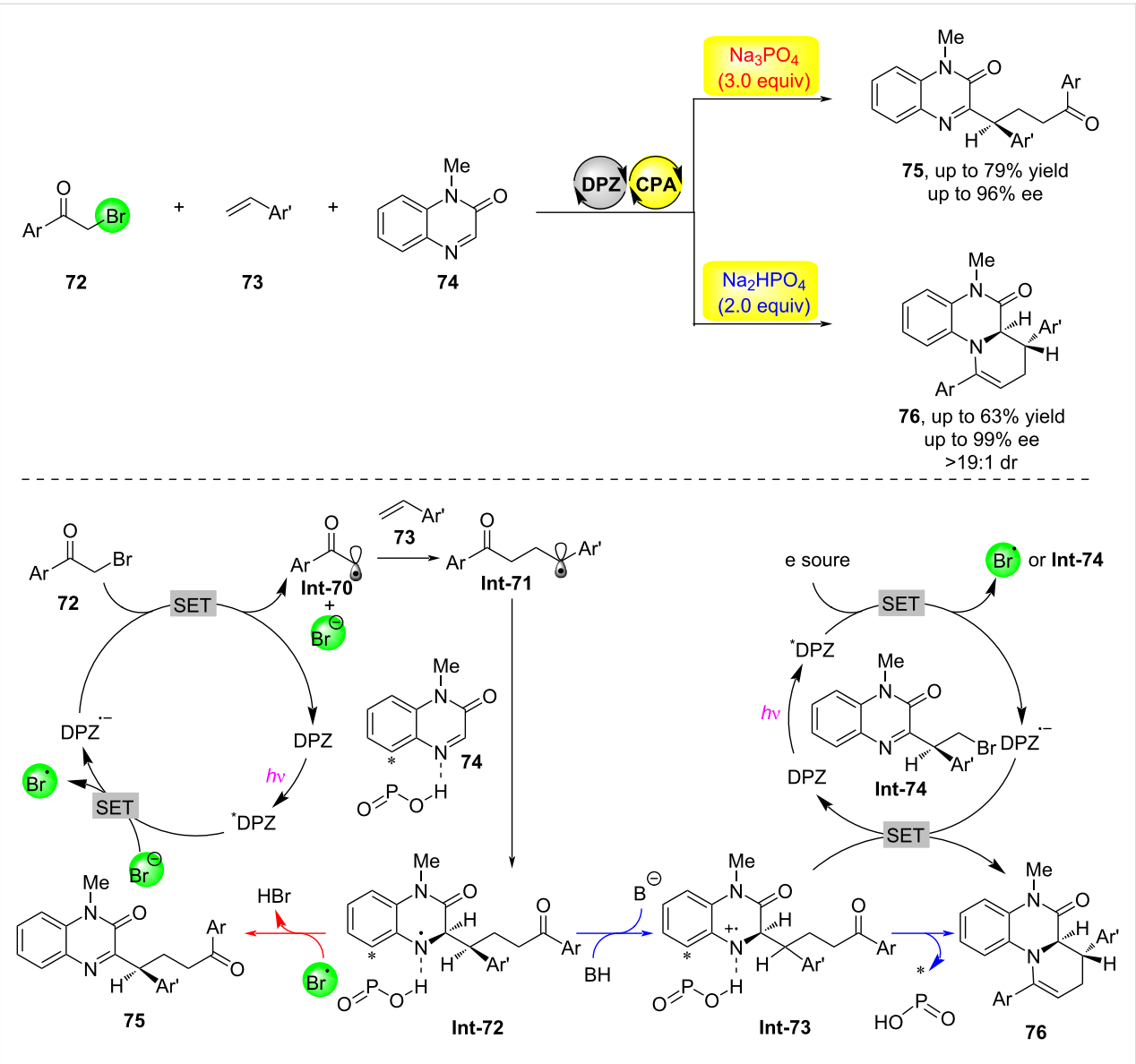

Scheme 20: Enantioselective chemodivergent three-component radical tandem reactions [49].

a possible mechanism for the reaction: first, DPZ is excited by light to form the excited state DPZ*, which then oxidizes bromide ions through single-electron transfer to generate corresponding radical anions. These radical anions undergo single-electron transfer with substrate **72** to form radical intermediate **Int-70**, completing the DPZ catalytic cycle. Intermediate **Int-70** adds to substrate **73** to form radical intermediate **Int-71**, which further adds to hydrogen-bond-activated substrate **74** to form hydrogen-bonded complex **Int-72**. When Na_3PO_4 is used as the inorganic base, bromine radicals abstract hydrogen to form product **75**; whereas when Na_2HPO_4 is used as the inorganic base, its weaker basicity leads to protonation of complex **Int-72** to form intermediate **Int-73**, which then preferentially undergoes single-electron transfer with the DPZ radical anion, followed by cyclization and dehydration to yield bicyclic product **76**.

Substrate control

Substrate control has emerged as a powerful strategy in organic synthesis, enabling precise manipulation of reaction pathways and stereochemical outcomes through the intrinsic structural and electronic features of the starting material. By exploiting preorganization, steric effects, or directing groups within the substrate, chemists can achieve high levels of regioselectivity, diastereoselectivity, and enantioselectivity without relying on external catalysts or additives. This approach has been successfully applied in the synthesis of complex natural products, pharmaceuticals, and functional materials, often streamlining multi-

step sequences and minimizing protecting-group strategies [50,51]. In 2016, Li and co-workers developed divergent coupling conditions for iminamides **77** with receptor-type diazo compounds **78** or **79** under ruthenium catalysis, generating indoles **81** and 3*H*-indoles **80**, respectively (Scheme 21) [52]. α-Diazo-β-ketoesters form indoles by cleaving the C(N_2)–C(acyl) bond, while diazomalonates form 3*H*-indoles through C–N-bond cleavage. Mechanistically, the cyclometalation of iminamides follows a concerted metalation–deprotonation (CMD) mechanism to generate ruthenium intermediate **Int-75**. Subsequently, diazo compound **78** or **79** coordinates with intermediate **Int-75**, followed by deazidation to form the ruthenium carbenoid species **Int-76**. The ruthenium–aryl bond in this intermediate migrates into the carbenoid unit, providing heptacyclic ruthenium ring intermediate **Int-77**. Intermediate **Int-78** is then formed via ruthenium migration insertion into the C=N bond from Ru–C(alkyl). For diazoketoester substrates, the final product **81** is released from **Int-78** through protonation, intramolecular nucleophilic addition, and subsequent release of one molecule of amide, reactivating the active ruthenium(II) catalyst. In contrast, for diazomalonates, intermediate **Int-78** releases ammonia with the help of Ru(II) or acetic acid, ultimately yielding 3*H*-indole **80**. This change in selectivity may be due to the reduced electrophilicity of the ester carbonyl.

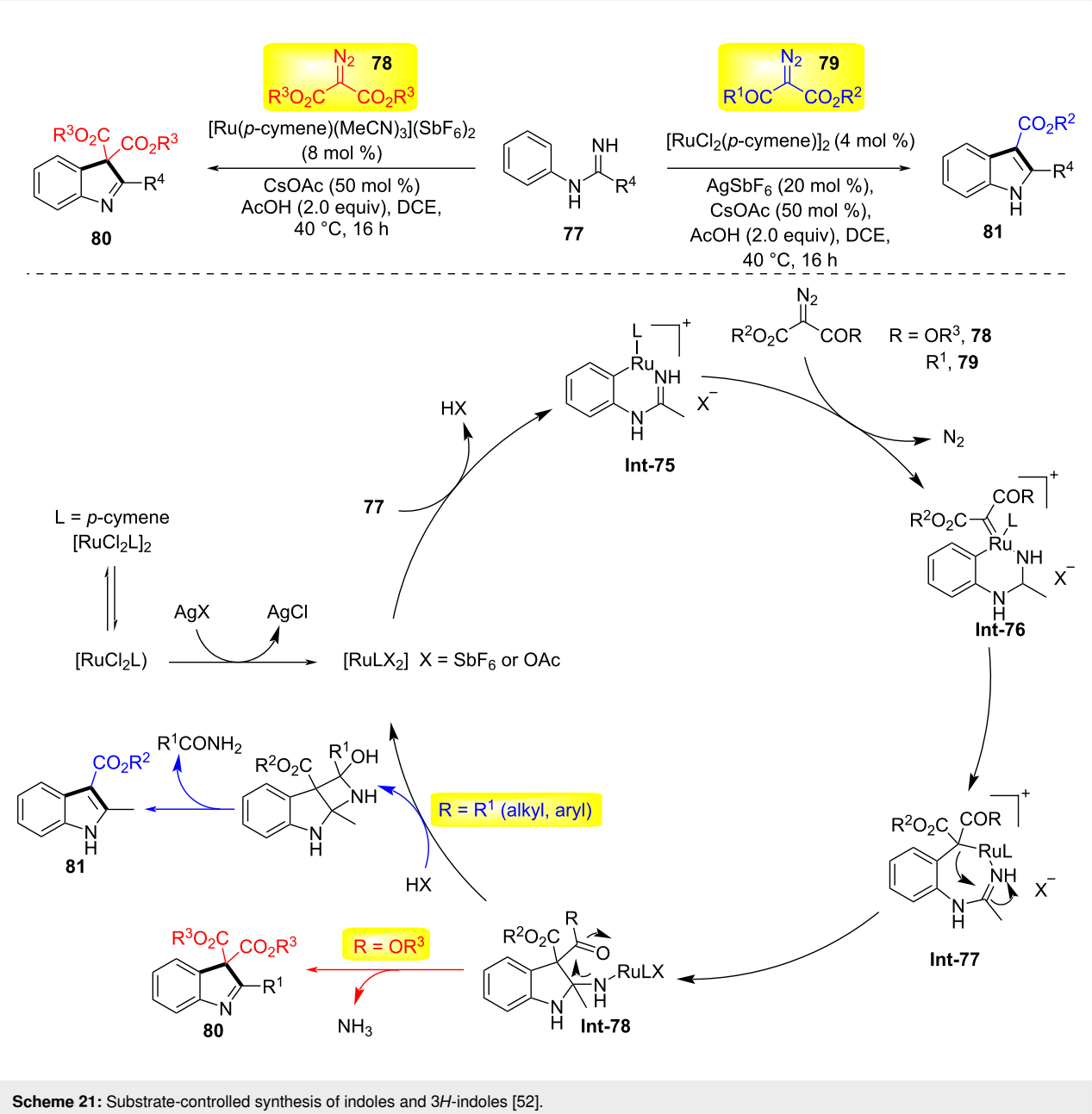

Scheme 21: Substrate-controlled synthesis of indoles and 3*H*-indoles [52].

In 2021, Dong and Xie reported the development of an azido Matteson reaction, which achieves carbene insertion into an N–B bond of aminoboranes **84** or **86** (Scheme 22) [53]. In this methodology, by controlling the carbene leaving group (alkyl chlorides/alkyl bromides) and the Lewis acid activator, a selective mono- or di-methylene insertion reaction can be carried out, generating α-/β-boryl-substituted tertiary organic amines **83** from simple secondary organic amines. Using *N*-alkyl-*N*-arylaminoboranes as the reactant, the reaction proceeds at −78 °C with CH_2Br_2 and *n*-BuLi, followed by a reaction with $ZnCl_2$ at room temperature. The product is then hydrolyzed with a NaOH solution of H_2O_2 to yield amino alcohols. The mechanism involves the formation of borate intermediate **Int-79** from substrate **83** under the action of CH_2BrLi. This is followed by an N-1,2-migration to form borate ester **86**, which then reacts with another molecule of CH_2BrLi to form the more stable borate **Int-80**. Subsequently, a C-1,2-migration leads to the formation of the double-insertion product **84**. If the amine portion is more electron-deficient or has more delocalized nitrogen electrons (such as indole substrates), **Int-79** is more stable at −78 °C, favoring the formation of the mono-insertion product **86**.

In 2022, Wu and colleagues reported a novel methodology for constructing α-ketoamides **90** or **92** and amides **91** through copper-catalyzed dicarbonylation and monocarbonylation reactions involving alkyl halides **88** (Scheme 23) [54]. Using alkyl bromides, CuBr as the catalyst, bpy as the ligand, $Co_2(CO)_8$ as the additive, Cs_2CO_3 as the base, and 1,4-dioxane as the solvent under 40 bar CO pressure at 80 °C, they successfully syn-

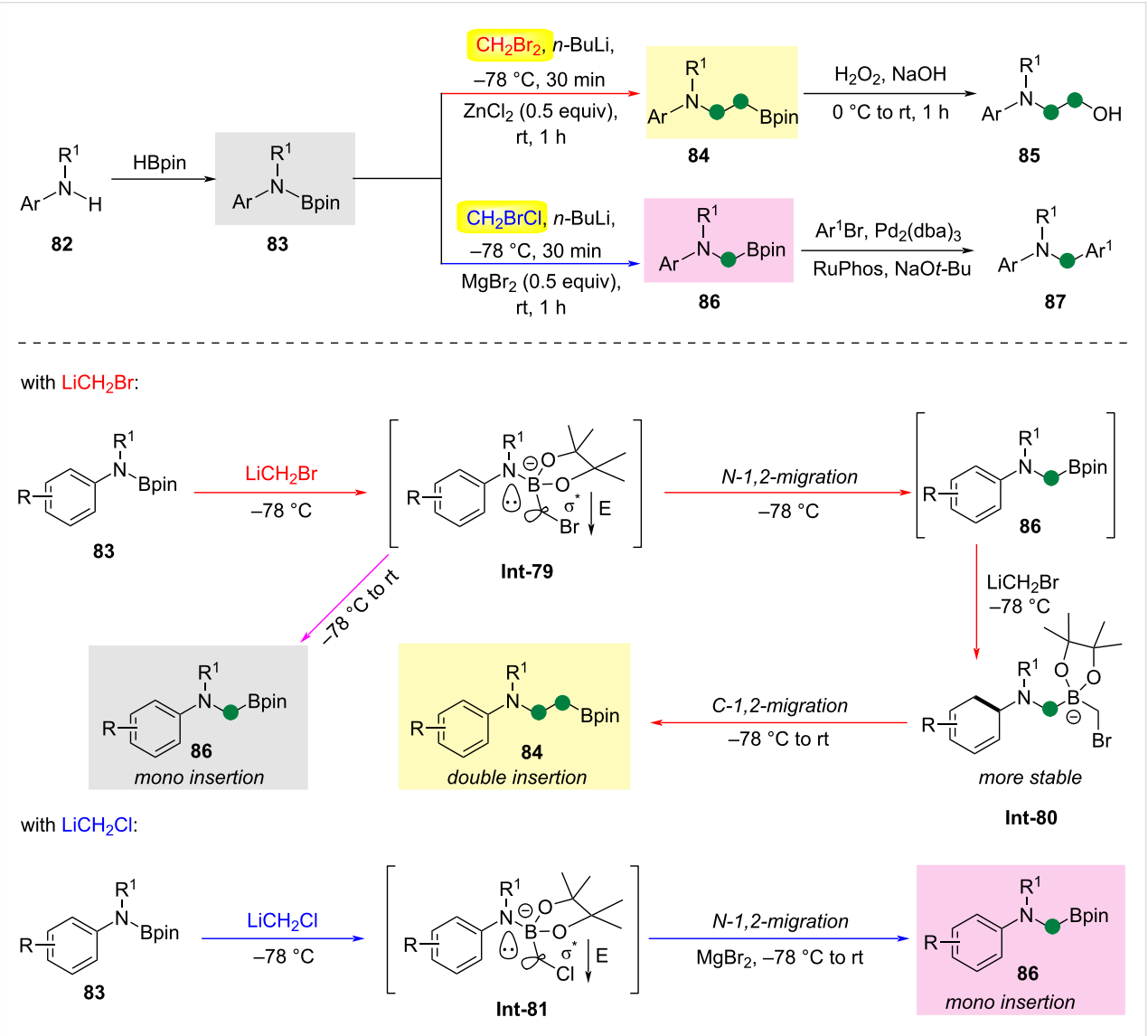

Scheme 22: Controlled mono- and double methylene insertions into nitrogen–boron bonds [53].

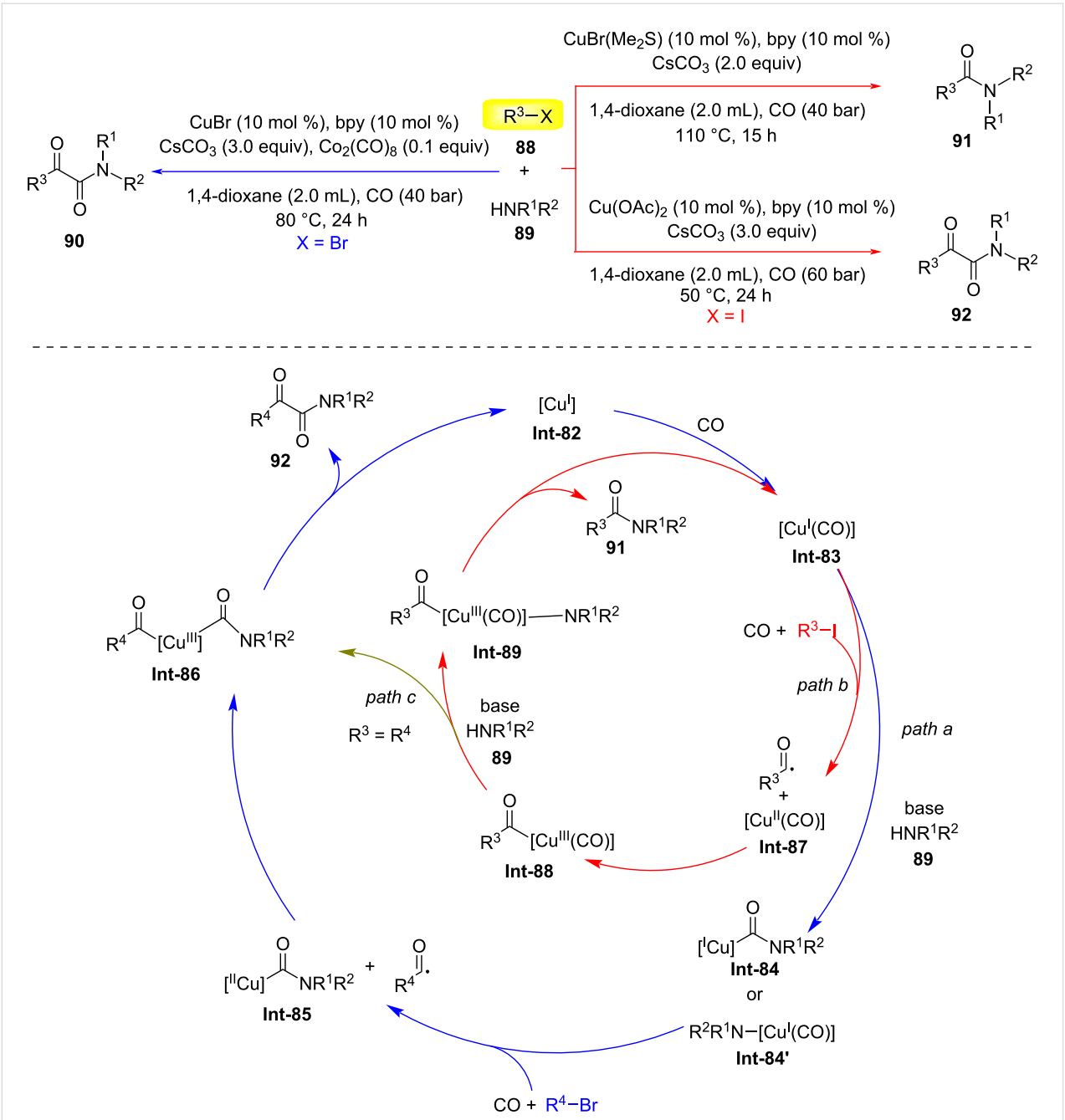

Scheme 23: Copper-catalyzed substrate-controlled carbonylative synthesis of α-keto amides and amides [54].

thesized α-ketoamides **90**. When alkyl iodides were used as substrates, both dicarbonylation and monocarbonylation processes occurred simultaneously with $Cu(OAc)_2$, favoring the dicarbonylation process. In contrast, using $CuBr(Me_2S)$ the monocarbonylation process was favored. Possible reaction mechanisms: First, CO coordinates with copper salts to form (carbonyl)copper species **Int-83**. Subsequently, in the presence of a base, the amine undergoes nucleophilic attack on the coordinated CO, generating (carbamoyl)copper complex **Int-84**. Then, alkyl bromide undergoes a single-electron-transfer (SET) process with **Int-84**, forming intermediate **Int-85** and an alkyl radical, which is captured by CO to yield an acyl radical. Alternatively, under the action of a base, the amine can undergo anionic ligand exchange with (carbonyl)copper species **Int-83**, generating an electron-rich amino copper(I) species **Int-84'**, which activates alkyl bromide through an SET process, followed by immediate insertion of CO to form complex **Int-85**. Nucleophilic activation of the acyl radical initiates through its

reaction with intermediate **Int-85**, generating the critical acyl(aminoacyl)copper species **Int-86**. Subsequent reductive elimination from this intermediate liberates the α-ketoamide product **92** while regenerating the catalytic species **Int-82**. Comparative kinetic analysis revealed a marked preference for alkyl iodide activation, as demonstrated by its substantially lower activation energy barrier compared to alkyl bromide analogs (path b). This energetic advantage facilitates preferential formation of intermediate **Int-87** via oxidative addition. Rapid coupling with the in situ-generated acyl radical produces copper-bound intermediate **Int-88**. Base-mediated anionic exchange then displaces the halide ligand with amine, yielding intermediate **Int-89**. Final reductive elimination from this species affords amide product **91** with concurrent regeneration of the catalyst **Int-83**. Notably, a competitive pathway emerges through alternative reactivity of **Int-88** (path c). The coordinated CO ligand undergoes nucleophilic attack by the amine, bypassing halide exchange to instead generate **Int-86**. This mechanistic crossover establishes a product dichotomy between α-ketoamide **92** and amide **91**, with the branching ratio governed by relative rates of base-mediated exchange versus CO activation at the copper center.

In 2022, the Jiang research team developed regulated SuFEx click chemistry between fluorosulfonyl imides and TMS-alkynes, enabling the rapid construction of S(VI)–C(sp^2) or S(VI)–C(sp) bonds efficiently (Scheme 24) [55]. This linkage utilizes the high bond dissociation energy (BDE =

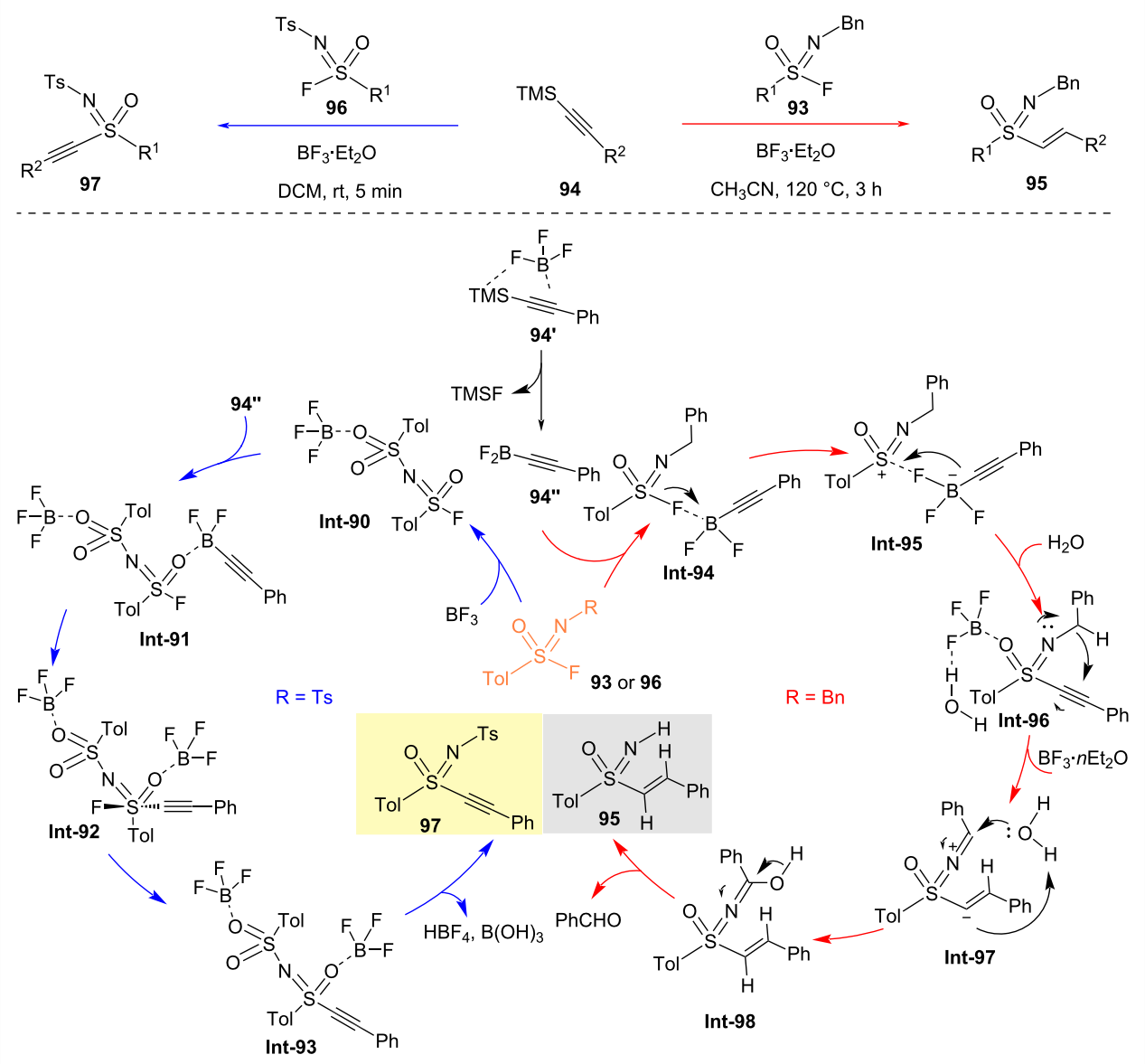

Scheme 24: Divergent sulfur(VI) fluoride exchange linkage of sulfonimidoyl fluorides and alkynes [55].

135 kcal/mol) of silicon–fluorine bonds, employing trifluoroborate as a fluorine transfer reagent to simultaneously cleave the S(VI)–F bond and activate the Si–C bond. DFT calculations indicate that the reaction proceeds via the formation of a difluoroborate phenylacetylene intermediate **94''** by in situ generation from boron trifluoride etherate and silicon-protected phenylacetylene **94**, which activates the S–F bond of the fluorosulfonyl imide to form sulfonyliminium cations **Int-95**. These then add to the activated phenylacetylene to construct the S–C bond, followed by intramolecular 1,5-hydrogen migration and aqueous workup to remove benzaldehyde, yielding the target sulfonylimine products.

Both original protoberberine and protonitidine alkaloids are characterized by an isoquinoline ring skeleton. An analysis of their molecular structures revealed that the two alkaloids share a basic structure, differing only in the junction of the B-ring. In 2021, Liu and Jiang designed new pyridyne precursors, which underwent cycloaddition reactions with substituted furans as diene component to produce the corresponding epoxy-cycloaddition adducts. The authors developed an Ir/Sc tandem catalytic reaction to convert these adducts into polysubstituted 3-haloisoquinolines **99** in one pot. After obtaining isoquinoline compounds **99** with different substituents and polysubstituted annular boronic acids **98**, a Suzuki coupling was employed to synthesize advanced isoquinoline intermediates **100**. Following this, a 6π electrocyclization reaction and nucleophilic reaction were developed to achieve C–C and C–N bond constructions, respectively, leading to the synthesis of differently substituted protonitidine alkaloids and protoberberine alkaloids (Scheme 25) [56].

Conclusion

Developing streamlined and versatile approaches for the rapid assembly of structurally diverse organic molecules represents a pivotal challenge in organic synthesis, pharmaceutical research, and advanced materials development. Recent advances in controllable/divergent synthesis methodologies, which enable

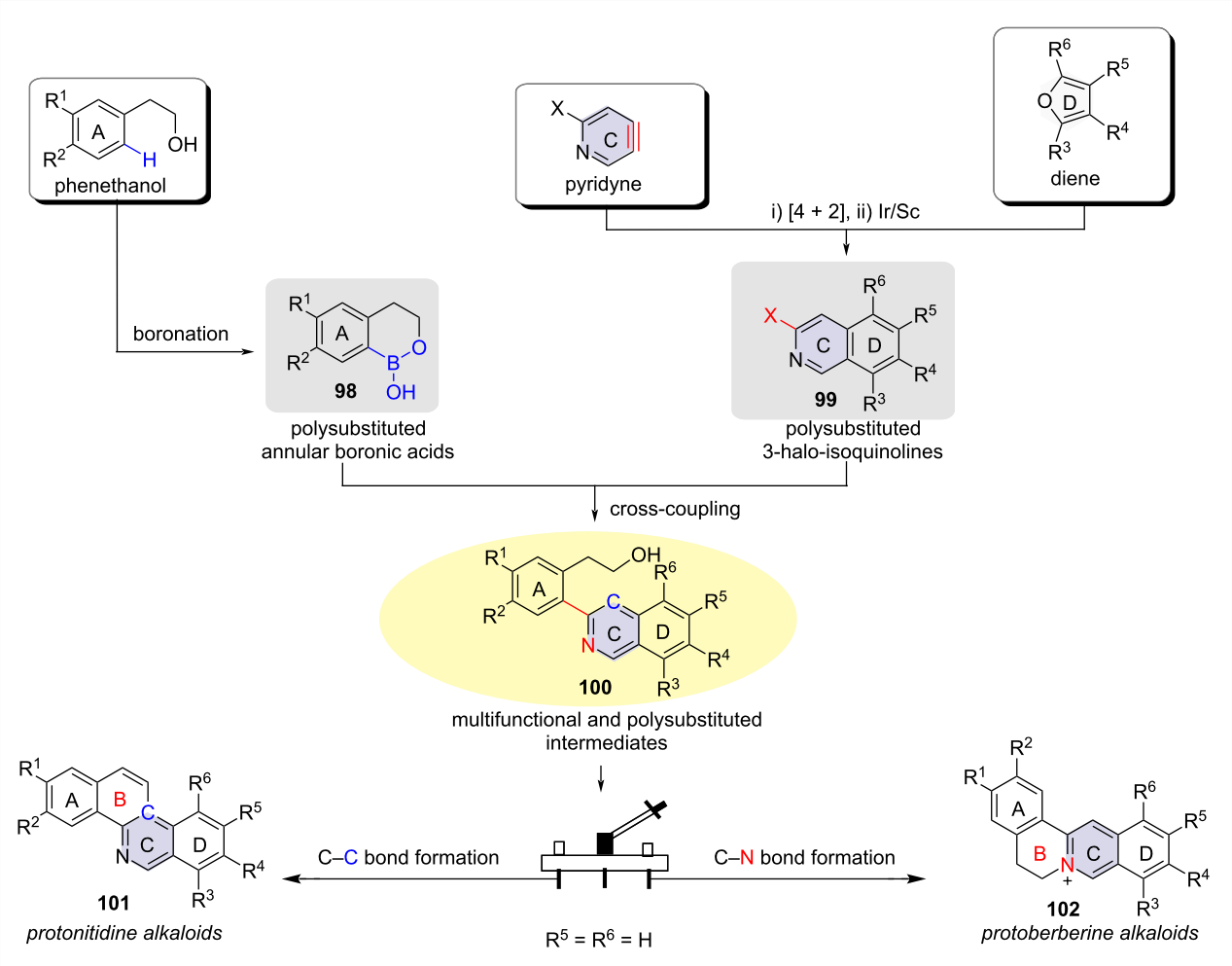

Scheme 25: Modular and divergent syntheses of protoberberine and protonitidine alkaloids [56].

the construction of variously functionalized architectures from common precursors, have emerged as particularly promising due to their inherent efficiency. Contemporary strategies for controlling reaction pathways and selectivity predominantly involve precise manipulation of catalytic systems (metal catalysts/ligands), reaction parameters (solvent, temperature, time), acid/base mediation, and strategic substrate engineering. This review systematically organizes recent breakthroughs according to critical control elements governing product divergence. Through mechanistic investigations of pivotal bond-forming steps and comparative analysis of representative case studies, we provide fundamental insights into the origin of selectivity variations and reaction pathway control. The discussion emphasizes structure–reactivity relationships and catalytic design principles that enable predictable access to distinct molecular architectures from shared synthetic intermediates. This review serves as a conceptualized platform for controllable/divergent synthesis, arousing more state-of-the-art tactics in chemical synthesis.

Funding

The authors are grateful for financial support provided by the NSFC (22125103, 22401095), Shanghai Rising-Star Program (24QB2704700), the STCSM (22JC1401000), and the China Postdoctoral Science Foundation (BX20230127).

Author Contributions

Jilei Cao: investigation. Leiyang Bai: investigation; writing – review & editing. Xuefeng Jiang: conceptualization; investigation; supervision; validation; writing – review & editing.

ORCID® iDs

Leiyang Bai - https://orcid.org/0000-0002-8159-4992
Xuefeng Jiang - https://orcid.org/0000-0002-1849-6572

Data Availability Statement

Data sharing is not applicable as no new data was generated or analyzed in this study.

References

1. Beletskaya, I. P.; Nájera, C.; Yus, M. *Chem. Rev.* **2018,** *118,* 5080–5200. doi:10.1021/acs.chemrev.7b00561
2. Nájera, C.; Foubelo, F.; Sansano, J. M.; Yus, M. *Org. Biomol. Chem.* **2020,** *18,* 1232–1278. doi:10.1039/c9ob02419k
3. Nájera, C.; Foubelo, F.; Sansano, J. M.; Yus, M. *Org. Biomol. Chem.* **2020,** *18,* 1279–1336. doi:10.1039/c9ob02597a
4. Katta, N.; Zhao, Q.-Q.; Mandal, T.; Reiser, O. *ACS Catal.* **2022,** *12,* 14398–14407. doi:10.1021/acscatal.2c04736
5. Nájera, C.; Beletskaya, I. P.; Yus, M. *Chem. Soc. Rev.* **2019,** *48,* 4515–4618. doi:10.1039/c8cs00872h
6. Beletskaya, I. P.; Nájera, C.; Yus, M. *Russ. Chem. Rev.* **2020,** *89,* 250–274. doi:10.1070/rcr4916
7. Mahatthananchai, J.; Dumas, A. M.; Bode, J. W. *Angew. Chem., Int. Ed.* **2012,** *51,* 10954–10990. doi:10.1002/anie.201201787
8. Lee, Y.-C.; Kumar, K.; Waldmann, H. *Angew. Chem., Int. Ed.* **2018,** *57,* 5212–5226. doi:10.1002/anie.201710247
9. Peng, J.-B.; Wu, X.-F. *Angew. Chem., Int. Ed.* **2018,** *57,* 1152–1160. doi:10.1002/anie.201709807
10. Cao, M.; Xie, H. *Chin. Chem. Lett.* **2021,** *32,* 319–327. doi:10.1016/j.cclet.2020.04.005
11. Chintawar, C. C.; Yadav, A. K.; Kumar, A.; Sancheti, S. P.; Patil, N. T. *Chem. Rev.* **2021,** *121,* 8478–8558. doi:10.1021/acs.chemrev.0c00903
12. Sakakibara, Y.; Murakami, K. *ACS Catal.* **2022,** *12,* 1857–1878. doi:10.1021/acscatal.1c05318
13. Pan, Q.; Ping, Y.; Kong, W. *Acc. Chem. Res.* **2023,** *56,* 515–535. doi:10.1021/acs.accounts.2c00771
14. Ke, Y.; Li, W.; Liu, W.; Kong, W. *Sci. China: Chem.* **2023,** *66,* 2951–2976. doi:10.1007/s11426-023-1533-y
15. Kumari, A.; Jain, A.; Rana, N. K. *Tetrahedron* **2024,** *150,* 133754. doi:10.1016/j.tet.2023.133754
16. Fuji, K.; Kawashima, K.; Mori, T.; Sekine, K.; Kuninobu, Y. *Org. Lett.* **2025,** *27,* 1614–1619. doi:10.1021/acs.orglett.4c04694
17. Long, Y.; Zhong, X.; Shi, M.; Wei, Y. *Chin. J. Chem.* **2025,** *43,* 1181–1189. doi:10.1002/cjoc.202401301
18. Zou, S.; Zhao, Z.; Yang, G.; Huang, H. *Nat. Commun.* **2024,** *15,* 10477. doi:10.1038/s41467-024-54328-5
19. Feng, M.; Tang, B.; Wang, N.; Xu, H.-X.; Jiang, X. *Angew. Chem., Int. Ed.* **2015,** *54,* 14960–14964. doi:10.1002/anie.201508340
20. Ding, D.; Mou, T.; Feng, M.; Jiang, X. *J. Am. Chem. Soc.* **2016,** *138,* 5218–5221. doi:10.1021/jacs.6b01707
21. Ding, D.; Zhu, G.; Jiang, X. *Angew. Chem., Int. Ed.* **2018,** *57,* 9028–9032. doi:10.1002/anie.201804788
22. Witkowski, D. C.; McVeigh, M. S.; Scherer, G. M.; Anthony, S. M.; Garg, N. K. *J. Am. Chem. Soc.* **2023,** *145,* 10491–10496. doi:10.1021/jacs.3c03102
23. Tang, X.; Tang, Y.; Peng, J.; Du, H.; Huang, L.; Gao, J.; Liu, S.; Wang, D.; Wang, W.; Gao, L.; Lan, Y.; Song, Z. *J. Am. Chem. Soc.* **2024,** *146,* 26639–26648. doi:10.1021/jacs.4c00252
24. Yang, F.; Chi, L.; Ye, Z.; Gong, L. *J. Am. Chem. Soc.* **2025,** *147,* 1767–1780. doi:10.1021/jacs.4c13321
25. Cheng, L.-J.; Mankad, N. P. *J. Am. Chem. Soc.* **2019,** *141,* 3710–3716. doi:10.1021/jacs.9b00068
26. Sun, Z.; Dai, M.; Ding, C.; Chen, S.; Chen, L.-A. *J. Am. Chem. Soc.* **2023,** *145,* 18115–18125. doi:10.1021/jacs.3c06253
27. Bai, L.; Ma, Y.; Jiang, X. *J. Am. Chem. Soc.* **2021,** *143,* 20609–20615. doi:10.1021/jacs.1c10498
28. Bai, L.; Li, J.; Jiang, X. *Chem* **2023,** *9,* 483–496. doi:10.1016/j.chempr.2022.10.021
29. Bai, L.; Jiang, X. *Chem Catal.* **2023,** *3,* 100752. doi:10.1016/j.checat.2023.100752
30. Wang, S.; Shi, L.; Chen, X.-Y.; Shu, W. *Angew. Chem., Int. Ed.* **2023,** *62,* e202303795. doi:10.1002/anie.202303795
31. Wang, X.; Xue, J.; Rong, Z.-Q. *J. Am. Chem. Soc.* **2023,** *145,* 15456–15464. doi:10.1021/jacs.3c03900
32. Lin, Z.; Ren, H.; Lin, X.; Yu, X.; Zheng, J. *J. Am. Chem. Soc.* **2024,** *146,* 18565–18575. doi:10.1021/jacs.4c04485
33. Zhu, H.; Zheng, H.; Zhang, J.; Feng, J.; Kong, L.; Zhang, F.; Xue, X.-S.; Zhu, G. *Chem. Sci.* **2021,** *12,* 11420–11426. doi:10.1039/d1sc03416b
34. Jain, A.; Kumari, A.; Shukla, K.; Selvakumar, S.; Rana, N. K. *ARKIVOC* **2023,** No. vi, 202211947. doi:10.24820/ark.5550190.p011.947

35. Zhou, Y.; Zhao, L.; Hu, M.; Duan, X.-H.; Liu, L. *Org. Lett.* **2023,** *25,* 5268–5272. doi:10.1021/acs.orglett.3c01787
36. Zhang, F.; Dutta, S.; Petti, A.; Rana, D.; Daniliuc, C. G.; Glorius, F. *Angew. Chem., Int. Ed.* **2025,** *64,* e202418239. doi:10.1002/anie.202418239
37. Huang, Z.; Zhang, C.; Zhou, P.; Wang, C.; Liang, T.; Zhao, S.; Zhang, Z. *J. Org. Chem.* **2025,** *90,* 1115–1125. doi:10.1021/acs.joc.4c02680
38. Kim, Y. L.; Yun, Y.; Choi, S.-M.; Kim, J. H. *Org. Chem. Front.* **2025,** *12,* 1452–1460. doi:10.1039/d4qo01980f
39. Wang, F.; Shi, X.; Zhang, Y.; Zhou, W.; Li, A.; Liu, Y.; Sessler, J. L.; He, Q. *J. Am. Chem. Soc.* **2023,** *145,* 10943–10947. doi:10.1021/jacs.3c01066
40. Hussain, Y.; Empel, C.; Koenigs, R. M.; Chauhan, P. *Angew. Chem., Int. Ed.* **2023,** *62,* e202309184. doi:10.1002/anie.202309184
41. Tian, Q.; Ge, J.; Liu, Y.; Wu, X.; Li, Z.; Cheng, G. *Angew. Chem., Int. Ed.* **2024,** *63,* e202409366. doi:10.1002/anie.202409366
42. Tu, H.-F.; Yang, P.; Lin, Z.-H.; Zheng, C.; You, S.-L. *Nat. Chem.* **2020,** *12,* 838–844. doi:10.1038/s41557-020-0489-1
43. Xu, Y.; Sun, M.; Xu, W.; Deng, G.; Liang, Y.; Yang, Y. *J. Am. Chem. Soc.* **2023,** *145,* 15303–15312. doi:10.1021/jacs.3c02875
44. Saha, S. K.; Bera, A.; Kumari, A.; Loitongbam, M.; Chakladar, D.; Rana, N. K. *Eur. J. Org. Chem.* **2025,** *28,* e202401448. doi:10.1002/ejoc.202401448
45. Milián, A.; Fernández-Rodríguez, M. A.; Merino, E.; Vaquero, J. J.; García-García, P. *Angew. Chem., Int. Ed.* **2022,** *61,* e202205651. doi:10.1002/anie.202205651
46. Wang, J.-W.; Liu, D.-G.; Chang, Z.; Li, Z.; Fu, Y.; Lu, X. *Angew. Chem., Int. Ed.* **2022,** *61,* e202205537. doi:10.1002/anie.202205537
47. Yu, S.; Zhou, X.; Tong, X. *ACS Catal.* **2025,** *15,* 72–80. doi:10.1021/acscatal.4c05561
48. Li, T.-R.; Cheng, B.-Y.; Wang, Y.-N.; Zhang, M.-M.; Lu, L.-Q.; Xiao, W.-J. *Angew. Chem., Int. Ed.* **2016,** *55,* 12422–12426. doi:10.1002/anie.201605900
49. Ma, C.; Shen, J.; Qu, C.; Shao, T.; Cao, S.; Yin, Y.; Zhao, X.; Jiang, Z. *J. Am. Chem. Soc.* **2023,** *145,* 20141–20148. doi:10.1021/jacs.3c08883
50. Chen, L.; Guo, L.-N.; Liu, S.; Liu, L.; Duan, X.-H. *Chem. Sci.* **2021,** *12,* 1791–1795. doi:10.1039/d0sc04399k
51. Tan, H.; Yu, S.; Yuan, X.; Chen, L.; Shan, C.; Shi, J.; Li, Y. *Nat. Commun.* **2024,** *15,* 3665. doi:10.1038/s41467-024-47952-8
52. Li, Y.; Qi, Z.; Wang, H.; Yang, X.; Li, X. *Angew. Chem., Int. Ed.* **2016,** *55,* 11877–11881. doi:10.1002/anie.201606316
53. Xie, Q.; Dong, G. *J. Am. Chem. Soc.* **2021,** *143,* 14422–14427. doi:10.1021/jacs.1c06186
54. Zhao, F.; Ai, H.-J.; Wu, X.-F. *Angew. Chem., Int. Ed.* **2022,** *61,* e202200062. doi:10.1002/anie.202200062
55. Zeng, D.; Ma, Y.; Deng, W.-P.; Wang, M.; Jiang, X. *Nat. Synth.* **2022,** *1,* 455–463. doi:10.1038/s44160-022-00060-1
56. Liu, K.; Jiang, X. *Org. Lett.* **2021,** *23,* 1327–1332. doi:10.1021/acs.orglett.0c04310

License and Terms

BEILSTEIN JOURNAL OF ORGANIC CHEMISTRY

A convergent synthetic approach to the tetracyclic core framework of khayanolide-type limonoids

Zhiyang Zhang[1], Jialei Hu[2,3], Hanfeng Ding[1,2], Li Zhang[*1] and Peirong Rao[*2]

Full Research Paper

Open Access

Address:
[1]School of Chemistry and Chemical Engineering, Zhejiang Sci-Tech University, Hangzhou 310018, China, [2]Department of Chemistry, Zhejiang University, Hangzhou 310058, China and [3]Hangzhou DAC Biotechnology Co., Ltd 369 Qiaoxin Road, Qiantang District, Hangzhou 310018, Zhejiang, China

Email:
Li Zhang[*] - lizhang@zstu.edu.cn; Peirong Rao[*] - prao@zju.edu.cn

* Corresponding author

Keywords:
enantioselective synthesis; interrupted Nazarov cyclization; khayanolide-type limonoids; tetracyclic framework

Beilstein J. Org. Chem. **2025,** *21,* 926–934.
https://doi.org/10.3762/bjoc.21.75

Received: 18 March 2025
Accepted: 25 April 2025
Published: 12 May 2025

Associate Editor: D. Y.-K. Chen

Abstract

A convergent approach for the enantioselective construction of an advanced intermediate containing the [5,5,6,6]-tetracyclic core framework of the khayanolide-type limonoids was described. The strategy features an acylative kinetic resolution of the benzylic alcohol, a 1,2-Grignard addition and an AcOH-interrupted Nazarov cyclization.

Introduction

Limonoids, a class of tetranortriterpenoids derived biosynthetically from oxidative truncation of apotirucallane or apoeuphane precursors coupled with subsequent β-furan annulation [1-6], constitute an architecturally sophisticated family of natural products. Based on their specific skeletal rearrangements, limonoids can be systematically categorized into four subfamilies: ring intact limonoids, ring-seco limonoids, rearranged limonoids and N-containing limonoids (Figure 1). Moreover, these molecules exhibit a remarkable pharmacological portfolio encompassing anticancer, antimicrobial, anti-inflammatory, and insect antifeedant activities [7-9], positioning them as compelling targets for both therapeutic development and agrochemical innovation. Furthermore, limonoids are also renowned for their extraordinary structural complexity. For instance, the phragmalin-type limonoids represent a significant category of highly oxygenated rearranged limonoids, which contain a distinctive octahydro-1*H*-2,4-methanoindene cage. The fascinating architectures and remarkable biological profiles of these compounds have attracted widespread attention from the synthetic community. In 1989, Corey and Hahl made a seminal contribution [10] to the field by completing the total synthesis of azadiradione (**1**). Following this, Ley and his team successfully synthesized azadirachtin (**2**) in 2007, a limonoid extensively utilized in organic agriculture [11]. In recent years, remarkable progress has been made on the total syntheses of various limonoids, with notable contributions from researchers such as Williams [12], Yamashita [13], Hao/Yang/Shen [14], Gong/Hao/Yang [15], Newhouse [16-19], Yang/Chen [20], Renata [21], Qin/Yu [22],

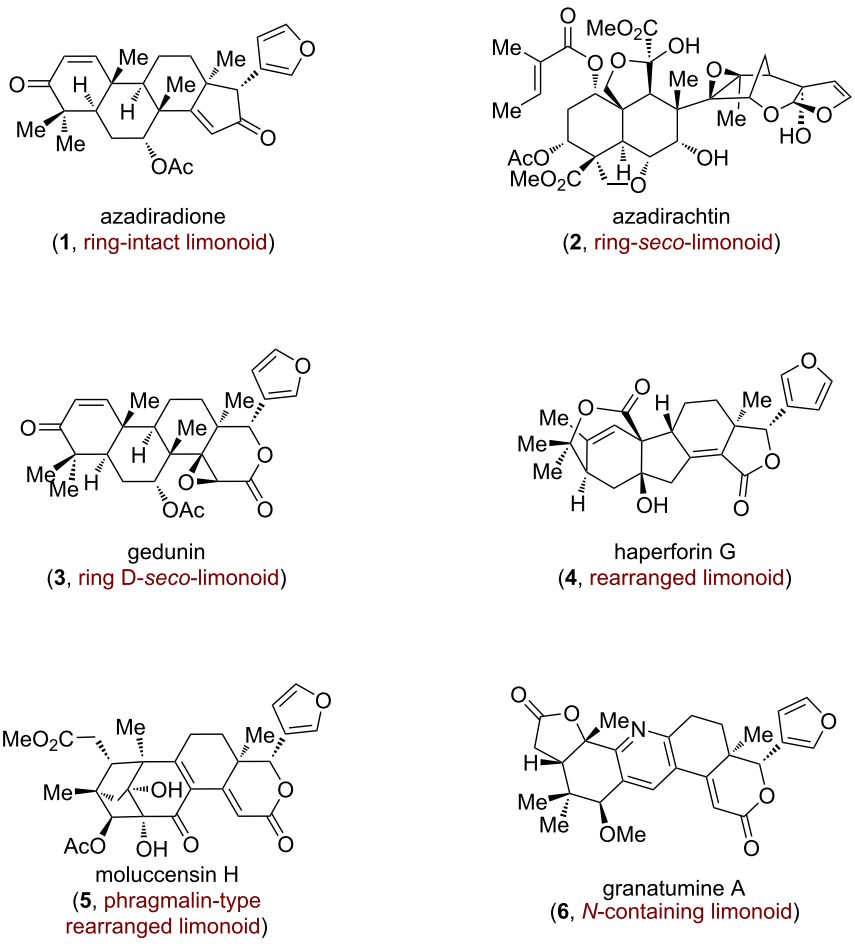

Figure 1: Representative limonoid triterpenes.

Ma [23], Watanabe [24], and Li [25]. Their groundbreaking work has provided valuable insights and inspired further research in synthetic chemistry involving limonoids.

Krishnolides A and C (**7** and **8**, respectively; Scheme 1A) were identified by Wu and co-workers from the seeds of a Krishna mangrove *Xylocarpus moluccensis* [26]. These two molecules belong to khayanolides, a class of rearranged phragmalin limonoids characterized by a structurally intricate tricyclo[4.2.1^{10,30}.1^{1,4}]decane ring system. Additionally, krishnolides A and C contain 9–11 stereogenic centers and exhibit diverse oxidation patterns. Their relative and absolute configurations were determined through NMR, HRESIMS and ECD experiments, as well as single crystal X-ray diffraction analysis. A preliminary investigation revealed that krishnolide A (**7**) exhibited unique anti-human immunodeficiency virus (HIV) activity, representing the first report of anti-HIV activity in khayanolide-type limonoids. However, the highly oxygenated and polycyclic scaffolds pose substantial challenges toward their total synthesis. Two synthetic studies were disclosed successively by Sarpong [27] and Jirgensons [28], both focusing on the construction of the unique methanoindene cage structure (A_1A_2B ring system). Building upon our previous syntheses of phragmalin-type limonoids [29], we herein disclose a convergent approach leveraging an AcOH-interrupted Nazarov cyclization to establish the [5,5,6,6]-tetracyclic scaffold with precise stereochemical fidelity.

Results and Discussion

Our retrosynthetic analysis toward krishnolides A (**7**) and C (**8**) is delineated in Scheme 1B. We hypothesized that these two molecules could be synthesized from diol **9** through a late-stage modification involving adjustment of the oxidation state and regioselective acylation. The formation of **9** was envisioned to proceed via an intramolecular pinacol coupling [30,31] of [5,5,6,6]-tetracycle **10**, which forges the A_2 ring while simultaneously installing the hydroxy group at C30. The latter intermediate could in turn be derived from dienone **11** by an AcOH-interrupted Nazarov cyclization [32-34], thereby establishing the B ring with the desired all-*cis* stereochemical configuration,

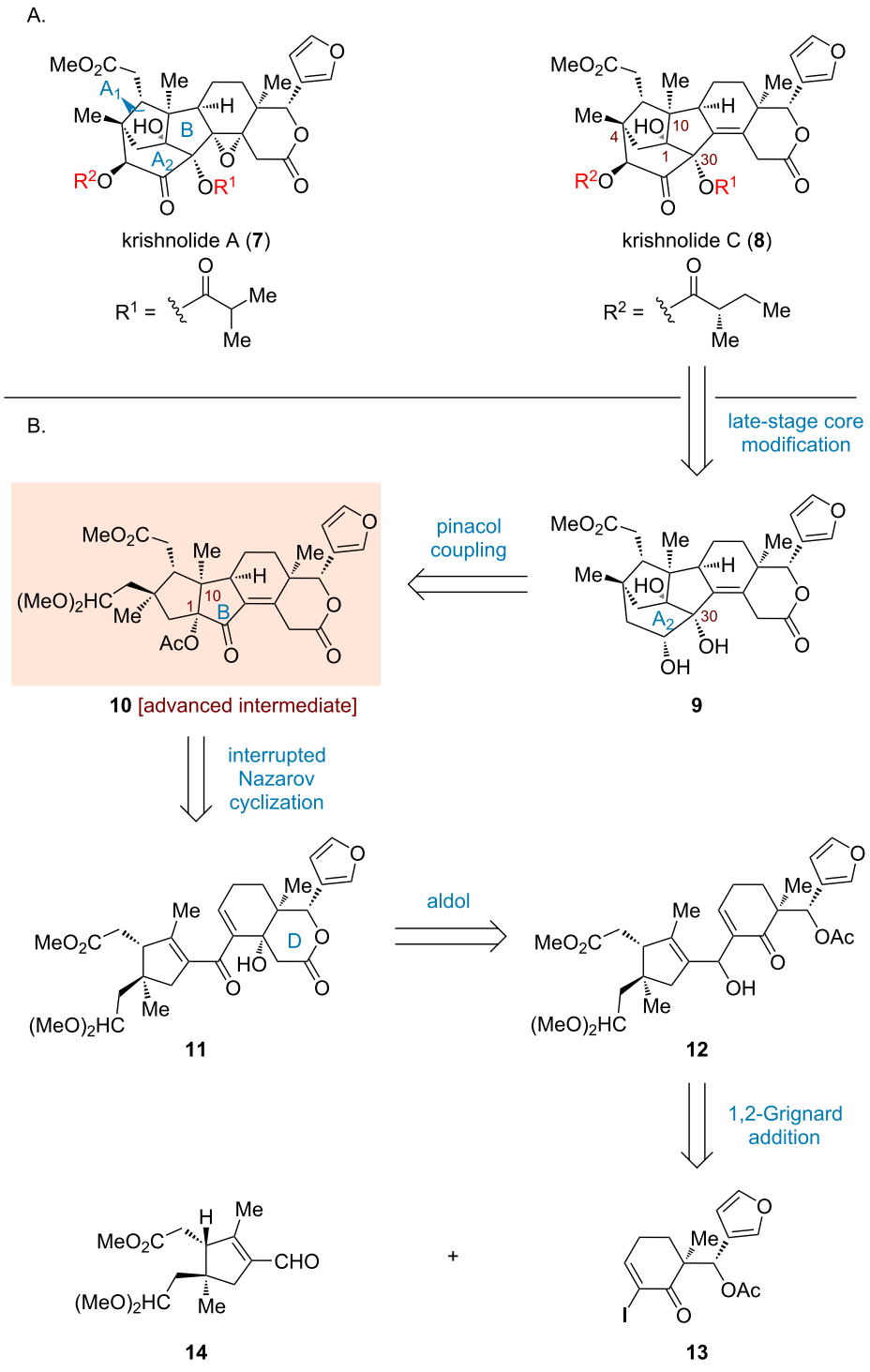

Scheme 1: Structures and retrosynthetic analysis of krishnolides A (**7**) and C (**8**).

including the quaternary carbon at C10 and the essential tertiary alcohol at C1. The β-hydroxylactone moiety (D ring) in **11** could be introduced through an intramolecular aldol condensation [35] of acetate **12**. Ultimately, the preparation of **12** could be traced back to aldehyde **14** through 1,2-Grignard addition with an organomagnesium reagent [36] prepared from α-iodoenone **13**.

Our synthesis began with the preparation of α-iodoenone **13** (Scheme 2). The α-monomethylation of cyclohexenone **15** was

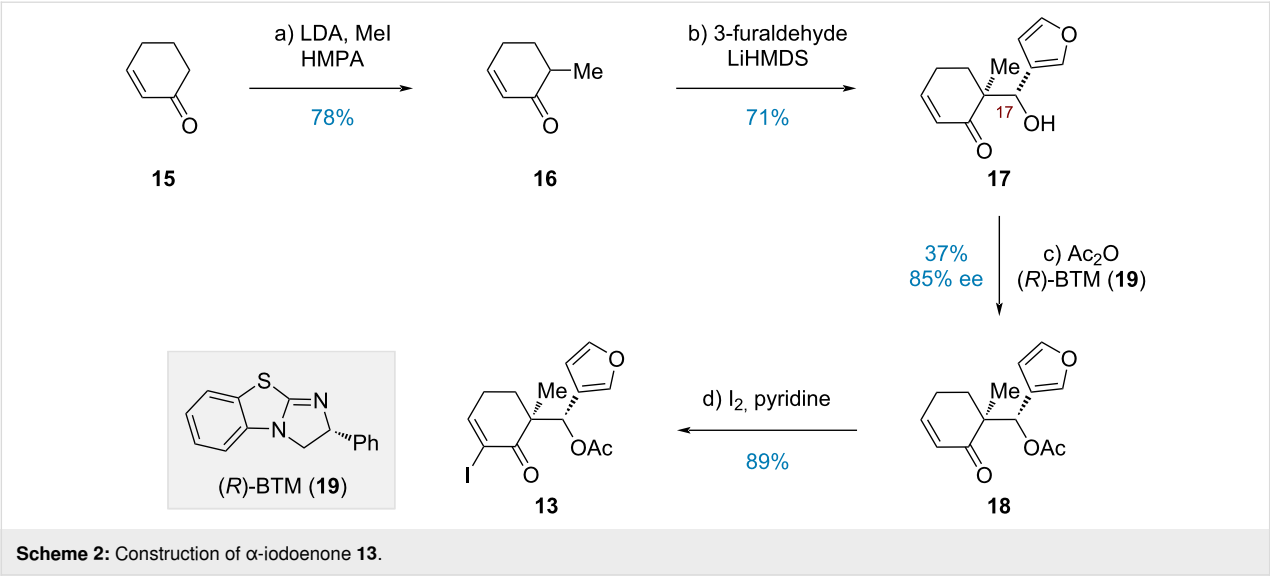

Scheme 2: Construction of α-iodoenone **13**.

efficiently carried out with LDA, HMPA, and MeI [37], producing enone **16** in 78% yield. Subsequently, a diastereoselective aldol reaction between **16** and 3-furaldehyde promoted by LiHMDS gave alcohol **17** with high regioselectivity (14:1 dr at C17) after an extensive screening of bases (LDA, NaHMDS, KHMDS, etc.). Drawing inspiration from the pioneering work of Birman [38], as well as Newhouse's applications [18,19], an acylative kinetic resolution of the alcohol was achieved by using (*R*)-BTM (**19**), furnishing acetate **18** with satisfactory efficiency and enantioselectivity (37% yield, 85% ee). Finally, iodination of **18** employing Johnsen's protocol (I_2, pyridine) [39] provided α-iodoenone **13** in 89% yield.

On the other hand, the synthesis of acetal aldehyde **14** commenced with bicyclic ketone **21**, which was prepared from (+)-Hajos–Parrish ketone in 49% yield over two steps (Scheme 3) [40-43]. Ensuring silyl enol etherification of the ketone at C29 coupled with IBX-mediated Nicolaou oxidation [44] furnished the corresponding enone in 72% yield (90% brsm). The methyl group at C10 was then introduced via a Michael addition (MeMgBr, CuI) to afford **22** in a yield of 65% (4:1 dr at C10). Initial attempts on the carbonyl 1,2-transposition protocol reported by Dong and co-workers were ineffective [45], leading to premature hydride termination and the formation of alkene **23**. As an alternative solution, by treating **22** with KHMDS and $PhNTf_2$, enol triflation took place successfully. The resultant triflate was coupled with *n*-Bu_3SnH to afford $\Delta^{1,29}$-alkene **23** in 83% yield over two steps. Subsequent hydroboration–oxidation by employing BH_3·THF proceeded smoothly, providing a 4.4:1 mixture of regioisomeric alcohols with the desired isomer being the major component, presumably due to the considerable steric hindrance from the quaternary carbon at C4. However, decagram-scale separation of these two isomers by chromatography proved troublesome. Fortunately, the distinct reactivity of those two alcohols toward oxidation allowed for the selective conversion of desired alcohol to ketone **24** using PCC, producing a 50% overall yield, while the recovered undesired alcohol could be reverted to **21** by Swern oxidation.

Direct enol triflation (Et_3N/Tf_2O, $NaH/PhNTf_2$, $DTBMP/Tf_2O$, etc.) of **24** led only to epimerization at C10 or slow decomposition of the starting material (see Supporting Information File 1, Table S1). Pleasingly, treating **24** with HMDS and TMSI regioselectively generated the expected TMS enol ether [46], which underwent a Li/Si exchange in the presence of MeLi followed by interception of the lithium enolate with $PhNTf_2$ to give enol triflate **25** in 59% overall yield. The following palladium-catalyzed methoxycarbonylation produced methyl ester **26** in a satisfactory yield of 84%. TIPS-protected allylic alcohol **28** was selected as the appropriate precursor for the α,β-unsaturated aldehyde and synthesized from **26** via a four-step transformation sequence, including deketalization, reduction, silylation of the primary alcohol and oxidation of the secondary alcohol. For the disconnection of the C2–C7 bond, a two-step protocol involving Rubottom oxidation and PIDA-promoted oxidative cleavage [47] was applied to deliver aldehyde **29**. Finally, a one-pot acetalization and desilylation effectively afforded the acetal alcohol, which was then oxidized with the aid of TPAP, furnishing acetal aldehyde **14** in 67% yield over two steps.

With the two fragments **13** and **14** in hand, the next stage was set for the construction of the target skeleton through a 1,2-addition (Scheme 4). Preliminary trials to generate organometallic species via Li/I exchange under various conditions (*n*-BuLi, *t*-BuLi, or *t*-BuLi in combination with $CeCl_3$ or $MgBr_2$) led to

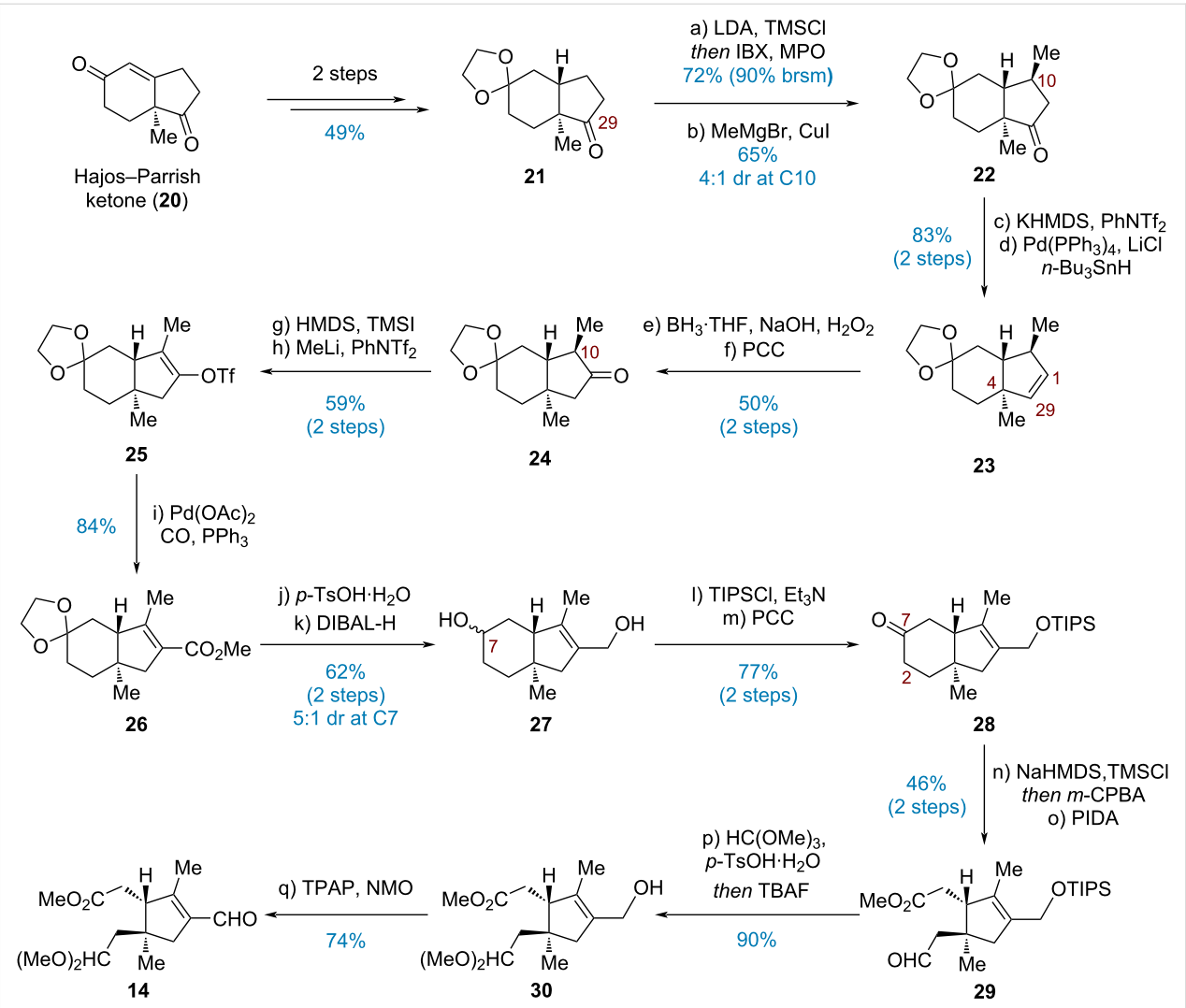

Scheme 3: Construction of aldehyde **14**.

rapid decomposition, likely due to inherent instability of α-iodoenone **13**. Inspired by the influential studies by Knochel [36] and Baran [48], we discovered that Mg/I exchange of **13** could be accomplished with iPrMgCl·LiCl at −78 °C. The resulting Grignard reagent reacted smoothly with aldehyde **14**, affording the corresponding adduct **12** in 58% yield (92% brsm). Since the newly created configuration at C30 was inconsequential, an intramolecular aldol reaction was directly carried out by treatment with LiHMDS to furnish β-hydroxylactone, which could be converted to dienone **11** through TPAP oxidation.

Having secured **11**, we proceeded to evaluate the pivotal Nazarov cyclization under a variety of conditions (Table 1). Initial trials under acid-mediated Nazarov conditions ($AlCl_3$, $BF_3{\cdot}Et_2O$ and Me_2AlCl) led to complete decomposition, while the exposure to AcOH resulted in recovery of the starting material (Table 1, entries 1–4). Recognizing the limitations of these approaches, we then turned to the milder photo-Nazarov cyclization, in which the UV-light sources were found to be critical. While irradiation at 365 or 313 nm failed to induce cyclization and only allowed recovery of the starting material (Table 1, entries 6 and 7), the disrotatory cyclization of **11** in the presence of AcOH by exposure to UV-light at 254 nm occurred exclusively to provide an inseparable mixture of **32** and **33** (Table 1, entry 5). Subsequent dehydration of the resultant mixture with $SOCl_2$ and pyridine yielded separable enones **34** (51%) and **10** (9%) over two steps. The structure of **10** was unequivocally determined through X-ray crystallographic analysis (ORTEP drawing, Scheme 4). Further optimization by elevating the reaction temperature did not noticeably alter the ratio of **32** and **33** (Table 1, entries 8 and 9). Moreover, attempts to apply interrupted Nazarov cyclization with H_2O under neutral conditions merely resulted in decomposition (Table 1,

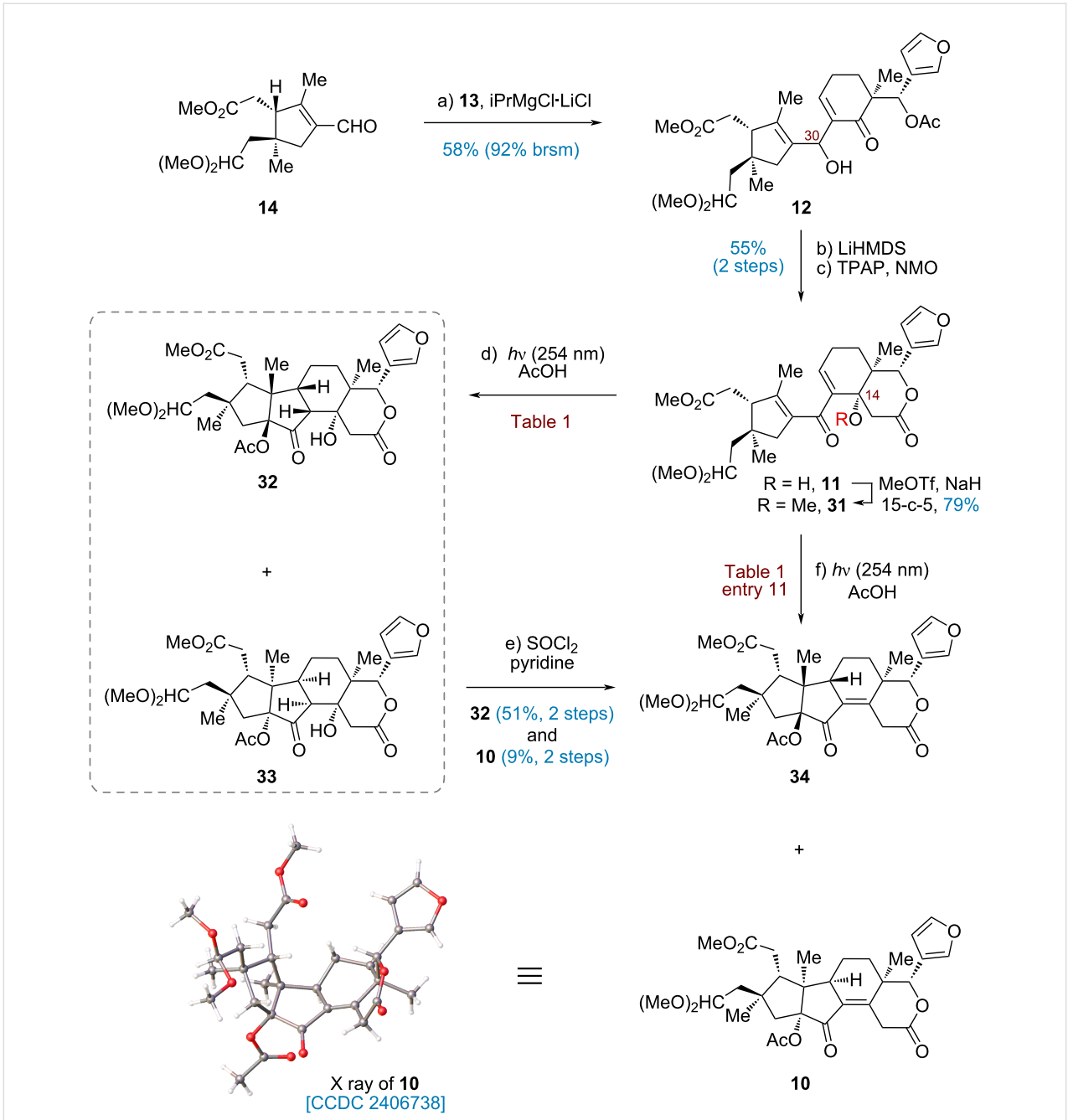

Scheme 4: Synthesis of the advanced intermediate **10** (in the X ray structure of **10** solvent molecule is omitted for clarity).

entry 10). To our delight, photoirradiation of the corresponding methyl ether **31** at 254 nm in the presence of AcOH at 20 °C led to a smooth cyclization, followed by spontaneous elimination, which produced the desired **10** as the single product, with no detection of **34** (Table 1, entry 11). This result presumably arises from the minimization of dipole–dipole repulsions between the carbonyl of the dienone moiety and the C14-OMe within the desired transition state (more details were discussed in our group's previous work [29]).

Conclusion

In conclusion, we have developed a convergent approach for the enantioselective assembly of an advanced intermediate en route to krishnolides A and C. Key steps of our strategy entail an acylative kinetic resolution of the alcohol, a 1,2-Grignard addition and an AcOH-interrupted Nazarov cyclization. Further elaboration of intermediate **10** to krishnolides A and C, as well as other khayanolide-type limonoids is currently ongoing, and the results will be disclosed in future reports.

Table 1: Optimization of the interrupted Nazarov cyclization.[a]

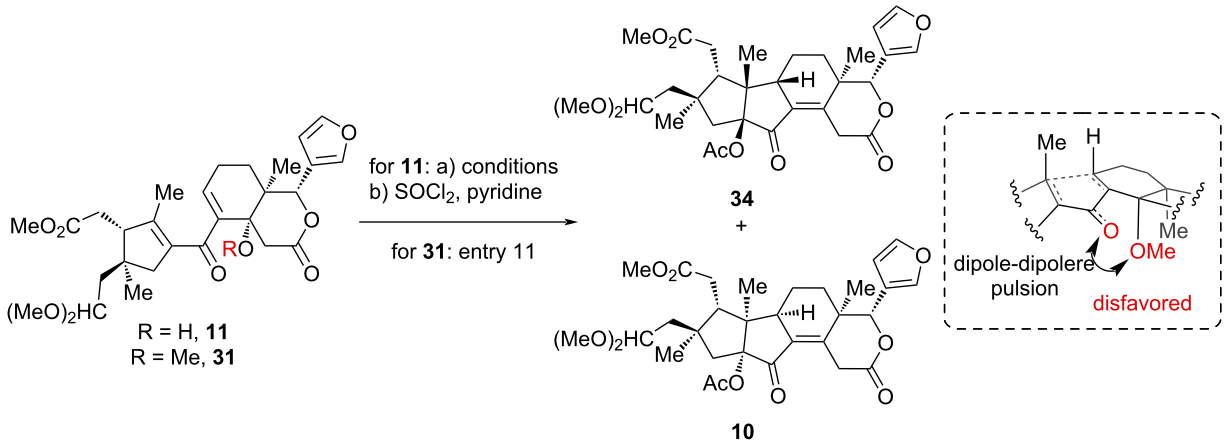

Entry	Conditions	Yield (%)[b]	
		34	**10**
1[c]	**11**, $AlCl_3$, DCE, 60 °C	0	0
2[c]	**11**, $BF_3{\cdot}Et_2O$, DCE, 60 °C	0	0
3[c]	**11**, Me_2AlCl, toluene, 100 °C	0	0
4	**11**, AcOH, DCE, 70 °C	0	0
5	**11**, 254 nm *hv*, AcOH, DCM, 20 °C	57	7
6[d]	**11**, 313 nm *hv*, AcOH, DCM, 20 °C	0	0
7[d]	**11**, 365 nm *hv*, AcOH, DCM, 20 °C	0	0
8	**11**, 254 nm *hv*, AcOH, DCE, 40 °C	54	8
9	**11**, 254 nm *hv*, AcOH, DCE, 70 °C	51	9
10[c]	**11**, 254 nm *hv*, H_2O, DCM, 20 °C	0	0
11	**31**, 254 nm *hv*, AcOH, DCM, 20 °C	0[e]	73[e]

[a]Reaction conditions: substrate (0.015 mmol), acid (2.0 equiv), solvent (5.0 mL). [b]Isolated yields over two steps involving Nazarov cyclization and dehydration. [c]Decomposition. [d]No reaction. [e]Isolated yields over Nazarov cyclization/elimination cascade.

Supporting Information

Deposition number 2406738 contains the supplementary crystallographic data for this paper. These data can be obtained free of charge via the joint Cambridge Crystallographic Data Centre (CCDC) and Fachinformationszentrum Karlsruhe Access Structures service.

Supporting Information File 1

Experimental procedures, NMR spectra and other characterization data for all new compounds.
[https://www.beilstein-journals.org/bjoc/content/supplementary/1860-5397-21-75-S1.pdf]

Acknowledgements

We thank Mr. Jiyong Liu from the Chemistry Instrumentation Center Zhejiang University for X-ray crystallographic analysis.

Funding

Financial support was provided by the National Natural Science Foundation of China (22125109, 22371250 and 22401251).

Author Contributions

Zhiyang Zhang: investigation; writing – original draft. Jialei Hu: investigation; methodology. Hanfeng Ding: conceptualization; funding acquisition; supervision; writing – original draft; writing – review & editing. Li Zhang: supervision. Peirong Rao: conceptualization; funding acquisition; investigation; writing – original draft.

ORCID® iDs

Hanfeng Ding - https://orcid.org/0000-0002-1781-4604
Peirong Rao - https://orcid.org/0009-0003-7405-9531

Data Availability Statement

All data that supports the findings of this study is available in the published article and/or the supporting information of this article.

Preprint

A non-peer-reviewed version of this article has been previously published as a preprint: https://doi.org/10.3762/bxiv.2025.19.v1

References

1. Heasley, B. *Eur. J. Org. Chem.* **2011,** 19–46. doi:10.1002/ejoc.201001218
2. Tan, Q.-G.; Luo, X.-D. *Chem. Rev.* **2011,** *111,* 7437–7522. doi:10.1021/cr9004023
3. Gualdani, R.; Cavalluzzi, M. M.; Lentini, G.; Habtemariam, S. *Molecules* **2016,** *21,* 1530. doi:10.3390/molecules21111530
4. Zhang, Y.; Xu, H. *RSC Adv.* **2017,** *7,* 35191–35220. doi:10.1039/c7ra04715k
5. Fu, S.; Liu, B. *Org. Chem. Front.* **2020,** *7,* 1903–1947. doi:10.1039/d0qo00203h
6. Luo, J.; Sun, Y.; Li, Q.; Kong, L. *Nat. Prod. Rep.* **2022,** *39,* 1325–1365. doi:10.1039/d2np00015f
7. Champagne, D. E.; Koul, O.; Isman, M. B.; Scudder, G. G. E.; Towers, G. H. N. *Phytochemistry* **1992,** *31,* 377–394. doi:10.1016/0031-9422(92)90003-9
8. Jain, D. C.; Tripathi, A. K. *Phytother. Res.* **1993,** *7,* 327–334. doi:10.1002/ptr.2650070502
9. Roy, A.; Saraf, S. *Biol. Pharm. Bull.* **2006,** *29,* 191–201. doi:10.1248/bpb.29.191
10. Corey, E. J.; Hahl, R. W. *Tetrahedron Lett.* **1989,** *30,* 3023–3026. doi:10.1016/s0040-4039(00)99392-4
11. Veitch, G. E.; Beckmann, E.; Burke, B. J.; Boyer, A.; Maslen, S. L.; Ley, S. V. *Angew. Chem., Int. Ed.* **2007,** *46,* 7629–7632. doi:10.1002/anie.200703027
12. Faber, J. M.; Eger, W. A.; Williams, C. M. *J. Org. Chem.* **2012,** *77,* 8913–8921. doi:10.1021/jo301182f
13. Yamashita, S.; Naruko, A.; Nakazawa, Y.; Zhao, L.; Hayashi, Y.; Hirama, M. *Angew. Chem., Int. Ed.* **2015,** *54,* 8538–8541. doi:10.1002/anie.201503794
14. Lv, C.; Yan, X.; Tu, Q.; Di, Y.; Yuan, C.; Fang, X.; Ben-David, Y.; Xia, L.; Gong, J.; Shen, Y.; Yang, Z.; Hao, X. *Angew. Chem., Int. Ed.* **2016,** *55,* 7539–7543. doi:10.1002/anie.201602783
15. Lv, C.; Tu, Q.; Gong, J.; Hao, X.; Yang, Z. *Tetrahedron* **2017,** *73,* 3612–3621. doi:10.1016/j.tet.2017.03.072
16. Schuppe, A. W.; Newhouse, T. R. *J. Am. Chem. Soc.* **2017,** *139,* 631–634. doi:10.1021/jacs.6b12268
17. Schuppe, A. W.; Huang, D.; Chen, Y.; Newhouse, T. R. *J. Am. Chem. Soc.* **2018,** *140,* 2062–2066. doi:10.1021/jacs.7b13189
18. Schuppe, A. W.; Zhao, Y.; Liu, Y.; Newhouse, T. R. *J. Am. Chem. Soc.* **2019,** *141,* 9191–9196. doi:10.1021/jacs.9b04508
19. Schuppe, A. W.; Liu, Y.; Gonzalez-Hurtado, E.; Zhao, Y.; Jiang, X.; Ibarraran, S.; Huang, D.; Wang, X.; Lee, J.; Loria, J. P.; Dixit, V. D.; Li, X.; Newhouse, T. R. *Chem* **2022,** *8,* 2856–2887. doi:10.1016/j.chempr.2022.09.012
20. Zhang, W.; Zhang, Z.; Tang, J.-C.; Che, J.-T.; Zhang, H.-Y.; Chen, J.-H.; Yang, Z. *J. Am. Chem. Soc.* **2020,** *142,* 19487–19492. doi:10.1021/jacs.0c10122
21. Li, J.; Chen, F.; Renata, H. *J. Am. Chem. Soc.* **2022,** *144,* 19238–19242. doi:10.1021/jacs.2c09048
22. Deng, H.; Deng, H.; Kim, C.; Li, P.; Wang, X.; Yu, Y.; Qin, T. *Nat. Synth.* **2023,** *3,* 378–385. doi:10.1038/s44160-023-00437-w
23. Jin, S. C.; Ma, D. W. *ChemRxiv* **2024**. doi:10.26434/chemrxiv-2024-dscn9
24. Mori, N.; Kitahara, T.; Mori, K.; Watanabe, H. *Angew. Chem., Int. Ed.* **2015,** *54,* 14920–14923. doi:10.1002/anie.201507935
25. Liu, X.; Xu, Y.; Li, L.; Li, J. *J. Am. Chem. Soc.* **2024,** *146,* 26243–26250. doi:10.1021/jacs.4c07956
26. Zhang, Q.; Satyanandamurty, T.; Shen, L.; Wu, J. *Mar. Drugs* **2017,** *15,* 333. doi:10.3390/md15110333
27. Lebold, T. P.; Gallego, G. M.; Marth, C. J.; Sarpong, R. *Org. Lett.* **2012,** *14,* 2110–2113. doi:10.1021/ol300647k
28. Becica, J.; Raciņš, O.; Ivanova, M.; Jirgensons, A. *J. Org. Chem.* **2023,** *88,* 10306–10309. doi:10.1021/acs.joc.3c00952
29. Rao, P.; Tang, D.; Xia, Q.; Hu, J.; Lin, X.; Xuan, J.; Ding, H. *J. Am. Chem. Soc.* **2025,** *147,* 3003–3009. doi:10.1021/jacs.4c16265
30. Hovey, M. T.; Cohen, D. T.; Walden, D. M.; Cheong, P. H.-Y.; Scheidt, K. A. *Angew. Chem., Int. Ed.* **2017,** *56,* 9864–9867. doi:10.1002/anie.201705308
31. Sasano, Y.; Koyama, J.; Yoshikawa, K.; Kanoh, N.; Kwon, E.; Iwabuchi, Y. *Org. Lett.* **2018,** *20,* 3053–3056. doi:10.1021/acs.orglett.8b01087
32. Grant, T. N.; Rieder, C. J.; West, F. G. *Chem. Commun.* **2009,** 5676–5688. doi:10.1039/b908515g
33. Yadykov, A. V.; Shirinian, V. Z. *Adv. Synth. Catal.* **2020,** *362,* 702–723. doi:10.1002/adsc.201901001
34. Trudel, V.; Tien, C.-H.; Trofimova, A.; Yudin, A. K. *Nat. Rev. Chem.* **2021,** *5,* 604–623. doi:10.1038/s41570-021-00304-2
35. Fernández-Mateos, A.; Grande Benito, M.; Pascual Coca, G.; Rubio González, R.; Tapia Hernández, C. *Tetrahedron* **1995,** *51,* 7521–7526. doi:10.1016/0040-4020(95)00375-i
36. Ren, H.; Krasovskiy, A.; Knochel, P. *Org. Lett.* **2004,** *6,* 4215–4217. doi:10.1021/ol048363h
37. Marques, F. A.; Lenz, C. A.; Simonelli, F.; Noronha Sales Maia, B. H. L.; Vellasco, A. P.; Eberlin, M. N. *J. Nat. Prod.* **2004,** *67,* 1939–1941. doi:10.1021/np049771x
38. Birman, V. B.; Li, X. *Org. Lett.* **2006,** *8,* 1351–1354. doi:10.1021/ol060065s
39. Johnson, C. R.; Adams, J. P.; Braun, M. P.; Senanayake, C. B. W.; Wovkulich, P. M.; Uskoković, M. R. *Tetrahedron Lett.* **1992,** *33,* 917–918. doi:10.1016/s0040-4039(00)91575-2
40. Daniewski, A. R.; Kiegiel, J. *Synth. Commun.* **1988,** *18,* 115–118. doi:10.1080/00397918808057826
41. Corey, E. J.; Huang, A. X. *J. Am. Chem. Soc.* **1999,** *121,* 710–714. doi:10.1021/ja983179a
42. Daniewski, A. R.; Liu, W. *J. Org. Chem.* **2001,** *66,* 626–628. doi:10.1021/jo0014414
43. Humphreys, D. J.; Newall, C. E.; Paskins, H. A.; Phillipps, G. H. *J. Chem. Soc., Perkin Trans. 1* **1978,** 15–19. doi:10.1039/p19780000015
44. Nicolaou, K. C.; Gray, D. L. F.; Montagnon, T.; Harrison, S. T. *Angew. Chem., Int. Ed.* **2002,** *41,* 996–1000. doi:10.1002/1521-3773(20020315)41:6<996::aid-anie996>3.0.co;2-i
45. Wu, Z.; Xu, X.; Wang, J.; Dong, G. *Science* **2021,** *374,* 734–740. doi:10.1126/science.abl7854
46. Moher, E. D.; Collins, J. L.; Grieco, P. A. *J. Am. Chem. Soc.* **1992,** *114,* 2764–2765. doi:10.1021/ja00033a087
47. Ohno, M.; Oguri, I.; Eguchi, S. *J. Org. Chem.* **1999,** *64,* 8995–9000. doi:10.1021/jo990704v
48. Cernijenko, A.; Risgaard, R.; Baran, P. S. *J. Am. Chem. Soc.* **2016,** *138,* 9425–9428. doi:10.1021/jacs.6b06623

License and Terms

BEILSTEIN JOURNAL OF ORGANIC CHEMISTRY

Recent total synthesis of natural products leveraging a strategy of enamide cyclization

Chun-Yu Mi‡, Jia-Yuan Zhai‡ and Xiao-Ming Zhang*

Review

Open Access

Address:
State Key Laboratory of Natural Product Chemistry & College of Chemistry and Chemical Engineering, Lanzhou University, Lanzhou 730000, P. R. China

Email:
Xiao-Ming Zhang* - zhangxiaom@lzu.edu.cn

* Corresponding author ‡ Equal contributors

Keywords:
alkaloid; cyclization; enamide; natural product; total synthesis

Beilstein J. Org. Chem. **2025,** *21,* 999–1009.
https://doi.org/10.3762/bjoc.21.81

Received: 24 February 2025
Accepted: 08 May 2025
Published: 22 May 2025

This article is part of the thematic issue "Concept-driven strategies in target-oriented synthesis".

Guest Editor: Y. Tang

Abstract

Enamides are distinctive amphiphilic synthons that can be strategically incorporated into cyclization reactions. The iminium species generated from enamides via nucleophilic addition or substitution are capable of engaging in further electrophilic additions or isomerization processes. Exploiting the multiple reactivities of enamides facilitates the development of diverse cyclization modes that provide entries to various *N*-heterocycles, some of which serve as key structural motifs in natural alkaloids. This review highlights recent advancements in enamide-based cyclization reactions, including enamide–alkyne cycloisomerization, [3 + 2] annulation, and polycyclization, with a particular emphasis on their pivotal role as a strategy in the total synthesis of natural products.

Introduction

The use of enamines as surrogates for enols in nucleophilic reactions has been well-documented for decades since their first report by Stork in the 1950s [1-3]. Compared with enols, enamines benefit from the lone pair of electrons on the nitrogen atom, which enhances the nucleophilicity of the alkene, enabling it to react with a broad range of electrophiles. This activation mode of carbonyl compounds has been so well-established that it is featured in nearly every organic chemistry textbook. However, despite their versatility, enamines themselves are not easily handling compounds in experimental settings. Their sensitivity to hydrolysis complicates their isolation and identification, and following the nucleophilic addition or substitution, the resulting iminium ions often undergo direct hydrolysis, preventing further use in a cascade nucleophilic addition. As a result, enamines are not ideal partners in tandem reactions for the synthesis of nitrogen-containing products. As analogues to enamines, the enamides contain an *N*-acyl group in place of the original alkyl group. The electron-withdrawing effect of the amide group delocalizes the nitrogen lone pair, thereby reducing the electron density and nucleophilicity of the enamide double bond. These features significantly diminish the reactivity of enamides as nucleophiles, rendering them more stable than

enamines. This stability is reflected in their frequent occurrence in natural products [4]. As a result, research on the synthetic applications of enamides has historically lagged behind that of enamines [5,6]. Beyond their use in hydrogenation reactions [7,8], the exploration of enamides' nucleophilic reactivity has only gained momentum in recent years. Inspired by pioneering work from various research groups [9-15], the potential of enamides in nucleophilic reactions has become recognized. Among them, enamide cyclizations have attracted considerable attention due to their promise in the total synthesis of alkaloids [16]. Notably, these valuable compounds can be employed as efficient synthons in enamide–alkyne cycloisomerization, [*n* + *m*] cycloadditions, pericyclic reactions, and radical cyclizations. A comprehensive review of these advancements up until 2015 has already been documented [16]. In this review, recent breakthroughs of these enamide cyclizations will be surveyed from the viewpoint of natural product synthesis. Leveraging the enamide–alkyne cycloisomerization cyclizations, *Lycopodium* alkaloids (−)-dihydrolycopodine, (−)-lycopodine, (+)-lycoposerramine Q, (+)-fawcettidine, (+)-fawcettimine, and (−)-phlegmariurine have been synthesized in a concise and efficient manner, while employment of the [2 + 3] cycloadditions or a polycyclization enables the elegant total synthesis of *Cephalotaxus* alkaloids cephalotaxine, cephalezomine H, (−)-cephalotaxine, (−)-cephalotine B, (−)-fortuneicyclidin A, (−)-fortuneicyclidin B, and (−)-cephalocyclidin A.

Unlike enamines, tertiary enamides can participate in cyclization reactions initial as nucleophiles, and upon protonation, alkenylation, or alkylation, the resultant iminium intermediates can serve as electrophiles. Due to the presence of an amide, the resulting iminiums from the enamides can be stabilized to take part in the second nucleophilic addition, though direct isomerization of the iminiums to the enamides is also possible (Figure 1). Guided by these principles, tandem reactions or annulations can be designed to efficiently access *N*-heterocycles. As the enamides are also easily accessible via condensations, applications of these nitrogen-containing building blocks in the synthesis of *N*-heterocycles are synthetically straightforward. When applied properly, these methods offer promising strategies for the total synthesis of complex natural products.

Review

Aza-Prins cyclization – total synthesis of (–)-dihydrolycopodine and (–)-lycopodine

Cyclizations of enamides can proceed via several distinct pathways. If protonation of the enamide occurs first, the resulting iminium ion can be readily captured by a wide variety of nucleophiles, including alkenes and alkynes. These *aza*-Prins cyclizations have potential applications in the synthesis of natural alkaloids, as exemplified by She's total synthesis of (−)-dihydrolycopodine and (−)-lycopodine [17]. These *Lycopodium* alkaloids have long been valued in traditional Chinese medicine for their therapeutic effects on skin disorders and as analgesics [18]. Preliminary biological evaluations also suggest their antipyretic and anticholinesterase activities [19]. As a prominent member of the lycopodine-type alkaloids, lycopodine features a characteristic tetracyclic structure with a bridged cyclohexanone. To address the challenges associated with constructing the complex ring systems of this structure, She and co-workers devised an intramolecular *aza*-Prins cyclization strategy to form both the bridge ring and the *N*-hetero quaternary center in a single step. As depicted in Scheme 1, key enamide **1** was prepared from (*R*)-pulegone in 6 steps. In the

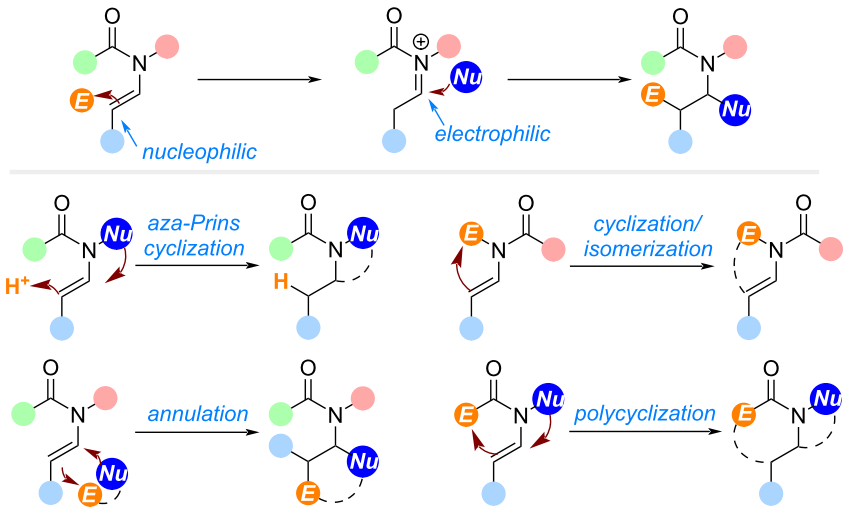

Figure 1: Reactivity of enamides and enamide cyclizations.

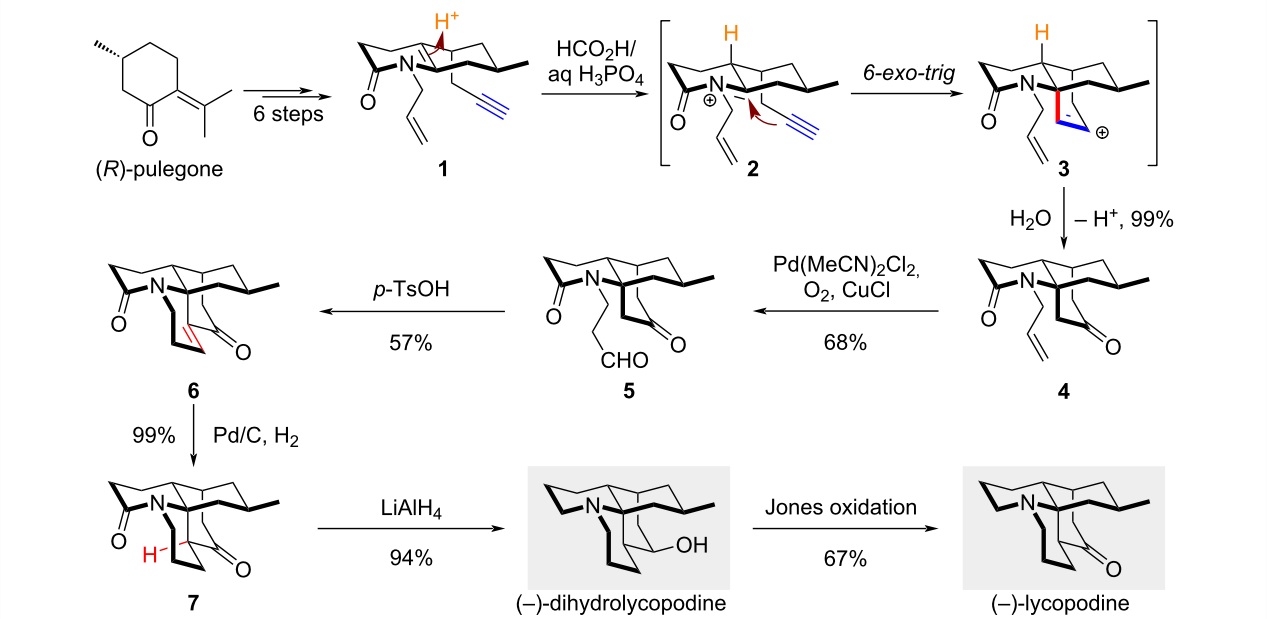

Scheme 1: Total synthesis of (–)-dihydrolycopodine and (–)-lycopodine.

presence of the weak acid H_3PO_4, protonation of **1** generates a stabilized iminium ion **2**, which then undergoes a *6-exo-trig* cyclization to deliver **4** after hydration of cation **3**. Notably, the terminal alkene remains intact during this process, and the initial protonation proceeds with full stereocontrol, rendering this transformation both highly chemo- and diastereoselective. From the cyclization result, it is presumed that the higher nucleophilicity of the alkyne functionality over the terminal alkene and the conformational strain of forming a bridge[3.2.1]bicycle might be responsible for a selective *6-exo-trig* cyclization.

From tricyclic compound **4**, *anti*-Markovnikov oxidation catalyzed by palladium led to the formation of aldehyde **5**. When treated with *p*-TsOH, the intramolecular aldol condensation of **5** provided the tetracyclic α,β-unsaturated enone **6** in 57% yield. Subsequent catalytic hydrogenation using Pd/C conditions delivered the hydrogen to the alkene from the less hindered face, producing ketone **7** with high diastereoselectivity. Final reduction of both the amide and ketone groups completed the total synthesis of (−)-dihydrolycopodine, which could then be further oxidized to (−)-lycopodine. The entire synthetic route hinges upon the development of a sterically congested *aza*-Prins cyclization, enabled by the presence of the enamide and its neighboring alkyne. Building on this strategy, the authors also accomplished the total synthesis of (−)-lycospidine A in only 10 steps [20], another *Lycopodium* alkaloid with a truncated tetracyclic skeleton and distinct oxidation levels, further highlighting the versatility and efficiency of the enamide *aza*-Prins approach.

Cyclization/isomerization – collective total synthesis of fawcettimine-type alkaloids

The bicyclic decahydroquinoline enamide motif can serve as a versatile precursor to access different types of tricyclic *N*-heterocycles. As demonstrated in the above work from She's group, the *aza*-Prins cyclization renders the α-position of enamide to be an active cyclization site, with the alkyne tether acting as the nucleophile. Since it is well-established that alkynes, when activated by transition metals such as gold or platinum, can also function as electrophiles, modulating the reactivity of the decahydroquinoline enamide motif to enable an enamide–alkyne cycloisomerization is also feasible. In this case, the initial nucleophilic cyclization of the enamide is followed by isomerization, shifting the cyclization site from the α- to the β-position of the enamide, resulting in the formation of a fused triangular ring system rather than a bridged tricycle. Building on this strategy, the same research group developed a divergent synthetic route that culminated in the concise and collective total synthesis of a series of fawcettimine-type *Lycopodium* alkaloids (Scheme 2) [21], which are well-known for their potent acetylcholinesterase (AChE) inhibitory activities [18].

In the presence of a catalytic amount of PPh_3AuCl and $AgSbF_6$, the enamide–alkyne cycloisomerization of bromo-substituted alkyne **8** proceeded via a *5-endo-dig* cyclization to afford tricyclic compound **10** through the formation of iminium intermediate **9**. The azepane ring was then constructed via an intramolecular reductive Heck reaction from vinyl bromide **10** with exclusive regioselectivity. Considering the strain of forming the

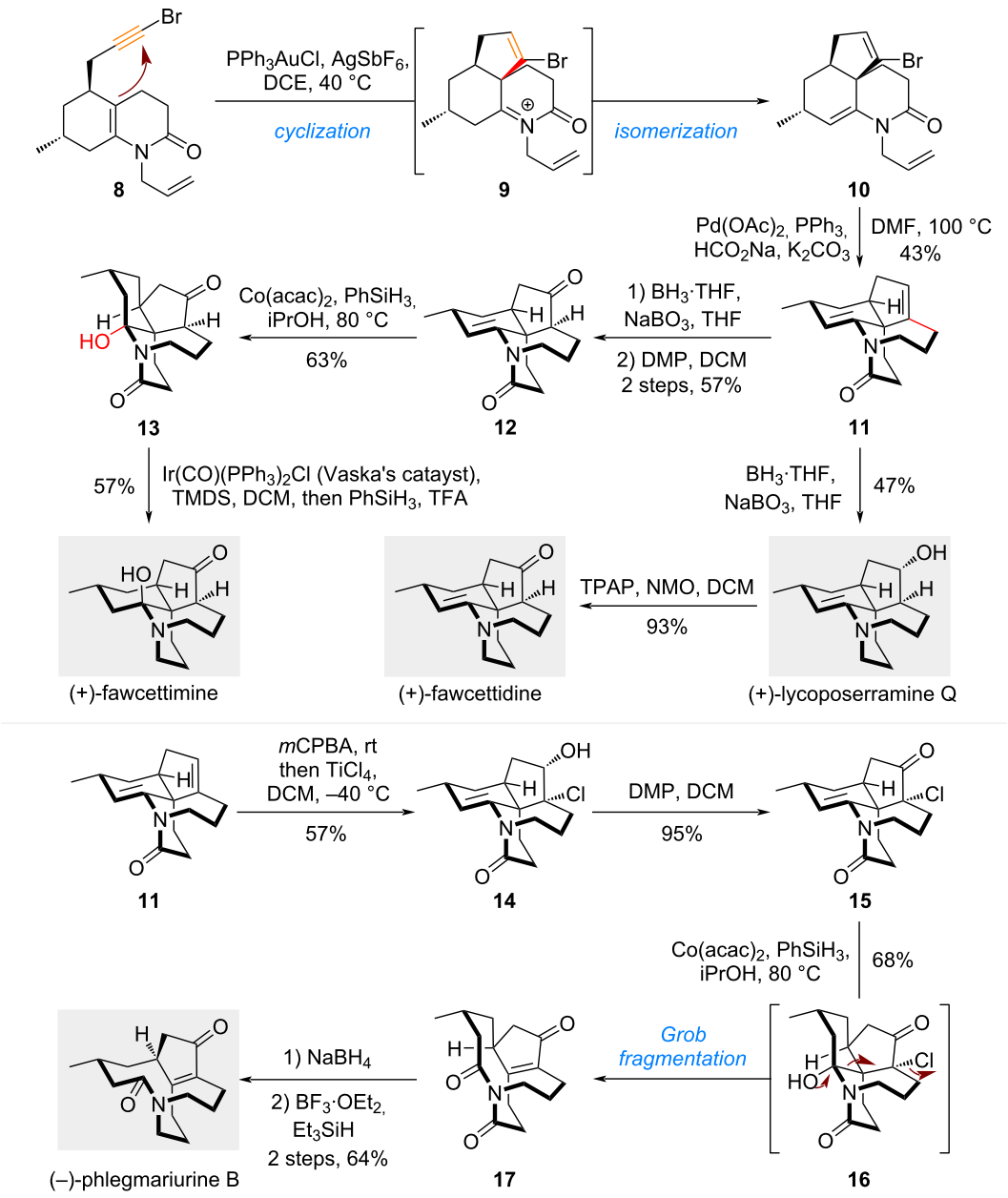

Scheme 2: Collective total synthesis of fawcettimine-type alkaloids.

7-membered ring, this highly efficient *7-endo-trig* (vs *6-exo-trig*) transannular Heck cyclization reaction was remarkable to be realized in a regioselective manner. From tetracyclic compound **11**, a one-pot facial and regioselective hydroboration/amide reduction followed by oxidation produced (+)-lycoposerramine Q, which was then converted to (+)-fawcettidine by Ley oxidation. Alternatively, hydroboration of **11** in mild conditions without the reduction of amide-generated ketone **12** after a subsequent Dess–Martin oxidation. Upon treatment of **12** with $Co(acac)_2$ and $PhSiH_3$ in iPrOH at 80 °C, the Mukaiyama hydration of enamide delivered hemiaminal **13**. Despite the incorrect configuration of the newly formed hydroxy group, it is considered inconsequential due to the reversibility of hemiaminal. Consequently, further reduction of the amide could complete the total synthesis of (+)-fawcettimine with in situ adjustment of the hemiaminal configuration.

The incorrect configuration observed in the Mukaiyama hydration also inspired the authors to develop a fragmentation process for the total synthesis of (−)-phlegmariurine B. A one-pot epoxidation/nucleophilic epoxide opening introduced both a hydroxy group and a chloride across the cyclopentene, produc-

ing **14** in 57% yield. After oxidation of alcohol **14** to ketone **15**, the Mukaiyama hydration then triggered a Grob fragmentation process of hemiaminal **16** and afforded the imide compound **17**. Final regioselective reduction of one of the two carbonyls on the imide completed the synthesis of (−)-phlegmariurine B.

Annulation

Total syntheses of cephalotaxine and cephalezomine H

The [2 + 3] annulation of enamides is a relatively underexplored reaction, particularly in the context of total synthesis. Its synthetic potential remains to be fully excavated, as it offers a modular approach for disassembling molecules into segments of comparable sizes. Recently, Fan's group reported the development of this annulation and applied it in the divergent total synthesis of *Cephalotaxus* alkaloids (Scheme 3) [22], including cephalotaxine whose ester, homoharringtonine, has been listed as an approved FDA drug for the treatment of chronic myeloid leukemia [23]. In their elegant study, an Au-catalyzed [2 + 3] annulation was utilized to transform enamine **18** and propargyl ester **19** into 1-azaspiro[4.4]nonane **20** with high diastereoselectivity. Notably, the combination of an *N*-heterocyclic carbene gold catalyst and a silver salt $AgSbF_6$ was found to be essential in guaranteeing the reactivity of the alkyne partner, probably due to the formation of a more acidic cationic gold complex. Following this annulation, reduction of the amide in **20**, catalytic hydrogenation of the alkene and the *N*-benzyl group, and subsequent nitrogen acylation yielded chloride **21** in a 42% total yield, setting the stage for the Witkop photocyclization. This transformation was carried out using a high-pressure mercury

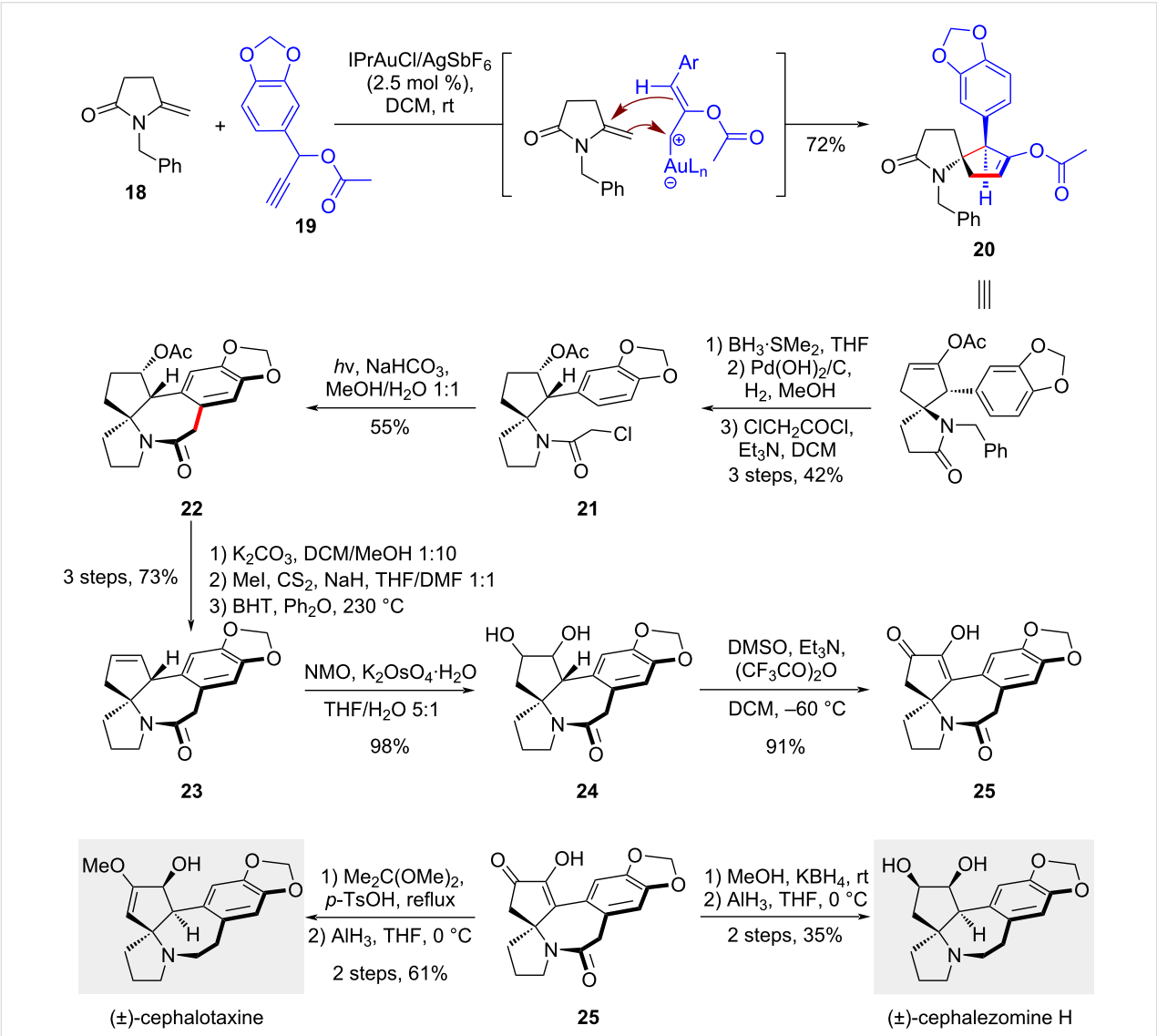

Scheme 3: Total syntheses of cephalotaxine and cephalezomine H.

vapor lamp to afford benzazepine **22**, completing the construction of the pentacyclic framework of the natural product. Subsequent functional group manipulations, including the Chugaev elimination of the hydroxy group on the cyclopentane ring, dihydroxylation, and oxidation of the diol to a diketone, produced intermediate **25** in its enol form. From this common intermediate, regioselective etherification at the less hindered position formed an enol ether. Final reduction of both the amide and the ketone using alane completed the total synthesis of cephalotaxine. Similarly, diastereoselective reduction of **25** with KBH_4 followed by alane reduction provided another alkaloid cephalezomine H.

Collective total syntheses of *Cephalotaxus* alkaloids

The cyclopentane ring in most *Cephalotaxus* alkaloids is characterized by the highest oxidation state within the pentacyclic framework. Installation of this cycle with suitable functional handles usually forms the key strategy of numerous total syntheses of these alkaloids [24-26]. Building upon earlier work, the same research group further advanced this approach by developing a Rh-catalyzed asymmetric [2 + 3] annulation of tertiary enamides with enoldiazoacetates, enabling highly efficient total syntheses of *Cephalotaxus* alkaloids (Scheme 4) [27]. In their recent study, the homopiperonyl alcohol **26** was transformed into tricyclic enamide **28** in five steps in a decagram scale. As no column chromatography was required during this process, the synthetic route is highly practical. The enantioselective annulation of tertiary enamide **28** with enoldiazoacetate **29** was then explored under the catalysis of a chiral dirhodium catalyst. While Doyle and co-workers had previously reported an elegant [2 + 3] cycloaddition of secondary enecarbamates [28], the extension of this reaction to enamides lacking an N–H group is a notable advancement. After extensive optimization, the chiral dirhodium catalyst **cat. 1** was found to be most capable in terms of both stereocontrol and efficiency. The use of 0.4% amount of **cat. 1** provided adduct **30** in 72% yield with 92% enantioselectivity, and the reaction could be scaled up to decagrams. Subsequent decarboxylation and recrystallization of the resulting ketone **31** yielded an enantiopure product (99% ee), which serves as a versatile intermediate for the divergent total synthesis of several *Cephalotaxus* alkaloids.

The α-hydroxylation of cyclopentanone, followed by amide reduction and methanol elimination in one-pot, produced (−)-cephalotaxine in 9 steps. Alternatively, Riley SeO_2 oxidation of **31**, benzylic bromination/hydrolyzation, facial selective ketone reduction, and epoxidation delivered compound **33** with the required oxidation level of the cyclopentane ring. In the final stages, Meinwald rearrangement/hemiketalization in a step-wise procedure, followed by amide reduction, completed the total synthesis of (−)-cephalotine B. Alternatively, after benzylic oxidation, the Meinwald rearrangement/aldol reaction gave rise to the bridge cyclic intermediate **35**, which can finally be converted into both (−)-fortuneicyclidin A and (−)-fortuneicyclidin B.

Polycyclization

Cyclization/Pictet–Spengler reaction

The hexahydropyrrolo[2,1-*a*]isoquinoline or tetrahydropyrrolo[2,1-*a*]isoquinolin-3(2*H*)-one framework is a pivotal core structure among various pyrrolo[2,1-*a*]isoquinoline alkaloids, exemplified by (+)-crispine, annosqualine, and erysotramidine, among others (Scheme 5) [29]. These bioactive alkaloids exhibit a broad spectrum of biological activities, including antitumor, antibacterial, antiviral, and antioxidizing properties. Previous synthetic strategies for these molecules typically rely on multi-step procedures to assemble the tricyclic core. However, the direct catalytic enantioselective formation of this scaffold from a linear precursor remains underexplored, despite the potential for such a tandem reaction to provide a more efficient route to these complex structures. In 2016, Wang and co-workers indigenously designed and developed a cyclization/Pictet–Spengler reaction cascade, leveraging the nucleophilicity of the tertiary enamides and the electrophilicity of the resulting acyliminium [30]. Unlike the monocyclization, which involves deprotonation of the acyliminium ion, the success of this polycyclization relies on the interception of the acyliminium ion by an aryl nucleophile, resulting in the formation of *N*-heterocyclic fused[6,6,5]tricycles. Optimization studies identified the tetraphenyl-substituted PyBox ligand **L1** as particularly effective in controlling the stereochemistry of the polycyclization, yielding high enantioselectivity for most substrates. As illustrated in Scheme 5, tertiary enamides with a tethered electron-rich arene could undergo cyclization to form products in high yields and excellent enantioselectivities. Notably, only a single diastereomer was produced in each case. The single-crystal X-ray crystallography revealed a *cis*-configuration for both the alkene and ketone substituents on the enamide, indicating that the intramolecular attack of the electron-rich arene on the acyliminium ion occurs from the *Si*-face. This stereochemical outcome is attributed to the steric discrepancy of the phenyl or *tert*-butyl group and the hydroxy group. The resulting tricyclic products could be further elaborated by elimination or amide reduction to yield hexahydropyrrolo[2,1-*a*]isoquinoline or tetrahydropyrrolo[2,1-*a*]isoquinolin-3(2*H*)-one frameworks, characteristic of alkaloids such as crispine analogs and erysotramidine.

Building on their previous work on cyclization/Pictet–Spengler reaction, the same group further designed cyclopentanone derived tertiary enamides as cyclization precursors (Scheme 6). The analogous polycyclization generated a tetracyclic *N*-hetero-

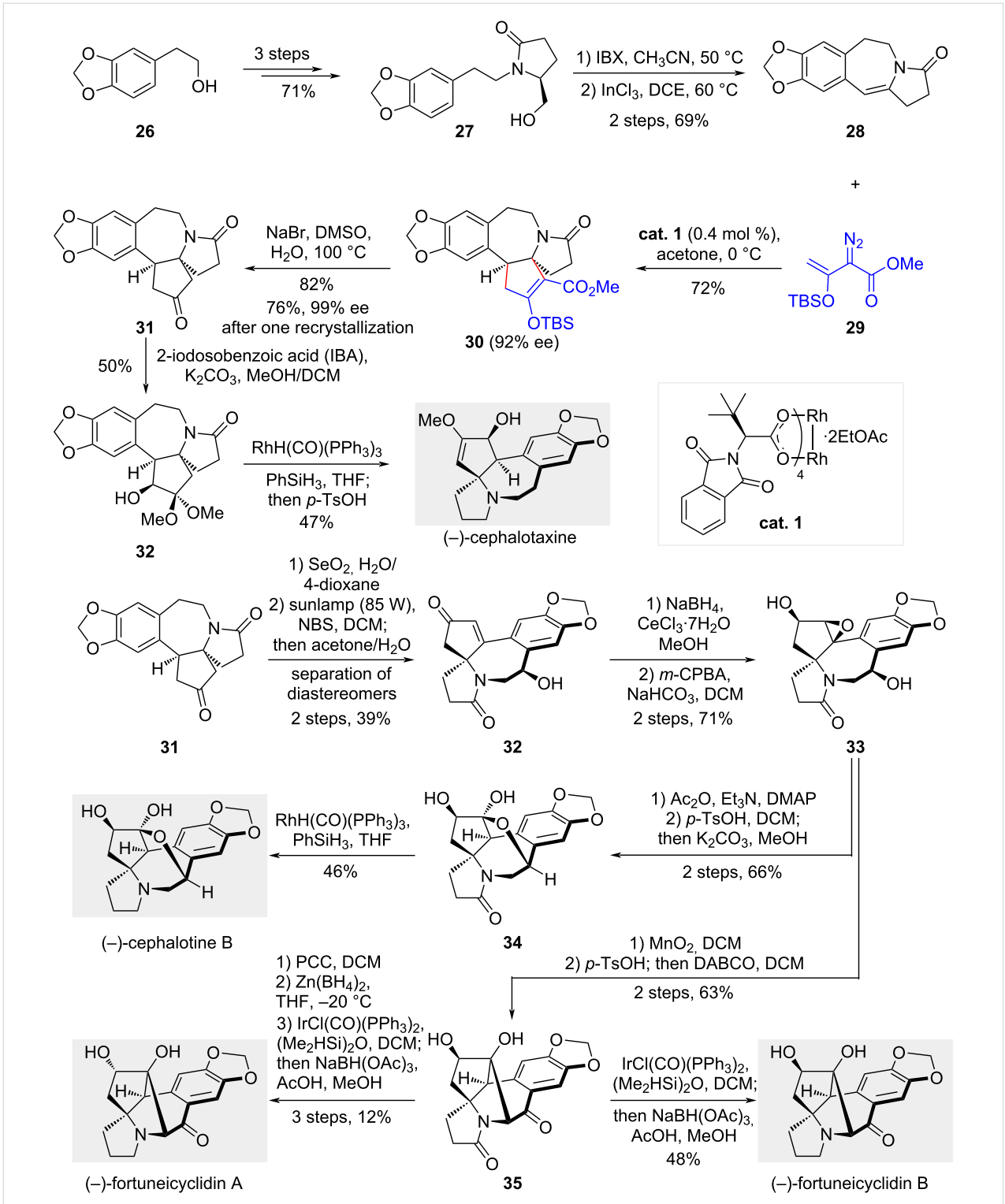

Scheme 4: Collective total syntheses of *Cephalotaxus* alkaloids.

cycle with three continuous stereogenic centers, one of them being an *aza*-quaternary carbon [31]. The resulting fused ring-system structurally resembles the nucleus of erysotramidine alkaloids, though it features a truncated cyclopentane rather than the characteristic cyclohexane or cyclohexene. In their optimization studies, the authors found the sequential catalysis of a chiral binol–Ti complex and $BF_3{\cdot}Et_2O$ to be the most efficient, providing products **39** in high yields with excellent

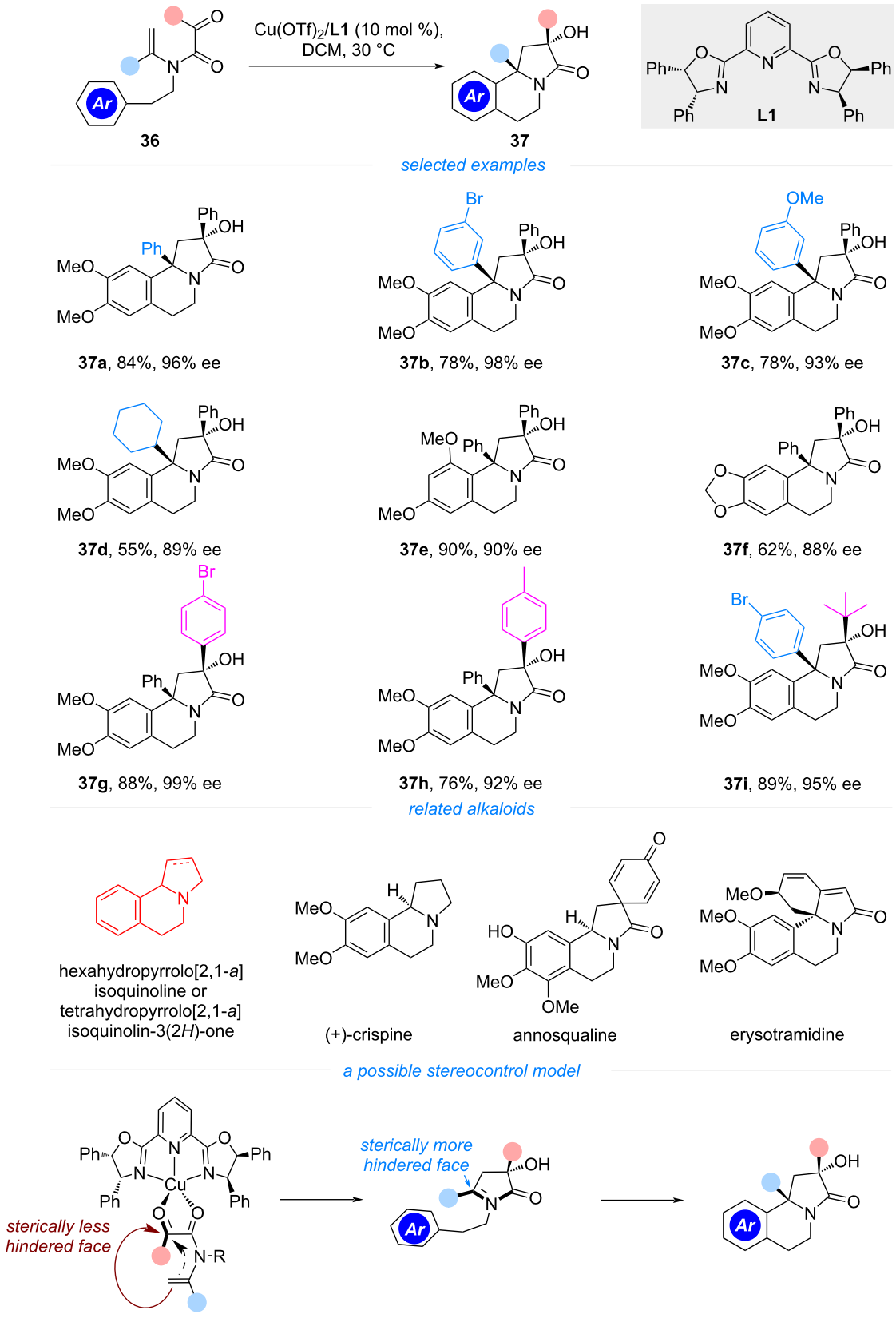

Scheme 5: Asymmetric tandem cyclization/Pictet–Spengler reaction of tertiary enamides.

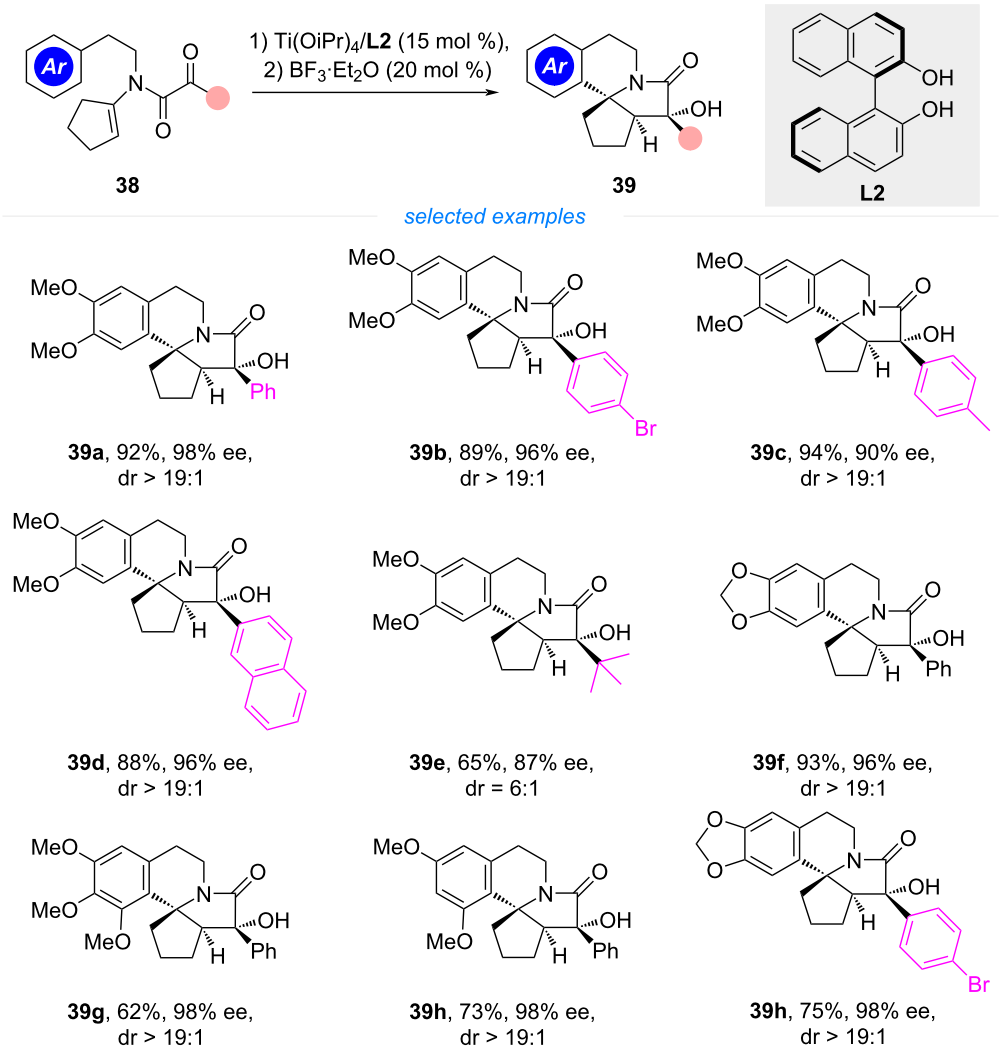

Scheme 6: Tandem cyclization/Pictet–Spengler reaction for the synthesis of chiral tetracyclic compounds.

diastereo- and enantioselectivities. The substituent on the enamide could be varied from aryl to *tert*-butyl groups, though the terminating aryl group still necessitates an electron-rich arene. As was found in their previous work, the steric hindrance of the phenyl or *tert*-butyl group was supposed to be responsible for the excellent diastereoselectivity observed in the second cyclization process. In their later studies, the authors also found cyclohexanone-derived tertiary enamides to be viable substrates for the polycyclization [32], affording erythrinane core skeletons in high yields. However, in these cases, the use of a chiral Cr(III)(salen)Cl complex in combination with $InCl_3$ was necessary to maintain a high level of stereocontrol.

Total synthesis of (−)-cephalocyclidin A

The bicyclic and tricyclic *N*-heterocycles without a fused arene are essential core structures in a wide array of alkaloids. A notable example is (−)-cephalocyclidin A, a cytotoxic pentacyclic cephalotaxus alkaloid [33,34]. Although the molecular structure contains a benzo-bridge ring system, disconnection of this bridge reveals a critical tricyclic *N*-heterocycle. To efficiently synthesize this tricycle, polycyclization of tertiary enamides is employed. Inspired by Wang's earlier work, Zhang and Tu's group developed a tandem cyclization/Mannich reaction to construct this architecture [35]. However, unlike the electron-rich arenes, the use of silyl enol ethers to terminate the second cyclization of the acyliminium intermediate would meet challenges associated with the instability of enolate derivatives. In their recent study, they successfully developed such a polycyclization taking advantage of a novel spiropyrroline-derived oxazole (SPDO) ligand (**L3**). As shown in Scheme 7, one-pot condensation of primary amine **40**, β-silyl substituted cyclopentanone **41**, and acyl chloride **42** produced enamide **43**. The polycyclization then took place under the catalysis of $Cu(OTf)_2$/

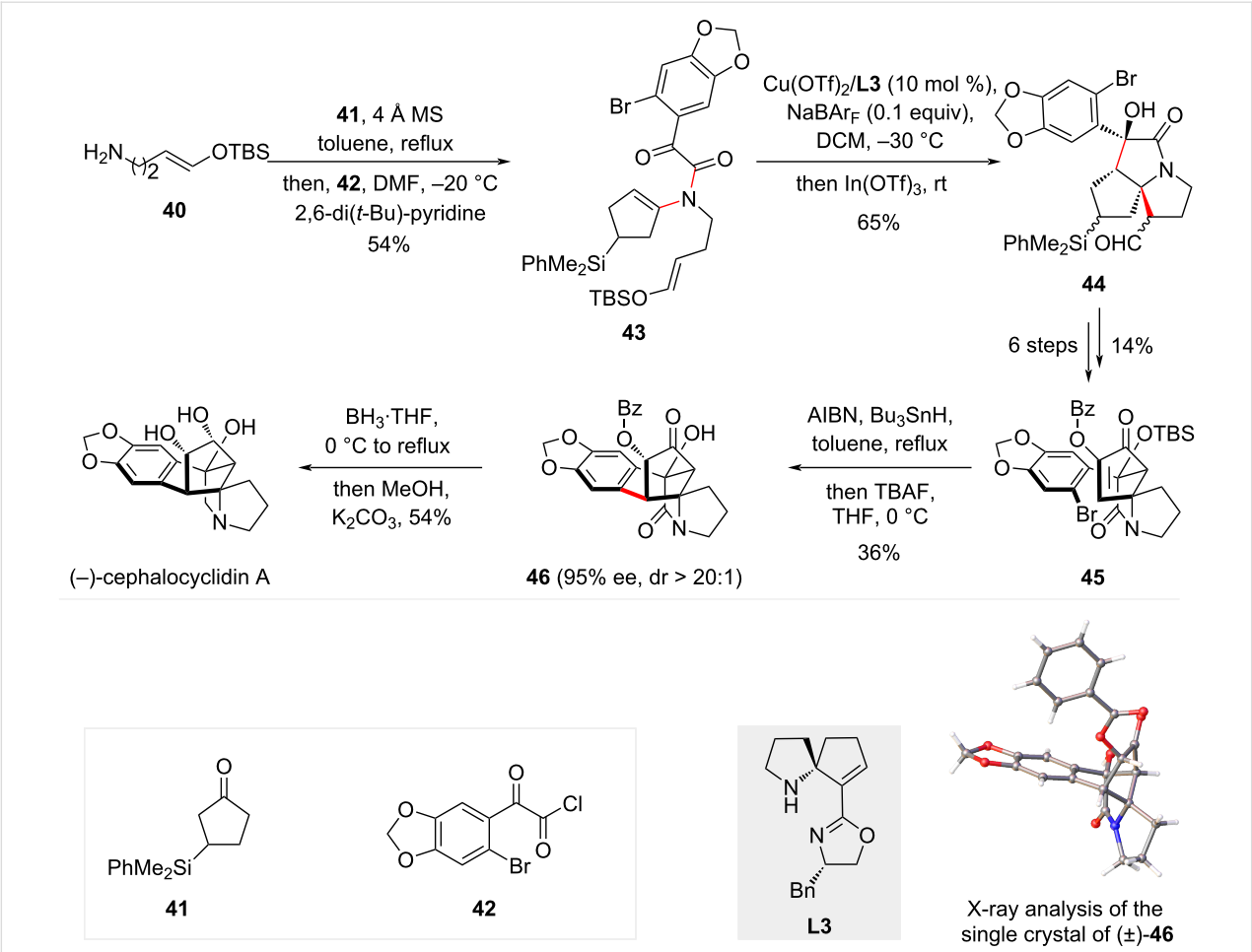

Scheme 7: Total synthesis of (–)-cephalocyclidin A.

L3 and $In(OTf)_3$, delivering tricyclic product **44** in high yield with excellent enantioselectivity. Despite formation of multiple diastereomers due to the presence of silyl and aldehyde groups on the tricycle, it is inconsequential as these groups are either removed or oxidized in subsequent steps. After adjustment of the oxidation levels, the cyclopentenone **45** obtained was subjected to an intramolecular Giese reaction, producing **46** with establishment of the bridge cycle [36,37]. The excellent diastereoselectivity in this radical cyclization was further rationalized by DFT calculations, which suggests an energy discrepancy of the hydrogen atom transfer process from different faces of the resulting α-hydroxyl radical. Final reduction of the ketone and amide followed by deprotection completed the total synthesis, giving rise to (−)-cephalocyclidin A in 10 steps from known compounds.

Conclusion

In summary, the perception of enamides as stable chemical entities with limited utilities in organic synthesis has evolved, and these compounds are now widely used in various cyclization reactions that play a pivotal role in the total synthesis of natural alkaloids. The nucleophilicity of enamides and the electrophilicity of the resulting acyliminium intermediates can be strategically manipulated in numerous ways to design cyclization and annulation reactions. Notably, these reactions – particularly tandem processes – are highly effective in constructing both fused and bridged ring systems, offering valuable new tools for chemical synthesis. Future advancements in the field could involve further applications of enamide cyclizations with other nucleophiles or in combination with other reaction patterns, potentially opening new avenues for the total synthesis of natural products.

Funding

We acknowledge NSFC (22371100, 22071147, and 92256303), the National Key R&D Program of China (2023YFA1506400, 2023YFA1506402, 2023YFA1506403), and The Science and Technology Major Program of Gansu Province of China (22ZD6FA006, 23ZDFA015, 24ZD13FA017) for financial supports.

ORCID® iDs

Xiao-Ming Zhang - https://orcid.org/0000-0002-9294-9672

Data Availability Statement

Data sharing is not applicable as no new data was generated or analyzed in this study.

References

1. Stork, G.; Terrell, R.; Szmuszkovicz, J. *J. Am. Chem. Soc.* **1954,** *76,* 2029–2030. doi:10.1021/ja01636a103
2. Stork, G.; Landesman, H. K. *J. Am. Chem. Soc.* **1956,** *78,* 5129–5130. doi:10.1021/ja01600a088
3. Stork, G.; Brizzolara, A.; Landesman, H.; Szmuszkovicz, J.; Terrell, R. *J. Am. Chem. Soc.* **1963,** *85,* 207–222. doi:10.1021/ja00885a021
4. Poulsen, T. B. *Acc. Chem. Res.* **2021,** *54,* 1830–1842. doi:10.1021/acs.accounts.0c00851
5. Carbery, D. R. *Org. Biomol. Chem.* **2008,** *6,* 3455–3460. doi:10.1039/b809319a
6. Beltran, F.; Miesch, L. *Synthesis* **2020,** *52,* 2497–2511. doi:10.1055/s-0040-1707403
7. Gopalaiah, K.; Kagan, H. B. *Chem. Rev.* **2011,** *111,* 4599–4657. doi:10.1021/cr100031f
8. Cabré, A.; Verdaguer, X.; Riera, A. *Chem. Rev.* **2022,** *122,* 269–339. doi:10.1021/acs.chemrev.1c00496
9. Matsubara, R.; Kobayashi, S. *Acc. Chem. Res.* **2008,** *41,* 292–301. doi:10.1021/ar700098d
10. Dake, G. R. *Synlett* **2012,** *23,* 814–824. doi:10.1055/s-0031-1290351
11. Gigant, N.; Chausset-Boissarie, L.; Gillaizeau, I. *Chem. – Eur. J.* **2014,** *20,* 7548–7564. doi:10.1002/chem.201402070
12. Wang, M.-X. *Chem. Commun.* **2015,** *51,* 6039–6049. doi:10.1039/c4cc10327k
13. Tong, S.; Wang, M.-X. *Synlett* **2021,** *32,* 1419–1427. doi:10.1055/a-1352-6358
14. Varlet, T.; Masson, G. *Chem. Commun.* **2021,** *57,* 4089–4105. doi:10.1039/d1cc00590a
15. Bouchet, D.; Varlet, T.; Masson, G. *Acc. Chem. Res.* **2022,** *55,* 3265–3283. doi:10.1021/acs.accounts.2c00540
16. Courant, T.; Dagousset, G.; Masson, G. *Synthesis* **2015,** *47,* 1799–1856. doi:10.1055/s-0034-1378706
17. Ma, D.; Zhong, Z.; Liu, Z.; Zhang, M.; Xu, S.; Xu, D.; Song, D.; Xie, X.; She, X. *Org. Lett.* **2016,** *18,* 4328–4331. doi:10.1021/acs.orglett.6b02072
18. Ma, X.; Gang, D. R. *Nat. Prod. Rep.* **2004,** *21,* 752–772. doi:10.1039/b409720n
19. Ortega, M. G.; Agnese, A. M.; Cabrera, J. L. *Phytomedicine* **2004,** *11,* 539–543. doi:10.1016/j.phymed.2003.07.006
20. Xu, S.; Zhang, J.; Ma, D.; Xu, D.; Xie, X.; She, X. *Org. Lett.* **2016,** *18,* 4682–4685. doi:10.1021/acs.orglett.6b02322
21. He, F.; Feng, S.; Zhao, Y.; Shi, H.; Duan, X.; Li, H.; Xie, X.; She, X. *Angew. Chem., Int. Ed.* **2022,** *61,* e202205439. doi:10.1002/anie.202205439
22. Ma, X.-Y.; An, X.-T.; Zhao, X.-H.; Du, J.-Y.; Deng, Y.-H.; Zhang, X.-Z.; Fan, C.-A. *Org. Lett.* **2017,** *19,* 2965–2968. doi:10.1021/acs.orglett.7b01202
23. Kantarjian, H. M.; O'Brien, S.; Cortes, J. *Clin. Lymphoma, Myeloma Leuk.* **2013,** *13,* 530–533. doi:10.1016/j.clml.2013.03.017
24. Weinreb, S. M.; Semmelhack, M. F. *Acc. Chem. Res.* **1975,** *8,* 158–164. doi:10.1021/ar50089a003
25. Chen, Y.; Li, W.-D. Z. *Chin. J. Org. Chem.* **2017,** *37,* 1885–1902. doi:10.6023/cjoc201705025
26. Jeon, H. *Asian J. Org. Chem.* **2021,** *10,* 3052–3067. doi:10.1002/ajoc.202100543
27. An, X.-T.; Ge, X.-M.; Liu, X.-Y.; Yang, Y.-H.; Zhao, X.-H.; Ma, X.-Y.; Peng, C.; Fan, Y.-J.; Qin, Y.; Fan, C.-A. *J. Am. Chem. Soc.* **2023,** *145,* 9233–9241. doi:10.1021/jacs.3c01572
28. Deng, Y.; Yglesias, M. V.; Arman, H.; Doyle, M. P. *Angew. Chem., Int. Ed.* **2016,** *55,* 10108–10112. doi:10.1002/anie.201605438
29. Yang, Y.-L.; Chang, F.-R.; Wu, Y.-C. *Helv. Chim. Acta* **2004,** *87,* 1392–1399. doi:10.1002/hlca.200490127
30. Xu, X.-M.; Zhao, L.; Zhu, J.; Wang, M.-X. *Angew. Chem., Int. Ed.* **2016,** *55,* 3799–3803. doi:10.1002/anie.201600119
31. Zhen, L.; Tong, S.; Zhu, J.; Wang, M.-X. *Chem. – Eur. J.* **2020,** *26,* 401–405. doi:10.1002/chem.201904596
32. Zhen, L.; Tong, S.; Zhu, J.; Wang, M.-X. *J. Org. Chem.* **2020,** *85,* 13211–13219. doi:10.1021/acs.joc.0c01992
33. Kobayashi, J.; Yoshinaga, M.; Yoshida, N.; Shiro, M.; Morita, H. *J. Org. Chem.* **2002,** *67,* 2283–2286. doi:10.1021/jo016327f
34. Kim, J. H.; Jeon, H.; Park, C.; Park, S.; Kim, S. *Angew. Chem., Int. Ed.* **2021,** *60,* 12060–12065. doi:10.1002/anie.202101766
35. Zhuang, Q.-B.; Tian, J.-R.; Lu, K.; Zhang, X.-M.; Zhang, F.-M.; Tu, Y.-Q.; Fan, R.; Li, Z.-H.; Zhang, Y.-D. *J. Am. Chem. Soc.* **2023,** *145,* 26550–26556. doi:10.1021/jacs.3c11178
36. Okada, K.; Ueda, H.; Tokuyama, H. *Org. Biomol. Chem.* **2022,** *20,* 5943–5947. doi:10.1039/d2ob00274d
37. Okada, K.; Ojima, K.-i.; Ueda, H.; Tokuyama, H. *J. Am. Chem. Soc.* **2023,** *145,* 16337–16343. doi:10.1021/jacs.3c05811

License and Terms

BEILSTEIN JOURNAL OF ORGANIC CHEMISTRY

Heterologous biosynthesis of cotylenol and concise synthesis of fusicoccane diterpenoids

Ye Yuan[‡1], Zhenhua Guan[‡2], Xue-Jie Zhang[‡1], Nanyu Yao[2], Wenling Yuan[2], Yonghui Zhang[*2], Ying Ye[*2] and Zheng Xiang[*1,3]

Letter

Open Access

Address:
[1]State Key Laboratory of Chemical Oncogenomics, Shenzhen Key Laboratory of Chemical Genomics, School of Chemical Biology and Biotechnology, Peking University Shenzhen Graduate School, Shenzhen 518055, P. R. China, [2]Hubei Key Laboratory of Natural Medicinal Chemistry and Resource Evaluation, School of Pharmacy, Tongji Medical College, Huazhong University of Science and Technology, Wuhan 430030, P. R. China and [3]Institute of Chemical Biology, Shenzhen Bay Laboratory, Shenzhen 518132, P. R. China

Email:
Yonghui Zhang[*] - zhangyh@mails.tjmu.edu.cn; Ying Ye[*] - ying_ye@hust.edu.cn; Zheng Xiang[*] - zxiang@pku.edu.cn

* Corresponding author ‡ Equal contributors

Keywords:
cotylenol; fusicoccane diterpenoids; heterologous biosynthesis; P450 oxidation; synthesis

Beilstein J. Org. Chem. **2025,** *21,* 1489–1495.
https://doi.org/10.3762/bjoc.21.111

Received: 30 January 2025
Accepted: 15 April 2025
Published: 21 July 2025

This article is part of the thematic issue "Concept-driven strategies in target-oriented synthesis".

Guest Editor: Y. Tang

Abstract

A novel strategy for the synthesis of fusicoccane diterpenoids is reported. By harnessing the biosynthetic pathways of brassicicenes and fusicoccins, cotylenol was produced in an engineered *Aspergillus oryzae* strain. We further achieved the concise synthesis of three fusicoccane diterpenoids, including alterbrassicicene E and brassicicenes A and R in 4 or 5 chemical steps from brassicicene I. This strategy lays the foundation for the preparation of fusicoccane diterpenoids and their analogues for biological studies.

Introduction

Fusicoccanes are a family of 5-8-5 tricyclic diterpenoid natural products that are produced by bacteria, fungi, algae, and plants (Figure 1a) [1-7]. Fusicoccanes possess a broad range of biological activities, including anticancer, anti-inflammatory, antimicrobial, antiparasitic, and plant growth regulating activities. For instance, cotylenin A (**1**) and fusicoccin A (**2**) function as molecular glues to stabilize the interactions between 14-3-3 proteins and their binding partners in plant and animal cells [8-12]. It has been reported that cotylenin A and its aglycone, cotylenol (**3**), induce differentiation in murine and human myeloid leukemia cells [13]. Cotylenin A and fusicoccin A also act synergistically with interferon-α or rapamycin to induce apoptosis in cancer cell lines [14-16]. However, cotylenin A cannot be produced by its natural source, *Cladosporium sp.* 501-7W, due to the loss of its ability to proliferate during preservation [17]. The important biological activities and complex structures of

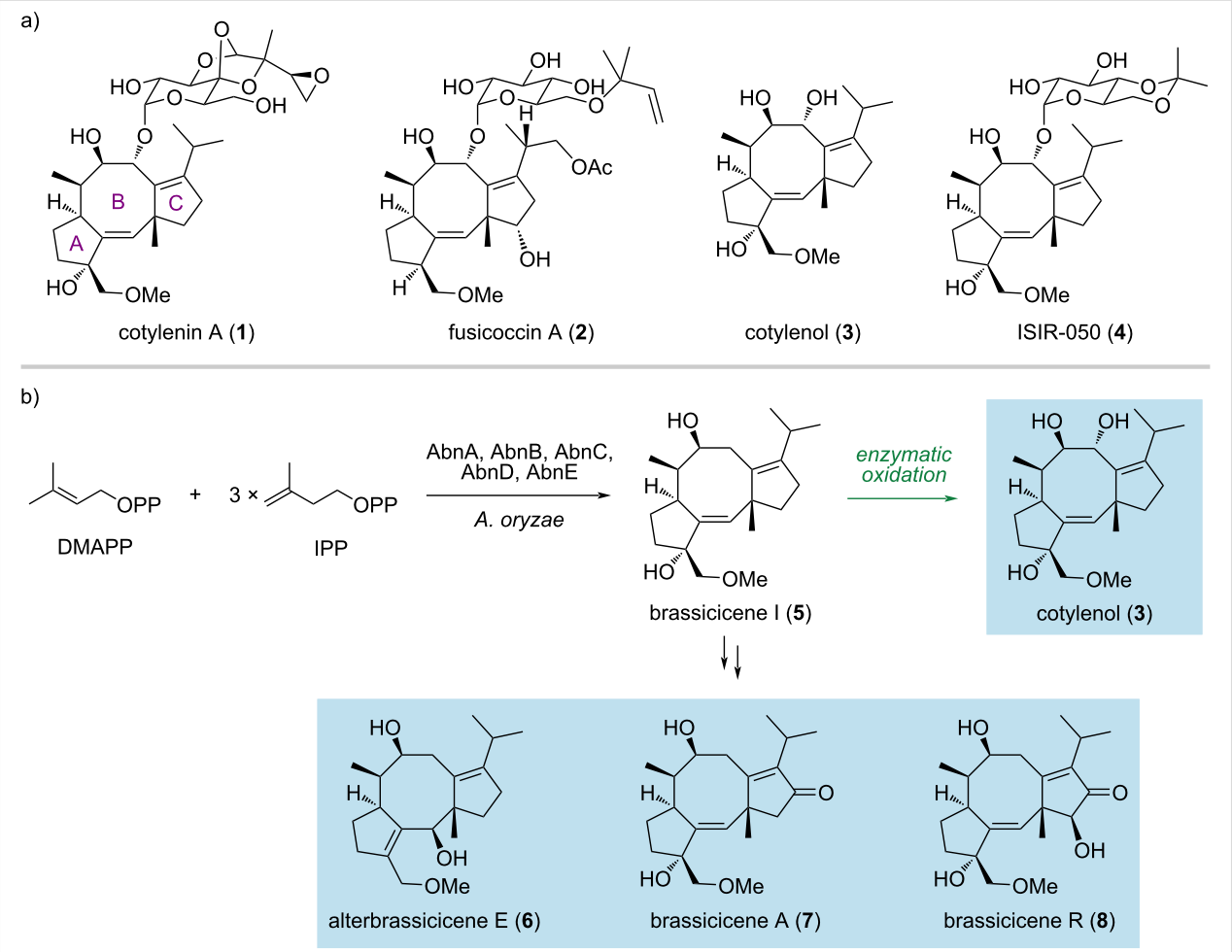

Figure 1: Selected fusicoccane diterpenoids and overview of this study. (a) Representative members of the fusicoccane diterpenoid family. (b) This work: heterologous biosynthesis of cotylenol (**3**) in an engineered *Aspergillus oryzae* strain and concise synthesis of fusicoccane diterpenoids.

fusicoccane diterpenoids have inspired several total syntheses, which range between 15 and 29 steps [18-26]. Most of these synthetic approaches rely on similar strategies, i.e., coupling of the A ring and the C ring followed by the formation of the B ring. Additionally, the semisynthesis of analogues of **1** has been reported and led to the discovery of ISIR-050 (**4**), which shows higher activity than cotylenin A in cell growth inhibition assays and less toxicity in single-agent treatments [27,28]. Recently, Jiang and Renata described a chemoenzymatic approach that combines the skeletal construction by chemical methods and enzymatic C–H oxidations [29]. The synthesis employs a catalytic Nozaki–Hiyama–Kishi reaction and a one-pot Prins cyclization/transannular hydride transfer to construct the 5-8-5 tricyclic scaffold. Enzymatic oxidations were used to install the hydroxy group at the C-3 position. Ten fusicoccanes were synthesized in 8–13 steps each. Despite these efforts, a strategy with limited chemical transformations is highly desirable and should enable the discovery of new fusicoccane derivatives with improved biological activity.

Inspired by the biosynthetic machinery of terpenoids, we have reported a hybrid synthetic strategy for accessing bioactive terpenoids by combining enzymatic terpene cyclization and chemical synthesis [30-33]. Briefly, the carbon scaffolds are forged by terpene cyclases, followed by concise chemical transformations to yield the desired natural products. Here, we describe heterologous biosynthesis of cotylenol by engineering the biosynthetic pathway of brassicicenes in *Aspergillus oryzae* and harnessing the promiscuity of a cytochrome P450 from the biosynthesis of fusicoccin A (Figure 1b). A key intermediate, brassicicenes I (**5**), was further used to achieve the collective synthesis of alterbrassicicene E (**6**), brassicicenes A (**7**) and R (**8**).

Results and Discussion

Fusicoccanes feature a characteristic dicyclopenta[*a*,*d*]cyclooctane (5-8-5) ring system that is biosynthesized from geranylgeranyl pyrophosphate (GGPP) via class I terpene cyclization (Figure 2a). To date, two fusicoccadiene synthases have been

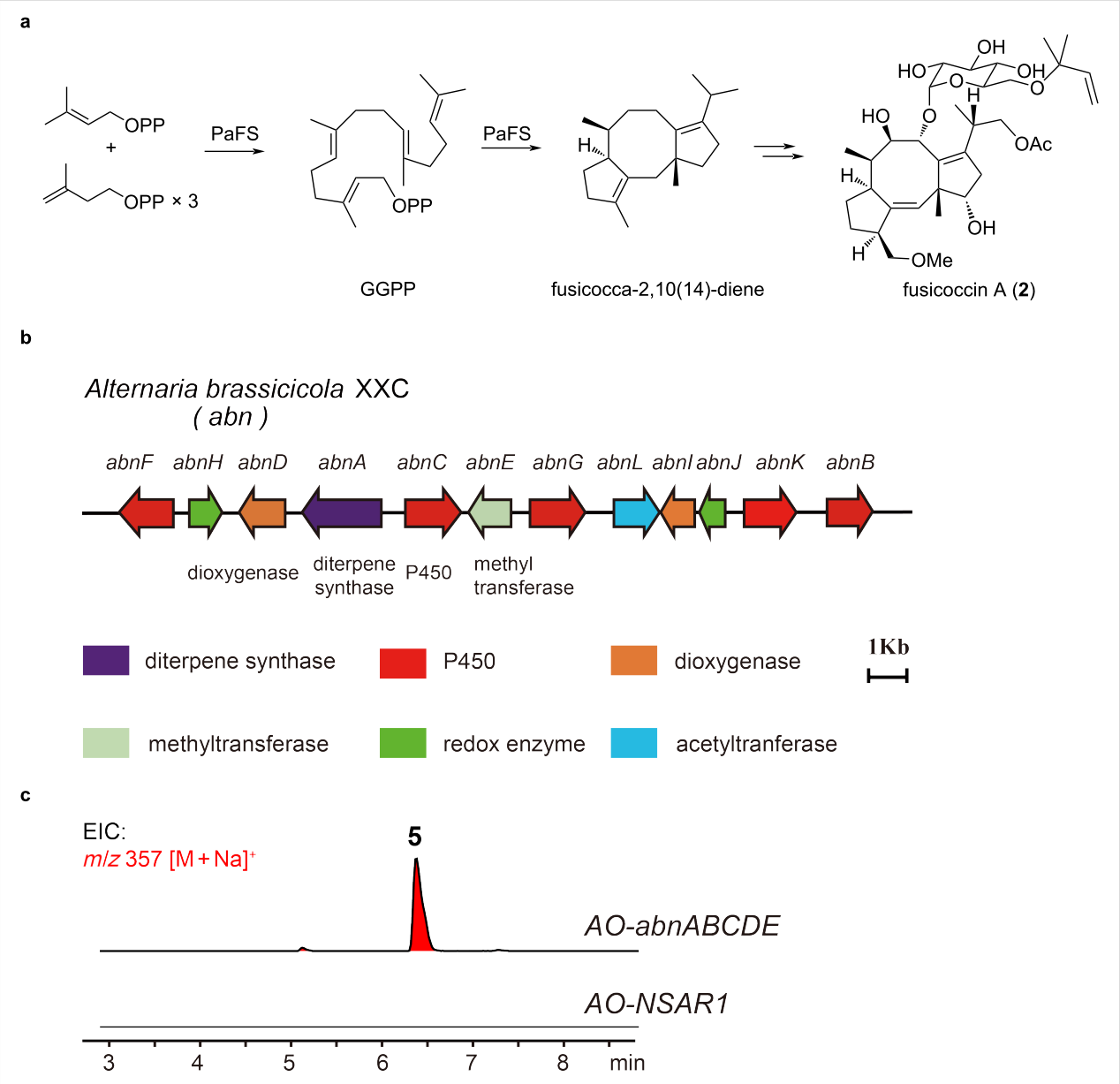

Figure 2: Heterologous production of brassicicene I in an engineered *A. oryzae* strain. (a) Biosynthesis of fusicoccin A in *Phomopsis (Fusicoccum) amygdali*. (b) Brassicicene BGC in *A. brassicicola* XXC. (c) Heterologous production of brassicicene I (**5**) in an engineered AO strain.

identified by the analysis of the brassicicene biosynthesis-related gene cluster (BGC) in *Alternaria brassicicola* and *Pseudocercospora fijiensis* [34,35]. The 5-8-5 tricyclic scaffold is transformed into various fusicoccane natural products catalyzed by P450s, dioxygenases, dehydrogenases, and reductases. Therefore, we propose to harness the biosynthetic pathway for brassicicenes, which share the same carbon skeleton and similar oxidation and unsaturation states as cotylenol and cotylenin A [36]. In a previous study, Oikawa and co-workers reported the identification of brassicicene BGC in *Pseudocercospora fijiensis* [37]. By heterologous expression of this BGC in *Aspergillus oryzae*, brassicicene I was produced by the transformant *AO-bscABCDE* at a titer of 5.5 mg/L. Recently, we identified a new BGC for brassicicenes, namely, *abn*, from the brassicicene-producing strain *A. brassicicola* XXC (Figure 2b) [38]. We constructed an *A. oryzae* strain with the homologous gene *abnABCDE*. As expected, compound **5** was produced at a titer of 8 mg/L (Figure 2c). By co-fermenting with Amberlite XAD-16, an enhanced yield of 30 mg/L was achieved, thus allowing further transformation into other natural products.

We next carried out the formal synthesis of cotylenin A and cotylenol (Figure 3a). Oxidation of brassicicene I with Dess–Martin reagent afforded intermediate **9** in 92% yield. The

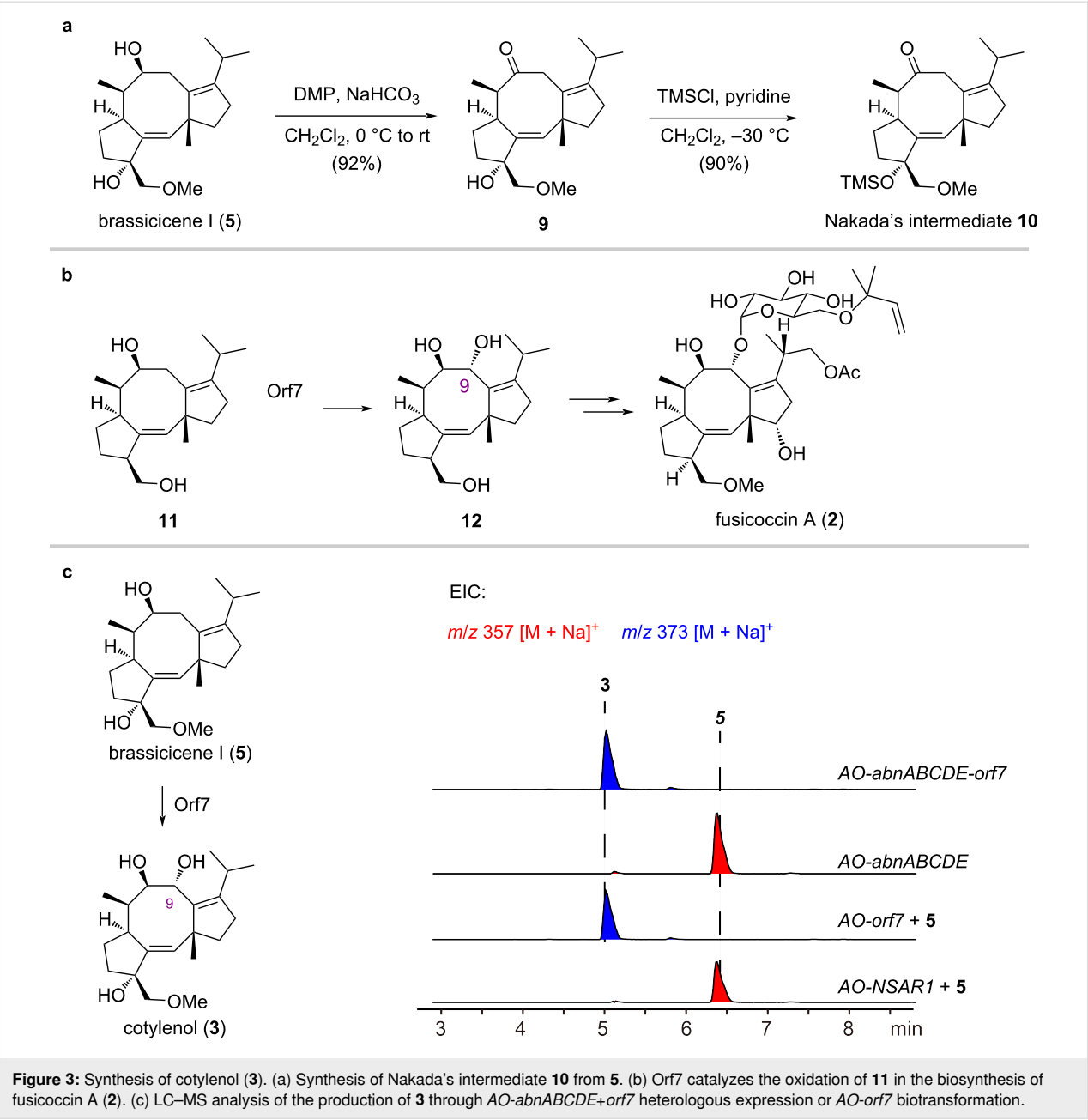

Figure 3: Synthesis of cotylenol (**3**). (a) Synthesis of Nakada's intermediate **10** from **5**. (b) Orf7 catalyzes the oxidation of **11** in the biosynthesis of fusicoccin A (**2**). (c) LC–MS analysis of the production of **3** through *AO-abnABCDE+orf7* heterologous expression or *AO-orf7* biotransformation.

tertiary hydroxy group of compound **9** was further protected with a TMS group to provide compound **10** in 90% yield, a key intermediate in the synthesis of cotylenol and cotylenin A by Nakada and co-workers [21]. However, installing the C9 hydroxy group requires the use of stoichiometric MoOPH [39], which raises toxicity and safety issues. Therefore, we sought an enzymatic method to selectively oxidize **5** at the C9 position. Dairi and co-workers reported that Orf7 oxidizes compound **11** at the C9 position in the biosynthesis of fusicoccin A (Figure 3b) [40]. Given the structural similarities between compound **5** and compound **11**, we hypothesized that Orf7 might also catalyze the hydroxylation of compound **5** at C9. Hence, we fed an *A. oryzae* strain that expressed the *orf7* gene with compound **5**. To our delight, compound **3** was obtained successfully (Figure 3c). To stably produce **3** by fermentation, we constructed an *A. oryzae* strain that integrates *abnABCDE* with *orf7*, achieving a yield of 60 mg/kg rice through rice fermentation.

We next targeted alterbrassicicene E (**6**), brassicicenes A (**7**) and R (**8**) (Scheme 1). The secondary hydroxy group of brassicicene I was selectively TBS-protected in the presence of TBSOTf and 2,6-lutidine to give compound **13** in 93% yield. Then, compound **13** underwent oxidative rearrangement with

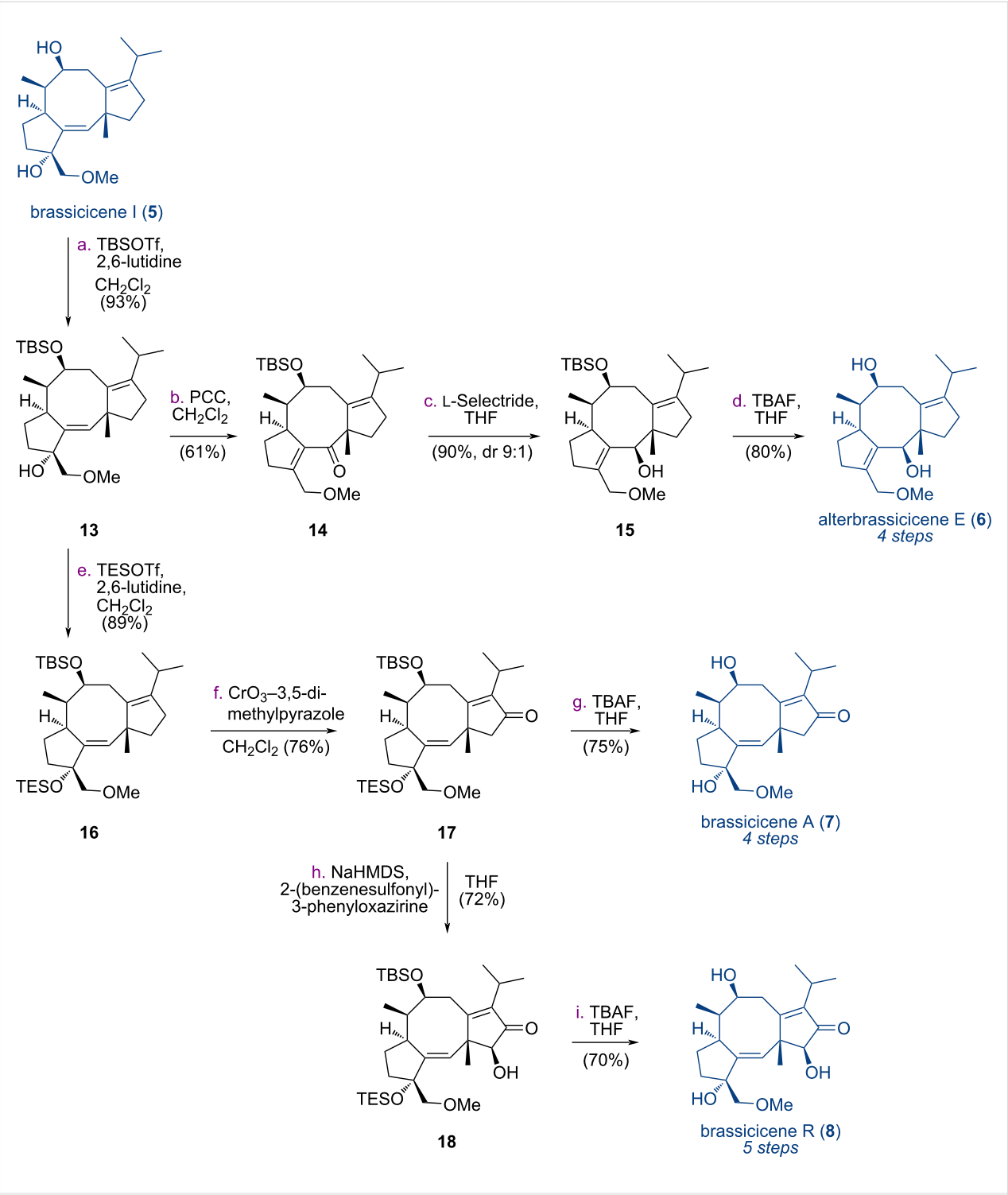

Scheme 1: Synthesis of alterbrassicicene E (**6**) and brassicicenes A (**7**) and R (**8**) from brassicicene I (**5**).

PCC to afford ketone **14** in 61% yield. Under Luche reduction conditions, compound **15** and its diastereomer were obtained in a total yield of 90% at a ratio of 1:0.7. To improve the diastereoselectivity, we examined other reduction conditions and found that L-Selectride afforded compound **15** in 90% yield with a dr of 9:1. Upon desilylation with TBAF, compound **15** was converted into alterbrassicicene E (**6**) in 80% yield. To synthesize brassicicenes A (**7**) and R (**8**), the tertiary hydroxy group of compound **13** was protected with a TES group to furnish compound **16** in 89% yield. By screening several condi-

tions, we found that allylic oxidation of compound **16** could be achieved in the presence of chromium trioxide–3,5-dimethylpyrazole complex [41] to provide compound **17** in 76% yield. After deprotection of the TBS and TES groups with TBAF, brassicicene A (**7**) was obtained in 75% yield. Compound **17** was subjected to α-hydroxylation from the less-hindered convex face using Davis's oxaziridine [25], furnishing intermediate **18** in 72% yield. After deprotection of the TBS and TES groups, brassicicene R (**8**) was obtained in 70% yield. Therefore, alterbrassicicene E (**6**) and brassicicenes A (**7**) and R (**8**) were synthesized from brassicicene I over 4 or 5 chemical steps.

Conclusion

In summary, the diverse biological activities and complex structures of fusicoccane diterpenoids have stimulated multiple elegant chemical syntheses. In contrast to these approaches, we harnessed the biosynthetic machinery of brassicicenes to produce brassicicene I in an engineered *A. oryzae* strain. Brassicicene I was further oxidized by a cytochrome P450 from the biosynthesis of fusicoccin A, thus leading to total biosynthesis of cotylenol in *A. oryzae*. Three fusicoccane diterpenoids, including alterbrassicicene E and brassicicenes A and R, were efficiently synthesized from brassicicene I in 4 or 5 chemical steps. This work lays the foundation for the preparation of fusicoccane natural products and exploration of their biological activities.

Supporting Information

Supporting Information File 1

Experimental data and copies of spectra.
[https://www.beilstein-journals.org/bjoc/content/supplementary/1860-5397-21-111-S1.pdf]

Acknowledgements

The authors thank Medical sub-center of analytical and testing center, Huazhong University of Science and Technology for measuring NMR spectroscopic data. The authors are very grateful to Professor Hideaki Oikawa (Hokkaido University, Sapporo, Japan) for providing *A. oryzae* NSAR1 heterologous expression system.

Funding

This work was financially supported by the National Key R&D Program of China (2021YFA0910500), the National Natural Science Foundation of China (22277035, 32000045, and 81973205), the Program for the National Natural Science Foundation for Distinguished Young Scholars (81725021), the Innovative Research Groups of the National Natural Science Foundation of China (81721005), the Fundamental Research Funds for the Central Universities (2020kfyXJJS083), the Sino-German Center for Research Promotion (M-0477), Key-Area Research and Development Program of Guangdong Province (2020B0303070002) and Shenzhen Science and Technology Program (KQTD20170330155106581).

ORCID® iDs

Zheng Xiang - https://orcid.org/0000-0003-2925-842X

Data Availability Statement

All data that supports the findings of this study is available in the published article and/or the supporting information of this article.

Preprint

A non-peer-reviewed version of this article has been previously published as a preprint: doi:10.26434/chemrxiv-2024-d4lpr

References

1. de Boer, A. H.; de Vries-van Leeuwen, I. J. *Trends Plant Sci.* **2012,** *17,* 360–368. doi:10.1016/j.tplants.2012.02.007
2. Ballio, A.; Chain, E. B.; De Leo, P.; Erlanger, B. F.; Mauri, M.; Tonolo, A. *Nature* **1964,** *203,* 297. doi:10.1038/203297a0
3. Sassa, T. *Agric. Biol. Chem.* **1971,** *35,* 1415–1418. doi:10.1271/bbb1961.35.1415
4. Sassa, T.; Ooi, T.; Nukina, M.; Ikeda, M.; Kato, N. *Biosci., Biotechnol., Biochem.* **1998,** *62,* 1815–1818. doi:10.1271/bbb.62.1815
5. Tang, Y.; Xue, Y.; Du, G.; Wang, J.; Liu, J.; Sun, B.; Li, X.-N.; Yao, G.; Luo, Z.; Zhang, Y. *Angew. Chem., Int. Ed.* **2016,** *55,* 4069–4073. doi:10.1002/anie.201600313
6. Li, F.; Lin, S.; Zhang, S.; Pan, L.; Chai, C.; Su, J.-C.; Yang, B.; Liu, J.; Wang, J.; Hu, Z.; Zhang, Y. *J. Nat. Prod.* **2020,** *83,* 1931–1938. doi:10.1021/acs.jnatprod.0c00165
7. Zhou, P.; Zhang, X.; Dai, C.; Yan, S.; Wei, M.; Feng, W.; Li, Q.; Liu, J.; Zhu, H.; Hu, Z.; Chen, C.; Zhang, Y. *J. Org. Chem.* **2022,** *87,* 7333–7341. doi:10.1021/acs.joc.2c00528
8. Ohkanda, J. *Chem. Lett.* **2021,** *50,* 57–67. doi:10.1246/cl.200670
9. Sengupta, A.; Liriano, J.; Bienkiewicz, E. A.; Miller, B. G.; Frederich, J. H. *ACS Omega* **2020,** *5,* 25029–25035. doi:10.1021/acsomega.0c01454
10. Molzan, M.; Kasper, S.; Röglin, L.; Skwarczynska, M.; Sassa, T.; Inoue, T.; Breitenbuecher, F.; Ohkanda, J.; Kato, N.; Schuler, M.; Ottmann, C. *ACS Chem. Biol.* **2013,** *8,* 1869–1875. doi:10.1021/cb4003464
11. Zheng, D.; Han, L.; Qu, X.; Chen, X.; Zhong, J.; Bi, X.; Liu, J.; Jiang, Y.; Jiang, C.; Huang, X. *J. Nat. Prod.* **2017,** *80,* 837–844. doi:10.1021/acs.jnatprod.6b00676
12. Kim, S.; Shin, D.-S.; Lee, T.; Oh, K.-B. *J. Nat. Prod.* **2004,** *67,* 448–450. doi:10.1021/np030384h
13. Asahi, K.-i.; Honma, Y.; Hazeki, K.; Sassa, T.; Kubohara, Y.; Sakurai, A.; Takahashi, N. *Biochem. Biophys. Res. Commun.* **1997,** *238,* 758–763. doi:10.1006/bbrc.1997.7385
14. Honma, Y.; Kasukabe, T.; Yamori, T.; Kato, N.; Sassa, T. *Gynecol. Oncol.* **2005,** *99,* 680–688. doi:10.1016/j.ygyno.2005.07.015

15. de Vries-van Leeuwen, I. J.; Kortekaas-Thijssen, C.; Nzigou Mandouckou, J. A.; Kas, S.; Evidente, A.; de Boer, A. H. *Cancer Lett.* **2010,** *293,* 198–206. doi:10.1016/j.canlet.2010.01.009
16. Kasukabe, T.; Okabe-Kado, J.; Honma, Y. *Cancer Sci.* **2008,** *99,* 1693–1698. doi:10.1111/j.1349-7006.2008.00867.x
17. Ono, Y.; Minami, A.; Noike, M.; Higuchi, Y.; Toyomasu, T.; Sassa, T.; Kato, N.; Dairi, T. *J. Am. Chem. Soc.* **2011,** *133,* 2548–2555. doi:10.1021/ja107785u
18. Liu, Y.; Hong, R. *Cell Rep. Phys. Sci.* **2024,** *5,* 102141. doi:10.1016/j.xcrp.2024.102141
19. Kato, N.; Okamoto, H.; Takeshita, H. *Tetrahedron* **1996,** *52,* 3921–3932. doi:10.1016/s0040-4020(96)00059-2
20. Williams, D. R.; Robinson, L. A.; Nevill, C. R.; Reddy, J. P. *Angew. Chem., Int. Ed.* **2007,** *46,* 915–918. doi:10.1002/anie.200603853
21. Uwamori, M.; Osada, R.; Sugiyama, R.; Nagatani, K.; Nakada, M. *J. Am. Chem. Soc.* **2020,** *142,* 5556–5561. doi:10.1021/jacs.0c01774
22. Chen, B.; Wu, Q.; Xu, D.; Zhang, X.; Ding, Y.; Bao, S.; Zhang, X.; Wang, L.; Chen, Y. *Angew. Chem., Int. Ed.* **2022,** *61,* e202117476. doi:10.1002/anie.202117476
23. Wang, Y.-Q.; Xu, K.; Min, L.; Li, C.-C. *J. Am. Chem. Soc.* **2022,** *144,* 10162–10167. doi:10.1021/jacs.2c04633
24. Sims, N. J.; Bonnet, W. C.; Lawson, D. M.; Wood, J. L. *J. Am. Chem. Soc.* **2023,** *145,* 37–40. doi:10.1021/jacs.2c12275
25. Chen, B.; Yang, Y.; Zhang, X.; Xu, D.; Sun, Y.; Chen, Y.; Wang, L. *Org. Lett.* **2023,** *25,* 8570–8574. doi:10.1021/acs.orglett.3c03355
26. Xie, S.; Chen, Y.; Zhang, Y.; Zhang, Z.; Hu, X.; Yan, C.; Xu, J. *Cell Rep. Phys. Sci.* **2024,** *5,* 101855. doi:10.1016/j.xcrp.2024.101855
27. Inoue, T.; Higuchi, Y.; Yoneyama, T.; Lin, B.; Nunomura, K.; Honma, Y.; Kato, N. *Bioorg. Med. Chem. Lett.* **2018,** *28,* 646–650. doi:10.1016/j.bmcl.2018.01.030
28. Ohkanda, J.; Kusumoto, A.; Punzalan, L.; Masuda, R.; Wang, C.; Parvatkar, P.; Akase, D.; Aida, M.; Uesugi, M.; Higuchi, Y.; Kato, N. *Chem. – Eur. J.* **2018,** *24,* 16066–16071. doi:10.1002/chem.201804428
29. Jiang, Y.; Renata, H. *Nat. Chem.* **2024,** *16,* 1531–1538. doi:10.1038/s41557-024-01533-w
30. You, Y.; Zhang, X.-J.; Xiao, W.; Kunthic, T.; Xiang, Z.; Xu, C. *Chem. Sci.* **2024,** *15,* 19307–19314. doi:10.1039/d4sc06060a
31. Xiao, W.; Wang, S.-J.; Yu, M.-Z.; Zhang, X.-J.; Xiang, Z. *Org. Biomol. Chem.* **2023,** *21,* 5527–5531. doi:10.1039/d3ob00206c
32. Mou, S.-B.; Xiao, W.; Wang, H.-Q.; Chen, K.-Y.; Xiang, Z. *Org. Lett.* **2021,** *23,* 400–404. doi:10.1021/acs.orglett.0c03894
33. Mou, S.-B.; Xiao, W.; Wang, H.-Q.; Wang, S.-J.; Xiang, Z. *Org. Lett.* **2020,** *22,* 1976–1979. doi:10.1021/acs.orglett.0c00325
34. Toyomasu, T.; Tsukahara, M.; Kaneko, A.; Niida, R.; Mitsuhashi, W.; Dairi, T.; Kato, N.; Sassa, T. *Proc. Natl. Acad. Sci. U. S. A.* **2007,** *104,* 3084–3088. doi:10.1073/pnas.0608426104
35. Minami, A.; Tajima, N.; Higuchi, Y.; Toyomasu, T.; Sassa, T.; Kato, N.; Dairi, T. *Bioorg. Med. Chem. Lett.* **2009,** *19,* 870–874. doi:10.1016/j.bmcl.2008.11.108
36. Guan, Z.; Yao, N.; Yuan, W.; Li, F.; Xiao, Y.; Rehmutulla, M.; Xie, Y.; Chen, C.; Zhu, H.; Zhou, Y.; Tong, Q.; Xiang, Z.; Ye, Y.; Zhang, Y. *Chem. Sci.* **2025,** *16,* 867–875. doi:10.1039/d4sc05963h
In parallel, we identified a biosynthetic pathway for cotylenol, cotylenins, from Talaromyces adpressus.
37. Tazawa, A.; Ye, Y.; Ozaki, T.; Liu, C.; Ogasawara, Y.; Dairi, T.; Higuchi, Y.; Kato, N.; Gomi, K.; Minami, A.; Oikawa, H. *Org. Lett.* **2018,** *20,* 6178–6182. doi:10.1021/acs.orglett.8b02654
38. Yuan, W.; Li, F.; Chen, Z.; Xu, Q.; Guan, Z.; Yao, N.; Hu, Z.; Liu, J.; Zhou, Y.; Ye, Y.; Zhang, Y. *Chin. Chem. Lett.* **2024,** *35,* 108788. doi:10.1016/j.cclet.2023.108788
39. Vedejs, E.; Engler, D. A.; Telschow, J. E. *J. Org. Chem.* **1978,** *43,* 188–196. doi:10.1021/jo00396a002
40. Noike, M.; Ono, Y.; Araki, Y.; Tanio, R.; Higuchi, Y.; Nitta, H.; Hamano, Y.; Toyomasu, T.; Sassa, T.; Kato, N.; Dairi, T. *PLoS One* **2012,** *7,* e42090. doi:10.1371/journal.pone.0042090
41. Salmond, W. G.; Barta, M. A.; Havens, J. L. *J. Org. Chem.* **1978,** *43,* 2057–2059. doi:10.1021/jo00404a049

License and Terms

BEILSTEIN JOURNAL OF ORGANIC CHEMISTRY

Chemical synthesis of glycan motifs from the antitumor agent PI-88 through an orthogonal one-pot glycosylation strategy

Shaokang Yang[1,2], Xingchun Sun[1,2], Hanyingzi Fan[2] and Guozhi Xiao[*2]

Full Research Paper

Open Access

Address:
[1]School of Chemistry and Chemical Engineering, Shaanxi Normal University, Xi'an, Shaanxi 710119, China and [2]State Key Laboratory of Phytochemistry and Natural Medicines, Kunming Institute of Botany, University of Chinese Academy of Sciences, Chinese Academy of Sciences, Kunming 650201, China

Email:
Guozhi Xiao[*] - xiaoguozhi@mail.kib.ac.cn

* Corresponding author

Keywords:
carbohydrates; chemical synthesis; glycosyl *ortho*-(1-phenylvinyl)benzoates; one-pot glycosylation; PI-88

Beilstein J. Org. Chem. **2025,** *21,* 1587–1594.
https://doi.org/10.3762/bjoc.21.122

Received: 26 June 2025
Accepted: 01 August 2025
Published: 06 August 2025

This article is part of the thematic issue "Concept-driven strategies in target-oriented synthesis".

Associate Editor: D. Y.-K. Chen

Abstract

Chemical synthesis of monophosphorylated glycan motifs from the antitumor agent PI-88 has been achieved through an orthogonal one-pot glycosylation strategy on the basis of glycosyl *ortho*-(1-phenylvinyl)benzoates, which not only accelerated synthesis, but also precluded the potential issues inherent to one-pot glycan assembly associated with thioglycosides. The following aspects were featured in synthetic approaches: 1) synthesis of trisaccharide and tetrasaccharide PI-88 glycans via [1 + 1 + 1] and [1 + 1 + 1 + 1] one-pot orthogonal glycosylation, respectively; 2) synthesis of PI-88 glycan motif pentasaccharide via [1 + 1 + 1] and [1 + 1 + 3] one-pot orthogonal glycosylation; 3) synthesis of hexasaccharide via [1 + 1 + 1] and [1 + 1 + 1 + 3] one-pot assembly.

Introduction

Carbohydrates as one of four essential biomolecules have been widely recognized as important targets for the development of carbohydrate-based therapeutics [1-18]. The example in point is the antitumor agent PI-88 (muparfostat), which retards tumor growth via inhibiting angiogenesis in two ways: 1) interaction with pro-angiogenic growth factors such as vascular endothelial growth factor (VEGF) and fibroblast growth factor (FGF) and 2) by prevention of the release of angiogenic growth factors from the extracellular matrix (ECM) via inhibition of heparanase [19-22]. PI-88 is a complex mixture of monophosphorylated, highly sulfated mannose glycans derived from the extracellular phosphomannan of *Pichia holstii* NRRL Y-2448 yeast [23-25], which had progressed to phase III clinical trials for post-resection hepatocellular carcinoma [26]. Interestingly, Ferro and co-workers revised the structure of PI-88 to **I** and **II** in 2017 via successful separation of oligosaccharide phosphate fractions by preparative ion-exchange chromatography (Scheme 1A) [27]. Besides the major components α(1→3)/

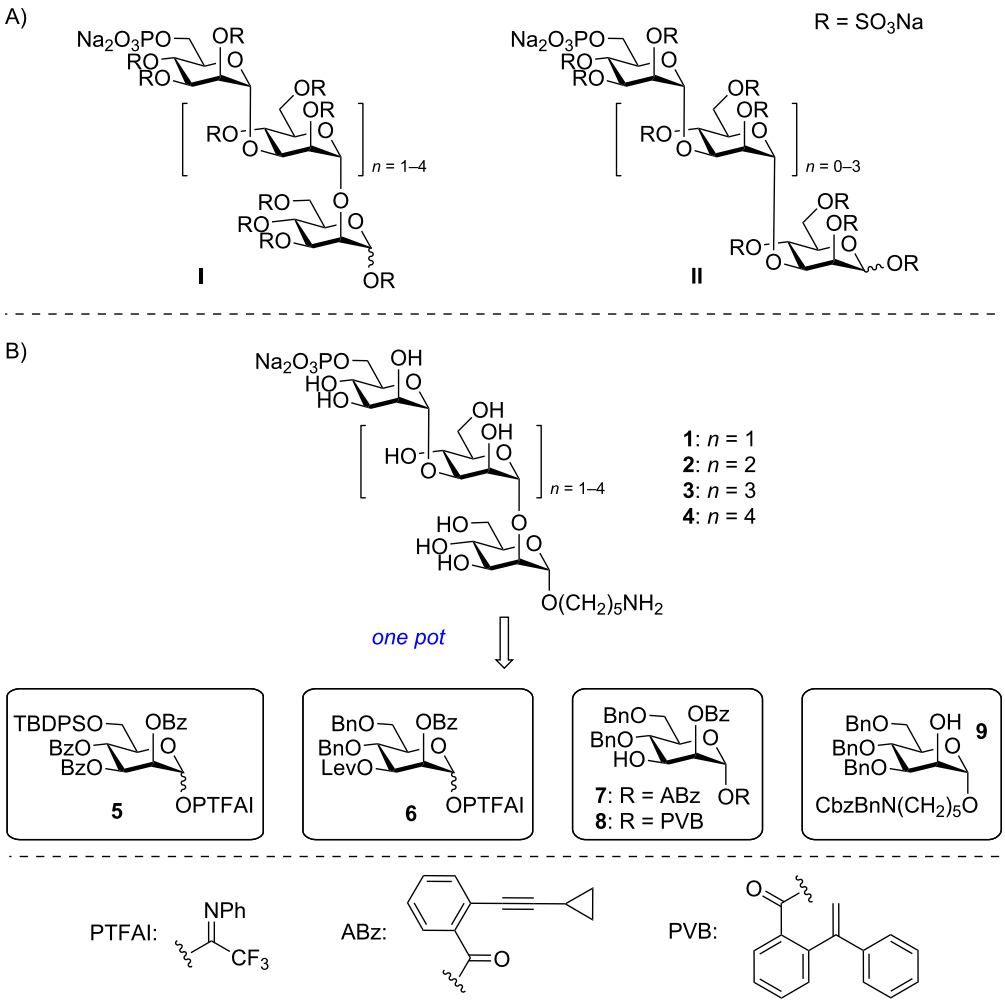

Scheme 1: (A) Glycan structures of PI-88 and (B) retrosynthetic analysis of PI-88 glycan motifs **1**–**4**.

α(1→2)-linked pentasaccharide (≈60%) and tetrasaccharide (≈30%) in **I**, the minor components of all α(1→3)-linked mannosides were also present in **II**.

During the past two decades, several strategies have been developed to synthesize glycan motifs from PI-88 [28-36]. In comparison with previous, traditional, and time-consuming synthesis of PI-88 glycan components, the one-pot glycan assembly strategy has some advantages, including: 1) acceleration of glycan synthesis, 2) avoidance of purification of intermediates during glycosylation intervals, and 3) reduction of chemical waste [37-42]. Recently, we introduced a new one-pot glycosylation strategy on the basis of recently developed glycosyl *ortho*-(1-phenylvinyl)benzoate (PVB) [43-45] donors from our group, which has been successfully applied to the streamline synthesis of various glycans from oligosaccharides to polysaccharides such as mannose-capped lipoarabinomannan motifs up to 101-mer from the *Mycobacterium tuberculosis* cell wall, nonadecasaccharide motif from *Ganoderma sinense*, and tridesaccharide motif from *Bacteroides vulgatus* lipopolysaccharides [46-56]. Here, we report the chemical synthesis of monophosphorylated glycan motifs **1**–**4** from PI-88 through an orthogonal one-pot glycosylation strategy via strategic combinations of glycosyl *N*-phenyltrifluoroacetimidates (PTFAI) [57,58], glycosyl *ortho*-(alkynylbenzoates) [59,60] (ABz), and glycosyl PVB, which precluded the potential issues inherent to one-pot glycosylation based on thioglycosides such as aglycone transfer [43-45,61].

Results and Discussion

Retrosynthetic analysis

Retrosynthetically, we envisaged that glycans **1**–**4** could be derived from monosaccharide building blocks Man PTFAI **5** and **6**, Man ABz **7**, Man PVB **8**, and Man **9** through orthogonal one-pot glycosylation strategy (Scheme 1B). The 2-*O*-Bz group in **5**–**8** served as the neighboring participating group for the

stereoselective construction of 1,2-*trans*-mannosidic bonds, while the 3-*O*-Lev group in **6** was the temporary protecting group for (1→3)-branching. The C6–OH group in **5** was protected as TBDPS group, which could be selectively replaced by the destined phosphate residue.

One-pot synthesis of glycans **1** and **2**

We commenced with the synthesis of monophosphorylated trisaccharide **1** (Scheme 2A). Glycosylation of mannosyl PTFAI **5** (1.2 equiv) with 3-OH in mannosyl PVB **8** (1.0 equiv) in the presence of TMSOTf as catalyst proceeded smoothly at 0 °C to room temperature, affording the α-Man-(1→3)-Man PVB disaccharide. The further coupling of the above PVB disaccharide with the poorly reactive 2-OH in mannoside **9** (0.9 equiv) under activation with NIS and TMSOTf at 0 °C to room temperature, successfully furnished the desired α-Man-(1→3)-α-Man-(1→3)-α-Man trisaccharide **10** in 87% yield in a one pot manner. Removal of TBDPS group in **10** with 70% HF·pyridine and subsequent phosphitylation of the resulting free alcohol with phosphoramidite **11** provided the desired phosphite, which was further oxidized by 3-chloroperoxybenzoic aicd (mCPBA) at −78 °C to 0 °C, producing the desired phosphorylated fully protected trisaccharide **12** in 79% overall yield over three steps. Removal of all protecting groups in trisaccharide **12** is a challenging task due to the presence of polar groups, including phosphoryl acid and amine groups [62]. After several optimizations, the following sequence was adopted to remove all Bn, Bz, and Cbz groups: 1) global hydrogenolysis of Bn and Cbz groups in **12** with $Pd(OH)_2$/C in a mixed solvent (THF/MeOH/AcOH/H_2O) and 2) saponification of all Bz groups with 1 M NaOH (dioxane/MeOH/H_2O, room temperature). The monophosphorylated trisaccharide **1** was obtained in 60% overall yield over two steps from **12** after purification over a Sephadex^{TM} LH-20 column. It was noted that the switch of deprotection sequences (first Bz groups, second Bn and Cbz groups) failed to efficiently produce trisaccharide **1**.

The synthesis of monophosphorylated tetrasaccharide **2** was next investigated (Scheme 2B). TMSOTf was used to activate Man PTFAI **5** (1.1 equiv) in the presence of mannosyl ABz **7** (1.0 equiv) at 0 °C to room temperature, readily producing the α-Man-(1→3)-Man ABz disaccharide. Yu glycosylation of the above ABz disaccharide with 3-OH in Man PVB **8** (0.9 equiv) under the catalysis of PhP_3AuOTf at room temperature successfully gave α-Man-(1→3)-α-Man-(1→3)-Man PVB trisaccharide, which was further coupled with the poorly reactive C2–OH in mannoside **9** (0.8 equiv) in the presence of NIS and TMSOTf at 0 °C to rt, uneventfully furnishing the desired tetrasaccharide α-Man-(1→3)-α-Man-(1→3)-α-Man-(1→2)-α-Man **13** in 69% yield in the same flask. The TBDPS-protected **13** was readily converted to phosphorylated protected tetrasaccharide **14** in 89% ovall yield over the following steps: 1) deprotection of the TBDPS group, 2) phosphitylation of the free alcohol with phosphoramidite **11** in the presence of 1*H*-tetrazole and 4 Å MS, and 3) oxidation of the phosphite by mCPBA. Hydrogenolysis of Bn and Cbz groups in **14** with $Pd(OH)_2$/C and subsequent saponification of all Bz groups with 1 M NaOH successfully produced monophosphorylated tetrasaccharide **2** in 63% overall yield.

One-pot synthesis of glycans **3** and **4**

Furthermore, we investigated the synthesis of monophosphorylated pentasaccharide **3** (Scheme 3). Orthogonal one-pot glycosylation of Man PTFAI **6** (1.2 equiv), Man PVB **8** (1.0 equiv), and mannoside **9** (0.9 equiv) readily generated α-Man-(1→3)-α-Man-(1→2)-α-Man trisaccharide **15** with 86% yield in one pot. The further sequential [1 + 1 + 3] one-pot orthogonal glycosylation of Man PTFAI **5** (1.1 equiv), Man PVB **8** (1.0 equiv), and trisaccharide **16** (0.9 equiv) derived from **15** via selective removal of the Lev group with $NH_2NH_2{\cdot}H_2O$ successfully generated the desired pentasaccharide α-Man-(1→3)-α-Man-(1→3)-α-Man -(1→3)-α-Man-(1→2)-α-Man **17** in 83% yield in a one-pot manner, which was readily converted to the phosphorylated protected pentasaccharide **18** in 92% overall yield via the switch of the TBDPS group with the phosphate group. First global deprotection of Bn and Cbz groups in **18** with $Pd(OH)_2$/C, followed by saponifications of all Bz groups with 1 M NaOH provided the desired monophosphorylated pentasaccharide **3** in 56% overall yield, which is the major glycan motif from PI-88.

Finally, the synthesis of the monophosphorylated hexasaccharide **4** was studied (Scheme 4). Orthogonal one-pot coupling of Man PTFAI **5** (1.1 equiv), Man ABz **7** (1.0 equiv), PVB **8** (0.9 equiv), and α-Man-(1→3)-α-Man-(1→2)-α-Man trisaccharide **16** (0.8 equiv) proceeded uneventfully, successfully producing the desired α-Man-(1→3)-α-Man-(1→3)-α-Man-(1→3)-α-Man-(1→3)-α-Man-(1→3)-α-Man-(1→2)-α-Man hexasaccharide **19** in 66% yield in the same flask. The TBDPS group in **19** was readily converted to a phosphate group in **20** with 88% overall yield over three steps. The desired monophosphorylated hexasaccharide **4** was obtained in 60% overall yield from **20** via sequential global deprotection of the Bn, Cbz, and Bz groups.

The structures of the synthetic glycan motifs **1**–**4** were supported by their ^1H and ^{13}C NMR spectra and MALDI–TOF as well as ESI mass spectra. In particular, the anomeric proton signals of **1**–**4** were highlighted in the ^1H NMR spectra of synthetic glycans motifs **1**–**4** (see Supporting Information File 1).

Conclusion

In summary, the monophosphorylated glycan motifs **1**–**4** from PI-88 have been collectively synthesized via a one-pot orthogo-

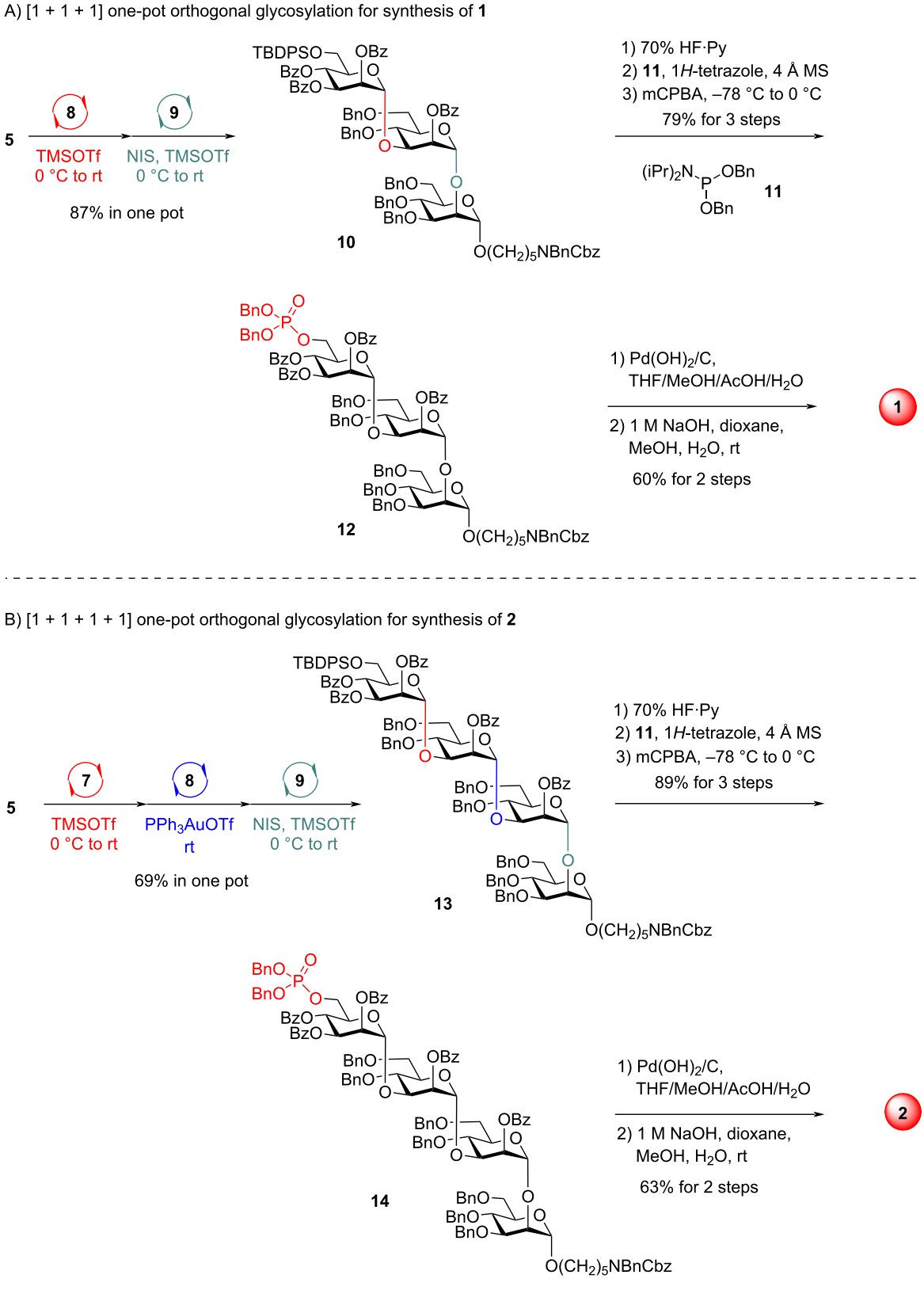

Scheme 2: One-pot synthesis of glycans **1** and **2**.

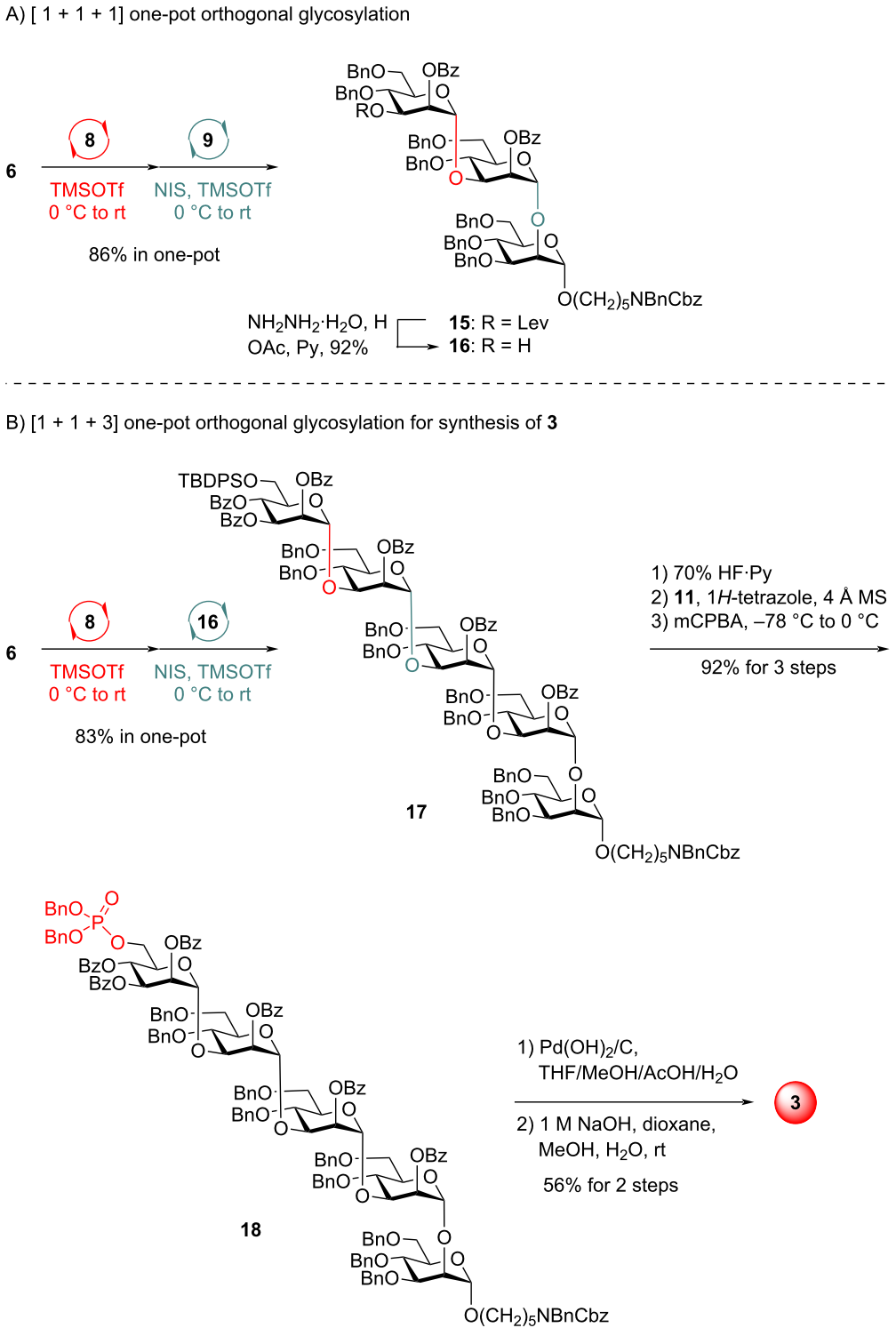

Scheme 3: One-pot synthesis of glycan **3**.

nal glycosylation strategy on the basis of glycosyl PVB, which avoids such issues as aglycon transfer inherent to one-pot glycosylations based on thioglycosides. Specifically, the following features were highlighted in our synthetic approach: 1) [1 + 1 + 1] one-pot orthogonal glycosylation for the synthesis of trisaccharide **1**; 2) [1 + 1 + 1 + 1] orthogonal one-pot

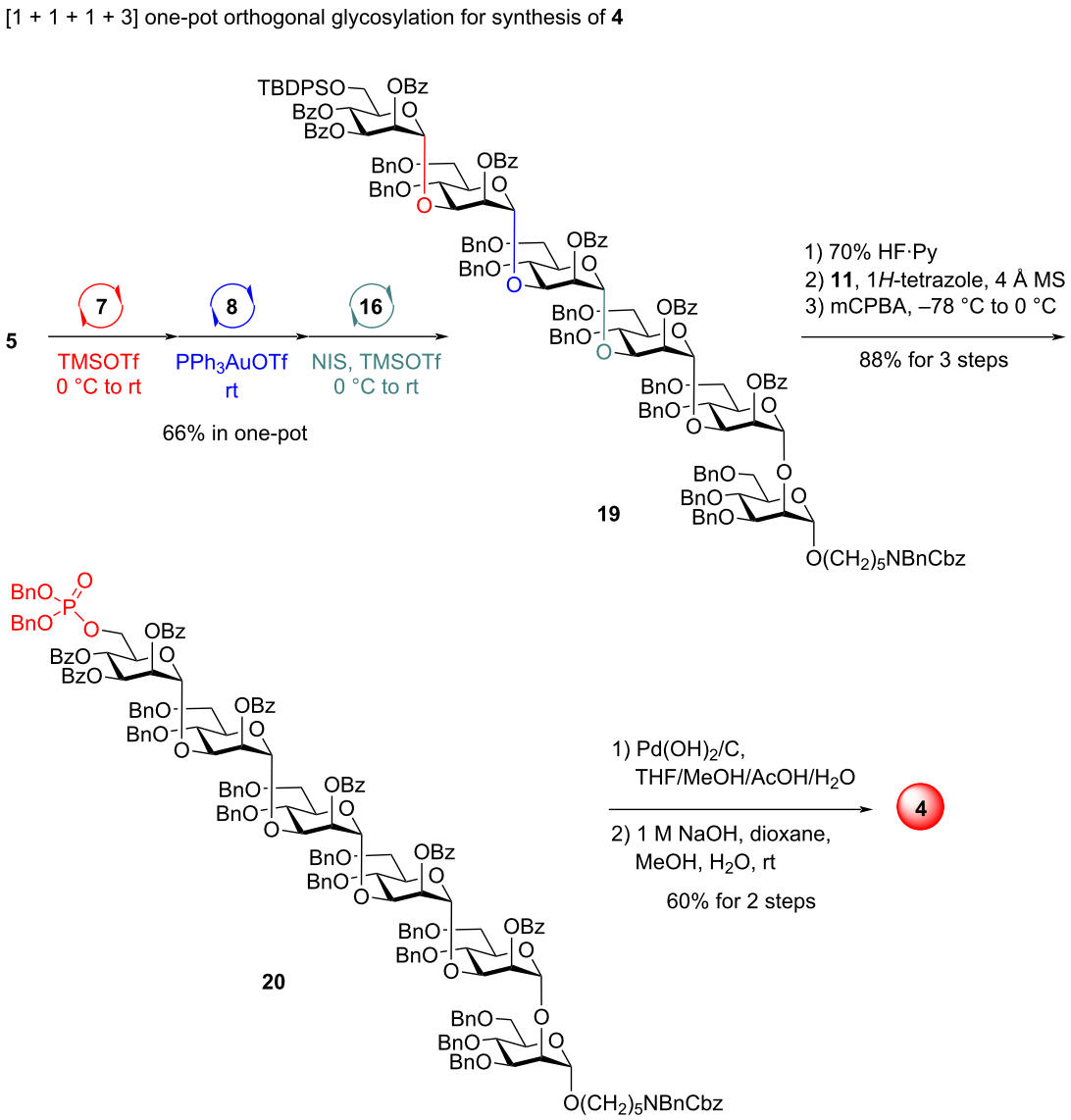

Scheme 4: One-pot synthesis of glycan **4**.

glycosylation for the synthesis of tetrasaccharide **2**; 3) [1 + 1 + 1] and [1 + 1 + 3] orthogonal one-pot assembly of pentasaccharide **3**; 4) [1 + 1 + 1] and [1 + 1 + 1 + 3] orthogonal one-pot assembly of hexasaccharide **4**.

Supporting Information

Supporting Information File 1

Experimental procedures and spectral data for all new compounds including ^{1}H NMR, ^{13}C NMR, and HRMS.
[https://www.beilstein-journals.org/bjoc/content/supplementary/1860-5397-21-122-S1.pdf]

Funding

The financial support from the National Natural Science Foundations of China (22322110), the Yunnan Revitalization Talent Support Program: Yunling Scholar Project, the Yunnan Fundamental Research Projects (grant NO. 202501AV070010), the Young Talents Project of High-level Talent Introduction Program of Yunnan Province and the Yunnan Province Science and Technology Department (202305AH340005) are greatly acknowledged.

ORCID® iDs

Shaokang Yang - https://orcid.org/0000-0002-8953-9672
Guozhi Xiao - https://orcid.org/0000-0002-4724-4390

Data Availability Statement

All data that supports the findings of this study is available in the published article and/or the supporting information of this article

References

1. Ramadan, S.; Mayieka, M.; Pohl, N. L. B.; Liu, J.; Hsieh-Wilson, L. C.; Huang, X. *Curr. Opin. Chem. Biol.* **2024,** *80,* 102455. doi:10.1016/j.cbpa.2024.102455
2. Qin, C.; Tian, G.; Hu, J.; Zou, X.; Yin, J. *Curr. Opin. Chem. Biol.* **2024,** *78,* 102424. doi:10.1016/j.cbpa.2023.102424
3. Wang, X.; Xiao, G. *Curr. Opin. Chem. Biol.* **2023,** *77,* 102387. doi:10.1016/j.cbpa.2023.102387
4. Shang, W.; Niu, D. *Acc. Chem. Res.* **2023,** *56,* 2473–2488. doi:10.1021/acs.accounts.3c00374
5. Wang, S.; Yang, Y.; Zhu, Q.; Lin, G.-Q.; Yu, B. *Curr. Opin. Chem. Biol.* **2022,** *69,* 102154. doi:10.1016/j.cbpa.2022.102154
6. Del Bino, L.; Østerlid, K. E.; Wu, D.-Y.; Nonne, F.; Romano, M. R.; Codée, J.; Adamo, R. *Chem. Rev.* **2022,** *122,* 15672–15716. doi:10.1021/acs.chemrev.2c00021
7. Li, J.; Nguyen, H. M. *Acc. Chem. Res.* **2022,** *55,* 3738–3751. doi:10.1021/acs.accounts.2c00636
8. Di Lorenzo, F.; Duda, K. A.; Lanzetta, R.; Silipo, A.; De Castro, C.; Molinaro, A. *Chem. Rev.* **2022,** *122,* 15767–15821. doi:10.1021/acs.chemrev.0c01321
9. Seeberger, P. H. *Chem. Rev.* **2021,** *121,* 3598–3626. doi:10.1021/acs.chemrev.0c01210
10. Krasnova, L.; Wong, C.-H. *J. Am. Chem. Soc.* **2019,** *141,* 3735–3754. doi:10.1021/jacs.8b11005
11. Kulkarni, S. S.; Wang, C.-C.; Sabbavarapu, N. M.; Podilapu, A. R.; Liao, P.-H.; Hung, S.-C. *Chem. Rev.* **2018,** *118,* 8025–8104. doi:10.1021/acs.chemrev.8b00036
12. Bennett, C. S.; Galan, M. C. *Chem. Rev.* **2018,** *118,* 7931–7985. doi:10.1021/acs.chemrev.7b00731
13. Panza, M.; Pistorio, S. G.; Stine, K. J.; Demchenko, A. V. *Chem. Rev.* **2018,** *118,* 8105–8150. doi:10.1021/acs.chemrev.8b00051
14. Leng, W.-L.; Yao, H.; He, J.-X.; Liu, X.-W. *Acc. Chem. Res.* **2018,** *51,* 628–639. doi:10.1021/acs.accounts.7b00449
15. Peng, P.; Schmidt, R. R. *Acc. Chem. Res.* **2017,** *50,* 1171–1183. doi:10.1021/acs.accounts.6b00518
16. Danishefsky, S. J.; Shue, Y.-K.; Chang, M. N.; Wong, C.-H. *Acc. Chem. Res.* **2015,** *48,* 643–652. doi:10.1021/ar5004187
17. Astronomo, R. D.; Burton, D. R. *Nat. Rev. Drug Discovery* **2010,** *9,* 308–324. doi:10.1038/nrd3012
18. Boltje, T. J.; Buskas, T.; Boons, G.-J. *Nat. Chem.* **2009,** *1,* 611–622. doi:10.1038/nchem.399
19. Kudchadkar, R.; Gonzalez, R.; Lewis, K. D. *Expert Opin. Invest. Drugs* **2008,** *17,* 1769–1776. doi:10.1517/13543784.17.11.1769
20. Khachigian, L. M.; Parish, C. R. *Cardiovasc. Drug Rev.* **2004,** *22,* 1–6. doi:10.1111/j.1527-3466.2004.tb00127.x
21. Chhabra, M.; Ferro, V. PI-88 and Related Heparan Sulfate Mimetic**s**. *Heparanase;* Advances in Experimental Medicine and Biology, Vol. 1221; Springer: Cham, Switzerland, 2020; pp 473–491. doi:10.1007/978-3-030-34521-1_19
22. Ferro, V.; Dredge, K.; Liu, L.; Hammond, E.; Bytheway, I.; Li, C.; Johnstone, K.; Karoli, T.; Davis, K.; Copeman, E.; Gautam, A. *Semin. Thromb. Hemostasis* **2007,** *33,* 557–568. doi:10.1055/s-2007-982088
23. Ferro, V.; Fewings, K.; Palermo, M. C.; Li, C. *Carbohydr. Res.* **2001,** *332,* 183–189. doi:10.1016/s0008-6215(01)00061-1
24. Yu, G.; Gunay, N. S.; Linhardt, R. J.; Toida, T.; Fareed, J.; Hoppensteadt, D. A.; Shadid, H.; Ferro, V.; Li, C.; Fewings, K.; Palermo, M. C.; Podger, D. *Eur. J. Med. Chem.* **2002,** *37,* 783–791. doi:10.1016/s0223-5234(02)01347-8
25. Elli, S.; Stancanelli, E.; Handley, P. N.; Carroll, A.; Urso, E.; Guerrini, M.; Ferro, V. *Glycobiology* **2018,** *28,* 731–740. doi:10.1093/glycob/cwy068
26. Chen, P.-J.; Lee, P.-H.; Han, K.-H.; Fan, J.; Cheung, T. T.; Hu, R.-H.; Paik, S. W.; Lee, W.-C.; Chau, G.-Y.; Jeng, L.-B.; Wang, H. J.; Choi, J. Y.; Chen, C.-L.; Cho, M.; Ho, M.-C.; Wu, C.-C.; Lee, K. S.; Mao, Y.; Hu, F.-C.; Lai, K.-L. *Ann. Oncol.* **2017,** *28,* v213. doi:10.1093/annonc/mdx369.008
27. Handley, P. N.; Carroll, A.; Ferro, V. *Carbohydr. Res.* **2017,** *446-447,* 68–75. doi:10.1016/j.carres.2017.05.008
28. Ventura, J.; Uriel, C.; Gómez, A. M.; López, J. C. *Carbohydr. Res.* **2022,** *516,* 108557. doi:10.1016/j.carres.2022.108557
29. Mong, K.-K. T.; Shiau, K.-S.; Lin, Y. H.; Cheng, K.-C.; Lin, C.-H. *Org. Biomol. Chem.* **2015,** *13,* 11550–11560. doi:10.1039/c5ob01786f
30. Liu, L.; Johnstone, K. D.; Fairweather, J. K.; Dredge, K.; Ferro, V. *Aust. J. Chem.* **2009,** *62,* 546. doi:10.1071/ch09015
31. Valerio, S.; Pastore, A.; Adinolfi, M.; Iadonisi, A. *J. Org. Chem.* **2008,** *73,* 4496–4503. doi:10.1021/jo8003953
32. Fairweather, J. K.; Hammond, E.; Johnstone, K. D.; Ferro, V. *Bioorg. Med. Chem.* **2008,** *16,* 699–709. doi:10.1016/j.bmc.2007.10.044
33. Namme, R.; Mitsugi, T.; Takahashi, H.; Ikegami, S. *Tetrahedron Lett.* **2005,** *46,* 3033–3036. doi:10.1016/j.tetlet.2005.03.016
34. Gu, G.; Wei, G.; Du, Y. *Carbohydr. Res.* **2004,** *339,* 1155–1162. doi:10.1016/j.carres.2004.01.020
35. Fairweather, J. K.; Karoli, T.; Ferro, V. *Bioorg. Med. Chem.* **2004,** *12,* 6063–6075. doi:10.1016/j.bmc.2004.09.005
36. Zhou, J.; Lv, S.; Zhang, D.; Xia, F.; Hu, W. *J. Org. Chem.* **2017,** *82,* 2599–2621. doi:10.1021/acs.joc.6b03017
37. Hu, C.; Wu, S.; He, F.; Cai, D.; Xu, Z.; Ma, W.; Liu, Y.; Wei, B.; Li, T.; Ding, K. *Angew. Chem., Int. Ed.* **2022,** *61,* e202202554. doi:10.1002/anie.202202554
38. Xiao, X.; Zeng, J.; Fang, J.; Sun, J.; Li, T.; Song, Z.; Cai, L.; Wan, Q. *J. Am. Chem. Soc.* **2020,** *142,* 5498–5503. doi:10.1021/jacs.0c00447
39. Cheng, C.-W.; Wu, C.-Y.; Hsu, W.-L.; Wong, C.-H. *Biochemistry* **2020,** *59,* 3078–3088. doi:10.1021/acs.biochem.9b00613
40. Huang, X.; Huang, L.; Wang, H.; Ye, X.-S. *Angew. Chem., Int. Ed.* **2004,** *43,* 5221–5224. doi:10.1002/anie.200460176
41. Zhang, Y.; Xiang, G.; He, S.; Hu, Y.; Liu, Y.; Xu, L.; Xiao, G. *Org. Lett.* **2019,** *21,* 2335–2339. doi:10.1021/acs.orglett.9b00617
42. Zhang, Y.; Chen, Z.; Huang, Y.; He, S.; Yang, X.; Wu, Z.; Wang, X.; Xiao, G. *Angew. Chem., Int. Ed.* **2020,** *59,* 7576–7584. doi:10.1002/anie.202000992
43. Li, P.; He, H.; Zhang, Y.; Yang, R.; Xu, L.; Chen, Z.; Huang, Y.; Bao, L.; Xiao, G. *Nat. Commun.* **2020,** *11,* 405. doi:10.1038/s41467-020-14295-z
44. He, H.; Xu, L.; Sun, R.; Zhang, Y.; Huang, Y.; Chen, Z.; Li, P.; Yang, R.; Xiao, G. *Chem. Sci.* **2021,** *12,* 5143–5151. doi:10.1039/d0sc06815b
45. Xiao, G. *Acc. Chem. Res.* **2025,** *58,* 2350–2363. doi:10.1021/acs.accounts.5c00387
46. Ma, Y.; Zhang, Y.; Huang, Y.; Chen, Z.; Xian, Q.; Su, R.; Jiang, Q.; Wang, X.; Xiao, G. *J. Am. Chem. Soc.* **2024,** *146,* 4112–4122. doi:10.1021/jacs.3c12815
47. Chen, Z.; Xiao, G. *J. Am. Chem. Soc.* **2024,** *146,* 17446–17455. doi:10.1021/jacs.4c05188

48. Zhang, Y.; Wang, L.; Zhou, Q.; Li, Z.; Li, D.; Yin, C.; Wang, X.; Xiao, G. *Angew. Chem., Int. Ed.* **2023,** *62,* e202301351. doi:10.1002/anie.202301351
49. Zhang, Y.; He, H.; Chen, Z.; Huang, Y.; Xiang, G.; Li, P.; Yang, X.; Lu, G.; Xiao, G. *Angew. Chem., Int. Ed.* **2021,** *60,* 12597–12606. doi:10.1002/anie.202103826
50. Zhang, Y.; Hu, Y.; Liu, S.; He, H.; Sun, R.; Lu, G.; Xiao, G. *Chem. Sci.* **2022,** *13,* 7755–7764. doi:10.1039/d2sc02176e
51. Shou, K.; Zhang, Y.; Ji, Y.; Liu, B.; Zhou, Q.; Tan, Q.; Li, F.; Wang, X.; Lu, G.; Xiao, G. *Chem. Sci.* **2024,** *15,* 6552–6561. doi:10.1039/d4sc01348d
52. Li, P.; Fan, H.; Tan, Q.; Xiao, G. *Org. Lett.* **2023,** *25,* 2788–2792. doi:10.1021/acs.orglett.3c00670
53. Sun, X.; Chen, Z.; Yang, R.; Wang, M.; Wang, X.; Zhang, Q.; Xiao, G. *Org. Lett.* **2023,** *25,* 7364–7368. doi:10.1021/acs.orglett.3c02842
54. Chen, Z.; Xiao, G. *Org. Lett.* **2023,** *25,* 7395–7399. doi:10.1021/acs.orglett.3c02898
55. Ma, Y.; Jiang, Q.; Wang, X.; Xiao, G. *Org. Lett.* **2022,** *24,* 7950–7954. doi:10.1021/acs.orglett.2c03081
56. Shou, K.; Liu, S.; Zhang, Y.; Xiao, G. *Chin. J. Chem.* **2024,** *42,* 1593–1598. doi:10.1002/cjoc.202400121
57. Yu, B.; Sun, J. *Chem. Commun.* **2010,** *46,* 4668. doi:10.1039/c0cc00563k
58. Yu, B.; Tao, H. *Tetrahedron Lett.* **2001,** *42,* 2405–2407. doi:10.1016/s0040-4039(01)00157-5
59. Li, Y.; Yang, Y.; Yu, B. *Tetrahedron Lett.* **2008,** *49,* 3604–3608. doi:10.1016/j.tetlet.2008.04.017
60. Yu, B. *Acc. Chem. Res.* **2018,** *51,* 507–516. doi:10.1021/acs.accounts.7b00573
61. Christensen, H. M.; Oscarson, S.; Jensen, H. H. *Carbohydr. Res.* **2015,** *408,* 51–95. doi:10.1016/j.carres.2015.02.007
62. Zhu, Q.; Shen, Z.; Chiodo, F.; Nicolardi, S.; Molinaro, A.; Silipo, A.; Yu, B. *Nat. Commun.* **2020,** *11,* 4142. doi:10.1038/s41467-020-17992-x

License and Terms

BEILSTEIN JOURNAL OF ORGANIC CHEMISTRY

Formal synthesis of a selective estrogen receptor modulator with tetrahydrofluorenone structure using [3 + 2 + 1] cycloaddition of yne-vinylcyclopropanes and CO

Jing Zhang[1], Guanyu Zhang[2], Hongxi Bai[2] and Zhi-Xiang Yu[*1,2]

Full Research Paper

Open Access

Address:
[1]Pingshan Translational Medicine Center, Shenzhen Bay Laboratory, Shenzhen, 518118, China and [2]Beijing National Laboratory of Molecular Sciences (BNLMS), Key Laboratory of Bioorganic Chemistry and Molecular Engineering, College of Chemistry, Peking University, Beijing, 100871, China

Email:
Zhi-Xiang Yu[*] - yuzx@pku.edu.cn

* Corresponding author

Keywords:
[3 + 2 + 1] cycloaddition; selective estrogen receptor modulators; synthesis; tetrahydrofluorenone

Beilstein J. Org. Chem. **2025,** *21,* 1639–1644.
https://doi.org/10.3762/bjoc.21.127

Received: 01 April 2025
Accepted: 29 July 2025
Published: 14 August 2025

This article is part of the thematic issue "Concept-driven strategies in target-oriented synthesis".

Guest Editor: C. Li

Abstract

A formal synthesis of product **VI** with tetrahydroflurenone structure as selective estrogen receptor modulator has been realized. The Rh-catalyzed [3 + 2 + 1] reaction of yne-vinylcyclopropanes and CO (20 mmol scale, in 87% yield) for building the 6/5/5 skeleton, and a Heck coupling reaction constructing the [3.2.1] framework, are the two key reactions in this 11-step synthesis.

Introduction

Estrogen receptors (ERs) [1,2] are widely distributed nuclear receptor proteins and include two subtypes, ERα [3,4] and ERβ [5,6]. These receptors can bind 17β-estradiol with similar affinity, facilitating the transfer of estrogen to various tissues in the body. Due to this, 17β-estradiol as non-selective ligand has been extensively studied in hormone replacement therapy (HRT). However, HRT produced some risks of breast and uterine cancer. Consequently, scientists then concentrated their efforts on developing selective estrogen receptor modulators (SERMs) that interact with intracellular ERs in a tissue-specific manner to reduce the risk of estrogen-related cancers and other complications. Now there is a growing consensus that specific ERβ agonists are safer than nonspecific modulators by avoiding ERα stimulation [7-9]. Therefore, searching for SERMs toward ERβ as agonist and/or antagonist [10,11] has become a research frontier for treating breast cancer, osteoporosis, cardiovascular disease, neuropathies, and other diseases.

Merck scientists found that molecules with tetrahydrofluorenone (6/5/6 tricyclic motif) can act as SERMs. For example, molecules **I** and **II** (Scheme 1A) displayed low nanomolar affinity for ERβ and have 75-fold selectivity of ERβ over Erα [12]. Molecules **III** and **IV** (Scheme 1A) with an additional pyrazole ring compared to **I** and **II** had good pharmacokinetic properties that had overcome the problems of rapid clearance and low oral bioavailability executed by previous molecules

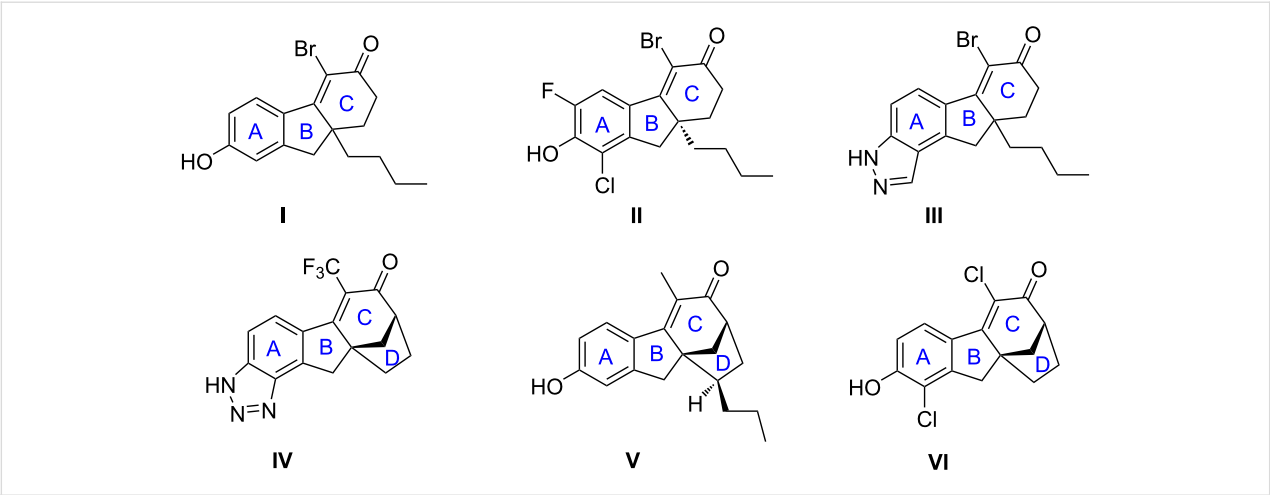

Scheme 1: Reported biologically active tetrahydrofluorenone-SERMs molecules.

[13,14]. A series of bridged tetrahydrofluorenone derivatives, represented by molecules **V** and **VI,** showed significant ERβ binding affinity and high selectivity [15-19].

So far, there are only two routes for accessing bridged tetrahydrofluorenone derivative **VI**. The first one shown in Scheme 2A includes a Robinson annulation to construct the **C** ring (cyclo-

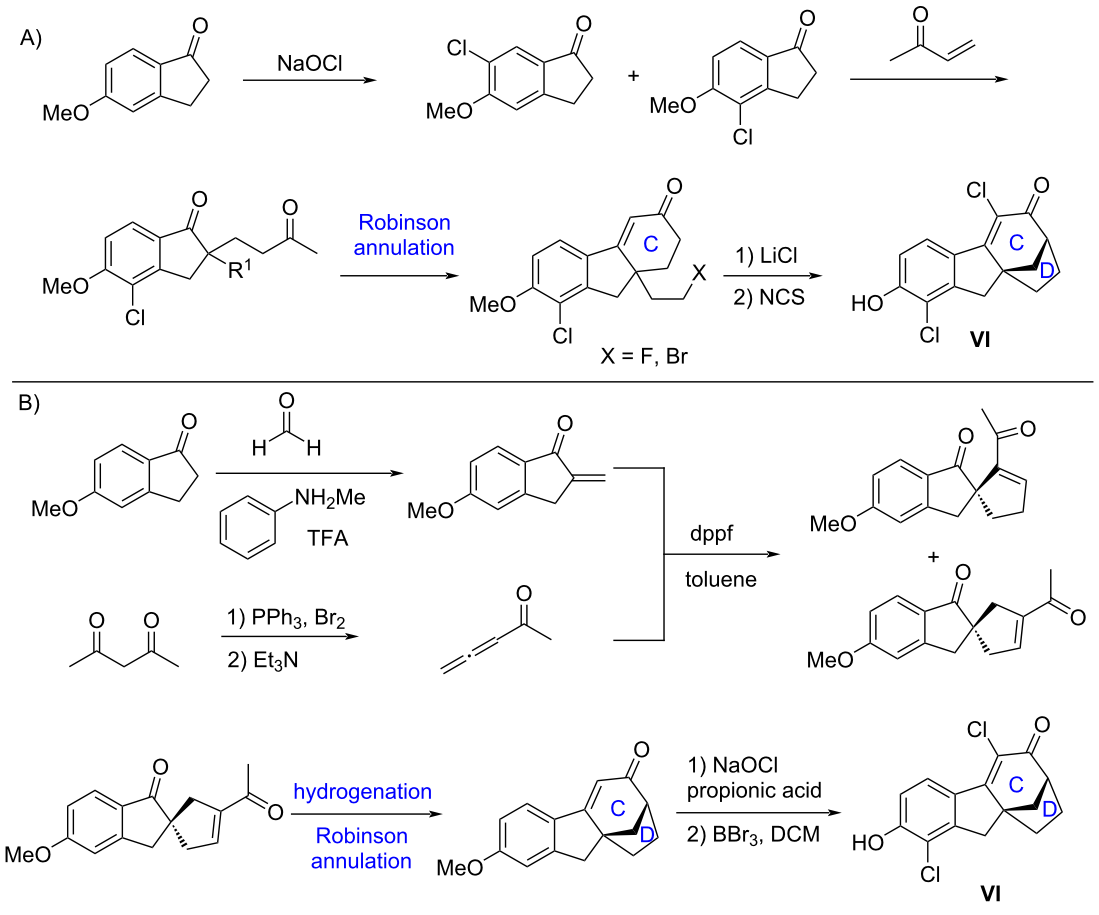

Scheme 2: Reported synthesis routes to SERMs molecule **VI**.

hexenone ring), and an intramolecular S_N2 reaction to build the D ring (five-membered ring) [15-18]. In 2013, Wallace and co-workers disclosed the second route for this molecule (Scheme 2B) [19], in which the five-membered ring B was formed by utilizing asymmetric Lu [3 + 2] cycloaddition reaction [20,21] between indanone and allenyl ketone. Then hydrogenation and Robinson annulation delivered the core of the target molecule. Some other excellent synthetic routes for tetrahydrofluorenone derivates have been developed [12-19] but finding new strategies for these molecules and their derivatives are still required for future medicinal investigations. Due to this, we decided to explore a new approach to **VI**, which is reported here.

Our approach is inspired by the Lei's synthesis of ent-kaurane diterpenoids (Scheme 3A) [22] which share the [3.2.1] motif as the SERMs in Scheme 1 do. Lei used a [3 + 2 + 1] reaction [23-28], which was developed in our group and has been applied in synthesis, coupled with stoichiometric Pd-mediated Heck reaction, concisely reaching the framework of their target natural products. We decided to use the same approach to synthesize **VI**, but we planned to use a catalytic Heck reaction by using a stronger nucleophile. As can be seen below, stoichiometric Heck reaction for **VI** failed because the present vinyl group of the [3 + 2 + 1] product does not have a methyl group in the terminal position, which could be the key to Lei's synthesis. Realizing the synthesis of **VI** would provide a practical strategy not only to our target here but also to other natural products with [3.2.1] framework such as songorine, beyerene, garryine and steviol shown in Scheme 3B.

Results and Discussion

Scheme 4 is the retrosynthetic analysis for the key intermediate **1**, which can reach the final compound **VI** via chlorination and demethylation [19]. Target molecule **1** can be accessed by decarboxylation reaction from compound **13**, prepared by an intramolecular Heck reaction between the β-ketoester and the vinyl group in compound **10**. Compound **10** can be realized by introducing an ester group in **9**, which is the [3 + 2 + 1] cycloadduct from **8** and CO using a Rh catalyst. The [3 + 2 + 1] substrate of yne-vinylcyclopropane (yne-VCP) **8** can be synthesized by Wittig reaction from cyclopropyl aldehyde **7**, in which the alkyne moiety is installed via Sonogashira coupling reaction using aryl iodide **5**. The cyclopropyl ring in **5** can be introduced via an S_N2 reaction of compound **2** with *tert*-butyl cyclopropanecarboxylate (**3**).

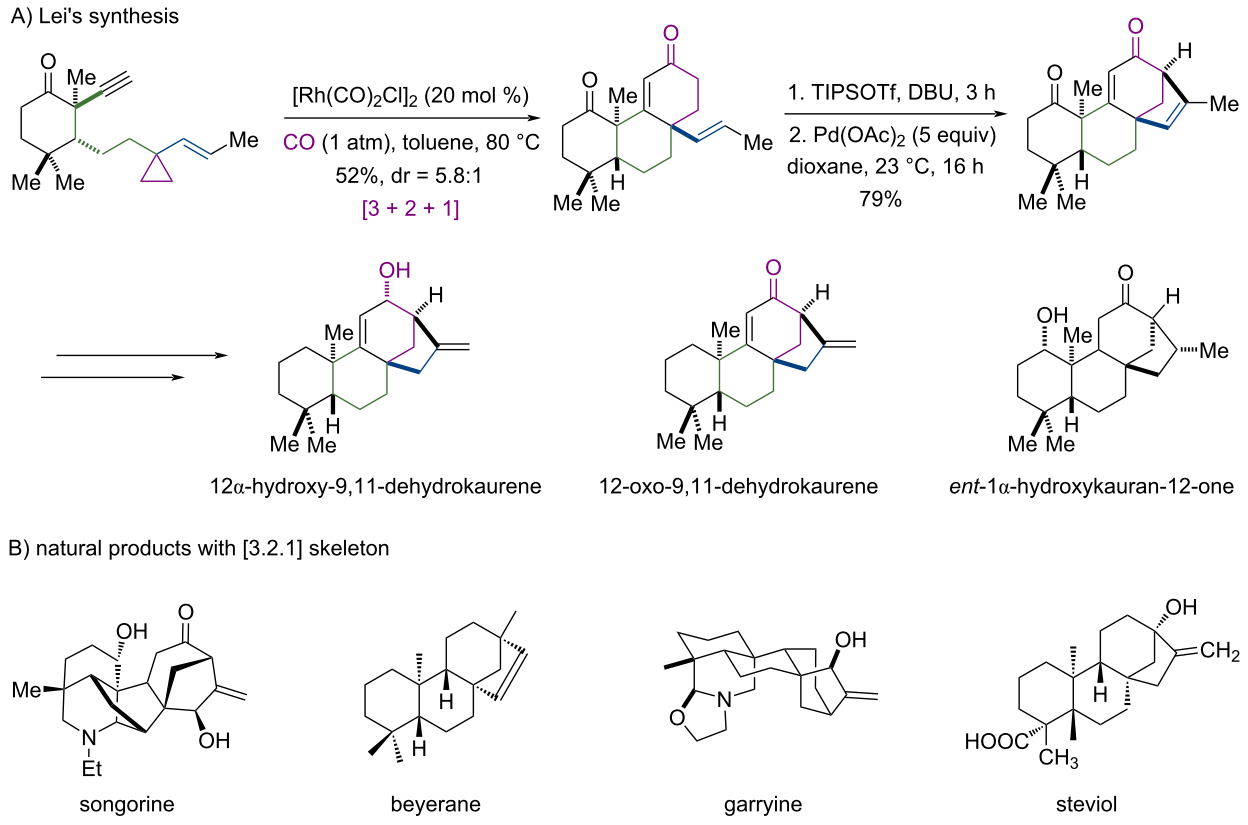

Scheme 3: Lei's synthesis of natural products of ent-kaurane diterpenoids (A), and natural products songorine, beyerene, garryine and steviol (B).

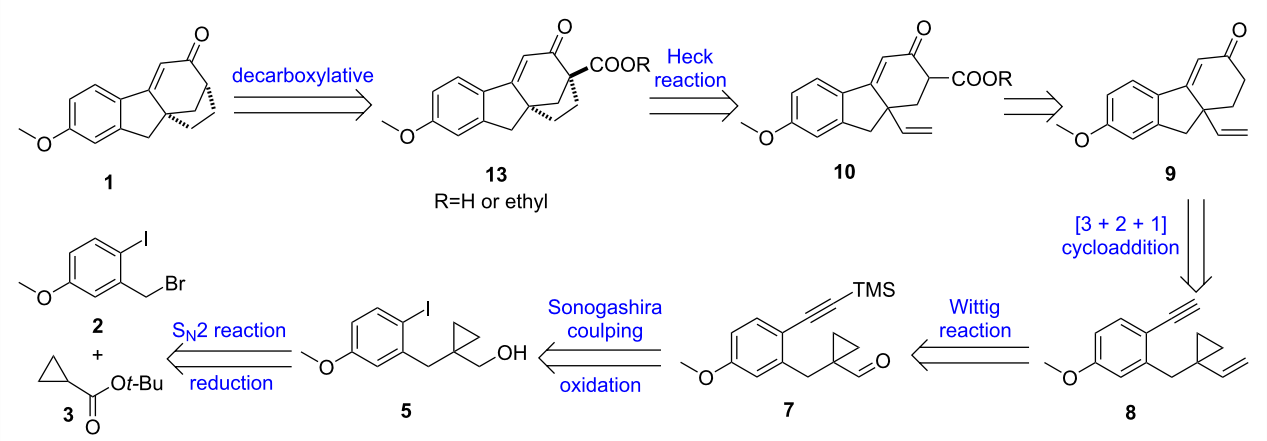

Scheme 4: Retrosynthetic analysis for the synthesis of **1**.

Scheme 5 summarizes the final successful execution of this route. The starting material **2** is a known compound [29] and can be prepared from readily available *m*-anisyl alcohol by using iodination and bromination reactions (see Supporting Information File 1 for the details). Subsequently, an S_N2 reaction between **2** and *tert*-butyl cyclopropanecarboxylate (**3**)

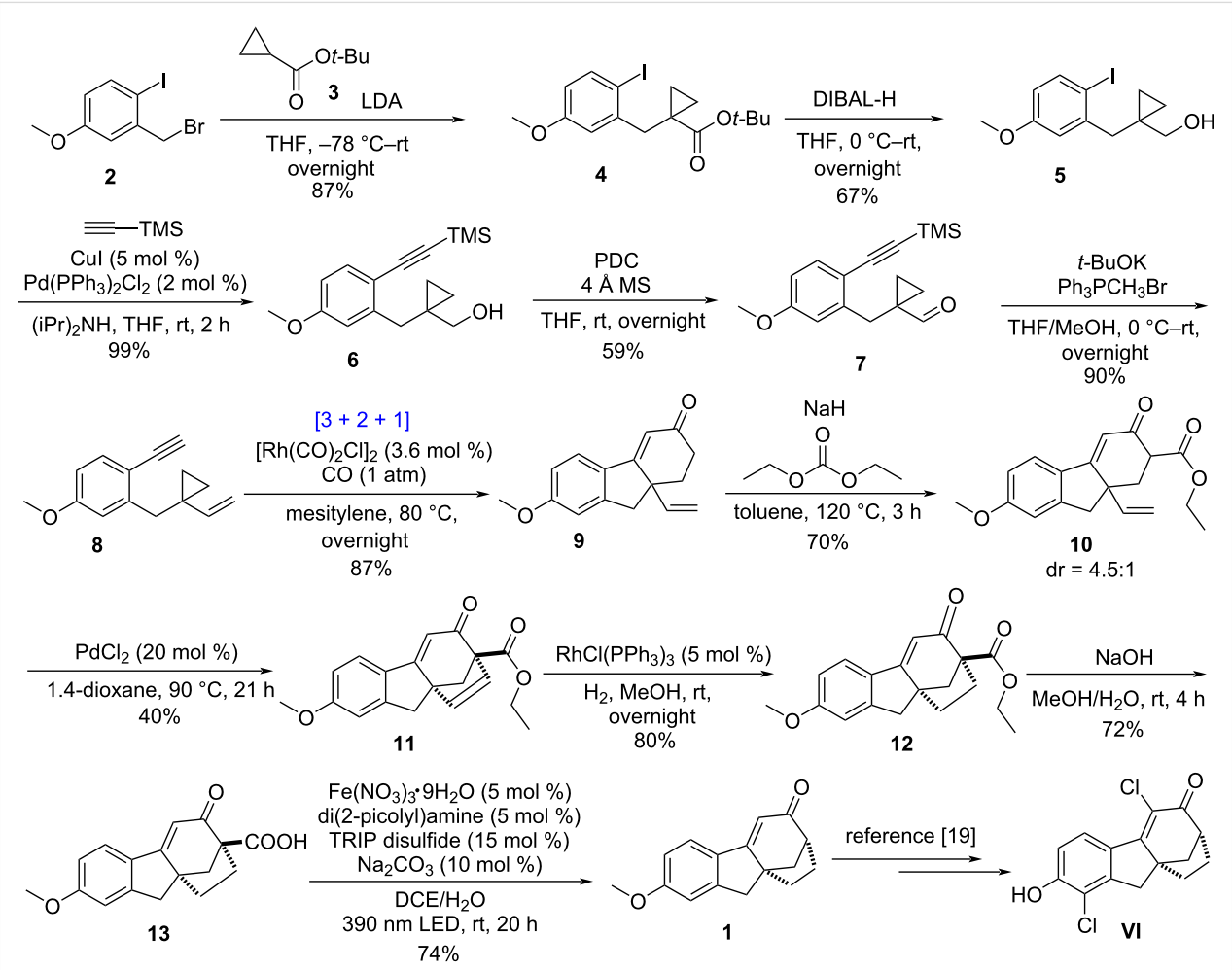

Scheme 5: Formal synthesis of SERMs molecule **VI**.

in the presence of LDA delivered product **4** in 87% yield with a cyclopropyl group. Then reducing the carboxylate group in **4** with DIBAL-H afforded alcohol **5** in 67% yield. Next, Sonogashira coupling reaction between **5** and trimethylsilylacetylene generated **6** with an alkyne moiety quantitatively. After that, the hydroxy group in **6** was oxidized into a carbonyl group, giving **7** in 59% yield. Then, under basic conditions, the aldehyde group in **7** was converted into a vinyl group via Wittig reaction, affording yne-VCP substrate **8** in 90% yield. During this process, the TMS protecting group was lost.

We then investigated the [3 + 2 + 1] reaction of **8** and CO. Applying the traditional solvent dioxane for the $[Rh(CO)_2Cl]_2$ catalyzed [3 + 2 + 1] reaction (the catalyst loading was increased from 5 mol % to 10 mol %) gave **9** in only 26% yield. To our delight, the reaction yield could be improved to 87% by using mesitylene [30] as the solvent and the loading of $[Rh(CO)_2Cl]_2$ catalyst can be reduced to 3.6 mol % (the reaction scale was 20.6 mmol).

After finishing the key [3 + 2 + 1] reaction, we focused on building the D ring in **1**. Initially, we tried to directly close the ring through addition of the α position of the carbonyl group to the bridgehead vinyl group through Heck reaction (using Pd catalyst), but disappointingly, all efforts failed to realize this goal. A stoichiometric version of the Heck reaction used by Lei did not work either. Maybe the terminal vinyl group in **9** has a lower reactivity compared to Lei's substrate (Scheme 3). We then decided to introduce an ester group at the α position of the carbonyl group in **9** to get compound **10**, which could have a more nucleophilic carbon better for the Heck reaction. **10** was obtained in 70% yield with a diastereomeric ratio of 4.5:1. Then, we screened various palladium catalysts and solvents to accomplish the target Heck coupling, finding that using 1,4-dioxane as the solvent and 20 mol % $PdCl_2$ as the catalyst, **11** could be obtained in 40% yield in the air. We tried by using more catalyst, or adding O_2 (or $CuCl_2$) as oxidant, but all these efforts did not give improved reaction yields (the reason for this was not known).

A hydrogenation reaction to reduce the C=C bond in **11** was then successfully applied, delivering product **12** in 80% yield (5 mol % $RhCl(PPh_3)_3$ catalyst and 1 atm hydrogen atmosphere were used). Next, we tested whether Krapcho decarboxylation reaction can convert **12** into **1** in one step. Unfortunately, failure was encountered here. This can be expected because the reaction site here is a bridge quaternary center (no such example was reported in literature for this) [31-33]. Due to this, we then converted the ester group in **12** into a carboxylic acid group, reaching **13** in 72% yield. Finally, photocatalytic decarboxylation [34] delivered the desired product **1** in 74% yield, realizing a formal synthesis of the selective estrogen receptor modulator **VI**.

Conclusion

In conclusion, we achieved a formal synthesis of SERM molecule VI through a 11-step process to its precursor, molecule **1**. Two key reactions have been applied here. The first one is a [3 + 2 + 1] reaction of yne-VCP and CO to build the 6/5/6 skeleton in 20 mmol scale with 87% yield. The second one is a Heck reaction between the β-ketoester and the vinyl group (coming from the [3 + 2 + 1] reaction) to form the [3.2.1] ring, the D ring of the target molecule. This route can provide new derivatives for further searching new SERMs. The synthetic strategy can be applied to other molecules with [3.2.1] framework. Of the same importance, the gram scale (4 g) of the [3 + 2 + 1] reaction with 87% reaction yield demonstrates the practical use of this reaction in synthesis.

Supporting Information

Supporting Information File 1

Experimental procedures, product characterizations, and copies of the ^1H and ^{13}C NMR spectra.
[https://www.beilstein-journals.org/bjoc/content/supplementary/1860-5397-21-127-S1.pdf]

Acknowledgements

We thank Zhiqiang Huang for testing the stoichiometric Heck reaction in this synthesis.

Funding

This research was supported by the National Natural Science Foundation of China (No.22331001).

Data Availability Statement

All data that supports the findings of this study is available in the published article and/or the supporting information of this article.

References

1. Paterni, I.; Granchi, C.; Katzenellenbogen, J. A.; Minutolo, F. *Steroids* **2014,** *90,* 13–29. doi:10.1016/j.steroids.2014.06.012
2. Dahlman-Wright, K.; Cavailles, V.; Fuqua, S. A.; Jordan, V. C.; Katzenellenbogen, J. A.; Korach, K. S.; Maggi, A.; Muramatsu, M.; Parker, M. G.; Gustafsson, J.-Å. *Pharmacol. Rev.* **2006,** *58,* 773–781. doi:10.1124/pr.58.4.8
3. Green, S.; Walter, P.; Kumar, V.; Krust, A.; Bornert, J.-M.; Argos, P.; Chambon, P. *Nature* **1986,** *320,* 134–139. doi:10.1038/320134a0
4. Greene, G. L.; Gilna, P.; Waterfield, M.; Baker, A.; Hort, Y.; Shine, J. *Science* **1986,** *231,* 1150–1154. doi:10.1126/science.3753802

5. Kuiper, G. G.; Enmark, E.; Pelto-Huikko, M.; Nilsson, S.; Gustafsson, J. A. *Proc. Natl. Acad. Sci. U. S. A.* **1996,** *93,* 5925–5930. doi:10.1073/pnas.93.12.5925
6. Mosselman, S.; Polman, J.; Dijkema, R. *FEBS Lett.* **1996,** *392,* 49–53. doi:10.1016/0014-5793(96)00782-x
7. Chang, E. C.; Frasor, J.; Komm, B.; Katzenellenbogen, B. S. *Endocrinology* **2006,** *147,* 4831–4842. doi:10.1210/en.2006-0563
8. Montanaro, D.; Maggiolini, M.; Recchia, A. G.; Sirianni, R.; Aquila, S.; Barzon, L.; Fallo, F.; Ando, S.; Pezzi, V. *J. Mol. Endocrinol.* **2005,** *35,* 245–256. doi:10.1677/jme.1.01806
9. Paruthiyil, S.; Parmar, H.; Kerekatte, V.; Cunha, G. R.; Firestone, G. L.; Leitman, D. C. *Cancer Res.* **2004,** *64,* 423–428. doi:10.1158/0008-5472.can-03-2446
10. Maximov, P. Y.; Lee, T. M.; Jordan, V. C. *Curr. Clin. Pharmacol.* **2013,** *8,* 135–155. doi:10.2174/1574884711308020006
11. Jordan, V. C. *Cancer Res.* **2001,** *61,* 5683–5687.
12. Wilkening, R. R.; Ratcliffe, R. W.; Tynebor, E. C.; Wildonger, K. J.; Fried, A. K.; Hammond, M. L.; Mosley, R. T.; Fitzgerald, P. M. D.; Sharma, N.; McKeever, B. M.; Nilsson, S.; Carlquist, M.; Thorsell, A.; Locco, L.; Katz, R.; Frisch, K.; Birzin, E. T.; Wilkinson, H. A.; Mitra, S.; Cai, S.; Hayes, E. C.; Schaeffer, J. M.; Rohrer, S. P. *Bioorg. Med. Chem. Lett.* **2006,** *16,* 3489–3494. doi:10.1016/j.bmcl.2006.03.098
13. Parker, D. L., Jr.; Meng, D.; Ratcliffe, R. W.; Wilkening, R. R.; Sperbeck, D. M.; Greenlee, M. L.; Colwell, L. F.; Lambert, S.; Birzin, E. T.; Frisch, K.; Rohrer, S. P.; Nilsson, S.; Thorsell, A.-G.; Hammond, M. L. *Bioorg. Med. Chem. Lett.* **2006,** *16,* 4652–4656. doi:10.1016/j.bmcl.2006.05.103
14. Wilkening, R. R.; Ratcliffe, R. W.; Fried, A. K.; Meng, D.; Sun, W.; Colwell, L.; Lambert, S.; Greenlee, M.; Nilsson, S.; Thorsell, A.; Mojena, M.; Tudela, C.; Frisch, K.; Chan, W.; Birzin, E. T.; Rohrer, S. P.; Hammond, M. L. *Bioorg. Med. Chem. Lett.* **2006,** *16,* 3896–3901. doi:10.1016/j.bmcl.2006.05.036
15. Wildonger, K. J.; Ratcliffe, R. W.; Mosley, R. T.; Hammond, M. L.; Birzin, E. T.; Rohrer, S. P. *Bioorg. Med. Chem. Lett.* **2006,** *16,* 4462–4466. doi:10.1016/j.bmcl.2006.06.043
16. Kinzel, O.; Fattori, D.; Muraglia, E.; Gallinari, P.; Nardi, M. C.; Paolini, C.; Roscilli, G.; Toniatti, C.; Gonzalez Paz, O.; Laufer, R.; Lahm, A.; Tramontano, A.; Cortese, R.; De Francesco, R.; Ciliberto, G.; Koch, U. *J. Med. Chem.* **2006,** *49,* 5404–5407. doi:10.1021/jm060516e
17. Parker, D. L., Jr.; Fried, A. K.; Meng, D.; Greenlee, M. L. *Org. Lett.* **2008,** *10,* 2983–2985. doi:10.1021/ol800971f
18. Maddess, M. L.; Scott, J. P.; Alorati, A.; Baxter, C.; Bremeyer, N.; Brewer, S.; Campos, K.; Cleator, E.; Dieguez-Vazquez, A.; Gibb, A.; Gibson, A.; Howard, M.; Keen, S.; Klapars, A.; Lee, J.; Li, J.; Lynch, J.; Mullens, P.; Wallace, D.; Wilson, R. *Org. Process Res. Dev.* **2014,** *18,* 528–538. doi:10.1021/op5000489
19. Wallace, D. J.; Reamer, R. A. *Tetrahedron Lett.* **2013,** *54,* 4425–4428. doi:10.1016/j.tetlet.2013.06.023
20. Wei, Y.; Shi, M. *Org. Chem. Front.* **2017,** *4,* 1876–1890. doi:10.1039/c7qo00285h
21. Liang, Y.; Liu, S.; Xia, Y.; Li, Y.; Yu, Z.-X. *Chem. – Eur. J.* **2008,** *14,* 4361–4373. doi:10.1002/chem.200701725
22. Wang, J.; Hong, B.; Hu, D.; Kadonaga, Y.; Tang, R.; Lei, X. *J. Am. Chem. Soc.* **2020,** *142,* 2238–2243. doi:10.1021/jacs.9b13722
23. Yang, J.; Xu, W.; Cui, Q.; Fan, X.; Wang, L.-N.; Yu, Z.-X. *Org. Lett.* **2017,** *19,* 6040–6043. doi:10.1021/acs.orglett.7b02656
24. Zhou, Y.; Qin, J.-L.; Xu, W.; Yu, Z.-X. *Org. Lett.* **2022,** *24,* 5902–5906. doi:10.1021/acs.orglett.2c02111
25. Bose, S.; Yang, J.; Yu, Z.-X. *J. Org. Chem.* **2016,** *81,* 6757–6765. doi:10.1021/acs.joc.6b00608
26. Jiao, L.; Lin, M.; Zhuo, L.-G.; Yu, Z.-X. *Org. Lett.* **2010,** *12,* 2528–2531. doi:10.1021/ol100625e
27. Feng, Y.; Yu, Z.-X. *J. Org. Chem.* **2015,** *80,* 1952–1956. doi:10.1021/jo502604p
28. Zhang, P.; Yu, Z.-X. *Acc. Chem. Res.* **2025,** *58,* 1065–1080. doi:10.1021/acs.accounts.4c00779
29. Ruiz, J.; Ardeo, A.; Ignacio, R.; Sotomayor, N.; Lete, E. *Tetrahedron* **2005,** *61,* 3311–3324. doi:10.1016/j.tet.2004.10.105
30. Huang, Z.; Jin, Y.; Zhao, S.; Zhang, P.; Liao, W.; Yu, Z.-X. *ACS Catal.* **2024,** *14,* 12734–12742. doi:10.1021/acscatal.4c03878
31. Moriyama, K.; Kuramochi, M.; Tsuzuki, S.; Fujii, K.; Morita, T. *Org. Lett.* **2021,** *23,* 268–273. doi:10.1021/acs.orglett.0c03546
32. Adepu, R.; Rambabu, D.; Prasad, B.; Meda, C. L. T.; Kandale, A.; Rama Krishna, G.; Malla Reddy, C.; Chennuru, L. N.; Parsa, K. V. L.; Pal, M. *Org. Biomol. Chem.* **2012,** *10,* 5554. doi:10.1039/c2ob25420d
33. González-Gómez, J. C.; Uriarte, E. *Synlett* **2002,** 2095–2097. doi:10.1055/s-2002-35569
34. Lu, Y.-C.; West, J. G. *Angew. Chem., Int. Ed.* **2023,** *62,* e202213055. doi:10.1002/anie.202213055

License and Terms

BEILSTEIN JOURNAL OF ORGANIC CHEMISTRY

Enantioselective desymmetrization strategy of prochiral 1,3-diols in natural product synthesis

Lihua Wei[‡1], Rui Yang[‡1], Zhifeng Shi[*2] and Zhiqiang Ma[*1]

Review

Open Access

Address:
[1]Key Lab of Functional Molecular Engineering of Guangdong Province, School of Chemistry & Chemical Engineering, South China University of Technology, Guangzhou 510641, P. R. China and [2]Medical Devices Research and Testing Center, South China University of Technology, Guangzhou 510006, P. R. China

Email:
Zhifeng Shi[*] - zhfs@scut.edu.cn; Zhiqiang Ma[*] - cezqma@scut.edu.cn

* Corresponding author ‡ Equal contributors

Keywords:
asymmetric synthesis; desymmetrization; 1,3-diols; natural product; total synthesis

Beilstein J. Org. Chem. **2025,** *21,* 1932–1963.
https://doi.org/10.3762/bjoc.21.151

Received: 27 May 2025
Accepted: 29 August 2025
Published: 18 September 2025

This article is part of the thematic issue "Concept-driven strategies in target-oriented synthesis".

Guest Editor: Y. Tang

Abstract

Enantioselective desymmetrization is employed as a powerful tool for the creation of chiral centers. Within this scope, the enantioselective desymmetrization of prochiral 1,3-diols, which generates chiral centers by enantioselective functionalization of one hydroxy group, offers beneficial procedures for accessing diverse structural motifs. In this review, we highlight a curated compilation of publications, focusing on the applications of enantioselective desymmetrization of prochiral 1,3-diols in the synthesis of natural products and biologically active molecules. Based on the reaction types, three strategies are discussed: enzymatic acylation, transition-metal-catalyzed acylation, and local desymmetrization.

Introduction

Natural products isolated from organisms are often asymmetric in their spatial structures, and these unique spatial structures are precisely what lead to their diverse biological activities [1-4]. For the synthesis of these natural products or bioactive molecules, chemists usually need to consider how to carry out asymmetric synthesis of them, driving the advancement of asymmetric methodologies [5-9].

Enantioselective desymmetrization of symmetric substrates has emerged as a pivotal methodology for the construction of chiral centers over the past few decades [10-13]. A series of reaction types have been developed, employing enzymes, metal complexes, or organocatalysts to convert prochiral or *meso* precursors into chiral motifs. Different from other strategies constructing chiral centers by formation of a new chemical bond at the central carbon, enantioselective desymmetrization is achieved through selective reaction at one of the symmetrical functional groups in the precursor, thereby breaking the symmetry and establishing a chiral center. Meanwhile, since the site where the reaction occurs is distant from the newly formed stereocenter, this strategy offers unique advantages, especially in the synthesis of complex molecules which are spatially crowded.

Among various types of substrates for enantioselective desymmetrization, symmetrical diols, especially prochiral 1,3-diols, are often prioritized for testing, because the two primary alcohols of the products (one of them is functionalized in an enantioselective manner) can be utilized for a series of transformations, including functionalization, chain elongation, ring formation, etc. Therefore, the enantioselective desymmetrization of diols has drawn considerable interest among synthetic chemists. Several comprehensive reviews [14-18] on the desymmetrization strategies for diols, including enzymatic desymmetrization and organocatalytic approaches, have been published in the past decade, most of which focus on the methodological development. Although there are reviews on desymmetrization in natural product synthesis [19-21], none of these have put emphasis on the desymmetrization of diols.

Prochiral 1,3-diols, as simple and practical substrates, have been widely used in developed desymmetrization methodologies with applications in the total synthesis of natural products and bioactive molecules, including enzymatic acylation, transition-metal-catalyzed acylation, and local desymmetrization. In this review, we cover total syntheses that utilize enantioselective desymmetrization of prochiral 1,3-diols.

Review

Desymmetrization via enzymatic acylation

Enzymatic reactions represent one of the most useful tools in total synthesis. Through combination with organic reactions, this chemo-enzymatic strategy has been successfully utilized in the synthesis of complex molecules [22,23]. Enzymatic reactions feature a convenient operation due to their relative insensitivity to water and oxygen, as well as a specificity to certain substrates, resulting in high enantioselectivity. However, since an enzymatic reaction generally produces only one of the two enantiomers, extensive enzyme screening is often required to access the desired enantiomer.

Among various types of enzymes, lipases have proven to be efficient for the desymmetrization of 1,3-diols. Lipases commonly share typical sequences of α-helices and β-strands and possess a catalytic triad consisting of serine (Ser), histidine (His), and aspartate (Asp) or glutamate (Glu). These three amino residues function as a nucleophile-base–acid catalytic system to facilitate esterification, and the general mechanism of a reaction catalyzed by lipases is illustrated in Scheme 1. Additionally, the diverse three-dimensional structures of lipases confer enantioselectivity in lipase-catalyzed esterification [24,25].

Moreover, their commercial availability makes lipases an attractive option for preparing optically pure intermediates in total synthesis. This section focuses on applications of lipase-catalyzed acylation of prochiral 1,3-diols in total synthesis.

Porcine pancreatic lipase (PPL)

PPL, a commercially available lipase isolated from fresh porcine pancreas [26], is one of the most widely used lipases for asymmetric acylation in total synthesis. In 1999, the Shishido

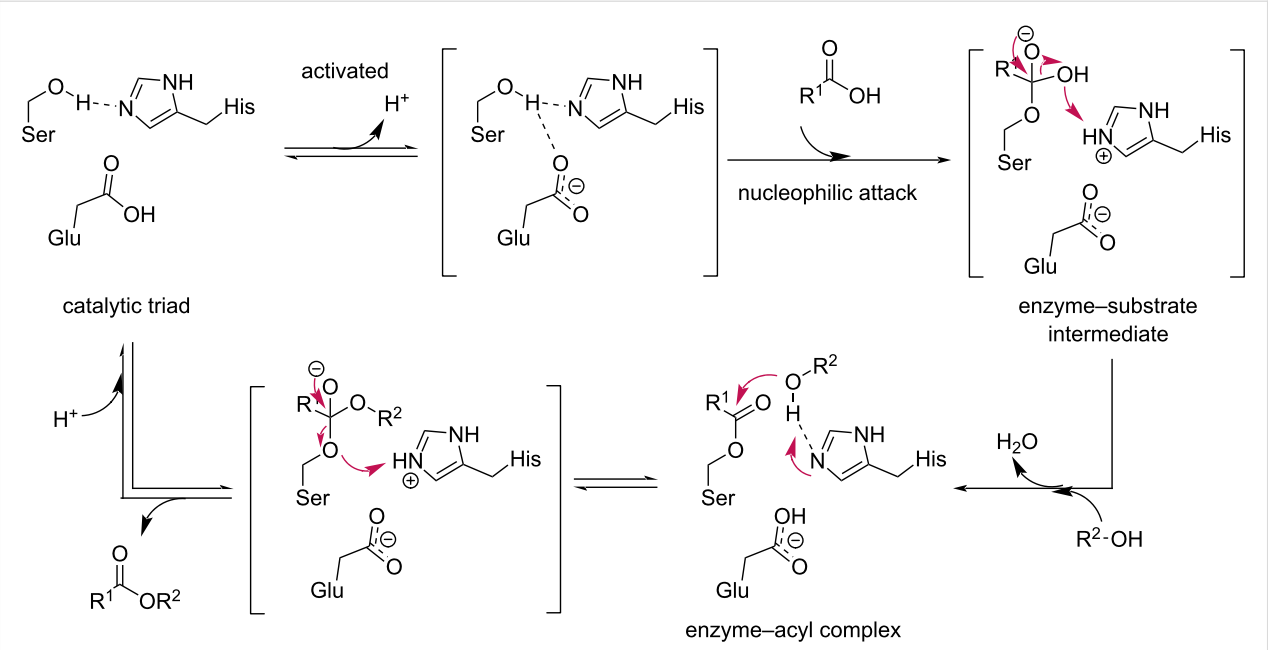

Scheme 1: General mechanism of a lipase-catalyzed esterification.

group completed the asymmetric synthesis of (−)-xanthorrhizol, a bioactive bisabolene-type sesquiterpenoid, employing a PPL-catalyzed acylation as the key step (Scheme 2) [27]. The prochiral diol **2** was synthesized from compound **1** in two steps. Subsequently, asymmetric acetylation of **2** catalyzed by PPL afforded (*R*)-**3** in 95% yield with 83% ee. The authors also used *Candida antarctica* lipase (CAL) in this transformation but with a suboptimal result ((*S*)-**3** in 19% yield with 94% ee). The monoacetate (*R*)-**3** was further converted into (−)-xanthorrhizol (**4**) in seven steps. Later in 2003, they further accomplished the synthesis of (+)-heliannuol D, a sesquiterpenoid isolated from sunflower (*Helianthus annuus* L. SH-222), starting from **4** [28]. A three-step sequence transformed **4** into diol **5**. Treatment of **5** with $Pd(OAc)_2$ and JohnPhos (**6**) induced cyclization, yielding bicyclic compound **7** with a 7-membered heterocycle. Final deprotection of the methoxymethyl (MOM) group in **7** afforded (+)-heliannuol D (**8**).

Having successfully applied PPL-catalyzed acetylation to the synthesis of (+)-heliannuol D, the Shishido group subsequently extended this strategy to other helianane-type sesquiterpenes. In 2003, they completed the enantioselective total synthesis of (−)-heliannuol A, another allelochemical sesquiterpenoid from *Helianthus annuus* L. SH-222 (Scheme 3a) [29]. The aryl iodide **9** was transformed into prochiral diol **10** in two steps. PPL-catalyzed desymmetrization of **10** with vinyl acetate yielded monoacetate (*R*)-**11** in 41% yield (94% brsm) with 78% ee. Diene **12** was prepared from (*R*)-**11** via a ten-step sequence. The following ring-closing metathesis (RCM) reaction catalyzed by Grubbs catalyst **13** converted **12** into the bicyclic compound **14**, which was transformed into (−)-heliannuol A (**15**) in three additional steps.

In 2006, the Shishido group further achieved the synthesis of heliannuol G and heliannuol H (Scheme 3b) [30]. Initially, the authors converted (*R*)-**11** into hydroquinone **16** through a seven-step sequence. The Pd-catalyzed intramolecular cyclization of **16** generated benzofuran **17** in 83% yield. After protecting the phenolic hydroxy group of **17**, cross-metathesis (CM) with allylic alcohol **18** catalyzed by **13** furnished intermediate **19**. Desilylation of **19** produced heliannuol G (**20**) and heliannuol H (**21**), with the structure of **21** confirmed by X-ray crystallographic analysis. Comparative analysis of the ^1H NMR data with authentic samples of the natural heliannuol G and heliannuol H enabled structural revision of these compounds, correcting prior misassignments in the literature [31,32]. Through enzyme-catalyzed asymmetric acetylation of prochiral 1,3-diols to access chiral building blocks (*R*)-**3** and (*R*)-**11**, Shishido's team completed a series of helianane-type sesquiterpenes. This pioneering work demonstrates the utility of prochiral 1,3-diols in the synthesis of natural products.

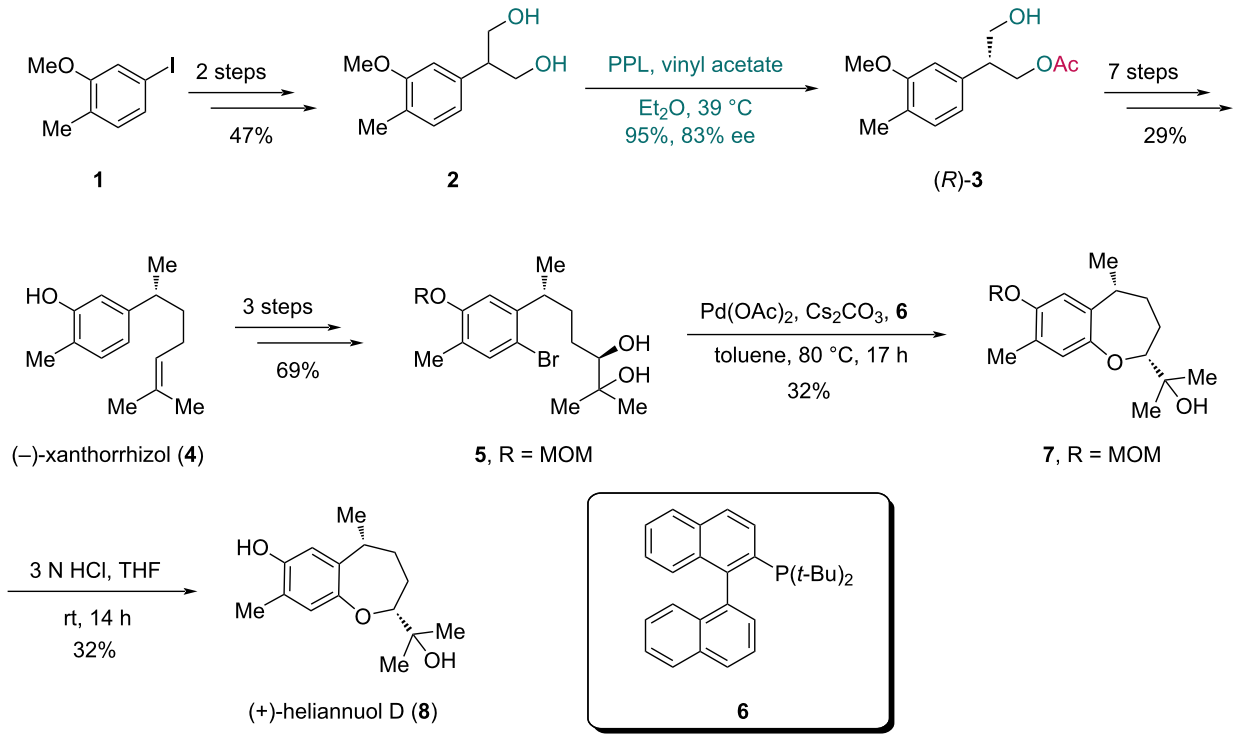

Scheme 2: Shishido's synthesis of (–)-xanthorrhizol (**4**) and (+)-heliannuol D (**8**).

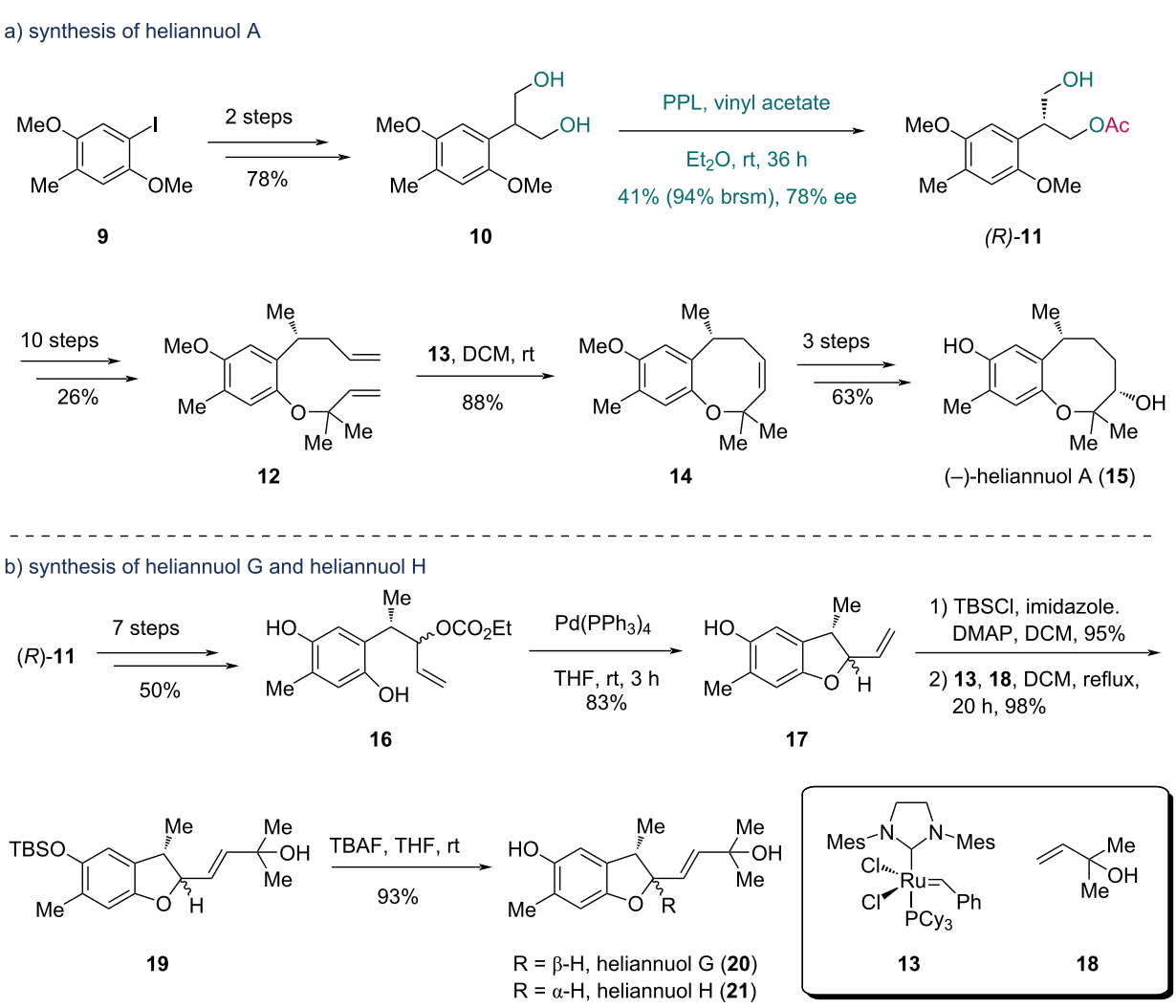

Scheme 3: Shishido's synthesis of a) (–)-heliannuol A (**15**) and b) heliannuol G (**20**) and heliannuol H (**21**).

In 2013, the first asymmetric synthesis of the norlignans hyperione A and *ent*-hyperione B was reported by the Deska group (Scheme 4) [33]. The synthesis commenced with a two-step conversion of ketone **22** to alkyne **23**. Pd-catalyzed Tsuji-type reaction with zinc reagent **24**, followed by acetonide hydrolysis, furnished allenic diol **25**. Treating allenic diol **25** with vinyl butanoate and PPL delivered monoester **26** in 92% yield (99% ee). The axial chirality was transferred to the C7' stereocenter through a Ag(I)-catalyzed cycloisomerization of the allenol, constructing the dihydrofuran ring. Lipase-catalyzed ester hydrolysis provided allylic alcohol **27**. Alcohol **28** was obtained from **27** in two steps, and was subsequently converted to hyperione A (**30**) and *ent*-hyperione B (**31**) by refluxing in toluene with Shvo's catalyst **29**. Notably, the authors found that hyperione A (**30**) could be obtained in higher yield and enantiopurity from alcohol **28** via a two-step sequence including oxidation and subsequent hydrogenation.

The Huang group reported their synthesis of (+)-brazilin and its racemic form in 2022 (Scheme 5) [34]. They first evaluated the feasibility of the Prins/Friedel–Crafts tandem reaction in the construction of the 6/6/5/6 tetracyclic skeleton, successfully completing the racemic synthesis of brazilin. For the asymmetric synthesis, the C3 chiral center of (+)-brazilin was established via enzymatic desymmetrization. Triol **33** was prepared from alcohol **32** in four steps. PPL-catalyzed desymmetrization of **33** afforded chiral monoester **34** in 95% yield with 62% ee. A two-step conversion of **34** gave diol **35**, which underwent Prins/Friedel–Crafts tandem cyclization to construct tetracyclic compound **36**. Final deprotection delivered (+)-brazilin (**37**).

Candida antarctica lipase (CAL)

CAL is a type of lipase originating from the yeast *Candida antarctica* and includes two enzymes, CAL-A and CAL-B [35,36]. Although a previous report [27] indicated that the

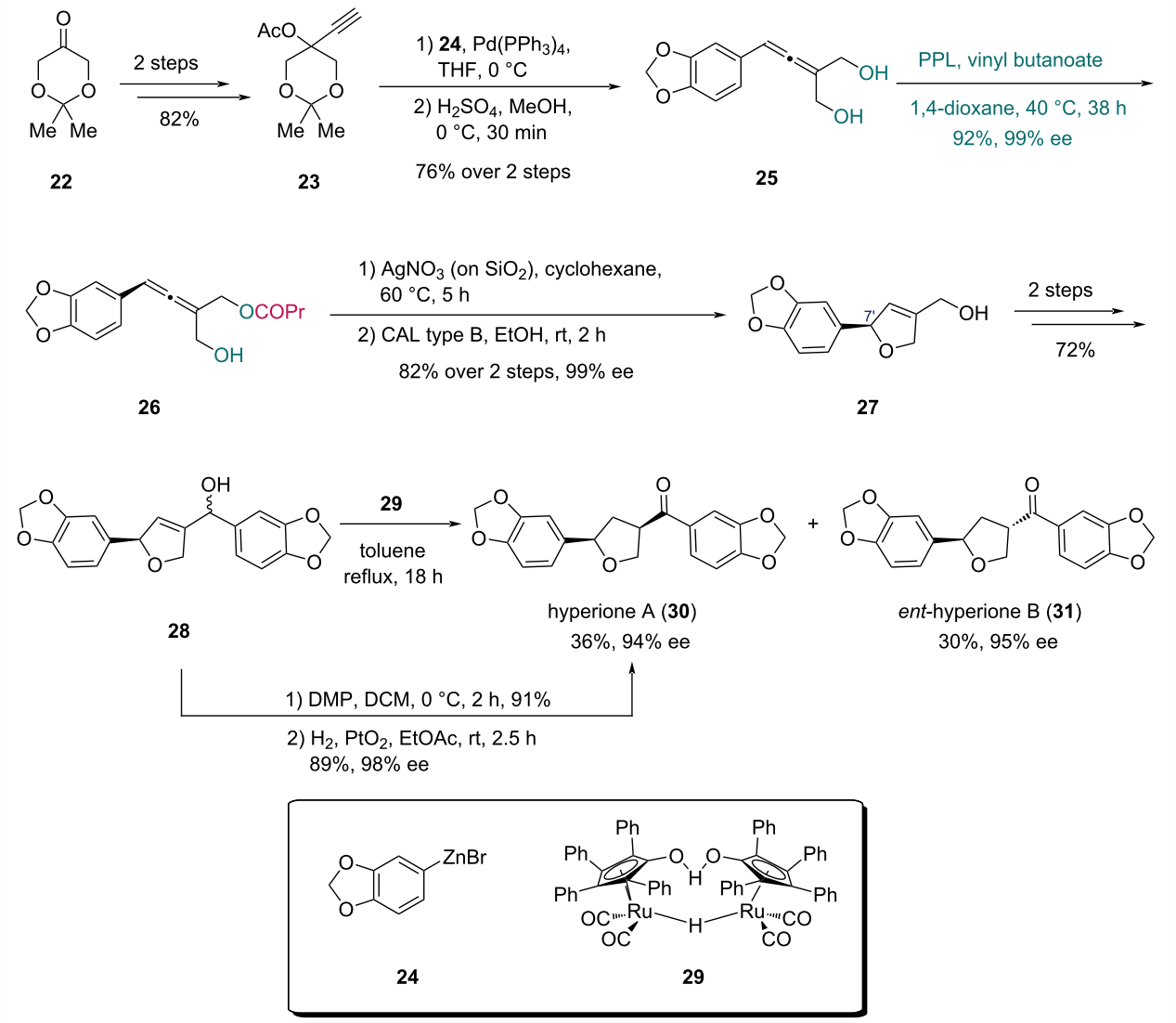

Scheme 4: Deska's synthesis of hyperione A (**30**) and *ent*-hyperione B (**31**).

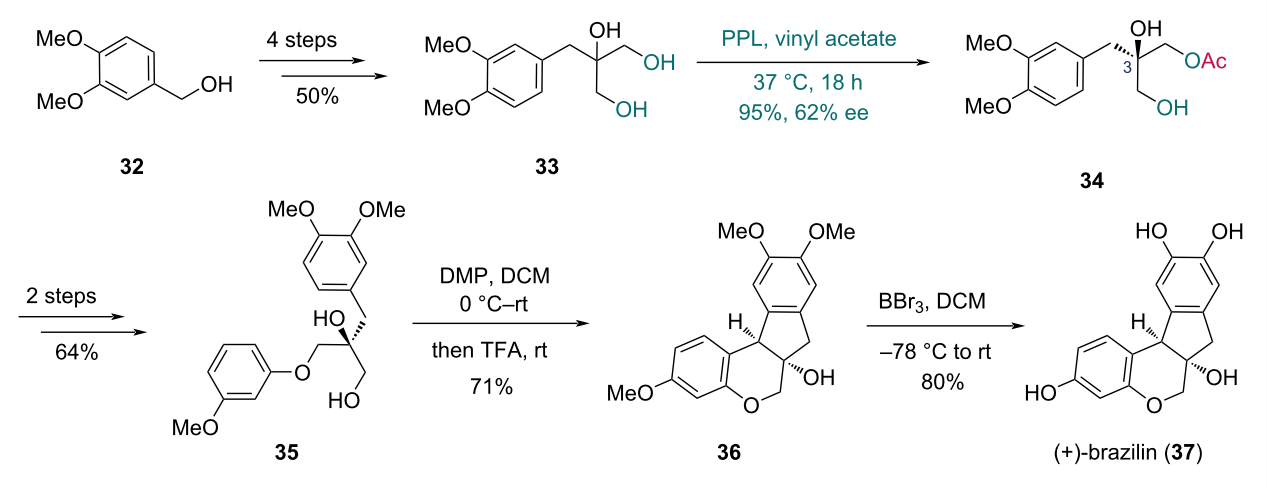

Scheme 5: Huang's synthesis of (+)-brazilin (**37**).

desymmetrization of prochiral diol **2** with CAL was ineffective, the Shishido group prepared optically active compound (*S*)-**11** via CAL-catalyzed asymmetric transesterification of the structurally similar diol **10**, thus completing the enantioselective synthesis of (−)-heliannuol D and (+)-heliannuol A (Scheme 6) [37]. The monoester (*S*)-**11** was isolated in 87% yield with >99% ee. A subsequent 17-step sequence provided epoxides **38** and **39**. Treatment of the mixture of **38** and **39** with 5% NaOH aqueous solution resulted in intramolecular [7-*exo*] and [8-*endo*] cyclization, furnishing the 7-membered cyclic ether **40** and 8-membered cyclic ether **41**, respectively. Finally, MOM deprotection produced (−)-heliannuol D (**42**) and (+)-heliannuol A (**43**).

In 2002, Chênevert and co-workers completed the total synthesis of (*S*)-α-tocotrienol, a natural isoform of vitamin E (Scheme 7) [38]. The authors used known triol **44** as the starting material. In the desymmetrization promoted by CAL, triol **44**

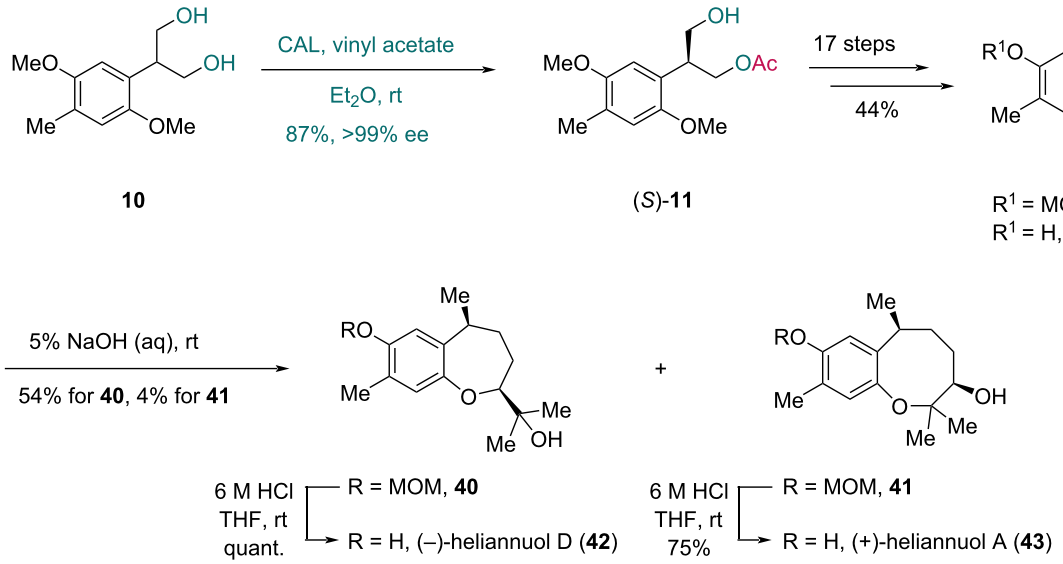

Scheme 6: Shishido's synthesis of (–)-heliannuol D (**42**) and (+)-heliannuol A (**43**).

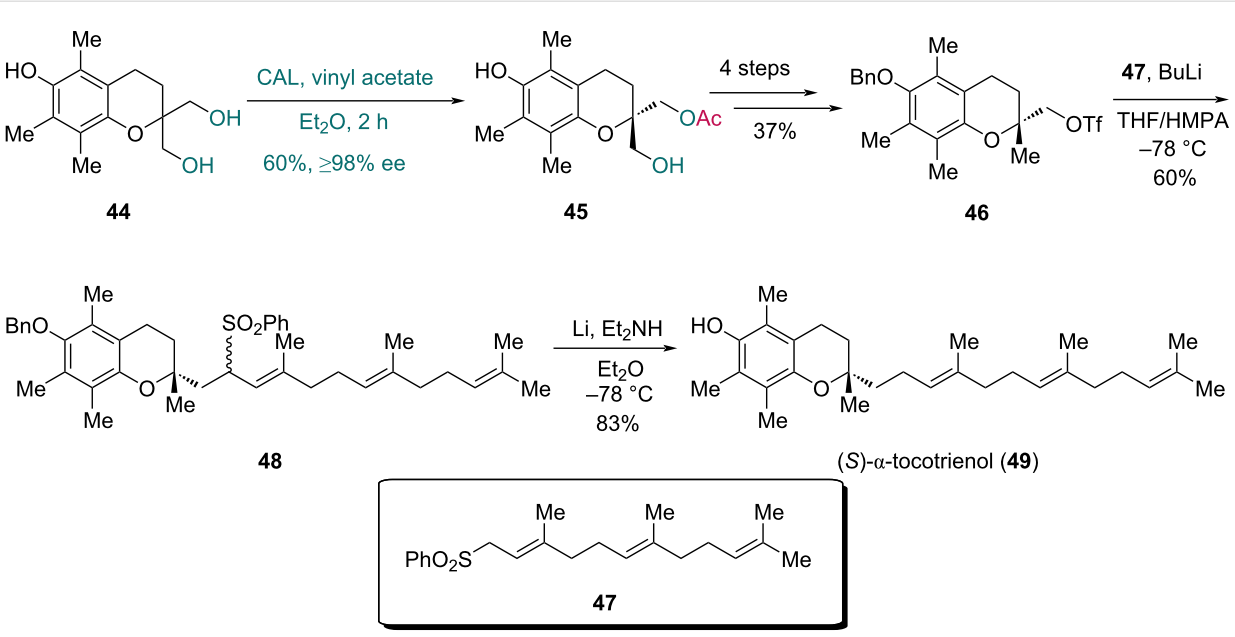

Scheme 7: Chênevert's synthesis of (*S*)-α-tocotrienol (**49**).

underwent a monoacetylation process, providing chiral compound **45** in 60% yield with over 98% ee. After a four-step conversion of **45** to triflate **46**, alkylation with sulfone **47** via treatment with butyllithium and hexamethylphosphoramide (HMPA) yielded the coupling product **48** as a mixture of diastereoisomers in 60% yield. Ultimately, single-electron reduction removed both the sulfone and benzyl groups of **48**, furnishing (*S*)-α-tocotrienol (**49**) in 83% yield.

Candida rugosa lipase (CRL)

The lipase CRL from *Candida rugosa,* another species of *Candida* genus*,* was used by the Kita group in their asymmetric synthesis of fredericamycin A in 2005 (Scheme 8) [39]. Different from their previous strategy [40] constructing the spiro chiral center via Lewis acid-mediated semi-pinacol rearrangement, this work involved a CRL-catalyzed desymmetrization of prochiral diol **51** (prepared from aldehyde **50** in four steps), providing monoester **53** in 57% yield with 83% ee. Notably, 1-ethoxyvinyl 2-furoate (**52**) was selected as the acyl donor in this step to suppress potential intramolecular acyl migration. To further improve the optical purity of monoester **53**, a *Pseudomonas aeruginosa* lipase-mediated kinetic resolution was performed with ethoxyvinyl butyrate **54**, ultimately achieving monoester **53** with 97% ee in 60% yield and the diester **53a**.

With enantioenriched monoester **53** in hand, the synthesis proceeded toward fredericamycin A (**60**) (Scheme 9). Dione **55**, which was prepared from **53** in six steps, underwent addition with alkyne **56** followed by acylation of the resulting hydroxy group with compound **57** to yield ketone **58**. A subsequent seven-step transformation involving acyl-group migration, [4 + 2] cycloaddition and aromatic Pummerer-type reaction, provided chiral spiro compound **59** with the 6/6/5/5/6/6 scaffold, and this intermediate was further elaborated to **60** in six additional steps.

Lipases from *Pseudomonas* genus

Pseudomonas is a genus of Gram-negative bacteria widely distributed in nature [41]. Some species within this genus produce lipases that effectively catalyze the desymmetrization of prochiral diols, which were used in total syntheses. In 2003, an enzymatic asymmetric acylation with PSA, a lipase from *Pseudomonas cepacia*, was adopted by Takabe and co-workers in their synthesis of (*E*)-3,7-dimethyl-2-octene-1,8-diol (isolated from *Danaus chrysippus*) (Scheme 10) [42]. Prepared from geraniol (**61**) in eight steps, diol **62** was converted to enantioenriched compound **63** in 75% yield with 90% ee in the presence of PSA. This intermediate was further advanced to (*E*)-3,7-dimethyl-2-octene-1,8-diol (**64**) over three steps.

Later in 2004, Takabe and co-workers accomplished the asymmetric synthesis of variabilin, a marine-derived furanosesterterpene (Scheme 11) [43]. The key C18 chiral center was established through lipase-mediated asymmetric transesterification. After substrates screening, diol **65** was selected and converted into monoester **66** in 95% yield with 98% ee using vinyl acetate and lipase PS from *Pseudomonas cepacia*. Four subsequent steps afforded sulfone **67**, and the following alkylation with fragment **68** in the presence of butyllithium and HMPA produced coupling product **69** in 84% yield. Finally, a six-step sequence completed the synthesis of (18*S*)-variabilin (**70**).

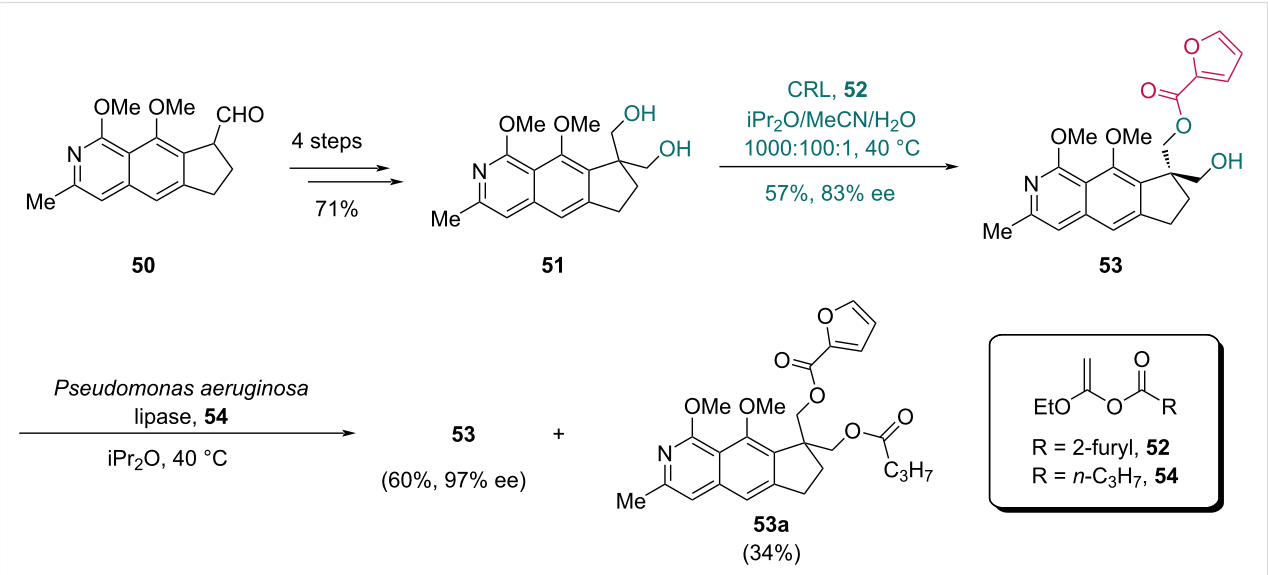

Scheme 8: Kita's synthesis of monoester **53**.

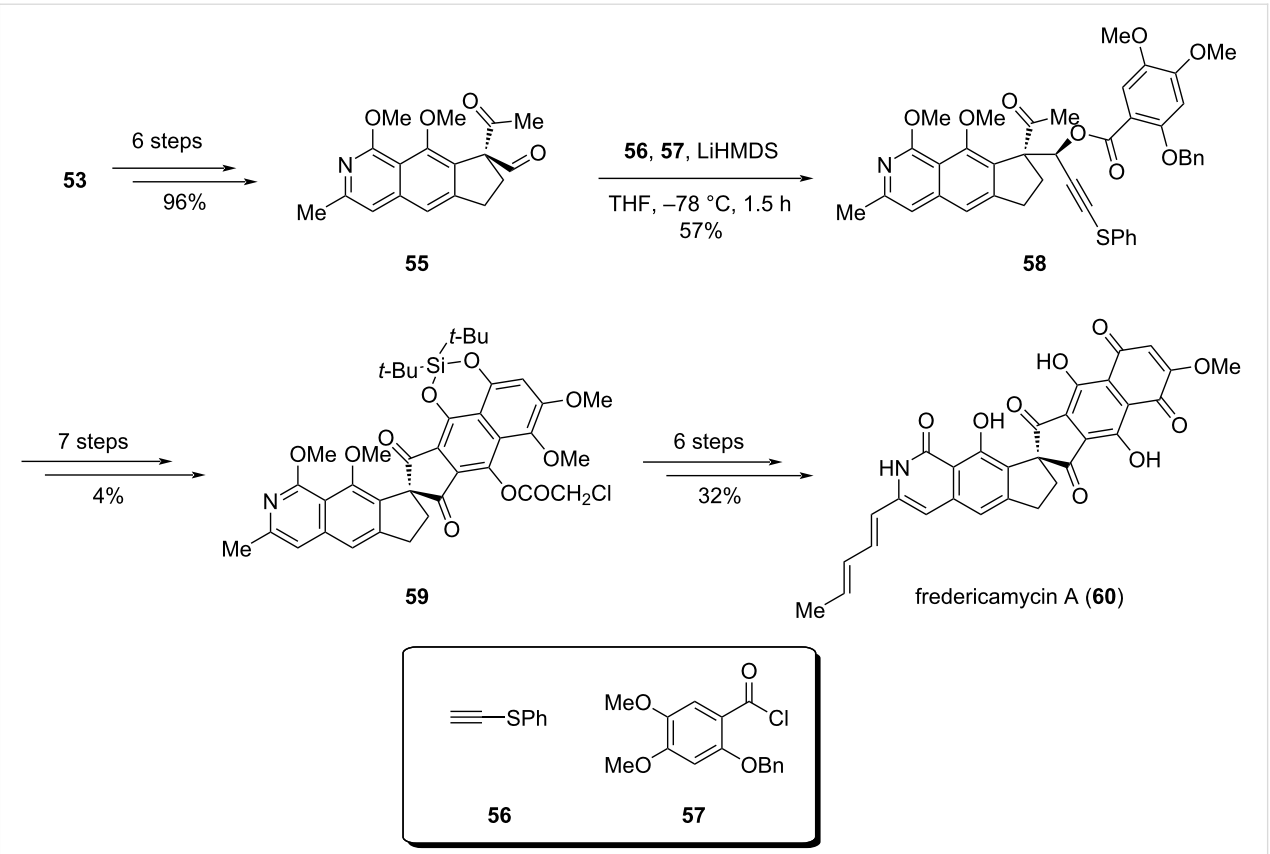

Scheme 9: Kita's synthesis of fredericamycin A (**60**).

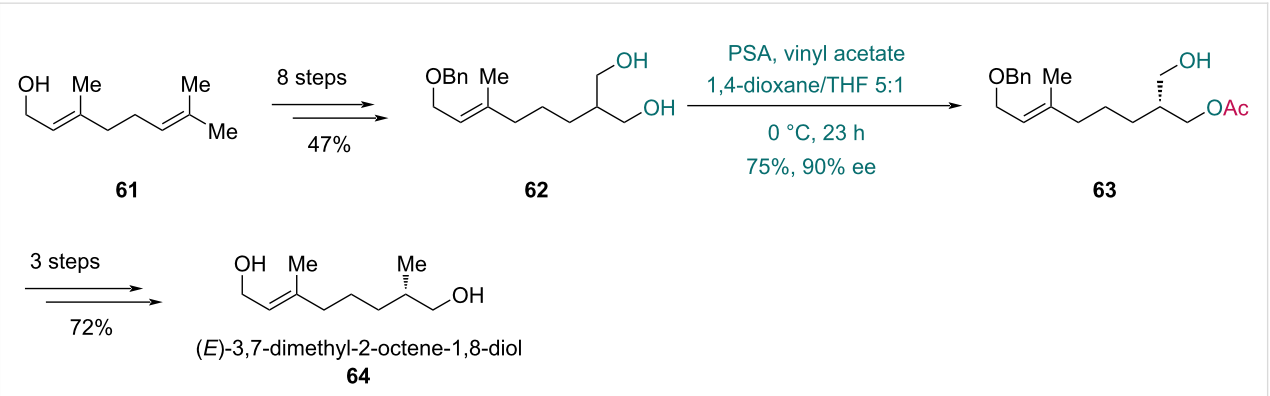

Scheme 10: Takabe's synthesis of (*E*)-3,7-dimethyl-2-octene-1,8-diol (**64**).

In 2010, Kawasaki and co-workers reported the asymmetric synthesis of both (*S*)-Rosaphen and (*R*)-Rosaphen to evaluate their odor profiles (Scheme 12) [44]. Diol **72** was prepared from bromide **71** in two steps. Lipase PS-mediated desymmetrization of **72** with vinyl butanoate provided monoester **73** in 90% yield with 97% ee. To obtain (*S*)-Rosaphen (**74**), monoester **73** was converted via mesylation followed by hydride reduction. In contrast, the synthesis of (*R*)-Rosaphen (**75**) required a four-step sequence comprising TBS protection, ester hydrolysis, mesylation, and hydride reduction.

In 2014, Tokuyama and co-workers accomplished the total synthesis of (−)-petrosin and (+)-petrosin, two marine-derived bisquinolizidine alkaloids [45]. They first completed the synthesis of (−)-petrosin (**84**) (Scheme 13a). Prochiral diol **77**, produced from diester **76** through reduction, was subjected to a

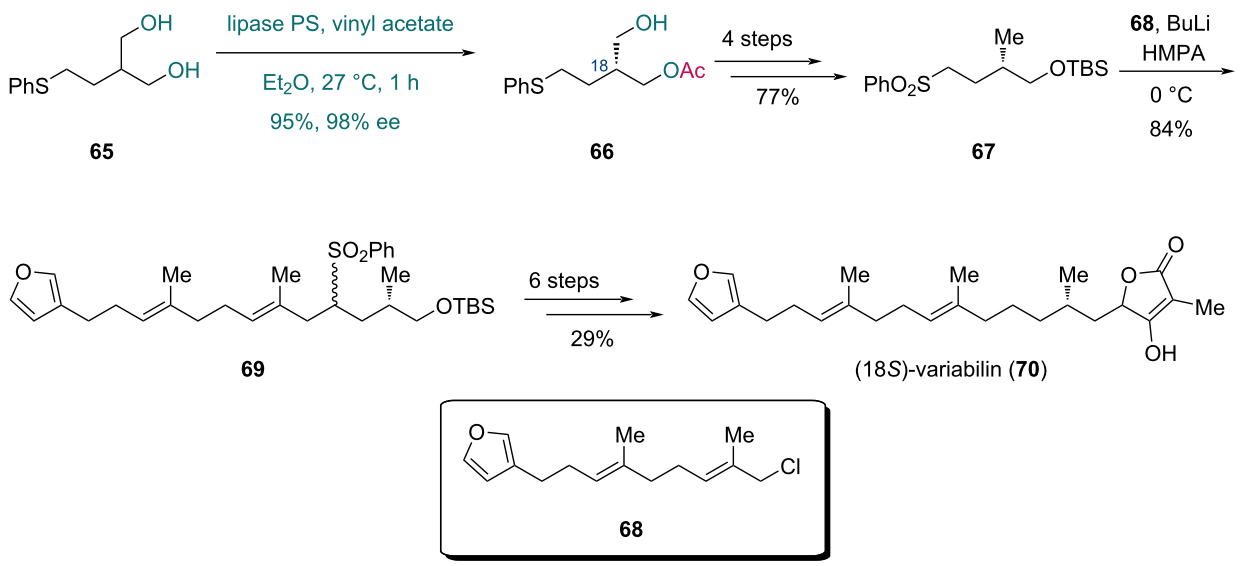

Scheme 11: Takabe's synthesis of (18*S*)-variabilin (**70**).

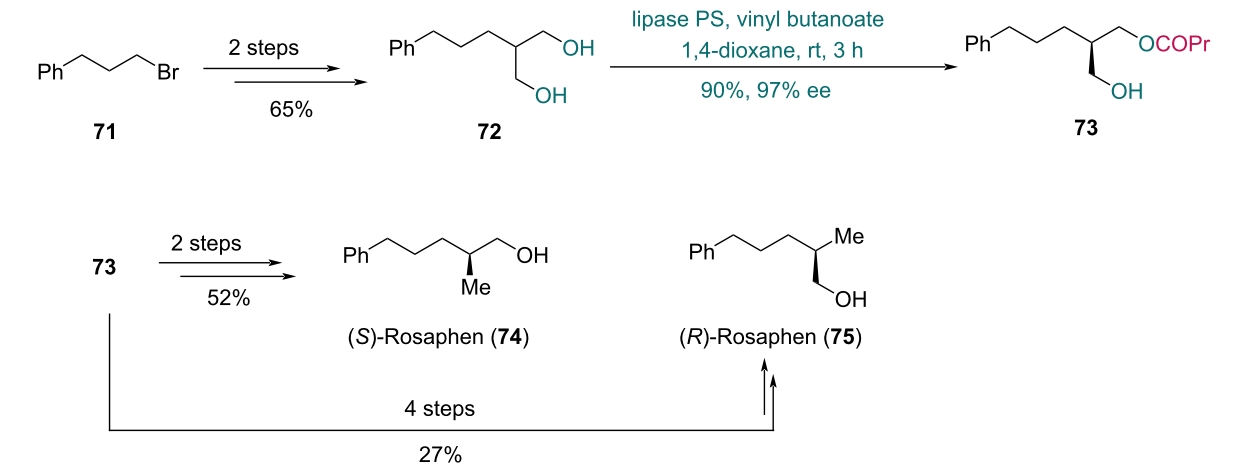

Scheme 12: Kawasaki's synthesis of (*S*)-Rosaphen (**74**) and (*R*)-Rosaphen (**75**).

lipase PS-mediated asymmetric transesterification. The resulting enantioenriched monoester, on hydroxy group protection with *tert*-butyldimethylsilyl chloride (TBSCl), yielded compound **78** in 84% yield over two steps with 99% ee. The TBS protection was crucial to prevent the potential racemization by intramolecular transesterification. Ester **79** was then prepared from **78** in eight steps. To complete the dimerization, fragments **80** and **81** were independently prepared from **79**. An intermolecular Suzuki–Miyaura coupling between **80** and **81** gave diester **82**. Through a ten-step sequence including an aza-Michael reaction, diester **82** was converted into diketone **83**, which was further transformed into (−)-petrosin (**84**) via RCM reaction and hydrogenation. For the synthesis of (+)-petrosin (**86**) (Scheme 13b), a similar strategy was adopted using compound **85** as the synthetic intermediate, which was prepared from diol **77** in a four-step sequence with 60% overall yield and 96% ee.

In 2003, the Fukuyama group realized the first total synthesis of leustroducsin B, a microbial metabolite with various biological activities, featuring a lipase AK (from *Pseudomonas fluorescens*)-mediated desymmetrization (Scheme 14) [46]. Starting with known compound **87**, the prochiral diol **88** was prepared in six steps. Subsequent asymmetric transesterification in the presence of vinyl acetate and lipase AK afforded the optically active acetate, which was followed by TBS protection of the free hydroxy group to give compound **89**, establishing the C8 chiral center in 86% yield over two steps with 90% ee. A further

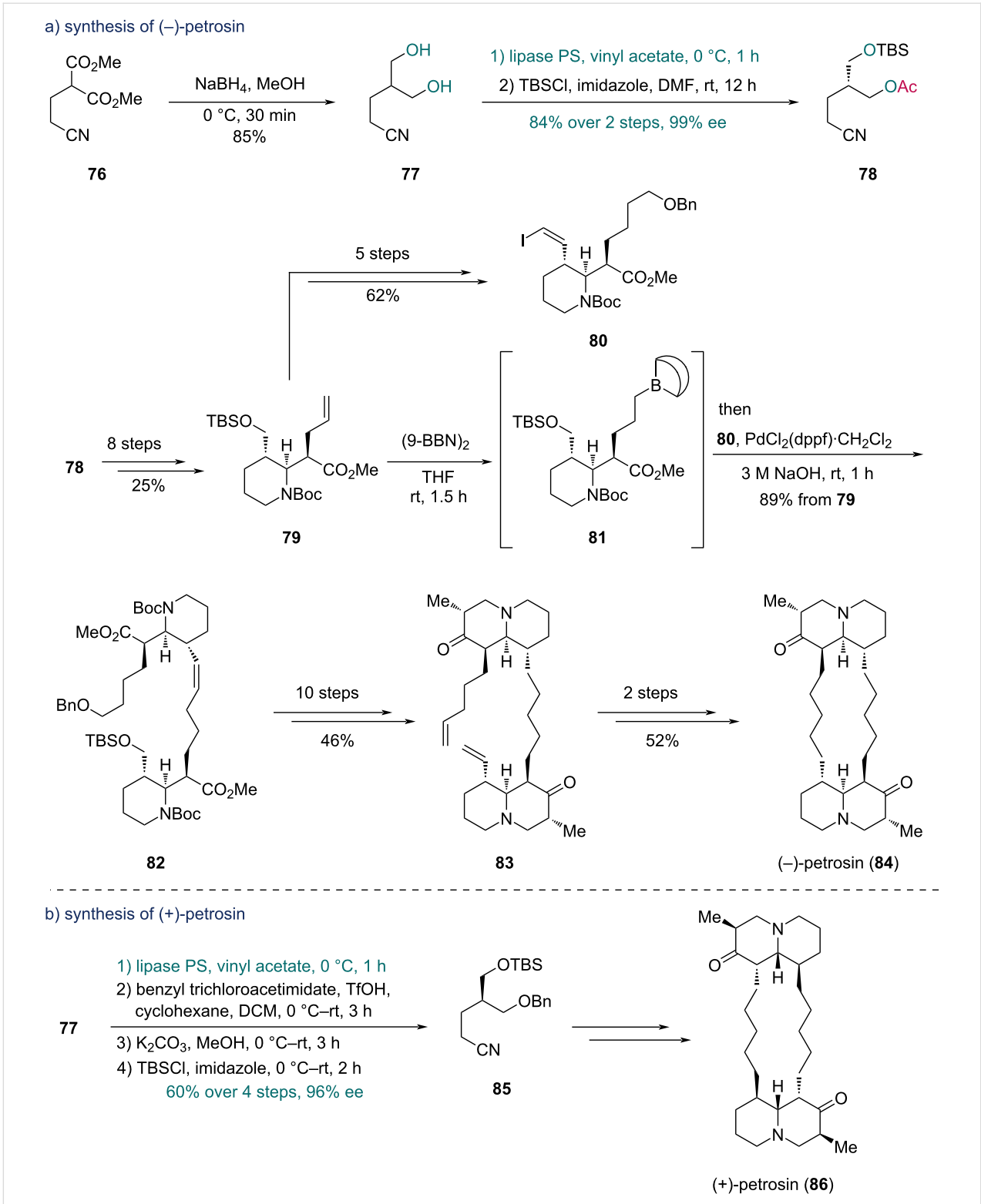

Scheme 13: Tokuyama's synthesis of a) (–)-petrosin (**84**) and b) (+)-petrosin (**86**).

14-step sequence furnished enone **90**, which underwent Evans aldol reaction with fragment **91**. After triethylsilyl (TES) protection of the resulting hydroxy group and auxiliary cleavage, thioester **92** was obtained. Five additional steps converted **92** into lactone **93**. Oxidative cleavage of the diol group in **93** and following coupling with fragment **94** gave compound

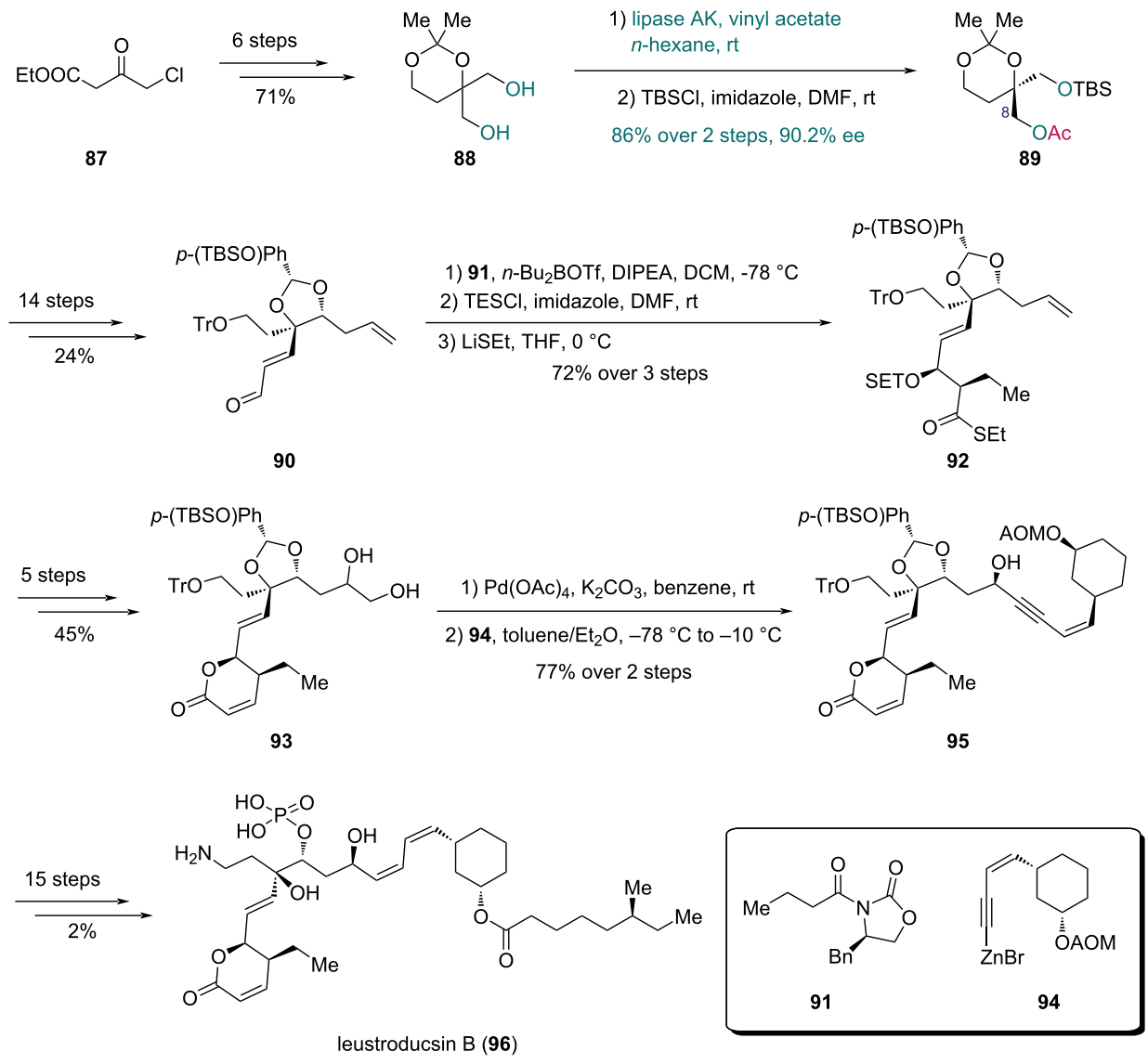

Scheme 14: Fukuyama's synthesis of leustroducsin B (**96**).

95, which was further elaborated to leustroducsin B (**96**) in 15 steps.

In 2013, Nanda and co-worker described the asymmetric synthesis of (−)-rasfonin, harnessing an enantioselective enzymatic desymmetrization with lipase AK and an enzymatic oxidative kinetic resolution to install stereocenters [47]. The synthesis commenced with the preparation of fragment **100** from ethylene glycol (**97**) (Scheme 15a). Through a four-step sequence, diol **98** was prepared from **97**, which underwent enzymatic desymmetrization with lipase AK in the presence of vinyl acetate to yield monoacetate **99** in 91% yield and 99% ee. This transformation established the C6' chiral center. Seven additional steps enabled the synthesis of fragment **100**. For the synthesis of fragment **106** (Scheme 15b), enzymatic hydrolysis of racemic diacetate **101** catalyzed by lipase PS-D (from *Pseudomonas cepacia*, immobilized on diatomite) was performed to deliver monoacetate **102** with the desired C7 chiral center in >99% ee. After four steps of functional group manipulations, alcohol **103** was subjected to enzymatic oxidative kinetic resolution with the bacterium *Gluconobacter oxydans*, producing alcohol **104** and acid **105**. The alcohol **104** with the desired C9 stereocenter was then converted into fragment **106** in nine steps, while acid **105** was recycled to **103** in two steps.

With the fragments **100** and **106** in hand, the synthesis of (−)-rasfonin proceeded via Yamaguchi esterification between the two fragments to obtain lactone **107** (Scheme 15c). A subse-

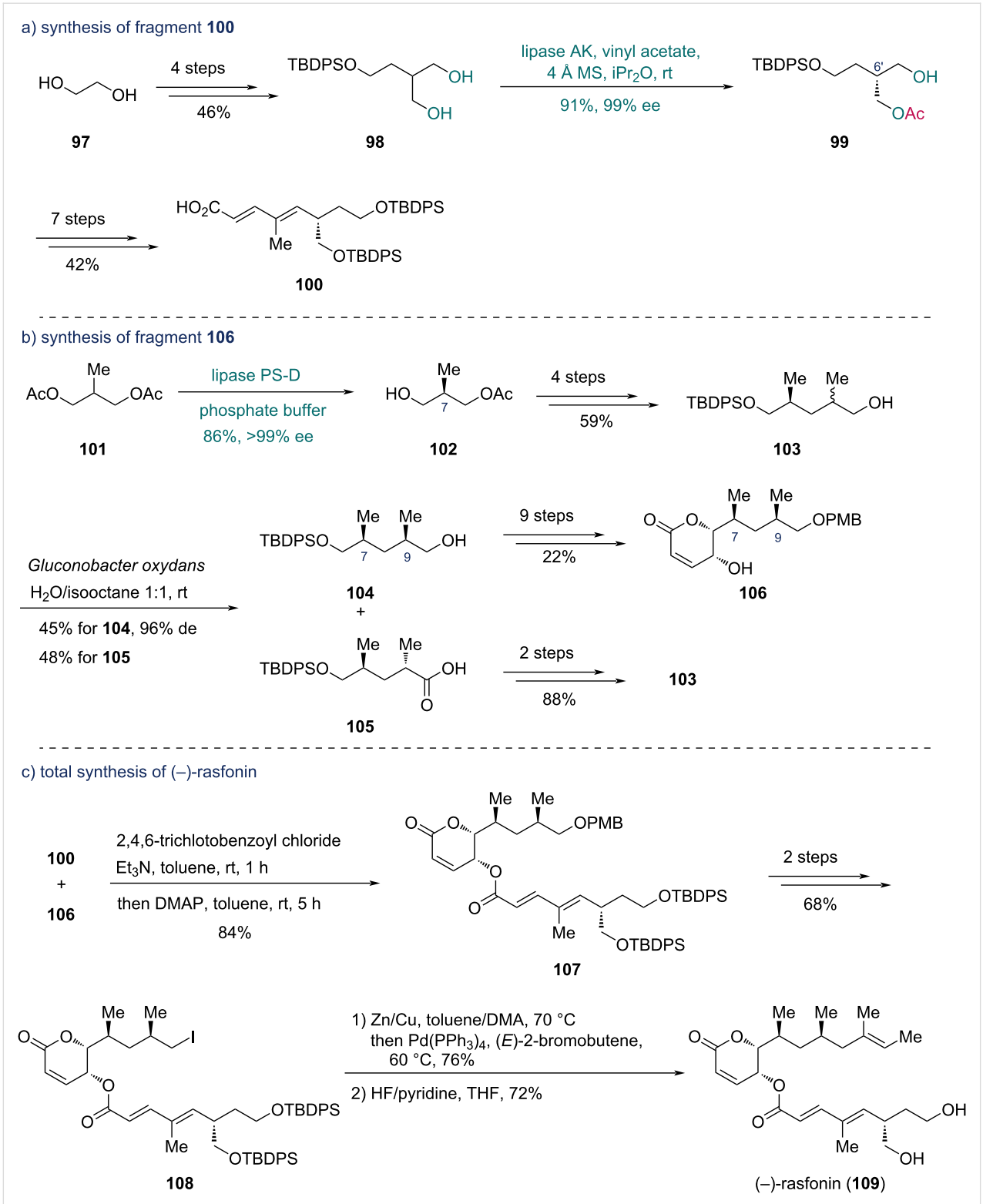

Scheme 15: Nanda's synthesis of a) fragment **100**, b) fragment **106** and c) (–)-rasfonin (**109**).

quent two-step transformation yielded compound **108**, which underwent Stille coupling with (*E*)-2-bromobutene followed by desilylation to afford (−)-rasfonin (**109**).

In 2009, Davies and co-workers disclosed the asymmetric synthesis of (+)-pilocarpine and (+)-isopilocarpine using an enzyme-catalyzed acetylation with *Pseudomonas fluorescens*

lipase (PFL) (Scheme 16) [48]. Treatment of diol **110** with PFL and vinyl acetate gave monoacetate **111** in 98% yield and >98% ee. Subsequently, monoacetate **111** was converted into compound **112** with a 1,3-dioxan-2-one moiety in three steps, which underwent Pd-catalyzed decarboxylation/carbonylation to form the lactone **113**. The *N*-methylimidazole ring was installed through a three-step sequence to give lactone **114**. Finally, hydrogenation of **114** provided (+)-pilocarpine (**115**) and (+)-isopilocarpine (**116**) in a ratio of 72:28. Treatment of the mixture with HNO_3 followed by recrystallization afforded the nitrate salt of **115** (**115**·HNO_3) in 70% yield from **114**.

In 2008, the Ōmura group completed the total synthesis of salinosporamide A, a marine-derived natural product with anticancer activity, featuring an enzymatic desymmetrization (Scheme 17) [49]. To establish the C4 chiral center, prochiral diol **118** (prepared from known compound **117**) was treated with lipase from *Pseudomonas* sp. (WAKO) and vinyl acetate, affording the corresponding monoacetate. Subsequent reaction with *tert*-butyldiphenylsilyl chloride (TBDPSCl) and imidazole provided compound **119** in 94% yield over two steps with 97% ee. Next, compound **120** was obtained in six steps from **119**. A stereoselective aldol reaction installed the cyclohexanone ring into **120**, and the resulting hydroxy group was protected to give ketone **121**. The γ-lactam moiety of compound **122** was then constructed in subsequent 12 steps. SmI_2-mediated intermolecular Reformatsky-type reaction with aldehyde **123** yielded compound **124**. Finally, salinosporamide A (**125**) was obtained through a 12-step sequence from **124**.

Desymmetrization via transition-metal-catalyzed acylation

Although enzymatic acylation reactions are widely employed in total synthesis, certain substrates are incompatible with acylation catalyzed by existing lipases. Inspired by enzymatic reactions, chemists have developed a series of catalysts composed of transition-metal cores and chiral ligands, which have been applied to various asymmetric reactions [50-52]. Compared to the enzymatic methods, the transition-metal-catalyzed approach may provide an advantage to access both enantiomers of the product in the same process by employing the antipodal ligand, as both enantiomers of the chiral ligand are normally accessible. Additionally, the substrate scope can be broadened by modifying the ligand's structure.

Early in 1984, Ichikawa and co-workers reported a Sn-mediated enantioselective acylation of glycerol derivatives [53]. Since then, desymmetrization strategies for prochiral 1,3-diols involving transition-metal-catalyzed acylation have been developed. Trost and co-workers then developed a Zn-based catalyst for asymmetric aldol reactions [54,55], later adapting it to the desymmetrization of 1,3-diols in 2003 [56]. Subsequent advances included Cu-based complexes developed by Kang and co-workers [57,58], first applied in total synthesis in 2008. In

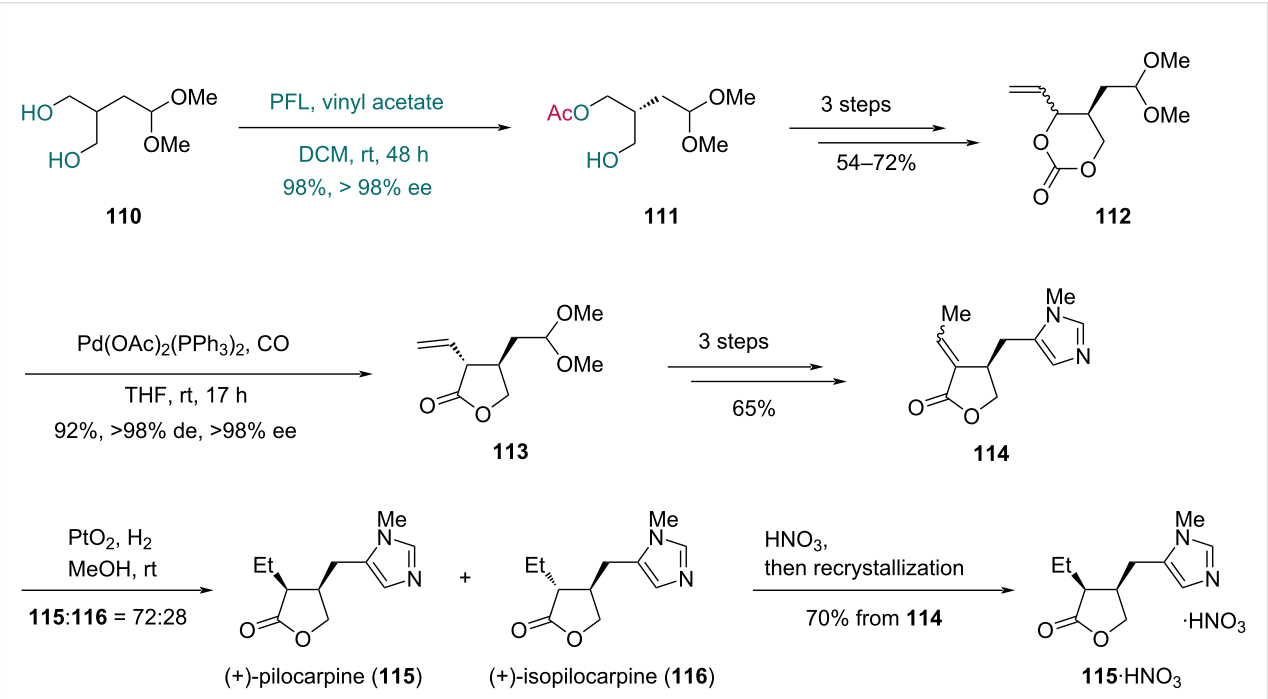

Scheme 16: Davies' synthesis of (+)-pilocarpine (**115**) and (+)-isopilocarpine (**116**).

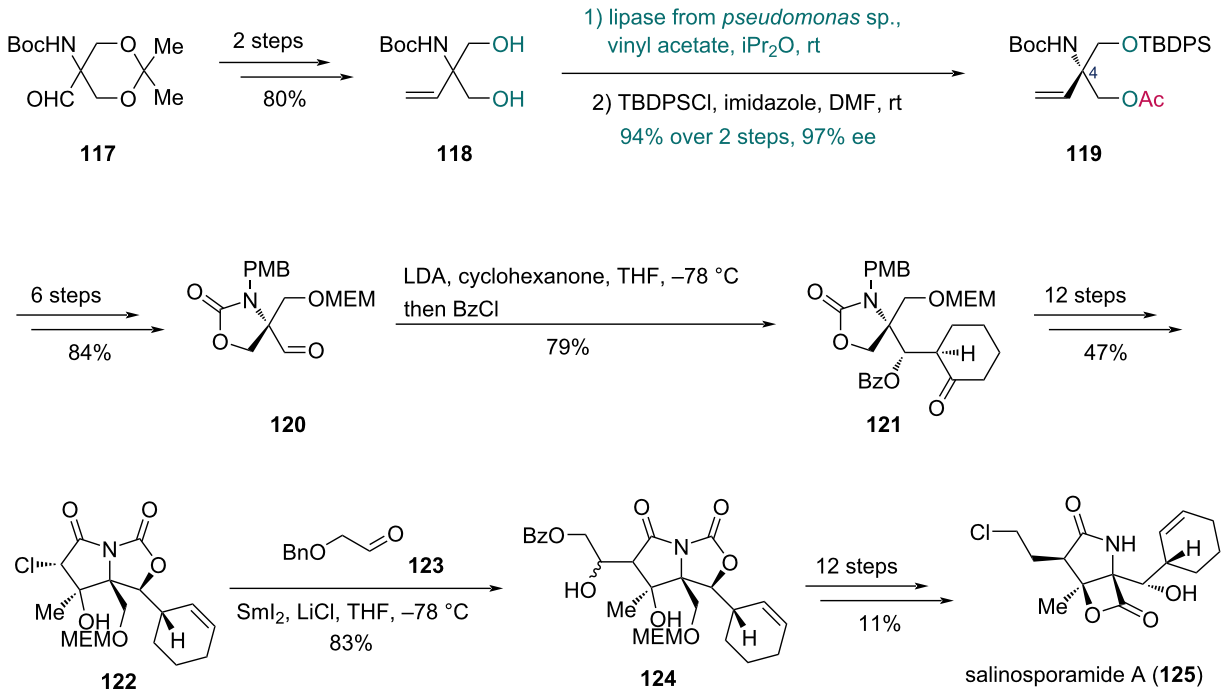

Scheme 17: Ōmura's synthesis of salinosporamide A (**125**).

this section, examples of transition-metal-catalyzed acylations of prochiral 1,3-diols in total synthesis are discussed, including Cu-catalyzed and Zn-catalyzed acylation reactions.

Cu-catalyzed acylation

In 2008, Kang and co-workers demonstrated the first use of Cu-catalyzed enantioselective acylation [57,58] in the synthesis of L-cladinose (Scheme 18) [59]. In the presence of catalyst **128**, triol **127**, prepared from compound **126** in two steps, was converted into (*R*)-**130** with 98% yield and 91% ee, which was subjected to a four-step sequence to give compound **131**. In this reaction, catalyst **128** proved most effective. As previously reported [57], installing a sterically demanding or electronically influential group on the pyridine moiety enhanced the reaction performance. However, excessively bulky substituents at C4 and substitutions at both C4 and C5 hindered the coordination between substrate and catalyst, and led to reduced enantioselectivity. As to the structure of **128**, the electronic effect of the bromo-substituted pyridine moiety favored complexation, while the phenyl substitution at C4 promoted a stable coordination-bond formation. Alternatively, (*S*)-**130** could be furnished using Cu complex **129** in the desymmetrization step with comparable efficiency (98% yield and 91% ee), and was likewise transformed into **131** in four steps. Epoxidation of **131** followed by methylation generated epoxide **132**. Construction of the lactone moiety commenced with the oxidative cleavage of the double bond, and the resulting carboxylic acid underwent intramolecular cyclization in the presence of $BF_3{\cdot}Et_2O$ to give lactone **133**. Subsequent hydride reduction induced rearrangement of **133** to form the pyranose skeleton of L-cladinose (**134**). Finally, the derivative, thiocladinoside **135** was then prepared from **134** in two additional steps.

The total synthesis of azithromycin [60] was reported shortly after completion of **135** (Scheme 19). For the synthesis of fragment **139**, epoxide **136** was first prepared from (*R*)-**130** in two steps. Parikh–Doering oxidation of **136** followed by addition with Et_2Zn in the presence of ligand **137** afforded alcohol **138**, which was subsequently converted into amine **139** via a seven-step sequence.

With the fragments **135** and **139** in hand, synthesis of the third fragment **146** was then pursued and further elaborated to complete the synthesis of azithromycin (Scheme 20). Triol **141** was first prepared in two steps from iodide **140**. Subsequent Cu-catalyzed desymmetrization with catalyst **129**, benzoyl chloride (BzCl) and Et_3N, enabled the synthesis of monobenzoate **142** in 94% yield along with 4% yield of its diastereomer (dr = 24:1). Following a four-step conversion of **142** to epoxide **143**, reductive cleavage produced a diol intermediate, which was subjected to chemoselective glycosylation with compound **144** to provide compound **145**. After a four-step transformation of **145**,

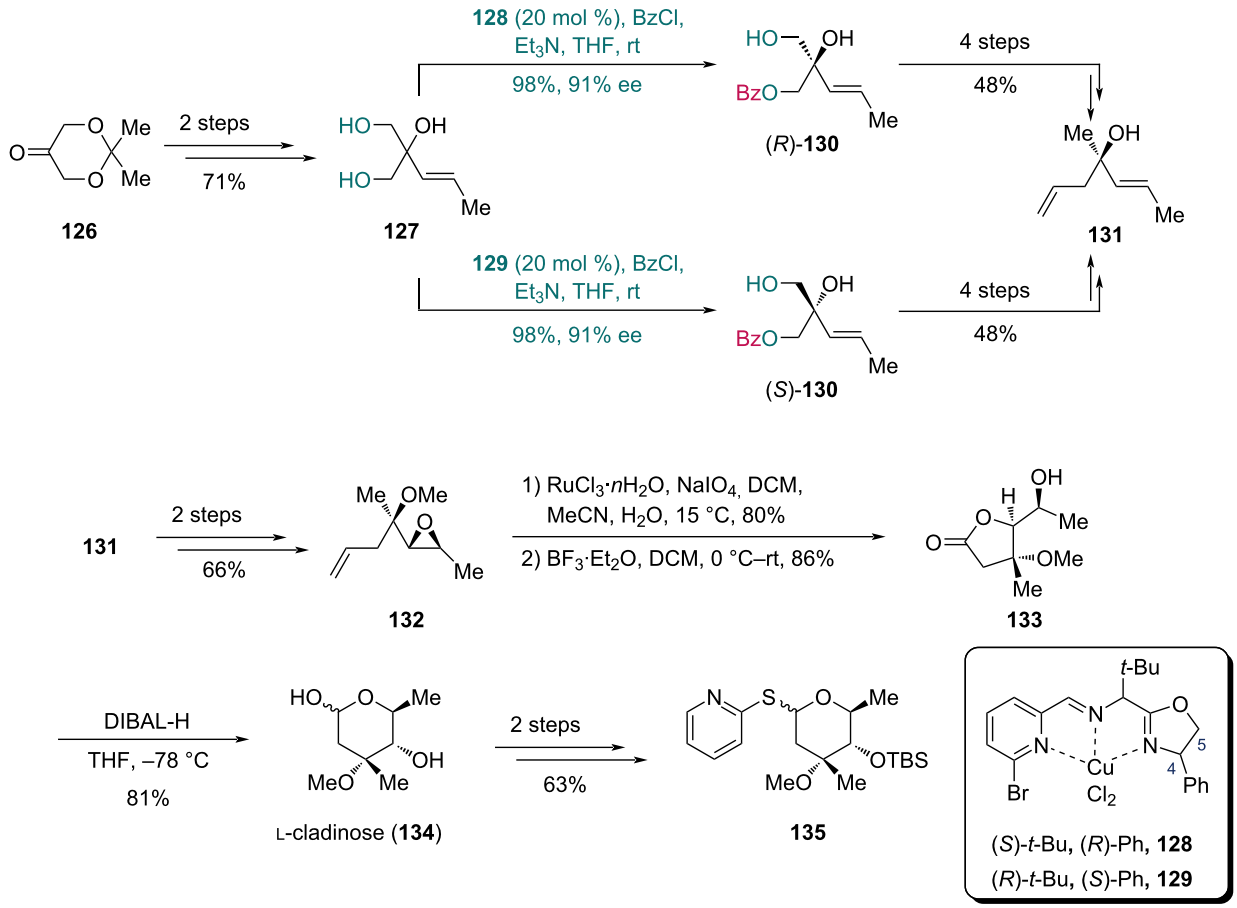

Scheme 18: Kang's synthesis of L-cladinose (**124**) and its derivative.

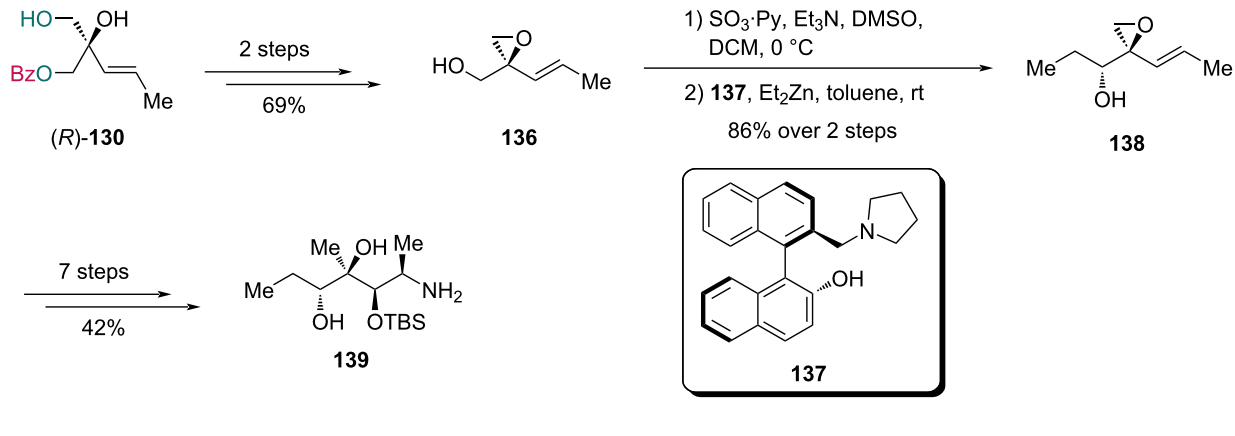

Scheme 19: Kang's preparation of fragment **139**.

compound **146** was oxidized with Dess-Martin periodinane (DMP). Subsequent reductive amination with fragment **139** provided an intermediate, which underwent the second reductive amination using formaldehyde. This one-pot process with concomitant deprotection afforded acid **147** in 70% yield over two steps. Macrocyclization of **147**, followed by glycosylation with

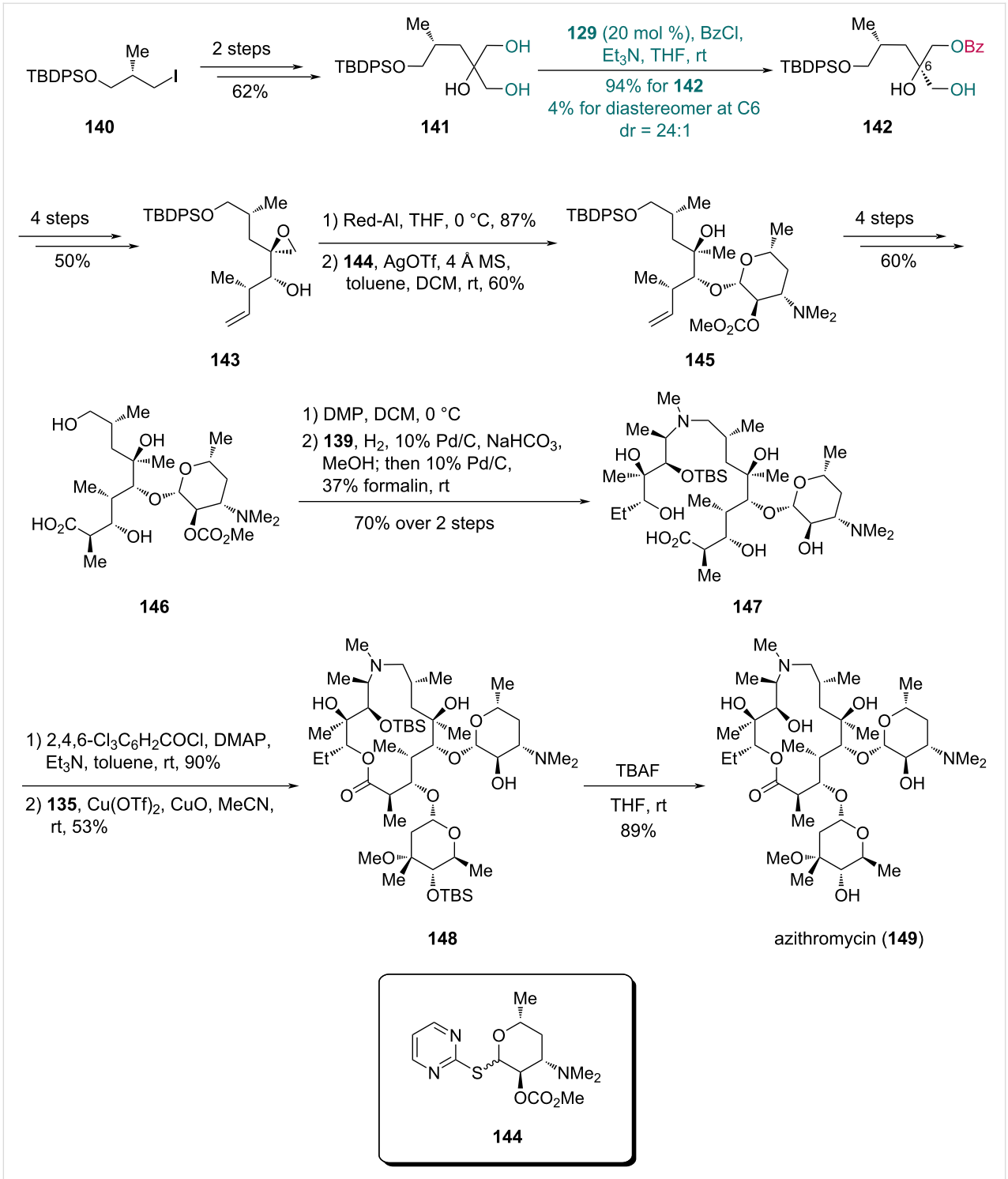

Scheme 20: Kang's synthesis of azithromycin (**149**).

135, gave compound **148**, which was converted into azithromycin (**149**) upon desilylation.

This desymmetrization strategy was also employed in the synthesis of (−)-dysiherbaine reported by Kang and co-workers in 2012 (Scheme 21) [61]. Their synthesis commenced with compound **150**, which was converted into triol **151** in two steps. Treatment of triol **151** with catalyst **128** furnished monobenzoate **152** in 96% yield and 97% de. Subsequently, monobenzoate **152** was transformed into diene **153** in five steps. The *cis*-

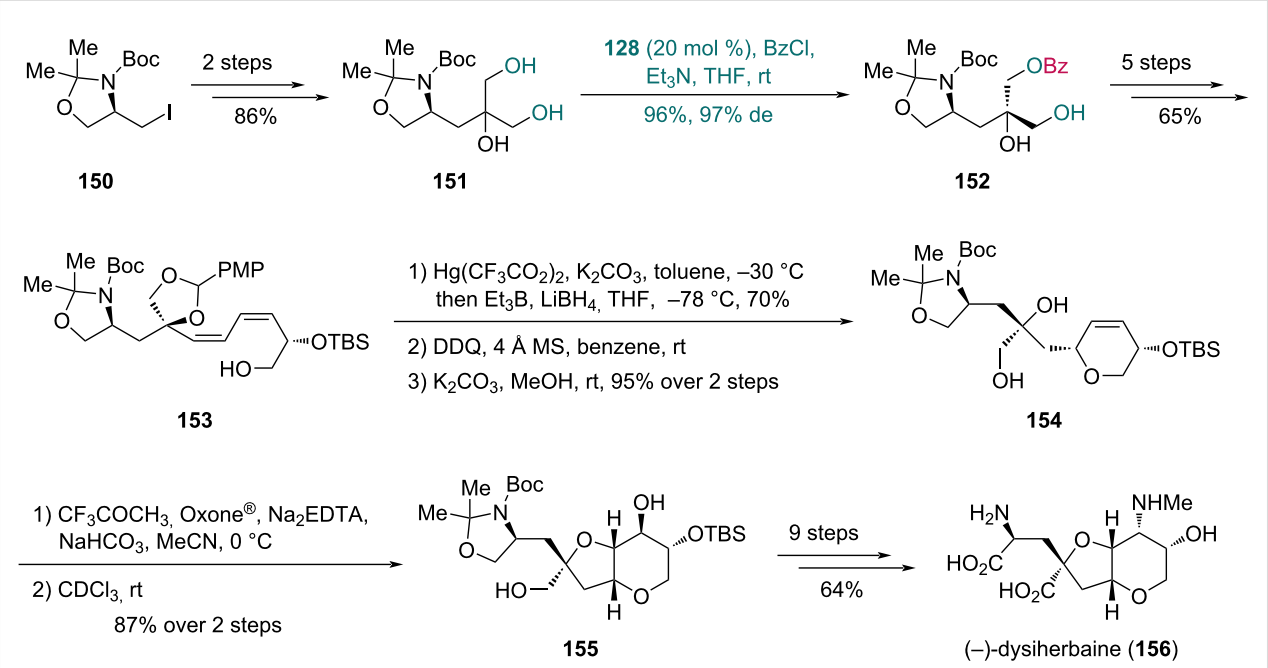

Scheme 21: Kang's synthesis of (–)-dysiherbaine (**156**).

3,6-disubstituted dihydropyran ring was assembled via a one-pot mercuriocyclization/reductive demercuration of **153** followed by two-step diol-deprotection to access compound **154**. Using trifluoromethylmethyldioxirane, which was generated in situ from trifluoroacetone, Oxone®, and disodium ethylenediaminetetraacetate dihydrate (Na_2EDTA), compound **154** underwent epoxidation followed by acid-mediated cyclization to yield bicyclic compound **155**. The synthesis was completed through a nine-step conversion of **155** to obtain (−)-dysiherbaine (**156**).

To construct the asymmetric quaternary carbon centers with an amino group, the Kang group developed a desymmetrization strategy for serinol derivatives using a bisoxazoline (BOX)–$CuCl_2$ complex as catalyst in 2008 [62]. They further applied this method in 2013 to the synthesis of (−)-kaitocephalin, a glutamate receptor antagonist from *Eupenicillium shearii* (Scheme 22) [63]. Diol **158**, which was accessed in two steps from diester **157**, underwent enantioselective monobenzoylation with complex **159** as catalyst to form benzoate **160** in 90% yield with 90% de. The size of the C4-substituent in the oxazoline moiety crucially influenced the enantioselectivity and conversion of the reaction: smaller substituents reduced the differential ability between two hydroxy groups, while bulky substituents hindered the formation of coordination bonds between the substrate and catalyst. As previously reported, with a suitable substituent at C4, an additional C5-substituent slightly enhanced the catalytic performance of the complex [62]. For diol **158**, the ligand with only isopropyl substitution at C4 proved effective with suitable size for the substrate–catalyst coordination. A subsequent two-step sequence enabled the sythesis of olefinic carbamate **161** from benzoate **160**. Treatment of **161** with $Hg(CF_3CO_2)_2$ induced mercuriocyclization, followed by reductive demercuration with $LiBH_4/Et_3B$ to construct the pyrrolidine ring of compound **162**. A three-step transformation of **162** yielded compound **163**, which was subjected to base-mediated cyclization with concomitant debenzoylation to deliver oxazolidinone **164**. Through a four-step sequence, oxazolidinone **164** was then converted into triester **165**, which was further transformed into (−)-kaitocephalin (**166**) as its diethylamine salt in three additional steps.

In Kang's synthesis of laidlomycin in 2016 (Scheme 23) [64], the BOX–$CuCl_2$ complex **168** effectively catalyzed the desymmetrization of triol **167**, affording monobenzoate **169** in 97% yield with 96% ee. For 2-alkyl-substituted glycerols like triol **167**, complex **168** is the most efficient catalyst as the BOX ligand with a benzyl substitution at C4 provided an appropriate size for the catalyst–substrate coordination [58]. The intermediate **169** was transformed into alcohol **170** in nine steps. Subsequent epoxidation of olefin in **170** followed by acid-mediated cyclization provided compound **171** bearing a tetrahydrofuran ring. An eight-step transformation then yielded compound **172**. Next, epoxidation of olefin of **172** with Shi's dioxirane (generated from ketone **173**) and the following acid-mediated cyclization formed another tetrahydrofuran ring. The resulting com-

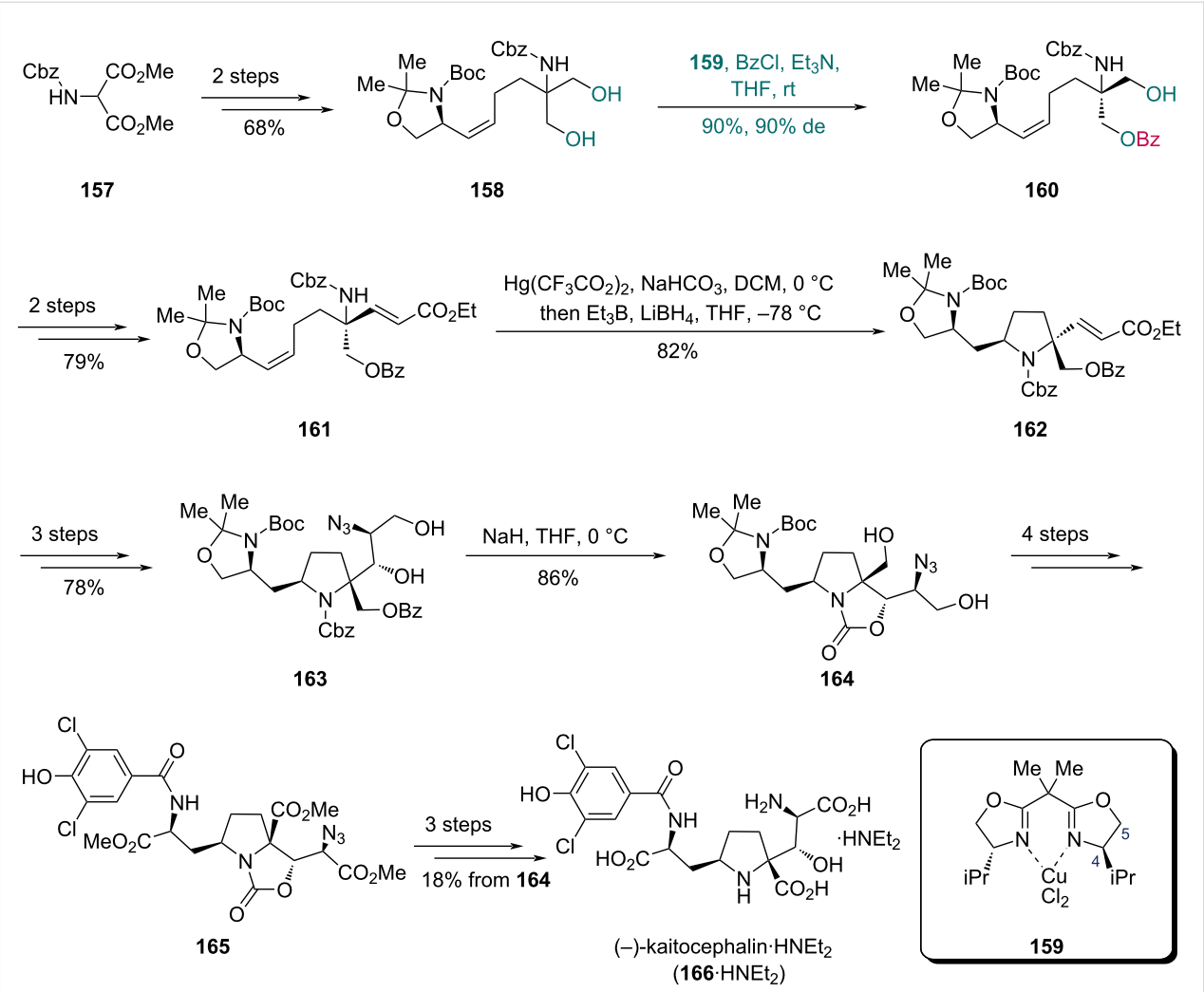

Scheme 22: Kang's synthesis of (–)-kaitocephalin (**166**).

pound was then converted into lactone **174** via 2,2,6,6-tetramethylpiperidin-1-oxyl (TEMPO)-mediated oxidation. Lactone **174** was then converted into aldehyde **175** in three steps, which underwent Horner–Wadsworth–Emmons (HWE) olefination with β-ketophosphonate **176** to produce *trans*-enone **177** as the sole product. Ester **178**, prepared in three steps from **177**, first underwent cyclization via hydrogenation to generate spiroketals as a 1:1 mixture. This intermediate was then isomerized under acidic conditions to the desired spiroketal **179**, which was ultimately converted into laidlomycin sodium salt (**180**) in two additional steps.

In 2011, the Kang group developed an enantioselective desymmetrization strategy for 2,2-disubstituted 1,3-propanediols catalyzed by a pyridinebisoxazoline (PyBOX)–$CuCl_2$ complex [65]. Snyder and co-workers applied this method to synthesize arboridinine, an indole alkaloid isolated from a Malaysian *Kopsia* species (Scheme 24) [66]. The synthesis commenced with *tert*-butyloxycarbonyl (Boc)-protected tryptamine **181**, which was converted into diol **182** in two steps. Initial attempts to forge the chiral center at C16 via enzyme-catalyzed monoacylation proved unsatisfactory and provided a low yield and ee (39% and 34%, respectively). In contrast, a $CuCl_2$ complex bearing a PyBOX-derived ligand **183** effectively catalyzed the desymmetrization of **182**, giving benzoate **185** in 72% yield. The C5-subsituents of ligand **183** are important to adjust the conformation of the ligand to provide suitable space for the smaller group. It is observed that the attachment of two *n*-butyl groups at the C5 position is beneficial for the reaction [65]. Although the ee of monobenzoate **185** was undetermined, azepinoindole **186** prepared in two steps from **185** exhibited 96% ee, indicating high enantioselectivity in the desymmetrization step. A four-step sequence was adopted to convert **186** into ynone **187**, which underwent a Ag-mediated 6-*endo-dig* cycli-

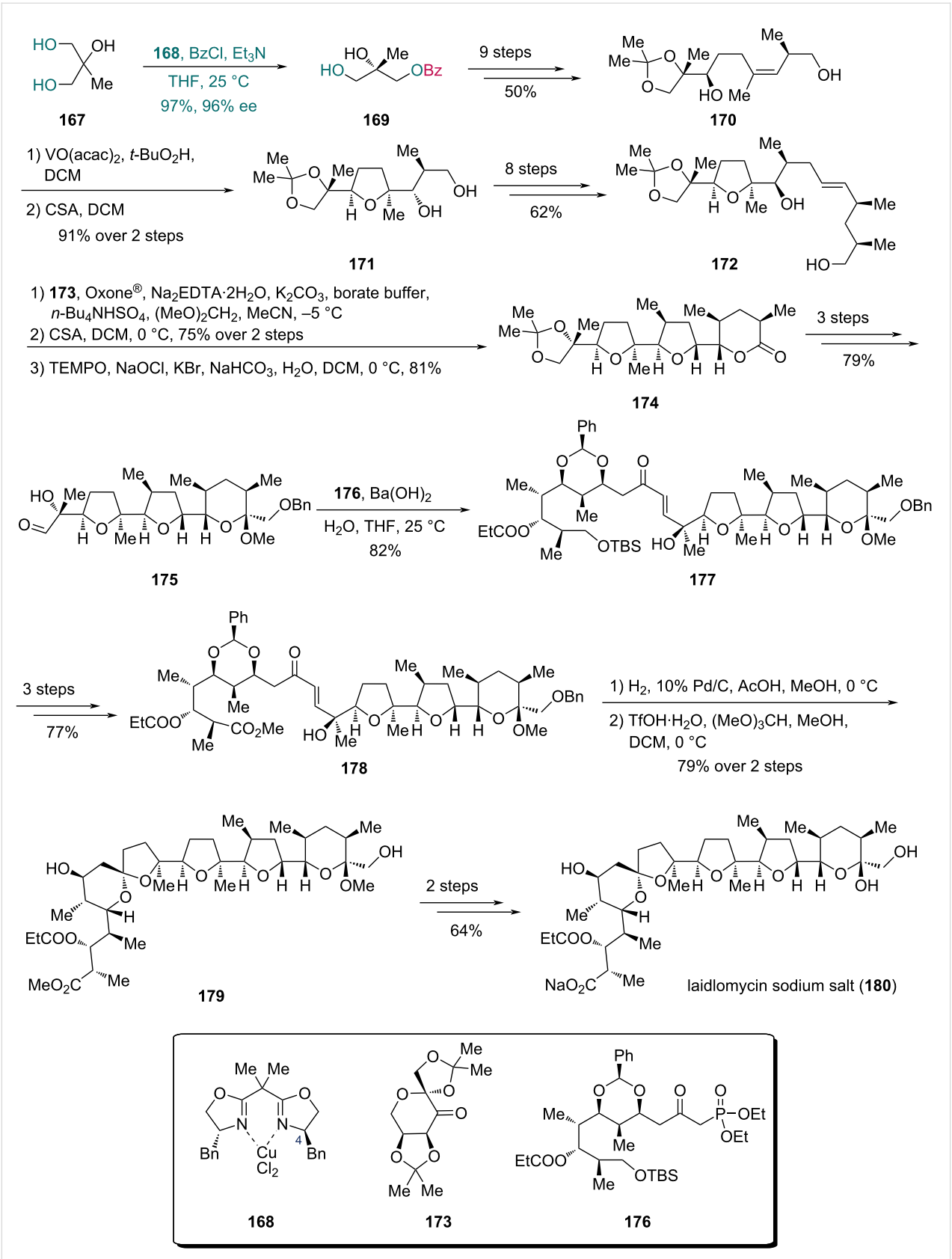

Scheme 23: Kang's synthesis of laidlomycin (**180**).

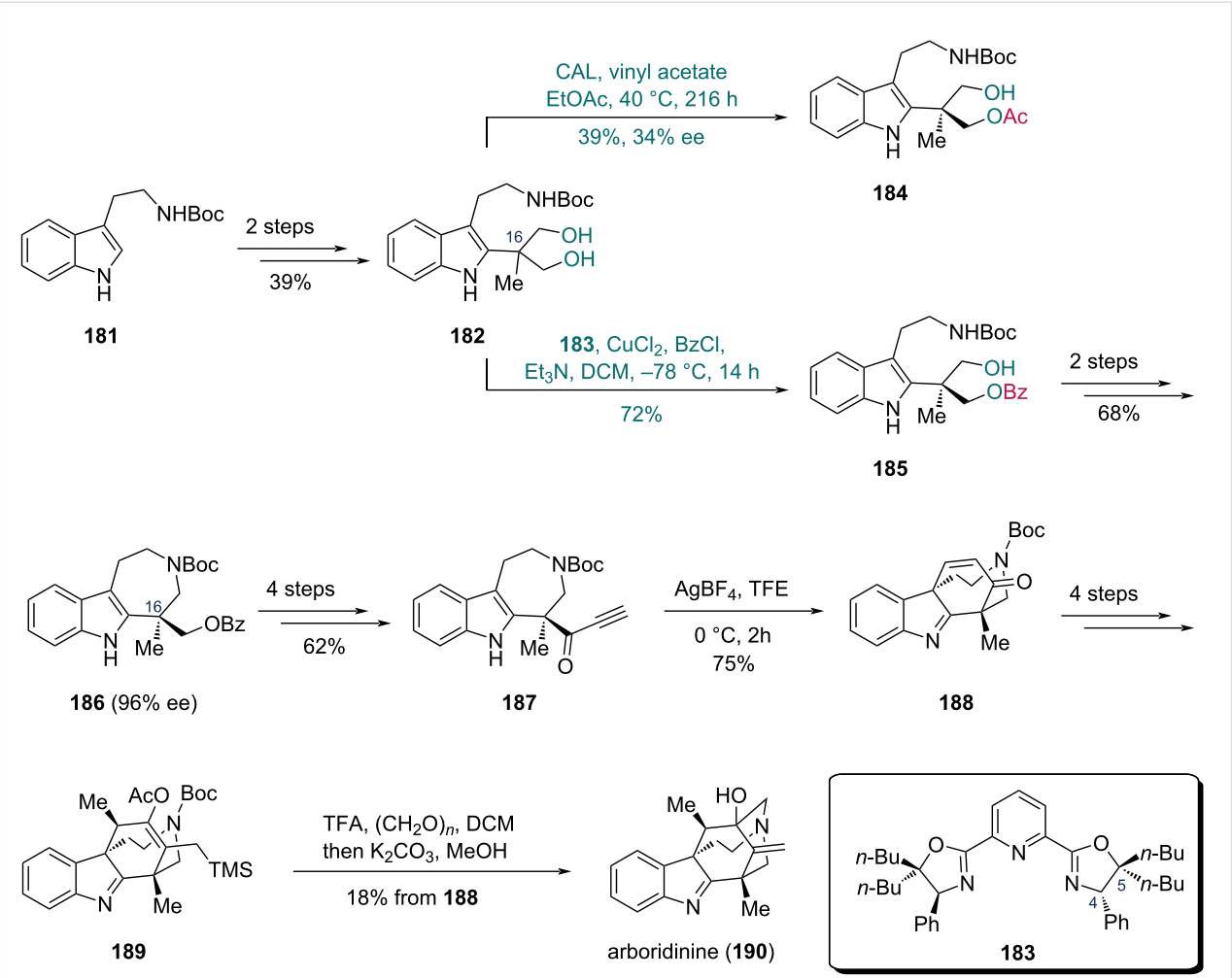

Scheme 24: Snyder's synthesis of arboridinine (**190**).

zation in trifluoroethanol (TFE) to produce enone **188** containing the tetracyclic core of arboridine. In the presence of trifluoroacetic acid (TFA) and paraformaldehyde, compound **189**, prepared from **188** in four steps, underwent aza-Prins cyclization to form the caged skeleton, and the following acetate hydrolysis afforded arboridinine (**190**) in 38% yield over two steps.

In 2024, Ma and co-workers accomplished their synthesis of (+)-alstrostine G with a Cu-catalyzed asymmetric desymmetrization as the key step (Scheme 25) [67]. Diol **192** with a 1,1-disubstituted tetrahydro-β-carboline (THBC) core was prepared from tryptamine derivative **191** via a two-step sequence comprising a Pictet–Spengler reaction followed by reduction. Screening of enantioselective monobenzoylation conditions revealed that using a Cu-based complex composed of 4-(1-naphthylbenzyl)-substituted BOX ligand **193** and $CuCl_2$ with Et_3N and BzCl in THF solution afforded optimal results in terms of both isolated yield and ee. Under these optimized conditions, diol **192** was transformed into monobenzoate **194** in 70% yield with 76% ee, and further recrystallization enhanced the enantiopurity to 97% ee with 61% yield. TBS protection of the hydroxy group in **194** afforded compound **195**. A three-step sequence comprising removal of the benzyl group, chemoselective *N*-alkylation with fragment **196**, and removal of the benzoyl group allowed the conversion of **195** into iodide **197**. Sequential oxidation of the alcohol, HWE reaction, and reduction of the resulting ester then provided compound **198**. In the presence of $Pd(OAc)_2$, PPh_3, and Et_3N in MeCN, the intramolecular Heck/hemiamination cascade reaction of **198** delivered the 5-*exo* cyclization product **199**, simultaneously constructing the fused D and E rings in a single transformation. Three additional steps converted **199** to hydroxy ketone **200**, which underwent SmI_2-mediated deoxygenation of **200** and ketone reduction to give compound **201**. Stereoselective hemiaminal ether formation promoted by $BF_3{\cdot}Et_2O$ with subsequent desilylation

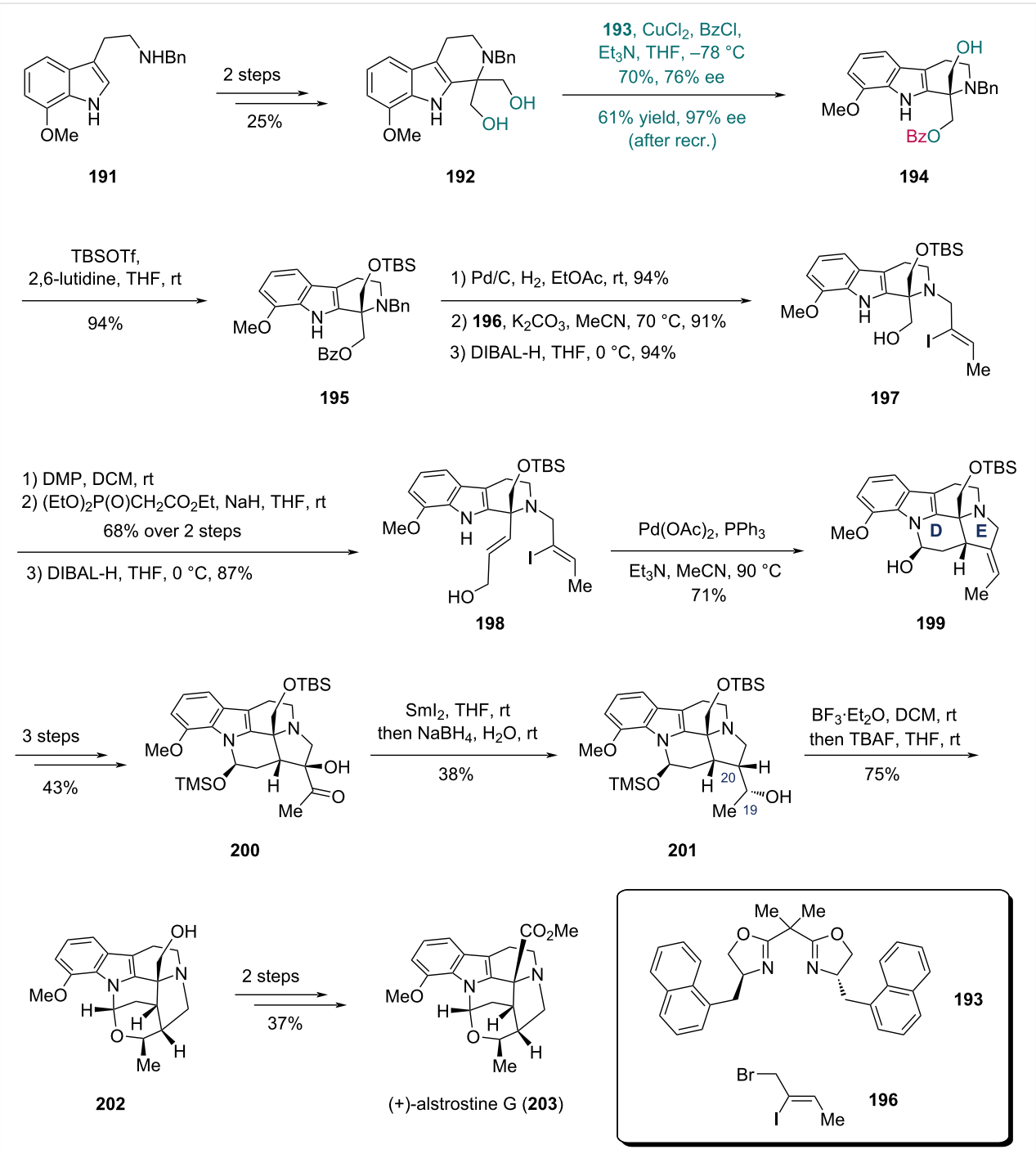

Scheme 25: Ma's synthesis of (+)-alstrostine G (**203**).

constructed the hexacyclic framework of alstrostine G, yielding compound **202**. Finally, (+)-alstrostine G (**203**) was obtained through a two-step sequence.

Zn-catalyzed acylation

Zn-based complexes are another class of effective catalysts used in desymmetrization of 1,3-diols, as reported by Trost and co-worker in 2003 [56]. In 2013, Trost et al. developed the synthesis of (−)-18-*epi*-peloruside A (Scheme 26) [68], and converted diol **204** into enantioenriched monobenzoate **206** using a catalyst composed of $ZnEt_2$ and ligand **205a**, affording the product in 99% yield and 86% ee. Although in their previous report [56], the ligand **205b** with a 4-biphenylyl substitution was more efficient than the phenyl-substituted **205a** in the

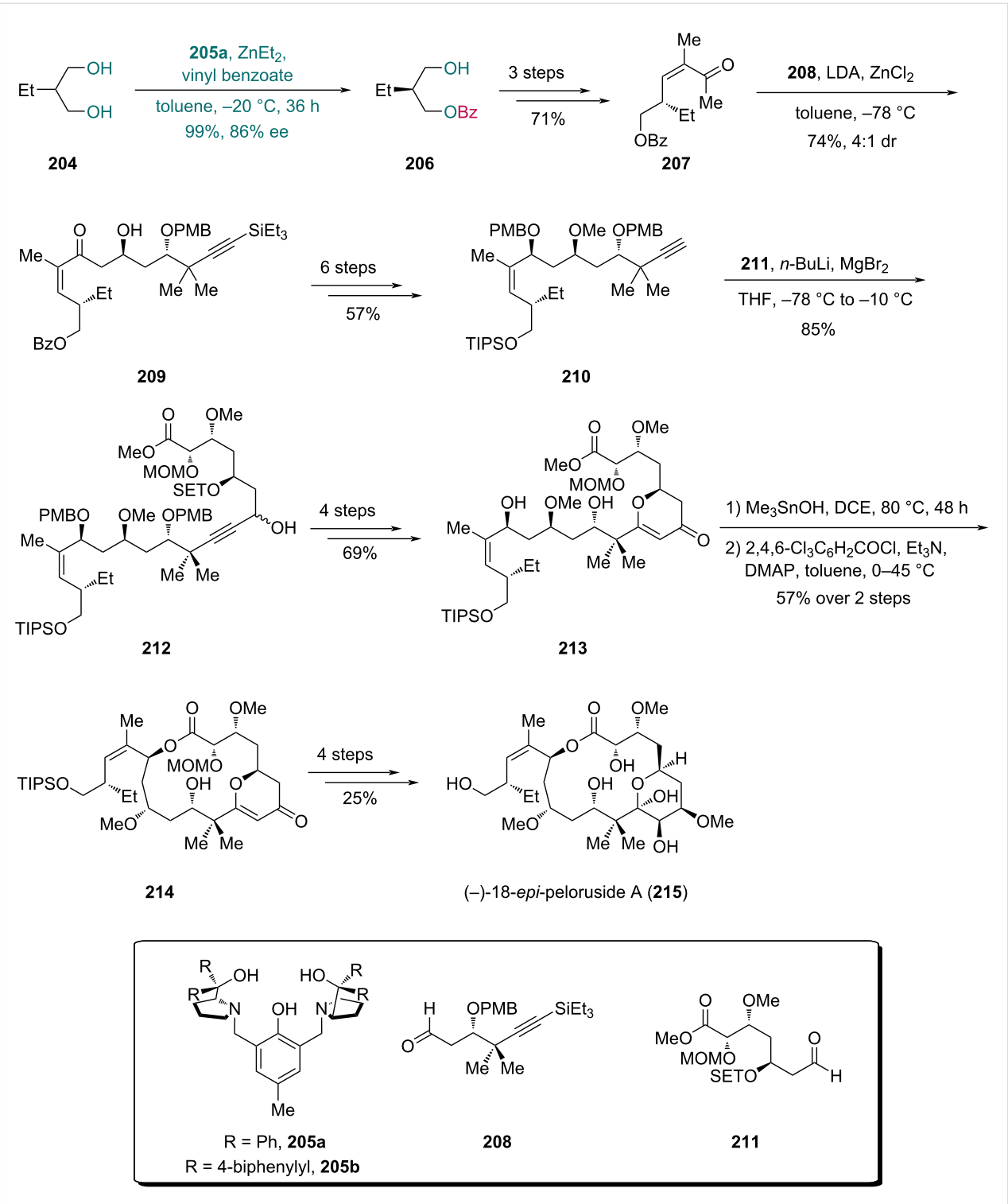

Scheme 26: Trost's synthesis of (–)-18-*epi*-peloruside A (**215**).

desymmetrization of 2-arylpropane-1,3-diols, ligand **205a** proved to be suitable for 2-ethylpropane-1,3-diol (**204**). A three-step sequence then furnished enone **207**, which underwent diastereoselective aldol reaction with fragment **208** to give compound **209**. Alkyne **210**, prepared from **209** in six steps, underwent addition with fragment **211** to yield compound **212**. Four subsequent steps, including oxidation of propargylic alcohol and cyclization between the hydroxy group and ynone,

provided compound **213** with a pyranone ring. Treatment of **213** with Me_3SnOH hydrolyzed the methyl ester, and intramolecular Yamaguchi esterification then led to lactone **214**, which was transformed into (−)-18-*epi*-peloruside A (**215**) in four steps.

In 2020, Lindel and co-workers reported their synthesis of (−)-dihydroraputindole D, featuring a Zn-catalyzed enantioselective benzoylation as the key step (Scheme 27) [69]. Using propargylic alcohol **217**, which was prepared from dihydroxyketone **216** in two steps, Sonogashira coupling with indoline **218** followed by acetylation afforded compound **219**. A Au-catalyzed cyclization and subsequent saponification with NaOMe gave indoline **220**. Three subsequent steps yielded diol **221**, which was treated with vinyl benzoate and a Zn-complex derived from Et_2Zn and phenol **205** to afford benzoate **222** in 91% yield with 84:16 er. Finally, an eight-step sequence provided (−)-dihydroraputindole D (**223**).

Local desymmetrization

Apart from enzymatic and transition-metal-catalyzed desymmetrization reactions, compounds with specific structures might also enable the desymmetrization by discriminating prochiral 1,3-diols in a diastereotopic manner. This strategy is termed as "local desymmetrization" [19,70].

In 1987, Iwata and co-workers completed the synthesis of (−)-talaromycin B and (+)-talaromycin A, two toxic metabolites from the fungus *Talaromyces stipitatus*, featuring asymmetric induction to forge chiral centers using a chiral sulfinyl group [71]. With their previously reported strategy [72], the chiral sulfinyl-containing diol **225** was prepared from diester **224** in eight steps (Scheme 28a). Treatment of **225** with $ZnCl_2$ afforded dioxabicyclic compound **226**. Regioselective hydrolysis of **226** with TFA yielded a dihydropyran intermediate, which was benzylated to deliver **227**. Desilylation of **227** gave diol **228**, which underwent intramolecular Michael reaction to form bicyclic compound **230** as a single stereoisomer (87% yield over two steps). This scaffold with the desired C6 chiral center was constructed via intermediate **229**, where the sulfinyl group induced K^+–oxygen chelation to form a six-membered transition state prior to protonation from the less hindered face. Acid-mediated epimerization at C9 of **230** yielded compound **231**, which was transformed into (−)-talaromycin B (**232**) in six steps. For (+)-talaromycin A (**235**) (Scheme 28b), a three-step transformation of **230** gave **233**, and subsequent isomerization at the C6 spirocenter with TFA produced compound **234**, which was converted into **235** in three additional steps.

The introduction of an inducing group such as a chiral sulfinyl group is effective in local desymmetrization, while substrates

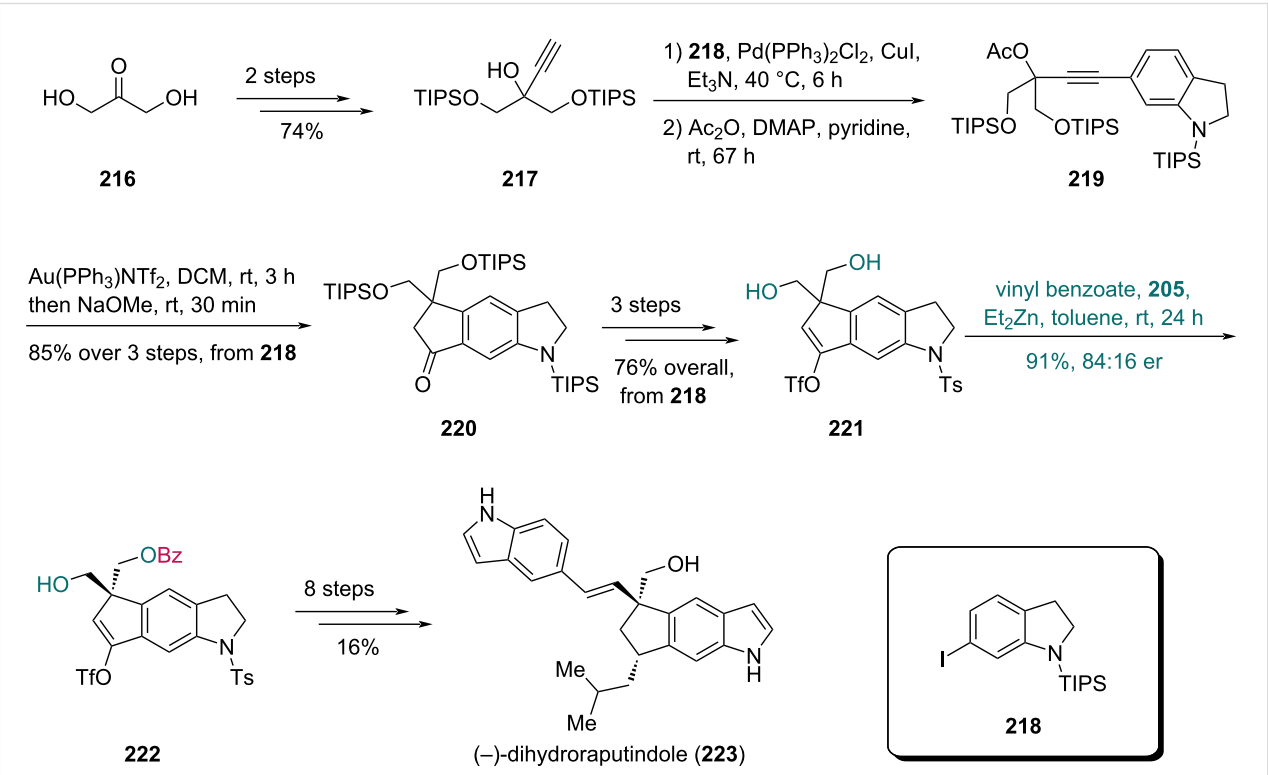

Scheme 27: Lindel's synthesis of (–)-dihydroraputindole (**223**).

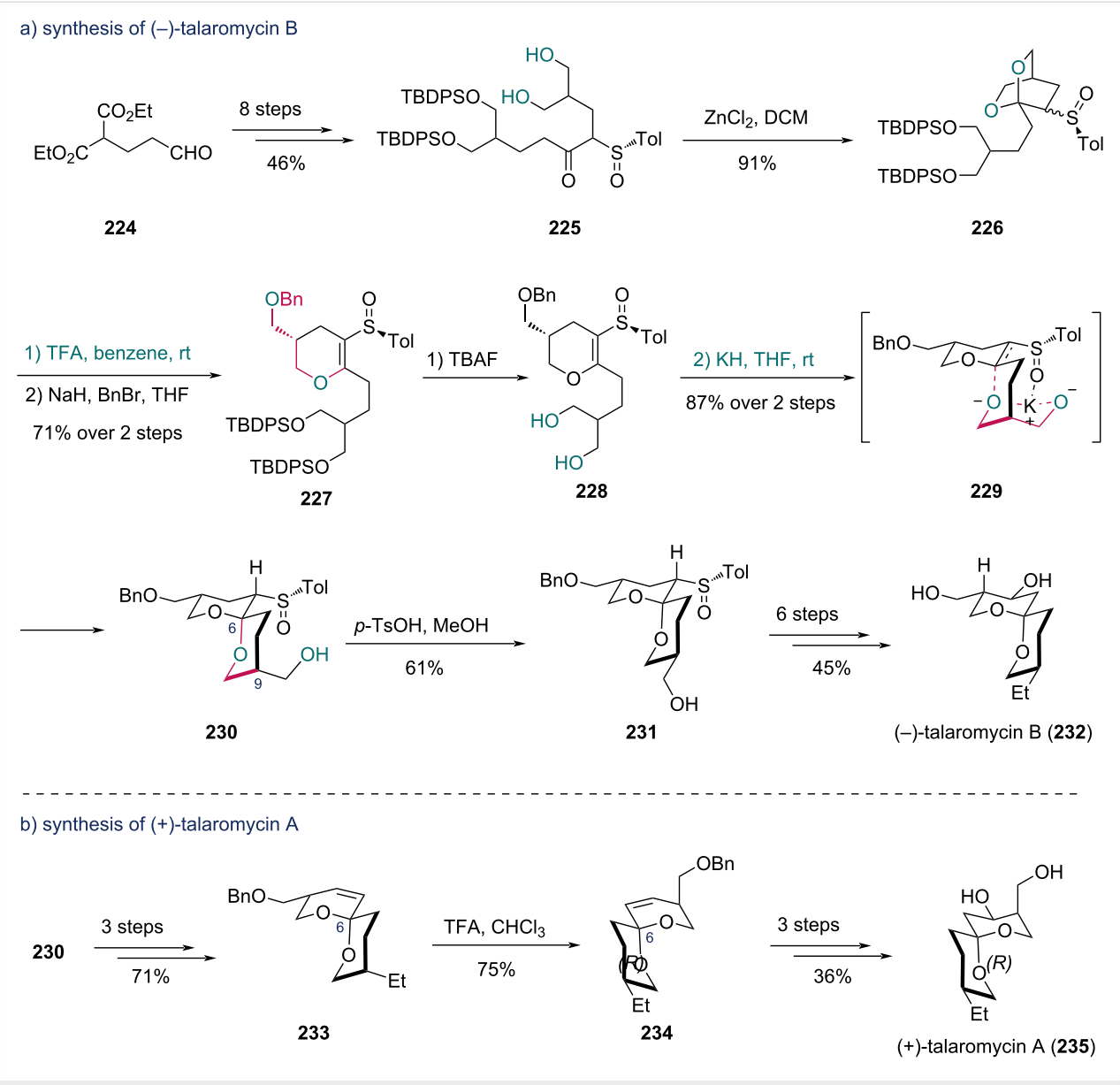

Scheme 28: Iwata's synthesis of a) (–)-talaromycin B (**232**) and b) (+)-talaromycin A (**235**).

bearing caged frameworks and multiple chiral centers can also realize the desymmetrization. The Cook group reported the first total synthesis of (−)-vincamajinine and (−)-11-methoxy-17-epivincamajine, featuring a stereospecific cyclization as the key step (Scheme 29a) [73,74]. To obtain the cyclization precursor **238**, the prochiral diol **237** was prepared from (+)-N_a-methylvellosimine (**236**) via a Tollens reaction. Subsequently, regioselective Ley–Griffith oxidation of **237** selectively targeted the C17 hydroxy group, affording aldehyde **238** in 78% yield with >10:1 dr. The high diastereoselectivity observed in the oxidation of the 1,3-diol indicated that the complex structure of the substrate could provide an environment of desymmetrization. The stereospecific cyclization of **238** was performed with trifluoroacetic acid (TFA) and Ac_2O, along with acetylation of the free hydroxy group, to deliver compound **239** in high yield. A further six-step sequence completed the synthesis of (−)-vincamajinine (**240**). With the same strategy, (−)-11-methoxy-17-epivincamajine (**245**) was prepared from (+)-N_a-methyl-16-epigardneral (**241**) (Scheme 29b). The synthesis of **244** was achieved through a similar sequence of steps: Tollens reaction of **241**, regioselective oxidation of diol **242**, and acidic cyclization of aldehyde **243**. Compound **244** was then converted into **245** in five additional steps.

The benzylic oxidative cyclization of indole derivatives mediated by 2,3-dichloro-5,6-dicyano-1,4-benzoquinone (DDQ) is

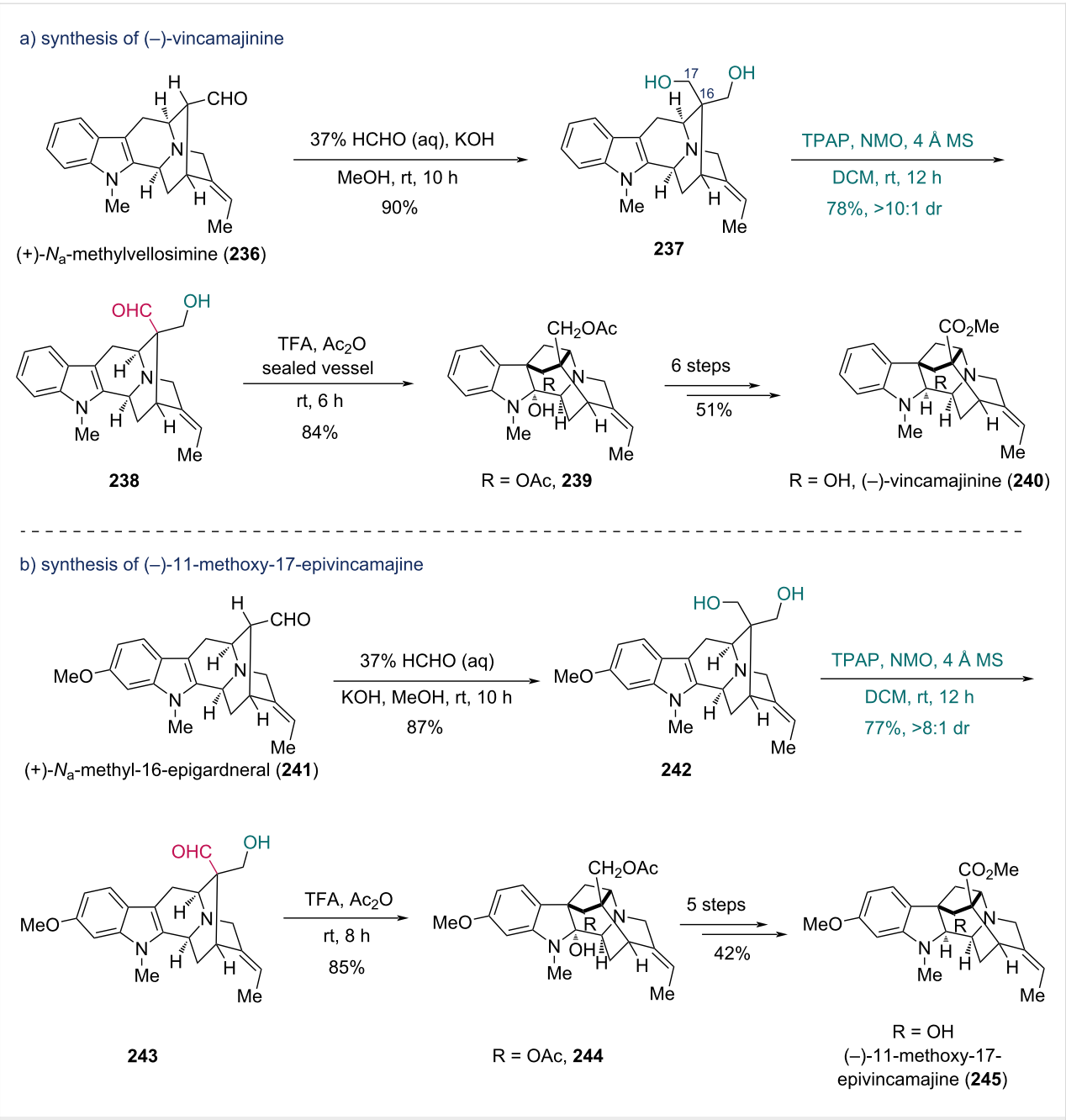

Scheme 29: Cook's synthesis of a) (–)-vincamajinine (**240**) and b) (–)-11-methoxy-17-epivincamajine (**245**).

an efficient strategy that the Cook group utilized in the total synthesis of several indole alkaloids [75-77]. In 2005, they reported the synthesis of vincamajine-related indole alkaloids, among which (+)-dehydrovoachalotine was prepared by a selective oxidative cyclization of a 1,3-diol moiety (Scheme 30) [74]. Treatment of the known prochiral diol **246** with DDQ first oxidized the benzylic C6 position to give intermediate **247**, followed by intramolecular attack of the hydroxy group to construct the tetrahydrofuran ring of compound **248**, establishing an expected C6 stereocenter and a chiral quaternary carbon center at C16. This desymmetrization was enabled due to the structural features of diol **246**, wherein the proximal hydroxy group was functionalized, while the distal hydroxy group remained intact. The synthesis of (+)-dehydrovoachalotine (**249**) was completed in two steps from **248**. Voachalotine (**250**) was further prepared from **249** in the presence of Et_3SiH and TFA [78].

Using the same strategy, the Cook group synthesized (−)-12-methoxy-N_b-methylvoachalotine, (+)-polyneuridine,

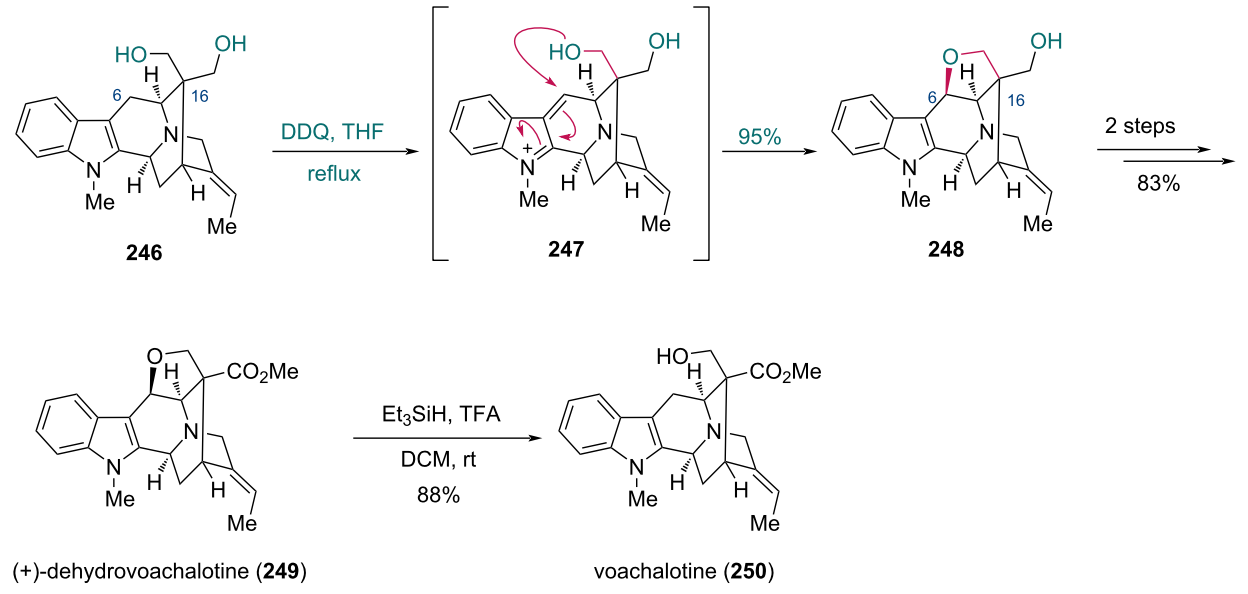

Scheme 30: Cook's synthesis of (+)-dehydrovoachalotine (**249**) and voachalotine (**250**).

(+)-polyneuridine aldehyde, and macusine A. In the synthesis of (−)-12-methoxy-N_b-methylvoachalotine (Scheme 31a) [78], (+)-12-methoxy-N_a-methylvellosimine (**252**) was first prepared in ten steps from aniline **251**, including a Larock indolization, Pictet–Spengler reaction, and Pd-catalyzed intramolecular cyclization. Tollens reaction of **252** gave diol **253**, which underwent DDQ-mediated oxidative cyclization to yield compound **254**. After a two-step conversion, the resulting compound **255** underwent reductive cleavage of the tetrahydrofuran ring with Et_3SiH/TFA, giving compound **256**. Exposure of **256** to MeI in THF provided the corresponding N_b-methiodide salt, which was subsequently converted into (−)-12-methoxy-N_b-methylvoachalotine (**257**) upon treatment with AgCl in 93% yield. For the synthesis of (+)-polyneuridine, macusine A, and (+)-polyneuridine aldehyde (Scheme 31b) [79], (+)-polyneuridine (**262**) was first prepared as the common intermediate for macusine A and (+)-polyneuridine aldehyde. From compound **258**, vellosimine (**259**) was synthesized in five steps and subsequently converted into diol **260** in three steps. Oxidative cyclization of **260** with DDQ afforded compound **261**, which was further transformed into **262** in three steps. Finally, macusine A (**263**) was prepared by methylation of **262** with MeI, while (+)-polyneuridine aldehyde (**264**) was synthesized directly from alcohol **262** via Corey–Kim oxidation.

The Trauner group also employed a similar strategy in the synthesis of stephadiamine in 2018 (Scheme 32) [80]. Starting from carboxylic acid **265**, compound **266** was prepared in a seven-step sequence. Then, the cascade cyclization was accomplished by treatment with NaOMe in MeOH, followed by H_2O, affording compound **267** in excellent yield and diastereoselectivity. A subsequent three-step sequence gave diol **268**. Under DDQ and AcOH conditions, the benzylic C11 position of **268** was first oxidized to generate intermediate **269**, followed by intramolecular nucleophilic attack of the hydroxy group. This stereoselective cyclization constructed the tetrahydropyran ring of pentacyclic compound **270** in 92% yield and established the stereocenter at the C7 position. Compound **271**, prepared from **270** in eight steps, was treated with *N*-bromosuccinimide (NBS) in a H_2O/THF solution to afford lactone **272** in 50% yield. Finally, **272** was converted to stephadiamine (**273**) in three steps.

In 2018, the Garg group completed the total synthesis of akuammiline alkaloids, including (−)-ψ-akuammigine (Scheme 33) [81]. The synthesis commenced with dibenzoate **274**, which underwent a Pd-catalyzed Trost desymmetrization using sulfonamide **275** and ligand **276**. Deprotection of the resulting adduct furnished alcohol **277**, which was subsequently converted to silyl enol ether **278** in two steps. Treatment of **278** with $(PMe_3)AuCl$ and AgOTf, followed by *p*-TsOH·H_2O, effected a Au-catalyzed cyclization to construct the bicyclic core. This intermediate was then transformed into enal **279** via epoxidation and Wittig olefination. Seven additional steps converted enal **279** to lactone **280**, which then underwent a reductive interrupted Fisher indolization with phenylhydrazine to give indoline **281**. To forge the C16 stereocenter and form the C–O bond at C2, diol **282** was prepared from **281** in six steps.

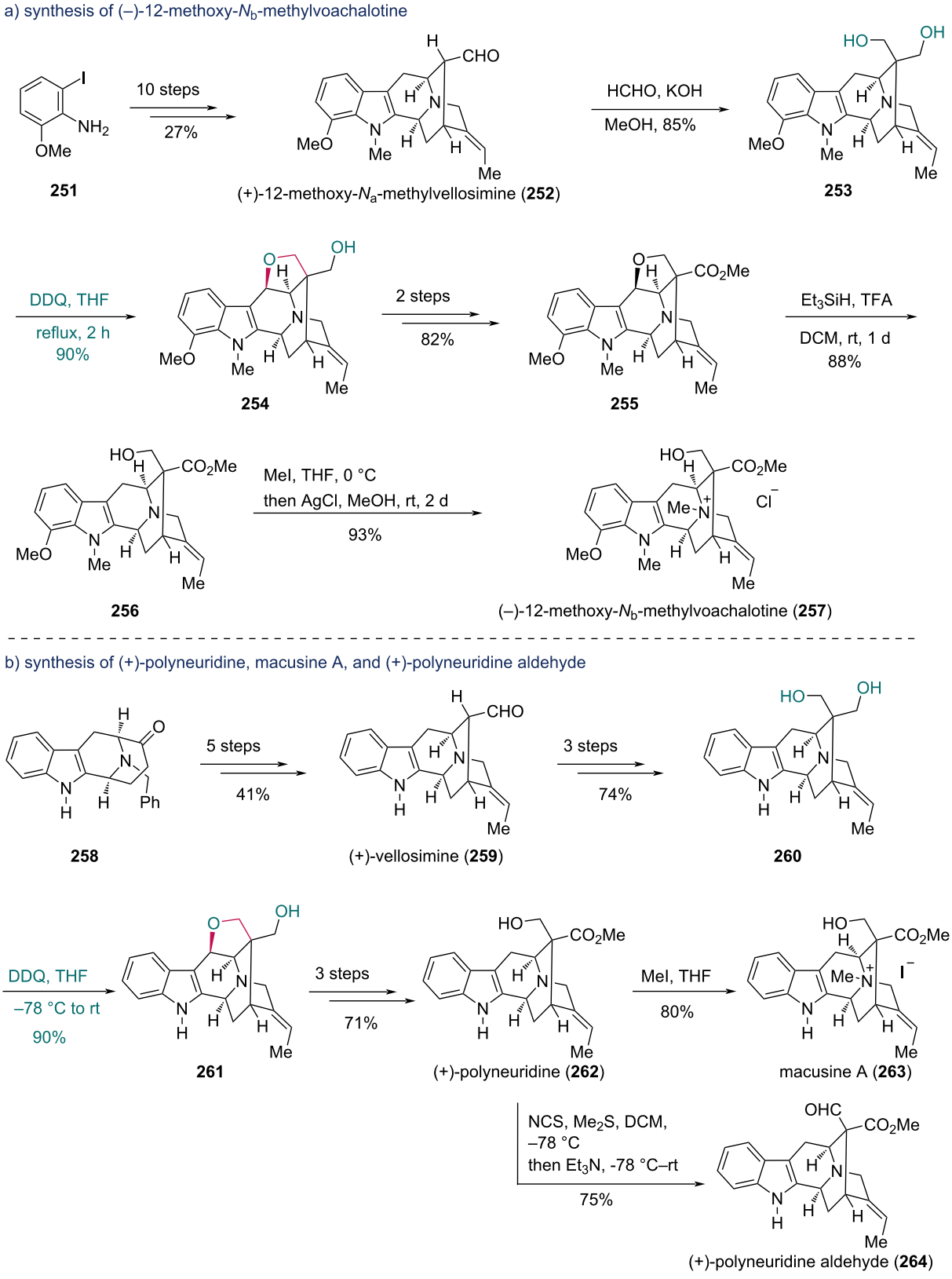

Scheme 31: Cook's synthesis of a) (–)-12-methoxy-N_b-methylvoachalotine (**257**) and b) (+)-polyneuridine, macusine A, and (+)-polyneuridine aldehyde (**264**).

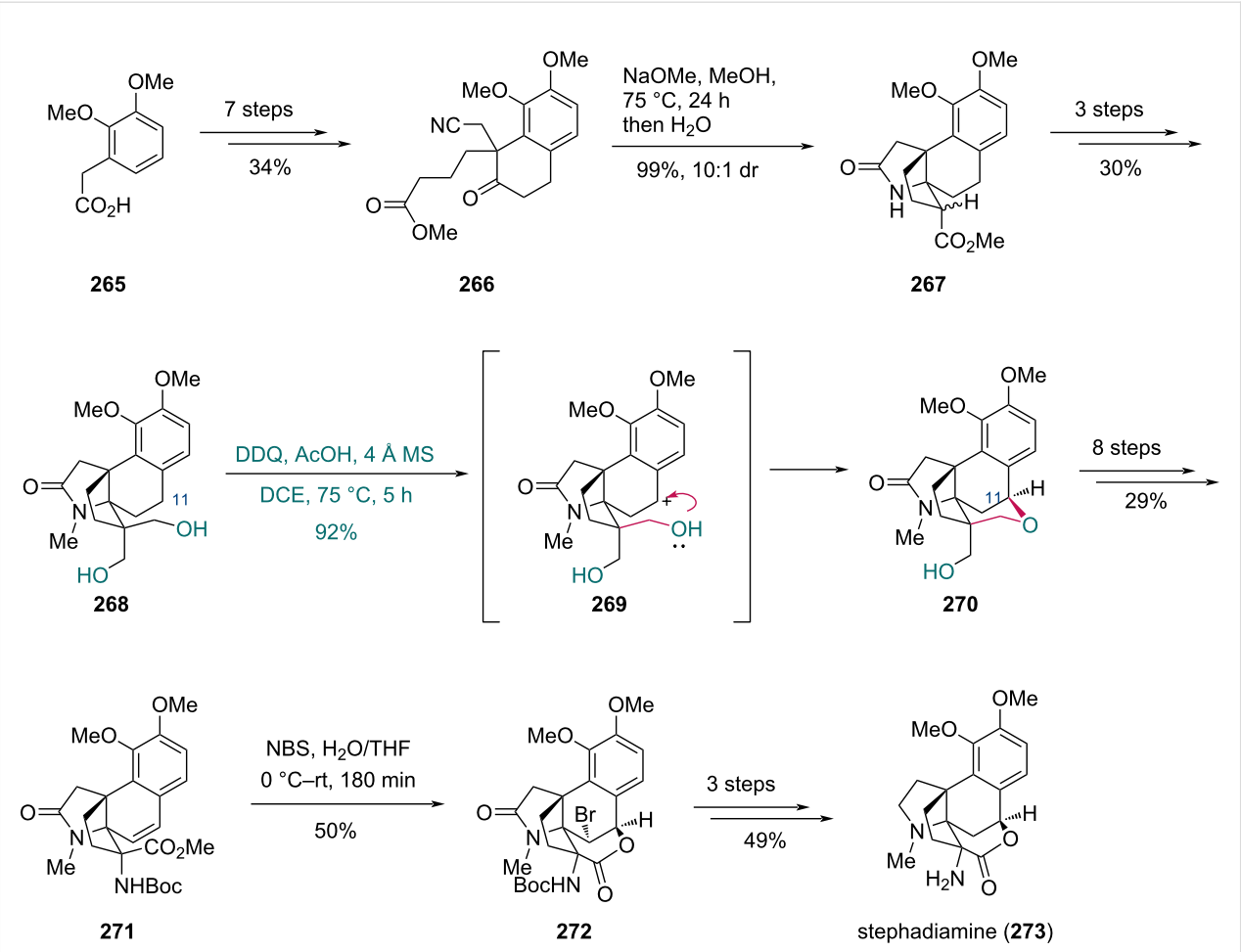

Scheme 32: Trauner's synthesis of stephadiamine (**273**).

Treatment of **282** with MeI/Cs_2CO_3 induced cyclization through putative indoleninium intermediate **283**, wherein one hydroxy group underwent nucleophilic attack on the C2 electrophilic center while the other remained unreacted, giving furoindoline **284** in 45% yield. A final two-step transformation completed the synthesis of (−)-ψ-akuammigine (**285**).

In 2021, the Ding group reported the total synthesis of two hetisine-type diterpenoids (+)-18-benzoyldavisinol and (+)-davisinol [82] (Scheme 34). Using diester **286** as a starting material, phenol **287** was prepared in six steps. Subsequent oxidative dearomatization-induced Diels–Alder cycloaddition with $PhI(OAc)_2$, delivered *endo*-cycloadduct **288** with high diastereoselectivity. Compound **288** was then treated with $Co(acac)_2$, 1,1,3,3-tetramethyldisiloxane (TMDSO), and O_2 in degassed iPrOH, undergoing a hydrogen-atom-transfer (HAT)-initiated redox radical cascade to give pentacyclic alcohol **289**, which was converted to C18/19 diol **290** in two steps. To differentiate the two hydroxy groups, the C18-alcohol was selectively protected by benzoylation using BzCN and 4-(dimethylamino)pyridine (DMAP) conditions, while the C19-alcohol was oxidized by TEMPO and *N*-chlorosuccinimide (NCS) subsequently. This two-step sequence provided ketoaldehyde **291** in 73% yield, demonstrating excellent site selectivity during the Bz protection. The assembly of the azabicyclic core was achieved in two steps from **291** via reductive amination followed by oxidative removal of the *p*-methoxybenzyl (PMB) group, giving heptacyclic compound **292**. Finally, (+)-18-benzoyldavisinol (**293**) was synthesized in two steps and subsequently deprotected to afford (+)-davisinol (**294**).

Conclusion

In conclusion, over the past few decades, the enantioselective desymmetrization of prochiral 1,3-diols has become an important tool for constructing chiral centers and applied in various total syntheses. Several strategies, including enzymatic acylation, transition-metal-catalyzed acylation, and local desym-

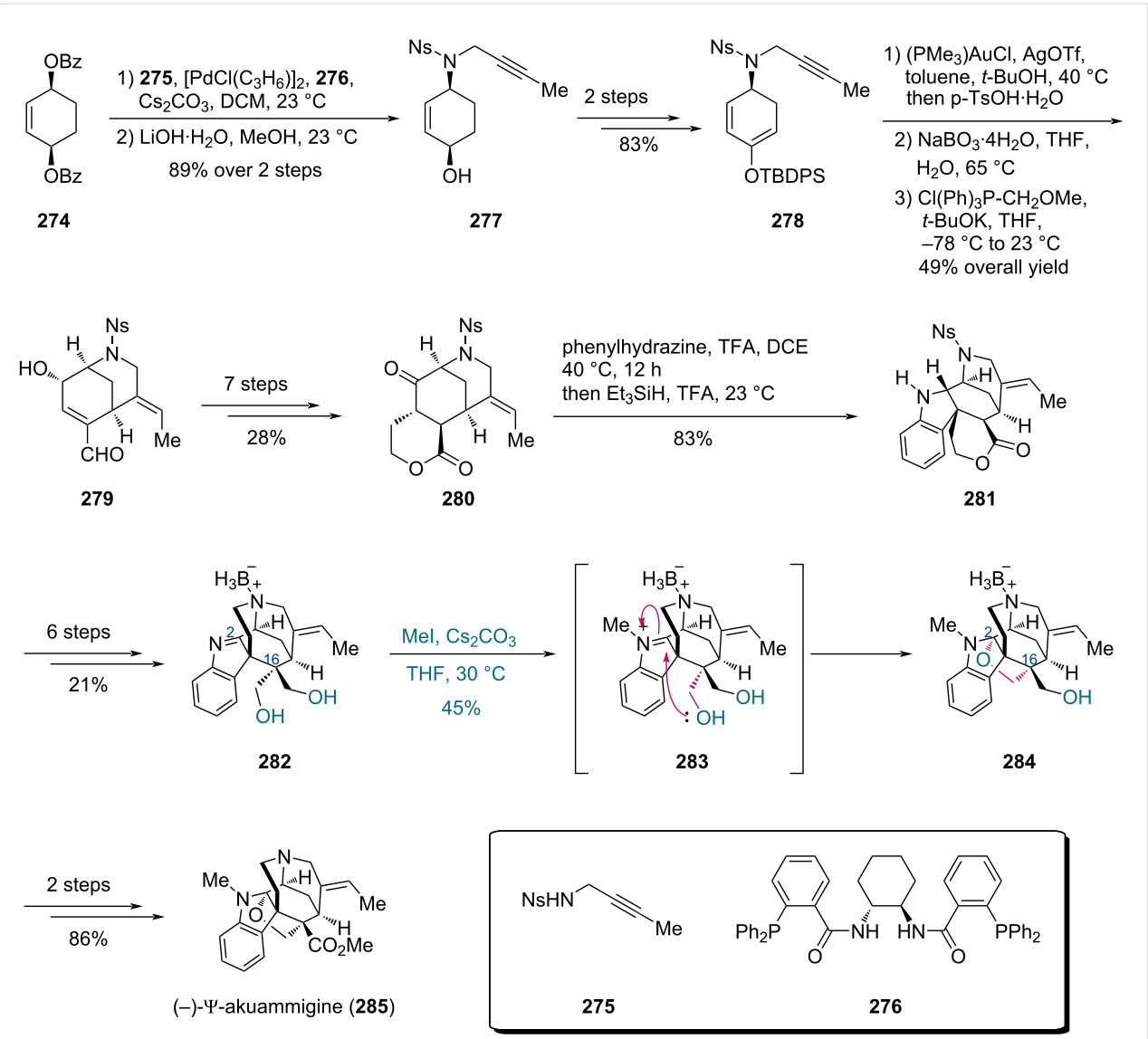

Scheme 33: Garg's synthesis of (–)-ψ-akuammigine (**285**).

metrization have been adopted by chemists to synthesize complex molecules. A general survey of these examples revealed that enzymatic acylations using lipases (such as PPL, CAL, CRL and those from the *Pseudomonas* genus) are generally operated in mild conditions achieving relatively high yield and enantioselectivity. However, due to the intrinsic structural limitations of lipases, accessing the desired enantiomer requires laborious screening of enzymes. In the case of transition-metal-catalyzed acylations, the enantioselective desymmetrization of prochiral 1,3-diols within complex structures can be realized using organometallic catalysts composed of copper or zinc salts and different types of chiral ligands. In general, the ability to control the stereoselectivity of the product by using the enantiomer of the ligand in transition-metal-catalyzed acylations is a notable advantage compared to enzymatic methods. In the case of local desymmetrization, the enantioselectivity of the reaction depends predominantly on the inherent properties of the substrate.

Although numerous examples of enantioselective desymmetrization reactions of prochiral 1,3-diols via metal-catalyzed and enzymatic methods have been reported, these transformations are mostly limited to the acylation of hydroxy groups. Other reaction types, such as sulfonylation, oxidation, and coupling, remain underdeveloped in this context, suggesting significant progress is still needed in the methodological development for the enantioselective desymmetrization of prochiral 1,3-diols.

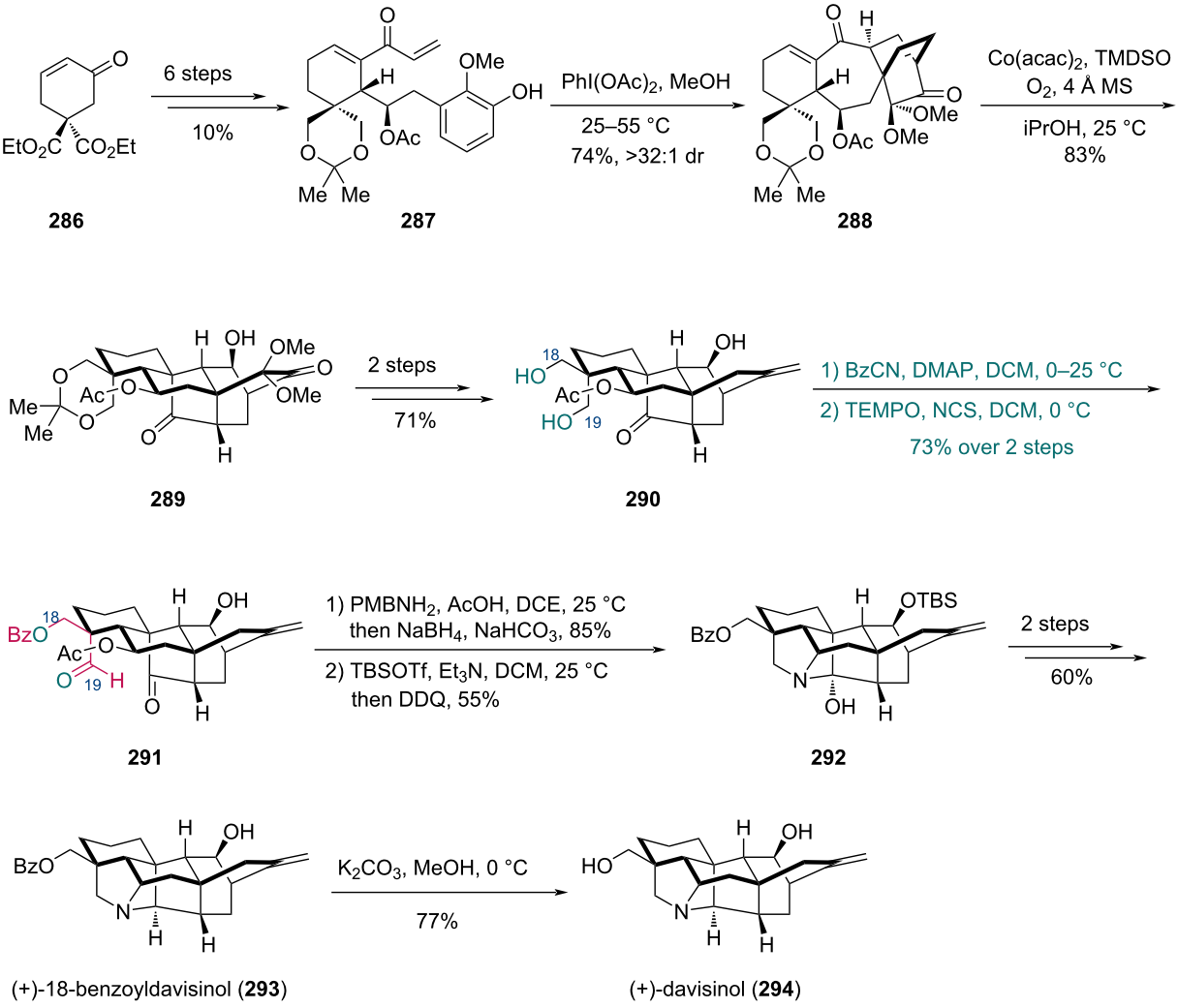

Scheme 34: Ding's synthesis of (+)-18-benzoyldavisinol (**293**) and (+)-davisinol (**294**).

Funding

We are grateful to the National Natural Science Foundation of China (22271099, 22471078 and 22071064) and the Guangdong Basic and Applied Basic Research Foundation (2024A1515012297) for the financial support.

ORCID® iDs

Zhiqiang Ma - https://orcid.org/0000-0002-3983-6636

Data Availability Statement

Data sharing is not applicable as no new data was generated or analyzed in this study.

References

1. McMorris, T. C.; Staake, M. D.; Kelner, M. J. *J. Org. Chem.* **2004,** *69,* 619–623. doi:10.1021/jo035084j
2. Rivas da Silva, A. C.; Lopes, P. M.; Barros de Azevedo, M. M.; Costa, D. C. M.; Alviano, C. S.; Alviano, D. S. *Molecules* **2012,** *17,* 6305–6316. doi:10.3390/molecules17066305
3. Zhai, W.; Zhang, L.; Cui, J.; Wei, Y.; Wang, P.; Liu, D.; Zhou, Z. *Chirality* **2019,** *31,* 468–475. doi:10.1002/chir.23075
4. Yamakoshi, H.; Ikarashi, F.; Minami, M.; Shibuya, M.; Sugahara, T.; Kanoh, N.; Ohori, H.; Shibata, H.; Iwabuchi, Y. *Org. Biomol. Chem.* **2009,** *7,* 3772–3781. doi:10.1039/b909646a
5. Parella, R.; Jakkampudi, S.; Zhao, J. C.-G. *ChemistrySelect* **2021,** *6,* 2252–2280. doi:10.1002/slct.202004196
6. Liu, X.-Y.; Qin, Y. *Green Synth. Catal.* **2022,** *3,* 25–39. doi:10.1016/j.gresc.2021.10.009
7. Chen, W.; Zhang, H. *Sci. China: Chem.* **2016,** *59,* 1065–1078. doi:10.1007/s11426-016-0055-0
8. Bai, L.; Ma, Y.; Jiang, X. *J. Am. Chem. Soc.* **2021,** *143,* 20609–20615. doi:10.1021/jacs.1c10498
9. Bai, L.; Li, J.; Jiang, X. *Chem* **2023,** *9,* 483–496. doi:10.1016/j.chempr.2022.10.021
10. Xu, P.; Zhou, F.; Zhu, L.; Zhou, J. *Nat. Synth.* **2023,** *2,* 1020–1036. doi:10.1038/s44160-023-00406-3

11. Zeng, X.-P.; Cao, Z.-Y.; Wang, Y.-H.; Zhou, F.; Zhou, J. *Chem. Rev.* **2016,** *116,* 7330–7396. doi:10.1021/acs.chemrev.6b00094
12. Lin, G.; Xu, J.; Song, Q. *Chin. J. Org. Chem.* **2024,** *44,* 3621–3638. doi:10.6023/cjoc202406029
13. Zhao, J.; Ge, Y.; He, C. *Chin. J. Org. Chem.* **2023,** *43,* 3352–3366. doi:10.6023/cjoc202305001
14. Nájera, C.; Foubelo, F.; Sansano, J. M.; Yus, M. *Tetrahedron* **2022,** *106–107,* 132629. doi:10.1016/j.tet.2022.132629
15. Yu, Z.; Li, Z.; Yang, C.; Gu, Q.; Liu, X. *Acta Chim. Sin. (Chin. Ed.)* **2023,** *81,* 955–966. doi:10.6023/a23040161
16. Yang, H.; Zheng, W.-H. *Tetrahedron Lett.* **2018,** *59,* 583–591. doi:10.1016/j.tetlet.2017.12.080
17. Suzuki, T. *Tetrahedron Lett.* **2017,** *58,* 4731–4739. doi:10.1016/j.tetlet.2017.10.048
18. Borissov, A.; Davies, T. Q.; Ellis, S. R.; Fleming, T. A.; Richardson, M. S. W.; Dixon, D. J. *Chem. Soc. Rev.* **2016,** *45,* 5474–5540. doi:10.1039/c5cs00015g
19. Horwitz, M. A. *Tetrahedron Lett.* **2022,** *97,* 153776. doi:10.1016/j.tetlet.2022.153776
20. Sugai, T.; Higashibayashi, S.; Hanaya, K. *Tetrahedron* **2018,** *74,* 3469–3487. doi:10.1016/j.tet.2018.05.053
21. Merad, J.; Candy, M.; Pons, J.-M.; Bressy, C. *Synthesis* **2017,** *49,* 1938–1954. doi:10.1055/s-0036-1589493
22. Cigan, E.; Eggbauer, B.; Schrittwieser, J. H.; Kroutil, W. *RSC Adv.* **2021,** *11,* 28223–28270. doi:10.1039/d1ra04181a
23. Chakrabarty, S.; Romero, E. O.; Pyser, J. B.; Yazarians, J. A.; Narayan, A. R. H. *Acc. Chem. Res.* **2021,** *54,* 1374–1384. doi:10.1021/acs.accounts.0c00810
24. Stergiou, P.-Y.; Foukis, A.; Filippou, M.; Koukouritaki, M.; Parapouli, M.; Theodorou, L. G.; Hatziloukas, E.; Afendra, A.; Pandey, A.; Papamichael, E. M. *Biotechnol. Adv.* **2013,** *31,* 1846–1859. doi:10.1016/j.biotechadv.2013.08.006
25. Liu, J.; Li, J.; Bai, L. *Acta Microbiol. Sin. (Engl. Transl.)* **2023,** *63,* 451–464. doi:10.13343/j.cnki.wsxb.20220380
26. Mendes, A. A.; Oliveira, P. C.; de Castro, H. F. *J. Mol. Catal. B: Enzym.* **2012,** *78,* 119–134. doi:10.1016/j.molcatb.2012.03.004
27. Sato, K.; Bando, T.; Shindo, M.; Shishido, K. *Heterocycles* **1999,** *50,* 11–15. doi:10.3987/com-98-s(h)4
28. Kishuku, H.; Yoshimura, T.; Kakehashi, T.; Shindo, M.; Shishido, K. *Heterocycles* **2003,** *61,* 125–131. doi:10.3987/com-03-s4
29. Kishuku, H.; Shindo, M.; Shishido, K. *Chem. Commun.* **2003,** 350–351. doi:10.1039/b211227b
30. Morimoto, S.; Shindo, M.; Yoshida, M.; Shishido, K. *Tetrahedron Lett.* **2006,** *47,* 7353–7356. doi:10.1016/j.tetlet.2006.08.014
31. Macías, F. A.; Varela, R. M.; Torres, A.; Molinillo, J. M. G. *J. Nat. Prod.* **1999,** *62,* 1636–1639. doi:10.1021/np990249y
32. Morimoto, S.; Shindo, M.; Shishido, K. *Heterocycles* **2005,** *66,* 69–73. doi:10.3987/com-05-s(k)21
33. Manzuna Sapu, C.; Deska, J. *Org. Biomol. Chem.* **2013,** *11,* 1376–1382. doi:10.1039/c2ob27073k
34. Xu, D.; Liu, J.; Han, X.; Huang, S.; Yang, X. *Synth. Commun.* **2022,** *52,* 724–732. doi:10.1080/00397911.2022.2047732
35. Nielsen, T. B.; Ishii, M.; Kirk, O. Lipases A and B from the yeast *Candida antarctica*. In *Biotechnological Applications of Cold-Adapted Organisms;* Margesin, R.; Schinner, F., Eds.; Springer: Berlin, Heidelberg, 1999; pp 49–61. doi:10.1007/978-3-642-58607-1_4
36. Kirk, O.; Christensen, M. W. *Org. Process Res. Dev.* **2002,** *6,* 446–451. doi:10.1021/op0200165
37. Takabatake, K.; Nishi, I.; Shindo, M.; Shishido, K. *J. Chem. Soc., Perkin Trans. 1* **2000,** 1807–1808. doi:10.1039/b003553j
38. Chênevert, R.; Courchesne, G. *Tetrahedron Lett.* **2002,** *43,* 7971–7973. doi:10.1016/s0040-4039(02)01865-8
39. Akai, S.; Tsujino, T.; Fukuda, N.; Iio, K.; Takeda, Y.; Kawaguchi, K.-i.; Naka, T.; Higuchi, K.; Akiyama, E.; Fujioka, H.; Kita, Y. *Chem. – Eur. J.* **2005,** *11,* 6286–6297. doi:10.1002/chem.200500443
40. Kita, Y.; Higuchi, K.; Yoshida, Y.; Iio, K.; Kitagaki, S.; Ueda, K.; Akai, S.; Fujioka, H. *J. Am. Chem. Soc.* **2001,** *123,* 3214–3222. doi:10.1021/ja0035699
41. Palleroni, N. J. Pseudomonas. In *Bergey's Manual of Systematics of Archaea and Bacteria;* Trujillo, M. E.; Dedysh, S.; DeVos, P.; Hedlund, B.; Kämpfer, P.; Rainey, F. A.; Whitman, W. B., Eds.; John Wiley & Sons, 2015; pp 1–105. doi:10.1002/9781118960608.gbm01210
42. Takabe, K.; Mase, N.; Hashimoto, H.; Tsuchiya, A.; Ohbayashi, T.; Yoda, H. *Bioorg. Med. Chem. Lett.* **2003,** *13,* 1967–1969. doi:10.1016/s0960-894x(03)00352-4
43. Takabe, K.; Hashimoto, H.; Sugimoto, H.; Nomoto, M.; Yoda, H. *Tetrahedron: Asymmetry* **2004,** *15,* 909–912. doi:10.1016/j.tetasy.2004.01.031
44. Kawasaki, M.; Toyooka, N.; Saka, T.; Goto, M.; Matsuya, Y.; Kometani, T. *J. Mol. Catal. B: Enzym.* **2010,** *67,* 135–142. doi:10.1016/j.molcatb.2010.07.019
45. Toya, H.; Satoh, T.; Okano, K.; Takasu, K.; Ihara, M.; Takahashi, A.; Tanaka, H.; Tokuyama, H. *Tetrahedron* **2014,** *70,* 8129–8141. doi:10.1016/j.tet.2014.08.009
46. Shimada, K.; Kaburagi, Y.; Fukuyama, T. *J. Am. Chem. Soc.* **2003,** *125,* 4048–4049. doi:10.1021/ja0340679
47. Bhuniya, R.; Nanda, S. *Tetrahedron* **2013,** *69,* 1153–1165. doi:10.1016/j.tet.2012.11.051
48. Davies, S. G.; Roberts, P. M.; Stephenson, P. T.; Storr, H. R.; Thomson, J. E. *Tetrahedron* **2009,** *65,* 8283–8296. doi:10.1016/j.tet.2009.07.010
49. Fukuda, T.; Sugiyama, K.; Arima, S.; Harigaya, Y.; Nagamitsu, T.; Omura, S. *Org. Lett.* **2008,** *10,* 4239–4242. doi:10.1021/ol8016066
50. Xiao, X.; Xu, K.; Gao, Z.-H.; Zhu, Z.-H.; Ye, C.; Zhao, B.; Luo, S.; Ye, S.; Zhou, Y.-G.; Xu, S.; Zhu, S.-F.; Bao, H.; Sun, W.; Wang, X.; Ding, K. *Sci. China: Chem.* **2023,** *66,* 1553–1633. doi:10.1007/s11426-023-1578-y
51. Olivo, G.; Cussó, O.; Costas, M. *Chem. – Asian J.* **2016,** *11,* 3148–3158. doi:10.1002/asia.201601170
52. Chen, J.; Song, W.; Lee, Y.-M.; Nam, W.; Wang, B. *Coord. Chem. Rev.* **2023,** *477,* 214945. doi:10.1016/j.ccr.2022.214945
53. Ichikawa, J.; Asami, M.; Mukaiyama, T. *Chem. Lett.* **1984,** *13,* 949–952. doi:10.1246/cl.1984.949
54. Trost, B. M.; Ito, H. *J. Am. Chem. Soc.* **2000,** *122,* 12003–12004. doi:10.1021/ja003033n
55. Trost, B. M.; Ito, H.; Silcoff, E. R. *J. Am. Chem. Soc.* **2001,** *123,* 3367–3368. doi:10.1021/ja003871h
56. Trost, B. M.; Mino, T. *J. Am. Chem. Soc.* **2003,** *125,* 2410–2411. doi:10.1021/ja029708z
57. Jung, B.; Kang, S. H. *Proc. Natl. Acad. Sci. U. S. A.* **2007,** *104,* 1471–1475. doi:10.1073/pnas.0607865104
58. Jung, B.; Hong, M. S.; Kang, S. H. *Angew. Chem., Int. Ed.* **2007,** *46,* 2616–2618. doi:10.1002/anie.200604977
59. Kim, H. C.; Youn, J.-H.; Kang, S. H. *Synlett* **2008,** 2526–2528. doi:10.1055/s-2008-1078046

60. Kim, H. C.; Kang, S. H. *Angew. Chem., Int. Ed.* **2009,** *48,* 1827–1829. doi:10.1002/anie.200805334
61. Celindro, N. C.; Kim, T. W.; Kang, S. H. *Chem. Commun.* **2012,** *48,* 6295–6297. doi:10.1039/c2cc32736h
62. Hong, M. S.; Kim, T. W.; Jung, B.; Kang, S. H. *Chem. – Eur. J.* **2008,** *14,* 3290–3296. doi:10.1002/chem.200701875
63. Lee, W.; Youn, J.-H.; Kang, S. H. *Chem. Commun.* **2013,** *49,* 5231–5233. doi:10.1039/c3cc42365d
64. Lee, W.; Kang, S.; Jung, B.; Lee, H.-S.; Kang, S. H. *Chem. Commun.* **2016,** *52,* 3536–3539. doi:10.1039/c5cc10673g
65. Lee, J. Y.; You, Y. S.; Kang, S. H. *J. Am. Chem. Soc.* **2011,** *133,* 1772–1774. doi:10.1021/ja1103102
66. Gan, P.; Pitzen, J.; Qu, P.; Snyder, S. A. *J. Am. Chem. Soc.* **2018,** *140,* 919–925. doi:10.1021/jacs.7b07724
67. Zhang, N.; Wang, C.; Xu, H.; Zheng, M.; Jiang, H.; Chen, K.; Ma, Z. *Angew. Chem., Int. Ed.* **2024,** *63,* e202407127. doi:10.1002/anie.202407127
68. Trost, B. M.; Michaelis, D. J.; Malhotra, S. *Org. Lett.* **2013,** *15,* 5274–5277. doi:10.1021/ol4024997
69. Fresia, M.; Kock, M.; Lindel, T. *Chem. – Eur. J.* **2020,** *26,* 12733–12737. doi:10.1002/chem.202002579
70. Horwitz, M. A.; Johnson, J. S. *Eur. J. Org. Chem.* **2017,** 1381–1390. doi:10.1002/ejoc.201601481
71. Iwata, C.; Fujita, M.; Moritani, Y.; Hattori, K.; Imanishi, T. *Tetrahedron Lett.* **1987,** *28,* 3135–3138. doi:10.1016/s0040-4039(00)96304-4
72. Iwata, C.; Fujita, M.; Moritani, Y.; Sugiyama, K.; Hattori, K.; Imanishi, T. *Tetrahedron Lett.* **1987,** *28,* 3131–3134. doi:10.1016/s0040-4039(00)96303-2
73. Yu, J.; Wearing, X. Z.; Cook, J. M. *J. Am. Chem. Soc.* **2004,** *126,* 1358–1359. doi:10.1021/ja039798n
74. Yu, J.; Wearing, X. Z.; Cook, J. M. *J. Org. Chem.* **2005,** *70,* 3963–3979. doi:10.1021/jo040282b
75. Wang, T.; Xu, Q.; Yu, P.; Liu, X.; Cook, J. M. *Org. Lett.* **2001,** *3,* 345–348. doi:10.1021/ol000331g
76. Cain, M.; Mantei, R.; Cook, J. M. *J. Org. Chem.* **1982,** *47,* 4933–4936. doi:10.1021/jo00146a021
77. Yu, J.; Wang, T.; Wearing, X. Z.; Ma, J.; Cook, J. M. *J. Org. Chem.* **2003,** *68,* 5852–5859. doi:10.1021/jo030116o
78. Zhou, H.; Liao, X.; Yin, W.; Ma, J.; Cook, J. M. *J. Org. Chem.* **2006,** *71,* 251–259. doi:10.1021/jo052081t
79. Yin, W.; Ma, J.; Rivas, F. M.; Cook, J. M. *Org. Lett.* **2007,** *9,* 295–298. doi:10.1021/ol062762q
80. Hartrampf, N.; Winter, N.; Pupo, G.; Stoltz, B. M.; Trauner, D. *J. Am. Chem. Soc.* **2018,** *140,* 8675–8680. doi:10.1021/jacs.8b01918
81. Picazo, E.; Morrill, L. A.; Susick, R. B.; Moreno, J.; Smith, J. M.; Garg, N. K. *J. Am. Chem. Soc.* **2018,** *140,* 6483–6492. doi:10.1021/jacs.8b03404
82. Yu, K.; Yao, F.; Zeng, Q.; Xie, H.; Ding, H. *J. Am. Chem. Soc.* **2021,** *143,* 10576–10581. doi:10.1021/jacs.1c05703

License and Terms

BEILSTEIN JOURNAL OF ORGANIC CHEMISTRY

Asymmetric total synthesis of tricyclic prostaglandin D2 metabolite methyl ester via oxidative radical cyclization

Miao Xiao[1], Liuyang Pu[1], Qiaoli Shang[1], Lei Zhu[2] and Jun Huang[*1]

Full Research Paper

Open Access

Address:
[1]School of Chemistry and Chemical Engineering, University of South China, Hengyang 421001, China and [2]College of Pharmacy, Third Military Medical University, Chongqing 200038, China

Email:
Jun Huang[*] - junhuang@usc.edu.cn

* Corresponding author

Keywords:
asymmetric total synthesis; oxidative radical cyclization; tricyclic prostaglandin D_2 metabolite methyl ester

Beilstein J. Org. Chem. **2025,** *21,* 1964–1972.
https://doi.org/10.3762/bjoc.21.152

Received: 31 July 2025
Accepted: 12 September 2025
Published: 24 September 2025

This article is part of the thematic issue "Concept-driven strategies in target-oriented synthesis".

Guest Editor: Y. Tang

Abstract

Prostaglandin D_2 (PGD_2) is a key pathophysiological mediator in many human diseases and biological pathways. Tricyclic prostaglandin D_2 metabolite methyl ester (tricyclic-PGDM methyl ester), the major urinary metabolite of PGD_2, can be used as a clinical indicator for PGD_2 overproduction. However, the limited amount of tricyclic-PGDM methyl ester available has prevented its practical use, and synthesis methods for tricyclic-PGDM methyl ester are required. Based on the utilization of oxidative radical cyclization for the stereoselective construction of the cyclopentanol subunit with three consecutive stereocenters, we describe an asymmetric total synthesis of tricyclic-PGDM methyl ester in 9 steps and 8% overall yield.

Introduction

Prostaglandins (PGs), a family of hormone-like lipid compounds, are ubiquitous natural products that control many essential biological processes in animals and humans [1-4]. In particular, prostaglandin D_2 (PGD_2, **3**) is a key pathophysiological mediator in a number of human diseases and biological pathways, such as systemic mastocytosis and inflammation. Therefore, the development of methods for sensitive detection of endogenous PGD_2 production and its stereoisomers are clinically important [5]. However, PGD_2 is rapidly metabolized with a short half-life, making the identification and quantification of its downstream metabolites a promising and reliable diagnostic tool. Tricyclic prostaglandin D_2 metabolite methyl ester (tricyclic-PGDM methyl ester, **4**), the major urinary metabolite of PGD_2, has been used as an indicator for PGD_2 overproduction. Roberts and associates established an assay for tricyclic-PGDM measurement using ^{18}O-labelled tricyclic-PGDM methyl ester **8**, which is an effective tool in clinical applications [6]. However, the scarcity of metabolite **4** has prevented it from being used more widely, and thus synthesis methods for **4** are required.

Compound **4** contains a cyclopentanol scaffold with stereogenicity at C8, C9, C11, and C12 (Scheme 1A). In addition, **4** is synthetically challenging because of the tricyclic ring system,

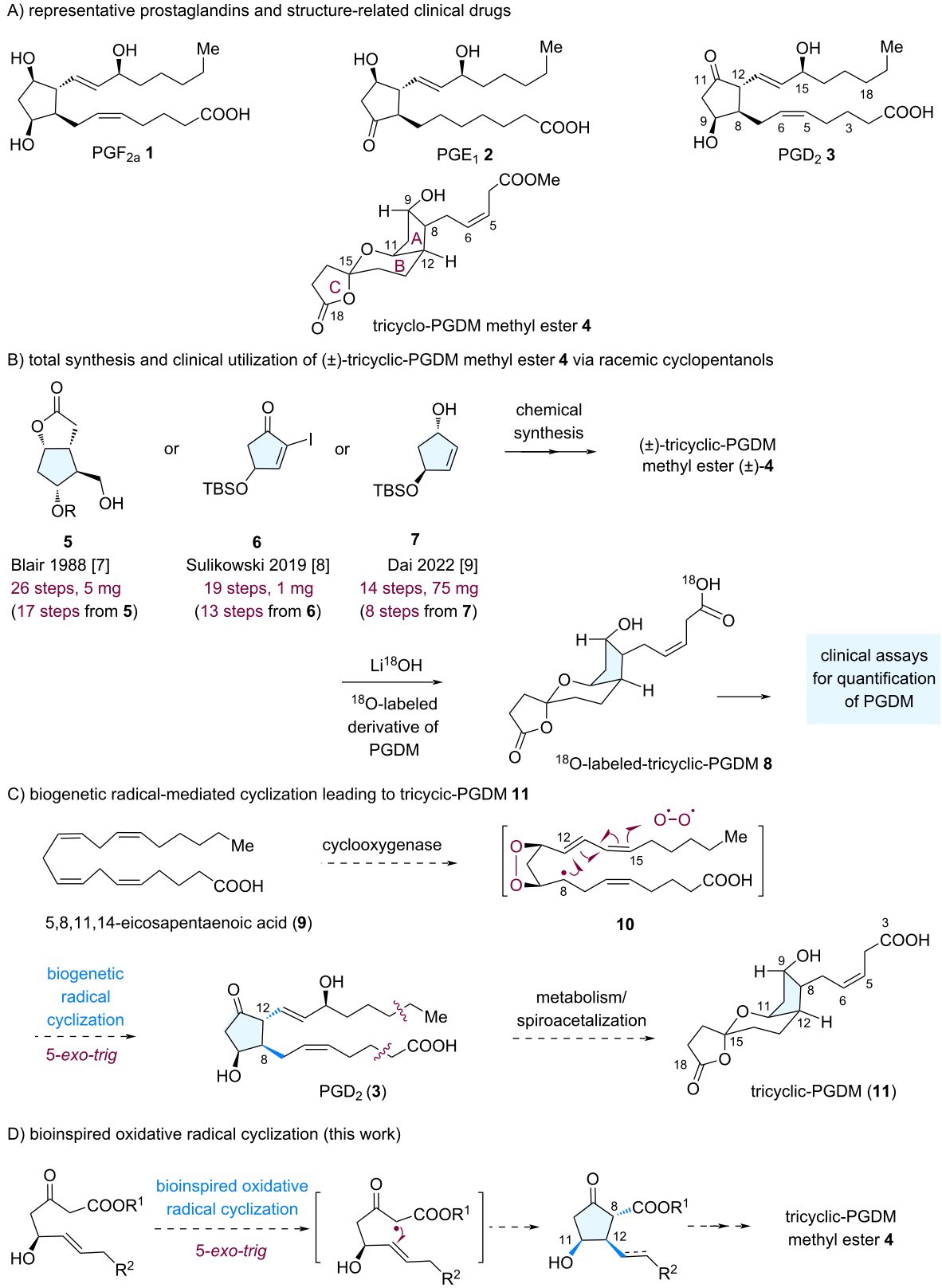

Scheme 1: Representative prostaglandins and general synthetic strategy toward PGDM methyl ester **4**.

spiroketal moiety (B, C-ring), and instability arising from dehydration of the hydroxy groups. Prior approaches to (±)-**4** have shown the feasibility of accessing this target molecule. Blair [7] and Sulikowski [8] reported the total synthesis of (±)-**4** from pentacyclic starting materials **5** and **6**, respectively (Scheme 1B). In 2021, Dai reported the total synthesis of (±)-**4** from cyclopentanol **7**, in which the bicyclic spiroketal moiety and (*Z*)-3-butenoate side chain were formed via a palladium-catalyzed carbonylative spirolactonization and *Z*-selective cross-metathesis, respectively [9]. In general, racemic cyclopentanol precursors (A ring system, prepared in 6–9 steps) have been used to form the polyfunctionalized tricyclic frameworks incorporating contiguous stereocenters.

In previous syntheses, the efficient construction of the cyclopentanol ring system with the appropriate functional groups in place for attaching the remaining groups is a highly important task for the asymmetric total synthesis of PGs and analogues [10-13]. The groups of Aggarwal [14], Hayashi [15], and Zhang [16] have reported bond-disconnection strategies for the total syntheses of PGs via organocatalysis, and enyne cycloisomerization, respectively. Thus, from a strategic viewpoint, developing alternative synthetic approaches for the stereoselective construction of the highly substituted cyclopentanol core framework in compound **4** may advance the efficient total synthesis of **4** and is required to explore alternative synthetic strategies for PGs and analogues [17].

Biosynthetically, **4** is proposed to arise via a 5-*exo*-*trig* biogenetic radical-mediated cyclization (Scheme 1C) [18,19]. Over the past five decades, the Snider oxidative radical reaction has been used as a powerful method for synthesizing complex natural products [20,21]. We envisaged that the A-ring in **4** could be constructed from the alkene-substituted β-keto ester precursor **A** via a bioinspired oxidative radical cyclization (Scheme 1D).

Herein, we report the full details of our efforts to stereoselectively access the *syn*-*anti*-cyclopentanol ring system with three vicinal stereogenic centers at C11, C12, and C8 via the oxidative radical cyclization that led to the asymmetric total synthesis of compound **4**.

Results and Discussion

First generation asymmetric total synthesis of tricyclic-PGDM methyl ester

The retrosynthetic analysis of tricyclic-PGDM methyl ester **4** is shown in Scheme 2. We expected to derive **4** from tricyclic substrate **12** via a side-chain installation at C8 [22]. The spiroketal

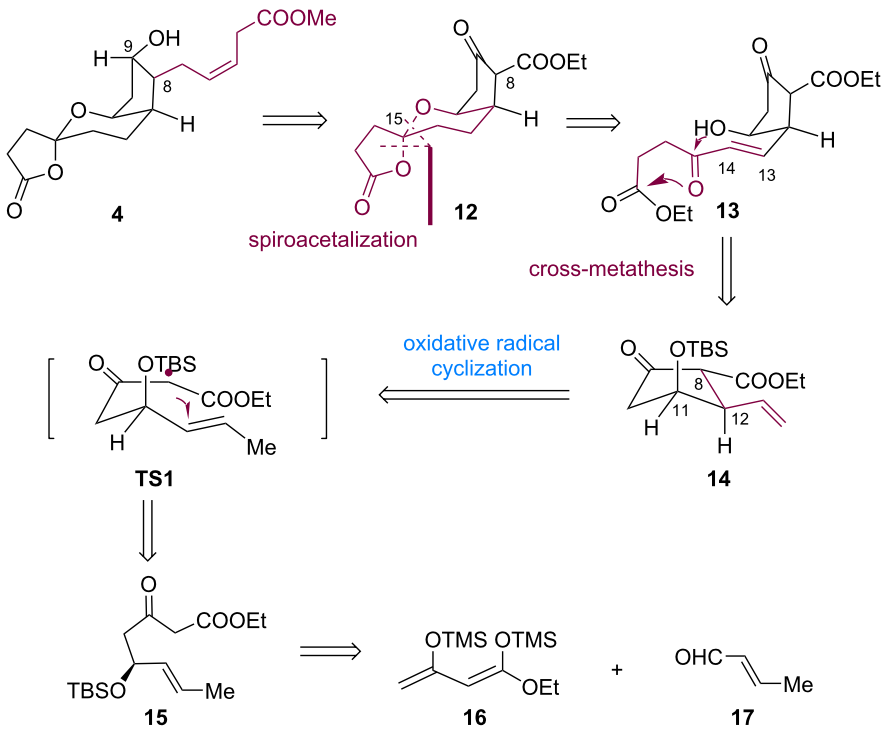

Scheme 2: Retrosynthetic analysis for the first generation synthesis of PGDM methyl ester **4**.

moiety in compound **12** could be obtained from compound **13** via a diastereoselective spiroketalization dictated by the anomeric effect [23] in the tricyclic scaffold. Compound **13** could be produced from olefin **14** via cross-metathesis. The regio- and diastereoselective connection of C8 and C12 in compound **14** could be realized through a transition-metal-mediated oxidative radical cyclization through **TS-1** from β-keto ester **15** [24]. The β-keto ester **15** was expected to be derived from compounds **16** and **17** via an asymmetric aldol reaction [25].

The first phase of the synthesis required the efficient preparation of compound **14**, for which a transition-metal-mediated oxidative radical cyclization of β-keto ester **15** was initially investigated (Scheme 3). Chan's diene (**16**) was subjected to condensation with freshly distilled aldehyde **17** in THF at room temperature, using a catalytic system comprising $Ti(OiPr)_4$/(*S*)-BINOL complex (2.0 mol %). Subsequent deprotection with pyridinium *p*-toluenesulfonate (PPTS) at 0 °C afforded the corresponding alcohol **18** in 89% yield with excellent enantioselectivity (98% ee) [25]. The hydroxy group in **18** was then protected via treatment with TBSCl in the presence of Et_3N in CH_2Cl_2, yielding β-keto ester **15** in 52% yield.

With diketone **15** in hand, we subsequently investigated the transition-metal-mediated oxidative radical cyclization for constructing cyclopentanone **14**. First, we used $Mn(OAc)_3{\cdot}2H_2O$/$Cu(OAc)_2{\cdot}H_2O$ [21] as the oxidant system to perform oxidative annulation of β-keto ester **15** in MeCN as solvent. However, only 9% of the desired product **14** was obtained after conducting the reaction at 50 °C for 36 h, and extensive decomposition

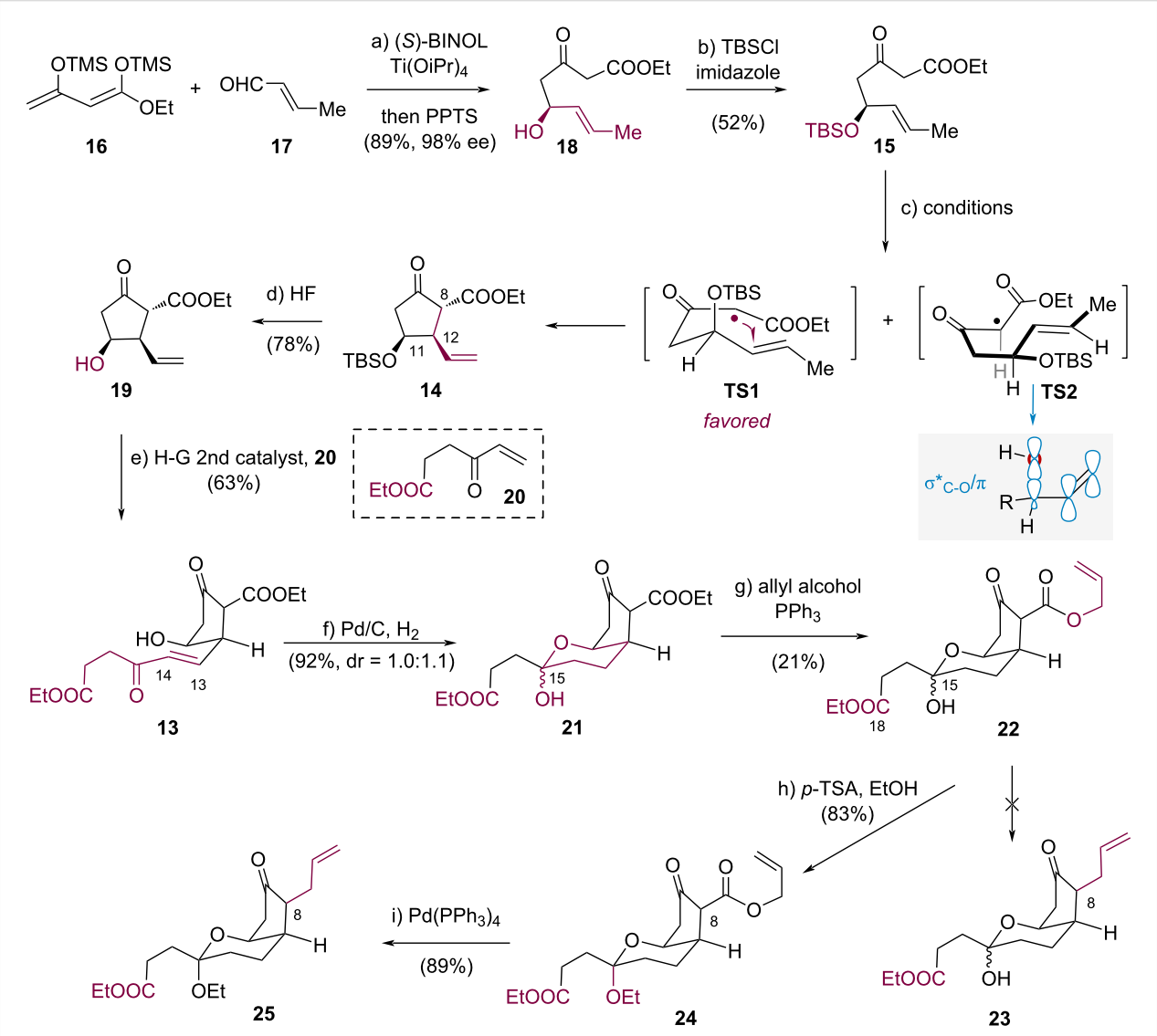

Scheme 3: Synthesis of bicyclic ketal **25**.

of the starting material β-keto ester **15** occurred (Table 1, entry 1). Solvent screening of EtOH [26], acetic acid [26], and hexafluoroisopropanol (HFIP) [27] demonstrated that HFIP afforded optimal results, delivering cyclopentanone **14** in 63% yield as a single diastereomer (Table 1, entry 4). To explain this diastereoselectivity, we hypothesize that the C–O bond, which occupies an axial position in the proposed transition state **TS-1**, could avert an additional hyperconjugative interaction ($\sigma^*_{C\text{-}O}/\pi$) that renders the reacting C=C bond electron-deficient [28], thereby lowering the energy barrier for electrophilic radical addition. Increasing the reaction temperature to 70 °C proved detrimental, yielding only trace amounts of product **14** (Table 1, entry 5). Finally, replacing $Mn(OAc)_3{\cdot}2H_2O/Cu(OAc)_2{\cdot}H_2O$ with other oxidants, such as ceric ammonium nitrate (CAN) [29,30] and $Fe(ClO_4)_3{\cdot}9H_2O$ [31], failed to afford desired product **14** (Table 1, entries 6 and 7).

To explore the synthesis of fully functionalized tricyclic core scaffold **12**, methods for incorporating the side chain at C14 and for the stereocontrolled introduction of the allyl moiety at C8 were developed. A straightforward transformation was designed involving a cross-metathesis of the C13–C14 double bond and a palladium-catalyzed decarboxylative allylation [32] as the key steps.

With **14** in hand, we investigated the feasibility of cross-metathesis of the C13–C14 double bond. Initially, compounds **14** and **20** were evaluated for the cross-metathesis of the olefin moiety in **14**. No reaction occurred and the desired product was not detected (not shown), presumably because of the steric hindrance from the TBS group. Following the removal of the silyl group, cyclopentanol **19** underwent the cross-metathesis reaction smoothly in the presence of the Hoveyda–Grubbs second-generation catalyst to afford the enone **13** in 63% yield with the desired *trans*-configuration. Enone **13** was then subjected to the Pd/C-catalyzed hydrogenation to give the thermodynamically favored bicyclic hemiketal **21** in 92% yield as an inseparable mixture of diastereomers at C-15 in a ratio of 1.0/1.1 (^{1}H NMR analysis).

Having established a route to the bicyclic hemiketal **21**, we investigated the stereoselective introduction of an allyl moiety at C8 for the synthesis of compound **25** according to the strategy in Scheme 3. Treatment of **21** with allyl alcohol and triphenylphosphine afforded transesterification product **22** in 21% yield [33], accompanied by unidentified decarboxylation by-products. A variety of standard conditions failed to promote the palladium-catalyzed decarboxylative allylation of allylic β-ketocarboxylate intermediate **22** (see Supporting Information File 1 for the details). Reasoning that the preferential coordination of the palladium catalyst with the hydroxy group at C15 and the carbonyl group at C18 in compound **22** may have deactivated the palladium catalyst [34], we protected the hydroxy group. Compound **22** was treated with *p*-toluenesulfonic acid (*p*-TSA) in EtOH at room temperature to afford ketal **24** in 83% yield as a single diastereomer. Subsequently, palladium-catalyzed decarboxylative allylation delivered compound **25** in 89% yield.

The efficiency of our first-generation strategy for asymmetric synthesis of **4** was unsatisfactory because it required nine steps to prepare bicyclic intermediate **25** with an overall yield of just 2.0%. This low efficiency prompted us to develop a more streamlined synthetic route for target compound **4**.

Table 1: Optimization of conditions to convert diketone **15** into cyclopentanone **14**.[a]

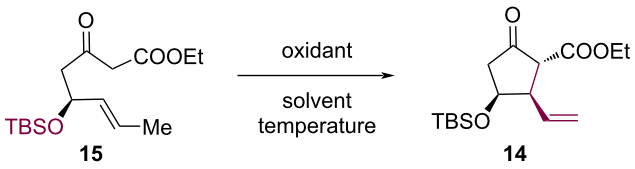

entry	oxidant	solvent	temp. (°C)	yield (%)
1	$Mn(OAc)_3{\cdot}2H_2O$ (2.2 equiv), $Cu(OAc)_2{\cdot}H_2O$ (1.1 equiv)	MeCN	50	9
2	$Mn(OAc)_3{\cdot}2H_2O$ (2.2 equiv), $Cu(OAc)_2{\cdot}H_2O$ (1.1 equiv)	EtOH	50	0
3	$Mn(OAc)_3{\cdot}2H_2O$ (2.2 equiv), $Cu(OAc)_2{\cdot}H_2O$ (1.1 equiv)	AcOH	50	12
4	$Mn(OAc)_3{\cdot}2H_2O$ (2.2 equiv), $Cu(OAc)_2{\cdot}H_2O$ (1.1 equiv)	HFIP	50	63
5	$Mn(OAc)_3{\cdot}2H_2O$ (2.2 equiv), $Cu(OAc)_2{\cdot}H_2O$ (1.1 equiv)	HFIP	70	trace
6	$Fe(ClO_4)_3{\cdot}9H_2O$ (2.2 equiv)	HFIP	50	0
7	CAN (2.2 equiv)	HFIP	50	0

[a]Step c in Scheme 3.

Second generation asymmetric total synthesis of tricyclic-PGDM methyl ester

Although the efficiency of the first-generation asymmetric total synthesis strategy was limited, the development of synthetic methods during this work, particularly the transition-metal-mediated oxidative radical cyclization for stereoselective assembly of the cyclopentanol scaffold bearing the C8, C11, and C12 contiguous stereogenic centers, provided important insights that influenced the design of our second-generation total synthesis. Compared with the Snider-type radical cyclization using stoichiometric amounts of metal oxidants, visible-light-induced photoredox-catalyzed radical cyclization strategies have emerged as an effective synthetic route for the stereocontrolled construction of diverse, highly functionalized bioactive and pharmaceutical molecules [35-37].

The herein adopted synthetic strategy, employing photoredox-catalyzed radical cyclization, is illustrated in Scheme 4. Compound **4** was expected to be derived from tricyclic substrate **26** via a *Z*-selective cross-metathesis [9]. The allyl group in compound **26** could be installed in β-keto ester **21** via sequential transesterification [33] and palladium-catalyzed decarboxylative allylation [32]. The regio- and diastereoselective connection of C8 and C12 in compound **21** could be realized through a photoredox-catalyzed radical cyclization of unactivated alkene-substituted β-ketoester **27**. This reaction was expected to involve a 5-*exo*-*trig* radical cyclization via transition state **TS-3** [38], in which the diastereoselectivity could be controlled by the stereoelectronic effect of the axial hydroxy group at C11 (Scheme 4) [28].

First, β-keto ester **21** was synthesized (Scheme 5). Cross-metathesis of allylic alcohol **18** and olefin **28** with the assistance of the Hoveyda–Grubbs second-generation catalyst delivered the desired product **27** in 68% yield. Having accessed the β-keto ester **27**, the photoredox-catalyzed oxidative radical cyclization of compound **27** was established on a 0.8 g scale, yielding compound **21** in 80% yield, as an inseparable mixture of diastereomers at C-15, the precursor for palladium-catalyzed decarboxylative allylation. The proposed mechanism to **21** involved the formation of an electron-deficient, resonance-stabilized radical species, followed by intramolecular alkylation of the unacti-

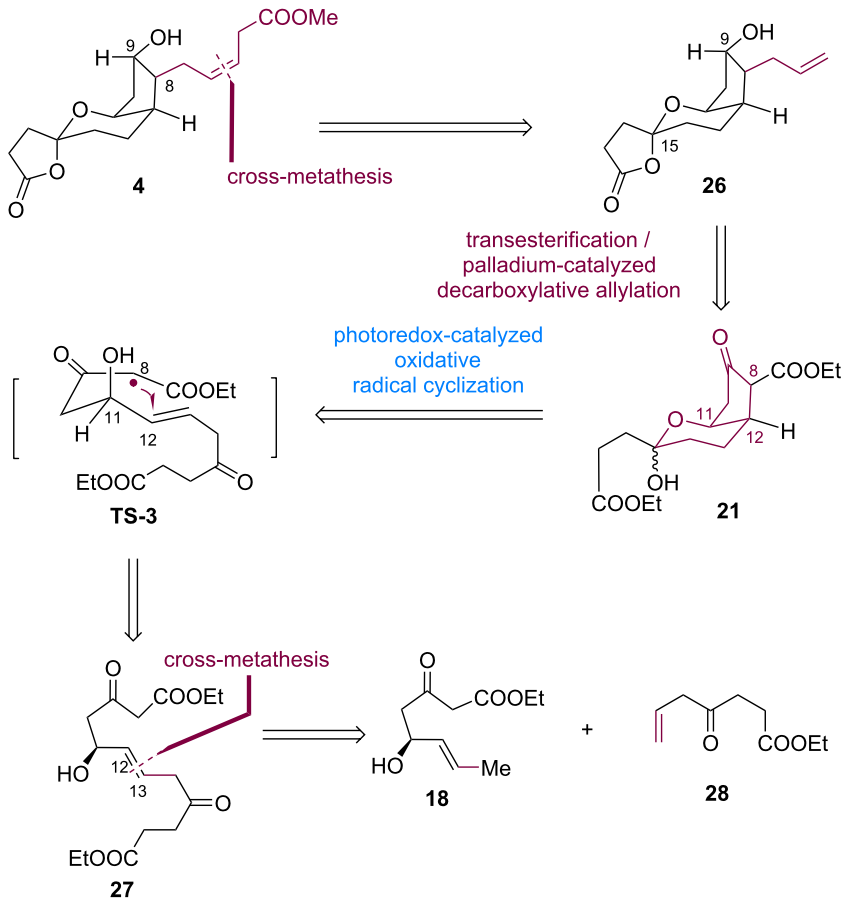

Scheme 4: Retrosynthetic analysis for the second-generation synthesis of tricyclic PGDM methyl ester **4**.

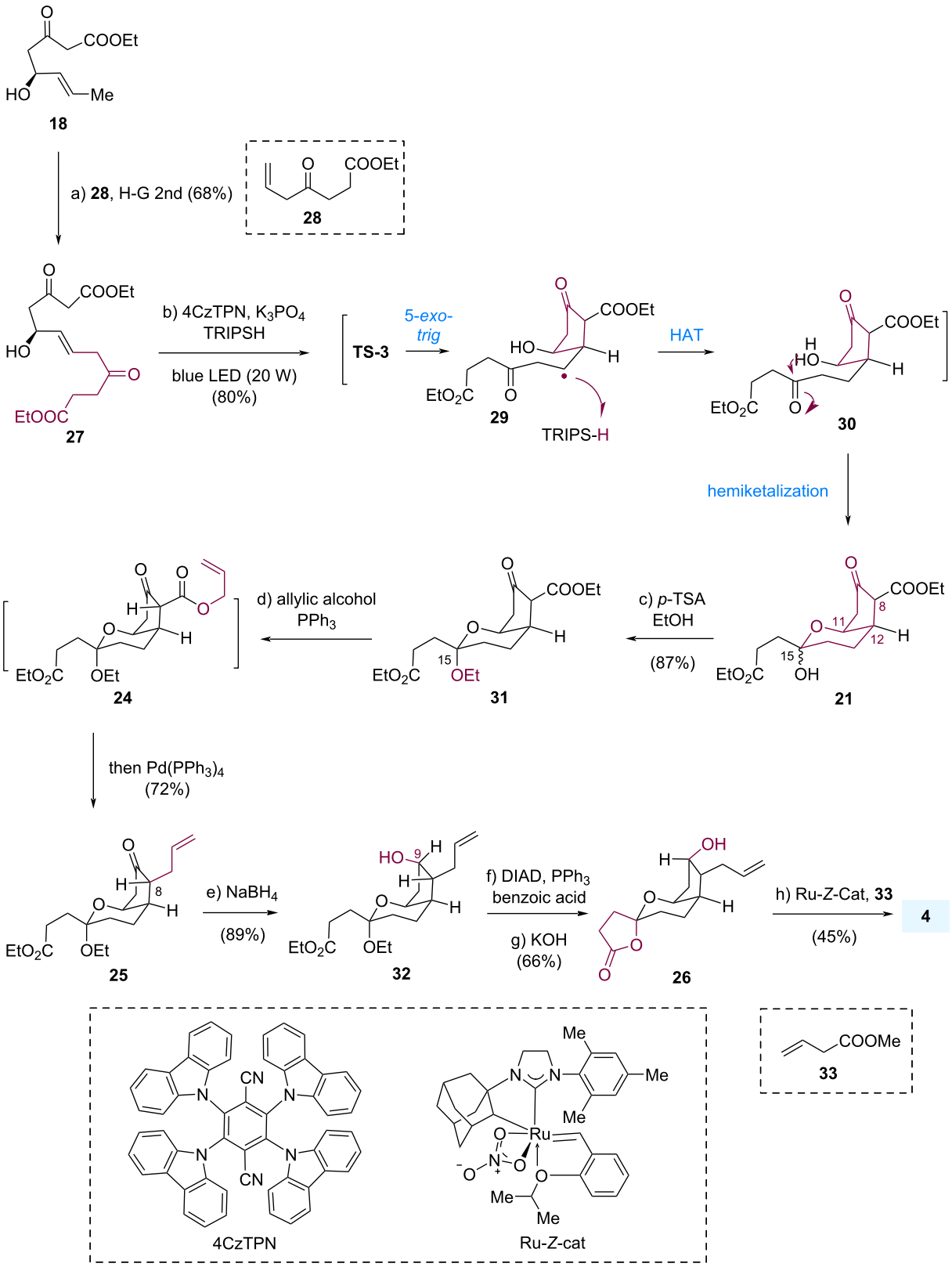

Scheme 5: Asymmetric total synthesis of tricyclic-PGDM methyl ester **4**.

vated alkene to generate radical **29** via a diastereoselective 5-*exo-trig* cyclization step. Radical intermediate **29** was trapped by 2,4,6-triisopropylbenzenethiol (TRIPSH) through a hydrogen atom transfer (HAT) process to afford intermediate **30** [39], which then cyclized to yield product **21**.

To install the allyl group at C8 with the desired stereochemistry, we treated compound **21** with *p*-TSA in EtOH at room temperature, and ketal **31** was obtained in 87% yield as a single diastereomer. Subsequently, one-pot transesterification and palladium-catalyzed decarboxylative allylation delivered compound **25** in 72% yield.

Next, we expected that we could perform a chemo- and diastereoselective reduction of the ketone to introduce the hydroxy group at C9 in a single step. However, the diastereoselective reduction of the ketone in **25** was challenging because the ketone was embedded in the concave face, which was more sterically hindered than the convex face. Common reductants, such as $NaBH_4$, DIBAL-H, and $LiAlH(O\textit{t}\text{-}Bu)_3$, provided product **32** with the opposite stereochemistry at C9. Therefore, alcohol **32** was subjected to a one-pot Mitsunobu reaction, hydrolyzation, and spirolactonization to give the corresponding alcohol **26** with inversed configuration at C9. Finally, terminal alkene **26** was transformed by Dai's Ru-catalyzed *Z*-selective cross-metathesis with **33** [9,40] to provide compound **4** in 8% overall yield over 9 steps starting from the readily available compound **16** [41].

Conclusion

In conclusion, we developed a synthetic strategy using a radical C_{sp3}–H cyclization, including Snider oxidative radical cyclization and photoredox-catalyzed radical cyclization, to construct cyclopentanols with three contiguous stereogenic centers in compound **4**. Our total synthesis also features an efficient cross-metathesis reaction to produce photoredox-catalyzed radical cyclization reaction precursor **27**, a one-pot transesterification and palladium-catalyzed decarboxylative allylation to install the side chain at C8, and a diastereoselective spirolactonization to generate the spiroketal moiety in **26**. This total synthesis is promising for divergent total syntheses of other PGs and structurally related pharmaceutical derivatives.

Supporting Information

Supporting Information File 1

Experimental procedures, characterization data and copies of ^1H and ^{13}C NMR spectra.
[https://www.beilstein-journals.org/bjoc/content/supplementary/1860-5397-21-152-S1.pdf]

Acknowledgements

We thank Prof. Zhen Yang (Peking University) for helpful discussion.

Funding

Financial support was supported by the National Natural Science Foundation of China (Grants No. 22371117), and the Science and Technology Innovation Program of Hunan Province (Grants No. 2022RC1106), and the Drug Research Project of university of South China (Grants No 211RGC012).

Author Contributions

Miao Xiao: conceptualization; data curation; formal analysis; investigation; methodology; visualization; writing – original draft; writing – review & editing. Liuyang Pu: formal analysis; investigation; methodology; validation. Qiaoli Shang: formal analysis; investigation; validation. Lei Zhu: data curation; software; validation. Jun Huang: conceptualization; data curation; formal analysis; funding acquisition; investigation; project administration; resources; supervision; writing – original draft; writing – review & editing.

ORCID® iDs

Jun Huang - https://orcid.org/0000-0003-1861-2390

Data Availability Statement

All data that supports the findings of this study is available in the published article and/or the supporting information of this article.

References

1. Gibson, K. H. *Chem. Soc. Rev.* **1977,** *6,* 489–510. doi:10.1039/cs9770600489
2. Curtis-Prior, P. B. *Prostaglandins: Biology and Chemistry of Prostaglandins and Related Eicosanoids;* Churchill Livingstone: Edinburgh, UK, 1988.
3. Funk, C. D. *Science* **2001,** *294,* 1871–1875. doi:10.1126/science.294.5548.1871
4. Dams, I.; Wasyluk, J.; Prost, M.; Kutner, A. *Prostaglandins Other Lipid Mediators* **2013,** *104–105,* 109–121. doi:10.1016/j.prostaglandins.2013.01.001
5. Liston, T. E.; Roberts, L. J., II. *J. Biol. Chem.* **1985,** *260,* 13172–13180. doi:10.1016/s0021-9258(17)38853-1
6. Morrow, J. D.; Prakash, C.; Awad, J. A.; Duckworth, T. A.; Zackert, W. E.; Blair, I. A.; Oates, J. A.; Jackson Roberts, L., II. *Anal. Biochem.* **1991,** *193,* 142–148. doi:10.1016/0003-2697(91)90054-w
7. Prakash, C.; Saleh, S.; Roberts, L. J.; Blair, I. A.; Taber, D. F. *J. Chem. Soc., Perkin Trans. 1* **1988,** 2821–2826. doi:10.1039/p19880002821
8. Kimbrough, J. R.; Austin, Z.; Milne, G. L.; Sulikowski, G. A. *Org. Lett.* **2019,** *21,* 10048–10051. doi:10.1021/acs.orglett.9b03983
9. Sims, H. S.; de Andrade Horn, P.; Isshiki, R.; Lim, M.; Xu, Y.; Grubbs, R. H.; Dai, M. *Angew. Chem., Int. Ed.* **2022,** *61,* e202115633. doi:10.1002/anie.202115633

10. Collins, P. W.; Djuric, S. W. *Chem. Rev.* **1993,** *93,* 1533–1564. doi:10.1021/cr00020a007
11. Das, S.; Chandrasekhar, S.; Yadav, J. S.; Grée, R. *Chem. Rev.* **2007,** *107,* 3286–3337. doi:10.1021/cr068365a
12. Peng, H.; Chen, F.-E. *Org. Biomol. Chem.* **2017,** *15,* 6281–6301. doi:10.1039/c7ob01341h
13. Corey, E. J.; Weinshenker, N. M.; Schaaf, T. K.; Huber, W. *J. Am. Chem. Soc.* **1969,** *91,* 5675–5677. doi:10.1021/ja01048a062
14. Coulthard, G.; Erb, W.; Aggarwal, V. K. *Nature* **2012,** *489,* 278–281. doi:10.1038/nature11411
15. Hayashi, Y.; Umemiya, S. *Angew. Chem., Int. Ed.* **2013,** *52,* 3450–3452. doi:10.1002/anie.201209380
16. Zhang, F.; Zeng, J.; Gao, M.; Wang, L.; Chen, G.-Q.; Lu, Y.; Zhang, X. *Nat. Chem.* **2021,** *13,* 692–697. doi:10.1038/s41557-021-00706-1
17. Ungrin, M. D.; Carrière, M.-C.; Denis, D.; Lamontagne, S.; Sawyer, N.; Stocco, R.; Tremblay, N.; Metters, K. M.; Abramovitz, M. *Mol. Pharmacol.* **2001,** *59,* 1446–1456. doi:10.1016/s0026-895x(24)12272-9
18. Sih, C. J.; Ambrus, G.; Foss, P.; Lai, C. J. *J. Am. Chem. Soc.* **1969,** *91,* 3685–3687. doi:10.1021/ja01041a065
19. Jahn, U.; Galano, J.-M.; Durand, T. *Angew. Chem., Int. Ed.* **2008,** *47,* 5894–5955. doi:10.1002/anie.200705122
20. Snider, B. B.; Mohan, R.; Kates, S. A. *J. Org. Chem.* **1985,** *50,* 3659–3661. doi:10.1021/jo00219a054
21. Snider, B. B. *Chem. Rev.* **1996,** *96,* 339–364. doi:10.1021/cr950026m
22. Šmit, B.; Rodić, M.; Pavlović, R. Z. *Synthesis* **2016,** *48,* 387–393. doi:10.1055/s-0035-1561285
23. Aho, J. E.; Pihko, P. M.; Rissa, T. K. *Chem. Rev.* **2005,** *105,* 4406–4440. doi:10.1021/cr050559n
24. Snider, B. B.; Patricia, J. J. *J. Org. Chem.* **1989,** *54,* 38–46. doi:10.1021/jo00262a016
25. Xu, Q.; Yu, J.; Han, F.; Hu, J.; Chen, W.; Yang, L. *Tetrahedron: Asymmetry* **2010,** *21,* 156–158. doi:10.1016/j.tetasy.2010.01.008
26. Snider, B. B.; Merritt, J. E.; Dombroski, M. A.; Buckman, B. O. *J. Org. Chem.* **1991,** *56,* 5544–5553. doi:10.1021/jo00019a014
27. Motiwala, H. F.; Armaly, A. M.; Cacioppo, J. G.; Coombs, T. C.; Koehn, K. R. K.; Norwood, V. M., IV; Aubé, J. *Chem. Rev.* **2022,** *122,* 12544–12747. doi:10.1021/acs.chemrev.1c00749
28. Chamberlin, A. R.; Mulholland, R. L., Jr.; Kahn, S. D.; Hehre, W. J. *J. Am. Chem. Soc.* **1987,** *109,* 672–677. doi:10.1021/ja00237a006
29. Nair, V.; Deepthi, A. *Chem. Rev.* **2007,** *107,* 1862–1891. doi:10.1021/cr068408n
30. Nair, V.; Mathew, J.; Prabhakaran, J. *Chem. Soc. Rev.* **1997,** *26,* 127–132. doi:10.1039/cs9972600127
31. Citterio, A.; Cerati, A.; Sebastiano, R.; Finzi, C.; Santi, R. *Tetrahedron Lett.* **1989,** *30,* 1289–1292. doi:10.1016/s0040-4039(00)72739-0
32. Tsuda, T.; Chujo, Y.; Nishi, S.; Tawara, K.; Saegusa, T. *J. Am. Chem. Soc.* **1980,** *102,* 6381–6384. doi:10.1021/ja00540a053
33. Yadav, J. S.; Reddy, B. V. S.; Krishna, A. D.; Reddy, C. S.; Narsaiah, A. V. *J. Mol. Catal. A: Chem.* **2007,** *261,* 93–97. doi:10.1016/j.molcata.2006.07.060
34. Strassfeld, D. A.; Chen, C.-Y.; Park, H. S.; Phan, D. Q.; Yu, J.-Q. *Nature* **2023,** *622,* 80–86. doi:10.1038/s41586-023-06485-8
35. Romero, K. J.; Galliher, M. S.; Pratt, D. A.; Stephenson, C. R. J. *Chem. Soc. Rev.* **2018,** *47,* 7851–7866. doi:10.1039/c8cs00379c
36. Pitre, S. P.; Weires, N. A.; Overman, L. E. *J. Am. Chem. Soc.* **2019,** *141,* 2800–2813. doi:10.1021/jacs.8b11790
37. Pitre, S. P.; Overman, L. E. *Chem. Rev.* **2022,** *122,* 1717–1751. doi:10.1021/acs.chemrev.1c00247
38. Forbes, K. C.; Crooke, A. M.; Lee, Y.; Kawada, M.; Shamskhou, K. M.; Zhang, R. A.; Cannon, J. S. *J. Org. Chem.* **2022,** *87,* 3498–3510. doi:10.1021/acs.joc.1c03055
39. Dénès, F.; Pichowicz, M.; Povie, G.; Renaud, P. *Chem. Rev.* **2014,** *114,* 2587–2693. doi:10.1021/cr400441m
40. Quigley, B. L.; Grubbs, R. H. *Chem. Sci.* **2014,** *5,* 501–506. doi:10.1039/c3sc52806e
41. Xiao, M.; Shang, Q.; Pu, L.; Wang, Z.; Zhu, L.; Yang, Z.; Huang, J. *JACS Au* **2025,** *5,* 1367–1375. doi:10.1021/jacsau.4c01268

License and Terms

BEILSTEIN JOURNAL OF ORGANIC CHEMISTRY

Bioinspired total syntheses of natural products: a personal adventure

Zhengyi Qin[1], Yuting Yang[1], Nuran Yan[1], Xinyu Liang[1], Zhiyu Zhang[1], Yaxuan Duan[1], Huilin Li[*1,2] and Xuegong She[*1]

Review

Open Access

Address:
[1]State Key Laboratory of Natural Product Chemistry, College of Chemistry and Chemical Engineering, Lanzhou University, Lanzhou 730000, P. R. China and [2]State Key Laboratory of Green Pesticide, Guizhou University, Guiyang 550025, P. R. China

Email:
Huilin Li[*] - lihuilin@lzu.edu.cn; Xuegong She[*] - shexg@lzu.edu.cn

* Corresponding author

Keywords:
bioinspired total synthesis; chabranol; gymnothelignans; monocerin; sarglamides; tabergingine

Beilstein J. Org. Chem. **2025,** *21,* 2048–2061.
https://doi.org/10.3762/bjoc.21.160

Received: 27 July 2025
Accepted: 24 September 2025
Published: 09 October 2025

This article is part of the thematic issue "Concept-driven strategies in target-oriented synthesis".

Associate Editor: D. Y.-K. Chen

Abstract

Bioinspired total synthesis represents an important concept to guide the designing of powerful synthetic strategies. Our group has a long-time interest and experience in designing synthetic strategies through analyzing the biosynthetic pathway of natural products. Recently, we have achieved an array of bioinspired total syntheses, which showed the great power of this approach in natural product synthesis. Documented herein is a review of these achievements which include the detailed process of how we develop these strategies. Specifically, bioinspired total synthesis of three types of natural products, namely diterpenoids (chabranol, and monocerin), alkaloids (indole, hydroquinoline, and monoterpenoid−indolidinoid hybrid), and gymnothelignans are discussed. Based on these achievements on bioinspired total synthesis, we provide some information on how to use this important strategy in natural product synthesis.

Introduction

Natural products are chemical substances generated within living organisms in nature. They are products of biotic evolution in which live survives from changes of Earth environment by changing themselves. Natural products play a pivotal role in biological transformations within organisms, and moreover, are of great value for human life by serving as food, cloth and medicine. It represents a longstanding goal in human history to obtain natural products and develop new applications. Traditionally, natural products are directly obtained from its natural source, such as sugar and vitamins. Since Wöhler's historic success [1] in converting widely believed "inorganic" materials into the "organic" compound urea, people began to be aware of the capability of mankind in making natural organic molecules. Since then, organic scientists are brave to challenge the complex organic structure of natural products given by nature [2-5]. To achieve the growing structural complexity of natural prod-

ucts, the synthetic capability have been increasing all the time by discovering and inventing a vast number of new organic reactions and methodologies [6]. However, could mankind become really stronger than Mother Nature one day? This question seems to have no answer as future is unpredictable. Maybe, Mother Nature could be our teacher and elevate our synthetic capability in some way.

In academia, learning from nature from the synthetic point of view has a very long history. A remarkable example is Robinson's tropinone synthesis early in 1917 [7] (Figure 1). This historic event may be ahead of its time and it allows rapid assembly of a complex natural product with a three-dimensional framework in a cascade way. Later, this was regarded as an artificial mimic in laboratory of the biochemical transformations in nature. In the 20th century, Woodward elevated the field of natural product total synthesis to the artistic status [8], and Corey drove it to a precise science full of chemical logics [6]. In this period, a lot of biomimetic total synthesis came out, such as Johnson's progesterone synthesis [9,10] Heathcock's synthesis of daphniphyllum alkaloids [11] and Nicolaou's synthesis of endiandric acids [12-15] (Figure 1). The bioinspired total synthesis literally showed the great power to gain complexity. In the 21st century, biomimetic or bioinspired synthesis has been widely realized as a powerful concept approach to natural product total synthesis, and a lot of total synthetic works of this kind have been reported.

A bioinspired approach represents many advantages to bring benefits to total synthesis. It could rapidly achieve complexity of the target molecule from a much simpler precursor in diverse forms of transformations such as cascade reaction, cycloaddition, and C–H functionalization, thereby, shorten the synthetic steps and gain efficiency. More significantly, since the exact biosynthetic pathway of a natural product is generally very complicated and hard to elucidate clearly, a biosynthetic pathway is basically proposed by the isolating scientist according to the structural analysis of the symbiotic natural products. The proposal lacks strong evidences, no matter it is scientifically reasonable or not. The bioinspired synthetic would provide evidences to support such a plausible biogenetic pathway through chemical transformations under simple biomimetic reaction conditions like acid, base, or visible light.

How to design a bioinspired approach may be most attractive to synthetic chemists. Recently, Tang [16] and Jia [17] independently reviewed their remarkable bioinspired total syntheses as accounts. Tang documented their longtime carrier of learning from nature aiming to achieve better results than nature. Jia categorized their works into three sections to showcase how they learn from nature, including 1) to mimic the key cyclization steps, 2) to mimic the revised biosynthetic pathway proposed, and 3) to mimic the skeletal diversification process. These three types of bioinspired synthesis probably lead this field to the lane of scientific logic, which would provide guidelines to design a bioinspired strategy.

Our group has a long-time of research experience on complex natural product synthesis. To achieve higher efficiency of synthesis, we inevitably exploited the concept of biomimetic or bioinspired total synthesis. Indeed, this approach has been proved to be of great power to access molecular complexity,

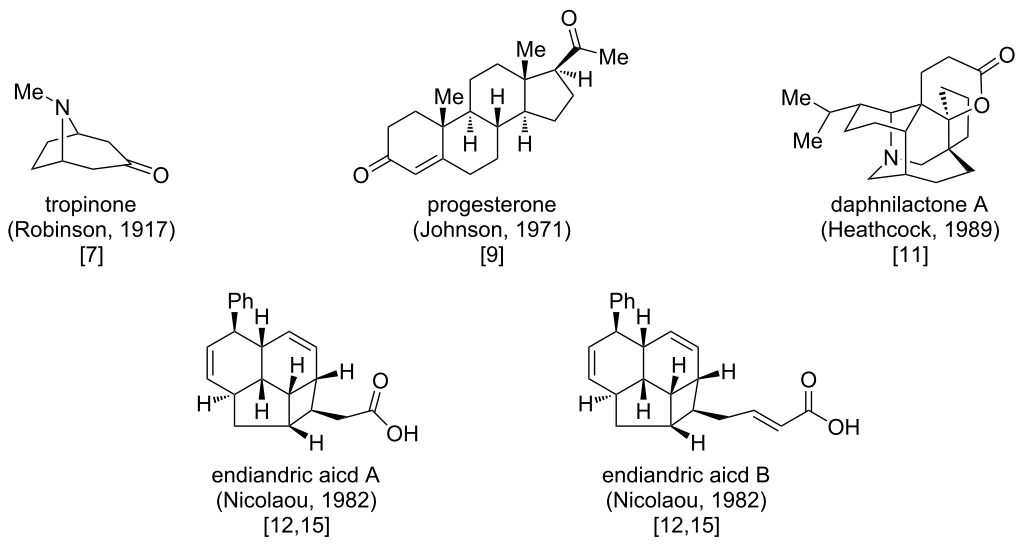

Figure 1: Representative natural products with biomimetic total synthesis.

and it is applicable to diverse types of natural products such as terpenoids, alkaloids, polyketides and lignans. Herein, we document our adventure of bioinspired total synthesis of natural products.

Review

Synthesis of chabranol

In 2009, Duh and co-workers investigated the ingredients of Formosan soft corals *Sinularia capillosa* Tixier-Durivault and *Nephthea chabroli* Audouin, collected from west pacific Dongsha Atoll and Siaoliouciou Island, providing two terpenoid natural products capillosanol and chabranol, respectively [18]. Chabranol was identified to contain a new bridged skeleton through extensive NMR experiments. However, no single-crystal X-ray diffraction analysis was conducted, making the structural determinations not that solid. It showed moderate cytotoxicity against P-388 (mouse lymphocytic leukemia). Attracted by the novel bridged structure and in order to further determine the structure, particularly the absolute configurations, we explored the total synthesis of chabranol [19].

Structurally, this molecule contains an oxa-[2.2.1] bridge, with two quaternary centers including one at the bridgehead position. To establish a proper strategy for total synthesis, we could, somehow, design its retrosynthetic analysis through diverse approaches to construct such a bicyclic skeleton. However, inspired by the biomimetic polycyclization of terpenoids, we sought to propose the biosynthetic pathway, which has not yet been reported in Duh's isolation report (Scheme 1a). In our proposal, the linear sesquiterpenoid *trans*-nerolidol (**1**) with a chiral tertiary alcohol undergoes dihydroxylation to generate triol **2**, which further proceeds a C–C bond cleavage to afford aldehyde **3**. This linear aldehyde would be activated by an acid to trigger a key Prins cyclization with the trisubstituted olefin through reaction model **3** and generate a putative tertiary carbocation to be trapped by the chiral alcohol, providing bicycle **4** stereoselectively. Finally, the last olefin would be oxidized to ketone, which gives chabranol.

According to this biosynthetic proposal, we thought that the Prins-triggered double cyclization would serve as a powerful

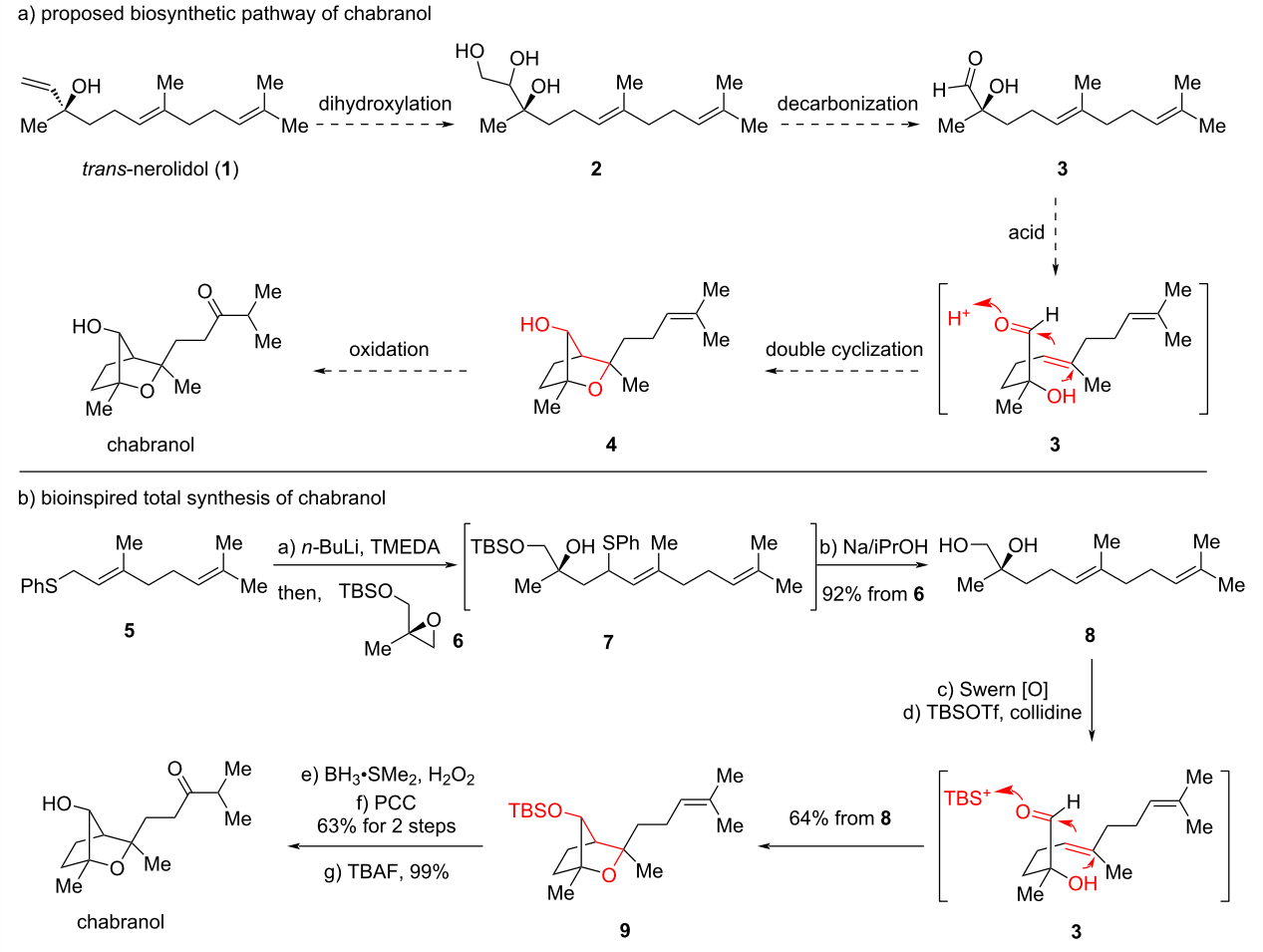

Scheme 1: Bioinspired total synthesis of chabranol (2010).

method to construct the bicycle in one step, and moreover, the proposed Prins-based double cyclization needs further supporting evidences of chemical transformations. Thus, a bioinspired total synthesis was investigated (Scheme 1b). Synthetically, we did not start from *trans*-nerolidol (**1**) to construct a C–C bond cleavage. Instead, a convergent coupling approach was selected to quickly access the aldehyde precursor. Phenyl sulfide **5**, derived from phenylthiol and geranyl bromide, coupled with chiral epoxide **6**, prepared through Sharpless epoxidation and TBS protection of 2-methylprop-2-en-1-ol, under strong basic conditions to generate intermediate **7** to further reduce the sulfide moiety with sodium, furnishing diol **8** with the loss of TBS protection in one pot. Oxidation of the primary alcohol using Swern oxidation gave the hydroxy aldehyde **3**, which was activated with a formal silicon cation to trigger the Prins cyclization terminated by the tertiary alcohol, affording silylated bicycle **9** directly through the designed bioinspired approach. This key reaction mimics the plausible biosynthetic pathway and demonstrates great efficiency and sole diastereoselectivity, showcasing the plausibility of the biosynthetic proposal. Further redox manipulations of the last olefin and deprotection ultimately provided chabranol. To clearly confirm the structure further, X-ray diffraction analysis of the derivative of bicycle **9** was obtained. This approach established the first total synthesis of chabranol in a concise way through the bioinspired Prins-triggered double cyclization strategy to rapidly construct the bicycle.

Total syntheses of natural products of the monocerin-family

Early in 1979, monocerin and 7-O-demethylmonocerin were elucidated from *Fusarium larvarum* [20]. Since then, a large group of analogues have been isolated from diverse fungal species [21-25] (Scheme 2). Along with the structural elucidation, biological studies of these molecules indicated that they exhibit a broad-spectrum activities including antifungal, insecticidal, plant pathogenic properties and phytotoxic activity. Structurally, these molecules basically contain an isocoumarin ring system and a five-carbon side chain. The side chain could further form a *cis*-substituted tetrahydrofuran (THF) moiety fused to the lactone with higher oxidation states. Notably, the phenyl ring contains three oxygen substituents in the form of alcohol and methoxy groups at different positions.

Biosynthetically, the THF ring was supposed to be formed through a benzylic oxidation to generate a *para*-quinone methide (*p*QM) intermediate. Using fusarentin 6-methyl ether as an example, *p*QM intermediate **10** would be generated. The C10 alcohol should successively undergo an oxa-Michael addition reaction to close the THF ring, providing 7-*O*-demethylmonocerin. Similarly, monocerin and 12-hydroxymonocerin were presumably generated from their corresponding precursors through similar oxidation and oxa-Michael addition reactions. Given the fact that quinone methides served as a powerful platform for the development of rich useful organic transformations, especially, through catalytic asymmetric methods [26], we intended to probe this biomimetic oxidative cyclization transformation [27,28].

In 2013, we first used monocerin as a model target molecule to initiate our study (Scheme 3a). Starting from benzaldehyde **11** with an isopropyl group on the hydroxy group in 4-position, Wittig reaction with $MOMPPh_3Cl$ and LDA gave the putative methyl enol ether, which could be directly converted into 1,3-dithiane **12** with propane-1,3-dithiol. Nucleophilic addition to chiral epoxide **13** and oxidative hydrolysis of 1,3-dithiane to ke-

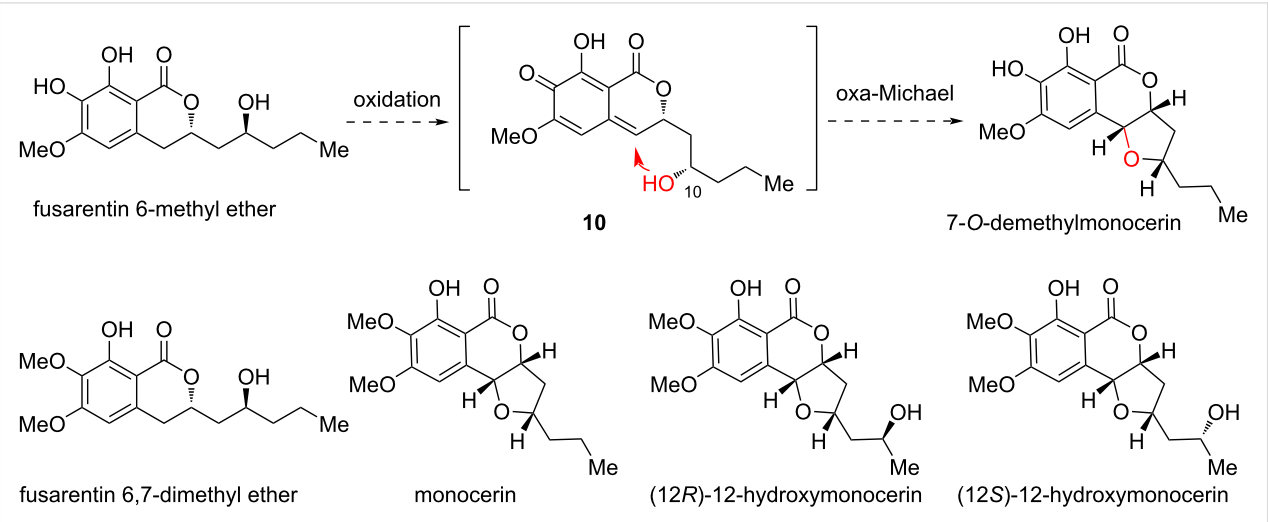

Scheme 2: Proposed biosynthetic pathway of monocerin-family natural products.

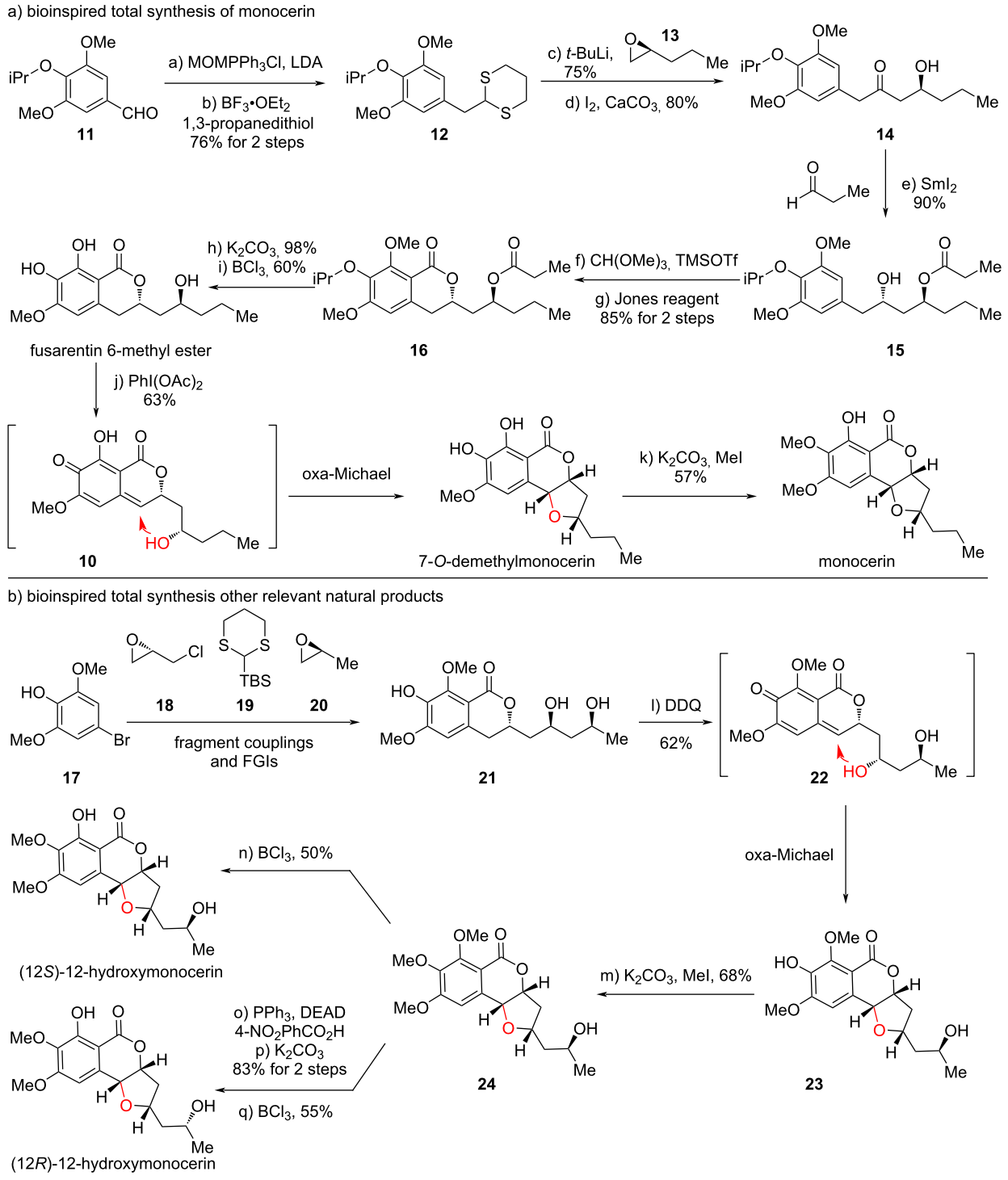

Scheme 3: Bioinspired total synthesis of monocerin-family molecules (2013).

tone delivered chiral β-hydroxyketone **14**. Evans–Tishchenko reduction of ketone using SmI_2 and propionaldehyde provided **15** diastereoselectively. Friedel–Crafts cyclization using trimethyl orthoformate and TMSOTf provided the cyclic acetal moiety to be oxidized with PDC, delivering the isocoumarin skeleton in **16**. Chemoselective removal of the ester with the lactone unreacted, which released the secondary alcohol, followed by BCl_3-promoted selective cleavage of the isopropyl and one methyl protection ultimately furnished thenatural product fusarentin 6-methyl ether.

With fusarentin 6-methyl ether in hand, we explored the bioinspired oxidation/oxa-Michael addition. This transformation was successfully achieved by using $PhI(OAc)_2$ as oxidant, providing 7-*O*-demethylmonocerin, containing the *cis*-substituted THF ring with sole diastereoselectivity. Site-selective mono-methylation gave rise to monocerin.

The bioinspired approach successfully found applications in the total synthesis of the monocerin-type natural products bearing a C10 alcohol. However, for other molecules with a C12 alcohol, it is unknown whether the C12 alcohol would bring challenges to the oxa-Michael addition or not. To investigate this, we used fragments **17**–**20** to access diol substrate **21**, through Smith's 1,3-dithiane linchpin coupling (Scheme 3b). To our delight, using DDQ as the optimal oxidizing reagent, the expected THF-containing product **23** was generated as a sole diastereoisomer, suggesting the *p*QM **22** underwent oxa-Michael addition only with the C10 alcohol. The free C12 alcohol did not affect this process, which further supported the probability of the proposed biosynthetic approach. Subsequently, site-selective methylation on phenol provided **24**, which further underwent *O*-directed demethylation to afford (12*S*)-hydroxymonocerin. On the other hand, a two-step protocol involving Mitsunobu reaction with an acid and base-promoted saponification inversed the C12 alcohol stereochemistry, which ultimately provided (12*R*)-hydroxymonocerin.

Total synthesis and bioinspired skeletal diversification of (12-MeO)-tabertinggine

In 2013, Kam and co-workers reported the discovery of two novel indole alkaloids voatinggine and tabertinggine from the plants of *Tabernaemontana* (Apocynaceae) genus in Malayan, which are literally widely distributed in tropical America, Africa, and Asia [29]. Given the fact that these plants are rich sources of bioactive alkaloids, voatinggine and tabertinggine with unprecedented skeletons are of great interests to synthetic chemists, since the biological studies are limited due to material scarcity in the nature.

Structurally, tabertinggine contains an aza-[3.2.1] bridged skeleton linked to indole C2 position. To rationalize how this unique structure is generated in nature (Scheme 4a), Kam proposed that tabertinggine might be biosynthetically generated from an ibogamine precursor keto-ibogamine through an indole oxidation and C21–N bond cleavage process to give intermediate **25**, which further undergoes a cyclization to form the C16–N bond and dehydration to generate the enone. By analyzing the structure, we supposed that there might exist an inversed pathway in which tabertinggine could be converted into the ibogamine aza-[2.2.2] bridged skeleton through intramolecular aza-Michael addition of the enone moiety to form the C21–N bond and a subsequent C16–N bond cleavage process (N-walking from C16 to C21) [30]. To investigate this proposal, we first developed the total synthesis of tabertinggine to obtain enough material for biogenetic skeletal diversification (Scheme 4b).

As shown in Scheme 4b, the total synthesis of tabertinggine started from the Pictet–Spengler cyclization of tryptamine **26a** with keto-diester intermediate **27** followed with a lactamization reaction in one-pot to access the γ-lactam moiety in product **28a**, which was obtained after Boc protection. Base-promoted aldol reaction of lactam **28a** with aldehyde **29** gave rise to alcohol **30a**, which subsequently underwent dehydroxylation protocol involving base-promoted mesylate elimination and catalytic hydrogenation reactions, providing **31a**. Reduction of lactam and ester in one pot with $LiAlH_4$ and acid-promoted hydrolysis of ketal protection to ketone furnished **32a**. Finally, oxidation of the primary alcohol to aldehyde followed by base-promoted aldol condensation reaction successfully provided tabertinggine. This approach achieved the first total synthesis of tabertinggine in only ten steps and capable of supplying enough material for the following skeletal diversifications.

With sufficient tabertinggine in hand, we treated it to Zn powder in AcOH to facilitate the N-walking transformation, and generated keto-ibogamine product **33** as a mixture of diastereomers (Scheme 4c). Then, reduction of ketone to methylene under Wolff–Kishner–Huang conditions provided ibogamine and its epimer in a 1:1.3 ratio. This result supported our proposal that tabertinggine might be the biogenetic precursor of ibogamine.

To further access some other natural products through skeletal diversifications, we found that some target molecules contain an OMe group at C12 position. So, 12-OMe-tabertinggine was prepared from C5-OMe-tryptamine **26b** just following the same route for synthesis of tatertinggine, and the yield of each step was basically comparable (Scheme 4b). Starting from 12-OMe-tabertinggine, Zn-promoted N-walking and ketone reduction provided ibogaine in 1:3 ratio with the major epimer. Indole oxidation with DMDO provided **34** as a single isomer, which further underwent a migratory rearrangement and afforded iboluteine. On the other hand, oxidation of ibogaine with molecular iodine achieved both indole and amine oxidations, delivering lactam **35**. Intermediate **35** could be oxidized with H_2O_2 through C–C bond cleavage to give natural product ervaoffine D. Thus, through the bioinspired skeletal diversifications of (12-OMe)-tabertinggine, four iboga alkaloids could be powerfully synthesized.

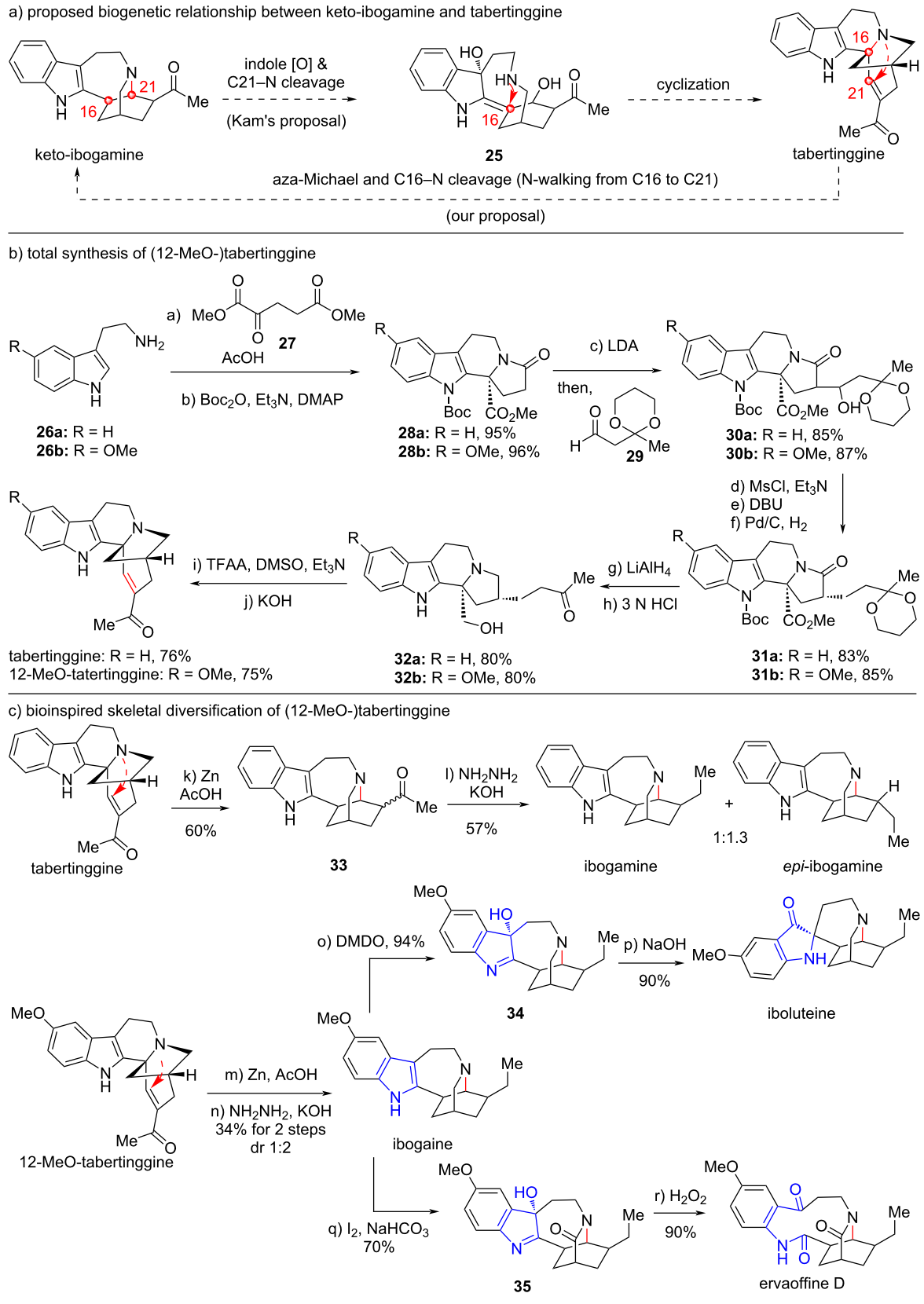

Scheme 4: Bioinspired skeletal diversification of (12-MeO-)tabertinggine (2016).

Bioinispired total synthesis of gymnothelignans

The *Gymnotheca* (Saururaceae) genus only contains two species of plants, *Gymnotheca chinensis* Decne and *Gymnotheca involucrate* Pei. These two plants are endemic in China, and have been used as medicinal herb for a long history to treat diseases such as dysentery, abdominal distention, edema, contusion, and strains [31]. Since 2012, Zhou and co-workers extensively investigated the ingredients of these plants, and have elucidated a huge number of lignan natural products with novel structural backbones [32-35] (Scheme 5a). Biologically, the gymnothelignans exhibit a broad-spectrum of properties such as antiviral, antifungal, and insecticidal activities.

Structurally, gymnothelignans included five types of common skeletons, namely eupomatilone, eupodienone, dibenzocyclooctene, and a novel spirocyclic and a linear skeleton (Scheme 5a). Notably, each of the skeleton comprises a series of members with diverse forms of oxidation states or dimers, and only one member is displayed. It is also worth noting that the former three types of lignans were isolated first from *Gymnotheca chinensis* Decne and the spirocyclic and linear members were latterly discovered from *Gymnotheca involucrate* Pei.

With respect to the biogenetic pathway of gymnothelignans, Zhou tentatively proposed a biosynthetic approach for the early isolated members of eupomatilone, eupodienone, and dibenzocyclooctene skeletons. We analyzed the structures and proposed a new biogenetic pathway of gymnothelignans with some differences to Zhou's proposal [36-39]. As shown in Scheme 5b, the dibenzylbutane skeleton might undergo benzylic oxidations and intramolecular dehydration to access a diaryltetrahydrofuran (THF) skeleton. Then, oxidation of one aryl group through phenol oxidation would generate a putative cyclohexadienone intermediate to be further captured by the other phenol to access eupodienone through a Friedel–Crafts reaction. Next, the cyclohexadienone moiety could be activated by an acid to undergo a rearrangement reaction to provide eupomatilone. The exocyclic THF ring might exist as diverse forms such as hemiacetal, acetal, lactone or acetal-linked dimer. The (hemi)acetal moiety could generate an oxa-carbenium cation triggered by an acid to proceed a Friedel–Crafts reaction to afford the dibenzocyclooctene skeleton. On the other hand, eupomatilone would undergo redox transformations to generate another oxa-carbenium cation to undergo a Friedel–Crafts reaction to form a spirocyclic skeleton. This oxa-carbenium cation could also undergo hydrolysis to provide a linear skeleton with a hydroxy ketone moiety, and this hydrolysis process is reversible. It is worth noting that Zhou explored the chemical conversion of the eupodienone skeleton to the eupomatilone skeleton through acid-promoted rearrangement under the conditions of H_2SO_4/MeOH, since their isolation of the natural products [32]. However, other critical bioinspired transformations have not yet been explored, which prompted us to initiate this study.

Guided by this biogenetic proposal, we conducted a series of reactions to probe the proposed key transformations (Scheme 6). Starting from the diaryl-THF-type precursor **36** with a phenol moiety, oxidation of the phenol with hypervalent iodine reagent PIDA generated the putative oxa-carbenium intermediate **37**, which successfully underwent the Friedel–Crafts cyclization to provide gymnothelignan N site-selectively [36] (Scheme 6a). The favored position of the Friedel–Crafts cyclization is literally the expected one, and it matches with the case in nature for generation of the natural product gymnothelignan N. This reaction successfully converts an open diaryl-THF-type precursor into an eupodienone skeleton. Our screened reaction conditions for the oxidative Friedel–Crafts cyclization were re-conducted by Lee and co-workers to show similar results for the synthesis of gymnothelignan N [40]. Then, we prepared the eupomatilone precursor **38** with a diphenyl and a lactone moiety through a stereoselective de novo approach [37]. The lactone was reduced with DIBAL-H to a semiketal, which was treated with the Lewis acid $BF_3{\cdot}OEt_2$ to generate the putative oxa-carbenium **39**. This cation triggered the Friedel–Crafts proposed cyclization with the electron-rich phenyl ring to give the dibenzocyclooctene product, which finally afforded the corresponding natural product gymnothelignan L after removal of the Bn protection (Scheme 6b). Interestingly, this transformation not only provided the expected skeleton, but also showed sole stereoselectivity in constructing the axially chiral diphenyl moiety. The obtained axial chirality is identical to the naturally occurring one. Almost at the same time, Soorukram and co-workers reported the same approach to access the dibenzocyclooctene member gymnothelignan V [41]. Next, we examined the bioinspired transformation of the linear skeleton to the spirocycle. By using chiral compound **40** with an acid-sensitive protecting group MEM on the alcohol as the precursor, the simple Brønsted acid TsOH successfully promoted the deprotection and dehydration to generate oxa-carbenium **41**, which subsequently proceeded the Friedel–Crafts cyclization to furnish gymnothespirolignan A in excellent yield and good diastereoselectivity [38] (Scheme 6c). The minor epimer is gymnothespirolignan C, another natural product of this family. This cascade reaction supports the proposed biogenetic pathway of the newly isolated novel siprocyclic gymnothelignans. The bioinspired double cyclization to forge the spirocycle in one step represents a comparably more powerful method to rapidly generate complexity, since the de novo synthesis approach by Cuny and co-workers [42] has inevitably met with a

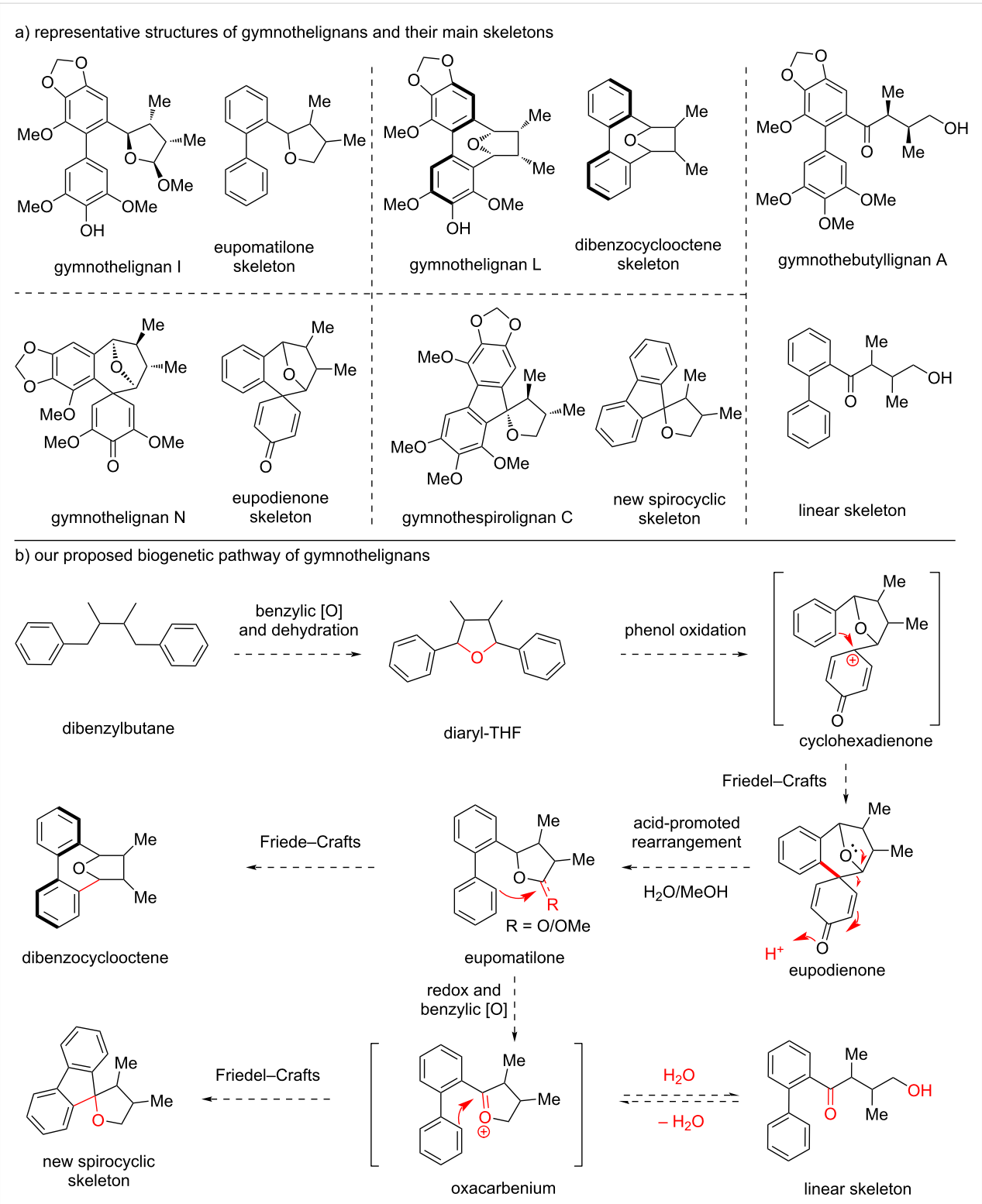

Scheme 5: Structures and our proposed biosynthetic pathway of gymnothelignans.

lot of problems on stereoselectivity although they started the synthesis from a tricyclic fluorenone to mainly focus on the construction of the THF system.

These bioinspired transformations served as solid evidences of chemical conversions to support the plausible biogenetic pathway of how the diverse skeletons of gymnothelignans were

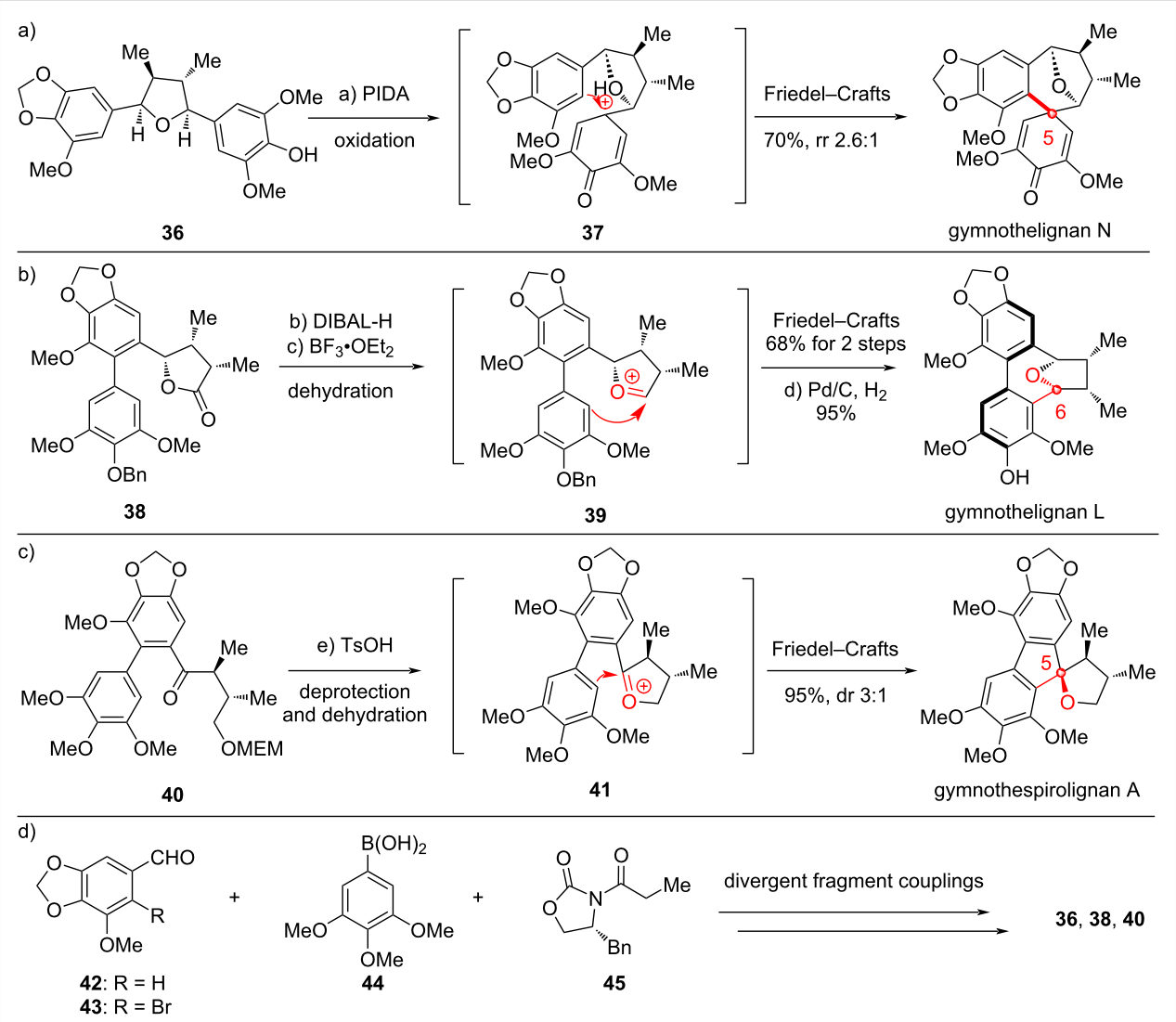

Scheme 6: Bioinspired total synthesis of gymnothelignans (2014–2025).

generated in nature. Moreover, these studies also provide powerful routes to the asymmetric total synthesis of these bioactive molecules. The precursors of the key bioinspired transformations **36**, **38** and **40** were efficiently synthesized from simple fragments aryl aldehyde **42** or **43**, phenylboronic acid **44** and chiral auxiliary-containing building block **45**, through divergent coupling approaches, and the stereocontrol with Evans oxazolidinone was always reliable to obtain an sole diastereomer (Scheme 6d).

Bioinspired concise and scalable total synthesis sarglamides

In 2023, Yue and co-workers investigated the ingredients of the Chinese folk medicine *Sarcandra glabra* subsp. *brachystachys*, and discovered a series of complex natural products named sargalmides A–E [43] (Scheme 7a). To clearly elucidate the complex structures, Yue and co-workers used multiple methods including extensive spectroscopic analysis (NMR, IR and MS), X-ray crystallography, quantum-chemical calculations, and chemical transformations. Biologically, these molecules exhibit antineuroinflammatory activity against lipopolysaccharide (LPS)-induced inflammation in BV-2 microglial cells. Structurally, these molecules generally have a tetracyclic backbone (A–D rings), among which AB rings form a bridged [2.2.2] carbocycle fused to CD rings. For sarglamides D and E, another oxygen-bridged E ring shows up at different positions. Overall, sarglamides A–E exhibit unusual unprecedented skeletons as they contain both monoterpenoid and indolidinoid subunits. Such a hybrid structure is rarely found in natural products.

Attracted by the structural uniqueness and to further confirm the structures, we initiated to explore the synthesis of these mole-

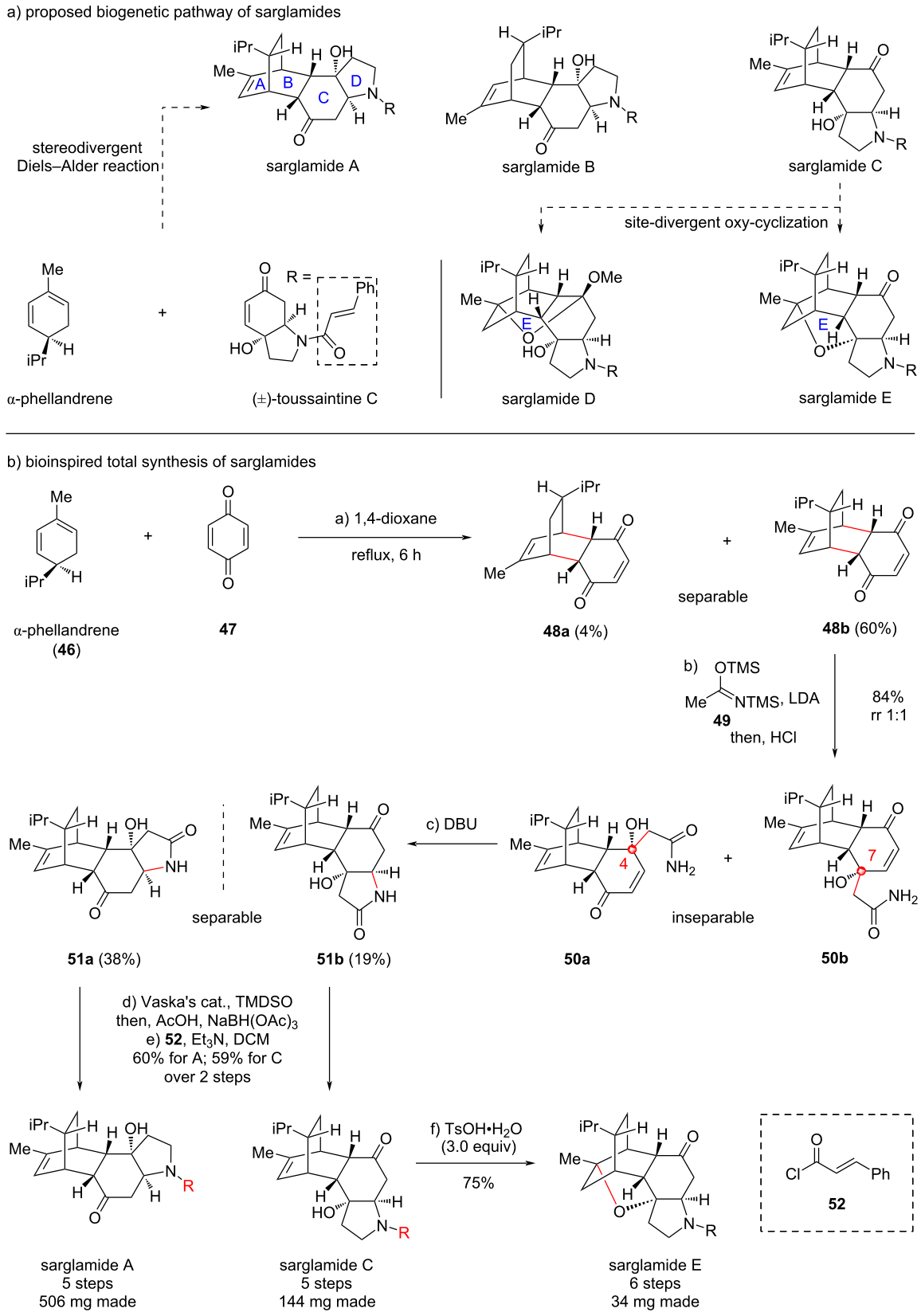

Scheme 7: Bioinspired total synthesis of sarglamides (2025).

cules. To design a practical retrosynthesis for these complex natural products, we analyzed the plausible biogenetic pathway of sarglamides to obtain some inspirations (Scheme 7a). Biogenetically, sarglamides A–C are generated directly from α-phellandrene and toussaintine C through stereodivergent Diels–Alder reactions, since the indolidinoid natural product toussaintine C is known and symbiotic with sarglamides. More importantly, a solid evidence to support this proposal is that toussaintine C was isolated as a racemic mixture, and sarglamides A and B are derived from one enantiomer of toussaintine C while sarglamides C–E are derived from the other one. The Diels–Alder cycloadditions are basically proceeded through *endo*-selectivity. The isopropyl group in α-phellandrene provided a steric effect to the cycloaddition. Then, sarglamides D and E arose from C through acid-promoted oxycyclizations. This biosynthetic approach rapidly constructs the complex structure from simple precursors, thus we intended to achieve the total synthesis of sarglamides through the bioinspired synthetic approach [44].

Initially, we prepared a bicyclic precursor similar with toussaintine C to react with α-phellandrene to mimic the bioinspired Diels–Alder reaction, which, however, showed no reactivity due to the strong steric hindrance. To decrease the steric effect, we finally used simple 1,4-benzoquinone to act as the dienophile, and the expected Diels–Alder reaction proceeded smoothly to provide the *endo* adducts **48a** and **48b**, in which **48b** was the major product dominated by the isopropyl steric effect. Isomers **48a** and **48b** were separable and determined through X-ray diffraction analysis. The major one **48b** was used for further study to install the pyrrolidine system. Thus, nucleophilic addition of an *N,O*-enolate, derived from precursor **49** with LDA, to the ketone functionality in **48b** was implemented to generate a pair of inseparable regioisomers **50a** and **50b**, arose from C4 and C7 additions, respectively. This result suggests that the addition fully went from the upper face and the left-oriented isopropyl showed no steric effect to control the regioselectivity. With free amide **50a** and **50b** in hand, the mixture was treated with DBU to promote aza-Michael addition to afford lactam compounds **51a** and **51b**, which became separable, gratifyingly. Finally, chemoselective reduction of lactam to amine with the more reactive ketone unreacted was successfully achieved. In this transformation, the iridium-catalyzed hydrosilylation of the lactam generated the corresponding *O*-silyl aminal, which was then treated with AcOH to afford the putative iminium cation to be chemoselectively reduced with $NaBH_3CN$ to ultimately reach the amine functionality. Through this protocol, the amine product was obtained, but it could not be isolated from silica gel for its high polarity. Thus, the extracted crude material of the amine was directly treated with cinnamoyl chloride under basic conditions to install the cinnamoyl side chain, delivering natural products sarglamides A and C independently. Sarglamide C was exposed to an acid to access sarglamides D and E with an oxyl-bridge. When a catalytic amount of TsOH was used, sarglamides D and E could be obtained with a 1:1 ratio, as conducted by Yue [43] and Tong [45] research groups. In our hand, we used an excess amount of TsOH (3.0 equiv), and found that sarglamide E was generated exclusively. Ultimately, a powerful total syntheses of complex polycyclic sarglamides A, C, D and E were established through a concise and protecting group-free approach, which was definitely inspired and utilized by the analysis of the biogenetic pathway of these natural products. Through this approach, a notable amount of natural products were made in one batch. The synthesis supports the proposed biogenetic pathway, and the *endo*-selective stereochemical outcome of the Diels–Alder reaction in the bioinspired synthesis fully matched with the proposed approach in nature.

Conclusion

The biomimetic or bioinspired total synthesis of natural product has gone a long way from more than one hundred years ago to today. By analyzing the plausible biogenetic pathway of natural products, one could literally obtain practical inspiration to guide the synthetic work. Utilization of this inspiration could dramatically decrease complexity of the target molecules, and ultimately lead to a powerful synthetic approach. By utilizing the concept of bioinspired total synthesis, our group has achieved the total synthesis of chabranol through a Lewis acid-promoted double cyclization, total synthesis of natural products of the monocerin-family through a benzylic oxidation and oxa-Michael addition reaction, total synthesis of (12-OMe-)tabertinggine converted it into other iboga alkaloids through skeletal diversifications, total synthesis of gymnothelignans of diverse skeletons through acid-promoted Friedel–Crafts cyclization, and the total synthesis of sarglamides through an *endo*-selective Diels–Alder reaction. These examples showcase the power of bioinspired strategies in total synthesis of complex natural products, and also provide the working model of how to utilize and develop a bioinspired total synthesis.

For a simple guidance of how to use the bioinspired total synthesis approach, one could go to figure out the symbiotic or structure-related members of the target natural product before the disconnection, and the structural similarities and differences between them would provide inspiration to the retrosynthetic disconnection pathway. Meanwhile, when a natural product or an advanced intermediate relevant to diverse naturally occurring molecules would be rationalized as a common connecting point of all molecules, a convergent strategy for collective total syntheses of natural products would be exploited through skeletal diversification. Meanwhile, symbiotic natural products involving site-, chemo-, and stereoselective patterns in

forming the polycycles could be trace back to same precursors or fragments, which would result in bioinspired total syntheses of natural products through controllable and selective chemical transformations. If there is only one single target molecule with an unprecedented skeleton, we can try to realize how the novel structure is generated in nature from known chiral pool molecules, thus a key cascade reaction to rapidly construct the novel framework would be biosynthetically applicable. This approach has found wide applications in total syntheses of newly-isolated terpenes.

There is no doubt that bioinspired total synthesis is currently a powerful and critical approach for complex natural product total synthesis. However, there still exist great challenges in the field, which would stimulate the discovery of new breakthroughs. Chemo- and regioselective employment of functionalities in a complex framework are formidable challenges for mankind since such transformations in nature are precisely induced by enzymes. Bioinspired functionalization of C–H bond in total synthesis is rarely developed and it represents another challenge, despite numerous methodologies have been invented. Moreover, bioinspired total synthesis involving visible light and enzymes are new significant trends in this field, and these techniques have demonstrated great power in achieving unprecedented selectivity and reactivity. Since nature still prevails in rapid generating molecular complexity and achieving selectivity, it is unarguably that the field of bioinspired total synthesis still has a long way to go.

Acknowledgements

We thank the graduate students in our group who undertook those research projects of bioinspired total synthesis and worked hard to achieve the final success.

Funding

This work is supported by the National Natural Science Foundation of China (NSFC 22231003, U24A20483 and 22171115), the Science and Technology Major Program of Gansu Province of China (24ZD13FA017, 23ZDFA015 and 22ZD6FA006), the State Key Laboratory of Green Pesticide and Guizhou University (GPLKF202505), and the Fundamental Research Funds for the Central Universities (FRFCU, lzujbky-2025-it46).

ORCID® iDs

Huilin Li - https://orcid.org/0000-0001-8088-6718
Xuegong She - https://orcid.org/0000-0002-3002-2433

Data Availability Statement

Data sharing is not applicable as no new data was generated or analyzed in this study.

References

1. Wöhler, F. *Ann. Phys. (Berlin, Ger.)* **1828,** *87,* 253–256. doi:10.1002/andp.18280870206
2. Kolbe, H. *Justus Liebigs Ann. Chem.* **1845,** *54,* 145–188. doi:10.1002/jlac.18450540202
3. Graebe, C.; Liebermann, C. *Ber. Dtsch. Chem. Ges.* **1869,** *2,* 332–334. doi:10.1002/cber.186900201141
4. Baeyer, A. *Ber. Dtsch. Chem. Ges.* **1878,** *11,* 1296–1297. doi:10.1002/cber.18780110206
5. Fischer, E. *Ber. Dtsch. Chem. Ges.* **1890,** *23,* 799–805. doi:10.1002/cber.189002301126
6. Corey, E. J.; Cheng, X.-M. *The Logic of Chemical Synthesis;* John Wiley & Sons: New York, NY, USA, 1989.
7. Robinson, R. *J. Chem. Soc., Trans.* **1917,** *111,* 762–768. doi:10.1039/ct9171100762
8. Woodward, R. B.; Eschenmoser, A. Vitamin B_{12}. In *Classics in Total Synthesis;* Nicolaou, K. C.; Sorensen, E. J., Eds.; Wiley-VCH: Weinheim, Germany, 1996; pp 99–136.
9. Johnson, W. S.; Gravestock, M. B.; McCarry, B. E. *J. Am. Chem. Soc.* **1971,** *93,* 4332–4334. doi:10.1021/ja00746a062
10. Gravestock, M. B.; Johnson, W. S.; McCarry, B. E.; Parry, R. J.; Ratcliffe, B. E. *J. Am. Chem. Soc.* **1978,** *100,* 4274–4282. doi:10.1021/ja00481a044
11. Ruggeri, R. B.; McClure, K. F.; Heathcock, C. H. *J. Am. Chem. Soc.* **1989,** *111,* 1530–1531. doi:10.1021/ja00186a075
12. Nicolaou, K. C.; Petasis, N. A.; Zipkin, R. E.; Uenishi, J. *J. Am. Chem. Soc.* **1982,** *104,* 5555–5557. doi:10.1021/ja00384a077
13. Nicolaou, K. C.; Petasis, N. A.; Uenishi, J.; Zipkin, R. E. *J. Am. Chem. Soc.* **1982,** *104,* 5557–5558. doi:10.1021/ja00384a078
14. Nicolaou, K. C.; Zipkin, R. E.; Petasis, N. A. *J. Am. Chem. Soc.* **1982,** *104,* 5558–5560. doi:10.1021/ja00384a079
15. Nicolaou, K. C.; Petasis, N. A.; Zipkin, R. E. *J. Am. Chem. Soc.* **1982,** *104,* 5560–5562. doi:10.1021/ja00384a080
16. Bao, R.; Zhang, H.; Tang, Y. *Acc. Chem. Res.* **2021,** *54,* 3720–3733. doi:10.1021/acs.accounts.1c00459
17. Chen, L.; Chen, P.; Jia, Y. *Acc. Chem. Res.* **2024,** *57,* 3524–3540. doi:10.1021/acs.accounts.4c00654
18. Cheng, S.-Y.; Huang, K.-J.; Wang, S.-K.; Wen, Z.-H.; Hsu, C.-H.; Dai, C.-F.; Duh, C.-Y. *Org. Lett.* **2009,** *11,* 4830–4833. doi:10.1021/ol901864d
19. Wang, X.; Zheng, J.; Chen, Q.; Zheng, H.; He, Y.; Yang, J.; She, X. *J. Org. Chem.* **2010,** *75,* 5392–5394. doi:10.1021/jo101016g
20. Grove, J. F.; Pople, M. *J. Chem. Soc., Perkin Trans. 1* **1979,** 2048–2051. doi:10.1039/p19790002048
21. Scott, F. E.; Simpson, T. J.; Trimble, L. A.; Vederas, J. C. *J. Chem. Soc., Chem. Commun.* **1984,** 756–758. doi:10.1039/c39840000756
22. Cuq, F.; Petitprez, M.; Herrmann-Gorline, S.; Klaebe, A.; Rossignol, M. *Phytochemistry* **1993,** *34,* 1265–1270. doi:10.1016/0031-9422(91)80013-q
23. Lim, C.-H. *Agric. Chem. Biotechnol. (Engl. Ed.)* **1999,** *42,* 45–47.
24. Sappapan, R.; Sommit, D.; Ngamrojanavanich, N.; Pengpreecha, S.; Wiyakrutta, S.; Sriubolmas, N.; Pudhom, K. *J. Nat. Prod.* **2008,** *71,* 1657–1659. doi:10.1021/np8004024
25. Zhang, W.; Krohn, K.; Draeger, S.; Schulz, B. *J. Nat. Prod.* **2008,** *71,* 1078–1081. doi:10.1021/np800095g
26. Li, X.; Li, Z.; Sun, J. *Nat. Synth.* **2022,** *1,* 426–438. doi:10.1038/s44160-022-00072-x

27. Fang, B.; Xie, X.; Zhao, C.; Jing, P.; Li, H.; Wang, Z.; Gu, J.; She, X. *J. Org. Chem.* **2013,** *78,* 6338–6343. doi:10.1021/jo400760q
28. Fang, B.; Xie, X.; Jing, P.; Zhao, C.; Li, H.; Ma, H.; She, X. *Tetrahedron* **2013,** *69,* 11025–11030. doi:10.1016/j.tet.2013.09.075
29. Nge, C.-E.; Gan, C.-Y.; Low, Y.-Y.; Thomas, N. F.; Kam, T.-S. *Org. Lett.* **2013,** *15,* 4774–4777. doi:10.1021/ol4021404
30. Zhao, G.; Xie, X.; Sun, H.; Yuan, Z.; Zhong, Z.; Tang, S.; She, X. *Org. Lett.* **2016,** *18,* 2447–2450. doi:10.1021/acs.orglett.6b00989
31. Zhang, Y. Q.; Zhang, Z. Y. *The Chinese Traditional Medicine Resources;* Science Press: Beijing, China, 1994; p 385.
32. He, D.; Ding, L.; Xu, H.; Lei, X.; Xiao, H.; Zhou, Y. *J. Org. Chem.* **2012,** *77,* 8435–8443. doi:10.1021/jo301225v
33. Xiao, S.-J.; Lei, X.-X.; Xia, B.; Xu, D.-Q.; Xiao, H.-P.; Xu, H.-X.; Chen, F.; Ding, L.-S.; Zhou, Y. *Tetrahedron Lett.* **2014,** *55,* 5949–5951. doi:10.1016/j.tetlet.2014.09.044
34. Xiao, S.-J.; Guo, D.-L.; Xia, B.; Allen, S.; Gu, Y.-C.; Chen, F.; Ding, L.-S.; Zhou, Y. *Planta Med.* **2016,** *82,* 723–728. doi:10.1055/s-0042-100915
35. Xiao, S.-J.; Zhang, M.-S.; Guo, D.-L.; Chen, F.; Zhou, Y.; Ding, L.-S. *Chin. Chem. Lett.* **2017,** *28,* 1049–1051. doi:10.1016/j.cclet.2016.12.011
36. Li, H.; Zhang, Y.; Xie, X.; Ma, H.; Zhao, C.; Zhao, G.; She, X. *Org. Lett.* **2014,** *16,* 4440–4443. doi:10.1021/ol501960j
37. Chen, P.; Huo, L.; Li, H.; Liu, L.; Yuan, Z.; Zhang, H.; Feng, S.; Xie, X.; Wang, X.; She, X. *Org. Chem. Front.* **2018,** *5,* 1124–1128. doi:10.1039/c8qo00026c
38. Yang, H.; Qin, Z.; Liang, X.; Yang, Y.; Xue, Y.; Duan, Y.; Wang, M.; Zhang, Z.; Li, H.; She, X. *J. Org. Chem.* **2025,** *90,* 3719–3726. doi:10.1021/acs.joc.4c03140
39. Hong, X.; Chen, P.; Li, H.; She, X. *Synlett* **2024,** *35,* 535–542. doi:10.1055/s-0042-1751416
40. Choi, H.; Choi, J.; Han, J.; Lee, K. *J. Org. Chem.* **2022,** *87,* 4316–4322. doi:10.1021/acs.joc.1c03167
41. Soorukram, D.; Pohmakotr, M.; Kuhakarn, C.; Reutrakul, V. *J. Org. Chem.* **2018,** *83,* 4173–4179. doi:10.1021/acs.joc.8b00164
42. Ali, G.; Cuny, G. D. *J. Org. Chem.* **2021,** *86,* 10517–10525. doi:10.1021/acs.joc.1c01159
43. Zhou, B.; Gong, Q.; Fu, Y.; Zhou, J.-S.; Zhang, H.-Y.; Yue, J.-M. *Org. Lett.* **2023,** *25,* 1464–1469. doi:10.1021/acs.orglett.3c00196
44. Wang, X.; Yang, Y.; Fang, J.; Duan, J.; Xie, X.; Li, H.; She, X. *J. Org. Chem.* **2025,** *90,* 709–715. doi:10.1021/acs.joc.4c02666
45. Kim, R.; Wu, Y.; Tong, R. *Chem. Sci.* **2024,** *15,* 12856–12860. doi:10.1039/d4sc03553d

License and Terms

BEILSTEIN JOURNAL OF ORGANIC CHEMISTRY

Further elaboration of the stereodivergent approach to chaetominine-type alkaloids: synthesis of the reported structures of aspera chaetominines A and B and revised structure of aspera chaetominine B

Jin-Fang Lü‡, Jiang-Feng Wu‡, Jian-Liang Ye and Pei-Qiang Huang*

Full Research Paper

Open Access

Address:
Department of Chemistry, Fujian Provincial Key Laboratory of Chemical Biology, College of Chemistry and Chemical Engineering, Xiamen University, Xiamen, Fujian 361005, P. R. China

Email:
Pei-Qiang Huang* - pqhuang@xmu.edu.cn

* Corresponding author ‡ Equal contributors

Keywords:
epoxidation; selective epimerization; stereodivergent synthesis; structural revision; tandem reaction

Beilstein J. Org. Chem. **2025,** *21,* 2072–2081.
https://doi.org/10.3762/bjoc.21.162

Received: 03 August 2025
Accepted: 26 September 2025
Published: 13 October 2025

This article is part of the thematic issue "Concept-driven strategies in target-oriented synthesis".

Guest Editor: C. Li

Abstract

We report herein the fourth generation of our synthetic strategy to chaetominine-type alkaloids featuring two modifications of the last step of our 4 to 6-step approach. Firstly, by employing EDCI/HOBt as the coupling system for the last step of the one-pot *O*-debenzylation–lactamization reaction, the overall yield of our previous total synthesis of (–)-isochaetominine A was increased from 25.4% to 30.8% over five steps. Secondly, a new protocol featuring the use of an aged solution of K_2CO_3/MeOH to quench the DMDO epoxidation-triggered cascade reaction was developed, which allowed the in situ selective mono- or double epimerization at C11/C14 as shown by the diastereodivergent synthesis of a pair of diastereomers of versiquinazoline H from its tripeptide precursor. This double epimerization at the last-step allowed the enantiodivergent synthesis of two enantiomers in either racemate form or two pure enantiomers from the same precursor. The former was demonstrated by the synthesis of alkaloid 14-*epi*-isochaetominine C that was used to determine the enantiomeric excess of the synthesized natural product (98.7% ee), while the latter was illustrated by the synthesis of both enantiomers of the alkaloid isochaetominine. Additionally, the reported structures of alkaloids aspera chaetominines A and B have been synthesized. Moreover, the four-step synthesis of the reported structure of aspera chaetominine B generated another diastereomer that was converted in one-pot to (–)-isochaetominine C, which turned out to be the revised structure of aspera chaetominine B.

Introduction

In contemporary organic chemistry, due to the widespread application of modern separation and analytical techniques, the structural elucidation and confirmation of natural products is no longer a motivation for the total synthesis [1]. Nevertheless, we also witness that each year, cases continue to be reported on the total synthesis

enabled revision of misassigned structures of natural products [1-9].

Efficiency is one of the major concerns in the field of total synthesis of natural products [10-20], which is not only essential for organic chemistry in its own right, but also crucial for drug discovery and structural revision of natural products. Although more and more diastereomeric and enantiomeric natural products have been discovered [21-32], and divergent synthetic methodology has attracted attention in recent years [33-38], diastereodivergent and enantiodivergent total synthesis remain rare [39-54]. This is the case for (−)-chaetominine (**1** in Figure 1), which is a hexacyclic quinazolinone alkaloid possessing four stereogenic centers, first isolated from a solid-substrate culture of *Chaetomium* sp. IFB-E015 [21]. Subsequently, several homologues, diastereomers, and enantiomers of chaetominine have been reported, which include: 1) pseudofischerine (**2**) [22], isolated from the fungus *Neosartorya pseudofischeri* S. W. Peterson, and from the marine-derived fungus *Pseudallescheria boydii* F19-1 [23]; 2) aniquinazoline D (**3**), isolated from marine-derived endophytic fungus *Aspergillus nidulans* [24]; 3) (–)-isochaetominines A–C (**4** - **6**) and (+)-14-*epi*-isochaetominine C (**7**), isolated from the solid-substrate culture of an *Aspergillus* sp. Fungus [25], and from other sources for (–)-isochaetominine C (**6**) [26-29]; 4) isochaetominine (**8**) from *Aspergillus fumigatus*, an endophytic fungus from the liverwort *Heteroscyphus tener* (Steph.) Schiffn. [30]; (–)-versiquinazoline H (**9**), isolated from the gorgonian (*Pseudopterogorgia* sp.)-derived fungus *Aspergillus versicolor* LZD-14-1 [31]; as well as 5) aspera chaetominines A and B (**12** and **13**), isolated from marine sponge associated fungus *Aspergillus versicolour* SCSIO XWS04 F52 [32]. All these alkaloids distinguish each other only by alkyl substituent at C11 and by relative stereochemistries at C2, C3, C11, and C14.

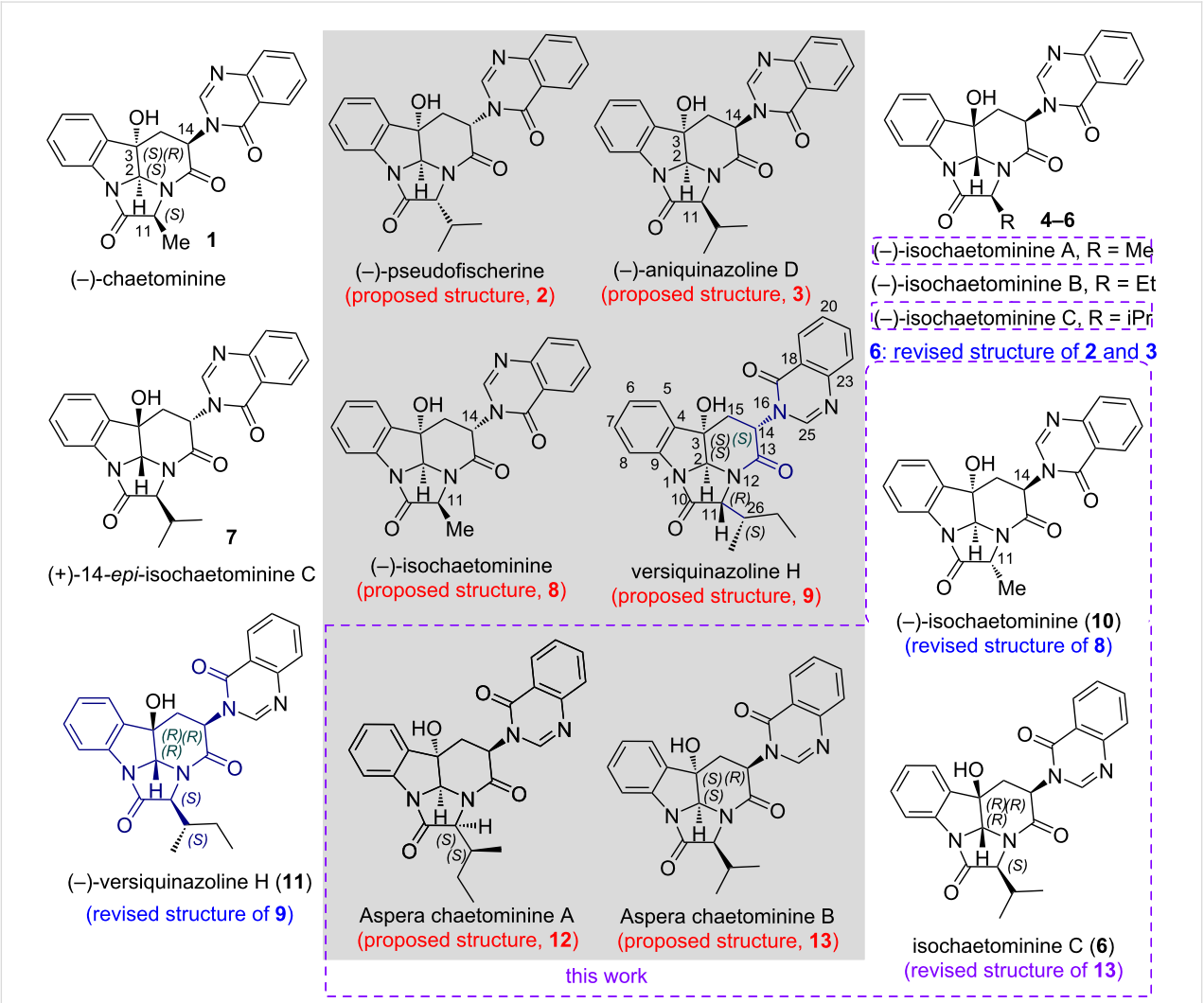

Figure 1: Structures of some reported chaetominine-type alkaloids and revised structures via our total syntheses.

Soon after the report of the isolation, structural elucidation, and bioactivity of (–)-chaetominine by Tan and co-workers [21], its synthesis has attracted attention of the synthetic community. The group of Snider [47], Evano [48,49], and Papeo [50] reported several elegant highly enantio- and diastereoselective total syntheses of this alkaloid from D-tryptophan. With our longstanding interest in the efficient total synthesis of natural products [10,55,56], in early 2009, our group disclosed a highly efficient four-step, enantioselective and diastereodivergent synthesis of (–)-chaetominine (**1**) and with one more step, of another diastereomer [57,58]. The strategy features a DMDO oxidation-triggered [59] double cyclization of an intermediate derived from D-tryptophan [60,61]. Subsequently, we developed a five-step total synthesis of (–)-chaetominine (**1**) and two diastereomers from L-tryptophan [62]. Taking advantages of the high efficiency and flexibility of our strategy [60], we have synthesized several natural and unnatural homologues and diastereomers of chaetominines [57,58,60-65]. This allowed us to revise the proposed structures of (–)-pseudofischerine (**2**) and (–)-aniquinazoline D (**3**) both to (–)-isochaetominine C (**6**), and that of isochaetominine (**8**) to **10** (11-*epi*-chaetominine). More recently, we have communicated the revision of the structure of versiquinazoline H to **11**. During and after the latter work, we undertook further investigation on the last step of our approach to chaetominine-type alkaloids, namely, the lactamization reaction for synthesizing 3,14-*cis*-chaetominines and the DMDO epoxidation-triggered double cyclization reaction. In addition, the synthesis of the recently reported natural products aspera chaetominines A and B (**12** and **13**) [32] was addressed. Herein, we report the full accounts of these investigations, which include: 1) an improved five-step total synthesis of (–)-isochaetominine A (**4**) and a diastereomer; 2) the diastereo- or enantiodivergent syntheses of chaetominine-family alkaloids and stereoisomers, and 3) the reported structures of aspera chaetominines A and B (**12** and **13**) and revised structure of aspera chaetominine B: **6** [(–)-isochaetominine C].

Results and Discussion

Improved five-step total synthesis of (–)-isochaetominine A

In our recent communication on the synthesis of versiquinazoline H (**11**) [65], we uncovered that the employment of EDCI/HOBt as the coupling system for the last step, namely, the *O*-debenzylation–lactamization reaction, afforded much higher yields than those using $(COCl)_2$/DIPEA in our previous synthesis of isochaetominines [63]. We realized that employing this lactamization protocol would significantly improve the synthetic efficiency of isochaetominines **4**–**6**. To showcase this possibility, the improved lactamization protocol was applied to compound **14**, an intermediate in our synthesis of (–)-isochaetominine A (**4**) [63]. Indeed, EDCI/HOBt-mediated lactamization of **14** derived amino acid (not shown) via debenzylation increased the yield of (–)-isochaetominine A (**4**) from 75% to 91% (Scheme 1). Thus, overall yield of the total synthesis of (–)-isochaetominine A (**4**) increased to 30.8% over five steps.

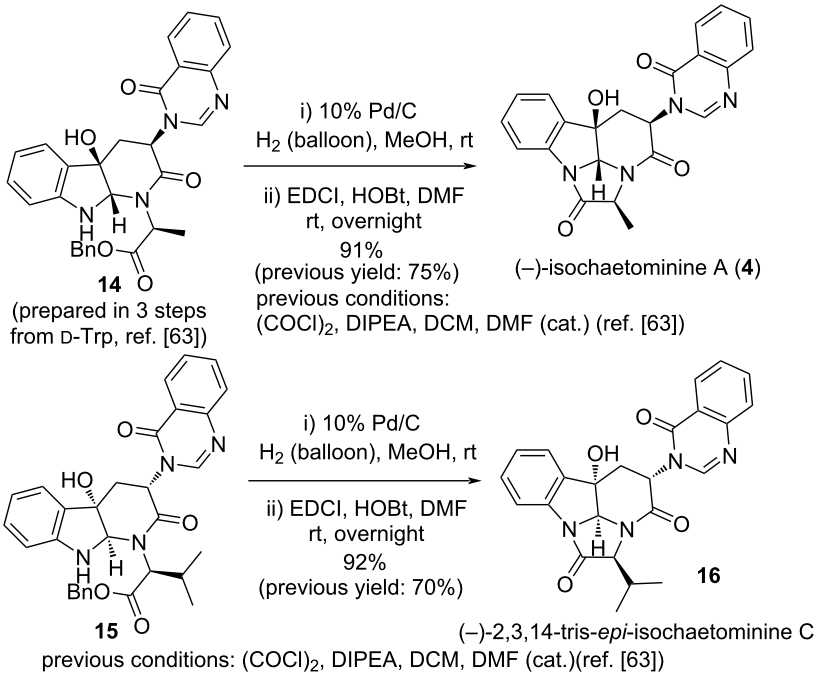

Scheme 1: Improved total synthesis of (–)-isochaetominine A (**4**) and diastereomer **16**.

Similarly, EDCI/HOBt-mediated lactamization of amino acid (not shown) derived from **15** [63] via debenzylation produced the known (–)-2,3,14-tris-*epi*-isochaetominine C (**16**) with a significantly increased 92% yield.

The epoxidation-triggered stereodivergent synthesis of diastereomers of versiquinazoline H: the fourth generation strategy

In all our previous syntheses of chaetominine and isochaetominine alkaloids [57,58,60-65], the key DMDO-oxidation triggered double cyclization always accompanied with a monocyclization product. It was anticipated that if we run the work-up procedure under more basic conditions, one would be able to obtain solely double cyclization products. Indeed, alternation of the work-up protocol by employing an aged solution of K_2CO_3/MeOH (stood at rt overnight, pH 11) to quench the DMDO oxidation reaction of intermediate **17** [65] yielded the thermodynamically stable C2/C11-*trans* and C3/C14-*trans* diastereomers **19** and **20** (dr = ca. 1:1) in a combined yield of 75% (Scheme 2). The ^{1}H NMR spectrum of this diastereomeric mixture shows only one set of resonance signals, but two sets of resonance signals were observed on the ^{13}C NMR spectrum. We have succeeded in preparing a single crystal from the oxidation products. Interestingly, the X-ray diffraction analysis [66] showed that the single crystal contained two diastereomers (**19**/**20**) with the structures displayed in Scheme 2. Similarly, the DMDO oxidation of diastereomers **18** followed by quenching the reaction with an aged solution of K_2CO_3/MeOH resulted in the formation of the same diastereomeric mixture **19** and **20** (dr = ca. 1:1) as that obtained from **17**.

Enantiodivergent syntheses of chaetominine-type alkaloids and antipodes in racemic or enantiomeric forms

Applying the newly developed quenching protocol featuring the use of an aged K_2CO_3/MeOH solution to the known

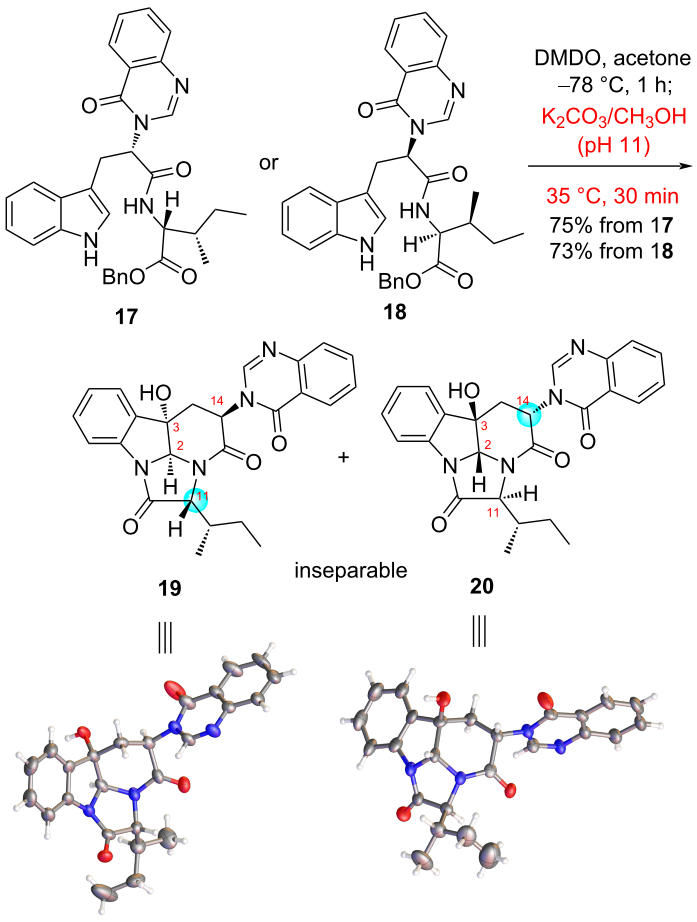

Figures abstracted from the single crystal structure of **19**/**20**

Scheme 2: Diastereoconvergent transformations of **17** and **18** into two diastereomers of versiquinazoline H.

compound **21** [63] resulted in the formation of an indistinguishable mixture of two double cyclization products (+)-14-*epi*-isochaetominine C (**7**) and its antipode (–)-**7** (ratio = ca. 1:1) in 75% yield (Scheme 3a). The optical rotation of this mixture is zero confirming that the reaction led to two enantiomers in almost equal quantities. To take advantage of this protocol, the enantiomeric excess (ee) of (+)-**7**, prepared in four steps from L-Trp [63], was determined to be 98.7%. It is worth mentioning that in the field of chiral drug R & D, the evaluation of bio-profiles of both enantiomers and racemic compound is required by the U.S. FDA. The result presented herein shows that by a late-stage racemization, one could obtain a racemic sample in just one step, instead of repeating the total synthesis from another enantiomeric chiral starting material or racemic one. On the basis of this consideration, such racemization represents a valuable "enantiodivergent synthesis".

Nevertheless, a more useful and generally acceptable enantiodivergent synthesis is the one that allows accessing two enantiomers both in pure form from only one enantiomer of a chiral starting material or a chiral ligand [33]. To demonstrate the value of our protocol in this regard, an enantiodivergent synthesis of isochaetominine (**10**) was envisioned. Previously, we have reported a four-step synthesis of (+)-isochaetominine (*ent*-**10**, previously known as *ent*-11-*epi*-chaetominine) in 32% yield starting from L-Trp and L-Ala [64]. In the last step of that total synthesis, the diastereomeric monocyclization product **22** was obtained as the major product (48% yield). Exposing this compound to an aged K_2CO_3/MeOH solution at 35 °C for 30 min resulted in the formation of C11/C14 double epimerization product (–)-isochaetominine [(–)-**10**] in 71% yield. Thus, we have achieved a really enantiodivergent synthesis of alkaloid (–)-isochaetominine [(–)-**10**] and its antipode (+)-**10** in just five total steps.

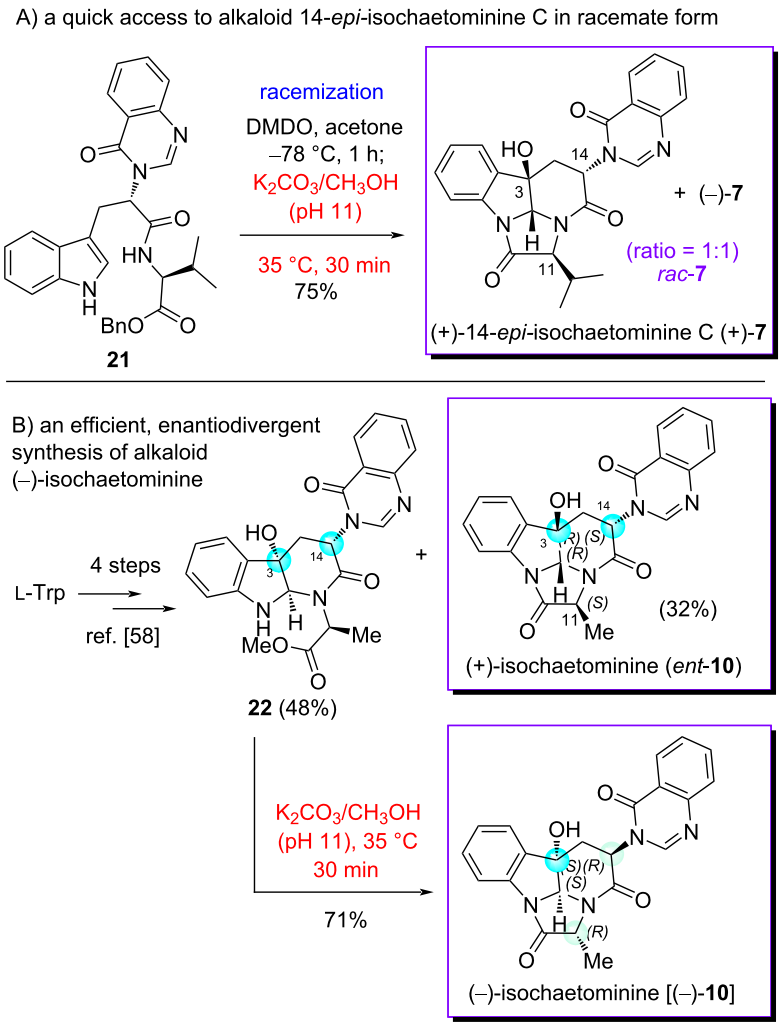

Scheme 3: Mono- and double epimerization-based enantiodivergent syntheses of chaetominine-type alkaloids and antipodes.

Synthesis of the proposed structures of aspera chaetominines A and B and revision of stereochemistry of aspera chaetominine B

Several years after we have had accomplished the abovementioned investigations, Liu and co-workers reported the isolation and structural elucidation of two new alkaloids, aspera chaetominines A (**12**) and B (**13**) from marine sponge associated fungus *Aspergillus versicolour* SCSIO XWS04 F52 [32]. They reported that both the two alkaloids showed cytotoxic activity against leukaemia K562 and colon cancer cells SW1116 with IC_{50} ranged from 7.5 to 12.5 μM, and significant protection against H1N1 virus-induced cytopathogenicity in MDCK cells with IC_{50} values of 15.5 and 24.5 μM, respectively. Attracted by both their structure and bioactivities, we anticipated their synthesis. The author determined the structure by means of spectroscopic (^{1}H, ^{13}C NMR, HSQC, HMBC, and ^{1}H-^{1}H COSY), and MS analysis, and claimed that "their absolute configuration was unambiguously determined by the comparison with the reported compound chaetominine (**1**)" [32]. The only information regarding the absolute configuration mentioned in the text is as follows: "aspera chaetominine A (**1**) was presumably biosynthesized from L-isoleucine, L-valine, anthranilic acid, and D-tryptophan". Such speculation regarding the absolute configurations is clearly not convincing. Moreover, neither optical rotation data nor melting point (both **12** and **13** were isolated as white powder) have been reported by Liu et al. [32]. Additionally, the solvents used for measuring ^{1}H and ^{13}C NMR are methanol-d_4 that is different from Tan's work [21] who used DMSO-d_6 to record ^{1}H and ^{13}C NMR spectra of (–)-chaetominine (**1**).

Thus we undertook the synthesis of the proposed structures of aspera chaetominines A (**12**) and B (**13**). By adopting our first-generation strategy [57,58,61], we re-synthesized tripepetide derivative **25** from D-tryptophan (D-Trp) and L-isoleucine (L-Ile) methyl ester hydrochloride salt (**24**) in three steps (Scheme 4). Treating **25** with DMDO followed by work-up with a saturated aqueous solution of Na_2SO_3 at 30 °C provided the proposed structure of aspera chaetominine A (**12**) and monocyclization product **26** in 31% and 45% yield, respectively. The spectral (^{1}H and ^{13}C NMR) data of our synthetic compound are different from those reported for the natural aspera chaetominine A, suggesting that the originally proposed stereochemistry for aspera chaetominine A (**12**) was incorrect. It is worth noting that compound **12** has been obtained in our previous investigation [65]. However, the ^{1}H and ^{13}C NMR spectra were recorded in DMSO-d_6 which prevent a direct comparison with the data of aspera chaetominine A.

We next addressed the synthesis of aspera chaetominine B (**13**). Employing our third-generation strategy featuring the employment of benzyl L-valinate as the coupling component [63], tripeptide derivative **28** was synthesized in three steps. Exposure of **28** to DMDO in acetone followed by treating the resulting intermediates with Na_2SO_3 produced the proposed structure of aspera chaetominine B (**13**) and monocyclization product **29** in

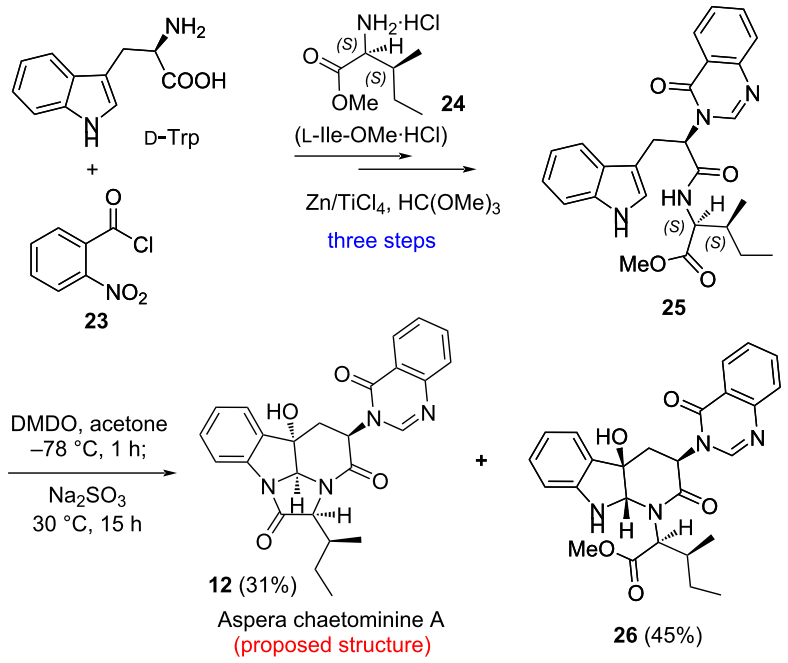

Scheme 4: Enantioselective synthesis of the proposed structure of aspera chaetominine A.

22% and 30% yield, respectively (Scheme 5). Once again, a comparison of the ^{1}H and ^{13}C NMR data of our synthetic compound **13** with those of the natural aspera chaetominine B showed that two compounds are different, indicating a misassignment of the structure (**13**) for aspera chaetominine B. To our delight, one-pot catalytic debenzylation–lactamization of **29** afforded lactamization product (–)-isochaetominine C (**6**). The ^{1}H and ^{13}C NMR data of compound **6** matched those of natural aspera chaetominine B suggesting that aspera chaetominine B is (–)-isochaetominine C (**6**), whose absolute configuration is tentatively assigned as 2*R*,3*R*,11*S*,14*R*. It is worth noting that compound **13** has been obtained in our previous investigation [63]. However, the ^{1}H and ^{13}C NMR spectra were recorded in DMSO-d_6 which prevent a direct comparison with the data of aspera chaetominine B.

Conclusion

In summary, we have elaborated our epoxidation-triggered diastereodivergent approach to chaetominine-type alkaloids. As shown by the synthesis of (–)-isochaetominine A, the previ-

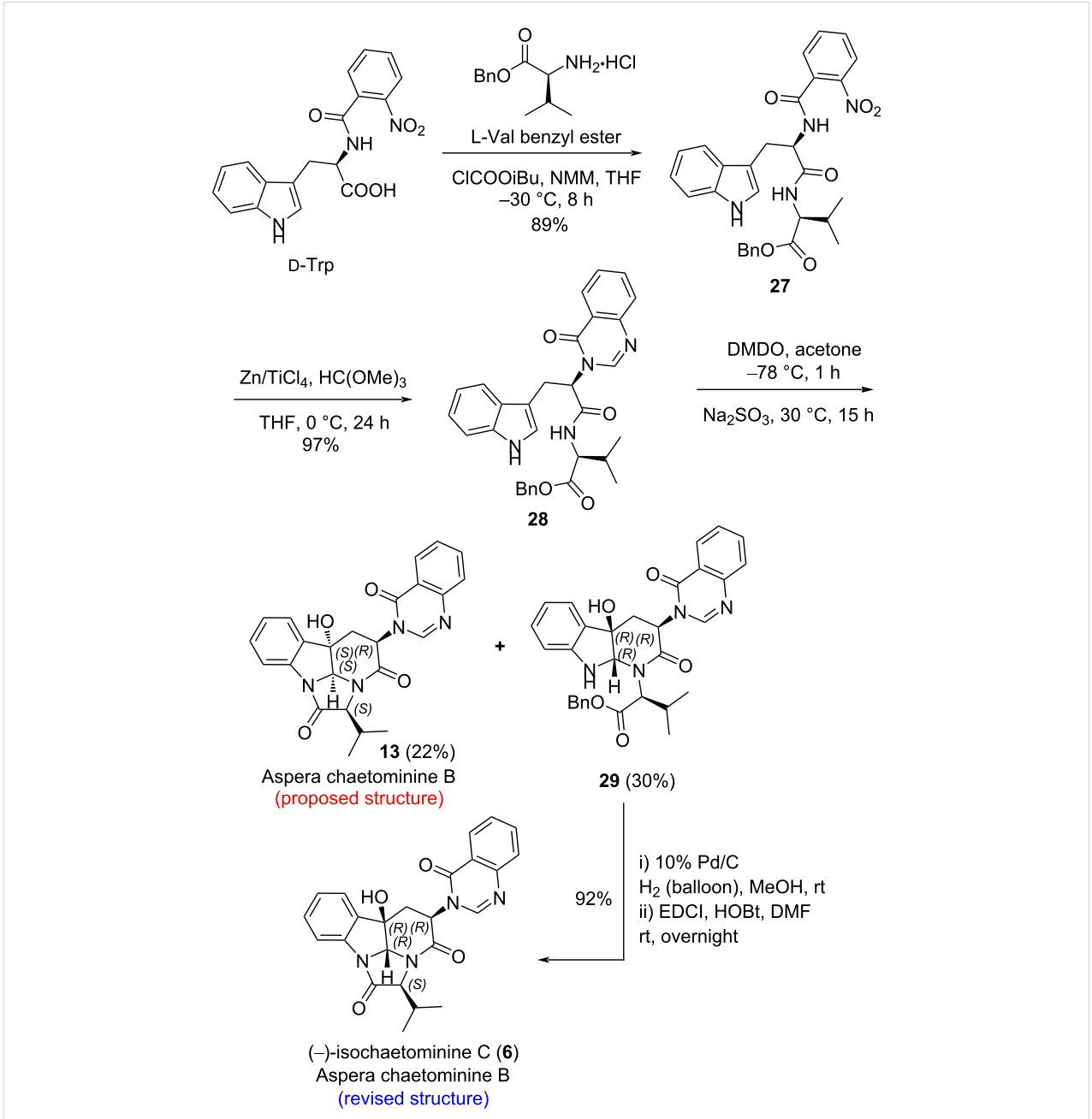

Scheme 5: Enantioselective syntheses of both the proposed and revised structures of aspera chaetominine B.

ously six-step total synthesis of 3,14-*cis* diastereomeric isochaetominines could be completed in five steps with higher yields. On the other hand, we have demonstrated that by simply alternating the quenching conditions for the key DMDO-epoxidation triggered double cyclization, one can realize: 1) a diastereoconvergent synthesis of two diastereomers of versiquinazoline H; 2) the enantiodivergent syntheses of racemic 14-*epi*-isochaetominine C, as well as (–)- and (+)-isochaetominine, respectively. This last-step enantiodivergent reaction allowed the one-step access to a racemic sample from a synthetic intermediate for determining the ee of a chaetominine-family alkaloid. Additionally, we have achieved the four-step enantioselective total synthesis of the proposed structure of aspera chaetominine A, and five-step enantioselective total synthesis of both the proposed and revised structures of aspera chaetominine B. The structure of aspera chaetominine B is revised to the known alkaloid (–)-isochaetominine C. Further application of this strategy to the total synthesis of natural products including the revised structure of aspera chaetominine A is in progress in our laboratory, and the results will be reported elsewhere in due course.

Supporting Information

Supporting Information File 1

General methods and materials, experimental procedures, characterization data, and copies of ^{1}H and ^{13}C NMR spectra of compounds **19/20**, **25**, **26**, **12**, **13**, and **6**.
[https://www.beilstein-journals.org/bjoc/content/supplementary/1860-5397-21-162-S1.pdf]

Acknowledgements

We thank Ms. Yan-Jiao Gao for technical assistance.

Funding

We are grateful for financial support of this work from the National Natural Science Foundation of China (22571267 and 21931010).

Author Contributions

Jin-Fang Lü: investigation; validation. Jiang-Feng Wu: data curation; methodology. Jian-Liang Ye: software. Pei-Qiang Huang: conceptualization; funding acquisition; methodology; writing – original draft; writing – review & editing.

ORCID® iDs

Jian-Liang Ye - https://orcid.org/0000-0003-1488-7311
Pei-Qiang Huang - https://orcid.org/0000-0003-3230-0457

Data Availability Statement

All data that supports the findings of this study is available in the published article and/or the supporting information of this article. Crystallographic data for **19**/**20** has been deposited at the Cambridge Crystallographic Data Centre (CCDC 1905613) and can be obtained from https://www.ccdc.cam.ac.uk/structures/.

References

1. Nicolaou, K. C.; Snyder, S. A. *Angew. Chem., Int. Ed.* **2005,** *44,* 1012–1044. doi:10.1002/anie.200460864
2. Guo, K.; Xia, L.; Xu, H.; Zheng, C. *Org. Biomol. Chem.* **2025,** *23,* 4578–4592. doi:10.1039/d5ob00282f
3. Yang, P.; Jia, Q.; Song, S.; Huang, X. *Nat. Prod. Rep.* **2023,** *40,* 1094–1129. doi:10.1039/d2np00034b
4. Shen, S.-M.; Appendino, G.; Guo, Y.-W. *Nat. Prod. Rep.* **2022,** *39,* 1803–1832. doi:10.1039/d2np00023g
5. Fuwa, H. *Org. Chem. Front.* **2021,** *8,* 3990–4023. doi:10.1039/d1qo00481f
6. Resa, S.; González, M.; Reyes, F.; Pérez-Victoria, I. *Org. Chem. Front.* **2024,** *11,* 306–314. doi:10.1039/d3qo01411h
7. Sikandar, A.; Popoff, A.; Jumde, R. P.; Mándi, A.; Kaur, A.; Elgaher, W. A. M.; Rosenberger, L.; Hüttel, S.; Jansen, R.; Hunter, M.; Köhnke, J.; Hirsch, A. K. H.; Kurtán, T.; Müller, R. *Angew. Chem., Int. Ed.* **2023,** *62,* e202306437. doi:10.1002/anie.202306437
8. Kim, T.; Kim, S.; Chung, G.; Park, K.; Han, S. *Org. Chem. Front.* **2023,** *10,* 5123–5129. doi:10.1039/d3qo01098h
9. Meng, Z.; Fürstner, A. *J. Am. Chem. Soc.* **2020,** *142,* 11703–11708. doi:10.1021/jacs.0c05347
10. Huang, P.-Q.; Yao, Z.-J.; Hsung, R. P., Eds. *Efficiency in Natural Product Total Synthesis;* John Wiley & Sons: Hoboken, NJ, USA, 2018. doi:10.1002/9781118940228
11. Lautié, E.; Russo, O.; Ducrot, P.; Boutin, J. A. *Front. Pharmacol.* **2020,** *11,* 397. doi:10.3389/fphar.2020.00397
12. Trost, B. M. *Science* **1991,** *254,* 1471–1477. doi:10.1126/science.1962206
13. Wender, P. A.; Verma, V. A.; Paxton, T. J.; Pillow, T. H. *Acc. Chem. Res.* **2008,** *41,* 40–49. doi:10.1021/ar700155p
14. Newhouse, T.; Baran, P. S.; Hoffmann, R. W. *Chem. Soc. Rev.* **2009,** *38,* 3010–3021. doi:10.1039/b821200g
15. Vaxelaire, C.; Winter, P.; Christmann, M. *Angew. Chem., Int. Ed.* **2011,** *50,* 3605–3607. doi:10.1002/anie.201100059
16. Dominguez-Huerta, A.; Dai, X.-J.; Zhou, F.; Querard, P.; Qiu, Z.; Ung, S.; Liu, W.; Li, J.; Li, C.-J. *Can. J. Chem.* **2019,** *97,* 67–85. doi:10.1139/cjc-2018-0357
17. Gao, Y.; Ma, D. *Acc. Chem. Res.* **2021,** *54,* 569–582. doi:10.1021/acs.accounts.0c00727
18. Zhang, W.; Lu, M.; Ren, L.; Zhang, X.; Liu, S.; Ba, M.; Yang, P.; Li, A. *J. Am. Chem. Soc.* **2023,** *145,* 26569–26579. doi:10.1021/jacs.3c06088
19. Zhao, J.-X.; Yue, J.-M. *Sci. China: Chem.* **2023,** *66,* 928–942. doi:10.1007/s11426-022-1512-0
20. Wang, F.; Xu, X.; Yan, Y.; Zhang, J.; Yang, Y. *Org. Chem. Front.* **2024,** *11,* 668–672. doi:10.1039/d3qo01835k
21. Jiao, R. H.; Xu, S.; Liu, J. Y.; Ge, H. M.; Ding, H.; Xu, C.; Zhu, H. L.; Tan, R. X. *Org. Lett.* **2006,** *8,* 5709–5712. doi:10.1021/ol062257t
22. Eamvijarn, A.; Kijjoa, A.; Bruyère, C.; Mathieu, V.; Manoch, L.; Lefranc, F.; Silva, A.; Kiss, R.; Herz, W. *Planta Med.* **2012,** *78,* 1767–1776. doi:10.1055/s-0032-1315301

23. Lan, W.-J.; Wang, K.-T.; Xu, M.-Y.; Zhang, J.-J.; Lam, C.-K.; Zhong, G.-H.; Xu, J.; Yang, D.-P.; Li, H.-J.; Wang, L.-Y. *RSC Adv.* **2016,** *6,* 76206–76213. doi:10.1039/c6ra06661e
24. An, C.-Y.; Li, X.-M.; Li, C.-S.; Wang, M.-H.; Xu, G.-M.; Wang, B.-G. *Mar. Drugs* **2013,** *11,* 2682–2694. doi:10.3390/md11072682
25. Liao, L.; You, M.; Chung, B. K.; Oh, D.-C.; Oh, K.-B.; Shin, J. *J. Nat. Prod.* **2015,** *78,* 349–354. doi:10.1021/np500683u
26. Lan, W.-J.; Fu, S.-J.; Xu, M.-Y.; Liang, W.-L.; Lam, C.-K.; Zhong, G.-H.; Xu, J.; Yang, D.-P.; Li, H.-J. *Mar. Drugs* **2016,** *14,* 18. doi:10.3390/md14010018
27. Paluka, J.; Kanokmedhakul, K.; Soytong, M.; Soytong, K.; Kanokmedhakul, S. *Fitoterapia* **2019,** *137,* 104257. doi:10.1016/j.fitote.2019.104257
28. Paluka, J.; Kanokmedhakul, K.; Soytong, M.; Soytong, K.; Yahuafai, J.; Siripong, P.; Kanokmedhakul, S. *Fitoterapia* **2020,** *142,* 104485. doi:10.1016/j.fitote.2020.104485
29. Ahammad Uz Zaman, K. H.; Hu, Z.; Wu, X.; Cao, S. *Tetrahedron Lett.* **2020,** *61,* 151730. doi:10.1016/j.tetlet.2020.151730
30. Xie, F.; Li, X.-B.; Zhou, J.-C.; Xu, Q.-Q.; Wang, X.-N.; Yuan, H.-Q.; Lou, H.-X. *Chem. Biodiversity* **2015,** *12,* 1313–1321. doi:10.1002/cbdv.201400317
31. Cheng, Z.; Lou, L.; Liu, D.; Li, X.; Proksch, P.; Yin, S.; Lin, W. *J. Nat. Prod.* **2016,** *79,* 2941–2952. doi:10.1021/acs.jnatprod.6b00801
32. Fredimoses, M.; Ai, W.; Lin, X.; Zhou, X.; Liao, S.; Pan, L.; Liu, Y. *Nat. Prod. Res.* **2025,** *39,* 566–578. doi:10.1080/14786419.2023.2275744
33. Krautwald, S.; Carreira, E. M. *J. Am. Chem. Soc.* **2017,** *139,* 5627–5639. doi:10.1021/jacs.6b13340
34. Ke, Y.; Li, W.; Liu, W.; Kong, W. *Sci. China: Chem.* **2023,** *66,* 2951–2976. doi:10.1007/s11426-023-1533-y
35. Wang, C.; Liu, N.; Wu, X.; Qu, J.; Chen, Y. *Chin. J. Chem.* **2024,** *42,* 599–604. doi:10.1002/cjoc.202300590
36. Tan, D.-X.; Zhou, J.; Gu, C.-Y.; Li, Z.-Y.; Shen, Y.-J.; Han, F.-S. *Chem* **2025,** *11,* 102440. doi:10.1016/j.chempr.2025.102440
37. Anagnostaki, E. E.; Zografos, A. L. *Chem. Soc. Rev.* **2012,** *41,* 5613–5625. doi:10.1039/c2cs35080g
38. Kourgiantaki, M.; Zografos, A. L. *Org. Lett.* **2025,** *27,* 5039–5043. doi:10.1021/acs.orglett.5c00485
39. Gennaiou, K.; Kelesidis, A.; Kourgiantaki, M.; Zografos, A. L. *Beilstein J. Org. Chem.* **2023,** *19,* 1–26. doi:10.3762/bjoc.19.1
40. Fernandes, R. A. *Chem. Commun.* **2023,** *59,* 12205–12230. doi:10.1039/d3cc03564f
41. Andres, R.; Wang, Q.; Zhu, J. *Angew. Chem., Int. Ed.* **2023,** *62,* e202301517. doi:10.1002/anie.202301517
42. Moore, M. J.; Qin, P.; Keith, D. J.; Wu, Z.-C.; Jung, S.; Chatterjee, S.; Tan, C.; Qu, S.; Cai, Y.; Stanfield, R. L.; Boger, D. L. *J. Am. Chem. Soc.* **2023,** *145,* 12837–12852. doi:10.1021/jacs.3c03710
43. Lee, J.; Chen, D. Y.-K. *Angew. Chem., Int. Ed.* **2019,** *58,* 488–493. doi:10.1002/anie.201811530
44. Li, Q.; Zhao, K.; Peuronen, A.; Rissanen, K.; Enders, D.; Tang, Y. *J. Am. Chem. Soc.* **2018,** *140,* 1937–1944. doi:10.1021/jacs.7b12903
45. Qiu, H.-B.; Qian, W.-J.; Yu, S.-M.; Yao, Z.-J. *Tetrahedron* **2015,** *71,* 370–380. doi:10.1016/j.tet.2014.10.062
46. Schafroth, M. A.; Zuccarello, G.; Krautwald, S.; Sarlah, D.; Carreira, E. M. *Angew. Chem., Int. Ed.* **2014,** *53,* 13898–13901. doi:10.1002/anie.201408380
47. Snider, B. B.; Wu, X. *Org. Lett.* **2007,** *9,* 4913–4915. doi:10.1021/ol7022483
48. Toumi, M.; Couty, F.; Marrot, J.; Evano, G. *Org. Lett.* **2008,** *10,* 5027–5030. doi:10.1021/ol802155n
49. Coste, A.; Karthikeyan, G.; Couty, F.; Evano, G. *Synthesis* **2009,** 2927–2934. doi:10.1055/s-0029-1216923
50. Malgesini, B.; Forte, B.; Borghi, D.; Quartieri, F.; Gennari, C.; Papeo, G. *Chem. – Eur. J.* **2009,** *15,* 7922–7929. doi:10.1002/chem.200900793
51. Tréguier, B.; Roche, S. P. *Org. Lett.* **2014,** *16,* 278–281. doi:10.1021/ol403281t
52. Deng, X.; Liang, K.; Tong, X.; Ding, M.; Li, D.; Xia, C. *Tetrahedron* **2015,** *71,* 3699–3704. doi:10.1016/j.tet.2014.09.029
53. Demertzidou, V. P.; Kourgiantaki, M.; Zografos, A. L. *Org. Lett.* **2024,** *26,* 4648–4653. doi:10.1021/acs.orglett.4c01374
54. Mazaraki, K.; Zangelidis, C.; Kelesidis, A.; Zografos, A. L. *Org. Lett.* **2024,** *26,* 11085–11089. doi:10.1021/acs.orglett.4c03504
55. Xu, F.-F.; Chen, J.-Q.; Shao, D.-Y.; Huang, P.-Q. *Nat. Commun.* **2023,** *14,* 6251. doi:10.1038/s41467-023-41846-x
56. Ji, K.-L.; He, S.-F.; Xu, D.-D.; He, W.-X.; Zheng, J.-F.; Huang, P.-Q. *Angew. Chem., Int. Ed.* **2023,** *62,* e202302832. doi:10.1002/anie.202302832
57. Huang, P.-Q.; Liu, L.-X.; Peng, Q.-L. Chinese patent: ZL 200910110953.2, **2009** (in Chinese) [Chem. Abstr. CN20091110953 20090122].
58. Peng, Q.-L.; Luo, S.-P.; Xia, X.-E.; Liu, L.-X.; Huang, P.-Q. *Chem. Commun.* **2014,** *50,* 1986–1988. doi:10.1039/c3cc48833k
59. El-Assaad, T. H.; Zhu, J.; Sebastian, A.; McGrath, D. V.; Neogi, I.; Parida, K. N. *Org. Chem. Front.* **2022,** *9,* 5675–5725. doi:10.1039/d2qo01005d
60. Geng, H.; Huang, P.-Q. *Chem. Rec.* **2019,** *19,* 523–533. doi:10.1002/tcr.201800079
61. Luo, S.-P.; Peng, Q.-L.; Xu, C.-P.; Wang, A.-E; Huang, P.-Q. *Chin. J. Chem.* **2014,** *32,* 757–770. doi:10.1002/cjoc.201400413
62. Xu, C.-P.; Luo, S.-P.; Wang, A.-E; Huang, P.-Q. *Org. Biomol. Chem.* **2014,** *12,* 2859–2863. doi:10.1039/c4ob00314d
63. Mao, Z.-Y.; Geng, H.; Zhang, T.-T.; Ruan, Y.-P.; Ye, J.-L.; Huang, P.-Q. *Org. Chem. Front.* **2016,** *3,* 24–37. doi:10.1039/c5qo00298b
64. Huang, P.-Q.; Mao, Z.-Y.; Geng, H. *Chin. J. Org. Chem.* **2016,** *36,* 315–324. doi:10.6023/cjoc201512015
65. Wu, J.-F.; Huang, P.-Q. *Chin. Chem. Lett.* **2020,** *31,* 61–63. doi:10.1016/j.cclet.2019.06.043
66. CCDC-1905613 (**19**/**20**) contains the supplementary crystallographic data for this paper. These data can be obtained free of charge from the Cambridge Crystallographic Data Centre via https://www.ccdc.cam.ac.uk/structures/.

License and Terms

BEILSTEIN JOURNAL OF ORGANIC CHEMISTRY

The application of desymmetric enantioselective reduction of cyclic 1,3-dicarbonyl compounds in the total synthesis of terpenoid and alkaloid natural products

Dong-Xing Tan[1] and Fu-She Han[*1,2]

Review

Open Access

Address:
[1]Changchun Institute of Applied Chemistry, Chinese Academy of Sciences, 5625 Renmin Street, Changchun, Jilin 130022, China and [2]School of Applied Chemistry and Engineering, University of Science and Technology of China, Hefei, Anhui 230026, China

Email:
Fu-She Han[*] - fshan@ciac.ac.cn.

* Corresponding author

Keywords:
alkaloids; cyclic 1,3-dicarbonyl compounds; desymmetrization; enantioselective reduction; terpenoids

Beilstein J. Org. Chem. **2025,** *21,* 2085–2102.
https://doi.org/10.3762/bjoc.21.164

Received: 30 July 2025
Accepted: 25 September 2025
Published: 14 October 2025

This article is part of the thematic issue "Concept-driven strategies in target-oriented synthesis".

Guest Editor: Y. Tang

Abstract

The desymmetric enantioselective reduction of cyclic 1,3-dicarbonyl compounds is a powerful tool for the construction of ring systems bearing multiple stereocenters including all-carbon quaternary stereocenters, which are widely useful chiral building blocks for the total synthesis of structurally complex natural products. On the other hand, terpenoids and alkaloids, with their intricate and diverse skeletal frameworks as well as the broad range of biological activities, have long been a major focus for synthetic chemists. Over the past fifteen years, significant progress has been made in the total synthesis of complex terpenoid and alkaloid natural products by strategically applying desymmetric enantioselective reduction. Advance before 2016 in this area has been overviewed in an elegant review article. Since then, a series of more challenging terpenoid and alkaloid natural products have been synthesized utilizing a desymmetric enantioselective reduction strategy of cyclic 1,3-dicarbonyl compounds as a key transformation. This review will summarize the application of this strategy in the total synthesis of terpenoid and alkaloid natural products from the year 2016 to 2025. We first focus on the synthesis of several terpenoids and alkaloids through the desymmetric enantioselective reduction of five-membered cyclic 1,3-dicarbonyl compounds. Subsequently, the utilization of six-membered cyclic 1,3-dicarbonyl compounds for the synthesis of some terpenoids natural products is described.

Introduction

Terpenoids and alkaloids are two major classes of highly important natural products because they usually exhibit diverse and important biological activities, such as antitumor, anti-inflammatory, and antiarrhythmic effects etc., and show potential to be developed into drug candidates or novel medications for treating human diseases [1-4]. However, their scarcity in nature

limits further research into their biological activities. Total synthesis is an important device to address the shortage of natural product sources. Nevertheless, the asymmetric total synthesis of terpenoid and alkaloid natural products presents significant challenges due to their complex and diverse ring systems and the presence of multiple stereocenters, including all-carbon quaternary stereocenters. Consequently, the development of novel methods and strategies to achieve efficient asymmetric total synthesis of complex terpenoid and alkaloid natural products has drawn considerable attention from synthetic chemists.

Over the past decades, the development of desymmetric enantioselective reduction strategy of cyclic 1,3-dicarbonyl compounds has invigorated the field of terpenoid and alkaloid natural products synthesis because of its multiple advantages. Specifically, such strategy allows for an efficient construction of multiple chiral centers by employing easily accessible or commercially available symmetric cyclic prochiral dicarbonyl substrates. In addition, various approaches could be used for the desymmetrization reactions such as enzyme catalytic-, organocatalyst-, and transition-metal-catalyzed reductions [5-7]. Advance about the synthesis of several terpenoid and alkaloid natural products (**1**–**5**, Figure 1) [8-11] has been achieved in this area as indicated by an elegant review in 2016 [12], which will not be discussed in this review.

Although only a limited number of terpenoids and alkaloids were synthesized by applying the desymmetric enantioselective reduction strategy of cyclic 1,3-dicarbonyl compounds before 2016, their success has provided a reference for the subsequent synthesis of other types of terpenoid and alkaloid natural products. In fact, over the past ten years, the number of terpenoid and alkaloid natural products synthesized utilizing this strategy has increased significantly compared to the period before 2016. However, there is currently a lack of systematic summary regarding the application of this strategy in the total synthesis of terpenoids and alkaloids over this time span. This review will provide a comprehensive overview of the recent advances (2016–2025), specially, we first summarize chronologically the application of desymmetric enantioselective reduction of five-membered cyclic 1,3-dicarbonyl compounds in the synthesis of terpenoid and alkaloid natural products **6**–**15** (Figure 2A). Subsequently, the advances in the utilization of six-membered cyclic 1,3-dicarbonyl compounds for the synthesis of terpenoid natural products **16**–**27** will be introduced in chronological order (Figure 2B). After that, a brief outlook of the desymmetric enantioselective reduction strategy of cyclic 1,3-dicarbonyl compounds in the total synthesis of natural products will be discussed. We hope this review can stimulate the methodology development and application of this strategy toward further improving the synthetic efficiency of natural product synthesis.

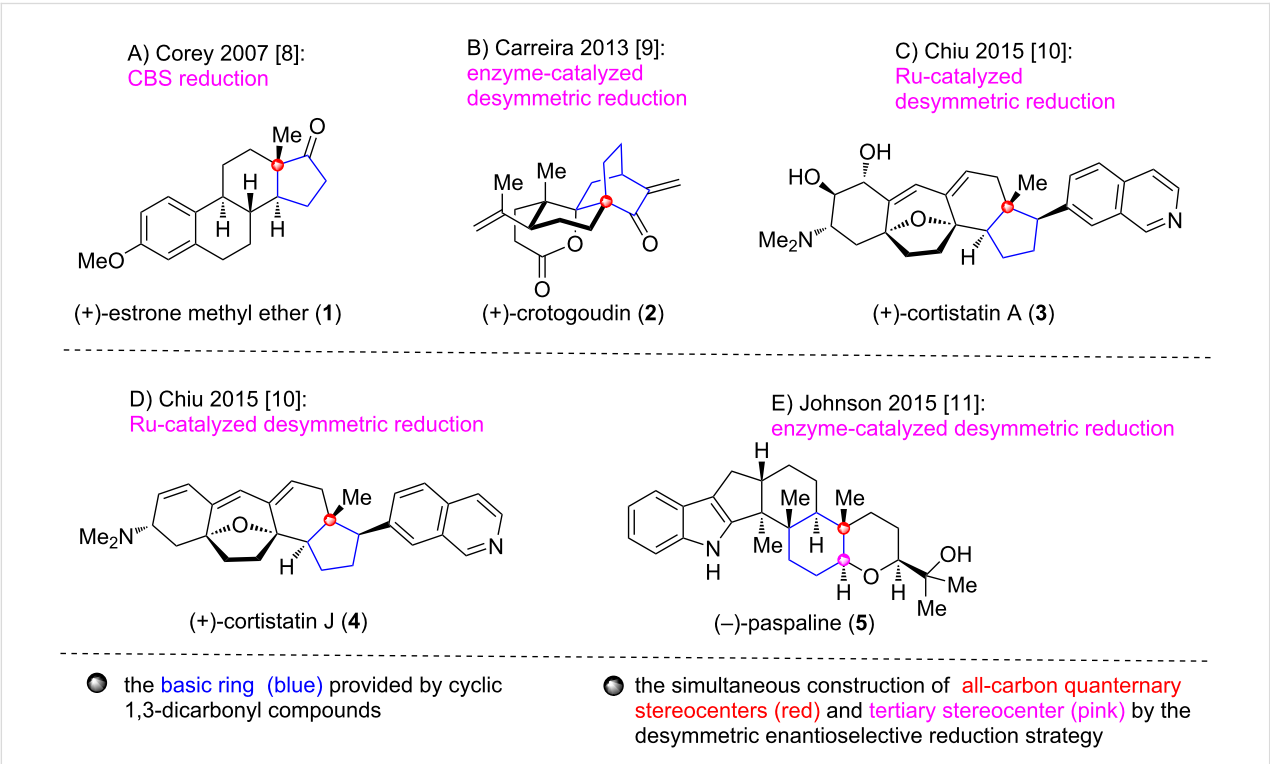

Figure 1: Several representative terpenoid and alkaloid natural products synthesized by applying desymmetric enantioselective reduction strategy of cyclic 1,3-dicarbonyl compounds before 2016.

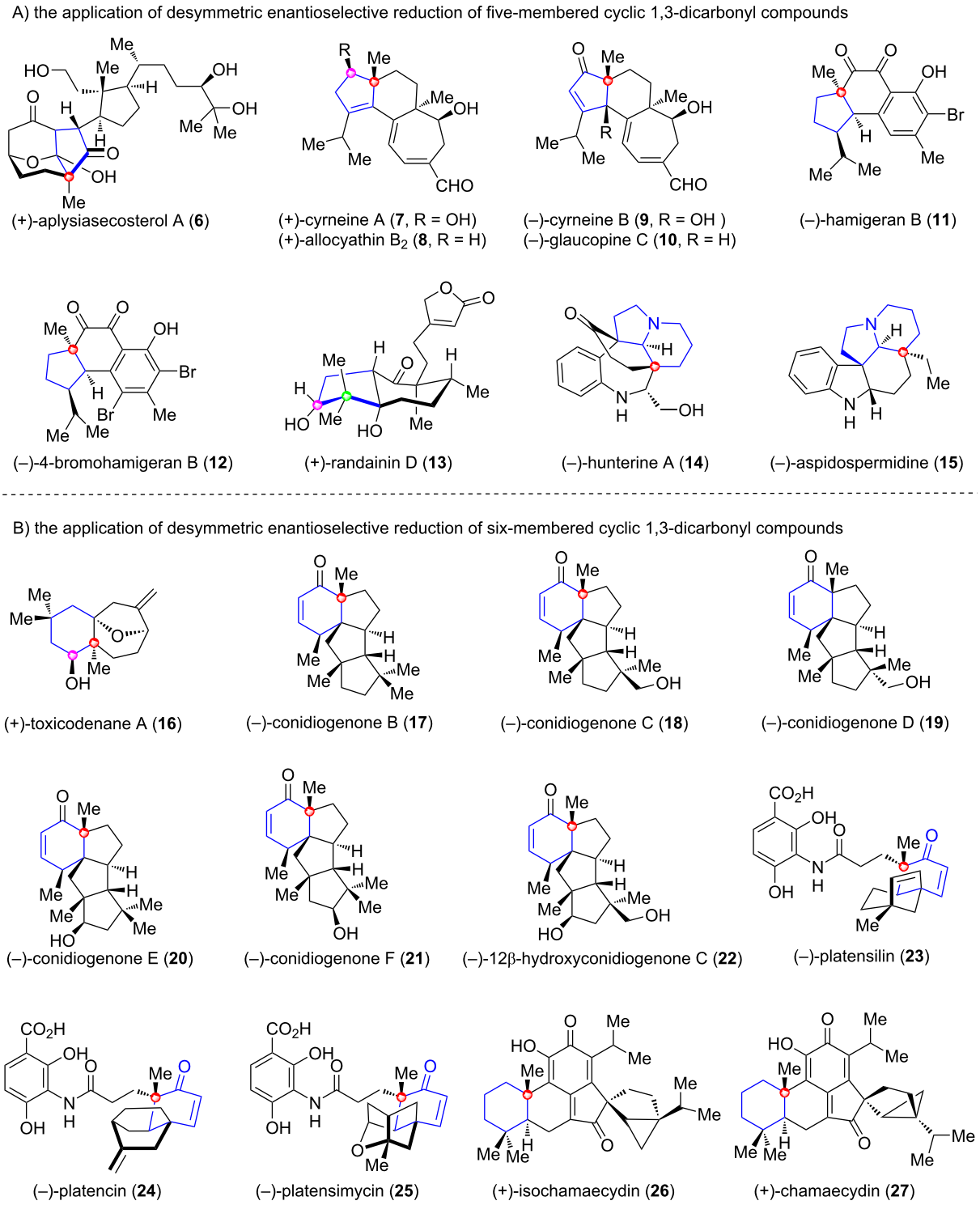

Figure 2: Selected terpenoid and alkaloid natural products synthesized by applying desymmetric enantioselective reduction strategy of cyclic 1,3-dicarbonyl compounds in 2016–2025.

Review

Total synthesis of terpenoid and alkaloid natural products through the desymmetric enantioselective reduction of five-membered cyclic 1,3-dicarbonyl compounds

Total synthesis of (+)-aplysiasecosterol A

(+)-Aplysiasecosterol A (**6**) is a secosteroid that was isolated from the sea hare *Aplysia kurodai* by Kita and Kigoshi in 2015 [13]. Due to its natural scarcity, the biological activity has not been explored. In 2018, Li and co-workers accomplished the first asymmetric total synthesis of (+)-aplysiasecosterol A (**6**) by employing a desymmetric enantioselective reduction strategy of 1,3-cyclopentanedione derivative as the key transformation [14].

Their synthesis features a highly efficient desymmetric enantioselective reduction of diketone **28** for preparing alcohol **30** under the CBS conditions [8] with (*S*)-**29** as the catalyst (Scheme 1) [14]. Notably, this reaction could be performed on multiple gram scales with satisfactory yield (72%) and ee value (92%). Protection of the alcohol group in **30** with TBSCl followed by modification of the terminal double bond afforded ketoaldehyde **31**. The 2-bromoallylation [15] of **31** with boronic ester **32** stereoselectively constructed the C3–OH group to give homoallylic alcohol **33**. Next, a successive manipulation by

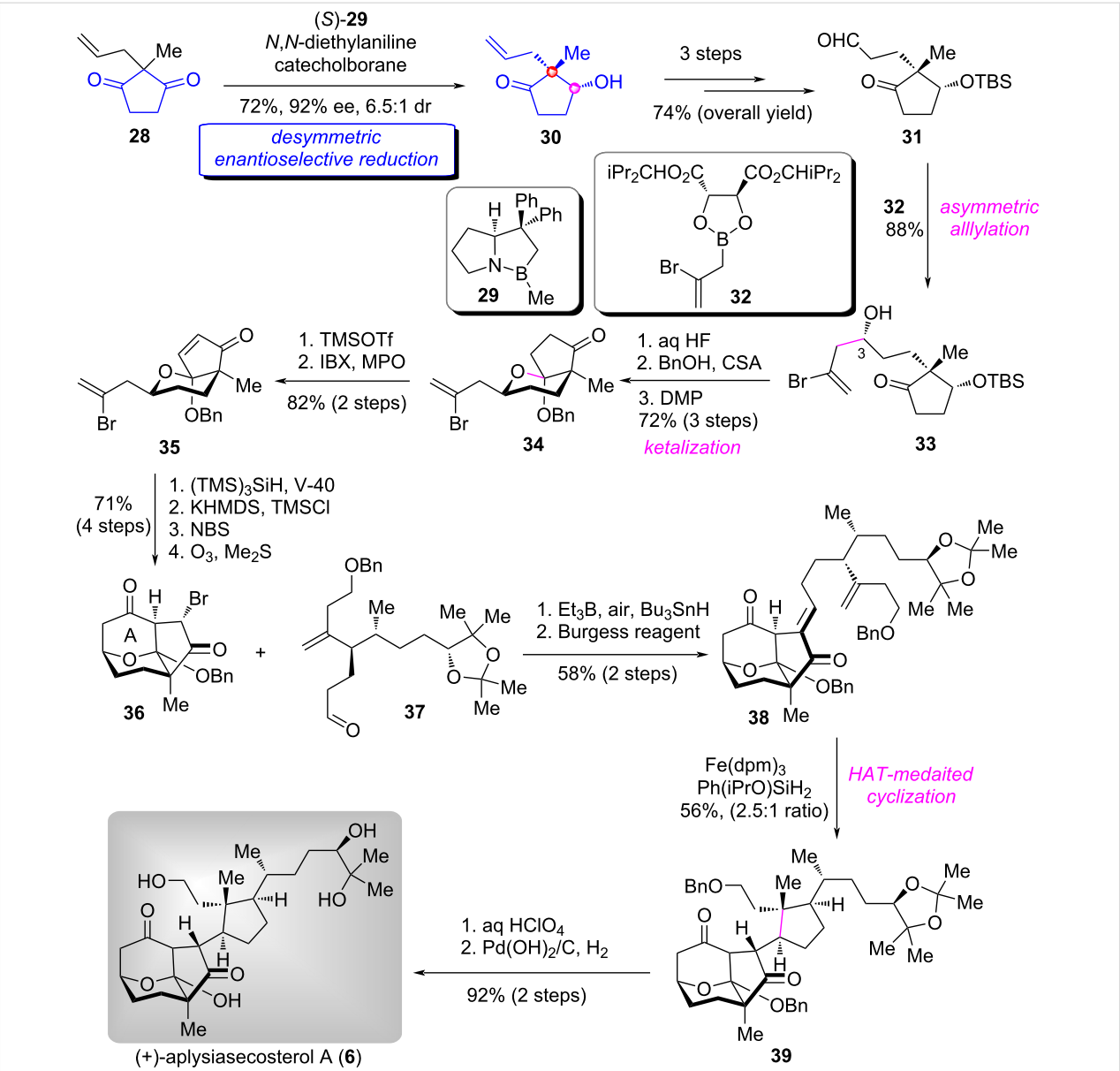

Scheme 1: The total synthesis of (+)-aplysiasecosterol A (**6**) by Li [14].

removal of TBS group, CSA-catalyzed ketalization, and DMP oxidation of the secondary alcohol to a ketone allowed for rapid construction of bicyclic ketone **34** in high overall yield. The oxidative dehydrogenation of **34** gave α,β-unsaturated bicyclic ketone **35** smoothly. Sequential A-ring construction and functional group modifications of **35** produced the diketone **36**. Subsequently, **36** and aldehyde **37**, which was prepared with 9 steps from commercially available (+)-citronellol, underwent a Reformatsky-type radical addition under the conditions of Et_3B/air/Bu_3SnH to deliver aldol product [16]. Dehydration of the secondary alcohol gave (*E*)-**38**. The HAT radical cyclization [17] of **38** in the presence of $Fe(dpm)_3$/$Ph(iPrO)SiH_2$ proceeded smoothly to furnish the tetracyclic product **39** in 56% yield with 2.5:1 ratio. Finally, removal of the acetonide and the Bn protecting group completed the total synthesis of (+)-aplysiasecosterol A (**6**).

Total synthesis of (+)-cyrneine A, (−)-cyrneine B, (−)-glaucopine C, and (+)-allocyathin B_2

The cyrneine diterpenoids represent an important subfamily of cyathane diterpenoids which possess a common 5-6-7 fused tricarbocyclic core with two all-carbon quaternary stereocenters. Many impressive syntheses have been reported to date [18-30]. In 2018, the group of Han accomplished the total synthesis of (+)-cyrneine A (**7**), (−)-cyrneine B (**9**), (−)-glaucopine C (**10**), and (+)-allocyathin B_2 (**8**) by a collective manner [31]. In their synthetic route, an enzyme-catalyzed desymmetric enantioselective reduction of 1,3-cyclopentanedione derivative was adopted as one of the key reactions, which facilitated the construction of the five-membered ring bearing an all-carbon quaternary center as the key chiral building block.

Their synthesis began with 1,3-dione **40** (Scheme 2) [31,32], allylation of this substrate with allylic bromide **41** afforded the 1,3-cyclopentanedione derivative **42**. Next, the baker's yeast-catalyzed desymmetric enantioselective reduction of **42** gave the α-hydroxyketone **43** in satisfactory yield and excellent stereoselectivity and diastereoselectivity on a decagram scale [33,34]. Functional group modifications and transformations of **43** produced hydroxyketone **44**. Due to the steric hindrance of this substrate, the subsequent Suzuki cross coupling reaction with 3-boronophenol proceeded in low yield. To address this issue, Han's group employed a novel palladacycle catalyst **45**, previously developed by their group [35-37]. This catalytic

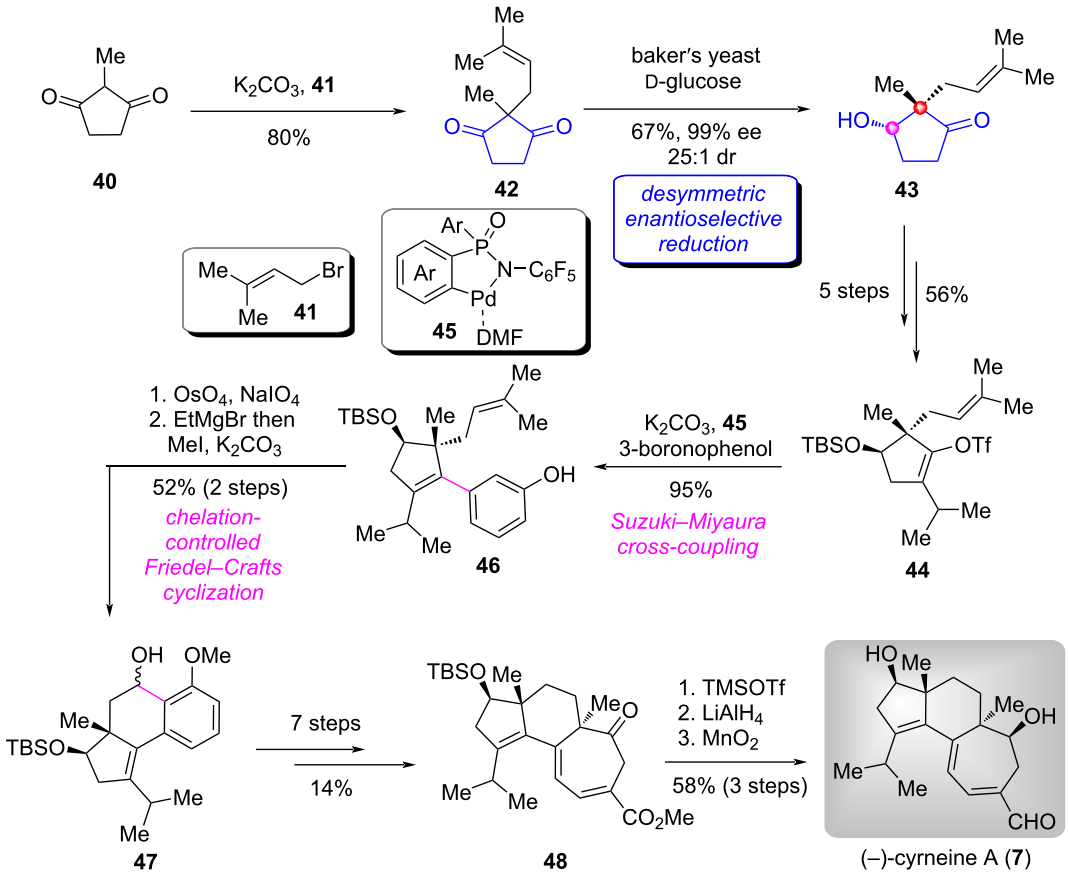

Scheme 2: The total synthesis of (−)-cyrneine A by Han [31].

system efficiently overcame the challenge and furnished the coupling product **46** in high yield. Oxidative cleavage of the double bond in **46** followed by Mg(II)-mediated chelation-controlled Friedel–Crafts cyclization delivered secondary alcohol **47**, which was elaborated to ketone **48** via a seven-step transformation. Finally, removal of the TBS group in **48** followed by a sequential reduction and selective oxidation of allylic primary alcohol achieved the total synthesis of (−)-cyrneine A (**7**).

The authors then moved forward to the synthesis of other target molecules (Scheme 3) [31,32]. Oxidation state adjustment of **48** led to the ketone **49**. Starting from this common intermediate, firstly, base-promoted double bond migration and oxidation at the γ-position gave tertiary alcohol **50**. Deprotection of acetyl in **50** followed by selective oxidation delivered (−)-cyrneine B (**9**). Secondly, a based-mediated concomitant double bond migration and deacetylation, and selective oxidation of allylic primary alcohol accomplished the total synthesis of (−)-glaucopine C (**10**). On the other hand, Barton–McCombie deoxygenation and isopropylation of **43** produced ketone **52**. Subsequently, by employing the same procedures for the synthesis of (−)-cyrneine A (**7**), the synthesis of (+)-allocyathin B_2 (**8**) could also be achieved smoothly from **52** by utilizing diketone **53** as the intermediate. The diverse syntheses of these terpenoids enabled by the desymmetric enantioselective reduction of cyclic 1,3-dicarbonyl compounds demonstrated the significance of the desymmetric reduction strategy in the synthesis of structurally complex natural products.

Total synthesis of (–)-hamigeran B and (–)-4-bromohamigeran B

(−)-Hamigeran B (**11**) and (−)-4-bromohamigeran B (**12**) were isolated from the sponge *Hamigera tarangaensis*, and show cytotoxicity against various tumor cells. Notably, compound **11** exhibits 100% inhibition against herpes and polio viruses without significant host cell cytotoxicity [38]. Since their isolation, the synthesis of **11** and **12** have been reported by many groups [39-50]. For an efficient synthesis of these two natural products, Han and co-workers [51] adopted an alternative route utilizing the desymmetric enantioselective reduction strategy of a 1,3-cyclopentanedione derivative as the key transformation. Both (−)-hamigeran B (**11**) and (−)-4-bromohamigeran B (**12**) were synthesized by a divergent manner with a longest linear sequence of 14 steps from the known symmetrical diketone **28**

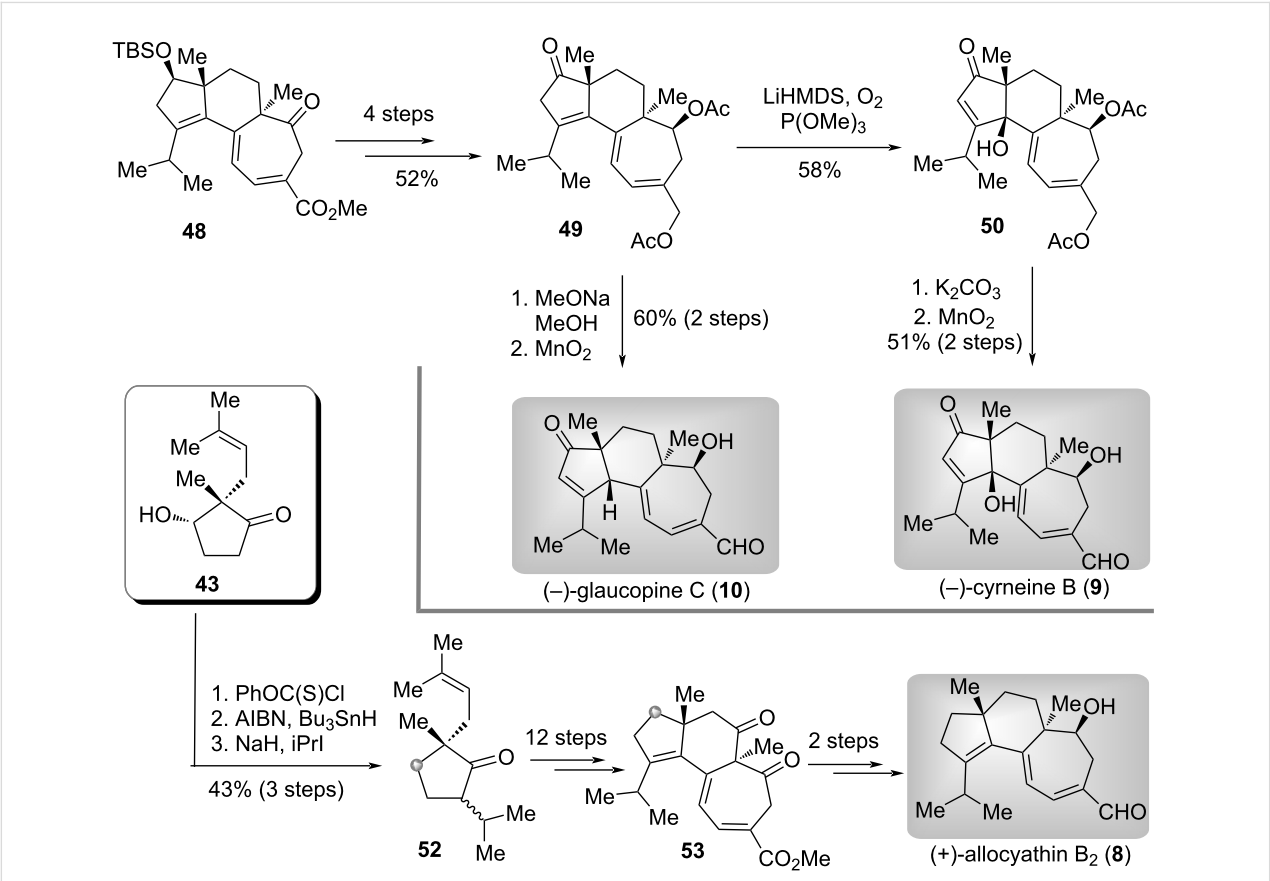

Scheme 3: The total syntheses of three cyrneine diterpenoids by Han [31,32].

(see Scheme 1) [14]. More importantly, this route allowed for the synthesis of target compounds at 100 mg scale in a single batch.

As shown in Scheme 4 [51], the enzyme-catalyzed desymmetric enantioselective reduction of **28**, afforded hydroxyketone **54** in 65% yield with >99% ee and 8–9:1 dr on multigram scale [34]. Functional group transformations of **54** in four steps produced sterically hindered allyl triflate **55**. By employing the palladacycle catalyst **45**-catalyzed Suzuki cross-coupling reaction of sterically hindered substrates developed by Han [35-37], the coupled product **57** was obtained in a satisfactory yield (72%) from **55** and pinacol boronate **56,** along with trace amounts of the double bond migrated side product **58** (**57**:**58** = ca. 15:1). Demethylation of **57** to phenolic intermediate followed by the construction of the B ring generated tricyclic core **59**. Subsequently, dihydroxylation of the doubled bond in the central six-membered ring using OsO_4/NMO gave diol, which was then subjected to acetylation of the two hydroxy groups and hydrogenation of C5=C6 double bond to afford triacetate **60** as a single diastereoisomer. Base-promoted hydrolysis and concomitant oxidation under oxygen atmosphere gave vicinal diketone **61**. Finally, the introduction of mono-bromo and di-bromo atoms achieved the total synthesis of (−)-hamigeran B (**11**) and (−)-4-bromohamigeran B (**12**), respectively.

Total synthesis of (+)-randainin D

(+)-Randainin D (**13**) is a representative member of a class of structurally intriguing diterpenoids containing a *trans*-hydroazulenone core and a C9-butenolide moiety isolated from *Callicarpa randaiensis* [52]. It exhibits inhibition of elastase release and superoxide-anion generation. In 2024, Baudoin and

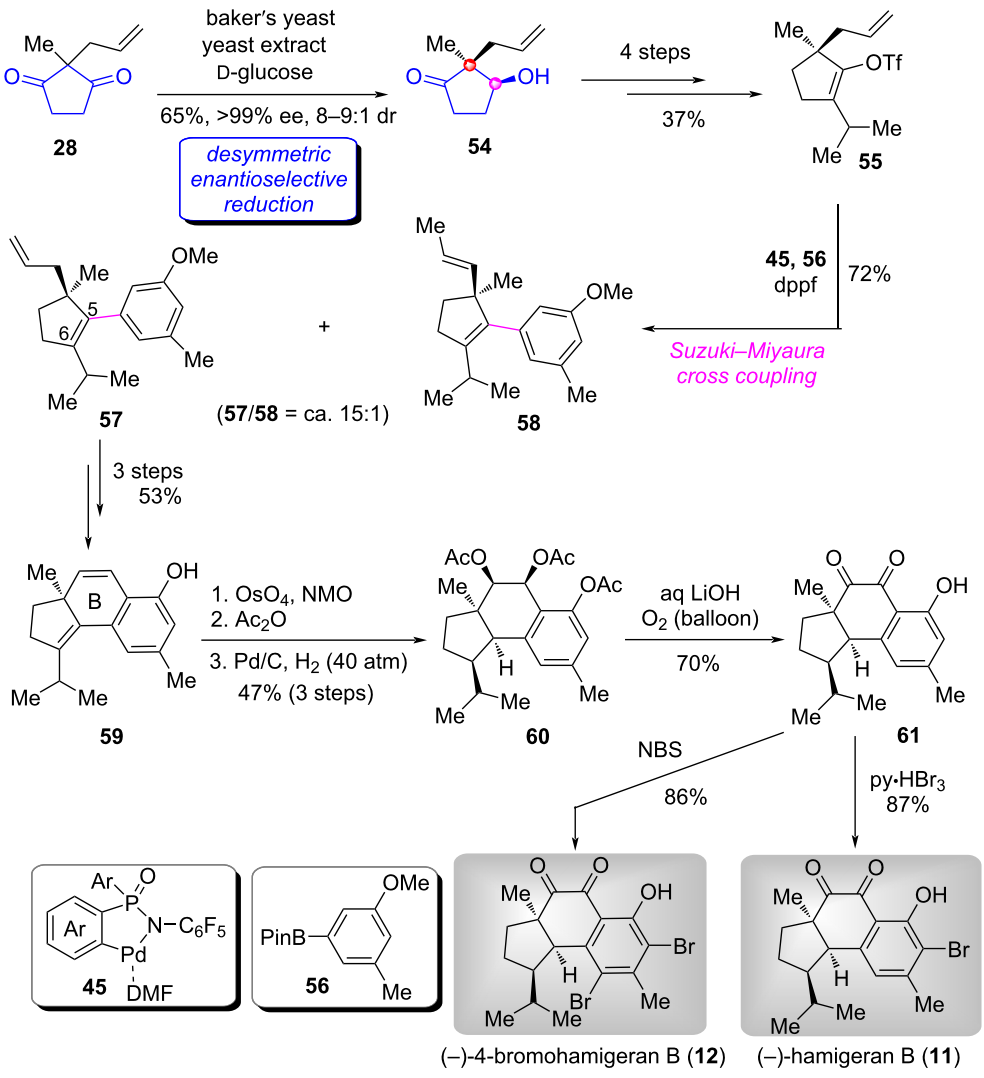

Scheme 4: The total synthesis of (−)-hamigeran B and (−)-4-bromohamigeran B by Han [51].

co-workers presented an efficient route for the first total synthesis (+)-randainin D (**13**) by utilizing an early-staged Ru-catalyzed desymmetric enantioselective reduction as the key transformation [53].

As shown in Scheme 5 [53], based on the reported method for asymmetric transfer hydrogenation of commercially available cyclopentadione **62** [54], the authors adapted an efficient method for the desymmetric enantioselective reduction of **62** using commercially available (*R*,*R*)-Ts-DENEB (**63**) as the catalyst and formic acid as the hydrogen donor, securing the desired secondary alcohol product in excellent enantioselectivity (99% ee). Protection of the alcohol group with TBDPSCl gave silyl ether **64** in high yield (79% for 2 steps). Subsequently, successive four manipulations including dehydrogenation, Morita–Baylis–Hillman reaction, protection of the resultant primary alcohol, and hydrogenation afforded ketone **65**. The $LaCl_3$·LiCl-promoted addition of **65** with Grignard reagent followed by TES protection of the resulting secondary alcohol, regioselective deprotection of the TES group and in situ oxidation provided aldehyde **66**. Next, **66** underwent the 1,2-addition of isopropenyllithium reagent (prepared from *n*-BuLi/tetraisopropenyltin (**67**) [55]) and DMP oxidation to afford ketone **68**. A three-step transformation including RCM, Mukaiyama hydration, and esterification, **68** was converted to methyl oxalate **69**. Irradiation of the reaction mixture **69** and lactone **70** at 456 nm with *fac*-Ir(ppy)$_3$ as the photocatalyst furnished a mixture of isomeric olefins. Finally, DBU-promoted the isomeric olefins conjugation and removal of the two silyl ether completed the first total synthesis of (+)-randainin D (**13**).

Total synthesis of (–)-hunterine A and (–)-aspidospermidine

(−)-Hunterine A (**14**) and (−)-aspidospermidine (**15**) are monoterpene indole alkaloids, which were isolated from *Hunteria zeylanica* and *Apocynaceae* plants, respectively [56,57]. Structurally, these two natural products both contain the fused polycyclic skeleton core bearing four consecutive stereocenters, two of which are all-carbon quaternary stereocenters. Such a skeletally extraordinary structure poses significant challenges for total synthesis. In 2024, Stoltz and co-workers finished the divergent enantioselective total synthe-

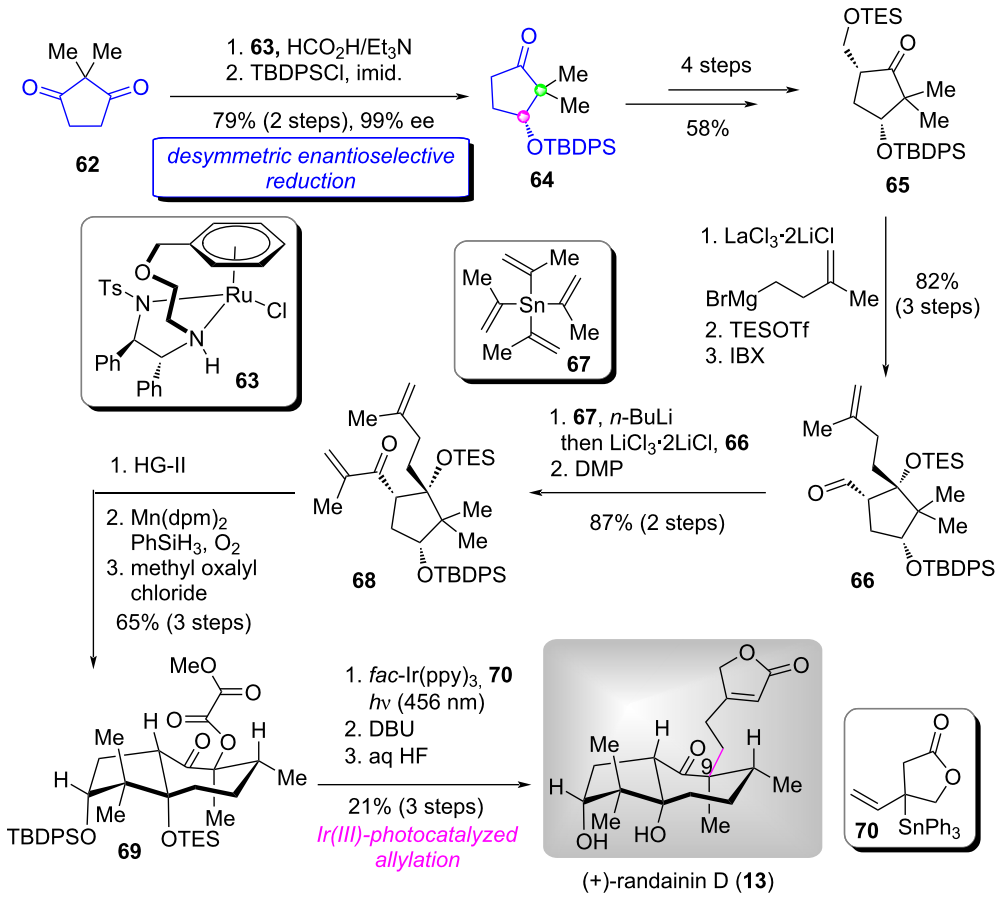

Scheme 5: The total synthesis of (+)-randainin D by Baudoin [53].

sis of (−)-hunterine A and (−)-aspidospermidine by utilizing a Ru-catalyzed desymmetric enantioselective reduction of bicyclic 1,3-diketone **72** for rapidly accessing the 5/5 bicyclic core skeleton containing two desired stereocenters [58]. The application of this strategy accelerated the synthesis of these two complex alkaloids within a longest linear sequence of 16 and 14 steps, respectively.

As shown in Scheme 6 [58], the Cu-catalyzed 1,4-conjugated addition of **71** [59] with vinylMgBr followed by intramolecular Claisen condensation furnished bicyclic diketone **72** on a gram scale. Notably, for such a bicyclic substrate, it is quite challenging to achieve desymmetric enantioselective reduction because the catalyst has difficulty identifying its *Re*- and *Si*-faces. After screening several reduction strategies, the authors identified a set of Ru-catalyzed transfer hydrogenation conditions [60,61] utilizing **73** as the catalyst that could be used for the desymmetric enantioselective reduction of **72**, affording the hydroxyketone **74** in 57% yield with 91% ee. Protection of the secondary alcohol in **74** followed by Beckmann rearrangement led to lactam **75**. Oxidation state modifications and functional group transformations of **75** afforded ketone **76**. Next, the 1,2-addition of **76** with vinyl iodine **77** and subsequent deprotection produced tertiary alcohol **78**. Starting from this common intermediate, on the one hand, through successive manipulations by diazotization and in situ azide substitution, $AgNO_3$-

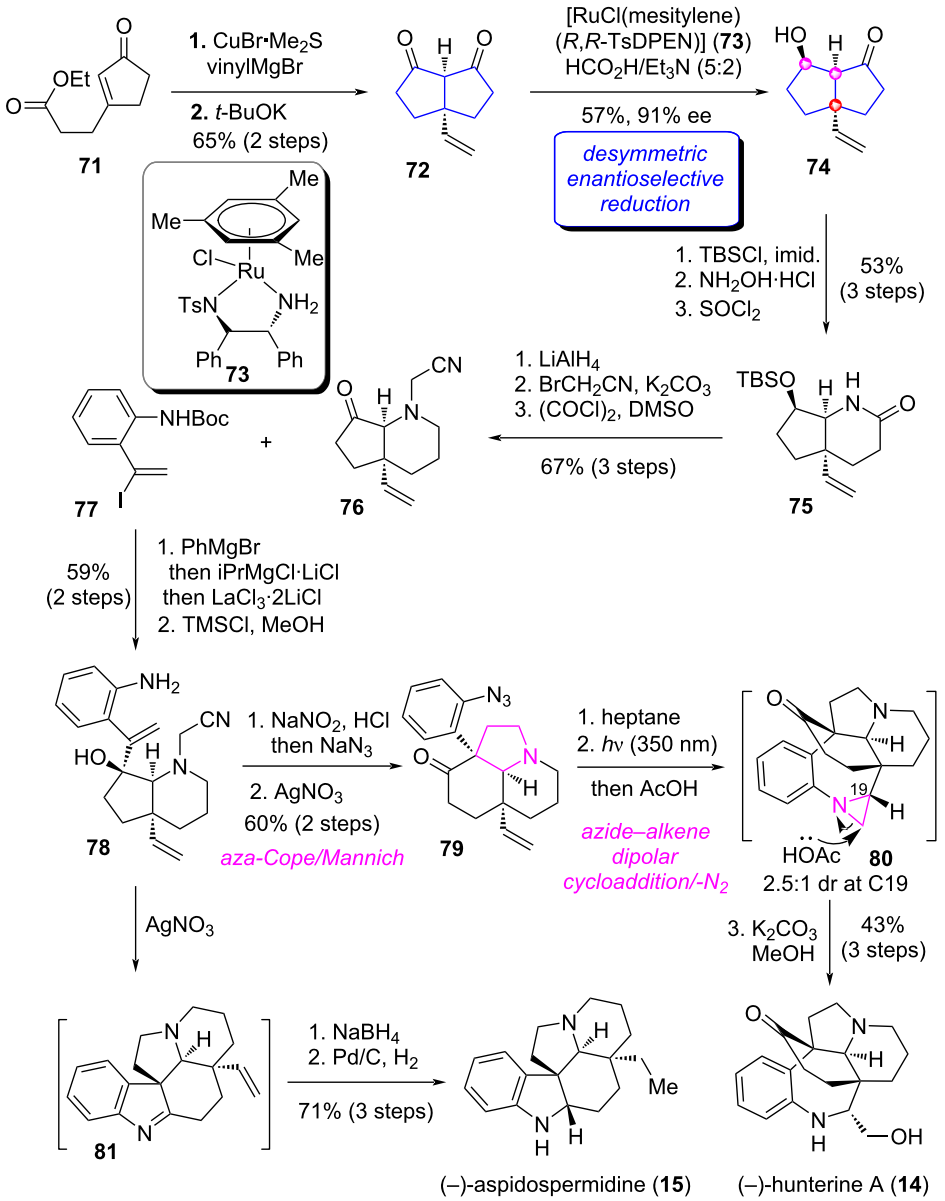

Scheme 6: The total synthesis of (−)-hunterine A and (−)-aspidospermidine by Stoltz [58].

mediated aza-Cope/Mannich [62] reaction delivered ketone **79**. Subsequently, a three-step operation including azide–alkene dipolar cycloaddition, irradiation of the resulting triazoline to aziridine **80** and in situ ring opening followed by deacetylation achieved the first total synthesis of (−)-hunterine A (**14**). On the other hand, aza-Cope/Mannich reaction of **78** produced imine intermediate **81**. Reduction and hydrogenation of **81** furnished the total synthesis of (−)-aspidospermidine (**15**).

Total synthesis of terpenoid natural products through the desymmetric enantioselective reduction of six-membered cyclic 1,3-dicarbonyl compounds

Total synthesis of (+)-toxicodenane A

The skeletally new sesquiterpenoids, toxicodenanes A–C and E (see representative structure **16** in Scheme 7) were isolated from *Toxicodendron vernicifluum* in 2013 to 2015 [63,64], whose structures feature the all-carbon bicyclic skeleton and four to seven contiguous stereocenters, posing significant challenges to their synthesis. Additionally, there is a lack of corresponding pharmacological activity studies. In 2021, the group of Han completed the first enantioselective total synthesis of (+)-toxicodenane A (**16**) and determined its absolute configuration by employing an early-stage desymmetric enantioselective reduction of a 1,3-cyclohexanedione derivative as the key transformation [65]. The application of this strategy markedly accelerated the synthesis of the complex molecule within a longest linear sequence of 9 steps from the commercially available material.

The synthesis began with the commercially available 1,3-cyclohexanedione **82** (Scheme 7) [65,66]. Accordingly, the α-dialkylation of **82** gave diketone **83**. Based on the conditions developed by the authors [67], namely, using *P*-stereogenic phosphinamide **84** as the catalyst and base **85** as the additive, the desymmetric enantioselective reduction of **83** proceeded smoothly to deliver the hydroxyketone **86** in 60% yield with 92% ee and 8.4:1 dr. A secondary hydroxy-directed Grignard reagent addition of **86** followed by selective protection, generated alcohol ester **87**. After one recrystallization, the ee value of **87** could be increased to 99%. Subsequently, TMSOTf-promoted transacetalation and in situ Prins cyclization produced the oxa-bridged product **88**. Finally, ozonolysis of **88** followed by Wittig reaction of the resultant ketone and subsequent reduction accomplished the total synthesis of (+)-toxicodenane

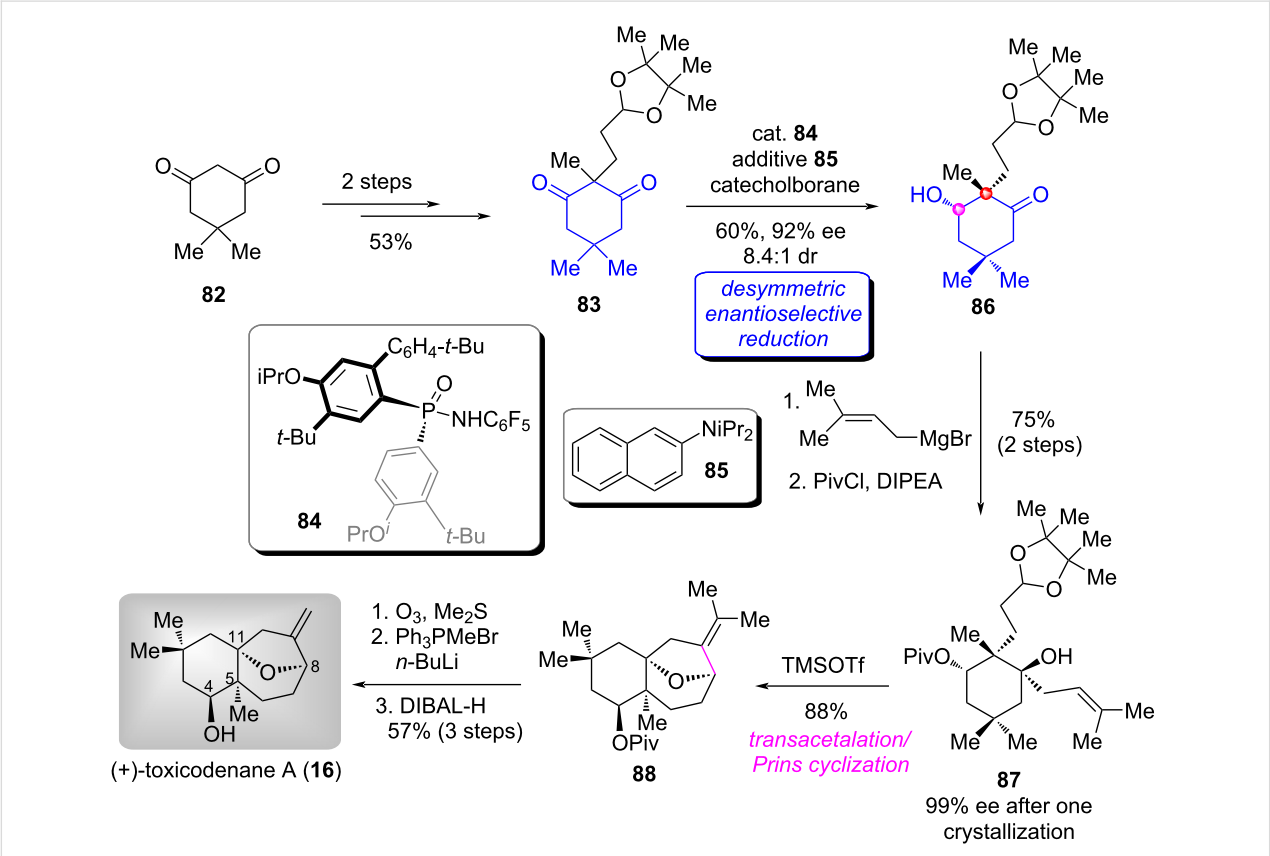

Scheme 7: The total synthesis of (+)-toxicodenane A by Han [65,66].

A (**16**). The authors eventually confirmed that the absolute configuration of (+)-**16** was 4*S*,5*S*,8*R*,11*R* based on the X-ray single-crystal analysis of its corresponding *p*-bromobenzoic ester (not shown).

Total synthesis of (–)-conidiogenones B–F and (–)-12β-hydroxyconidiogenone C

Conidiogenones are unique diterpenoids which possess a highly congested 6/5/5/5-fused framework with four all-carbon quaternary centers isolated from *Penicillium cylopium* and exhibit various biological properties [68]. The intriguing structure and interesting biological properties have attracted continued synthetic attention [69-71]. In a 2023 report, the group of Lee and Han adopted an early-stage desymmetric enantioselective reduction of 1,3-cyclohexanedione derivative **89** as the key transformation [72]. Both (−)-conidiogenones B–F (**17**–**21**) and (−)-12β-hydroxyconidiogenone C (**22**) were synthesized in a divergent manner.

Their synthetic route began with the known terminal alkyne cyclohexanedione **89** [73]. As illustrated in Scheme 8 [72], the easily prepared substrate underwent the CBS reduction condi-

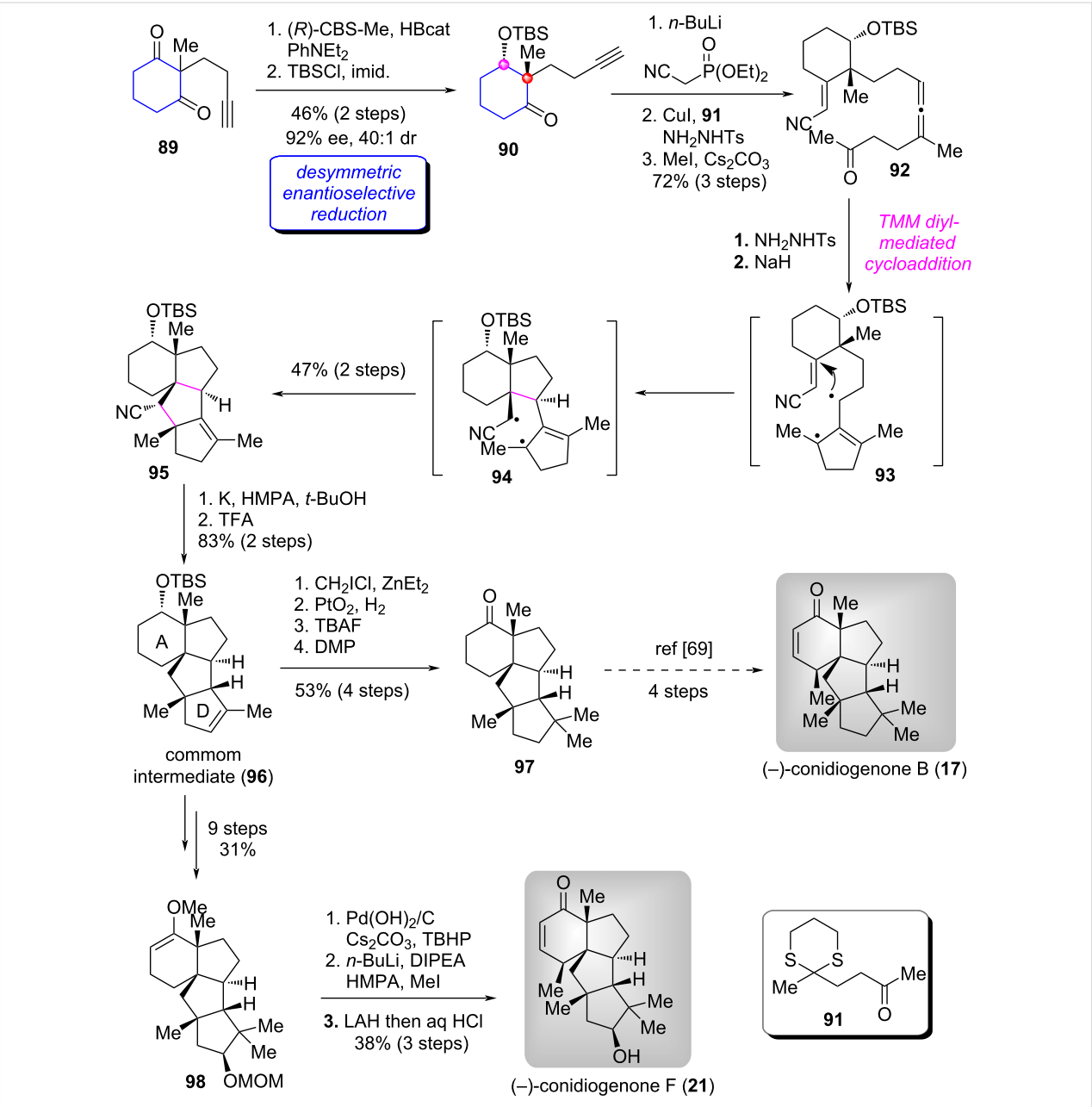

Scheme 8: The formal total synthesis of (–)-conidiogeone B and total synthesis of (–)-conidiogeone F by Lee and Han [72].

tions and protection of the resulting secondary alcohol with TBSCl to afforded silyl ether ketone **90** in 46% yield (two steps, dr = 40:1, 92% ee) [8]. Horner–Wadsworth–Emmons (HWE) reaction of **90** followed by Cu-carbene migratory insertion [74] with ketone **91** and deprotection of the dithiane group delivered alleneketone **92**. Sequential treatment of **92** with $TsNHNH_2$ and NaH, the trimethylenemethane (TMM) diyl-mediated cycloaddition via intermediates **93** and **94** proceeded uneventfully to form the tetracyclic product **95**. Next, reductive decyanation [75] and double bond migration of **95** produced common intermediate **96**, which was elaborated to ketone **97** [69] via four functional group manipulations, thereby achieving the formal total synthesis of (−)-conidiogenone B (**17**). On the other hand, functionalization and derivatization were performed on the A- and D-rings of **96**, respectively, delivering the methyl enol ether **98**. Finally, allylic oxidation [76], α-methylation and reduction of **98** followed by hydrolysis accomplished the first total synthsis of (−)-conidiogenone F (**21**).

After achieving the aforementioned success, the authors continued to utilize **96** as the common intermediate to synthesize other target natural products (Scheme 9) [72]. Firstly, the allylic oxidation and Luche reduction of **96** afforded primary alcohol **99**, which was elaborated to (−)-conidiogenone D (**19**) via ten functional group manipulations. Secondly, the allylic oxidation of **96** with CrO_3/3,5-DMP produced ketone **100**. The 1,4-conjugate addition of **100** with MeI followed by Luche reduction provided the secondary alcohol **101**. A-ring modifications in **101** completed the first total synthesis of (−)-conidiogenone E (**20**). One the other hand, a two-step transformation involving the 1,4-conjugate addition utilizing vinylMgBr and Luche reduction, **100** was converted to secondary alcohol **102** (dr = 2:1). Finally, functional group modifications of A- and D-rings furnished the total syntheses of (−)-conidiogenone C (**18**) and (−)-12β-hydroxyconidiogenone C (**22**), respectively.

Total syntheses of (–)-platensilin, (–)-platencin, and (–)-platensimycin

(−)-Platensilin (**23**), (−)-platencin (**24**), and (−)-platensimycin (**25**) are structurally unique meroterpenoids containing rigid bicycle [3.2.1] or [2.2.2]-octane cage core. They present promising drug leads for both antidiabetic and antibacterial therapies.

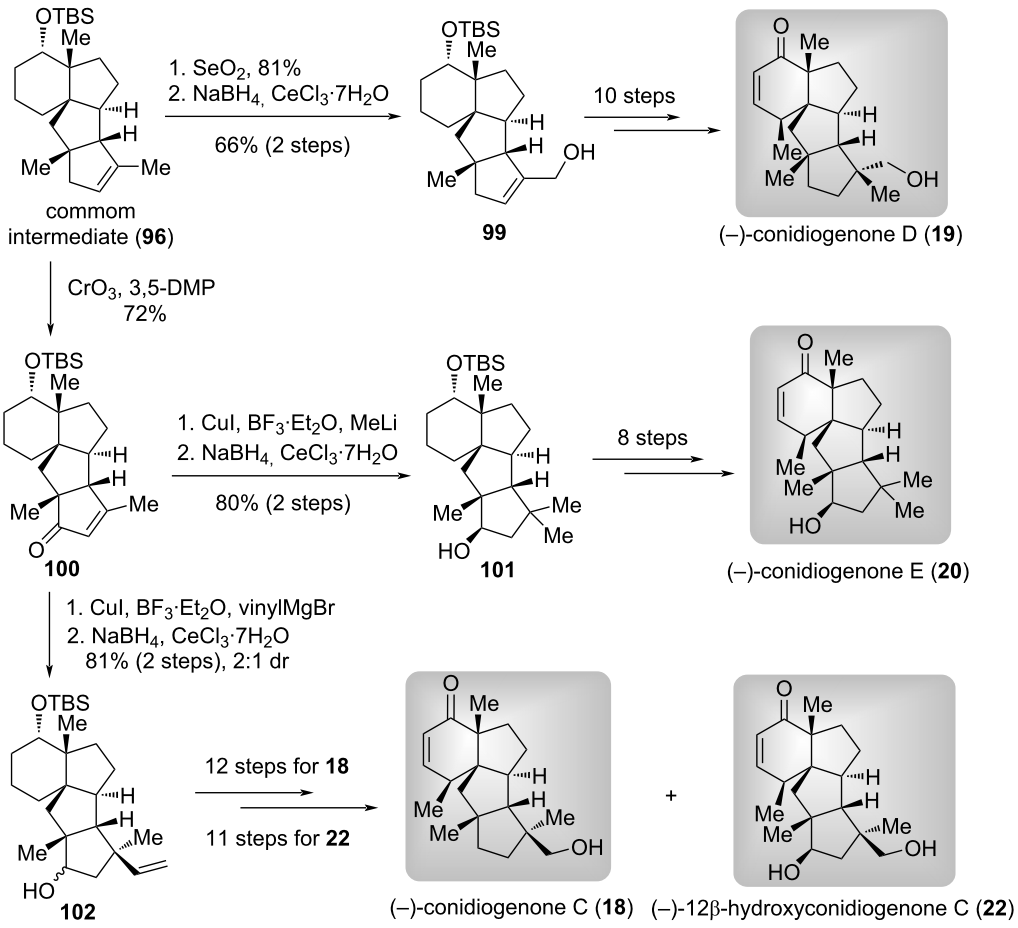

Scheme 9: The total syntheses of four conidiogenones natural products by Lee and Han [72].

The intriguing structural features and potential bioactivities have stimulated tremendous synthetic efforts [77-81]. In 2024, the group of Lou and Xu presented a unified and efficient route for the syntheses of (−)-platensilin, (−)-platencin, and (−)-platensimycin by utilizing a desymmetric enantioselective reduction of 1,3-cyclohexanedione derivative strategy [82].

The synthesis of (−)-platensilin (**23**) is shown in Scheme 10 [82]. Brewer's yeast (YSC-2)-promoted desymmetric enantioselective reduction of 1,3-cyclohexanedione derivative **103** proceeded smoothly to produce hydroxyketone **104** in excellent diastereoselectivity and enantioselectivity [9,11]. Ozonolysis of the double bond in **104** followed by Purdie methylation with Ag_2O/MeI, base-mediated vinyl triflation, and Pd-catalyzed Suzuki–Miyaura cross coupling with pinacol boronate **105** delivered diene **106**. Next, The Et_2AlCl-catalyzed intermolecular Diels–Alder reaction of **106** with methacrolein **107** afforded the common intermediate **108** in high yield. Sequential Grignard reagent addition and acid-promoted ethoxy elimination provided the separable planar diene **109** (dr = 1:1), which underwent a Mn-catalyzed HAT hydrogenation to give (15*R*)-**110** and (15*S*)-**110** in 65% and 54% yield, respectively. Subsequently, ten functional group manipulations of the diastereomeric mixture **110** produced ketoester **111**. Finally, the introduction of conjugated double bond in **111** followed by hydrolysis of the methyl ester to carboxylic acid and DCC-mediated condensation with **112** accomplished the total synthesis of (−)-platensilin (**23**).

Based on the aforementioned successful work, the authors focused on the synthesis of (−)-platencin (**24**) and (−)-platensimycin (**25**) (Scheme 11) [82]. Accordingly, Wittig reaction of **108** followed by 1,4-elimination and intramolecular Diels–Alder reaction generated tricyclo[3.2.1.$0^{2,7}$]-octene **113**. A two-step transformation including HAT hydrogenation and acetal C–H oxidation with $RuCl_3$/$NaIO_4$, **113** was converted into ketoester **114**. The TFA-mediated C13–C15 bond cleavage of **114** proceed smoothly to give ring-opening products, which underwent dehydration with Martin's sulfurane to afford the known intermediate **115** [83] and terminal alkene **116** (C12–C13 bond-cleaved byproduct). Thus, the formal total synthesis of (−)-platencin (**24**) was achieved. On the other hand, epoxidation of **113** followed by acid-mediated regioselective ring-opening and in situ allylic substitution with MeOH produced [3.2.1] bridged ring product **117**, which was transformed into ketone **118** via nine functional group manipulations.

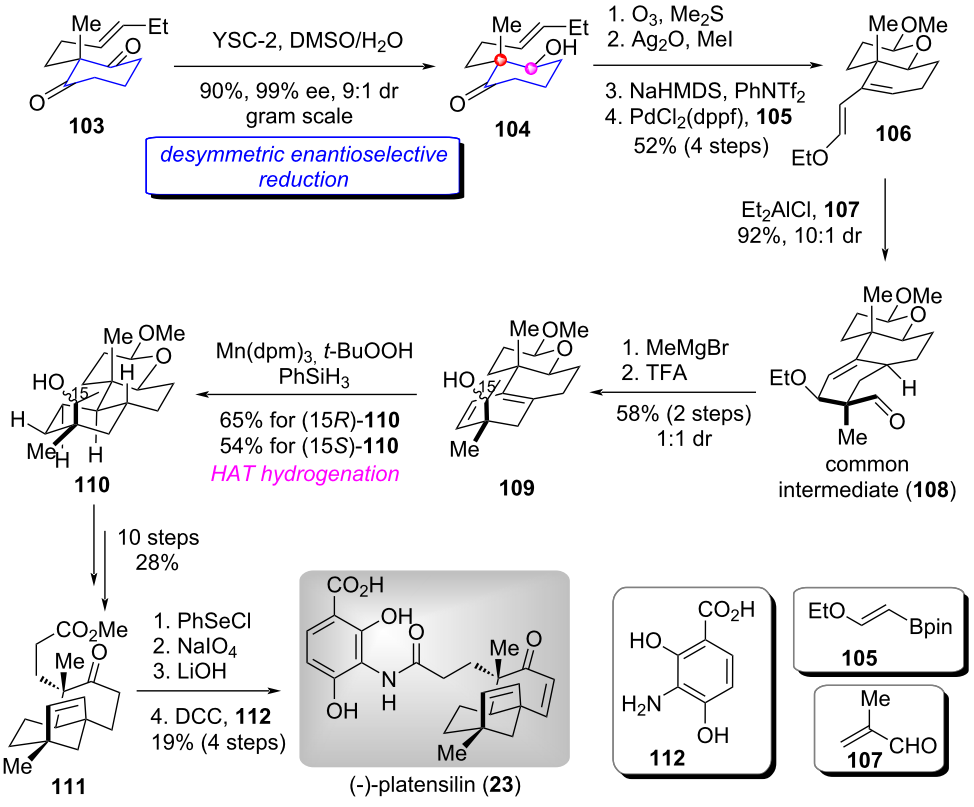

Scheme 10: The total synthesis of (−)-platensilin by Lou and Xu [82].

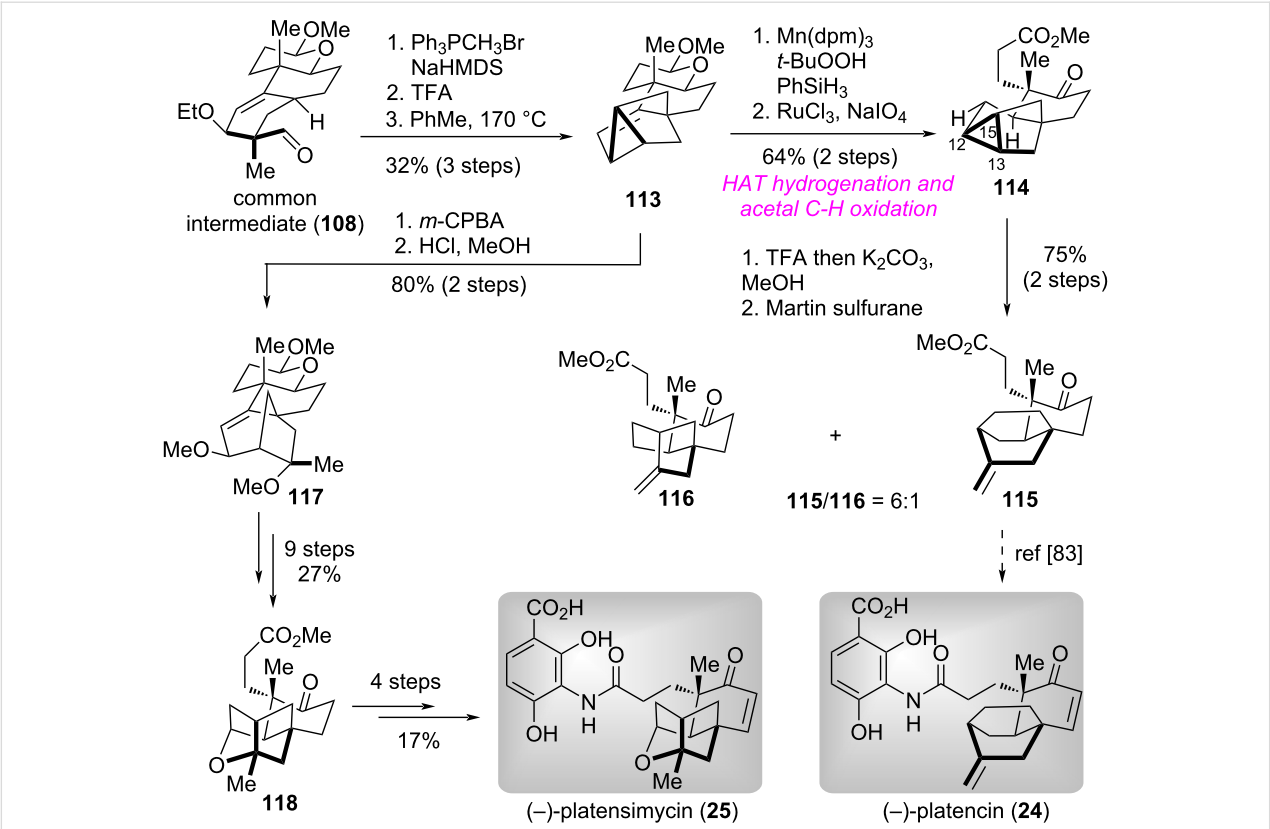

Scheme 11: The total synthesis of (–)-platencin and (–)-platensimycin by Lou and Xu [82].

Finally, by employing the same reaction procedures as those utilized in the total synthesis of (−)-platensilin (**23**), the authors accomplished the total synthesis of (−)-platensimycin (**25**).

Total synthesis of (+)-isochamaecydin and (+)-chamaecydin

(+)-Isochamaecydin (**26**) and (+)-chamaecydin (**27**) are represented members of the cryptoquinonemethides isolated from the seed of *chamaecyparis obtusa* Endl. genus [84]. This two compounds possess the unprecedented spiroannulated 6/6/6/5/5/3 (A/B/C/D/E/F) hexacarbocyclic motif and exhibit significant antifeedant activity against the pest insect *Spodoptera litura* [85]. In a very recent report, Han and co-workers accomplished the first catalytic asymmetric total syntheses of **26** and **27** via a modular and convergent strategy [86]. The key to their successful synthesis depended on the method application of a desymmetric enantioselective reduction of a 1,3-cyclohexanedione derivative as the key transformation.

Their synthesis began with the known 1,3-cyclohexanedione **119** (Scheme 12) [86]. Initially, for the construction of the crucial B ring bearing an all-carbon quaternary stereocenter, the authors employed a method they had previously reported [35,67]. Namely, the *P*-stereogenic phosphinamide (**84**, see Scheme 7)-catalyzed desymmetric enantioselective reduction of **119**. Hydroxyketone **120** could be acquired in 60% yield with 93% ee. Subsequently, the Grignard addition of the ketone in **120** provided diene intermediate, which was converted to bicyclic secondary alcohol **121** via RCM reaction/hydrogenation and dehydration/hydrogenation. Oxidation states adjustment and functional group transformations of **121** generated bromodiene **122**. Next, the metal–halogen exchange/intermolecular addition of **122** with aldehyde (+)-**123** and in situ $PtCl_2$-promoted hydrolysis and hydration gave tricyclic product **124**. The $BnMe_3NOH$-mediated intramolecular Michael/aldol cascade reaction of **124** constructed the C/D rings, followed by dehydration to afford pentacyclic product **125**. Finally, a five-step operation including the 1,2-addition of **125** with iPrLi, PCC oxidation of the resulting tertiary alcohol, oxidative aromatization and in situ neutralization/oxidation, acid-mediated 1,6-addition with H_2O, and stereoselective cyclopropanation accomplished the first total synthesis of (+)-isochamaecydin (**26**).

On the other hand, starting from **122** and (−)-**123,** the authors adopted the same procedures as for the synthesis of **125** to obtain the pentacyclic product **126**, which underwent the same functional group transformations for the synthesis of (+)-**26** to

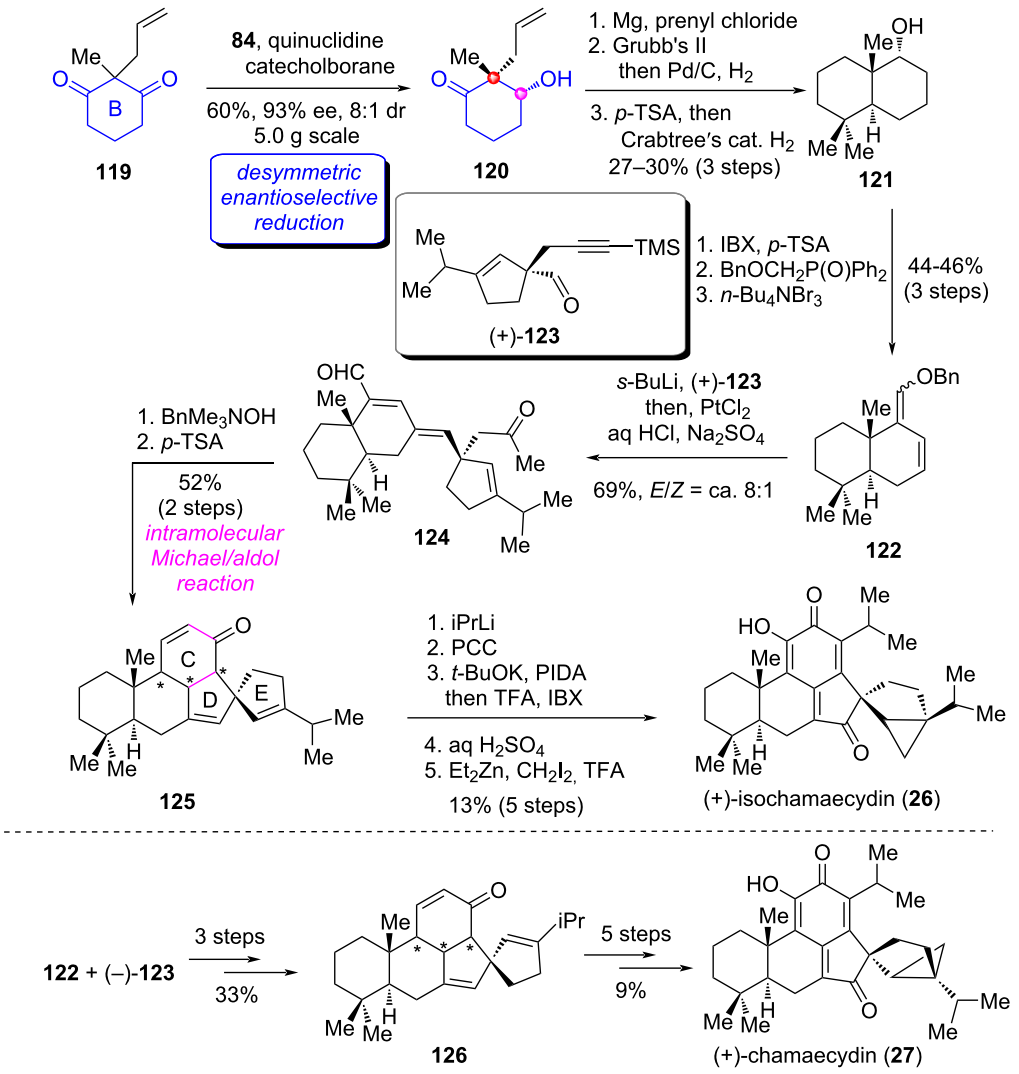

Scheme 12: The total synthesis of (+)-isochamaecydin and (+)-chamaecydin by Han [86].

complete the first total synthesis of (+)-chamaecydin (**27**). The successful collective total synthesis of the two structurally complex natural products demonstrated the high efficiency of the modular synthetic strategy based on the desymmetric enantioselective reduction of cyclic 1,3-dicarbonyl compounds.

Summary and Outlook

In this review, we summarized the application of desymmetric enantioselective reduction of cyclic 1,3-dicarbonyl compounds in the total synthesis of a series of terpenoid and alkaloid natural products reported between 2016 and 2025. It was evident that the application frequency of this strategy in the synthesis of terpenoid and alkaloid natural products has increased significantly over these ten years compared to the period before 2016. Notably, the substrates of desymmetric enantioselective reduction were no longer limited to monocyclic 1,3-dicarbonyl compounds but could also be extended to bicyclic dicarbonyl compounds. The diversification of substrates enabled this strategy to provide a novel alternative for the synthetic design of structurally more complex natural products. More importantly, from these previous works, it could be observed that the early-stage application of desymmetric enantioselective reduction could efficiently provide access to enantiomerically enriched intermediates with multiple stereocenters containing an all-carbon quaternary chiral center. Taking aforementioned advantages of this strategy, the synthetic efficiency was significantly improved.

Despite remarkable progress has been made, there is still a long way to go before the strategy achieves maturity for applications in natural products. Specifically, challenges remain in improving the enantioselectivity and diastereoselectivity of the desym-

metric enantioselective reduction of some complex substrates, as well as suppressing the double reduction by-products and developing new types of catalysts. Moreover, the application of desymmetric enantioselective reduction of chain dicarbonyl compounds in natural products synthesis remains largely undeveloped although several desymmetric enantioselective reduction studies utilizing malonate ester as substrates have been achieved [87-89]. Nevertheless, we believed on the basis of these pioneering works of the development of new reagents and methodologies for desymmetric enantioselective reduction based on the novel dicarbonyl substrates, as well as their applications in the synthesis of various complex natural products will become a focal point in the field of organic synthetic chemistry.

Funding

Financial support from the National Natural Science Foundation of China (grant no. 22071235, 22101276, 22471261) is gratefully acknowledged.

Author Contributions

Dong-Xing Tan: writing – original draft. Fu-She Han: writing – review & editing.

ORCID® iDs

Dong-Xing Tan - https://orcid.org/0000-0002-9858-9997
Fu-She Han - https://orcid.org/0000-0003-0456-7461

Data Availability Statement

Data sharing is not applicable as no new data was generated or analyzed in this study.

References

1. Sun, H.-D.; Huang, S.-X.; Han, Q.-B. *Nat. Prod. Rep.* **2006,** *23,* 673–698. doi:10.1039/b604174d
2. Liu, M.; Wang, W.-G.; Sun, H.-D.; Pu, J.-X. *Nat. Prod. Rep.* **2017,** *34,* 1090–1140. doi:10.1039/c7np00027h
3. O'Connor, S. E.; Maresh, J. J. *Nat. Prod. Rep.* **2006,** *23,* 532–547. doi:10.1039/b512615k
4. Aoki, S.; Watanabe, Y.; Tanabe, D.; Setiawan, A.; Arai, M.; Kobayashi, M. *Tetrahedron Lett.* **2007,** *48,* 4485–4488. doi:10.1016/j.tetlet.2007.05.003
5. Brooks, D. W.; Mazdiyasni, H.; Chakrabarti, S. *Tetrahedron Lett.* **1984,** *25,* 1241–1244. doi:10.1016/s0040-4039(01)80123-4
6. Shimizu, M.; Yamada, S.; Fujita, Y.; Kobayashi, F. *Tetrahedron: Asymmetry* **2000,** *11,* 3883–3886. doi:10.1016/s0957-4166(00)00378-5
7. Hashiguchi, S.; Fujii, A.; Takehara, J.; Ikariya, T.; Noyori, R. *J. Am. Chem. Soc.* **1995,** *117,* 7562–7563. doi:10.1021/ja00133a037
8. Yeung, Y.-Y.; Chein, R.-J.; Corey, E. J. *J. Am. Chem. Soc.* **2007,** *129,* 10346–10347. doi:10.1021/ja0742434
9. Breitler, S.; Carreira, E. M. *Angew. Chem., Int. Ed.* **2013,** *52,* 11168–11171. doi:10.1002/anie.201305822
10. Kuang, L.; Liu, L. L.; Chiu, P. *Chem. – Eur. J.* **2015,** *21,* 14287–14291. doi:10.1002/chem.201502890
11. Sharpe, R. J.; Johnson, J. S. *J. Am. Chem. Soc.* **2015,** *137,* 4968–4971. doi:10.1021/jacs.5b02631
12. Zeng, X.-P.; Cao, Z.-Y.; Wang, Y.-H.; Zhou, F.; Zhou, J. *Chem. Rev.* **2016,** *116,* 7330–7396. doi:10.1021/acs.chemrev.6b00094
13. Kawamura, A.; Kita, M.; Kigoshi, H. *Angew. Chem., Int. Ed.* **2015,** *54,* 7073–7076. doi:10.1002/anie.201501749
14. Lu, Z.; Zhang, X.; Guo, Z.; Chen, Y.; Mu, T.; Li, A. *J. Am. Chem. Soc.* **2018,** *140,* 9211–9218. doi:10.1021/jacs.8b05070
15. Hara, S.; Yamamoto, Y.; Fujita, A.; Suzuki, A. *Synlett* **1994,** 639–640. doi:10.1055/s-1994-22956
16. Nozaki, K.; Oshima, K.; Utimoto, K. *Tetrahedron Lett.* **1988,** *29,* 1041–1044. doi:10.1016/0040-4039(88)85330-9
17. Lo, J. C.; Yabe, Y.; Baran, P. S. *J. Am. Chem. Soc.* **2014,** *136,* 1304–1307. doi:10.1021/ja4117632
18. Nakada, M. *Chem. Rec.* **2014,** *14,* 641–662. doi:10.1002/tcr.201402019
19. Ward, D. E.; Gai, Y.; Qiao, Q. *Org. Lett.* **2000,** *2,* 2125–2127. doi:10.1021/ol006026c
20. Ward, D. E.; Shen, J. *Org. Lett.* **2007,** *9,* 2843–2846. doi:10.1021/ol070994z
21. Trost, B. M.; Dong, L.; Schroeder, G. M. *J. Am. Chem. Soc.* **2005,** *127,* 2844–2845. doi:10.1021/ja0435586
22. Trost, B. M.; Dong, L.; Schroeder, G. M. *J. Am. Chem. Soc.* **2005,** *127,* 10259–10268. doi:10.1021/ja051547m
23. Waters, S. P.; Tian, Y.; Li, Y.-M.; Danishefsky, S. J. *J. Am. Chem. Soc.* **2005,** *127,* 13514–13515. doi:10.1021/ja055220x
24. Enquist, J. A., Jr.; Stoltz, B. M. *Nature* **2008,** *453,* 1228–1231. doi:10.1038/nature07046
25. Pfeiffer, M. W. B.; Phillips, A. J. *J. Am. Chem. Soc.* **2005,** *127,* 5334–5335. doi:10.1021/ja0509836
26. Reddy, T. J.; Bordeau, G.; Trimble, L. *Org. Lett.* **2006,** *8,* 5585–5588. doi:10.1021/ol062304h
27. Snider, B. B.; Vo, N. H.; ONeil, S. V.; Foxman, B. M. *J. Am. Chem. Soc.* **1996,** *118,* 7644–7645. doi:10.1021/ja9615379
28. Snider, B. B.; Vo, N. H.; O'Neil, S. V. *J. Org. Chem.* **1998,** *63,* 4732–4740. doi:10.1021/jo9804700
29. Tori, M.; Toyoda, N.; Sono, M. *J. Org. Chem.* **1998,** *63,* 306–313. doi:10.1021/jo971514s
30. Piers, E.; Gilbert, M.; Cook, K. L. *Org. Lett.* **2000,** *2,* 1407–1410. doi:10.1021/ol0057333
31. Wu, G.-J.; Zhang, Y.-H.; Tan, D.-X.; Han, F.-S. *Nat. Commun.* **2018,** *9,* 2148. doi:10.1038/s41467-018-04480-6
32. Wu, G.-J.; Zhang, Y.-H.; Tan, D.-X.; He, L.; Cao, B.-C.; He, Y.-P.; Han, F.-S. *J. Org. Chem.* **2019,** *84,* 3223–3238. doi:10.1021/acs.joc.8b03138
33. Csuk, R.; Glaenzer, B. I. *Chem. Rev.* **1991,** *91,* 49–97. doi:10.1021/cr00001a004
34. Brooks, D. W.; Mazdiyasni, H.; Grothaus, P. G. *J. Org. Chem.* **1987,** *52,* 3223–3232. doi:10.1021/jo00391a009
35. Du, Z.-J.; Guan, J.; Wu, G.-J.; Xu, P.; Gao, L.-X.; Han, F.-S. *J. Am. Chem. Soc.* **2015,** *137,* 632–635. doi:10.1021/ja512029x
36. Guan, J.; Wu, G.-J.; Han, F.-S. *Chem. – Eur. J.* **2014,** *20,* 3301–3305. doi:10.1002/chem.201303056
37. Wu, G.-J.; Han, F.-S.; Zhao, Y.-L. *RSC Adv.* **2015,** *5,* 69776–69781. doi:10.1039/c5ra12742d
38. Wellington, K. D.; Cambie, R. C.; Rutledge, P. S.; Bergquist, P. R. *J. Nat. Prod.* **2000,** *63,* 79–85. doi:10.1021/np9903494

39. Nicolaou, K. C.; Gray, D.; Tae, J. *Angew. Chem., Int. Ed.* **2001,** *40,* 3679–3683. doi:10.1002/1521-3773(20011001)40:19<3679::aid-anie3679>3.0.co;2-t
40. Nicolaou, K. C.; Gray, D. L. F.; Tae, J. *J. Am. Chem. Soc.* **2004,** *126,* 613–627. doi:10.1021/ja030498f
41. Clive, D. L. J.; Wang, J. *Angew. Chem., Int. Ed.* **2003,** *42,* 3406–3409. doi:10.1002/anie.200351519
42. Clive, D. L. J.; Wang, J. *Tetrahedron Lett.* **2003,** *44,* 7731–7733. doi:10.1016/j.tetlet.2003.08.089
43. Clive, D. L. J.; Wang, J. *J. Org. Chem.* **2004,** *69,* 2773–2784. doi:10.1021/jo030347v
44. Trost, B. M.; Pissot-Soldermann, C.; Chen, I.; Schroeder, G. M. *J. Am. Chem. Soc.* **2004,** *126,* 4480–4481. doi:10.1021/ja0497025
45. Trost, B. M.; Pissot-Soldermann, C.; Chen, I. *Chem. – Eur. J.* **2005,** *11,* 951–959. doi:10.1002/chem.200400558
46. Taber, D. F.; Tian, W. *J. Org. Chem.* **2008,** *73,* 7560–7564. doi:10.1021/jo8010683
47. Mukherjee, H.; McDougal, N. T.; Virgil, S. C.; Stoltz, B. M. *Org. Lett.* **2011,** *13,* 825–827. doi:10.1021/ol102669z
48. Jiang, B.; Li, M.-m.; Xing, P.; Huang, Z.-g. *Org. Lett.* **2013,** *15,* 871–873. doi:10.1021/ol400030a
49. Lin, H.; Xiao, L.-J.; Zhou, M.-J.; Yu, H.-M.; Xie, J.-H.; Zhou, Q.-L. *Org. Lett.* **2016,** *18,* 1434–1437. doi:10.1021/acs.orglett.6b00369
50. Kuwata, K.; Fujita, R.; Hanaya, K.; Higashibayashi, S.; Sugai, T. *Tetrahedron* **2018,** *74,* 740–745. doi:10.1016/j.tet.2017.12.054
51. Cao, B.-C.; Wu, G.-J.; Yu, F.; He, Y.-P.; Han, F.-S. *Org. Lett.* **2018,** *20,* 3687–3690. doi:10.1021/acs.orglett.8b01490
52. Cheng, H.-H.; Cheng, Y.-B.; Hwang, T.-L.; Kuo, Y.-H.; Chen, C.-H.; Shen, Y.-C. *J. Nat. Prod.* **2015,** *78,* 1823–1828. doi:10.1021/acs.jnatprod.5b00012
53. Vyhivskyi, O.; Baudoin, O. *J. Am. Chem. Soc.* **2024,** *146,* 11486–11492. doi:10.1021/jacs.4c02224
54. Kreutziger, J.; Jäger, A.; Metz, P. *ARKIVOC* **2023,** No. v, 43–53. doi:10.24820/ark.5550190.p011.915
55. Rim, C.; Son, D. Y. *ARKIVOC* **2006,** No. ix, 265–291. doi:10.3998/ark.5550190.0007.909
56. Zhang, J.; Liu, Z.-W.; Ao, Y.-L.; Hu, L.-J.; Wei, C.-J.; Zhang, Q.-H.; Yuan, M.-F.; Wang, Y.; Zhang, Q.-W.; Ye, W.-C.; Zhang, X.-Q. *J. Org. Chem.* **2019,** *84,* 14892–14897. doi:10.1021/acs.joc.9b01835
57. Ma, H.; Xie, X.; Jing, P.; Zhang, W.; She, X. *Org. Biomol. Chem.* **2015,** *13,* 5255–5259. doi:10.1039/c5ob00228a
58. Hicks, E. F.; Inoue, K.; Stoltz, B. M. *J. Am. Chem. Soc.* **2024,** *146,* 4340–4345. doi:10.1021/jacs.3c13590
59. Kim, S.; Lee, P. H. *Tetrahedron Lett.* **1988,** *29,* 5413–5416. doi:10.1016/s0040-4039(00)82882-8
60. Fujii, A.; Hashiguchi, S.; Uematsu, N.; Ikariya, T.; Noyori, R. *J. Am. Chem. Soc.* **1996,** *118,* 2521–2522. doi:10.1021/ja954126l
61. Monnereau, L.; Cartigny, D.; Scalone, M.; Ayad, T.; Ratovelomanana-Vidal, V. *Chem. – Eur. J.* **2015,** *21,* 11799–11806. doi:10.1002/chem.201501884
62. Dunn, T. B.; Ellis, J. M.; Kofink, C. C.; Manning, J. R.; Overman, L. E. *Org. Lett.* **2009,** *11,* 5658–5661. doi:10.1021/ol902373m
63. He, J.-B.; Luo, J.; Zhang, L.; Yan, Y.-M.; Cheng, Y.-X. *Org. Lett.* **2013,** *15,* 3602–3605. doi:10.1021/ol4014415
64. He, J.-B.; Lu, Q.; Cheng, Y.-X. *Helv. Chim. Acta* **2015,** *98,* 1004–1008. doi:10.1002/hlca.201400390
65. Qin, X.-L.; Wu, G.-J.; Han, F.-S. *Org. Lett.* **2021,** *23,* 8570–8574. doi:10.1021/acs.orglett.1c03293
66. Qin, X.-L.; Wu, G.-J.; Han, F.-S. *J. Org. Chem.* **2022,** *87,* 3223–3233. doi:10.1021/acs.joc.1c02928
67. Qin, X.-L.; Li, A.; Han, F.-S. *J. Am. Chem. Soc.* **2021,** *143,* 2994–3002. doi:10.1021/jacs.1c00277
68. Roncal, T.; Cordobés, S.; Ugalde, U.; He, Y.; Sterner, O. *Tetrahedron Lett.* **2002,** *43,* 6799–6802. doi:10.1016/s0040-4039(02)01493-4
69. Hou, S.-H.; Tu, Y.-Q.; Wang, S.-H.; Xi, C.-C.; Zhang, F.-M.; Wang, S.-H.; Li, Y.-T.; Liu, L. *Angew. Chem., Int. Ed.* **2016,** *55,* 4456–4460. doi:10.1002/anie.201600529
70. Hu, P.; Chi, H. M.; DeBacker, K. C.; Gong, X.; Keim, J. H.; Hsu, I. T.; Snyder, S. A. *Nature* **2019,** *569,* 703–707. doi:10.1038/s41586-019-1179-2
71. Xu, B.; Xun, W.; Su, S.; Zhai, H. *Angew. Chem., Int. Ed.* **2020,** *59,* 16475–16479. doi:10.1002/anie.202007247
72. Kim, J.; Lee, S.; Han, S.; Lee, H.-Y. *Chem* **2023,** *9,* 1270–1280. doi:10.1016/j.chempr.2023.01.018
73. Kim, M. J.; Lee, S.; Kang, T.; Baik, M.-H.; Lee, H.-Y. *Eur. J. Org. Chem.* **2020,** 609–617. doi:10.1002/ejoc.201901700
74. Hossain, M. L.; Ye, F.; Zhang, Y.; Wang, J. *J. Org. Chem.* **2013,** *78,* 1236–1241. doi:10.1021/jo3024686
75. Torneiro, M.; Fall, Y.; Castedo, L.; Mouriño, A. *Tetrahedron Lett.* **1992,** *33,* 105–108. doi:10.1016/s0040-4039(00)77685-4
76. Yu, J.-Q.; Corey, E. J. *J. Am. Chem. Soc.* **2003,** *125,* 3232–3233. doi:10.1021/ja0340735
77. Tiefenbacher, K.; Mulzer, J. *Angew. Chem., Int. Ed.* **2008,** *47,* 2548–2555. doi:10.1002/anie.200705303
78. Nicolaou, K. C.; Chen, J. S.; Edmonds, D. J.; Estrada, A. A. *Angew. Chem., Int. Ed.* **2009,** *48,* 660–719. doi:10.1002/anie.200801695
79. Palanichamy, K.; Kaliappan, K. P. *Chem. – Asian J.* **2010,** *5,* 668–703. doi:10.1002/asia.200900423
80. Saleem, M.; Hussain, H.; Ahmed, I.; van Ree, T.; Krohn, K. *Nat. Prod. Rep.* **2011,** *28,* 1534–1579. doi:10.1039/c1np00010a
81. Tian, K.; Deng, Y.; Li, Y.; Duan, Y.; Huang, Y. *Chin. J. Org. Chem.* **2018,** *38,* 2348–2362. doi:10.6023/cjoc201805062
82. Gao, Z.-X.; Wang, H.; Su, A.-H.; Li, Q.-Y.; Liang, Z.; Zhang, Y.-Q.; Liu, X.-Y.; Zhu, M.-Z.; Zhang, H.-X.; Hou, Y.-T.; Li, X.; Sun, L.-R.; Li, J.; Xu, Z.-J.; Lou, H.-X. *J. Am. Chem. Soc.* **2024,** *146,* 18967–18978. doi:10.1021/jacs.4c02256
83. Yoshimitsu, T.; Nojima, S.; Hashimoto, M.; Tanaka, T. *Org. Lett.* **2011,** *13,* 3698–3701. doi:10.1021/ol2013439
84. Hirose, Y.; Hasegawa, S.; Ozaki, N.; Iitaka, Y. *Tetrahedron Lett.* **1983,** *24,* 1535–1538. doi:10.1016/s0040-4039(00)81702-5
85. Fukushima, J.-i.; Yatagai, M.; Ohira, T. *J. Wood Sci.* **2002,** *48,* 326–330. doi:10.1007/bf00831355
86. Zhang, Y.-H.; Deng, L.-H.; Tan, D.-X.; Han, F.-S. *Angew. Chem., Int. Ed.* **2025,** *64,* e202423944. doi:10.1002/anie.202423944
87. Xu, P.; Huang, Z. *Nat. Chem.* **2021,** *13,* 634–642. doi:10.1038/s41557-021-00715-0
88. Zheng, Y.; Zhang, S.; Low, K.-H.; Zi, W.; Huang, Z. *J. Am. Chem. Soc.* **2022,** *144,* 1951–1961. doi:10.1021/jacs.1c12404
89. Xu, P.; Liu, S.; Huang, Z. *J. Am. Chem. Soc.* **2022,** *144,* 6918–6927. doi:10.1021/jacs.2c01380

BEILSTEIN JOURNAL OF ORGANIC CHEMISTRY

Electrochemical cyclization of alkynes to construct five-membered nitrogen-heterocyclic rings

Lifen Peng[1], Ting Wang[1], Zhiwen Yuan[1], Bin Li[2], Zilong Tang[1], Xirong Liu[*3,4], Hui Li[4], Guofang Jiang[4], Chunling Zeng[*3,4], Henry N. C. Wong[*2] and Xiao-Shui Peng[*2]

Review

Open Access

Address:
[1]Key Laboratory of Theoretical Organic Chemistry and Functional Molecule of Ministry of Education, School of Chemistry and Chemical Engineering, Hunan University of Science and Technology, Xiangtan, Hunan 411201, P. R. China, [2]School of Science and Engineering, Shenzhen Key Laboratory of Innovative Drug Synthesis, The Chinese University of Hong Kong, Shenzhen, Shenzhen 518172, P. R. China, [3]Hunan Norchem Pharmaceutical Company, Ltd., Changsha 410000, P. R. China and [4]College of Chemistry and Chemical Engineering, Hunan University, Changsha 410082, P. R. China

Email:
Xirong Liu[*] - liuxirong@norchem-pharma.com;
Chunling Zeng[*] - zengchunling@norchem-pharma.com;
Henry N. C. Wong[*] - hncwong@cuhk.edu.hk;
Xiao-Shui Peng[*] - xspeng@cuhk.edu.cn

* Corresponding author

Keywords:
alkyne; catalysis; cyclization; electrochemistry; five-membered ring

Beilstein J. Org. Chem. **2025,** *21,* 2173–2201.
https://doi.org/10.3762/bjoc.21.166

Received: 24 July 2025
Accepted: 01 October 2025
Published: 16 October 2025

This article is part of the thematic issue "Concept-driven strategies in target-oriented synthesis".

Guest Editor: C. Li

Abstract

Organic five-membered rings have shown significant applications in the fields of organic synthesis, natural products, organic materials and pharmaceuticals for their unique characteristics. Electrochemical construction of five-membered rings from alkynes attracted increasing attention due to the notable advantages of electrochemical transformations and facile access of alkynes. Indole skeletons were constructed successfully through electrochemical intramolecular coupling of ethynyl-involved ureas, annulation of *o*-arylalkynylanilines, cyclization of 2-ethynylanilines, selenocyclization of diselenides with 2-ethynylanilines as well as C–H indolization of 2-alkynylanilines with 3-functionalized indoles. Isoindolones were synthesized successfully by electrochemical annulation of benzamides with terminal alkynes, 5-*exo*-*dig* aza-cyclization of 2-alkynylbenzamides as well as reductive cascade annulation of *o*-alkynylbenzamides. Pyrroles and imidazoles were formed efficiently via electrochemical annulation of alkynes with enamides and tandem Michael addition/azidation/cyclization of alkynes, amines and azides, respectively. Imidazopyridines could be obtained by electrochemical [3 + 2] cyclization of heteroarylamines. The electrochemical oxidative [3 + 2] cycloaddition of secondary propargyl alcohols was a simple and efficient access towards 1,2,3-triazoles. In this review, electrochemical cyclizations of alkynes to construct five-membered rings are highlighted. Firstly, the property and application of five-membered rings are simply introduced. After presenting the usefulness of alkynes and the general progress of electrochemical transformations, electrochemical cyclization reactions of alkynes towards five-membered rings are classified and presented in detail. Based on different types of five-

membered rings, electrochemical construction of indoles, isoindolinones, indolizines, oxazoles, imidazoles, pyrroles, imidazoles and 1,2,3-triazoles are summarized and the possible reaction mechanisms are disclosed if available.

Introduction

Organic five-membered rings, an essential class of organic compounds, not only are frequently used as important starting materials, intermediates or ligands in organic synthesis [1-14] but also are critical moieties in natural products [15-18], organic materials [19] and pharmaceuticals [20-24] due to their unique chemical, electrical, optical, pharmacological and biological properties. Gracilioether F and cryptotrione have fused and spiro five-membered rings, respectively [25,26]. Strepsesquitriol bearing bridged five-membered rings was firstly synthesized by Li in 2024 [27]. The green fluorescent protein (GFP) core chromophore (*o*-LHBDI) displayed a potential application in organic light emitting diodes [28]. Formyl oxazolidine (V12) was a potential candidate to protect maize from herbicide harm [29]. Thiadiazole-linked thioacetamide (S5) exhibited exceptional inhibitory activity against *Synechocystis* sp. PCC6803 and Cy-FBP/SBPase [30]. Pyrrolidine compound MSC2530818 could be potentially used as an inhibitor of cyclin dependent kinase (CDK8) [31]. Sulfonamide-*N*-benzoxaborole analog GSK8175 is an inhibitor against hepatitis C virus (HCV) [20] (Figure 1).

The construction of five-membered rings obtained growing attention [32-38], and alkynes [39-55] have been extensively applied as facilely available starting materials to build five-membered rings for their hybrid structures with appropriate reactivities [56-59]. For example, cyclizations of silyloxyenyne [60], anionic cyclization of enediyne [61], [3 + 2] reductive cycloadditions of enal-alkyne [62], [2 + 2 + 1] cycloaddition of acetylenes [63] and cyclization of 1,6-enyne [64] were efficient approaches towards five-membered rings. Since Faraday synthesized hydrocarbons by employing electric current to an acetate solution [65], the use of electricity to promote a reaction grew up gradually [56-74]. In the past decades, the electrochemical organic reactions [75-88] which utilized an external applied voltage to accelerate transformations far from thermodynamic equilibria have emerged abundantly with the consideration of green chemistry [89-92]. Redox-active organic compounds, transition metal coordinating compounds and even an electrode surface were commonly employed as catalysts in the electrochemical transformations [93,94]. Electrochemical transformations used renewable and clean electricity as a source of electrons and electron holes to generate radical species, showing several superiorities such as safety, economy, high selectivity, scalability, mild reaction conditions, powerful efficiency, environment-friendly and sustainability [95-100]. Numerous electrochemical constructions of cyclic compounds from alkynes have been developed. For examples, 2-aryl-3-sulfonyl-functionalized quinoline was formed by an electrochemical annulation of benzoxazinanone and *p*-arylsulfonyl hydrazide [101]. The electro-oxidative annulation of alkyne and benzamide afforded chiral pyridine-*N*-oxide [102], isoquinoline was synthesized successfully via electrochemical annulation of alkyne and benzamide [103] or imidate [104], electrochemical annulation of alkyne and acrylamide afforded α-pyrone and α-pyridone [105], sultam-fused pyridinone [106] as well as cyclicphosphinic amide [107] were produced by electrochemical cyclization of alkyne. Especially, the electrochemical organic transformation of alkyne was widely applied to build five-membered rings. For example, benzimidazole-fused isoindole was generated by electrochemical

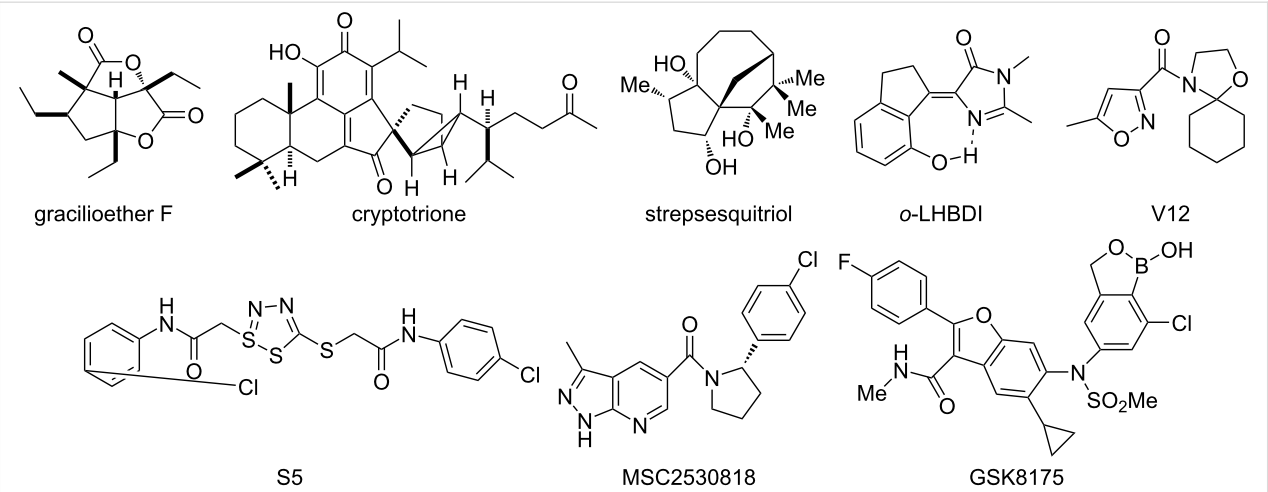

Figure 1: Natural products and functional molecules possessing five-membered rings.

[4 + 1] annulation of alkynoate with arylbenzimidazole [108], and the electrochemical *ortho*-annulation of 2-alkynylbenzenesulfonamide gave the corresponding five-membered heterocycle [106].

In recent years, a few reviews about the electrochemical cyclization of alkynes and electrochemical synthesis of cyclic compounds have emerged. The electrochemical functionalization of alkynes was highlighted by Ahmed in 2019 [109], Zhang described radical annulation of 1,*n*-enynes under photo/electrochemical reaction conditions in 2023 [110], the electrochemical formation of heterocycles was summarized by Sindhu in 2022 [98] and sustainable syntheses of heterocycles from alkyne annulations through C–H activations were reported by Ackermann in 2024 [111]. Although few examples about the electrochemical formation of five-membered rings from alkynes were included in the above reviews [106,111], a systemic review on electrochemical construction of five-membered rings from alkynes was in high need due to the importance of five-membered rings and the advantages of electrochemical transformations. In this review, we summarize the advance on electrochemical construction of five-membered rings from alkynes systematically. According to different types of five-membered rings, the electrochemical construction of five-membered rings from alkynes are mainly classified into the following categories: (a) construction of indoles, (b) construction of isoindolinones and indolizines, (c) construction of oxazoles and imidazoles, (d) construction of pyrroles, imidazoles and 1,2,3-triazoles. Literature on the electrochemical formation of five-membered rings from alkynes in this review was collected up to June 2025. We apologize to the authors if their contributions were not involved here due to the limitations of the search tools and profiles applied.

Review

Construction of indoles

Indoles, exhibiting interesting photoelectric properties and biological activities, were widely applied in organic synthesis, pharmacology and organic materials science [112-136]. Recently, Shi has disclosed the synthesis or transformation of indoles and developed indole-derived platform molecules [137-161]. Besides, electrochemical cyclization of alkynes is also an important access towards indoles. In 2016, Xu reported the electrochemical intramolecular coupling of urea derivatives to form substituted indoles (Scheme 1) [162]. Using [Cp_2Fe] (5 mol %) as the redox catalyst, the intramolecular coupling of ureas **1** proceeded smoothly in an undivided cell (reticulated vitreous carbon (RVC) anode, Pt cathode, 5 mA), forming the desired indoles **2** in high yields. The reaction showed good compatibility with various functional groups like phenyl, furyl, alkenyl and alkyl at the acetylene moieties, producing **2a**–**d** in 66%–87% yields. Boc-amino ester (**2e**), dipeptide (**2f**), apivalate ester (**2g**) and ethinyl estradiol (**2h**) skeletons were also tolerated well. According to the previous works [163] and the experimental results, the authors proposed a plausible mechanism. Firstly, the anodic oxidation of [Cp_2Fe] generated [$Cp_2Fe]^+$ along with cathodic reduction of MeOH to H_2 and MeO^- acting as a base. Deprotonation of **1a** using MeO^- produced the anion **A**, which underwent single-electron transfer (SET) with [$Cp_2Fe]^+$ to give the nitrogen-centered radical **B** with regeneration of [Cp_2Fe] [164-172]. Then, the 6-*exo-dig* cyclization of **B** obtained the vinyl radical **C** [173] that proceeded cyclization with the aryl species to form the radical **D**. Eventually, the rearomatization of **D** by eliminating one proton along with electron afforded **2a**. This protocol, proceeding smoothly without noble-metal catalyst and oxidant, was an economic and efficient protocol compared with the previous method [174-184].

The ruthenium-accelerated electrochemical dehydrogenative annulation of alkyne with an aniline derivative was also an efficient method to build the indole frame (Scheme 2) [185]. In the presence of KPF_6 and NaOAc, subjection of alkyne **3** and aniline **4** to [$RuCl_2$(*p*-cyneme)]$_2$-catalyzed electrochemical annulation formed the titled indole **5** successfully. After studying the reaction in details, the best reaction conditions were acquired as following: a mixture of aniline **4** (0.3 mmol), alkyne **3** (0.6 mmol), [$RuCl_2$(*p*-cymene)]$_2$ (0.03 mmol), KPF_6 (0.06 mmol) and NaOAc (0.06 mmol) in H_2O/iPrOH (1:1, 6 mL), refluxing under electrolysis (RVC anode, Pt cathode, 10 mA) for 1.8–3.9 h. This reaction was compatible with anilines with either electron-donating (MeO, Me) or electron-withdrawing (F, Br, CF_3) groups on the phenyl cycle to generate the corresponding products **5b**–**f** in moderate to excellent yields. The internal alkynes incorporated with phenyl and ethyl, butyl and thienyl were applicable in this transformation, leading to the formation of **5g** and **5h** in 89% and 63% yield, respectively. Based on the results of control experiments and the previous reports [186], a plausible reaction mechanism was deduced. Firstly, treatment of [$RuCl_2$(*p*-cymene)]$_2$ with NaOAc afforded the ruthenium diacetate species **A**, which underwent complexation with **4** and reversible C–H activation to give the six-membered intermediate **C**. Substitution of the acetate ligand in **C** by **3** caused the generation of complex **D**. The six-membered ruthenacycle **E** was then obtained by migratory insertion of acetylene into the Ru–C bond. Finally, reductive elimination of **E** formed the target indole **5** and a Ru(0) species **F** that was oxidized on the RVC anode to regenerate **A**. This electrochemical formation of indole, using easily available reactants and proceeding successfully under aqueous solution with simple undivided cell, was a green and convenient route towards indole.

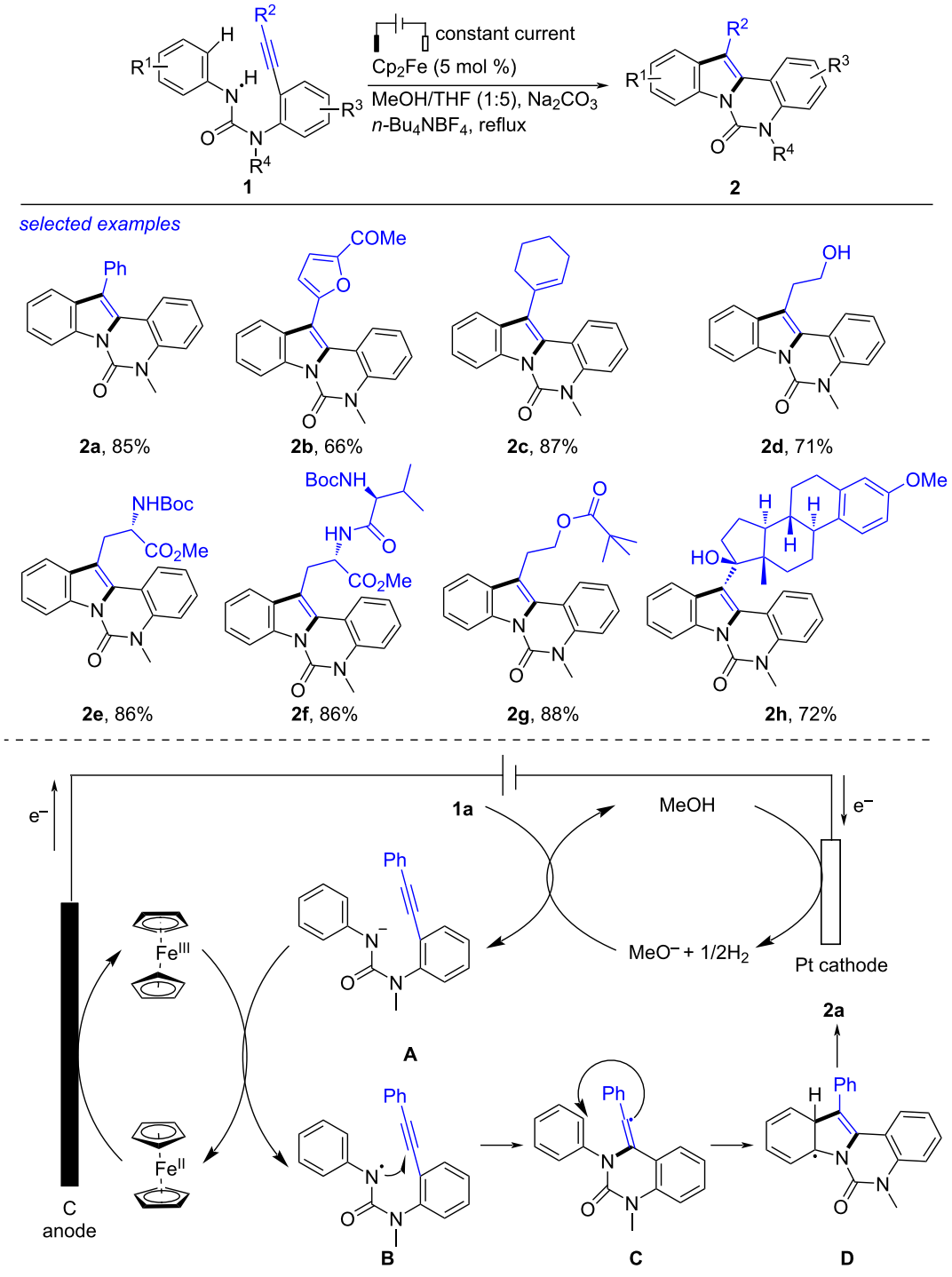

Scheme 1: Electrochemical intramolecular coupling of ureas to form indoles.

A series of skeletally diverse indoles were obtained successfully via electrochemical annulations of *o*-arylalkynylanilines (Scheme 3) [187]. In an undivided cell (Pt anode, Pt cathode, 10 mA), treatment of *o*-arylalkynylanilines **6** with ammonium halides (NH_4X, X = I, Br, Cl) gave the C3-halogenated indoles **7** in moderate to excellent yields. When KI was used instead of NH_4X, naphtho[1′,2′:4,5]furo[3,2-*b*]indoles **8** were generated in 43–72% yields. Performing the electrochemical bicyclization of **6'** with NH_4I in acetone yielded naphtho[1′,2′:5,6][1,3]oxazino[3,4-*a*]indoles **9** in moderate

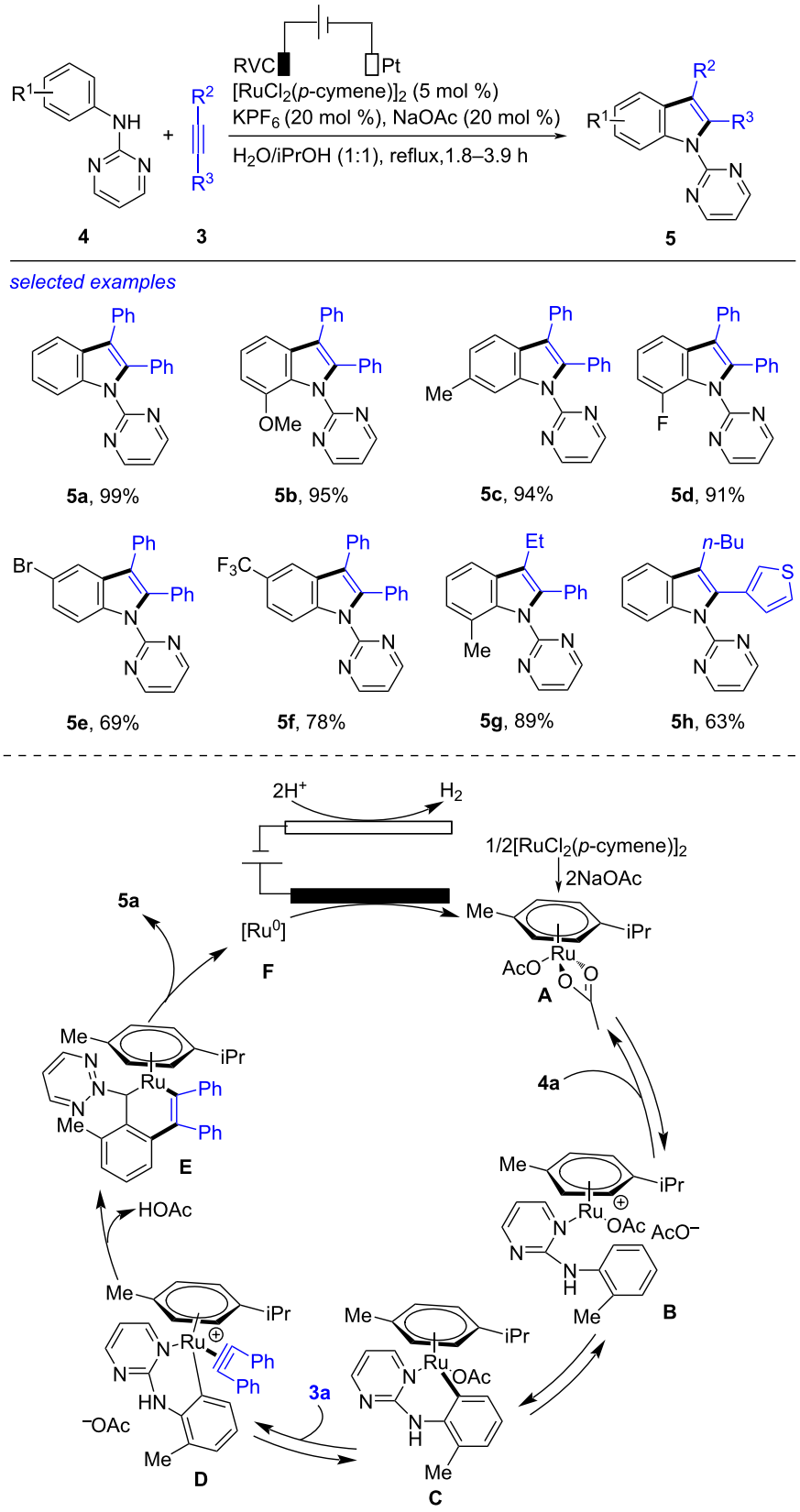

Scheme 2: Electrochemical dehydrogenative annulation of alkynes with anilines.

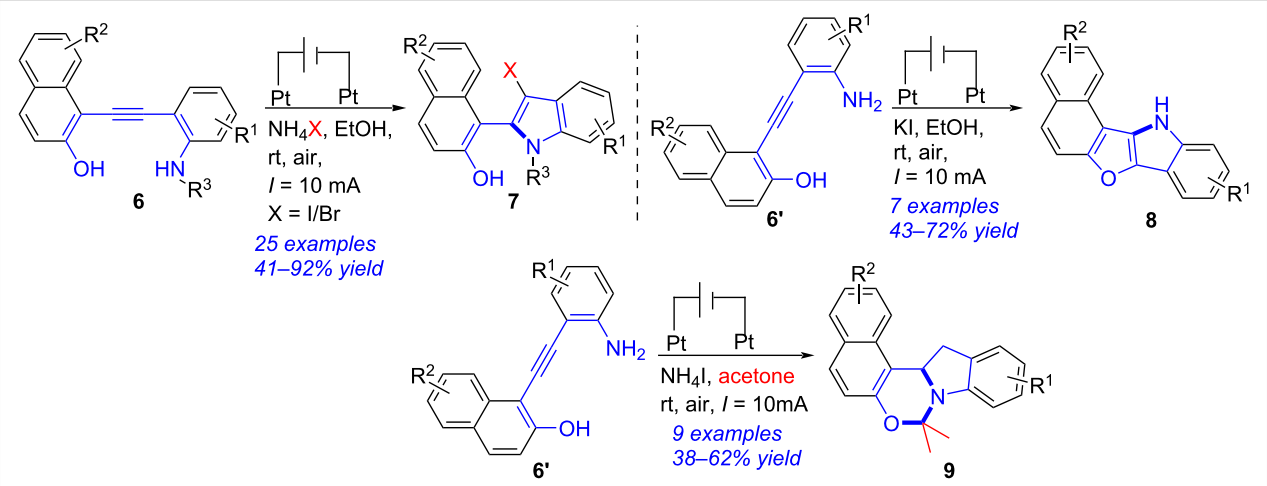

Scheme 3: Electrochemical annulations of *o*-arylalkynylanilines.

yields. It was worth mentioning that this report provided a switchable and green synthetic methodology for skeletally diverse indoles.

Divergent electrochemical cyclization of 2-ethynylanilines was developed to synthesize indoles and iodoindoles (Scheme 4) [188]. Treatment of 2-ethynylanilines **10** with KI in DMSO/H_2O in an undivided cell (Pt electrodes, 10 mA, 4.0 F/mol) afforded 3-iodoindoles **11** in satisfactory yields. When an alternative cell (Cu electrodes, 10 mA, 0.1 F/mol) was applied, the target indoles **12** were obtained in excellent yields. On the basis of control experiments and previous studies [189-200], the authors proposed a possible reaction mechanism. For the synthesis of **11a** in Pt plate electrodes, two-electron anodic oxidation of I^- formed I^+. Addition of I^+ to C≡C in **10** resulted in the production of **A**. Meanwhile, continuous reduction of H_2O at the cathode formed H_2 and HO^-. The *anti*-nucleophilic attack of the N atom in **A** and the following HO^- facilitated deprotonation and formed the corresponding 3-iodoindole **11a**. Excessive-reduction (a minor side-reaction) of **11a** took place as well in certain instances, resulting in the formation of **12a**. And for the generation of **12a** in Cu rod electrodes, the Cu anode was expected to liberate Cu^+ into the reaction mixture. The reaction of this Cu^+ with DMSO and I^- afforded $(DMSO)_nCuI$, which was coordinated with C≡C to give **B**. The intermediate **C** was obtained by cyclization of **B** and deprotonation. Further protonation of **C** afforded **12a** and regenerated $(DMSO)_nCuI$. Notably, this reaction, using KI as the only additive and performing under ambient conditions in a non-volatile aqueous solvent, was a simple, selective, efficient and sustainable electrosynthesis of indole derivatives.

3-Selenylindoles were also formed by electrochemical selenocyclization of diselenides and 2-ethynylanilines (Scheme 5) [201]. After probing the reaction systematically, the optimal conditions were afforded as following: a mixture of 2-ethynylaniline **13** (0.2 mmol), diselenide **14** (0.13 mmol), n-Bu_4NPF_6 (0.04 mmol) and MeCN (5.0 mL), under electrolysis (Pt plate electrodes, 5 mA, 1.87 F/mol) at rt for 2–4 h. 2-Ethynylanilines with either electron-withdrawing (CN, CF_3, Br, COOMe) or electron-donating (Me, OMe) groups at the phenyl cycle of aniline were tolerated well under these conditions, producing the corresponding **15b–g** in 81–98% yield. This reaction also showed high compatibility with 2-naphthyl (**15h**), 2-thiophenyl (**15i**), ferrocenyl (**15j**), cyclohexenyl (**15k**) and *tert*-butyl (**15l**) incorporated at the ethynyl moiety. According to the results of control experiments, a plausible mechanism was presented. Firstly, one-electron oxidation of **14a** occurred to give a radical cation $PhSeSePh^{\bullet+}$ at the anode. The subsequent cleavage of Se–Se bond formed a radical $PhSe^\bullet$ and a cation $PhSe^+$. Further additional oxidation of $PhSe^\bullet$ yielded another $PhSe^+$, which worked as the major reactive species and quickly added to C≡C in **13a** to form intermediate **A**. Finally, **A** proceeded an intramolecular nucleophilic attack by N and deprotonation to finish **15a**. The other possible pathway was radical route, in which $PhSe^\bullet$ dimerized to reform **14a** or added to C≡C bond in **13a** to afford **B**. The subsequent anodic oxidation of **B** gave **C**, which underwent nucleophilic cyclization/deprotonation to form the target **15a**. Meanwhile, H^+ was continually reduced at the cathode to give by-product H_2. This transformation, completing under short reaction time and conditions with a low equivalent of charges with high yields and good substrate scope, was a convenient, efficient, practical and a sustainable strategy for the preparation of 3-selenylindoles.

In 2023, Satyanarayana also described a similar electrochemical cascade approach towards 3-selenylindoles from 2-alkynylanilines (Scheme 6) [202]. When graphite was used as anode,

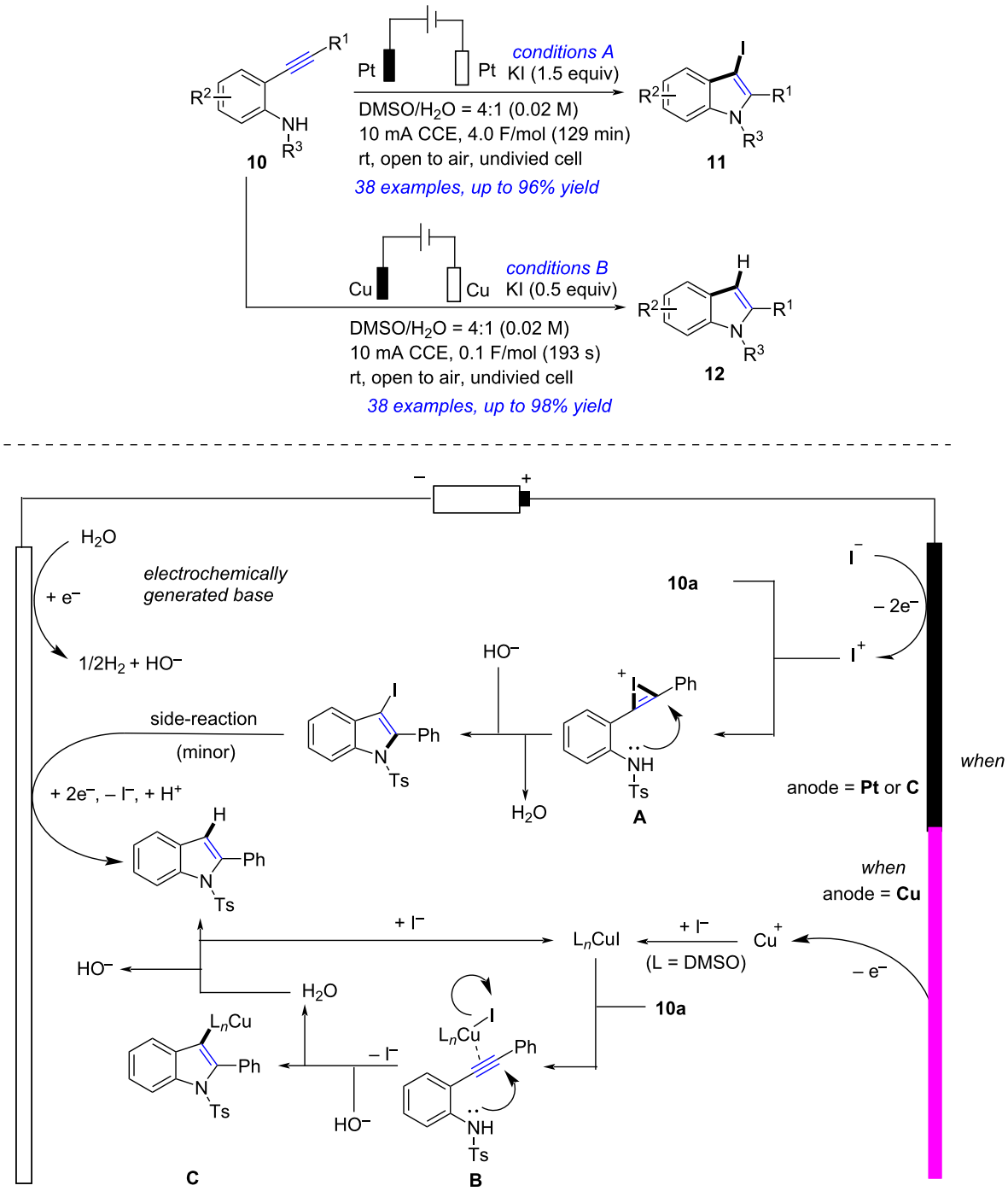

Scheme 4: Electrochemical cyclization of 2-ethynylanilines.

platinum as cathode and $LiClO_4$ as electrolyte, the electrochemical oxidative cyclization of 2-alkynylaniline **16** and diselenide **17** occurred to form desired 3-selenylindole **18** in satisfactory yields with wide substance scope. Based on control experiments and previous references [203], a possible reaction mechanism was outlined. Firstly, the anodic oxidation of **17a** formed phenylselenium cation **C** and phenylselenium radical **B** through radical cation species **A**. Simultaneously, the cathodic reduction of **17a** generated anion **D** and radical **B**. Then, addition of **B** with the alkyne portion in **16a** gave a radical intermediate **E**, which proceeded a one-electron oxidation followed by nucleophilic addition and then deprotonation to yield the desired **18a** via intermediate **G**. Another possible pathway is that phenylselenium cation **C** attacked **16a** afforded the alkenyl cation **G**,

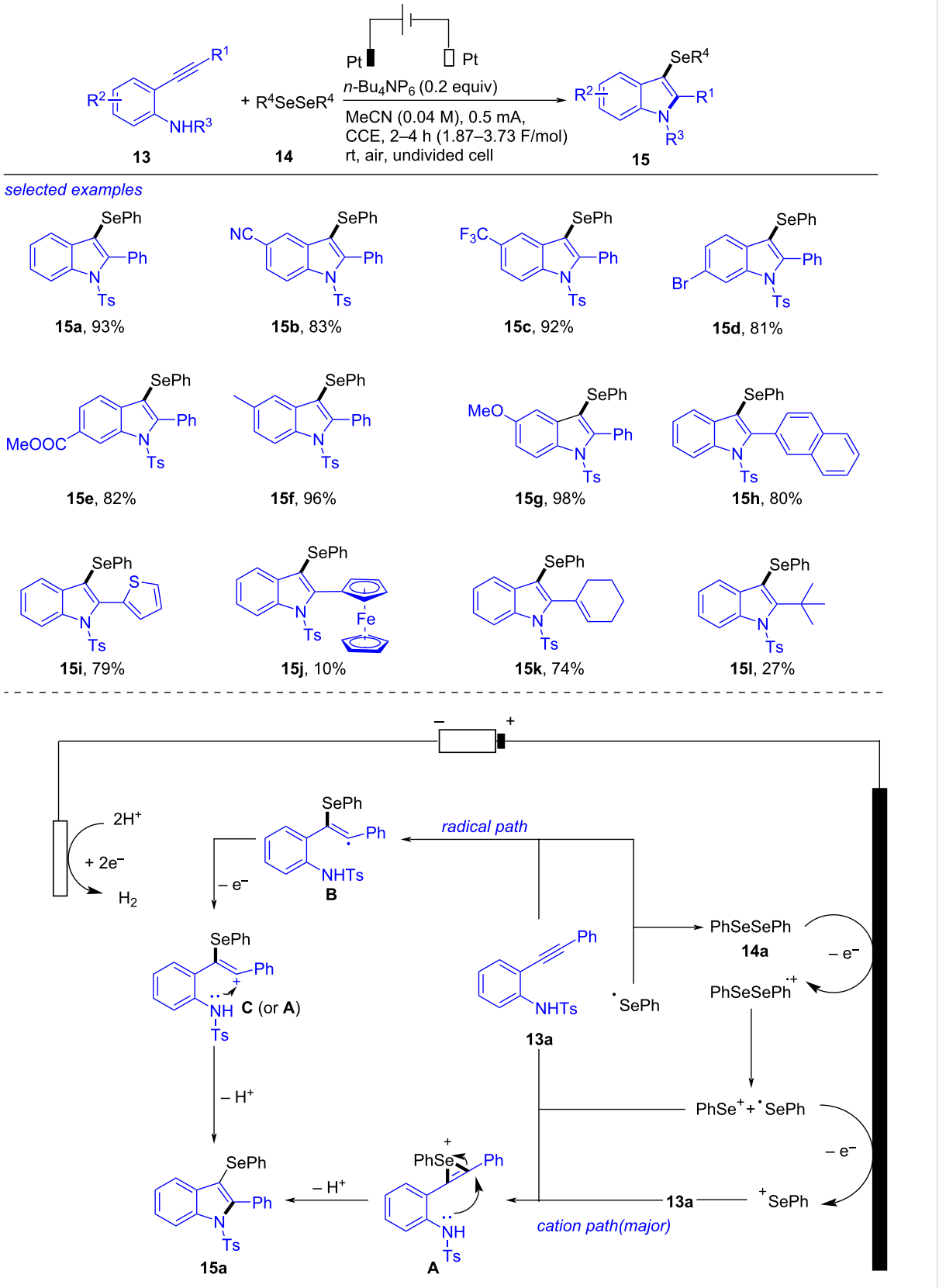

Scheme 5: Electrochemical selenocyclization of diselenides and 2-ethynylanilines.

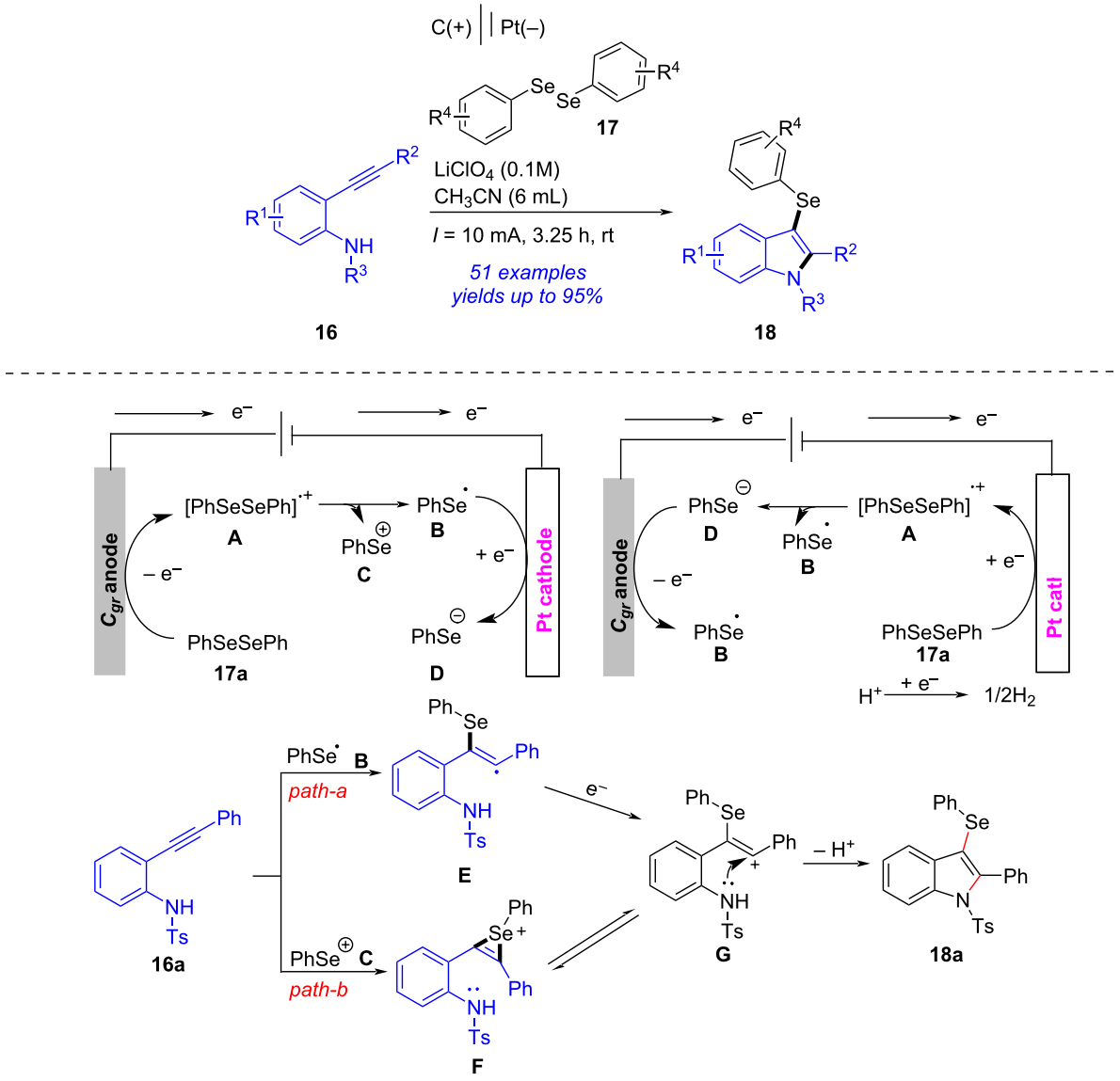

Scheme 6: Electrochemical cascade approach towards 3-selenylindoles.

which underwent cyclization and deprotonation to produce **18a**. It should be noted that this conversion proceeded under metal, oxidant, and base-free conditions.

An electrochemical enantioselective tandem C–H indolization of 2-alkynylanilines with 3-functionalized indoles towards 2,3′-biindolyl atropisomers was achieved by Zeng in 2025 (Scheme 7) [204]. After screening the reaction carefully, the optimal conditions were gained as following: a mixture 3-functionalized indole **19** (0.08 mmol), 2-alkynylaniline **20** (0.12 mmol), (*R*)-**Rh1** (5 mol %), *n*-Bu_4NOAc (0.08 mmol), 1-adamantane carboxylic acid (1-$AdCO_2H$, 0.08 mmol) and MeOH/$CHCl_3$ (1:1, 2 mL), under electrolysis (graphite felt (GF) anode and graphite (C) cathode, 2 mA, 5.6 F/mol) at rt for 6 h. The authors also proposed the reaction mechanism on basis of experimental results and previous literature [205,206]. Firstly, the ligand exchange between (*R*)-**Rh1** and *n*-Bu_4NOAc or 1-$AdCO_2H$ gave a chiral active catalyst **A**. The irreversible base-prompted C–H activation of **A** with **19a** yielded a five-membered rhodacycle **B**, which underwent alkyne coordination followed by nucleophilic cyclization with **20a** to give the biindolyl–Rh species **D**. The reductive elimination of **D** produced the bisindole-ligated CpxRhI intermediate **E**, which performed anodic oxidation to finish **21a** and regenerate **A**. Notably, this protocol was an efficient and sustainable approach to synthesize 2,3′-biindolyl atropisomers and could be potentially applied in manufacture of functional materials, bioactive molecules and chiral ligands.

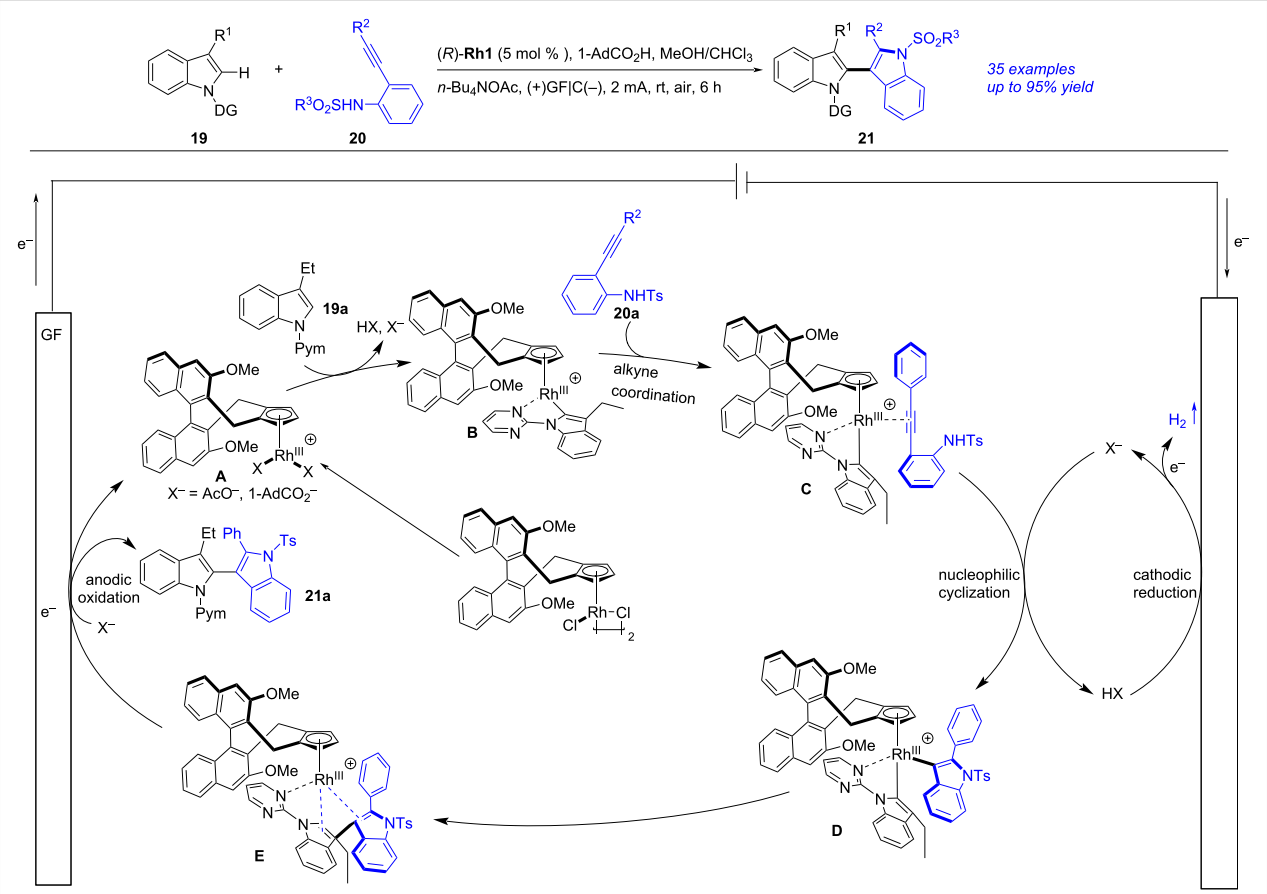

Scheme 7: Electrochemical C–H indolization.

Construction of isoindolinones and indolizines

An electrochemical and copper-catalyzed annulation of benzamides and terminal alkynes was established for the synthesis of isoindolones by Ackermann in 2019 (Scheme 8) [207]. After screening the reaction carefully, the optimum conditions were presented as following: a mixture of benzamide **22** (0.25 mmol), alkyne **23** (0.50 mmol), NaOPiv (0.25 mmol), $Cu(OAc)_2$-H_2O (0.0125 mmol) and *N*,*N*-dimethylacetamide (DMA, 4.0 mL), under electrolysis (RVC anode, Pt cathode, 6.0 mA) at 100 °C for 6 h. According to the experimental results, a proposed mechanism was outlined. Firstly, treatment of NaOPiv (0.25 mmol) with $Cu(OAc)_2$-H_2O formed $Cu(OPiv)_2$. Coordination of **22** with $Cu(OPiv)_2$ and the following anodic copper(II) oxidation provided copper(III) carboxylate intermediate **B**. Facile carboxylate-promoted C–H activation and ligand exchange with **23** formed the copper(III) species **D**, which underwent metalation/reductive elimination to generate intermediate **E** along with the formation of Cu(OPiv) which was transformed to $Cu(OPiv)_2$ by oxidation at the anode. Finally, the cyclization of **E** afforded target isoindolone **24**. Notably, this reaction was the first example of electrochemical copper-catalyzed oxidative cyclization of alkyne which was enabled by C–H alkynylation of electron-deficient benzamide.

In 2022, Ye presented an electrochemical synthesis of isoindolinone through 5-*exo*-*dig* aza-cyclization of 2-alkynylbenzamide (Scheme 9) [208]. By applying carbon cloth as anode, Pt as cathode and *n*-Bu_4NOAc as electrolyte, the 5-*exo*-*dig*/6-*endo*-*dig* cyclization of 2-alkynylbenzamide **25** occurred to form the corresponding isoindolinone **26** in reasonable yields. According to the experimental results and previous investigations [209-211], the proposed reaction mechanism was described. Initially, proton-coupled electron transfer took place between *n*-Bu_4NOAc and 2-(phenylethynyl)-*N*-tosylbenzamide (**25a**) to afford the amidyl radical **B**, which then proceeded intramolecular 5-*exo*-*dig* radical annulation to form the five-membered intermediate **C**. The oxidation of **C** followed by capturing an AcO^- generated the intermediate **E**, which was converted into triacetate adduct **F** through anodic oxidation and AcO^- capture. The hydrolysis of **F** then occurred to afford the final product **26a**. This protocol featured with some advantages such as without any oxidants and metal catalysts, simple operation, good yields, high selectivity and wide substrate scope.

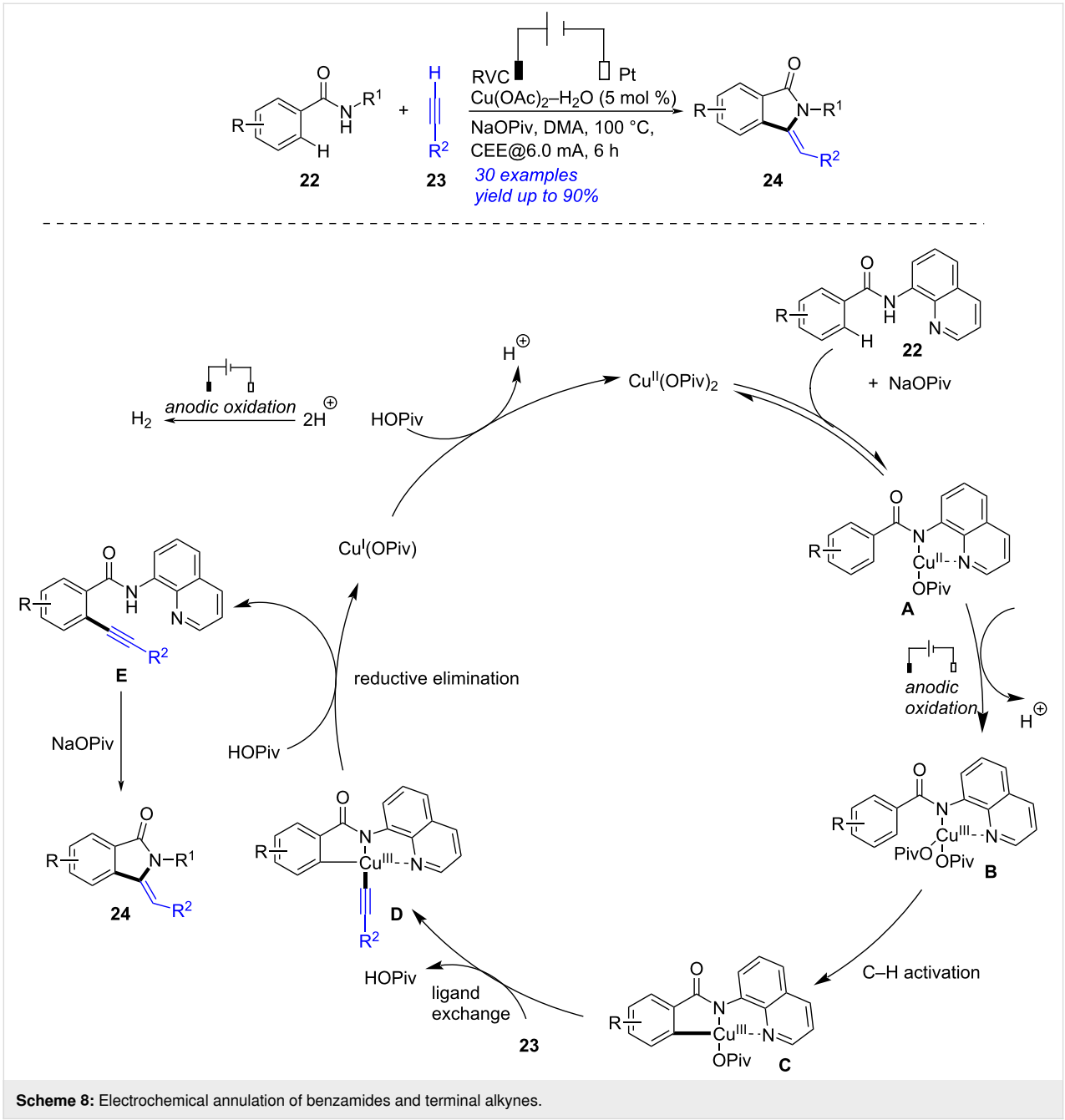

Scheme 8: Electrochemical annulation of benzamides and terminal alkynes.

Isoindolinone could be also obtained by electrochemical reductive cascade annulation of *o*-alkynylbenzamide (Scheme 10) [212]. Under 10 mA constant current with two platinum plate as electrodes and *n*-Bu_4NPF_6 as electrolyte, the reductive cascade cyclization of *o*-alkynylbenzamide **27** proceeded smoothly in the presence of *N*,*N*-diisopropylethylamine (DIPEA) to give the corresponding isoindolinone **28** in 32–90% yield. A plausible reaction mechanism was presented according to the experimental results and earlier works [213,214]. Firstly, the proton coupled electron transfer (PCET) procedure of **27** formed the amidyl radical **B**, which performed 5-*exo*-*dig* *N*-radical addition into the C≡C bond to generate the cyclic species **C**. The radical anion **D** was then obtained via single electron reduction of **C** at the cathode. The subsequent protonation of **D** gave α-aminyl radical **E** [215-217], which was converted into the anion **F** by further cathodic reduction. The subsequent protonation of **F** occurred to complete the formation of **28**. This approach, applying electrolyte as the proton sources, avoided the use of reductants and metal catalysts efficiently.

In 2022, Guo developed an electrochemical intramolecular 1,2-amino oxygenation of alkyne to access indolizine (Scheme 11)

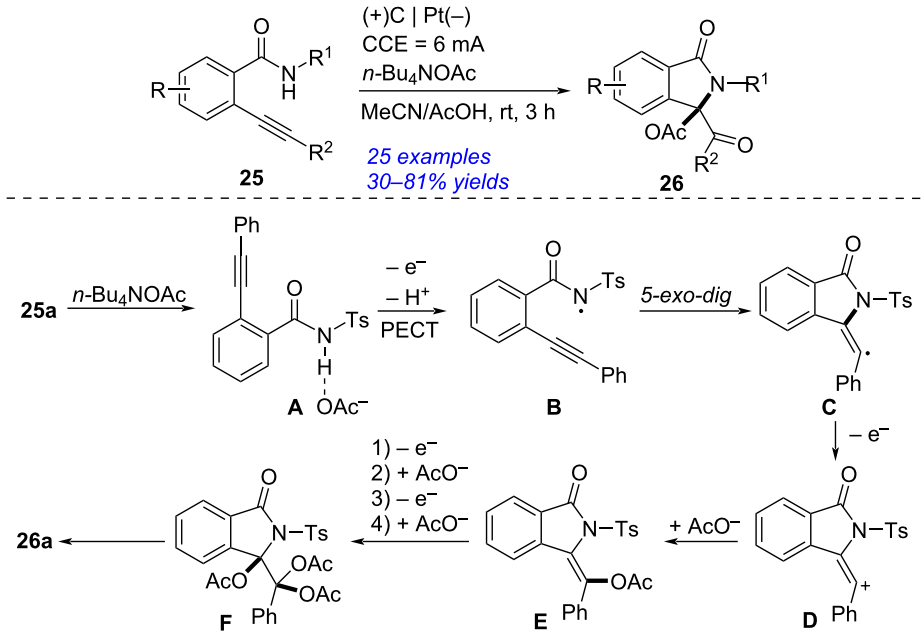

Scheme 9: Electrochemical synthesis of isoindolinone by 5-*exo-dig* aza-cyclization.

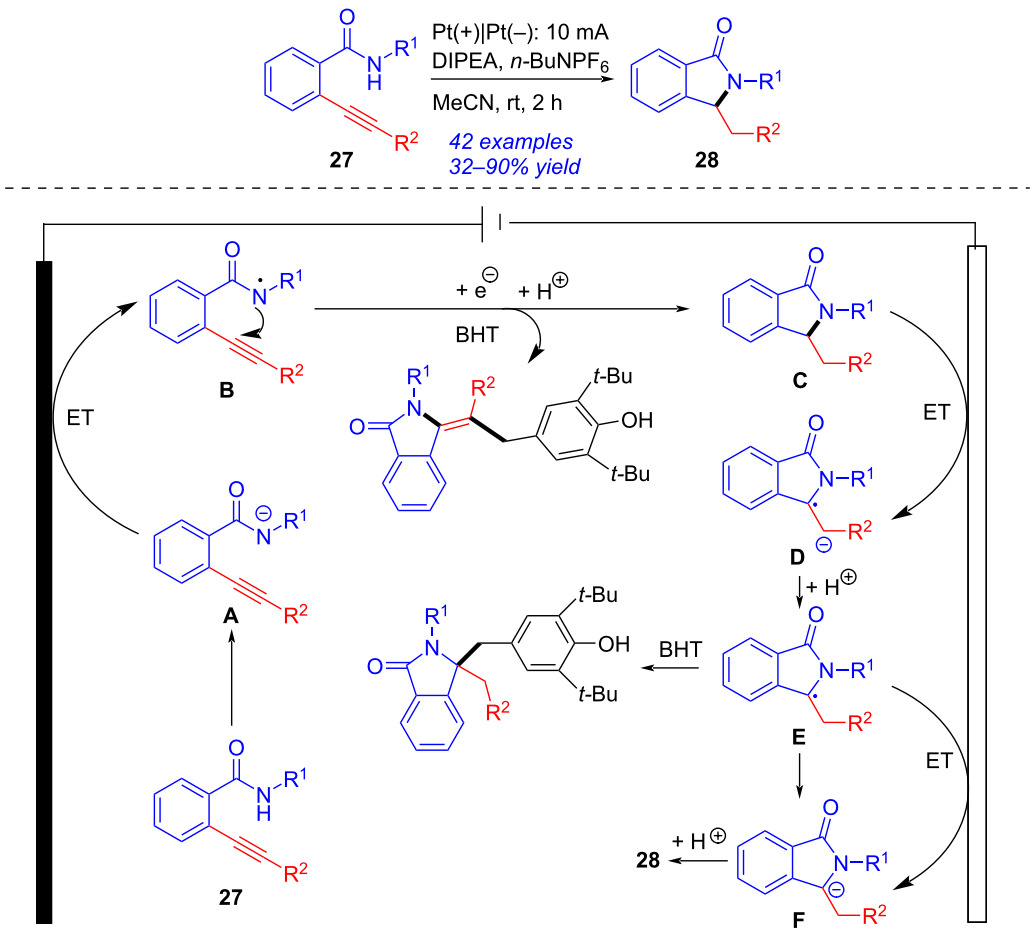

Scheme 10: Electrochemical reductive cascade annulation of *o*-alkynylbenzamide.

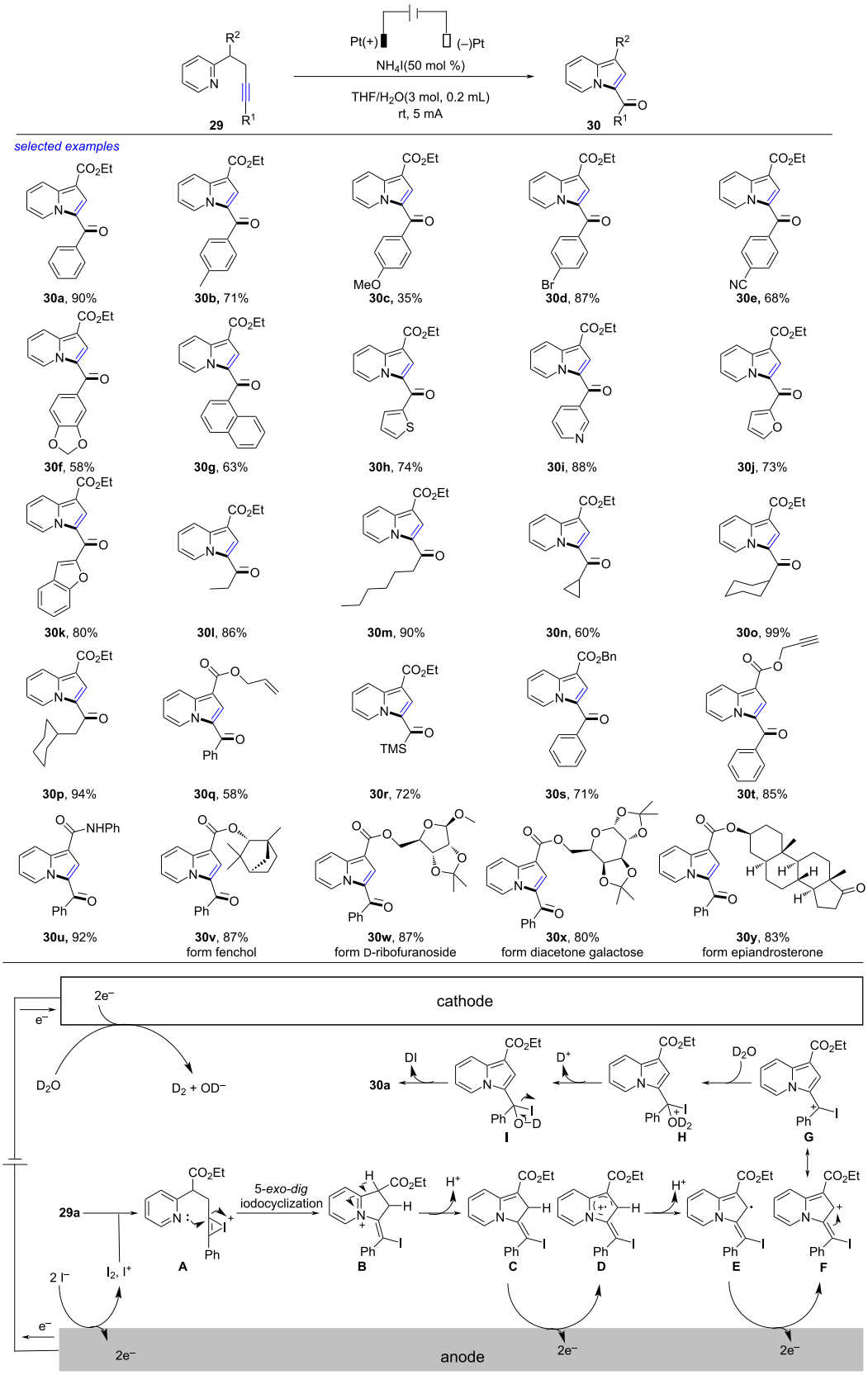

Scheme 11: Electrochemical intramolecular 1,2-amino oxygenation of alkyne.

[218]. Under electrolysis (two platinum plate as electrodes, NH_4I as electrolyte and electrocatalyst, 5 mA, 8.4 F/mol), the aminooxygenation of alkyne **29** underwent efficiently to form the desired indolizine **30** in good to excellent yield. The reaction was compatible with many groups involved at the ethyne moiety like substituted phenyl (**30b–e**), benzodioxole (**30f**), naphthyl (**30g**), thienyl (**30h**), pyridinyl (**30i**), furyl (**30j**), benzofuranyl (**30k**), alkyl (**30l**, **30m**), cycloalkyl (**30n–p**) and trimethylsilyl (**30r**). This reaction was also compatible with benzyl ester (**30s**), propynyl ester (**30t**), phenylamide (**30u**) as well as natural product-derived and pharmaceutical skeletons: fenchol (**30v**), D-ribofuranoside (**30w**), diacetone galactose (**30x**), and epiandrosterone (**30y**). Based on the experimental results, a possible reaction mechanism was disclosed. Initially, the anodic oxidation of I^- formed I^+ or I_2. Coordination of **29a** with I^- produced the iodonium species **A**, which was transformed to vinyl iodide **B** by intramolecular 5-*exo*-*dig* iodocyclization. The deprotonation/anodic oxidation of **B** gave the radical cation **D** via **C**. The second deprotonation/anodic oxidation produced **F**, which was transformed into stable cationic resonance **G** quickly. The nucleophilic attack of D_2O formed **H**, which underwent dedeuteration and elimination of DI to form **30a** with reduction of deuterated water to generate deuteroxyl ions (OD^-) and deuterium gas (D_2) at the cathode. This method, using iodide salts as electrolyte and redox mediator and proceeding in aqueous solution with pleasure yields, was a simple, convenient, powerful, environmentally benign and sustainable electrooxidative approach towards indolizine.

Construction of oxazoles and imidazoles

Without any additional oxidants and catalysts, an electrochemical multicomponent reaction of nitrile, xanthene, terminal alkyne and water to synthesize oxazole was established by Li in 2023 (Scheme 12) [219]. After examining the reaction carefully, the optimized reaction conditions were obtained as follows: a mixture of alkyne **31** (0.3 mmol), xanthene **32** (0.45 mmol), CH_3CN (5.0 mL), H_2O (0.3 mmol) and *n*-Bu_4NBF_4 (0.45 mmol), under electrolysis (Pt plate as electrodes, 5 mA) at air for 10 h. Electron-donating (Me, Et, *t*-Bu and OMe) or electron-withdrawing (Cl, Br and F) groups involved phenylacetylenes, 1-ethynylnaphthalene and 2-ethynylthiophene were tolerated well under these reaction conditions, resulting in the formation of the corresponding oxazoles (**33b–j**) in 43–80% yields. Xanthenes bearing Me, *t*-Bu, MeO, Ph, Cl, CF_3 and naphthyl groups were applicable as well, generating the desired **33k–r** in moderate yields. According to the results of control experiments and previous studies [220-231], a proposed mechanism for this reaction was depicted. Firstly, the anodic oxidation of **32a** took place to give a radical cation species **A** that proceeded deprotonation to give benzylic radical intermediate **B**. Further oxidation of **B** afforded a cationic intermediate **C**, which was converted into **D** through nucleophilic addition of **31a**. Trapping **D** by the weak nucleophile H_2O formed the by-product **34**, while trapping of **D** by CH_3CN generated species **E**, which was trapped by H_2O and formed intermediate **F**. Furthermore, oxidation of **F** at the anode produced radical cation **G** [232]. The following intramolecular cyclization/anode oxidation produced intermediate **I** that was then deprotonated to yield the target **33a**. Compared to the previous reported methods [233-254], this approach exhibited the following advantages like without metal catalysts and external oxidants, atom economy, facile access of starting materials, etc.

In 2024, Cho succeeded in the preparation of trifluoromethylated oxazoles through in-situ aminotrifluoromethylation/cyclization of alkynes (Scheme 13) [255]. Under electrolysis (graphite as electrodes, tetra-*n*-butylammonium salt ($TBAPF_6$) as electrolyte, *N*,*N*,*N*,*N*-tetramethylethylenediamine (TMEDA) as mediator, 4.28 V), the four-component reaction of alkynes **35**, $NaSO_2CF_3$, nitriles and residual water proceeded efficiently to form titled trifluoromethylated oxazoles **36** in moderate to excellent yields. A proposed mechanism was established on basis of control experiments. Firstly, the anodic oxidation of $NaSO_2CF_3$ gave a trifluoromethyl radical, which was then added to **35a**, affording alkenyl intermediate **A**. In the presence of TMEDA, oxidation of **A** yielded $\mathbf{A}^+$, which was then trapped by $MeCN/H_2O$ to form the CF_3-enamide intermediate **B**. The subsequent cyclization/oxidation of **B** offered oxazoline radical intermediate **C**, which was transformed to the target **36a** through anodic oxidation/deprotonation. This transformation, implementing under mild conditions, was an efficient and straightforward protocol towards oxazoles.

An electrochemical and selenium-catalyzed construction of 2,1-benzoxazole through cyclization of *o*-nitrophenylacetylene was achieved by Pan in 2021 (Scheme 14) [256]. After examining the reaction in details, the best conditions were disclosed as following: a mixture of *o*-nitrophenylacetylene **37** (0.3 mmol), diphenyl diselenide (0.03 mmol), Et_4NPF_6 (0.15 mmol) and CH_3CN (10 mL), under electrolysis (graphite cathode and platinum anode, 1.6 V) at rt. Based on the experimental results and the reported studies [257,258], the authors deduced a plausible reaction mechanism. Initially, the anodization of diphenyl diselenide produced phenylselenium radical **A** and selenium cation **B**, the single-electron transfer on the anode could also transformed **A** into **B**. Addition of **B** to **37a** formed the intermediate **C** that underwent intramolecular nucleophilic cyclization to give **D**. The fracture of the N–O bond in **D** yielded **E**. Elimination of selenium cation **A** from **E** and the following cyclization afforded **38a**. This transformation, combining selenium catalysis and organic electrosynthesis,

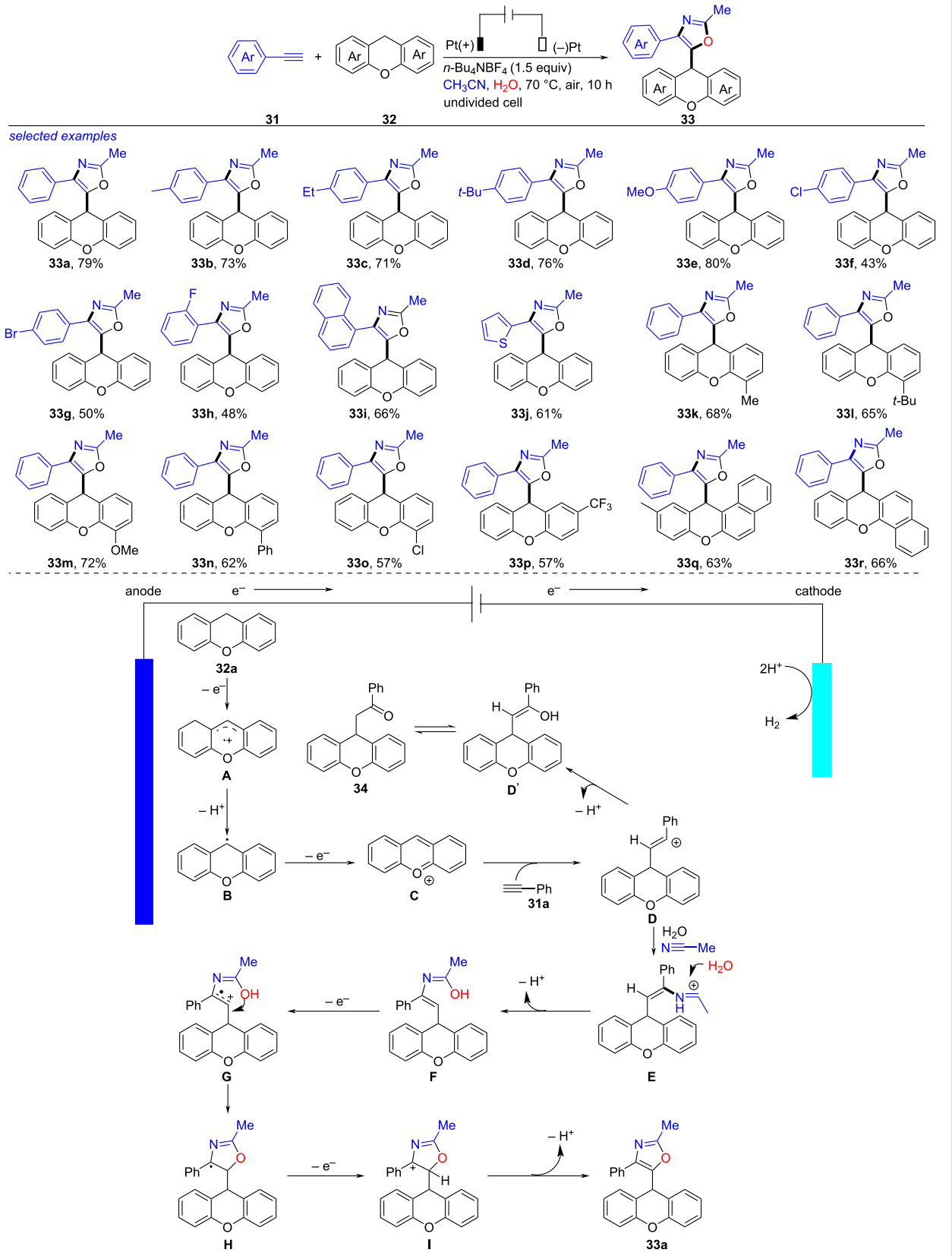

Scheme 12: Electrochemical multicomponent reaction of nitrile, (thio)xanthene, terminal alkyne and water.

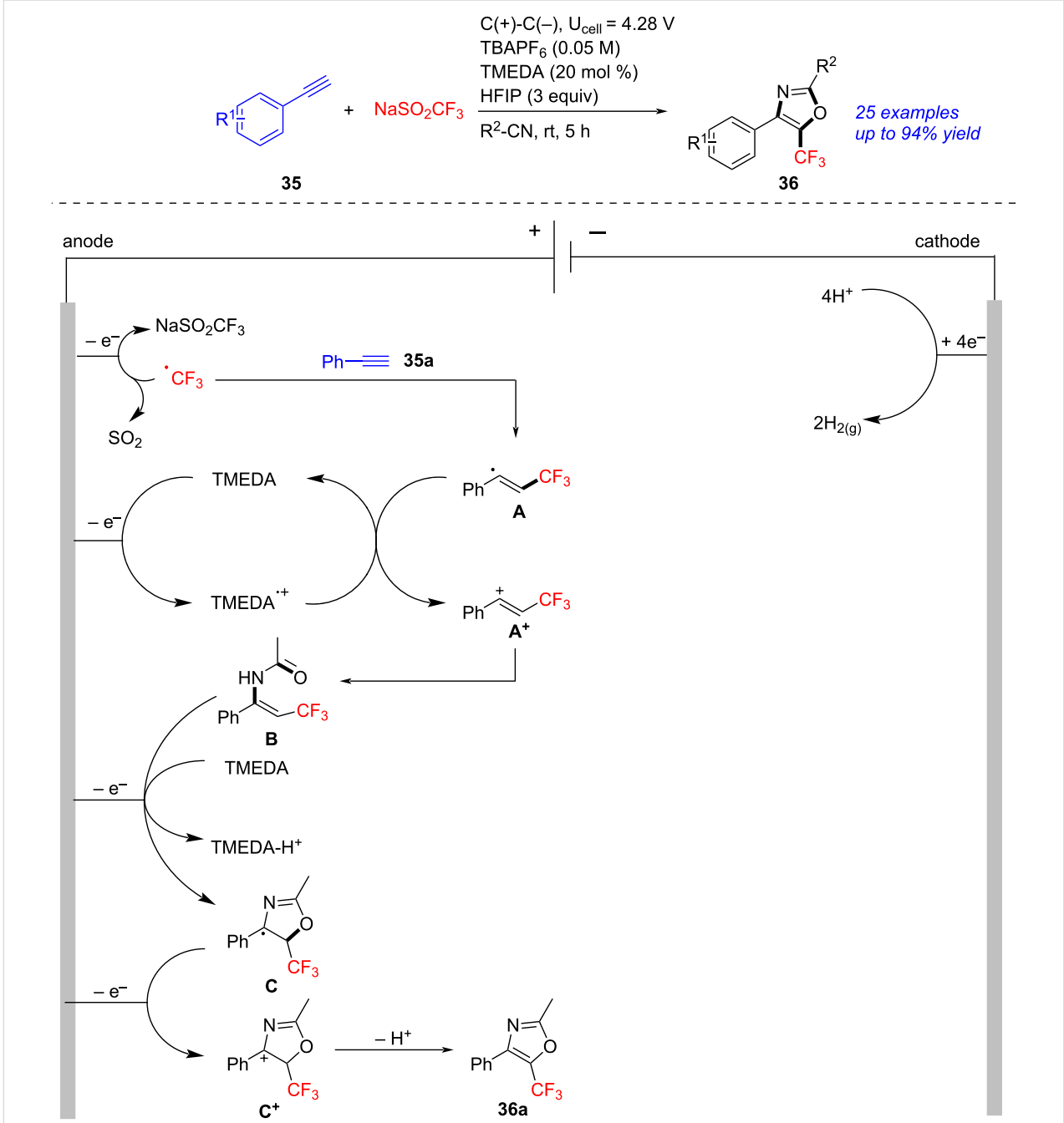

Scheme 13: Electrochemical aminotrifluoromethylation/cyclization of alkynes.

proceeded smoothly at rt without external oxidants and metal catalysts.

Construction of pyrroles, imidazoles and 1,2,3-triazoles

A series of indeno[1,2-*c*]pyrroles were synthesized successfully through electrochemical annulation of alkynyl enaminones by Zhao in 2022 (Scheme 15) [259]. After examining the reaction carefully, the best reaction conditions were obtained as following: alkynyl enaminone **39** (0.2 mmol), $LiClO_4$ (0.3 M) and NaI (0.1 M) in MeCN (6 mL) at 80 °C under electrolysis (Pt plate as electrodes, 10 mA) at rt for 20 h. Alkynyl enaminones bearing substituted phenyl, naphthyl, cyclopropyl and *n*-butyl groups at the amino moiety were tolerated well under these conditions, resulting in the formation of indeno[1,2-*c*]pyrroles **40b–g** in 63–97% yields. Alkynyl enaminones containing phenyl, trimethylsilyl and *n*-butyl groups at the ethynyl terminal were also applicable to produce the desired **40h–j** in

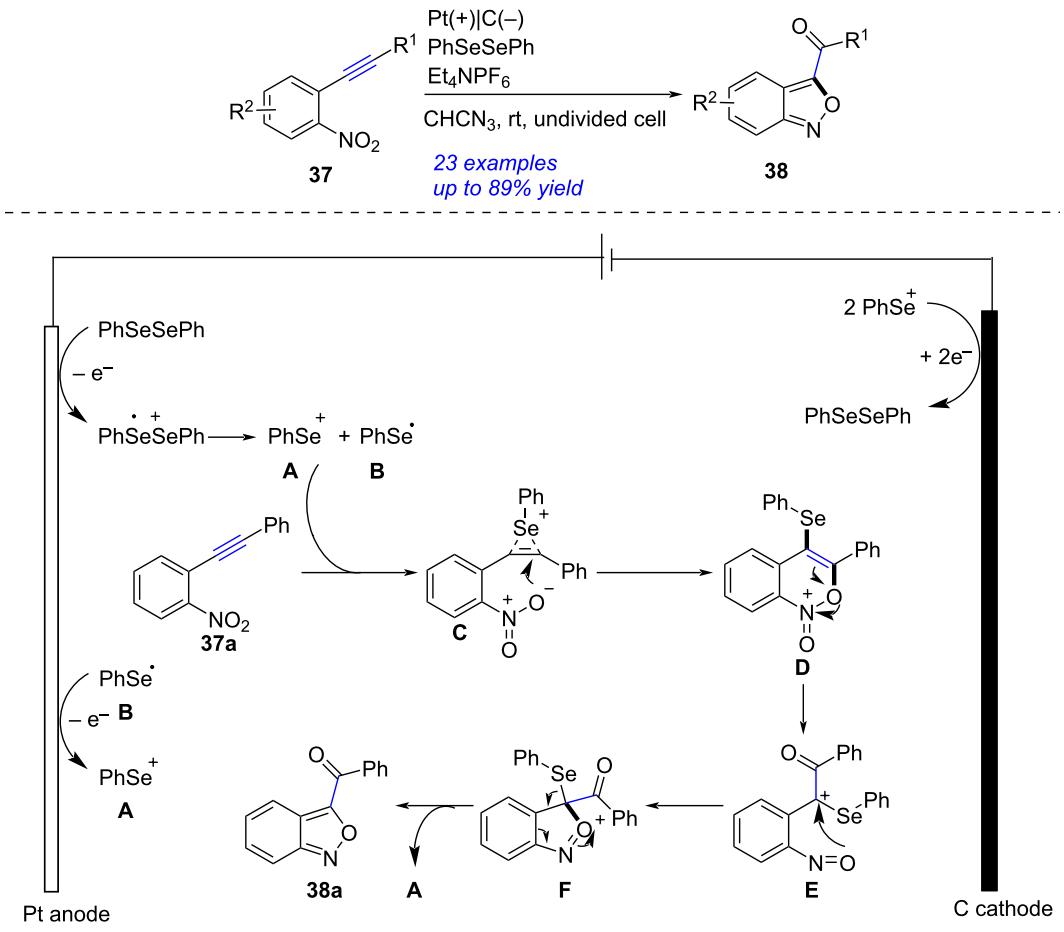

Scheme 14: Electrochemical cyclization of *o*-nitrophenylacetylene.

satisfactory yields. Based on the results of control experiments and previous works [260-265], a proposed mechanism was also presented. Initially, I^- was oxidized to $I^•$ at the anode. A vinyl radical intermediate **A** was produced through reaction of $I^•$ with **39a**. The following intramolecular cyclization formed the species **B**, which was oxidized at the anode to generate imine intermediate **C**. Simultaneously, treatment of **39a** with I^+ and the following intramolecular nucleophilic cyclization produced **C**. The elimination of a proton from **C** afforded the intermediate **D**. In the presence of 1,8-diazabicyclo[5.4.0]undec-7-ene (DBU), the intramolecular nucleophilic substitution of **D** afforded target indeno[1,2-*c*]pyrrole **40a** along with eliminating I. Notably, this oxidant-free and catalyst-free approach could be potentially applied in the pharmaceutical manufacture.

A Rh-promoted synthesis of pyrroles through annulation of alkynes and enamides was demonstrated by Ackermann in 2023 (Scheme 16) [266]. Using GF as anode, Pt as cathode, NaOAc as the electrolyte and $[Cp^*Rh(MeCN)_3](SbF_6)_2$ as the catalyst, the annulation between alkyne **41** and enamide **42** succeeded, forming the corresponding pyrrole **43** in good yield. Although this transformation employing electricity as a sustainable and green oxidant, noble metal catalyst (Rh) was required to achieve reasonable yields.

An electrochemical synthesis of imidazoles through tandem Michael addition/azidation/intramolecular cyclization of alkynes, amines and azides was realized by Chen in 2022 (Scheme 17) [267]. After investigating the reaction in details, the optimum reaction conditions were acquired as following: a mixture of alkyne **44** (0.5 mmol), amine **45** (0.5 mmol), azidotrimethylsilane ($TMSN_3$, 1.5 mmol), *n*-Bu_4NBF_4 (0.1 M), KI (1 mmol) and DMSO (5.0 mL), under electrolysis (Pt plate as electrodes, 9 mA) at rt for 9 h. The reaction was compatible with numerous amines such as substituted benzylamines **46b–d**, 1-(2-naphthyl)methanamine **46e**, 3,4-methylenedioxybenzylamine **46f**, furfurylamine **46g** and 2-thiophenemethylamine **46h**. Alkynes with ester and trifluoromethyl groups worked well under this reaction, leading to the corresponding imidazoles **46i–k** in moderate yields. With the consideration of exper-

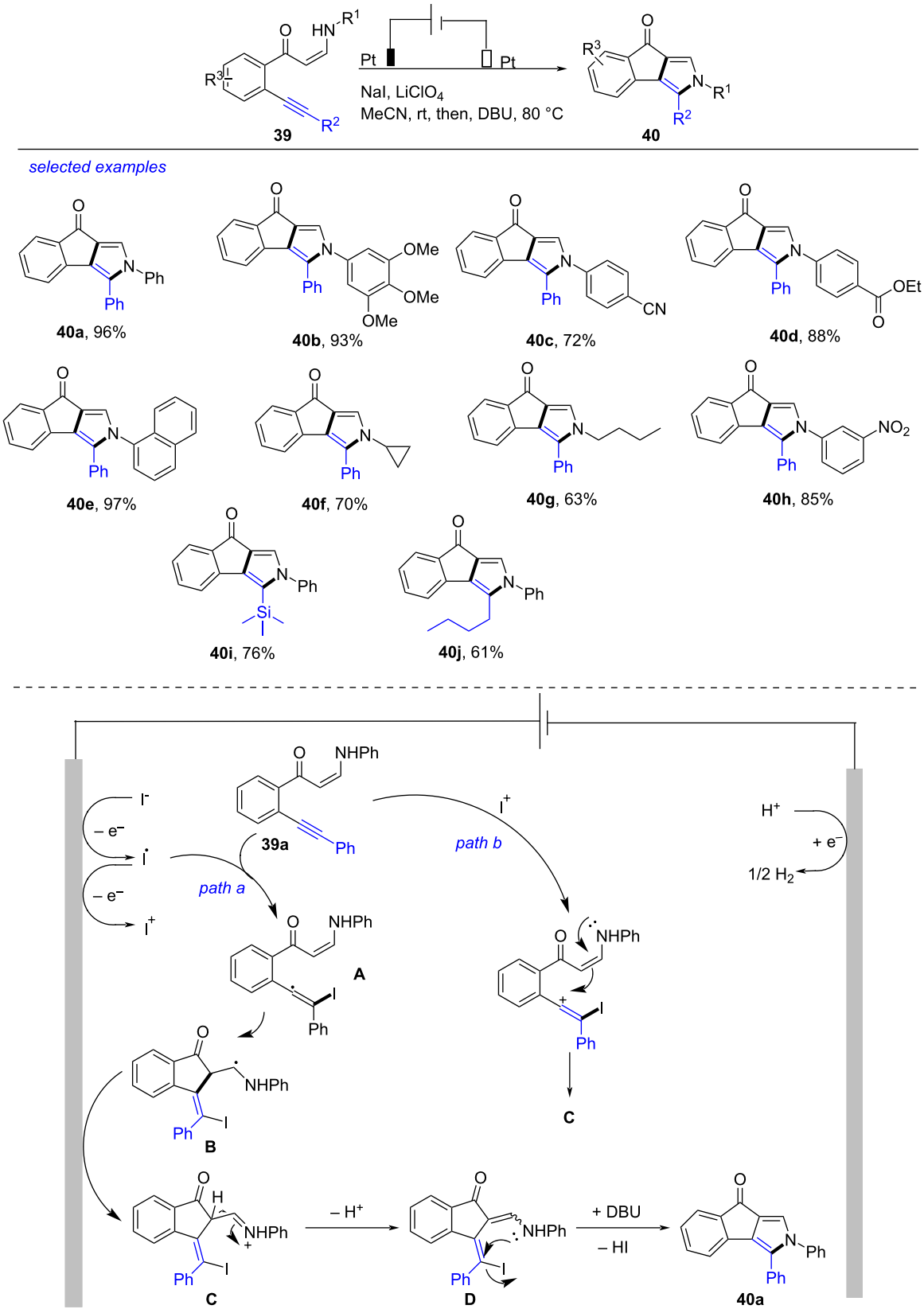

Scheme 15: Electrochemical annulation of alkynyl enaminones.

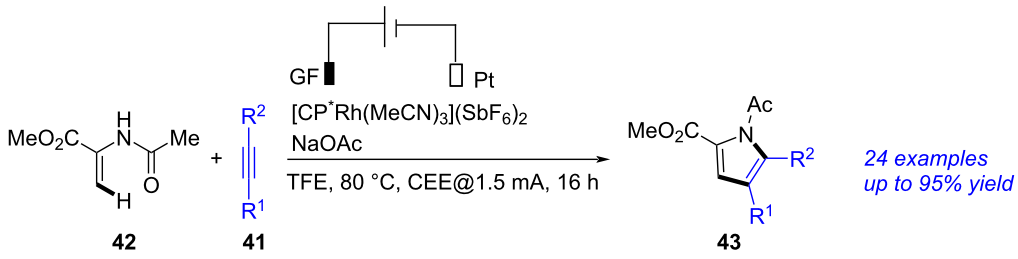

Scheme 16: Electrochemical annulation of alkyne and enamide.

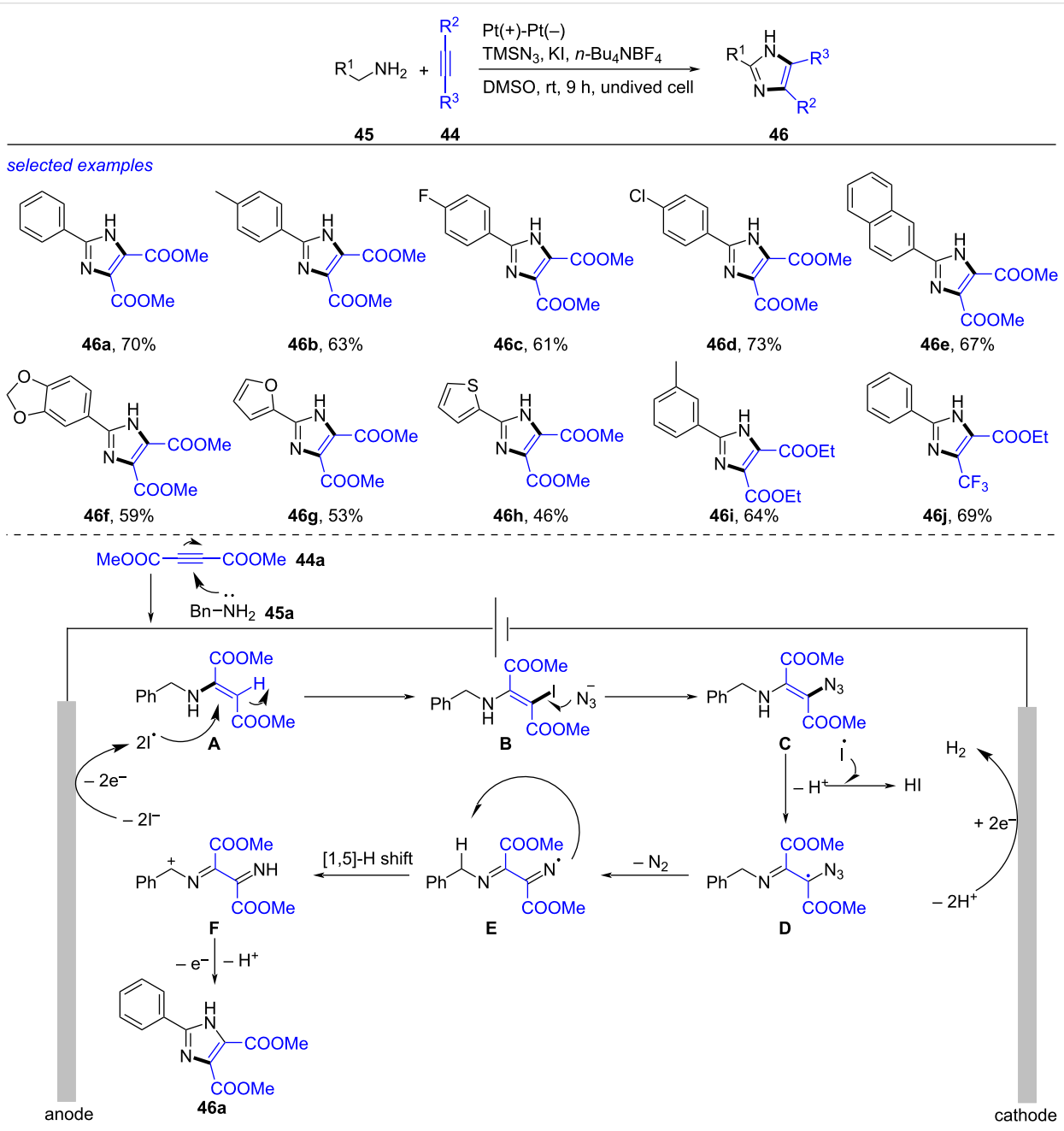

Scheme 17: Electrochemical tandem Michael addition/azidation/cyclization.

imental results and the reported literature [268,269], a proposed reaction mechanism was disclosed. Firstly, treatment of **44a** with **45a** formed **A**. Oxidation of I^- produced $I^•$ that reacted with **A** to generate iodide **B**. Attachment of **B** by N_3^- gave intermediate **C**. A free radical species **E** was obtained from **C** through oxidation and elimination of N_2 via intermediate **D**. The subsequent [1,5]-H shift generated α-amino radical **F**, which was converted into the final product **46a** by oxidation and cyclization. This reaction avoided the use of metal catalysts and oxidants, but the yields remained to improve.

An electrochemical [3 + 2] cyclization of heteroarylamine to access imidazopyridine was achieved by Xu in 2017 (Scheme 18) [270]. When RVC was used as anode, platinum as cathode and Et_4NBF_4 as electrolyte, the tetraarylhydrazine-(**47**)-catalyzed cyclization of heteroarylamine **48** succeeded, forming the corresponding imidazopyridine **49** in up to 94% yield with broad substance scope. The authors also presented a possible mechanism for this transformation. Firstly, the anodic oxidation of **47** formed a radical-cation species **A** along with the generation of OH^- through reduction of H_2O at the cathode. In the presence of OH^-, deprotonation of **48** underwent smoothly to generate the anion species **B**. The single-electron transfer from **B** to **A** gave amidyl radical **C** with the regeneration of **47**. The 5-*exo*-*dig* annulation of **C** provided vinyl radical intermediate **D**. The radical in **D** reacted with the pyridyl N atom regioselectively to form a tricyclic radical **E**, which proceeded one-electron oxidation/hydrolysis afforded **49**. Additionally, the imidazopyridines could be constructed through electrochemical intramolecular [3 + 2] annulation of carbamates as well [271]. Notably, the above approach provided imidazopyridines in high yields under aqueous solution without any metal catalysts.

Early in 2008, an electrochemical copper(I)-catalyzed azide–alkyne cycloaddition (CuAAC) to access 1,2,3-triazole was realized by Finn [272]. But the copper catalyst was still required in that procedure. In 2023, Bera presented an electrochemical oxidative [3 + 2] cycloaddition of secondary propargyl alcohol to access 1,2,3-triazole (Scheme 19) [273]. After probing the reaction systematically, the optimal conditions were presented as following: a mixture of propargyl alcohol **50** (0.7 mmol), NaN_3 (2.8 mmol), *n*-Bu_4NI (0.5 mmol) and MeCN (10 mL) under electrolysis (graphite rod as anode, stainless-steel plate as cathode, 11 mA) at rt for 10 h. According to the

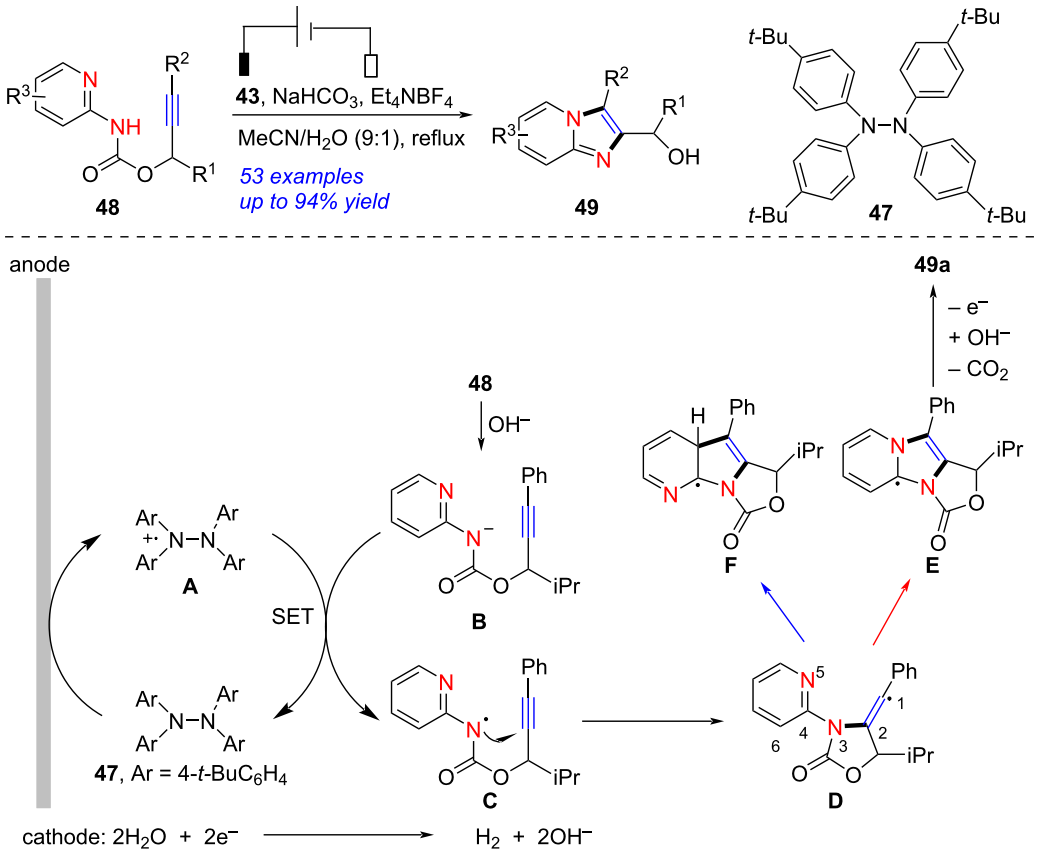

Scheme 18: Electrochemical [3 + 2] cyclization of heteroarylamines.

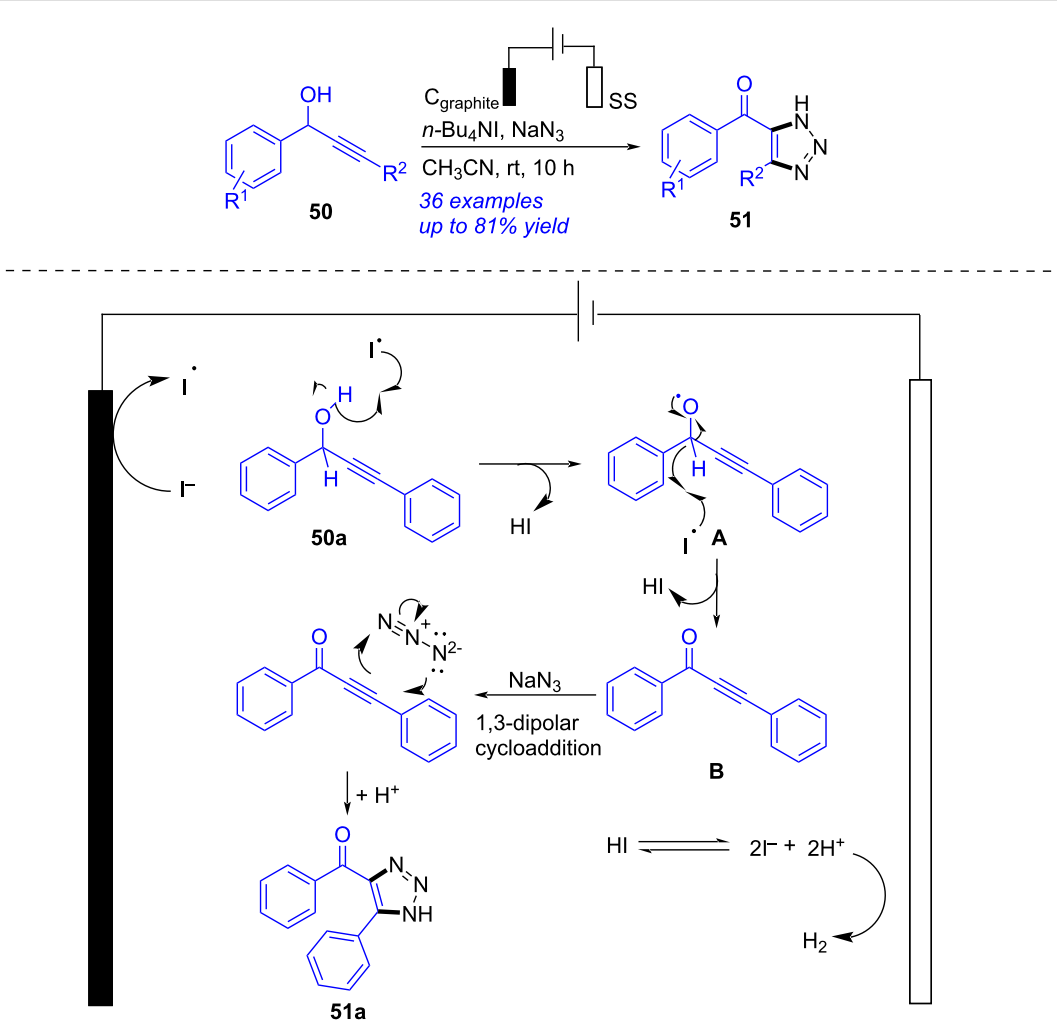

Scheme 19: Electrochemical CuAAC to access 1,2,3-triazole.

experimental results and density functional theory (DFT) calculations, a plausible mechanism for this reaction was proposed. Firstly, oxidation of I^- at the anode afforded $I^•$, which abstracted a hydrogen atom from **50a** to form the intermediate **A** with elimination of HI as a by-product. The second abstraction of a hydrogen atom generated ketone **B**, which then underwent 1,3-dipolar cycloaddition to produce **51a**. This report produced 1,2,3-triazole without any metal catalysts, but the reaction time was relatively long, and the yield remained to enhance.

Conclusion and Outlook

In conclusion, the construction of organic five-membered rings attracted popular attention due to their distinctive properties and wide applications. Alkynes were extensively used as starting materials or intermediates for the synthesis of five-membered rings. Recently, the electrochemical synthesis of organic five-membered rings from alkynes have been developed due to the superiorities of electrochemical transformations. Indole skeletons were obtained successfully through electrochemical coupling of urea derivatives, dehydrogenative annulation of alkynes with anilines, annulation of *o*-arylalkynylanilines, cyclization of 2-ethynylanilines, selenocyclization of diselenides with 2-ethynylanilines, and enantioselective tandem C–H indolization of 2-alkynylanilines with 3-functionalized indoles. The electrochemical and copper-catalyzed annulation of benzamides and terminal alkynes formed isoindolones in high yields. Isoindolinone could be also afforded via electrochemical 5-*exo*-*dig* aza-cyclization of 2-alkynylbenzamides and reductive cascade annulation of *o*-alkynylbenzamides. An electrochemical intramolecular 1,2-amino oxygenation of alkynes provided indolizines in reasonable yields. The electrochemical multicomponent reaction was also developed for the construction of oxazole. Pyrrole could be prepared by electrochemical annulation of alkynes with enamides. Electrochemical [3 + 2] cyclization of heteroarylamine was an efficient access towards

imidazopyridine. The electrochemical oxidative [3 + 2] cycloaddition of secondary propargyl alcohol produced 1,2,3-triazole. In most of these above reactions, the target cyclic products were obtained in high yields with wide substance scope without any metal catalysts and accessional oxidants.

Although these above electrochemical transformations of alkynes are powerful and green protocols to construct five-membered rings, the development of other reactions to form organic five-membered rings from alkynes and application of the above reported approaches to construct other organic rings are still needed, and the following scientific topics would be focused: (1) the development of a simple, sustainable and electrochemical procedure to synthesize organic rings from alkynes bearing heteroatoms such as ynamides and thioalkynes would be enhanced in future research; (2) since axial chirality is critical in natural products and pharmaceuticals, it would be significant to apply the electrochemical annulation of alkynes in formation of organic rings with axial chirality; (3) to satisfy the requirements of green and sustainable chemistry, it could be necessary to develop the electrochemical transformations of alkynes towards organic rings in aqueous solution, ionic liquid or deep eutectic solvents (DESs) with recycle of solvents and electrolytes.

Table 1: About the Authors.

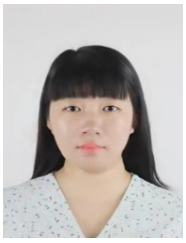

Lifen Peng received her Ph.D. under the supervision of Prof. Akihiro Orita and Prof. Junzo Otera at Okayama University of Science, Japan, in 2014. She moved to The Chinese University of Hong Kong and joined Prof. Henry N. C. Wong's group in Oct. 2014. She became a lecturer at Hunan University of Science and Technology in 2015, and was promoted to an associate professor in 2020. Her research interest is transition metal catalysis, synthesis of alkynes and heterocycles.

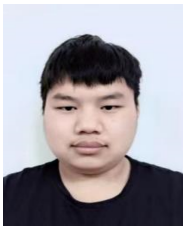

Ting Wang received his BS degree at Huaihua University in June 2023. He joined Prof. Lifen Peng's group and did Master's research at Hunan University of Science and Technology in September 2023. Currently, he is a postgraduate student at Hunan University of Science and Technology majoring in chemical. His research interests mainly focused on transition-metal catalysis, synthesis of alkynes and heterocycles.

Zhiwen Yuan is an undergraduate student at College of Chemistry and Chemical Engineering, Hunan University of Science and Technology, majoring in applied chemistry. His hometown is Ji'an city Jiangxi province. He took part in Prof. Lifen Peng's group in 2022. Now, he did organic experiments after the class. His current research interest is organic reactions, including transition metal catalysis, the coupling reaction of alkyne, synthesis of cyclic alkynes and heterocycles.

Bin Li is an undergraduate student majoring in chemistry at the School of Science and Engineering, The Chinese University of Hong Kong, Shenzhen. He joined Prof. Henry N. C. Wong and Prof. Xiaoshui Peng's group in 2023, in which he conducted research on organic synthesis of natural and non-natural molecules. His research interests are focusing on syntheses of functionally important organic molecules.

Zilong Tang received his Ph.D. under the supervision of Prof. Leon Ghosez at University of Louvain, Belgium in 2004. He joined Prof. Myrargue's group as a postdoctor at University of Paris XI in France. He is an executive director of the Hunan Chemical Society, a chairman of Fine Chemical Professional Committee of Hunan Chemical Society, a high-level talent in Xiangtan and excellent supervisor of HUST. His interest is pharmacochemistry and organic synthesis.

Table 1: About the Authors. (continued)

Xirong Liu is a chairman of Hunan Norchem Pharmaceutical Co., Ltd. Currently, he is a Ph.D. student at College of Chemistry and Chemical Engineering, Hunan University, doing his thesis under the supervision of Professor Guofang Jiang. He obtained a M. Sc. degree from West China Medical University. His current research interests focus on the enzyme-catalyzed synthesis of steroids, and bioactive natural products.

Hui Li received her BS degree at Hunan University of Science and Technology in June 2022. She did Master's research at Hunan University in September 2022. She received her Master's degree majoring in chemical engineering under the supervision of Prof. Xinhua Xu at Hunan University in 2025. Her research interests mainly focused on transition-metal catalysis, green organic reactions and the synthesis of natural products.

Guofang Jiang obtained his Ph.D. from Shanghai Institute of Organic Chemistry, Chinese Academy of Sciences in 1999. Then he moved to Hunan University. From 2002 to 2004, he did his postdoctoral research fellowship at Kyoto University. After that, he returned to Hunan University. He is now a professor and doctoral supervisor at Hunan University. His research is focused on organic synthesis, fine chemicals, biomimetic catalysis, functional materials, electrocatalytic oxidation treatment for wastewater.

Chunling Zeng received his Ph.D. under the supervision of Prof. Xinhua Xu at Hunan University in 2023. He obtained a B. Sc. degree from Hunan University of Chinese Medicine, and his M. Sc. degree from Sichuan University. He spends 15 years as a researcher (2010–now) at Hunan Norchem Pharmaceutical Co., Ltd. His current research interests focus on the enzyme-catalyzed synthesis of steroids and green synthetic chemistry.

Henry N. C. Wong was born in Hong Kong and obtained his B.Sc. degree from The Chinese University of Hong Kong and his Ph.D. degree from University College London (with Prof. Franz Sondheimer) in 1976. After two years at Harvard University as a postdoctoral associate with Prof. Robert B. Woodward, he returned to University College London as a Ramsay Memorial Fellow. From 1980 to 1982, Wong did research at the Shanghai Institute of Organic Chemistry, the Chinese Academy of Sciences. In 1982, he returned to Hong Kong and is now an Emeritus Professor of Chemistry and a Research Professor therein. Concurrently, he is also X. Q. Deng Presidential Chair Professor at The Chinese University of Hong Kong (Shenzhen). His research interests are concerned with syntheses of natural and non-natural molecules as well as synthetic methodologies.

Xiao-Shui Peng received his B.Sc. and M.Sc. degrees from Lanzhou University in 1999 and 2002, respectively, under the guidance of Prof. Xin-Fu Pan. In 2006, he obtained his Ph.D. from The Chinese University of Hong Kong, where he worked on the total synthesis of pallavicinin under the supervision of Prof. Henry Wong. After completing his postdoctoral research fellowship with Prof. K. C. Nicolaou and Prof. David Y. K. Chen on the cortistatins project at CSL@Biopolis, Singapore, he returned to The Chinese University of Hong Kong in 2009 as a Research Assistant Professor and then was a Research Associate Professor until 2020. He is now an Associate Professor at The Chinese University of Hong Kong (Shenzhen). His research is focused on the development of novel “bioinspired” strategies and methodologies for the total synthesis of structurally complex and biologically significant natural products.

Funding

This work was supported by the National Natural Science Foundation of China (NSFC) (Nos. 22271243, 21802040 and 21971219), the Research Program and Guangdong Leading Talent Program for Guangdong Introducing Innovative and Entrepreneurial Teams (No. 2021ZT090195) and its matching funding from the Longgang Government, Shenzhen Science, Technology and Innovation Committee for the Shenzhen Key

Laboratory Scheme (No. ZDSYS20220507161600001), the Leading Talent Scheme of the "Pearl River Talent Recruitment Program" of Guangdong Province (No. 2021CX020028), the CAS-Croucher Funding Scheme for Joint Laboratories 2024 (CAS24402/CAS24CU02), the Research Foundation of Education Bureau of Hunan Province, China (No. 24B0448).

Author Contributions

Lifen Peng: conceptualization; funding acquisition; supervision; writing – original draft; writing – review & editing. Ting Wang: writing – original draft. Zhiwen Yuan: writing – original draft. Bin Li: writing – original draft. Zilong Tang: writing – original draft. Xirong Liu: supervision; writing – review & editing. Hui Li: writing – original draft. Guofang Jiang: supervision; writing – original draft. Chunling Zeng: supervision; writing – original draft; writing – review & editing. Henry N. C. Wong: conceptualization; supervision; writing – review & editing. Xiao-Shui Peng: conceptualization; funding acquisition; supervision; validation; writing – review & editing.

ORCID® iDs

Bin Li - https://orcid.org/0009-0000-2399-6734
Henry N. C. Wong - https://orcid.org/0000-0002-3763-3085
Xiao-Shui Peng - https://orcid.org/0000-0001-9528-8470

Data Availability Statement

Data sharing is not applicable as no new data was generated or analyzed in this study.

References

1. Ye, X.-S.; Li, W.-K.; Wong, H. N. C. *J. Am. Chem. Soc.* **1996,** *118,* 2511–2512. doi:10.1021/ja953747b
2. Mirzaei, A.; Peng, X.-S.; Wong, H. N. C. *Org. Lett.* **2019,** *21,* 3795–3798. doi:10.1021/acs.orglett.9b01250
3. Song, Z. Z.; Wong, H. N. C. *J. Org. Chem.* **1994,** *59,* 33–41. doi:10.1021/jo00080a009
4. Yang, Z.; Liu, H. B.; Lee, C. M.; Chang, H. M.; Wong, H. N. C. *J. Org. Chem.* **1992,** *57,* 7248–7257. doi:10.1021/jo00052a046
5. Chan, K.-F.; Wong, H. N. C. *Org. Lett.* **2001,** *3,* 3991–3994. doi:10.1021/ol010196n
6. Yim, H.-K.; Wong, H. N. C. *J. Org. Chem.* **2004,** *69,* 2892–2895. doi:10.1021/jo030385e
7. Ye, X.-S.; Wong, H. N. C. *J. Org. Chem.* **1997,** *62,* 1940–1954. doi:10.1021/jo962191n
8. Song, Z. Z.; Ho, M. S.; Wong, H. N. C. *J. Org. Chem.* **1994,** *59,* 3917–3926. doi:10.1021/jo00093a025
9. Liu, J.-H.; Chan, H.-W.; Wong, H. N. C. *J. Org. Chem.* **2000,** *65,* 3274–3283. doi:10.1021/jo991531c
10. Takahashi, T.; Kuzuba, Y.; Kong, F.; Nakajima, K.; Xi, Z. *J. Am. Chem. Soc.* **2005,** *127,* 17188–17189. doi:10.1021/ja0561789
11. Li, X.; Gao, Z.-W.; Chen, C.; Wang, X.-N.; Han, Y.-F. *J. Am. Chem. Soc.* **2025,** *147,* 6367–6372. doi:10.1021/jacs.4c18599
12. Aikawa, K.; Okamoto, T.; Mikami, K. *J. Am. Chem. Soc.* **2012,** *134,* 10329–10332. doi:10.1021/ja3032345
13. Dzwiniel, T. L.; Stryker, J. M. *J. Am. Chem. Soc.* **2004,** *126,* 9184–9185. doi:10.1021/ja047852+
14. Wang, J.; Li, Y.-F.; Du, J.; Huang, S.; Ding, C.-H.; Wong, H. N. C.; Hou, X.-L. *Org. Lett.* **2022,** *24,* 1561–1565. doi:10.1021/acs.orglett.2c00253
15. Zhou, Y.-G.; Wong, H. N. C.; Peng, X.-S. *J. Org. Chem.* **2020,** *85,* 967–976. doi:10.1021/acs.joc.9b02918
16. Yu, P.; Yang, Y.; Zhang, Z. Y.; Mak, T. C. W.; Wong, H. N. C. *J. Org. Chem.* **1997,** *62,* 6359–6366. doi:10.1021/jo970476+
17. Liu, J.-H.; Yang, Q.-C.; Mak, T. C. W.; Wong, H. N. C. *J. Org. Chem.* **2000,** *65,* 3587–3595. doi:10.1021/jo9915224
18. Abe, H.; Aoyagi, S.; Kibayashi, C. *J. Am. Chem. Soc.* **2000,** *122,* 4583–4592. doi:10.1021/ja9939284
19. Yan, H.; Wang, Y.; Huo, F.; Yin, C. *J. Am. Chem. Soc.* **2023,** *145,* 3229–3237. doi:10.1021/jacs.2c13223
20. Chong, P. Y.; Shotwell, J. B.; Miller, J.; Price, D. J.; Maynard, A.; Voitenleitner, C.; Mathis, A.; Williams, S.; Pouliot, J. J.; Creech, K.; Wang, F.; Fang, J.; Zhang, H.; Tai, V. W.-F.; Turner, E.; Kahler, K. M.; Crosby, R.; Peat, A. J. *J. Med. Chem.* **2019,** *62,* 3254–3267. doi:10.1021/acs.jmedchem.8b01719
21. Renneberg, D.; Dervan, P. B. *J. Am. Chem. Soc.* **2003,** *125,* 5707–5716. doi:10.1021/ja0300158
22. Wang, L.; Woods, K. W.; Li, Q.; Barr, K. J.; McCroskey, R. W.; Hannick, S. M.; Gherke, L.; Credo, R. B.; Hui, Y.-H.; Marsh, K.; Warner, R.; Lee, J. Y.; Zielinski-Mozng, N.; Frost, D.; Rosenberg, S. H.; Sham, H. L. *J. Med. Chem.* **2002,** *45,* 1697–1711. doi:10.1021/jm010523x
23. Wang, G. T.; Chen, Y.; Wang, S.; Gentles, R.; Sowin, T.; Kati, W.; Muchmore, S.; Giranda, V.; Stewart, K.; Sham, H.; Kempf, D.; Laver, W. G. *J. Med. Chem.* **2001,** *44,* 1192–1201. doi:10.1021/jm000468c
24. Martinez Botella, G.; Salituro, F. G.; Harrison, B. L.; Beresis, R. T.; Bai, Z.; Shen, K.; Belfort, G. M.; Loya, C. M.; Ackley, M. A.; Grossman, S. J.; Hoffmann, E.; Jia, S.; Wang, J.; Doherty, J. J.; Robichaud, A. J. *J. Med. Chem.* **2015,** *58,* 3500–3511. doi:10.1021/acs.jmedchem.5b00032
25. Shen, X.-Y.; Peng, X.-S.; Wong, H. N. C. *Org. Lett.* **2016,** *18,* 1032–1035. doi:10.1021/acs.orglett.6b00161
26. Lyu, M.-Y.; Zhong, Z.; Lo, V. K.-Y.; Wong, H. N. C.; Peng, X.-S. *Angew. Chem., Int. Ed.* **2020,** *59,* 19929–19933. doi:10.1002/anie.202009255
27. Li, L.-Z.; Huang, Y.-R.; Xu, Z.-X.; He, H.-S.; Ran, H.-W.; Zhu, K.-Y.; Han, J.-C.; Li, C.-C. *J. Am. Chem. Soc.* **2024,** *146,* 24782–24787. doi:10.1021/jacs.4c09384
28. Hsu, Y.-H.; Chen, Y.-A.; Tseng, H.-W.; Zhang, Z.; Shen, J.-Y.; Chuang, W.-T.; Lin, T.-C.; Lee, C.-S.; Hung, W.-Y.; Hong, B.-C.; Liu, S.-H.; Chou, P.-T. *J. Am. Chem. Soc.* **2014,** *136,* 11805–11812. doi:10.1021/ja5062856
29. Ding, Y.; Zhao, D.-M.; Kang, T.; Shi, J.; Ye, F.; Fu, Y. *J. Agric. Food Chem.* **2023,** *71,* 7654–7668. doi:10.1021/acs.jafc.3c00467
30. Zuo, L.; Huang, S.; He, Y.; Zhang, L.; Cheng, G.; Feng, Y.; Han, Q.; Ge, L.; Feng, L. *J. Agric. Food Chem.* **2023,** *71,* 11834–11846. doi:10.1021/acs.jafc.3c01913
31. Czodrowski, P.; Mallinger, A.; Wienke, D.; Esdar, C.; Pöschke, O.; Busch, M.; Rohdich, F.; Eccles, S. A.; Ortiz-Ruiz, M.-J.; Schneider, R.; Raynaud, F. I.; Clarke, P. A.; Musil, D.; Schwarz, D.; Dale, T.; Urbahns, K.; Blagg, J.; Schiemann, K. *J. Med. Chem.* **2016,** *59,* 9337–9349. doi:10.1021/acs.jmedchem.6b00597

32. Doerksen, R. S.; Hodík, T.; Hu, G.; Huynh, N. O.; Shuler, W. G.; Krische, M. J. *Chem. Rev.* **2021,** *121,* 4045–4083. doi:10.1021/acs.chemrev.0c01133
33. Meng, W.; Brigance, R. P.; Chao, H. J.; Fura, A.; Harrity, T.; Marcinkeviciene, J.; O'Connor, S. P.; Tamura, J. K.; Xie, D.; Zhang, Y.; Klei, H. E.; Kish, K.; Weigelt, C. A.; Turdi, H.; Wang, A.; Zahler, R.; Kirby, M. S.; Hamann, L. G. *J. Med. Chem.* **2010,** *53,* 5620–5628. doi:10.1021/jm100634a
34. Hartz, R. A.; Ahuja, V. T.; Sivaprakasam, P.; Xiao, H.; Krause, C. M.; Clarke, W. J.; Kish, K.; Lewis, H.; Szapiel, N.; Ravirala, R.; Mutalik, S.; Nakmode, D.; Shah, D.; Burton, C. R.; Macor, J. E.; Dubowchik, G. M. *J. Med. Chem.* **2023,** *66,* 4231–4252. doi:10.1021/acs.jmedchem.3c00133
35. De Cesco, S.; Deslandes, S.; Therrien, E.; Levan, D.; Cueto, M.; Schmidt, R.; Cantin, L.-D.; Mittermaier, A.; Juillerat-Jeanneret, L.; Moitessier, N. *J. Med. Chem.* **2012,** *55,* 6306–6315. doi:10.1021/jm3002839
36. Gong, Y.-D.; Lee, T. *J. Comb. Chem.* **2010,** *12,* 393–409. doi:10.1021/cc100049u
37. Yuan, Y.; Du, L.; Tan, R.; Yu, Y.; Jiang, J.; Yao, A.; Luo, J.; Tang, R.; Xiao, Y.; Sun, H. *J. Med. Chem.* **2022,** *65,* 7770–7785. doi:10.1021/acs.jmedchem.2c00083
38. Motati, D. R.; Amaradhi, R.; Ganesh, T. *Org. Chem. Front.* **2021,** *8,* 466–513. doi:10.1039/d0qo01079k
39. Neto, J. S. S.; Zeni, G. *Org. Biomol. Chem.* **2020,** *18,* 4906–4915. doi:10.1039/d0ob00670j
40. Tóth, B. L.; Amos, S. G. E.; Kleij, A. W. *Org. Chem. Front.* **2025,** *12,* 1326–1339. doi:10.1039/d4qo02143f
41. Sun, K.; Sagisaka, K.; Peng, L.; Watanabe, H.; Xu, F.; Pawlak, R.; Meyer, E.; Okuda, Y.; Orita, A.; Kawai, S. *Angew. Chem., Int. Ed.* **2021,** *60,* 19598–19603. doi:10.1002/anie.202102882
42. Peng, L.; Chen, J.; Chen, Y.; Lu, H.; Okuda, Y.; Tang, Z.; Orita, A.; Qiu, R.; Yin, S.-F. *Eur. J. Org. Chem.* **2024,** *27,* e202301146. doi:10.1002/ejoc.202301146
43. Peng, L.; Yuan, Z.; Tang, Z.; Zeng, C.; Xu, X. *Chem. Rec.* **2023,** *23,* e202300242. doi:10.1002/tcr.202300242
44. Peng, L.; Zhao, Y.; Okuda, Y.; Le, L.; Tang, Z.; Yin, S.-F.; Qiu, R.; Orita, A. *J. Org. Chem.* **2023,** *88,* 3089–3108. doi:10.1021/acs.joc.2c02876
45. Zeng, C.; Yuan, Z.; Jiao, Y.; Peng, L.; Tang, Z.; Xu, X. *Eur. J. Org. Chem.* **2023,** *26,* e202300733. doi:10.1002/ejoc.202300733
46. Hu, Z.; Peng, L.; Qiu, R.; Orita, A. *Chin. J. Org. Chem.* **2020,** *40,* 3112–3119. doi:10.6023/cjoc202005094
47. Peng, L.; Li, R.; Tang, Z.; Chen, J.; Yi, R.; Xu, X. *Tetrahedron* **2017,** *73,* 3099–3105. doi:10.1016/j.tet.2017.04.009
48. Peng, L.; Hu, Z.; Wang, H.; Wu, L.; Jiao, Y.; Tang, Z.; Xu, X. *RSC Adv.* **2020,** *10,* 10232–10244. doi:10.1039/d0ra01286f
49. Rao, Y.; Xu, L.; Zhou, M.; Yin, B.; Osuka, A.; Song, J. *Angew. Chem., Int. Ed.* **2022,** *61,* e202206899. doi:10.1002/anie.202206899
50. Shu, H.; Guo, M.; Wang, M.; Zhou, M.; Zhou, B.; Xu, L.; Rao, Y.; Yin, B.; Osuka, A.; Song, J. *Angew. Chem., Int. Ed.* **2022,** *61,* e202209594. doi:10.1002/anie.202209594
51. Kawai, S.; Sadeghi, A.; Feng, X.; Lifen, P.; Pawlak, R.; Glatzel, T.; Willand, A.; Orita, A.; Otera, J.; Goedecker, S.; Meyer, E. *ACS Nano* **2013,** *7,* 9098–9105. doi:10.1021/nn403672m
52. Moll, N.; Schuler, B.; Kawai, S.; Xu, F.; Peng, L.; Orita, A.; Otera, J.; Curioni, A.; Neu, M.; Repp, J.; Meyer, G.; Gross, L. *Nano Lett.* **2014,** *14,* 6127–6131. doi:10.1021/nl502113z
53. Kawai, S.; Sadeghi, A.; Xu, F.; Peng, L.; Orita, A.; Otera, J.; Goedecker, S.; Meyer, E. *ACS Nano* **2015,** *9,* 2574–2583. doi:10.1021/nn505876n
54. Kawai, S.; Krejčí, O.; Foster, A. S.; Pawlak, R.; Xu, F.; Peng, L.; Orita, A.; Meyer, E. *ACS Nano* **2018,** *12,* 8791–8797. doi:10.1021/acsnano.8b05116
55. Xu, F.; Nishida, T.; Shinohara, K.; Peng, L.; Takezaki, M.; Kamada, T.; Akashi, H.; Nakamura, H.; Sugiyama, K.; Ohta, K.; Orita, A.; Otera, J. *Organometallics* **2017,** *36,* 556–563. doi:10.1021/acs.organomet.6b00781
56. Welker, M. E. *Chem. Rev.* **1992,** *92,* 97–112. doi:10.1021/cr00009a004
57. Aubert, C.; Buisine, O.; Malacria, M. *Chem. Rev.* **2002,** *102,* 813–834. doi:10.1021/cr980054f
58. Xu, F.; Zhang, S.-Y.; Li, Y.-P.; Huo, J.-Q.; Zeng, F.-W. *Chem. Commun.* **2025,** *61,* 1729–1747. doi:10.1039/d4cc05807k
59. Huang, B. *Green Chem.* **2024,** *26,* 11773–11796. doi:10.1039/d4gc04495a
60. Brazeau, J.-F.; Zhang, S.; Colomer, I.; Corkey, B. K.; Toste, F. D. *J. Am. Chem. Soc.* **2012,** *134,* 2742–2749. doi:10.1021/ja210388g
61. Eshdat, L.; Berger, H.; Hopf, H.; Rabinovitz, M. *J. Am. Chem. Soc.* **2002,** *124,* 3822–3823. doi:10.1021/ja0174074
62. Herath, A.; Montgomery, J. *J. Am. Chem. Soc.* **2006,** *128,* 14030–14031. doi:10.1021/ja0660249
63. Fukuyama, T.; Nakashima, N.; Okada, T.; Ryu, I. *J. Am. Chem. Soc.* **2013,** *135,* 1006–1008. doi:10.1021/ja312654q
64. Miura, T.; Shimada, M.; Murakami, M. *J. Am. Chem. Soc.* **2005,** *127,* 1094–1095. doi:10.1021/ja0435079
65. Faraday, M. *Ann. Phys. (Berlin, Ger.)* **1834,** *109,* 481–520. doi:10.1002/andp.18341093102
66. Zhang, L.; Zhang, Z.; Zhang, J.; Li, K.; Mo, F. *Green Chem.* **2018,** *20,* 3916–3920. doi:10.1039/c8gc02026d
67. Vijh, A. K.; Conway, B. E. *Chem. Rev.* **1967,** *67,* 623–664. doi:10.1021/cr60250a003
68. Knolle, J.; Schäfer, H. J. *Angew. Chem., Int. Ed. Engl.* **1975,** *14,* 758. doi:10.1002/anie.197507581
69. Cardoso, D. S. P.; Šljukić, B.; Santos, D. M. F.; Sequeira, C. A. C. *Org. Process Res. Dev.* **2017,** *21,* 1213–1226. doi:10.1021/acs.oprd.7b00004
70. Lund, H. *J. Electrochem. Soc.* **2002,** *149,* S21. doi:10.1149/1.1462037
71. Francke, R.; Little, R. D. *Chem. Soc. Rev.* **2014,** *43,* 2492–2521. doi:10.1039/c3cs60464k
72. Yoshida, J.-i.; Murata, T.; Isoe, S. *Tetrahedron Lett.* **1986,** *27,* 3373–3376. doi:10.1016/s0040-4039(00)84799-1
73. Yoshida, J.-i.; Isoe, S. *Tetrahedron Lett.* **1987,** *28,* 6621–6624. doi:10.1016/s0040-4039(00)96929-6
74. Yoshida, J.-i.; Sugawara, M.; Kise, N. *Tetrahedron Lett.* **1996,** *37,* 3157–3160. doi:10.1016/0040-4039(96)00516-3
75. Hou, Z.-W.; Mao, Z.-Y.; Melcamu, Y. Y.; Lu, X.; Xu, H.-C. *Angew. Chem.* **2018,** *130,* 1652–1655. doi:10.1002/ange.201711876
76. Ye, Z.; Ding, M.; Wu, Y.; Li, Y.; Hua, W.; Zhang, F. *Green Chem.* **2018,** *20,* 1732–1737. doi:10.1039/c7gc03739b
77. Li, J.; Huang, W.; Chen, J.; He, L.; Cheng, X.; Li, G. *Angew. Chem., Int. Ed.* **2018,** *57,* 5695–5698. doi:10.1002/anie.201801106
78. Tang, S.; Wang, D.; Liu, Y.; Zeng, L.; Lei, A. *Nat. Commun.* **2018,** *9,* 798. doi:10.1038/s41467-018-03246-4
79. Zeng, L.; Li, H.; Tang, S.; Gao, X.; Deng, Y.; Zhang, G.; Pao, C.-W.; Chen, J.-L.; Lee, J.-F.; Lei, A. *ACS Catal.* **2018,** *8,* 5448–5453. doi:10.1021/acscatal.8b00683

80. Sauermann, N.; Meyer, T. H.; Ackermann, L. *Chem. – Eur. J.* **2018,** *24,* 16209–16217. doi:10.1002/chem.201802706
81. Meyer, T. H.; Oliveira, J. C. A.; Sau, S. C.; Ang, N. W. J.; Ackermann, L. *ACS Catal.* **2018,** *8,* 9140–9147. doi:10.1021/acscatal.8b03066
82. Mei, R.; Sauermann, N.; Oliveira, J. C. A.; Ackermann, L. *J. Am. Chem. Soc.* **2018,** *140,* 7913–7921. doi:10.1021/jacs.8b03521
83. Mei, R.; Koeller, J.; Ackermann, L. *Chem. Commun.* **2018,** *54,* 12879–12882. doi:10.1039/c8cc07732k
84. Xiong, P.; Xu, H.-H.; Song, J.; Xu, H.-C. *J. Am. Chem. Soc.* **2018,** *140,* 2460–2464. doi:10.1021/jacs.8b00391
85. Gao, X.; Wang, P.; Wang, Q.; Chen, J.; Lei, A. *Green Chem.* **2019,** *21,* 4941–4945. doi:10.1039/c9gc02118c
86. Zhang, L.-B.; Geng, R.-S.; Wang, Z.-C.; Ren, G.-Y.; Wen, L.-R.; Li, M. *Green Chem.* **2020,** *22,* 16–21. doi:10.1039/c9gc03290h
87. Zhang, M.-M.; Sun, Y.; Wang, W.-W.; Chen, K.-K.; Yang, W.-C.; Wang, L. *Org. Biomol. Chem.* **2021,** *19,* 3844–3849. doi:10.1039/d1ob00079a
88. Wang, Y.; Oliveira, J. C. A.; Lin, Z.; Ackermann, L. *Angew. Chem., Int. Ed.* **2021,** *60,* 6419–6424. doi:10.1002/anie.202016895
89. Wu, L.; Peng, L.; Hu, Z.; Jiao, Y.; Tang, Z. *Curr. Org. Synth.* **2020,** *17,* 271–281. doi:10.2174/1570179417666200316124107
90. Peng, L.; Hu, Z.; Lu, Q.; Tang, Z.; Jiao, Y.; Xu, X. *Chin. Chem. Lett.* **2019,** *30,* 2151–2156. doi:10.1016/j.cclet.2019.05.063
91. Peng, L.; Hu, Z.; Tang, Z.; Jiao, Y.; Xu, X. *Chin. Chem. Lett.* **2019,** *30,* 1481–1487. doi:10.1016/j.cclet.2019.04.008
92. Li, H.; Yi, S.-Y.; Zeng, C.; Liu, X.; Peng, L.; Xu, X.; Wong, H. N. C.; Peng, X.-S. *Green Synth. Catal.* **2025,** in press. doi:10.1016/j.gresc.2025.05.008
93. Lee, K. J.; Elgrishi, N.; Kandemir, B.; Dempsey, J. L. *Nat. Rev. Chem.* **2017,** *1,* 0039. doi:10.1038/s41570-017-0039
94. Jackson, M. N.; Surendranath, Y. *Acc. Chem. Res.* **2019,** *52,* 3432–3441. doi:10.1021/acs.accounts.9b00439
95. Sen, P. P.; Dagar, N.; Singh, S.; Roy, V. J.; Pathania, V.; Raha Roy, S. *Org. Biomol. Chem.* **2020,** *18,* 8994–9017. doi:10.1039/d0ob01874k
96. Han, X.; Zhang, N.; Li, Q.; Zhang, Y.; Das, S. *Chem. Sci.* **2024,** *15,* 13576–13604. doi:10.1039/d4sc02512a
97. Hashmi, S. Z.; Bareth, D.; Dwivedi, J.; Kishore, D.; Alvi, P. A. *RSC Adv.* **2024,** *14,* 18192–18246. doi:10.1039/d4ra02812k
98. Devi, S.; Jyoti; Kiran; Wadhwa, D.; Sindhu, J. *Org. Biomol. Chem.* **2022,** *20,* 5163–5229. doi:10.1039/d2ob00572g
99. Novaes, L. F. T.; Liu, J.; Shen, Y.; Lu, L.; Meinhardt, J. M.; Lin, S. *Chem. Soc. Rev.* **2021,** *50,* 7941–8002. doi:10.1039/d1cs00223f
100. Shi, Y.; Xia, C.; Huang, Y.; He, L. *Chem. – Asian J.* **2021,** *16,* 2830–2841. doi:10.1002/asia.202100800
101. Ma, Q.; Li, M.; Chen, Z.; Ni, S.-F.; Wright, J. S.; Wen, L.-R.; Zhang, L.-B. *Green Chem.* **2022,** *24,* 4425–4431. doi:10.1039/d2gc00151a
102. Zhang, Y.; Liu, S.-L.; Li, T.; Xu, M.; Wang, Q.; Yang, D.; Song, M.-P.; Niu, J.-L. *ACS Catal.* **2024,** *14,* 1–9. doi:10.1021/acscatal.3c04853
103. Li, T.; Shi, L.; Wang, X.; Yang, C.; Yang, D.; Song, M.-P.; Niu, J.-L. *Nat. Commun.* **2023,** *14,* 5271. doi:10.1038/s41467-023-40978-4
104. Kong, W.-J.; Finger, L. H.; Messinis, A. M.; Kuniyil, R.; Oliveira, J. C. A.; Ackermann, L. *J. Am. Chem. Soc.* **2019,** *141,* 17198–17206. doi:10.1021/jacs.9b07763
105. Xing, Y.-K.; Chen, X.-R.; Yang, Q.-L.; Zhang, S.-Q.; Guo, H.-M.; Hong, X.; Mei, T.-S. *Nat. Commun.* **2021,** *12,* 930. doi:10.1038/s41467-021-21190-8
106. Shi, Z.; Dong, S.; Liu, T.; Wang, W.-Z.; Li, N.; Yuan, Y.; Zhu, J.; Ye, K.-Y. *Chem. Sci.* **2024,** *15,* 2827–2832. doi:10.1039/d3sc05229j
107. Liu, T.; Zhang, W.; Xu, C.; Xu, Z.; Song, D.; Qian, W.; Lu, G.; Zhang, C.-J.; Zhong, W.; Ling, F. *Green Chem.* **2023,** *25,* 3606–3614. doi:10.1039/d3gc00455d
108. Huang, Y.-T.; Barve, I. J.; Pawar, G. P.; Sun, C.-M. *J. Org. Chem.* **2023,** *88,* 10916–10924. doi:10.1021/acs.joc.3c00937
109. Martins, G. M.; Shirinfar, B.; Hardwick, T.; Murtaza, A.; Ahmed, N. *Catal. Sci. Technol.* **2019,** *9,* 5868–5881. doi:10.1039/c9cy01312a
110. Cai, Z.; Trienes, S.; Liu, K.; Ackermann, L.; Zhang, Y. *Org. Chem. Front.* **2023,** *10,* 5735–5745. doi:10.1039/d3qo01482g
111. Kushwaha, P.; Saxena, A.; von Münchow, T.; Dana, S.; Saha, B.; Ackermann, L. *Chem. Commun.* **2024,** *60,* 12333–12364. doi:10.1039/d4cc03871a
112. Tu, M.-S.; Chen, K.-W.; Wu, P.; Zhang, Y.-C.; Liu, X.-Q.; Shi, F. *Org. Chem. Front.* **2021,** *8,* 2643–2672. doi:10.1039/d0qo01643h
113. Sheng, F.-T.; Wang, J.-Y.; Tan, W.; Zhang, Y.-C.; Shi, F. *Org. Chem. Front.* **2020,** *7,* 3967–3998. doi:10.1039/d0qo01124j
114. Li, T.-Z.; Liu, S.-J.; Tan, W.; Shi, F. *Chem. – Eur. J.* **2020,** *26,* 15779–15792. doi:10.1002/chem.202001397
115. Zhang, Y.-C.; Jiang, F.; Shi, F. *Acc. Chem. Res.* **2020,** *53,* 425–446. doi:10.1021/acs.accounts.9b00549
116. Li, C.; Xu, D.-N.; Ma, C.; Mei, G.-J.; Shi, F. *J. Org. Chem.* **2018,** *83,* 9190–9200. doi:10.1021/acs.joc.8b01217
117. Wang, H.-Q.; Xu, M.-M.; Wan, Y.; Mao, Y.-J.; Mei, G.-J.; Shi, F. *Adv. Synth. Catal.* **2018,** *360,* 1850–1860. doi:10.1002/adsc.201800150
118. Zhu, Z.-Q.; Yu, L.; Sun, M.; Mei, G.-J.; Shi, F. *Adv. Synth. Catal.* **2018,** *360,* 3109–3116. doi:10.1002/adsc.201800688
119. Zhang, H.; Shi, F. *Chin. J. Org. Chem.* **2022,** *42,* 3351–3372. doi:10.6023/cjoc202203018
120. Jiang, X.-L.; Wu, S.-F.; Wang, J.-R.; Mei, G.-J.; Shi, F. *Adv. Synth. Catal.* **2018,** *360,* 4225–4235. doi:10.1002/adsc.201800829
121. Mei, G.-J.; Shi, F. *Chem. Commun.* **2018,** *54,* 6607–6621. doi:10.1039/c8cc02364f
122. Ma, C.; Zhou, J.-Y.; Zhang, Y.-Z.; Jiao, Y.; Mei, G.-J.; Shi, F. *Chem. – Asian J.* **2018,** *13,* 2549–2558. doi:10.1002/asia.201800620
123. Zhang, H.-H.; Wang, C.-S.; Li, C.; Mei, G.-J.; Li, Y.; Shi, F. *Angew. Chem., Int. Ed.* **2017,** *56,* 116–121. doi:10.1002/anie.201608150
124. Jiang, F.; Zhao, D.; Yang, X.; Yuan, F.-R.; Mei, G.-J.; Shi, F. *ACS Catal.* **2017,** *7,* 6984–6989. doi:10.1021/acscatal.7b02279
125. Ma, C.; Zhang, T.; Zhou, J.-Y.; Mei, G.-J.; Shi, F. *Chem. Commun.* **2017,** *53,* 12124–12127. doi:10.1039/c7cc06547g
126. Mei, G.-J.; Bian, C.-Y.; Li, G.-H.; Xu, S.-L.; Zheng, W.-Q.; Shi, F. *Org. Lett.* **2017,** *19,* 3219–3222. doi:10.1021/acs.orglett.7b01336
127. Zhu, Z.-Q.; Shen, Y.; Liu, J.-X.; Tao, J.-Y.; Shi, F. *Org. Lett.* **2017,** *19,* 1542–1545. doi:10.1021/acs.orglett.7b00351
128. Zhu, Z.-Q.; Yin, L.; Wang, Y.; Shen, Y.; Li, C.; Mei, G.-J.; Shi, F. *Org. Chem. Front.* **2017,** *4,* 57–68. doi:10.1039/c6qo00446f
129. Wu, J.-L.; Wang, J.-Y.; Wu, P.; Mei, G.-J.; Shi, F. *Org. Chem. Front.* **2017,** *4,* 2465–2479. doi:10.1039/c7qo00649g
130. He, Y.-Y.; Sun, X.-X.; Li, G.-H.; Mei, G.-J.; Shi, F. *J. Org. Chem.* **2017,** *82,* 2462–2471. doi:10.1021/acs.joc.6b02850
131. Mei, G.-J.; Shi, F. *J. Org. Chem.* **2017,** *82,* 7695–7707. doi:10.1021/acs.joc.7b01458
132. Xu, M.-M.; Wang, H.-Q.; Wan, Y.; Wang, S.-L.; Shi, F. *J. Org. Chem.* **2017,** *82,* 10226–10233. doi:10.1021/acs.joc.7b01731

133. Sun, X.-X.; Li, C.; He, Y.-Y.; Zhu, Z.-Q.; Mei, G.-J.; Shi, F. *Adv. Synth. Catal.* **2017,** *359,* 2660–2670. doi:10.1002/adsc.201700203
134. Jiang, X.-L.; Liu, S.-J.; Gu, Y.-Q.; Mei, G.-J.; Shi, F. *Adv. Synth. Catal.* **2017,** *359,* 3341–3346. doi:10.1002/adsc.201700487
135. Zhao, J.-J.; Tang, M.; Zhang, H.-H.; Xu, M.-M.; Shi, F. *Chem. Commun.* **2016,** *52,* 5953–5956. doi:10.1039/c6cc00920d
136. Sun, X.-X.; Zhang, H.-H.; Li, G.-H.; Meng, L.; Shi, F. *Chem. Commun.* **2016,** *52,* 2968–2971. doi:10.1039/c5cc09145d
137. Li, T.-Z.; Liu, S.-J.; Sun, Y.-W.; Deng, S.; Tan, W.; Jiao, Y.; Zhang, Y.-C.; Shi, F. *Angew. Chem., Int. Ed.* **2021,** *60,* 2355–2363. doi:10.1002/anie.202011267
138. Wan, X.; Sun, M.; Wang, J.-Y.; Yu, L.; Wu, Q.; Zhang, Y.-C.; Shi, F. *Org. Chem. Front.* **2021,** *8,* 212–223. doi:10.1039/d0qo00699h
139. Liu, S.-J.; Chen, Z.-H.; Chen, J.-Y.; Ni, S.-F.; Zhang, Y.-C.; Shi, F. *Angew. Chem., Int. Ed.* **2022,** *61,* e202112226. doi:10.1002/anie.202112226
140. Wang, J.-Y.; Sun, M.; Yu, X.-Y.; Zhang, Y.-C.; Tan, W.; Shi, F. *Chin. J. Chem.* **2021,** *39,* 2163–2171. doi:10.1002/cjoc.202100214
141. Chen, K.-W.; Chen, Z.-H.; Yang, S.; Wu, S.-F.; Zhang, Y.-C.; Shi, F. *Angew. Chem., Int. Ed.* **2022,** *61,* e202116829. doi:10.1002/anie.202116829
142. Yang, S.; Wang, H.-Q.; Gao, J.-N.; Tan, W.-X.; Zhang, Y.-C.; Shi, F. *Eur. J. Org. Chem.* **2022,** e202200878. doi:10.1002/ejoc.202200878
143. Hang, Q.-Q.; Wu, S.-F.; Yang, S.; Wang, X.; Zhong, Z.; Zhang, Y.-C.; Shi, F. *Sci. China: Chem.* **2022,** *65,* 1929–1937. doi:10.1007/s11426-022-1363-y
144. Sheng, F.-T.; Yang, S.; Wu, S.-F.; Zhang, Y.-C.; Shi, F. *Chin. J. Chem.* **2022,** *40,* 2151–2160. doi:10.1002/cjoc.202200327
145. Wang, H.-Q.; Wu, S.-F.; Yang, J.-R.; Zhang, Y.-C.; Shi, F. *J. Org. Chem.* **2023,** *88,* 7684–7702. doi:10.1021/acs.joc.2c02303
146. Shi, Y.-C.; Yan, X.-Y.; Wu, P.; Jiang, S.; Xu, R.; Tan, W.; Shi, F. *Chin. J. Chem.* **2023,** *41,* 27–36. doi:10.1002/cjoc.202200503
147. Wu, P.; Yu, L.; Gao, C.-H.; Cheng, Q.; Deng, S.; Jiao, Y.; Tan, W.; Shi, F. *Fundam. Res.* **2023,** *3,* 237–248. doi:10.1016/j.fmre.2022.01.002
148. Chen, Z.-H.; Li, T.-Z.; Wang, N.-Y.; Ma, X.-F.; Ni, S.-F.; Zhang, Y.-C.; Shi, F. *Angew. Chem., Int. Ed.* **2023,** *62,* e202300419. doi:10.1002/anie.202300419
149. Zhang, J.-Y.; Chen, J.-Y.; Gao, C.-H.; Yu, L.; Ni, S.-F.; Tan, W.; Shi, F. *Angew. Chem., Int. Ed.* **2023,** *62,* 202305450. doi:10.1002/anie.202305450
150. Yang, S.; Huang, J.-B.; Wang, D.-H.; Wang, N.-Y.; Chen, Y.-Y.; Ke, X.-Y.; Chen, H.; Ni, S.-F.; Zhang, Y.-C.; Shi, F. *Precis. Chem.* **2024,** *2,* 208–220. doi:10.1021/prechem.4c00008
151. Li, T.; Liu, S.; Wu, S.; Cheng, Q.; Chen, Q.; Jiao, Y.; Zhang, Y.; Shi, F. *Sci. China: Chem.* **2024,** *67,* 2629–2636. doi:10.1007/s11426-023-1927-3
152. Wang, J.-Y.; Gao, C.-H.; Ma, C.; Wu, X.-Y.; Ni, S.-F.; Tan, W.; Shi, F. *Angew. Chem., Int. Ed.* **2024,** *63,* e202316454. doi:10.1002/anie.202316454
153. Lai, B.-W.; Qu, S.-Y.; Yin, Y.-X.; Li, R.; Dong, K.; Shi, F. *J. Org. Chem.* **2024,** *89,* 10197–10211. doi:10.1021/acs.joc.4c01080
154. Liu, S.-J.; Li, T.-Z.; Wang, N.-Y.; Cheng, Q.; Jiao, Y.; Zhang, Y.-C.; Shi, F. *Org. Chem. Front.* **2024,** *11,* 4812–4819. doi:10.1039/d4qo01047g
155. Li, T.-Z.; Wu, S.-F.; Wang, N.-Y.; Hong, C.-S.; Zhang, Y.-C.; Shi, F. *J. Org. Chem.* **2024,** *89,* 12559–12575. doi:10.1021/acs.joc.4c01489
156. Wu, P.; Zhang, W.-T.; Yang, J.-X.; Yu, X.-Y.; Ni, S.-F.; Tan, W.; Shi, F. *Angew. Chem., Int. Ed.* **2024,** e202410581. doi:10.1002/anie.202410581
157. Liu, S.-Y.; Fan, L.; Zhu, Z.-Q.; Shi, F. *J. Org. Chem.* **2024,** *89,* 16791–16803. doi:10.1021/acs.joc.4c02101
158. Wang, N.-Y.; Gao, S.; Shu, Z.-D.; Cheng, B.-B.; Ma, C.; Zhang, Y.-C.; Shi, F. *Sci. China: Chem.* **2025,** *68,* 3130–3137. doi:10.1007/s11426-024-2472-2
159. Ye, L.-H.; Cheng, X.; Zhu, Z.-Q.; Shi, F. *Eur. J. Org. Chem.* **2025,** *28,* e202401405. doi:10.1002/ejoc.202401405
160. Lai, B.-W.; Zhang, H.-H.; Yao, B.-X.; Li, R.; Ni, S.-F.; Dong, K.; Shi, F. *Angew. Chem., Int. Ed.* **2025,** *64,* e202507804. doi:10.1002/anie.202507804
161. Zhang, H.-H.; Yang, C.; Tian, H.-C.; Dong, K.; Shi, F. *Eur. J. Org. Chem.* **2025,** *28,* e202500193. doi:10.1002/ejoc.202500193
162. Hou, Z.-W.; Mao, Z.-Y.; Zhao, H.-B.; Melcamu, Y. Y.; Lu, X.; Song, J.; Xu, H.-C. *Angew. Chem., Int. Ed.* **2016,** *55,* 9168–9172. doi:10.1002/anie.201602616
163. Zhu, L.; Xiong, P.; Mao, Z.-Y.; Wang, Y.-H.; Yan, X.; Lu, X.; Xu, H.-C. *Angew. Chem., Int. Ed.* **2016,** *55,* 2226–2229. doi:10.1002/anie.201510418
164. Nicolaou, K. C.; Baran, P. S.; Zhong, Y.-L.; Barluenga, S.; Hunt, K. W.; Kranich, R.; Vega, J. A. *J. Am. Chem. Soc.* **2002,** *124,* 2233–2244. doi:10.1021/ja012126h
165. Janza, B.; Studer, A. *J. Org. Chem.* **2005,** *70,* 6991–6994. doi:10.1021/jo0509399
166. Wang, Y.-F.; Chen, H.; Zhu, X.; Chiba, S. *J. Am. Chem. Soc.* **2012,** *134,* 11980–11983. doi:10.1021/ja305833a
167. Li, Z.; Song, L.; Li, C. *J. Am. Chem. Soc.* **2013,** *135,* 4640–4643. doi:10.1021/ja400124t
168. Hu, X.-Q.; Chen, J.-R.; Wei, Q.; Liu, F.-L.; Deng, Q.-H.; Beauchemin, A. M.; Xiao, W.-J. *Angew. Chem., Int. Ed.* **2014,** *53,* 12163–12167. doi:10.1002/anie.201406491
169. Choi, G. J.; Knowles, R. R. *J. Am. Chem. Soc.* **2015,** *137,* 9226–9229. doi:10.1021/jacs.5b05377
170. Miller, D. C.; Choi, G. J.; Orbe, H. S.; Knowles, R. R. *J. Am. Chem. Soc.* **2015,** *137,* 13492–13495. doi:10.1021/jacs.5b09671
171. Jahn, U.; Hartmann, P. *Chem. Commun.* **1998,** 209–210. doi:10.1039/a706879d
172. Kafka, F.; Holan, M.; Hidasová, D.; Pohl, R.; Císařová, I.; Klepetářová, B.; Jahn, U. *Angew. Chem., Int. Ed.* **2014,** *53,* 9944–9948. doi:10.1002/anie.201403776
173. Fuentes, N.; Kong, W.; Fernández-Sánchez, L.; Merino, E.; Nevado, C. *J. Am. Chem. Soc.* **2015,** *137,* 964–973. doi:10.1021/ja5115858
174. Stuart, D. R.; Bertrand-Laperle, M.; Burgess, K. M. N.; Fagnou, K. *J. Am. Chem. Soc.* **2008,** *130,* 16474–16475. doi:10.1021/ja806955s
175. Stuart, D. R.; Alsabeh, P.; Kuhn, M.; Fagnou, K. *J. Am. Chem. Soc.* **2010,** *132,* 18326–18339. doi:10.1021/ja1082624
176. Shi, Z.; Zhang, C.; Li, S.; Pan, D.; Ding, S.; Cui, Y.; Jiao, N. *Angew. Chem., Int. Ed.* **2009,** *48,* 4572–4576. doi:10.1002/anie.200901484
177. Chen, J.; Pang, Q.; Sun, Y.; Li, X. *J. Org. Chem.* **2011,** *76,* 3523–3526. doi:10.1021/jo1025546
178. Wang, H.; Grohmann, C.; Nimphius, C.; Glorius, F. *J. Am. Chem. Soc.* **2012,** *134,* 19592–19595. doi:10.1021/ja310153v
179. Ackermann, L.; Lygin, A. V. *Org. Lett.* **2012,** *14,* 764–767. doi:10.1021/ol203309y

180. Song, W.; Ackermann, L. *Chem. Commun.* **2013,** *49,* 6638–6640. doi:10.1039/c3cc43915a
181. Zhang, G.; Yu, H.; Qin, G.; Huang, H. *Chem. Commun.* **2014,** *50,* 4331–4334. doi:10.1039/c3cc49751h
182. Larock, R. C.; Yum, E. K. *J. Am. Chem. Soc.* **1991,** *113,* 6689–6690. doi:10.1021/ja00017a059
183. Larock, R. C.; Yum, E. K.; Refvik, M. D. *J. Org. Chem.* **1998,** *63,* 7652–7662. doi:10.1021/jo9803277
184. Caron, S.; Dugger, R. W.; Ruggeri, S. G.; Ragan, J. A.; Ripin, D. H. B. *Chem. Rev.* **2006,** *106,* 2943–2989. doi:10.1021/cr040679f
185. Xu, F.; Li, Y.-J.; Huang, C.; Xu, H.-C. *ACS Catal.* **2018,** *8,* 3820–3824. doi:10.1021/acscatal.8b00373
186. Ackermann, L. *Acc. Chem. Res.* **2014,** *47,* 281–295. doi:10.1021/ar3002798
187. Zhang, J.; Shi, S.-Q.; Hao, W.-J.; Dong, G.-Y.; Tu, S.-J.; Jiang, B. *J. Org. Chem.* **2021,** *86,* 15886–15896. doi:10.1021/acs.joc.0c02898
188. Huang, B.; Chen, G.; Zhang, H.; Tang, X.; Yuan, J.; Lu, C.; Wang, J. *Org. Chem. Front.* **2023,** *10,* 3515–3521. doi:10.1039/d3qo00512g
189. Barluenga, J.; Trincado, M.; Rubio, E.; González, J. M. *Angew. Chem., Int. Ed.* **2003,** *42,* 2406–2409. doi:10.1002/anie.200351303
190. Amjad, M.; Knight, D. W. *Tetrahedron Lett.* **2004,** *45,* 539–541. doi:10.1016/j.tetlet.2003.10.207
191. Li, Y.-L.; Li, J.; Yu, S.-N.; Wang, J.-B.; Yu, Y.-M.; Deng, J. *Tetrahedron* **2015,** *71,* 8271–8277. doi:10.1016/j.tet.2015.09.005
192. Hiroya, K.; Itoh, S.; Sakamoto, T. *J. Org. Chem.* **2004,** *69,* 1126–1136. doi:10.1021/jo035528b
193. Yin, Y.; Ma, W.; Chai, Z.; Zhao, G. *J. Org. Chem.* **2007,** *72,* 5731–5736. doi:10.1021/jo070681h
194. Okuma, K.; Seto, J.-i.; Sakaguchi, K.-i.; Ozaki, S.; Nagahora, N.; Shioji, K. *Tetrahedron Lett.* **2009,** *50,* 2943–2945. doi:10.1016/j.tetlet.2009.03.210
195. McNulty, J.; Keskar, K. *Eur. J. Org. Chem.* **2014,** 1622–1629. doi:10.1002/ejoc.201301368
196. Song, S.; Huang, M.; Li, W.; Zhu, X.; Wan, Y. *Tetrahedron* **2015,** *71,* 451–456. doi:10.1016/j.tet.2014.12.007
197. Chen, Z.; Shi, X.-X.; Ge, D.-Q.; Jiang, Z.-Z.; Jin, Q.-Q.; Jiang, H.-J.; Wu, J.-S. *Chin. Chem. Lett.* **2017,** *28,* 231–234. doi:10.1016/j.cclet.2016.07.022
198. Chaisan, N.; Kaewsri, W.; Thongsornkleeb, C.; Tummatorn, J.; Ruchirawat, S. *Tetrahedron Lett.* **2018,** *59,* 675–680. doi:10.1016/j.tetlet.2018.01.014
199. Huang, B.; Yang, C.; Zhou, J.; Xia, W. *Chem. Commun.* **2020,** *56,* 5010–5013. doi:10.1039/c9cc09869k
200. Seavill, P. W.; Holt, K. B.; Wilden, J. D. *Green Chem.* **2018,** *20,* 5474–5478. doi:10.1039/c8gc03262a
201. Zhang, M.; Luo, Z.; Tang, X.; Yu, L.; Pei, J.; Wang, J.; Lu, C.; Huang, B. *Org. Biomol. Chem.* **2023,** *21,* 8918–8923. doi:10.1039/d3ob01502e
202. Dapkekar, A. B.; Satyanarayana, G. *Chem. Commun.* **2023,** *59,* 8719–8722. doi:10.1039/d3cc02294c
203. Kim, Y. J.; Kim, D. Y. *Org. Lett.* **2019,** *21,* 1021–1025. doi:10.1021/acs.orglett.8b04041
204. Peng, Z.-H.; Huang, P.; Li, A.; Yang, M.; Li, Z.; Li, Y.; Qin, S.; Cai, J.; Wang, S.; Zhou, Z.; Yi, W.; Gao, H.; Zeng, Z. *ACS Catal.* **2025,** *15,* 1422–1430. doi:10.1021/acscatal.4c06594
205. Zeng, Z.; Goebel, J. F.; Liu, X.; Gooßen, L. J. *ACS Catal.* **2021,** *11,* 6626–6632. doi:10.1021/acscatal.1c01127
206. Tian, M.; Bai, D.; Zheng, G.; Chang, J.; Li, X. *J. Am. Chem. Soc.* **2019,** *141,* 9527–9532. doi:10.1021/jacs.9b04711
207. Tian, C.; Dhawa, U.; Scheremetjew, A.; Ackermann, L. *ACS Catal.* **2019,** *9,* 7690–7696. doi:10.1021/acscatal.9b02348
208. Shi, Z.; Li, N.; Wang, W.-Z.; Lu, H.-K.; Yuan, Y.; Li, Z.; Ye, K.-Y. *Org. Biomol. Chem.* **2022,** *20,* 4320–4323. doi:10.1039/d2ob00637e
209. Ding, D.; Xu, L.; Wei, Y. *J. Org. Chem.* **2022,** *87,* 4912–4917. doi:10.1021/acs.joc.1c02681
210. Lei, W.-L.; Yang, B.; Zhang, Q.-B.; Yuan, P.-F.; Wu, L.-Z.; Liu, Q. *Green Chem.* **2018,** *20,* 5479–5483. doi:10.1039/c8gc02766h
211. Yang, Z.; Lu, F.; Li, H.; Zhang, Y.; Lin, W.; Guo, P.; Wan, J.; Shi, R.; Wang, T.; Lei, A. *Org. Chem. Front.* **2020,** *7,* 4064–4068. doi:10.1039/d0qo01161d
212. Reddy, M. B.; Prabhu, S.; Anandhan, R. *Chem. Commun.* **2023,** *59,* 11125–11128. doi:10.1039/d3cc03350c
213. Qin, Y.; Lu, J.; Zou, Z.; Hong, H.; Li, Y.; Li, Y.; Chen, L.; Hu, J.; Huang, Y. *Org. Chem. Front.* **2020,** *7,* 1817–1822. doi:10.1039/d0qo00547a
214. Li, J.; He, L.; Liu, X.; Cheng, X.; Li, G. *Angew. Chem., Int. Ed.* **2019,** *58,* 1759–1763. doi:10.1002/anie.201813464
215. Li, B.; Ge, H. *Sci. Adv.* **2019,** *5,* eaaw2774. doi:10.1126/sciadv.aaw2774
216. Huang, B.; Sun, Z.; Sun, G. *eScience* **2022,** *2,* 243–277. doi:10.1016/j.esci.2022.04.006
217. Yu, E.; Kim, H.; Park, C.-M. *Adv. Synth. Catal.* **2022,** *364,* 4088–4096. doi:10.1002/adsc.202200847
218. Yang, Q.-L.; Ma, R.-C.; Li, Z.-H.; Li, W.-W.; Qu, G.-R.; Guo, H.-M. *Org. Chem. Front.* **2022,** *9,* 4990–4997. doi:10.1039/d2qo00904h
219. Yang, N.; Li, A.; Gao, H.; Liao, L.-M.; Yang, Y.-P.; Wang, P.-L.; Li, H. *Green Chem.* **2023,** *25,* 5128–5133. doi:10.1039/d2gc04782a
220. Chen, X.; Liu, H.; Gao, H.; Li, P.; Miao, T.; Li, H. *J. Org. Chem.* **2022,** *87,* 1056–1064. doi:10.1021/acs.joc.1c02346
221. Gao, H.; Chen, X.; Wang, P.-L.; Shi, M.-M.; Shang, L.-L.; Guo, H.-Y.; Li, H.; Li, P. *Org. Chem. Front.* **2022,** *9,* 1911–1916. doi:10.1039/d1qo01925b
222. Zhong, Q.; Gao, H.; Wang, P.-L.; Zhou, C.; Miao, T.; Li, H. *Molecules* **2022,** *27,* 4967. doi:10.3390/molecules27154967
223. Li, C.; Ding, R.; Guo, H.-Y.; Xia, S.; Shu, L.; Wang, P.-L.; Li, H. *Green Chem.* **2022,** *24,* 7883–7888. doi:10.1039/d2gc02204d
224. Lin, M.-Y.; Xu, K.; Jiang, Y.-Y.; Liu, Y.-G.; Sun, B.-G.; Zeng, C.-C. *Adv. Synth. Catal.* **2018,** *360,* 1665–1672. doi:10.1002/adsc.201701536
225. Yang, Y.-Z.; Song, R.-J.; Li, J.-H. *Org. Lett.* **2019,** *21,* 3228–3231. doi:10.1021/acs.orglett.9b00947
226. Li, K.-J.; Jiang, Y.-Y.; Xu, K.; Zeng, C.-C.; Sun, B.-G. *Green Chem.* **2019,** *21,* 4412–4421. doi:10.1039/c9gc01474h
227. Yuan, Y.; Qiao, J.; Cao, Y.; Tang, J.; Wang, M.; Ke, G.; Lu, Y.; Liu, X.; Lei, A. *Chem. Commun.* **2019,** *55,* 4230–4233. doi:10.1039/c9cc00975b
228. Yang, Y.-Z.; Wu, Y.-C.; Song, R.-J.; Li, J.-H. *Chem. Commun.* **2020,** *56,* 7585–7588. doi:10.1039/d0cc02580a
229. Liang, Y.; Niu, L.; Liang, X.-A.; Wang, S.; Wang, P.; Lei, A. *Chin. J. Chem.* **2022,** *40,* 1422–1428. doi:10.1002/cjoc.202200020
230. Wei, B.; Qin, J.-H.; Yang, Y.-Z.; Xie, Y.-X.; Ouyang, X.-H.; Song, R.-J. *Org. Chem. Front.* **2022,** *9,* 816–821. doi:10.1039/d1qo01714d
231. Wei, W.-J.; Zhong, Y.-J.; Feng, Y.-F.; Gao, L.; Tang, H.-T.; Pan, Y.-M.; Ma, X.-L.; Mo, Z.-Y. *Adv. Synth. Catal.* **2022,** *364,* 726–731. doi:10.1002/adsc.202101289
232. Bao, L.; Liu, C.; Li, W.; Yu, J.; Wang, M.; Zhang, Y. *Org. Lett.* **2022,** *24,* 5762–5766. doi:10.1021/acs.orglett.2c02252
233. Cornforth, J. W.; Huang, H. T. *J. Chem. Soc.* **1948,** 1969–1971. doi:10.1039/jr9480001969

234. Wasserman, H. H.; Vinick, F. J. *J. Org. Chem.* **1973,** *38,* 2407–2408. doi:10.1021/jo00953a028
235. Doyle, M. P.; Buhro, W. E.; Davidson, J. G.; Elliott, R. C.; Hoekstra, J. W.; Oppenhuizen, M. *J. Org. Chem.* **1980,** *45,* 3657–3664. doi:10.1021/jo01306a023
236. Dalla Vechia, L.; de Souza, R. O. M. A.; de Mariz e Miranda, L. S. *Tetrahedron* **2018,** *74,* 4359–4371. doi:10.1016/j.tet.2018.07.010
237. Cano, I.; Álvarez, E.; Nicasio, M. C.; Pérez, P. J. *J. Am. Chem. Soc.* **2011,** *133,* 191–193. doi:10.1021/ja109732s
238. He, W.; Li, C.; Zhang, L. *J. Am. Chem. Soc.* **2011,** *133,* 8482–8485. doi:10.1021/ja2029188
239. Li, X.; Huang, L.; Chen, H.; Wu, W.; Huang, H.; Jiang, H. *Chem. Sci.* **2012,** *3,* 3463–3467. doi:10.1039/c2sc21041j
240. Xu, Z.; Zhang, C.; Jiao, N. *Angew. Chem., Int. Ed.* **2012,** *51,* 11367–11370. doi:10.1002/anie.201206382
241. Odabachian, Y.; Tong, S.; Wang, Q.; Wang, M.-X.; Zhu, J. *Angew. Chem., Int. Ed.* **2013,** *52,* 10878–10882. doi:10.1002/anie.201305506
242. Saito, A.; Taniguchi, A.; Kambara, Y.; Hanzawa, Y. *Org. Lett.* **2013,** *15,* 2672–2675. doi:10.1021/ol4009816
243. Zhang, L.; Zhao, X. *Org. Lett.* **2015,** *17,* 184–186. doi:10.1021/ol5030986
244. Rassadin, V. A.; Boyarskiy, V. P.; Kukushkin, V. Y. *Org. Lett.* **2015,** *17,* 3502–3505. doi:10.1021/acs.orglett.5b01592
245. Mallick, R. K.; Prabagar, B.; Sahoo, A. K. *J. Org. Chem.* **2017,** *82,* 10583–10594. doi:10.1021/acs.joc.7b02124
246. Yagyu, T.; Takemoto, Y.; Yoshimura, A.; Zhdankin, V. V.; Saito, A. *Org. Lett.* **2017,** *19,* 2506–2509. doi:10.1021/acs.orglett.7b00742
247. Yang, W.; Zhang, R.; Yi, F.; Cai, M. *J. Org. Chem.* **2017,** *82,* 5204–5211. doi:10.1021/acs.joc.7b00386
248. Pan, J.; Li, X.; Qiu, X.; Luo, X.; Jiao, N. *Org. Lett.* **2018,** *20,* 2762–2765. doi:10.1021/acs.orglett.8b00992
249. Ma, J.-W.; Wang, Q.; Wang, X.-G.; Liang, Y.-M. *J. Org. Chem.* **2018,** *83,* 13296–13307. doi:10.1021/acs.joc.8b02111
250. Liao, L.; Zhang, H.; Zhao, X. *ACS Catal.* **2018,** *8,* 6745–6750. doi:10.1021/acscatal.8b01595
251. Dubovtsev, A. Y.; Dar'in, D. V.; Kukushkin, V. Y. *Adv. Synth. Catal.* **2019,** *361,* 2926–2935. doi:10.1002/adsc.201900097
252. Yuan, G.; Zhu, Z.; Gao, X.; Jiang, H. *RSC Adv.* **2014,** *4,* 24300–24303. doi:10.1039/c4ra03865g
253. Wang, Y.; Zhao, X.-J.; Wu, X.; Zhang, L.; Li, G.; He, Y. *ChemElectroChem* **2022,** *9,* e202200378. doi:10.1002/celc.202200378
254. Sattler, L. E.; Hilt, G. *Chem. – Eur. J.* **2021,** *27,* 605–608. doi:10.1002/chem.202004140
255. Jang, J.; Cho, E. J. *Adv. Synth. Catal.* **2024,** *366,* 3450–3454. doi:10.1002/adsc.202400461
256. Wang, L.-W.; Feng, Y.-F.; Lin, H.-M.; Tang, H.-T.; Pan, Y.-M. *J. Org. Chem.* **2021,** *86,* 16121–16127. doi:10.1021/acs.joc.1c00012
257. Mallick, S.; Baidya, M.; Mahanty, K.; Maiti, D.; De Sarkar, S. *Adv. Synth. Catal.* **2020,** *362,* 1046–1052. doi:10.1002/adsc.201901262
258. Asao, N.; Sato, K.; Yamamoto, Y. *Tetrahedron Lett.* **2003,** *44,* 5675–5677. doi:10.1016/s0040-4039(03)01357-1
259. Zhao, Y.; Fan, Y.; Meng, X.; Kang, X.; Ji, Z.; Yan, S.; Tian, L. *J. Org. Chem.* **2022,** *87,* 11131–11140. doi:10.1021/acs.joc.2c01373
260. Wen, J.; Shi, W.; Zhang, F.; Liu, D.; Tang, S.; Wang, H.; Lin, X.-M.; Lei, A. *Org. Lett.* **2017,** *19,* 3131–3134. doi:10.1021/acs.orglett.7b01256
261. Zhang, Y.; Liu, X.-K.; Wu, Z.-G.; Wang, Y.; Pan, Y. *Org. Biomol. Chem.* **2017,** *15,* 6901–6904. doi:10.1039/c7ob01637a
262. Hua, J.; Fang, Z.; Xu, J.; Bian, M.; Liu, C.; He, W.; Zhu, N.; Yang, Z.; Guo, K. *Green Chem.* **2019,** *21,* 4706–4711. doi:10.1039/c9gc02131k
263. Pfeifer, L.; Gouverneur, V. *Org. Lett.* **2018,** *20,* 1576–1579. doi:10.1021/acs.orglett.8b00321
264. Takeda, Y.; Kajihara, R.; Kobayashi, N.; Noguchi, K.; Saito, A. *Org. Lett.* **2017,** *19,* 6744–6747. doi:10.1021/acs.orglett.7b03497
265. Barluenga, J.; Rodriguez, M. A.; Campos, P. J. *J. Org. Chem.* **1990,** *55,* 3104–3106. doi:10.1021/jo00297a027
266. Homölle, S. L.; Stangier, M.; Reyes, E.; Ackermann, L. *Precis. Chem.* **2023,** *1,* 382–387. doi:10.1021/prechem.3c00061
267. Zhou, K.; Xia, S.; Liu, Y.; Chen, Z. *Org. Biomol. Chem.* **2022,** *20,* 7840–7844. doi:10.1039/d2ob01501c
268. Ma, H.; Zhang, X.; Chen, L.; Yu, W. *J. Org. Chem.* **2017,** *82,* 11841–11847. doi:10.1021/acs.joc.7b01361
269. Patel, S. M.; P., E. P.; Bakthadoss, M.; Sharada, D. S. *Org. Lett.* **2021,** *23,* 257–261. doi:10.1021/acs.orglett.0c03269
270. Hou, Z.-W.; Mao, Z.-Y.; Melcamu, Y. Y.; Lu, X.; Xu, H.-C. *Angew. Chem., Int. Ed.* **2018,** *57,* 1636–1639. doi:10.1002/anie.201711876
271. Hou, Z.-W.; Mao, Z.-Y.; Xu, H.-C. *Org. Biomol. Chem.* **2021,** *19,* 8789–8793. doi:10.1039/d1ob01644j
272. Hong, V.; Udit, A. K.; Evans, R. A.; Finn, M. G. *ChemBioChem* **2008,** *9,* 1481–1486. doi:10.1002/cbic.200700768
273. Bandyopadhyay, M.; Bhadra, S.; Pathak, S.; Menon, A. M.; Chopra, D.; Patra, S.; Escorihuela, J.; De, S.; Ganguly, D.; Bhadra, S.; Bera, M. K. *J. Org. Chem.* **2023,** *88,* 15772–15782. doi:10.1021/acs.joc.3c01836

License and Terms

BEILSTEIN JOURNAL OF ORGANIC CHEMISTRY

Pathway economy in cyclization of 1,*n*-enynes

Hezhen Han[1,2,3], Wenjie Mao[1,2,3], Bin Lin[1,2,3], Maosheng Cheng[*1,3], Lu Yang[*1,2,3] and Yongxiang Liu[*1,2,3]

Review

Open Access

Address:
[1]Key Laboratory of Structure-Based Drug Design and Discovery (Shenyang Pharmaceutical University), Ministry of Education, Shenyang 110016, P. R. China, [2]Wuya College of Innovation, Shenyang Pharmaceutical University, Shenyang 110016, P. R. China and [3]Institute of Drug Research in Medicine Capital of China, Benxi 117000, P. R. China

Email:
Maosheng Cheng[*] - mscheng@syphu.edu.cn;
Lu Yang[*] - yanglusyphu@163.com;
Yongxiang Liu[*] - yongxiang.liu@syphu.edu.cn

* Corresponding author

Keywords:
economical synthesis; 1,*n*-enynes; pathway economy; small-molecule skeletons

Beilstein J. Org. Chem. **2025,** *21,* 2260–2282.
https://doi.org/10.3762/bjoc.21.173

Received: 31 July 2025
Accepted: 09 October 2025
Published: 27 October 2025

This article is part of the thematic issue "Concept-driven strategies in target-oriented synthesis".

Guest Editor: Y. Tang

Abstract

This review presents a paradigm-shifting "pathway economy" strategy for 1,*n*-enyne cyclization, enabling divergent construction of complex molecular architectures from a single substrate class. Through mechanistic-guided modulation of catalysts, solvents, ligands, and angle strain, this approach achieves unprecedented reaction pathway control while demonstrating superior temporal and step efficiency compared to conventional methods. The work establishes a sustainable framework for rapid molecular diversification, offering transformative potential for green chemistry and pharmaceutical applications. By unifying mechanistic insights with practical synthetic design, this review provides valuable guidance for future innovations in precision organic synthesis.

Introduction

As organic synthesis concepts continue to evolve, economical synthesis remains a foundational principle for synthetic chemists [1-7]. The essence of economical synthesis lies in the conservation of materials and time, thereby facilitating the synthesis of target molecules at lower cost while minimizing environmental pollution through minimized waste generation.

In 1991, Trost first introduced the concept of “atom economy”, proposing that an ideal reaction should incorporate all atoms of the reactants, thereby enabling more efficient utilization of limited raw materials [1,2]. Two years later, Wender proposed “step economy” advocating optimized synthetic routes and strategies to minimize the number of steps required for constructing target molecules [3,4]. In 2008, “redox economy” was introduced by Baran [5]. Similar to “atom and step economies”, this concept emphasizes prioritizing the minimization of redox manipulations during synthesis to achieve linear and stable progression of oxidation states in intermediates. In recent years, “pot economy” and “time economy” were proposed by Hayashi, underscoring the importance of reducing the time required for

reaction processes and conducting multistep reactions within a single pot (Scheme 1a) [6,7].

Contemporary organic synthesis is progressively approaching ideal synthesis – achieving highly functionalized target molecular frameworks in a single step. This paradigm circumvents cumbersome late-stage functional group manipulations and perfectly aligns with the principles of step economy, time economy, and redox economy.

Over the past few decades, chemists have rapidly directed this efficient synthetic paradigm toward diverse targets by skillfully regulating reaction components such as solvents, catalysts, ligands and so on. Unlike traditional “one-to-one” reactions, pathway-controlled “one-to-many” transformations synthesize multiple products from single intermediates, dramatically reducing preparation time and reagent requirements (Scheme 1b). As an exceptionally significant reaction, 1,*n*-enyne cyclization is capable of constructing a variety of complex small-molecule frameworks, including fused and bridged rings, thereby serving as a potent tool in the syntheses of natural products and pharmaceuticals. Our group has pioneered the concept of "pathway economy" by systematically regulating reaction parameters (solvent, substituent, ligand, catalyst) in 1,*n*-enyne cyclizations, enabling efficient "one-to-many" transformations that drastically reduce synthetic steps and resource consumption.

Review

Solvent-controlled cyclization of 1,*n*-enynes

Solvents play a multifaceted regulatory role in chemical transformations, exerting kinetic modulation through solvation

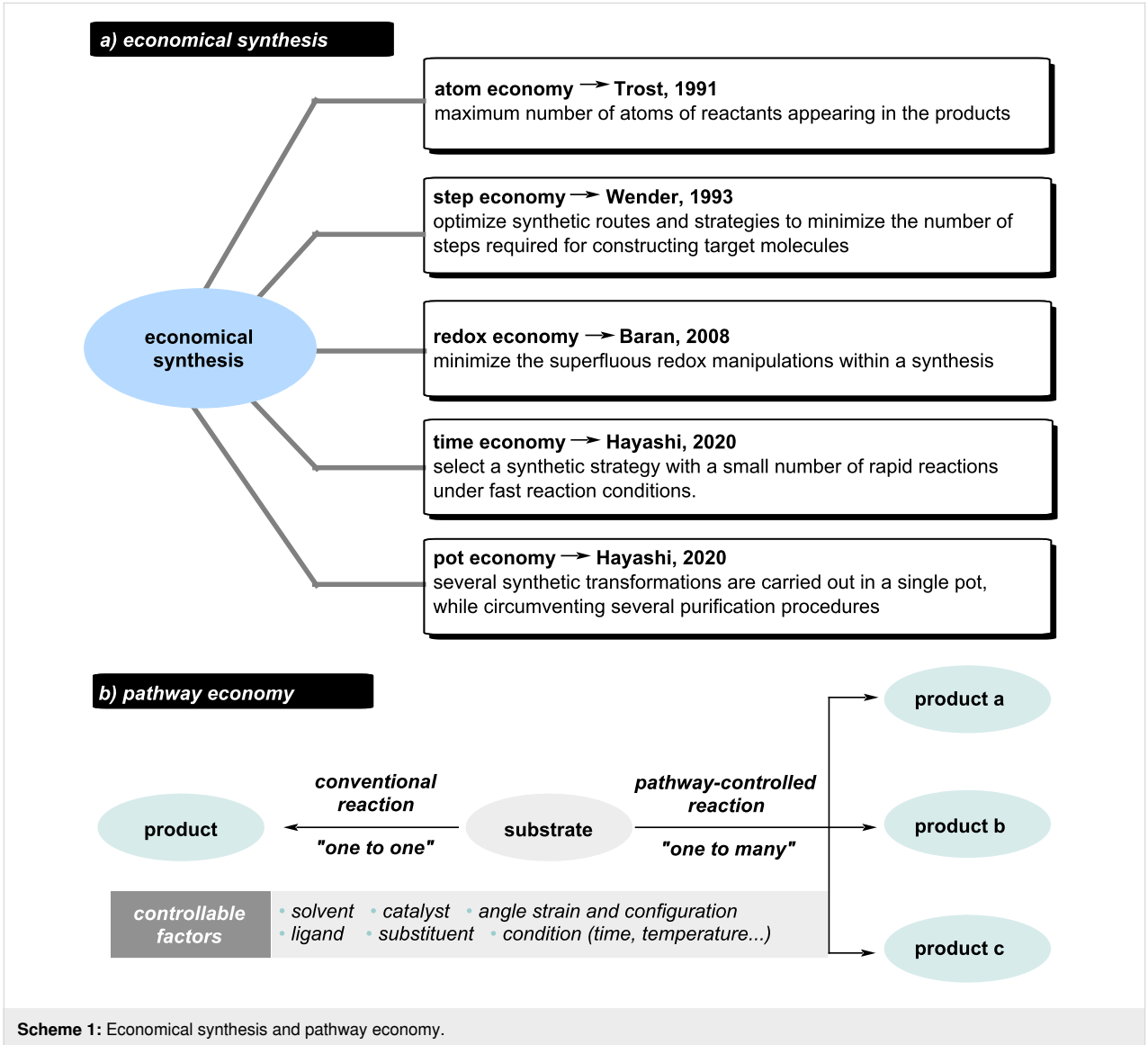

Scheme 1: Economical synthesis and pathway economy.

effects on activation barriers and reaction rates, dictating thermodynamic equilibria that govern product distribution, and enabling precise reaction pathway regulation via selective stabilization of critical transition states. This integrated control framework provides a rational basis for designing reaction conditions to optimize selectivity and efficiency in organic synthesis. In 2014, the Liu group developed an Au(I)-catalyzed cascade cyclization strategy for synthesizing polysubstituted naphthalenes using 1,5-enynes **1** as substrates involving alkyne alkoxylation and dienol ether aromaticity-driven processes (Scheme 2) [8]. The reaction pathway was decisively influenced by the choice of solvent. Under gold catalysis, with toluene as the solvent and 2 equiv of methanol serving as the nucleophile, the reaction proceeded via 5-*endo*-dig cyclization. This pathway involved enol ether attack on the gold-activated alkyne, leading to the formation of oxonium intermediate **2**. Subsequently, nucleophilic addition of methanol culminated in the formation of indene motif **5** (Scheme 2, path a). When methanol served dual roles as solvent and nucleophile, the gold-catalyzed intermolecular Markovnikov addition of methanol to the gold-activated alkyne proceeded to afford dienol intermediate **4**. The intermediate **4** subsequently underwent a regioselective 6-*endo*-trig cyclization, generating the naphthalene core **7** (Scheme 2, path b). In the following years, Liu and co-workers discovered that the protonation of intermediate **2** triggered its conversion to intermediate **3**, which subsequently underwent oxidation with oxygen, resulting in the generation of an indenone skeleton **6** [9]. This tunability achieved efficient and regioselective syntheses of indene, indenone, and naphthalene derivatives from simple aromatic 1,5-enyne substrates.

In 2020, a solvent-controlled strategy for Au(I)-catalyzed divergent syntheses of phenanthrene and dihydrophenanthrene derivatives was developed by the Rodríguez group (Scheme 3) [10]. In dichloromethane (DCM), gold(I)-catalyzed alkyne activation initiated 6-*endo*-dig cyclization of the conjugated alkene. Subsequent alkyl migration formed four-membered ring intermediate **9**, which underwent fragmentation and rearrangement to yield phenanthrene derivative **10** (Scheme 3, path a). When tetrahydrofuran (THF) was used as solvent, the proton elimination and protodeauration led to the formation of dihydrophenanthrene **12** due to solvent effects (Scheme 3, path b). This pathway-controlled approach for the syntheses of phenanthrenes complemented the established protocols.

In 2020, Mutra et al. achieved a radical initiated intramolecular cascade cyclization of 1,*n*-enynes to provide structurally diverse heterocycles (Scheme 4) [11]. Solvent selection dictated divergent reaction pathways under I_2/TBHP oxidation. When an acetonitrile/water mixed solvent was used, iodine radical addition to the alkyne preferentially initiated 6-*endo*-trig cyclization, affording iodinated homoallylic alcohol piperidines **15** (Scheme 4, path a). Conversely, cyclopropane-annulated pyrrolidines **17** were constructed using methanol as solvent through

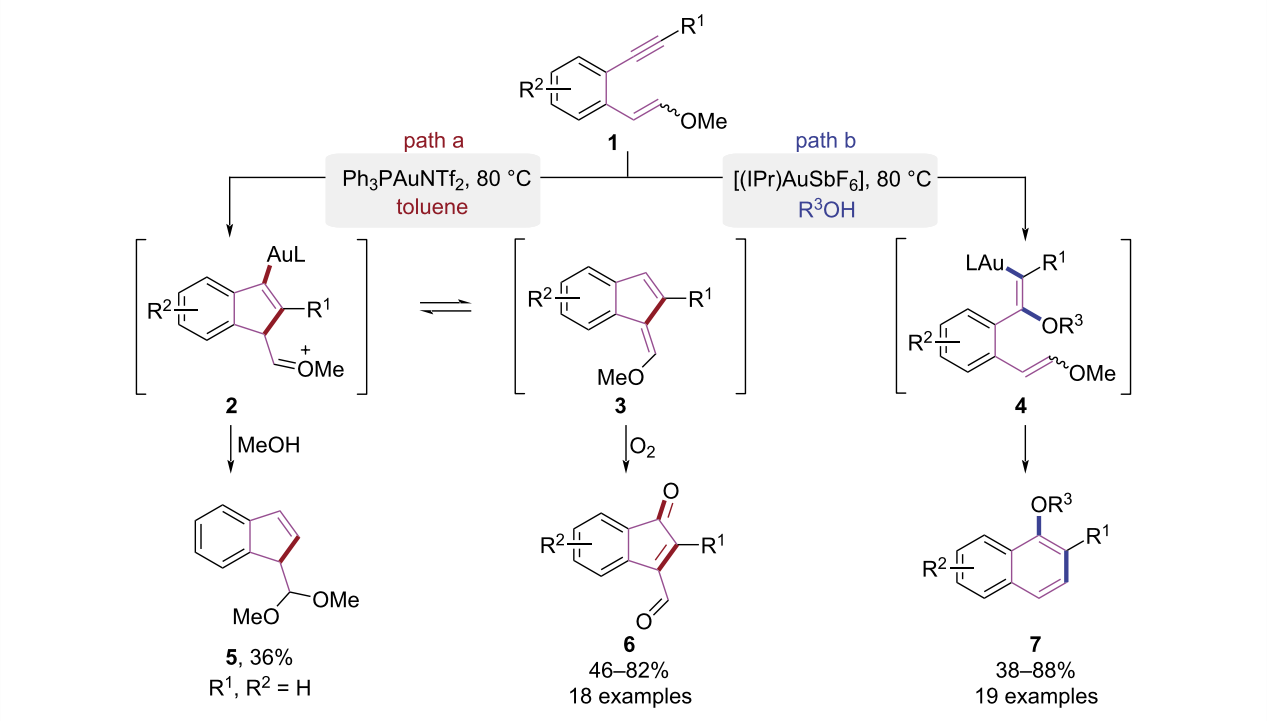

Scheme 2: Au(I)-catalyzed cascade cyclization paths of 1,5-enynes.

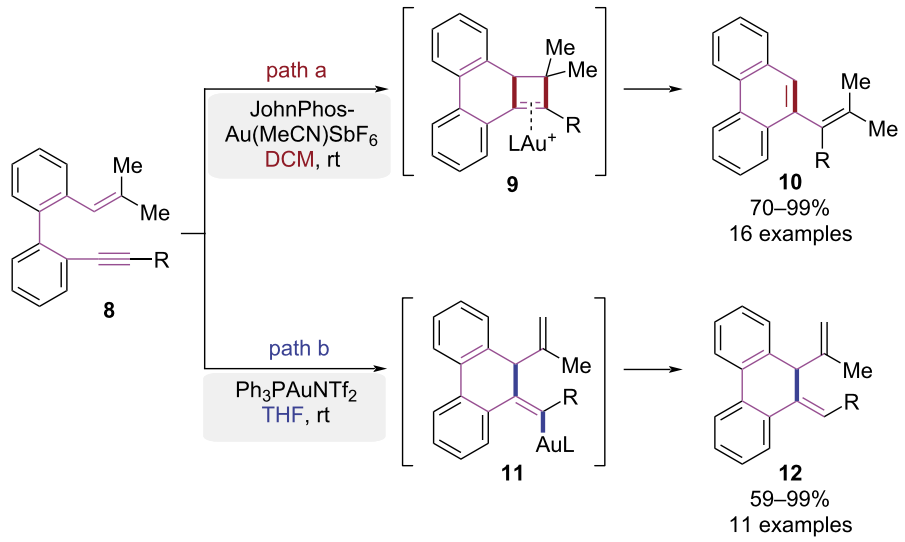

Scheme 3: Au(I)-catalyzed cyclization paths of 1,7-enynes.

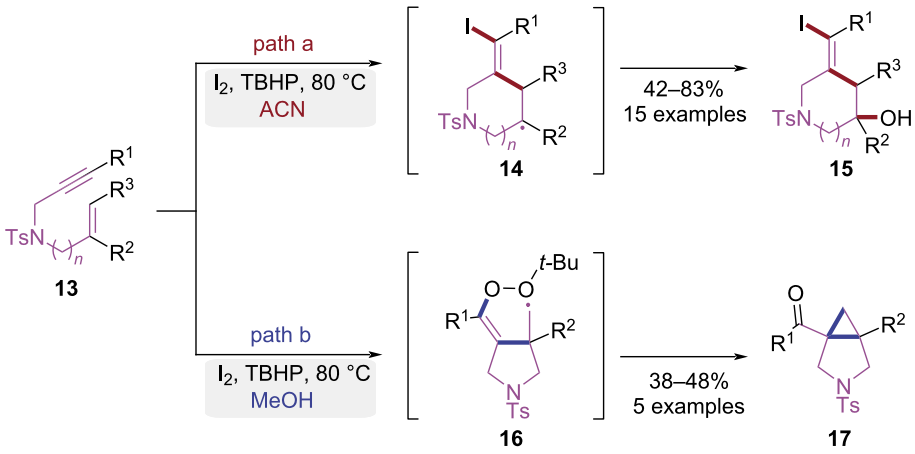

Scheme 4: I_2/TBHP-mediated radical cycloisomerization paths of 1,*n*-enyne.

hydroxyl radical-mediated 5-*exo*-trig cyclization pathway (Scheme 4, path b). This metal-free methodology delivered synthetically versatile iodinated homoallylic alcohols bearing piperidine motifs and pyrrolidine-fused cyclopropanes. Importantly, the reaction was carried out with high operational simplicity and environmental compatibility under mild reaction conditions.

In 2024, Chan and co-workers achieved an innovative gold-catalyzed cascade cycloisomerization of 3-allyloxy-1,6-diynes to access cyclopropane- and cyclobutane-fused benzofurans/chromanols (Scheme 5) [12]. In this study, solvent polarity and trace water were identified as key parameters governing the reaction pathway. In THF with trace water, water served as a nucleophile that participated in the reaction, triggering hydroxylation of cyclopropanation intermediate **19** and affording cyclopropane-fused chromanol products **20** (Scheme 5, path a). In anhydrous 1,2-dichloroethane (DCE), gold(I)-catalyzed cyclopropanation of 1,6-enyne initiated a cascade involving 1,5-enyne addition, consecutive 1,2-alkyl migrations, and Friedel–Crafts alkylation, efficiently constructing the pentacyclic fused benzofuran framework **21** (Scheme 5, path b). Above two analogues were prepared on a gram scale, converted into valuable synthetic intermediates, and used to successfully modify diverse bioactive scaffolds via late-stage functionalization, collectively demonstrating the method's synthetic utility.

In 2025, the Das group developed a palladium-catalyzed cycloisomerization of 2-alkynylbenzoate-cyclohexadienone that

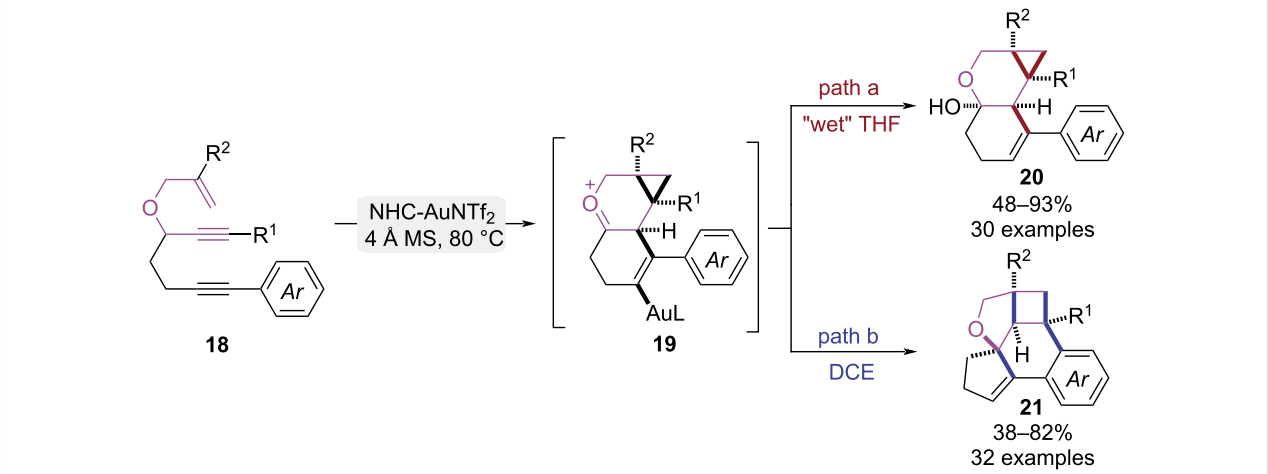

Scheme 5: Au(I)-catalyzed cycloisomerization paths of 3-allyloxy-1,6-diynes.

enables solvent-controlled selective syntheses of two polycyclic compounds (Scheme 6) [13]. Using $PdCl_2$ as the catalyst and DMF as the solvent, substrate **22** underwent a 6-*endo*-dig cyclization and subsequent enone insertion, forming a palladium–carbon bond intermediate. Protonolysis yielded isocoumarin-fused dihydrochromenone skeleton **24** (Scheme 6, path a). When DMSO was employed instead, the strongly coordinating solvent diverted the reaction towards 5-*exo*-dig cyclization, furnishing a *Z*-configured tetrasubstituted alkene product **26** (Scheme 6, path b). The isocoumarin-fused dihydrochromenones prepared by this strategy could be further derivatized (e.g., via borylation, epoxidation), establishing a versatile platform for accessing fused-ring natural products.

Substituent-controlled cyclization of 1,*n*-enynes

In transition metal-catalyzed cyclization reactions, the electronic properties and steric hindrance of substituents serve as critical switches for determining reaction pathway selection. Chemists have developed sophisticated synthetic strategies for programmable assembly of complex small molecular framework by leveraging substituent electronic and steric effects.

In 2006, the Shibata group reported a gold-catalyzed cyclization approach using aromatic enyne derivatives, where substituent control governed the stereoselective syntheses of naphthalene and indene cores (Scheme 7) [14]. When the alkyne

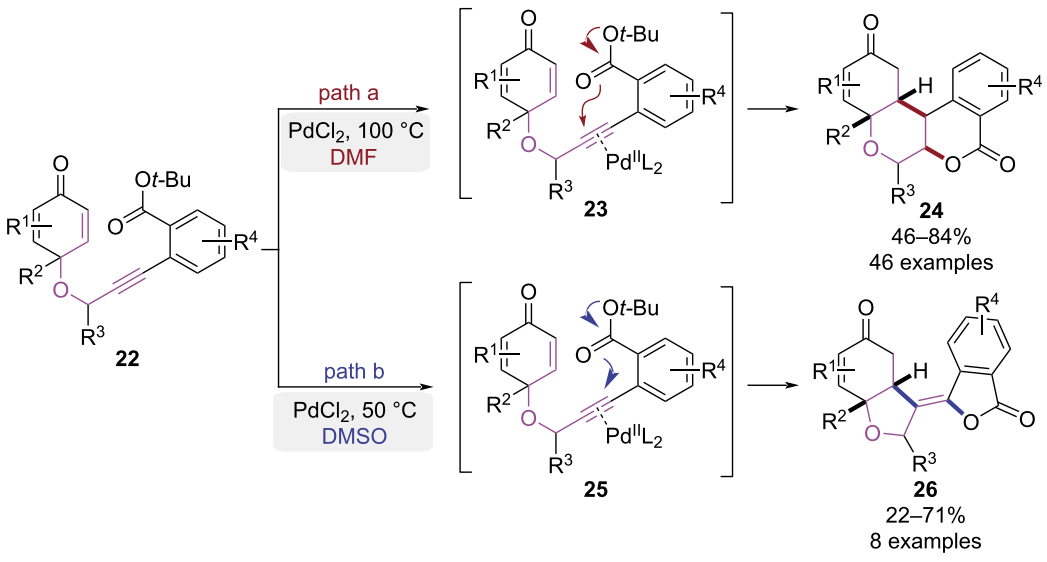

Scheme 6: Pd(II)-catalyzed cycloisomerization paths of 2-alkynylbenzoate-cyclohexadienone.

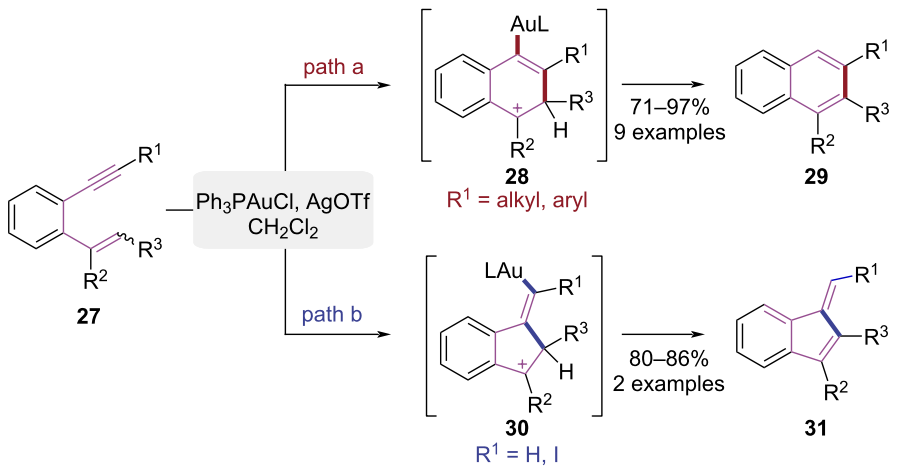

Scheme 7: Stereoselective cyclization of 1,5-enynes.

terminus of the substrate **27** bore an alkyl or aryl substituent, the $Ph_3PAuCl/AgOTf$-catalyzed 6-*endo*-dig cyclization and subsequent deprotonation furnished 1,3-disubstituted or 1,2,3-trisubstituted naphthalenes **29** (Scheme 7, path a). When the alkyne terminus was iodo-substituted or unsubstituted, the 5-*exo*-dig cyclization pathway proceeded via selective activation of the iodoalkyne, generating 1-methyleneindene derivatives **31** (Scheme 7, path b). This work provided a novel approach for constructing substituted naphthalene and indene frameworks via gold-catalyzed cycloisomerization of 1,5-enynes.

In 2016, Liu et al. achieved the stereoselective syntheses of furofuran and furopyran scaffolds from propargyl vinyl ethers under gold(I) catalysis through a substituent-controlled strategy (Scheme 8) [15]. Substrates with heteroaryl substituents underwent 6-*endo*-dig cyclization via gold-heteroatom coordination, furnishing the lactone-fused pyran scaffold **34** (Scheme 8, path a). Substrates with aryl substituents at the terminal alkyne proceeded via a gold(I)-catalyzed propargyl-Claisen rearrangement, generating a β-allenic intermediate **35**. This intermediate underwent a Markovnikov-type nucleophilic addition followed by a 5-*exo*-trig cyclization to stereoselectively construct the furo[3,2-*b*]furan bicyclic framework **36** (Scheme 8, path b). The substituent-controlled gold(I)-catalyzed cycloisomerization of propargyl vinyl ethers provides a highly efficient platform for the divergent synthesis of functionalized furofuran and furopyran. Meanwhile, the preliminary antifungal assessment of these compounds underscored the synthetic value of this method.

In 2017, the Liu group established a precise control over cyclization sequences of 1,2-diphenylacetylenes by modulating the

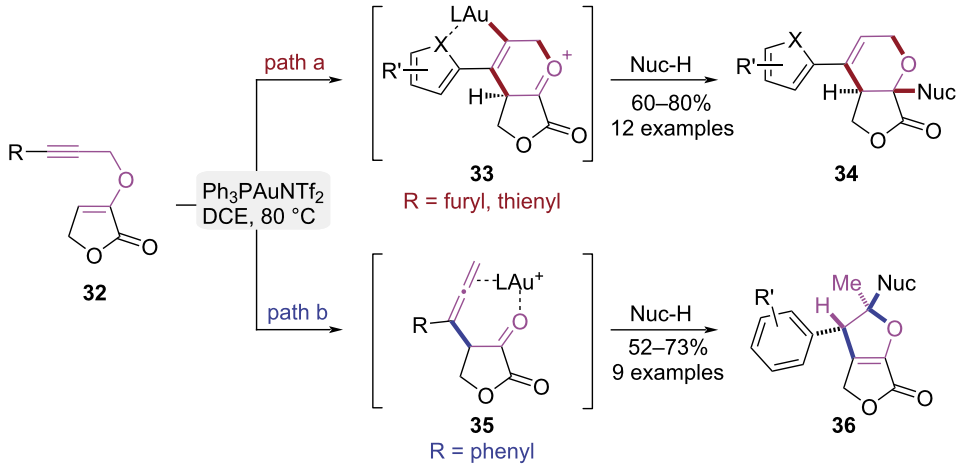

Scheme 8: Substituent-controlled cycloisomerization of propargyl vinyl ethers.

nitrogen-substitution patterns, enabling divergent syntheses of benzo[*a*]carbazole and indeno[1,2-*c*]quinoline derivatives (Scheme 9) [16]. When the nitrogen atom was substituted with strong electron-withdrawing groups, a nucleophilic attack to gold(I)-activated alkyne generated intermediate **38**, with subsequent 6-*endo*-trig cyclization affording benzo[*a*]carbazole **39** (Scheme 9, path a). Conversely, the activated alkyne was attacked by enol ether to yield intermediate **40** when using substrates with unsubstituted nitrogen. Concurrent oxygen-involved cyclization then furnished indeno[1,2-*c*]quinoline **41** (Scheme 9, path b). This work established a pathway-controlled strategy for efficient access to benzo[*a*]carbazole and indeno[1,2-*c*]quinoline derivatives.

In 2019, the Liu group developed a gold-catalyzed tandem cycloisomerization, offering controllable synthesis of either indolo[2,3-*a*]quinolizine or indolizino[8,7-*b*]indole derivatives (Scheme 10) [17]. When the indole nitrogen of the substrate

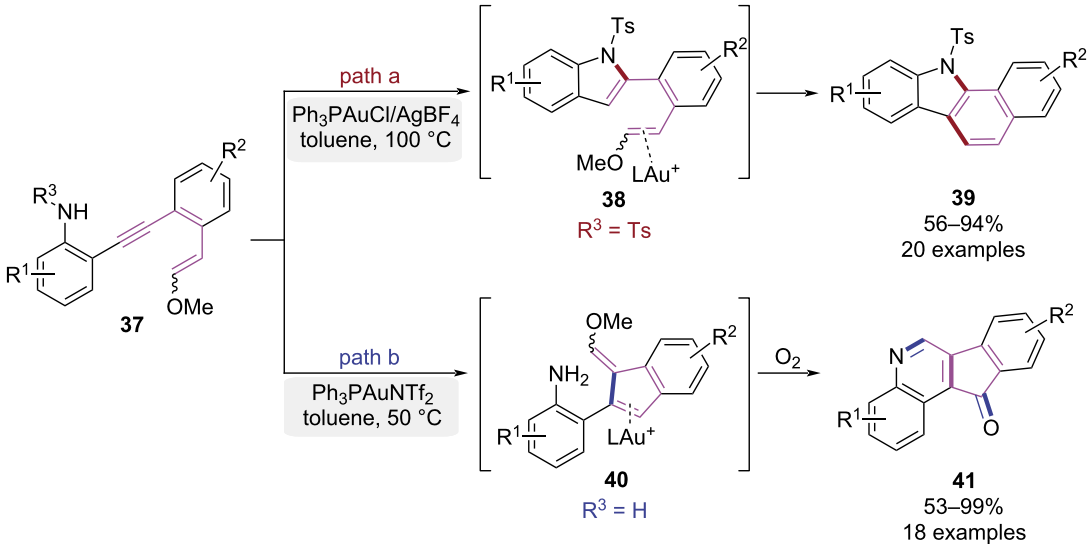

Scheme 9: Au(I)-catalyzed pathway-controlled domino cyclization of 1,2-diphenylethynes.

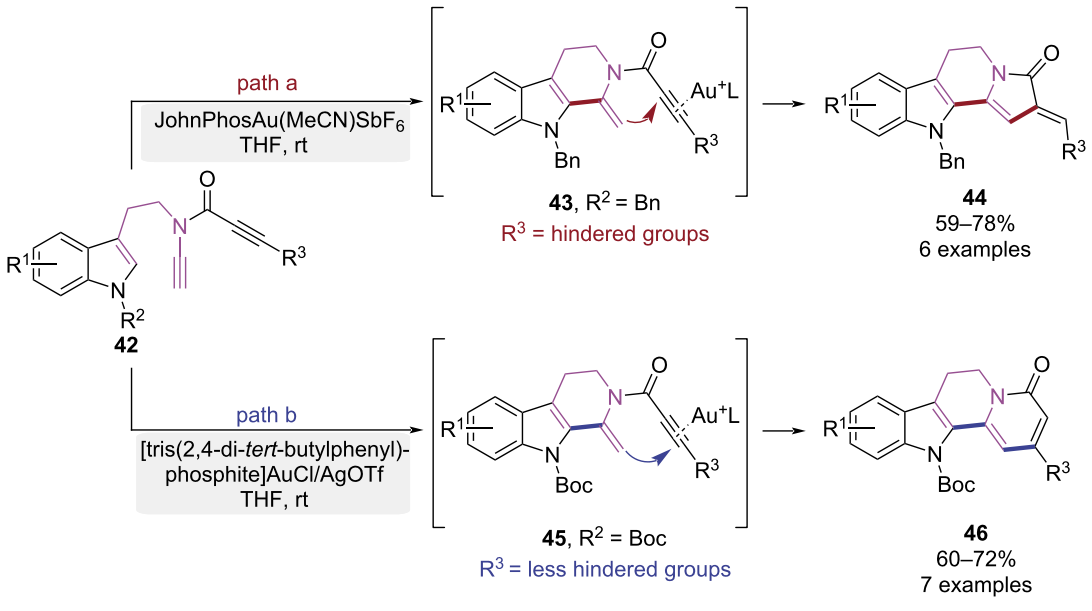

Scheme 10: Au(I)-catalyzed tandem cyclo-isomerization of tryptamine-*N*-ethynylpropiolamide.

was substituted with electron-donating groups (EDGs) and the alkyne of propiolamide was equipped with a bulky substituent, the 6-*exo*-dig cyclization was initially triggered under gold(I)-catalysis, leading to intermediate **43**. Then the indolizino[8,7-*b*]indole skeleton **44** ultimately was constructed via a tandem 5-*exo*-dig cyclization (Scheme 10, path a). When the indole nitrogen was strategically functionalized with an electron-withdrawing groups (EWGs) and the alkyne of propiolamide was modified with a less bulky substituent. A 6-*exo*-dig cyclization yielded intermediate **45**. Finally, a tandem 6-*endo*-dig cyclization enabled the successful assembly of the indolo[2,3-*a*]quinolizine framework **46** (Scheme 10, path b). This controllable approach provided an efficient synthetic pathway for the related natural products.

In 2020, a gold-catalyzed divergent synthesis of bicyclo[3.2.1]oct-2-ene and bicyclo[3.3.1]nonadiene derivatives from 1,6-cyclohexenynes was reported by Davenel et al. (Scheme 11) [18]. The pathway selectivity was regulated by modulating substituents on the terminal alkyne. When the alkyne was unsubstituted, the vinylidene intermediate **48** was generated via a 5-*exo*-dig cyclization, which subsequently underwent protonolysis to yield the bicyclo[3.2.1]oct-2-ene product **49** (Scheme 11, path a). When aryl or alkyl substituents were introduced on the alkyne moiety, a more stable vinylidene intermediate **50** was formed via a 6-*endo*-dig cyclization, ultimately leading to the generation of the bicyclo[3.3.1]nonadiene product **51** (Scheme 11, path b). DFT calculations confirmed that the cyclization pathways were controlled by the influence of substituents on the stability of the intermediates. This work expanded the scope of gold-catalyzed reactions through systematic cycloisomerization studies of 1,6-enynes and an ethyl 4-oxocyclohexanecarboxylate-derived 1,7-enyne.

In 2021, the Shibata group reported a gold-catalyzed ring isomerization strategy to synthesize medium-sized nitrogen heterocycles (Scheme 12) [19]. The seven-membered dibenzo[*b*,*d*]azepine and eight-membered dibenzo[*b*,*d*]azocine frameworks were successfully obtained through the modulation of alkyne terminal substituents. Under the catalysis of IPrAuCl/$AgSbF_6$, substrates bearing unsubstituted terminal alkynes underwent 7-*exo*-dig cyclization driven by the strong nucleophilicity of the 3,5-dimethoxyphenyl group, exclusively affording dibenzo[*b*,*d*]azepine **54** (Scheme 12, path a). Conversely, substrates with aryl-substituted internal alkynes underwent exclusive 8-*endo*-dig cyclization, efficiently delivering the strained dibenzo[*b*,*d*]azocine **56** (Scheme 12, path b). Distinct activation modes governed the selectivity, where regioselective terminal gold coordination triggered 7-*exo*-dig cyclization in terminal alkynes, whereas internal alkynes favored the 8-*endo*-dig pathway due to steric constraints and carbocation stability. This strategy facilitated efficient and selective synthesis of macrocyclic amines, with precise ring size control via substituent modulation.

In 2021, Liu group reported a $BiCl_3$-mediated controllable cyclization of tryptamine-derived ynamides to synthesize two types of indole alkaloid skeletons (Scheme 13) [20]. For alkyl-substituted alkynes, the ynamide activated by $BiCl_3$ was attacked by indole's C3-position to form spirocyclic intermediate **58**. Subsequent 1,2-migration then exclusively delivered tricyclic indole derivative **59** featuring an exocyclic *Z*-alkene (Scheme 13, path a). When the terminal substituent of the alkyne was an aryl group, C3-selective cyclization was triggered under $BiCl_3$ catalysis to generate tricyclic iminium **60**. Subsequent aryl-assisted Mannich cyclization efficiently assembled the pentacyclic spiroindole framework **61** (Scheme 13,

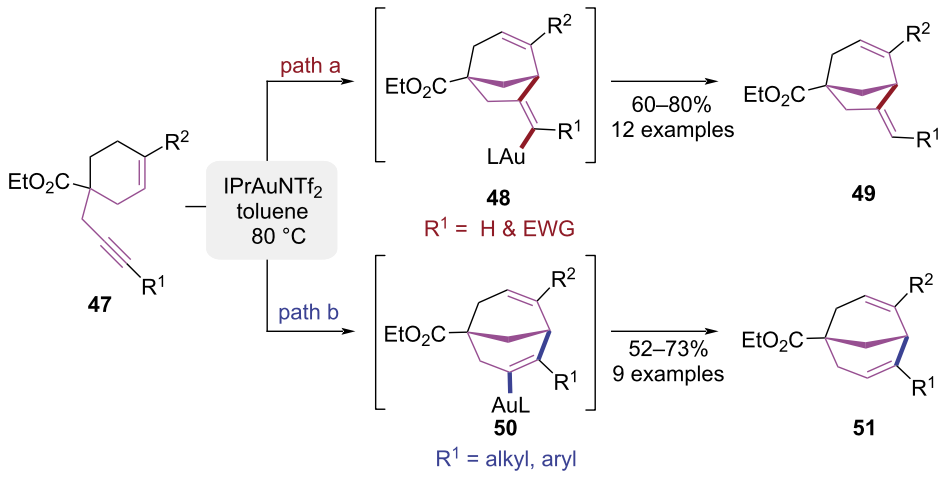

Scheme 11: Au(I)-catalyzed tunable cyclization of 1,6-cyclohexenylalkyne.

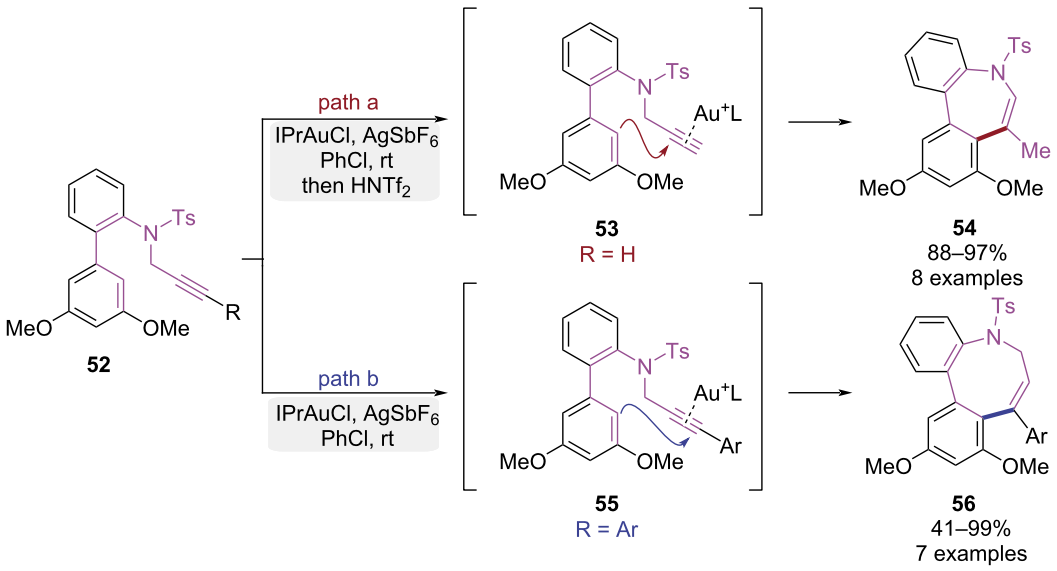

Scheme 12: Substituent-controlled 7-*exo*- and 8-*endo*-dig-selective cyclization of 2-propargylaminobiphenyl derivatives.

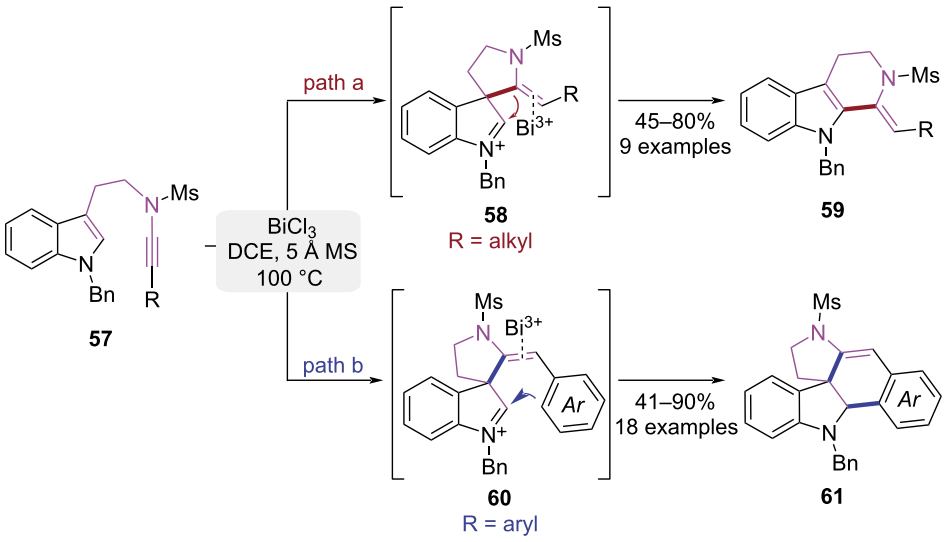

Scheme 13: $BiCl_3$-catalyzed cycloisomerization of tryptamine-ynamide derivatives.

path b). The controllability of this cyclization process arose from the steric and electronic effects of the aryl group, where the π–π interactions and rigid structure of the aryl group facilitated the stabilization of the five-membered spiro ring. This work presents an efficient synthetic approach for two structurally complex classes of pentacyclic spiroindolines and tricyclic indoles of pharmacological significance.

In 2023, the Liu group reported a controllable cyclization strategy for indole substrates featuring a 1,6-enyne motif, which afforded selective access to four indole derivatives through modulation of the alkyne's terminal substituents and nucleophile type (Scheme 14) [21,22]. The gold(I) catalyst activated the unsubstituted terminal alkynes to initiate a 5-*exo*-dig cyclization, generating a spiro[indoline-3,3′-pyrrolidine] intermediate **62** (Scheme 14, path a). When a less nucleophilic indole was used as the nucleophile, a Wagner–Meerwein rearrangement occurred, leading to the formation of a pyrido[4,3-*b*]indole product **63**. When Hantzsch ester (HEH) was used as the nucleophile, the imine intermediate **62** was reduced to product

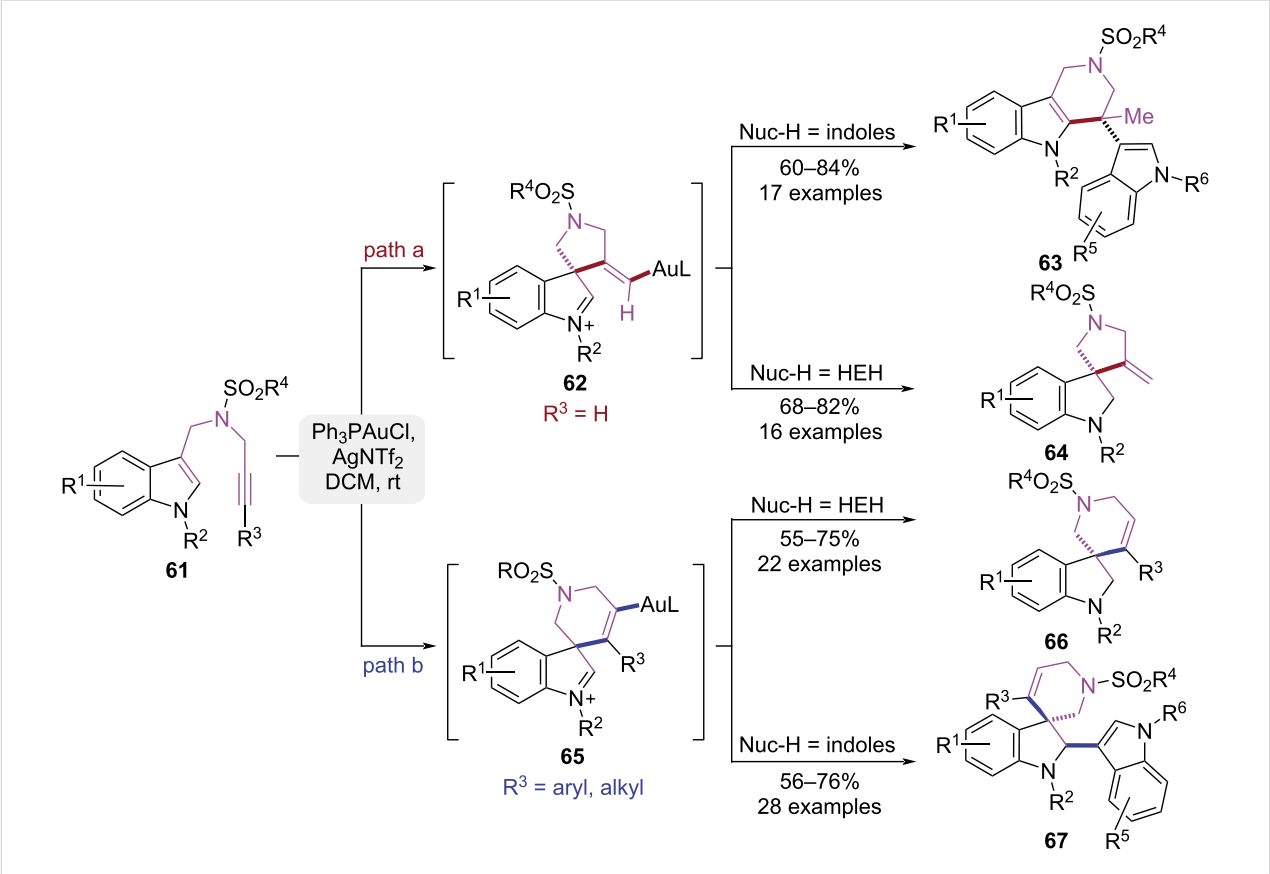

Scheme 14: Au(I)-mediated substituent-controlled cycloisomerization of 1,6-enynes.

64. In contrast, when the alkyne was substituted with a phenyl group, the reaction shifted toward a 6-*endo*-dig cyclization pathway due to steric and electronic effects (Scheme 14, path b). When HEH was employed as the nucleophile, a spiro[indoline-3,3′-piperidine] framework **66** was formed. When indole acted as nucleophile, the stable imine–gold–aryl cation–π–π interaction precluded rearrangement and promoted the capture of imine to form spiro[indoline-3,3′-pyridine] derivatives **67**. The $Ph_3PAuCl/AgNTf_2$-catalyzed cyclization of *N*-propargyl-tethered amide enynes efficiently afforded four distinct heterocyclic scaffolds, which established a versatile platform for synthesizing structurally diverse indoline frameworks.

Ligand-controlled cyclization of 1,*n*-enynes

The core function of catalyst ligands lies in their ability to precisely modulate catalyst performance through electronic and steric effects. The ligands could enhance catalytic activity and efficiency while enabling fine control over chemo-, regio-, stereo-, and enantioselectivity of reactions. Ligands enhance both the thermal/chemical stability and solubility profiles of catalysts in specific reaction media. Thus, ligands function as a regulatory nexus for the rational design and optimization of highly effective, selective homogeneous catalytic systems. In 2013, Barriault and co-workers demonstrated that strategic modulation of steric and electronic ligand parameters within gold(I)-catalyzed cyclization pathways enables the selective assembly of polycyclic aromatic heterocycles (Scheme 15) [23]. Catalysts bearing the strong σ-donating IPr ligand exhibited a marked preference for the 5-*exo*-dig cyclization pathway, affording five-membered ring product **70** (Scheme 15, path a). When a bulky Me_4XPhos ligand was employed, the reaction favored 6-*endo*-dig cyclization, yielding a six-membered ring product **72** (Scheme 15, path b). This observed selectivity arose from differential stabilization of transition states by ligands, thereby enabling the Au(I)-catalyzed cyclization to directly access bioactive heterocyclic frameworks commonly encountered in natural products and pharmaceutical agents.

In 2013, Chan and co-workers reported a ligand-controlled cycloisomerization of 1,7-enyne esters affording the selective synthesis of *cis*-tetrahydropyridinones and δ-diketones (Scheme 16) [24]. When NHC-ligated gold catalysts were employed, a cascade sequence comprising 1,3-acyloxy migration, 6-*exo*-trig cyclization, and 1,5-acyl migration proceeded, affording δ-diketone-substituted *cis*-1,2,3,6-tetrahydropyridine derivatives **75** (Scheme 16, path a). The phosphine-ligated cata-

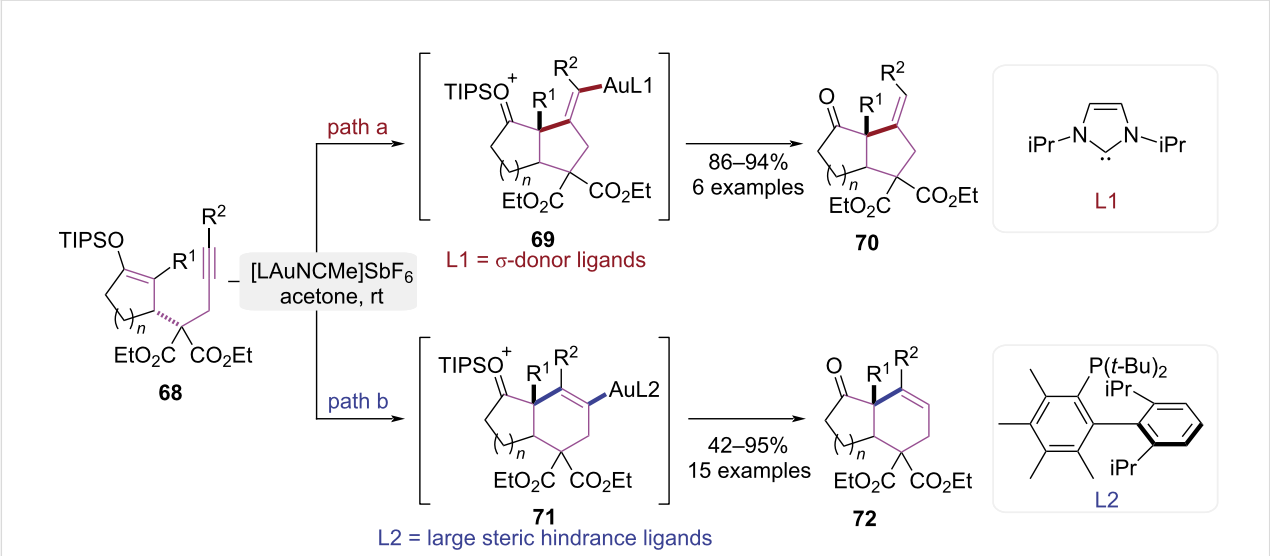

Scheme 15: Ligand-controlled regioselective cyclization of 1,6-enynes.

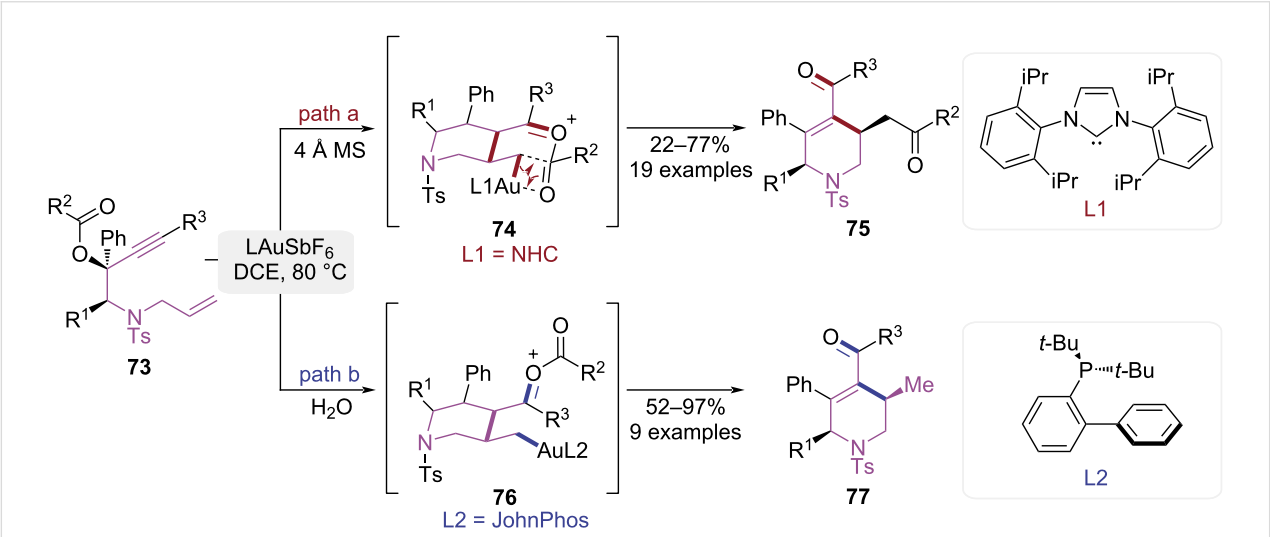

Scheme 16: Ligand-dependent cycloisomerization of 1,7-enyne esters.

lysts promoted an alternative pathway cascade involving 1,3-acyloxy migration, 6-*exo*-trig cyclization, and hydrolysis, exclusively producing *cis*-tetrahydropyridin-4-one derivatives **77** (Scheme 16, path b). Mechanistic studies revealed that intermediate **74** could be stabilized by NHC ligands to facilitate 1,5-acyl migration, whereas phosphine ligands could accelerate proton dissociation in intermediate **76** to drive hydrolysis. This methodology tolerates structurally diverse 1,7-enyne esters and generates defined *cis*-1,2,3,6-tetrahydropyridine scaffolds, which serve as synthetic intermediates for complex natural products and pharmacologically relevant heterocyclic frameworks.

In 2016, Jiang group achieved *ortho*- and *para*-selective cyclization of methoxyamide-functionalized alkynes via ligand-controlled steric and electronic modifications (Scheme 17) [25]. When a flexible electron-deficient phosphate ligand **L1** was utilized, the Au(I)-catalyzed cyclization of substrates **78** resulted in the formation of *ortho*-cyclized products **80**, enabled by coordination to both the directing group and alkyne (Scheme 17, path a). However, the rigid electron-rich XPhos ligand (**L2**) promoted *para*-cyclization due to steric constraints and π–π stacking to yield dihydroquinoline derivatives **82** (Scheme 17, path b). This ligand-controlled Au(I)-catalyzed intramolecular hydroarylation overcame key challenges of poor

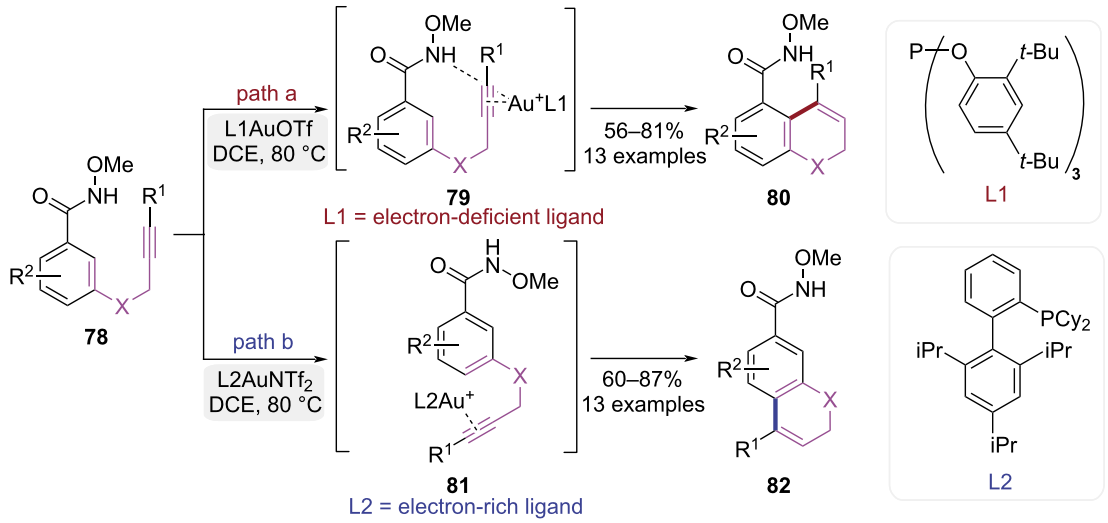

Scheme 17: Ligand-controlled cycloisomerization of 1,5-enynes.

regioselectivity and limited applicability to electron-deficient substrates.

In 2018, a gold-catalyzed divergent cyclization to access heteropolycyclic frameworks was reported by the Shi group (Scheme 18) [26]. Ph_3PAuCl/AgOTf catalyzed a tandem 7-*exo*-dig cyclization followed by a cyclobutyl ring expansion process, yielding intermediate **84**. The deprotonation followed by protonolysis-mediated gold elimination delivered the ring-expanded product **85** (Scheme 18, path a). When a bulkier ligand was used, steric constraints promoted intramolecular Friedel–Crafts cyclization via intermediate **84** to form spiropolycycle **86** (Scheme 18, path b). The ligand-dependent gold(I)-catalyzed cyclization provided modular access to therapeutically significant fused polycyclic heterocyclic scaffolds via regioselective ring expansion/cycloisomerization sequences.

In 2019 and 2020, Liu and co-workers achieved pathway-controlled cyclization–isomerization of tryptamine-ynamides using ligand-influenced silver catalytic systems (Scheme 19) [27-29]. To circumvent decomposition caused by the inherent high reactivity of ynamides under catalytic conditions, the authors attenuated the silver catalyst's activity through ligand addition. This allowed for a umpolung addition of the substrate **87**, affording six-membered spirocyclic intermediate **88**. When the NFSI was used as ligand without nucleophiles, the tricyclic azepinoindole **89** was obtained via a Wagner–Meerwein rearrangement from the six-membered spirocyclic intermediate **88**. The addition of

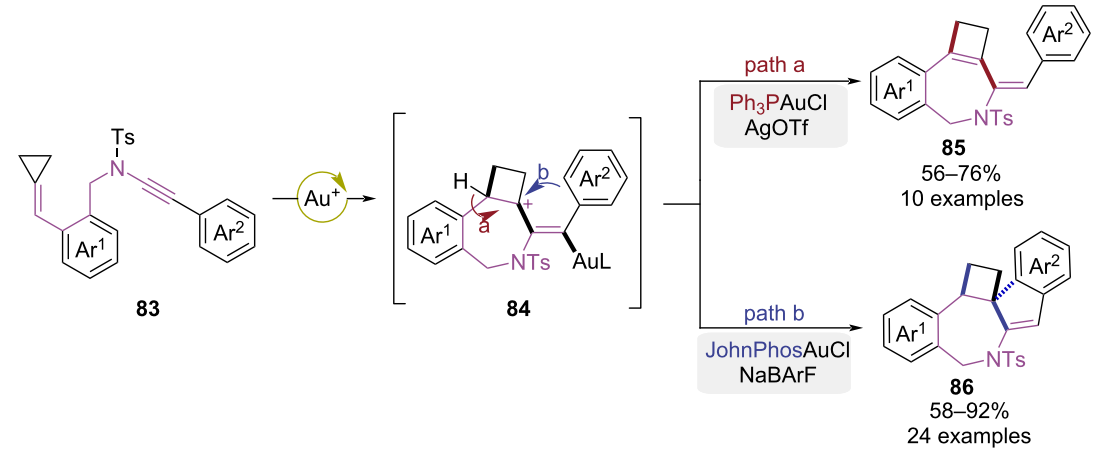

Scheme 18: Ligand-controlled cyclization strategy of alkynylamide tethered alkylidenecyclopropanes.

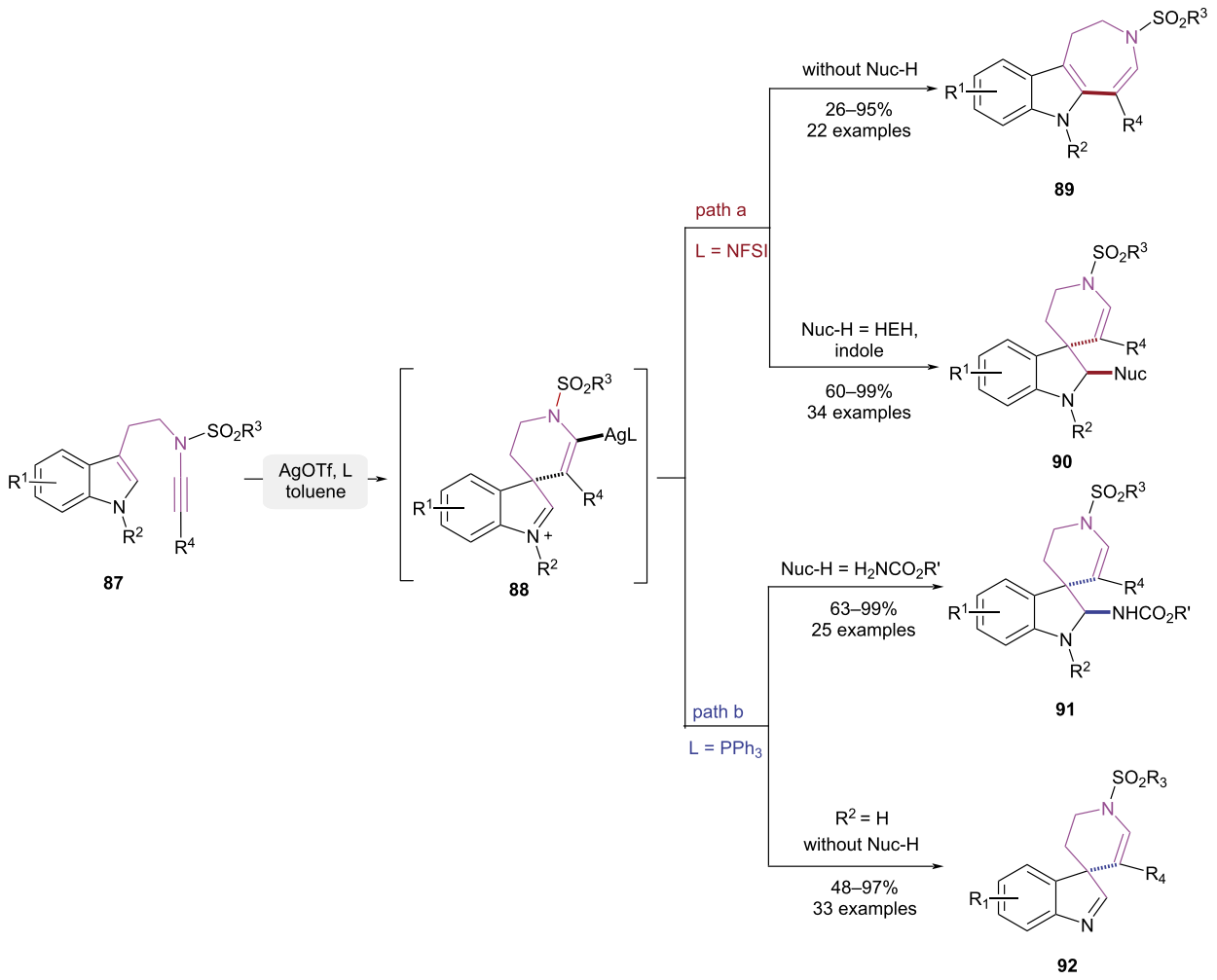

Scheme 19: Ag(I)-mediated pathway-controlled cycloisomerization of tryptamine-ynamides.

Hantzsch ester or indole as the nucleophile effectively trapped the imine intermediate **88**, preventing Wagner–Meerwein rearrangement and yielding spirocyclic indole framework **90** (Scheme 19, path a). When PPh_3 was used as the ligand and amides as nucleophiles, the spirocyclic indole framework **91** was obtained via the capture of imine intermediate **88**. When the PPh_3 was used as ligand in the absence of nucleophiles, the substrate **87** with an unprotected indole nitrogen facilitated the formation of intermediate **88**, enabling its stable isolation and subsequent affordance of the spirocyclic indole-derived imine product **92** (Scheme 19, path b). The suppression of Wagner–Meerwein rearrangement was attributed to the lower Lewis acidity of PPh_3 relative to NFSI, which emerged as the critical determinant in this reaction.

Catalyst-controlled cyclization of 1,*n*-enynes

The core function of a catalyst lies in providing a new, energetically more favorable pathway for the reaction. Different catalytic systems, with their unique physical structures, chemical compositions, and electronic properties, could form distinct intermediates or transition states with reactants, thereby fundamentally altering the reaction pathway. Therefore, many research groups have made significant contributions to the divergent synthesis of small-molecule frameworks by modulating catalyst types to steer reaction pathways.

In 2006, the Echavarren group reported an intramolecular gold-catalyzed cyclization of indole-alkynes, achieving control over the annulation pathway through modulation of Au oxidation state (Scheme 20) [30,31]. The seven-membered heterocycles **95** was formed via Au(I)-catalyzed 7-*exo*-dig cyclization of *N*-propargyl tryptamines **93** (Scheme 20, path a). However, the indoloazocines **97** was afforded by Au(III)-catalyzed 8-*endo*-dig cyclization via intermediated **96** (Scheme 20, path b). Interestingly, prolonged reaction time under Au(I) catalysis facilitated the formation of olefin intermediate **98**, which then under-

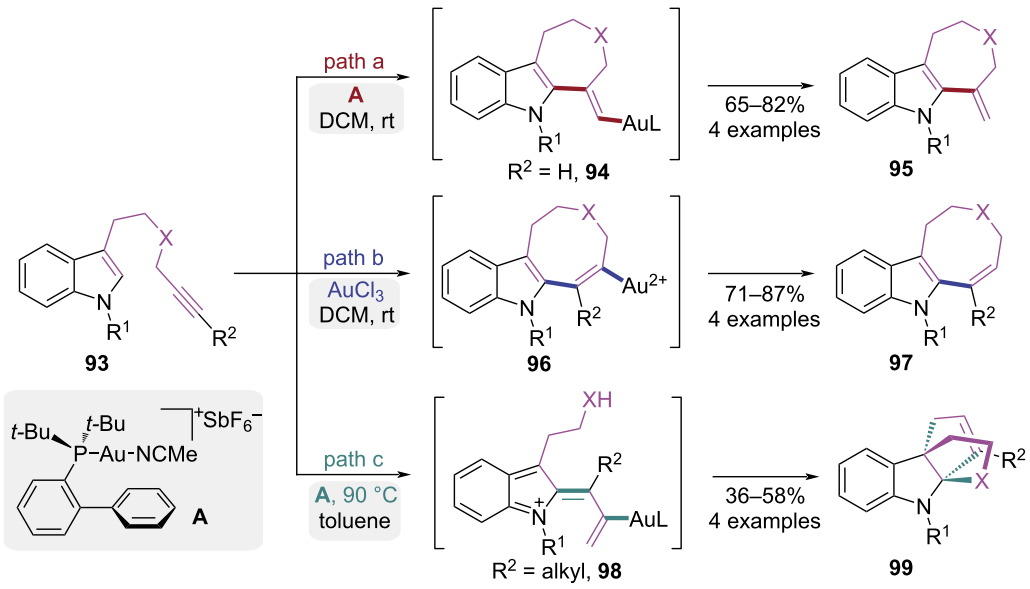

Scheme 20: Gold-catalyzed cycloisomerization of indoles with alkynes.

went further Au(I)-catalyzed transformation to afford tetracyclic products **99** (Scheme 20, path c). This allenylation reaction provided efficient access to functionalized indole derivatives by regulating catalyst systems and substituent patterns.

In 2010, the Iwasawa group established a stereoselective synthetic strategy toward bicyclo[4.3.0]nonane frameworks via geminal carbo-functionalization of 3-siloxy-1,3-dien-7-ynes (Scheme 21) [32]. A stereoselective sequence initiated by 5-*exo*-dig cyclization and Michael addition under cationic gold catalysis to generate strained bicyclic gold-carbene complex **101**, which was transformed to metastable intermediate **102** via stereospecific 1,2-alkyl migration. After protodemetalation, the bicyclo[4.3.0]nonane compounds **103** were obtained (Scheme 21, path a). Interestingly, the gold-catalyzed cyclization of *E*/*Z* mixture of **100** afforded bicyclo[4.3.0]nonanes **103** with configurations distinct from those generated through thermal Diels–Alder cycloaddition of (*Z*)-**100**. However, when

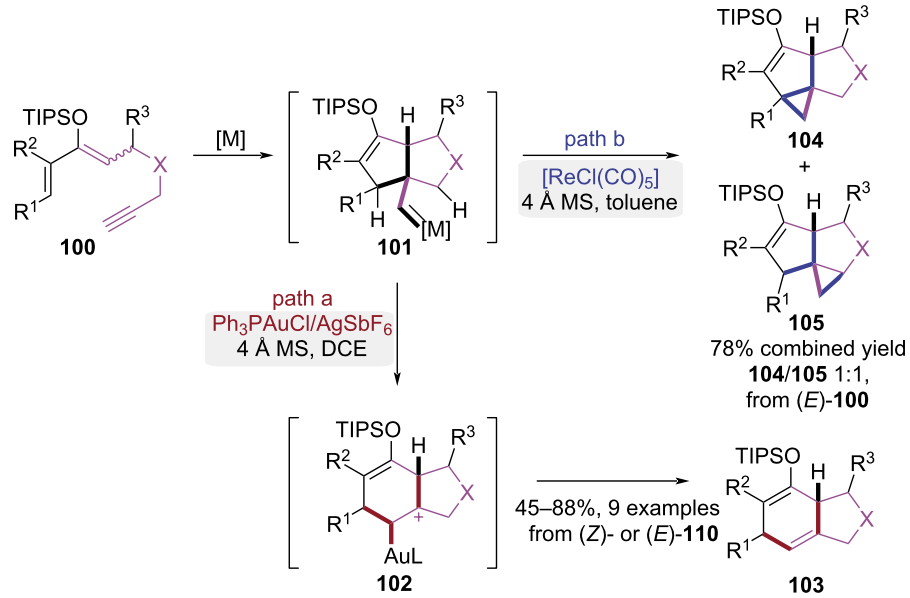

Scheme 21: Catalyst-dependent cycloisomerization of dienol silyl ethers.

[$ReCl(CO)_5$] was used as the catalyst, a regioselective C–H bond insertion pathway was observed for substrate (*E*)-**100**, leading to the formation of tricyclic products **104** and **105** (Scheme 21, path b). This strategy employed transition metal-catalyzed carbene intermediates to mediate stereoselective cyclization, affording bicyclo[4.3.0]nonane derivatives with configurations distinct from Diels–Alder adducts.

In 2013, Alami and co-workers demonstrated catalyst-dependent cycloisomerization of aromatic enynes **106** (Scheme 22) [33]. When $Ph_3PAuNTf_2$ was employed as the catalyst, a 6-*endo*-dig cyclization occurred after the alkyne was electrophilically activated, leading to the formation of aryl naphthalene derivatives **108** (Scheme 22, path a). However, when the PdI_2/dppp catalytic system was used, the reaction pathway changed significantly. The (*E*)-benzofulvene product **110** was exclusively generated through palladium-catalyzed C–H activation followed by a 5-*exo*-dig cyclization (Scheme 22, path b). This study established a general method for the divergent syntheses of phenylnaphthalenes and benzofulvenes from aromatic enyne precursors, where product selectivity was controlled by the catalytic system employed.

In 2014, Ma and co-workers disclosed a regioselective synthetic strategy for carbazole derivatives, where the directionality of alkyl migration was modulated by the choice of transition metal catalysts (Scheme 23) [34]. When the $Ph_3PAuCl/AgBF_4$ system was employed, the alkyne underwent an intramolecular

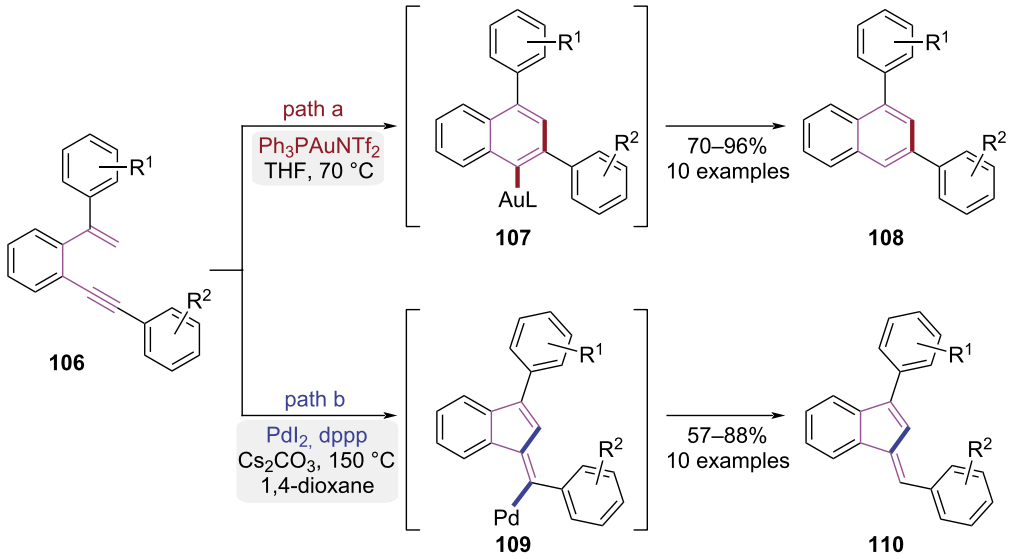

Scheme 22: Cycloisomerization of aromatic enynes governed by catalyst.

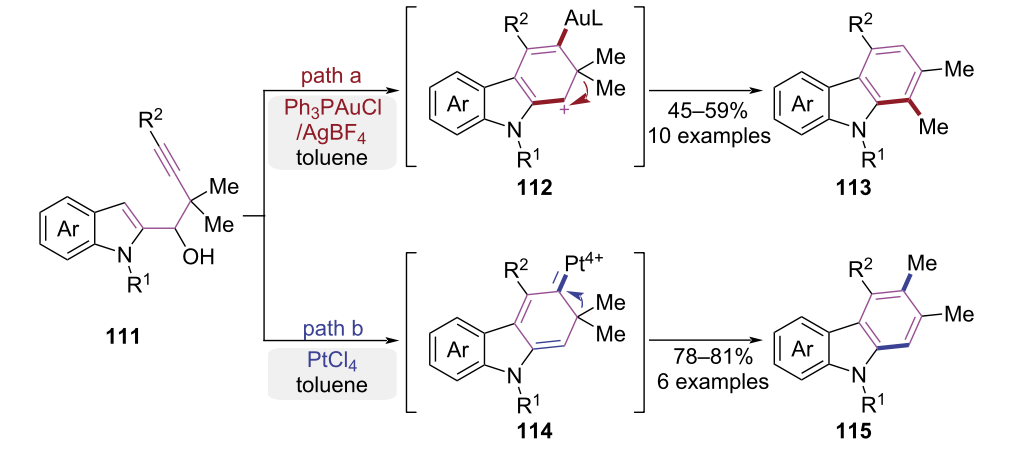

Scheme 23: Catalyst-dependent 1,2-migration in cyclization of 1-(indol-2-yl)-3-alkyn-1-ols.

nucleophilic attack by the C-3 position of indole to form a carbocation intermediate **112**. This intermediate underwent a Wagner–Meerwein-type 1,2-alkyl migration, ultimately leading to the construction of carbazole **113** (Scheme 23, path a). In contrast, the utilization of $PtCl_4$ as a catalyst induced a distinct reaction pathway involving a platinum carbene intermediate **114**. This intermediate underwent a different 1,2-alkyl shift, leading to the selective formation of carbazole derivative **115** (Scheme 23, path b). Collectively, these findings demonstrate that the choice of transition metal catalyst critically governs the regioselectivity of 1,2-alkyl migration processes, thereby providing a strategic approach for the efficient synthesis of structurally diverse polysubstituted carbazoles.

In 2015, Menon et al. developed a pathway-controllable gold-catalyzed cycloisomerization for the divergent syntheses of 2-sulfonylmethylpyrroles and 1,2-dihydropyridine derivatives (Scheme 24) [35]. The substrate **116** was initially transformed to a β-allene imine intermediate **117** via a gold-catalyzed propargyl-Claisen rearrangement. When the gold(I) complex [JohnPhosAu(CH_3CN)SbF_6] was employed, a subsequent 5-*exo*-dig cyclization followed by aromatization steps occurred, ultimately affording the 2-sulfonylmethylpyrrole **118** (Scheme 24, path a). Conversely, utilization of the Ph_3PAuCl/$AgSbF_6$ catalytic system induced a different reaction pathway. Tautomerization of intermediate **117** produced an *aza*-triene species, which underwent a 6π-*aza*-electrocyclization to afford 1,2-dihydropyridine derivatives **119** (Scheme 24, path b). This work established a divergent cycloisomerization of *N*-propargyl-*N*-vinyl sulfonamides governed by catalyst, delivering structurally distinct 2-sulfonylmethylpyrroles and dihydropyridine products with high selectivity.

In 2015, the Sanz group developed a gold(I)-catalyzed regioselective cyclization strategy leading to divergent syntheses of indenes and polycyclic compounds (Scheme 25) [36]. The sub-

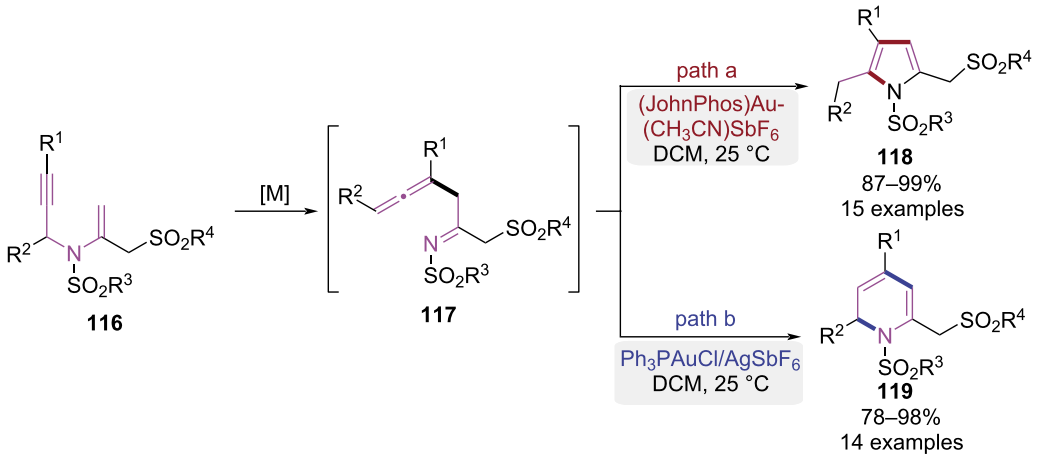

Scheme 24: Gold-catalyzed cycloisomerization of *N*-propargyl-*N*-vinyl sulfonamides.

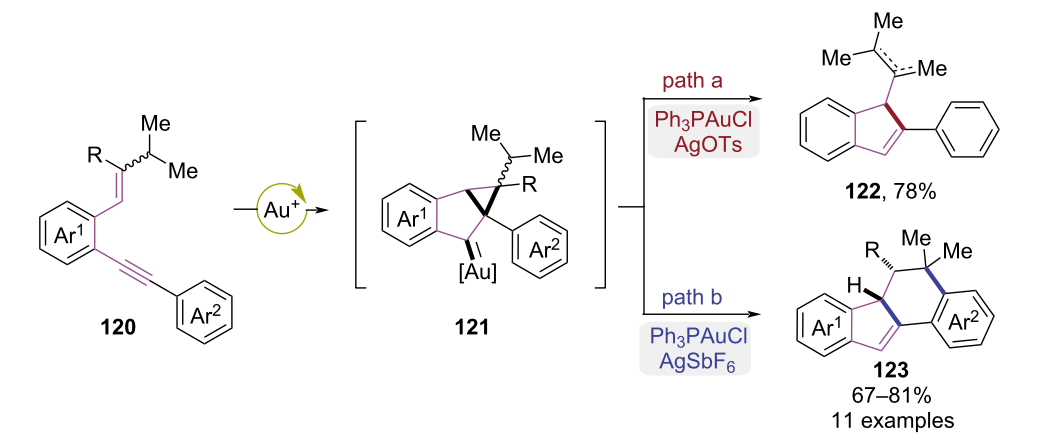

Scheme 25: Gold(I)-mediated enantioselective cycloisomerizations of *ortho*-(alkynyl)styrenes.

strates **120** featuring an isopropyl substituent was transformed to a carbene intermediate **121** via a gold-catalyzed 5-*endo*-dig cyclization. When the $Ph_3PAuCl/AgOTs$ system was used, indene derivative **122** was obtained by deprotonation (Scheme 25, path a). In contrast, 1,2-hydrogen migration was favored using the $Ph_3PAuCl/AgSbF_6$ system, ultimately resulting in the formation of dihydrobenzo[*a*]fluorenes **123** via Friedel–Crafts alkylation (Scheme 25, path b).

In 2018, the Shi research group developed an innovative intramolecular cyclization strategy using 1,6-enynes as substrates for the synthesis of 1,2-dihydroquinoline derivatives (Scheme 26) [37]. Selective synthesis of 1,2-dihydroquinolines bearing cyclobutene or methylenecyclopropane frameworks was enabled by precise tuning of gold and silver catalysts. The intermediate **125** was generated via gold(I)-catalyzed nucleophilic cyclization, which underwent intramolecular rearrangement and subsequent ring expansion process to yield the product **126** (Scheme 26, path a). In contrast, a similar nucleophilic cyclization of the alkene was triggered by the silver catalyst, which preserved the intact methylenecyclopropane skeleton and yielded product **128** (Scheme 26, path b). The metal-dependent selectivity was attributed to differences in alkyne activation modes between gold and silver. The gold catalyst induced linear coordination of the alkyne to generate a carbenoid species, while silver ions favored formation of a π-activated intermediate.

In 2018, the Liu group demonstrated a pathway-controlled approach using tryptamine ynamides bearing Michael acceptor moieties as substrates (Scheme 27) [38,39]. Under strong Brønsted acid catalysis, protonation of the carbonyl group was

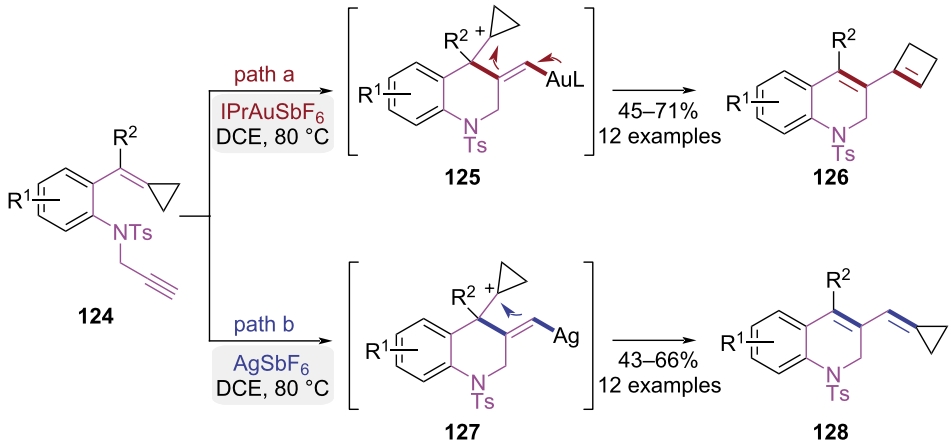

Scheme 26: Catalyst-controlled intramolecular cyclization of 1,7-enynes.

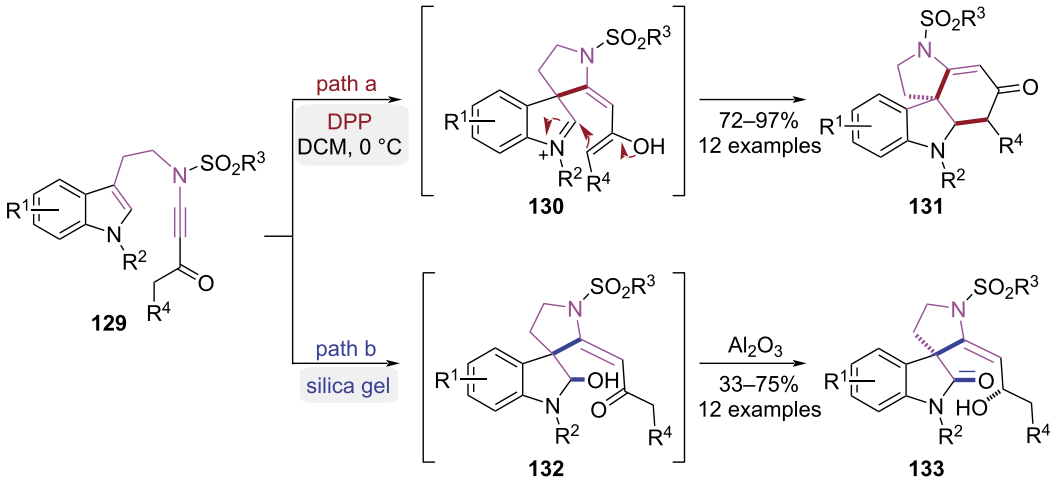

Scheme 27: Brønsted acid-catalyzed cycloisomerizations of tryptamine ynamides.

achieved, which facilitated a Michael addition between the electron-rich indole C3-position and the activated ynamide. This sequence resulted in the formation of spiroindoleninium intermediate **130** (Scheme 27, path a). Subsequent intramolecular Mannich cyclization proceeded, yielding the 1*H*-pyrrolo[2,3-*d*]carbazole derivatives **131**. When silica gel was utilized as the catalytic medium, the same Michael addition happened to generate the spiroindoleninium intermediate. This transient species was subsequently trapped by water physisorbed in the silica gel, forming hemiaminal adduct **132**. A 1,5-hydride shift was then mediated by Al_2O_3, ultimately affording the spiro[indoline-3,3′-pyrrolidin]-2-one derivatives **133** (Scheme 27, path b). Through precise acid catalyst selection, the reaction pathways were strategically modulated to afford efficient construction of both 1*H*-pyrrolo[2,3-*d*]carbazole derivatives and spiro[indoline-3,3'-pyrrolidin]-2-one derivatives.

In 2019, the Ye group reported a copper-catalyzed stereospecific tandem cyclization of indolyl homopropargyl amides for the construction of bridged aza[*n*.2.1] frameworks (Scheme 28) [40]. The copper catalyst, acting as a σ,π-dual activator, induced a 5-*endo*-dig cyclization to form a vinylcopper intermediate **135**. Subsequently, a protodemetalation process first occurred, followed by an intramolecular Friedel–Crafts alkylation, ultimately resulting in the assembly of product **136** (Scheme 28, path a). Notably, a systematic screening of transition-metal catalysts revealed that structurally distinct products were obtainable from the same substrate under gold catalysis (Scheme 28, path b). When $IPrAuNTf_2$ was used as the catalyst, product **138** was obtained via a 6-*exo*-dig cyclization, whereas when $Ph_3PAuNTf_2$ was employed as the catalyst, product **139** was exclusively obtained through a hydroarylation/isomerization/elimination pathway. This work disclosed an unprecedented copper-catalyzed tandem process initiated by *endo*-cyclization of indolyl homopropargyl amides, enabling atom-economical synthesis of therapeutically significant bridged aza[*n*.2.1] skeletons.

Angle strain and configuration-controlled cyclization of 1,*n*-enynes

In cyclization reactions, angle strain and configuration exert pronounced effects on reaction pathways. These substrate-specific geometric parameters directly dictate transition state formation during ring closure. Recent advances demonstrated that deliberate manipulation of angle strain and configuration enabled divergent skeletal outcomes under identical reaction conditions.

In 2016, the Liu group achieved unconventional Au(I)-catalyzed 6-*endo*-trig cyclization by modulating the angle strain of the enol ether (Scheme 29) [41]. In previous studies [42], propargylic vinyl ethers **140** underwent Au(I)-catalyzed propargyl-Claisen rearrangement to form an allene intermediate **141**, which subsequently underwent 5-*exo*-trig cyclization to construct polysubstituted furan compounds **142**. Liu et al. discovered that the regioselectivity of cyclization could be completely altered by introducing a cyclic structure to modify the bond angle of the enol ether, exclusively yielding furopyran de-

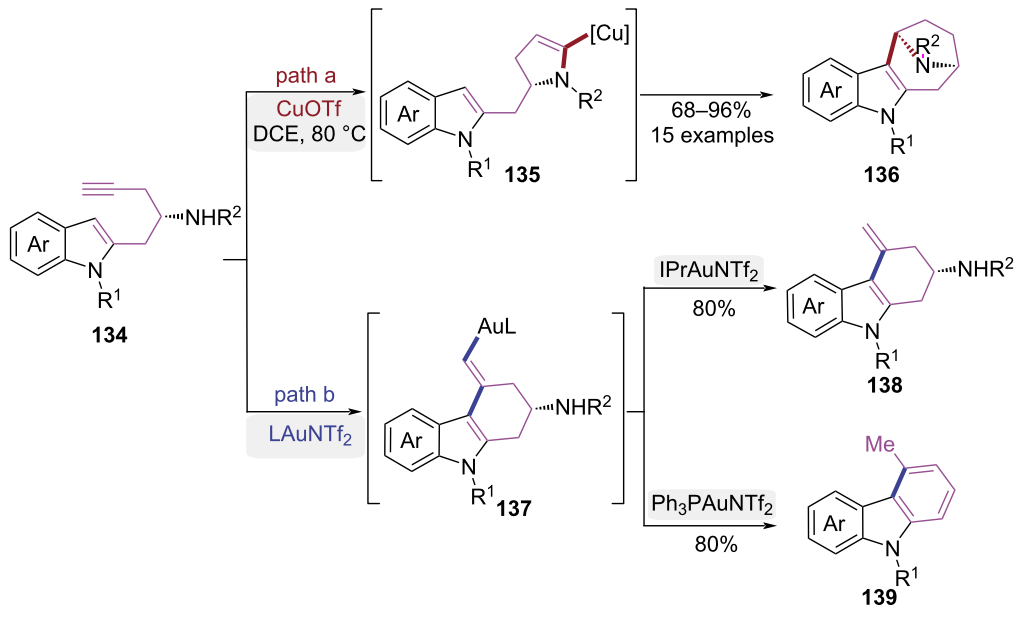

Scheme 28: Catalyst-controlled cyclization of indolyl homopropargyl amides.

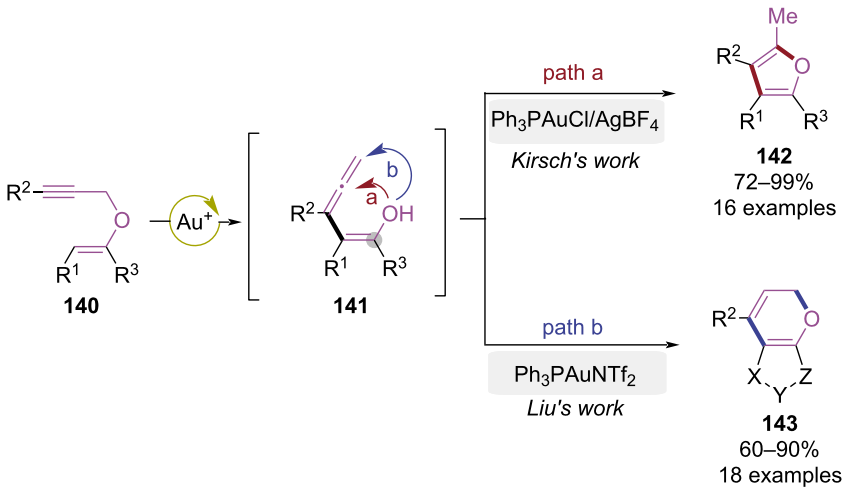

Scheme 29: Angle strain-dominated 6-*endo*-trig cyclization of propargyl vinyl ethers.

rivative **143** via 6-*endo*-trig cyclization. This pioneering study altered Au(I)-catalyzed 5-*exo*-trig cyclization preference through angle strain modulation, establishing an efficient strategy for the synthesis of furopyran derivatives.

In 2018, Su and co-workers developed a gold-catalyzed cyclization strategy for the synthesis of 1,2- and 2,3-fused quinazolinones, which was controlled by the angle strain of a key carbon atom in the substrate (Scheme 30) [43]. Experimental results showed intramolecular cyclization depended on the hybridization state of the carbon adjacent to quinazolinone's amino group. When this carbon atom was in a sp^2 hybridization state, the C3 position of the indole attacked the inner side of the triple bond under the action of a gold catalyst, leading to a 6-*exo*-dig cyclization to yield 1,2-fused quinazolinones **146** (Scheme 30, path a). When the carbon atom was in a sp^3 hybridization state, the C3 position of the indole attacked the outer side of the triple bond, resulting in a 7-*endo*-dig cyclization to produce 2,3-fused quinazolinones **148** (Scheme 30, path b). This hybridization-controlled annulation strategy enabled efficient access to rutaecarpine core structures, demonstrating notable utility in the synthesis of this biologically significant alkaloid.

In 2020, Sanz and co-workers developed a gold(I)-catalyzed strategy achieving stereoselective construction of alkylidenecyclopentenes and benzene derivatives (Scheme 31) [44].

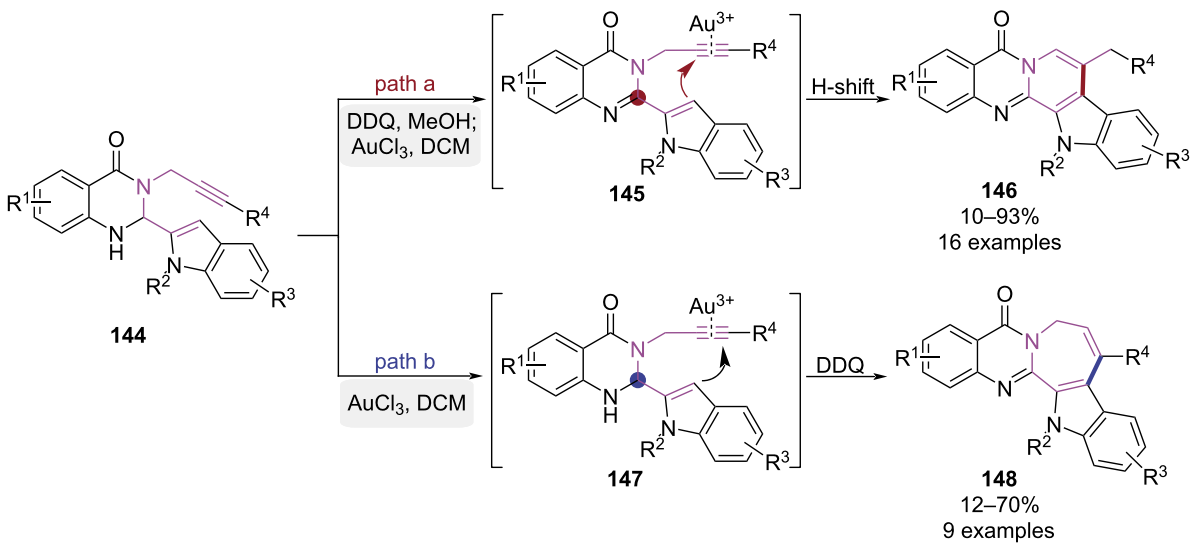

Scheme 30: Angle strain-controlled cycloisomerization of alkyn-tethered indoles.

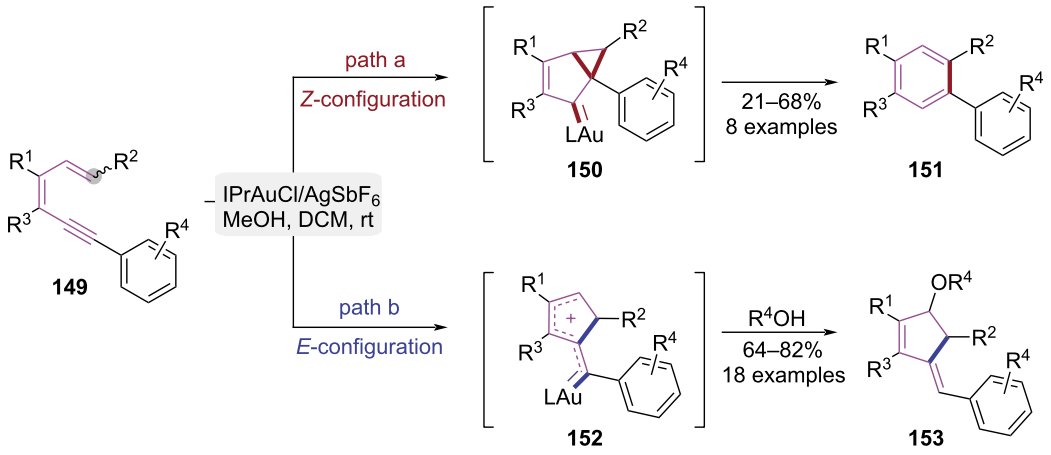

Scheme 31: Geometrical isomeration-dependent cycloisomerization of 1,3-dien-5-ynes.

Notably, this study pioneered the regio- and stereoselective 5-*exo*-dig alkoxycyclization of 1,5-enynes via gold(I) catalysis. The cyclization mode was controlled by the configuration of the double bond in the substrate. In *Z*-configured substrates, steric constraints promoted 5-*endo*-dig cyclization, generating bicyclo[3.1.0]hexane intermediate **150**. Subsequent aromatization and ring expansion afforded benzene derivatives **151** (Scheme 31, path a). Conversely, *E*-configured substrates underwent gold-catalyzed alkyne activation, triggering terminal alkene 5-*exo*-dig cyclization to form carbocationic intermediate **152**. Alcohols nucleophilically trapped intermediate **152**, affording alkylidenecyclopentenes **153** with high diastereoselectivity (Scheme 31, path b). By clarifying *E*/*Z*-configuration-dependent cyclization mechanisms, this work introduced the gold(I)-catalyzed 5-*exo*-dig cyclization of 1,3-dien-5-ynes, gaining insights into regioselective control principles for gold catalysis.

Temperature-controlled cyclization of 1,*n*-enynes

Temperature, a pivotal thermodynamic parameter, not only governs reaction kinetics but also determines reaction pathways. Typically, kinetic product formation is favored at lower temperatures via pathways with reduced activation barriers, while thermodynamic products dominate under elevated thermal conditions. Recent advancements have yielded novel cyclization methodologies enabling pathway control through precise temperature regulation. In 2016, the Liao group reported a temperature-regulated strategy enabling the controlled synthesis of nitrogen-containing heterocycles via reaction pathway modulation (Scheme 32) [45]. Under catalysis of $Cu(OAc)_2$ and HOAc, the substrate was subjected to decyanation and followed copper-promoted [2 + 2] cycloaddition that yielded cyclobutene intermediate **155**. Carbocation rearrangement and hydrogen elimination then occurred, affording 3-azabicyclo[4.1.0]hepta-2,4-diene

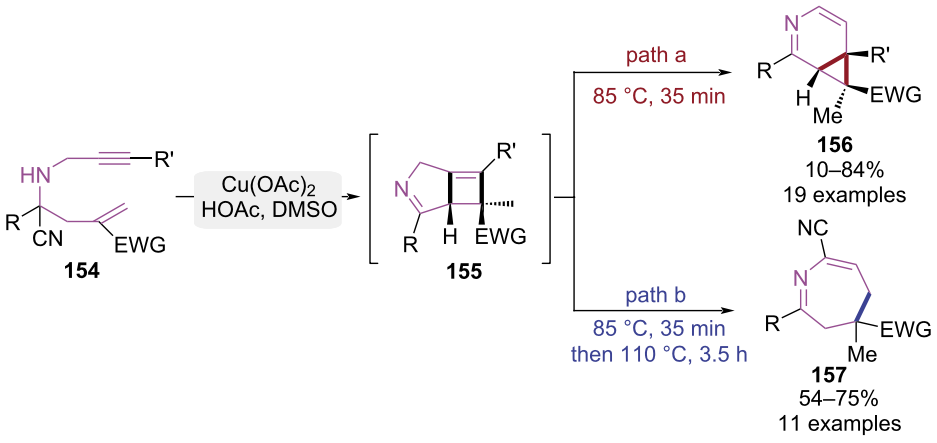

Scheme 32: Temperature-controlled cyclization of 1,7-enynes.

derivatives **156**. In contrast, when the temperature was raised to 110 °C, intermediate **155** underwent a 6π electrocyclic ring-opening, which was trapped by in situ-generated cyanide ions to form 4,5-dihydro-3*H*-azepines **157**.

In 2021, the Zhou group reported a nickel-catalyzed cyclization strategy using *N*-(*o*-ethynylaryl)acrylamides as substrates, achieving divergent access to dihydrocyclobuta[*c*]quinolin-3-ones and benzo[*b*]azocin-2-ones (Scheme 33) [46]. The reaction pathway was governed by thermal modulation, wherein 60 °C initiated nickel-mediated intramolecular [2 + 2] cycloaddition to form dihydrocyclobuta[*c*]quinolin-3-one framework **164**. Conversely, when the temperature was elevated to 140 °C, thermal ring-expansion of the four-membered intermediate was induced through C–C bond cleavage/reorganization, affording the eight-membered benzo[*b*]azocin-2-one product **165**. This methodology was distinguished by operational simplicity, high efficiency, and scalable synthesis. Moreover, temperature modulation achieved rapid access to cyclic compounds with distinct ring sizes.

In 2022, biphenyl-embedded 1,3,5-trien-7-ynes were employed by the García group to construct borylated polycyclic products via a temperature-controlled boracyclization reaction mediated by BCl_3 (Scheme 34) [47]. At 0 °C, BCl_3-mediated activation of the alkyne triggered an intramolecular [2 + 2] cycloaddition, generating a boron-chlorine intermediate **167**. Subsequent treatment with triethylamine/pinacol induced ring closure, affording the phenanthreno[1,3-*b*]cyclobutane borate ester **168**. In contrast, when the temperature was elevated to 60 °C, the reac-

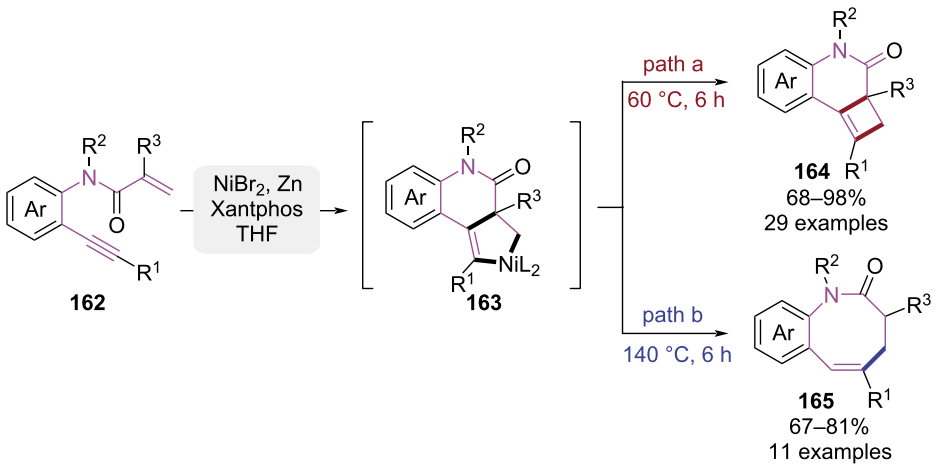

Scheme 33: Cycloisomerizations of *n*-(*o*-ethynylaryl)acrylamides through temperature modulation.

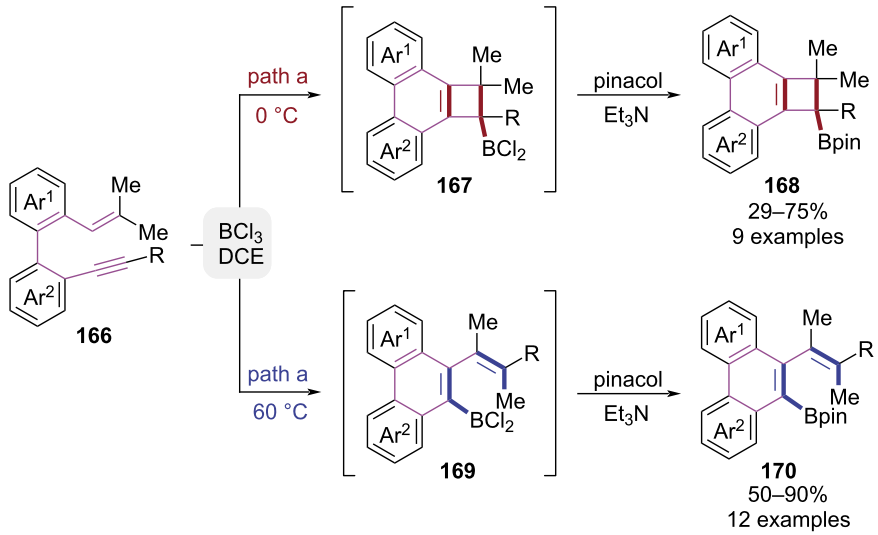

Scheme 34: Temperature-controlled boracyclization of biphenyl-embedded 1,3,5-trien-7-ynes.

tion underwent a BCl_3-driven skeletal rearrangement involving methyl migration and alkyne cleavage to form the boronated phenanthrene framework **170**. It is worth mentioning that a unique skeleton rearrangement, supported by DFT calculations, was proposed in this work, which was unprecedented in $BiCl_3$-promoted cyclization.

Conclusion

This comprehensive review has systematically delineated the conceptual framework and innovative applications of pathway economy in the cyclization chemistry of 1,*n*-enynes. The strategic integration of pathway economy principles not only redefines reaction design paradigms but also establishes a sustainable platform for precision organic synthesis. By judiciously modulating reaction parameters – including solvent polarity, catalyst architecture, ligand electronic effects, and substrate strain effects – chemists can achieve unprecedented control over reaction pathways. This approach enables divergent access to complex molecular architectures from a unified substrate platform, as exemplified by recent breakthroughs in polycyclic skeleton construction and stereo-divergent cyclization.

The implementation of pathway economy fosters significant advancements in green chemistry by minimizing synthetic steps, reducing waste generation, and enhancing atom economy. Notably, this strategy has demonstrated remarkable potential in pharmaceutical synthesis, where the rapid generation of molecular diversity from simple precursors is paramount. Looking forward, the fusion of pathway economy with machine learning algorithms and high-throughput experimentation holds promise for accelerating reaction optimization. Furthermore, expanding this concept to other reaction manifolds – such as electrocyclic processes and photoredox catalysis – may uncover new avenues for molecular innovation. The pursuit of pathway-economical synthesis represents a paradigm shift toward sustainable and intellectually rewarding synthetic methodologies, with far-reaching implications for both fundamental science and industrial applications.

Funding

The authors are grateful to the Joint Fund for Regional Innovation and Development, National Natural Science Foundation of China (U23A20525), National Natural Science Foundation of China (22277082), Educational Department of Liaoning Province (LJ232510163001), and Liaoning Provincial Foundation of Natural Science (2025-BS-0753) for financial support. The authors acknowledge the Program for the Innovative Research Team of the Ministry of Education and the Program for the Liaoning Innovative Research Team in University.

Author Contributions

Hezhen Han: investigation; writing – original draft. Wenjie Mao: investigation. Bin Lin: validation. Maosheng Cheng: funding acquisition; supervision. Lu Yang: visualization; writing – review & editing. Yongxiang Liu: conceptualization; writing – review & editing.

ORCID® iDs

Lu Yang - https://orcid.org/0000-0001-9727-4849

Data Availability Statement

Data sharing is not applicable as no new data was generated or analyzed in this study.

References

1. Trost, B. M. *Science* **1991,** *254,* 1471–1477. doi:10.1126/science.1962206
2. Trost, B. M. *Angew. Chem., Int. Ed. Engl.* **1995,** *34,* 259–281. doi:10.1002/anie.199502591
3. Wender, P. A.; Croatt, M. P.; Witulski, B. *Tetrahedron* **2006,** *62,* 7505–7511. doi:10.1016/j.tet.2006.02.085
4. Wender, P. A. *Nat. Prod. Rep.* **2014,** *31,* 433–440. doi:10.1039/c4np00013g
5. Burns, N. Z.; Baran, P. S.; Hoffmann, R. W. *Angew. Chem., Int. Ed.* **2009,** *48,* 2854–2867. doi:10.1002/anie.200806086
6. Hayashi, Y. *Chem. Sci.* **2016,** *7,* 866–880. doi:10.1039/c5sc02913a
7. Hayashi, Y. *J. Org. Chem.* **2021,** *86,* 1–23. doi:10.1021/acs.joc.0c01581
8. Liu, Y.; Guo, J.; Liu, Y.; Wang, X.; Wang, Y.; Jia, X.; Wei, G.; Chen, L.; Xiao, J.; Cheng, M. *Chem. Commun.* **2014,** *50,* 6243–6245. doi:10.1039/c4cc00464g
9. Guo, J.; Peng, X.; Wang, X.; Xie, F.; Zhang, X.; Liang, G.; Sun, Z.; Liu, Y.; Cheng, M.; Liu, Y. *Org. Biomol. Chem.* **2018,** *16,* 9147–9151. doi:10.1039/c8ob02582g
10. Milián, A.; García-García, P.; Pérez-Redondo, A.; Sanz, R.; Vaquero, J. J.; Fernández-Rodríguez, M. A. *Org. Lett.* **2020,** *22,* 8464–8469. doi:10.1021/acs.orglett.0c03067
11. Mutra, M. R.; Dhandabani, G. K.; Li, J.; Wang, J.-J. *Chem. Commun.* **2020,** *56,* 2051–2054. doi:10.1039/c9cc07820g
12. Wang, Z.; Chen, J.; Yu, L.; Zhang, C.; Rao, W.; Chan, P. W. H. *Org. Lett.* **2024,** *26,* 2635–2640. doi:10.1021/acs.orglett.4c00705
13. Rai, A.; Bajpai, P.; Gamidi, R. K.; Vanka, K.; Das, U. *Org. Lett.* **2025,** *27,* 5429–5434. doi:10.1021/acs.orglett.5c01396
14. Shibata, T.; Ueno, Y.; Kanda, K. *Synlett* **2006,** 0411–0414. doi:10.1055/s-2006-926261
15. Liu, Y.; Jin, S.; Wang, Y.; Cui, S.; Peng, X.; Niu, Y.; Du, C.; Cheng, M. *Chem. Commun.* **2016,** *52,* 6233–6236. doi:10.1039/c6cc01770c
16. Peng, X.; Zhu, L.; Hou, Y.; Pang, Y.; Li, Y.; Fu, J.; Yang, L.; Lin, B.; Liu, Y.; Cheng, M. *Org. Lett.* **2017,** *19,* 3402–3405. doi:10.1021/acs.orglett.7b01358
17. Liu, C.; Sun, Z.; Xie, F.; Liang, G.; Yang, L.; Li, Y.; Cheng, M.; Lin, B.; Liu, Y. *Chem. Commun.* **2019,** *55,* 14418–14421. doi:10.1039/c9cc05667j
18. Davenel, V.; Nisole, C.; Fontaine-Vive, F.; Fourquez, J.-M.; Chollet, A.-M.; Michelet, V. *J. Org. Chem.* **2020,** *85,* 12657–12669. doi:10.1021/acs.joc.0c01841

19. Ito, M.; Takaki, A.; Okamura, M.; Kanyiva, K. S.; Shibata, T. *Eur. J. Org. Chem.* **2021,** 1688–1692. doi:10.1002/ejoc.202001643
20. Lin, X.-T.; Zhao, C.; Wang, D.-R.; Wu, G.-C.; Chen, G.-S.; Chen, S.-J.; Ren, H.; Deng, D.-S.; Xu, Y.-B.; Hu, X.-W.; Liu, Y.-L. *Adv. Synth. Catal.* **2022,** *364,* 890–896. doi:10.1002/adsc.202101232
21. Zhu, J.; Li, J.; Zhang, L.; Sun, S.; Wang, Z.; Li, X.; Yang, L.; Cheng, M.; Lin, B.; Liu, Y. *J. Org. Chem.* **2023,** *88,* 5483–5496. doi:10.1021/acs.joc.2c03104
22. Zhu, J.; Li, J.; Zhang, L.; Sun, S.; Yang, L.; Fu, J.; Sun, H.; Cheng, M.; Lin, B.; Liu, Y. *J. Org. Chem.* **2023,** *88,* 10586–10598. doi:10.1021/acs.joc.3c00604
23. Barabé, F.; Levesque, P.; Sow, B.; Bellavance, G.; Bétournay, G.; Barriault, L. *Pure Appl. Chem.* **2013,** *85,* 1161–1173. doi:10.1351/pac-con-13-01-02
24. Rao, W.; Sally; Koh, M. J.; Chan, P. W. H. *J. Org. Chem.* **2013,** *78,* 3183–3195. doi:10.1021/jo400121j
25. Ding, D.; Mou, T.; Feng, M.; Jiang, X. *J. Am. Chem. Soc.* **2016,** *138,* 5218–5221. doi:10.1021/jacs.6b01707
26. Zhang, J.-h.; Wei, Y.; Shi, M. *Org. Chem. Front.* **2018,** *5,* 2980–2985. doi:10.1039/c8qo00907d
27. Liang, G.; Ji, Y.; Liu, H.; Pang, Y.; Zhou, B.; Cheng, M.; Liu, Y.; Lin, B.; Liu, Y. *Adv. Synth. Catal.* **2020,** *362,* 192–205. doi:10.1002/adsc.201901175
28. Liang, G.; Pang, Y.; Ji, Y.; Zhuang, K.; Li, L.; Xie, F.; Yang, L.; Cheng, M.; Lin, B.; Liu, Y. *J. Org. Chem.* **2020,** *85,* 3010–3019. doi:10.1021/acs.joc.9b02839
29. Chen, Y.; Wang, Z.; Zhao, W.; Sun, S.; Yang, L.; Zhang, J.; Zhang, D.; Cheng, M.; Lin, B.; Liu, Y. *Chem. Commun.* **2022,** *58,* 3051–3054. doi:10.1039/d1cc07298f
30. Ferrer, C.; Echavarren, A. M. *Angew. Chem., Int. Ed.* **2006,** *45,* 1105–1109. doi:10.1002/anie.200503484
31. Ferrer, C.; Amijs, C. H. M.; Echavarren, A. M. *Chem. – Eur. J.* **2007,** *13,* 1358–1373. doi:10.1002/chem.200601324
32. Kusama, H.; Karibe, Y.; Onizawa, Y.; Iwasawa, N. *Angew. Chem., Int. Ed.* **2010,** *49,* 4269–4272. doi:10.1002/anie.201001061
33. Aziz, J.; Frison, G.; Le Menez, P.; Brion, J.-D.; Hamze, A.; Alami, M. *Adv. Synth. Catal.* **2013,** *355,* 3425–3436. doi:10.1002/adsc.201300746
34. Qiu, Y.; Ma, D.; Kong, W.; Fu, C.; Ma, S. *Org. Chem. Front.* **2014,** *1,* 62–67. doi:10.1039/c3qo00006k
35. Undeela, S.; Thadkapally, S.; Nanubolu, J. B.; Singarapu, K. K.; Menon, R. S. *Chem. Commun.* **2015,** *51,* 13748–13751. doi:10.1039/c5cc04871k
36. Sanjuán, A. M.; Rashid, M. A.; García-García, P.; Martínez-Cuezva, A.; Fernández-Rodríguez, M. A.; Rodríguez, F.; Sanz, R. *Chem. – Eur. J.* **2015,** *21,* 3042–3052. doi:10.1002/chem.201405789
37. Jiang, B.; Wei, Y.; Shi, M. *Org. Chem. Front.* **2018,** *5,* 2091–2097. doi:10.1039/c8qo00358k
38. Wang, Y.; Lin, J.; Wang, X.; Wang, G.; Zhang, X.; Yao, B.; Zhao, Y.; Yu, P.; Lin, B.; Liu, Y.; Cheng, M. *Chem. – Eur. J.* **2018,** *24,* 4026–4032. doi:10.1002/chem.201705189
39. Wang, Y.; Wang, X.; Lin, J.; Yao, B.; Wang, G.; Zhao, Y.; Zhang, X.; Lin, B.; Liu, Y.; Cheng, M.; Liu, Y. *Adv. Synth. Catal.* **2018,** *360,* 1483–1492. doi:10.1002/adsc.201701576
40. Tan, T.-D.; Zhu, X.-Q.; Bu, H.-Z.; Deng, G.; Chen, Y.-B.; Liu, R.-S.; Ye, L.-W. *Angew. Chem., Int. Ed.* **2019,** *58,* 9632–9639. doi:10.1002/anie.201904698
41. Jin, S.; Jiang, C.; Peng, X.; Shan, C.; Cui, S.; Niu, Y.; Liu, Y.; Lan, Y.; Liu, Y.; Cheng, M. *Org. Lett.* **2016,** *18,* 680–683. doi:10.1021/acs.orglett.5b03641
42. Suhre, M. H.; Reif, M.; Kirsch, S. F. *Org. Lett.* **2005,** *7,* 3925–3927. doi:10.1021/ol0514101
43. Kong, X.-F.; Zhan, F.; He, G.-X.; Pan, C.-X.; Gu, C.-X.; Lu, K.; Mo, D.-L.; Su, G.-F. *J. Org. Chem.* **2018,** *83,* 2006–2017. doi:10.1021/acs.joc.7b02956
44. Virumbrales, C.; Suárez-Pantiga, S.; Marín-Luna, M.; Silva López, C.; Sanz, R. *Chem. – Eur. J.* **2020,** *26,* 8443–8451. doi:10.1002/chem.202001296
45. Xu, Q.-Q.; Hou, Q.-L.; Liu, W.; Wang, H.-J.; Liao, W.-W. *Org. Lett.* **2016,** *18,* 3854–3857. doi:10.1021/acs.orglett.6b01864
46. Li, Q.; Cai, Y.; Hu, Y.; Jin, H.; Chen, F.; Liu, Y.; Zhou, B. *Chem. Commun.* **2021,** *57,* 11657–11660. doi:10.1039/d1cc04750g
47. Milián, A.; Fernández-Rodríguez, M. A.; Merino, E.; Vaquero, J. J.; García-García, P. *Angew. Chem., Int. Ed.* **2022,** *61,* e202205651. doi:10.1002/anie.202205651

License and Terms

BEILSTEIN JOURNAL OF ORGANIC CHEMISTRY

Recent advances in Norrish–Yang cyclization and dicarbonyl photoredox reactions for natural product synthesis

Peng-Xi Luo, Jin-Xuan Yang, Shao-Min Fu* and Bo Liu*

Review

Open Access

Address:
College of Chemistry, Sichuan University, 29 Wangjiang Rd., Chengdu, Sichuan 610064, China

Email:
Shao-Min Fu* - fsm09@aliyun.com; Bo Liu* - chembliu@scu.edu.cn

* Corresponding author

Keywords:
dicarbonyls; natural product; Norrish–Yang cyclization; photoredox; total synthesis

Beilstein J. Org. Chem. **2025,** *21,* 2315–2333.
https://doi.org/10.3762/bjoc.21.177

Received: 30 July 2025
Accepted: 07 October 2025
Published: 30 October 2025

This article is part of the thematic issue "Concept-driven strategies in target-oriented synthesis".

Guest Editor: C. Li

Abstract

In recent years, the Norrish–Yang cyclization and related photoredox reactions of dicarbonyls have been extensively utilized in natural product synthesis. This review summarizes the latest advancements in these reactions for constructing terpenoids, alkaloids, and antibiotics. Through Norrish–Yang cyclization, dicarbonyls (e.g., 1,2-diketones and α-keto amides) can efficiently construct sterically hindered ring structures, which can further undergo ring-opening or rearrangement reaction to assemble complex molecular frameworks. Additionally, quinone photoredox reactions involving single-electron transfer (SET) processes provide novel strategies for the stereoselective synthesis of useful structures such as spiroketals. This review, drawing on examples from recently reported natural product syntheses, elaborates on reaction mechanisms, factors governing regioselectivity and stereoselectivity, and the impact of substrate structures on reaction pathways. These reactions not only serve as robust tools for the streamlined synthesis of natural products but also establish a solid foundation for subsequent pharmaceutical investigations.

Introduction

In the 1930s, Norrish documented the photodecomposition of aldehydes and ketones [1-3]. These studies revealed distinct reaction types, with the Norrish type II reaction being one of the most extensively characterized. The mechanism underlying the Norrish type II reaction proceeds via the following steps (Scheme 1a): photoexcitation of carbonyl compound **A** generates an excited singlet state, which undergoes intersystem crossing (ISC) to form the excited triplet state **B**. An intramolecular 1,5-hydrogen atom transfer (HAT) then ensues, producing the 1,4-diradical **C**, which can be converted into diverse products such as alkenes and enols (Scheme 1a). Notably, the 1,4-diradical intermediate is also capable of cyclization through radical coupling to form cyclobutanol **D**, a process systematically expanded upon by Yang's group at the University of Chicago [4], which later became known as the Norrish–Yang cyclization. In recent years, dicarbonyls, specifically 1,2-di-

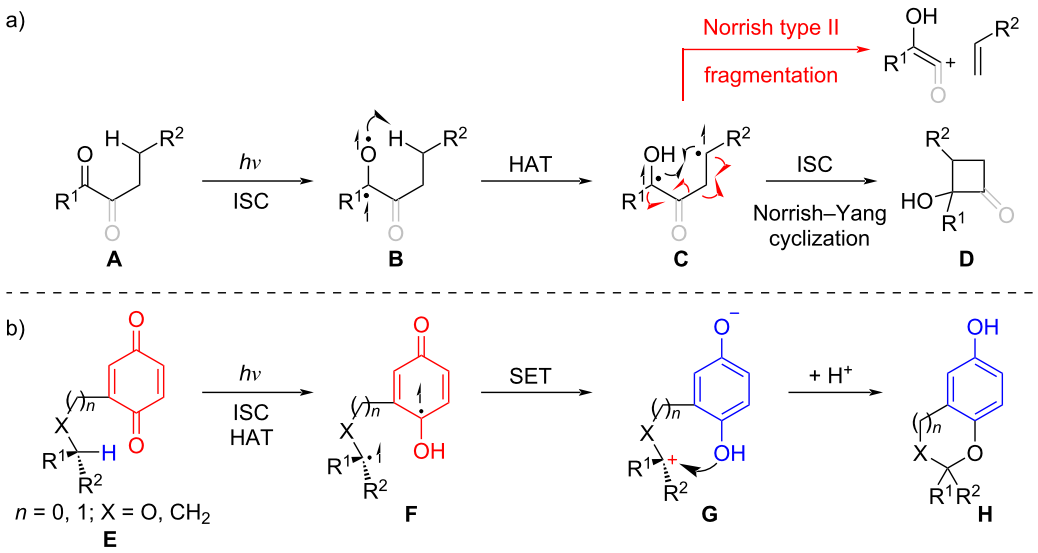

Scheme 1: a) The mechanism of Norrish type II reaction and Norrish–Yang cyclization; b) The mechanism of the dicarbonyls photoredox reaction.

ketones, α-keto esters, α-keto amides, 1,4-quinones, and 1,2-quinones in this context, have emerged as versatile substrates in Norrish–Yang cyclizations, finding widespread application in natural products synthesis. Compared to monoketones, dicarbonyls (e.g., 1,2-diketones) offer distinct advantages: (1) they generally favor Norrish–Yang cyclization over the competing unproductive Norrish type II fragmentation pathway; (2) the long excitation wavelength of 1,2-diketones ($\lambda_{max} \approx 450$ nm) enables their selective activation in the presence of other photochemically excitable groups [5,6]. Furthermore, the resulting α-hydroxy-β-lactams or 2-hydroxycyclobutanones can function either as inherent structural motifs in target natural products or as strained reactive intermediates, facilitating C–H functionalization via four-membered ring opening [6-11]. Quinones display distinct photochemical reactivities among dicarbonyl compounds, as they not only undergo Norrish–Yang cyclization but also engage in photorearrangement, photoreduction, and photoredox cyclization reactions [12-16]. The last of these, first reported in 1965 [17], has been the subject of extensive studies by Suzuki's group [18]. In contrast to the direct radical coupling in Norrish–Yang cyclization, the distal biradical **F**, formed from quinone **E** through a pathway analogous to that of **C** in the photoredox process, subsequently undergoes intramolecular SET to generate a zwitterion **G**. This intermediate is then trapped by the proximal phenol, yielding the cyclization product **H** (Scheme 1b). Notably, the quinone is reduced, while the proximal C–H bond is subject to oxidation. Building on these mechanistic insights and the synthetic merits of dicarbonyls, Norrish–Yang cyclization and related photoredox reactions have been serving as powerful tools for constructing complex molecular architectures. Centered on the structural diversity and synthetic relevance of target natural products, this review is divided into three main sections: terpenoids, alkaloids, and antibiotics. Each section highlights the recent application of Norrish–Yang cyclization and related photoredox reactions in their total synthesis or model studies. Earlier literature pertaining to Norrish type I and II reactions in natural product synthesis has been comprehensively reviewed by Majhi [19] and thus lies beyond the scope of this article.

Review

1 Terpenoids

1.1 (+)-Cyclobutastellettolide B

(+)-Cyclobutastellettolide B (**13**), featuring an unusual 6/6/4-fused tricyclic core with six stereocenters – including three contiguous quaternary stereocenters – was first isolated by Stonik et al. in 2019 from a *Stelletta sp*. sponge collected in Vietnamese waters [20]. This compound significantly elevates reactive oxygen species levels in murine peritoneal macrophages (73 ± 12%) and exhibits potential as a lead for developing immunomodulatory agents. In 2021, Yang's group reported a concise enantioselective total synthesis of (+)-cyclobutastellettolide B, employing a late-stage biomimetic Norrish–Yang cyclization to construct the highly compact cyclobutanone motif [21]. The task commenced with epoxide **2** (Scheme 2), which was accessible via a known five-step protocol from geranyl acetate (**1**). Compound **2** was advanced to **3** using a tandem cyclization developed by the Yang group [22]. Installation of the hydroxymethyl group in **4** was achieved through sequential formylation and reduction. Compound **4** then

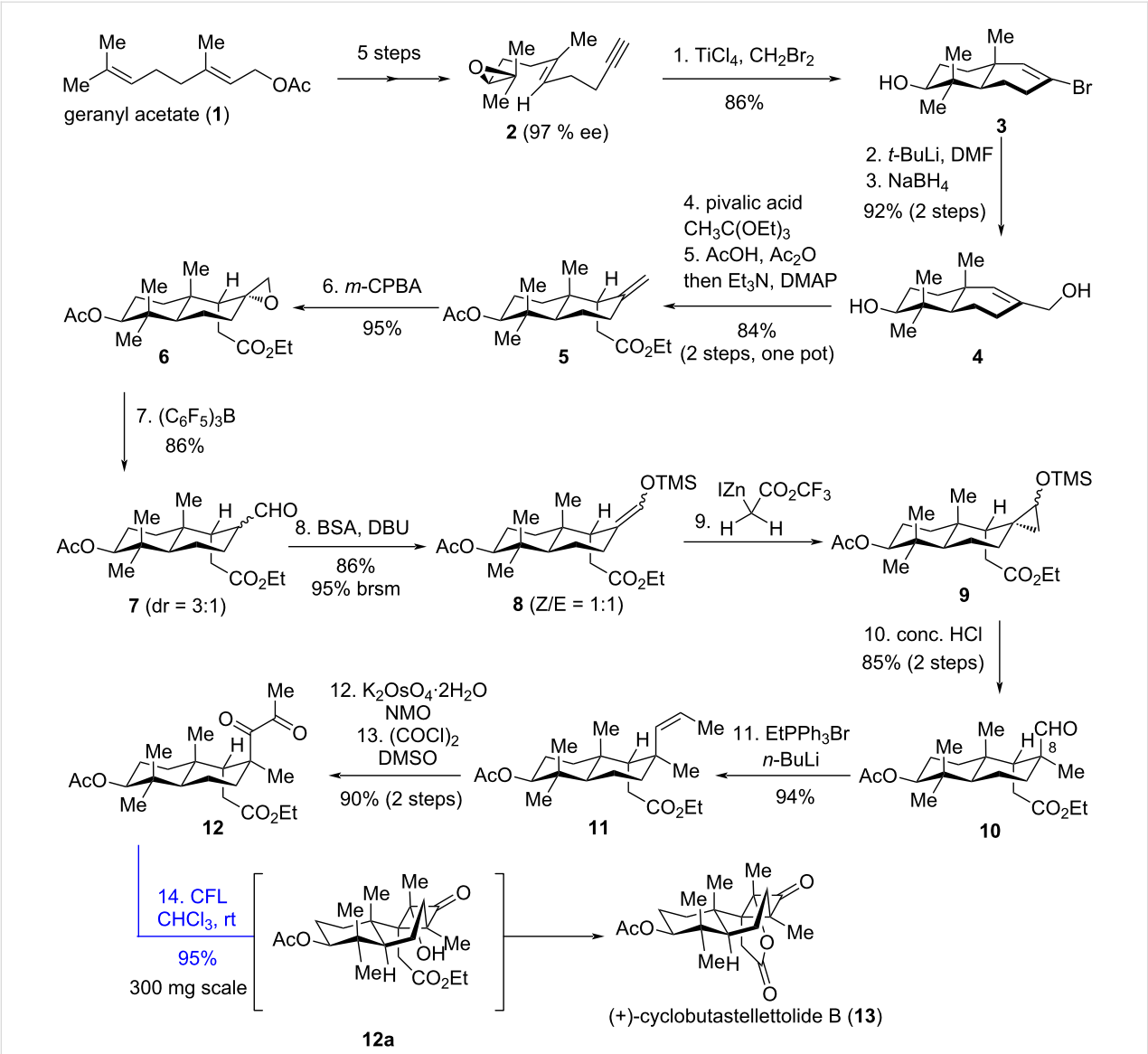

Scheme 2: Total synthesis of (+)-cyclobutastellettolide B.

underwent a one-pot, substrate-controlled diastereoselective Johnson–Claisen rearrangement/acetylation to install ester **5**. Treating **5** with *m*-CPBA (*meta*-chloroperoxybenzoic acid) induced epoxidation, which was then followed by a Meinwald rearrangement to accomplish aldehyde **7**. From **7**, a sequence involving silyl enol ether formation, Simmons–Smith cyclopropanation, and acid-mediated regioselective ring-opening installed the C8 quaternary methyl group in **10**. Subsequent transformation of **10** via sequential Wittig reaction, dihydroxylation, and Swern oxidation generated 1,2-diketone **12**, thus setting the stage for the Norrish–Yang reaction.

Finally, irradiation of **12** with a compact fluorescent lamp (CFL) completed (+)-cyclobutastellettolide B (**13**) as the sole product in 95% yield. This transformation proceeded via sequential regio- and stereoselective Norrish–Yang annulation, followed by intramolecular lactonization mediated by **12a**. Notably, when the ethyl ester in **12** was replaced with a methyl group to form **14** with R = Et (Scheme 3), photoreaction of **14** led to **15** in 95% yield. This product arises from a Norrish–Yang cyclization/1,2-methyl migration cascade of **14** via intermediate **14a**. Intriguingly, the substrate with R = H (**14'**) underwent only Norrish–Yang cyclization (95% yield) without 1,2-methyl migration [23]. It is hypothesized that the substituent at C9 in compound **14** drives this migration, due to the highly sterically congested environment – exacerbated by the 1,3-strain between the methyl groups at C10 and C14. The observed 1,2-methyl migration also underscores the critical role

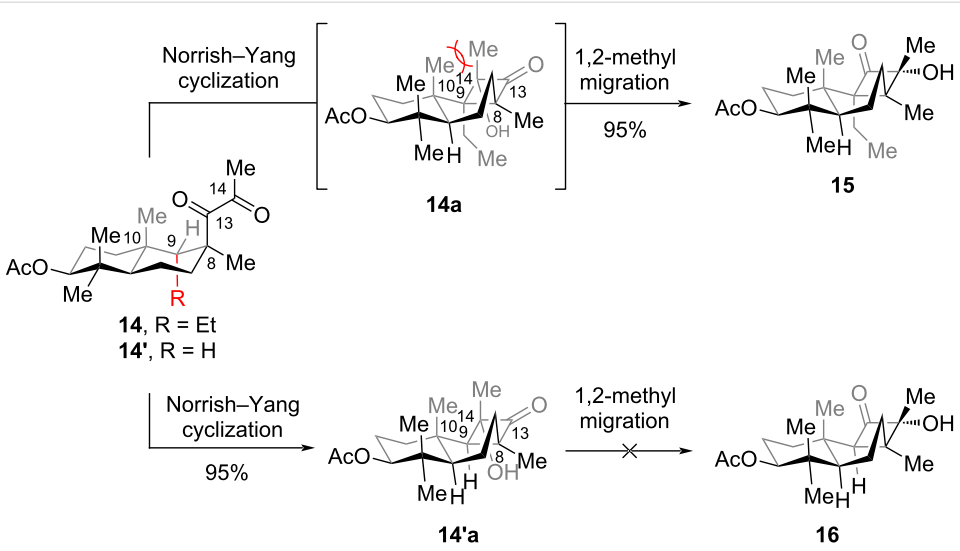

Scheme 3: Norrish–Yang cyclization and 1,2-methyl migration.

of the preinstalled ester group in **12**: it suppresses potential methyl migration, enabling the total synthesis of **13** via in situ intramolecular lactonization as a key step.

Computational and experimental studies reveal that the regio- and stereoselectivity of the Norrish−Yang cyclization are governed by the influence of the methyl group at C10: (1) In terms of regioselectivity, the 1,3-strain between the methyl group at C10 and the substituent at C8 restricts the free rotation of the C8–C13 bond (although this steric hindrance can be circumvented through chair–boat isomerization of the six-membered ring, the barrier for this isomerization is relatively high), resulting in a conformational preference at C8 that favors 1,5-HAT occurring at C9. (2) In terms of stereoselectivity, the steric hindrance between the spin center at C14 and the axial methyl group at C10 restricts the rotation around the C13–C14 bond, thereby enabling the diradical to undergo coupling stereoselectively.

As a key late-stage step in this total synthesis, the Norrish–Yang photocyclization exhibits high chemoselectivity and efficiency. It regulates selectivity through C–H bond dissociation energy and restricted bond rotation, constructing a 6/6/4 fused ring system with three contiguous quaternary carbons. Moreover, the reaction can be performed on a 300 mg scale, balancing selectivity, efficiency, and practicality.

1.2 Synthetic study toward phainanoids

Phainanoids are highly modified triterpenoids first isolated from *Phyllanthus hainanensis* by Yue's group [24,25]. Biologically, these molecules exhibit intriguing immunosuppressive activities, with phainanoid F (**17**) standing out as the most potent: it inhibits the proliferation of T and B lymphocytes with an IC_{50} value of 2.04 ± 0.01 nM. Structurally, phainanoids are characterized by a highly modified dammarane-type triterpenoid core, featuring an unprecedented 4,5-spirocyclic B/C ring system and a [4,3,1]propellane F/G/H ring fragment. In 2024, Yang's group achieved the construction of the ABCDE pentacyclic skeleton of phainanoids, leveraging Norrish–Yang cyclization to accomplish the regio- and stereoselective assembly of the rigid, sterically congested benzofuranone-based 4,5-spirocycle [26]. Starting from Wieland–Miescher ketone (**18**, Scheme 4), the synthesis proceeded through a sequence of transformations: the nonconjugated carbonyl was chemoselectively protected as ketal **19**; the unprotected ketone then underwent α-methylation to provide **20**; and subsequent conversion of the ketone in **20** to the vinyl iodide in **21** – via hydrazone formation, lithium–halogen exchange, and final nucleophilic substitution – secured the Norrish–Yang cyclization precursor **22**. Following systematic optimization of reaction conditions, irradiation of **22** with 100 W blue LEDs at room temperature constructed a single diastereoisomer **23** in 90% yield. From **23**, the ABCDE pentacyclic skeleton of phainanoids (**27**) was ultimately established via a Mitsunobu reaction, intramolecular nucleophilic substitution with in situ-generated aryllithium, and protecting group manipulations.

Notably, under Mitsunobu conditions, **23** – with its C9 ketal remaining intact – led to **28** and **29** in 40% total yield, with a 1:2.5 ratio favoring the undesired regioisomer **29** (Scheme 5a). These two isomers arise from S_N2 and S_N2' mechanisms, respectively. Furthermore, when **30** (bearing a saturated C5–C6 bond) was subjected to Norrish–Yang cyclization conditions (Scheme 5b), the two methyl groups at C4 initially underwent

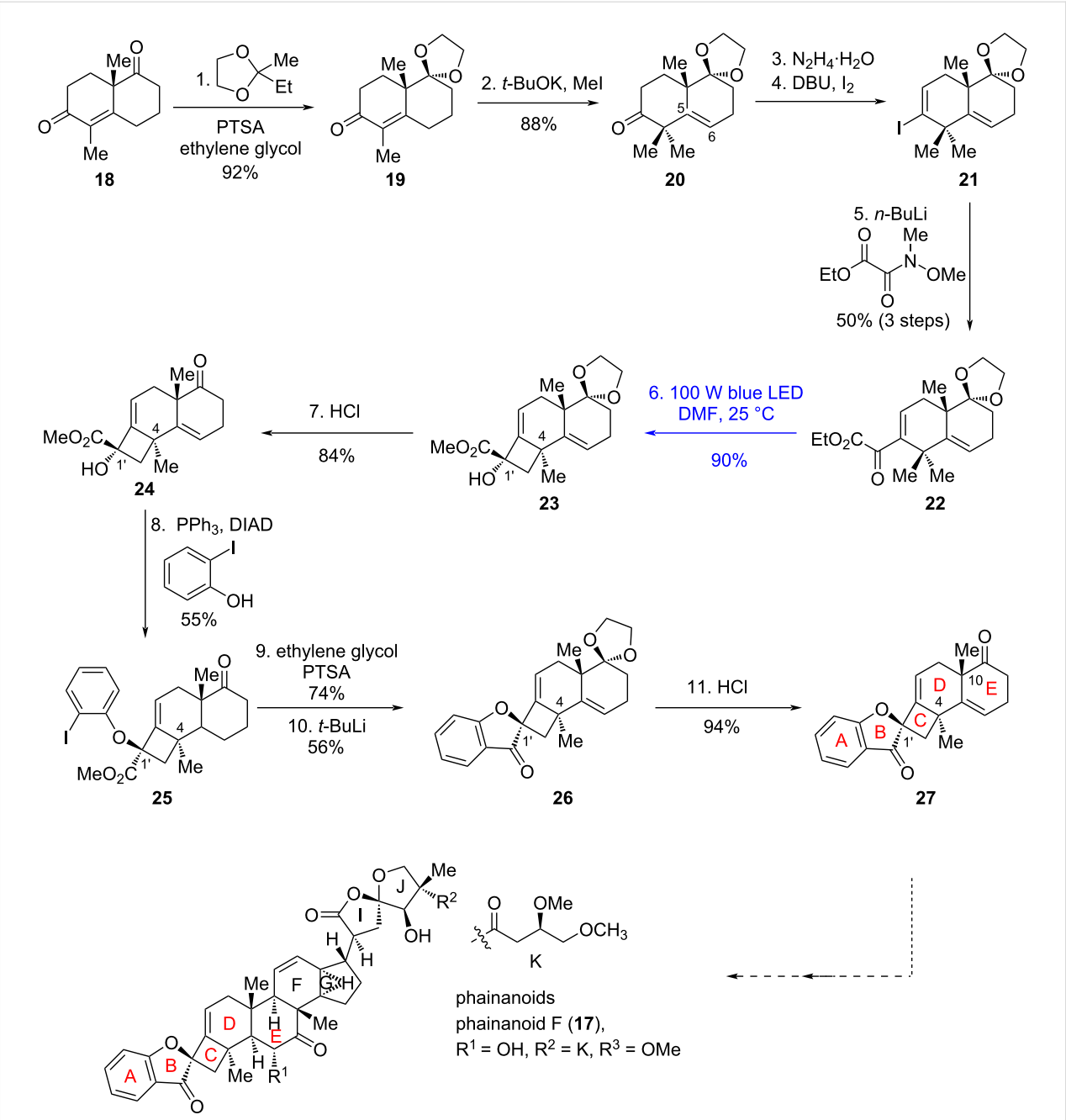

Scheme 4: Synthetic study toward phainanoids.

non-selective 1,5-HAT, resulting in a loss of both regio- and stereoselectivity. In both cases, the functional groups on the ring E likely exert a significant influence on the conformation of the substrates, thereby modulating their reactivities. Density functional theory calculations show that **22** prefers to proceed its annulation through **TS22b** ($\Delta\Delta G^{\ddagger}$ = 0) to afford **23** rather than that via **TS22a** ($\Delta\Delta G^{\ddagger}$ = 1.5 kcal/mol). In contrast, annulation of **30** undergoes through the low barrier difference between **TS30b** ($\Delta\Delta G^{\ddagger}$ = 0.3 kcal/mol) and **TS30a** ($\Delta\Delta G^{\ddagger}$ = 0), resulting in the formation of **31** as a 1:1 mixture of regioisomers (Scheme 5c). In this work, to address unsatisfactory C4 stereochemistry in initial synthesis, the authors introduced a double bond to alter substrate conformation, enabling stereochemical inversion of the Norrish–Yang reaction. This achieved efficient construction of benzofuranone-based 4,5-spirocycles with contiguous all-carbon quaternary centers, offering a conformational regulation protocol for stereocontrol in complex polycyclic systems.

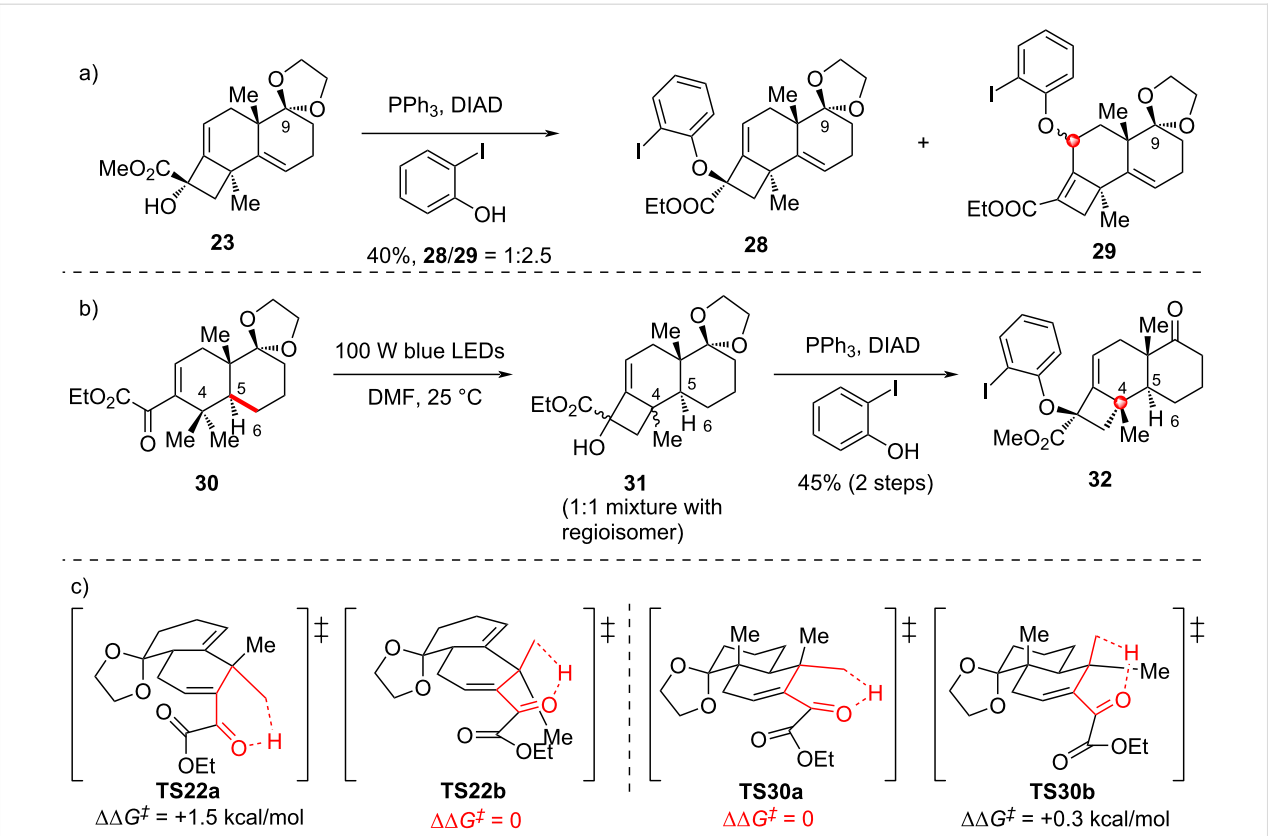

Scheme 5: a) Mitsunobu reaction of the C9 ketal; b) Norrish–Yang cyclization of the saturated C5–C6; c) calculated Gibbs free energy difference (ΔΔ*G*‡) for 1,5-HAT processes of **22** and **30**.

1.3 Avarane-type meroterpenoids

In 2024, Yang's and Zhang's groups employed a quinone-based, acid-promoted Norrish–Yang cyclization to achieve the stereoselective construction of multiple avarane-type meroterpenoids [27], including dysiherbol A (**33**) [28], dysifragilone A (**34**) [29], dysideanone B (**35**) [30], dysideanone E (**36**) [28], and the core structure of septosone B (**37**) [31] (Scheme 6). All these compounds were first isolated from South China Sea sponges of the genus *Dysidea* by Lin's group. Dysiherbol A (**33**) exhibits NF-κB inhibitory activity (IC_{50} = 0.49 μM) and cytotoxicity against the human myeloma cell line NCI H-929 (IC_{50} = 0.58 μM). Dysifragilone A (**34**) displays stronger inhibition of NO production than hydrocortisone, with an IC_{50} of 6.6 μM. Dysideanone B (**35**) shows cytotoxicity against HeLa and HepG2 human cancer cell lines, with IC_{50} values of 7.1 and 9.4 μM, respectively. Septosone B (**37**), featuring an unusual spiro[4.5]decane scaffold, exhibits NF-κB inhibitory activity with an IC_{50} of 27 μM.

Given that **33**–**37** were isolated from the same genus, Yang's group proposed that they might share a common biosynthetic precursor. Leveraging this insight and their knowledge of the Norrish–Yang reaction, they hypothesized that irradiating neoavarone (**44**) would trigger a quinone-based Norrish–Yang cyclization, enabling divergent synthesis of these meroterpenoids (or their core structures). In Yang's divergent total synthesis, Wieland–Miescher ketone (**18**) served as the starting material. Selective acetalization of the non-conjugated ketone in **18**, followed by diastereoselective α-alkylation, produced **38**. A Wittig reaction and subsequent deketalization converted the ketone in **38** to the terminal alkene **39**, allowing for subsequent sequential chemoselective hydrogenations: first, hydrogenation of the *exo*-olefin using Wilkinson's catalyst proceeded with moderate diastereoselectivity; this was followed by Mn(III)-catalyzed metal-hydride hydrogen atom (MHAT) transfer to reduce the endocyclic olefin, forming **41** as a single diastereomer. Subsequent transformations – including a Wittig reaction, demethylation, and oxidation of the resulting phenol to a *p*-benzoquinone – advanced **41** to neoavarone (**44**). After screening various Lewis acids (including $AlCl_3$, $Mg(OTf)_2$, $Yb(OTf)_3$, etc.), it was finally found that treatment of **44** with irradiation at 422 nm in the presence of the optimal Lewis acid $LaCl_3$ furnished the natural products dysiherbol A (**33**) and dysideanone E (**36**), along with the core structures of dysifragilone A (**45**), dysideanone B (**46**), and septosone B (**47**) in the highest total yield of 88% and product divergence. In compari-

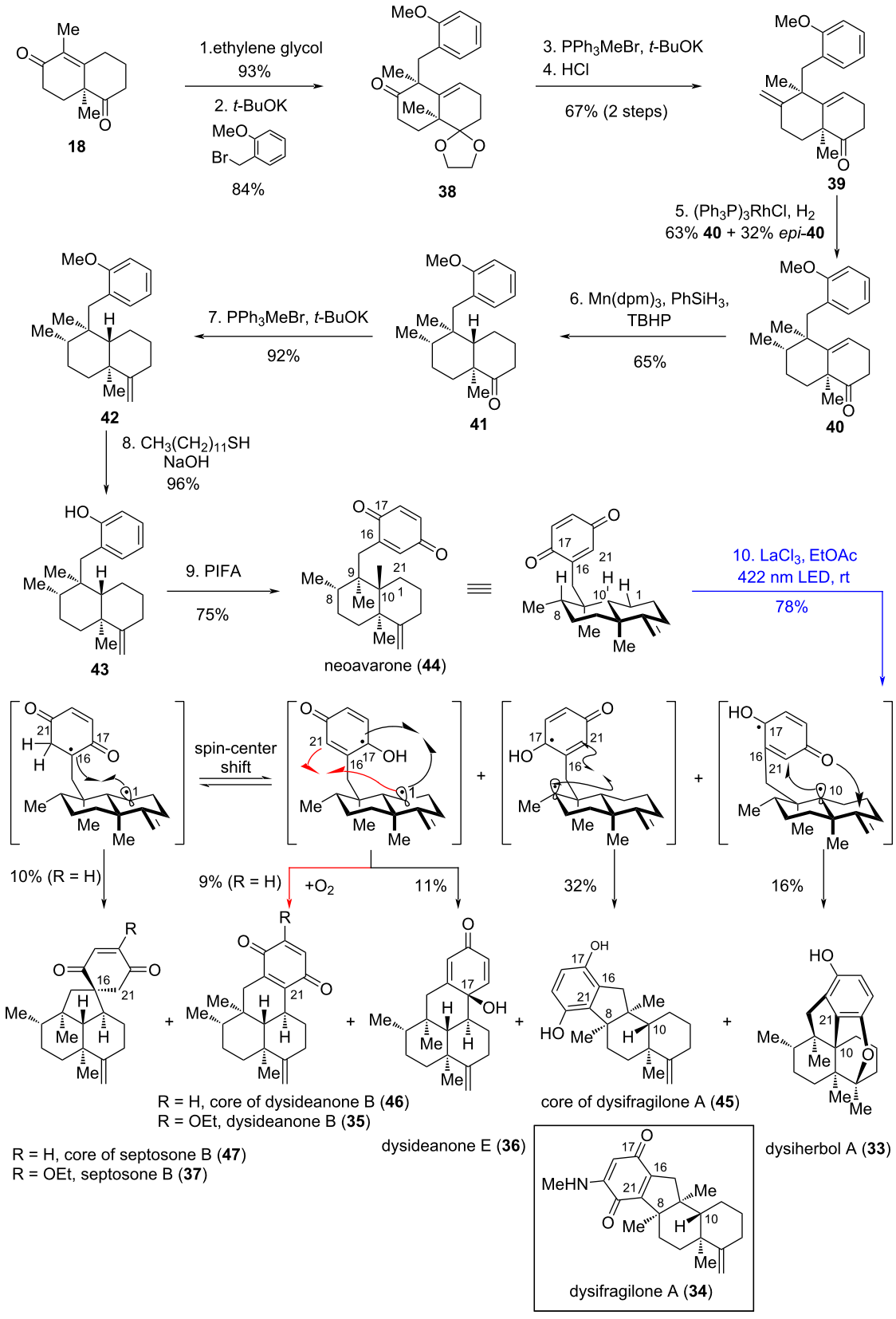

Scheme 6: Total synthesis of avarane-type meroterpenoids.

son, the total yield in the absence of any Lewis acid was 66%. Dysifragilone A (**34**) was obtained over four steps from **45**, while dysideanone B (**35**) was completed from **46** via oxidative ethoxylation. The diversity of the key photoreaction stems from three factors: (1) the ability of the excited quinone moiety in **44** to abstract hydrogen atoms from distinct positions; (2) delocalization of the semiquinone radical; (3) the involvement of a spin-center-shift (SCS) process in forming the core of septosone B (**47**) [32,33]. The influence of Lewis acids is partially attributable to two effects: (1) the observed elongation of the lifetime of the singlet excited state (from 0.846 ± 0.015 ns to 0.912 ± 0.014 ns), which reduces undesired photophysical cycles and thereby enhances selectivity; and (2) promotion of subsequent ground-state processes [34,35].

In this work, the authors innovatively applied the Norrish–Yang reaction of *p*-benzoquinone to the synthesis of avarane-type meroterpenoids. Starting from the common precursor quinone, they generated diverse biradical intermediates via regioselective hydrogen transfer (δ-H or ε-H), further constructing various C–C bonds. This enabled efficient synthesis of the core skeletons of five natural products. The divergent strategy significantly reduces redundant synthetic steps, embodies synthetic economy of "one precursor for multiple targets", and provides a valuable scheme for building structurally diverse natural product libraries.

1.4 Gracilisoids A–I

In 2025, Li's group exemplified the “Isolation-Synthesis-Functionality” research concept for a new class of sesterterpenoids, namely gracilisoids A–I (**49–57**) [36]. Gracilisoids A–E (**49–53**) were isolated from the ethnomedicinal plant *Eurysolen gracilis* of the Lamiaceae, while UPLC-MS/MS analysis of the crude leaf extract indicated trace amounts of gracilisoids F–I (**54–57**) in the plant material. Li’s group pursued the divergent total synthesis of **49–57** via a bioinspired strategy, incorporating a Norrish–Yang cyclization/α-hydroxyketone rearrangement tandem reaction and late-stage biomimetic photooxidation as key steps. The synthetic endeavour began with the total synthesis of **49**, which served as both the envisioned precursor for Norrish–Yang cyclization and the divergent starting point for accessing the other eight natural products (**50–57**). As an initial lead, two commercially available starting materials: (−)-citronellal (**58**) and diosgenin were employed (Scheme 7). (–)-Citronellal (**58**) was first converted to **59** via enantioselective intramolecular aldehyde α-alkylation using MacMillan's protocol, subsequently undergoing Shi's asymmetric epoxidation to give rise to epoxide **60** as a 3:1 mixture of diastereomers. These were not separated until step 8 due to poor separability at this stage. Concurrently, diosgenin was then processed through a known two-step sequence to **61**, followed by Mitsunobu reaction, ester reduction, thioether oxidation, and silylation of the primary alcohol to furnish sulfone **64**. The two key fragments – aldehyde **60** and sulfone **64** – were merged via Julia–Kocienski olefination to construct alkene **65**. Treatment of **65** with $(C_6F_5)_3B$ triggered a Meinwald rearrangement, generating aldehyde **66**. Nucleophilic addition, oxidation of the resulting alcohol, and base-promoted epimerization at C6 of **67**' delivered **67**. Subsequent dihydroxylation of the alkene in **67** and protection of the resulting 1,2-diol as a cyclic carbonate delivered **68**. A one-pot desilylation/oxidation of **67** produced an aldehyde, which was subject to selective nucleophilic addition in the presence of a ketone, allowing for access to the furan precursor **68** [37]. Oxidation–cyclization–aromatization of **68** with Dess–Martin periodinane (DMP) constructed the southern furan moiety of **69**. Finally, hydrolysis of the carbonate followed by oxidation of the resulting diol completed the Norrish–Yang cyclization precursor gracilisoid A (**49**).

Irradiation of **49** under anaerobic conditions with a CFL, followed by treatment with silica gel, successfully generated a pair of separable regioisomers: gracilisoid F (**54**) in 42% yield and gracilisoid H (**56**) in 40% yield, respectively (Scheme 8). Here, light triggered a regiodivergent Norrish–Yang cyclization, while the acidic nature of silica gel sufficiently promoted an α-hydroxy ketone rearrangement. This type of rearrangement was also observed in Yang’s total synthesis of (+)-cyclobutastellettolide B (**13**) as described above [21]. The driving force for the rearrangement is proposed to stem from 1,2-strain between the substituents at C13/C10 and C13/C7, consistent with observations from Yang's work [21].

Next, peroxides **54a** and **56a** (Scheme 9) – formed via [4 + 2] cycloaddition of singlet oxygen with the southern furan moiety in gracilisoid F (**54**) and gracilisoid H (**56**), respectively – served as branching points in the downstream divergent synthesis. Kornblum–DeLaMare-type rearrangement of **54a** and **56a** assembled gracilisoids B (**50**) and D (**52**), respectively. Alternatively, nucleophilic addition of MeOH to **54a** and **56a**, followed by ring-opening elimination, arrived at the corresponding γ-keto aldehyde intermediates **72**/**73**. Subsequent intramolecular aldol cyclization of these intermediates furnished gracilisoids C/G (**51**/**55**) and E/I (**53**/**57**), respectively.

In this work, inspired by the biosynthetic pathway of natural products, the authors employed a tandem Norrish–Yang photocyclization and α-hydroxy ketone rearrangement as the key step to construct the unique bicyclo[3.2.0]heptane skeleton

of gracilisoids. This strategy ingeniously leverages the high selectivity of photochemical reactions and the strain-release property of rearrangement reactions, enabling the precise con-

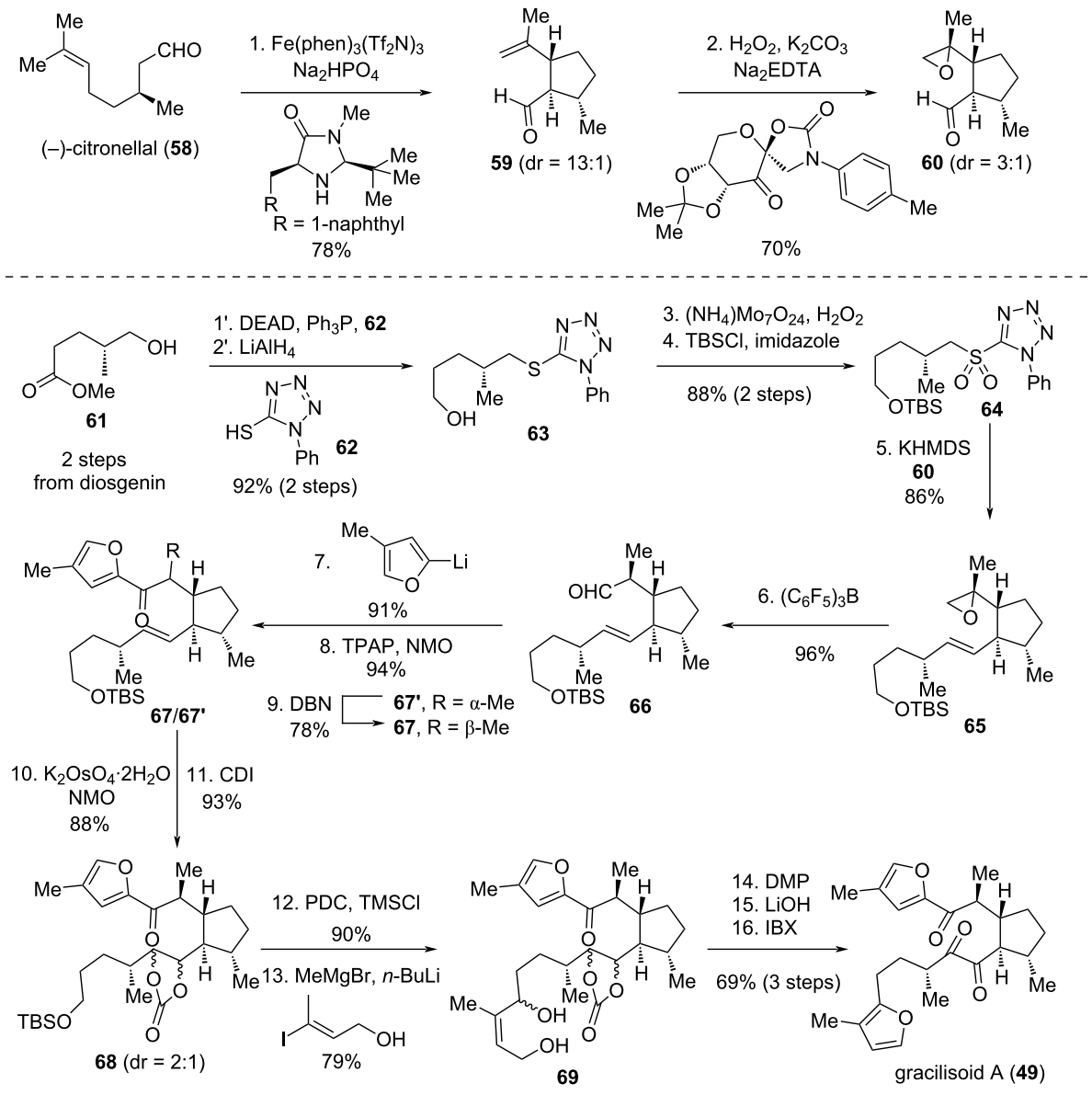

Scheme 7: Total synthesis of gracilisoid A.

struction of multiple stereocenters in one step and overcoming the synthetic challenges posed by contiguous quaternary carbon centers and sterically congested structures in complex bicyclic systems.

2 Alkaloids

2.1 Lycoplatyrine A

In 2020, Sarpong's group disclosed their progress toward a robust and broadly applicable strategy for the C–H functionalization of piperidines and related saturated *N*-heterocycles. This approach involves lactamization via Norrish–Yang cyclization, followed by a strain-release Pd-catalyzed C–C cleavage/cross-coupling protocol [9,11]; the strategy was subsequently applied to the total synthesis of lycoplatyrine A (**89**) in 2021 [38]. Isolated by Low's group [39], lycoplatyrine A (**89**) belongs to the lycodine-type *Lycopodium* alkaloids – a structurally diverse class of natural products found in plants of the widely distributed genus *Lycopodium*. Guided by biosynthetic hypotheses, Sarpong's group envisioned a divergent total synthesis of five lycodine-type *Lycopodium* alkaloids (including lycoplatyrine A (**89**)) used *N*-Boc-β-obscurine (**83**) as a late-stage common intermediate. Compound **83** was readily accessible via previously reported protocols [40], which featured a diastereoselective formal [3 + 3] cycloaddition between **76** and **81** as the key step. This cycloaddition constructs the three contiguous stereocenters and two C–C bonds of **83** (Scheme 10). Building block

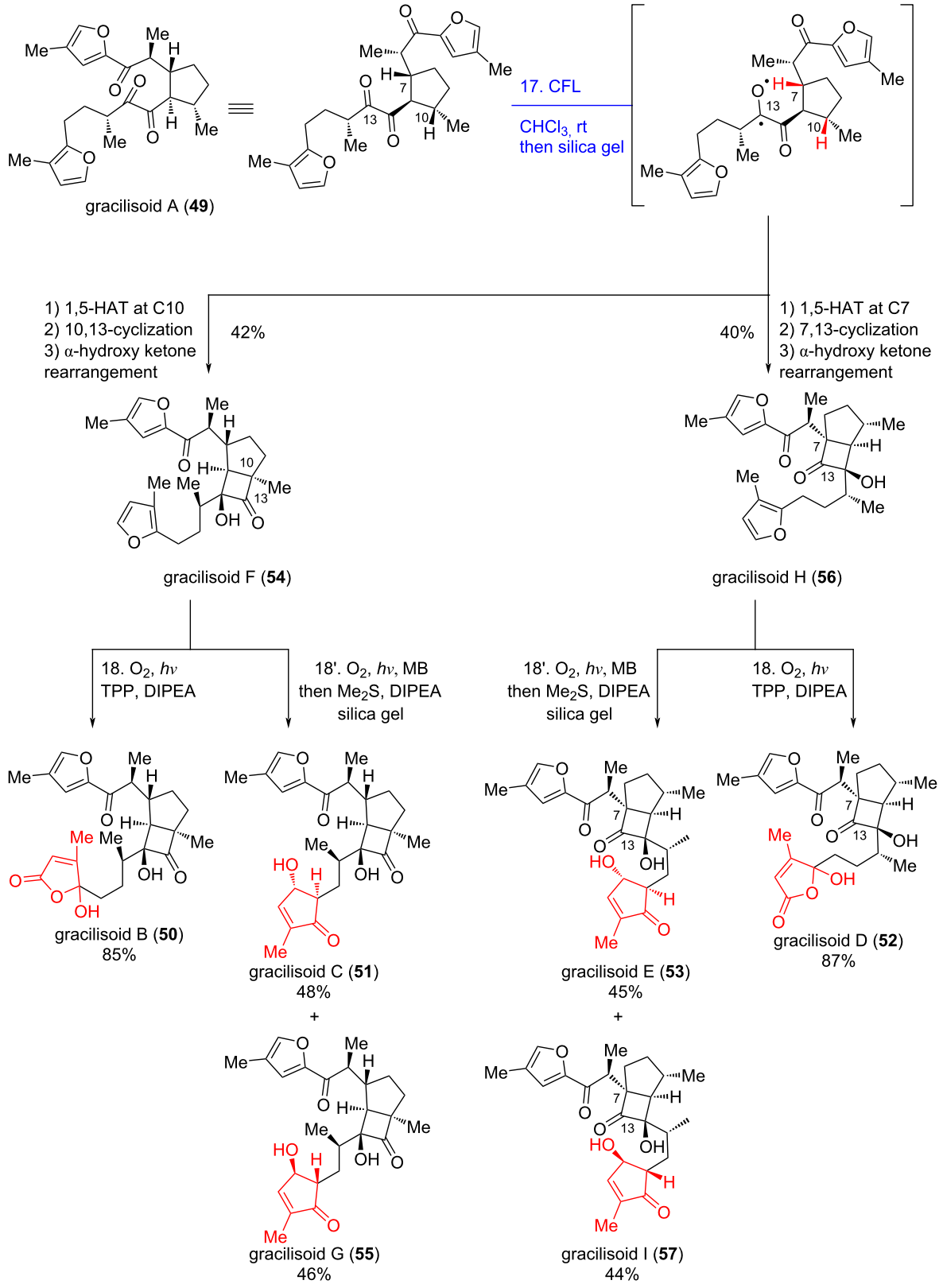

Scheme 8: Divergent total synthesis of gracilisoids B–I.

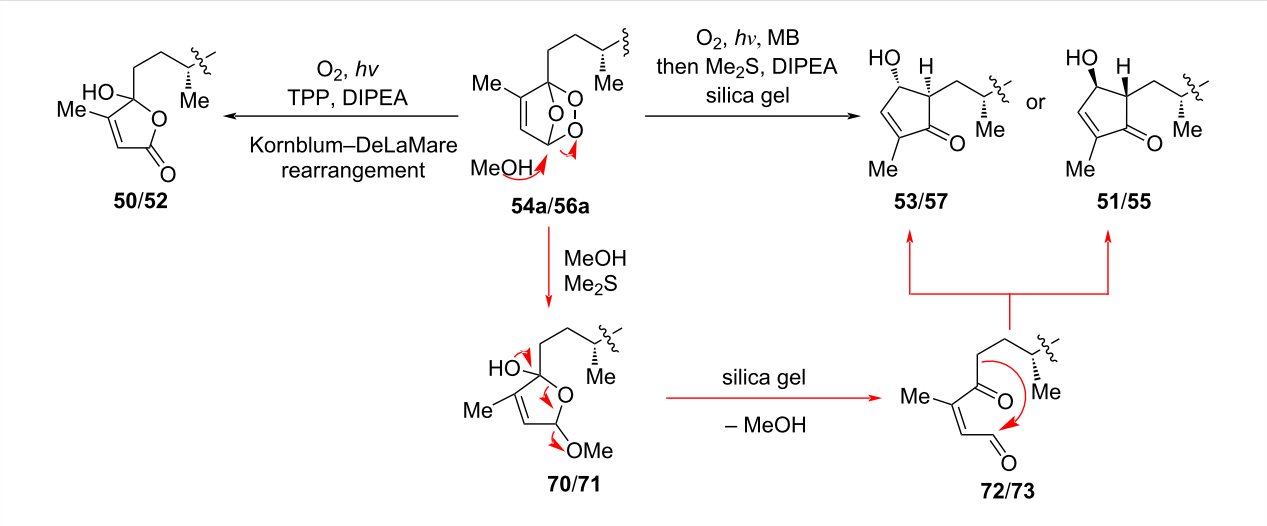

Scheme 9: Mechanism of the late-stage biomimetic photooxidation.

76 was first obtained in 18% overall yield from β-ketoester **74** through a sequence involving Michael addition, decarboxylation, nitrile hydration, and cyclization under vacuum. Aminoketal **81** – a direct precursor to the oxygen-sensitive α,β-unsaturated iminium **81a** – was prepared from (+)-pulegone (**77**) through a six-step manipulation involving epoxidation, epoxide opening with sodium thiophenolate and subsequent concomitant retro-aldol, sulfoxidation, a one pot α-alkylation with acrylonitrile proceeding to thermal *syn*-elimination of phenylsulfenic acid, ketone protection as ketal and nitrile reduction. The two building blocks (**76** and **81**) were then merged through the desired formal [3 + 3]-cycloaddition to generate *N*-desmethyl-α-obscurine (**82**), presumably via in situ-generated intermediates **76a** and **81a**, respectively. Subsequent Boc protection of the cyclic amine in **82**, followed by dehydrogenation, delivered compound **83** in 49% yield over three steps. Pyridone **83** could be funneled into pyridine **85** through *O*-triflation followed by Pd-catalyzed reductive detriflation. Ir-catalyzed *meta*-selective C–H borylation of **85**, followed by bromodeborylation of the pyridine ring, constructing **86** – setting the stage for the group's key reaction, in which α-hydroxy-β-lactams (e.g., **87**) serve as surrogates for α-metalated *N*-heterocycles in Pd-catalyzed coupling with aryl halides. Both enantiomers of **87** (only one shown in Scheme 10) participated in a Pd-catalyzed stereoretentive coupling at C2 with aryl bromide **86**, yielding **88** as a single diastereomer. Manipulation of the protecting group of **88** arrived at lycoplatyrine A (**89**). Notably, **87** and related α-hydroxy-β-lactams were obtained via Norrish–Yang cyclization of the corresponding neat α-keto amides in the solid state under blue LED irradiation. Solid-state reactions differ from solution-phase processes due to restraints on molecular motions imposed by the crystal lattice, thereby avoiding side reactions caused by unrestricted molecular motions in solution [41]. It has also been demonstrated that for crystalline 1,2-diketones, the rigid lattice structure locks molecules into a specific conformation, limiting access to certain γ-hydrogens for abstraction and thus enhancing regioselectivity [42]. Enantiopure **87** was obtained by preparative chiral supercritical fluid chromatography (SFC) resolution of the racemate, while racemic **87** was synthesized on a gram scale in 47% yield from **90** via a Norrish–Yang reaction.

However, under the established photochemical conditions for generating **87**, the corresponding pyrrolidine-derived species **93** is not formed (Scheme 11). In contrast, solution-phase irradiation of the same pyrrolidine-derived phenyl keto amide substrate **91** with blue LEDs produces the pyrrolidine-fused 4-oxazolidinone (*N*,*O*-acetal) **92**, precluding preparation of the pyrrolidine analog of lycoplatyrine A (**94**) by this method. Compound **92** is presumably formed via either the radical mechanism [41] or possibly undergoes SET to form a zwitterion as an intermediate step prior to cyclization [35,43,44]. It is noted that such molecular motions (rotations) are possible in solution but prevented by crystal-lattice restraints in the solid state [37].

In this synthesis, Sarpong et al. utilized the Norrish–Yang reaction to construct a β-lactam, an α-metallated piperidine equivalent, overcoming poor yields and stereoselectivity in traditional methods. Its palladium-catalyzed cross-coupling with 2-bromolycodine via β-lactam C–C cleavage enabled stereoretentive coupling, efficiently synthesizing lycoplatyrine A and its epimers. This strategy merges photochemical selectivity with cross-coupling efficiency, avoiding reactive metal incompatibility and enabling precise stereocontrol for chiral nitrogen heterocycles.

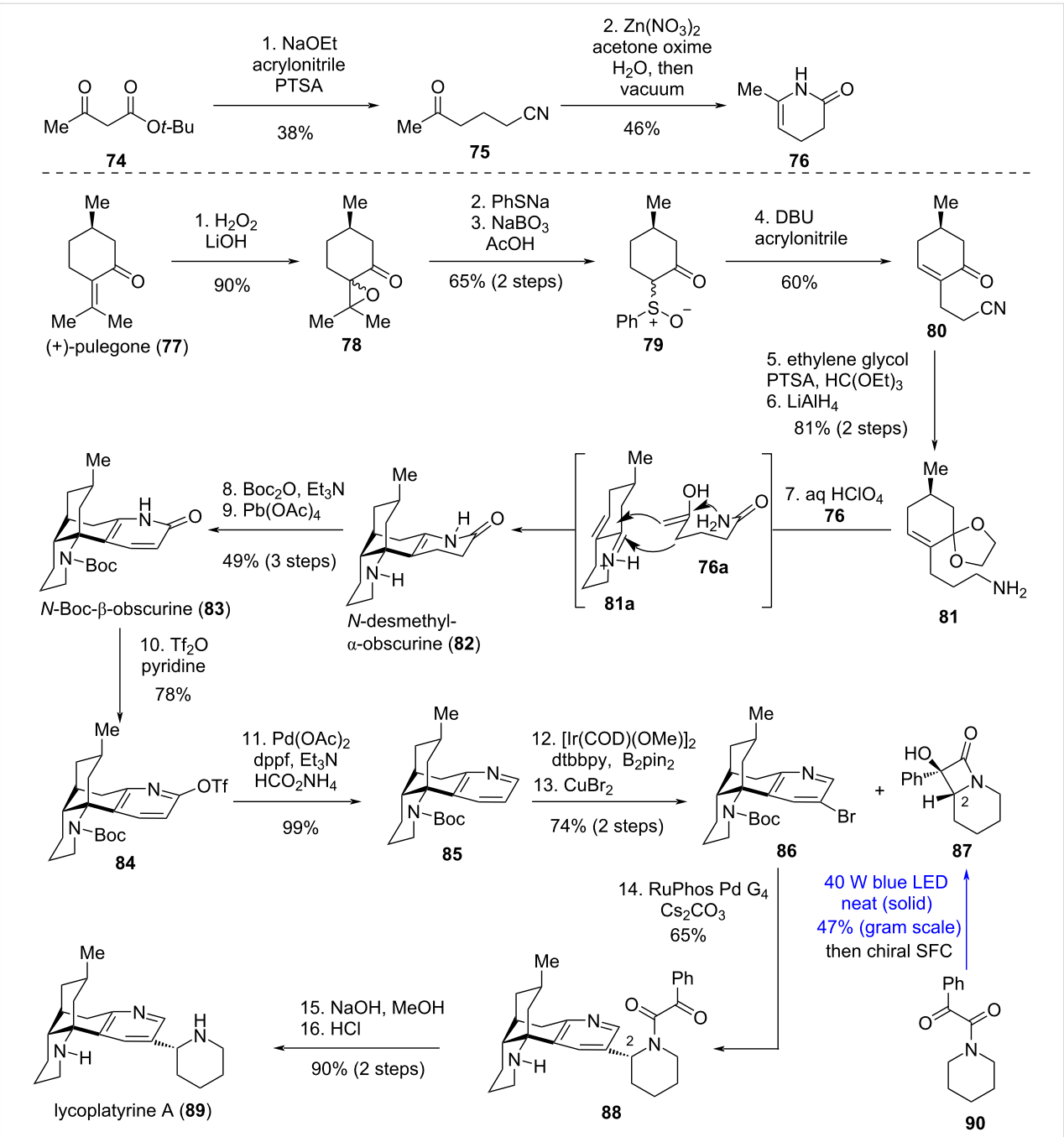

Scheme 10: Asymmetric total synthesis of lycoplatyrine A.

3 Antibiotics

3.1 Synthetic study toward γ-rubromycin

Since 2017, Suzuki's group has developed a stereoretentive photoredox reaction of naphthoquinones initiated by Norrish type-II hydrogen abstraction [45-51]. The mechanism involves three consecutive photoinduced events: (1) hydrogen abstraction by the excited quinone to generate a biradical species; (2) intramolecular SET process converting the biradical to the corresponding zwitterion; (3) oxy-cyclization to afford the product. This process constitutes an intramolecular redox reaction, wherein the quinone is reduced to a hydroquinone while the proximal C–H bond is oxidized to a C–O bond. Although related photoredox reactions had precedents [9], no systematic studies on their scope and limitations had been reported. Suzuki's group optimized the reaction conditions and thoroughly explored the substrate scope, encompassing 1,5-HAT and 1,6-HAT of 1,4-naphthoquinones as well as 1,5-HAT of 1,2-naphthoquinones (Scheme 12). Ultimately, this approach

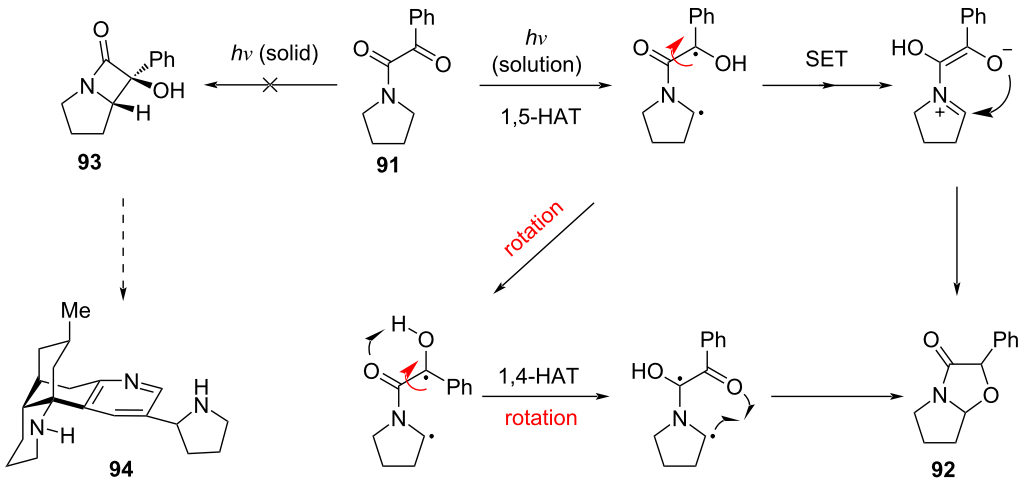

Scheme 11: Photoreaction of pyrrolidine-derived phenyl keto amide.

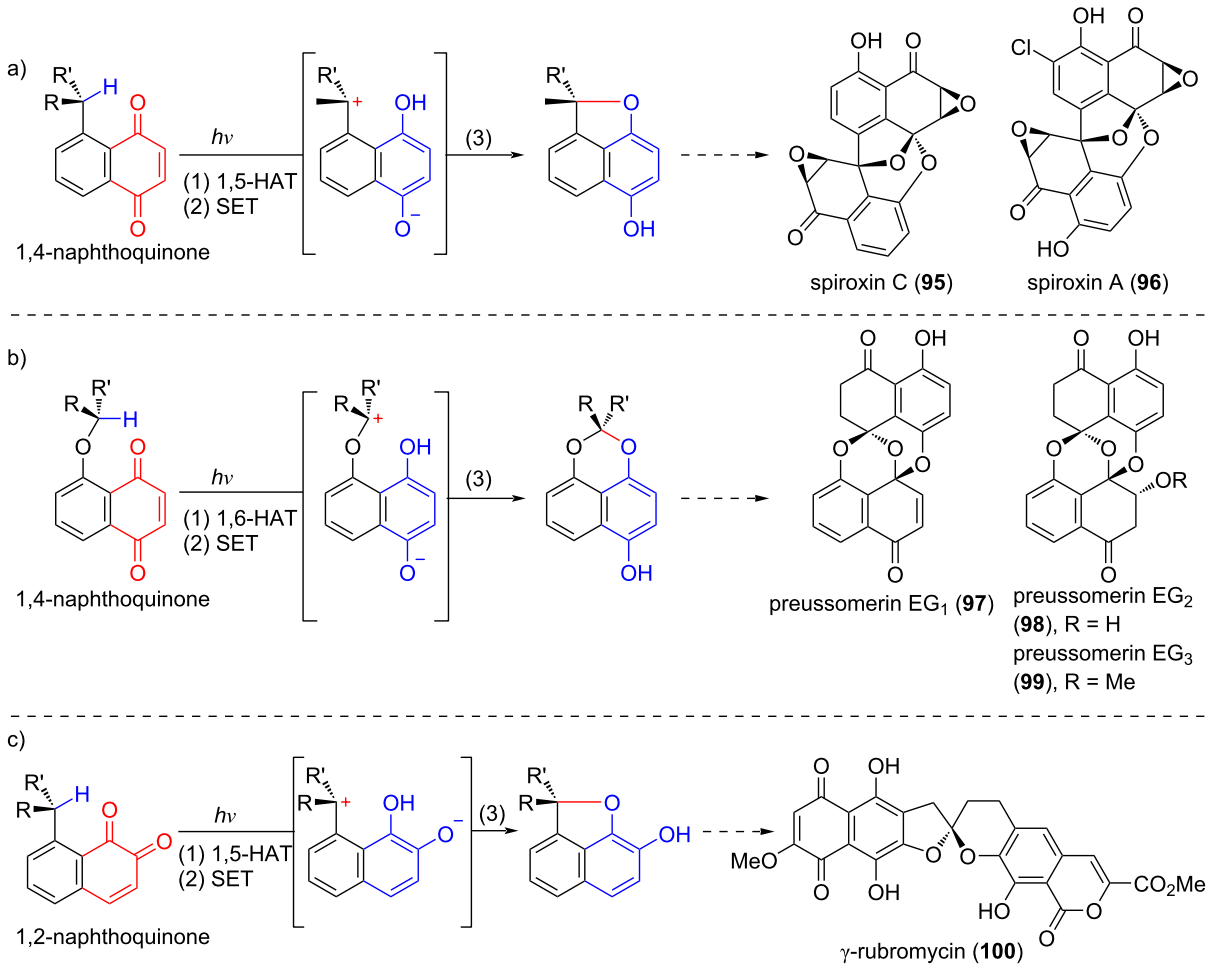

Scheme 12: Photoredox reactions of naphthoquinones.

enabled the total synthesis of spiroxin C (**95**) [45], spiroxin A (**96**) [48], preussomerin EG_1 (**97**), preussomerin EG_2 (**98**), and preussomerin EG_3 (**99**) [49], alongside model studies on γ-rubromycin (**100**) [50,51].

γ-Rubromycin (**100**) is a prominent member of the rubromycin family of natural products, characterized by a [5,6]-bisbenzannulated spiroketal moiety as its central structural motif. This key feature is critical to its potent biological activities, including strong inhibition of human telomerase [52], as well as its established roles as an effective antibiotic and HIV-1 reverse transcriptase inhibitor [53,54]. In 2018, Suzuki's group employed their developed photoredox reaction to carry out a model study on the chiral [5,6]-spiroketal core of γ-rubromycin [50]. 1,2-Naphthoquinone **106** was selected as the model substrate for the photoredox reaction (Scheme 13a). Lawsone (**101**) underwent reductive alkylation with aldehyde **102**, producing **103**, which was then protected as its OMOM ether to yield **104**. One-pot hydrogenation of quinone **104** afforded the corresponding hydroquinone, which, upon subsequent methylation, furnished **105**. Removal of the MOM group from **105** followed by oxidation of the resulting phenol delivered 1,2-naphthoquinone **106**. Notably, enantiomer (−)-**106** could be prepared from (+)-**105**, which was in turn obtained by preparative HPLC on a chiral stationary phase from (±)-**105**. Following extensive screening, it was found that photoirradiation of quinone (−)-**106** under the optimized conditions (300 W Xe lamp, MeOH/CH_3CN = 3:1, −78 °C) induced the formation of the five-membered ring, forming spiroacetal (−)-**107** in 68% yield with nearly complete configurational integrity (98% ee). This high stereoselectivity is attributed to three factors: (1) polar solvents enhance yields by accelerating electron transfer for zwitterionic intermediate (e.g., (−)-**106b** or (+)-1**06b**) formation; (2) protic solvents (e.g., MeOH) improve ee values through H-bonding stabilization, which reduces intermediate flexibility; (3) low temperatures enhance the optical purity by slowing conformational changes without compromising the reaction rate. These rationales for stereoretention are equally applicable to photoredox reactions of other substrates (vide infra), and therefore will be omitted there.

In 2024, Suzuki's group further explored the feasibility of their photoredox strategy for constructing the γ-rubromycin spiroacetal core using multi-functionalized 1,2-naphthoquinone substrates [51]. This study focused on substituent effects of methoxy groups at different positions (C5–C8) on the naphthoquinone chromophore (Scheme 13b). Key findings revealed that substrates bearing methoxy groups at C5, C6, or C8 (**108a**, **108b**, **108d**) underwent the desired photochemical reaction (Scheme 13b), yielding spiroacetals **109a**, **109b**, and **109d** following CAN (cerium(IV) ammonium nitrate) oxidation. In contrast, C7-methoxy-substituted analogs (**108c**, **108e**) remained unreactive. Reactivity correlated with UV–vis absorption profiles: reactive substrates exhibited λ_{max} < 460 nm (yellow-orange), whereas unreactive ones showed λ_{max} > 460 nm (dark red-purple). This suggests insufficient excitation energy for Norrish type-II hydrogen abstraction in the latter. Such chromophore-dependent reactivity provides critical insights for designing viable intermediates in the total synthesis of γ-rubromycin, emphasizing the need to avoid C7-oxygenation at early stages.

3.2 Preussomerins

Preussomerins EG_1 (**97**), EG_2 (**98**), and EG_3 (**99**) – isolated from the endophytic fungus *Edenia gomezpompae* in *Callicarpa acuminata* – exhibit strong antifungal activity against phytopathogens such as *Phytophthora* and *Fusarium*. Among these, preussomerin EG_1 (**97**) is the most potent, with IC_{50} values of 57.71×10^{-5} M against *Phytophthora parasitica*, 5.61×10^{-5} M against *Phytophthora capsici*, and 1.45×10^{-5} M against *Fusarium oxysporum*, while showing no significant inhibition (>5.75×10^{-4} M) against *Alternaria solani* [55]. In 2023, Suzuki's group pioneered the enantioselective total syntheses of preussomerins **97**–**99** through their photoredox strategy [49]. This study addressed the key challenge of controlling spiroacetal stereoselectivity through a 1,6-HAT process – a less favorable pathway compared to the previously employed 1,5-HAT. Initial feasibility studies revealed that the non-brominated substrate exhibited poor reactivity in the photochemical 1,6-HAT reaction (Scheme 14), as its unreactive conformer **J** dominated the equilibrium. In contrast, the brominated analogue achieved high efficiency: the bulky bromine atom sterically biased the population toward the reactive conformer **I**, where the benzylic C–H bond is optimally positioned for 1,6-HAT.

Therefore, (*S*)-**113** was selected as the precursor for the key photoredox reaction (Scheme 15). To prepare this, a Mitsunobu reaction between two known compounds – (*R*)-**110** and **111** – afforded (*S*)-**112** (>99% ee after recrystallization), which was then oxidized to yield the key naphthoquinone (*S*)-**113**. As expected, the photoredox reaction of (*S*)-**113** proceeded efficiently under blue LED irradiation (448 nm) in CH_3CN/CH_2Cl_2 at room temperature, delivering spiroacetal (*S*)-**114** with complete retention of configuration (>99% ee). The subsequent one-pot acetylation generated (*S*)-**115** in 83% overall yield over three steps from (*S*)-**112**. The following functional group manipulations of (*S*)-**115** – including debenzylation/debromination, ketone reduction, hydroquinone oxidation, and alcohol oxidation – led to the labile ketone **118**. Completion of preussomerin EG_3 (**99**) from **118** relied on a simple sequence including a formal intramolecular 1,6-addition, followed by si-

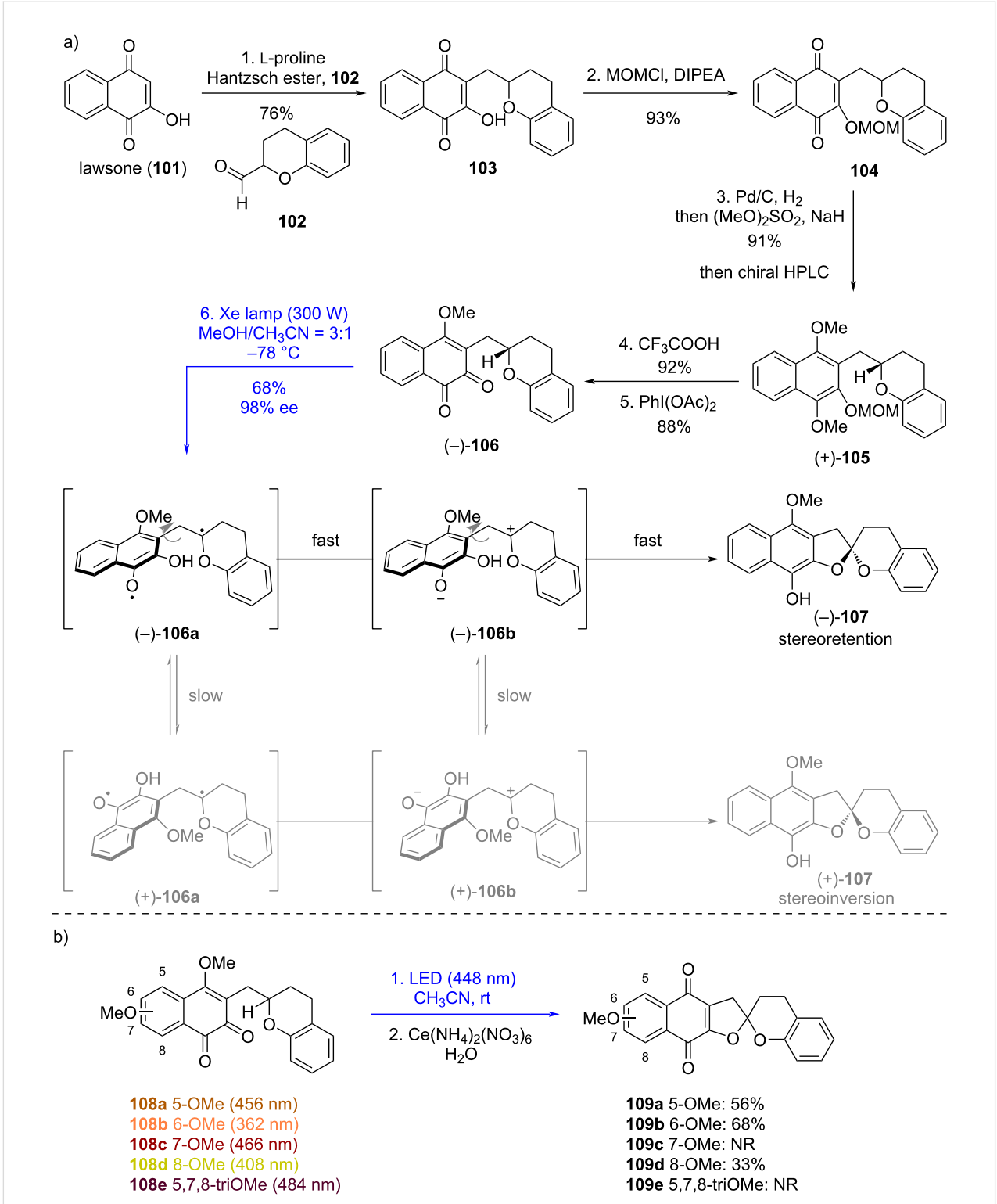

Scheme 13: Synthetic study toward γ-rubromycin.

multaneous methanol trapping of the resulting electrophilic quinone. Notably, **116** resisted oxidation to **118**, presumably due to carbonyl-induced π-electron depletion, whereas compound **118** proved resistant to direct conversion into preussomerin EG_3 (**99**) under various conditions. Alternatively, preussomerin EG_1 (**97**) was obtained in 83% yield over two

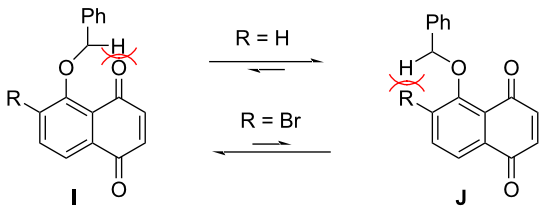

Scheme 14: Substituent-dependent conformational preferences.

steps from preussomerin EG_3 (**99**) via TMSOTf/Et_3N-mediated β-elimination of methanol followed by desilylation. Finally, stereoselective epoxidation and reductive opening of the oxirane ring enabled the total synthesis of preussomerin EG_2 (**98**) from preussomerin EG_1 (**97**) in 88% yield over two steps.

In this synthesis, the stereospecific intramolecular photoredox reaction of naphthoquinones overcame the limitation of poor stereoselectivity in traditional photochemical reactions, repre-

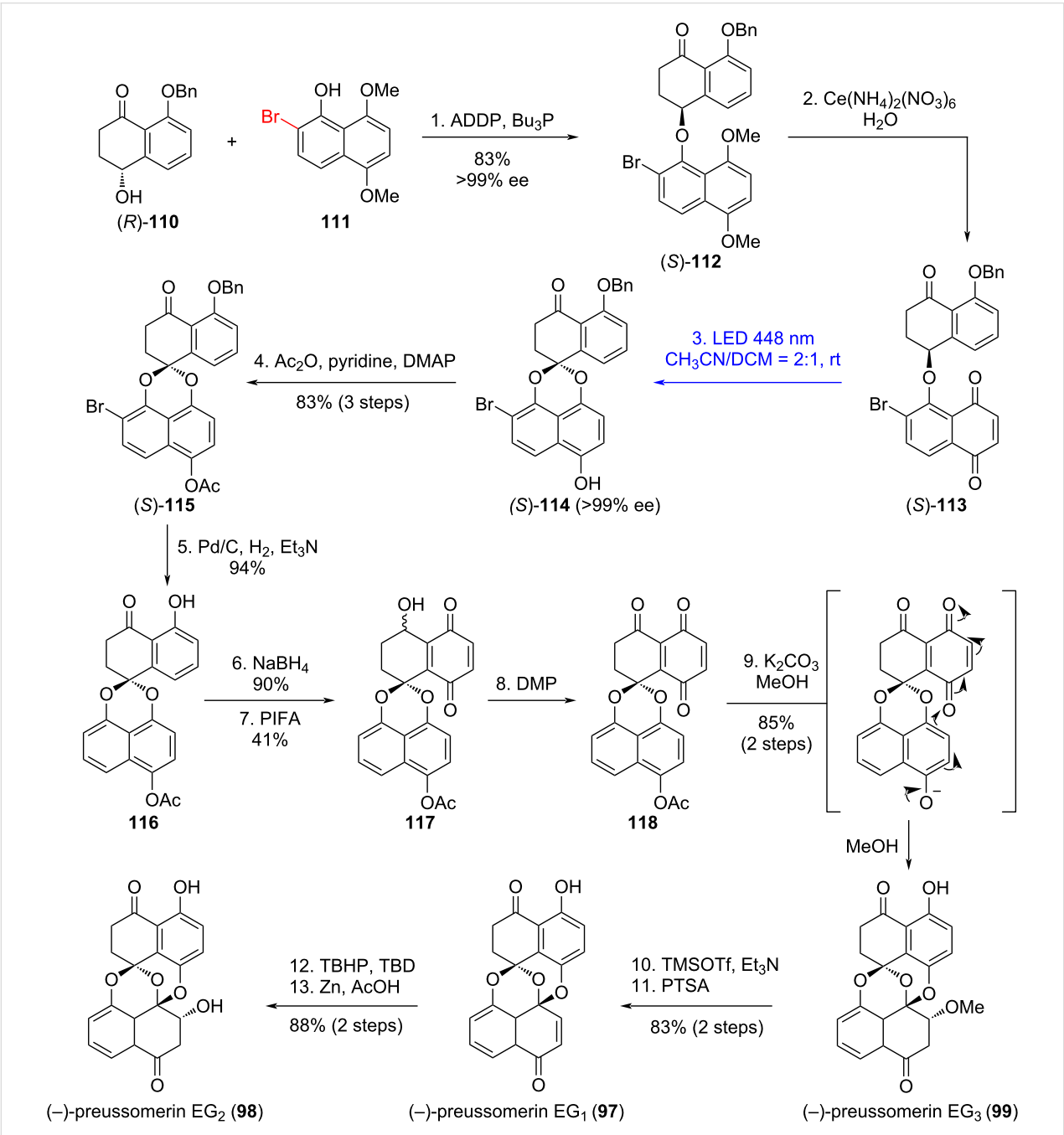

Scheme 15: Total synthesis of preussomerins EG_1, EG_2, and EG_3.

senting the first application of naphthoquinone photoredox processes to the stereospecific construction of complex spirocyclic structures. Its ingenuity lies in utilizing the inherent conformational constraints of the substrate instead of external chiral catalysts, which not only simplifies the reaction system but also solves the challenge of precisely controlling contiguous chiral centers in polycyclic systems.

Conclusion

This review systematically summarizes the latest advancements in the Norrish–Yang cyclization and related photoredox reactions of dicarbonyls, with a focus on their applications in the total synthesis of bioactive natural products. It highlights the distinct photochemical behaviors of various dicarbonyls, including 1,2-diketones, α-keto esters, α-keto amides, 1,4-quinones, and 1,2-quinones, emphasizing their unique roles in constructing diverse substructures. However, the reaction faces challenges in terms of regioselectivity and stereoselectivity, which are mainly attributed to the influence of substrate structure, substituent effects, and steric hindrance. Meanwhile, for multifunctional group substrates, the presence of potential competitive hydrogen transfer sites tends to lead to the formation of non-target cyclized products, further reducing the reaction specificity. Dicarbonyls are excellent substrates for Norrish–Yang cyclization and related photoredox reactions, owing to their ability to undergo selective activation under mild conditions (e.g., long-wavelength irradiation) – a feature that minimizes competing fragmentation pathways. Notably, different dicarbonyl substrates exhibit distinct reactivity patterns, enabling the construction of diverse architectures including sterically hindered cyclobutanes, spiroketals, and fused polycycles. However, the potential of dicarbonyls in photoreactions warrants further exploration. Future research could investigate a broader range of dicarbonyl substrates to uncover new reactivity modes and expand the structural diversity of accessible natural product scaffolds. Additionally, the highly reactive strained four-membered rings generated from these reactions present exciting opportunities for further functionalization. Studying their downstream transformations – particularly under catalytic conditions – may lead to novel strategies for C–H functionalization and fragment coupling, ultimately advancing the field of target-oriented synthesis. Combining Norrish–Yang reaction with flow chemistry technology to realize the continuous operation of the reaction can improve the safety and controllability of the reaction, and at the same time, it is also conducive to the rapid optimization of reaction conditions and scale-up production. Finally, the Norrish–Yang reaction can utilize artificial intelligence to assist in designing reaction routes in the future, and through big data analysis and machine learning algorithms to quickly screen and optimize reaction conditions, substrate structures, and predict reaction results, it will accelerate the development of new Norrish–Yang reaction systems in the total synthesis of complex bioactive natural products.

Acknowledgements

This work was supported by the National Natural Science Foundation of China (NSFC, 22471181, 22371192) and Fundamental Research Funds for the Central Universities.

Author Contributions

Peng-Xi Luo: writing – original draft. Jin-Xuan Yang: writing – original draft. Shao-Min Fu: writing – review & editing. Bo Liu: writing – review & editing.

ORCID® iDs

Shao-Min Fu - https://orcid.org/0000-0002-7095-0672

Data Availability Statement

Data sharing is not applicable as no new data was generated or analyzed in this study.

References

1. Norrish, R. G. W.; Appleyard, M. E. S. *J. Chem. Soc.* **1934,** 874–880. doi:10.1039/jr9340000874
2. Norrish, R. G. W.; Bamford, C. H. *Nature* **1936,** *138,* 1016. doi:10.1038/1381016a0
3. Norrish, R. G. W.; Bamford, C. H. *Nature* **1937,** *140,* 195–196. doi:10.1038/140195b0
4. Yang, N. C.; Yang, D.-D. H. *J. Am. Chem. Soc.* **1958,** *80,* 2913–2914. doi:10.1021/ja01544a092
5. Urry, W. H.; Trecker, D. J. *J. Am. Chem. Soc.* **1962,** *84,* 118–120. doi:10.1021/ja00860a034
6. Kamijo, S.; Hoshikawa, T.; Inoue, M. *Tetrahedron Lett.* **2010,** *51,* 872–874. doi:10.1016/j.tetlet.2009.12.027
7. Yoshioka, S.; Nagatomo, M.; Inoue, M. *Org. Lett.* **2015,** *17,* 90–93. doi:10.1021/ol503291s
8. Kawamata, T.; Nagatomo, M.; Inoue, M. *J. Am. Chem. Soc.* **2017,** *139,* 1814–1817. doi:10.1021/jacs.6b13263
9. Roque, J. B.; Kuroda, Y.; Jurczyk, J.; Xu, L.-P.; Ham, J. S.; Göttemann, L. T.; Amber, C.; Adpressa, D.; Saurí, J.; Joyce, L. A.; Musaev, D. G.; Yeung, C. S.; Sarpong, R. *ACS Catal.* **2020,** *10,* 2929–2941. doi:10.1021/acscatal.9b04551
10. Ham, J. S.; Park, B.; Son, M.; Roque, J. B.; Jurczyk, J.; Yeung, C. S.; Baik, M.-H.; Sarpong, R. *J. Am. Chem. Soc.* **2020,** *142,* 13041–13050. doi:10.1021/jacs.0c04278
11. Xu, L.-P.; Roque, J. B.; Sarpong, R.; Musaev, D. G. *J. Am. Chem. Soc.* **2020,** *142,* 21140–21152. doi:10.1021/jacs.0c10220
12. Orlando, C. M.; Mark, H.; Bose, A. K.; Manhas, M. S. *J. Am. Chem. Soc.* **1967,** *89,* 6527–6532. doi:10.1021/ja01001a027
13. Orlando, C. M., Jr.; Mark, H.; Bose, A. K.; Manhas, M. S. *J. Org. Chem.* **1968,** *33,* 2512–2516. doi:10.1021/jo01270a076
14. Iwamoto, H.; Takuwa, A.; Hamada, K.; Fujiwara, R. *J. Chem. Soc., Perkin Trans. 1* **1999,** 575–582. doi:10.1039/a809530b
15. Fónagy, O.; Szabó-Bárdos, E.; Horváth, O. *J. Photochem. Photobiol., A* **2021,** *407,* 113057. doi:10.1016/j.jphotochem.2020.113057

16. Ando, Y.; Suzuki, K. *Chem. – Eur. J.* **2018,** *24,* 15955–15964. doi:10.1002/chem.201801064
17. Cameron, D. W.; Giles, R. G. F. *Chem. Commun. (London)* **1965,** 573–574. doi:10.1039/c19650000573
18. Ando, Y.; Suzuki, K. *Tetrahedron* **2023,** *139,* 133448. doi:10.1016/j.tet.2023.133448
19. Majhi, S. *Photochem. Photobiol. Sci.* **2021,** *20,* 1357–1378. doi:10.1007/s43630-021-00100-3
20. Kolesnikova, S. A.; Lyakhova, E. G.; Kalinovsky, A. I.; Berdyshev, D. V.; Pislyagin, E. A.; Popov, R. S.; Grebnev, B. B.; Makarieva, T. N.; Minh, C. V.; Stonik, V. A. *J. Nat. Prod.* **2019,** *82,* 3196–3200. doi:10.1021/acs.jnatprod.9b00824
21. Zhang, Z.; Chen, S.; Tang, F.; Guo, K.; Liang, X.-T.; Huang, J.; Yang, Z. *J. Am. Chem. Soc.* **2021,** *143,* 18287–18293. doi:10.1021/jacs.1c08880
22. Liang, X.-T.; Chen, J.-H.; Yang, Z. *J. Am. Chem. Soc.* **2020,** *142,* 8116–8121. doi:10.1021/jacs.0c02522
23. Tang, F.; Zhang, Z.; Yang, Z. *Tetrahedron Lett.* **2024,** *145,* 155161. doi:10.1016/j.tetlet.2024.155161
24. Fan, Y.-Y.; Zhang, H.; Zhou, Y.; Liu, H.-B.; Tang, W.; Zhou, B.; Zuo, J.-P.; Yue, J.-M. *J. Am. Chem. Soc.* **2015,** *137,* 138–141. doi:10.1021/ja511813g
25. Fan, Y.-Y.; Gan, L.-S.; Liu, H.-C.; Li, H.; Xu, C.-H.; Zuo, J.-P.; Ding, J.; Yue, J.-M. *Org. Lett.* **2017,** *19,* 4580–4583. doi:10.1021/acs.orglett.7b02181
26. Zhou, Y.-K.; Zhang, Z.-Y.; Liu, H.-Y.; Li, Y.-H.; Zhang, Z.-C.; Chen, J.-H.; Yang, Z. *Org. Lett.* **2024,** *26,* 8217–8221. doi:10.1021/acs.orglett.4c02411
27. Liu, B.-Y.; Zhang, Z.-C.; Song, Z.-L.; Yuan, H.-Y.; Li, Y.-H.; Zhang, Z.-C.; Yang, Z. *Angew. Chem., Int. Ed.* **2025,** *64,* e202415249. doi:10.1002/anie.202415249
28. Jiao, W.-H.; Shi, G.-H.; Xu, T.-T.; Chen, G.-D.; Gu, B.-B.; Wang, Z.; Peng, S.; Wang, S.-P.; Li, J.; Han, B.-N.; Zhang, W.; Lin, H.-W. *J. Nat. Prod.* **2016,** *79,* 406–411. doi:10.1021/acs.jnatprod.5b01079
29. Jiao, W.-H.; Xu, T.-T.; Zhao, F.; Gao, H.; Shi, G.-H.; Wang, J.; Hong, L.-L.; Yu, H.-B.; Li, Y.-S.; Yang, F.; Lin, H.-W. *Eur. J. Org. Chem.* **2015,** 960–966. doi:10.1002/ejoc.201403487
30. Jiao, W.-H.; Xu, T.-T.; Yu, H.-B.; Chen, G.-D.; Huang, X.-J.; Yang, F.; Li, Y.-S.; Han, B.-N.; Liu, X.-Y.; Lin, H.-W. *J. Nat. Prod.* **2014,** *77,* 346–350. doi:10.1021/np4009392
31. Gui, Y.-H.; Jiao, W.-H.; Zhou, M.; Zhang, Y.; Zeng, D.-Q.; Zhu, H.-R.; Liu, K.-C.; Sun, F.; Chen, H.-F.; Lin, H.-W. *Org. Lett.* **2019,** *21,* 767–770. doi:10.1021/acs.orglett.8b04019
32. Wessig, P.; Muehling, O. *Eur. J. Org. Chem.* **2007,** 2219–2232. doi:10.1002/ejoc.200600915
33. Zhang, F.-L.; Li, B.; Houk, K. N.; Wang, Y.-F. *JACS Au* **2022,** *2,* 1032–1042. doi:10.1021/jacsau.2c00051
34. Görner, H.; Wolff, T. *Photochem. Photobiol.* **2008,** *84,* 1224–1230. doi:10.1111/j.1751-1097.2008.00339.x
35. Zhan, T.; Yang, L.; Chen, Q.; Weng, R.; Liu, X.; Feng, X. *CCS Chem.* **2023,** *5,* 2101–2110. doi:10.31635/ccschem.022.202202405
36. Zheng, Y.; Teng, L.-L.; Zhou, T.-T.; Liu, Z.-W.; Guo, K.; Li, H.; Li, T.; Wang, L.-L.; Liu, Y.; Li, S.-H. *Angew. Chem., Int. Ed.* **2025,** *64,* e202421497. doi:10.1002/anie.202421497
37. Huang, X.; Song, L.; Xu, J.; Zhu, G.; Liu, B. *Angew. Chem., Int. Ed.* **2013,** *52,* 952–955. doi:10.1002/anie.201208687
38. Haley, H. M. S.; Payer, S. E.; Papidocha, S. M.; Clemens, S.; Nyenhuis, J.; Sarpong, R. *J. Am. Chem. Soc.* **2021,** *143,* 4732–4740. doi:10.1021/jacs.1c00457
39. Yeap, J. S.-Y.; Lim, K.-H.; Yong, K.-T.; Lim, S.-H.; Kam, T.-S.; Low, Y.-Y. *J. Nat. Prod.* **2019,** *82,* 324–329. doi:10.1021/acs.jnatprod.8b00754
40. Fischer, D. F.; Sarpong, R. *J. Am. Chem. Soc.* **2010,** *132,* 5926–5927. doi:10.1021/ja101893b
41. Aoyama, H.; Hasegawa, T.; Omote, Y. *J. Am. Chem. Soc.* **1979,** *101,* 5343–5347. doi:10.1021/ja00512a039
42. Alvarez-Dorta, D.; León, E. I.; Martín, Á.; Kennedy, A. R.; Pérez-Martín, I.; Shankland, K.; Suárez, E. *J. Org. Chem.* **2022,** *87,* 14940–14947. doi:10.1021/acs.joc.2c01855
43. Aoyama, H.; Sakamoto, M.; Kuwabara, K.; Yoshida, K.; Omote, Y. *J. Am. Chem. Soc.* **1983,** *105,* 1958–1964. doi:10.1021/ja00345a049
44. Chesta, C. A.; Whitten, D. G. *J. Am. Chem. Soc.* **1992,** *114,* 2188–2197. doi:10.1021/ja00032a038
45. Ando, Y.; Hanaki, A.; Sasaki, R.; Ohmori, K.; Suzuki, K. *Angew. Chem., Int. Ed.* **2017,** *56,* 11460–11465. doi:10.1002/anie.201705562
46. Suzuki, K.; Ando, Y.; Matsumoto, T. *Synlett* **2017,** *28,* 1040–1045. doi:10.1055/s-0036-1589001
47. Ando, Y.; Wakita, F.; Ohmori, K.; Suzuki, K. *Bioorg. Med. Chem. Lett.* **2018,** *28,* 2663–2666. doi:10.1016/j.bmcl.2018.05.056
48. Ando, Y.; Tanaka, D.; Sasaki, R.; Ohmori, K.; Suzuki, K. *Angew. Chem., Int. Ed.* **2019,** *58,* 12507–12513. doi:10.1002/anie.201906762
49. Ando, Y.; Ogawa, D.; Ohmori, K.; Suzuki, K. *Angew. Chem., Int. Ed.* **2023,** *62,* e202213682. doi:10.1002/anie.202213682
50. Wakita, F.; Ando, Y.; Ohmori, K.; Suzuki, K. *Org. Lett.* **2018,** *20,* 3928–3932. doi:10.1021/acs.orglett.8b01475
51. Ando, Y.; Ogawa, D.; Wakita, F.; Suzuki, K.; Ohmori, K. *Synlett* **2024,** *35,* 441–444. doi:10.1055/a-2113-0212
52. Ueno, T.; Takahashi, H.; Oda, M.; Mizunuma, M.; Yokoyama, A.; Goto, Y.; Mizushina, Y.; Sakaguchi, K.; Hayashi, H. *Biochemistry* **2000,** *39,* 5995–6002. doi:10.1021/bi992661i
53. Brockmann, H.; Renneberg, K.-H. *Naturwissenschaften* **1953,** *40,* 59–60. doi:10.1007/bf00596449
54. Puder, C.; Loya, S.; Hizi, A.; Zeeck, A. *Eur. J. Org. Chem.* **2000,** 729–735. doi:10.1002/(sici)1099-0690(200003)2000:5<729::aid-ejoc729>3.0.co;2-2
55. Macías-Rubalcava, M. L.; Hernández-Bautista, B. E.; Jiménez-Estrada, M.; González, M. C.; Glenn, A. E.; Hanlin, R. T.; Hernández-Ortega, S.; Saucedo-García, A.; Muria-González, J. M.; Anaya, A. L. *Phytochemistry* **2008,** *69,* 1185–1196. doi:10.1016/j.phytochem.2007.12.006

BEILSTEIN JOURNAL OF ORGANIC CHEMISTRY

Comparative analysis of complanadine A total syntheses

Reem Al-Ahmad[1] and Mingji Dai[*1,2]

Review

Open Access

Address:
[1]Department of Chemistry, Emory University, Atlanta, Georgia 30322, United States and [2]Department of Pharmacology and Chemical Biology, School of Medicine, Emory University, Atlanta, Georgia 30322, United States

Email:
Mingji Dai[*] - mingji.dai@emory.edu

* Corresponding author

Keywords:
biomimetic synthesis; C–H functionalization; complanadine; *lycopodium* alkaloid; skeletal editing; total synthesis; transition metal catalysis

Beilstein J. Org. Chem. **2025,** *21,* 2334–2344.
https://doi.org/10.3762/bjoc.21.178

Received: 30 July 2025
Accepted: 02 October 2025
Published: 30 October 2025

This article is part of the thematic issue "Concept-driven strategies in target-oriented synthesis".

Associate Editor: D. Y.-K. Chen

Abstract

In this review, we summarize and compare four total syntheses of complanadine A, a complex and pseudo-dimeric *lycopodium* alkaloid with promising neurotrophic activity and potential for pain management. These four total syntheses are from the groups of Siegel, Sarpong, Tsukano, and Dai. Each of the four total syntheses contains innovative strategies and creative tactics, reflecting how emerging synthetic capabilities and concepts can positively impact natural product total synthesis.

Introduction

Natural products, owing to their structural complexity, diversity, and therapeutic potential, have continued to serve as inspirations for the development of novel synthetic methodologies and strategies. In turn, these methodological and strategic advancements have significantly improved the efficiency and step-economy of natural product total synthesis. This symbiotic relationship has also helped to accelerate natural product biological evaluation and the subsequent biomedical development [1]. *Lycopodium* alkaloids are one of the largest families of natural products [2], from which famous molecules such as the huperzines have been discovered and advanced into human clinical trials as acetylcholinesterase inhibitors for treating Alzheimer's disease [3]. Among the *lycopodium* family, complanadine A (**1**, Scheme 1) and its natural congeners such as complanadines B (**2**), D (**3**), and E (**4**) were isolated by Kobayashi and co-workers from the club moss *Lycopodium complanatum* [4-7]. They discovered that complanadine A exhibited neurotrophic activity by enhancing the mRNA expression level for nerve growth factor (NGF) biosynthesis in 1321N1 human astrocytoma cells and NGF production in human glial cells, rendering complanadine A a promising lead compound for neurological disorder treatment. Later, complanadine A was also identified as a lead compound for pain management by Siegel and co-workers [8]. They discovered one of its potential cellular targets as the Mas-related G protein-coupled receptor (GPCR) X2 (MrgprX2), which is highly expressed in neurons and functions as a modulator of pain. Complanadine A serves as a selective agonist of MrgprX2.

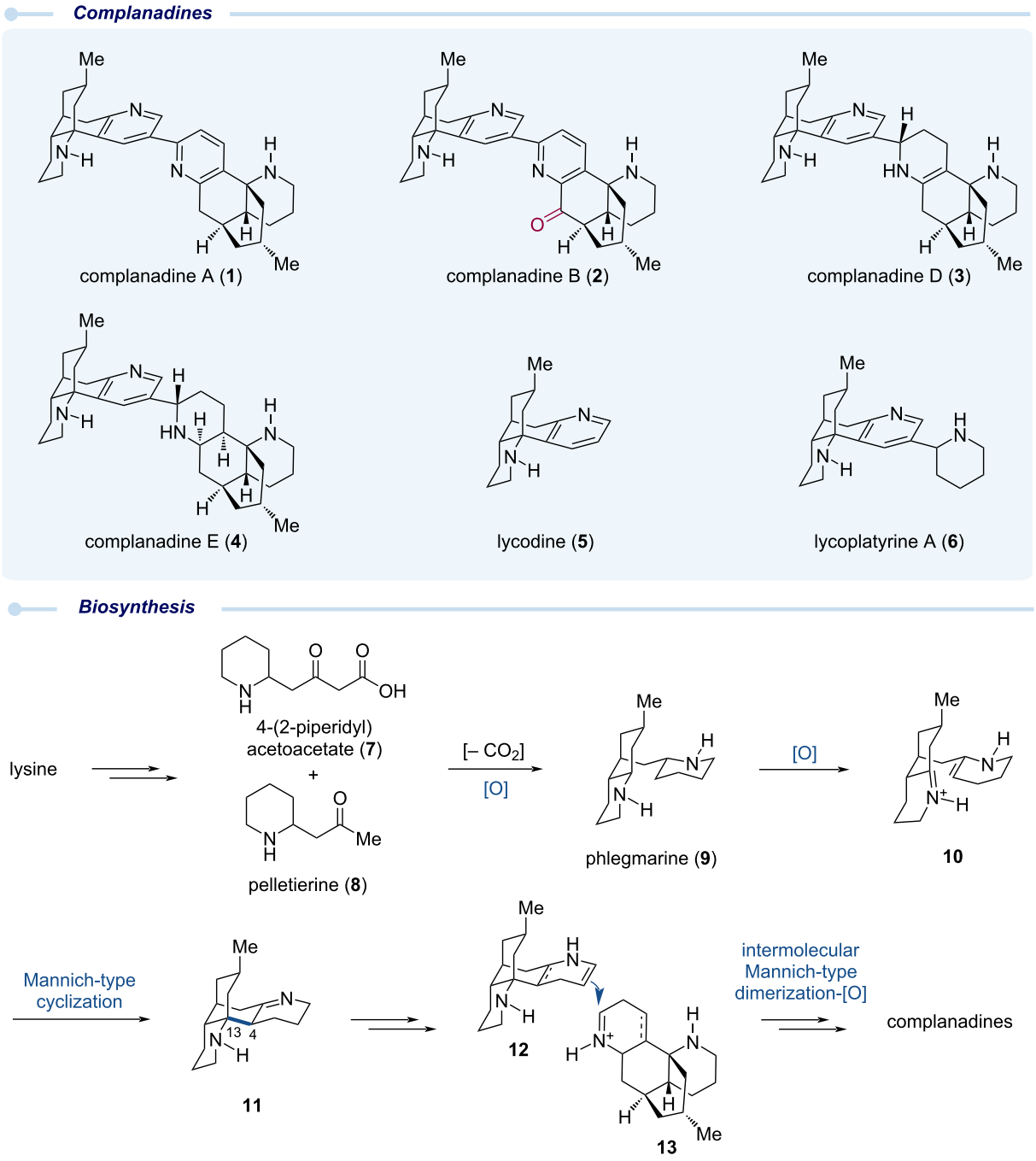

Scheme 1: Complanadine natural products and their plausible biosynthesis.

Structurally, complanadine A is an unsymmetrical dimer of the tetracyclic lycodine (**5**) via a C2–C3' linkage [9,10]. Complanadine B is a mono-oxidized analog and complanadines D and E are partially reduced analogs. In addition, natural analogs such as lycoplatyrine A (**6**), isolated as a mixture of diastereomers, were discovered as derivatives of lycodine and an amino acid [11]. Biosynthetically, lysine was proposed to be the starting point of these *lycopodium* alkaloids [12]. Lysine could be advanced to 4-(2-piperidyl)acetoacetate (**7**) and pelletierine (**8**), which would react with each other to deliver phlegmarine (**9**). Double oxidation of **9** would give **10** for a subsequent intramolecular Mannich-type cyclization to forge the C4–C13 bond and produce **11**, which could be further converted to **12** and **13** for an intermolecular Mannich-type dimerization to form the C2–C3' linkage [13]. Further oxidation state adjustment would give complanadines A, B, D, and E.

Since their isolation, the complanadines, especially complanadine A, have attracted a significant amount of synthetic attention due to their unique structural features and promising therapeutic potential. To date, four total syntheses of complanadine A have been reported from the groups of Siegel [14,15], Sarpong [16], Tsukano [17], and Dai [18], together with one synthetic study from Lewis and co-workers [19]. In this review article, we summarize these four total syntheses, comparatively analyze their strategic novelty and differences, and highlight the impact of enabling methodologies and concepts on the overall efficiency and economy of each total synthesis [20].

Review

The Siegel total synthesis – 2010

In 2010, Siegel and co-workers reported their total synthesis of complanadine A (Scheme 2). Their synthesis centres on two transition metal-catalyzed alkyne–alkyne–nitrile [2 + 2 + 2] cycloadditions to forge the two pyridine rings encoded by complanadine A [21]. Notably, the C2–C3' linkage of complanadine A is embedded within the symmetrical bis(trimethylsilyl)butadiyne starting material, elegantly circumventing the challenges associated with the direct construction of this key connection. This strategic maneuver differentiates Siegel's synthesis from the other three reported approaches. Overall, their synthesis highlights the impact of enabling transition metal catalysis on natural product total synthesis.

The Siegel synthesis starts with chiral pool molecule (+)-pulegone (**14**), which encodes the first stereocenter of the entire sequence. (+)-Pulegone was converted to compound **15** in four steps. Subsequent conjugate addition of the lithium anion of TMS-acetonitrile to **15,** followed by careful one-pot protonation of the resulting enolate with ethyl salicylate and TMS removal with CsF, gave **16** bearing three properly arranged substituents. Grignard 1,2-addition to ketone **16**, followed by acetylation of the resulting propargylic alcohol afforded **17** which was further advanced to **18** via copper-catalyzed selective displacement of the propargyl acetate with benzylamine and hydrolysis of the primary acetate. The primary alcohol of **18** was activated with PPh_3/CCl_4, triggering an intramolecular cyclization to afford alkyne–nitrile **19** for the first [2 + 2 + 2] cycloaddition with bis(trimethylsilyl)butadiyne (**20**). This transformation proceeded smoothly under thermal conditions with $CpCo(CO)_2$ to afford **21** as the major regioisomer (rr = 25:1) [22]. Removal of the two TMS groups and reinstallation of a single TMS on the alkyne provided pyridyl-alkyne **22** for the second [2 + 2 + 2] cycloaddition reaction which proved nontrivial, with the protecting group on the secondary amine of the alkyne-nitrile moiety and the choice of ligand playing crucial roles. Specifically, when using **19** as the alkyne-nitrile partner, the undesired regioisomer (2,2'-bipyridyl product) was obtained as the major product. Switching the alkyne-nitrile partner from **19,** bearing a benzyl group, to the formyl-substituted partner **23**, combined with addition of 8 equivalents of PPh_3, successfully inverted the regioselectivity and gave the desired cycloadduct **24** as the major product in 56% yield. From here on, removal of the TMS group with TBAF, followed by hydrogenolytic removal of the benzyl group and acidic hydrolysis of the formyl group, completed Siegel's total synthesis of complanadine A. In addition, this synthetic route enabled Siegel and co-workers to determine the first biological target of complanadine A. Screening against a panel of cell surface GPCRs revealed that complanadine A acts as a selective agonist of MrgprX2, while the monomer lycodine showed no significant activity towards this target. This finding highlights the importance of complanadine A's pseudo-dimeric structural motif for its biological function.

The Sarpong total synthesis – 2010

In the same year (2010), Sarpong and co-workers reported their total synthesis of complanadine A (Scheme 3). Their synthesis features a biomimetic cascade reaction to rapidly establish the tetracyclic skeleton of complanadine A and an iridium-catalyzed site-selective pyridine C–H borylation followed by a Suzuki–Miyaura cross coupling to forge the C2–C3' linkage. Their synthesis achieves a high degree of synergy between classic transformations and modern synthetic capabilities, highlighting the importance of biomimetic strategies in total synthesis [23-25].

The Sarpong synthesis utilized (+)-pulegone (**14**) as the starting point as well. They first advanced (+)-pulegone to primary amine **25** with a masked enone moiety, which upon treatment with $HClO_4$ underwent ketone release and amine-ketone condensation to form iminium ion **27**. Under the same acidic conditions, enamide **26** underwent hydrolysis and tautomerization to form enol **28**. Conjugate addition of enol **28** to iminium ion **27** gave **29** for the subsequent intramolecular Mannich cyclization to deliver **30**, which continued with an amide-ketone condensation to finally produce **31** in this highly efficient one-step biomimetic cascade sequence. The secondary amine of **31** was selectively protected as a Boc carbamate and the dihydropyridone moiety was oxidized to a pyridone with $Pb(OAc)_4$. Pyridone **32** was prepared in 55% from **25** and **26** in three steps. Triflation of the pyridone gave **33** with a triflate at the C2 position for cross coupling to form the C2–C3' linkage. At this stage, the Sarpong group needed to install a functional group at the C3 position of the pyridine. They creatively solved this challenge with an Ir-catalyzed regioselective C–H borylation developed simultaneously by Ishiyama, Miyaura, Hartwig, and co-workers and Smith and co-workers [26,27]. First, the triflate group of **33** was removed by a Pd-catalyzed reduction with am-

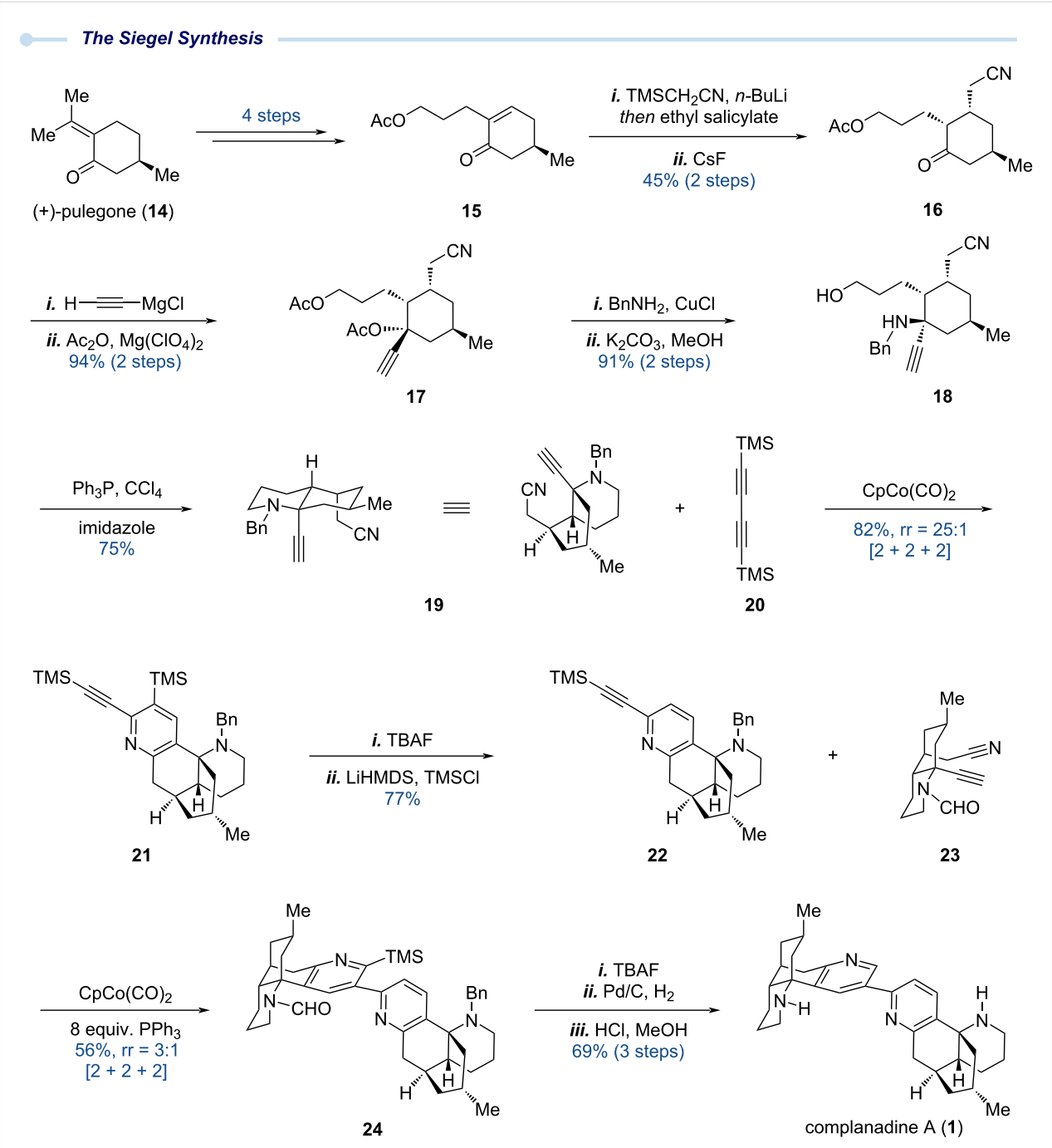

Scheme 2: The Siegel total synthesis of complanadine A enabled by [2 + 2 + 2] cycloadditions.

monium formate as the reducing reagent. The resulting Boc-protected lycodine **34** underwent Ir-catalyzed C3–H borylation mainly guided by steric factors to provide boronic ester **35** in 75% yield. With the boronic ester handle at the C3 position, the subsequent Suzuki–Miyaura cross coupling between **35** and **33** occurred smoothly to deliver pseudo-dimer **36**, which upon acidic removal of the two Boc protecting groups completed the Sarpong total synthesis of complanadine A.

Efficient access of key coupling intermediates **33** and **34** further enabled Sarpong and co-workers to successfully synthesize other *lycopodium* alkaloids. For example, to synthesize complanadine B with mono-oxidation at one of the two benzylic positions, they started with benzylic oxidation of **34** using SeO_2 to provide **37**, which was further oxidized to pyridine *N*-oxide **38**. Treatment of **38** with $POCl_3$ in DMF delivered 2-chloropyridine **39** for the subsequent Suzuki–Miyaura

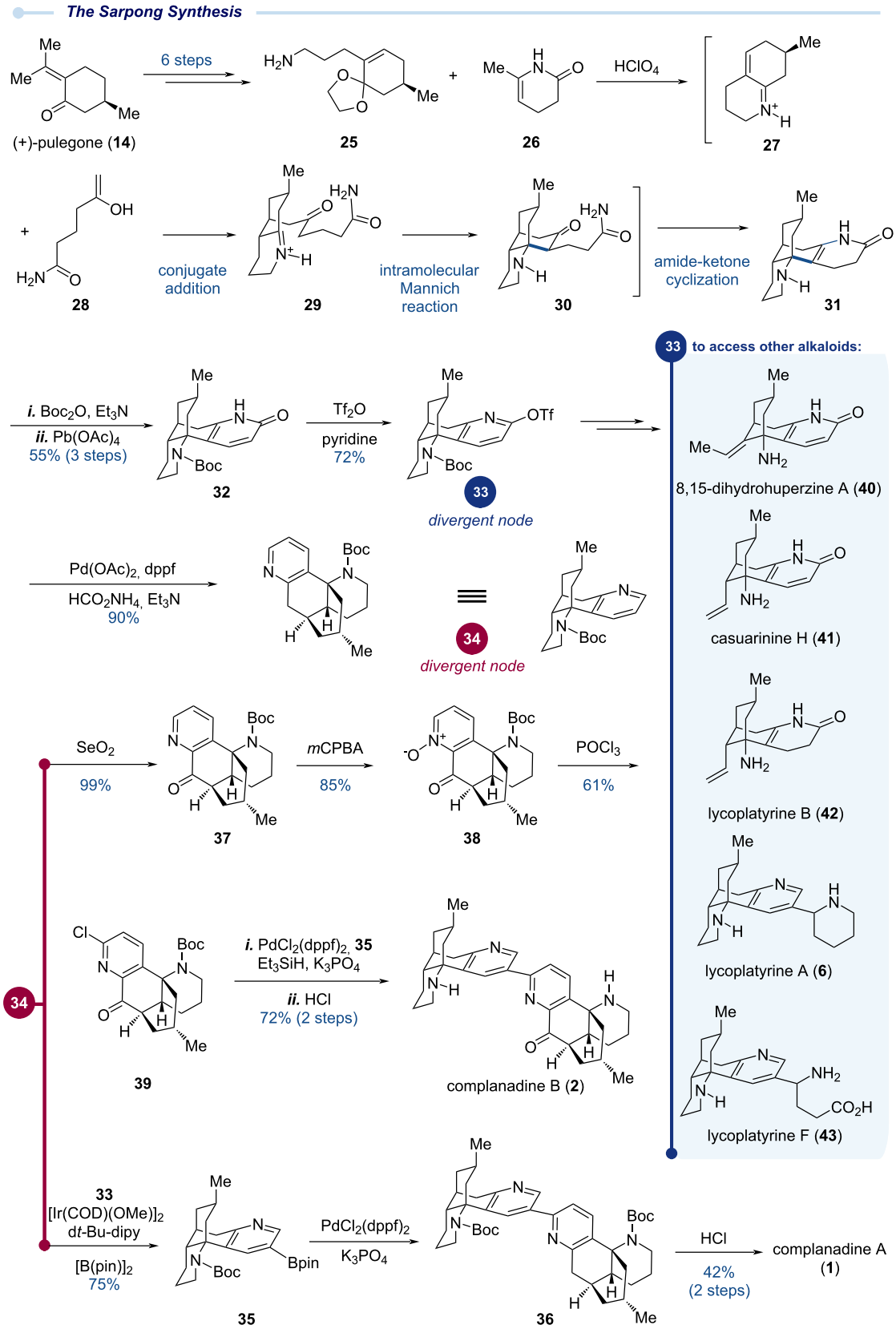

Scheme 3: The Sarpong total synthesis of complanadine A enabled by a biomimetic strategy and C–H activation.

cross coupling with **35** to form the C2–C3' linkage. Boc removal then completed their total synthesis of complanadine B [28]. Notably, while complanadine B could be derived from complanadine A via a selective enzymatic oxidation, attempts to achieve this transformation using chemical methods were unsuccessful. For instance, treatment of **36** with SeO_2 gave a mono-oxidation product at the undesired benzylic position. In addition, from **33** or **35**, Sarpong and co-workers prepared several other *lycopodium* alkaloids including 8,15-dihydrohuperzine A (**40**), casuarinine H (**41**), lycoplatyrines B (**42**), A (**6**), and F (**43**, existing as a mixture of diastereomers) via either a creative "degradation" of the piperidine ring or cross-coupling reactions at the pyridine C3 position [29].

The Tsukano total synthesis – 2013

In 2013, Tsukano and co-workers reported their total synthesis of complanadines A and B (Scheme 4). Their synthesis utilizes a Diels–Alder reaction and an intramolecular Heck reaction to build the two six-membered carbocycles embedded in the bicyclo[3.3.1]nonane ring system of complanadine A and a pyridine *N*-oxide directed *ortho* C–H arylation to forge the C2–C3' linkage.

As shown in Scheme 4, they first prepared diene **44** and dienophile **45** for a thermal Diels–Alder cycloaddition, which afforded a mixture of stereo- (*endo*/*exo*) and regioisomers, among which the desired product **46** was obtained in 45% yield as a racemic mixture. After triflation of the free hydroxy group of **46** to provide **47**, an intramolecular Heck reaction was employed to close the second six-membered carbocycle to deliver **48** in 73% yield. The Diels–Alder reaction and Heck reaction quickly set up the tetracyclic skeleton for subsequent peripheral modifications. First, the ketone functionality of **48** was reduced to a methylene group via a sequence of Luche reduction and Barton–McCombie deoxygenation. The extra ethyl carboxylate was removed via a sequence of LiOH hydrolysis and a Curtius rearrangement using DPPA to form the corresponding acyl azide. Ketone **50** was produced in 98% yield over two steps. The newly formed ketone functionality enabled the introduction of the desired methyl group at its α-position to afford **51** in racemic form. This seemingly straightforward α-methylation turned out to be quite challenging. Tsukano and co-workers eventually utilized a two-step sequence to solve this problem, namely, TMS enol ether formation followed by trapping the enol ether with MeI in presence of benzyltrimethylammonium fluoride (BTAF). At this stage, to prepare optically active natural product, the racemic mixture of **51** was separated using chiral HPLC to afford (+)-**51** and (−)-**51**, which were used to prepare both enantiomers of complanadine A for biological evaluations. With optically active **51** in hand, its extra ketone functionality was reduced via thioacetalization (**51** → **52**) and radical reduction (**52** → **53**) to provide **53**, a diverging point to access C–H arylation partners **54** and **55**. *m*CPBA oxidation of **53** afforded pyridine *N*-oxide **54**. The Ir-catalyzed C–H borylation used in the Sarpong synthesis was again utilized here to introduce a boronic ester at the C3 position, which was further converted to 3-bromopyridine **55** with $CuBr_2$. With both **54** and **55**, Tsukano and co-workers employed a remarkable pyridine *N*-oxide directed C–H arylation method developed by Fagnou et al. to forge the C2–C3' bipyridyl linkage and produce **56** in good yield [30]. From **56**, a one-pot Cbz removal and pyridine *N*-oxide reduction completed their total synthesis of complanadine A. In addition, **56** also served as a key intermediate for their synthesis of complanadine B, which was achieved via a sequence of Boekelheide rearrangement (**56** → **57**), acetate hydrolysis, DMP oxidation and Cbz removal. Based on these results, Tsukano and co-workers suggested that a mono-*N*-oxide intermediate could be involved in the biosynthesis of these dimeric complanadine alkaloids. Importantly, access to both enantiomers of **51** allowed Tsukano and co-workers to prepare both enantiomers of complanadine A. Their further biological evaluation of the complanadines and several synthetic intermediates revealed that the pseudo-dimeric structure, absolute configuration, and oxidation level are important for the observed neurotrophic activity, providing a strong foundation for future analog design and synthesis [31].

The Dai total synthesis – 2021

In 2021, eleven years after the first two total syntheses of complanadine A, Dai and co-workers reported their total synthesis of complanadine A (Scheme 5). Their synthesis features a novel single-atom skeletal editing strategy [32,33] to form the pyridine from a pyrrole and a similar pyridine *N*-oxide directed *ortho* C–H arylation to forge the C2–C3' linkage as the Tsukano synthesis, but with a much less reactive 3-chloropyridine as the cross-coupling partner.

As shown in Scheme 5, the Dai synthesis starts with compound **58** which can be prepared from (+)-pulegone in three steps or via an organocatalyzed tandem sequence in one step. The terminal olefin of **58** was then converted to a primary azide via an anti-Markovnikov hydroazidation reaction with a combination of **59** and $TMSN_3$ recently developed by Xu and co-workers [34]. Mukaiyama conjugate addition between **60** and **61** promoted by Tf_2NH followed by a one-pot enol ether hydrolysis gave **62** as a mixture of inconsequential stereoisomers. Subsequent oxidative cleavage of the terminal olefin of **62** using ozonolysis followed by Paal–Knorr pyrrole synthesis delivered **63**, which was unstable and spontaneously cyclized to provide **64**. Compound **64** was then advanced to tetracyclic intermediate **67** in a one-pot tandem process, which initiated with Staudinger azide reduction with PPh_3 to form a primary

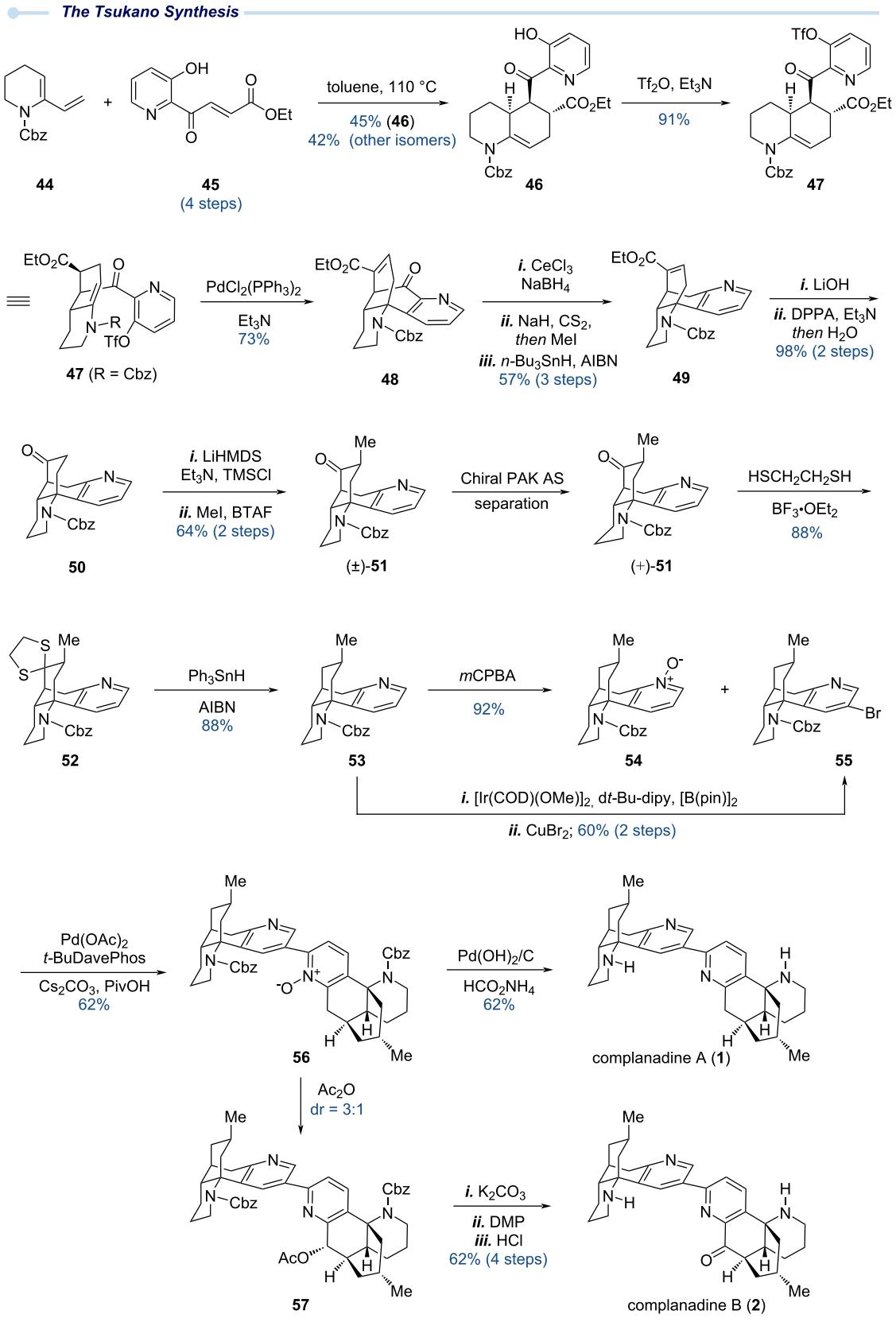

Scheme 4: The Tsukano total synthesis of complanadine A enabled by Diels–Alder cycloaddition, Heck cyclization, and directed C–H arylation.

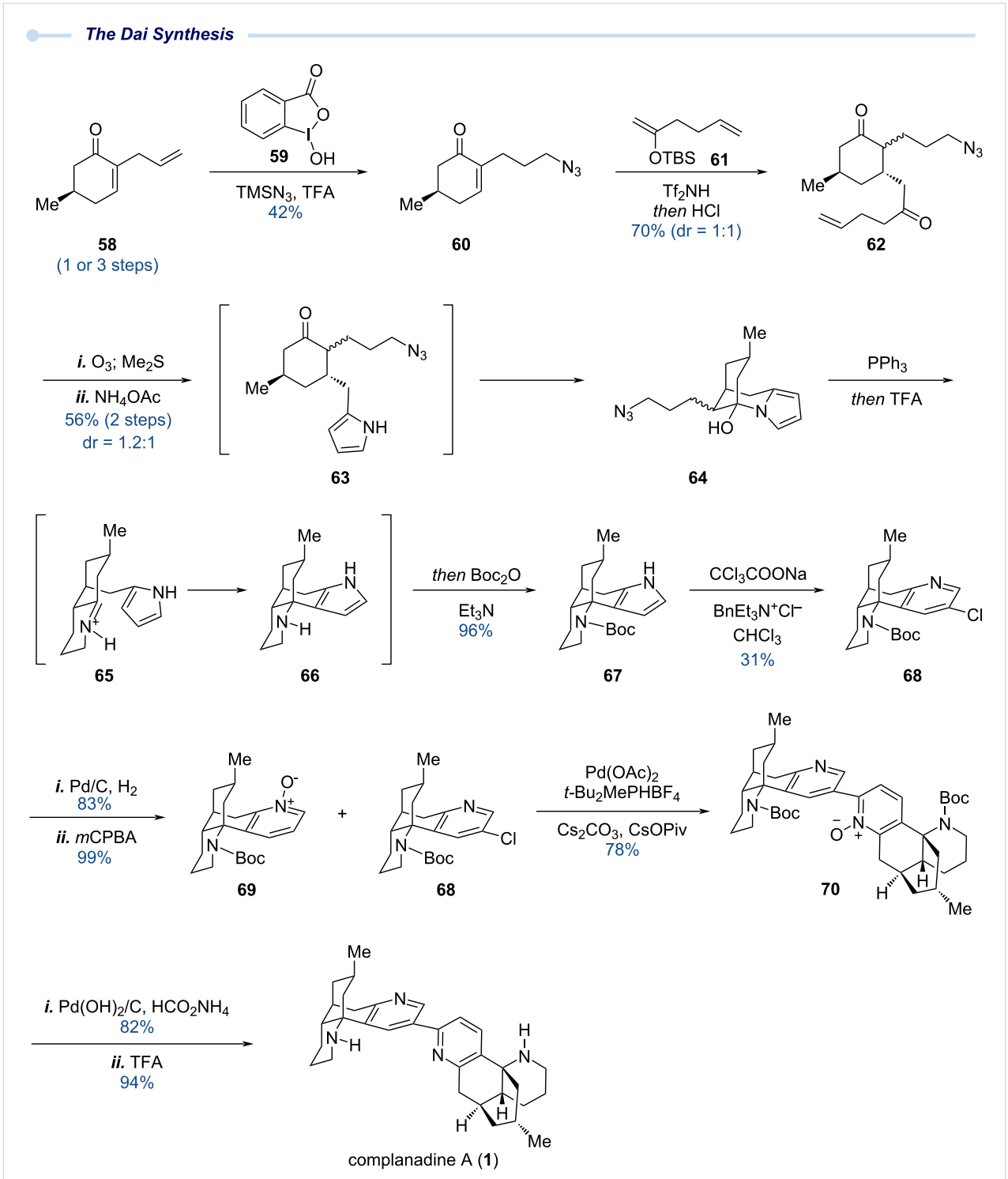

Scheme 5: The Dai total synthesis of complanadine A using single-atom skeletal editing.

amine. After reversible hemiaminal opening and amine–ketone condensation, iminium ion **65** was produced for the next pyrrole nucleophilic addition to form a strategically important C–C bond and afford **66**, which was protected as Boc carbamate in the same pot to give **67** in 96% yield from **64**. In this tandem sequence, the nucleophilicity of the electron-rich pyrrole group is essential for the key C–C bond formation. In the next step, the pyrrole group was converted to the pyridine group encoded by the natural product. This single-atom skeletal editing step (**67** → **68**) was achieved using the Ciamician–Dennstedt rear-

rangement, a reaction discovered back in 1881 [35]. Furthermore, this rearrangement positioned a chloride handle at the desired site for the next C–H arylation. Part of **68** was then converted to pyridine *N*-oxide via Pd/C-catalyzed dechlorination and *m*CPBA oxidation. While a similar C–H arylation strategy was used in the Tsukano synthesis, the 3-chloropyridine **68** used in the Dai synthesis exhibited much lower reactivity compared to the 3-bromopyridine **55** used in the Tsukano synthesis. Thus, a set of new reaction conditions was needed. To solve this reactivity issue, a protocol developed by Stoltz et al. in their jorunnamycin synthesis [$Pd(OAc)_2$, *t*-$Bu_2MePHBF_4$, Cs_2CO_3, and CsOPiv in toluene at 130 °C] was utilized to afford the C–H arylation in 78% yield with a 1:4 ratio of **68**/**69** [36]. Subsequent reduction of the pyridine *N*-oxide with $Pd(OH)_2$/C and H_2 followed by acidic Boc removal completed their total synthesis of complanadine A (**1**). In addition, 3-chloropyridine **68** enabled Dai and co-workers to prepare simplified analogs of complanadine A for biological evaluation [13].

Conclusion

As summarized in Scheme 6, four complanadine A total syntheses were reviewed here. Toward the same target molecule, four

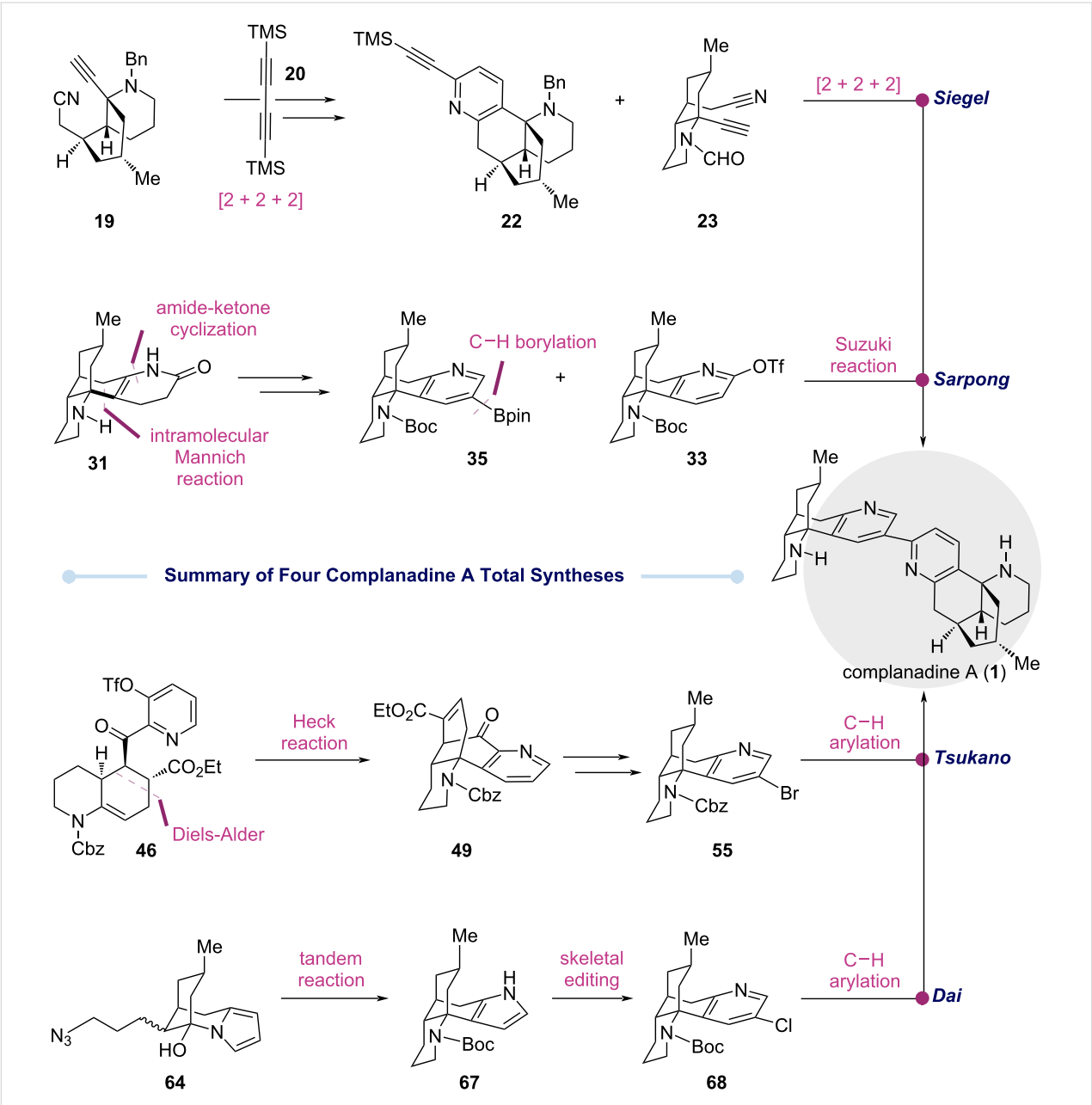

Scheme 6: Comparative summary of the four complanadine A total syntheses.

strategically unique and different approaches were developed. The Siegel synthesis harnesses the power and efficiency of two Co-mediated [2 + 2 + 2] cycloadditions to build the C2–C3'-bipyridyl moiety encoded by complanadine A. The Sarpong synthesis leverages a biomimetic approach to rapidly assemble the tetracyclic core skeleton and the newly developed C–H borylation to install a boronic ester handle at the desired position for a Suzuki–Miyaura cross coupling to build the C2–C3' linkage which was hidden in bis(trimethylsilyl)butadiyne (**20**) of the Siegel synthesis. Both the groups of Tsukano and Dai utilized a pyridine *N*-oxide directed C–H arylation to forge the C2–C3' linkage, but the approaches to prepare the C–H arylation precursors they employed differ completely. In the Tsukano synthesis, a Diels–Alder reaction and an intramolecular Heck reaction were used to build the key ring systems of complanadine A. In the Dai synthesis, they used an electron-rich and nucleophilic pyrrole as the precursor of the electron-deficient pyridine to enable a tandem sequence involving an intramolecular nucleophilic addition of the pyrrole to an iminium ion to form a key C–C bond. The pyrrole group was then converted to the desired pyridine via a single-atom skeletal editing using the 145-year-old Ciamician–Dennstedt rearrangement, completing its long overdue debut in total synthesis. Overall, each of these four total syntheses showcase innovative strategies and creative and enabling tactics including modern transition metal catalysis, C–H activation methods, biomimetic synthesis, classic rearrangements, skeletal editing logic, and others. In addition, these efforts enabled the identification of the potential cellular target of complanadine A, validation of its neurotrophic activity, establishment of preliminary structure activity relationships, and generation of synthetic analogs, all of which pave the way for further study and development of this unique natural product and/or its analogs.

Funding

We thank NIH GM128570 for financial support.

Author Contributions

Reem Al-Ahmad: conceptualization; writing – original draft; writing – review & editing. Mingji Dai: conceptualization; funding acquisition; project administration; supervision; writing – original draft; writing – review & editing.

ORCID® iDs

Reem Al-Ahmad - https://orcid.org/0000-0001-7591-3371

Data Availability Statement

Data sharing is not applicable as no new data was generated or analyzed in this study.

References

1. Nicolaou, K. C.; Hale, C. R. H. *Natl. Sci. Rev.* **2014,** *1,* 233–252. doi:10.1093/nsr/nwu001
2. Ma, X.; Gang, D. R. *Nat. Prod. Rep.* **2004,** *21,* 752–772. doi:10.1039/b409720n
3. Tun, M. K. M.; Herzon, S. B. *J. Exp. Pharmacol.* **2012,** *4,* 113–123. doi:10.2147/jep.s27084
4. Kobayashi, J.; Hirasawa, Y.; Yoshida, N.; Morita, H. *Tetrahedron Lett.* **2000,** *41,* 9069–9073. doi:10.1016/s0040-4039(00)01630-0
5. Morita, H.; Ishiuchi, K.; Haganuma, A.; Hoshino, T.; Obara, Y.; Nakahata, N.; Kobayashi, J. *Tetrahedron* **2005,** *61,* 1955–1960. doi:10.1016/j.tet.2005.01.011
6. Ishiuchi, K.; Kubota, T.; Ishiyama, H.; Hayashi, S.; Shibata, T.; Mori, K.; Obara, Y.; Nakahata, N.; Kobayashi, J. *Bioorg. Med. Chem.* **2011,** *19,* 749–753. doi:10.1016/j.bmc.2010.12.025
7. Ishiuchi, K.; Kubota, T.; Mikami, Y.; Obara, Y.; Nakahata, N.; Kobayashi, J. *Bioorg. Med. Chem.* **2007,** *15,* 413–417. doi:10.1016/j.bmc.2006.09.043
8. Johnson, T.; Siegel, D. *Bioorg. Med. Chem. Lett.* **2014,** *24,* 3512–3515. doi:10.1016/j.bmcl.2014.05.060
9. Heathcock, C. H.; Kleinman, E. F.; Binkley, E. S. *J. Am. Chem. Soc.* **1982,** *104,* 1054–1068. doi:10.1021/ja00368a024
10. Azuma, M.; Yoshikawa, T.; Kogure, N.; Kitajima, M.; Takayama, H. *J. Am. Chem. Soc.* **2014,** *136,* 11618–11621. doi:10.1021/ja507016g
11. Yeap, J. S.-Y.; Lim, K.-H.; Yong, K.-T.; Lim, S.-H.; Kam, T.-S.; Low, Y.-Y. *J. Nat. Prod.* **2019,** *82,* 324–329. doi:10.1021/acs.jnatprod.8b00754
12. Wang, J.; Zhang, Z.-K.; Jiang, F.-F.; Qi, B.-W.; Ding, N.; Hnin, S. Y. Y.; Liu, X.; Li, J.; Wang, X.-h.; Tu, P.-F.; Abe, I.; Morita, H.; Shi, S.-P. *Org. Lett.* **2020,** *22,* 8725–8729. doi:10.1021/acs.orglett.0c03339
13. Martin, B. S.; Ma, D.; Saito, T.; Gallagher, K. S.; Dai, M. *Synthesis* **2024,** *56,* 107–117. doi:10.1055/a-2107-5159
14. Yuan, C.; Chang, C.-T.; Axelrod, A.; Siegel, D. *J. Am. Chem. Soc.* **2010,** *132,* 5924–5925. doi:10.1021/ja101956x
15. Yuan, C.; Chang, C.-T.; Siegel, D. *J. Org. Chem.* **2013,** *78,* 5647–5668. doi:10.1021/jo400695c
16. Fischer, D. F.; Sarpong, R. *J. Am. Chem. Soc.* **2010,** *132,* 5926–5927. doi:10.1021/ja101893b
17. Zhao, L.; Tsukano, C.; Kwon, E.; Takemoto, Y.; Hirama, M. *Angew. Chem., Int. Ed.* **2013,** *52,* 1722–1725. doi:10.1002/anie.201208297
18. Ma, D.; Martin, B. S.; Gallagher, K. S.; Saito, T.; Dai, M. *J. Am. Chem. Soc.* **2021,** *143,* 16383–16387. doi:10.1021/jacs.1c08626
19. Uosis-Martin, M.; Pantoş, G. D.; Mahon, M. F.; Lewis, S. E. *J. Org. Chem.* **2013,** *78,* 6253–6263. doi:10.1021/jo401014n
20. Newhouse, T.; Baran, P. S.; Hoffmann, R. W. *Chem. Soc. Rev.* **2009,** *38,* 3010–3021. doi:10.1039/b821200g
21. Varela, J. A.; Saá, C. *Chem. Rev.* **2003,** *103,* 3787–3802. doi:10.1021/cr030677f
22. Varela, J. A.; Castedo, L.; Saá, C. *J. Am. Chem. Soc.* **1998,** *120,* 12147–12148. doi:10.1021/ja982832r
23. de la Torre, M. C.; Sierra, M. A. *Angew. Chem., Int. Ed.* **2004,** *43,* 160–181. doi:10.1002/anie.200200545
24. Razzak, M.; De Brabander, J. K. *Nat. Chem. Biol.* **2011,** *7,* 865–875. doi:10.1038/nchembio.709
25. Bao, R.; Zhang, H.; Tang, Y. *Acc. Chem. Res.* **2021,** *54,* 3720–3733. doi:10.1021/acs.accounts.1c00459

26. Ishiyama, T.; Takagi, J.; Ishida, K.; Miyaura, N.; Anastasi, N. R.; Hartwig, J. F. *J. Am. Chem. Soc.* **2002,** *124,* 390–391. doi:10.1021/ja0173019
27. Cho, J.-Y.; Tse, M. K.; Holmes, D.; Maleczka, R. E., Jr.; Smith, M. R., III. *Science* **2002,** *295,* 305–308. doi:10.1126/science.1067074
28. Newton, J. N.; Fischer, D. F.; Sarpong, R. *Angew. Chem., Int. Ed.* **2013,** *52,* 1726–1730. doi:10.1002/anie.201208571
29. Haley, H. M. S.; Payer, S. E.; Papidocha, S. M.; Clemens, S.; Nyenhuis, J.; Sarpong, R. *J. Am. Chem. Soc.* **2021,** *143,* 4732–4740. doi:10.1021/jacs.1c00457
30. Campeau, L.-C.; Rousseaux, S.; Fagnou, K. *J. Am. Chem. Soc.* **2005,** *127,* 18020–18021. doi:10.1021/ja056800x
31. Zhao, L.; Tsukano, C.; Kwon, E.; Shirakawa, H.; Kaneko, S.; Takemoto, Y.; Hirama, M. *Chem. – Eur. J.* **2017,** *23,* 802–812. doi:10.1002/chem.201604647
32. Al-Ahmad, R.; Dai, M. *Acc. Chem. Res.* **2025,** *58,* 1392–1406. doi:10.1021/acs.accounts.5c00030
33. Jurczyk, J.; Woo, J.; Kim, S. F.; Dherange, B. D.; Sarpong, R.; Levin, M. D. *Nat. Synth.* **2022,** *1,* 352–364. doi:10.1038/s44160-022-00052-1
34. Li, H.; Shen, S.-J.; Zhu, C.-L.; Xu, H. *J. Am. Chem. Soc.* **2019,** *141,* 9415–9421. doi:10.1021/jacs.9b04381
35. Ciamician, G. L.; Dennstedt, M. *Ber. Dtsch. Chem. Ges.* **1881,** *14,* 1153–1163. doi:10.1002/cber.188101401240
36. Welin, E. R.; Ngamnithiporn, A.; Klatte, M.; Lapointe, G.; Pototschnig, G. M.; McDermott, M. S. J.; Conklin, D.; Gilmore, C. D.; Tadross, P. M.; Haley, C. K.; Negoro, K.; Glibstrup, E.; Grünanger, C. U.; Allan, K. M.; Virgil, S. C.; Slamon, D. J.; Stoltz, B. M. *Science* **2019,** *363,* 270–275. doi:10.1126/science.aav3421

License and Terms

BEILSTEIN JOURNAL OF ORGANIC CHEMISTRY

Synthetic study toward vibralactone

Liang Shi, Jiayi Song, Yiqing Li, Jia-Chen Li, Shuqi Li, Li Ren, Zhi-Yun Liu* and Hong-Dong Hao*

Letter

Open Access

Address:
Shaanxi Key Laboratory of Natural Products & Chemical Biology, College of Chemistry & Pharmacy, Northwest A&F University, Yangling, Shaanxi 712100, China

Email:
Zhi-Yun Liu* - liuzhiy@nwafu.edu.cn; Hong-Dong Hao* - hongdonghao@nwafu.edu.cn

* Corresponding author

Keywords:
alkylidene carbene; C–H insertion; total synthesis; vibralactone

Beilstein J. Org. Chem. **2025,** *21,* 2376–2382.
https://doi.org/10.3762/bjoc.21.182

Received: 27 July 2025
Accepted: 21 October 2025
Published: 04 November 2025

This article is part of the thematic issue "Concept-driven strategies in target-oriented synthesis".

Guest Editor: Y. Tang

Abstract

A synthetic study toward vibralactone, a potent inhibitor of pancreatic lipase, is reported. The synthesis of the challenging all-carbon quaternary center within the cyclopentene ring was achieved through intramolecular alkylidene carbene C–H insertion.

Introduction

β-Lactones have attracted continuous interest and have been widely utilized as key intermediates in the synthesis of natural products and polymers due to their innate ring strain [1-6]. Moreover, several natural products and their derivatives containing β-lactone as key structural moiety have been isolated and demonstrate potent bioactivities [7] (Figure 1). For example, lactacystin (**1**) which was isolated by Ōmura and co-workers [8,9], is a potent and selective proteasome inhibitor; its active form is the synthetic precursor omuralide (**2**) [10,11]. Similarly, salinosporamide (**3**), a marine natural product isolated by Fenical and co-workers [12], also acts as a proteasome inhibitor and displays more potent in vitro cytotoxicity than omuralide (**2**). Anisatin (**4**), which contains a characteristic spiro β-lactone has been identified as a noncompetitive antagonist of GABA-gated ion channels [13]. Tetrahydrolipstatin (**5**) is a potent pancreatic lipase inhibitor and has been developed into an antiobesity drug marketed under the generic name Orlistat. Vibralactone (**6**), which was isolated by Liu and co-workers from Basidiomycete *Boreostereum vibrans*, features a fused β-lactone with a cyclopentene ring containing an all-carbon quaternary center [14], and inhibits pancreatic lipase with an IC_{50} of 0.4 μg/mL. Several congeners with varying oxidation state, as well as related β-hydroxy acids or esters have also been isolated from the culture broth of the basidiomycete [15-21]. Additionally, a series of vibralactone homodimers and oxime esters **10**–**12** were reported by the groups of Liu and Zhang, respectively [22,23]. Through modification of the primary hydroxy group, a structure-based optimization of vibralactone (**6**) was carried out by Liu and co-workers and yielded several potent pancreatic lipase inhibitors with nanomolar IC_{50} values [24], further supporting vibralactone as a promising lead compound warranting further investigation.

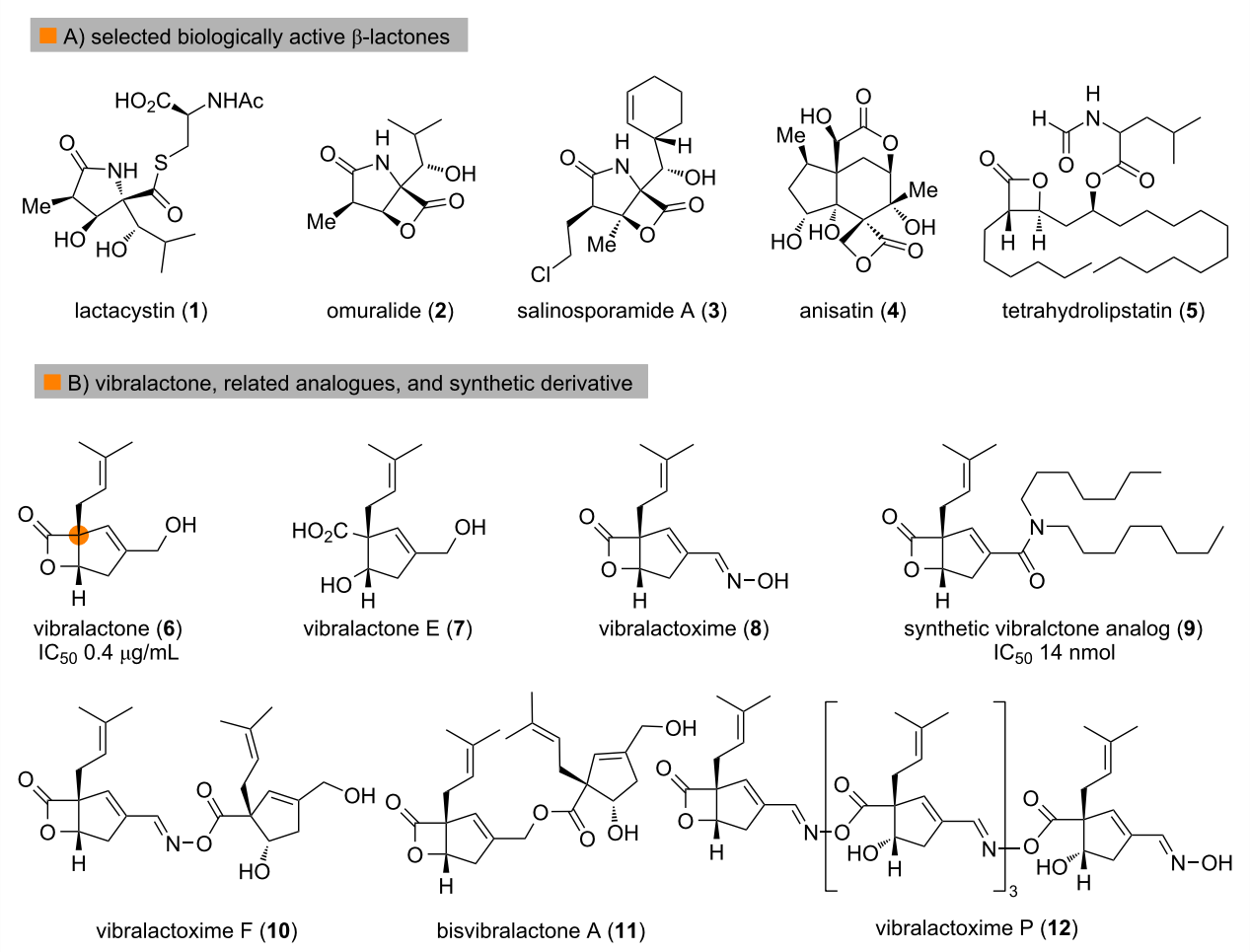

Figure 1: Selected representative natural products and derivatives with β-lactone moiety.

Although vibralactone (**6**) is a relatively small natural product, its molecular structure features a unique 4/5-fused bicyclic β-lactone with an all-carbon quaternary center and two trisubstituted olefin moieties. It is therefore not surprising that this compound has attracted considerable interest from both the chemical biology and synthetic chemistry communities. Sieber and co-workers disclosed that vibralactone can target ClpP1 and ClpP2 and it could be utilized as a probe to study the activity and structure of the ClpP1P2 complex from *Listeria monocytogenes* [25]. Previously, Snider and co-worker reported the first total synthesis of vibralactone (**6**) employing Birch reductive alkylation, intramolecular aldol reaction and late-stage lactonization as key steps [26] (Scheme 1). Subsequently, they achieved the asymmetric synthesis of vibralactone (**6**) based on the asymmetric Birch reduction–alkylation methodology developed by the Schultz group [27,28]. In 2016, Brown and co-workers described an efficient synthetic route featuring a novel Pd-catalyzed β-lactone formation [29]. In addition to these approaches, Nelson and co-workers reported a very concise and impressive total synthesis of vibralactone involving photochemical valence isomerization of substituted pyrone, cyclopropanation, and ring expansion [30]. Zeng, Liu and co-workers investigated the biosynthetic pathway of vibralactone (**6**). They established that 4-hydroxybenzoate serves as the direct ring precursor of vibralactone and the β-lactone moiety was formed via vibralactone cyclase (VibC)-catalyzed cyclization [31-34]. This is a fascinating cyclization as the all-carbon quaternary center is formed in the last step. Given that the β-lactone moiety may act as a potential covalent inhibitor toward target proteins and that the sterically congested bicyclic skeleton presents a significant synthetic challenge, we herein report our synthetic study toward vibralactone.

Impressed by the unexpected biosynthetic pathway, our synthetic strategy also aimed to construct the quaternary center in the late stage. The retrosynthetic analysis of vibralactone (**6**) is descripted in Scheme 2. Initially, we proposed that vibralactone could be synthesized from lactone **13** through allylic oxidation and cross metathesis. For the construction of the cyclopentene ring, an alkylidene carbene-mediated C–H insertion would be

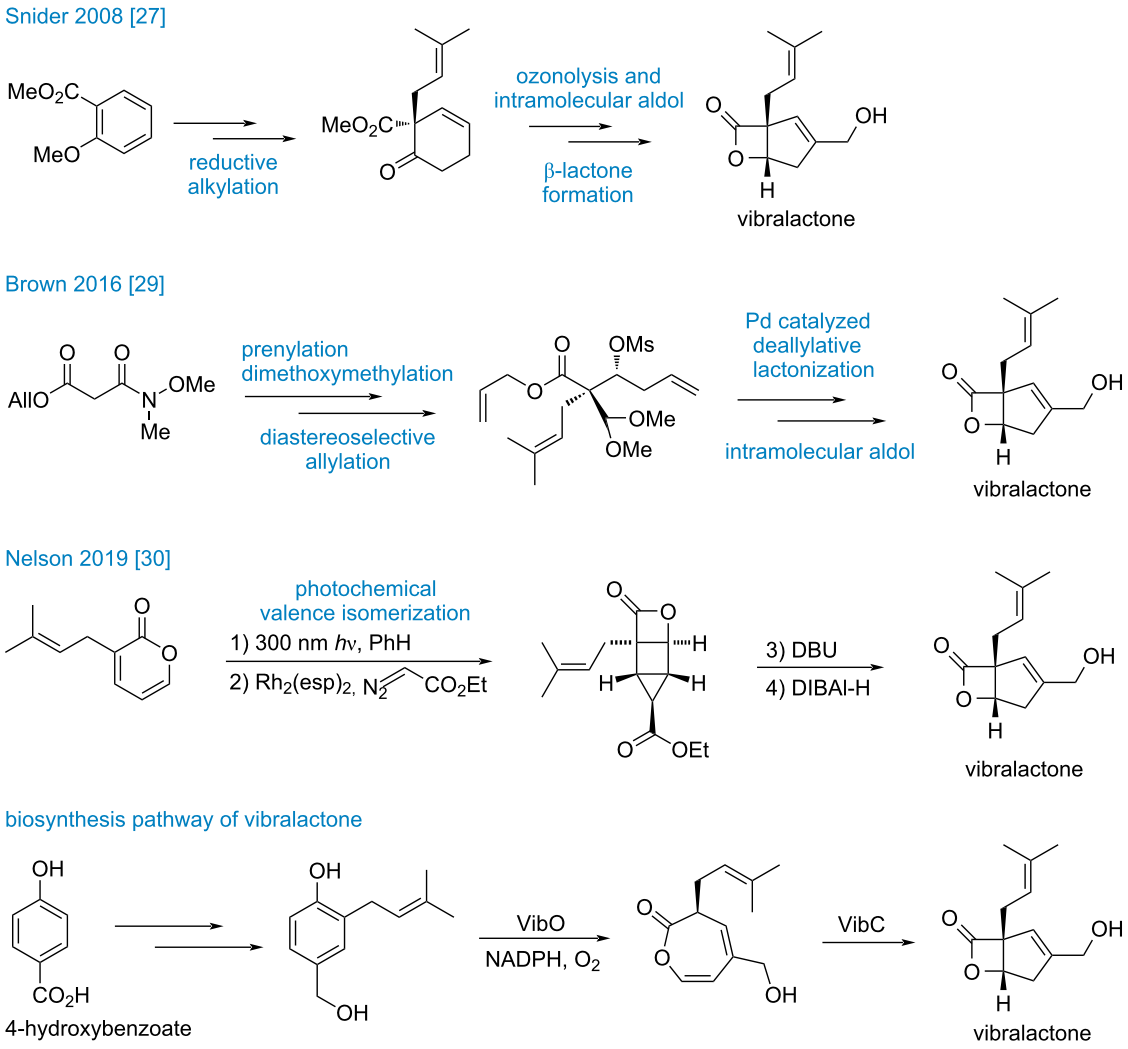

Scheme 1: Previous syntheses of vibralactone (**6**).

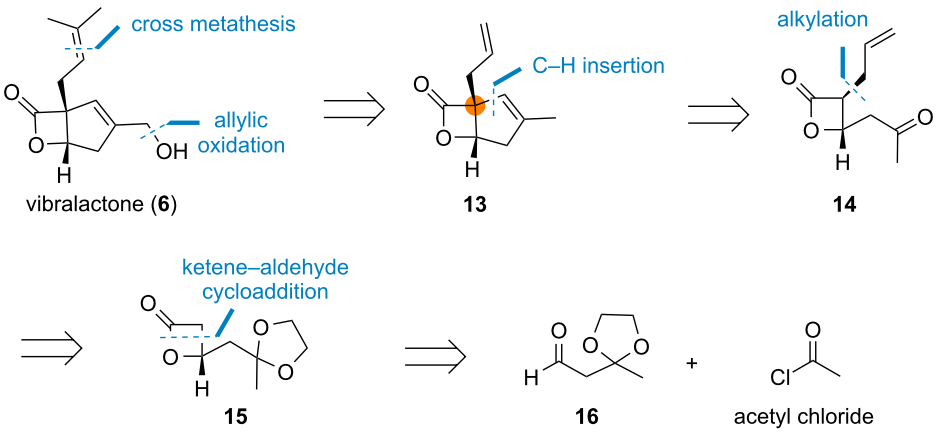

Scheme 2: Retrosynthetic analysis of vibralactone (**6**).

applied [35]. The synthetic route could be traced back to β-lactone **14**, which contains two continuous stereogenic centers with *trans* configuration. This intermediate was intended to be prepared through allylation [36] with its precursor **15** accessible from aldehyde **16** and acetyl chloride through ketene–aldehyde [2 + 2] cycloaddition [37].

Results and Discussion

Our synthetic route commenced from the known aldehyde **16** which is readily accessed in a single step from commercially available fructone [38] (Scheme 3). Following an efficient *O*-trimethylsilylquinine-catalyzed ketene–aldehyde cycloaddition and subsequent alkylation [36], **17** was synthesized. From **17**, it was envisioned that the bicyclic skeleton could be efficiently constructed through ketal deprotection followed by C–H insertion. However, when attempting to remove the ketal protecting group, only decomposition of the starting material was observed. A plausible explanation for this outcome is that the β-lactone ring, located at the β-position of the methyl ketone, may undergo facile β-elimination, although the corresponding enone product was not isolated. Facing a dead-end, the synthetic route to precursor **14** needed to be revised. From **15**, after sodium methoxide-mediated ring opening of lactone, the Fráter–Seebach alkylation [39-41] was applied to afford β-hydroxy ester **18**. At this stage, the ketal moiety was removed and the resulting intermediate underwent Wittig olefination to yield vinyl chloride **20**. Subsequent hydrolysis and intramolecular esterification furnished intermediate **21**, which was then subjected to C–H insertion [42-44]. To our disappointment, this ring closure still did not proceed to form the all-carbon quaternary center and only decomposition of **21** was observed. The failure is likely due to the sterically hindered environment of the substituted β-lactone ring which precludes the C–H insertion or deprotonation of the β-lactone and interrupted the generation of the alkylidene carbene. Therefore, we modified the synthetic sequence and opted to construct the five-membered ring prior to β-lactone formation, identifying intermediate **19** as a potentially suitable precursor.

From **19**, after treatment with lithiotrimethylsilyldiazomethane [45], only tetrahydrofuran **22** was isolated via a formal [4 + 1] annulation pathway [46] (Scheme 4). Since the hydroxy group interrupted the C–H insertion, it was protected as the TES ether **23** and subjected to the same conditions. However, the reaction only afforded the C–Si insertion product **24** [47].

Based on the above results, although the β-lactone was converted into the linear methyl ester **19** to decrease the potential steric hinderance associated with the fused bicyclic skeleton, substrates containing a free hydroxy group or the corresponding TES ether still failed to close the cyclopentene ring. In this scenario, it was necessary to explore additional protecting groups for the hydroxy functionality. Furthermore, given that alkylidene carbenes are electron-deficient and highly electrophilic, electron-rich C–H bonds are more prone to undergo C–H insertion [48]. Following this analysis, commencing from **20**,

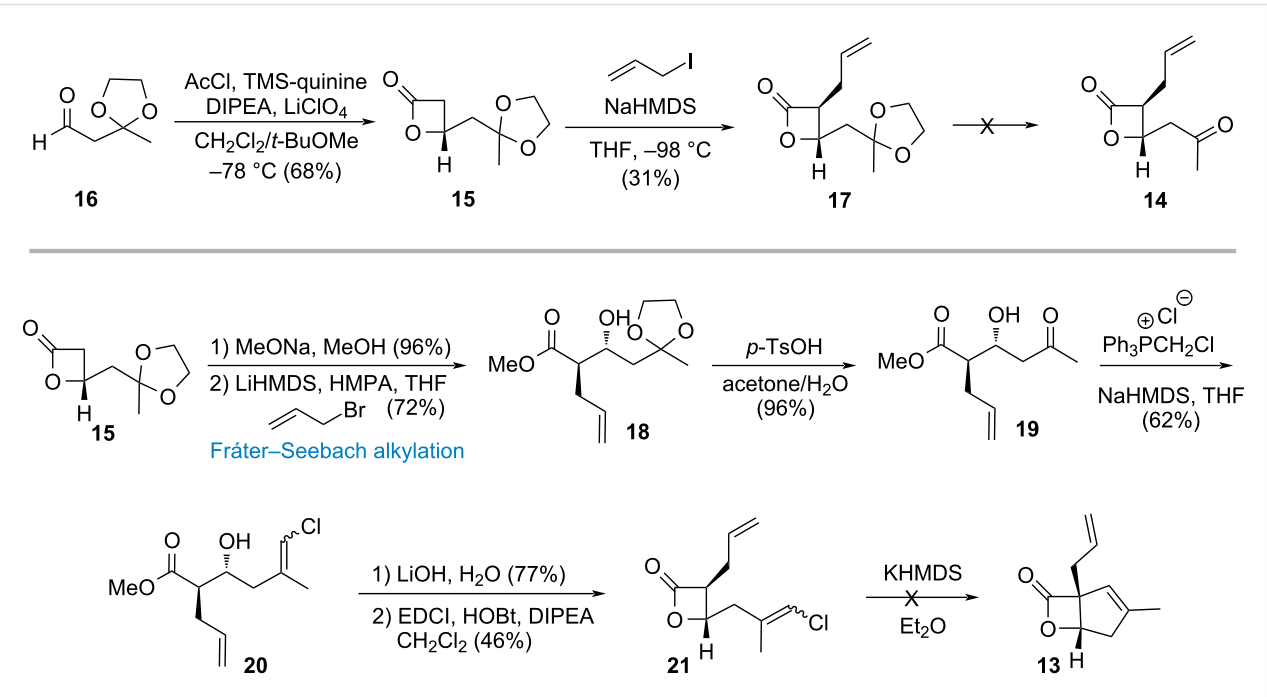

Scheme 3: Synthetic study toward vibralactone (**6**) in the present of β-lactone.

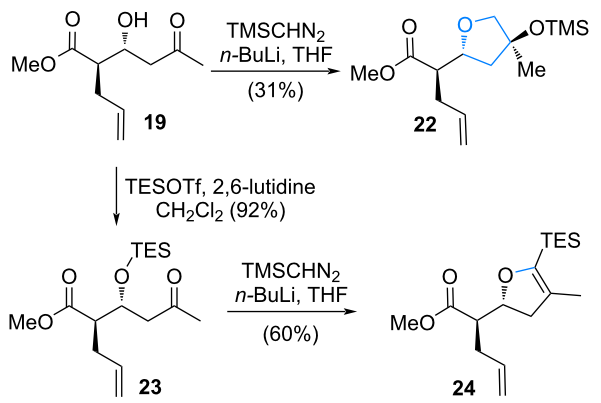

Scheme 4: C–H insertion utilizing linear precursor **19**.

after reduction, the 1,3-diol intermediate was transformed into acetonide **25** (Scheme 5). Subsequently, the desired five-membered ring was successfully constructed through the in situ-generated alkylidene carbene **26** followed by C–H insertion; herein lies a significant electronic effect influencing this crucial step. With this key intermediate in hand, β-hydroxy acid **29** was synthesized through deprotection, IBX oxidation, and Pinnick–Lindgren–Kraus oxidation and the β-lactone **13** was subsequently obtained through activation of the carboxylic acid. Although we successfully constructed the molecular scaffold of vibralactone (**6**), however, the need to open, reduce, oxidize, and reform the β-lactone lengthened the route beyond initial expectations. Currently an alternative approach towards synthesizing compound **25** is actively being pursued with aims to streamline the overall synthesis.

Conclusion

In summary, we have developed an approach to assemble the bicyclic skeleton of vibralactone (**6**) utilizing an intramolecular alkylidene carbene C–H insertion as key step. The insights gained from this study illustrate how diverse reactivity patterns and electrophilic characteristics of alkylidene carbenes influence ring closure outcomes. As intermediate **13** may serve as a valuable precursor to vibralactone (**6**) and other congeners such as vibralactone E (**7**), an alternative synthetic route toward **13** is currently being carried out in our laboratory and will be reported in due course.

Supporting Information

Supporting Information File 1

Characterization data and ^{1}H NMR, ^{13}C NMR spectra of the compounds.
[https://www.beilstein-journals.org/bjoc/content/supplementary/1860-5397-21-182-S1.pdf]

Acknowledgements

The authors sincerely acknowledge all of the anonymous reviewers for their valuable comments and suggestions.

Funding

We are grateful for financial support from the Qin Chuangyuan Innovation and Entrepreneurship Talent Project (No. QCYRCXM-2022-218), the Natural Science Research Program of Shaanxi Province of China (2024JC-YBMS-641) and Natural Science Foundation of China (Grant No. 22471221).

Author Contributions

Liang Shi: conceptualization; data curation; formal analysis; investigation; visualization. Jiayi Song: formal analysis; investigation. Yiqing Li: investigation. Jia-Chen Li: investigation. Shuqi Li: investigation. Li Ren: conceptualization; formal analysis; funding acquisition; investigation; project administration.

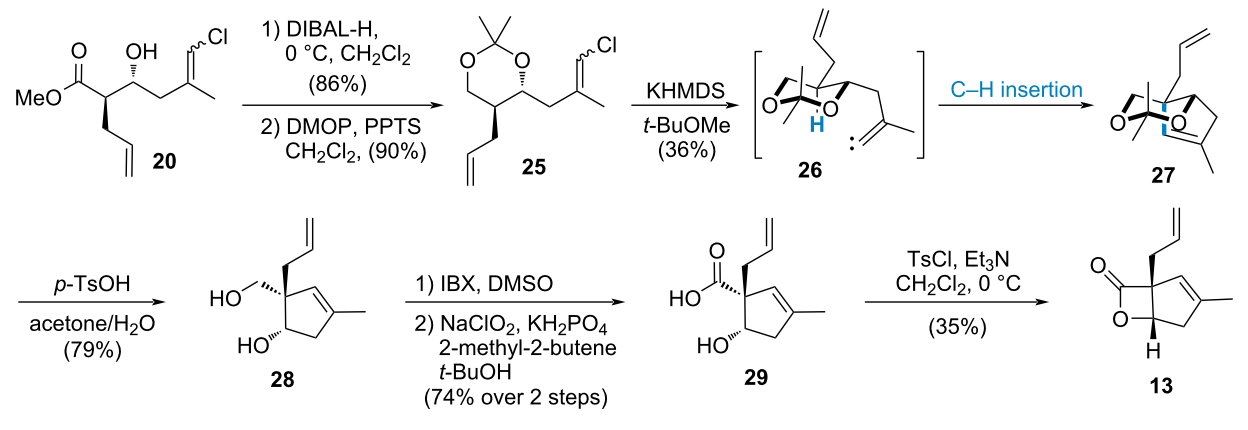

Scheme 5: Construction the bicyclic skeleton of vibralactone (**6**) through C–H insertion.

Zhi-Yun Liu: formal analysis; funding acquisition. Hong-Dong Hao: conceptualization; formal analysis; funding acquisition; investigation; project administration; resources; supervision; writing – original draft; writing – review & editing.

ORCID® iDs

Jia-Chen Li - https://orcid.org/0009-0004-9448-7303
Zhi-Yun Liu - https://orcid.org/0000-0001-6558-7437
Hong-Dong Hao - https://orcid.org/0000-0002-9236-3727

Data Availability Statement

All data that supports the findings of this study is available in the published article and/or the supporting information of this article.

References

1. Wang, X.; Wang, Z.; Ma, X.; Huang, Z.; Sun, K.; Gao, X.; Fu, S.; Liu, B. *Angew. Chem., Int. Ed.* **2022,** *61,* e202200258. doi:10.1002/anie.202200258
2. Guo, Z.; Bao, R.; Li, Y.; Li, Y.; Zhang, J.; Tang, Y. *Angew. Chem., Int. Ed.* **2021,** *60,* 14545–14553. doi:10.1002/anie.202102614
3. Leverett, C. A.; Purohit, V. C.; Johnson, A. G.; Davis, R. L.; Tantillo, D. J.; Romo, D. *J. Am. Chem. Soc.* **2012,** *134,* 13348–13356. doi:10.1021/ja303414a
4. Fukuyama, T.; Xu, L. *J. Am. Chem. Soc.* **1993,** *115,* 8449–8450. doi:10.1021/ja00071a065
5. Young, M. S.; LaPointe, A. M.; MacMillan, S. N.; Coates, G. W. *J. Am. Chem. Soc.* **2024,** *146,* 18032–18040. doi:10.1021/jacs.4c04716
6. Tian, J.-J.; Li, R.; Quinn, E. C.; Nam, J.; Chokkapu, E. R.; Zhang, Z.; Zhou, L.; Gowda, R. R.; Chen, E. Y.-X. *Nature* **2025,** *643,* 967–974. doi:10.1038/s41586-025-09220-7
7. Robinson, S. L.; Christenson, J. K.; Wackett, L. P. *Nat. Prod. Rep.* **2019,** *36,* 458–475. doi:10.1039/c8np00052b
8. Ōmura, S.; Fujimoto, T.; Otoguro, K.; Matsuzaki, K.; Moriguchi, R.; Tanaka, H.; Sasaki, Y. *J. Antibiot.* **1991,** *44,* 113–116. doi:10.7164/antibiotics.44.113
9. Ōmura, S.; Matsuzaki, K.; Fujimoto, T.; Kosuge, K.; Furuya, T.; Fujita, S.; Nakagawa, A. *J. Antibiot.* **1991,** *44,* 117–118. doi:10.7164/antibiotics.44.117
10. Corey, E. J.; Reichard, G. A.; Kania, R. *Tetrahedron Lett.* **1993,** *34,* 6977–6980. doi:10.1016/s0040-4039(00)61575-7
11. Corey, E. J.; Li, W.-D. Z. *Chem. Pharm. Bull.* **1999,** *47,* 1–10. doi:10.1248/cpb.47.1
12. Feling, R. H.; Buchanan, G. O.; Mincer, T. J.; Kauffman, C. A.; Jensen, P. R.; Fenical, W. *Angew. Chem., Int. Ed.* **2003,** *42,* 355–357. doi:10.1002/anie.200390115
13. Shenvi, R. A. *Nat. Prod. Rep.* **2016,** *33,* 535–539. doi:10.1039/c5np00160a
14. Liu, D.-Z.; Wang, F.; Liao, T.-G.; Tang, J.-G.; Steglich, W.; Zhu, H.-J.; Liu, J.-K. *Org. Lett.* **2006,** *8,* 5749–5752. doi:10.1021/ol062307u
15. Jiang, M.-Y.; Wang, F.; Yang, X.-L.; Fang, L.-Z.; Dong, Z.-J.; Zhu, H.-J.; Liu, J.-K. *Chem. Pharm. Bull.* **2008,** *56,* 1286–1288. doi:10.1248/cpb.56.1286
16. Jiang, M.-Y.; Zhang, L.; Dong, Z.-J.; Yang, Z.-L.; Leng, Y.; Liu, J.-K. *Chem. Pharm. Bull.* **2010,** *58,* 113–116. doi:10.1248/cpb.58.113
17. Chen, H.-P.; Zhao, Z.-Z.; Yin, R.-H.; Yin, X.; Feng, T.; Li, Z.-H.; Wei, K.; Liu, J.-K. *Nat. Prod. Bioprospect.* **2014,** *4,* 271–276. doi:10.1007/s13659-014-0029-z
18. Chen, H.-P.; Jiang, M.-Y.; Zhao, Z.-Z.; Feng, T.; Li, Z.-H.; Liu, J.-K. *Nat. Prod. Bioprospect.* **2018,** *8,* 37–45. doi:10.1007/s13659-017-0147-5
19. Aqueveque, P.; Céspedes, C. L.; Becerra, J.; Dávila, M.; Sterner, O. *Z. Naturforsch., C: J. Biosci.* **2015,** *70,* 97–102. doi:10.1515/znc-2015-5005
20. Kang, H.-S.; Kim, J.-P. *J. Nat. Prod.* **2016,** *79,* 3148–3151. doi:10.1021/acs.jnatprod.6b00647
21. Wei, J.; Li, Z.-X.; Peng, G.-K.; Li, X.; Chen, H.-P.; Liu, J.-K. *Nat. Prod. Bioprospect.* **2025,** *15,* 20. doi:10.1007/s13659-025-00505-y
22. Chen, H.-P.; Zhao, Z.-Z.; Li, Z.-H.; Dong, Z.-J.; Wei, K.; Bai, X.; Zhang, L.; Wen, C.-N.; Feng, T.; Liu, J.-K. *ChemistryOpen* **2016,** *5,* 142–149. doi:10.1002/open.201500198
23. Liang, Y.; Li, Q.; Wei, M.; Chen, C.; Sun, W.; Gu, L.; Zhu, H.; Zhang, Y. *Bioorg. Chem.* **2020,** *99,* 103760. doi:10.1016/j.bioorg.2020.103760
24. Wei, K.; Wang, G.-Q.; Bai, X.; Niu, Y.-F.; Chen, H.-P.; Wen, C.-N.; Li, Z.-H.; Dong, Z.-J.; Zuo, Z.-L.; Xiong, W.-Y.; Liu, J.-K. *Nat. Prod. Bioprospect.* **2015,** *5,* 129–157. doi:10.1007/s13659-015-0062-6
25. Zeiler, E.; Braun, N.; Böttcher, T.; Kastenmüller, A.; Weinkauf, S.; Sieber, S. A. *Angew. Chem., Int. Ed.* **2011,** *50,* 11001–11004. doi:10.1002/anie.201104391
26. Zhou, Q.; Snider, B. B. *Org. Lett.* **2008,** *10,* 1401–1404. doi:10.1021/ol800118c
27. Zhou, Q.; Snider, B. B. *J. Org. Chem.* **2008,** *73,* 8049–8056. doi:10.1021/jo8015743
28. Schultz, A. G. *Chem. Commun.* **1999,** 1263–1271. doi:10.1039/a901759c
29. Leeder, A. J.; Heap, R. J.; Brown, L. J.; Franck, X.; Brown, R. C. D. *Org. Lett.* **2016,** *18,* 5971–5973. doi:10.1021/acs.orglett.6b03007
30. Nistanaki, S. K.; Boralsky, L. A.; Pan, R. D.; Nelson, H. M. *Angew. Chem., Int. Ed.* **2019,** *58,* 1724–1726. doi:10.1002/anie.201812711
31. Zhao, P.-J.; Yang, Y.-L.; Du, L.; Liu, J.-K.; Zeng, Y. *Angew. Chem., Int. Ed.* **2013,** *52,* 2298–2302. doi:10.1002/anie.201208182
32. Yang, Y.-L.; Zhou, H.; Du, G.; Feng, K.-N.; Feng, T.; Fu, X.-L.; Liu, J.-K.; Zeng, Y. *Angew. Chem., Int. Ed.* **2016,** *55,* 5463–5466. doi:10.1002/anie.201510928
33. Feng, K.-N.; Yang, Y.-L.; Xu, Y.-X.; Zhang, Y.; Feng, T.; Huang, S.-X.; Liu, J.-K.; Zeng, Y. *Angew. Chem., Int. Ed.* **2020,** *59,* 7209–7213. doi:10.1002/anie.202000710
34. Feng, K.-N.; Zhang, Y.; Zhang, M.; Yang, Y.-L.; Liu, J.-K.; Pan, L.; Zeng, Y. *Nat. Commun.* **2023,** *14,* 3436. doi:10.1038/s41467-023-39108-x
35. Taber, D. F. *Eur. J. Org. Chem.* **2022,** e202200032. doi:10.1002/ejoc.202200032
36. Parsons, P. J.; Cowell, J. K. *Synlett* **2000,** 107–109. doi:10.1055/s-2000-6448
37. Zhu, C.; Shen, X.; Nelson, S. G. *J. Am. Chem. Soc.* **2004,** *126,* 5352–5353. doi:10.1021/ja0492900
38. Velazquez, D. G.; Luque, R. *Tetrahedron Lett.* **2011,** *52,* 7004–7007. doi:10.1016/j.tetlet.2011.10.112
39. Fráter, G. *Helv. Chim. Acta* **1979,** *62,* 2825–2828. doi:10.1002/hlca.19790620832
40. Fráter, G.; Müller, U.; Günther, W. *Tetrahedron* **1984,** *40,* 1269–1277. doi:10.1016/s0040-4020(01)82413-3

41. Seebach, D.; Wasmuth, D. *Helv. Chim. Acta* **1980,** *63,* 197–200. doi:10.1002/hlca.19800630118
42. Grainger, R. S.; Owoare, R. B. *Org. Lett.* **2004,** *6,* 2961–2964. doi:10.1021/ol048911r
43. Esmieu, W. R.; Worden, S. M.; Catterick, D.; Wilson, C.; Hayes, C. J. *Org. Lett.* **2008,** *10,* 3045–3048. doi:10.1021/ol8010166
44. Munro, K. R.; Male, L.; Spencer, N.; Grainger, R. S. *Org. Biomol. Chem.* **2013,** *11,* 6856–6862. doi:10.1039/c3ob41390j
45. Ohira, S.; Okai, K.; Moritani, T. *J. Chem. Soc., Chem. Commun.* **1992,** 721–722. doi:10.1039/c39920000721
46. Shen, Y.; Li, L.; Pan, Z.; Wang, Y.; Li, J.; Wang, K.; Wang, X.; Zhang, Y.; Hu, T.; Zhang, Y. *Org. Lett.* **2015,** *17,* 5480–5483. doi:10.1021/acs.orglett.5b02845
47. Miwa, K.; Aoyama, T.; Shioiri, T. *Synlett* **1994,** 461–462. doi:10.1055/s-1994-22891
48. Grainger, R. S.; Munro, K. R. *Tetrahedron* **2015,** *71,* 7795–7835. doi:10.1016/j.tet.2015.06.053

License and Terms

BEILSTEIN JOURNAL OF ORGANIC CHEMISTRY

Synthesis of the tetracyclic skeleton of *Aspidosperma* alkaloids via PET-initiated cationic radical-derived interrupted [2 + 2]/*retro*-Mannich reaction

Ru-Dong Liu[1], Jian-Yu Long[1], Zhi-Lin Song[1], Zhen Yang[*1,2,3] and Zhong-Chao Zhang[*1,4]

Full Research Paper

Open Access

Address:
[1]Laboratory of Chemical Genomics, School of Chemical Biology and Biotechnology, Peking University Shenzhen Graduate School, Shenzhen 518055, China, [2]Key Laboratory of Bioorganic Chemistry and Molecular Engineering of Ministry of Education and Beijing National Laboratory for Molecular Science, and Peking-Tsinghua Centre for Life Sciences, Peking University, Beijing 100871, China, [3]Shenzhen Bay Laboratory, Shenzhen 518055, China and [4]Key Laboratory of Structure-Based Drug Design & Discovery of Ministry of Education, Shenyang Pharmaceutical University, Liaoning Shenyang 110016, China

Email:
Zhen Yang[*] - zyang@pku.edu.cn; Zhong-Chao Zhang[*] - zc_zhang@pku.edu.cn

* Corresponding author

Keywords:
Aspidosperma alkaloids; [2 + 2]-cycloaddition/*retro*-Mannich reaction; DFT study; photoinduced electron transfer

Beilstein J. Org. Chem. **2025,** *21,* 2470–2478.
https://doi.org/10.3762/bjoc.21.189

Received: 08 August 2025
Accepted: 27 October 2025
Published: 10 November 2025

This article is part of the thematic issue "Concept-driven strategies in target-oriented synthesis".

Guest Editor: C. Li

Abstract

Natural products with topologically complex architectures are important sources in drug discovery. The pursuit of conciseness and efficiency in the total synthesis of natural products promotes continuous innovation and the development of new reactions and strategies. In this work, a PET-initiated cationic radical-derived interrupted [2 + 2]/*retro*-Mannich reaction of N-substituted cyclobutenone provided a facile approach to the direct construction of the ABCE tetracyclic framework of *Aspidosperma* alkaloids. DFT calculations showed that the rate-determining step of the key PET reaction involved C19–C12 bond formation and C19–C3 bond cleavage. Investigation of the bond length changes along the IRC path, spin density, and NBO analysis indicated that this process is neither strictly concerted nor stepwise, but falls in between, and involves a formal 1,3-C shift.

Introduction

Photochemical reactions, which enable the construction of topologically complex architectures from simple building blocks, have attracted considerable attention in recent decades. Numerous approaches to natural product synthesis have been reported in which a photochemical transformation represents a key step [1-3]. In this context, the photochemical [2 + 2] cycloaddition and subsequent fragmentation of the resulting cyclobutane provides a valuable strategy for synthesizing natural and unnat-

ural products from simple building blocks [4]. Three distinct photoinitiated approaches have been established for the formation of the [2 + 2] cycloadducts: direct irradiation [5,6], energy transfer (EnT) [7], and photoinduced electron transfer (PET, or photoredox catalysis) processes [8-10].

Cyclobutenone (**A**) is a versatile C4 synthon [11] – its [2 + 2] photocyclization yields **B**, featuring a strained bicyclo[2.2.0]hexane unit [12], which can fragment to form **C** (Figure 1a) [13,14]. However, competitive C1–C4 bond cleavage under irradiation or heating leads to ketene **D**, which can undergo cycloaddition with an alkene to yield **E**. This fragmentation pathway dominates under various conditions (e.g., transition-metal catalysis, nucleophilic addition) and is driven by ring-strain release [11].

PET, an alternative to direct excitation and EnT, enables the formation of unique radical intermediates [9,10]. We previously demonstrated the Ir-catalyzed [2 + 2] cyclization/*retro*-Mannich reaction of a tryptamine-substituted cyclopentenone **F**, which led to the formation of indoline **J** (Figure 1b) [15]. Unlike other reported methods [16-18], the PET reaction of **F** generates the cationic radical **G**, which initiates formation of **H**, which has a strained bicyclo [3.2.0]heptane core. Strain release of **H** triggers a downstream radical-driven *retro*-Mannich reaction, which ultimately results in the formation of **J** via reductive quenching of intermediate **I**.

As part of our current interest in the synthesis of complex natural products via photochemical reactions, we decided to achieve such an unusual bond cleavage (Figure 1a, path A) of cyclobutenone by generating a radical cation species via a PET reaction. The synthetic plan is shown in Figure 1c and includes a PET-initiated [2 + 2] cyclization of the tryptamine-substituted cyclobutenone **K** to form the radical cation **L**, which has a highly functionalized and rigid bicyclo[2.2.0]hexane core. Fragmentation of the C3–C19 bond would afford a redox-active intermediate which upon further reductive quenching would lead to the tetracyclic indoline **M**, which was expected to serve as a common intermediate for the total synthesis of *Aspidosperma* alkaloids. These alkaloids constitute a large family of structurally complex compounds, which incorporate a pentacyclic ABCDE skeleton (Figure 1d, **1**–**8**) [19-23]. However, the formation of intermediate **L** is challenging because its ring-strain energy (Figure 1e, 52.1 kcal/mol) is higher than that of its counterpart, i.e. the bicyclo[3.2.0]heptane motif (28.3 kcal/mol) in **H** [24].

Herein, we report our recent results on the development of a novel strategy for the stereoselective construction of the tetracyclic core of *Aspidosperma* alkaloids. Our method involves an Ir-catalyzed PET reaction of **K** for the stereoselective formation of the *cis*-configured BC bicyclic core with an all-carbon quaternary center [25,26]. Computational studies suggest that the observed tandem PET reaction of **K** proceeds via an unusual 1,3-C shift to afford **M**, i.e. through an interrupted [2 + 2] cyclization/*retro*-Mannich reaction.

Results and Discussion

Conditions optimization

Our study commenced with the evaluation of the proposed PET-based tandem [2 + 2] cyclization/*retro*-Mannich reaction. We selected compound **10a**, which has a spiro-pentacyclic core, as the target to be synthesized via the proposed PET reaction of substrate **9a** (Table 1). Substrate **9a** can be synthesized from tryptamine and a substituted cyclobutane-1,3-dione according to a published protocol [27].

Initially, we focused on identifying catalysts that could promote the proposed PET reaction of **9a** on the basis of our previous results [15]. The reaction was performed in MeCN in the presence of photocatalysts under blue light-emitting diode (LED) irradiation at 30 °C. The results are listed in Table 1. Catalysts **I** [28], **II** [29], and **III** [30] gave the desired product **10a**, with catalyst **I** giving the best result (Table 1, entries 1–3). The necessities of irradiation and the presence of a photocatalyst were also defined (Table 1, entries 4 and 5). However, use of the other tested catalysts did not give the desired product under the reaction conditions (see Supporting Information File 1 for details). Next, we evaluated the effects of different solvents on the production of **10a** in the presence of catalyst **I**. Changing the solvent to MeOH, tetrahydrofuran (THF), and dichloromethane (DCM) resulted in decreased yields and substrate conversions, and intense substrate decomposition (Table 1, entries 6–8). These results showed that MeCN is the best solvent for the reaction.

Finally, we investigated the effects of an alternative N-substituent in the indole moiety, and the reaction time and temperature on the photocyclization results. Boc-substituted substrate **9f** was subjected to the optimized conditions, which resulted in both a lower conversion and yield (Table 1, entry 9). In contrast, when the reaction of **9f** was performed in a mixed MeCN/toluene 10:1 solvent, the conversion of substrate **9f** to product **10f** decreased, but the yield increased to 56% (Table 1, entry 10) compared with that in entry 9 (42%). These results indicate that Cbz is a more effective protecting group than Boc under the profiled conditions. The effects of the reaction temperature on the outcome of the PET reaction of **9a** were investigated. Among the conditions screened (Table 1, entries 11–13), the reaction in MeCN at 30 °C for 24 h gave the best result, namely a quantitative conversion and 90% yield.

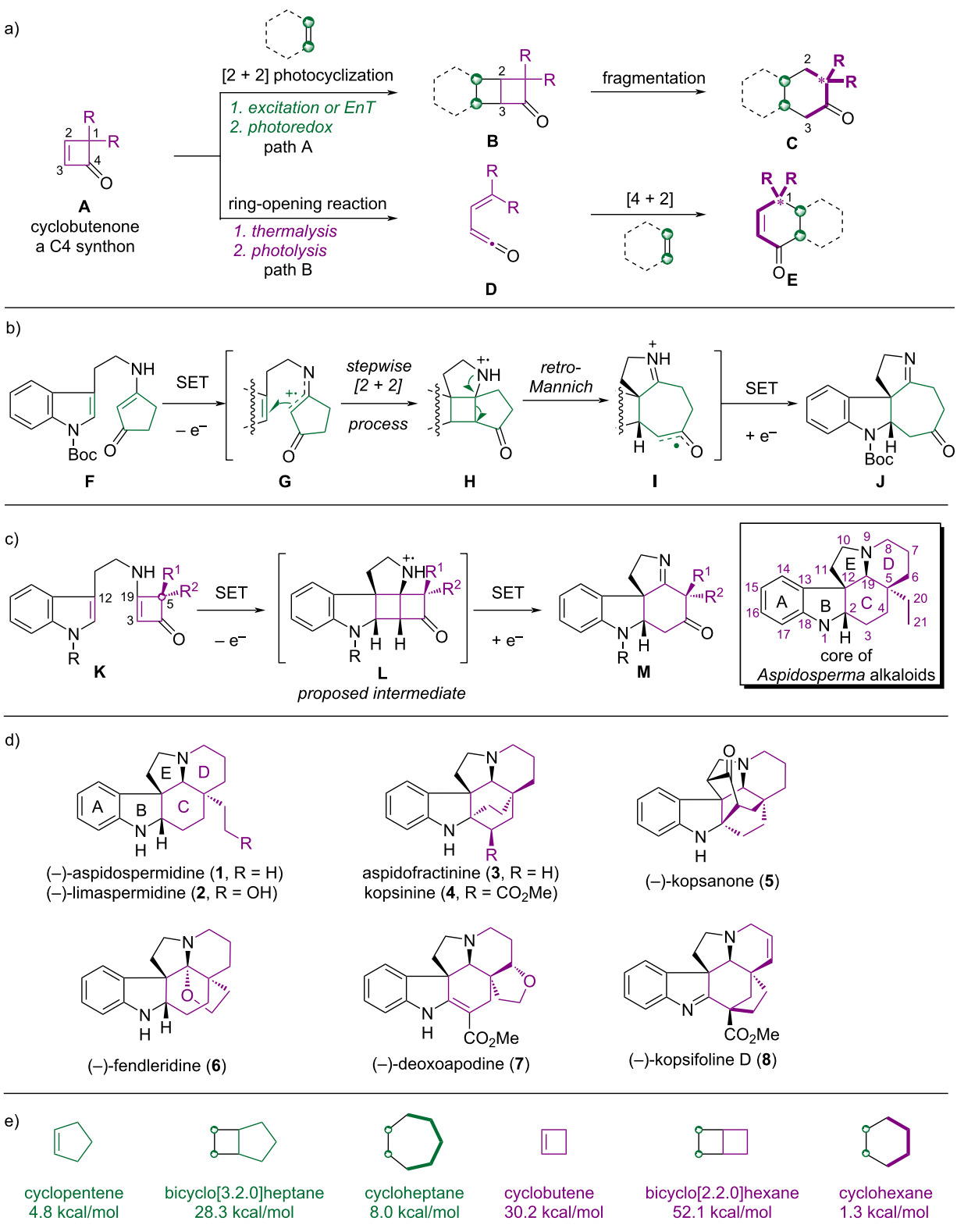

Figure 1: Synthetic plan. a) General model of cyclobutenone bond cleavage; b) our previously reported method; c) plan for indole *Aspidosperma* alkaloid synthesis; d) naturally occurring *Aspidosperma* alkaloids; e) ring strain energy of cyclopentene, bicyclo[3.2.0]heptane, cycloheptane, cyclobutene, bicyclo[2.2.0]hexane and cyclohexane.

Table 1: Conditions screening.[a]

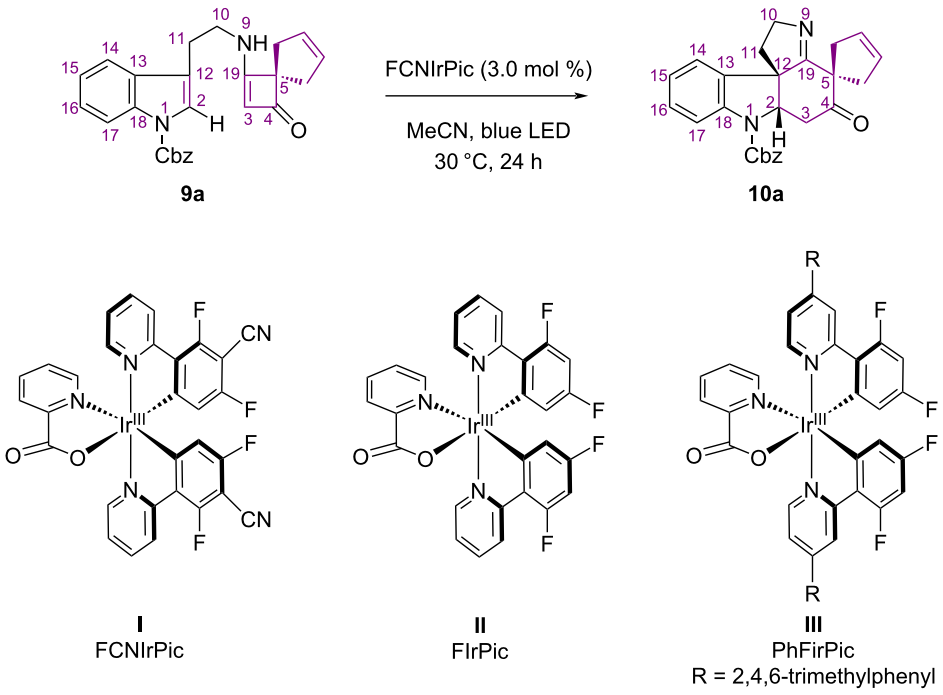

Entry	Photocatalyst	Solvent	Temp.	Conv./yield (%)
1	FCNIrPic (**I**)	MeCN	30 °C	100/86[b]
2	FirPic (**II**)	MeCN	30 °C	83/26
3	PhFIrPic (**III**)	MeCN	30 °C	65/43
4	in dark	MeCN	30 °C	<5/n.d.
5	no catalyst	MeCN	30 °C	<5/n.d.
6	FCNIrPic (**I**)	MeOH	30 °C	84/23
7	FCNIrPic (**I**)	THF	30 °C	30/20
8	FCNIrPic (**I**)	DCM	30 °C	59/35
9	FCNIrPic (**I**)	MeCN	30 °C	86/42[c]
10	FCNIrPic (**I**)	MeCN/PhMe	30 °C	67/56[c,d]
11	FCNIrPic (**I**)	MeCN	10 °C	100/60
12	FCNIrPic (**I**)	MeCN	20 °C	100/66
13	FCNIrPic (**I**)	MeCN	40 °C	90/50

[a]Reaction conditions: A 15 mL glass vial was charged with **9a** (0.1 mmol) and a photocatalyst (3.0 mol %) in an appropriate solvent (5.0 mL), and irradiated by two blue LEDs (center wavelength 455 nm; light intensity, 0.21 W/cm^2). The yield and conversion were determined by ^{1}H NMR spectroscopy with 1,3,5-trimethoxybenzene as the internal standard. [b]Isolated yield = 86%. [c]Cbz is replaced by -Boc (**9f**). [d]V_{MeCN}/V_{PhMe} = 10:1.

Substrate scope

With the optimal conditions in hand, we then explored the substrate scope. Targeting on the total synthesis of *Aspidosperma* alkaloids, different tryptamine-substituted cyclobutenones **9a**–**n** were prepared and reacted under the optimal conditions. The results are shown in Scheme 1. Substrate **9a**, which contains a spiro-cyclopentene moiety, delivered the best result and gave **10a** in 86% isolated yield. When C15 or C16 was substituted with a chlorine atom, **10b** and **10c** were obtained in 70% and 72% yield, respectively. However, when C15 was substituted with a methyl group, the yield of **10d** decreased slightly to 63%. Product **10e**, which has two contiguous quaternary stereogenic centers at C2 and C12, was obtained in 74% yield without a significant change in the yield, which indicates that steric hindrance at C2 has a limited effect on the reactivity. However, when the steric hindrance of the protecting group was increased by replacing –Cbz with –Boc, the activity of the PET reaction decreased, which resulted in a lower yield of **10f** (45%). In the case of substrate **9g**, which has a stereogenic centre at C10, photocyclization afforded **10g** in moderate yield and with excel-

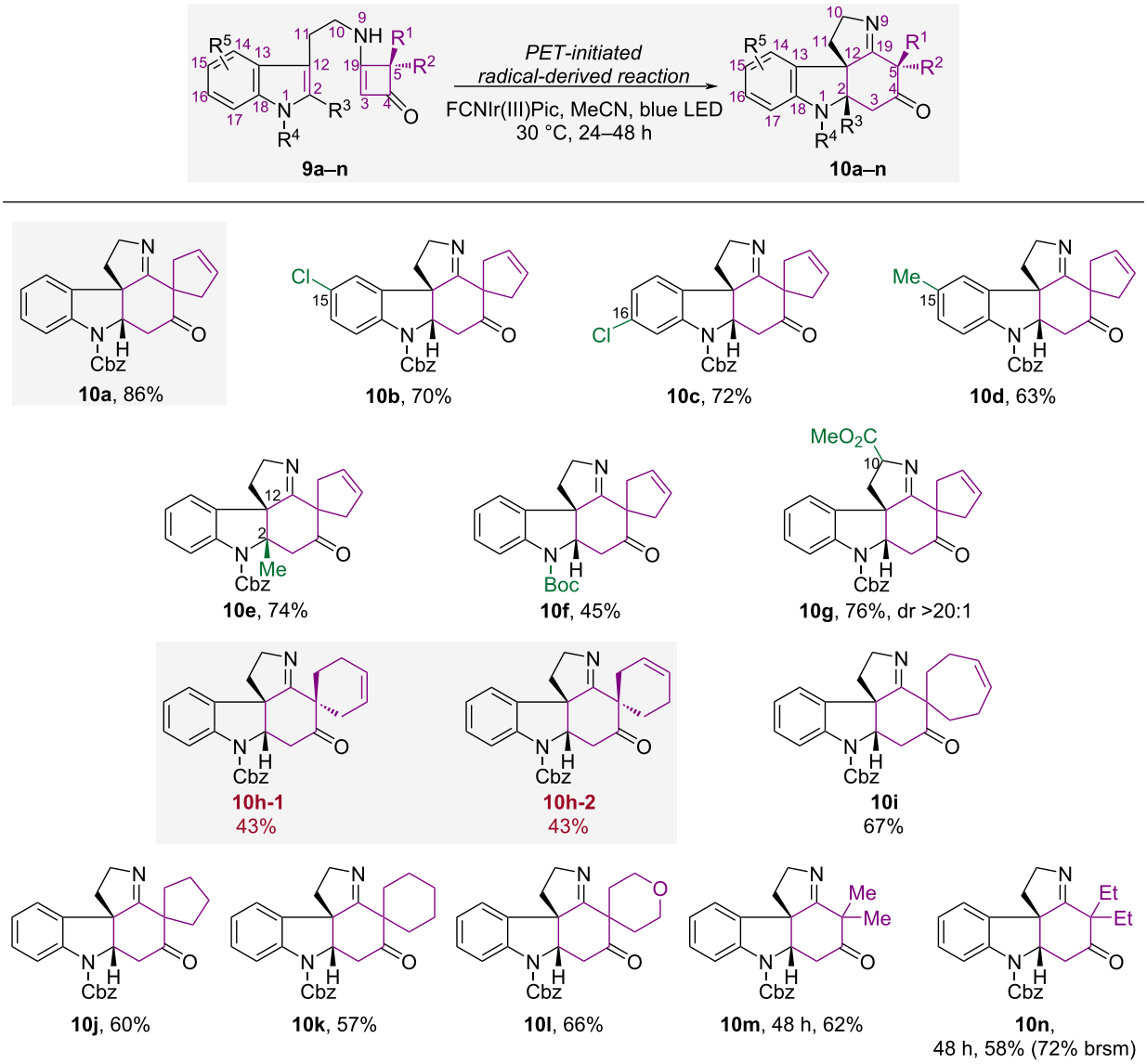

Scheme 1: Substrate scope.

lent diastereoselectivity (76% yield, dr >20:1). This indicates that the reaction is controlled by the substrate conformation.

To investigate the effects of the spirocyclic ring size on the photocyclization, substrates **9h** and **9i** were prepared and subjected to the optimal conditions. The PET reaction of **9h** with a spiro-cyclohexene unit gave a pair of separable isomers, **10h-1** and **10h-2**, in 86% yield and a 1:1 ratio. The reaction of **9i**, which bears a spiro-cycloheptene moiety, afforded the annulated product **10i** in 67% yield. This indicates that an increase in the spirocyclic ring size negatively affects the photocyclization outcome. We expanded the reaction scope by synthesizing substrates **9j–l**, which contain various types of saturated spirocycles. As anticipated, **10j**, **10k**, and **10l** were obtained in moderate yields (57–66%) under the standard reaction conditions. When substrates **9m** and **9n**, which have a *gem*-dimethyl and *gem*-diethyl group, respectively, were used, their PET reactions required a longer reaction time to achieve full conversion. The resulting products **10m** and **10n** were obtained in yields of 62% and 58%, respectively.

Computational study

The synthesis of (±)-aspidospermidine (**1**) and (±)-limaspermidine (**2**) showcased the effectiveness of our strategy for constructing complex monoterpene indole alkaloids [26]. In this work, we turned our attention to investigating the mechanistic intricacies of the key PET reaction for formation of the unique bicyclo[2.2.0]hexane unit present in the proposed intermediate

L (Figure 1). In the presence of the excited photocatalyst [FCNIr(III)Pic]*, the substrate participates in an oxidative single-electron transfer (SET) process, which leads to the formation of **IN1**. The radical cation **IN1** served as the reference point for DFT investigations. As illustrated in Figure 2a, facilitated by a favorable radical cation–π interaction [31], **IN1**

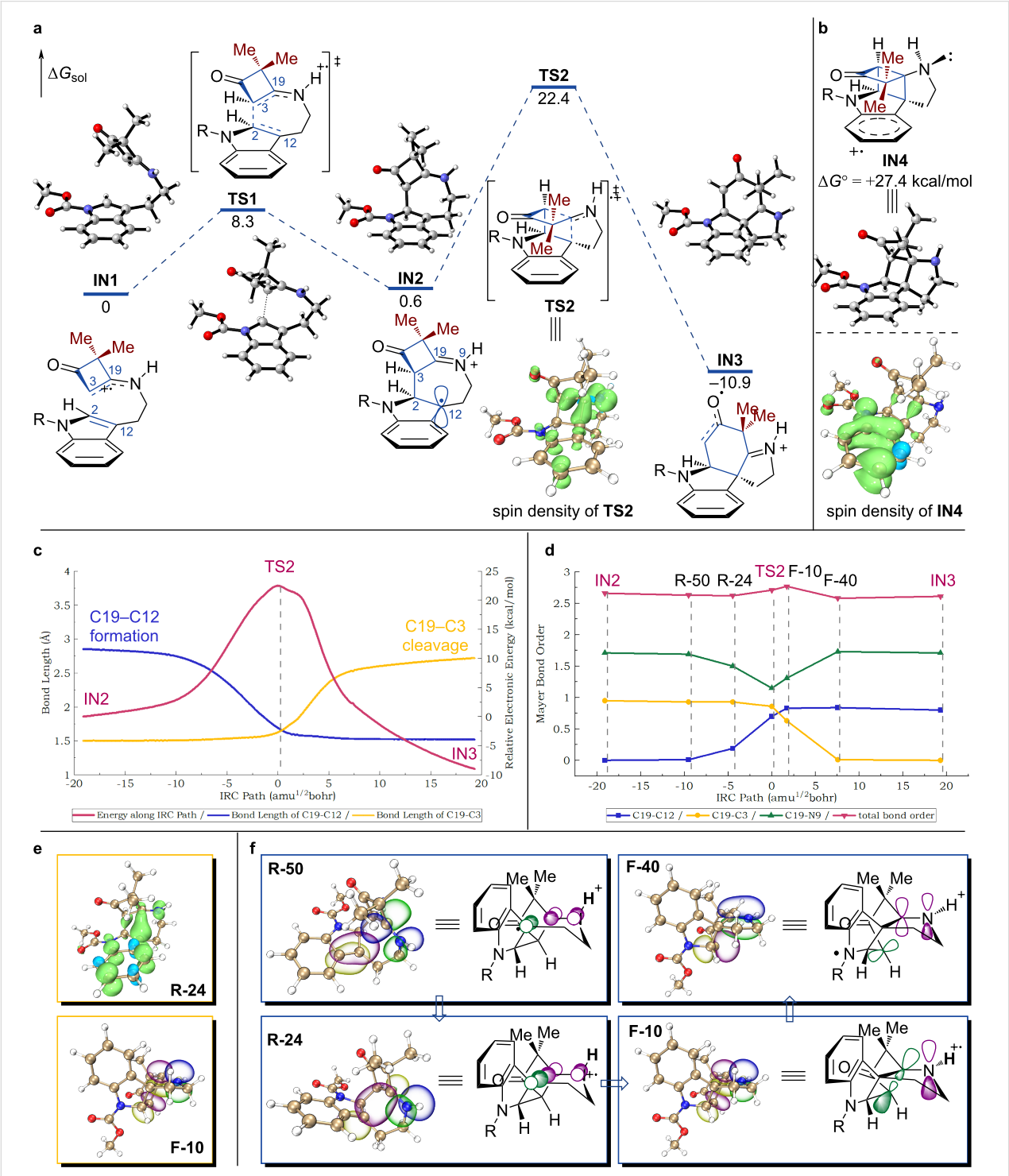

Figure 2: Computational study. a) Energy profiles from **IN1** to **IN3** and spin density of **TS2** (isovalue = 0.004), solvated (SMD) Gibbs free energies were calculated at the B3LYP-D3/def2-tzvp//B3LYP/6-31G(d) level in MeCN. b) Spin density of **IN4** (isovalue = 0.004). c) IRC analysis of **TS2** (red line) and bond-length changes of C19–C3 (yellow line) and C19–C12 (blue line) along IRC path. d) Mayer bond order changes of selected structures along IRC path. e) Spin-density analyses of **R-24** and **F-10** (isovalue = 0.004). f) NBO analyses of the selected transient structures (isovalue = 0.04).

proceeds to the first radical addition transition state (**TS1**), with an energy barrier of 8.3 kcal/mol. This leads to the formation of benzyl radical **IN2**, which has a boat-like seven-membered ring. This structural feature may facilitate formation of the C19–C12 bond, even in the presence of critical steric hindrance between the C5 quaternary carbon and the indole moiety.

Further DFT investigation proved challenging because of the peculiar features that the potential energy surface (PES) exhibits in the rate-determining step, which involves both formation of the C19–C12 bond and cleavage of the C19–C3 bond. This process has an energy barrier of 21.8 kcal/mol via **TS2**, and results in direct formation of **IN3**, which can undergo reductive SET in the presence of $[FCNIr(II)Pic]^-$. This leads to the regeneration of [FCNIr(III)Pic] to complete the catalytic cycle and formation of the final product via proton transfer. Intrinsic reaction coordinate (IRC) analysis showed the reaction coordinate connecting the transition state **TS2**, the reactant (**IN2**), and the C19–C3 bond cleavage product **IN3** wells (Figure 2c).

Possible intermediates with a bicyclo[2.2.0]hexane unit located on the PES minimum were investigated by performing two-dimensional scans of simplified structures to find a minimum. When the nonbonding sp^3 orbital of the N atom is positioned antiperiplanar to the adjacent C19–C3 bond, an intermediate **IN4** with a bicyclo[2.2.0]hexane unit was successfully located. However, the Gibbs free energy of **IN4** (ΔG° = +27.4 kcal/mol) is significantly higher than the activation energy of **TS2** ($\Delta G^\ddagger$ = 22.4 kcal/mol). This energy difference can be attributed to a subtle discrepancy between the spin localizations of **IN4** and **TS2**. As depicted in Figure 2b, the spin density of **IN4** is predominantly concentrated at the benzene ring, whereas in **TS2** it is primarily localized at C19, C12, C3, and N9 (Figure 2a) [32]. Therefore, the intermediacy of **IN4** was ruled out.

We assume that the overlap between the sp^2-hybridized N spin center and σ* (C19–C3) in **TS2**, and the ring-strain release of the transient bicyclo[2.2.0]hexane unit, play essential roles that enable the reaction to occur. Thus, natural bond orbital (NBO) [33] and Mayer bond order [34,35] analyses were performed to determine the hyperconjugative interactions in the intermediates, transition states, and transient structures along the IRC path (Figure 2c and 2d). In the early stage of this process (Figure 2f, **IN2** → **R-50** → **R-24** → **TS2**), formation of the C19–C3 bond arises from the orbital overlap between the p orbital of the C19 atom (Figure 2e, **R-24**) and the $\pi_{(C3=N9)}$* orbital. During this process, the bond order of C19–C12 increases, but no significant change is observed for C19–C3. This leads to the formation of a nonbonding p orbital at the N9 atom (Figure 2e, **F-10**). Further geometrical adjustment and conformational restriction of the transient structure enable the N9 nonbonding p orbital to align parallel to the $\sigma_{(C19–C3)}$* orbital (Figure 2f, **TS2** → **F-10** → **F-40** → **IN3**), which reinforces the hyperconjugative interaction. Facilitated by the bond stretching and bond-angle bending of the transient structure with a pseudo bicyclo[2.2.0]hexane unit, the favorable hyperconjugative interaction ultimately leads to cleavage of the C19–C3 bond (**TS2** → **IN3**) and release of the ring strain.

DFT analysis hereby explains that the orbital symmetry involved in this process does not conform to a sigmatropic rearrangement reaction [36]. Inspection of the changes in the bond lengths (Figure 2c) and Mayer bond orders (Figure 2d) along the IRC path clearly show that C19–C12 bond formation and C19–C3 bond cleavage are asynchronous. On the basis of these premises, we assume that the process **IN2** → **IN3** is neither strictly concerted nor stepwise [37,38]. This can be attributed to the inherent ring-strain release in the transient structure located on the PES and the hyperconjugative interaction between the N9 nonbonding p orbital and $\sigma_{(C19–C3)}$* during geometrical distortions. This ambiguous mechanistic feature suggests an unusual 1,3-C shift, and indicates that this reaction proceeds via a PET-initiated interrupted [2 + 2]/*retro*-Mannich process.

Conclusion

In summary, a PET-initiated cationic radical-derived interrupted [2 + 2]/*retro*-Mannich reaction has been developed for constructing the ABCE tetracyclic cores of *Aspidosperma* alkaloids from tryptamine-substituted cyclobutenones. Importantly, this methodology has already been successfully applied in the total syntheses of (±)-aspidospermidine and (±)-limaspermidine using **10a** and **10h** as substrates, respectively [26]. The functionalized C5 atom in the formed ABCE tetracyclic core provides potential opportunities for accessing more complex indole alkaloids. The extensive DFT study indicated that the observed PET-initiated cationic radical-derived reaction proceeds via an unconventional formal 1,3-C shift, which is neither concerted nor stepwise. These findings shed light on the mechanistic innovation of a PET-initiated radical-derived reaction that was driven by the ring-strain release.

Supporting Information

Supporting Information File 1

Experimental procedures, characterization data, NMR spectra, and computational study.
[https://www.beilstein-journals.org/bjoc/content/supplementary/1860-5397-21-189-S1.pdf]

Funding

This work was supported by the National Science Foundation of China (Grant Nos. 22171013), Guangdong Natural Science Foundation (Grant Nos. 2020B0303070002), Shenzhen Basic Research Program (Grant No. JCYJ 20180302180215524), Shenzhen-Hong Kong Institute of Brain Science-Shenzhen Fundamental Research Institutions (2024SHIBS0004), Key Laboratory of Structure-Based Drug Design & Discovery of Ministry of Education, Shenyang Pharmaceutical Universit (SY2024KF-02), the research grants from the Major Program of Shenzhen Bay Laboratory, and the Shenzhen Outstanding Talents Training Fund.

Author Contributions

Ru-Dong Liu: investigation; validation. Jian-Yu Long: investigation. Zhi-Lin Song: investigation. Zhen Yang: conceptualization; funding acquisition; project administration; supervision; validation; visualization; writing – original draft; writing – review & editing. Zhong-Chao Zhang: data curation; funding acquisition; methodology; supervision; writing – original draft; writing – review & editing.

ORCID® iDs

Zhi-Lin Song - https://orcid.org/0009-0009-7524-4898
Zhen Yang - https://orcid.org/0000-0001-8036-934X
Zhong-Chao Zhang - https://orcid.org/0000-0001-5017-5691

Data Availability Statement

All data that supports the findings of this study is available in the published article and/or the supporting information of this article.

Preprint

A non-peer-reviewed version of this article has been previously published as a preprint: https://doi.org/10.3762/bxiv.2025.50.v1

References

1. Bach, T.; Hehn, J. P. *Angew. Chem., Int. Ed.* **2011,** *50,* 1000–1045. doi:10.1002/anie.201002845
2. Kärkäs, M. D.; Porco, J. A., Jr.; Stephenson, C. R. J. *Chem. Rev.* **2016,** *116,* 9683–9747. doi:10.1021/acs.chemrev.5b00760
3. Pitre, S. P.; Overman, L. E. *Chem. Rev.* **2022,** *122,* 1717–1751. doi:10.1021/acs.chemrev.1c00247
4. Winkler, J. D.; Bowen, C. M.; Liotta, F. *Chem. Rev.* **1995,** *95,* 2003–2020. doi:10.1021/cr00038a010
5. Baldwin, J. E. Thermal Cyclobutane Ring Formation. *Comprehensive Organic Synthesis;* Pergamon Press: Oxford, UK, 1991; Vol. 5, pp 63–84. doi:10.1016/b978-0-08-052349-1.00120-7
6. Poplata, S.; Tröster, A.; Zou, Y.-Q.; Bach, T. *Chem. Rev.* **2016,** *116,* 9748–9815. doi:10.1021/acs.chemrev.5b00723
7. Großkopf, J.; Kratz, T.; Rigotti, T.; Bach, T. *Chem. Rev.* **2022,** *122,* 1626–1653. doi:10.1021/acs.chemrev.1c00272
8. Takahashi, Y.; Okitsu, O.; Ando, M.; Miyashi, T. *Tetrahedron Lett.* **1994,** *35,* 3953–3956. doi:10.1016/s0040-4039(00)76711-6
9. Ravelli, D.; Protti, S.; Fagnoni, M. *Chem. Rev.* **2016,** *116,* 9850–9913. doi:10.1021/acs.chemrev.5b00662
10. Romero, N. A.; Nicewicz, D. A. *Chem. Rev.* **2016,** *116,* 10075–10166. doi:10.1021/acs.chemrev.6b00057
11. Chen, P.-h.; Dong, G. *Chem. – Eur. J.* **2016,** *22,* 18290–18315. doi:10.1002/chem.201603382
12. Wiberg, K. B. *Angew. Chem., Int. Ed. Engl.* **1986,** *25,* 312–322. doi:10.1002/anie.198603121
13. Paquette, L. A.; Schwartz, J. A. *J. Am. Chem. Soc.* **1970,** *92,* 3215–3217. doi:10.1021/ja00713a066
14. Wilson, S. R.; Phillips, L. R.; Pelister, Y.; Huffman, J. C. *J. Am. Chem. Soc.* **1979,** *101,* 7373–7379. doi:10.1021/ja00518a040
15. Mu, X.-P.; Li, Y.-H.; Zheng, N.; Long, J.-Y.; Chen, S.-J.; Liu, B.-Y.; Zhao, C.-B.; Yang, Z. *Angew. Chem., Int. Ed.* **2021,** *60,* 11211–11216. doi:10.1002/anie.202101104
16. Schell, F. M.; Cook, P. M. *J. Org. Chem.* **1984,** *49,* 4067–4070. doi:10.1021/jo00195a041
17. Winkler, J. D.; Muller, C. L.; Scott, R. D. *J. Am. Chem. Soc.* **1988,** *110,* 4831–4832. doi:10.1021/ja00222a053
18. Zhu, M.; Zhang, X.; Zheng, C.; You, S.-L. *Acc. Chem. Res.* **2022,** *55,* 2510–2525. doi:10.1021/acs.accounts.2c00412 and references cited therein.
19. Zhao, S.; Sirasani, G.; Andrade, R. B. Aspidosperma and Strychnos alkaloids: Chemistry and biology. *The Alkaloids: Chemistry and Biology;* Academic Press: Cambridge, MA, USA, 2021; Vol. 86, pp 1–143. doi:10.1016/bs.alkal.2021.05.001
20. Sears, J. E.; Boger, D. L. *Acc. Chem. Res.* **2016,** *49,* 241–251. doi:10.1021/acs.accounts.5b00510
21. Pritchett, B. P.; Stoltz, B. M. *Nat. Prod. Rep.* **2018,** *35,* 559–574. doi:10.1039/c7np00069c
22. Wang, Y.; Xie, F.; Lin, B.; Cheng, M.; Liu, Y. *Chem. – Eur. J.* **2018,** *24,* 14302–14315. doi:10.1002/chem.201800775
23. Saya, J. M.; Ruijter, E.; Orru, R. V. A. *Chem. – Eur. J.* **2019,** *25,* 8916–8935. doi:10.1002/chem.201901130
24. Khoury, P. R.; Goddard, J. D.; Tam, W. *Tetrahedron* **2004,** *60,* 8103–8112. doi:10.1016/j.tet.2004.06.100 Ring strain energy calculations were performed in B3LYP-D3/def2-SVP level according to the reported method.
25. Quasdorf, K. W.; Overman, L. E. *Nature* **2014,** *516,* 181–191. doi:10.1038/nature14007
26. Long, J.; Liu, R.; Mu, X.; Song, Z.; Zhang, Z.; Yang, Z. *Org. Lett.* **2024,** *26,* 2960–2964. doi:10.1021/acs.orglett.4c00540
27. Brand, S.; de Candole, B. C.; Brown, J. A. *Org. Lett.* **2003,** *5,* 2343–2346. doi:10.1021/ol034701n
28. D'Andrade, B. W.; Datta, S.; Forrest, S. R.; Djurovich, P.; Polikarpov, E.; Thompson, M. E. *Org. Electron.* **2005,** *6,* 11–20. doi:10.1016/j.orgel.2005.01.002
29. Adachi, C.; Kwong, R. C.; Djurovich, P.; Adamovich, V.; Baldo, M. A.; Thompson, M. E.; Forrest, S. R. *Appl. Phys. Lett.* **2001,** *79,* 2082–2084. doi:10.1063/1.1400076
30. Kozhevnikov, V. N.; Zheng, Y.; Clough, M.; Al-Attar, H. A.; Griffiths, G. C.; Abdullah, K.; Raisys, S.; Jankus, V.; Bryce, M. R.; Monkman, A. P. *Chem. Mater.* **2013,** *25,* 2352–2358. doi:10.1021/cm4010773
31. Yamada, S. *Chem. Rev.* **2018,** *118,* 11353–11432. doi:10.1021/acs.chemrev.8b00377
32. Humphrey, W.; Dalke, A.; Schulten, K. *J. Mol. Graphics* **1996,** *14,* 33–38. doi:10.1016/0263-7855(96)00018-5
33. *NBO 7.0;* Theoretical Chemistry Institute, University of Wisconsin: Madison, WI, USA, 2018.

34. Mayer, I. *Chem. Phys. Lett.* **1983,** *97,* 270–274. doi:10.1016/0009-2614(83)80005-0
35. Lu, T.; Chen, F. *J. Comput. Chem.* **2012,** *33,* 580–592. doi:10.1002/jcc.22885
36. Woodward, R. B.; Hoffmann, R. *The conservation of orbital symmetry;* Verlag Chemie: Weinheim, Germany, 1970. doi:10.1016/b978-1-4832-3290-4.50006-4
37. López, C. S.; Faza, O. N.; Álvarez, R.; de Lera, Á. R. *J. Org. Chem.* **2006,** *71,* 4497–4501. doi:10.1021/jo0603274
38. Smentek, L.; Hess, B. A., Jr. *J. Am. Chem. Soc.* **2010,** *132,* 17111–17117. doi:10.1021/ja1039133

License and Terms

BEILSTEIN JOURNAL OF ORGANIC CHEMISTRY

Rapid access to the core of malayamycin A by intramolecular dipolar cycloaddition

Yilin Liu[‡1], Yuchen Yang[‡2], Chen Yang[2], Sha-Hua Huang[*1], Jian Jin[*2] and Ran Hong[*2]

Full Research Paper

Open Access

Address:
[1]Faculty of Chemical Engineering and Energy Technology, Shanghai Institute of Technology, 100 Haiquan Road, Shanghai 201418, P.R. China and [2]State Key Laboratory of Chemical Biology, Shanghai Institute of Organic Chemistry, Chinese Academy of Sciences, 345 Lingling Road, Shanghai 200032, P.R. China

Email:
Sha-Hua Huang[*] - shahua@sit.edu.cn; Jian Jin[*] - jianjin@sioc.ac.cn; Ran Hong[*] - rhong@sioc.ac.cn

* Corresponding author ‡ Equal contributors

Keywords:
dipolar cycloaddition; elimination; fungicide; nucleoside; oxazoline

Beilstein J. Org. Chem. **2025,** *21,* 2542–2547.
https://doi.org/10.3762/bjoc.21.196

Received: 30 August 2025
Accepted: 07 November 2025
Published: 17 November 2025

This article is part of the thematic issue "Concept-driven strategies in target-oriented synthesis".

Associate Editor: D. Y.-K. Chen

Abstract

We have streamlined a dipolar cycloaddition approach to assemble the core of malayamycin A and other related uracil nucleosides possessing the common bicyclic perhydrofuropyran framework. The latent functionality strategy employing oxazoline to unmask the 1,2-hydroxyamine moiety proves feasible, eliminating the need for alkene functionalization required in previous endeavours. This current strategy provides a reliable platform for accessing diverse uracil nucleosides and their derivatives, facilitating the development of potent fungicides.

Introduction

Modern agriculture relies on various effective fungicides to combat crop diseases for achieving significant gains [1]. However, the long-term and widespread use of chemicals and biological agents has led to a rapid emergence of resistance, which in turn diminishes the national-wide and even global-wide food security. Moreover, toxins produced by fungi in diseased crops have serious impacts on animal and human health [2]. There remains high demand to develop new antifungal compounds as alternatives to existing fungicides as well as enhancing the control spectrum and persistence [3].

A group of scientists at Syngenta reported a bicyclic perhydrofuropyran C-nucleoside malayamycin A (**1**) from the soil bacterium *Streptomyces malaysiensis* [4] (Figure 1). This novel compound was found to inhibit the sporulation of *Stagonospora nodorum* (Berk) Castell and Germano that were identified as the culprit of wheat glume blotch disease [5]. Furthermore, malayamycin functions as a broad-spectrum fungicide with an unusually higher potency in planta than in vitro, suggesting that its mode of action may not be consistent with those of known fungicide classes. This encouraging character-

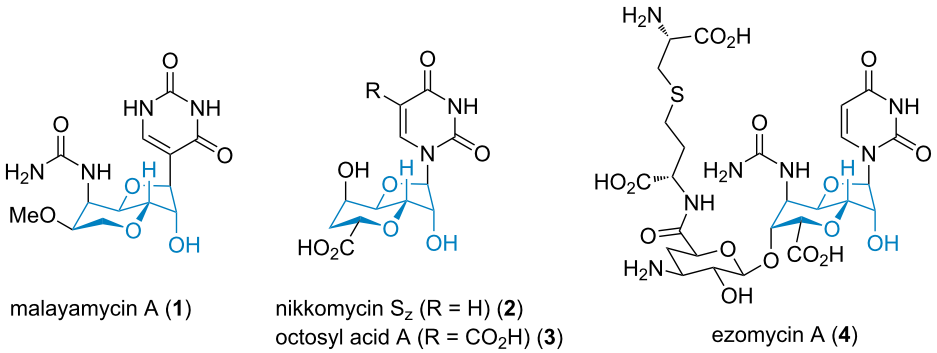

Figure 1: Selected natural uracil-containing nucleosides (the key perhydrofuropyran core highlighted in blue).

istic indicates its potential to overcome resistance to other fungicides [6-8].

Structurally, malayamycin A belongs to a class of modified nucleosides that mimic UDP (uridine 5′-diphosphate)-linked metabolites and exhibit intriguing bioactivities (**2**–**4**, Figure 1). These antifungal nucleoside agents have been received great attention from the scientific community and several elegant syntheses have been disclosed [9-15]. Specifically, Hanessian and co-workers reported the first total synthesis and structural determination of malaymycin A (**1**) as well as the subsequent design of structural analogues for biological evaluation [16-20]. Preliminary structure–activity relationship (SAR) studies revealed that fungicidal activity is highly dependent on the nature and stereochemistry of substituents, as well as the heterocyclic anomeric unit. Uncertainty regarding the mode of action, along with inadequate synthetic approaches toward a lead compound, remains elusive.

The well-established synthetic route reported by Hanessian and co-workers began with D-ribonolactone which bears three contiguous stereogenic centers (Scheme 1A). The pyran ring was constructed by a RCM reaction [16]. Subsequent functionalization of the alkene to install the 1,2-*cis*-hydroxy amine required 6 steps from the sterically more demanding side. In continuing our recent interest in accessing unusual monosaccharides and applying dipolar cycloaddition to construct various bioactive compounds [21-27], we intended to develop a practical strategy to access the perhydrofuropyran core of malayamycin A and other uracil nucleosides to enable future rapid derivatization (Scheme 1B). The bicyclic intermediate **5** will be converted into the final target after installation of the

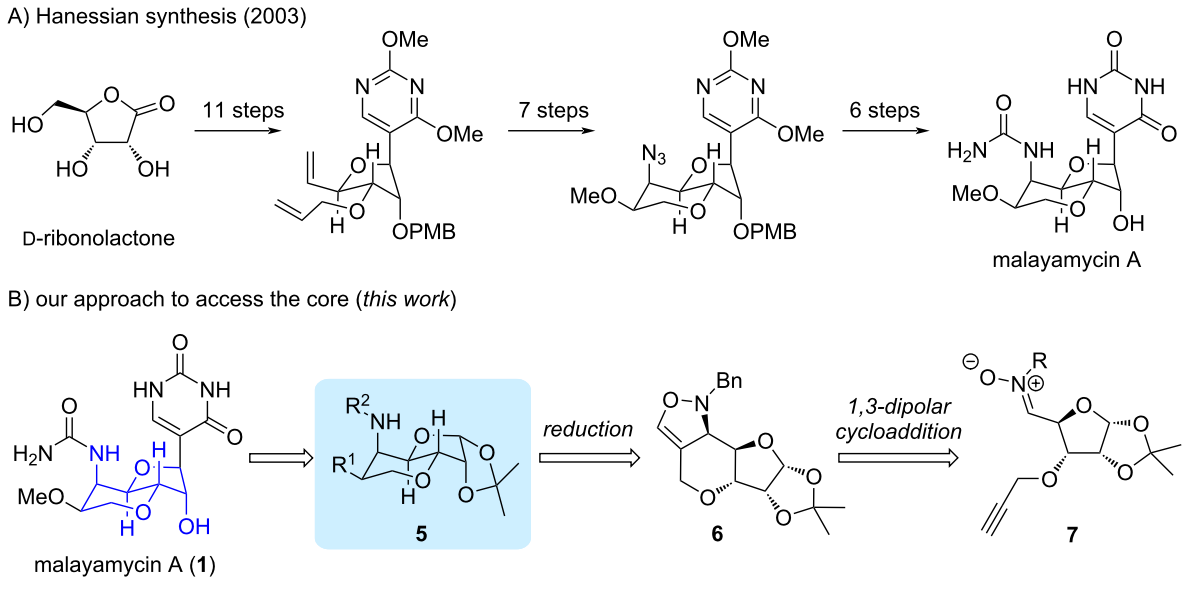

Scheme 1: Synthetic strategies toward malayamycin A. (A) Previous synthetic route. (B) Our strategy toward the core skeleton.

urea and uracil motifs. Accordingly, a nitrone-based latent functionality approach [28] would be tunable from fully substituted tetrahydrofuran-derived nitrone **7**. The *cis*-1,2-hydroxy amine could be derived from oxazoline **6** through cleavage of the N–O bond, oxidation and Baeyer–Villiger oxidation. The starting functional groups (including alkyne and nitrone) for the proposed oxazoline were established in literature precedents [29-31]. Moreover, the readily available intermediate **8** [32] bearing three defined stereogenic centers is secured from the commercial source.

Results and Discussion

Based on the known protocol [33], diacetone-D-allofuranose **8** was first introduced with a propargyl group (Scheme 2A). Upon treatment of AcOH to afford diol **9**, oxidative cleavage with Shing's protocol ($NaIO_4$ on silica gel) [34] proceeded smoothly to deliver the aldehyde which was immediately subjected to the condensation reaction with benzylhydroxylamine. The corresponding nitrone **10** then underwent an intramolecular cycloaddition. Adduct **11** was isolated as the major product in 42% yield for 2 steps. Comprehensive NMR analysis revealed the undesired stereochemistry at C3 due to a possible chair-like transition state like **10a** (Scheme 2B). This phenomenon is consistent with the observations from previous syntheses [31,35,36]. We anticipated that late-stage epimerization might invert the configuration once the acyl group is revealed at the C2 position. Therefore, dihydroxylation [37] readily converted alkene **11** to diol **12** as a mixture of inseparable isomers. Without purification, oxidative cleavage with $NaIO_4$ resulted in a compound with strong UV absorption, which was eventually identified as enone **14** (Scheme 3). It is assumed that the formyloxy group on the N atom in the unstable intermediate **13** serves as electron-withdrawing group to facilitate fragmentation when removal of the acidic proton at C2 was initiated.

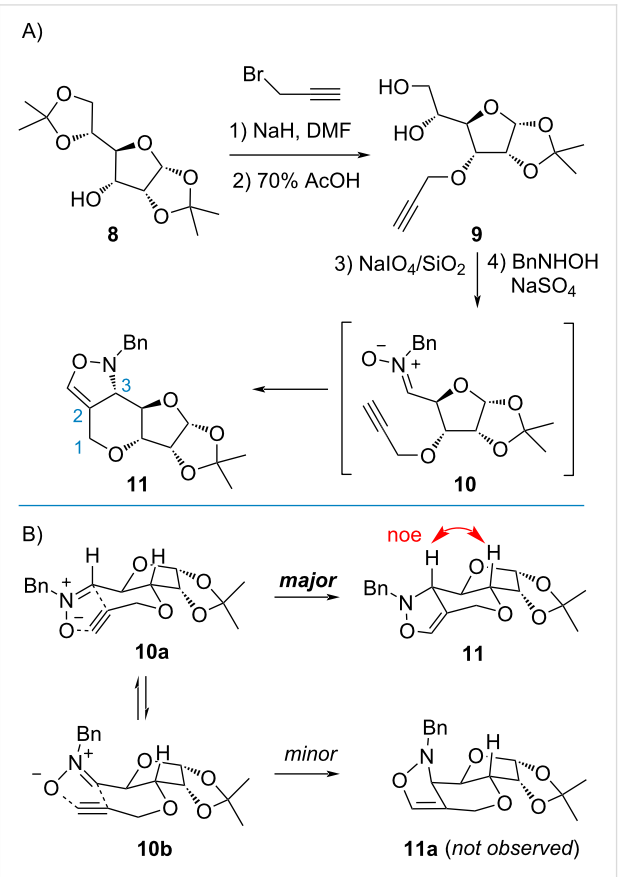

Scheme 2: Rational for intramolecular dipolar cycloaddition.

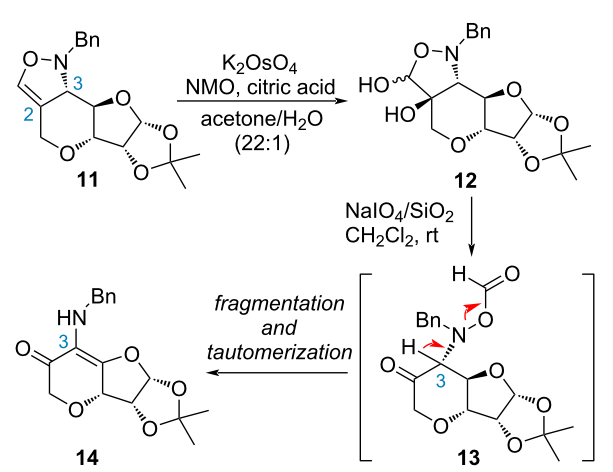

Scheme 3: Proposed pathway for the enone formation.

Although the reduction of enone **14** could provide the requisite stereoisomer, the rigid conformation of such bicyclic [4.3.0]-ring necessitates tedious optimization to properly install three continuous tertiary centers (C2, C3, and C4). To circumvent the influence of the electron-withdrawing group on the nitrogen atom, we anticipated that cleaving the N–O bond prior to breaking the C2–C2' bond would be feasible. However, several conditions to cleave the N–O bond in **11** or **12** had not yielded any successful outcome. Therefore, we turned to adjust the synthetic sequence to switch the oxidation states at C2 and C3 (Scheme 4). It should be noted that compound **16** [38] was obtained as a stereoisomeric mixture of olefin, resulting from the use of crotyl bromide as a mixture of geometric isomers. After installation of the crotyl group, hydrolysis of the acetonide group and oxidative cleavage of diol **16**, oxime **17** was prepared through the condensation of the aldehyde with hydroxylamine in overall 59% yield. Upon oxidation with $NaClO{\cdot}5H_2O$, the in situ-generated nitrile *N*-oxide immediately underwent intramolecular dipolar cycloaddition to deliver the cycloadducts **18** in good yield as a mixture of two inseparable diastereoisomers. This telescoped step was readily performed on a gram scale without interrupted purification of the nitrile oxide.

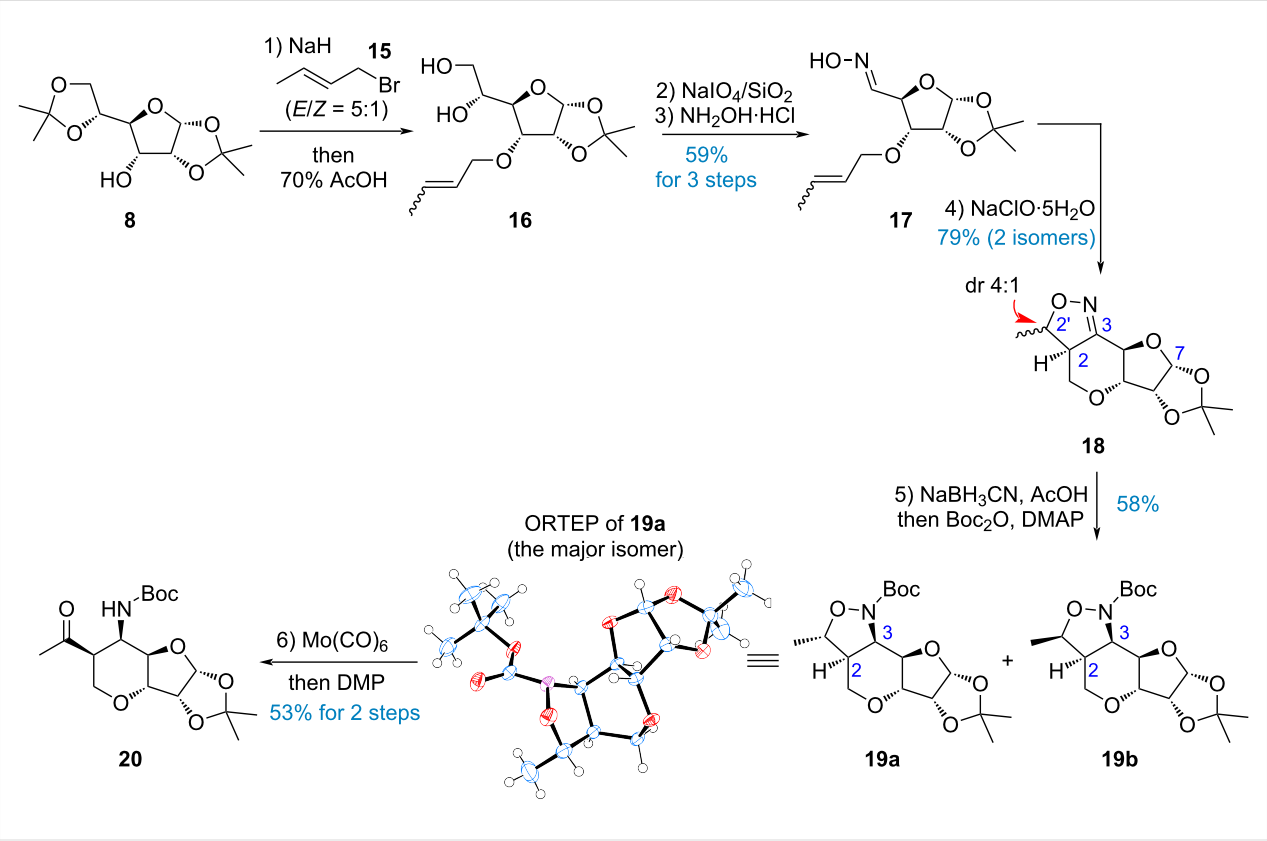

Scheme 4: Modified route to access the core of malayamycins.

At this stage, it is not clear that the diastereomeric ratio (dr 4:1) may share with the same configuration at the C2 or C2' position. The mixture of **18** was subjected to reduction of the imine motif by $NaBH_3CN$ in AcOH–MeOH and immediately protected with the Boc group. The isolated yield of **19** was moderate because the anomeric carbon at C7 is associated with an acid-sensitive acetonide group. The structural determination of the major product **19a** was accomplished by comprehensive NMR spectroscopy and further unambiguously confirmed by X-ray analysis (see Supporting Information File 1 for details). The following reductive cleavage of the N–O bond was carried out by $Mo(CO)_6$ in refluxing CH_3CN [39]. Subsequent oxidation of the resulting secondary alcohol with Dess–Martin periodinane (DMP) [40] afforded methyl ketone **20** in 53% yield for 2 steps. Moreover, the minor isomer **19b** also underwent the above two-step sequence, yielding a product identical to **20** (the synthetic route is not shown). This indicates that the pair of diastereomers essentially differs only at the C2' position arised from the isomeric mixture of crotyl bromide **15**. It is also worth noting that both stereoisomers derived from the INOC cycloaddition can be converted to a single stereoisomer of **20**.

With all required stereogenic centers embedded in the 6-5 *trans*-fused bicyclic skeleton, the remaining problem is converting C to O to install the secondary alcohol at C2 with retention of the β-configuration. The programmed Baeyer–Villiger (BV) oxidation would be a feasible transformation to furnish all necessary functional groups for the completion of the core skeleton in malayamycins. To our surprise, it turns out very challenging for the BV oxidation. Several oxidants were examined and the desired acetate **21** remains inaccessible (Scheme 5) [41]. We assumed the steric hinderance of the Boc protecting group might have a great impact to the reactivity of ketone. Investigation along this line is currently on the way.

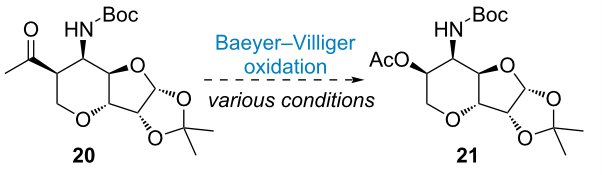

Scheme 5: Attempting the Baeyer–Villiger reaction.

Conclusion

In summary, we have streamlined the rapid construction of the core perhydrofuropyran skeleton of malayamycin A and other

related uracil nucleosides via a dipolar cycloaddition. The latent functionality strategy employing oxazoline to reveal the *cis*-1,2-hydroxyamine moiety proves to be feasible, circumventing the lengthy route for alkene functionalization required in previous syntheses. Although the target-oriented synthesis toward malayamycins remains to be complished and several steps need to be improved, the current strategy provides a reliable platform to access various uracil nucleosides and derivatives for developing potent fungicides.

Supporting Information

Supporting Information File 1

Experimental procedures and compound characterization data.
[https://www.beilstein-journals.org/bjoc/content/supplementary/1860-5397-21-196-S1.pdf]

Acknowledgements

We thank Dr. Min Shao (Shanghai University) for assistance of X-ray analysis.

Funding

Financial support from the National Natural Science Foundation of China (22271194 and U24A20484) is highly appreciated.

Conflict of Interest

The authors declare no conflict of interest.

Author Contributions

Yilin Liu: data curation; formal analysis; investigation; writing – original draft. Yuchen Yang: formal analysis; investigation; methodology; writing – review & editing. Chen Yang: formal analysis; investigation; methodology; writing – original draft; writing – review & editing. Sha-Hua Huang: conceptualization; funding acquisition; project administration; supervision; writing – review & editing. Jian Jin: conceptualization; project administration; writing – review & editing. Ran Hong: conceptualization; formal analysis; funding acquisition; project administration; writing – original draft; writing – review & editing.

ORCID® iDs

Jian Jin - https://orcid.org/0000-0001-9685-3355

Data Availability Statement

Data generated and analyzed during this study is available from the corresponding author upon reasonable request.

References

1. Steffens, J. J.; Pell, E. J.; Tien, M. *Curr. Opin. Biotechnol.* **1996,** *7,* 348–355. doi:10.1016/s0958-1669(96)80043-7
2. Yin, Y.; Miao, J.; Shao, W.; Liu, X.; Zhao, Y.; Ma, Z. *Phytopathology* **2023,** *113,* 707–718. doi:10.1094/phyto-10-22-0370-kd
3. Serpi, M.; Ferrari, V.; Pertusati, F. *J. Med. Chem.* **2016,** *59,* 10343–10382. doi:10.1021/acs.jmedchem.6b00325
4. Benner, J. P.; Boehlendorf, B. G. H.; Kipps, M. R.; Lambert, N. E. P.; Luck, R.; Molleyres, L. P.; Neff, S.; Schuez, T. C.; Stanley, P. D. Biocidal compounds and their preparation. WO Pat. Appl. WO2003062242A1, July 31, 2003.
5. Li, W.; Csukai, M.; Corran, A.; Crowley, P.; Solomon, P. S.; Oliver, R. P. *Pest Manage. Sci.* **2008,** *64,* 1294–1302. doi:10.1002/ps.1632
6. Winn, M.; Goss, R. J. M.; Kimura, K.-i.; Bugg, T. D. H. *Nat. Prod. Rep.* **2010,** *27,* 279–304. doi:10.1039/b816215h
7. Chen, S.; Kinney, W. A.; Van Lanen, S. *World J. Microbiol. Biotechnol.* **2017,** *33,* 66. doi:10.1007/s11274-017-2233-6
8. McErlean, M.; Liu, X.; Cui, Z.; Gust, B.; Van Lanen, S. G. *Nat. Prod. Rep.* **2021,** *38,* 1362–1407. doi:10.1039/d0np00064g
9. Zhang, D.; Miller, M. J. *Curr. Pharm. Des.* **1999,** *5,* 73–99. doi:10.2174/1381612805666230109204948
10. Datta, A. Synthetic Studies on Antifungal Peptidyl Nucleoside Antibiotics. In *Chemical Synthesis of Nucleoside Analogues;* Merino, P., Ed.; John Wiley & Sons: Hoboken, NJ, USA, 2013; pp 819–846. doi:10.1002/9781118498088.ch18
11. Danishefsky, S.; Hungate, R. *J. Am. Chem. Soc.* **1986,** *108,* 2486–2487. doi:10.1021/ja00269a080
12. Danishefsky, S. J.; Hungate, R.; Schulte, G. *J. Am. Chem. Soc.* **1988,** *110,* 7434–7440. doi:10.1021/ja00230a024
13. Knapp, S.; Thakur, V. V.; Madduru, M. R.; Malolanarasimhan, K.; Morriello, G. J.; Doss, G. A. *Org. Lett.* **2006,** *8,* 1335–1337. doi:10.1021/ol0600382
14. Fan, S.; Jiang, T.; Lv, T.; Liu, J.; Wang, X. *Org. Lett.* **2023,** *25,* 4355–4358. doi:10.1021/acs.orglett.3c01494
15. Fan, S.; Jiang, T.; Siddique, M. N.; Zhang, L.; Liu, J.; Wang, X. *Org. Lett.* **2023,** *25,* 7832–7835. doi:10.1021/acs.orglett.3c03087
16. Hanessian, S.; Marcotte, S.; Machaalani, R.; Huang, G. *Org. Lett.* **2003,** *5,* 4277–4280. doi:10.1021/ol030095k
17. Hanessian, S.; Huang, G.; Chenel, C.; Machaalani, R.; Loiseleur, O. *J. Org. Chem.* **2005,** *70,* 6721–6734. doi:10.1021/jo050727b
18. Hanessian, S.; Marcotte, S.; Machaalani, R.; Huang, G.; Pierron, J.; Loiseleur, O. *Tetrahedron* **2006,** *62,* 5201–5214. doi:10.1016/j.tet.2005.12.066
19. Loiseleur, O.; Schneider, H.; Huang, G.; Machaalani, R.; Sellès, P.; Crowley, P.; Hanessian, S. *Org. Process Res. Dev.* **2006,** *10,* 518–524. doi:10.1021/op0600299
20. Hanessian, S.; Ritson, D. J. *J. Org. Chem.* **2006,** *71,* 9807–9817. doi:10.1021/jo061904r
21. Meng, Y.; Tao, S.; Wu, X.-Y.; Huang, S.-H.; Hong, R. *Org. Lett.* **2023,** *25,* 1929–1934. doi:10.1021/acs.orglett.3c00461
22. Chen, H.; Lin, Z.; Meng, Y.; Li, J.; Huang, S.-H.; Hong, R. *Org. Lett.* **2023,** *25,* 6429–6433. doi:10.1021/acs.orglett.3c02449
23. Peng, Y.; Lin, Z.; Zhu, L.; Han, S.; Huang, S.-H.; Hong, R. *Chin. J. Chem.* **2024,** *42,* 841–845. doi:10.1002/cjoc.202300618
24. Liu, Y.; Zhao, J.; Hong, R. *Org. Lett.* **2024,** *26,* 4666–4671. doi:10.1021/acs.orglett.4c01411
25. Wang, Y.; Lin, Z.; Huang, S.-H.; Zhu, L.; Hong, R. *Chin. J. Org. Chem.* **2025,** *45,* 1021–1029. doi:10.6023/cjoc202406048

26. Lin, Z.; Wu, L.; Yang, S.; Zhu, L.; Hong, R.; Huang, S.-H. *Org. Lett.* **2025,** *27,* 6222–6226. doi:10.1021/acs.orglett.5c01926
27. Liu, Y.; Yang, C.; Huang, S.-H.; Hong, R. *Eur. J. Org. Chem.* **2025,** *28,* e202500768. doi:10.1002/ejoc.202500768
28. Fernandes, R. A. Latent Functionality. In *Protecting-Group-Free Organic Synthesis: Improving Economy and Efficiency;* Fernandes, R. A., Ed.; John Wiley & Sons: Hoboken, NJ, USA, 2018; pp 229–257. doi:10.1002/9781119295266.ch9
29. Shing, T. K. M.; Leung, G. Y. C. *Tetrahedron* **2002,** *58,* 7545–7552. doi:10.1016/s0040-4020(02)00577-x
30. Bhattacharjee, A.; Datta, S.; Chattopadhyay, P.; Ghoshal, N.; Kundu, A. P.; Pal, A.; Mukhopadhyay, R.; Chowdhury, S.; Bhattacharjya, A.; Patra, A. *Tetrahedron* **2003,** *59,* 4623–4639. doi:10.1016/s0040-4020(03)00634-3
31. Popik, O.; Grzeszczyk, B.; Staszewska-Krajewska, O.; Furman, B.; Chmielewski, M. *Org. Biomol. Chem.* **2020,** *18,* 2852–2860. doi:10.1039/d0ob00228c
32. Trifonova, A.; Földesi, A.; Dinya, Z.; Chattopadhyaya, J. *Tetrahedron* **1999,** *55,* 4747–4762. doi:10.1016/s0040-4020(99)00147-7
33. Jana, S. *Indian J. Chem., Sect. B: Org. Chem. Incl. Med. Chem.* **2007,** *45B,* 1648–1657.
34. Zhong, Y.-L.; Shing, T. K. M. *J. Org. Chem.* **1997,** *62,* 2622–2624. doi:10.1021/jo9621581
35. Padwa, A. *Angew. Chem., Int. Ed. Engl.* **1976,** *15,* 123–136. doi:10.1002/anie.197601231
36. Nair, V.; Suja, T. D. *Tetrahedron* **2007,** *63,* 12247–12275. doi:10.1016/j.tet.2007.09.065
37. Dupau, P.; Epple, R.; Thomas, A. A.; Fokin, V. V.; Sharpless, K. B. *Adv. Synth. Catal.* **2002,** *344,* 421–433. doi:10.1002/1615-4169(200206)344:3/4<421::aid-adsc421>3.0.co;2-f
38. Chatterjee, A.; Bhattacharya, P. K. *J. Org. Chem.* **2006,** *71,* 345–348. doi:10.1021/jo051414j
39. Nagireddy, J. R.; Tranmer, G. K.; Carlson, E.; Tam, W. *Beilstein J. Org. Chem.* **2014,** *10,* 2200–2205. doi:10.3762/bjoc.10.227
40. Dess, D. B.; Martin, J. C. *J. Org. Chem.* **1983,** *48,* 4155–4156. doi:10.1021/jo00170a070
41. Fatima, S.; Zahoor, A. F.; Khan, S. G.; Naqvi, S. A. R.; Hussain, S. M.; Nazeer, U.; Mansha, A.; Ahmad, H.; Chaudhry, A. R.; Irfan, A. *RSC Adv.* **2024,** *14,* 23423–23458. doi:10.1039/d4ra03914a

License and Terms

BEILSTEIN JOURNAL OF ORGANIC CHEMISTRY

Ni-promoted reductive cyclization cascade enables a total synthesis of (+)-aglacin B

Si-Chen Yao[1], Jing-Si Cao[1], Jian Xiao[*2], Ya-Wen Wang[1] and Yu Peng[*1]

Letter

Open Access

Address:
[1]School of Chemistry, Southwest Jiaotong University, Chengdu 610031, People's Republic of China and [2]School of Materials and Environment Engineering, Chengdu Technological University, Chengdu 611730, People's Republic of China

Email:
Jian Xiao[*] - xiaojian@swjtu.edu.cn; Yu Peng[*] - pengyu@swjtu.edu.cn

* Corresponding author

Keywords:
aryltetralin; conjugate addition; cyclolignan; nickel; reductive coupling

Beilstein J. Org. Chem. **2025,** *21,* 2548–2552.
https://doi.org/10.3762/bjoc.21.197

Received: 29 August 2025
Accepted: 03 November 2025
Published: 18 November 2025

This article is part of the thematic issue "Concept-driven strategies in target-oriented synthesis".

Guest Editor: Y. Tang

Abstract

The total synthesis of bioactive (+)-aglacin B was achieved. The key steps include an asymmetric conjugate addition reaction induced by a chiral auxiliary and a nickel-promoted reductive tandem cyclization of the elaborated β-bromo acetal, which led to the efficient construction of the aryltetralin[2,3-*c*]furan skeleton embedded in this natural product.

Introduction

Proksch and co-workers isolated aglacins A, B, C, and E (**1**–**4**, Figure 1) from the methanolic extract of stem bark of *Aglaia cordata* Hiern from the tropical rain forests of the Kalimantan region (Indonesia) [1,2]. These cyclic ether natural products belong to the typical aryltetralin lignans, which have already attracted broad attention from the synthetic community [3-5]. Zhu and co-workers disclosed a concise synthesis of (±)-aglacins B (**2**) and C (**3**), featuring a visible light-catalyzed radical cation cascade for the formation of the C8–C8′ and C2–C7′ bonds [6]. Subsequently, they improved the reaction conditions to achieve the racemic synthesis of aglacins A (**1**) and E (**4**) as well [7]. In 2021, the Gao group described the total synthesis of both enantiomers of aglacins A (**1**), B (**2**), and E (**4**) by asymmetric photoenolization/Diels–Alder reactions as the key steps for the construction of the C7–C8 and C7′–C8′ bonds [8].

During the past decade, we had developed nickel-catalyzed or -promoted reductive coupling/cyclization reactions for the formation of inter- or intramolecular carbon–carbon bonds under mild conditions [9-12], and strategically applied this method for the divergent syntheses of some natural products [13-17]. Herein, we report our recent advance to a total synthesis of (+)-aglacin B (**2**), which relies on a non-photocatalysis approach.

Results and Discussion

Retrosynthetic analysis of (+)-aglacin B

Based on the retrosynthetic analysis shown in Scheme 1, both C8′–C8 and C7–C1 bonds in (+)-aglacin B (**2**) could be constructed in one-step from the β-bromo acetal **5** by a Ni-promoted tandem radical cyclization, and a subsequent

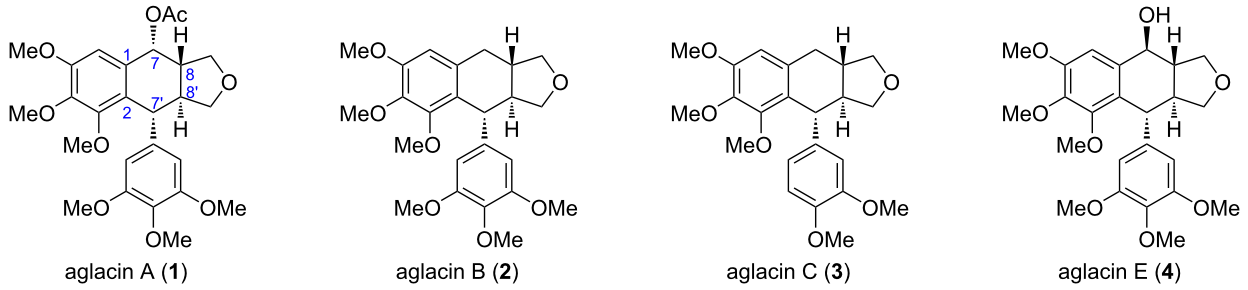

Figure 1: The structures of aglacins A, B, C, and E.

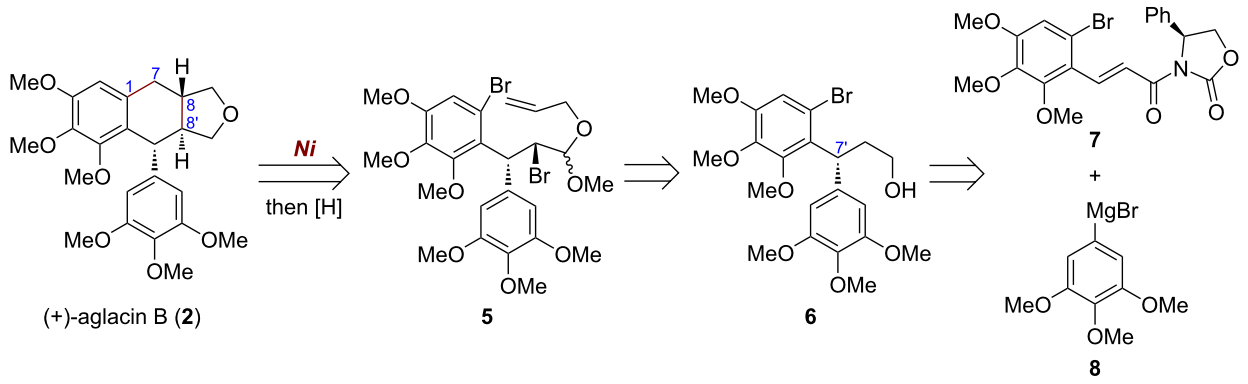

Scheme 1: Retrosynthetic analysis of (+)-aglacin B (**2**).

acetal reduction under acidic conditions then can complete the total synthesis of this molecule. The cyclization precursor **5** could be prepared from the primary alcohol **6** through transforming functional groups of the alkyl chain and installing an allyl group. It was envisioned that the diarylmethine stereocenter at C7′ in **6** could be formed by an Evans' auxiliary-induced asymmetric conjugate addition of α,β-unsaturated acyl oxazolidinone **7** with 3,4,5-trimethoxyphenylmagnesium bromide (**8**). Both of these two building blocks could be conveniently prepared from commercially available 2,6-dimethoxyphenol [18,19].

Synthesis of cyclization precursor **5** and (+)-aglacin B

As shown in Scheme 2, the forward synthesis began with a triethyl phosphonoacetate-mediated Horner–Wadsworth–Emmons (HWE) reaction of *o*-bromobenzaldehyde **9** derived from 2,6-dimethoxyphenol (Supporting Information File 1). The generated ester **10** was then converted into the corresponding acyl chloride by saponification and subsequent reaction with pivaloyl chloride. The resulting acyl chloride was then trapped by (*S*)-4-phenyl-2-oxazolidinone (**11**) to produce the desired α,β-unsaturated amide **7**. Next, the asymmetric conjugate addition was carried out [20,21]. The in situ generated aryl–copper(I) species was obtained under the action of CuBr·Me_2S with Grignard reagent **8**, and then added to a THF solution of the α,β-unsaturated acyl oxazolidinone **7** at −48 °C. This reaction demonstrated an excellent diastereocontrol for **12** (dr = 20:1), and could easily proceed on a scale of ten grams (Supporting Information File 1). For the reduction of the chiral auxiliary in **12**, $NaBH_4$ in THF/H_2O proved to be the optimal conditions, giving the primary alcohol **6** in 80% yield. Subsequently, oxidation of this alcohol by IBX followed by reaction with $CH(OMe)_3$ afforded acetal **17**, which was then subjected to a CH_2Cl_2 solution of TMSOTf and iPr_2NEt. A mixture of enol methyl ethers **18** were thus produced by an elimination reaction. Eventually, a site-selective bromination of the double bond over the electron-rich benzene rings with 2,4,4,6-tetrabromo-2,5-cyclohexadienone (TBCD) in CH_2Cl_2 followed by reaction with allyl alcohol, provided β-bromo acetal **5** in 30% overall yield starting from alcohol **6**.

With a successful preparation of the cyclization precursor **5**, the designed nickel-promoted reductive tandem cyclization was

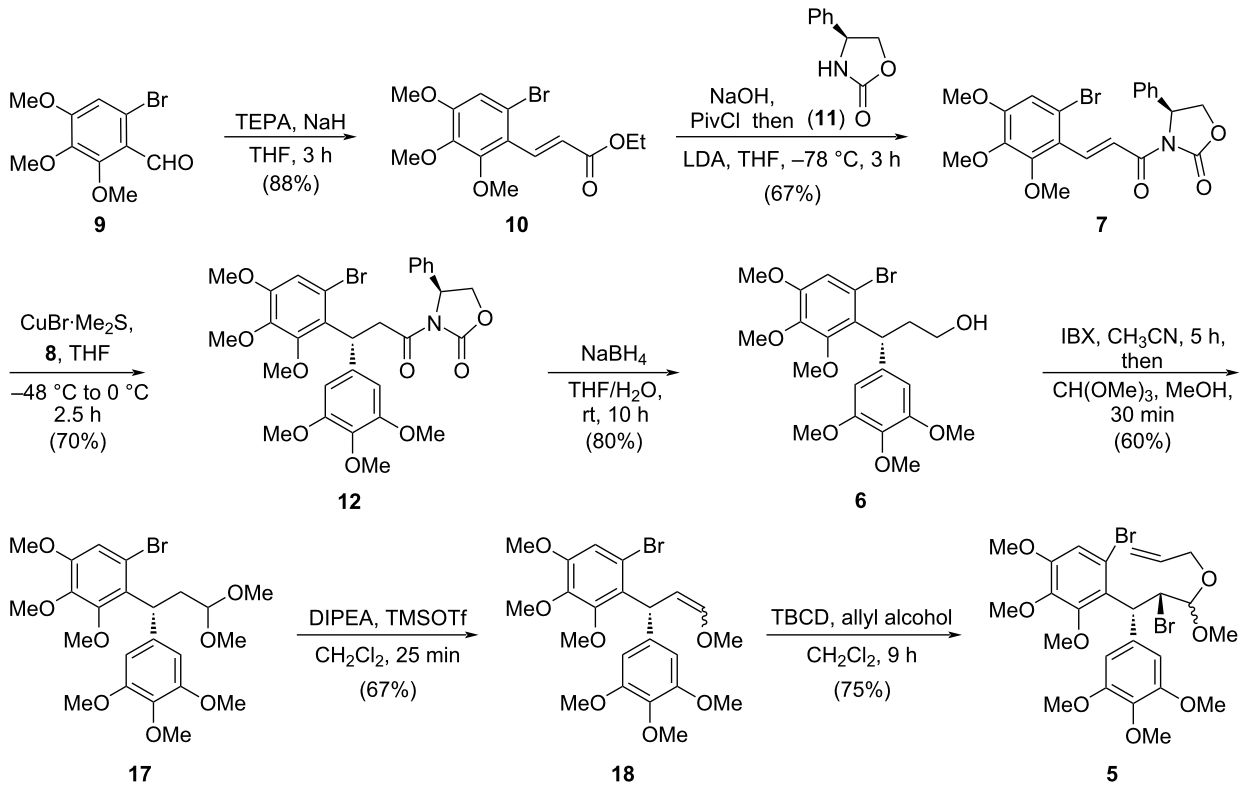

Scheme 2: Synthesis of cyclization precursor **5**.

pursued (Scheme 3). By slightly modifying the reaction conditions of our previous studies [11,12], the expected bicyclization of **5** occurred smoothly, resulting in an efficient construction of the *trans*-tetrahydronaphtho[2,3-*c*]furan skeleton embedded in **13**, which could be separated from the other diastereomer [14] by flash column chromatography in 30% yield. The stereocon-

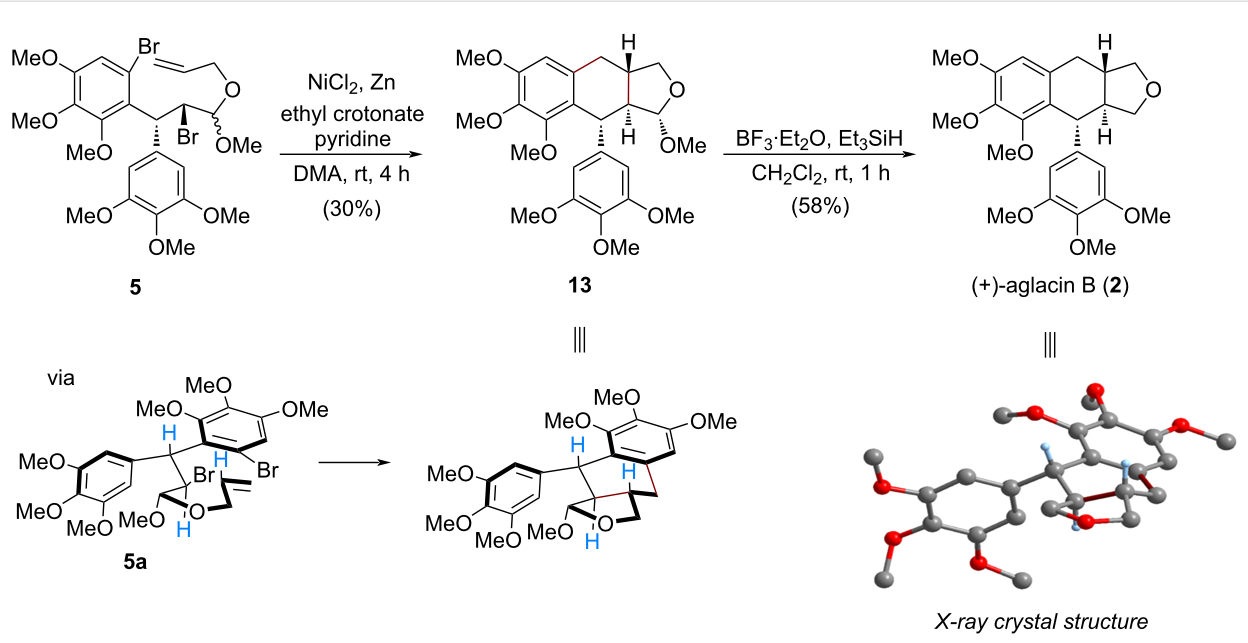

Scheme 3: Synthesis of (+)-aglacin B (**2**).

trolled formation of aryltetralin **13** could be attributed to an adoption of a *pseudo*-half-chair conformation **5a**. Finally, the final step towards the total synthesis of (+)-aglacin B (**2**) was achieved by treatment with $BF_3{\cdot}Et_2O$ as the Lewis acid and Et_3SiH as the hydrogen source [22], affording this natural product in 58% isolated yield. NMR data of the synthetic sample were found to be in agreement with those of previous literature (Tables S1 and S2, Supporting Information File 1). Moreover, the newly synthesized (+)-aglacin B (**2**) formed single crystals, and a corresponding X-ray diffraction analysis (inset in Scheme 3, selected H atoms have been omitted for clarity, and Table S3, Supporting Information File 1) unambiguously confirmed its precise structure with three continuous chiral centers.

Conclusion

In summary, the total synthesis of (+)-aglacin B, a typical aryltetralin natural product [23,24], was completed from 2,6-dimethoxyphenol. The key Ni-promoted reductive cyclization cascade of a β-bromo acetal with an allyl tether, smoothly established the tetrahydronaphtho[2,3-*c*]furan core of this molecule in a new fashion.

Supporting Information

Supporting Information File 1

Experimental procedures, characterization data, and copies of $^1H/^{13}C$ NMR spectra.
[https://www.beilstein-journals.org/bjoc/content/supplementary/1860-5397-21-197-S1.pdf]

Acknowledgements

We thank the Analytical and Testing Center of Southwest Jiaotong University for the NMR test.

Funding

The National Natural Science Foundation of China (Nos. 22071200 and 22471224).

ORCID® iDs

Yu Peng - https://orcid.org/0000-0002-3862-632X

Data Availability Statement

All data that supports the findings of this study is available in the published article and/or the supporting information of this article.

References

1. Wang, B.-G.; Ebel, R.; Nugroho, B. W.; Prijono, D.; Frank, W.; Steube, K. G.; Hao, X.-J.; Proksch, P. *J. Nat. Prod.* **2001,** *64,* 1521–1526. doi:10.1021/np0102962
2. Wang, B.-G.; Ebel, R.; Wang, C.-Y.; Wray, V.; Proksch, P. *Tetrahedron Lett.* **2002,** *43,* 5783–5787. doi:10.1016/s0040-4039(02)01180-2
3. Yao, S.-C.; Xiao, J.; Nan, G.-M.; Peng, Y. *Tetrahedron Lett.* **2023,** *115,* 154309. doi:10.1016/j.tetlet.2022.154309
4. Zhang, H.-Q.; Yan, C.-X.; Xiao, J.; Wang, Y.-W.; Peng, Y. *Org. Biomol. Chem.* **2022,** *20,* 1623–1636. doi:10.1039/d1ob02457d
5. Reynolds, R. G.; Nguyen, H. Q. A.; Reddel, J. C. T.; Thomson, R. J. *Nat. Prod. Rep.* **2022,** *39,* 670–702. doi:10.1039/d1np00057h
6. Xiang, J.-C.; Wang, Q.; Zhu, J. *Angew. Chem., Int. Ed.* **2020,** *59,* 21195–21202. doi:10.1002/anie.202007548
7. Xiang, J.-C.; Fung, C.; Wang, Q.; Zhu, J. *Nat. Commun.* **2022,** *13,* 3481. doi:10.1038/s41467-022-31000-4
8. Xu, M.; Hou, M.; He, H.; Gao, S. *Angew. Chem., Int. Ed.* **2021,** *60,* 16655–16660. doi:10.1002/anie.202105395
9. Yan, C.-S.; Peng, Y.; Xu, X.-B.; Wang, Y.-W. *Chem. – Eur. J.* **2012,** *18,* 6039–6048. doi:10.1002/chem.201200190
10. Peng, Y.; Xu, X.-B.; Xiao, J.; Wang, Y.-W. *Chem. Commun.* **2014,** *50,* 472–474. doi:10.1039/c3cc47780k
11. Peng, Y.; Xiao, J.; Xu, X.-B.; Duan, S.-M.; Ren, L.; Shao, Y.-L.; Wang, Y.-W. *Org. Lett.* **2016,** *18,* 5170–5173. doi:10.1021/acs.orglett.6b02665
12. Xiao, J.; Cong, X.-W.; Yang, G.-Z.; Wang, Y.-W.; Peng, Y. *Chem. Commun.* **2018,** *54,* 2040–2043. doi:10.1039/c8cc00001h
13. Peng, Y.; Luo, L.; Yan, C.-S.; Zhang, J.-J.; Wang, Y.-W. *J. Org. Chem.* **2013,** *78,* 10960–10967. doi:10.1021/jo401936v
14. Xiao, J.; Cong, X.-W.; Yang, G.-Z.; Wang, Y.-W.; Peng, Y. *Org. Lett.* **2018,** *20,* 1651–1654. doi:10.1021/acs.orglett.8b00408
15. Luo, L.; Zhai, X.-Y.; Wang, Y.-W.; Peng, Y.; Gong, H. *Chem. – Eur. J.* **2019,** *25,* 989–992. doi:10.1002/chem.201805682
16. Cao, J.-S.; Zeng, J.; Xiao, J.; Wang, X.-H.; Wang, Y.-W.; Peng, Y. *Chem. Commun.* **2022,** *58,* 7273–7276. doi:10.1039/d2cc02221d
17. Liu, Z.-H.; Xiao, J.; Zhai, Q.-Q.; Tang, X.; Xu, L.-J.; Zhuang, Z.-Y.; Wang, Y.-W.; Peng, Y. *Chem. Commun.* **2024,** *60,* 694–697. doi:10.1039/d3cc05312a
18. Percec, V.; Holerca, M. N.; Nummelin, S.; Morrison, J. J.; Glodde, M.; Smidrkal, J.; Peterca, M.; Rosen, B. M.; Uchida, S.; Balagurusamy, V. S. K.; Sienkowska, M. J.; Heiney, P. A. *Chem. – Eur. J.* **2006,** *12,* 6216–6241. doi:10.1002/chem.200600178
19. Massé, P.; Choppin, S.; Chiummiento, L.; Colobert, F.; Hanquet, G. *J. Org. Chem.* **2021,** *86,* 3033–3040. doi:10.1021/acs.joc.0c02489
20. Andrews, R. C.; Teague, S. J.; Meyers, A. I. *J. Am. Chem. Soc.* **1988,** *110,* 7854–7858. doi:10.1021/ja00231a041
21. Chen, C.-y.; Reamer, R. A. *Org. Lett.* **1999,** *1,* 293–294. doi:10.1021/ol990608g
22. Mason, J. D.; Terwilliger, D. W.; Pote, A. R.; Myers, A. G. *J. Am. Chem. Soc.* **2021,** *143,* 11019–11025. doi:10.1021/jacs.1c03529
23. Chen, Y.; Yun, Z.; Quynh Nguyen, T.; Wang, J.; Tang, Y. *CCS Chem.* **2025,** in press. doi:10.31635/ccschem.025.202505994
24. Xu, W.-X.; Peng, Z.; Gu, Q.-X.; Zhu, Y.; Zhao, L.-H.; Leng, F.; Lu, H.-H. *Nat. Synth.* **2024,** *3,* 986–997. doi:10.1038/s44160-024-00564-y

BEILSTEIN JOURNAL OF ORGANIC CHEMISTRY

Total syntheses of highly oxidative *Ryania* diterpenoids facilitated by innovations in synthetic strategies

Zhi-Qi Cao, Jin-Bao Qiao* and Yu-Ming Zhao*

Review

Open Access

Address:
Key Laboratory of Applied Surface and Colloid Chemistry of MOE & School of Chemistry and Chemical Engineering, Shaanxi Normal University, Xi'an, 710119, China

Email:
Jin-Bao Qiao* - qiaojb21@snnu.edu.cn; Yu-Ming Zhao* - ymzhao@snnu.edu.cn

* Corresponding author

Keywords:
natural products; *Ryania* diterpenoids; synthetic strategy; total synthesis

Beilstein J. Org. Chem. **2025,** *21,* 2553–2570.
https://doi.org/10.3762/bjoc.21.198

Received: 22 September 2025
Accepted: 07 November 2025
Published: 19 November 2025

This article is part of the thematic issue "Concept-driven strategies in target-oriented synthesis".

Associate Editor: D. Y.-K. Chen

Abstract

Innovations in synthetic methods and strategic design serve as the primary driving forces behind the advancement of organic synthetic chemistry. With rapidly evolving organic synthesis technologies, a diverse array of novel methods and sophisticated strategies continues to emerge. These approaches not only complement and synergize with one another but also significantly enhance synthetic efficiency, reduce costs, and provide robust solutions to challenges encountered in the synthesis of complex molecular architectures. *Ryania* diterpenes are natural products characterized by intricate structures and high oxidation states. Biological studies have revealed that the family member ryanodine has a specific regulatory effect on myocardial calcium ion channels (PyR). Since only a limited number of compounds have been reported to act by modifying this receptor, ryanodine and its derivatives are potential therapeutic agents for treating cardiovascular diseases. This article focuses on reviewing the efficient application of ring-construction methods and synthetic strategies in the total synthesis of highly oxidized *Ryania* diterpenoid natural products, emphasizing the pivotal role of novel synthetic methods and strategic innovations.

Introduction

Organic synthesis, as a cornerstone of chemical research, is dedicated to constructing complex natural products or target molecules from simple and readily available starting materials via a series of precise and efficient chemical reactions. This field serves not only as a vital tool for molecular structure validation and the discovery of new reaction mechanisms but also as a fundamental driving force behind advances in related disciplines such as pharmaceutical science. Throughout this endeavor, innovations in methods and strategies function as an engine, consistently pushing the boundaries of the discipline. From the early synthesis of simple molecules to the current precise assembly of complex natural products and functional

materials, the iteration of methods and optimization of strategies have always been key to breaking through synthetic bottlenecks.

Since Nobel laureate E. J. Corey proposed the revolutionary concept of "retrosynthetic analysis" [1], the design of synthetic strategies has built upon this core intellectual framework: starting from the target molecule, a stepwise deconstruction guided by reverse logic leads to a series of structurally simple and readily accessible precursor compounds [2]. Based on this philosophy, chemists have developed a variety of classical synthetic strategies to address target molecules with diverse structural features. For instance, "divergent synthesis" employs a universal chiral advanced intermediate, systematically deriving multiple structurally related natural products through functional group transformations and oxidation-state adjustments [3,4]. This approach efficiently constructs compound family libraries, greatly facilitating drug screening and structure–activity relationship (SAR) studies. Conversely, the "biomimetic synthesis" strategy mimics nature's enzyme-catalyzed pathways to construct target molecules in the laboratory, offering milder reaction conditions and more concise synthetic steps, while demonstrating excellent atom economy and step economy [5-7].

These powerful and diverse methods continuously drive synthetic chemistry forward through deep integration and synergistic application. This article focuses on the total synthesis of highly oxidized *Ryania* diterpenoid natural products, systematically reviewing the synthetic strategies and ring-construction methods employed therein while providing an in-depth analysis of the innovation of classical methods, the application of emerging technologies, and the enhancements in synthetic efficiency achieved through multi-strategy integration. The aim is to offer readers a clear understanding of the developmental trajectory and future trends in the total synthesis of natural products from this family.

Natural products derived from the *Ryania* genus comprise a class of structurally intricate polycyclic diterpenoids isolated from the Central and South American shrub *Ryania speciosa* (Scheme 1) [8-14]. Research on these compounds dates back to 1943 when the American pharmaceutical company Merck developed a novel insecticide, Ryanex, from the stems and leaves of the plant. In 1948, Folkers and colleagues reported the isolation of the first bioactive member of this family – ryanodine (**1**) [8]. Due to limitations in technical capabilities at the time, its absolute configuration remained undetermined. Over the subse-

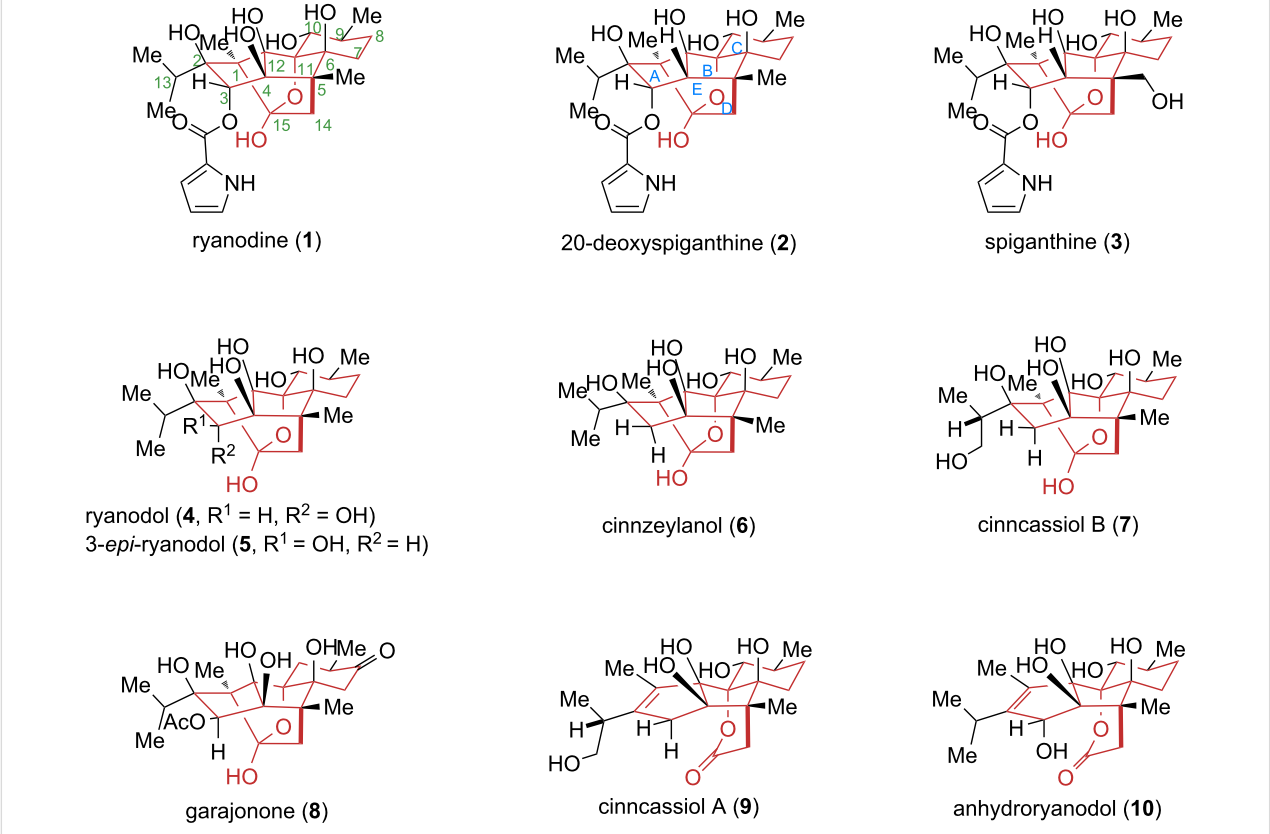

Scheme 1: Representative *Ryania* diterpenoids and their derivatives.

quent two decades, its hydrolysis product ryanodol (**4**) and several structurally related analogs were isolated sequentially [9-14]. The absolute configurations of both **1** and **4** were ultimately elucidated in 1968 by Wiesner and co-workers using a combination of chemical degradation and X-ray crystallography [14]. Notably, in 2016, Inoue's group at the University of Tokyo reconciled discrepancies through comparative analysis of experimental and natural product data, confirming the correct structure of ryanodol to be 3-*epi*-ryanodol (**5**), thereby revising the previously accepted configuration [15]. Since then, numerous analogs based on the ryanodol scaffold have been identified and characterized. As of now, 18 natural products from this family have been successfully isolated and structurally established [16-18].

Structurally, ryanodine (**1**) and related diterpenoid natural products feature a 6-5-5-5-6 pentacyclic core skeleton containing 11 stereocenters, eight of which are quaternary carbons. A key structural feature is the assembly of a polycyclic cage-like framework via multiple C–C and C–O bonds, incorporating a labile hemiketal moiety. Furthermore, the presence of multiple oxygenated quaternary carbons classifies these molecules among the most highly oxidized diterpenoid natural products reported in the literature.

In terms of biological activity, ryanodine (**1**) exhibits high specificity and regulatory effects on ryanodine receptors (RyRs) [19,20]. It is among the few small organic molecules identified to date that can modulate these receptors. Dysfunctions of RyRs are closely associated with various diseases: mutations in RyRs can cause genetic disorders such as malignant hyperthermia and central nervous system disorders; altered expression of RyR2 and RyR3 is linked to the pathogenesis of neurodegenerative diseases like Alzheimer's disease. Notably, as a critical calcium ion channel in cardiac muscle, RyRs are intimately involved in the development and progression of cardiovascular diseases [21-24]. Additionally, compounds such as cinnzeylanol (**6**), cinncassiol B (**7**), and cinncassiol A (**9**) exhibit various potential biological activities, including insecticidal, ion channel modulatory, and immunosuppressive effects [25-29].

Review

Synthetic research on *Ryania* diterpenoid natural products

Ryania diterpenoids have garnered sustained interest in the synthetic chemistry community due to their complex, unique molecular structures and potential biological activities. This has motivated extensive research that has led to notable advances. This review summarizes total synthesis efforts of various research groups on *Ryania* diterpenoid natural products, focusing on strategic methods for assembling the 6-5-5-5-6 pentacyclic core skeleton. Furthermore, it examines the integration and synergy of multiple synthetic approaches in constructing this intricate framework, emphasizing their value in addressing highly challenging synthetic endeavors.

Deslongchamps' total synthesis of ryanodol (**4**) and 3-*epi*-ryanodol (**5**)

In 1979, the Canadian organic chemist Deslongchamps, after a decade of dedicated research, successfully achieved the first total synthesis of the non-naturally produced ryanodol (**4**) and its dehydrated derivative, anhydroryanodol (**10**) [30] (Scheme 2). Given the highly complex fused-ring system and the stereochemical challenges posed by multiple chiral centers, the author utilized the Diels–Alder reaction, a prominent representative of pericyclic reactions [31-44], to control the formation of the crucial C5 chiral center precisely. Subsequent oxidative cleavage of the carbon–carbon double bond introduced in the Diels–Alder reaction, followed by an intramolecular aldol reaction, efficiently constructed the ABC tricyclic core skeleton of the target molecule. This achievement transformed a simple monocyclic precursor into a complex fused-ring skeleton, vividly demonstrating the application value of the multi-reaction synergistic strategy in natural product synthesis.

The specific synthetic route is as follows: Starting from the chiral compound (*S*)-carvone, four simple transformations yield the enone intermediate **11**. This intermediate undergoes an intermolecular [4 + 2] cycloaddition with diene **12**, generating two sets of regioselective products in an approximate ratio of 1:1. The product with the correct relative configuration undergoes hydrolysis of its spirocyclic lactone moiety under basic conditions to yield **13**, establishing the critical C5 chiral center. Under acidic conditions, intermediate **13** undergoes ketal deprotection followed by successive intramolecular aldol reactions, smoothly constructing the A ring to afford compound **14**. Subsequent protection of the vicinal diol and aldehyde functionalities in **14** provides an intermediate that, after Baeyer–Villiger oxidation and subsequent tungsten-promoted reverse epoxidation, forms lactone **15**. Ozonolysis of **15** cleaves the double bond, and a subsequent transannular aldol reaction efficiently assembles the B and C rings, yielding the ABC tricyclic core **16**. Further manipulations included the introduction of a methyl group at C9, adjustments of the oxidation state, and the installation of a mesylate group at C10, leading to compound **19**. This intermediate is converted to lactone **20** via base-promoted Grob fragmentation followed by acid-mediated MOM deprotection. Epoxidation of the C10–C11 double bond in **20**, lactone hydrolysis-promoted epoxide ring opening, and inversion of the C10 hydroxy configuration, yield the key intermediate **21**, thereby completing the construction of the D ring. Adjustments of func-

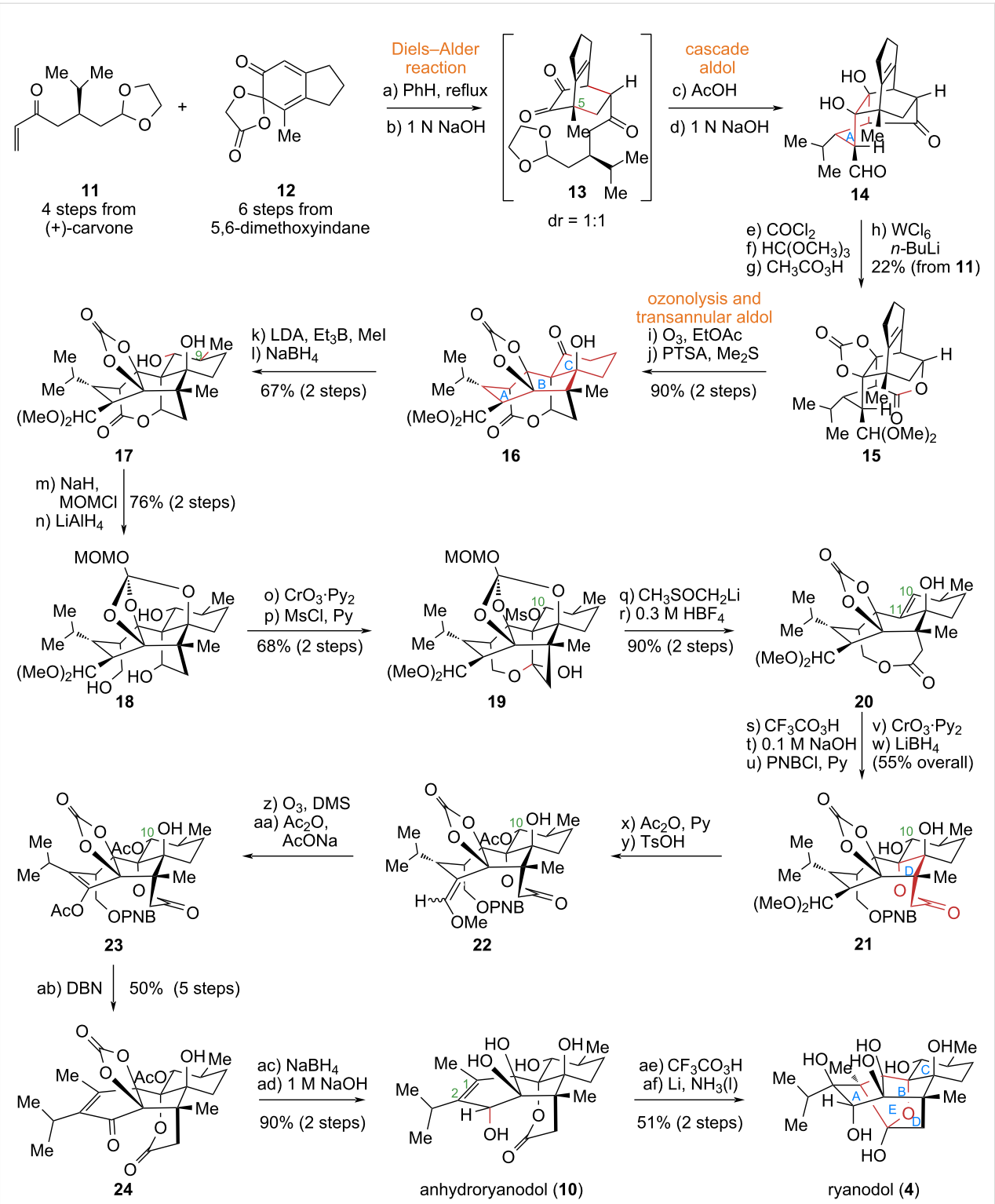

Scheme 2: Deslongchamps's total synthesis of ryanodol (**4**).

tional groups and oxidation states at multiple sites then afford anhydroryanodol (**10**). Finally, epoxidation of the C1–C2 double bond followed by Li/NH_3-promoted reductive cyclization constructs the E ring of the molecular core, successfully completing the first asymmetric total synthesis of ryanodol (**4**) in 41 steps.

To elucidate the role of the C15 hemiacetal hydroxy group in ryanodine (**1**)-type diterpenoid natural products in binding to ryanodine receptors, the authors initially proposed reducing the lactone moiety in anhydroryanodine (not shown) to the corresponding hemiacetal. However, common reducing agents proved ineffective for lactone reduction. Leveraging previous findings, the authors implemented an alternative strategy involving two sequential intramolecular reductive cyclizations to invert the configuration of the C3 secondary hydroxy group, successfully achieving the conversion of ryanodol (**4**) to 3-*epi*-ryanodol (**5**) and 3-*epi*-ryanodine (**30**) [45].

The specific synthetic route is as follows (Scheme 3): Beginning with ryanodol (**4**), an acid-promoted fragmentation yields anhydroryanodol (**10**). Subjecting compound **10** to Li/NH_3 conditions induces the first intramolecular reductive cyclization, affording hemiacetal **27**. This intermediate is then transformed via a one-pot sequence involving epoxidation, fragmentation, and re-epoxidation to give epoxide **29**. A second intramolecular reductive cyclization of **29** under Li/NH_3 forms the intramolecular oxa-bridged ring, culminating in the first total synthesis of 3-*epi*-ryanodol (**5**) and 3-*epi*-ryanodine (**30**). The subsequent biological evaluation revealed that **30** possesses only 1% of the affinity of ryanodine (**1**) for ryanodine receptors (RyRs).

Inoue's total synthesis of ryanodine, ryanodol, 3-*epi*-ryanodol, cinnzeylanol, and cinncassiols A,B

In 2014, the Inoue group at the University of Tokyo reported a synthetic strategy for ryanodol (**4**) that leveraged substrate symmetry design, employing intramolecular radical coupling and olefin metathesis as key steps [46] (Scheme 4). Recognizing an embedded symmetric motif within the complex pentacyclic target, the authors designed a simplified C_2-symmetric tricyclic intermediate, (±)-**33**, which was efficiently synthesized in 13 steps from commercial starting materials **31** and **32** by capitalizing on its molecular symmetry. A notable feature of this sequence was the simultaneous construction of four quaternary carbon centers (C1, C4, C5, and C12) and the core AB bicyclic skeleton, markedly improving synthetic efficiency. Subsequent oxidative desymmetrization of the C14–C15 olefin in (±)-**33** established the sterically hindered C11 quaternary carbon center. An α-alkoxy bridgehead radical addition then installed an allyl fragment, and ring-closing metathesis (RCM) smoothly formed the C ring to complete the core skeleton. The

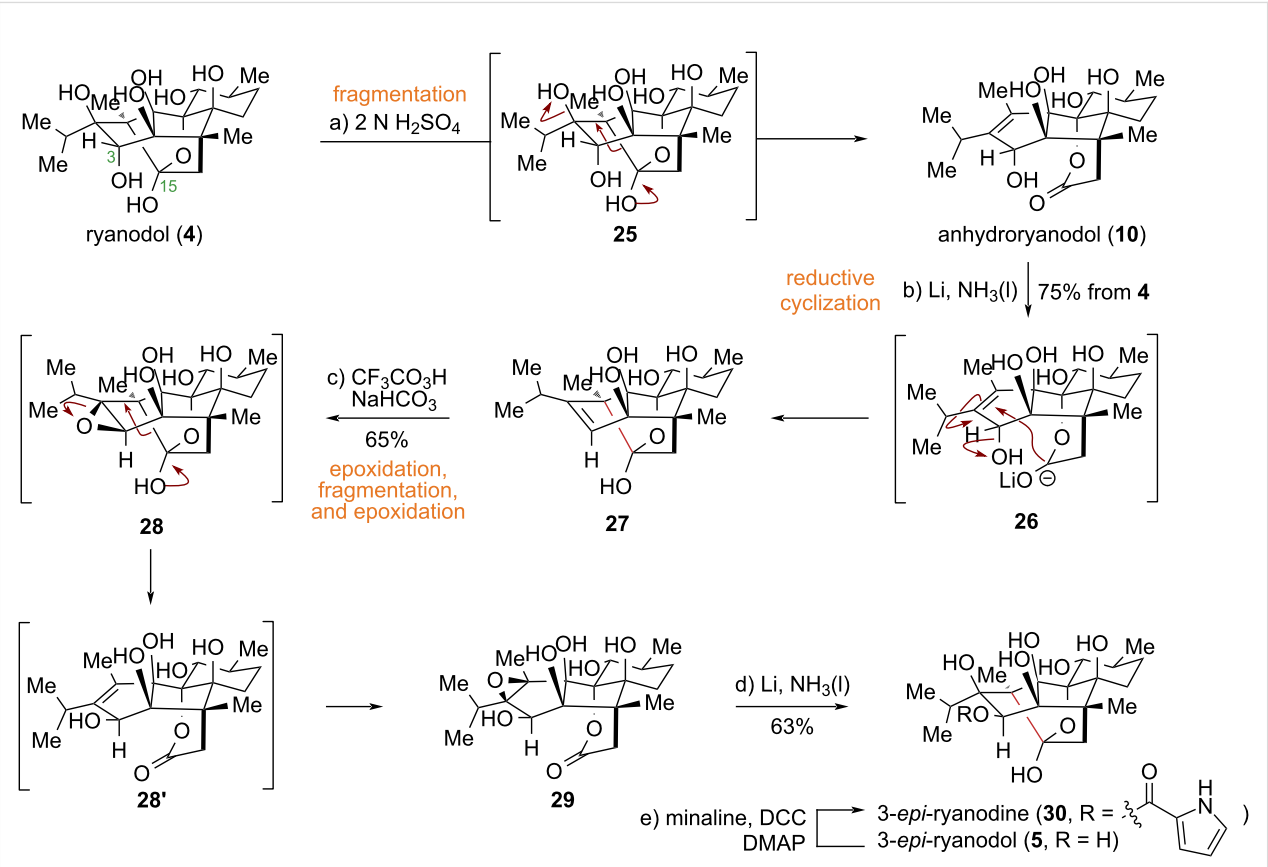

Scheme 3: Deslongchamps's total synthesis of 3-*epi*-ryanodol (**5**).

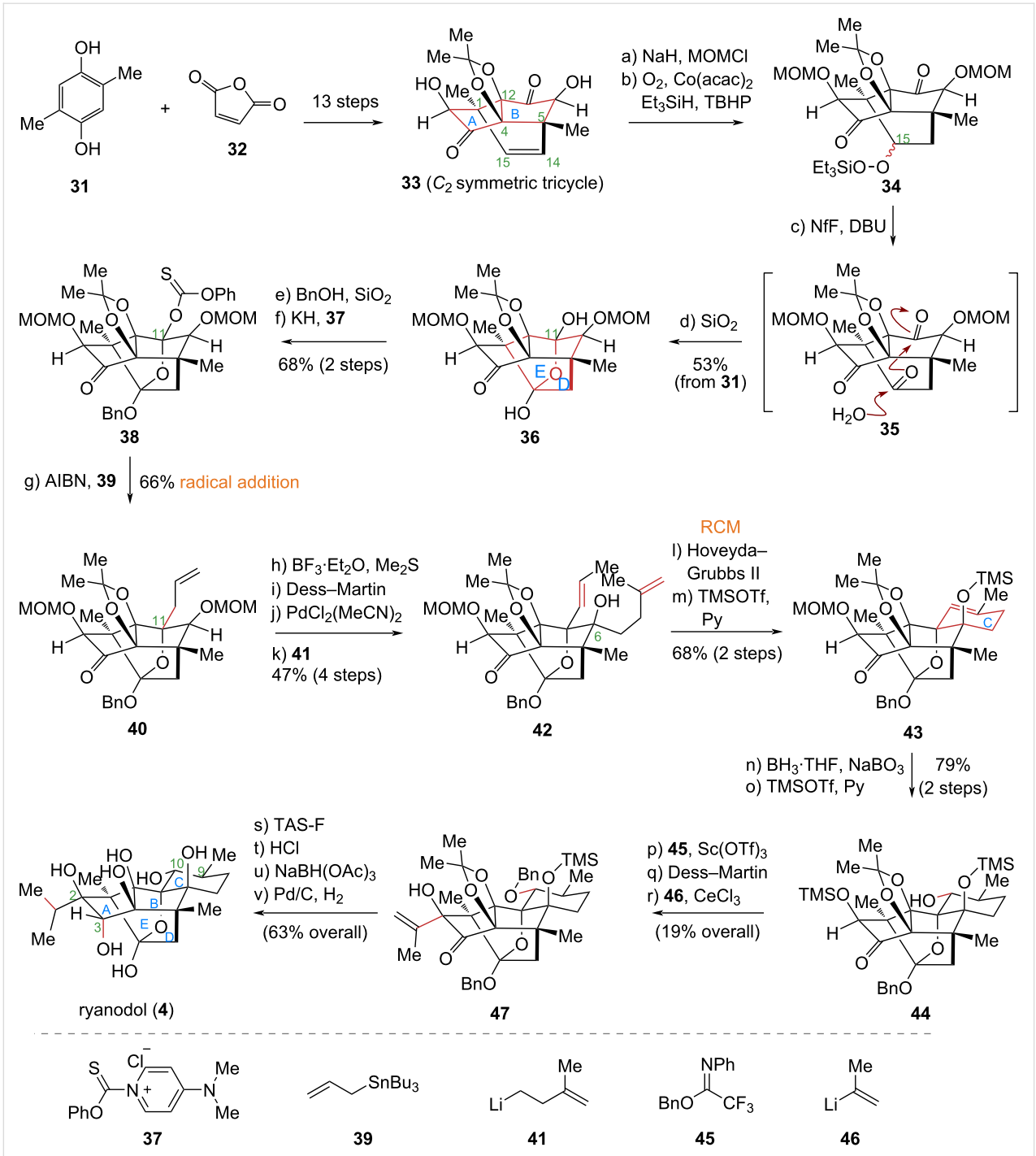

Scheme 4: Inoue's total synthesis of ryanodol (**4**).

total synthesis was finalized by installing the four remaining stereocenters (C2, C3, C9, and C10).

The specific synthetic route is as follows: Commercially available compounds **31** and **32** were converted to the C_2-symmetric **33** over 13 steps, enabling construction of the AB bicyclic skeleton in the target molecules. Compound **33** then underwent Mukaiyama hydration to adjust the C15 oxidation state, followed by water-promoted consecutive hemiacetalization to construct the oxa[3.2.1]-bridged ring system, thereby forming the D and E rings. Subsequently, the introduction of a tertiary hydroxy thiocarbonate at C11 afforded compound **38**. Under thermal conditions, **38** underwent smooth introduction of an allyl fragment via intermolecular radical addition reaction with

allyltributylstannane, yielding compound **40**. After isomerization of the C11 allyl double bond and introduction of a C6 isobutenyl group, the resulting diene **42** underwent RCM catalyzed by the Hoveyda–Grubbs catalyst to form the pentacyclic skeleton **43**, thus completing the C ring of the natural product's core structure. Finally, multisite functional group modifications and oxidation state adjustments enabled the total synthesis of ryanodol (**4**) in 35 steps.

Ryanodine (**1**), a prominent member of the *Ryanoid* diterpene natural product family, exhibits remarkable insecticidal and pharmacological activities and serves as a potent modulator of intracellular calcium release channels. In contrast to ryanodol (**4**), compound **1** possesses a pyrrole-2-carboxylate ester moiety at the C3 position. This ester group can be cleaved via hydrolysis to yield **4**. However, the reverse transformation – the synthesis of ryanodine (**1**) from ryanodol (**4**) – had long eluded chemists. The primary challenge involved the selective installation of the bulky pyrrole unit onto the sterically congested C3 secondary hydroxy group within a polyfunctionalized, polyhydroxylated framework. In 2016, building upon prior work, the Inoue group reported the first total synthesis of ryanodine from ryanodol [47] (Scheme 5). Their strategy utilized a novel boronate protecting group to mask the four *syn*-oriented hydroxy groups. A critical step was the in-situ generation of the pyrrole-2-carboxylate unit from a glycine ester and 1,3-bis(dimethylamino)allylium tetrafluoroborate, which was then coupled to the C3 hydroxy group via Yamaguchi esterification. Global deprotection subsequently afforded ryanodine (**1**) in 10 steps, thus achieving this critical synthetic transformation.

Although the interaction of ryanodine with intracellular calcium release channels has been extensively studied, the mechanisms of action of other ryanoid diterpenoid natural products remain poorly understood. Elucidating the structure–activity relationships (SAR) of these compounds is essential for identifying the functional groups critical for their biological activity, thereby facilitating targeted molecular optimization. In 2016, the Inoue group accomplished the total synthesis of cinncassiol A (**9**) and B (**7**), cinnzeylanol (**6**), and 3-*epi*-ryanodol (**5**) through precisely controlled reactions with high stereoselectivity [15] (Scheme 6). Their approach allowed for the introduction of diverse substituents at the C2 position and precise modulation of oxidation states at other sites, including C3. The synthesis of 3-*epi*-ryanodol (**5**) commenced with compound **44**. After the protection of the C10 secondary hydroxy group, a sterically controlled, face-selective reduction of the C3 carbonyl, a silyl transform, and oxidation of the C2 secondary hydroxy group afforded intermediate **54**. This sequence successfully installed the C3 hydroxy group with the requisite stereochemistry for 3-*epi*-ryanodol (**5**). Subsequent introduction of an isopropyl group at C2 and global deprotection yielded the natural product. Similarly, starting from **57**, installation of an allyl group at C2, followed by oxidative cleavage, reduction, and deprotection,

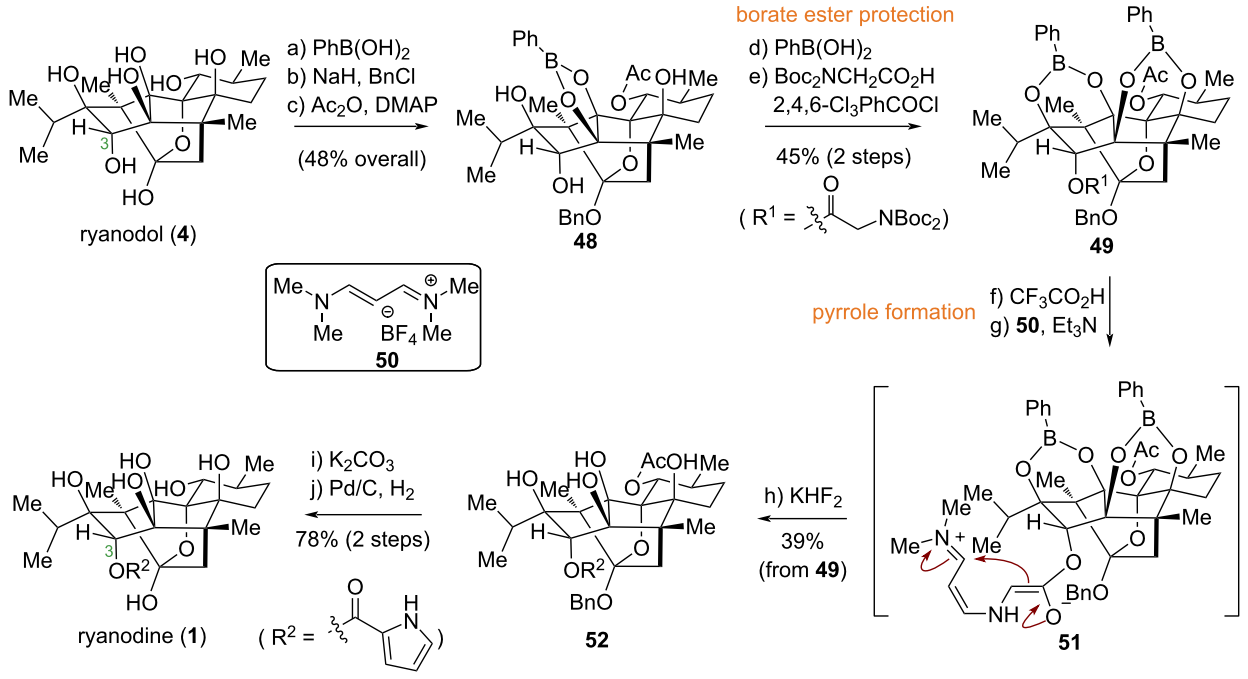

Scheme 5: Inoue's total synthesis of ryanodine (**1**) from ryanodol (**4**).

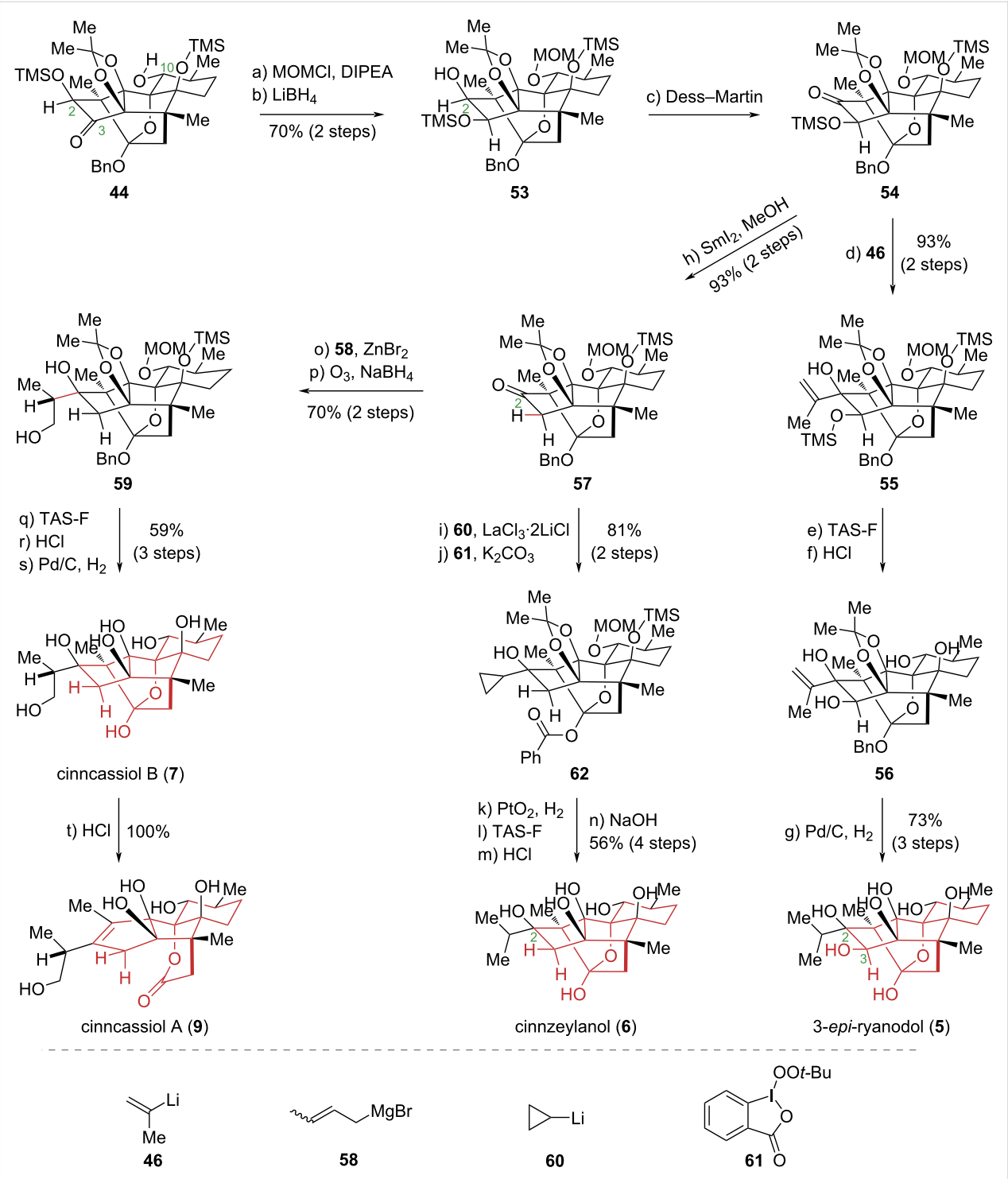

Scheme 6: Inoue's total synthesis of cinncassiol A (**9**), cinncassiol B (**7**), cinnzeylanol (**6**), and 3-*epi*-ryanodol (**5**).

provided cinncassiol B (**7**). Subjecting this compound to an acid-promoted fragmentation reaction then completed the total synthesis of cinncassiol A (**9**). Furthermore, from intermediate **57**, the introduction of an isopropyl group at C2 and subsequent deprotection furnished cinnzeylanol (**6**).

Reisman's total synthesis of (+)-ryanodine (**1**), (+)-20-deoxyspiganthine (**2**), and (+)-ryanodol (**4**)

In 2016, the Reisman group at Caltech reported an asymmetric total synthesis of (+)-ryanodol (**4**) in just 15 steps, highlighting the Pauson–Khand cyclization and a selenium dioxide-medi-

ated selective oxidation as key transformations [48] (Scheme 7). To construct the multi-substituted five-membered ring in the target molecule, the authors strategically employed the Pauson–Khand reaction – a powerful method for building five-membered rings. This single [2 + 2 + 1] cycloaddition step efficiently converted a simple linear precursor into a complex bicyclic system. Subsequent late-stage modifications of the enone skeleton introduced multiple chiral centers, significantly enhancing overall synthetic efficiency. A further highlight of this work was the development of a selenium dioxide-mediated regioselective oxidation. Leveraging the existing chiral centers in the molecular framework, this strategy allowed for the simultaneous installation of the desired oxidation states at three distinct positions (C3, C4, C12) in a single step. This obviated the need for protecting groups and individual oxidation state adjustments, greatly streamlining the synthesis of this polyhydroxylated diterpene and underscoring the reaction's utility in improving synthetic efficiency.

The specific synthetic route commenced from (−)-pulegone. After introducing oxidation states at C6 and C10 and installing an alkynyl group at C11, oxidative cleavage of a double bond yielded the key propargylic alcohol intermediate **66**. This compound underwent a 1,2-addition with alkynyl Grignard reagent **67**, and the resulting adduct was subjected to AgOTf-catalyzed lactonization to successfully construct the D ring of target molecular framework. Next, a 1,4-addition reaction introduced a vinyl group to compound **68**, affording compound **70**. A Pauson–Khand cyclization of **70** under $[RhCl(CO)_2]_2$/CO conditions smoothly furnished the ABCD tetracyclic core skeleton **71**. Treatment of **71** with SeO_2 effected a multi-site sequential oxidation, and subsequent triflation yielded triflate **73**. Finally, compound **73** underwent a sequence of transformations: introduction of an isopropyl group at C2, directed reduction of the C3 carbonyl, epoxidation of the C1–C2 double bond, and Li/NH_3-promoted reductive cyclization to construct the core E ring, completing the asymmetric total synthesis of (+)-ryanodol (**4**).

The 800-fold greater binding affinity of (+)-ryanodine (**1**) for cardiac ryanodine receptors (RyRs) compared to its hydrolysis product, (+)-ryanodol (**4**), indicates that the pyrrole-2-carboxyl-

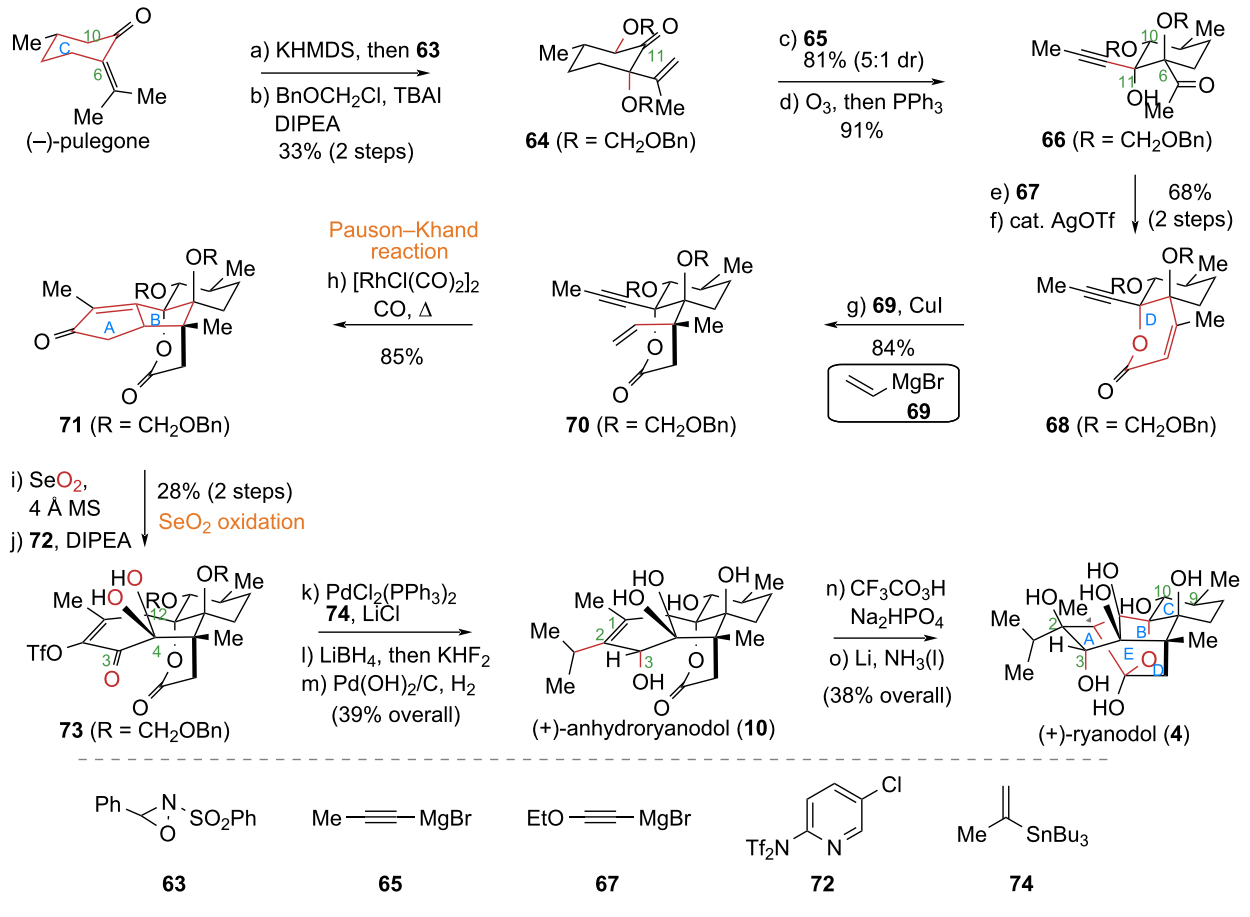

Scheme 7: Reisman's total synthesis of (+)-ryanodol (**4**).

ate unit at the C3 position is critical for receptor binding, as established by structure–activity relationship (SAR) studies [28]. However, the direct and selective modification of the highly sterically hindered C3 hydroxy group within this polyhydroxylated molecular framework has posed a significant synthetic challenge, impeding the preparation of derivatives for SAR exploration. In 2017, the Reisman group addressed this issue by drawing upon an analysis of Deslongchamps's prior synthetic work [45] (Scheme 8). They hypothesized that utilizing an intermediate from the synthesis of anhydroryanodol (**10**), which features a less hindered C3 hydroxy group, would circumvent the chemoselectivity problems. Their strategy involved first installing the pyrrole carboxylate unit on this more accessible position, followed by constructing the ketal moiety of the ryanodine skeleton via an established single-electron reductive cyclization to complete the total synthesis. This strategic inversion of the synthetic sequence enabled direct acylation of anhydroryanodol derivatives, facilitating the introduction of the key pyrrole-2-carboxylate unit. This method effectively resolved a major obstacle in the synthesis of ryanodine (**1**) and established a versatile approach for introducing diverse C3 ester substituents for future SAR studies [49].

The synthesis commenced from advanced intermediate **71** (from their prior work). Sequential SeO_2-mediated oxidation, triflation, and introduction of an isopropenyl group afforded compound **75**. Subsequent protection of the vicinal diol as a boronic ester and diastereoselective reduction of the C3 carbonyl group yielded compound **76**. Esterification with acylating reagent **77** under basic conditions, followed by boronic ester

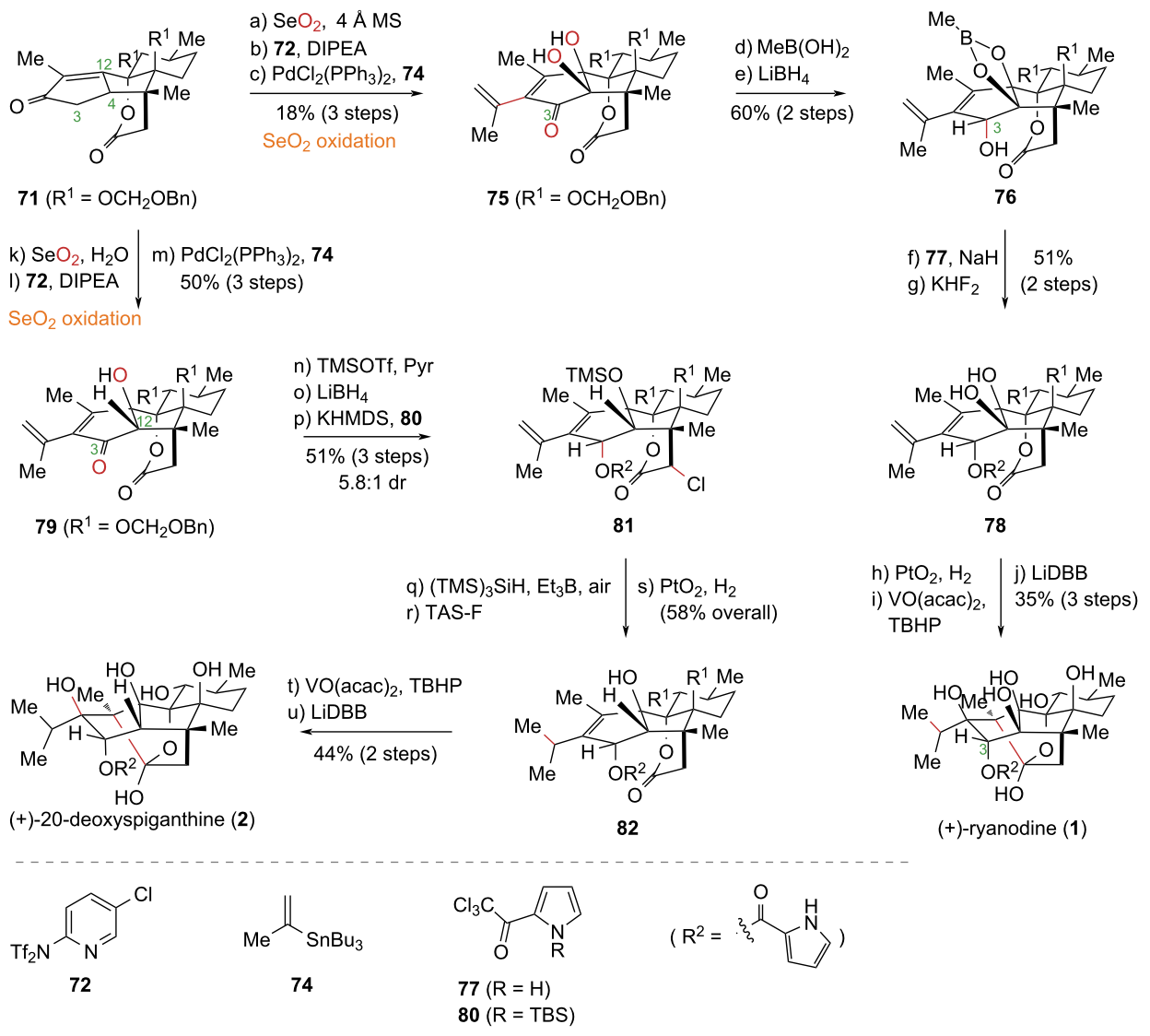

Scheme 8: Reisman's total synthesis of (+)-ryanodine (**1**) and (+)-20-deoxyspiganthine (**2**).

removal, provided compound **78**. Finally, a sequence comprising terminal alkene reduction, epoxidation of the tetrasubstituted alkene, and LiDBB-promoted intramolecular reductive cyclization and deprotection completed the asymmetric total synthesis of (+)-ryanodine (**1**) in 17 steps. Notably, the additive used in the SeO_2 oxidation critically influenced the reaction outcome [50,51]. Employing 4 Å molecular sieves afforded product **75** with oxidation states installed at both the C4 and C12 positions. In contrast, using H_2O as an additive yielded product **79**, bearing a single oxidation state at the C12 position. Leveraging this regioselective oxidation, the authors achieved the total synthesis of (+)-20-deoxyspiganthine (**2**) from compound **71**. Thus, **71** was converted to **79** via selective SeO_2 oxidation (with H_2O), triflation, and isopropenyl installation. After protecting the C12 tertiary alcohol and performing a diastereoselective reduction of the C3 ketone, the acyl pyrrole group was introduced to yield **81**. During acyl pyrrole installation, excess KHMDS enolized the lactone to suppress lactone-C3 hydroxy transesterification. However, α-chlorination of the ester carbonyl was unavoidable. Finally, reductive dechlorination, terminal alkene reduction, and intramolecular reductive cyclization culminated in the completion of the first asymmetric total synthesis of (+)-20-deoxyspiganthine (**2**) in 19 steps.

Micalizio's formal total synthesis of ryanodol (**4**)

In 2020, the Micalizio group at the University of California, San Diego, achieved the total synthesis of anhydroryanodol (**10**) and a formal synthesis of ryanodol (**4**) through a key low-valent titanium-mediated intramolecular stereoselective coupling of alkynes with 1,3-dicarbonyl compounds [52] (Scheme 9). To construct the oxygenated fused-ring system with contiguous stereocenters characteristic of the target molecule, the authors strategically implemented this methodology. This approach efficiently established two carbon–carbon and four carbon–oxygen bonds while introducing four contiguous stereocenters, successfully assembling the highly functionalized AB ring system. This work not only demonstrates the efficacy of the titanium-mediated intramolecular alkyne-1,3-diketone coupling but also provides a novel strategic approach for synthesizing natural products within this structural class.

The synthesis commenced from commercially available compound **83**. Sequential alkyne difunctionalization, furyl group installation, Achmatowicz rearrangement, and subsequent functional group manipulations provided intermediates **84** and **85**. C5-acylation and methylation under kinetically controlled conditions followed by Sonogashira coupling yielded cyclization precursor **89**. Treatment of **89** with $Ti(OiPr)_4$/iPrMgCl promoted the intramolecular stereoselective alkyne–1,3-dicarbonyl coupling, resulting in the construction of the AB ring system. This transformation afforded tricyclic compound **91** as the major product, accompanied by minor amounts of by-product **90**. Subjecting **91** to epoxidation of the tetrasubstituted alkene followed by Grieco elimination yielded diene **92**. Subsequent oxidation of the hemiacetal, saponification of the lactone, intramolecular epoxide opening, and Hoveyda–Grubbs (II)-catalyzed RCM afforded tetracyclic compounds **94** and its transesterification product **93**, thus establishing the core C and D rings. Base-mediated equilibration fully converted **93** into lactone **94**. Finally, selective hydroxy protection in **94**, diastereoselective introduction of the C10 secondary alcohol, and global deprotection completed the total synthesis of anhydroryanodol (**10**). Application of established Deslongchamps and Reisman protocols then enabled the formal synthesis of ryanodol (**4**) in 22 steps.

Zhao's total synthesis of garajonone (**8**) and formal syntheses of ryanodol (**4**) and ryanodine (**1**)

Traditional total synthesis strategies often follow a linear, stepwise approach – analogous to "climbing a staircase" – where each successive step involves functional group interconversions and protecting group manipulations, culminating in low overall efficiency. In contrast, Baran's "two-phase" synthesis strategy emulates nature's "cyclization–functionalization" logic [53,54]. This approach is akin to "taking an elevator", prioritizing the rapid assembly of the molecular core skeleton before undertaking precise late-stage functionalization. This strategy has proven highly successful for synthesizing complex terpenoids, as exemplified by the Baran group's 2013 total synthesis of ingenol [55]. Typically, the biosynthesis of polycyclic diterpenes occurs in two distinct phases: an initial cyclase-mediated cyclization phase to form the carbon framework, followed by an oxidase-catalyzed phase to install the requisite oxidation states. Inspired by this general biosynthetic pathway, the Zhao group employed a similar two-phase strategy to achieve the first total synthesis of the *Ryania* diterpenoid garajonone (**8**) in 2025 [56] (Scheme 10).

Key achievements of this synthesis include: (1) application of palladium-catalyzed Heck/carbonylative cascade cyclization to efficiently construct the core tricyclic carbon skeleton, and (2) systematic oxidation state manipulation of this scaffold to precisely introduce its dense array of oxygenated stereocenters. The construction of the C6 quaternary stereocenter represented a particularly formidable challenge in the late stage. This was successfully accomplished via an epoxide ring-opening/tandem lactonization/olefin hydration sequence. In total, 12 consecutive redox manipulations (7 oxidations and 5 reductions) established all stereocenters, with subsequent functional group transformations completing the total synthesis of garajonone (**8**).

The synthesis commenced with the preparation of key cyclization precursor **98** via Barbier coupling and Babler–Dauben oxi-

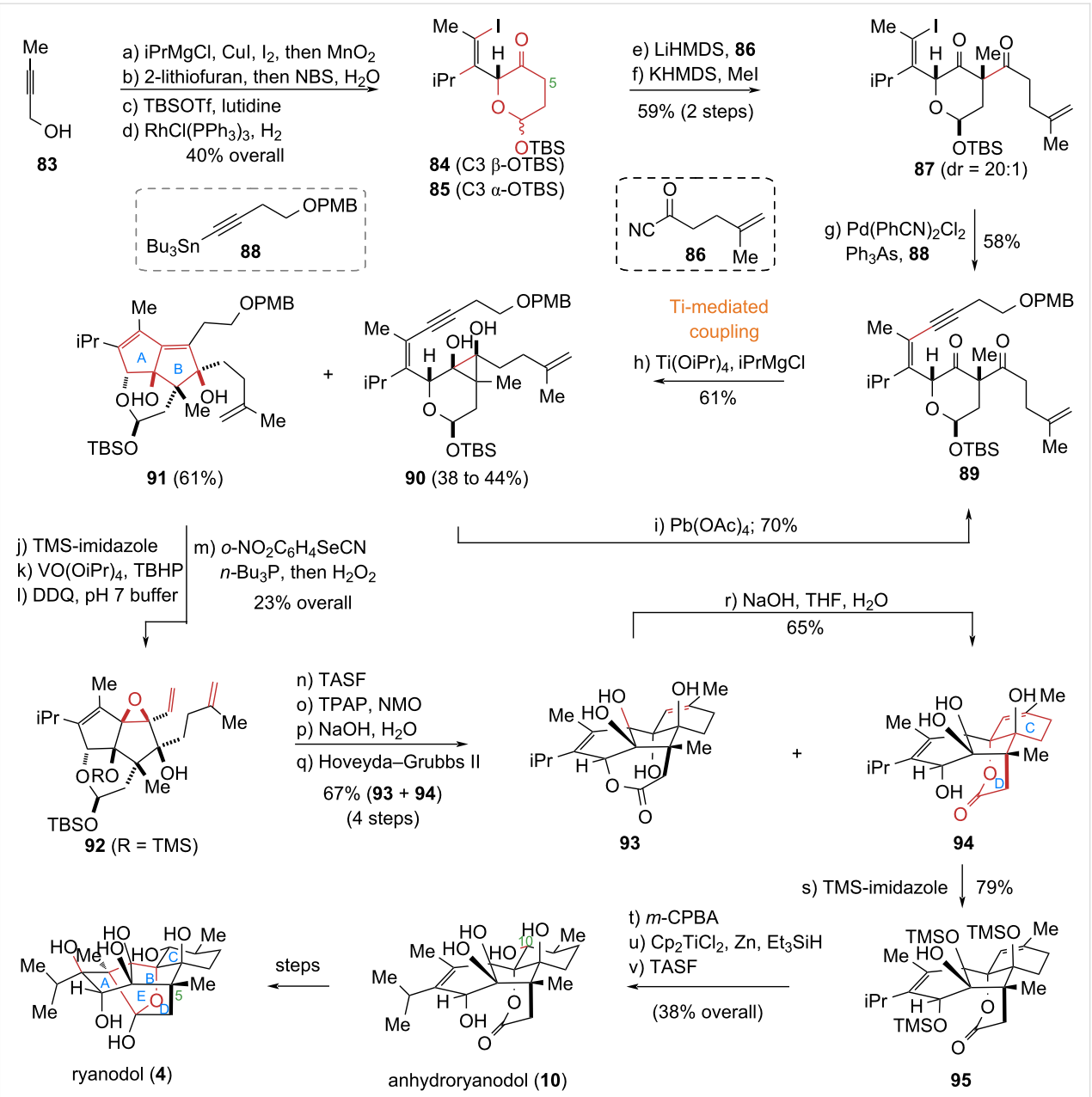

Scheme 9: Micalizio's formal total synthesis of ryanodol (**4**).

dative rearrangement. A pivotal palladium-catalyzed Heck/carbonylative cyclization then efficiently furnished the ABC tricyclic core **99**. Notably, adding *N*-formylsaccharin under a CO atmosphere significantly suppressed side reactions, yielding the cyclized product in excellent yield and selectivity. This indicates that *N*-formylsaccharin, beyond acting as a CO-releasing agent, may function as a ligand in the catalytic cycle to regulate the palladium catalyst's activity and stability. While its mechanism remains incompletely understood, this additive's unique efficacy in such transformations is unprecedented. Subsequent steps involved hydroxylation of the double bond and the protection of the vicinal diol as a dimethyl ketal giving ester **100**. Oxidative dehydrogenation, benzyl deprotection and ester hydrolysis produced carboxylic acid **101**, which upon oxidative dearomatization yielded dienone **102**, thus completing the D-ring. Regioselective epoxidation to **103** and reduction (using Adams' catalyst) through intermediate **104** gave lactone **105**. A retro-*oxa*-Michael/intramolecular transesterification sequence produced mono-enone **106**, whose hydration installed the C6 stereocenter to yield **107**. Further protecting group and oxidation state adjustments afforded lactone **108**, which was transformed via an intramolecular S_N2' reaction (single-electron

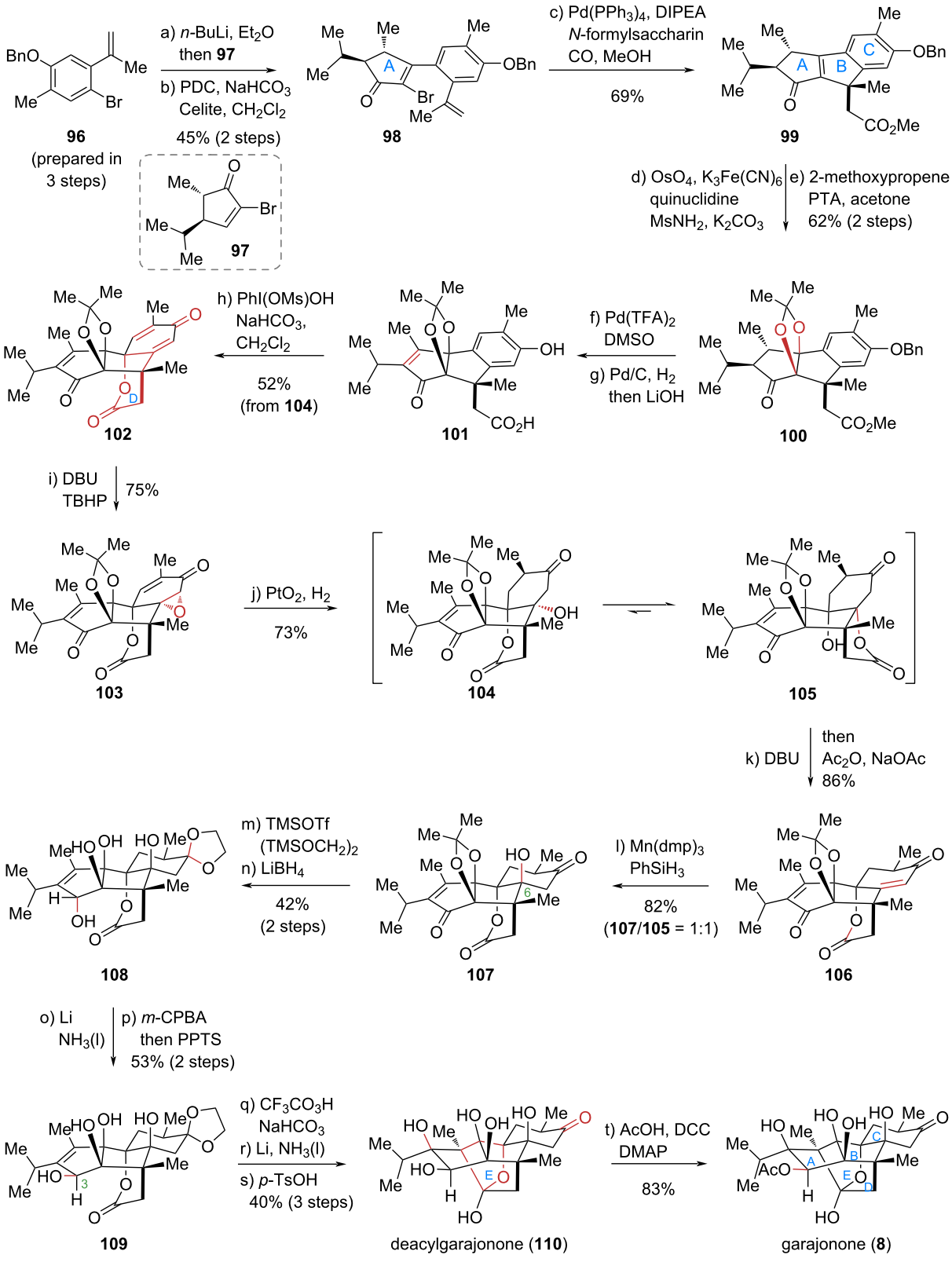

Scheme 10: Zhao's total synthesis of garajonone (**8**).

reduction), *m*-CPBA epoxidation, acid-promoted fragmentation, and face-selective hydroxylation at C3 to yield **109**. A final sequence of epoxidation, single-electron reductive cyclization, and ethylene glycol deprotection delivered hemiketal **110**, completing the E-ring formation. Finally, selective acetylation of the secondary hydroxy group culminated in the first total synthesis of garajonone (**8**) in 20 steps.

The structural diversity of ryanodine-type diterpenoid natural products arises primarily from variations in oxidation patterns and stereochemical configurations, particularly at the C3, C8, and C10 positions. These subtle structural differences present substantial challenges in developing a unified synthetic strategy capable of accessing diverse members of this family. The Zhao group recently achieved the first total synthesis of the *Ryania* diterpenoid garajonone (**8**) and its epimer 3-*epi*-garajonone. Unlike the representative ryanodine diterpenoids and analogs prepared by Inoue, Reisman, and Micalizio, these compounds feature oxidation at the C8 position instead of the more conventional C10 site. Capitalizing on this oxidative divergence, they investigated whether a common advanced intermediate could be selectively functionalized to install either C8 or C10 oxidation, followed by subsequent oxidation state adjustments and functional group manipulations to accomplish the total synthesis of the target natural products [57] (Scheme 11). Based on retrosynthetic analysis of previous routes, they employed common intermediate **103** as the starting material. Key transformations included regioselective and stereoselective alkene epoxidation, organoselenium-mediated reductive cleavage of the α,β-epoxy ketone, and a hydroxy-directed stereospecific Mukaiyama hydration. These operations successfully introduced the C6 and C10 oxidation states, enabling the synthesis of the representative *Ryania* diterpenoid degradation product anhydroryanodol (**10**) and the formal total syntheses of ryanodol (**4**) and ryanodine (**1**). This work establishes the first unified synthetic approach for ryanodine-type diterpenoids with varying oxidation patterns and provides a robust platform for synthesizing other family members and their structural analogues.

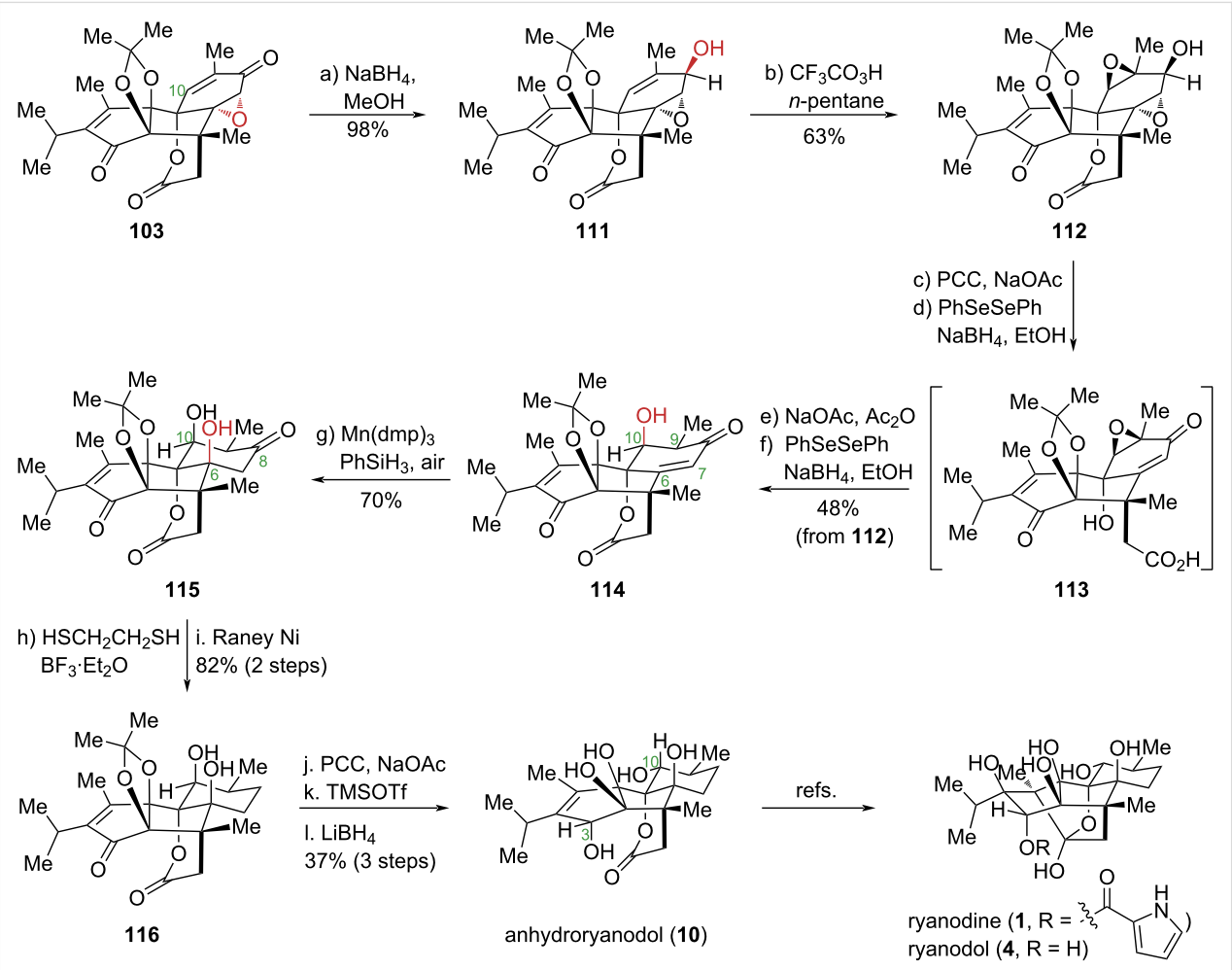

Scheme 11: Zhao's formal total synthesis of ryanodol (**4**) and ryanodine (**1**).

The synthetic sequence commenced with common intermediate **103** as the starting material. Stereoselective reduction of **103** yielded compound **111** as a single diastereomer. Systematic optimization of reaction conditions revealed that oxidation with freshly prepared trifluoroperacetic acid in *n*-pentane converted **111** to bis-epoxide **112** with excellent stereoselectivity and yield. Subjecting **112** to oxidation and organoselenium-mediated regioselective α,β-epoxy ketone opening, followed by intramolecular transesterification and elimination, provided carboxylic acid **113** in a single operation. Subsequent activation of **113** with acetic anhydride, relactonization, and organoselenium-mediated regioselective epoxide opening yielded mono-enone **114**, successfully installing the key C9 and C10 chiral centers with the required oxidation states. Notably, the bis-epoxy ketone exhibited distinct reactivity under ring-opening conditions compared to mono-epoxy substrates, presumably due to steric constraints. Leveraging the directing ability of the C10 hydroxy group, stereospecific Mukaiyama hydration of the C6–C7 double bond was achieved, furnishing compound **115** and establishing the correct C6 configuration. This transformation represents the first reported example of a hydroxy-directed Mukaiyama hydration reaction. The C8 carbonyl group was then protected as its 1,3-dithiolane derivative by treatment with 1,2-ethanedithiol. Without purification, the resulting intermediate was directly subjected to Raney nickel desulfurization, reducing the C8 carbonyl to a methylene group and delivering compound **116**. Finally, oxidation of the secondary alcohol, dimethyl ketal deprotection, and hydroxy-directed reduction installed the C3 hydroxy group and inverted the C10 stereochemistry, thereby completing the total synthesis of anhydroryanodol (**10**). By applying established strategies developed by Deslongchamps and Reisman to this intermediate, they enabled the formal total syntheses of ryanodol (**4**) and ryanodine (**1**).

Summary and Outlook

Ryania diterpenoid natural products continue to attract considerable research interest due to their intricate chemical architectures and distinctive biological properties. Through decades of dedicated effort, synthetic chemists have accomplished the total synthesis of several members within this family that share a common core scaffold yet exhibit diverse oxidation patterns and stereochemical configurations, with ryanodine (**1**) representing a landmark example (Table 1).

Table 1: The total synthesis of *Ryania* diterpenoids (1979–2025).

NPs[a]	Research group	Year	Key strategy/steps
ryanodol	Deslongchamps	1979	• Diels–Alder reaction • intramolecular aldol • transannular aldol • reductive cyclization
	Inoue	2014	• desymmetric strategy • Mukaiyama hydration • bridgehead radical addition • ring-closing metathesis
	Reisman	2016	• chiral pool strategy • intramolecular Pauson–Khand • SeO_2-mediated regioselective oxidation • reductive cyclization
	Micalizio	2020	• formal synthesis • Ti-mediated coupling • selective epoxy opening • ring-closing methathesis
	Zhao	2025	• formal synthesis • Pd-catalyzed Heck/carbonylative cascade • oxidative dearomatization • directed Mukaiyama hydration
3-*epi*-ryanodol	Deslongchamps	1993	• Diels–Alder reaction • intramolecular aldol • transannular aldol • reductive cyclization • epoxidation/fragmentation cascade
	Inoue	2016	• desymmetric strategy • Mukaiyama hydration • bridgehead radical addition • ring-closing metathesis

Table 1: The total synthesis of *Ryania* diterpenoids (1979–2025). (continued)

3-*epi*-ryanodine	Deslongchamps	1993	• Diels–Alder reaction • intramolecular aldol • transannular aldol • reductive cyclization • epoxidation/fragmentation cascade • late-stage pyrrole-2-carboxylate formation
ryanodine	Inoue	2016	• desymmetric strategy • Mukaiyama hydration • bridgehead radical addition • ring-closing metathesis • borate ester protection • in-situ pyrrole formation
	Reisman	2017	• chiral pool strategy • intramolecular Pauson–Khand • SeO_2-mediated regioselective oxidation • early-stage pyrrole-2-carboxylate formation • reductive cyclization
cinnzeylanol	Inoue	2016	• desymmetric strategy • Mukaiyama hydration • radical addition • ring-closing metathesis • introduction of isopropyl
cinncassiol A	Inoue	2016	• desymmetric strategy • Mukaiyama hydration • radical addition • ring-closing metathesis • selective 1,2-addition
cinncassiol B	Inoue	2016	• desymmetric strategy • Mukaiyama hydration • radical addition • ring-closing metathesis • selective 1,2-addition
20-deoxyspiganthine	Reisman	2017	• chiral pool strategy • intramolecular Pauson–Khand • SeO_2-mediated regioselective oxidation • early-stage pyrrole-2-carboxylate formation • reductive cyclization
garajonone	Zhao	2025	• two-phase strategy • Pd-catalyzed Heck/carbonylative cascade • oxidative dearomatization • selective redox • reductive cyclization

[a]NPs = natural product or its epimer.

This review has highlighted synthetic investigations of *Ryania* diterpenoids by various research groups, encompassing brief discussions of their isolation, structural elucidation, and biological activities. Particular emphasis has been placed on analyzing the strategic designs and key synthetic transformations employed in existing total syntheses, aiming to provide readers with a comprehensive overview of the current state of total synthesis achievements for this natural product family while stimulating further innovation in synthetic methodology. Evidently, the synthesis of *Ryania* diterpenoids remains one of the most formidable challenges in contemporary synthetic chemistry. The development of more efficient and broadly applicable synthetic strategies leveraging these complex molecular architectures continues to be a primary objective for synthetic chemists. Achieving this goal will require persistent innovation to transcend conventional synthetic paradigms and advance synthetic methods toward enhanced efficiency, precision, and sustainability. Concurrently, biological investigations of this natural product family remain relatively underdeveloped. Systematic evaluation of biological activities and structure–activity relationships, along with deeper exploration of the potential biological functions and practical applications of highly oxidized *Ryania* diterpenoids, will constitute crucial directions for future research.

Funding

We acknowledge the National Natural Science and Foundation of China (22022106, 22201168, 22371176) and Fundamental

Research Funds for the Central Universities (GK202308003) for financial supports.

Author Contributions

Zhi-Qi Cao: investigation; writing – original draft. Jin-Bao Qiao: writing – original draft; writing – review & editing. Yu-Ming Zhao: supervision; writing – review & editing.

ORCID® iDs

Yu-Ming Zhao - https://orcid.org/0000-0003-0337-2558

Data Availability Statement

Data sharing is not applicable as no new data was generated or analyzed in this study.

References

1. Corey, E. J. *Angew. Chem., Int. Ed. Engl.* **1991,** *30,* 455–465. doi:10.1002/anie.199104553
2. Corey, E. J.; Cheng, X.-M. *The Logic of Chemical Synthesis;* John Wiley & Sons: New York, NY, USA, 1995.
3. Boger, D. L.; Brotherton, C. E. *J. Org. Chem.* **1984,** *49,* 4050–4055. doi:10.1021/jo00195a035
4. Li, L.; Chen, Z.; Zhang, X.; Jia, Y. *Chem. Rev.* **2018,** *118,* 3752–3832. doi:10.1021/acs.chemrev.7b00653
5. Poupon, E.; Nay, B. *Biomimetic Organic Synthesis, Volumes 1&2;* Wiley-VCH: Weinheim, Germany, 2011. doi:10.1002/9783527634606
6. de la Torre, M. C.; Sierra, M. A. *Angew. Chem., Int. Ed.* **2004,** *43,* 160–181. doi:10.1002/anie.200200545
7. Razzak, M.; De Brabander, J. K. *Nat. Chem. Biol.* **2011,** *7,* 865–875. doi:10.1038/nchembio.709
8. Rogers, E. F.; Koniuszy, F. R.; Shavel, J., Jr.; Folkers, K. *J. Am. Chem. Soc.* **1948,** *70,* 3086–3088. doi:10.1021/ja01189a074
9. Kelly, R. B.; Whittingham, D. J.; Wiesner, K. *Can. J. Chem.* **1951,** *29,* 905–910. doi:10.1139/v51-105
10. Kelly, R. B.; Whittingham, D. J.; Wiesner, K. *Chem. Ind.* **1952,** 857.
11. Wiesner, K.; Valenta, Z.; Findlay, J. A. *Tetrahedron Lett.* **1967,** *8,* 221–223. doi:10.1016/s0040-4039(00)90521-5
12. Srivastava, S. N.; Przybylska, M. *Can. J. Chem.* **1968,** *46,* 795–797. doi:10.1139/v68-133
13. Wiesner, K. *Adv. Org. Chem.* **1972,** *8,* 295–316.
14. Wiesner, K. *Collect. Czech. Chem. Commun.* **1968,** *33,* 2656–2665. doi:10.1135/cccc19682656
15. Koshimizu, M.; Nagatomo, M.; Inoue, M. *Angew. Chem., Int. Ed.* **2016,** *55,* 2493–2497. doi:10.1002/anie.201511116
16. Totini, C. H.; Umehara, E.; Reis, I. M. A.; Lago, J. H. G.; Branco, A. *Chem. Biodiversity* **2023,** *20,* e202300947. doi:10.1002/cbdv.202300947
17. Meng, L.; Qiao, J.-B.; Zhao, Y.-M. *Chin. J. Org. Chem.* **2025,** *45,* 804–813. doi:10.6023/cjoc202409037
18. Zhang, B.; Zhao, J.; Li, S.; Liang, H.; Hao, X.; Zhang, Y. *Nat. Prod. Rep.* **2025,** in press. doi:10.1039/d5np00052a
19. Lanner, J. T. Ryanodine Receptor Physiology and Its Role in Disease. In *Calcium Signaling;* Islam, M., Ed.; Advances in Experimental Medicine and Biology, Vol. 740; Springer: Dordrecht, Netherlands, 2012; pp 217–234. doi:10.1007/978-94-007-2888-2_9
20. Kelliher, M.; Fastbom, J.; Cowburn, R. F.; Bonkale, W.; Ohm, T. G.; Ravid, R.; Sorrentino, V.; O'Neill, C. *Neuroscience* **1999,** *92,* 499–513. doi:10.1016/s0306-4522(99)00042-1
21. Wehrens, X. H. T.; Marks, A. R., Eds. *Ryanodine Receptors: Structure, Function and Dysfunction in Clinical Disease;* Springer Science & Business Media: Boston, MA, USA, 2005. doi:10.1007/b100805
22. Betzenhauser, M. J.; Marks, A. R. *Pfluegers Arch.* **2010,** *460,* 467–480. doi:10.1007/s00424-010-0794-4
23. Mackrill, J. J. *Biochem. Pharmacol.* **2010,** *79,* 1535–1543. doi:10.1016/j.bcp.2010.01.014
24. Van Petegem, F. *J. Biol. Chem.* **2012,** *287,* 31624–31632. doi:10.1074/jbc.r112.349068
25. Li, J. W.-H.; Vederas, J. C. *Science* **2009,** *325,* 161–165. doi:10.1126/science.1168243
26. Newman, D. J.; Cragg, G. M. *J. Nat. Prod.* **2012,** *75,* 311–335. doi:10.1021/np200906s
27. Butler, M. S.; Robertson, A. A. B.; Cooper, M. A. *Nat. Prod. Rep.* **2014,** *31,* 1612–1661. doi:10.1039/c4np00064a
28. Sutko, J. L.; Airey, J. A.; Welch, W.; Ruest, L. *Pharmacol. Rev.* **1997,** *49,* 53–98. doi:10.1016/s0031-6997(24)01313-9
29. Zeng, J.; Xue, Y.; Shu, P.; Qian, H.; Sa, R.; Xiang, M.; Li, X.-N.; Luo, Z.; Yao, G.; Zhang, Y. *J. Nat. Prod.* **2014,** *77,* 1948–1954. doi:10.1021/np500465g
30. Bélanger, A.; Berney, D. J. F.; Borschberg, H.-J.; Brousseau, R.; Doutheau, A.; Durand, R.; Katayama, H.; Lapalme, R.; Leturc, D. M.; Liao, C.-C.; MacLachlan, F. N.; Maffrand, J.-P.; Marazza, F.; Martino, R.; Moreau, C.; Saint-Laurent, L.; Saintonge, R.; Soucy, P.; Ruest, L.; Deslongchamps, P. *Can. J. Chem.* **1979,** *57,* 3348–3354. doi:10.1139/v79-547
31. Diels, O.; Alder, K. *Justus Liebigs Ann. Chem.* **1928,** *460,* 98–122. doi:10.1002/jlac.19284600106
32. Jiang, X.; Wang, R. *Chem. Rev.* **2013,** *113,* 5515–5546. doi:10.1021/cr300436a
33. Foster, R. A. A.; Willis, M. C. *Chem. Soc. Rev.* **2013,** *42,* 63–76. doi:10.1039/c2cs35316d
34. Xie, M.; Lin, L.; Feng, X. *Chem. Rec.* **2017,** *17,* 1184–1202. doi:10.1002/tcr.201700006
35. Oliveira, B. L.; Guo, Z.; Bernardes, G. J. L. *Chem. Soc. Rev.* **2017,** *46,* 4895–4950. doi:10.1039/c7cs00184c
36. Yu, M.; Danishefsky, S. J. *J. Am. Chem. Soc.* **2008,** *130,* 2783–2785. doi:10.1021/ja7113757
37. Nicolaou, K. C.; Becker, J.; Lim, Y. H.; Lemire, A.; Neubauer, T.; Montero, A. *J. Am. Chem. Soc.* **2009,** *131,* 14812–14826. doi:10.1021/ja9073694
38. Peng, F.; Danishefsky, S. J. *J. Am. Chem. Soc.* **2012,** *134,* 18860–18867. doi:10.1021/ja309905j
39. Yin, J.; Wang, C.; Kong, L.; Cai, S.; Gao, S. *Angew. Chem., Int. Ed.* **2012,** *51,* 7786–7789. doi:10.1002/anie.201202455
40. Yuan, C.; Du, B.; Deng, H.; Man, Y.; Liu, B. *Angew. Chem., Int. Ed.* **2017,** *56,* 637–640. doi:10.1002/anie.201610484
41. Huang, J.; Gu, Y.; Guo, K.; Zhu, L.; Lan, Y.; Gong, J.; Yang, Z. *Angew. Chem., Int. Ed.* **2017,** *56,* 7890–7894. doi:10.1002/anie.201702768
42. Liu, D.-D.; Sun, T.-W.; Wang, K.-Y.; Lu, Y.; Zhang, S.-L.; Li, Y.-H.; Jiang, Y.-L.; Chen, J.-H.; Yang, Z. *J. Am. Chem. Soc.* **2017,** *139,* 5732–5735. doi:10.1021/jacs.7b02561
43. Sara, A. A.; Um-e-Farwa; Saeed, A.; Kalesse, M. *Synthesis* **2022,** *54,* 975–998. doi:10.1055/a-1532-4763
44. Rana, A.; Mishra, A.; Awasthi, S. K. *RSC Adv.* **2025,** *15,* 4496–4525. doi:10.1039/d4ra07989b

45. Ruest, L.; Deslongchamps, P. *Can. J. Chem.* **1993,** *71,* 634–638. doi:10.1139/v93-084
46. Nagatomo, M.; Koshimizu, M.; Masuda, K.; Tabuchi, T.; Urabe, D.; Inoue, M. *J. Am. Chem. Soc.* **2014,** *136,* 5916–5919. doi:10.1021/ja502770n
47. Masuda, K.; Nagatomo, M.; Inoue, M. *Chem. Pharm. Bull.* **2016,** *64,* 874–879. doi:10.1248/cpb.c16-00214
48. Chuang, K. V.; Xu, C.; Reisman, S. E. *Science* **2016,** *353,* 912–915. doi:10.1126/science.aag1028
49. Xu, C.; Han, A.; Virgil, S. C.; Reisman, S. E. *ACS Cent. Sci.* **2017,** *3,* 278–282. doi:10.1021/acscentsci.6b00361
50. Dibrell, S. E.; Maser, M. R.; Reisman, S. E. *J. Am. Chem. Soc.* **2020,** *142,* 6483–6487. doi:10.1021/jacs.9b13818
51. Dibrell, S. E.; Tao, Y.; Reisman, S. E. *Acc. Chem. Res.* **2021,** *54,* 1360–1373. doi:10.1021/acs.accounts.0c00858
52. Du, K.; Kier, M. J.; Stempel, Z. D.; Jeso, V.; Rheingold, A. L.; Micalizio, G. C. *J. Am. Chem. Soc.* **2020,** *142,* 12937–12941. doi:10.1021/jacs.0c05766
53. Chen, K.; Baran, P. S. *Nature* **2009,** *459,* 824–828. doi:10.1038/nature08043
54. Kanda, Y.; Nakamura, H.; Umemiya, S.; Puthukanoori, R. K.; Murthy Appala, V. R.; Gaddamanugu, G. K.; Paraselli, B. R.; Baran, P. S. *J. Am. Chem. Soc.* **2020,** *142,* 10526–10533. doi:10.1021/jacs.0c03592
55. Jørgensen, L.; McKerrall, S. J.; Kuttruff, C. A.; Ungeheuer, F.; Felding, J.; Baran, P. S. *Science* **2013,** *341,* 878–882. doi:10.1126/science.1241606
56. Qiao, J.-B.; Meng, L.; Pei, J.-Y.; Shao, H.; Zhao, Y.-M. *Angew. Chem., Int. Ed.* **2025,** *64,* e202417647. doi:10.1002/anie.202417647
57. Meng, L.; Pei, J.-Y.; Qiao, J.-B.; Zhao, Y.-M. *Org. Lett.* **2025,** *27,* 2521–2525. doi:10.1021/acs.orglett.5c00604

License and Terms

BEILSTEIN JOURNAL OF ORGANIC CHEMISTRY

Recent advances in total synthesis of illisimonin A

Juan Huang and Ming Yang*

Review

Open Access

Address:
State Key Laboratory of Natural Product Chemistry, College of Chemistry and Chemical Engineering, Lanzhou University, 222 South Tianshui Road, Lanzhou, Gansu Province 730000, China

Email:
Ming Yang* - yangming@lzu.edu.cn

* Corresponding author

Keywords:
bioinspired synthesis; biosynthetic pathway; *Illicium* sesquiterpene; illisimonin A; total synthesis

Beilstein J. Org. Chem. **2025,** *21,* 2571–2583.
https://doi.org/10.3762/bjoc.21.199

Received: 31 August 2025
Accepted: 05 November 2025
Published: 20 November 2025

This article is part of the thematic issue "Concept-driven strategies in target-oriented synthesis".

Associate Editor: D. Y.-K. Chen

Abstract

Illicium sesquiterpenes are a large class of highly oxygenated and sterically congested sesquiterpenoids isolated from the genus *Illicium*. Illisimonin A stands out as one of the most structurally intricate members of this family, featuring a novel bridged tricyclo[5.2.1.$0^{1,5}$]decane carbon framework designated as the “illisimonane” skeleton. This core ring system is further embellished by additional bridging via a γ-lactone and a γ-lactol ring, resulting in a caged pentacyclic scaffold with a 5/5/5/5/5 ring arrangement. The compound demonstrates neuroprotective activity by mitigating oxygen-glucose deprivation-induced cell injury in SH-SY5Y cells. Since its isolation in 2017, illisimonin A has garnered significant interest from the synthetic chemistry community. To date, five research groups have accomplished the total synthesis of illisimonin A. This review offers a comprehensive overview of its isolation, proposed biosynthetic pathway and the synthetic strategies employed in its total synthesis.

Introduction

The genus *Illicium*, the sole member of the family Illiciaceae, is a rich source of sesquiterpenoid natural products. To date, a wide variety of sesquiterpenes have been isolated from this genus, among which *Illicium* sesquiterpenes represent a prominent group. Since the first isolation of anisatin in 1952 [1], more than 100 *Illicium* sesquiterpenes have been isolated from over 40 species of *Illicium* [2]. Based on their carbon skeletons, they can be classified into the following types: *allo*-cedrane, anislactone, *seco*-prezizaane and illisimonane (Figure 1). The illismonane-type is the most recent identified. The *seco*-prezizaane-type can be further divided into six subtypes according to their lactone patterns, namely anisatin-subtype, pseudoanisatin-subtype, pseudomajucin-subtype, cycloparvifloralone-subtype, majucin-subtype, and miwanensin-subtype (Figure 1). The seminal work by the Fukuyama group demonstrated that some of these natural products exhibit potent neurite outgrowth-promoting activity in primary cultured rat cortical neurons, which has attracted considerable interest from synthetic chemists. Although the intricate structures of this family have posed significant challenges to chemical synthesis, more than 30 total syntheses of *Illicium* sesquiterpenes have been reported until now [3-25].

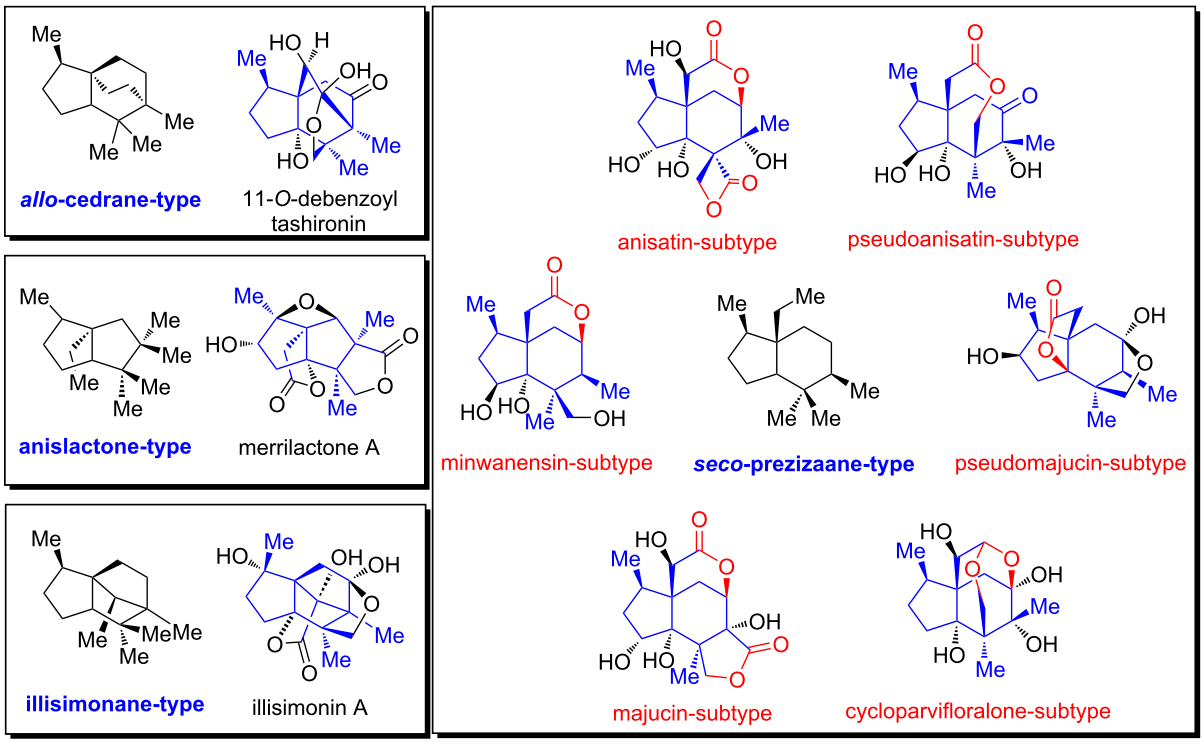

Figure 1: The categorization of *Illicium* sesquiterpenes and representative natural products.

In 2017, Yu and co-workers isolated a new *Illicium* sesquiterpene, namely illisimonin A, from the fruits of *Illicium simonsii* [26]. Unlike other *Illicium* sesquiterpenes, illisimonin A features an unprecedented bridged tricyclo[5.2.1.$0^{1,5}$]decane carbon framework that incorporates a highly strained *trans*-pentalene subunit. This carbon ring system is further bridged with a γ-lactone and a γ-lactol ring, forming a caged pentacyclic scaffold with a 5/5/5/5/5 ring arrangement. Illisimonin A was thus classified as an illisimonane-type *Illicium* sesquiterpene, and its carbon skeleton was designated as "illisimonane skeleton". The absolute configuration of (−)-illisimonin A was determined to be 1*R*,4*R*,5*R*,6*R*,7*S*,9*S*,10*S* by comparing the calculated electronic circular dichroism (EDC) spectrum with experimental CD data (Figure 2). Biological evaluation revealed that illisimonin A exhibits neuroprotective effects against oxygen-glucose deprivation-induced cell injury in SH-SY5Y cells, suggesting its potential as a lead compound for the treatment of neurodegenerative diseases.

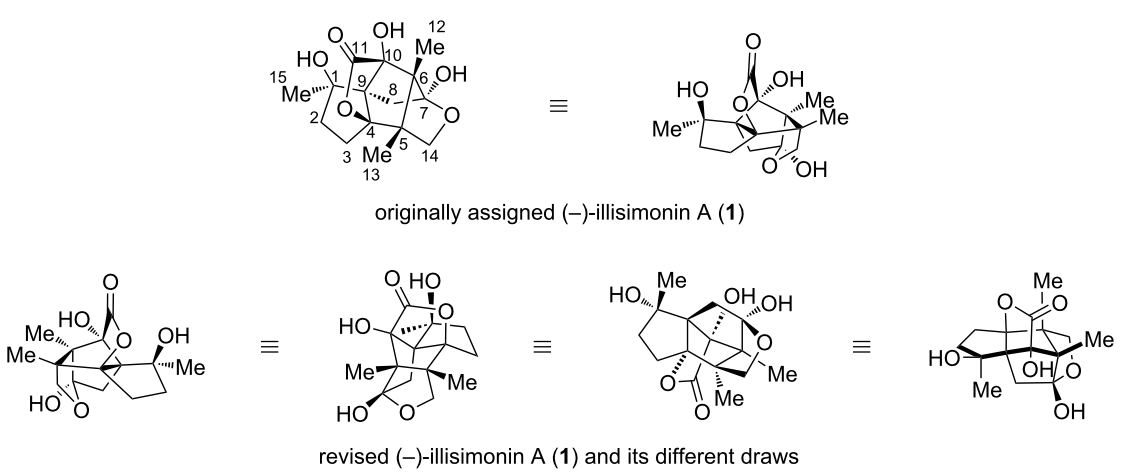

Figure 2: The original assigned (–)-illisimonin A, revised (–)-illisimonin A, and their different draws.

The possible biosynthetic pathway of illisimonin A was also proposed by Yu and co-workers, as illustrated in Scheme 1. The proposed biosynthetic pathway clarifies the relationship between illisimonin A and other *Illicium* sesquiterpenes. *Allo*-cedrane-type, *seco*-prezizaane-type and illismonane-type *Illicium* sesquiterpenes are all biosynthesized from farnesyl diphosphate (**2**) through a series of cationic cyclizations and migrations. The 5/6/6 tricarbocyclic *allo*-cedrane framework **6** serves as the key biogenetic intermediate for both the *seco*-prezizaane and illismonane skeletons. The conversion of the *allo*-cedrane skeleton to the illismonane skeleton was hypothesized to proceed via a 1,2-alkyl migration of intermediate **9** to **10**. However, subsequent density functional theory (DFT) calculations by the Tantillo group on rearrangements of potential biosynthetic precursors revealed that structure **10** corresponds to a transition state rather than a stable intermediate of the 1,2-alkyl migration [27]. Their study further indicated that only certain precursors with certain specific oxidation patterns are competent to undergo this rearrangement.

The same as other *Illicium* sesquiterpenes, the highly oxgenated and strained skeleton of illisimonin A has posed a significant challenge to synthetic chemists. To date, the research groups of Rychnovsky [28], Kalesse [29], Yang [30], Dai [31] and Lu [32] have achieved the total synthesis of this molecule. Notable, Rychnovsky and co-workers revised the absolute configuration of (−)-illisimonin A to 1*S*,4*S*,5*S*,6*S*,7*R*,9*R*,10*R*. This review summarizes the reported synthetic routes toward illisimonin A, including uncompleted approaches.

Review

Rychnovsky's synthesis and the absolute configuration revision of (–)-illisimonin A

In 2019, Rychnovsky's group reported the first total synthesis of illisimonin A [28]. Recognizing that the strained *trans*-pentalene moiety in the molecule is challenging to construct directly, the team adopted a strategy involving rearrangement from the more accessible *cis*-pentalene isomer. They first assembled the

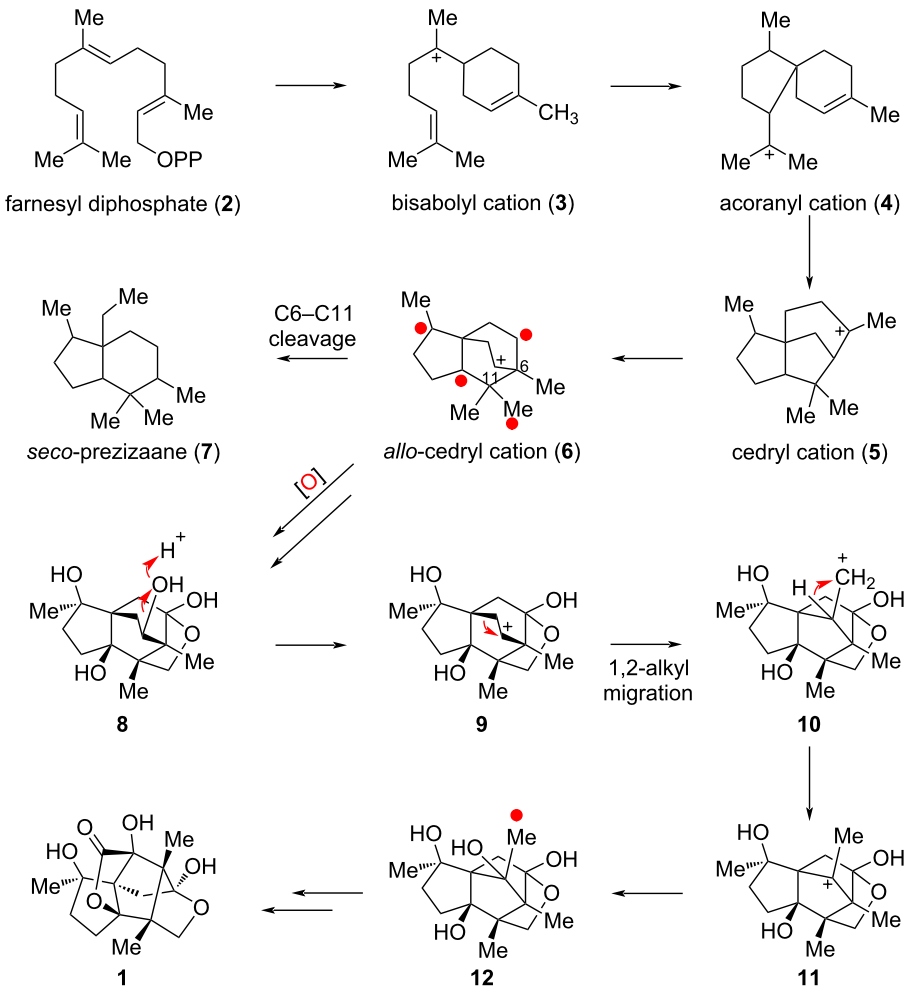

Scheme 1: Proposed biosynthetic pathway of illisimonin A by Yu et al.

cis-pentalene core through an elegant intramolecular Diels–Alder (IMDA) reaction. Subsequently, the conversion from *cis* to *trans*-pentalene was achieved via a semipinacol rearrangement. Finally, a White–Chen C–H oxidation [33-35] was employed to install the lactone ring, thereby completing the synthesis.

The synthesis began with commercially available compound **19** and known compound **20** (Scheme 2). These were joined via an intermolecular aldol reaction to give adduct **21**, obtained as a 1.7:1 mixture of diastereomers after protection of one of the carbonyl groups in **19** as enol ether with BOMCl. A silyl-tethered intramolecular Diels–Alder reaction of the in situ generated **22** constructed the tricyclo[5.2.1.0^{1,5}]decane core bearing a *cis*-pentalene unit, yielding compound **23**, which was subsequently subjected to a one-pot desilylation to afford **24**. Reduction of both the ester and ketone functionalities in **24**, followed by selective protection of the primary alcohol and re-oxidation of the secondary alcohol to ketone, furnished compound **25** in three steps. The ketone in **25** was then converted to vinyl iodide **26** via hydrazine formation followed by iodination using Barton's method. Subsequent Bouvealt aldehyde synthesis and

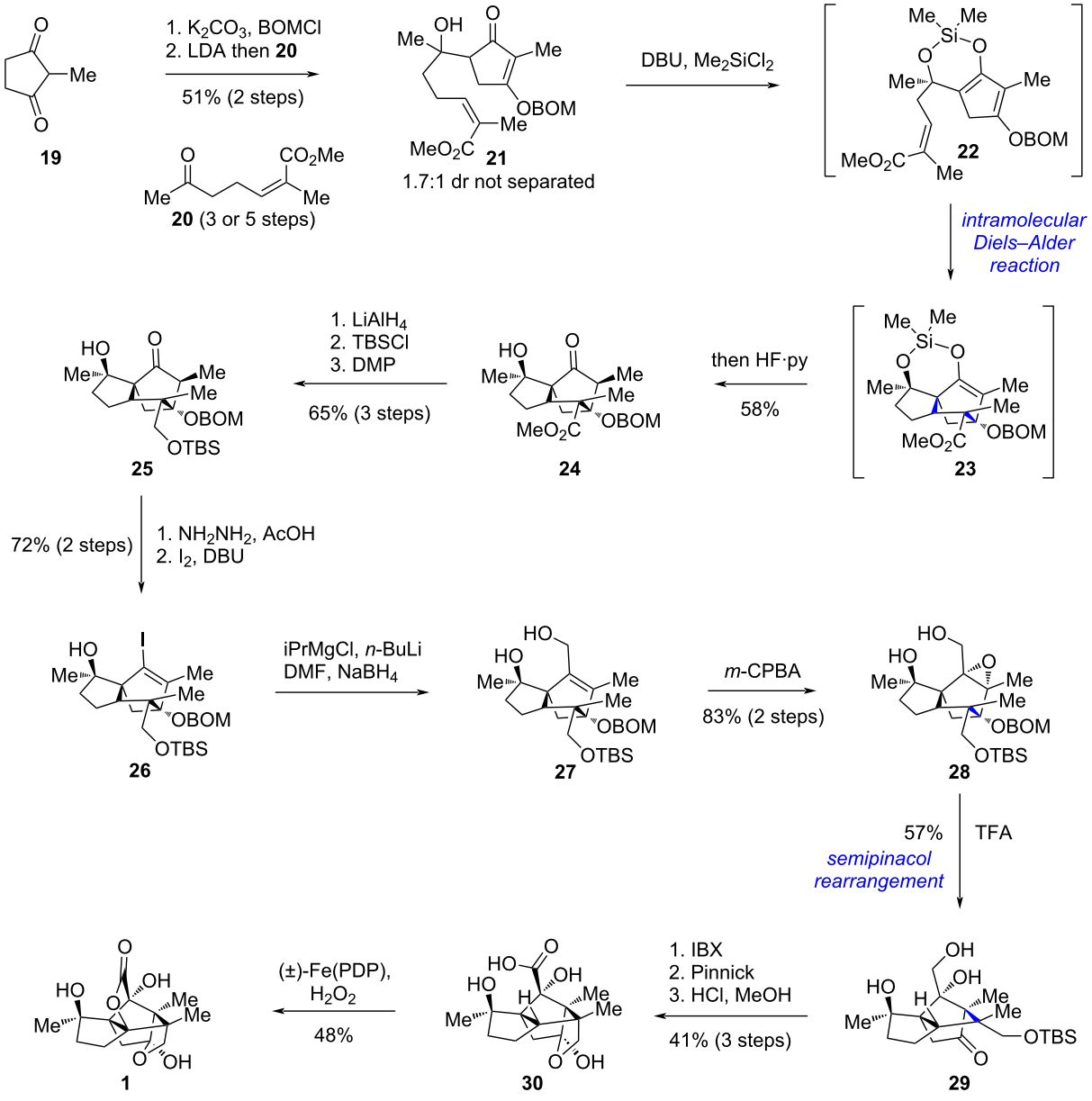

Scheme 2: Rychnovsky's racemic synthesis of illisimonin A (**1**).

in situ reduction delivered allylic alcohol **27**. Epoxidation of **27** with *m*-CPBA afforded the rearrangement precursor **28**. Protonic acid-promoted semipinacol rearrangement of **28** enabled the rearrangement of *cis*-pentalene to *trans*-pentalene, delivering intermediate **29**, which possesses the same carbon skeleton as the natural product. Further oxidation of the primary alcohol to a carboxylic acid, accompanied by TBS deprotection, afforded hemiketal **30**. Finally, a White−Chen C–H oxidation [33-35] of **30** installed the lactone, completing the synthesis of racemic illisimonin A (**1**).

Noting that the C1 configuration of illisimonin A was opposite to that of other *Illicium* sesquiterpenes, Rychnovsky's group sought to confirm the absolute configuration of the natural product. They resolved racemic intermediate **27** by derivatization with (*S*)-1-(1-naphthyl)ethyl isocyanate, followed by separation of the resulting diastereomers via silica gel chromatography (Scheme 3). By converting diastereomer **32** to (−)-illisimonin A, the absolute configuration of the natural product was conclusively revised to 1*S*,4*S*,5*S*,6*S*,7*R*,9*R*,10*R*.

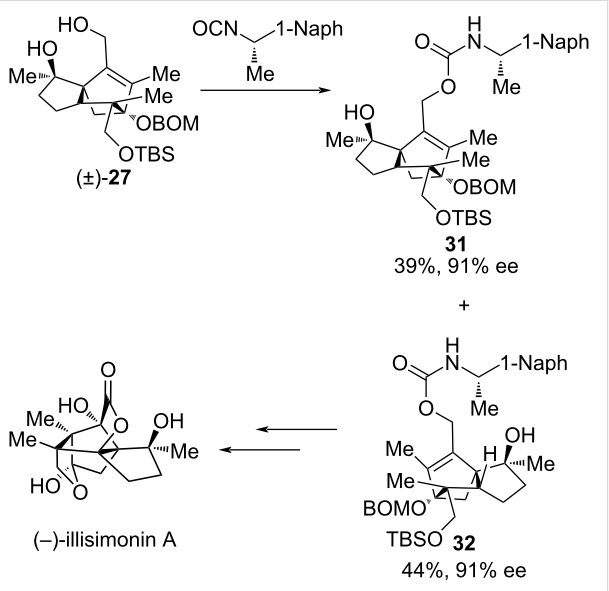

Scheme 3: The absolute configuration revision of (–)-illisimonin A.

Kalesse's asymmetric synthesis of illisimonin A

In 2023, Kalesse and co-workers reported an asymmetric synthetic route to illisimonin A [29]. The Kalesse group also noticed the strained *trans*-pentalene in illisimonin A. Since there is a spiro substructure hidden inside the natural product's cage-like ring system, Kalesse's group chose to construct this architecture first using a tandem Nazarov/ene cyclization [36]. The *cis*-pentalene was subsequently assembled via a Ti(III)-mediated epoxide–ketone coupling reaction.

Starting from the known enantioenriched compound **33**, a nickel-catalyzed hydrocyanation of the terminal alkyne was performed. Subsequent protection of the tertiary alcohol with TESOTf and reduction of the resulting cyanide to an aldehyde afforded compound **34** (Scheme 4). Addition of isopropenyllithium to aldehyde **34**, followed by TES deprotection and oxidation of the secondary alcohol, yielded the cyclization precursor **35**. A $B(C_6F_5)_3$-catalyzed tandem Nazarov/ene cyclization of **35** provided the key spirocyclic intermediate **37**. The tertiary alcohol was protected in situ with TESOTf to suppress retro-aldol side reactions. Notably, prior TES deprotection of the cyclization precursor was essential, as the TES-protected analogue of **35** failed to deliver the desired spirocycle **38** under the Nazarov cyclization conditions. α-Oxidation of **38** with molecular oxygen afforded **39**, which was then converted to **40** via formation of a chloromethyl silyl ether, deprotonation, and intramolecular addition to ketone. Treatment of the silacycle with MeMgCl cleaved the Si–O bond and subsequent intramolecular nucleophilic substitution of the chloride with the adjacent hydroxy group yielded TMS-epoxide **41**. Protonic acid-mediated opening of the TMS-epoxide, accompanied by TES deprotection, afforded enal **42**. To avoid the chemoselectivity issues in the subsequent allylic oxidation and radical cyclization steps, enal **42** was converted to **43** by reduction of the aldehyde and protection of the resultant diol with Ph_2SiCl_2. Allylic oxidation of **43** with **44** [37] afforded the enone in 22% yield (63% brsm) or 50% yield after four cycles with recovery of starting material. Selective epoxidation of the isopropenyl group with *m*-CPBA delivered cyclization precursor **45** as an inseparable mixture of diastereomers (dr = 1:2.1). A Cp_2TiCl-mediated cyclization of **45** constructed the tricyclo[5.2.1.$0^{1,5}$]decane core with a *cis*-pentalene unit. The product was further processed into rearrangement precursor **46** (as an inseparable mixture, dr = 1:1.6) by TBS protection of the primary alcohol and epoxidation of the alkene with *m*-CPBA. Unlike Rychnovsky's substrate, epoxy alcohol **46** underwent rearrangement only under Lewis acidic conditions to furnish **47**. Selective TES deprotection with HF afforded Rychnovsky's intermediate **29**. (−)-Illisimonin A was obtained in 13% yield over the same 4-step sequence as reported by Rychnovsky's group. An alternative 4-step endgame starting from **47** was also developed, albeit with a lower overall yield of 3%.

Yang's bioinspired synthesis of illisimonin A

In 2023, Yang and co-workers reported a bioinspired divergent synthesis of illisimonin A and merrilactone A, which belonged to illisimonane-type and anislactone-type *Illicium* sesquiterpenes, respectively [30]. They proposed that a deeper understanding of the biosynthetic pathway of *Illicium* sesquiterpenes could facilitate a divergent total synthesis of this family of natural products, even among members with distinct carbon

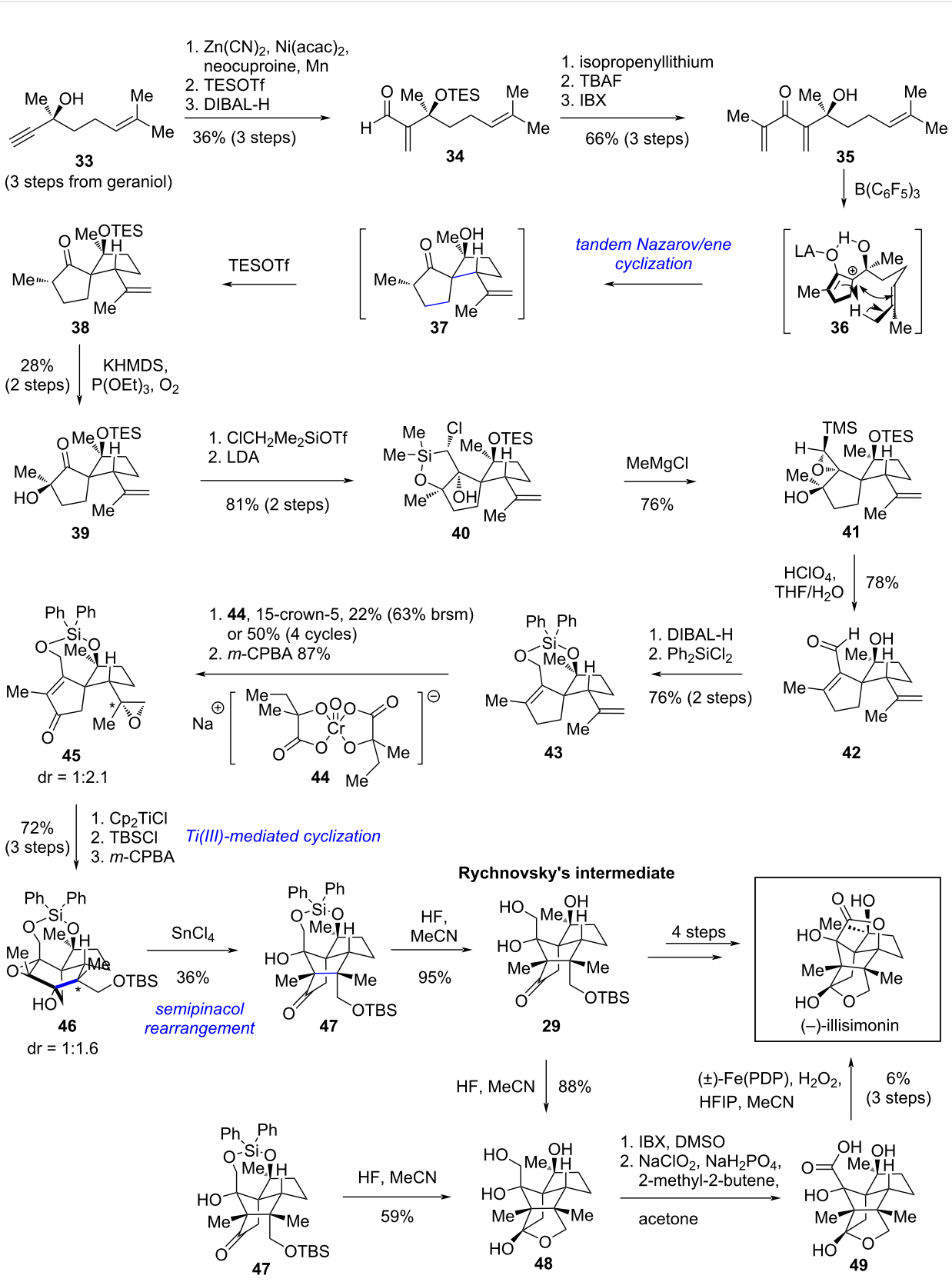

Scheme 4: Kalesse's asymmetric synthesis of (–)-illisimonin A.

skeletons. Since previously proposed biosynthetic pathways lacked key mechanistic details – particularly the critical reactions responsible for skeletal diversity – Yang and co-workers first introduced a comprehensive and detailed biosynthetic pathway for *Illicium* sesquiterpenes, with the route to illisimonin A depicted in Scheme 5. The transformations from farnesyl diphosphate to the *allo*-cedryl cation were consistent with earlier reports [2,26], though the configurations of the intermediates were clearly delineated. The authors proposed that dicarbonyl compound **50** serves as the key intermediate diverging to all *Illicium* sesquiterpenes, with a retro-Dieckmann condensation and aldol reaction identified as the key steps enabling the transformation from the *allo*-cedrane skeleton to the illisimonane framework.

Inspired by the proposed biosynthetic pathway, Yang et al. designed a synthetic route as shown in Scheme 6. Starting from the known compound **53**, a Tsuji–Trost allylation was employed to introduce another side chain, affording a diene intermediate. A subsequent ring-closing metathesis (RCM) reaction formed the cyclopentene ring, and one pot protection of both carbonyl groups with ethylene glycol provided bis-ketal **55**. Notably, due to steric hindrance, only one carbonyl group could be protected prior to the RCM step. Oxidative cleavage of the cyclopentene followed by Pinnick oxidation of the resulting aldehyde to the carboxylic acid and esterification yielded ketoester **56**. Dieckmann condensation of **56**, esterification of the resulting enolate with **57**, and subsequent one-pot partial deketalization afforded carbonate **58**. A palladium-catalyzed decarboxylative alkenylation reaction was then carried out across the less hindered face of the six-membered ring to connect C5 and C6. Selective deprotonation and triflation at the C4 carbonyl group provided enol triflate **59**. An intramolecular reductive Heck reaction of **59** enabled the transannular connection between C4 and C5, generating key intermediate **60**, which possesses the same carbon skeleton as the proposed biosynthetic key intermediate **50** and contains the suitable functional groups for further elaboration. Mukaiyama hydration of **60** introduced a tertiary alcohol at the C4 position, yielding retro-Dieckmann precursor **61**. Subsequent retro-Dieckmann condensation under basic conditions, deprotection of the PMP group, and selective ketalization of the C11 carbonyl group afforded compound **62**. The C1 methyl group was installed via enol triflate formation followed by a palladium-catalyzed coupling reaction with $AlMe_3$. The carbonyl group at C8, required for the subsequent aldol reaction, was introduced by enolate oxidation

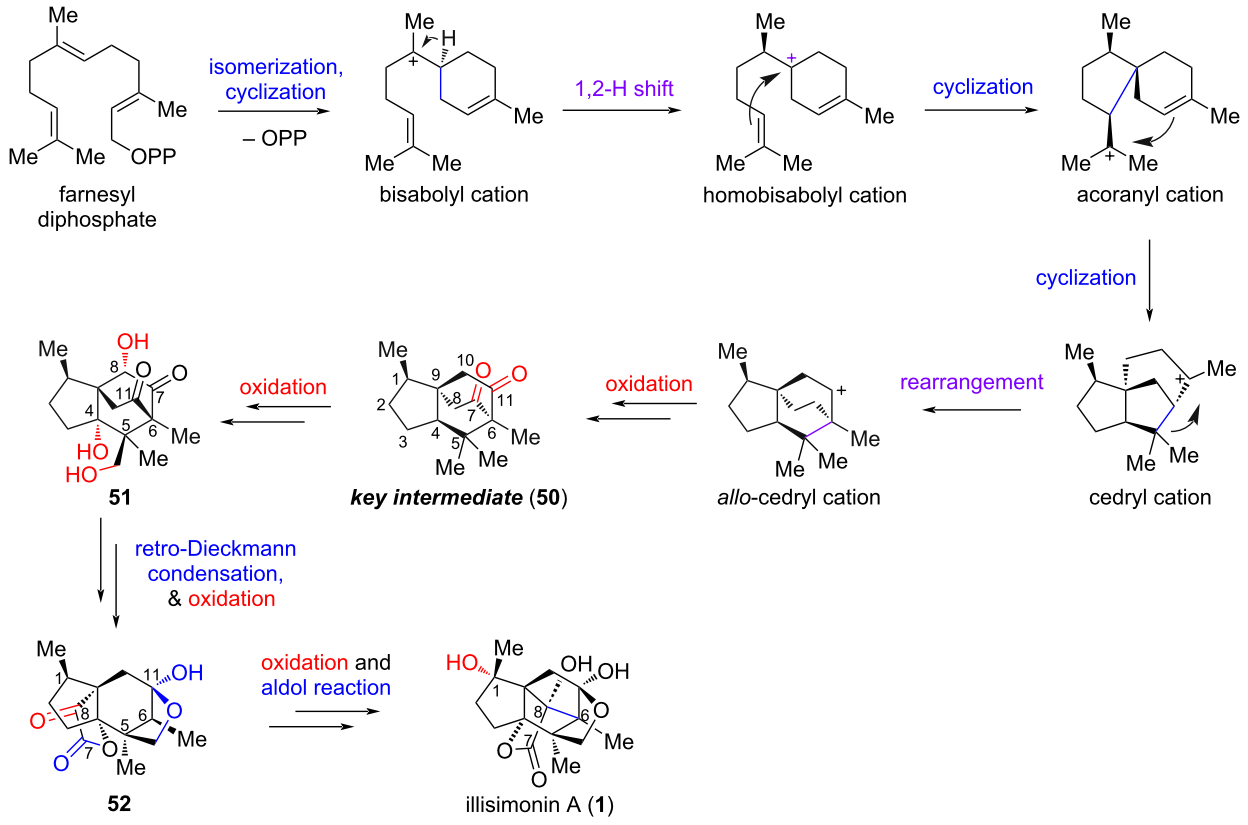

Scheme 5: Yang group proposed biosynthetic pathway of illisimonin A.

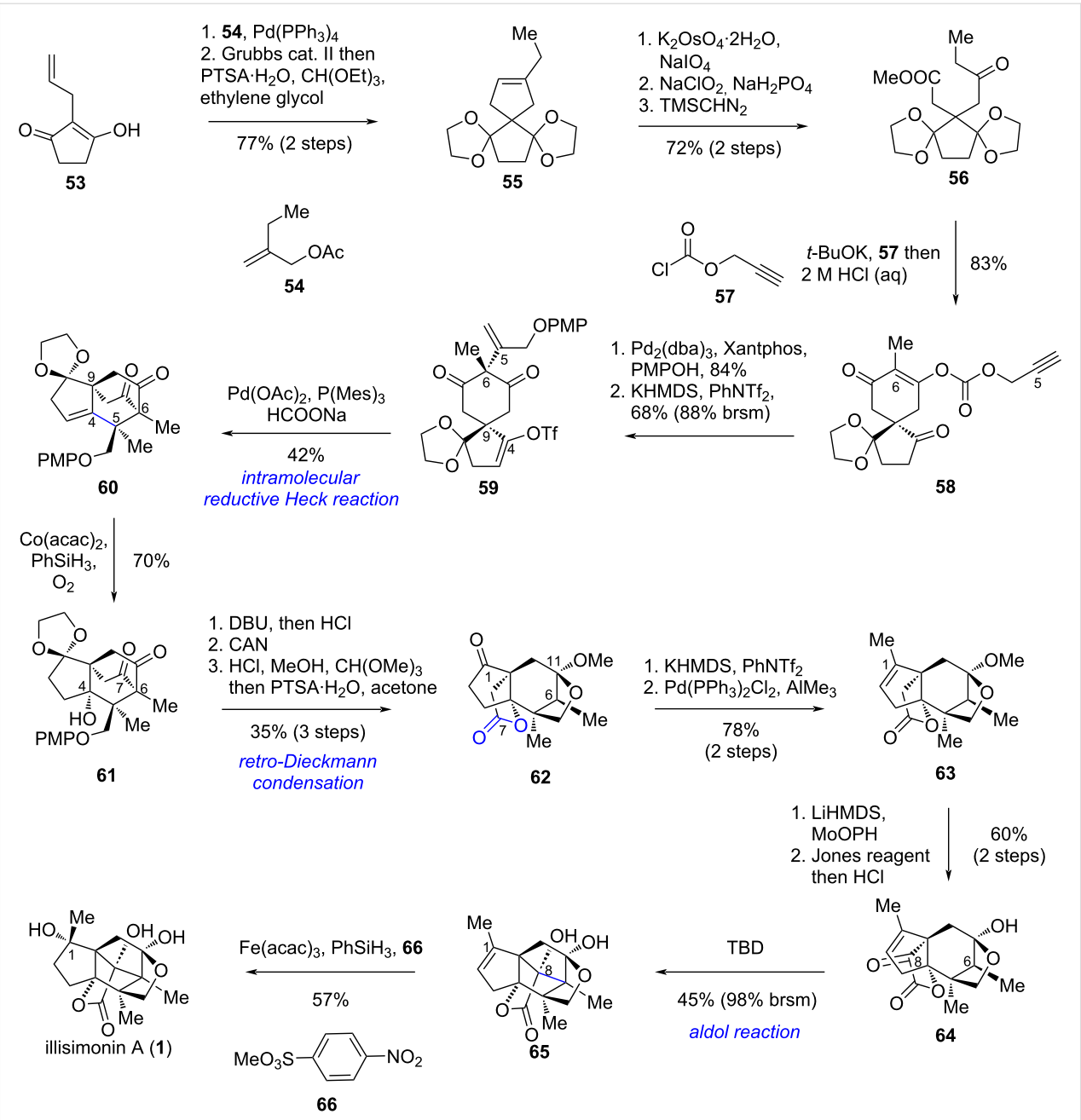

Scheme 6: Yang's bioinspired synthesis of illisimonin A.

followed by Jones oxidation. Hydrolysis of the ketal at C11 afforded ketoester **64**. A TBD (1,5,7-triazabicyclo[4.4.0]dec-5-ene)-catalyzed intramolecular aldol reaction connected C6 and C8, assembling the *trans*-pentalene ring and affording the core carbon framework of illisimonin A. The C1 hydroxy group was initially introduced by a Mukaiyama hydration reaction using O_2 as the stoichiometric oxidant; however, illisimonin A was obtained only as a minor product. When O_2 was replaced with the nitroaromatic compound **66** [38], the diastereoselectivity was reversed, thereby providing illisimonin A in 57% yield as a single diastereomer. The authors proposed that a hydrogen bond between the nitro group of **66** and the C8 hydroxy group could be responsible for this reversal in selectivity.

Dai's asymmetric synthesis of (−)-illisimonin A

In 2025, Dai and co-workers accomplished an asymmetric total synthesis of (−)-illisimonin A in 16 steps from (*S*)-carvone (**67**) using a pattern-recognition strategy and five sequential olefin transpositions [31].

Starting from (*S*)-carvone (**67**), reaction with allyl bromide introduced an allyl group to give **68**, which was then converted to the bicyclic compound **69** via a ring-closing metathesis (RCM) reaction followed by one-pot epimerization at the α-position of the carbonyl group (Scheme 7). Chemoselective epoxidation of the enone double bond in **69** yielded epoxide **70**. A Wittig reaction of **70** with (methoxymethyl)triphenylphosphonium chloride and *t*-BuOK generated a methyl enol ether, which

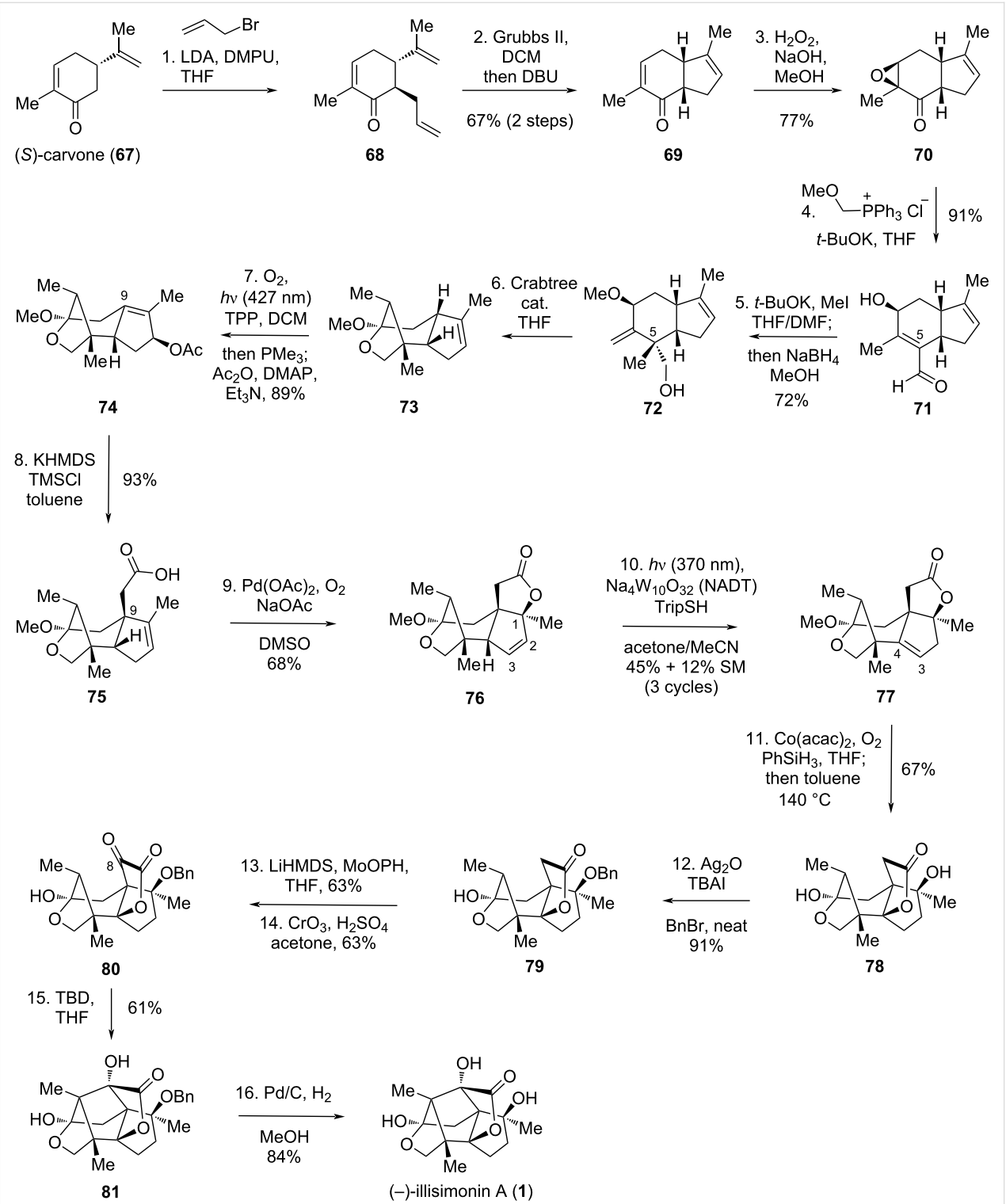

Scheme 7: Dai's asymmetric synthesis of (–)-illisimonin A.

was unstable in the presence of the epoxide. During aqueous workup, simultaneous hydrolysis of the enol ether and epoxide ring-opening afforded **71**. To install the all-carbon quaternary center at C5, compound **71** was treated with *t*-BuOK and MeI, enabling the deprotonation of the α,β-unsaturated aldehyde and methylation at C5; this step also facilitated protection of the secondary alcohol. The aldehyde was reduced in the same pot to give **72**. Isomerization of the allylic methyl ether to an enol methyl ether was achieved using Crabtree's catalyst in refluxing THF. Subsequent ketalization with the primary alcohol yielded the bridged ketal **73**. A Schenck ene reaction on **73** induced the second olefin isomerization, generating an allylic alcohol that was acetylated in situ to provide **74**. An Ireland–Claisen rearrangement facilitated the third olefin transposition, concurrently forming an all-carbon quaternary center at C9 and affording carboxylic acid **75**. The fourth olefin transposition was achieved via a palladium-catalyzed oxidative lactonization, yielding **76** with a newly established quaternary center at C1 and isomerization of the double bond to C2=C3. Photocatalyzed isomerization of the C2–C3 double bond in **76** to C3=C4 furnished **77** [39,40]. A Mukaiyama hydration introduced a hydroxy group at C4, accompanied by *trans*-esterification to give lactone **78**. The resulting tertiary alcohol was protected as its benzyl ether to afford **79**. A two-step oxidation protocol, analogous to Yang's method, introduced the C8 carbonyl group, yielding **80**. The final ring was closed via an intramolecular aldol reaction following Yang's conditions [30], assembling the *trans*-pentalene to give **81**. Finally, deprotection of the benzyl ether delivered (−)-illisimonin A (**1**).

Lu's gram-scale synthesis of illisimonin A

In 2025, the Lu group reported a gram-scale total synthesis of illisimonin A in 15 steps from commercially available starting materials [32]. This synthesis features a pentafulvene-based intramolecular [6 + 2] cycloaddition [41,42] and a nitroso-Diels–Alder reaction [43] as key steps.

The route began with the esterification of pentafulvenol **82** to give β-ketoester **83**, which was subsequently converted to the sterically encumbered tricyclic lactone **84** via an intramolecular [6 + 2] cycloaddition (Scheme 8). Attempts to achieve an asymmetric version of the cycloaddition were unsuccessful. Treatment of the lactone with MeMgBr, followed by mesylation and elimination of the resulting hemiacetal, afforded enol ether **85**.

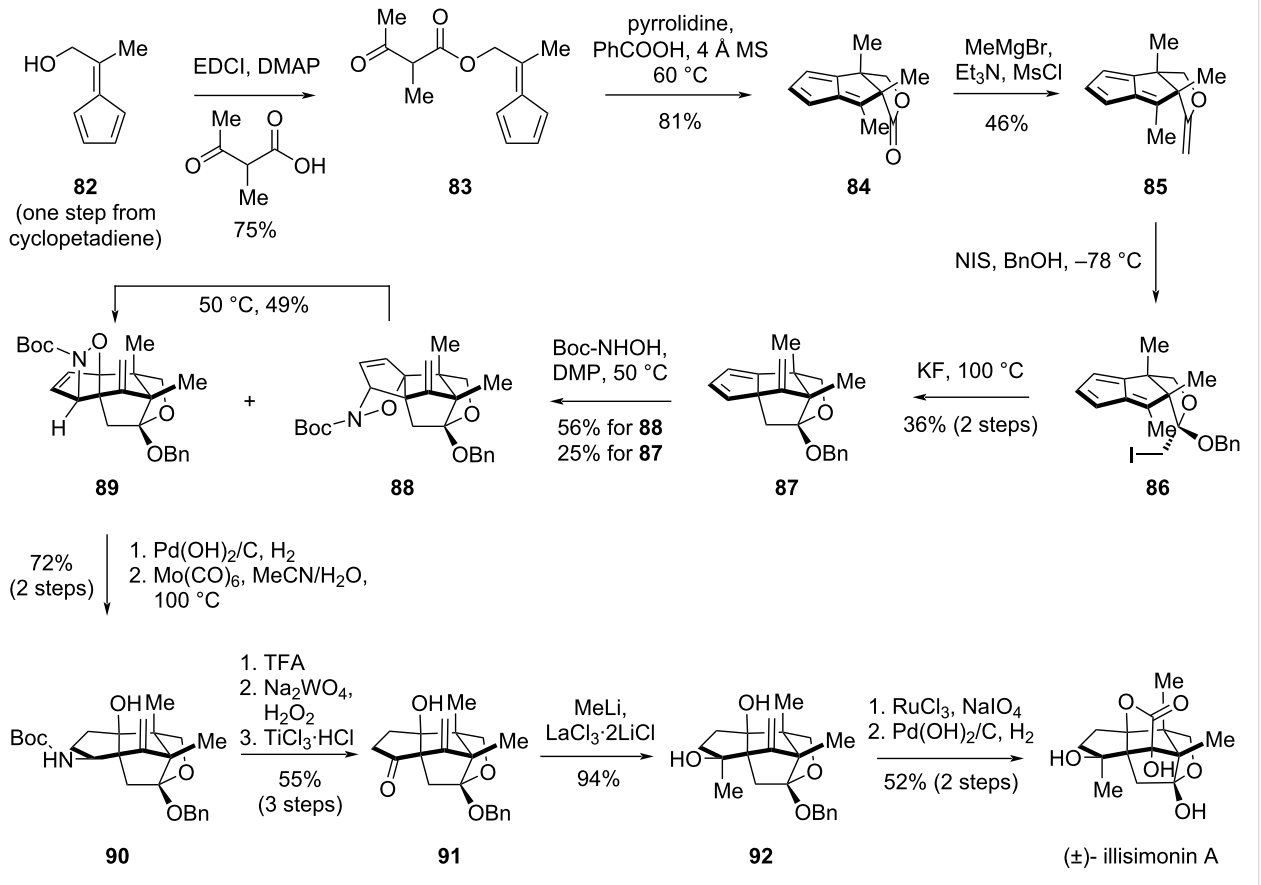

Scheme 8: Lu's total synthesis of illisimonin A.

Reaction of **85** with iodine and BnOH enabled the intermolecular iodoetherification to yield ketal **86**. A KF-promoted intramolecular alkylation of the cyclopentadiene moiety then delivered compound **87**. To introduce the C4 hydroxy group and C1 functional handle for further elaboration, a nitroso-Diels–Alder reaction of **87** was employed, generating both the kinetic product **88** and the desired thermodynamic product **89**. Heating **88** promoted a retro-Diels–Alder/Diels–Alder equilibrium, favoring the more stable isomer **89**. Palladium-catalyzed hydrogenation of the 1,2-disubstituted alkene in **89**, followed by $Mo(CO)_6$-mediated N–O bond cleavage afforded carbamate **90**. The carbamate was converted to a carbonyl group via Boc deprotection with TFA, oxidation of the resulting amine to the oxime with Na_2WO_4 and H_2O_2, and subsequent reduction with $TiCl_3$·HCl to give **91**. The $LaCl_3$·2LiCl-mediated methyl addition to the carbonyl group installed the tertiary alcohol at C1, yielding intermediate **92**. The α-hydroxy lactone was constructed through RuO_4-mediated oxidation, forming the pentacyclic core. Finally, debenzylation of the resulting pentacyclic compound under palladium-catalyzed hydrogenation provided (±)-illisimonin A. Notably, the authors were able to obtain 1.8 g of the natural product in a single run.

The successful total synthesis of illisimonin A by the Lu group was preceded by instructive setbacks, primarily in constructing the *trans*-fused 5/5 ring system. As depicted in Scheme 9, compound **85** was first transformed into the pentacyclic diene intermediate **93** via a two-step sequence. Subsequent [4 + 2] cycloaddition of **93** with singlet oxygen yielded an unstable endoperoxide adduct **94**, which rearranged to diketone **95**. A five-step sequence, featuring an intramolecular aldol reaction to assemble the pentacyclic core and the installation of the C1 methyl group, then afforded compound **96**. However, subjecting **96** to the singlet oxygen cycloaddition again led to rearrangement, producing diketones **98** and **99**. The solution was found by employing a nitroso-Diels–Alder reaction with dienophile **87**, which provided a stable adduct and ultimately enabled the completion of the synthesis. This strategic pivot offers a key lesson for handling fragile cycloaddition adducts.

Suzuki's synthetic effort towards illisimonin A

A synthetic study aimed at constructing the tricyclo[5.2.1.$0^{1,5}$]decane core of illisimonin A was reported by Suzuki and co-workers in 2021 [44]. Their work proposed that this core structure could be generated from a highly oxidized *allo*-cedrane moiety through a tandem retro-Claisen/aldol reaction.

Beginning with compound **100**, a 6-step sequence afforded *ortho*-quinone **101** (Scheme 10). Heating **101** promoted an intramolecular Diels–Alder reaction, affording **102** and **103** in 91% yield with a 1:6 ratio. The major product **103** was selected to investigate the tandem retro-Claisen/aldol reaction. Hydrolysis of the enol methyl ether in **103** under acidic conditions delivered triketone **104**. Subsequent treatment of **104** with aqueous NaOH facilitated a retro-Claisen reaction, yielding the intermediate **106**, which subsequently underwent an intramolecular aldol reaction to form the five-membered ring. The resulting carboxylic acid was then esterified with $TMSCHN_2$ to furnish ester **107**, which possesses the characteristic tricyclo[5.2.1.$0^{1,5}$]decane core of illisimonin A.

Conclusion

Over the past seventy years, ongoing chemical investigations of the *Illicium* species have led to the discovery of a great number of *Illicium* sesquiterpenes. The sterically congested and highly oxygenated skeleton of *allo*-cedrane-type, anislactone-type, and *seco*-prezizaane-type *Illicium* sesquiterpenes have attracted

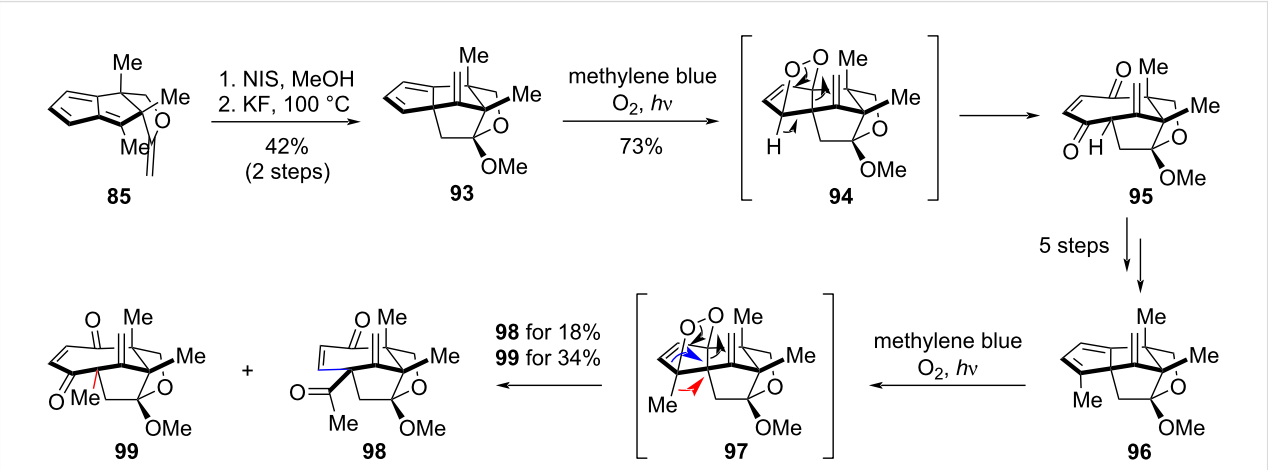

Scheme 9: Initial efforts toward the total synthesis of illisimonin A by the Lu Group.

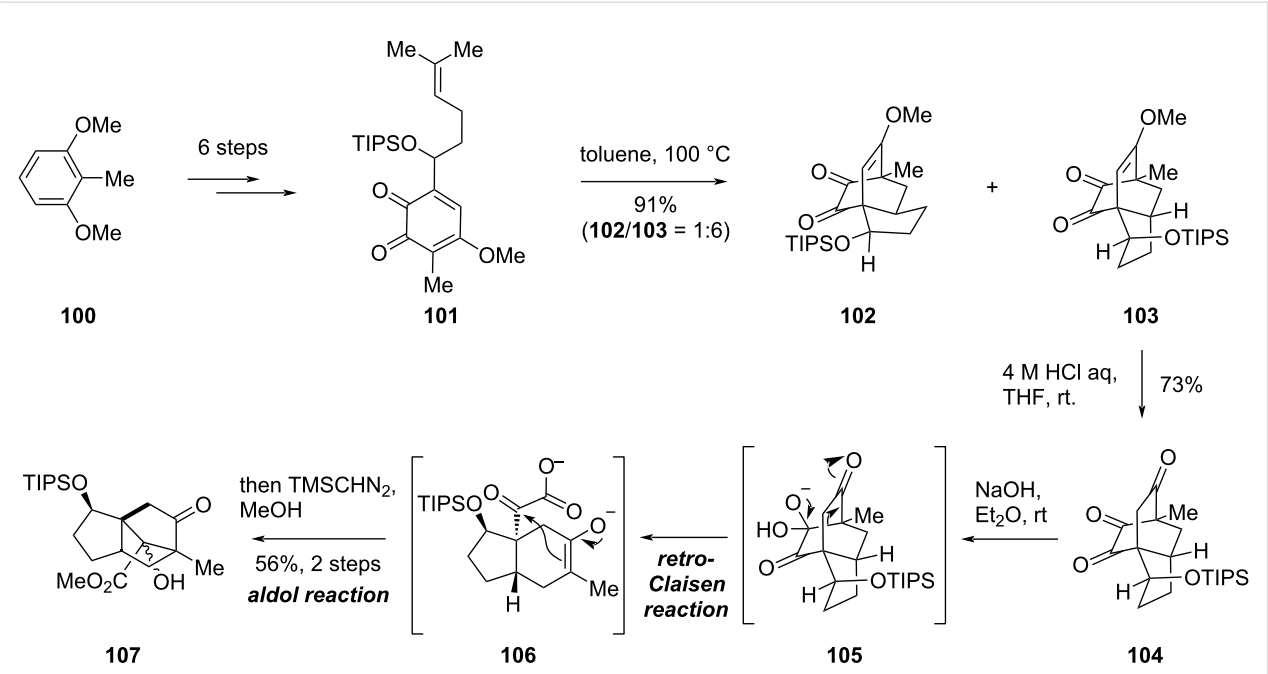

Scheme 10: Suzuki's synthetic effort towards illisimonin A.

significant interest from synthetic chemists, resulting in numerous elegant total syntheses of molecules within this family. The recent identification of illisimonin A has further expanded the structural diversity of *Illicium* sesquiterpenes. Its tricyclo[5.2.1.$0^{1,5}$]decane core, which contains a strained *trans*-pentalene subunit, presents new synthetic challenges. A breakthrough in the total synthesis of illisimonin A was achieved by Rychnovsky and co-workers through a rearrangement strategy that also led to the correction of its absolute configuration. Kalesse and co-workers accomplished the first asymmetric total synthesis of (−)-illisimonin A based on strategies involving spiro substructure assembly and rearrangement. Consideration of the biosynthetic pathway of illisimonin A inspired Yang and co-workers to develop a bioinspired synthetic route. Employing a pattern-recognition strategy, Dai and co-workers achieved the second asymmetric total synthesis of (−)-illisimonin A in 16 steps. Lu and co-workers realized the shortest and gram-scale total synthesis of racemic illisimonin A in 15 steps by leveraging a higher-order cycloaddition. Although various synthetic strategies have been developed, only two of them are asymmetric. Designing a more efficient and asymmetric synthetic route remains a worthwhile pursuit.

Funding

Financial Support was provided by the Department of Science and Technology of Gansu Province (22ZD6FA006, 23ZDFA015, 24ZD13FA017 and 24ZDFA003), the National Natural Science Foundation of China (22322105 and 22571126), the Fundamental Research Funds for the Central Universities (lzujbky-2023-ey01), and the Wen Kui Foundation.

ORCID® iDs

Ming Yang - https://orcid.org/0000-0001-6107-6226

Data Availability Statement

Data sharing is not applicable as no new data was generated or analyzed in this study.

References

1. Lane, J. F.; Koch, W. T.; Leeds, N. S.; Gorin, G. *J. Am. Chem. Soc.* **1952,** *74,* 3211–3215. doi:10.1021/ja01133a002
2. Fukuyama, Y.; Huang, J. M. Chemistry and neurotrophic activity of seco-prezizaane- and anislactone-type sesquiterpenes from Illicium species. In *Studies in Natural Products Chemistry;* Atta-ur-Rahman, Ed.; Bioactive Natural Products (Part L), Vol. 32; Elsevier: Amsterdam, Netherlands, 2005; pp 395–427. doi:10.1016/s1572-5995(05)80061-4
3. Urabe, D.; Inoue, M. *Tetrahedron* **2009,** *65,* 6271–6289. doi:10.1016/j.tet.2009.06.010
4. Xu, J.; Lacoske, M. H.; Theodorakis, E. A. *Angew. Chem., Int. Ed.* **2014,** *53,* 956–987. doi:10.1002/anie.201302268
5. Li, L.; Shen, Y.; Zhang, Y. *Chin. J. Org. Chem.* **2016,** *36,* 439–446. doi:10.6023/cjoc201511054
6. Condakes, M. L.; Novaes, L. F. T.; Maimone, T. J. *J. Org. Chem.* **2018,** *83,* 14843–14852. doi:10.1021/acs.joc.8b02802
7. Hung, K.; Condakes, M. L.; Novaes, L. F. T.; Harwood, S. J.; Morikawa, T.; Yang, Z.; Maimone, T. J. *J. Am. Chem. Soc.* **2019,** *141,* 3083–3099. doi:10.1021/jacs.8b12247

8. Dooley, C. J., III; Rychnovsky, S. D. *Org. Lett.* **2022,** *24,* 3411–3415. doi:10.1021/acs.orglett.2c01207
9. Cook, S. P.; Polara, A.; Danishefsky, S. J. *J. Am. Chem. Soc.* **2006,** *128,* 16440–16441. doi:10.1021/ja0670254
10. Mehta, G.; Maity, P. *Tetrahedron Lett.* **2011,** *52,* 1749–1752. doi:10.1016/j.tetlet.2011.02.012
11. Ohtawa, M.; Krambis, M. J.; Cerne, R.; Schkeryantz, J. M.; Witkin, J. M.; Shenvi, R. A. *J. Am. Chem. Soc.* **2017,** *139,* 9637–9644. doi:10.1021/jacs.7b04206
12. Tong, J.; Xia, T.; Wang, B. *Org. Lett.* **2020,** *22,* 2730–2734. doi:10.1021/acs.orglett.0c00689
13. Birman, V. B.; Danishefsky, S. J. *J. Am. Chem. Soc.* **2002,** *124,* 2080–2081. doi:10.1021/ja012495d
14. Inoue, M.; Sato, T.; Hirama, M. *J. Am. Chem. Soc.* **2003,** *125,* 10772–10773. doi:10.1021/ja036587+
15. Meng, Z.; Danishefsky, S. J. *Angew. Chem., Int. Ed.* **2005,** *44,* 1511–1513. doi:10.1002/anie.200462509
16. Inoue, M.; Sato, T.; Hirama, M. *Angew. Chem., Int. Ed.* **2006,** *45,* 4843–4848. doi:10.1002/anie.200601358
17. Mehta, G.; Singh, S. R. *Angew. Chem., Int. Ed.* **2006,** *45,* 953–955. doi:10.1002/anie.200503618
18. He, W.; Huang, J.; Sun, X.; Frontier, A. J. *J. Am. Chem. Soc.* **2007,** *129,* 498–499. doi:10.1021/ja068150i
19. He, W.; Huang, J.; Sun, X.; Frontier, A. J. *J. Am. Chem. Soc.* **2008,** *130,* 300–308. doi:10.1021/ja0761986
20. Shi, L.; Meyer, K.; Greaney, M. F. *Angew. Chem., Int. Ed.* **2010,** *49,* 9250–9253. doi:10.1002/anie.201005156
21. Chen, J.; Gao, P.; Yu, F.; Yang, Y.; Zhu, S.; Zhai, H. *Angew. Chem., Int. Ed.* **2012,** *51,* 5897–5899. doi:10.1002/anie.201200378
22. Liu, W.; Wang, B. *Chem. – Eur. J.* **2018,** *24,* 16511–16515. doi:10.1002/chem.201804195
23. Shen, Y.; Li, L.; Xiao, X.; Yang, S.; Hua, Y.; Wang, Y.; Zhang, Y.-w.; Zhang, Y. *J. Am. Chem. Soc.* **2021,** *143,* 3256–3263. doi:10.1021/jacs.1c00525
24. Huffman, B. J.; Chu, T.; Hanaki, Y.; Wong, J. J.; Chen, S.; Houk, K. N.; Shenvi, R. A. *Angew. Chem., Int. Ed.* **2022,** *61,* e202114514. doi:10.1002/anie.202114514
25. Fu, P.; Liu, T.; Shen, Y.; Lei, X.; Xiao, T.; Chen, P.; Qiu, D.; Wang, Z.; Zhang, Y. *J. Am. Chem. Soc.* **2023,** *145,* 18642–18648. doi:10.1021/jacs.3c06442
26. Ma, S.-G.; Li, M.; Lin, M.-B.; Li, L.; Liu, Y.-B.; Qu, J.; Li, Y.; Wang, X.-J.; Wang, R.-B.; Xu, S.; Hou, Q.; Yu, S.-S. *Org. Lett.* **2017,** *19,* 6160–6163. doi:10.1021/acs.orglett.7b03050
27. McCulley, C. H.; Tantillo, D. J. *J. Am. Chem. Soc.* **2020,** *142,* 6060–6065. doi:10.1021/jacs.9b12398
28. Burns, A. S.; Rychnovsky, S. D. *J. Am. Chem. Soc.* **2019,** *141,* 13295–13300. doi:10.1021/jacs.9b05065
29. Etling, C.; Tedesco, G.; Di Marco, A.; Kalesse, M. *J. Am. Chem. Soc.* **2023,** *145,* 7021–7029. doi:10.1021/jacs.3c01262
30. Gong, X.; Huang, J.; Sun, X.; Chen, Z.; Yang, M. *Angew. Chem., Int. Ed.* **2023,** *62,* e202306367. doi:10.1002/anie.202306367
31. Xu, B.; Zhang, Z.; Dai, M. *J. Am. Chem. Soc.* **2025,** *147,* 17592–17597. doi:10.1021/jacs.5c05409
32. Zhu, L.; Li, J.; Lu, Z. *J. Am. Chem. Soc.* **2025,** *147,* 23417–23421. doi:10.1021/jacs.5c07921
33. Chen, M. S.; White, M. C. *Science* **2007,** *318,* 783–787. doi:10.1126/science.1148597
34. Bigi, M. A.; Reed, S. A.; White, M. C. *J. Am. Chem. Soc.* **2012,** *134,* 9721–9726. doi:10.1021/ja301685r
35. White, M. C.; Zhao, J. *J. Am. Chem. Soc.* **2018,** *140,* 13988–14009. doi:10.1021/jacs.8b05195
36. Etling, C.; Tedesco, G.; Kalesse, M. *Chem. – Eur. J.* **2021,** *27,* 9257–9262. doi:10.1002/chem.202101041
37. Wilde, N. C.; Isomura, M.; Mendoza, A.; Baran, P. S. *J. Am. Chem. Soc.* **2014,** *136,* 4909–4912. doi:10.1021/ja501782r
38. Bhunia, A.; Bergander, K.; Daniliuc, C. G.; Studer, A. *Angew. Chem., Int. Ed.* **2021,** *60,* 8313–8320. doi:10.1002/anie.202015740
39. Occhialini, G.; Palani, V.; Wendlandt, A. E. *J. Am. Chem. Soc.* **2022,** *144,* 145–152. doi:10.1021/jacs.1c12043
40. Palani, V.; Wendlandt, A. E. *J. Am. Chem. Soc.* **2023,** *145,* 20053–20061. doi:10.1021/jacs.3c06935
41. Wu, T. C.; Houk, K. N. *J. Am. Chem. Soc.* **1985,** *107,* 5308–5309. doi:10.1021/ja00304a065
42. Hayashi, Y.; Gotoh, H.; Honma, M.; Sankar, K.; Kumar, I.; Ishikawa, H.; Konno, K.; Yui, H.; Tsuzuki, S.; Uchimaru, T. *J. Am. Chem. Soc.* **2011,** *133,* 20175–20185. doi:10.1021/ja108516b
43. Carosso, S.; Miller, M. J. *Org. Biomol. Chem.* **2014,** *12,* 7445–7468. doi:10.1039/c4ob01033g
44. Suzuki, T.; Nagahama, R.; Fariz, M. A.; Yukutake, Y.; Ikeuchi, K.; Tanino, K. *Organics* **2021,** *2,* 306–312. doi:10.3390/org2030016

License and Terms

BEILSTEIN JOURNAL OF ORGANIC CHEMISTRY

Chemoenzymatic synthesis of the cardenolide rhodexin A and its aglycone sarmentogenin

Fuzhen Song[1], Mengmeng Zheng[2], Dongkai Wang[1], Xudong Qu[3] and Qianghui Zhou[*1]

Letter

Open Access

Address:
[1]Engineering Research Center of Organosilicon Compounds & Materials (Ministry of Education), Hubei Key Lab on Organic and Polymeric OptoElectronic Materials, College of Chemistry and Molecular Sciences, The Institute for Advanced Studies, TaiKang Center for Life and Medical Sciences and State Key Laboratory of Metabolism and Regulation in Complex Organisms, Wuhan University, Wuhan, 430072, China, [2]School of Life Sciences, Shanghai University, Shanghai, 200444, China and [3]State Key Laboratory of Microbial Metabolism and School of Life Sciences and Biotechnology, Zhangjiang Institute for Advanced Study, Shanghai Jiao Tong University, Shanghai, 200240, China

Email:
Qianghui Zhou[*] - qhzhou@whu.edu.cn

* Corresponding author

Keywords:
cardiac glycosides; C–H hydroxylation; chemoenzymatic synthesis; Mukaiyama hydration; protecting-group-free synthesis

Beilstein J. Org. Chem. **2025,** *21,* 2637–2644.
https://doi.org/10.3762/bjoc.21.204

Received: 28 August 2025
Accepted: 21 November 2025
Published: 03 December 2025

This article is part of the thematic issue "Concept-driven strategies in target-oriented synthesis".

Associate Editor: D. Y.-K. Chen

Abstract

Herein, we report a concise chemoenzymatic synthesis of the cardenolide rhodexin A in 9 steps and the first protecting-group-free synthesis of its aglycone sarmentogenin in 7 steps from 17-deoxycortisone. The synthesis features a scalable enzymatic C_{14}–H α-hydroxylation, a Bestmann ylide-enabled one-step construction of the butenolide motif, a late stage Mukaiyama hydration, and a stereoselective C11 carbonyl reduction.

Introduction

Cardiac glycosides (CGs) are widely distributed natural products, generated by plants and amphibians [1]. Structurally, they are composed of an aglycone-steroidal moiety, an unsaturated lactone ring attached to the C17 position, and a glycosyl moiety in general. It is believed that CGs can increase cardiac contractility by inhibiting the sodium–potassium adenosine triphosphatase (Na^+/K^+ ATPase) of the plasma membrane [2]. The well-known CGs, such as digoxin, digitoxin, ouabain, and oleandrin have been used in clinical treatment for heart failure for a long time (Figure 1) [3-5]. The bioactivity of CGs is primarily determined by the lactone ring, with the sugar residue critically influencing their toxicological profile [6]. This is evident as the free aglycone facilitates absorption and metabolism, and specific moieties like rhamnose can enhance CG potency markedly by more than 25 times [1,7]. In addition, the -OH groups on the steroids' structure also play an important

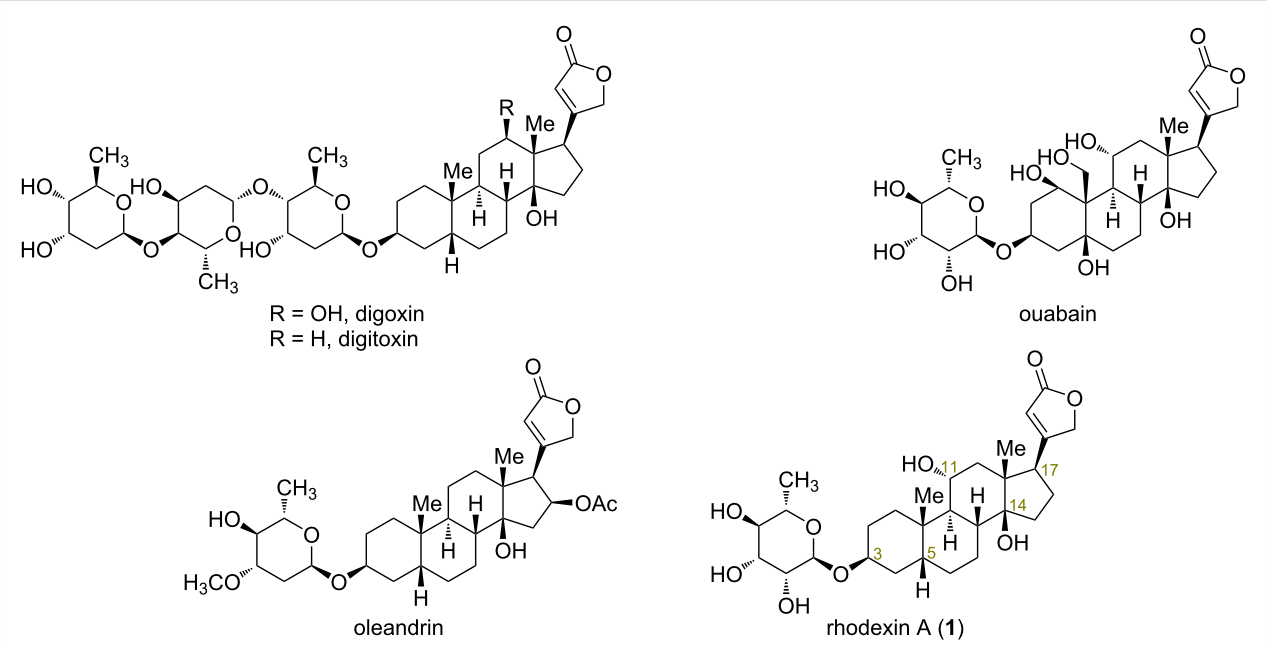

Figure 1: Representative CGs with promising biological activities.

role on their activity. However, these compounds are mainly isolated from plants or animals, which not only causes damage to the environment, but also greatly restricts further research for their pharmaceutical applications. Therefore, substantial synthetic efforts have been devoted towards the preparation of these valuable targets recently [8-17].

Rhodexin A was firstly isolated from the leaves and roots of the Japanese evergreen plant *Rohdea japonica* in 1951, and was also discovered in several other plants later [18]. Rhodexin A is the only natural CG that exhibits both cardiotonic activity and strong inhibitory activity on human leukemia K562 cells with an IC_{50} = 19 nM [19]. In addition, rhodexin A exhibits a strong antiproliferation activity due to the ability to inhibit the synthesis of hypoxia inducible factor 1 (HIF-1α) [20]. Thus, rhodexin A shows high value in medicinal research. Structurally, rhodexin A consists of two parts, the cardenolide aglycon – sarmentogenin and L-rhamnose connected by the C3–O bond. In the steroidal skeleton, both the A/B and C/D rings are *cis* fused, which is different from common steroids. Besides, the steroidal skeleton is moderately oxidized at the C3, C11, and C14 positions. The introduction of the hydroxy groups and the glycoside in a stereocontrolled manner makes the synthesis of rhodexin A a challenging task. Currently, there are only a few reports about the synthesis of rhodexin A [20-22]. In 2011, the Jung group finished the first total synthesis of rhodexin A in 26 steps [20]. In this work, an elegant inverse-electron demand Diels–Alder (IEDDA) reaction was utilized to successfully construct the BCD tricyclic structure with the correct configuration of the four contiguous stereocenters in just one step. However, the requirement of a series of protecting group manipulations undermined the step-economy and overall synthetic efficiency of this route. Therefore, the development of more efficient syntheses of rhodexin A is of great significance.

Recently, chemoenzymatic syntheses of steroids have made excellent progress, which can enormously shorten the synthetic routes and increase the overall efficiency [23-27]. Considering the common steroidal skeleton, we envisioned a chemoenzymatic strategy for the concise synthesis of rhodexin A and the retrosynthetic analysis is shown in Scheme 1. We envisaged rhodexin A (**1**) could be assembled from two fragments, sarmentogenin (**2**) and the L-rhamnose donor, through a late-stage glycosylation. The aglycon **2** can be derived from the Δ14 olefin intermediate **3** via Mukaiyama hydration and several functional group transformations. In turn, **3** would be generated from the key C14α-hydroxylated intermediate **4** via an elimination process. For the synthesis of **4**, an enzymatic C14–H α-hydroxylation of 17-deoxycortisone (**5**) could be adopted, as described in our recent work [27]. Notably, **5** can be readily obtained from the inexpensive commercial steroid cortisone via a two-step process [27].

Results and Discussion

Following the retrosynthetic analysis, we started the first step to prepare the C14α-hydroxylated steroidal intermediate **4** from 17-deoxycortisone (**5**). Delightfully, based on our previous study on enzymatic α-hydroxylation of C_{14}–H of common

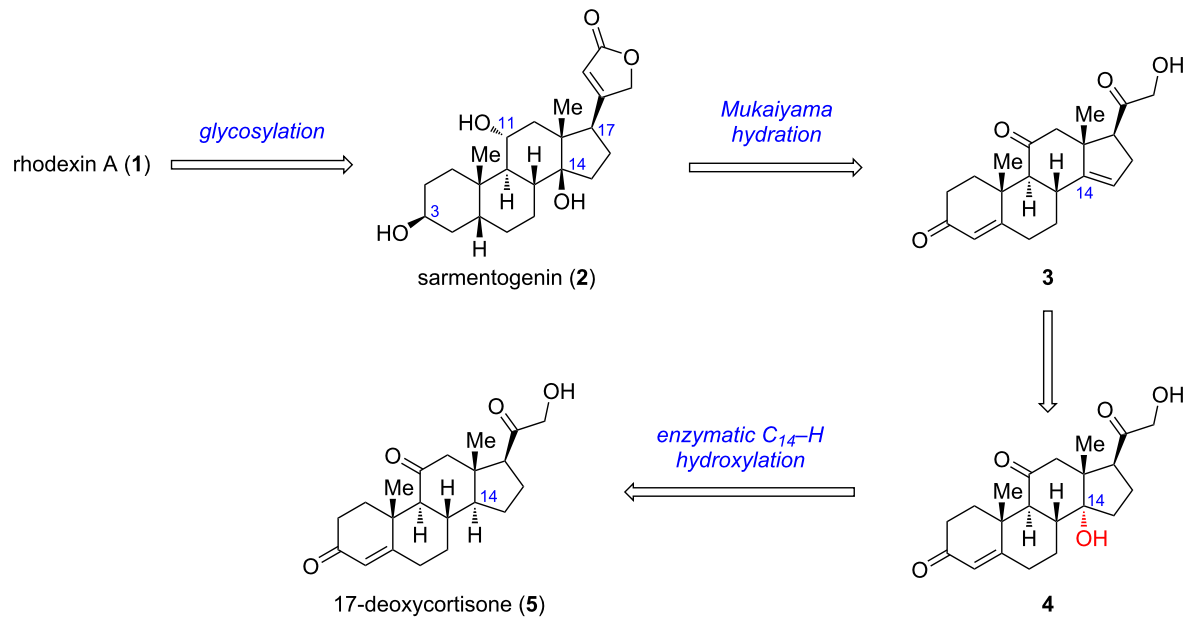

Scheme 1: Retrosynthetic analysis of rhodexin A and sarmentogenin.

steroids [27], compound **4** could be successfully obtained in 69% yield by using the biocatalyst CYP14A mutant. However, the maximum substrate loading was only 0.1 g/L, which was not sufficient for the enrichment of **4**. Thus, we changed our focus to another microorganism *Thamnostylum piriforme NBRC 6117*, which could act as whole cell biocatalyst to oxidize progesterone at the C14 position [28]. Fortunately, 17-deoxycortisone **5** could also be transformed into **4** in 65% yield after incubation in the *Thamnostylum piriforme NBRC 6117* liquid medium (Table 1, entry 1). Notably, a major C9 α-hydroxylated side product **4'** was also generated in 30% yield, which could be readily separated by column chromatography.

Table 1: Optimization of the fermentation conditions of the biocatalytic C_{14}–H α-hydroxylation.

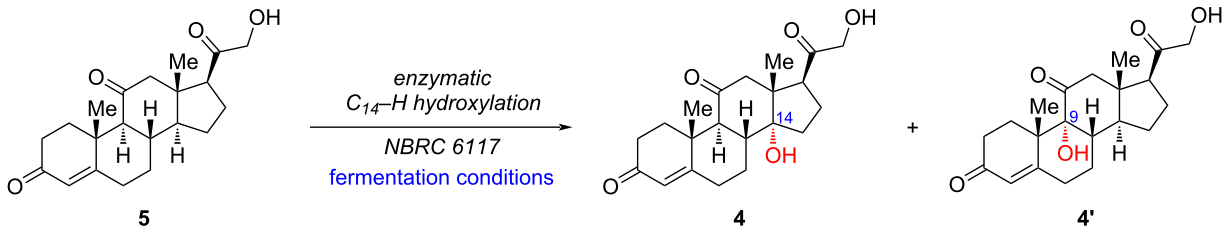

Entry	Substrate loading (g/L)	Additive	Time (d)	Yield of **4** (%)[a]	Yield of **4'** (%)[a]
1	0.1	–	1	65	30
2	0.25	–	2	64	32
3	0.5	–	4	30	18
4	0.5	HP-β-CD	3	60	34
5	1.0	HP-β-CD	4	52	26
6	**1.0**	**HP-β-CD tween 80**	**4**	**64**	**30**
7	2.0	HP-β-CD tween 80	6	28	15

[a]Isolated yields were reported.

Based on the above preliminary results, we subsequently performed extensive optimization of fermentation conditions for a scalable synthesis of **4**. As shown in Table 1, when the substrate loading was increased to 0.25 g/L, a much longer reaction time (2 days) was required to allow complete conversion, affording **4** in 64% yield (Table 1, entry 2). However, at a higher concentration (0.5 g/L), a significant amount of starting compound **5** remained unconverted even after 4 days, and only 30% of **4** was isolated (Table 1, entry 3). To our delight, upon adding 2-hydroxypropyl-β-cyclodextrin (HP-β-CD) [29] as the solubilizer to the fermentation broth, a complete conversion of **5** was achieved within 3 days to afford **4** in 60% yield (Table 1, entry 4). When the substrate loading was further increased to 1.0 g/L in the presence of HP-β-CD, there was a small amount of starting material remained after 4 days of fermentation (Table 1, entry 5). Delightfully, after adding 1% Tween 80 to the above fermentation broth, a complete conversion was observed in 4 days, and compound **4** was obtained in 64% yield (Table 1, entry 6). However, further increasing the substrate concentration to 2.0 g/L resulted in a much lower conversion rate owing to inhibited microbial growth (Table 1, entry 7). Therefore, the conditions from Table 1, entry 6 were identified as the optimized fermentation conditions that secured the gram-scale synthesis of **4** effortlessly.

With compound **4** in sufficient quantities at hands, we next focused on transforming it into the pivotal C14 β-hydroxylated steroidal intermediate. As shown in Scheme 2, a $BF_3{\cdot}Et_2O$-promoted elimination afforded the 14-olefinated intermediate **3** in a moderate yield. However, the following Mukaiyama hydration to introduce the C14 β-hydroxy group was unsuccessful. Owing to the reactive C17 side chain including an α-hydroxycarbonyl group, a set of side reactions (e.g., reduction of the C20 carbonyl, hydrogenation of Δ^4 and Δ^{14} double bonds, etc.) occurred under the Mukaiyama hydration conditions [30,31]. Therefore, it was necessary to alter the side chain before installing the C14 β-OH group.

The revised synthetic route is described in Scheme 2. At first, **4** was subjected to a Pd/C-catalyzed hydrogenation to afford the desired A/B-*cis* fused intermediate **7** along with its C5 epimer as a 2:1 separable mixture in a quantitative yield. By treating **7** with the Bestmann ylide reagent [20], the key intermediate **8** bearing a butenolide motif was obtained in 76% yield. Next, with the aid of the strong Lewis acid $Bi(OTf)_3$, the regioselective elimination of **8** was achieved to produce the Δ^{14} olefin intermediate **9** in 86% yield. Afterwards, we evaluated the reactivity of **9** towards typical Mukaiyama hydration conditions [30-32] to install the C14 β-hydroxy group. However, only a trace amount of the undesired C14α-hydroxylated product **10** was obtained. Additional optimizations regarding the transition-metal catalyst, hydrogen source and solvent all failed to improve the results. Therefore, we decided to perform the Mukaiyama hydration on advanced intermediates. Next, a K-selectride-promoted chemo- and stereoselective reduction of the C3 carbonyl of **9** was realized to solely deliver **11** in 85% yield [33]. Then, **11** was subjected to Mukaiyama hydration conditions. Under the $Fe(acac)_3$-catalyzed anaerobic conditions [30], **11** was transformed into the C14 hydroxylated intermediate **12** as epimeric mixture in 42% yield and dr = 1:5, among which the undesired 14α-hydroxy epimer was the major component. Interestingly, the use of $Co(acac)_2$ or $Mn(acac)_2$ as the catalyst [31,32] instead of $Fe(acac)_3$ could reverse the diastereomeric ratio of the C14-hydroxylated products to dr = 1.5–1.7:1 and increased the yield to 48–58% as well. Nevertheless, the unsatisfactory diastereoselectivity urged us to explore a late-stage Mukaiyama hydration. To this end, we next performed the thermodynamic C11-carbonyl reduction by dissolved lithium metal in liquid NH_3 solution, and the C11 α-hydroxylated intermediate **13** was obtained as a single diastereoisomer in 54% yield. Lastly, as expected, a $Co(acac)_2$-catalyzed Mukaiyama hydration of **13** afforded the desired natural product sarmentogenin (**2**) in 69% yield with high diastereoselectivity (dr = 14β/14α = 6.7:1), and the minor component 14-*epi*-sarmentogenin could be readily separated. Notably, our work represents the first protecting-group-free synthesis [34,35] of sarmentogenin in just 7 steps from 17-deoxycortisone.

With the aglycone sarmentogenin (**2**) in hand, we first tried the synthesis of rhodexin A through direct glycosylation of **2** by the L-rhamnose donor 2,3,4-tri-*O*-benzoyl-α-L-rhamnopyranosyl trichloroacetimidate (**14**). However, the selective glycosylation at the C3-hydroxy group of **2** was a formidable challenge since competitive glycosylations of the other hydroxy groups of **2** could not be avoided, resulting in a complex mixture including mono-, di-, and triglycosylated products (Scheme 3A). Thus, both C11–OH and C14–OH needed to be masked before glycosylation. Based on this thought, we selected intermediate **11** as a suitable substrate for glycosylation. To our delight, as shown in Scheme 3B, with TMSOTf as the promoter, the glycosylation between **11** and **14** proceeded smoothly in a stereospecific manner, delivering the key intermediate **15** in 98% yield. Subsequently, treating **15** under $Mn(acac)_2$-catalyzed Mukaiyama hydration conditions yielded the key C14 β-hydroxylated intermediate **16** in 53% yield, accompanied by the separable C14 α-OH epimer in 27% yield. Later on, we assumed to achieve the deprotection of the sugar motif and the reduction of the C11 carbonyl of **16** simultaneously under Li–NH_3(l) conditions, which would directly afford the final natural product rhodexin A in one step. Just as expected, when directly subjecting **16** to the abovementioned conditions, rhodexin A was indeed afforded albeit in only 10% yield. The

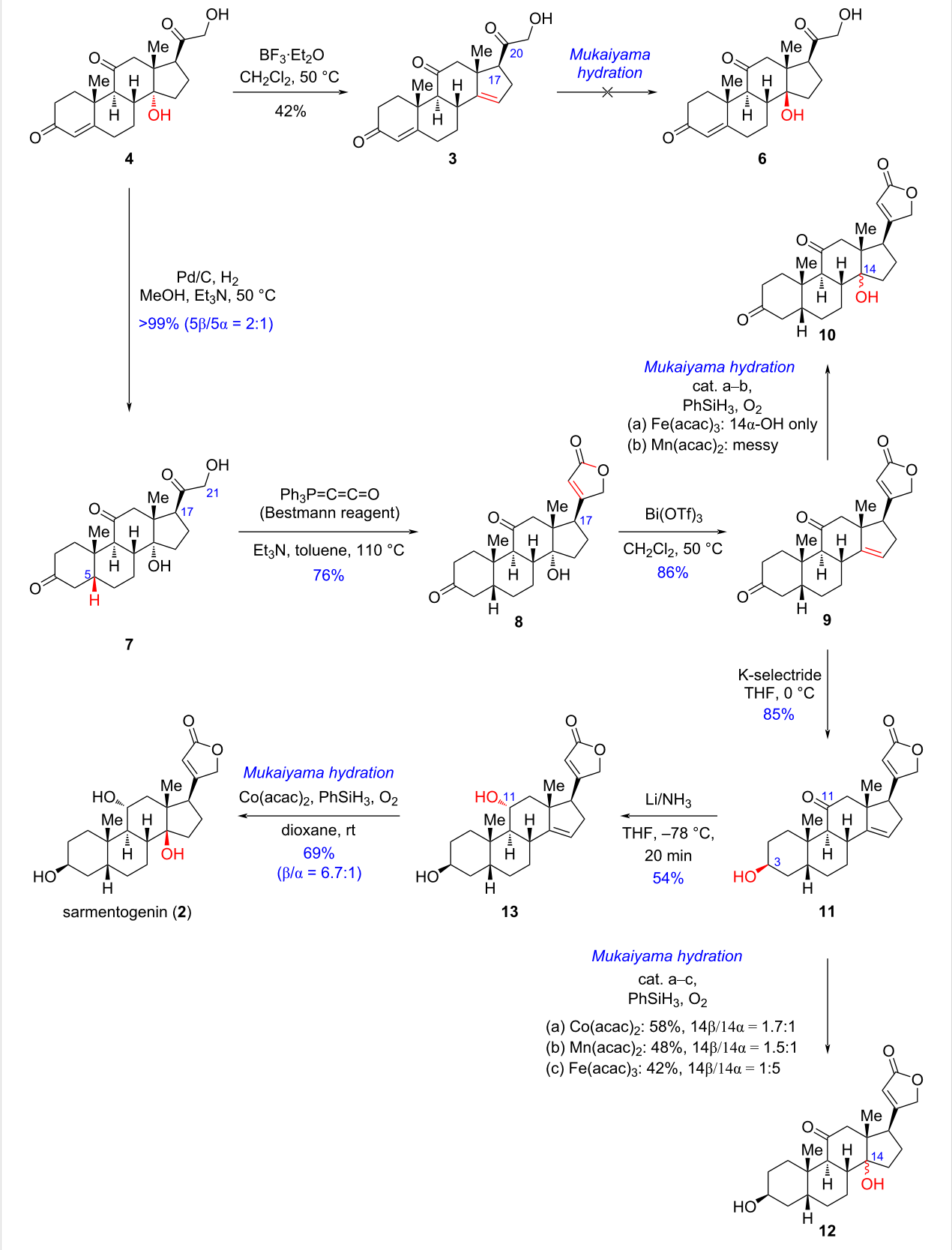

Scheme 2: Chemoenzymatic synthesis of sarmentogenin (**2**).

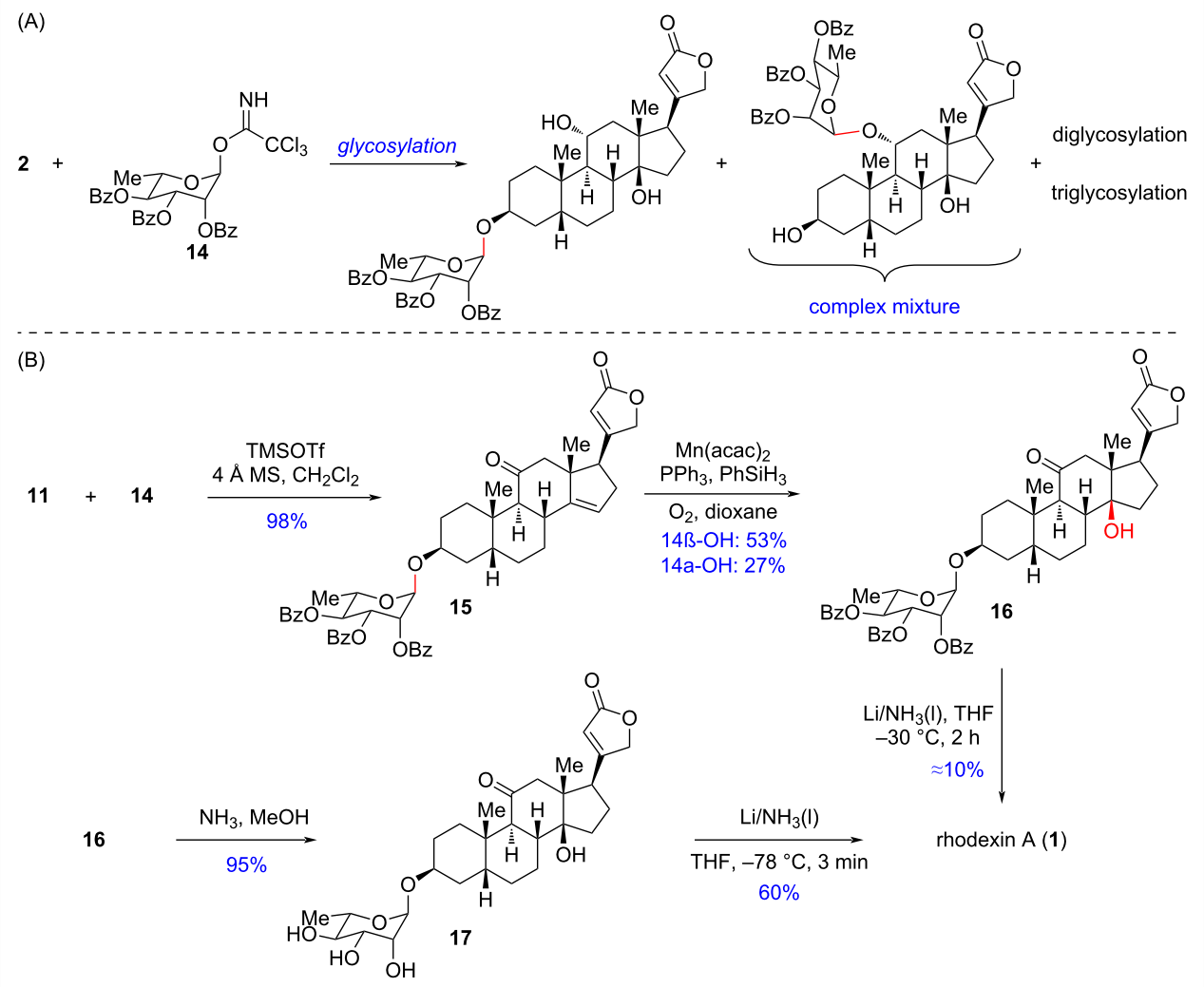

Scheme 3: Synthesis of rhodexin A.

required longer reaction time and elevated temperature to achieve deprotection of the sugar motif resulted in an over-reduction of the butenolide motif. The low efficiency of this reaction prompted us to pursue an alternative two-step approach. First, we performed the deprotection to remove all the Bz groups of **16** by NH_3/MeOH, furnishing the saccharide **17** in 95% yield. Eventually, the quick stereospecific C11 carbonyl reduction by Li–NH_3(l) was accomplished in just 3 minutes to afford rhodexin A in 60% isolated yield. The synthetic sample exhibited identical NMR spectroscopic data to the literature precedent [20], which confirmed the completion of the chemoenzymatic synthesis of rhodexin A in 9 steps from 17-deoxycortisone.

Conclusion

In summary, we have completed a concise chemoenzymatic synthesis of cardenolide rhodexin A in 9 steps and the first protecting-group-free synthesis of its aglycone sarmentogenin (**2**) in 7 steps from 17-deoxycortisone. The key steps include a scalable enzymatic C_{14}–H α-hydroxylation, a Bestmann ylide-enabled one-step construction of the butenolide motif, a late-stage Mukaiyama hydration, and a stereoselective C11 carbonyl reduction. We believe this chemoenzymatic synthetic strategy will inspire future endeavors towards the practical synthesis of complex steroids and other bioactive natural products.

Supporting Information

Supporting Information File 1

Experimental details and spectral data for all new compounds.
[https://www.beilstein-journals.org/bjoc/content/supplementary/1860-5397-21-204-S1.pdf]

Acknowledgements

The authors are grateful to Prof. Wenqing Chen (WHU) and Prof. Kui Hong (WHU) for sharing the instruments.

Funding

This work was supported by the National Natural Science Foundation of China (Grant No. 22325106) and the TaiKang Center for Life and Medical Sciences.

ORCID® iDs

Xudong Qu - https://orcid.org/0000-0002-3301-8536

Data Availability Statement

All data that supports the findings of this study is available in the published article and/or the supporting information of this article.

References

1. Botelho, A. F. M.; Pierezan, F.; Soto-Blanco, B.; Melo, M. M. *Toxicon* **2019,** *158,* 63–68. doi:10.1016/j.toxicon.2018.11.429
2. Langford, S. D.; Boor, P. J. *Toxicology* **1996,** *109,* 1–13. doi:10.1016/0300-483x(95)03296-r
3. El-Seedi, H. R.; Khalifa, S. A. M.; Taher, E. A.; Farag, M. A.; Saeed, A.; Gamal, M.; Hegazy, M.-E. F.; Youssef, D.; Musharraf, S. G.; Alajlani, M. M.; Xiao, J.; Efferth, T. *Pharmacol. Res.* **2019,** *141,* 123–175. doi:10.1016/j.phrs.2018.12.015
4. Gao, H.; Popescu, R.; Kopp, B.; Wang, Z. *Nat. Prod. Rep.* **2011,** *28,* 953–969. doi:10.1039/c0np00032a
5. Zhong, Y.; Zhao, C.; Wu, W.-Y.; Fan, T.-Y.; Li, N.-G.; Chen, M.; Duan, J.-A.; Shi, Z.-H. *Eur. J. Med. Chem.* **2020,** *189,* 112038. doi:10.1016/j.ejmech.2020.112038
6. Brown, L.; Thomas, R.; Watson, T. *Naunyn-Schmiedeberg's Arch. Pharmacol.* **1986,** *332,* 98–102. doi:10.1007/bf00633205
7. Cornelius, F.; Kanai, R.; Toyoshima, C. *J. Biol. Chem.* **2013,** *288,* 6602–6616. doi:10.1074/jbc.m112.442137
8. Heasley, B. *Chem. – Eur. J.* **2012,** *18,* 3092–3120. doi:10.1002/chem.201103733
9. Michalak, M.; Michalak, K.; Wicha, J. *Nat. Prod. Rep.* **2017,** *34,* 361–410. doi:10.1039/c6np00107f
10. Khatri, H. R.; Carney, N.; Rutkoski, R.; Bhattarai, B.; Nagorny, P. *Eur. J. Org. Chem.* **2020,** 755–776. doi:10.1002/ejoc.201901466
11. Fu, S.; Liu, B. *Org. Chem. Front.* **2020,** *7,* 1903–1947. doi:10.1039/d0qo00203h
12. Sun, J.; Chen, Y.; Ragab, S. S.; Gu, W.; Tang, Z.; Tang, Y.; Tang, W. *Angew. Chem., Int. Ed.* **2023,** *62,* e202303639. doi:10.1002/anie.202303639
13. Renata, H.; Zhou, Q.; Baran, P. S. *Science* **2013,** *339,* 59–63. doi:10.1126/science.1230631
14. Urabe, D.; Asaba, T.; Inoue, M. *Chem. Rev.* **2015,** *115,* 9207–9231. doi:10.1021/cr500716f
15. Mukai, K.; Urabe, D.; Kasuya, S.; Aoki, N.; Inoue, M. *Angew. Chem., Int. Ed.* **2013,** *52,* 5300–5304. doi:10.1002/anie.201302067
16. Mukai, K.; Kasuya, S.; Nakagawa, Y.; Urabe, D.; Inoue, M. *Chem. Sci.* **2015,** *6,* 3383–3387. doi:10.1039/c5sc00212e
17. Bai, H.; Gu, W.; Zhao, D.; Xu, G.; Tang, W. *Green Synth. Catal.* **2025,** *6,* 267–274. doi:10.1016/j.gresc.2023.12.001
18. Nawa, H. *Proc. Jpn. Acad.* **1951,** *27,* 436–440. doi:10.2183/pjab1945.27.436
19. Masuda, T.; Oyama, Y.; Yamamoto, N.; Umebayashi, C.; Nakao, H.; Toi, Y.; Takeda, Y.; Nakamoto, K.; Kuninaga, H.; Nishizato, Y.; Nonaka, A. *Biosci., Biotechnol., Biochem.* **2003,** *67,* 1401–1404. doi:10.1271/bbb.67.1401
20. Jung, M. E.; Yoo, D. *Org. Lett.* **2011,** *13,* 2698–2701. doi:10.1021/ol200796r
21. Jung, M. E.; Chu, H. V. *Tetrahedron Lett.* **2011,** *52,* 4512–4514. doi:10.1016/j.tetlet.2011.06.114
22. Jung, M. E.; Guzaev, M. *J. Org. Chem.* **2013,** *78,* 7518–7526. doi:10.1021/jo400909t
23. Zheng, M.; Lin, Z.; Lin, S.; Qu, X. *Eur. J. Org. Chem.* **2024,** *27,* e202301066. doi:10.1002/ejoc.202301066
24. Zhao, Y.; Zhang, B.; Sun, Z. Q.; Zhang, H.; Wang, W.; Wang, Z. R.; Guo, Z. K.; Yu, S.; Tan, R. X.; Ge, H. M. *ACS Catal.* **2022,** *12,* 9839–9845. doi:10.1021/acscatal.2c02185
25. Wang, J.; Zhang, Y.; Liu, H.; Shang, Y.; Zhou, L.; Wei, P.; Yin, W.-B.; Deng, Z.; Qu, X.; Zhou, Q. *Nat. Commun.* **2019,** *10,* 3378. doi:10.1038/s41467-019-11344-0
26. Peng, Y.; Gao, C.; Zhang, Z.; Wu, S.; Zhao, J.; Li, A. *ACS Catal.* **2022,** *12,* 2907–2914. doi:10.1021/acscatal.1c05776
27. Song, F.; Zheng, M.; Wang, J.; Liu, H.; Lin, Z.; Liu, B.; Deng, Z.; Cong, H.; Zhou, Q.; Qu, X. *Nat. Synth.* **2023,** *2,* 729–739. doi:10.1038/s44160-023-00280-z
28. Hu, S.-h.; Genain, G.; Azerad, R. *Steroids* **1995,** *60,* 337–352. doi:10.1016/0039-128x(95)00006-c
29. Malanga, M.; Szemán, J.; Fenyvesi, É.; Puskás, I.; Csabai, K.; Gyémánt, G.; Fenyvesi, F.; Szente, L. *J. Pharm. Sci.* **2016,** *105,* 2921–2931. doi:10.1016/j.xphs.2016.04.034
30. Bhunia, A.; Bergander, K.; Daniliuc, C. G.; Studer, A. *Angew. Chem., Int. Ed.* **2021,** *60,* 8313–8320. doi:10.1002/anie.202015740
31. Cheng, M.-J.; Zhong, L.-P.; Gu, C.-C.; Zhu, X.-J.; Chen, B.; Liu, J.-S.; Wang, L.; Ye, W.-C.; Li, C.-C. *J. Am. Chem. Soc.* **2020,** *142,* 12602–12607. doi:10.1021/jacs.0c05479
32. Mukaiyama, T.; Yamada, T. *Bull. Chem. Soc. Jpn.* **1995,** *68,* 17–35. doi:10.1246/bcsj.68.17
33. Kaplan, W.; Khatri, H. R.; Nagorny, P. *J. Am. Chem. Soc.* **2016,** *138,* 7194–7198. doi:10.1021/jacs.6b04029
34. Zhou, Q.; Chen, X.; Ma, D. *Angew. Chem., Int. Ed.* **2010,** *49,* 3513–3516. doi:10.1002/anie.201000888
35. Hui, C.; Chen, F.; Pu, F.; Xu, J. *Nat. Rev. Chem.* **2019,** *3,* 85–107. doi:10.1038/s41570-018-0071-1

BEILSTEIN JOURNAL OF ORGANIC CHEMISTRY

Advances in Zr-mediated radical transformations and applications to total synthesis

Hiroshige Ogawa and Hugh Nakamura*

Review

Open Access

Address:
The Hong Kong University of Science and Technology (HKUST), Clear Water Bay, New Territories, Hong Kong SAR, China

Email:
Hugh Nakamura* - hnakamura@ust.hk

* Corresponding author

Keywords:
halogen atom transfer; photoredox; radical; total synthesis; zirconium

Beilstein J. Org. Chem. **2026,** *22,* 71–87.
https://doi.org/10.3762/bjoc.22.3

Received: 07 October 2025
Accepted: 18 December 2025
Published: 05 January 2026

This article is part of the thematic issue "Concept-driven strategies in target-oriented synthesis".

Guest Editor: C. Li

Abstract

Radical reactions, which have been reported in large numbers in recent years, have exerted major influence across fields where organic synthesis plays a central role, including pharmaceuticals, agrochemicals, materials chemistry, organic semiconductors, and organic thin-film solar cells. These areas are intimately linked to human life; thus, advances in organic synthesis are essential for improving human well-being. Nearly two centuries after the seminal 1828 synthesis of urea from inorganic precursors – often regarded as the birth of organic synthesis – the field continues to evolve rapidly and to exert profound impact on society. A retrospective of almost 200 years of organic synthesis shows that the development and discovery of two-electron ionic transformations dominated the early stages. Over time, pericyclic reactions exemplified by the Woodward–Hoffmann rules and one-electron radical processes became prominent research topics. Today, many of these classical transformations have been further refined to afford reactions that are cheaper, safer, and less toxic. In this context, we focus on mild radical reactions mediated by zirconium (Zr), which has recently attracted attention because of its low toxicity and ease of handling. We discuss the utility of Zr in such radical processes and consider prospects for future development.

Introduction

Zirconium, a transition metal in the same group as titanium, has been employed across research fields and in medical applications owing to its distinctive physical and chemical properties [1]. Among its notable physical attributes is its high corrosion resistance: metallic zirconium is exceptionally stable toward acids and bases at ambient temperature and is less susceptible to corrosion than titanium. Its low toxicity and excellent biocompatibility have historically supported the use of zirconium in jewelry and in metal trading for investment. As an oxide, zirconium dioxide (ZrO_2) is also widely used as a white pigment in cosmetics and as a material for artificial teeth, reflecting its long-standing presence in everyday life.

Regarding supply, zirconium is typically obtained from silicate minerals ($ZrSiO_4$) in igneous rocks, which are widely distributed in the Earth's crust. Consequently, compared with certain rare metals whose sources are limited – such as iridium, rhodium, palladium, platinum, and ruthenium – zirconium is relatively inexpensive and readily available. Zirconium was first discovered by Klaproth in 1789 and subsequently isolated by Berzelius in 1824. In 1952, Wilkinson and Birmingham synthesized zirconium-containing organometallic compounds, pioneering research in organozirconium chemistry [2]. In 1974, Schwartz et al. reported the Schwartz reagent, which remains widely used today as a reducing agent [3] (Figure 1). In recent years, this accessibility, together with advances in radical chemistry, has motivated many researchers to investigate control of radical reactions using zirconium.

A particularly important physical property of zirconium is its large bond dissociation energy (BDE). Although zirconium shares many characteristics with titanium as a group-congener transition metal, it is known to form stronger bonds in several cases. For example, the Ti–O BDE is reported as 115 kcal·mol^{-1}, whereas the Zr–O BDE is 132 kcal·mol^{-1} [4]; likewise, Ti–Br and Zr–Br BDEs are 79 and 90 kcal·mol^{-1}, respectively [5]. Despite being a congener of titanium, zirconium exhibits substantially higher BDEs (Figure 1).

Building on this characteristic, a range of one-electron processes mediated by zirconium has been reported in recent years. In 2024, Ota and Yamaguchi published a review on radical reactions catalyzed by zirconium complexes [6]. Their review provides a comprehensive summary, particularly of photo-redox reactions involving zirconium catalysis. In the present review, we focus on three aspects: 1) Zr-mediated stoichiometric radical reactions 2) Zr-catalyzed radical reactions 3) Applications of Zr-mediated reactions in total synthesis. To apply these reactions to total synthesis, high functional group compatibility is required. Thus, the insights gained here can be used to assess the potential of zirconium-catalyzed radical reactions.

Review

Zr-mediated stoichiometric radical reactions

Traditionally, the use of Zr complexes in organic reactions had been limited to two-electron processes; however, the first example of a Zr-mediated radical reaction was reported by Oshima et al. in 2001. They reported an intramolecular radical cyclization using Schwartz's reagent (Scheme 1) [7,8]. When compound **2**, bearing an alkyl halide and an olefin moiety, was treated with triethylborane and Schwartz's reagent in tetrahydrofuran, a halogen atom transfer (XAT) occurred at the alkyl halide, generating alkyl radical **3**. This radical subsequently underwent intramolecular addition to the olefin, affording the cyclized

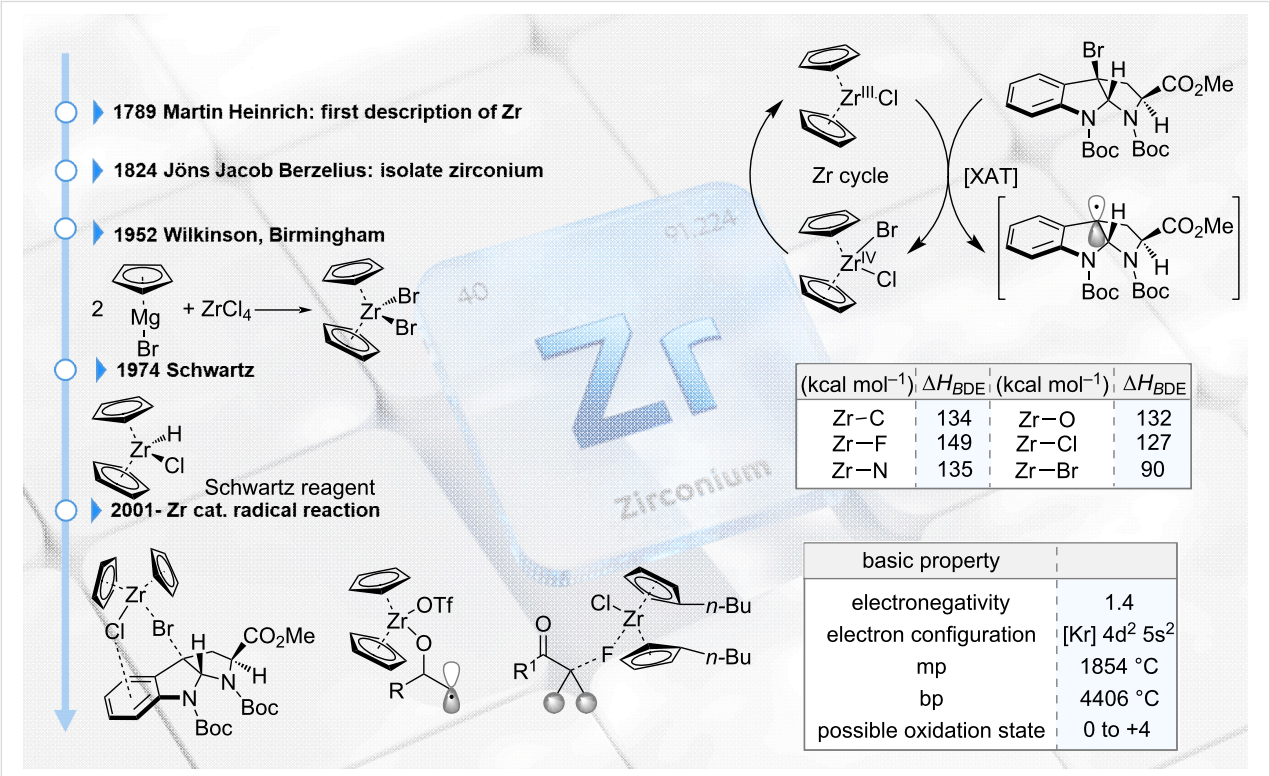

Figure 1: Historical background of zirconium and its physical properties. Image depicted in the background of Figure 1 was purchased from iStock.com/Just_Super. This content is not subject to CC BY 4.0.

acetal product **4**. The reaction proceeded efficiently across a range of substrates bearing various substituents at R^1–R^4, delivering the desired cyclized products **4a–f** in good yields. The proposed mechanism is illustrated in Scheme 1C. Initially, Schwartz's reagent reacts with triethylborane to generate a low-valent zirconium complex **5**. This complex abstracts the halogen atom from the alkyl halide, forming alkyl radical **8**. The radical then cyclizes onto the olefin, and the resulting radical intermediate undergoes hydrogen atom transfer (HAT) from Schwartz's reagent to furnish product **4d**.

In 2017, Kishi et al. reported a radical-based ketone synthesis employing zirconocene and a nickel catalyst (Scheme 2A) [9]. Traditional anion-based ketone syntheses (e.g., Grignard or RLi reagents) are often unsuitable for complex molecules due to the strongly basic conditions required. As an alternative, dithiane-based ketone synthesis has long been used, but it suffers from drawbacks in terms of step economy [10,11]. To address these limitations, the authors developed a radical-based one-pot ketone synthesis that proceeds under mild conditions.

When thioester **11** and alkyl iodide **10** were subjected to nickel catalysis in the presence of zirconocene dichloride and zinc dust, intermolecular coupling occurred to afford ketone **12** in good yields. This reaction was applicable to substrates bearing β-alkoxy substituents, which are typically problematic under anionic conditions, delivering the desired ketones **12** in good yields. The reaction also tolerated a wide range of protecting groups, including esters, carbamates, and silyl ethers, without degradation (**10f–k**). Neopentyl iodide **10l** and secondary alkyl iodide **10m** were also competent substrates, although tertiary alkyl iodide **10n** failed to give the desired products. In substrate **10o** containing both iodide and bromide, selective activation of the alkyl iodide was observed, affording the coupled product in 96% yield. Furthermore, the reaction proceeded smoothly in the presence of alcohols **10p–q** and carboxylic acid **10r**, demonstrating excellent functional group tolerance.

The proposed mechanism is shown in Scheme 2C. Zirconocene dichloride is first reduced by zinc dust to generate Zr^{II}. The resulting low-valent zirconium species reacts with the alkyl iodide to form a metal-centered radical intermediate. This species undergoes transmetallation with a Ni^{II} complex generated by oxidative addition of the thioester to Ni^0. Finally, reductive elimination from Ni^{II} furnishes the ketone. Given the strong Zr–S bond (BDE = 137 kcal/mol) [12], zirconocene is thought to play a key role in facilitating the oxidative addition of Ni^0 to the thioester and accelerating the whole process.

Zr-mediated catalytic radical reactions

In recent years, numerous chemical transformations employing photoredox catalysts in combination with catalytic amounts of zirconium complexes have been reported. In this section, representative examples of such reactions are summarized and described.

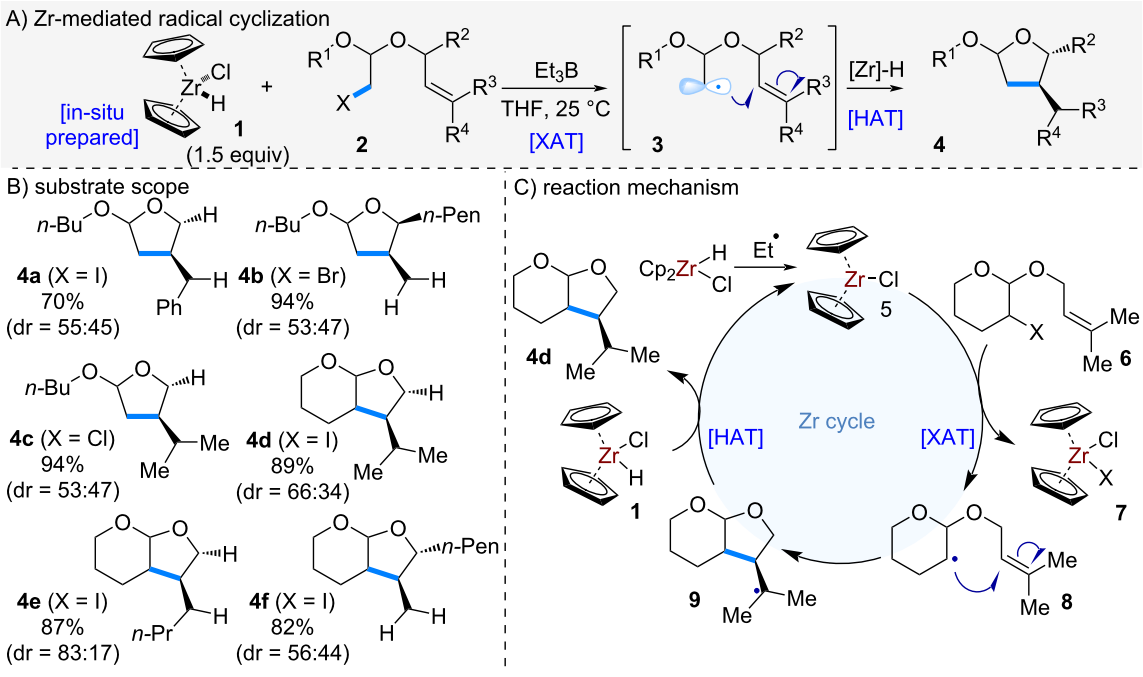

Scheme 1: Zr-mediated radical cyclization.

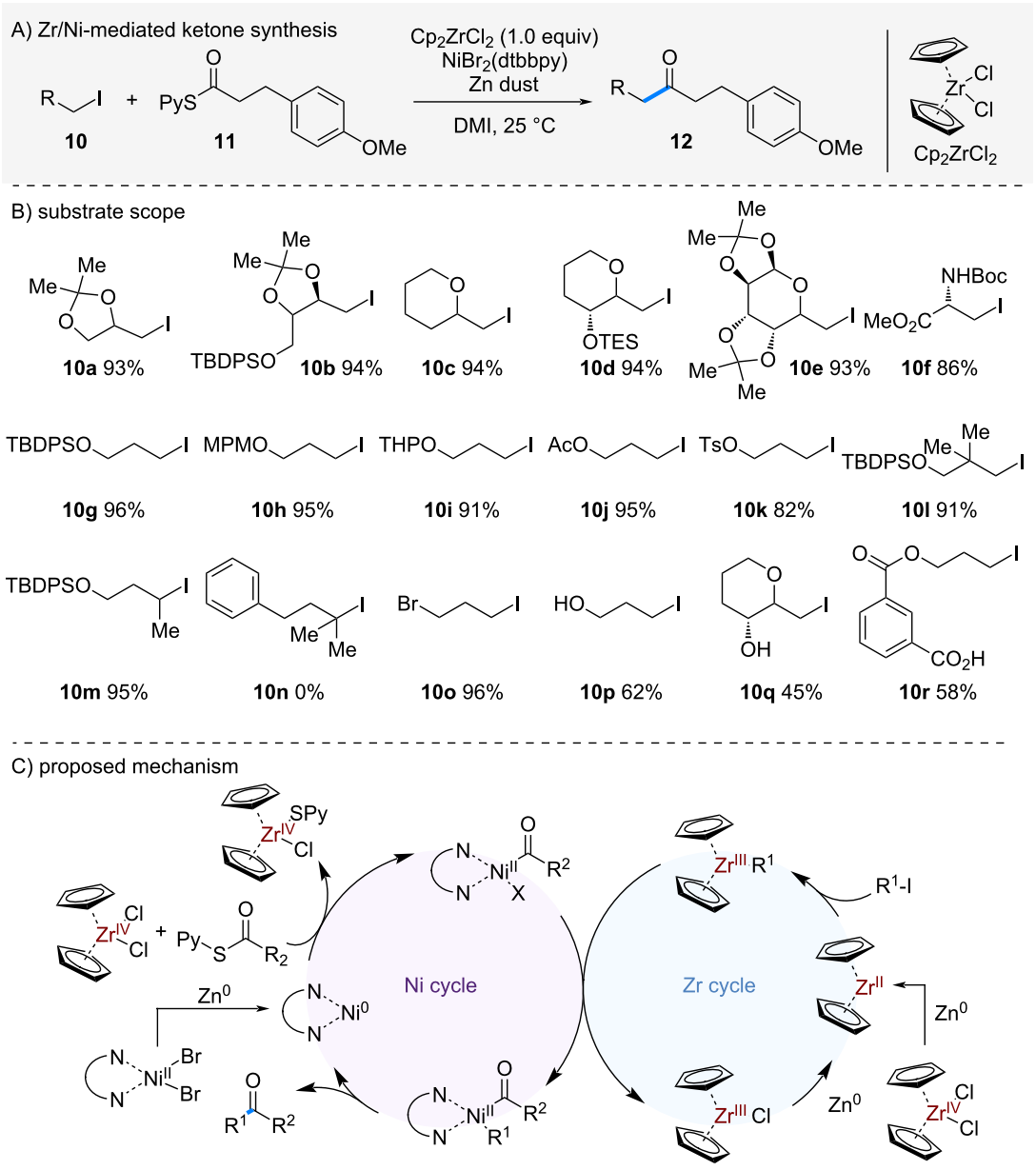

Scheme 2: Ni/Zr-mediated one-pot ketone synthesis.

In 2007, Oshima et al. reported the zirconocene-catalyzed alkylative dimerization of 2-methylene-1,3-dithiane (Scheme 3) [13]. When alkyl halide **13** was treated with Schwartz's reagent in the presence of butylmagnesium bromide, the generation of an alkyl radical via XAT process and its subsequent radical addition to 2-methylene-1,3-dithiane (**14**) proceeded, affording radical intermediate **15**. This radical intermediate rapidly underwent homodimerization to give *vic*-bis(dithiane) **16**. The reaction could be applied to both tertiary and secondary alkyl halides, providing the corresponding *vic*-bis(dithiane) derivatives **16a**–**d**.

In 2018, Milsmann et al. reported the dimerization of benzyl bromide using a zirconium complex as a photosensitizer (Scheme 4) [14]. Heating a zirconium precursor with the pincer-type ligand **17**, which can be synthesized in three steps from commercially available materials, in benzene afforded the Zr(^{R}CNN)$_2$ complex **18**. Investigation of the photoredox properties of the synthesized complex revealed trends similar to those of known photosensitizers, suggesting its potential utility as a photosensitizer [15]. Accordingly, the Zr(^{Me}CNN)$_2$ complex was employed as a photosensitizer, together with compound **22** as a sacrificial reductant, in the dimerization of benzyl

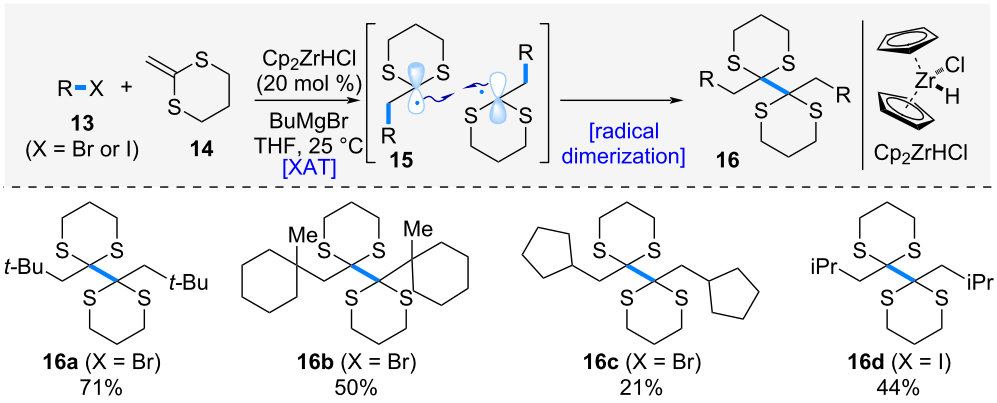

Scheme 3: Zirconocene-catalyzed alkylative dimerization of 2-methylene-1,3-dithiane.

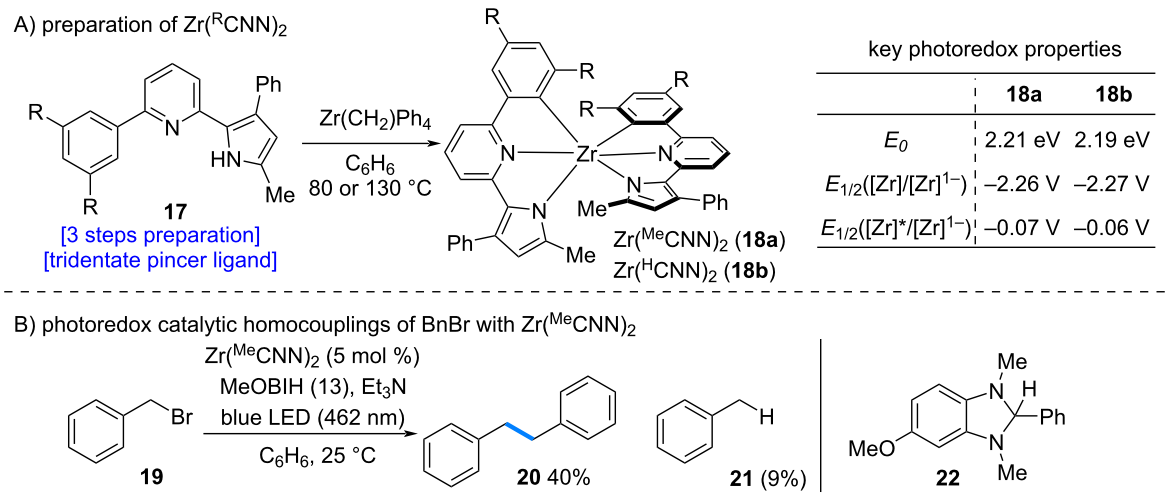

Scheme 4: Zirconium complexes as a photoredox catalyst.

bromide (**19**). The desired dimerized product **20** was obtained in 40% yield. This study highlights the potential of zirconium complexes as a photoredox catalyst, pointing to promising opportunities for further development in this area.

In 2022, Ota and Yamaguchi et al. reported the zirconocene-catalyzed ring-opening of epoxides using $Cp_2Zr(OTf)_2$·THF (Scheme 5) [4]. Traditionally, such transformations are carried out with low-valent titanium catalysts, which typically proceed via more substituted alkyl radicals to afford compound **25** as a major product [16-20]. In contrast, this study revealed that the strong affinity of zirconium for oxygen reverses this trend, leading instead to compound **24** as a predominant product.

The generality of the reaction was demonstrated with a variety of unsymmetrical epoxides (Scheme 5B). Both monosubstituted epoxides **23a–e** and di- and trisubstituted epoxides **23f–h** underwent ring opening with regioselectivity opposite to that observed in conventional systems, affording the corresponding alcohols. Moreover, the method was successfully applied to complex molecules such as allose (**23i**) and cholesterol (**23k**), delivering the desired alcohols in good yields with excellent regioselectivity.

The proposed mechanism is shown in Scheme 5C. Homolytic cleavage of the C–O bond in the epoxide generates a strong Zr–O bond, while the resulting alkyl radical abstracts a hydrogen atom from 1,4-cyclohexadiene to furnish the alcohol product. The active species $Cp_2Zr^{III}(OTf)$ is then regenerated via single-electron transfer (SET) from the Ir photocatalyst.

Notably, the addition of thiourea **26** significantly improved the regioselectivity in this reaction. According to NMR experiments, coordination of thiourea **26** to the Zr center was sug-

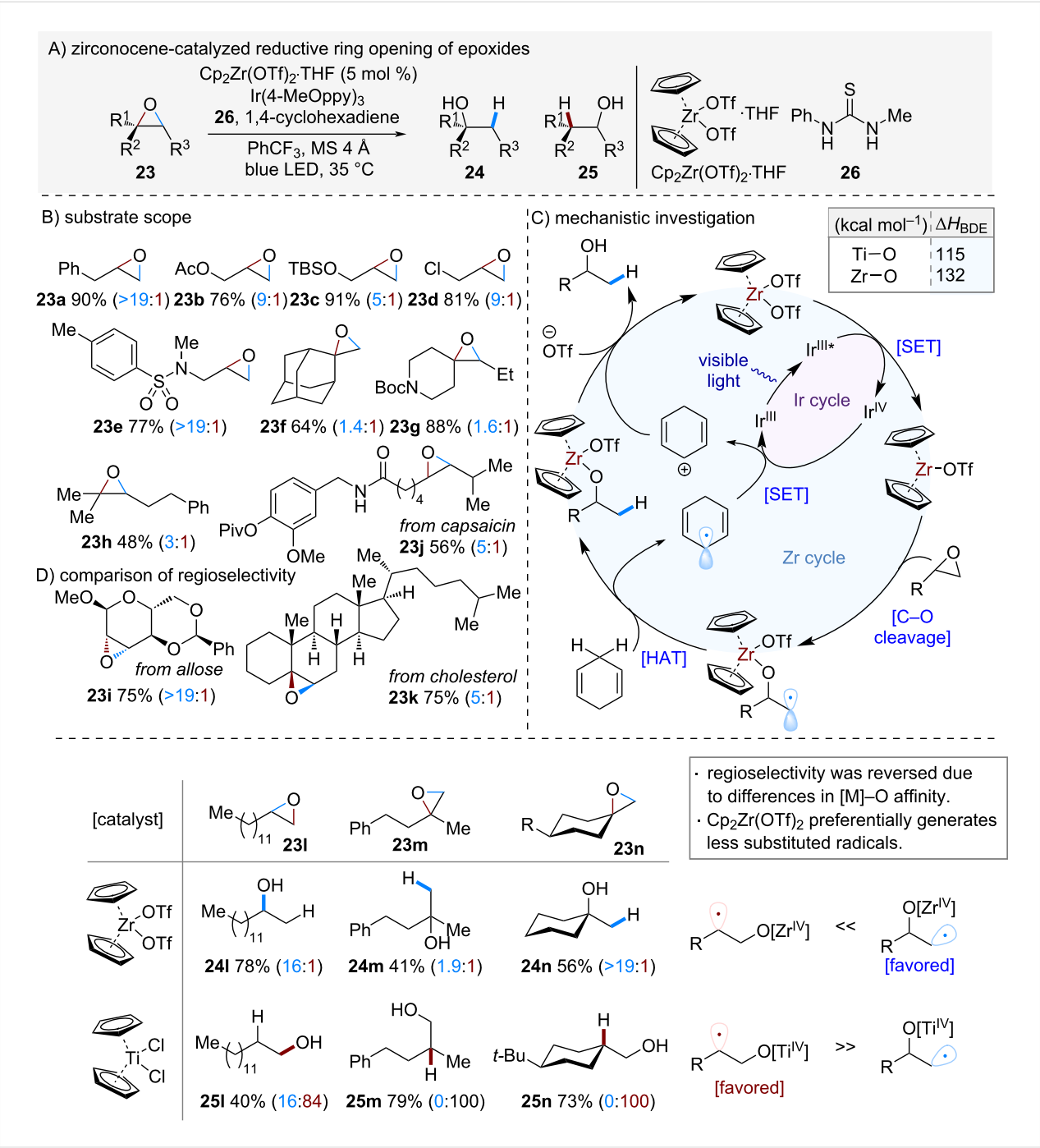

Scheme 5: Zr-catalyzed reductive ring opening of epoxides.

gested. This effect is considered to have tuned the reactivity of the Zr-catalyst, thereby having a positive effect on the reaction process.

Finally, the regioselectivity of epoxide ring opening was compared between low-valent titanocene and zirconocene catalysts using substrates **23l**–**n**. In both cases, the regioselectivity was found to be reversed. With titanocene, the reaction proceeds through the more stable, substituted radical, whereas with zirconocene, the high oxygen affinity of zirconium is the key factor driving the opposite regioselectivity.

In a related study, Ota and Yamaguchi et al. reported the regioselective ring-opening of oxetanes using zirconocene catalysis (Scheme 6) [21]. Treatment of oxetane **27** with zirconocene in the presence of an Ir-photoredox catalyst led to ring opening via

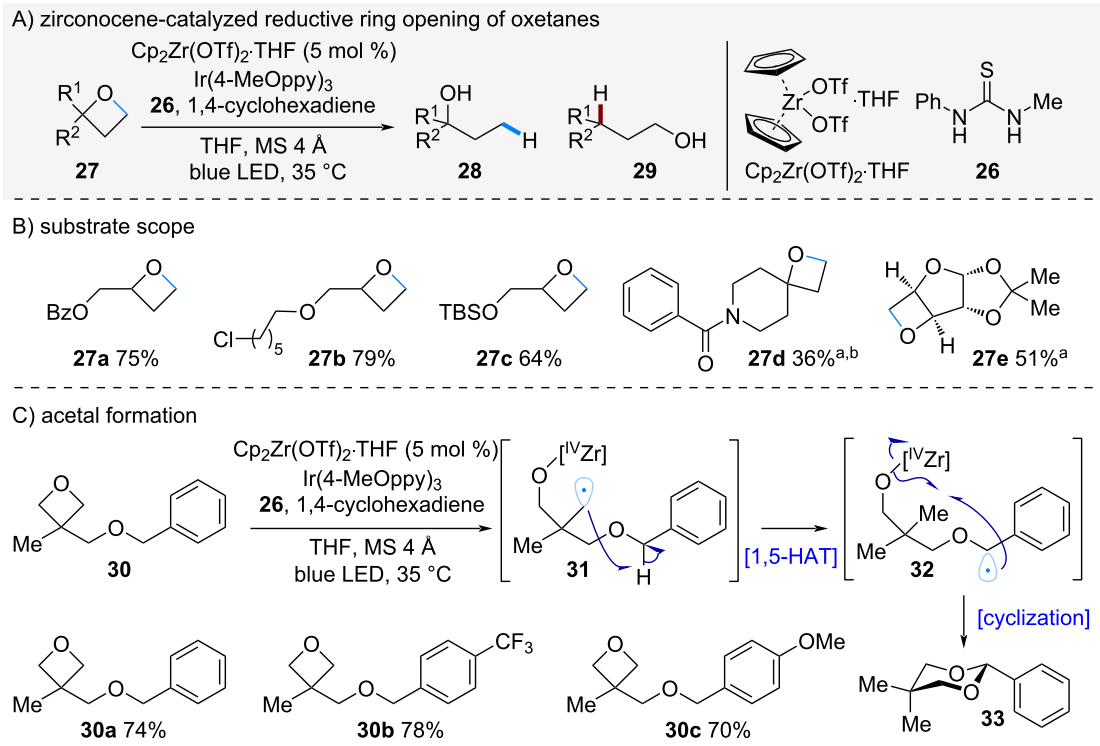

Scheme 6: Zr-catalyzed reductive ring opening of oxetanes. [a]10 mol % of $Cp_2Zr(OTf)_2$·THF was used. [b]$PhCF_3$ was used as a solvent.

the less substituted radical intermediate, affording the corresponding alcohol **28**. In contrast, when substrates bearing a benzylic alcohol moiety at the α-position were subjected to the same conditions, the reaction proceeded through radical intermediate **31**, which underwent a 1,5-hydrogen atom transfer (1,5-HAT) followed by intramolecular C–O bond formation to give the cyclic acetal **33**. This transformation was applicable to a range of oxetanes **30a–c** bearing benzylic alcohol derivatives, each affording the corresponding cyclic acetals in good yields.

In 2023, Ota and Yamaguchi et al. reported the hydrogenation of alkyl chlorides via halogen atom transfer (XAT) mediated by zirconocene bistosylate (Scheme 7A) [22]. Alkyl chlorides are inexpensive and readily available feedstocks; however, their chemical transformation has been challenging due to the high bond dissociation energy of the C–Cl bond compared to the C–Br and C–I bonds [12]. Motivated by the strong affinity of zirconium for halogens, they developed a catalytic system to address this issue. Treatment of alkyl chloride **34** with zirconocene bistosylate in the presence of an Ir-photoredox catalyst promoted halogen atom transfer to generate alkyl radical **35**. This radical then abstracted a hydrogen atom from 1,4-cyclohexadiene, affording the hydrogenated product **36**. The reaction proved broadly applicable to a wide range of alkyl chlorides.

For example, primary alkyl chlorides bearing functional groups such as amides (**34b**), esters (**34c**), ketones (**34d**), and phosphoesters (**34e**) underwent smooth hydrogenation to give the corresponding alkanes in good yields. Secondary (**34f–h**) and tertiary alkyl chlorides (**34i–k**) also reacted smoothly. Moreover, the method was successfully applied to complex molecules, including valine (**34l**), caffeine (**34m**), and glucofuranoside (**34n**), giving the desired products in good yields.

The catalytic system was further extended to the borylation of alkyl chlorides. (Scheme 7B). Under XAT conditions with $B_2(cat)_2$, the in situ-generated alkyl radical was trapped by diborane compound to form intermediate **39**, which was subsequently converted into pinacol boronate **40** upon treatment with pinacol in the presence of Et_3N. This transformation was likewise applicable to a broad range of alkyl chlorides, affording the corresponding alkylboronates **40a–j** in good yields.

The bibenzyl skeleton is commonly found in numerous natural products and bioactive compounds [23-25], and the development of efficient synthetic methods for its construction remains in high demand. Benzyl chlorides, which are inexpensive and readily available, have attracted attention as promising feedstocks. Against this background, Ota and Yamaguchi et al. in 2025 reported the dimerization of benzyl chlorides using

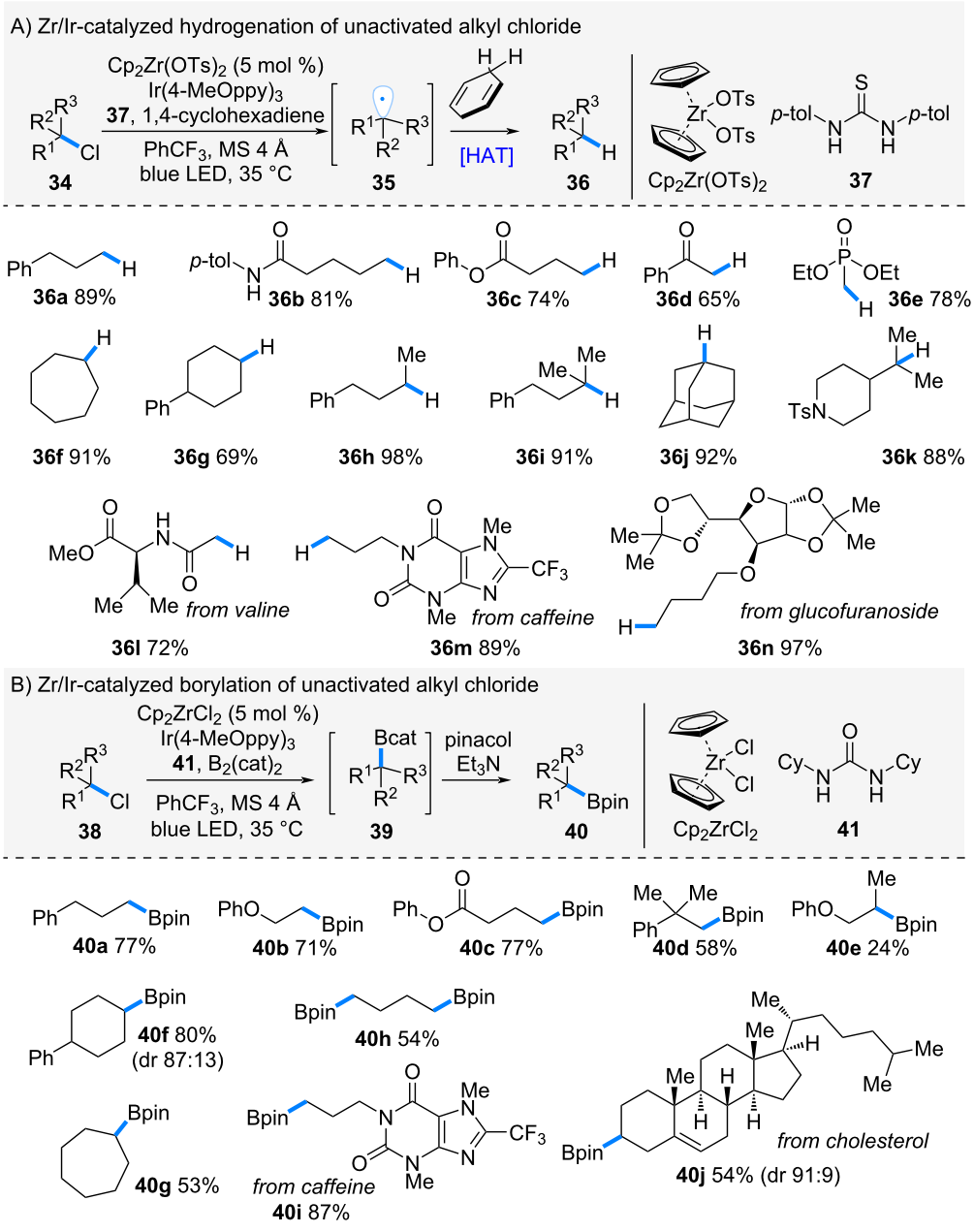

Scheme 7: Zr-catalyzed halogen atom transfer of alkyl chlorides.

zirconocene in combination with a photoredox catalyst (Scheme 8A) [26]. Treatment of benzyl chlorides with zirconocene dichloride in the presence of an Ir-photoredox catalyst promoted halogen atom transfer (XAT) from the C–Cl bond to generate benzyl radical **43**. Subsequent radical homocoupling afforded the desired bibenzyl dimer **44**.

The reaction proceeded efficiently regardless of the electronic character of the aromatic ring (Scheme 8B, **44a**–**c**). Furthermore, substrates containing various heteroaromatic motifs such as thiophene (**44d**), indole (**44e**), and oxazole (**44f**) also underwent smooth dimerization. The method applied to secondary alkyl chlorides, both acyclic (**44h**) and cyclic (**44i** and **44j**), as well as to benzyl chlorides derived from bioactive molecules such as fenofibrate (**44k**) and celestoride (**44l**), all of which furnished the corresponding dimers in excellent yields.

The proposed reaction mechanism is shown in Scheme 8C. Upon photoexcitation, the Ir^{III}* reduces Zr^{IV} to Zr^{III}. The resulting low-valent zirconium species abstracts a chlorine atom

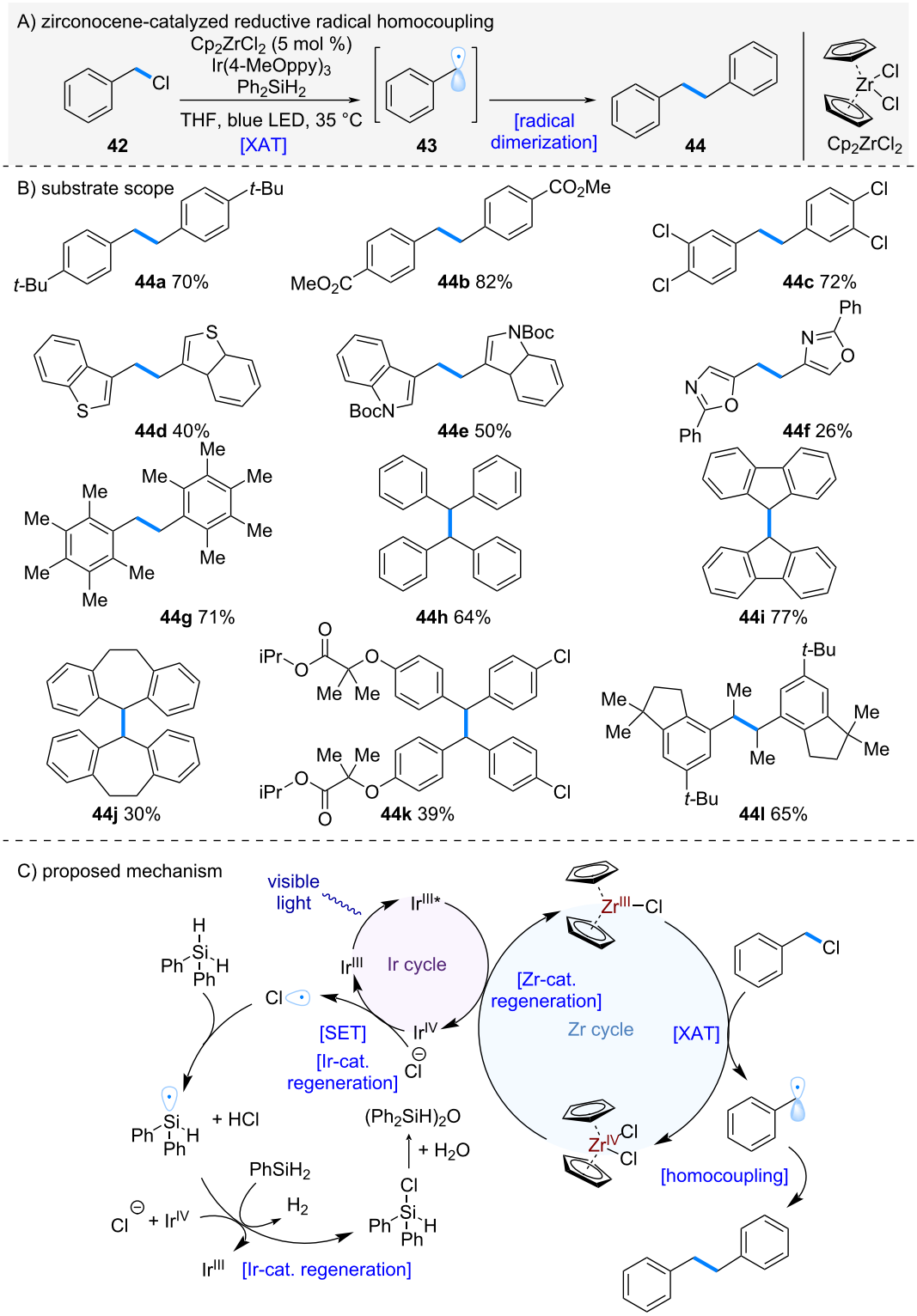

Scheme 8: Zr-catalyzed radical homo coupling of alkyl chlorides.

from the alkyl chloride, generating a benzyl radical, which undergoes homocoupling to give the desired dimer. The addition of $PhSiH_2$ was found to be beneficial, serving two roles: (1) scavenging HCl generated in the reaction, and (2) trapping chlorine radicals to form silyl radicals, which are subsequently oxidized by Ir^{IV}, thereby regenerating Ir^{III}.

In 2024, Ota and Yamaguchi et al. reported a zirconocene-mediated defluorination and subsequent functionalization of α-fluorocarbonyl compounds via halogen atom transfer (XAT) (Scheme 9A) [27]. Conventional defluorination reactions had largely been limited to trifluoromethyl groups, which possess relatively positive reduction potentials [28-34]. On the other hand, reductive transformations of monofluoroalkyl groups have been considered difficult due to their negative reduction potentials. In contrast, the authors focused on the comparatively small bond dissociation energy (BDE) of C(sp^3)–F bonds. Based on the hypothesis that this property could enable C–F bond functionalization via a halogen-atom transfer (XAT) mechanism, they initiated the development of monofluoroalkyl group functionalization.

Upon visible-light irradiation in the presence of an Ir photocatalyst and dibutylzirconocene, α-fluorocarbonyl compounds **45** underwent XAT with low-valent zirconium species to generate alkyl radicals **46**. When γ-terpinene was employed as a hydrogen donor, the radicals were reduced to the corresponding alkanes **47**. Alternatively, in the presence of olefins, radical addition proceeded smoothly to furnish functionalized products **48**. This methodology proved broadly applicable to a wide range of α-fluorocarbonyl substrates and olefins (Scheme 9B).

In 2025, Ota and Yamaguchi et al. reported a zirconocene-mediated selective cleavage of C–O bonds (Scheme 10A) [35]. The authors had previously demonstrated regioselective ring-opening reactions of epoxides and oxetanes by exploiting the strong affinity of zirconium for oxygen atoms [4,21]. Building on this concept, they envisioned that a similar reaction system could be applied to the homolytic cleavage of C–O bonds in alcohols and ethers.

When benzyl alcohol and ether derivatives **49** were treated with zirconocene in the presence of a photoredox catalyst, homolytic C–O bond cleavage occurred, generating alkyl radicals **50**. These radicals abstracted a hydrogen atom from γ-terpinene, affording the corresponding alkanes. In this reaction, oxo-bridged dimeric zirconocene was employed. This catalytic system was first reported by Romero and co-workers and used for ketone reduction to alcohols [36]. The reaction was applic-

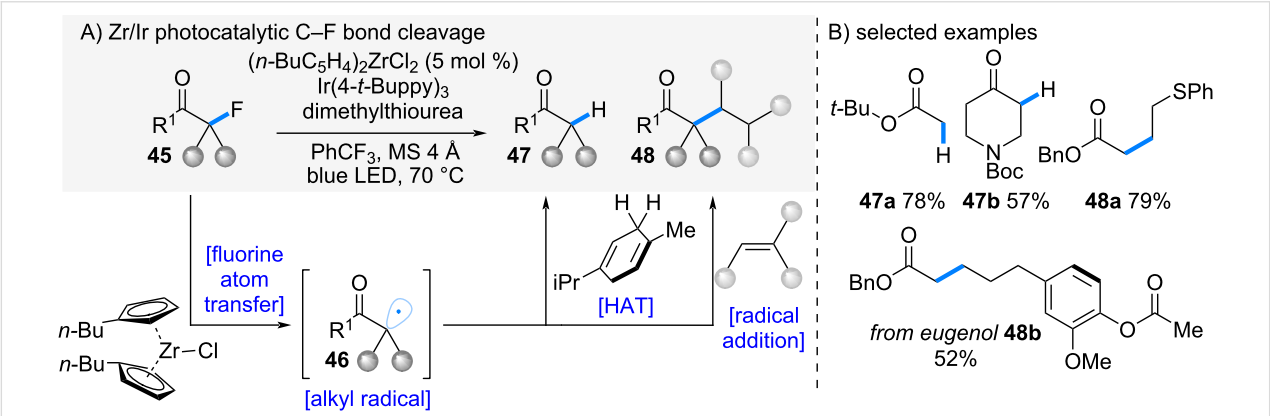

Scheme 9: Zr-catalyzed fluorine atom transfer.

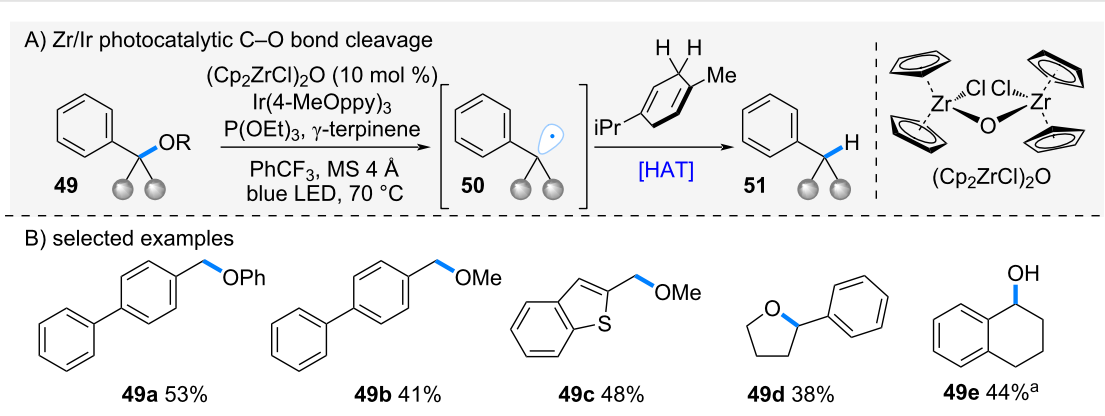

Scheme 10: Zr-catalyzed C–O bond cleavage. [a]Yield without the use of $P(OEt)_3$.

able to a range of benzyl alcohols and ethers **49a–e**, delivering the desired alkanes in moderate yields. Furthermore, when substrates containing multiple C–O bonds **49d** were employed, the reaction proceeded selectively at the benzylic position, giving the hydrogenated products with high site selectivity.

Zr-catalyzed radical reaction in the total synthesis of complex natural products

This section presents examples of zirconium-mediated reactions applied to the synthesis of complex molecules. For application in total synthesis, high functional group tolerance and mild reaction conditions are required. Accordingly, this section may provide helpful insight into the potential of zirconium-complex-mediated chemical transformations.

Kishi et al. explored the application of their developed ketone synthesis (Scheme 2) [9] to the total synthesis of the halichondrin family of natural products (Scheme 11) [37,38]. Ketone **57**, an intermediate in the synthesis of halichondrins, bears a β-alkoxy substituent, which raises concerns about potential epimerization via a retro-oxa-Michael/oxa-Michael pathway (Scheme 11A). To address this issue, the authors first examined

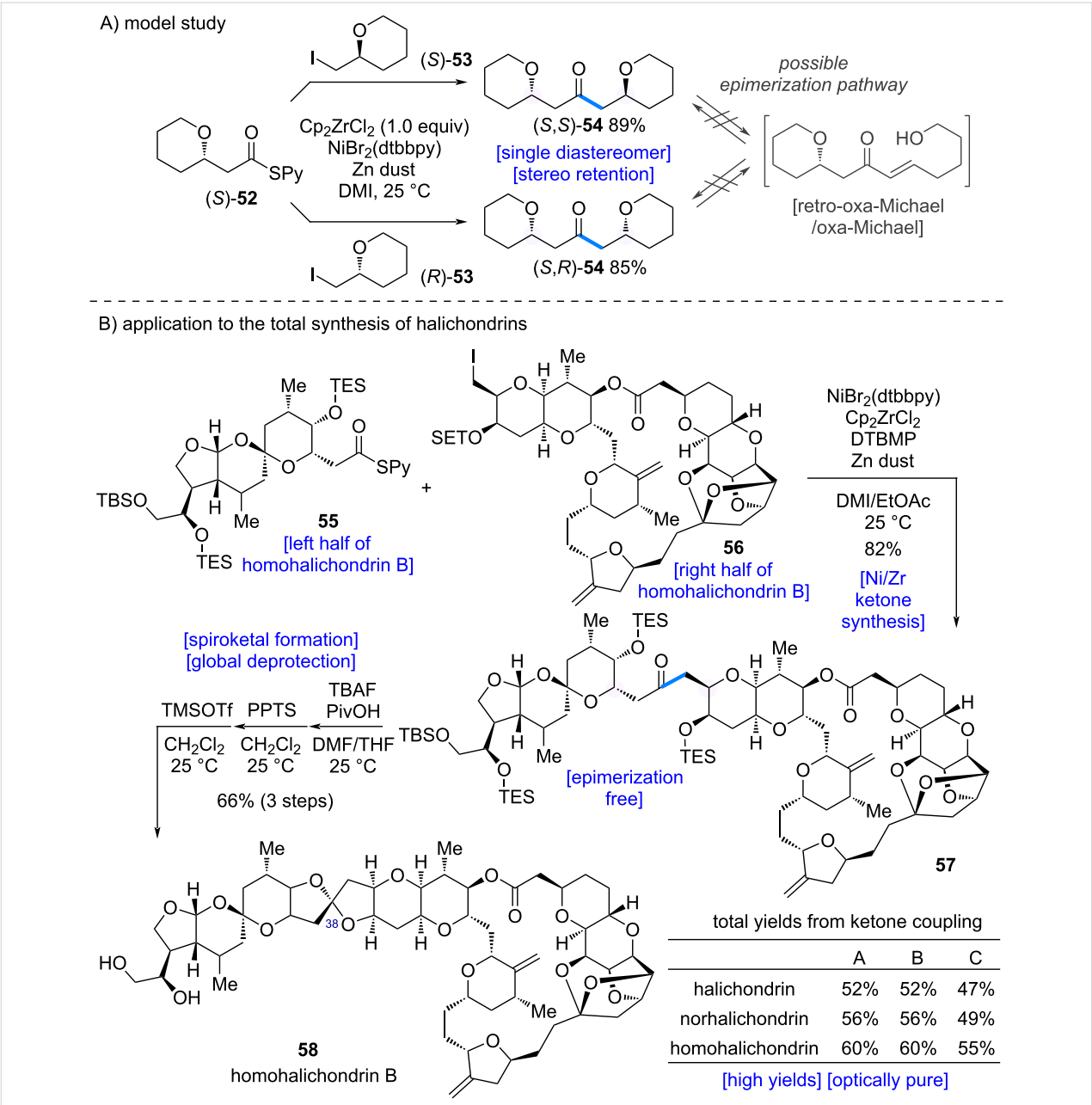

Scheme 11: Application to the total synthesis of halichondrins.

a model system. When β-alkoxythioesters (*S*)-**52** were coupled with chiral alkyl iodides (*S*)-**53** and (*R*)-**53** under the developed conditions, the desired β-alkoxy ketones **54** were obtained in good yields without epimerization, affording optically pure products. These results suggested that the developed reaction would be applicable to halichondrin synthesis.

The Zr/Ni-mediated ketone synthesis was then applied to the total synthesis of homohalichondrin B (**58**, Scheme 11B). Using a fragment corresponding to homohalichondrin B, the coupling reaction furnished ketone **57** in 82% yield. No epimerization at the β-position was observed, and **57** was obtained as a single product. Subsequent removal of the silyl protecting group under PivOH buffer/TBAF conditions, followed by PPTS treatment, enabled spiroketal formation. Finally, epimerization at C38 with TMSOTf completed the total synthesis of homohalichondrin B (**58**).

This synthetic strategy proved broadly applicable to multiple members of the halichondrin family, enabling the efficient synthesis of nine natural products: halichondrins A–C, norhalichondrins A–C, and homohalichondrins A–C. The Zr/Ni-mediated one-pot ketone synthesis developed by the Kishi group thus offers significant advantages over traditional methods, proceeding under mild conditions with easily prepared starting materials. Its versatility highlights the potential for broad application in drug discovery and the development of new materials.

In 2025, the Nakamura group achieved the first total synthesis of cyctetryptomycins A and B by employing a zirconium catalyst (Scheme 12) [5]. The synthesis commenced with the dimerization of 3-bromotryptophan derivative **59**. As an initial step, the authors sought to develop a mild and scalable method for the dimerization of **59** to afford the dimerized product **61** (Scheme 12A). A screening of various zirconocene catalysts revealed that a sterically bulky dibutylzirconocene catalyst (10 mol %) was particularly effective. Interestingly, the addition of 1,2-bis(diphenylphosphino)ethane (DPPE) (10 mol %) proved to be crucial for the success of the reaction.

DFT calculations suggested that in the transition state (**TS1**), a Cl–π interaction between the chlorine atom on the zirconocene catalyst and the aromatic ring of the substrate facilitated rapid halogen atom transfer (XAT), generating a radical at the C3 position of tryptophan. The resulting radical species underwent fast dimerization to furnish the desired dimer **61**.

This zirconocene-catalyzed dimerization proceeded smoothly under remarkably mild conditions at room temperature, suggesting broad applicability. Indeed, the reaction was shown to tolerate a wide substrate scope, with various 3-bromotryptophan derivatives **59** successfully undergoing dimerization (Scheme 12B).

The proposed mechanism is outlined in Scheme 12C. Zirconocene(IV) is reduced by Zn dust to generate Zr^{III}, which then promotes halogen atom transfer from the 3-bromotryptophan derivative **59** to form a radical species. Radical dimerization subsequently affords the desired product **61a**.

Mechanistic studies also revealed that $ZnCl_2$, a byproduct of the catalytic cycle, exerts a detrimental effect on the reaction. Specifically, $ZnCl_2$ coordinates with the two Boc groups of the substrate, raising the reduction potential from −1.1 V to −0.9 V. This shift increases the susceptibility of the benzylic radical intermediate to over-reduction, leading to undesired anionic species. To address this issue, DPPE was found to be effective: it captures $ZnCl_2$ to form complex **60**, thereby suppressing the increase in reduction potential and stabilizing the radical pathway.

The DFT calculations are shown in Scheme 13A. The activation barrier for the XAT process was calculated to be $\Delta G^{\ddagger}$ = 8.0 kcal/mol, indicating that this process can proceed spontaneously around room temperature. Moreover, the transition state (**TS1**) suggested the presence of a Cl–π interaction, which facilitates the facile XAT process. Since this step is accompanied by the formation of a strong Zr–Br bond [12], the overall process is exothermic (ΔG_{rxn} = −22.6 kcal/mol) and provides the thermodynamic driving force for the reaction.

Next, control experiments were conducted to evaluate the effect of Zn salts on the reaction (Scheme 13B). The standard dimerization conditions were applied to 3-bromotryptophan derivative **59b**, providing the desired dimer **61b** in 65% yield. The addition of 1 equivalent of $ZnCl_2$ reduced the yield to 31%. Furthermore, when $ZnCl_2$ (1 equiv) was added in the absence of dppe, the yield dropped further to 21%, and the over-reduced byproduct **62** was obtained in 72% yield. These results suggest that $ZnCl_2$ promotes the formation of the over-reduced compound **62**. Notably, the transformation does not require specialized equipment, such as a glovebox, and can be performed on a 100 g scale without difficulty. From a practical standpoint, this feature highlights the method's utility compared to existing approaches.

The established Zr-catalyzed dimerization was next applied to the total synthesis of the cyctetryptomycins (Scheme 14, **76** and **77**). The developed dimerization protocol proved scalable to 100 g scale, affording 40 g of the desired dimer **61b** in 47% yield. Subsequent removal of the two Boc groups with TMSI,

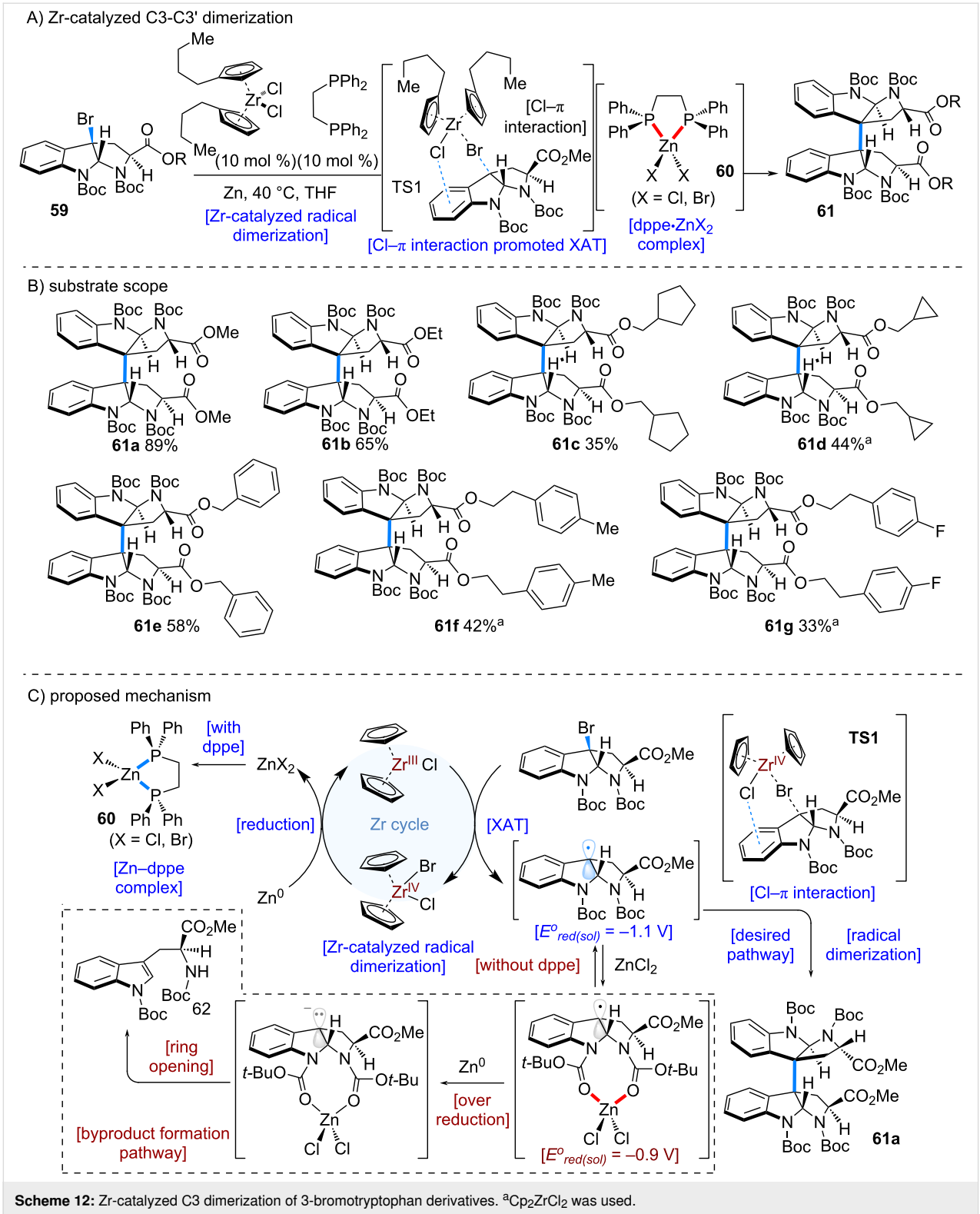

Scheme 12: Zr-catalyzed C3 dimerization of 3-bromotryptophan derivatives. [a]Cp_2ZrCl_2 was used.

followed by HATU-mediated amide coupling with various amino acids **65**–**67**, furnished the diketopiperazine precursors **68**–**70**. Heating these precursors under flash vacuum pyrolysis conditions at 230 °C led to the removal of the Boc group and intramolecular dehydration–condensation, thereby constructing the diketopiperazine core and enabling the total syntheses of ditryptophenaline (**70**), dibrevianamide F (**71**), and tetratryptomycin A (**72**).

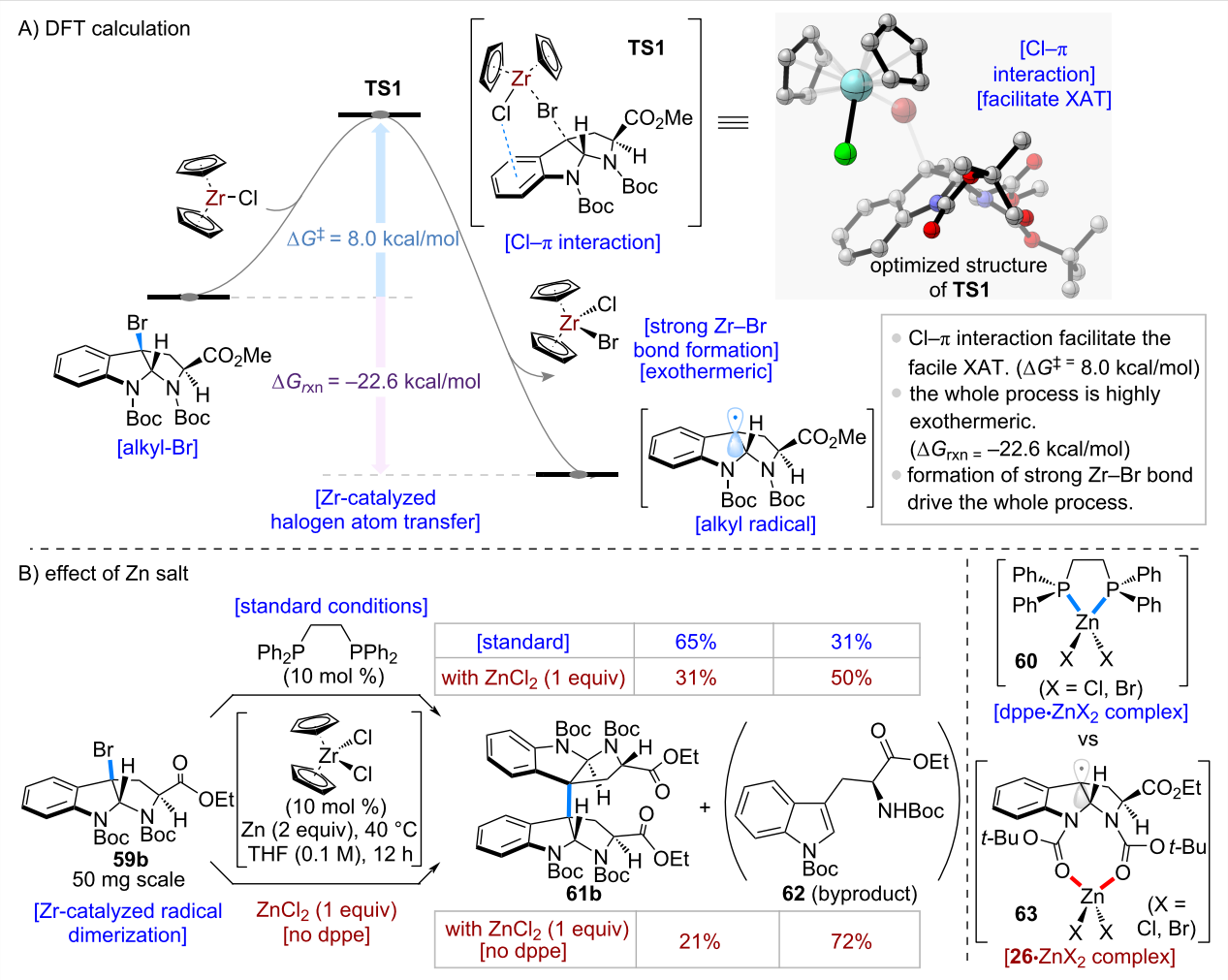

Scheme 13: Mechanistic studies.

Notably, this strategy enabled the preparation of tetratryptomycin A (**72**) on a multigram scale, providing a total of 21 g of tetratryptomycin A (**72**).

The synthesized tetratryptomycin A (**72**) was then employed in the total synthesis of cyctetryptomycins (**76** and **77**). Under chemical oxidation conditions, undesired over-oxidation occurred, and no cyclized product was detected. In contrast, enzymatic oxidation using CttpC successfully promoted the desired transformation, affording a separable mixture of cyctetryptomycin A (**76**) and cyctetryptomycin B (**77**). In this way, the total synthesis of the cyctetryptomycins (**76** and **77**) was accomplished. The development of a practical and scalable dimerization method of C3 bromo tryptophan derivative was crucial for this total synthesis.

Conclusion

Since the first organozirconium reagent was synthesized by Wilkinson and Birmingham in 1954 [2], zirconium has been widely employed in the field of organic synthesis. This widespread use is underpinned by zirconium's abundance in the Earth's crust and its low toxicity, among other advantageous properties.

Traditionally, its applications have predominantly involved two-electron processes via hydrozirconation. In recent years, however, single-electron transformations mediated by zirconium complexes have begun to emerge. This review systematically highlights the groundbreaking radical mechanisms involving zirconium complexes that have been reported. Zirconium exhibits unique characteristics – such as a strong affinity for heteroatoms – that offer the potential to enable chemical transformations previously unsolved.

Nevertheless, compared to other transition metals like nickel and palladium, the development of zirconium-based catalysis is still in its early stages, leaving ample room for further exploration. The application of zirconium catalysts in radical reac-

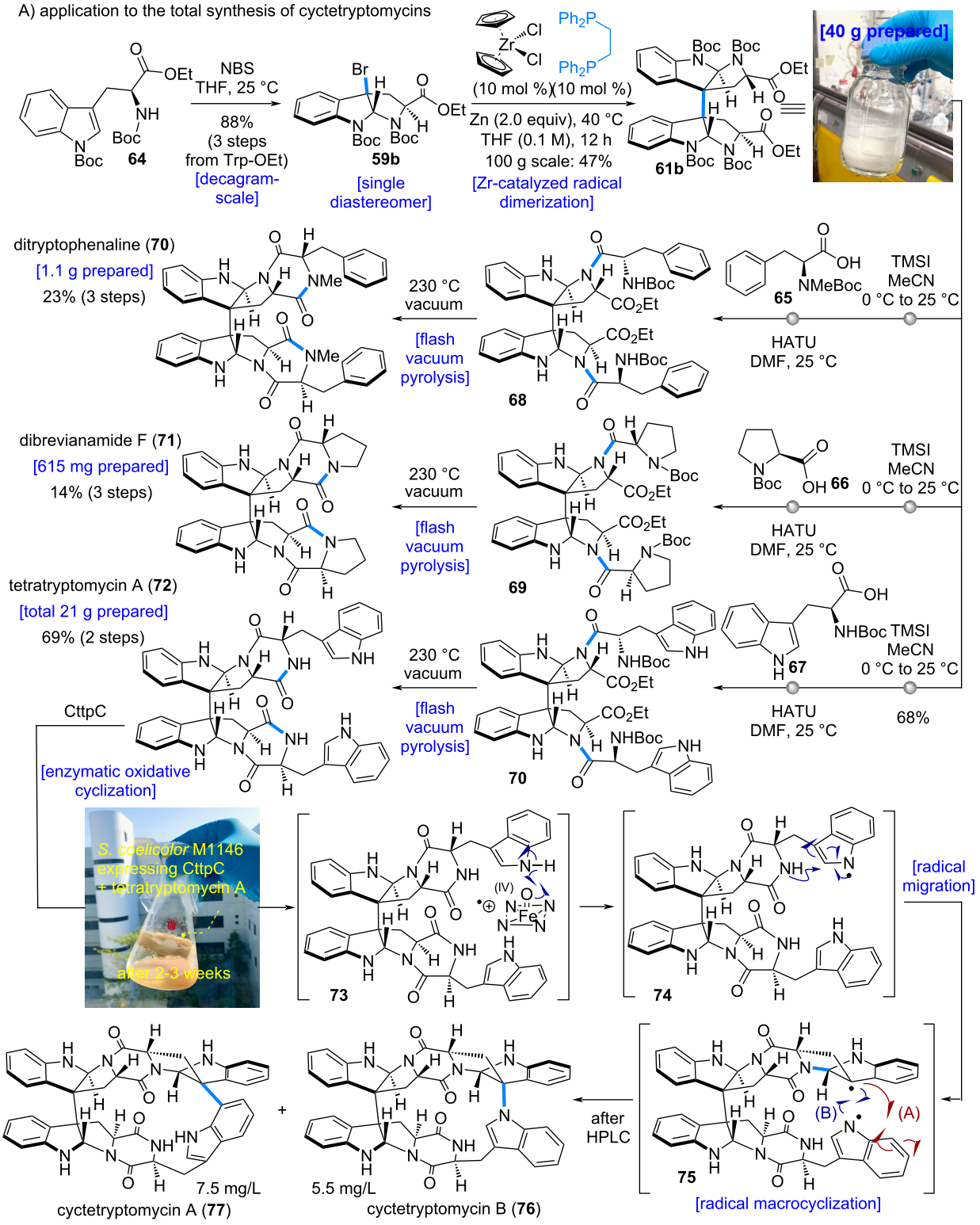

Scheme 14: Application to the total synthesis of cyctetryptomycins. A photo of compound **61b** was taken by the authors (Ogawa, H. and Nakamura, H.). This content is not subject to CC BY 4.0. A photo of "S. coelicolor M1146 expressing CttpC + tetratryptomycin A after 2–3 weeks" was reproduced from [5] (© 2024 L. Yu et al., published by Wiley-VCH GmbH, distributed under the terms of the Creative Commons Attribution 4.0 International License, https://creativecommons.org/licenses/by/4.0/

tions is expected to make significant contributions to diverse fields, including drug discovery and the development of advanced functional materials. This review will provide a conceptual foundation for future research in this promising area.

Acknowledgements

The image depicted in the background of the graphical abstract was purchased from iStock.com/Just_Super. This content is not subject to CC BY 4.0.

Author Contributions

Hiroshige Ogawa: conceptualization; writing – original draft; writing – review & editing. Hugh Nakamura: conceptualization; supervision; writing – original draft; writing – review & editing.

ORCID® iDs

Hugh Nakamura - https://orcid.org/0000-0001-5475-7883

Data Availability Statement

Data sharing is not applicable as no new data was generated or analyzed in this study.

References

1. Nielsen, R. H.; Schlewitz, J. H.; Nielsen, H. Zirconium and Zirconium Compounds. *Kirk-Othmer Encyclopedia of Chemical Technology;* John Wiley & Sons: Hoboken, NJ, USA, 2013; pp 1–46. doi:10.1002/0471238961.26091803.a01.pub3
2. Wilkinson, G.; Birmingham, J. M. *J. Am. Chem. Soc.* **1954,** *76,* 4281–4284. doi:10.1021/ja01646a008
3. Hart, D. W.; Schwartz, J. *J. Am. Chem. Soc.* **1974,** *96,* 8115–8116. doi:10.1021/ja00833a048
4. Aida, K.; Hirao, M.; Funabashi, A.; Sugimura, N.; Ota, E.; Yamaguchi, J. *Chem* **2022,** *8,* 1762–1774. doi:10.1016/j.chempr.2022.04.010
5. Yu, L.; Ogawa, H.; Li, S.; Lam Cheung, T.; Liu, W.; Yan, D.; Matsuda, Y.; Kobayashi, Y.; Guo, Z.; Ikeda, K.; Hamlin, T. A.; Yamazaki, K.; Qian, P.-Y.; Nakamura, H. *Angew. Chem., Int. Ed.* **2025,** *64,* e202414295. doi:10.1002/anie.202414295
6. Ota, E.; Aida, K.; Yamaguchi, J. *Chem. Lett.* **2024,** *53,* upae095. doi:10.1093/chemle/upae095
7. Fujita, K.; Yorimitsu, H.; Oshima, K. *Bull. Chem. Soc. Jpn.* **2004,** *77,* 1727–1736. doi:10.1246/bcsj.77.1727
8. Fujita, K.; Nakamura, T.; Yorimitsu, H.; Oshima, K. *J. Am. Chem. Soc.* **2001,** *123,* 3137–3138. doi:10.1021/ja0032428
9. Ai, Y.; Ye, N.; Wang, Q.; Yahata, K.; Kishi, Y. *Angew. Chem., Int. Ed.* **2017,** *56,* 10791–10795. doi:10.1002/anie.201705520
10. Yus, M.; Nájera, C.; Foubelo, F. *Tetrahedron* **2003,** *59,* 6147–6212. doi:10.1016/s0040-4020(03)00955-4
11. Smith, A. B., III; Adams, C. M. *Acc. Chem. Res.* **2004,** *37,* 365–377. doi:10.1021/ar030245r
12. Luo, Y.-R. *Comprehensive Handbook of Chemical Bond Energies,* 1st ed.; CRC Press: Boca Raton, FL, USA, 2007. doi:10.1201/9781420007282
13. Yoshida, S.; Yorimitsu, H.; Oshima, K. *J. Organomet. Chem.* **2007,** *692,* 3110–3114. doi:10.1016/j.jorganchem.2006.12.029
14. Zhang, Y.; Petersen, J. L.; Milsmann, C. *Organometallics* **2018,** *37,* 4488–4499. doi:10.1021/acs.organomet.8b00388
15. Zhang, Y.; Petersen, J. L.; Milsmann, C. *J. Am. Chem. Soc.* **2016,** *138,* 13115–13118. doi:10.1021/jacs.6b05934
16. Gansäuer, A.; Barchuk, A.; Keller, F.; Schmitt, M.; Grimme, S.; Gerenkamp, M.; Mück-Lichtenfeld, C.; Daasbjerg, K.; Svith, H. *J. Am. Chem. Soc.* **2007,** *129,* 1359–1371. doi:10.1021/ja067054e
17. Gansäuer, A.; Fleckhaus, A.; Lafont, M. A.; Okkel, A.; Kotsis, K.; Anoop, A.; Neese, F. *J. Am. Chem. Soc.* **2009,** *131,* 16989–16999. doi:10.1021/ja907817y
18. Klare, S.; Gordon, J. P.; Gansäuer, A.; RajanBabu, T. V.; Nugent, W. A. *Tetrahedron* **2019,** *75,* 130662. doi:10.1016/j.tet.2019.130662
19. Fernández-Mateos, A.; Encinas Madrazo, S.; Herrero Teijón, P.; Rubio González, R. *J. Org. Chem.* **2009,** *74,* 3913–3918. doi:10.1021/jo900479v
20. Barrero, A. F.; Quílez del Moral, J. F.; Sánchez, E. M.; Arteaga, J. F. *Org. Lett.* **2006,** *8,* 669–672. doi:10.1021/ol052849w
21. Ota, E.; Yamaguchi, J.; Aida, K. *Synlett* **2024,** *35,* 451–454. doi:10.1055/s-0041-1738454
22. Okita, T.; Aida, K.; Tanaka, K.; Ota, E.; Yamaguchi, J. *Precis. Chem.* **2023,** *1,* 112–118. doi:10.1021/prechem.2c00002
23. Harrowven, D. C.; Kostiuk, S. L. *Nat. Prod. Rep.* **2012,** *29,* 223–242. doi:10.1039/c1np00080b
24. Keylor, M. H.; Matsuura, B. S.; Stephenson, C. R. J. *Chem. Rev.* **2015,** *115,* 8976–9027. doi:10.1021/cr500689b
25. Zhang, X.; Chen, W.; Du, Y.; Su, P.; Qiu, Y.; Ning, J.; Liu, M. *J. Ethnopharmacol.* **2021,** *276,* 114143. doi:10.1016/j.jep.2021.114143
26. Tajima, R.; Tanaka, K.; Aida, K.; Ota, E.; Yamaguchi, J. *Precis. Chem.* **2025,** *3,* 43–50. doi:10.1021/prechem.4c00077
27. Takimoto, H.; Aida, K.; Nishimoto, Y.; Yokogawa, D.; Ota, E.; Yamaguchi, J. *ChemRxiv* **2024**. doi:10.26434/chemrxiv-2024-ssj00
28. Chen, K.; Berg, N.; Gschwind, R.; König, B. *J. Am. Chem. Soc.* **2017,** *139,* 18444–18447. doi:10.1021/jacs.7b10755
29. Luo, Y.-C.; Tong, F.-F.; Zhang, Y.; He, C.-Y.; Zhang, X. *J. Am. Chem. Soc.* **2021,** *143,* 13971–13979. doi:10.1021/jacs.1c07459
30. Sugihara, N.; Suzuki, K.; Nishimoto, Y.; Yasuda, M. *J. Am. Chem. Soc.* **2021,** *143,* 9308–9313. doi:10.1021/jacs.1c03760
31. Kynman, A. E.; Elghanayan, L. K.; Desnoyer, A. N.; Yang, Y.; Sévery, L.; Di Giuseppe, A.; Tilley, T. D.; Maron, L.; Arnold, P. L. *Chem. Sci.* **2022,** *13,* 14090–14100. doi:10.1039/d2sc04192h
32. Wang, T.; Zong, Y.-Y.; Huang, T.; Jin, X.-L.; Wu, L.-Z.; Liu, Q. *Chem. Sci.* **2023,** *14,* 11566–11572. doi:10.1039/d3sc03771a
33. Huang, J.; Gao, Q.; Zhong, T.; Chen, S.; Lin, W.; Han, J.; Xie, J. *Nat. Commun.* **2023,** *14,* 8292. doi:10.1038/s41467-023-44097-y
34. Ghosh, S.; Qu, Z.-W.; Roy, S.; Grimme, S.; Chatterjee, I. *Chem. – Eur. J.* **2023,** *29,* e202203428. doi:10.1002/chem.202203428
35. Aida, K.; Tajima, R.; Ota, E.; Yamaguchi, J. *Tetrahedron Lett.* **2025,** *169,* 155741. doi:10.1016/j.tetlet.2025.155741
36. Kehner, R. A.; Hewitt, M. C.; Bayeh-Romero, L. *ACS Catal.* **2022,** *12,* 1758–1763. doi:10.1021/acscatal.2c00079
37. Kranthikumar, R.; Kishi, Y. *Org. Lett.* **2024,** *26,* 7105–7109. doi:10.1021/acs.orglett.4c02297
38. Yahata, K.; Ye, N.; Ai, Y.; Iso, K.; Kishi, Y. *Angew. Chem., Int. Ed.* **2017,** *56,* 10796–10800. doi:10.1002/anie.201705523

BEILSTEIN JOURNAL OF ORGANIC CHEMISTRY

Total synthesis of natural products based on hydrogenation of aromatic rings

Haoxiang Wu and Xiangbing Qi*

Review

Open Access

Address:
National Institute of Biological Sciences, Beijing. No. 7, Science Park Road, Zhongguancun Life Science Park, Changping District, 102206 Beijing, China

Email:
Xiangbing Qi* - qixiangbing@nibs.ac.cn

* Corresponding author

Keywords:
aromatic rings; dearomatization; hydrogenation; natural products; total synthesis

Beilstein J. Org. Chem. **2026,** *22,* 88–122.
https://doi.org/10.3762/bjoc.22.4

Received: 01 October 2025
Accepted: 19 December 2025
Published: 07 January 2026

This article is part of the thematic issue "Concept-driven strategies in target-oriented synthesis".

Guest Editor: Y. Tang

Abstract

Arenes and heteroarenes are easily available building blocks in organic chemistry, and saturation the aromatic ring facilitates synthetic chemists to efficiently synthesize natural products with complex three-dimensional structures. Recent advances in catalyst and ligand design have enabled unprecedented progress in the catalytic hydrogenation of (hetero)aromatic systems. Quinoline, isoquinoline, pyridine, and related substrates can now be reduced with high efficiency and stereoselectivity, providing efficient access to saturated and partially saturated architectures vital to synthetic chemistry. Furthermore, catalytic asymmetric aromatic hydrogenation has facilitated the asymmetric total synthesis of complex natural products and pharmaceutical agents. This review highlights recent advances in catalytic (hetero)arene hydrogenation, with a focus on its application in natural product synthesis.

Introduction

For decades, a principal objective in natural product synthesis has been the development and utilization of efficient methods to access molecular frameworks with defined stereochemical complexity [1]. Natural products, such as taxol [2], strychnine [3-5], and tetrodotoxin [6-8], which contain complex three-dimensional structures, make total synthesis challenging. The retrosynthetic analysis [9], alongside the evolution of methodologies such as “two-phase synthesis” [10], “biomimetic synthesis” [11], or “protecting-group-free synthesis” [12], has progressively streamlined synthetic strategies. The integration of photochemistry [13] and electrochemistry [14] into total synthesis has further extended the realm. Synthesis of complex natural product structures can promote the discovery of new reactions and the generation of new strategies [15]. However, despite careful design, the primary building blocks used in natural product syntheses are often difficult to prepare or scale-up, constrained by subtle chemical reactivity, functional group compatibility, and control of stereoselectivity. Together, these factors continue to shape the pursuit of concise and practical synthetic routes to complex natural products [16,17].

Arenes and heteroarenes have long been readily accessible, as many can be obtained through industrial synthesis or microbial fermentation. The diverse reactivity of aromatic compounds has made them indispensable starting materials in synthetic and medicinal chemistry [18-20]. In recent years, promoted by the rapid development of asymmetric catalysis, a wealth of reactions applicable to aromatic systems – including substitution reactions, transition-metal-coupling reactions, and even dearomatization [21-23] – have been reported, further extending their utility in complex molecule synthesis.

Saturated heterocycles containing sp^3-hybridized carbons play a pivotal role in natural products as well as pharmaceutical agents, as their three-dimensional structures enable more precise interactions in biological systems [24]. Among the various strategies to access these saturated frameworks, catalytic hydrogenation of unsaturated arenes stands out as the most efficient one: it directly transforms planar sp^2 systems into three-dimensional sp^3-rich scaffolds via the shortest possible synthetic route, embodying both step economy and atom economy (Scheme 1) [25].

Although oxidative dearomatization has been a widely studied and powerful approach in synthetic chemistry [21,26-28], researchers have gradually recognized its inherent limitations, including narrow substrate scope, poor selectivity, and low functional group compatibility. Under the circumstance of atom economy and concise synthesis, catalytic hydrogenation of (hetero)arenes has re-emerged as an attractive and practical alternative, offering a complementary pathway to transform planar aromatic systems into saturated or partially saturated, three-dimensional structures.

Key challenges in hydrogenation of aromatic rings

The catalytic hydrogenation of arenes offers a powerful route to disrupt aromaticity and access synthetically valuable intermediates. However, its implementation in strategic synthesis has been hindered by the persistent challenge of controlling selectivity across diverse substrate electronic environments [29]. Reactivity is governed by the electron density of arenes, which directly influences kinetics and product distributions [30,31]. The inability to generically modulate this interaction has confined most catalytic systems to narrow substrate scopes. Addressing this limitation requires the design of catalysts that achieve precise electronic complementarity, enabling selective activation across a broad spectrum of aromatic compounds (Scheme 2) [32].

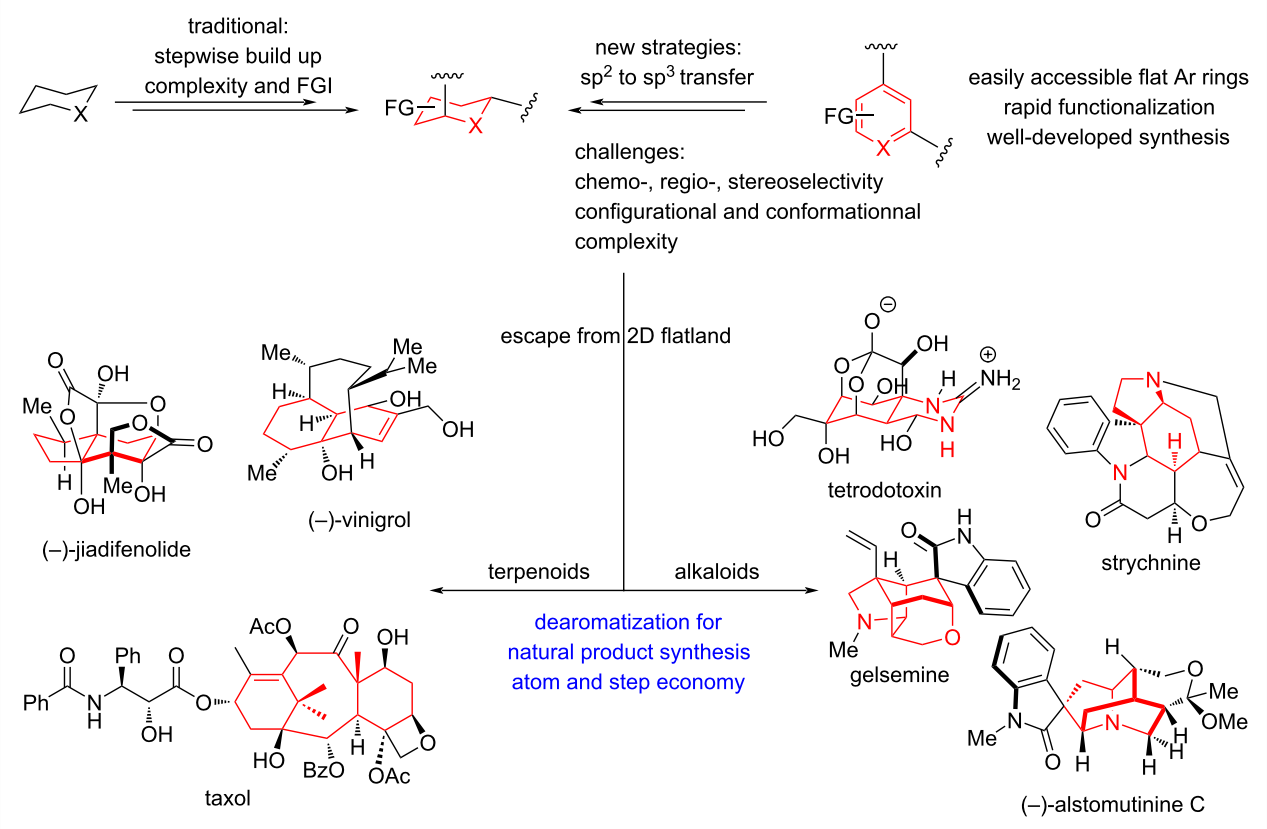

Scheme 1: The association between dearomatization and natural product synthesis.

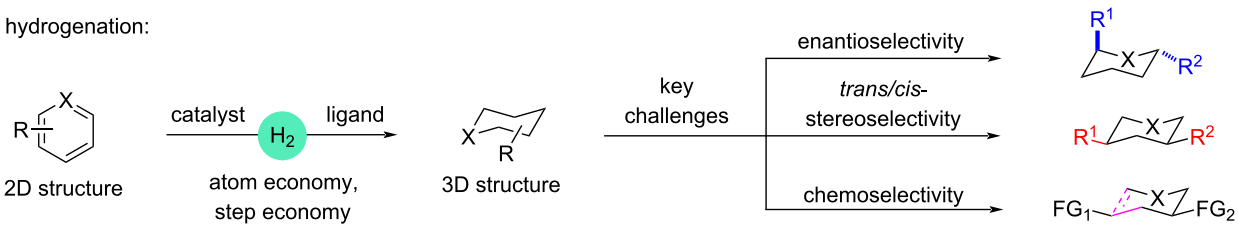

Scheme 2: Key challenges in hydrogenation of aromatic rings.

From the standpoint of scalable synthesis, catalyst cost is a major bottleneck in aromatic hydrogenation. Most state-of-the-art systems depend on expensive transition metals such as platinum, ruthenium, or palladium, inflating the cost of large-scale applications. In addition, precious-metal catalysts often display poor selectivity, while heteroatoms in heteroarenes – acting as Lewis bases – tend to coordinate to the metal center and complicate catalysis. Consequently, designing cost-effective catalytic systems with enhanced efficiency, particularly for the selective hydrogenation of complex substrates, remains an essential direction for future research [33].

Hydrogenation of arenes has rapidly evolved from a specialized transformation into a broadly enabling strategy in complex molecule synthesis, yet a unified perspective connecting recent methodological advances with their strategic applications in the total synthesis of natural products remains lacking. Although several reviews discuss catalyst development for (hetero)arene hydrogenation, they typically treat the topic from a purely methodological angle and seldom address its growing influence on retrosynthetic analysis [30,32,34-36]. Meanwhile, the capability to convert flat, readily accessible aromatic feedstocks into stereochemically defined, three-dimensional scaffolds with exceptional step and atom economy has begun to reshape how to design synthetic routes toward architecturally complex natural products.

The past five years have witnessed significant methodological evolution in the hydrogenation of (hetero)arenes. However, a systematic analysis correlating catalyst innovation with its application in complex natural product synthesis – remains lacking. This review would offer a strategic framework for synthetic chemists and identifies prevailing challenges and future opportunities of the field.

Review

The methodologies in hydrogenation of aromatic rings

Encompassing both homogeneous and heterogeneous systems, the hydrogenation of (hetero)arenes has become a cornerstone of modern synthesis for constructing saturated carbocycles and heterocycles [37]. When an appropriate ligand is paired with a transition-metal catalyst, stereoselective hydrogenation of aromatic rings becomes achievable, enabling access to reduced products with well-defined configurations [38]. Although the repertoire of ligands capable of exerting precise stereocontrol remains limited, each provides distinct advantages that suit different metals and reaction conditions. From the perspective of the catalyst itself, a central scientific challenge is how to maintain high catalytic activity throughout the reaction, while preventing deactivation caused by coordination of heteroatoms that may be present in the reduced products.

While the following subsections categorize hydrogenation strategies by substrate class (monocyclic vs fused; heterocycle vs carbocycle), all catalytic systems must still address the fundamental selectivity challenges inherent to arene reduction – chemo-, regio-, and stereoselectivity. Chemoselectivity becomes particularly demanding when reducible groups such as olefins or carbonyls are present, often requiring fine-tuning of the reaction conditions to prevent overreduction. Disruption of aromaticity also creates multiple potential reduction sites, and subtle electronic or substituent differences can lead to regioisomers, especially in polysubstituted or fused systems. In addition, converting a planar sp^2-hybridized-atoms-enriched framework into three-dimensional sp^3-hybridized-atoms-enriched architectures inherently generates new stereocenters, making stereocontrol essential in asymmetric variants. As highlighted in the methods below, recent advances in catalyst and ligand design showcase complementary solutions to these selectivity issues, with each substrate class imposing its own opportunities on hydrogenation outcomes.

With these considerations in mind, the following section categorizes catalytic hydrogenation strategies by arene substrate type and highlights representative examples that illustrate recent synthetic advances [35,36].

Hydrogenation of monocyclic aromatic rings

Hydrogenation of heterocyclic aromatic rings: Despite the widespread application of six-membered aromatic heterocycles

in various fields of organic chemistry, reports on their catalytic hydrogenation are relatively rare. This is partly due to the high stability of six-membered aromatic heterocycles, such as pyridine, making it difficult to interrupt the aromaticity under mild conditions [34]. Furthermore, the heteroatoms (such as nitrogen and oxygen atoms) within the saturated heterocycles exhibit strong Lewis basicity, potentially complexing and deactivating catalysts. Consequently, the catalytic hydrogenation of six-membered aromatic heterocycles such as pyridine often requires the introduction of substituents or activation of the aromatic heterocycle to facilitate hydrogenation.

Between 2020 and 2021, the research groups of Zhang [39], Bao [40], Zhou [41], and Glorius [42] reported four different methods for the reductive hydrogenation of pyridine or pyridine derivatives (Scheme 3). By activating pyridine to a pyridinium salt, the hydrogenated product can be efficiently obtained in the presence of metal catalysts including Pd or Ir and different ligands. In 2021 and 2022, Wang and co-workers reported two impressive hydroboration–hydrogenation reactions catalyzed by FLP (triarylphenylborane) that reduced pyridine compounds **11** or **15** to dihydropyridine compounds **12** or chiral piperidine **17** (Scheme 3) [43,44]. Mechanistic studies demonstrated that the nitrogen atoms present in both pyridine and piperidine complexed with the triarylborane, cleaving the H–H bond and reducing the pyridine. In 2022, Xiao and co-workers reported a study on the conversion of isolated pyridinium salts **18**, **20** to piperidine compounds using $[CpRhCl_2]_2$ as a metal catalyst and formic acid as a hydrogen source (Scheme 3) [45]. Different with other previous studies, this method allows for substituents at the 3-position of pyridine, enabling the rapid preparation of chiral piperidine compounds. It should be noted that in the presence of water, the reaction would undergo transamination with the pyridinium nitrogen moiety while inducing chirality on the ring.

Hydrogenation of carbocyclic aromatic rings: In 2021, Andersson and co-workers reported a rhodium-catalyst precursor capable of operating in both homogeneous and heterogeneous phases to achieve asymmetric complete hydrogenation of vinyl aromatics – a long-standing challenge in arene reduction (Scheme 4) [46]. By tuning the ratio of phosphine ligand to rhodium precursor, they controlled the formation of distinct catalytic species, which remained mutually compatible, and rationalized facial selectivity through insights from asymmetric styrene hydrogenation. In 2024, Glorius and co-workers developed a chemoselective hydrogenation strategy capable of selectively reducing benzene rings in the presence of pyridine rings (Scheme 4) [47]. Supported by fragment-based screening across a broad substrate set, their method efficiently provides cyclohexane and piperidine frameworks commonly found in bioactive molecules and pharmaceutical intermediates. In the same year, Yu and co-worker described another mild and convenient approach to reduce monocyclic aromatic rings (Scheme 4) [48]. Using $[Rh(nbd)Cl]_2$ and Pd/C as catalysts, aromatic hydrocarbons with various functional groups can be hydrogenated at room temperature and 1 atmosphere of hydrogen, thus simplifying the reaction operation and cost.

Hydrogenation of fused aromatic rings

Hydrogenation of the heterocycle part: Quinoline, one of the most accessible heteroaromatic feedstocks from natural and commercial sources, has long attracted interest in both synthetic and medicinal chemistry. A central challenge, however, is the selective catalytic hydrogenation of quinolines to the synthetically valuable partially or fully saturated derivatives [49]. Over the past years, several research groups worldwide have reported significant progress toward addressing these selectivity and reactivity issues (Scheme 5 and Scheme 6). Nevertheless, despite these advances, the field still suffers from fundamental limitations in terms of substrate scope, stereoselectivity, and scalability, leaving ample room for innovation in catalyst design and mechanistic understanding.

Fan and co-workers have long been dedicated to the asymmetric catalysis of chiral diamine ruthenium complexes. In 2020, they reported the efficient hydrogenation of the polycyclic aromatic compound PyBQ to PyBTHQ using this catalyst in HFIP (Scheme 5) [50]. Under the optimized conditions, only the heteroaromatic part of quinoline was reduced selectively, while the benzene ring and pyridine remained unchanged. In 2020, Beller and co-workers used a manganese catalyst to achieve the hydrogenation of the nitrogen heterocyclic moiety in quinoline, that yielded the target product in near-quantitative amounts [51]. In 2021, the research groups of Sun [52] and Zhang [53] reported the use of iridium or manganese as catalysts to convert quinoline derivatives into tetrahydroquinolines by using dihydrogen or formic acid as the hydrogen source. In 2021 and 2024, Liu and co-workers demonstrated that with [NNP-Mn] catalysts, the hydrogenation of quinoline and its derivatives can proceed with high regio- and stereoselectivity [54,55] (Scheme 5).

In 2022, Stoltz and co-workers reported for the first time the reduction of 1,3-disubstituted isoquinoline compounds **45** to *trans*-quinoxalines **46** (Scheme 6) [56]. By using iridium catalysts and commercially available chiral JosiPhos ligands, a batch of enantioriched *trans*-tetrahydroisoquinolines could be prepared efficiently and stereoselectively. In 2023, Chen in collaboration with Zhang, reported a simple and efficient rhodium–thiourea-catalyzed asymmetric hydrogenation reaction for the synthesis of highly optically pure tetrahydroquinox-

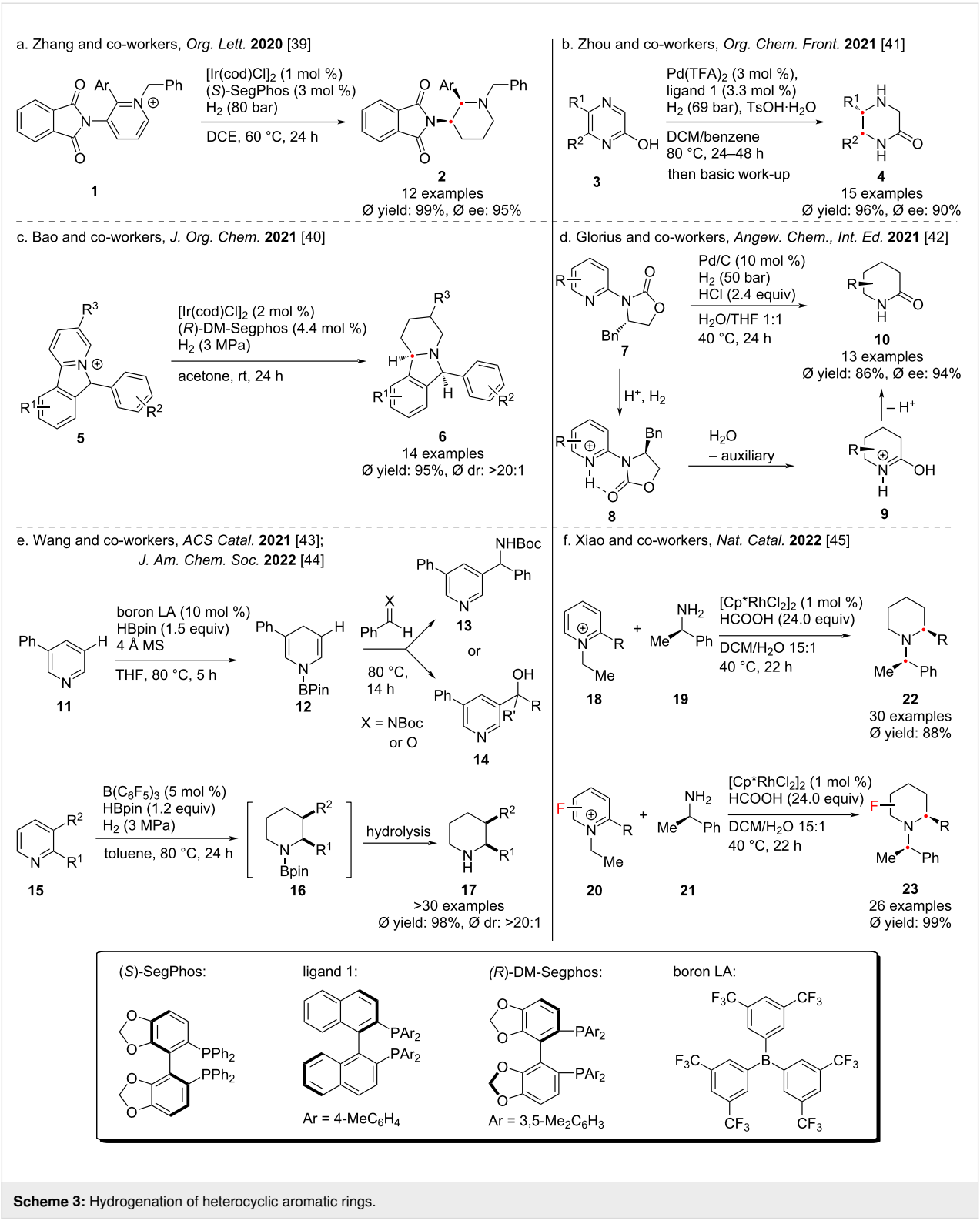

Scheme 3: Hydrogenation of heterocyclic aromatic rings.

aline **48** and dihydroquinoxalinones **50** (Scheme 6) [57]. Due to the mild conditions and broad substrate range, the reaction was scaled up to the gram scale with high yield and high enantioselectivity. Recently, Du and co-workers reported a transition-metal-free asymmetric transfer hydrogenation reaction (Scheme 6) [58]. Under a hydrogen atmosphere, using chiral phosphoric acid and achiral borane as catalysts, they synthesized 2-substituted quinoxalines **52** in high yield.

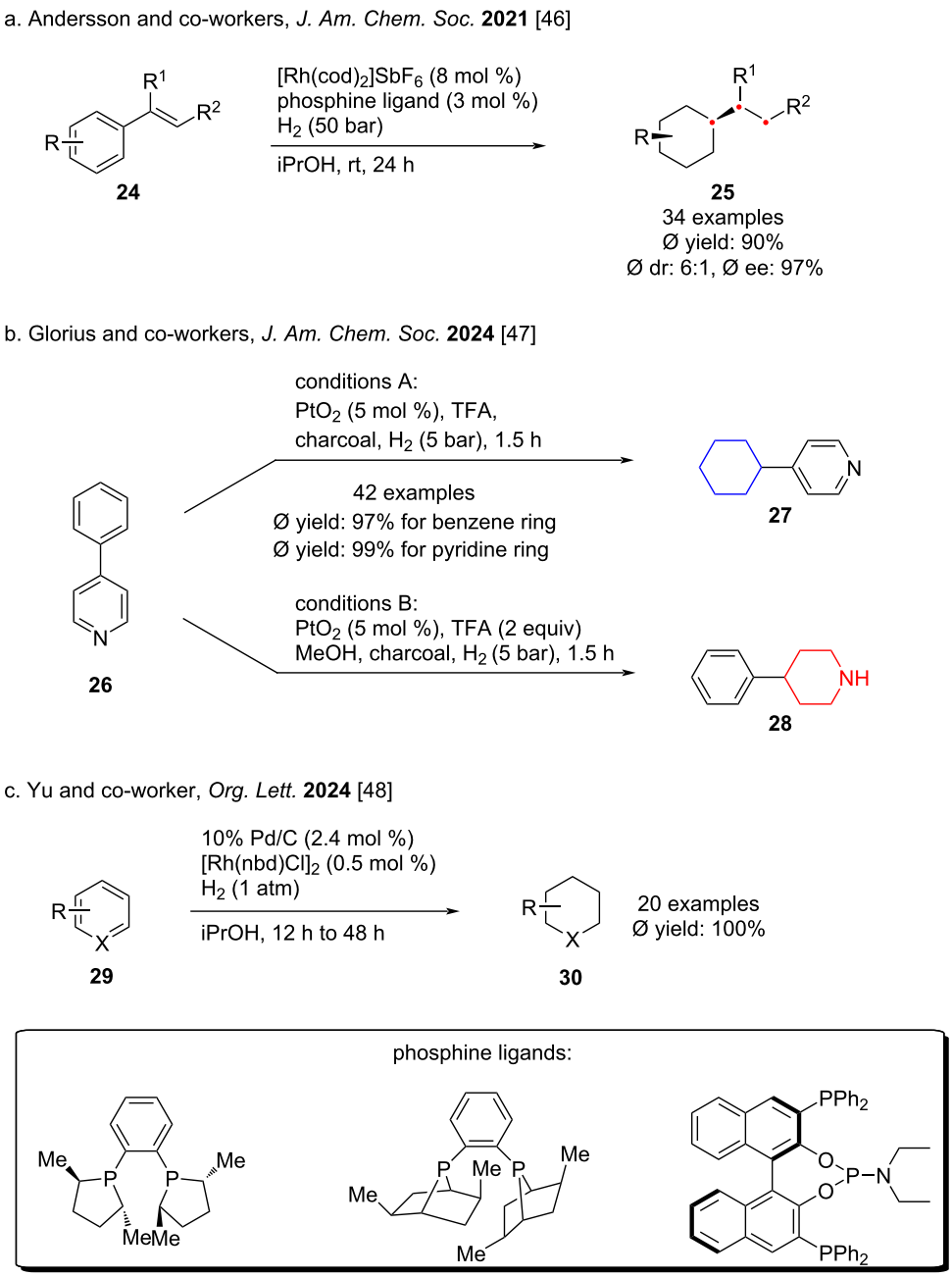

Scheme 4: Hydrogenation of the carbocyclic aromatic rings.

For benzofuran, indole and other heteroarenes, hydrogenation of these easily accessible building blocks is rare. In 2020, Ding and co-workers demonstrated the selective reduction of benzoannelated five-membered heteroaromatic compounds **53** while retaining the benzene ring structure using an iridium catalyst to selectively hydrogenate indoles and benzofurans (Scheme 7) [59]. The hydrogenated products were obtained in 90% yield with 98% ee on average. In 2024, Yin and co-workers reported an innovative palladium-catalyzed asymmetric hydrogenation reaction (Scheme 7) [60]. Using an acid-assisted dynamic kinetic resolution method, they obtained a series of chiral indolines **56** containing exocyclic stereocenters in high yields and excellent enantioselectivity. Mechanistic studies of the reaction revealed that the dynamic kinetic resolution process relies on the rapid interconversion of the enantiomers in the racemic substrate, which in turn relies on the acid-promoted isomerization between the aromatic indole and the nonaromatic exocyclic enamine intermediate. Very recently, Chen and co-workers reported that using a Mn catalyst with different PNN-ligands, multi-nitrogen heteroaromatic compounds,

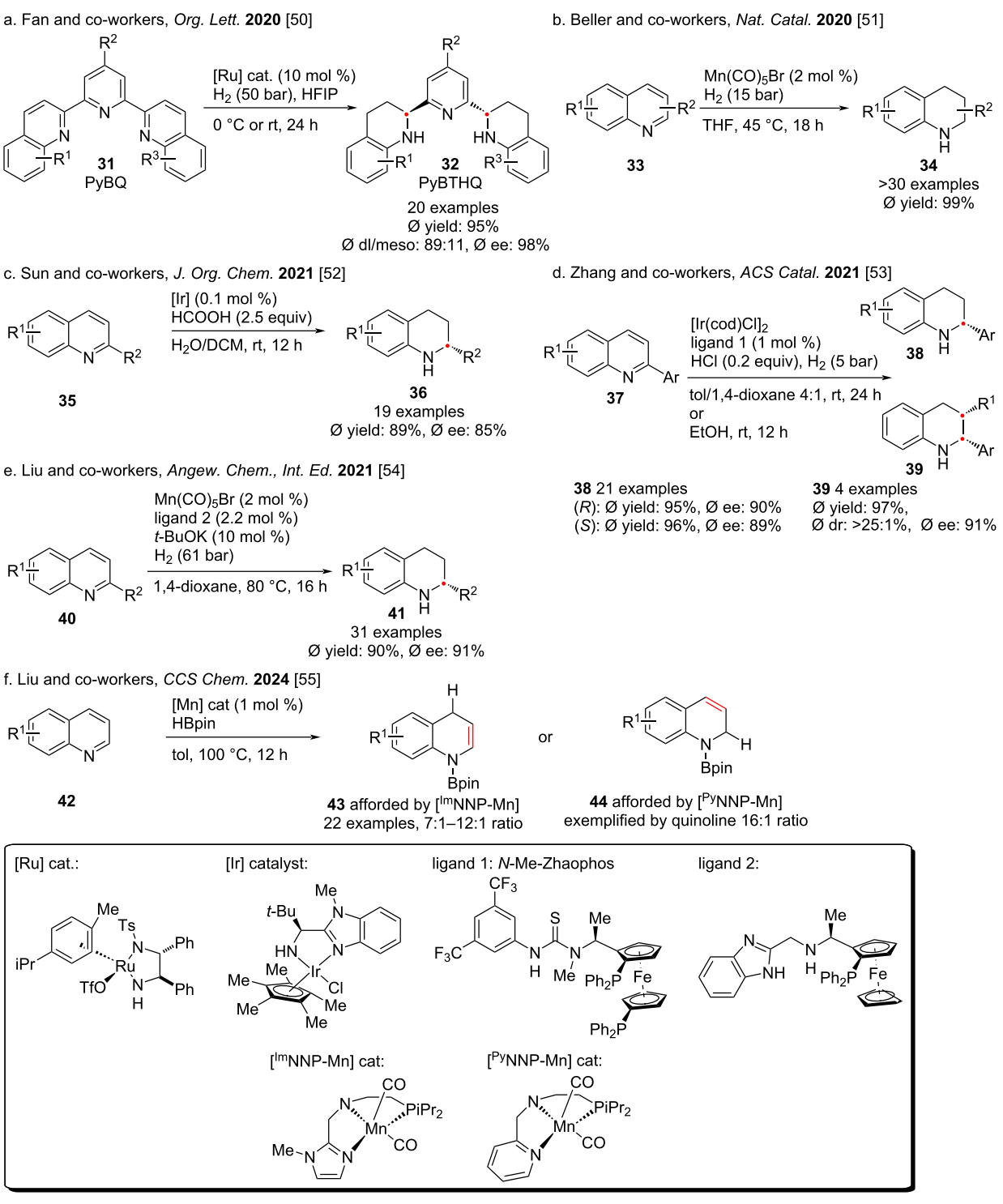

Scheme 5: Hydrogenation of the heterocycle part in bicyclic aromatic rings.

including substituted pyrazolo[1,5-*a*]pyrimidines, pyrrolo[1,2-*a*]pyrazines, and imidazo[1,2-*a*]pyrazines can be hydrogenated efficiently, providing the corresponding reduced products with high enantioselectivity, reactivity, and broad substrate scope [61].

Hydrogenation of the carbocycle part: The hydrogenation of the benzene ring in bicyclic aromatic systems has always been very challenging, since the aromaticity of the benzene ring is stronger than that of heteroaromatic rings, and the lack of heteroatoms in the ring makes it even

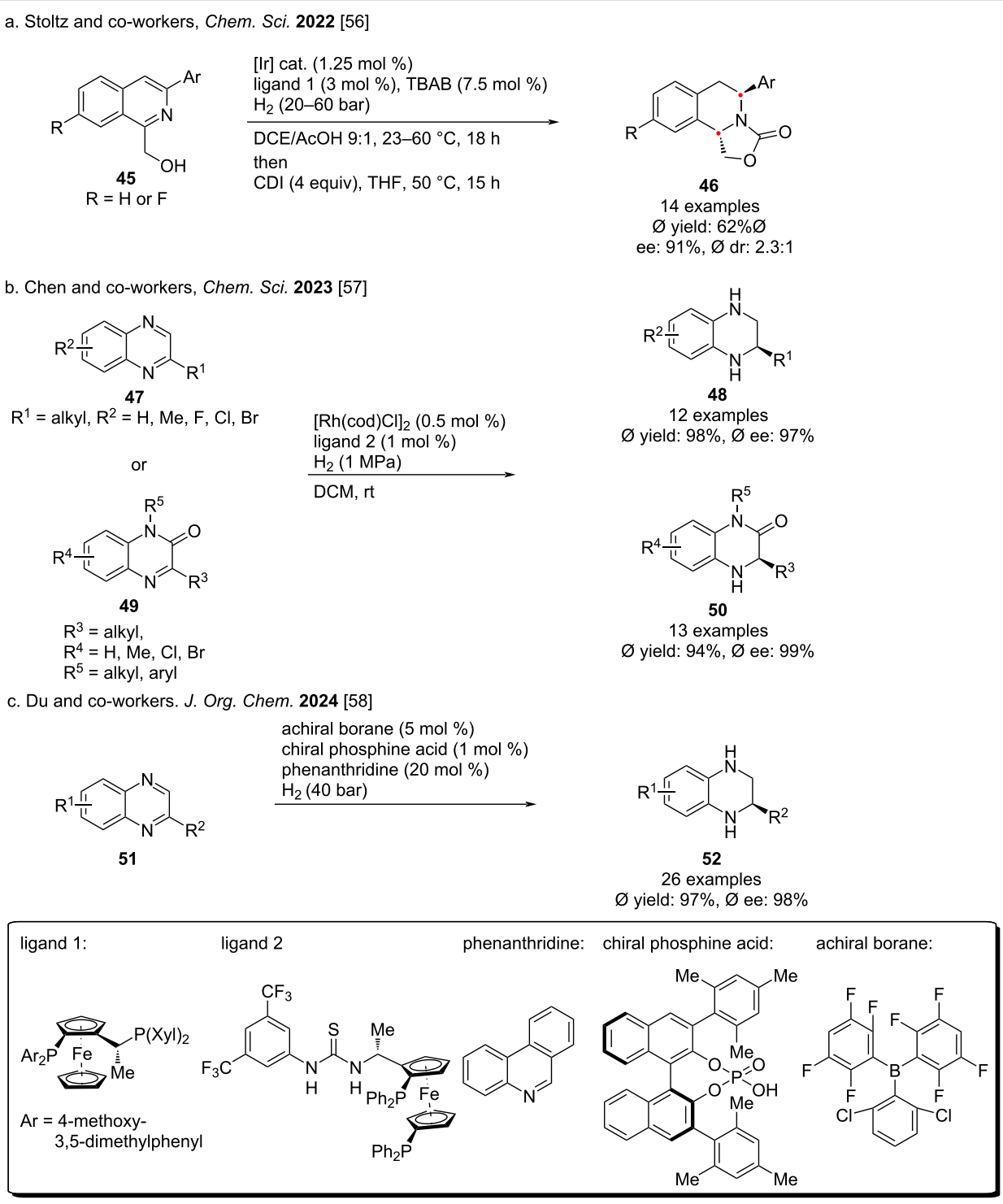

Scheme 6: Hydrogenation of the heterocycle part in bicyclic aromatic rings.

more difficult for the substrate to coordinate with the metal catalyst.

In 2021, Glorius and co-workers reported an enantio- and diastereoselective complete hydrogenation of substituted benzofurans **65** in a one-pot cascade reaction (Scheme 8) [62]. This method facilitates the controlled installation of up to six new stereocenters, producing architecturally complex 6–5 fused ring systems. The key points lie in the utility of a chiral homogeneous ruthenium-*N*-heterocyclic carbene complex, as well as an

a. Ding and co-workers, *Chem. – Eur. J.* **2020** [59]

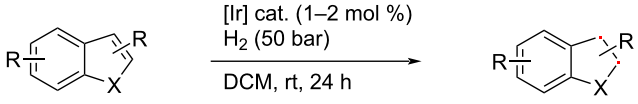

53
X = NBoc, NTs, O, SO_2

54
28 examples
Ø yield: 90%, Ø ee: 98%

b. Yin and co-workers, *J. Am. Chem. Soc.* **2024** [60]

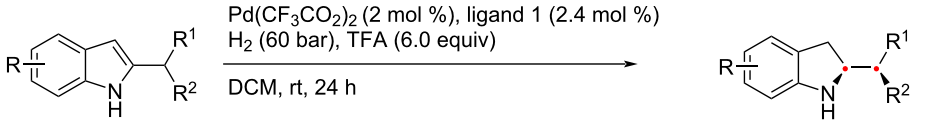

55

56
32 examples
Ø yield: 94%, Ø ee: >99%

c. Chen and co-workers, *Org. Lett.* **2025** [61]

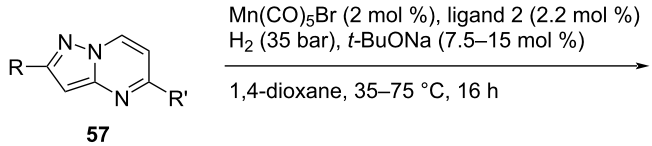

57

58
13 examples
Ø yield: 99%, Ø ee: 97%

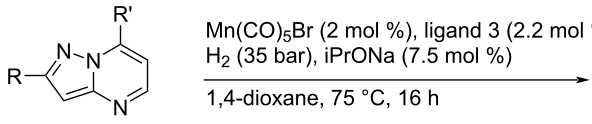

59

60
15 examples
Ø yield: 99%, Ø ee: 98%

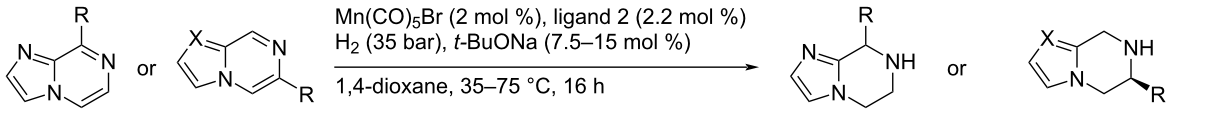

61

62
X = C or N

63
moderate % ee

64
5 examples
Ø yield: 99%, Ø ee: 91%

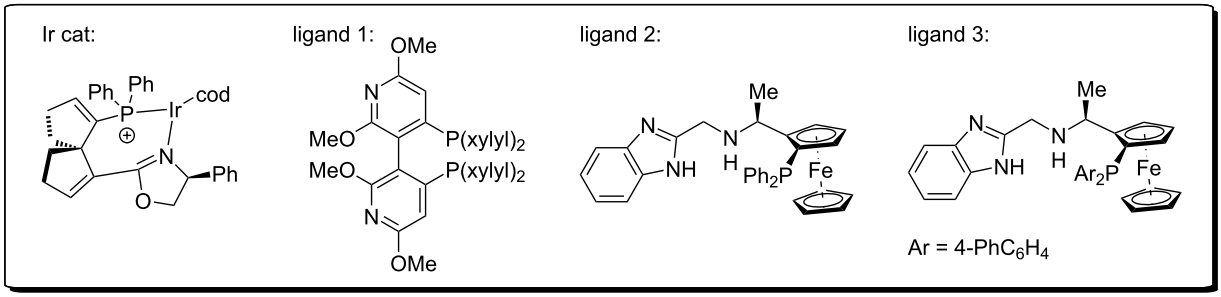

Scheme 7: Hydrogenation of benzofuran, indole, and their analogues.

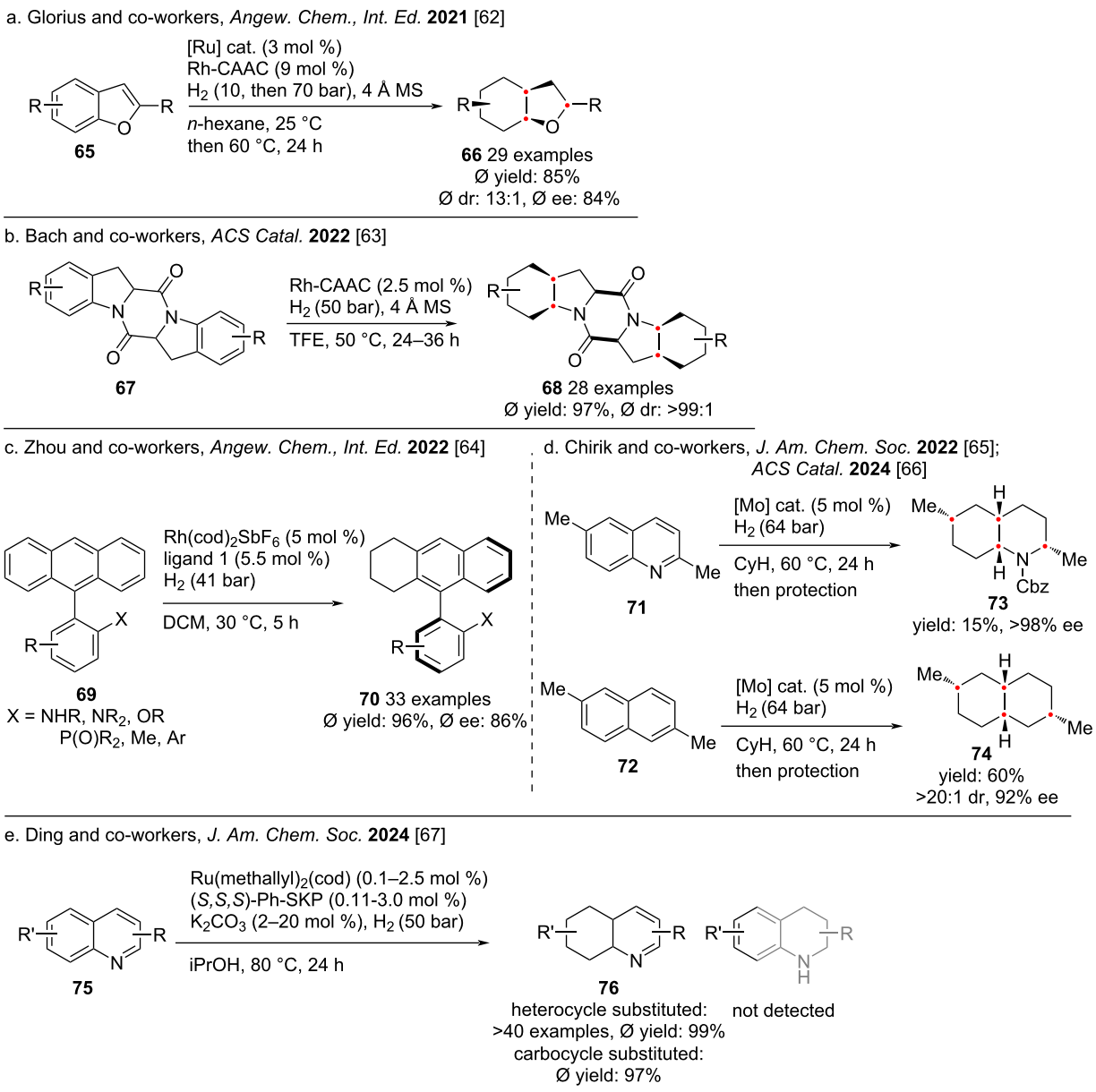

Scheme 8: Hydrogenation of benzofuran, indole, and their analogues.

in-situ activated rhodium catalyst. In 2022, Bach and co-workers reported a modular approach for the highly diastereoselective hydrogenation of symmetrical 2,5-DKP (2,5-dipiperazinone) **67** using a rhodium complex (Scheme 8) [63]. The saturated pentacyclic compound **68** was obtained in high yield and excellent diastereoselectivity. The hydrogen atoms in the final product were all arranged in *cis* configuration. Key features of the reaction include high functional group tolerance and excellent stereocontrol. In the same year, Zhou and co-workers reported a rhodium/bisphosphine-catalyzed asymmetric hydrogenation reaction of all-carbon aromatic rings **69** (Scheme 8) [64]. Through desymmetrization or kinetic resolution, a series of axially chiral cyclic compounds with high enantioselectivity could be synthesized. In addition, the authors also obtained central chiral cyclic compounds by asymmetric hydrogenation of phenanthrene with directing groups.

In 2022 and 2024, Chirik and co-workers reported the use of molybdenum as a metal catalyst to completely hydrogenate substituted naphthalene to saturated 6–6 fused bicycle (Scheme 8) [65,66]. The target decahydronaphthalene was obtained in high yield and high enantioselectivity. In 2024, Ding and co-workers reported a method for the selective hydrogenation of the carbon ring in quinoline to generate hexahydroquinoline using a Ru catalyst (Scheme 8) [67]. When (*S,S,S*)-DKP was used as a ligand, the hydrogenation of the carbon ring was highly selective.

Reduction of aromatic rings via hydride or electron transfer pathways

Beyond catalytic hydrogenation, aromatic rings can also be reduced through hydride-based or electron-transfer pathways, which provide complementary modes of reactivity that are often orthogonal to metal-catalyzed hydrogenation systems. Classical dissolving-metal reductions such as the Birch reduction convert arenes into 1,4-dihydro intermediates via sequential electron transfer and protonation, enabling regioselective partial dearomatization that is difficult to achieve under hydrogenation conditions. Likewise, hydride reagents – including $NaBH_3CN$, DIBAL-H, and other aluminum or borohydride derivatives – have been widely employed for the selective reduction of activated aromatic cations (e.g., pyridinium, quinolinium, or benzopyrylium salts), offering mild and chemoselective access to partially or fully saturated heterocycles. More recent advances in single-electron transfer (SET) chemistry, particularly those mediated by photoredox catalysts or electrochemical systems, have expanded the toolbox further by enabling reductive dearomatization under exceptionally mild conditions and with high functional-group compatibility. Collectively, these hydride- and electron-transfer approaches enrich the landscape of arene reduction by providing tunable control over regioselectivity, degree of saturation, and stereochemical induction – features that are increasingly leveraged in total synthesis to access complex, three-dimensional natural products [68-70].

Total synthesis based on hydrogenation of aromatic rings

Beyond catalyst and substrate diversity, arene hydrogenation fundamentally proceeds through either partial or complete loss of aromaticity. Partial hydrogenation delivers dihydro- or tetrahydro intermediates that retain useful unsaturation for further transformation. Complete hydrogenation typically requires stronger reductive conditions or more reactive catalyst–ligand systems to overcome higher aromatic stabilization energies. Thus, chemoselectively distinguishing between partial and complete reduction is crucial: depending on the substrate, the catalyst must either halt the process at a defined stage or drive it to full saturation without affecting other functionalities. The following sections highlight representative examples of both modes in complex molecule synthesis.

Total synthesis of (±)-keramaphidin B by Baldwin, 1996

Although the methodologies for aromatic ring hydrogenations have only recently flourished, the reduction of aromatic rings to obtain saturated aliphatic or heterocyclic rings and their subsequent application in the total synthesis of natural products has a long history. A brilliant early work is Baldwin's total synthesis of the macrocyclic diamine natural product (±)-keramaphidin B in the year of 1996 (Scheme 9) [71,72].

Starting from compounds **77** and **78**, Baldwin and co-workers converted them into pyridine derivative **79** in high yield over three steps including a Wittig reaction and tosylation. Subsequent reduction with sodium borohydride furnished the dimer **80** bearing partially reduced pyridine rings. From **80**, intermediate **81** was prepared via a Polonovski–Polish reaction and isomerization, which, when adopting the proper conformation, spontaneously underwent an intramolecular [4 + 2] cycloaddition to construct the unsaturated bridged ring of (±)-keramaphidin B in a single transformation. Subsequently, the iminium ion **83** was reduced, completing the total synthesis of (±)-keramaphidin B. Although the yield of the [4 + 2] cycloaddition step is not ideal, this work on (±)-keramaphidin B exemplifies the application of an aromatic ring hydrogenation strategy in the total synthesis of natural products and its promising development potential.

Total synthesis of ergolines by Vollhardt (1994), Boger (2015), and Smith (2023)

Dearomative ionic hydrogenations have been widely applied in alkaloid synthesis, including that of the ergot alkaloids – a bio-

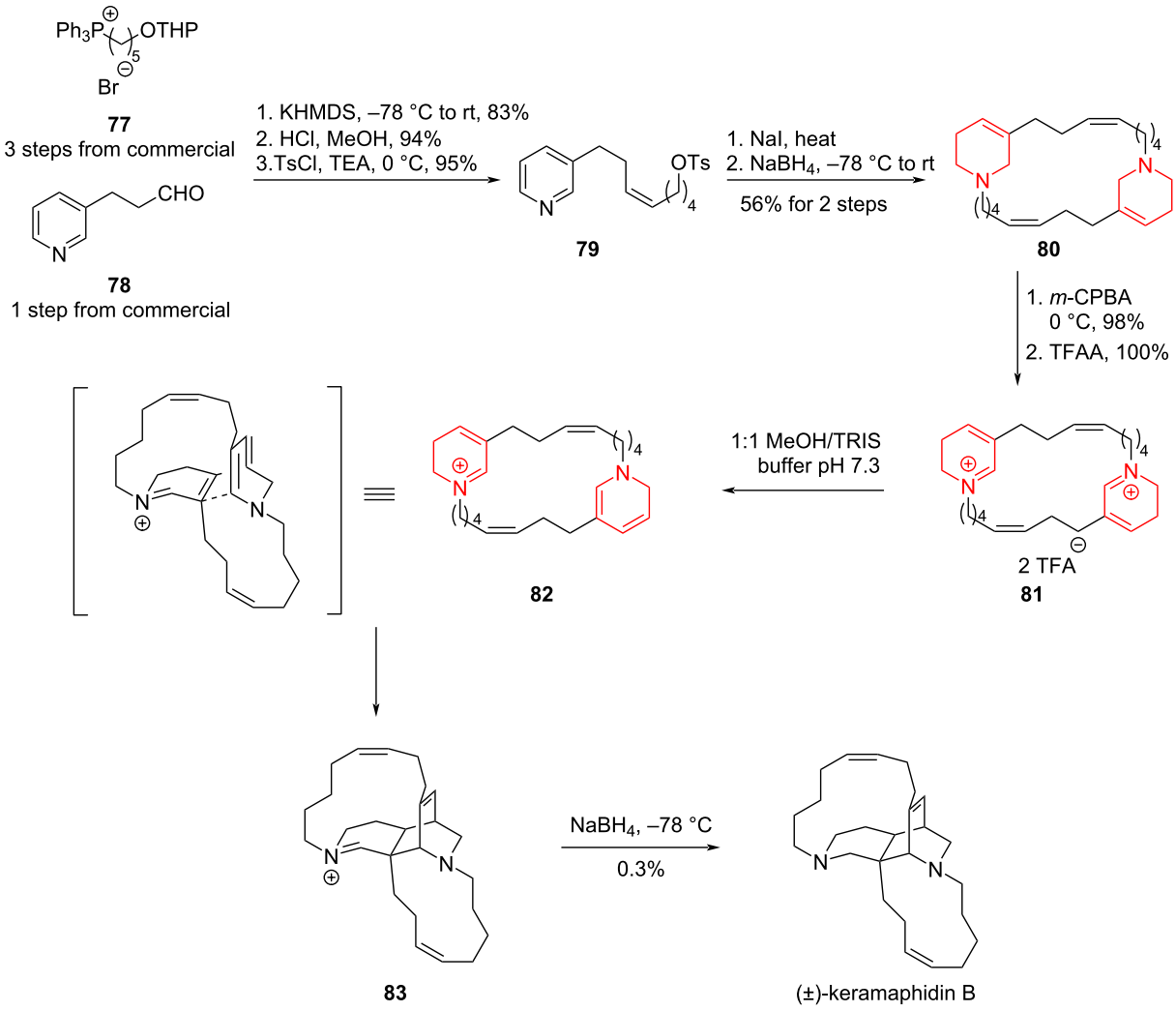

Scheme 9: Total synthesis of (±)-keramaphidin B by Baldwin and co-workers.

active compounds family with a long synthetic history [73]. In the synthesis of (±)-LSD by Vollhardt and co-workers, the pyridine part was constructed by a Co-catalyzed [2 + 2 + 2] cycloaddition between alkyne **84** and nitrile **85**, constructing the ergoline core **86**. Methylation with MeOTf provided pyridinium **87**, and subsequent $NaBH_4$-mediated hydrogenation selectively generated the tetrahydropyridine and completed the synthesis of (±)-LSD (Scheme 10) [74,75].

In the synthesis of (±)-dihydrolysergic acid, Boger and co-workers constructed the tetracyclic core via an inverse-electron demand Diels–Alder cycloaddition between an enamine derived from ketone **88** and triazine, giving pyridine **90** in 75% yield over two steps [76]. Alkylation with MeI furnished pyridinium **91**, which was hydrogenated in two steps with $NaBH_3CN$ to the fully saturated piperidine **92**. Acidic removal of the benzoyl group triggered auto-oxidation to the indole, and subsequent hydrolysis of methyl ester delivered the target (±)-dihydrolysergic acid (Scheme 11).

Smith and co-workers recently reported a six-step synthesis of (±)-lysergic acid [77]. In contrast to previous approaches, the pyridine was introduced via a magnesium–halogen exchange of pyridyl iodide **93**, followed by addition to aldehyde **94**. Subsequent reduction of the resulting benzylic alcohol with TFA/Et_3SiH afforded pyridine **95**, which underwent a one-pot sequence of indole protection, methylation, and hydrogenation to furnish tetrahydropyridine **96**. In contrast to Vollhardt's synthesis, the unsaturation was misaligned with that of the natural product, most likely arising from protonation during reduction or an isomerization event. Kinetic translocation of the double bond to the correct position enabled an intramolecular Heck reaction, a transformation originally developed by Fukuyama (Scheme 12) [78].

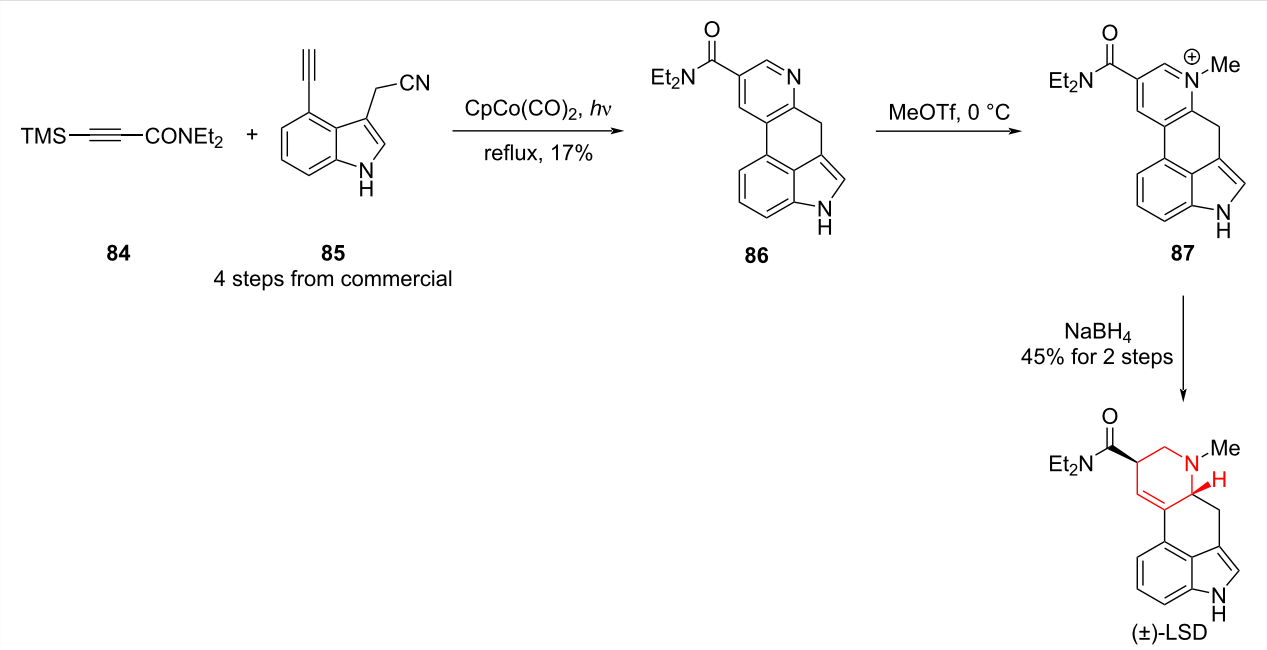

Scheme 10: Total synthesis of (±)-LSD by Vollhardt and co-workers.

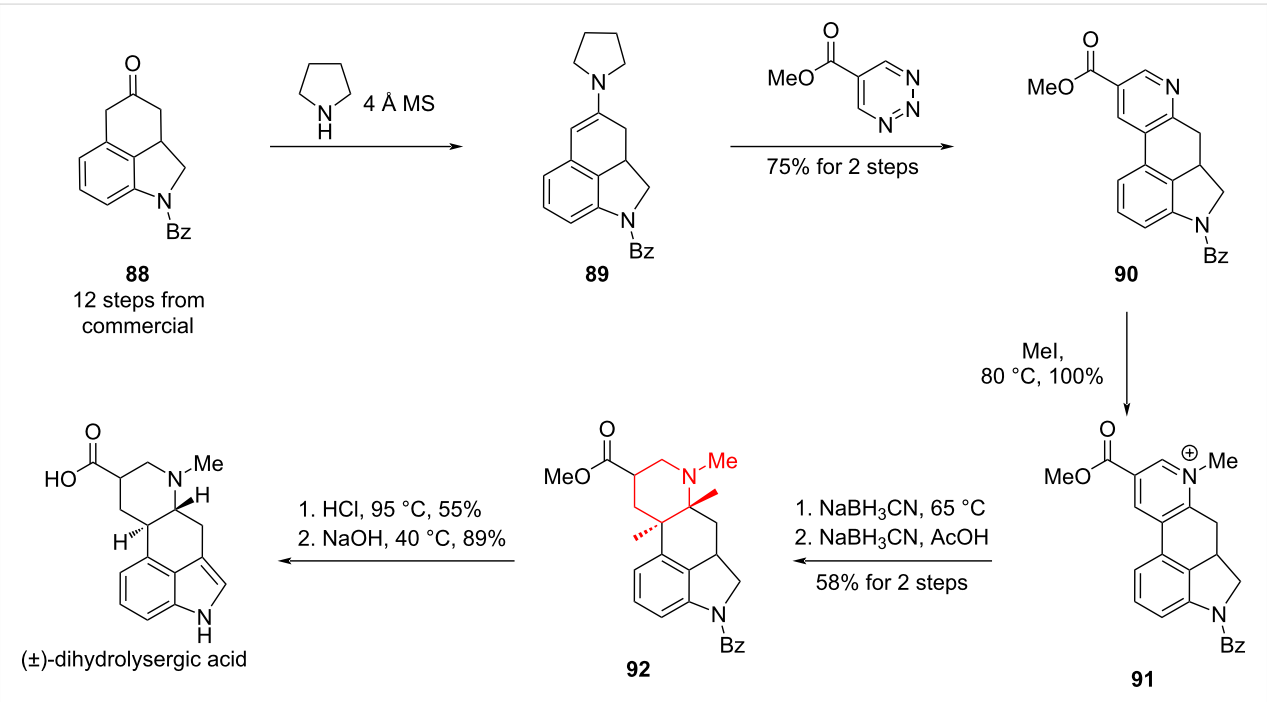

Scheme 11: Total synthesis of (±)-dihydrolysergic acid by Boger and co-workers.

Hydrogenation of (−)-tabersonine to (−)-decahydrotabersonine by Catherine Dacquet, 1997

An unavoidable challenge for aromatic ring hydrogenations is controlling the stereochemistry of the product during the hydrogenation reduction process. In 1997, Dacquet and co-workers conducted a hydrogenation reduction of the natural product (−)-tabersonine using platinum dioxide as a catalyst in the presence of perchloric acid to obtain (−)-decahydrotabersonine, a product with a completely reduced aromatic ring (Scheme 13) [79]. Through the structural characterization of the product, the authors found that the hydrogenation was highly stereoselective,

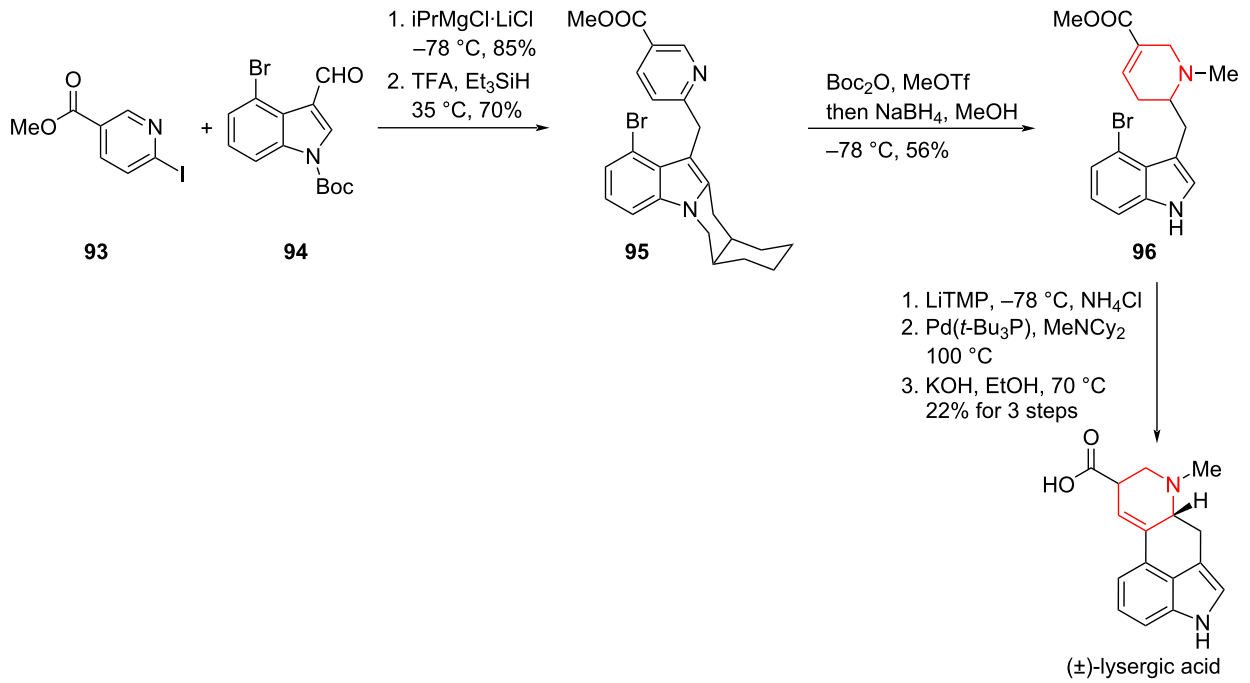

Scheme 12: Total synthesis of (±)-lysergic acid by Smith and co-workers.

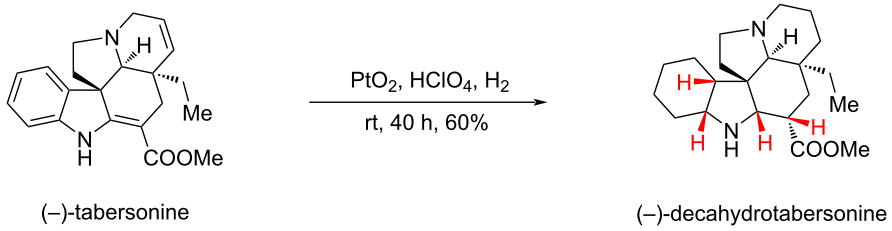

Scheme 13: Hydrogenation of (–)-tabersonine to (–)-decahydrotabersonine by Catherine Dacquet and co-workers.

yielding only *cis*-hydrogenated products. This suggests that substrate induction during hydrogenation could effectively direct the process, enabling stereoselective product formation.

Total synthesis of (±)-nominine by Natsume, 2004

Natural products with complex ring systems, such as bridged rings, spirocycles or highly rigid ring systems, have long captivated synthetic chemists. Designing and completing the total synthesis of these molecules not only leads to the development and application of novel methodologies but also elevates the field to a new level, embodying the artistry of synthesis [80]. In 2004, Natsume and co-workers achieved the first total synthesis of the hepta-ring-containing natural product (±)-nominine applying a palladium-catalyzed intramolecular α-acylation and Birch reduction as key steps (Scheme 14) [81,82].

Starting with a simple trisubstituted benzene **97**, they obtained the ketal **98** in 39% yield over six steps. The authors then utilized their own palladium-catalyzed intramolecular α-acylation followed by protection of the carbonyl group to obtain the diketal **99**. Birch reduction of **99** afforded the enone, which was then subjected to a Luche reduction to get the allylic alcohol **100**. A Johnson–Claisen rearrangement and Lewis acid-promoted acetal–ene reaction provided the tetracyclic skeleton **101**. With **101** in hands, a 6 step transformation afforded the alkyne **102** in an overall yield of 45%. After obtaining **102**, the authors used a free radical reaction to initiate a one-step *6-exo-trig* cyclization, constructing the [2.2.2]-bridged ring within the (+)-nominine followed by protection of the primary alcohol as mesylate. Using lithium bromide as the bromine source, an S_N2 reaction was performed, and the allylic position was oxidized

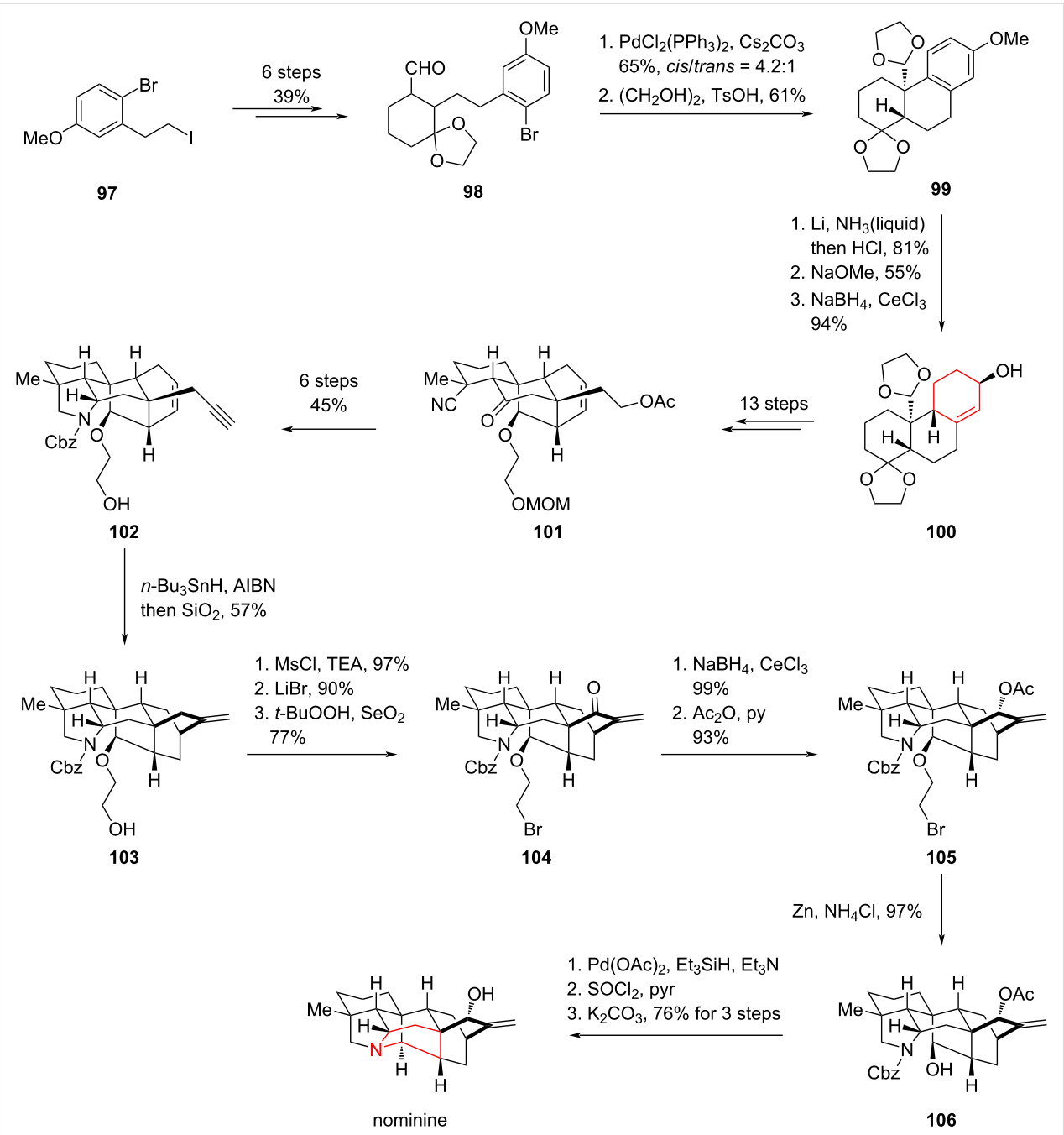

Scheme 14: Total synthesis of (±)-nominine by Natsume and co-workers.

with *tert*-butyl peroxide and selenium dioxide to generate the enone **104**. After obtaining **104**, the unsaturated ketone was stereoselectively reduced to a specifically oriented hydroxy group using a Luche reduction, which was then protected with acetic anhydride to yield **105**. Compound **105** then gave rise to the tertiary alcohol **106** in the presence of zinc powder and ammonium chloride. Finally, through a sequence of removal of the Cbz protecting group, alcohol chlorination, proximal nucleophilic substitution, and deprotection of the secondary alcohol, the first total synthesis of nominine was completed. Although the synthetic route seemed to be lengthy, this challenging total synthesis provided a promising strategy for the subsequent synthesis of this family of natural products.

Total synthesis of (+)-nominine by Gin, 2006

Only two years after Natsume completed the total synthesis of (+)-nominine, Gin and co-workers reported another total synthesis of (+)-nominine via a brilliant dearomatization strategy

(Scheme 15) [83]. Starting from a *para*-disubstituted benzene **107** and an unsaturated aldehyde **108**, they obtained **109** via a Staudinger aza-Wittig reaction. Compound **109** isomerized to the internal salt **110** in the presence of TFA, and **110** spontaneously underwent two different transition states to give the intramolecular [5 + 2] products **111** and **112**, respectively. While the

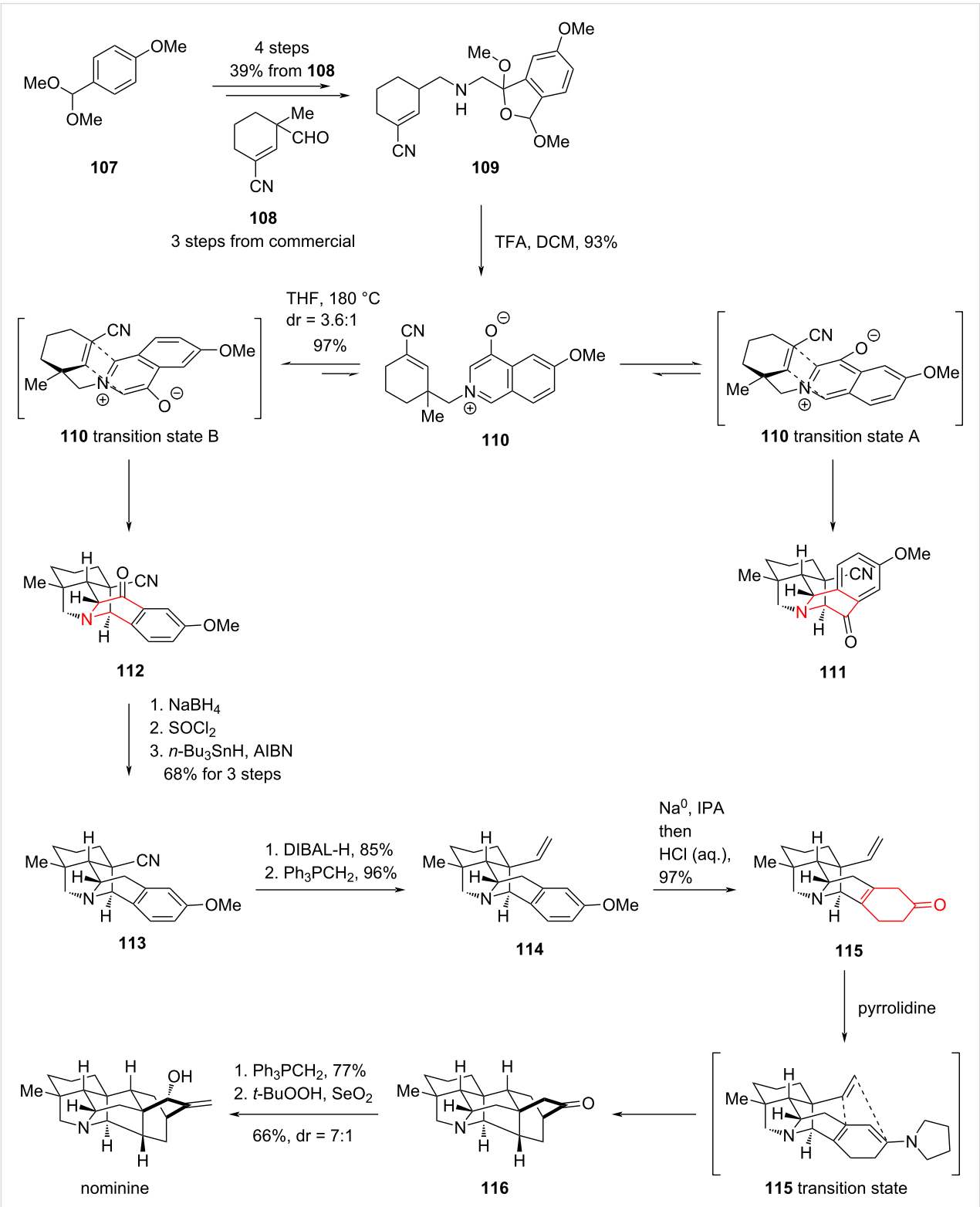

Scheme 15: Total synthesis of (+)-nominine by Gin and co-workers.

desired cycloadduct **112** was formed as the minor constituent (**112**/**111** = 1:3.6), the isomeric ratio was verified to be the result of thermodynamic selection. The cycloaddition process is reversible under the conditions, thereby permitting iterative thermal re-equilibration of the undesired cycloadduct **111**, which enhanced the formation of **112** while minimizing material loss.

Cycloadduct **112** was converted to **113** in high yield through a three-step sequence of carbonyl hydroboration, alcohol chlorination with thionyl chloride, and radical reduction. Subsequently, reduction of the cyanide group with DIBAL-H and a Wittig reaction afford alkene **114** in 82% yield. Sodium metal was then used as a single-electron reducing agent to provide the second cycloaddition precursor **115**, which was converted to the enamine. The enamine spontaneously underwent an intramolecular cycloaddition to yield the highly rigid [2.2.2]-bridged ring skeleton in ketone **116**. Finally, nominine was generated via a two-step sequence comprising a Wittig reaction followed by *tert*-butyl peroxide/selenium dioxide-mediated allylic oxidation, thereby completing another impressive total synthesis. Relative to Natsume's strategy, Gin and co-workers leveraged two intramolecular cycloaddition reactions to efficiently construct the carbon framework, resulting in a efficient total synthesis of nominine.

Total synthesis of (±)-lemonomycinone and (±)-renieramycin by Magnus, 2005

Tetrahydroisoquinoline alkaloids have long captivated chemical and biological interest; among them, lemonomycin and renieramycins (A–S) are especially notable for their potent antitumor and antimicrobial activities [84]. In 2005, Magnus and co-worker achieved the total synthesis of two bis-tetrahydroisoquinoline natural products, (±)-lemonomycinone and (±)-renieramycin, featuring as key steps a dearomative nucleophilic addition and diastereoselective hydrogenation of a dihydroisoquinoline (Scheme 16) [85].

Starting from pentasubstituted isoquinoline **117**, the authors utilized a dearomative nucleophilic addition to indirectly reduce

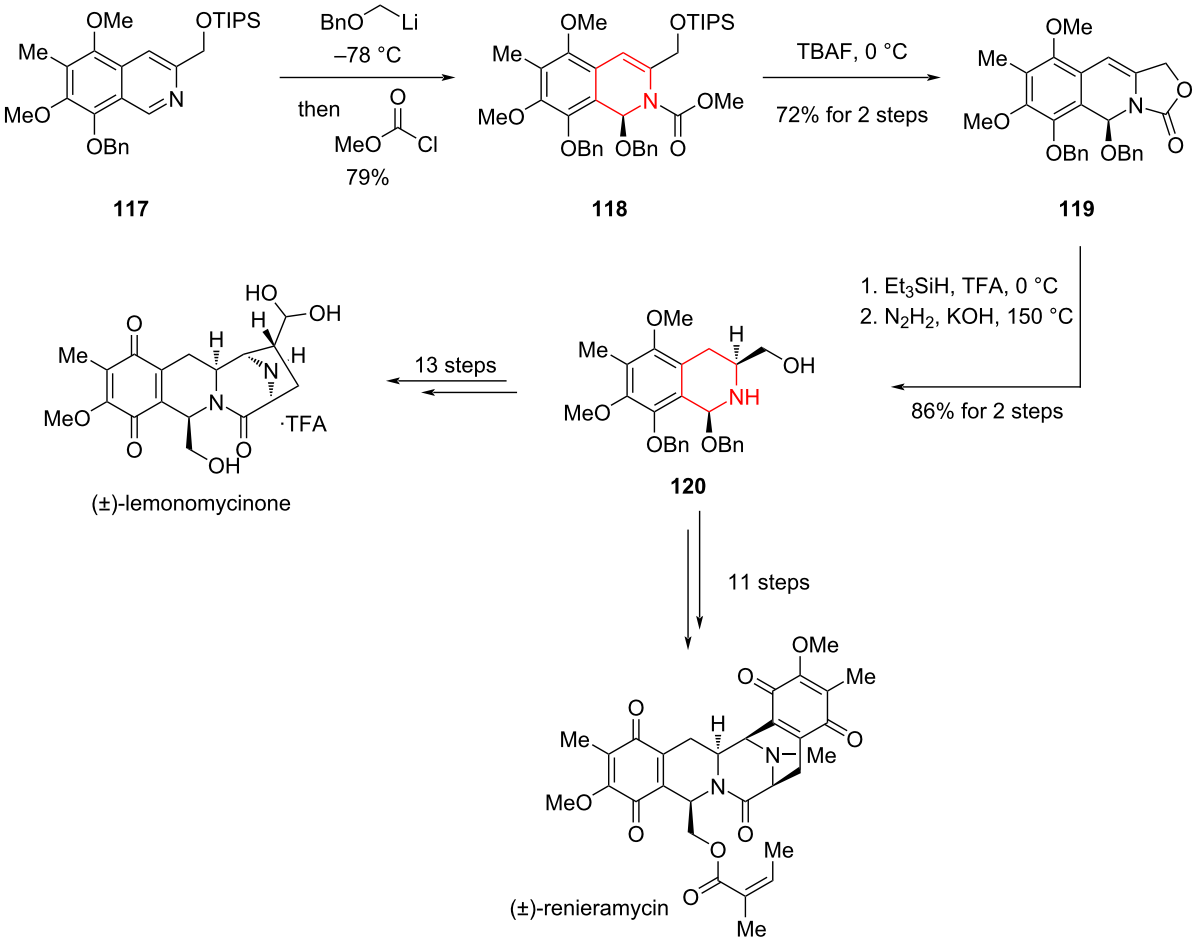

Scheme 16: Total synthesis of (±)-lemonomycinone and (±)-renieramycin by Magnus.

the heteroaromatic ring of the isoquinoline to yield compound **118**. This was followed by desilylation with TBAF and spontaneous intramolecular cyclization to yield the tricyclic **119**. With **119** in hand, the double bond was diastereoselectively hydrogenated using Et_3SiH and TFA, followed by hydrazinolysis to generate alcohol **120**. Starting from the common intermediate **120**, the total syntheses of renieramycin and lemonomycinone were accomplished through 11 and 13 steps, respectively.

Total synthesis to the alkaloids GB13 by Sarpong, 2009

In 2009, Sarpong and co-workers reported a total synthesis of the galbulimima alkaloid GB13. Mander and co-workers had already completed an earlier total synthesis of GB13 in 2003 [86]. However, a key difference between the Sarpong and Mander strategies lies in the construction of the piperidine ring: Sarpong's route features a catalytic hydrogenation of a pyridine precursor, whereas Mander's strategy relied on an Eschenmoser fragmentation as well as a reductive amination (Scheme 17) [87].

Pyridine analogue **121** was converted to tetracyclic compound **123** via a 1,2-addition. A five-step transformation, including allylic hydroxy group transposition, olefin hydrogenation, and DMP oxidation, provided diketone **125**. The two carbonyl groups in **125** were then chemoselectively and stereoselectively reduced using rhodium as a catalyst to yield hydroxylated ketone **126**. A further three-step transformation provided the catalytic hydrogenation precursor **127**. Catalytic hydrogenation of **127** yielded the piperidine ring with a dr ratio of 8:1, completing the total synthesis of GB13 in overall 18 steps.

Total synthesis to the alkaloids GB13 by Shenvi, 2022

In 2022, Shenvi and co-workers completed another concise and efficient total synthesis of GB13 (Scheme 18) [88]. Starting from pyridine derivatives **129**, they obtained the key intermediate **131** via a Simmon–Smith reaction and a bimetallic-mediated photocatalytic radical coupling reaction. Intermediate **132** was then constructed by Friedel–Crafts alkylation using diethylaluminum chloride as a Lewis acid. The pyridine ring was then

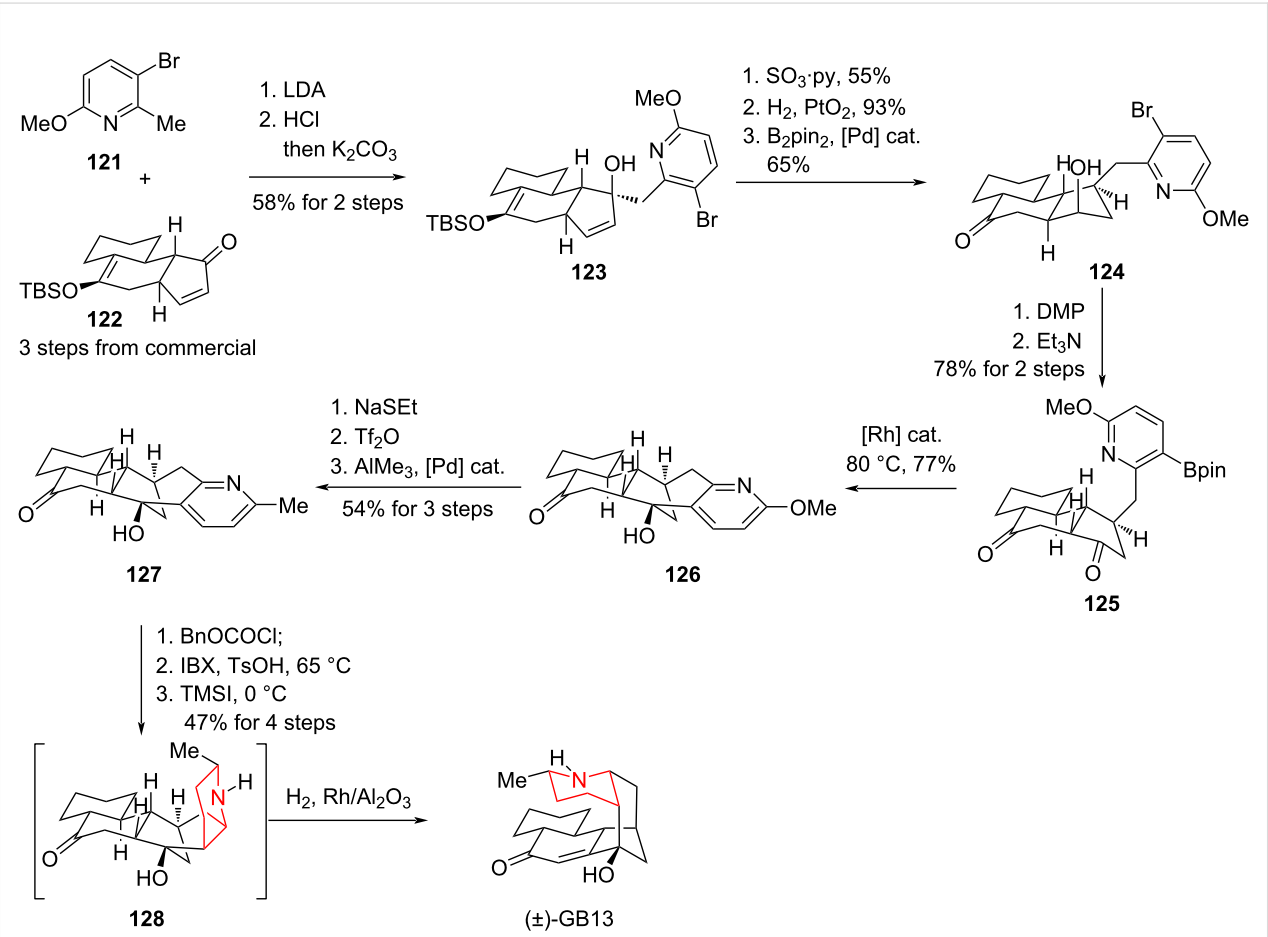

Scheme 17: Total synthesis of GB13 by Sarpong and co-workers.

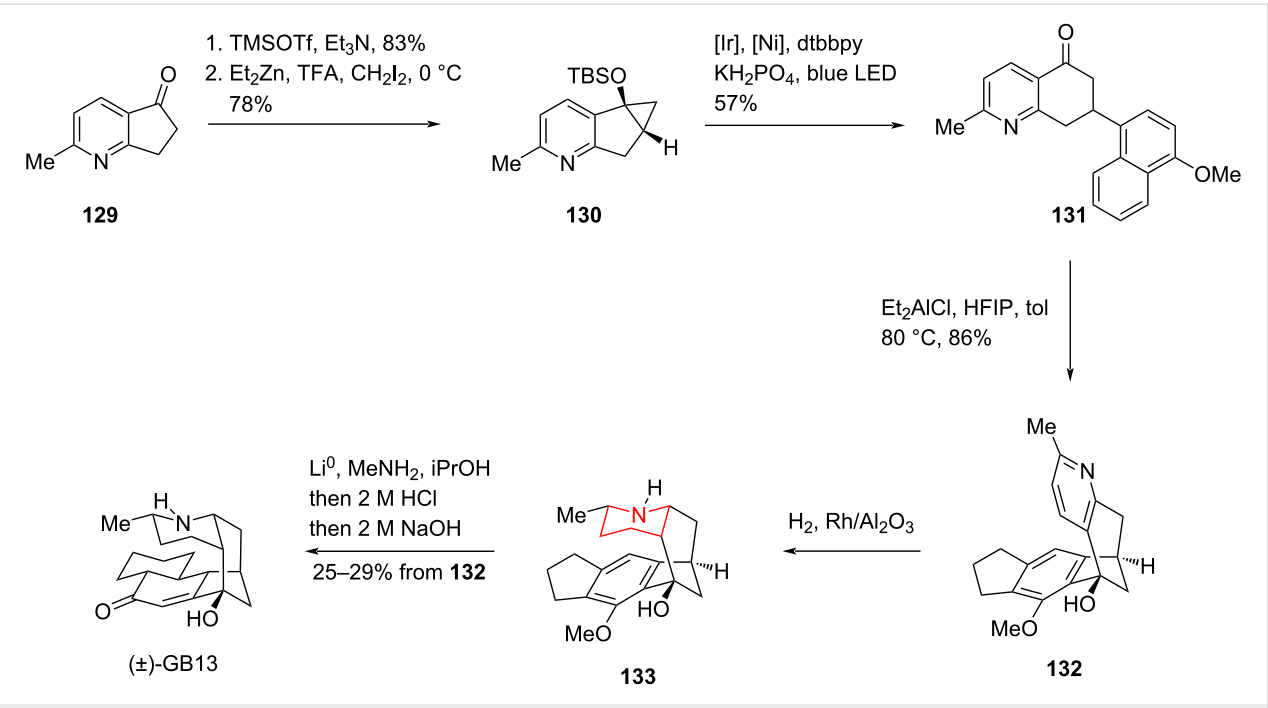

Scheme 18: Total synthesis of GB13 by Shenvi and co-workers.

hydrogenated to the piperidine by direct hydrogenation, and the benzene ring was then reduced to an unsaturated ketone structure by Birch reduction, completing the highly efficient total synthesis of GB13 in 6 steps with an overall yield of 10%.

Total synthesis of (±)-corynoxine and (±)-corynoxine B by Xia, 2014

In 2014, Xia and co-workers completed an outstanding total synthesis of (±)-croynoxine and (±)-croynoxine B, two oxindoline-type tetracyclic natural products [89]. Starting from 2-oxoindole derivative **134** and the 3-substituted pyridine **135**, the pyridinium salt **136** was synthesized, which perfomed as a key substrate for the aerobic oxidation. The formation of the tetracyclic 3-spirooxindole structure **137** was achieved through a transition-metal-free intramolecular cross-dehydrogenative coupling. With **137** in hand, a sequence of transformations including ketone reduction with $NaBH_4$, Johnson–Claisen rearrangement, enol ester formation, and methylation afforded **140**. Finally, hydrogenation of **140** via PtO_2/H_2 generated the target molecule (±)-corynoxine, and under acidic conditions, (±)-corynoxine could be isomerized to (±)-corynoxine B (Scheme 19).

Total synthesis of (+)-serratezomine E, (±)-serralongamine A and (–)-huperzine N by Bonjoch, 2015 and 2016

In 2015, Bonjoch and co-workers reported a method for the selective hydrogenation of an exocyclic double bond conjugated to an aromatic ring [90]. For the pyridine derivative **141**, rhodium catalysis provided the chiral reduction product in quantitative yield and excellent stereoselectivity. Leveraging this unique reaction strategy, Bonjoch completed the total synthesis of the tricyclic natural product serratezomine E and the putative structure of huperzine N (Scheme 20).

Starting from simple 5-aminopentanoic acid (**144**), they synthesized the reduction precursor **145** in 53% yield over six steps. Subsequent catalytic hydrogenation afforded the diastereomeric product **146** in high yield. With compound **146** in hand, they completed the total synthesis of serratezomine E through a three-step sequence comprising removal of the Ts group, acetylation, and pyridine hydrogenation. Simultaneously, starting from **149**, they employed a similar route involving rhodium-catalyzed double-bond reduction, nitrogen methylation, pyridine reduction, and formation of the nitrogen oxide to give the putative structure of huperzine N.

In 2016, Bonjoch and co-workers reported another synthesis work to revise the structure of huperzine N. Similar to their previous study, the synthesis started with a 1,3-dicarbonyl compound **154** to synthesize the hydrogenation precursor **155**. A three-step process, including hydrogenation of the olefin, hydride reduction and methylation, afforded (±)-serralongamine A. With (±)-serralongamine A in hand, huperzine N and N-*epi*-huperzine N could be obtained via a reduction–oxidation sequence [91] (Scheme 21).

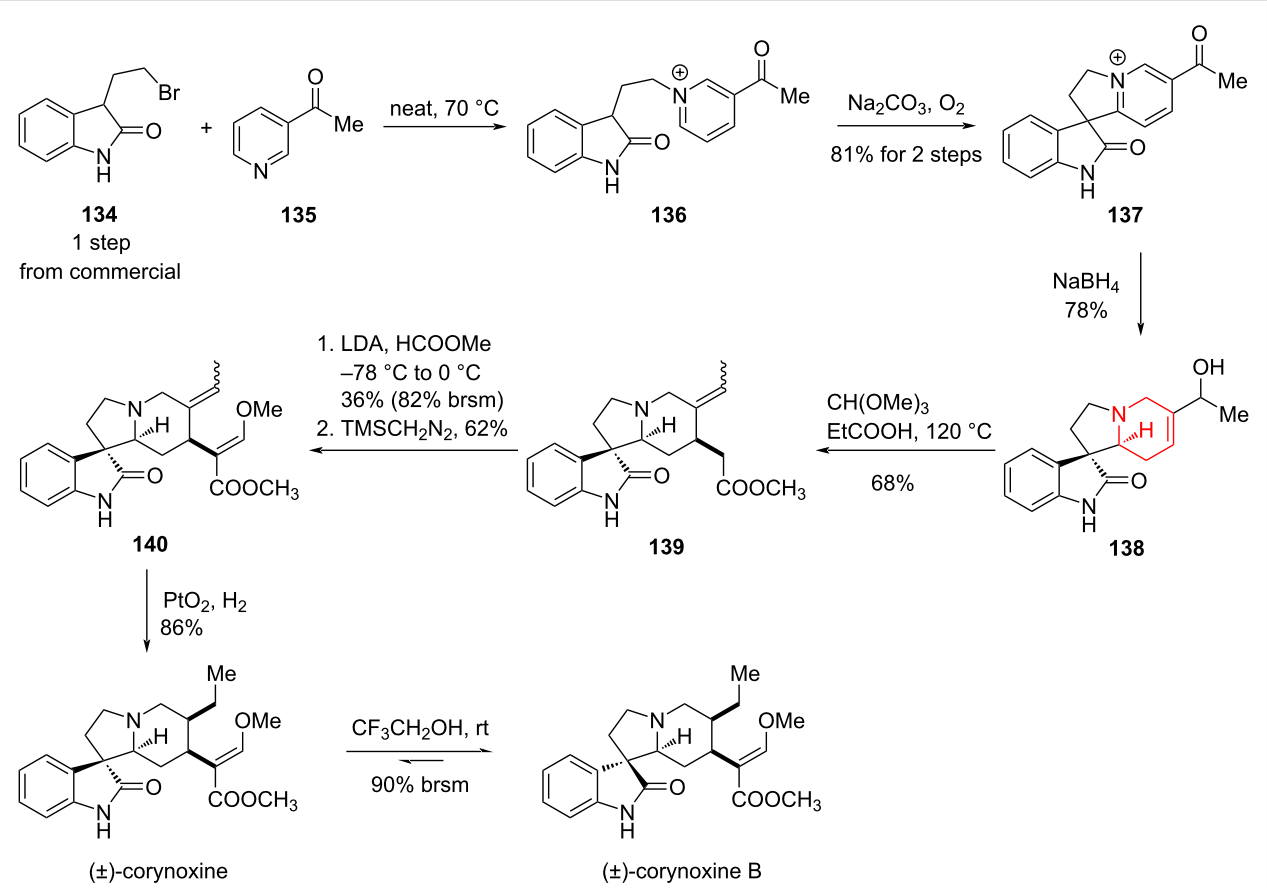

Scheme 19: Total synthesis of (±)-corynoxine and (±)-corynoxine B by Xia and co-workers.

Asymmetric synthesis towards indenopiperidine core of an 11-β-HSD-1 inhibitor, 2016

Growing interest has focused on inhibiting 11-β-hydroxysteroid dehydrogenase type 1 (11-β-HSD-1), a key enzyme that alleviates insulin resistance by lowering cortisol production. Compound **157** emerged as a promising 11-β-HSD-1 inhibitor candidate. In 2016, researchers from Boehringer Ingelheim Pharmaceuticals and the University of Pennsylvania reported a concise and stereoselective synthesis of **157**, which strategically combined a Pd-catalyzed pyridine C–H acylation and an Ir-catalyzed asymmetric hydrogenation of the aromatic core [92].

The synthesis began with the coupling of trisubstituted benzene **158** and 2-substituted pyridine **159**, furnishing the bicyclic intermediate **160**. Three subsequent steps (74% overall yield) then provided the key hydrogenation precursor **161**. Hydrogenation of **161** under heterogeneous catalytic conditions (Pd/C, Pt/C, Raney Ni, Rh/C, Ru/C) proved inefficient, giving complex mixtures that included partially or fully hydrogenated pyridines, over-reduced products and even dimers of reduced species.

The authors proposed that the cyano substituent on the benzene ring might coordinate with or deactivate the metal catalysts, or undergo reduction under the reaction conditions, thereby diminishing catalytic activity. To address this challenge, they hydrolyzed the cyano group to an amide (**162**) under acidic conditions, which then allowed successful Pd/C-mediated hydrogenation to **163**. Subsequent dehydration with $POCl_3$ and chiral resolution using D-DBTA provided the optically enriched compound **165** (Scheme 22).

While this approach rendered catalytic hydrogenation feasible, it also increased the complexity of the synthetic route, limiting its suitability for large-scale preparation of **157**. Consequently, the authors redirected their efforts toward homogeneous catalytic hydrogenation, a field that has seen rapid progress in recent years. Upon converting **161** into the zwitterionic salt **166**, extensive screening revealed that iridium catalysis with MeO-BoQPhos afforded the highest stereoselectivity. This approach furnished the reduced product **167** in high yield. After five further transformations (overall yield: 67%), the final coupling with a benzimidazole fragment efficiently delivered the target compound **157** (Scheme 23).

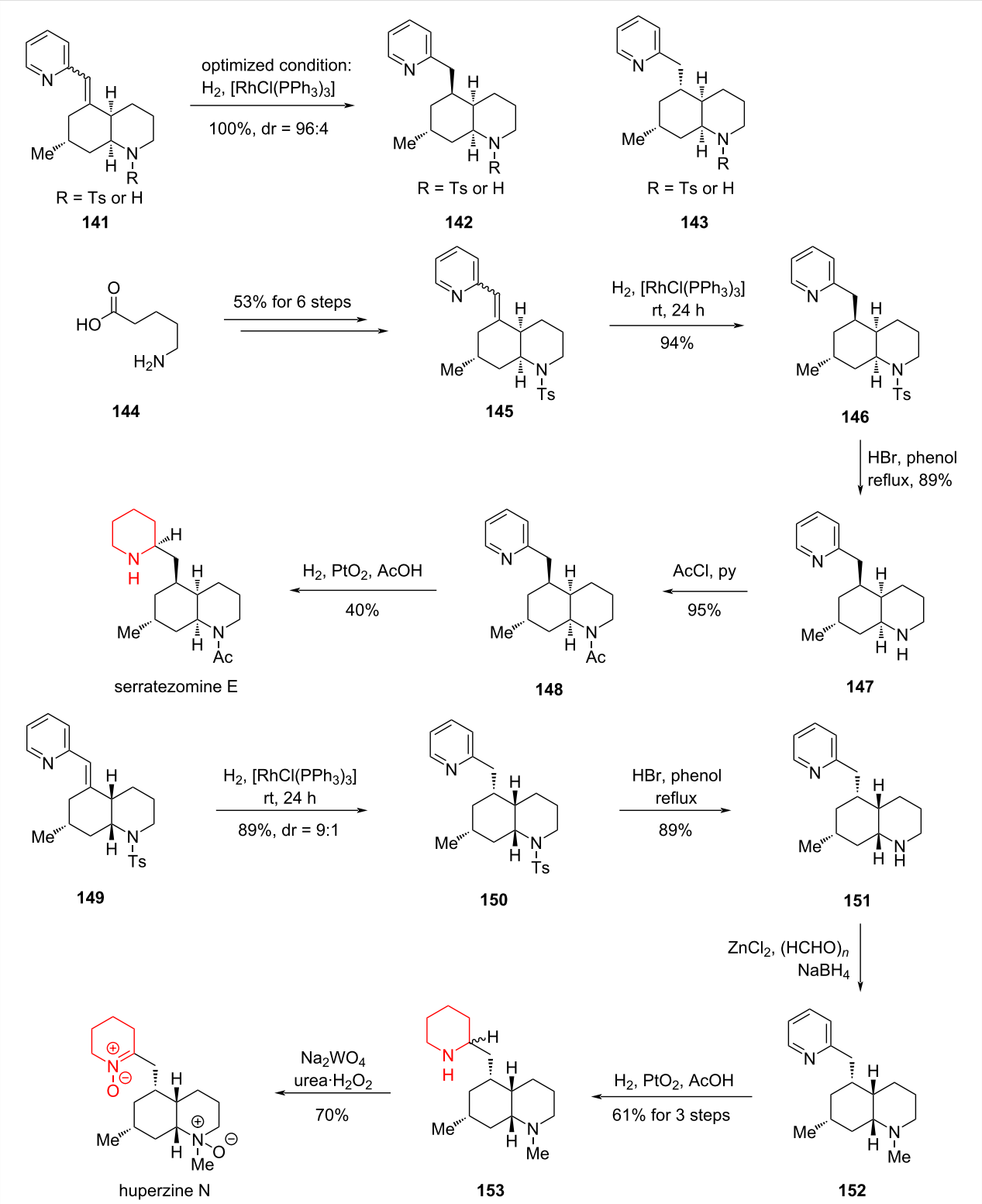

Scheme 20: Total synthesis of (+)-serratezomine E and the putative structure of huperzine N by Bonjoch and co-workers.

This study highlights the pivotal role of controlled aromatic hydrogenation, especially of pyridine derivatives, in modern drug discovery, and illustrates how the choice of the catalytic system (heterogeneous vs homogeneous) together with functional group management can decisively shape the success of complex molecule synthesis.

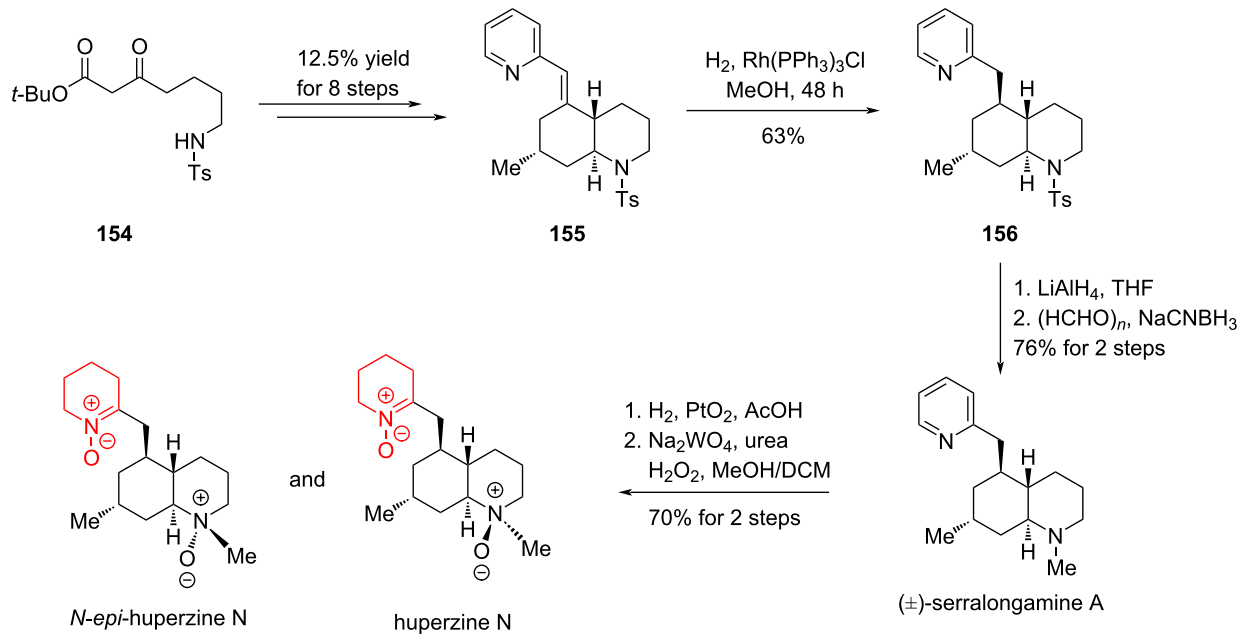

Scheme 21: Total synthesis of (±)-serralongamine A and the revised structure of huperzine N and N-*epi*-huperzine N.

Total synthesis of jorunnamycin A and jorumycin by Stoltz, 2019

The bistetrahydroisoquinoline (bis-THIQ) alkaloids, a class of polycyclic natural products with significant physiological activities, have drawn sustained interest from synthetic chemists worldwide due to their pronounced antibacterial and anticancer properties. Since their discovery, bis-THIQ scaffolds have been constructed primarily through the Pictet–Spengler reaction, a cyclization strategy that continues to be widely employed in total synthesis. In 2019, Stoltz and co-workers developed an elegant substrate-directed asymmetric hydrogenation approach to construct the bis-THIQ framework, achieving the concise total syntheses of two structurally complex natural products [93] (Scheme 24).

Starting from the polysubstituted aromatic precursors **170** and **172**, the Stoltz group accomplished the synthesis of *N*-oxide **171** and isoquinoline compound **173** in two steps with 76% and 42% yield, respectively. These intermediates were then elaborated through a four-step sequence to afford the coupled intermediate **174** in 23% overall yield, which served as the substrate for catalytic hydrogenation.

During the hydrogenation of compound **174**, Stoltz and co-workers observed that the addition of the first two molecules of hydrogen to the substrate proceeded with high stereoselectivity. They proposed that this selectivity arises from chelation between the nitrogen and oxygen atoms from the substrate and the metal catalyst, which fixed the conformation of the polycyclic scaffold. As a result, the top face is sterically less favored, thereby hydrogen approaches from the opposite face. The subsequent addition of another two equivalents of hydrogen also supported this mechanistic hypothesis. Based on this stereochemical control, the Stoltz team successfully obtained the asymmetric hydrogenation product **176**, which spontaneously underwent intramolecular cyclization to furnish the bridged cyclic compound **177**.

With compound **177** in hand, a series of three transformations, including hydroxylation of aryl halide, partial lactam reduction with cyanide trapping, and oxidation of the phenol, enabled the total synthesis of jorunnamycin A in 15 steps. The acetylation of the hydroxy group in jorunnamycin A followed by cyano hydrolysis led to the total synthesis of another natural product, jorumycin.

Total synthesis of (–)-finerenone by Aggarwal, 2021

(−)-Finerenone is a non-steroidal mineralocorticoid receptor antagonist currently under investigation for the treatment of chronic kidney disease (CKD) associated with type 2 diabetes. Its molecular structure features a rare dihydronaphthyridine core, which presents a unique synthetic challenge. Given that (−)-finerenone is presently undergoing phase III clinical trials, the development of efficient and scalable methods for constructing the dihydronaphthyridine scaffold has become a focal point of interest in synthetic chemistry. In 2020, Aggarwal and

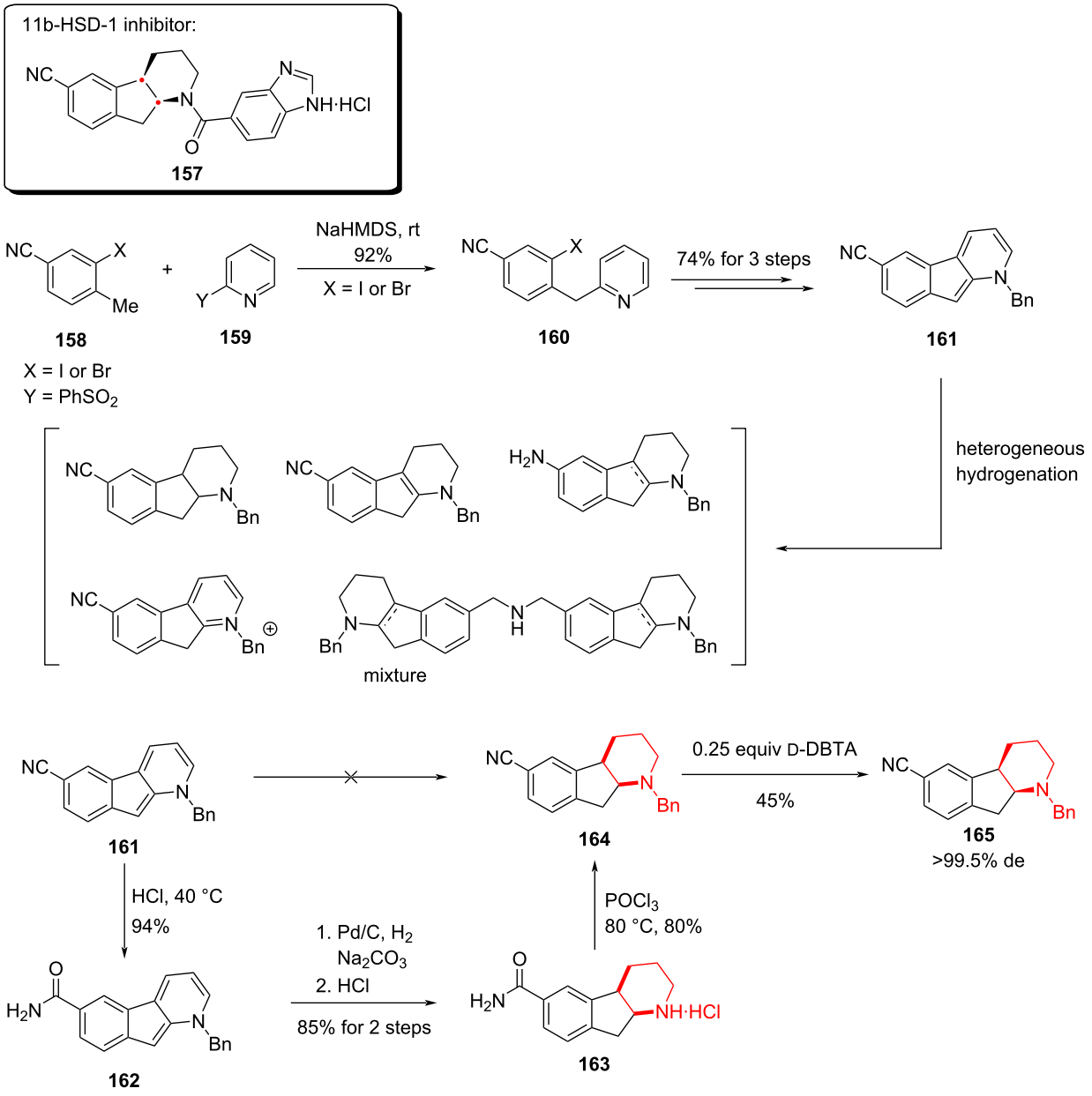

Scheme 22: Early attempts to indenopiperidine core.

co-workers reported a concise and enantioselective synthesis of (−)-finerenone via an asymmetric hydrogen atom transfer (HAT) strategy, completing the total synthesis in just six steps with high efficiency and stereoselectivity [94].

Starting from the 2-pyridone derivative **178**, the authors synthesized the bicyclic intermediate **179** in four steps with an overall yield of 31%. Initially, they attempted a formal [4 + 2] cycloaddition between **179** and a 1,3-dicarbonyl compound, catalyzed by the chiral phosphoric acid (*R*)-TRIP, aiming to construct (−)-finerenone in a single step. However, this approach delivered the target compound in only 19% yield and a low 15% ee (Scheme 25). Given that high enantiopurity is critical for subsequent clinical studies, the authors needed to revise their strategy.

Instead of pursuing a direct asymmetric cyclization, they performed a formal [4 + 2] cycloaddition between **179** and the dicarbonyl compound, followed by in-situ oxidation of the resulting intermediate **180** to afford compound **181** in a one-pot

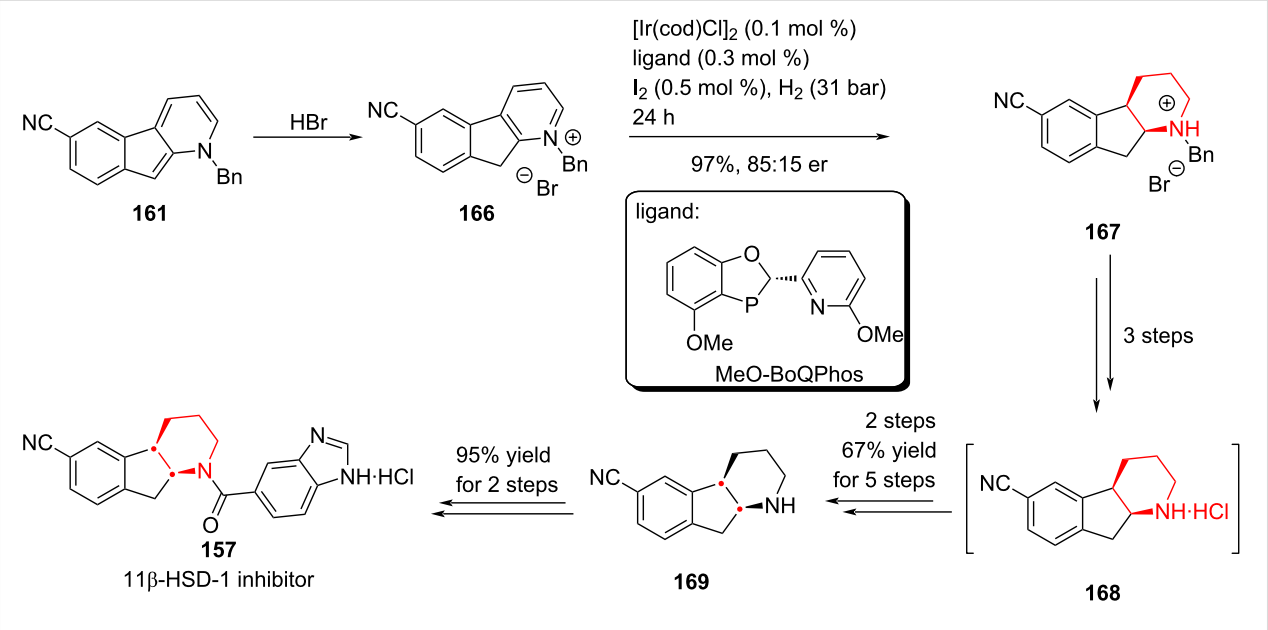

Scheme 23: Homogeneous hydrogenation and completion of the synthesis.

sequence. At this step, the key challenge was to obtain (−)-finerenone with high enantioselectivity through asymmetric hydrogenation of intermediate **181** (Scheme 25).

During attempts to reduce intermediate **181** via asymmetric hydrogen atom transfer (HAT), the authors found that **181** exists as a racemic mixture, with chirality originating from its axially chiral biaryl structure. Owing to the steric hindrance introduced by substituents, **181** exists as a pair of atropisomers, which inspired a new strategy for achieving asymmetric hydrogenation.

The authors proposed that the two atropisomers exhibit different reactivity and selectivity under catalytic conditions, enabling a process of kinetic resolution. More importantly, they envisioned that this inherent resolution could be transformed into a dynamic kinetic resolution, thereby allowing for the selective formation of optically enriched finerenone.

Subsequent experiments confirmed this hypothesis: by employing chiral phosphoric acids of different configurations as catalysts, the authors successfully obtained (+)-finerenone in 42% yield with 94% ee, and (−)-finerenone in 67–82% yield with 94:6 er, respectively (Scheme 26).

Total synthesis of (+)-*N*-methylaspidospermidine by Smith and Grigolo, 2022

In 2021 and 2022, Smith, Grigolo and co-workers reported a total synthesis of the monoterpene indole alkaloid *N*-methylaspidospermidine (Scheme 27) [95,96].

In a single-step reaction, pyridine **182** was activated with 2-chloroethyl triflate and the resulting pyridinium salt was dearomatized with a Grignard reagent to produce ketone **184**. In this step, the Grignard nucleophile added regio- and diastereoselectively at the 2-position of the pyridinium, consistent with established reactivity models from prior studies [97]. A three-step sequence involved Raney Ni hydrogenation of the dihydropyridine, TFA-mediated indole deprotection, and base-promoted formation of a C3 quaternary carbon center provided piperidine compound **185**. The resulting intermediate was trapped with a side chain enolate (derived from a methyl ketone), successfully constructing the pentacyclic aspidospermidine core. The next three steps comprised nitrogen methylation, ketone reduction, and hydroxyl elimination to afford **186**. In the final two steps, an ethyl group was introduced via Fe-mediated HAT and sulfone cleavage. This 10-step asymmetric synthesis demonstrates that, in the case of indole monoterpene alkaloids, the rational application of aromatic ring hydrogenation can markedly reduce step count and enhance overall efficiency.

Total synthesis of matrine-type alkaloids by Reisman, 2022

The tetracyclic alkaloids (+)-matrine and (+)-isomatrine, isolated from *Sophora flavescens*, are thought to originate biosynthetically from (−)-lysine. In 2022, Reisman and co-workers reported a pyridine hydrogenation strategy that provided collective access to matrine-type alkaloids [98]. That same year, Sherburn and co-workers described a complementary synthesis employing an aza-Diels–Alder cycloaddition followed by olefin hydrogenation [99].

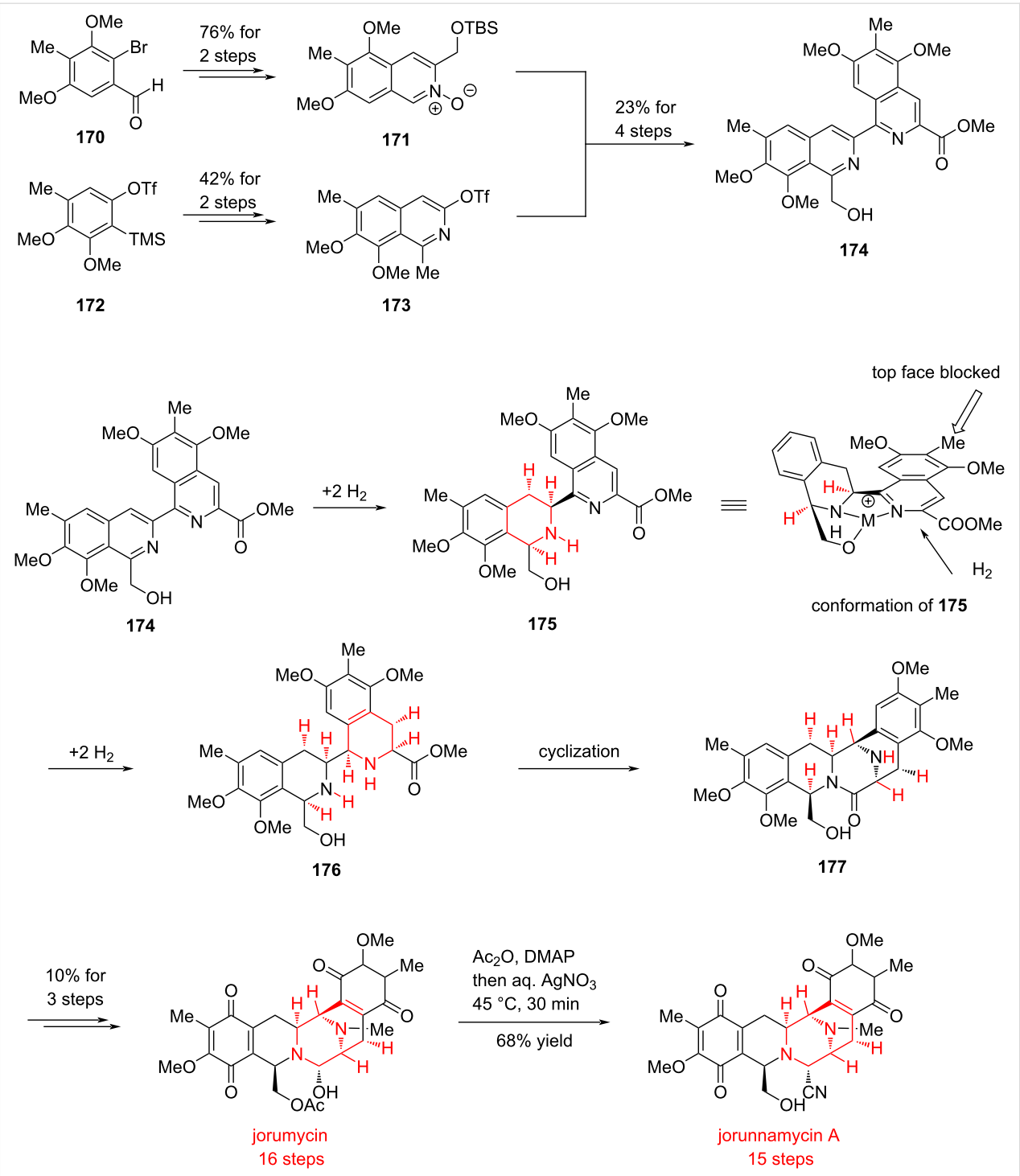

Scheme 24: Total synthesis of jorunnamycin A and jorumycin by Stoltz and co-workers.

Starting from pyridine and glutaryl chloride, tetracyclic intermediate **192** was efficiently generated in a single step through sequential nucleophilic attack and intramolecular cyclization. (+)-Isomatrine was subsequently synthesized through catalytic hydrogenation via Rh/C, LAH reduction, and tertiary amine oxidation (Scheme 28).

After synthesizing (+)-isomatrine, the effects of catalyst type, loading, temperature, and reaction time on the hydrogenation process were systematically examined. The results revealed that appropriate tuning of the conditions enabled the selective synthesis of different natural products, including (+)-matrine, (+)-allomatrine, and other tetracyclic alkaloids, thereby

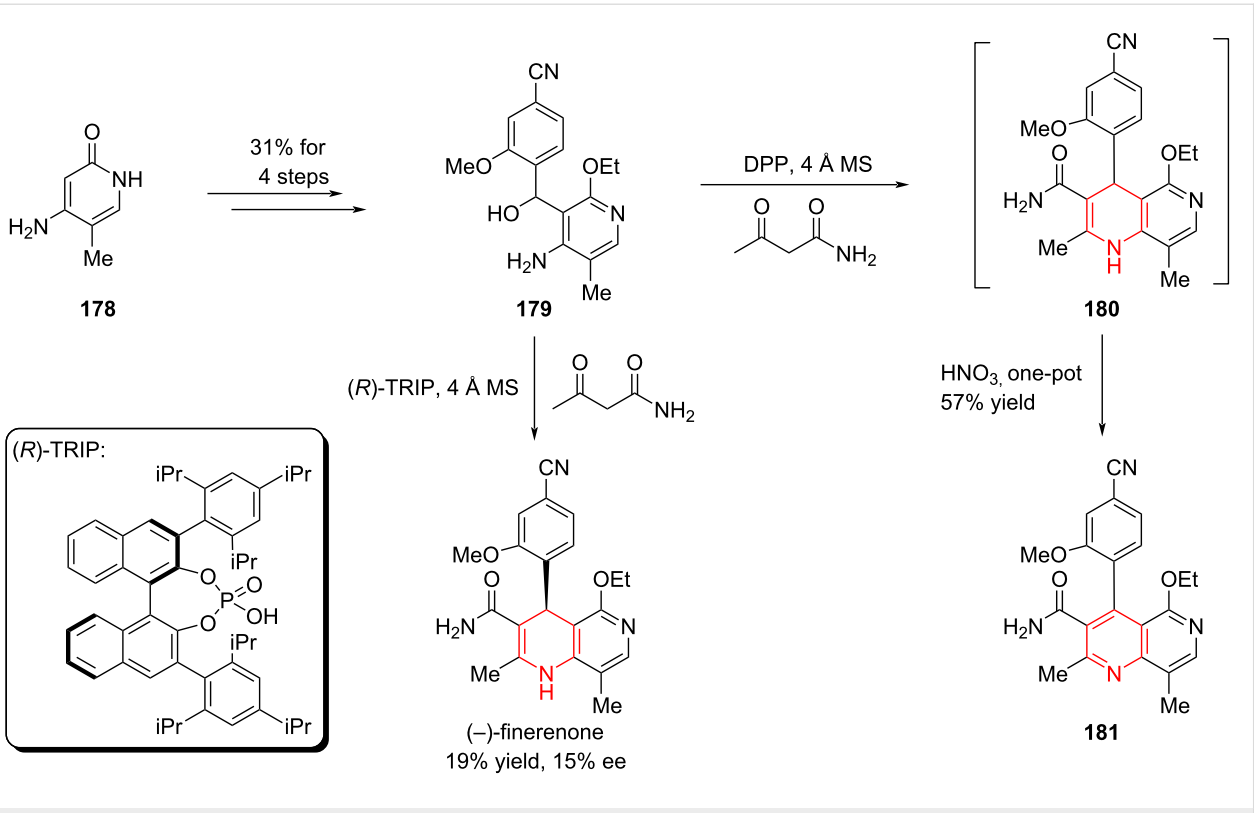

Scheme 25: Early attempt towards (–)-finerenone by Aggarwal and co-workers.

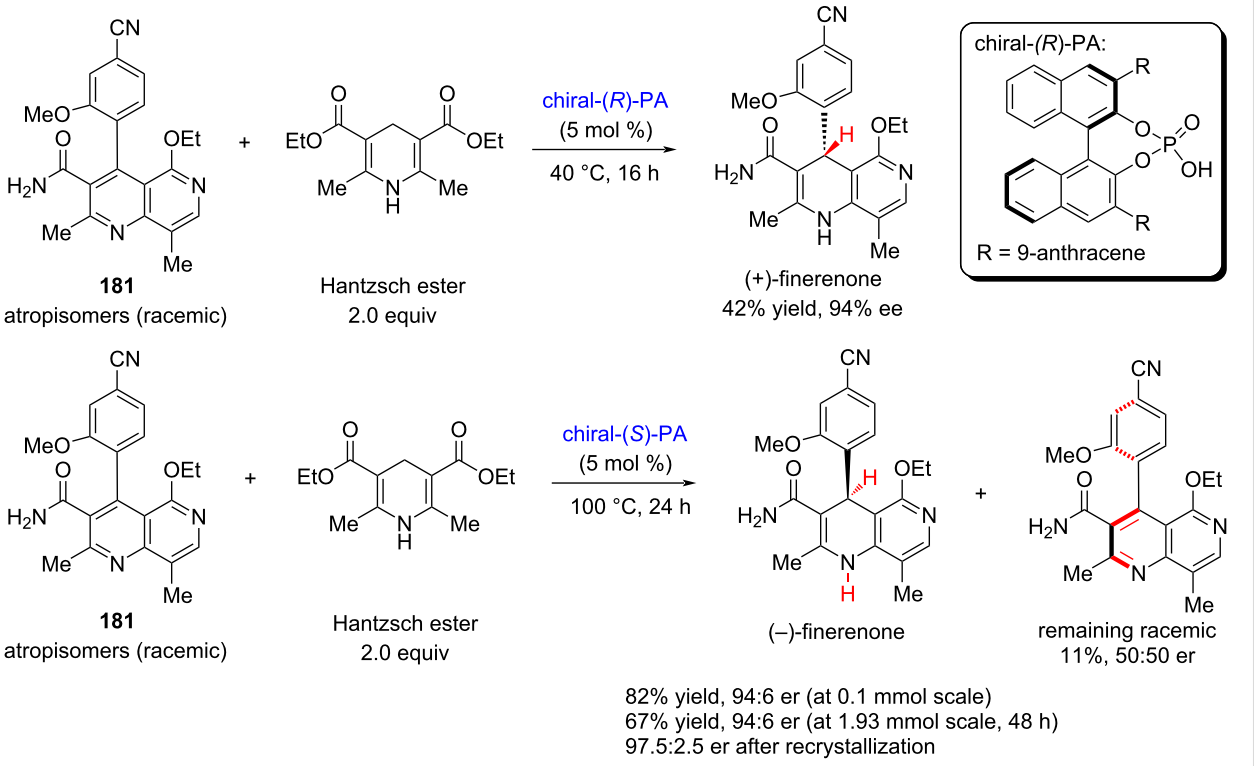

Scheme 26: Enantioselective synthesis towards (–)-finerenone.

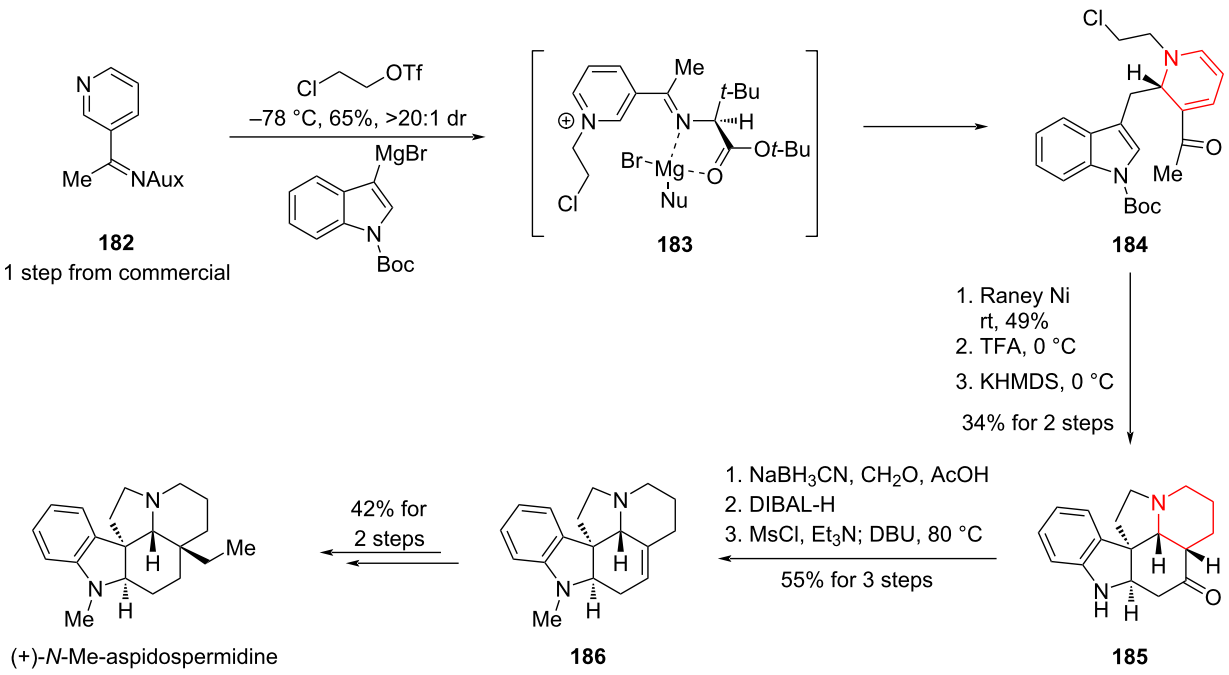

Scheme 27: Total synthesis of (+)-*N*-methylaspidospermidine by Smith, Grigolo and co-workers.

achieving an efficient collective synthesis of matrine-type alkaloids.

Asymmetric total synthesis of senepodine F by Ishikawa, 2023

Lycopodium alkaloids, isolated from plants of the *Lycopodium* genus (*Lycopodiaceae* family), represent a vast and structurally diverse family of natural products. To date, over 500 members of this family have been reported, with some known to exhibit acetylcholinesterase inhibitory activity and other notable bioactivities. Their architecturally complex and unique polycyclic frameworks have attracted sustained interest from synthetic, natural product, and medicinal chemists alike. In 2023, Ishikawa and co-workers reported the first asymmetric total synthesis of (−)-senepodine F, a tetracyclic *Lycopodium* alkaloid (Scheme 29) [100].

The synthesis commenced with a stereoselective Diels–Alder reaction between compounds **194** and **195** under asymmetric amine catalysis, directly affording the bicyclic intermediate **196**, which was further elaborated over seven steps (overall yield: 74%) to give **197**. In parallel, the authors adopted Glorius' protocol, applying an Evans chiral auxiliary to achieve asymmetric catalytic hydrogenation of the pyridine derivative **198**, delivering the lactam **199** in 66% yield and with excellent enantioselectivity (96% ee). Subsequent transformations over six steps (overall yield: 71%) provided the piperidine building block **200**.

Coupling of the key fragments **197** and **200** was achieved in two steps (77% yield), affording alkyne intermediate **201**. This was followed by a sequence of strategic functional group manipulations, including a pivotal intramolecular S_N2 cyclization, ultimately completing the total synthesis of (−)-senepodine F. Notably, this work also led to the structural revision of the originally assigned natural product, as reported in earlier isolation studies.

Hydrogenation strategy in total synthesis by Qi, 2023 and 2024

Indole-containing natural products have long attracted considerable interest in synthetic chemistry, owing to their pronounced biological activities and the biosynthetic relevance of indole as a key metabolite in diverse pathways. These biosynthetic processes frequently inspire new synthetic methodologies and retrosynthetic strategies. Simple indole derivatives – such as indole-3-acetic acid, tryptophan, and indole-2-carboxylic acid – are accessible on a large scale via biological routes. Nevertheless, for arenes containing both a benzene ring and a heteroaromatic core, achieving regioselective catalytic hydrogenation that discriminates between the phenyl and heteroaromatic moieties remains a persistent challenge.

A recent work by Qi and co-workers has substantially advanced the selective hydrogenation of indole-containing compounds. Systematic tuning of reaction parameters such as catalyst loading, solvent, reaction time, and temperature enabled the

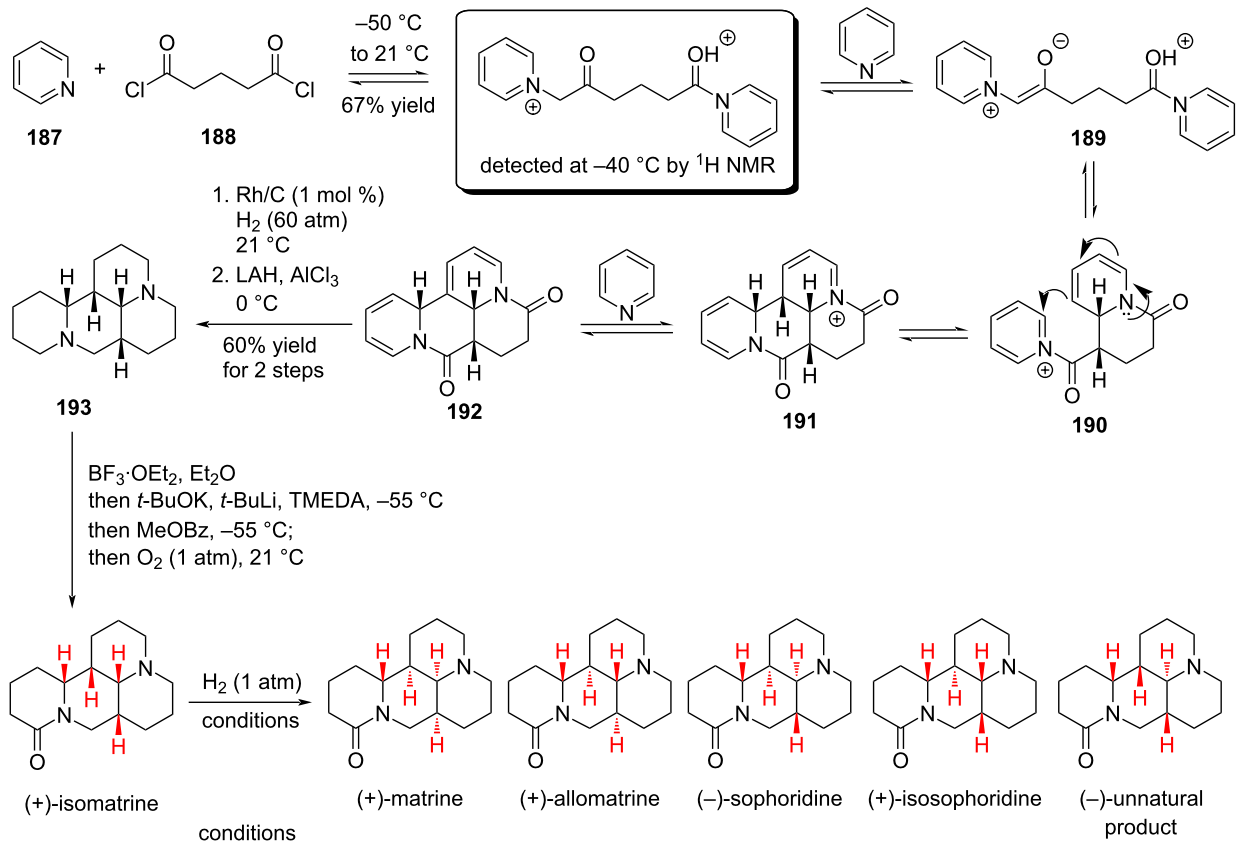

conditions	(+)-matrine	(+)-allomatrine	(–)-sophoridine	(+)-isosophoridine	(–)-unnatural product
10 mol % Rh/C 98 °C, 1 h	32%	60%	0%	0%	0%
10 mol % Rh/C 98 °C, 2 h	15%	83%	0%	0%	0%
110 mol % PtO_2 98 °C, 15 min	6%	10%	10%	29%	14%
10 mol % Pd/C 98 °C, 15 min	0%	11%	0%	55%	19%
110 mol % PtO_2 80 °C, 24 h	0%	18%	0%	33%	40%

Scheme 28: Dearomatization approach towards matrine-type alkaloids.

selective access to diverse hydrogenated products. These developments have established a valuable foundation for the total synthesis of indole-derived alkaloids, facilitating more concise and efficient synthetic routes (Scheme 30) [101].

As an illustration, compound **203** underwent hydrogenation with 50 wt % Pd/C in HFIP/THF 50:1 to give the debenzyloxylated product **204** in 48% yield. The reaction selectively reduced the indole ring while preserving the conjugated olefin adjacent to the carbonyl group, thereby providing a valuable synthetic handle that was exploited in the formal synthesis of pancracine.

Skeletal rearrangements enable the rapid conversion of simple molecules into complex architectures and represent a powerful strategy in natural product synthesis. Qi and co-workers recently reported a one-pot reaction featuring a double oxidative rearrangement cascade of furans and indoles followed by nucleophilic cyclization. This methodology was applied to the formal synthesis of rhynchophylline/isorhynchophylline and the first total syntheses of (±)-(7*R*)- and (±)-(7*S*)-geissoschizol oxindoles (Scheme 31) [102].

In the presence of NBS as the oxidant, precursor **206** undergoes an aza-Achmatowicz rearrangement to give the monobromi-

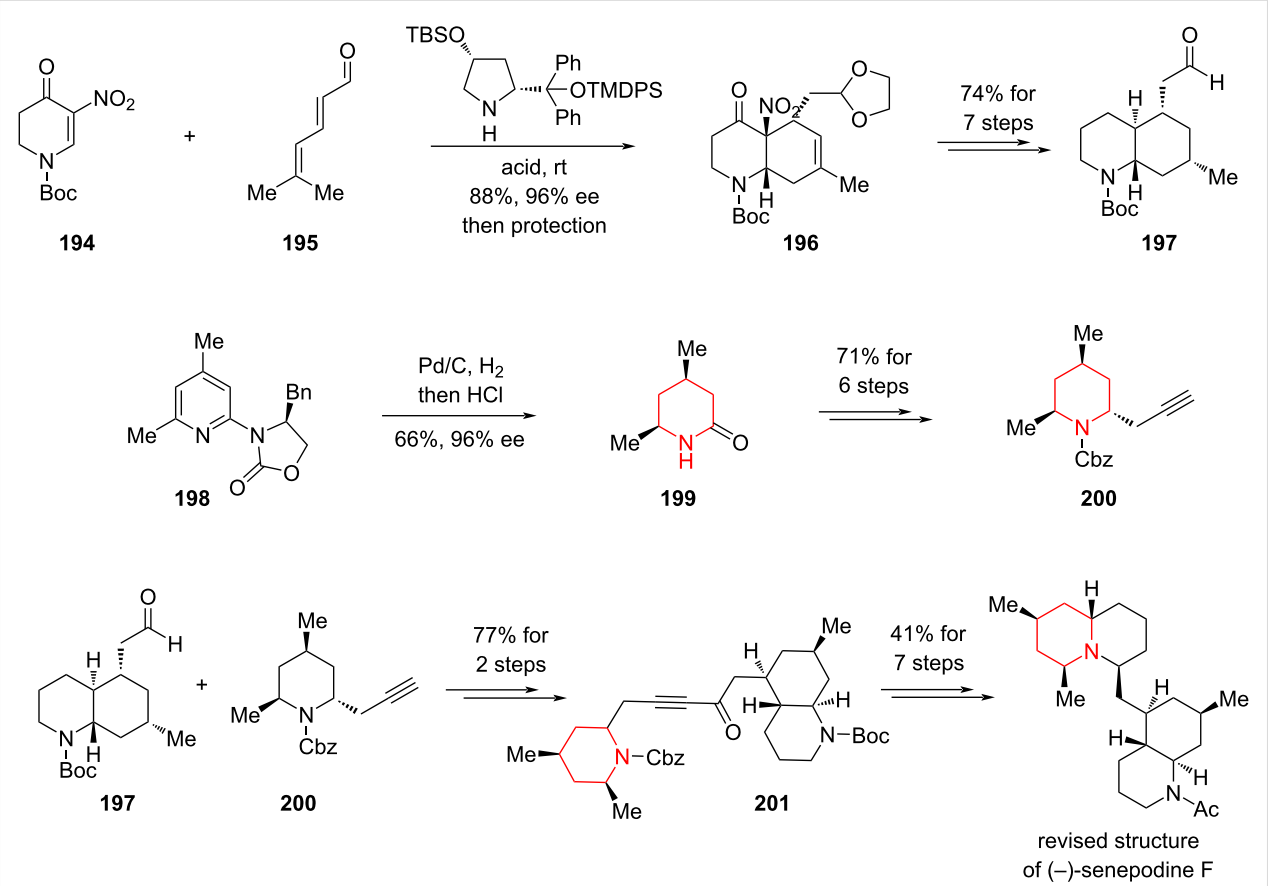

Scheme 29: Asymmetric total synthesis to (–)-senepodine F via an asymmetric hydrogenation of pyridine.

nated intermediate **207**, which upon treatment with $NaHCO_3$ furnishes the spirocyclic scaffold **208**. From this versatile intermediate, a range of oxindole natural products can be accessed. Notably, compound **208** also can be selectively hydrogenated either at the pyridine or indole ring by adjusting the reaction conditions, thereby enabling divergent access to a range of related natural products.

Total synthesis of annotinolide B via sequential quinoline dearomatization, Smith, 2025

Very recently, Smith and co-workers disclosed an elegant total synthesis of the cyclobutane-containing Lycopodium alkaloid annotinolide B (Scheme 32) [103]. Beginning from bromo-substituted quinoline **216**, the authors prepared methyl ester **217** through a concise three-step sequence. A key photochemical dearomatization – originally developed by Ma and co-workers in 2023 – then transformed **217** into dihydroquinoline **219**, accompanied by a minor amount of tetrahydroquinoline **218** [104]. Subsequent transformations over five steps delivered protected intermediate **220** with a primary alcohol group, which was debenzylated and the resulting pyridone intermediate subjected to oxidative cyclization to provide tricyclic intermediate **221**. From this scaffold, a sequence comprising olefin hydrogenation, a [2 + 2] cycloaddition, Pd-catalyzed reduction, Vaska's catalyst-mediated amide reduction, and final lactonization furnished annotinolide B in 20 steps and 2.7% overall yield.

Conclusion

Over the past decade, advances in catalyst platforms and ligand architecture have transformed arene hydrogenation from a niche reactivity into a broadly general strategy. Enantioselective hydrogenations now encompass quinolines, isoquinolines, benzofurans, pyridines, and related heteroarenes, with stereocontrol enabled by finely tuned ligand classes – N-heterocyclic carbenes, chiral diamines, bisoxazolines, bisphosphines, and pincer frameworks. These systems create discriminating steric/electronic environments and compatible H_2-activation manifolds that deliver site-, chemo-, and enantioselectivity even in the presence of coordinating heteroatoms.

Critically, these developments have moved beyond method demonstration to strategic application in complex settings. Arene hydrogenation is increasingly used to install multiple stereocenters in a single operation, streamline protecting-group

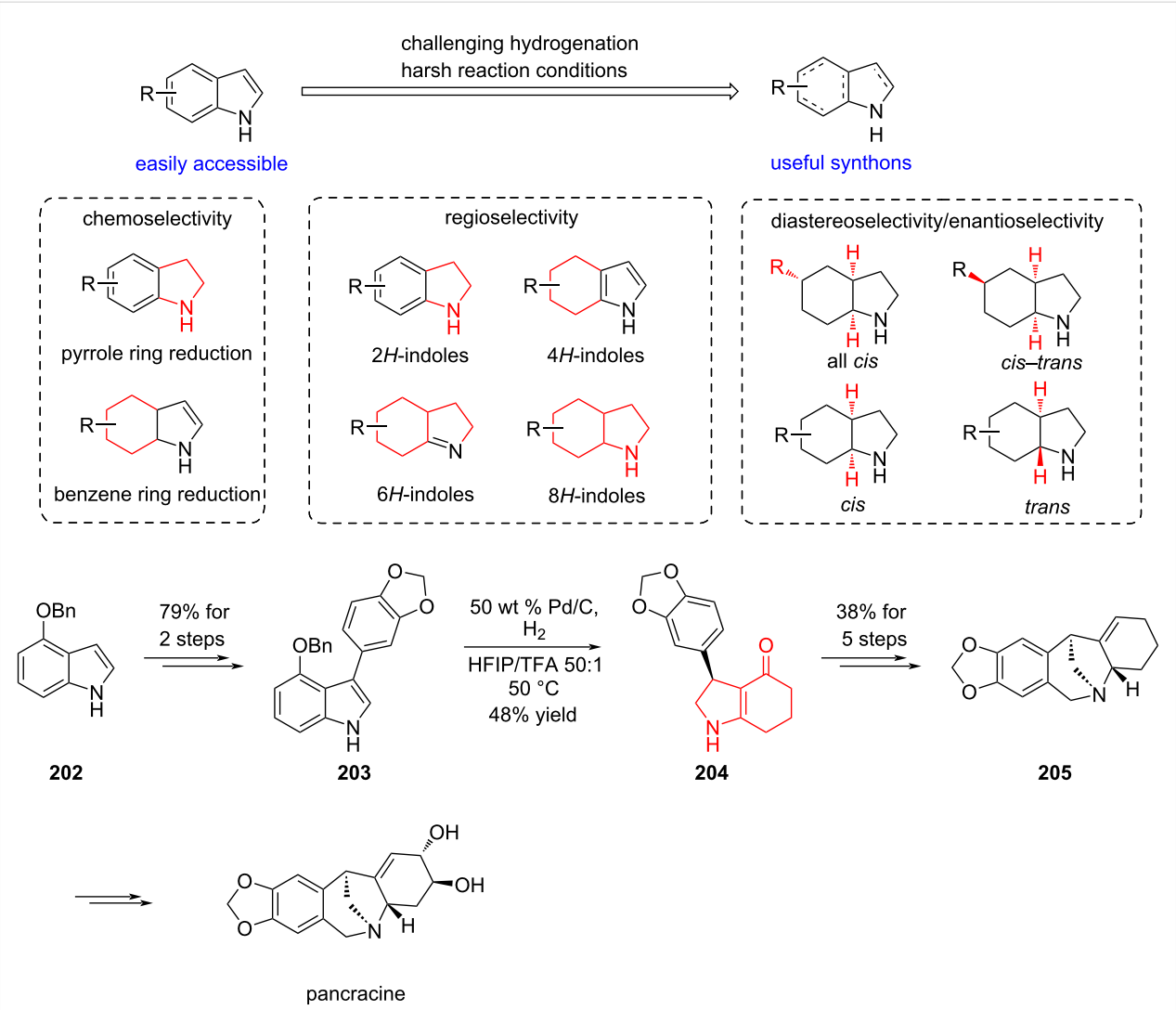

Scheme 30: Selective hydrogenation of indole derivatives and application.

and redox economies, and unlock divergent routes from common intermediates – thereby improving step economy and scalability in total synthesis and medicinal chemistry. For example, Stoltz and co-workers leveraged a substrate-directed asymmetric hydrogenation of isoquinolines to accomplish concise total syntheses of jorunnamycin A and jorumycin, providing a compelling alternative to the Pictet–Spengler reaction and underscoring the strategic value of arene hydrogenation in modern synthesis.

Despite the impressive advances achieved thus far, several fundamental questions remain unresolved and continue to shape the research frontier. A critical issue concerns the influence of substituents with distinct electronic and steric properties on hydrogenation reactivity and selectivity; subtle differences in substitution patterns can dramatically alter reaction pathways, yet predictive models remain underdeveloped. Equally important is the role of heteroatoms, whose tendency to coordinate to transition-metal centers may attenuate catalytic activity or redirect selectivity. Even the archetypal aromatic substrate – benzene – poses a formidable challenge: achieving asymmetric hydrogenation under mild and practical conditions remains an unmet goal. Beyond these challenges, the broader problems of chemo-, regio-, and stereoselectivity underscore the need for new paradigms in catalyst design.

Looking ahead, future progress will hinge on three interrelated directions. First, the deployment of earth-abundant, inexpensive metals will be essential to reduce cost and ensure sustainability, thereby expanding the scope of practical applications. Second, innovation in catalyst and ligand architecture must aim not only at higher levels of stereo- and site-selectivity but also

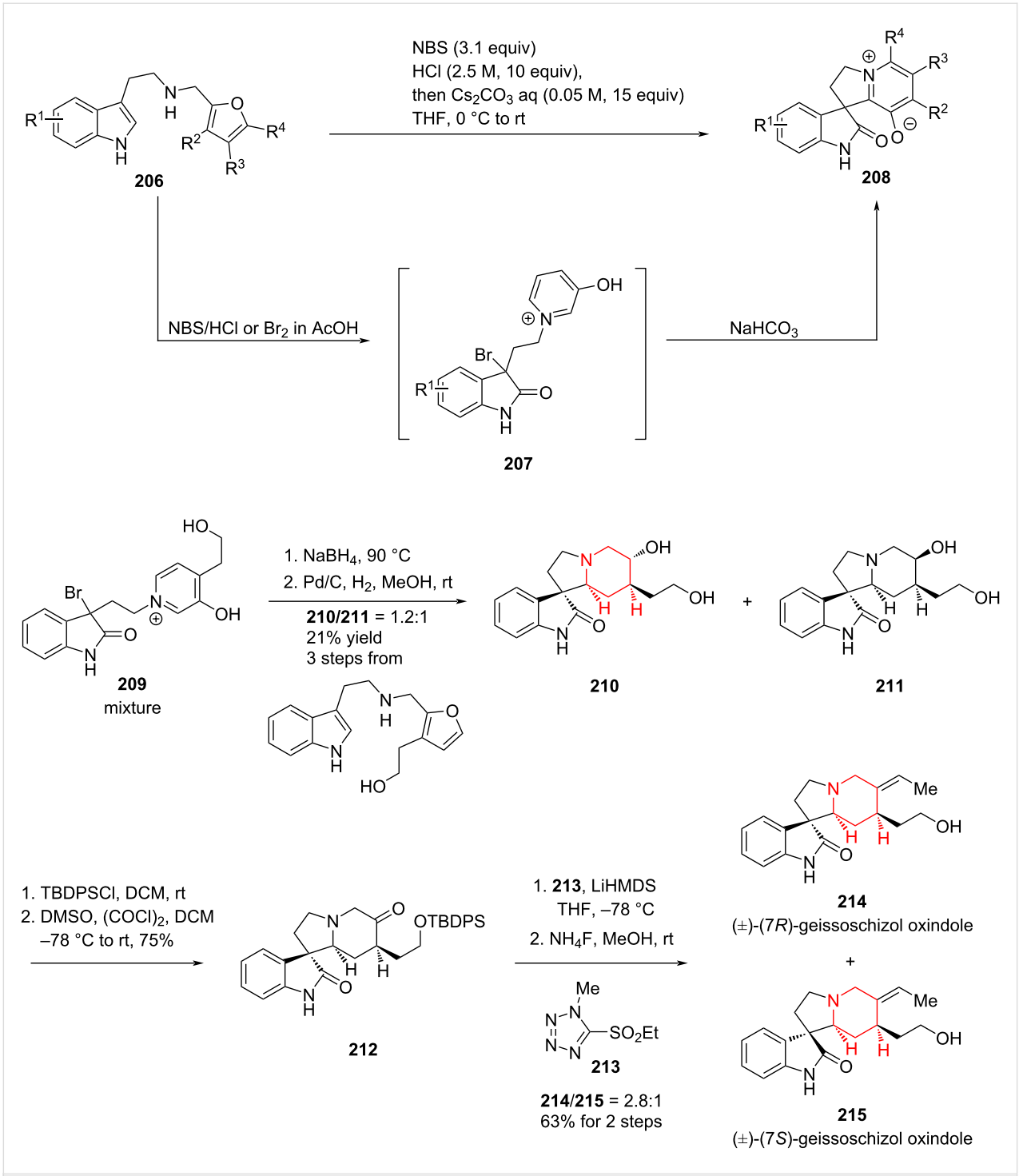

Scheme 31: Synthetic approaches to the oxindole alkaloids by Qi and co-workers.

at expanding functional group tolerance and enabling transformations previously considered inaccessible. Third, deeper mechanistic insight into the interplay between substituents, electronic structure, and catalyst behavior is urgently required, as this knowledge will guide the rational design of more general catalytic systems.

With sustained methodological innovation, asymmetric hydrogenation of arenes is poised to evolve from a specialized transformation into a central strategy in synthesis. Its impact will likely extend far beyond methodological studies, driving progress in the streamlined construction of natural products, the design of bioactive molecules, and the discovery of new thera-

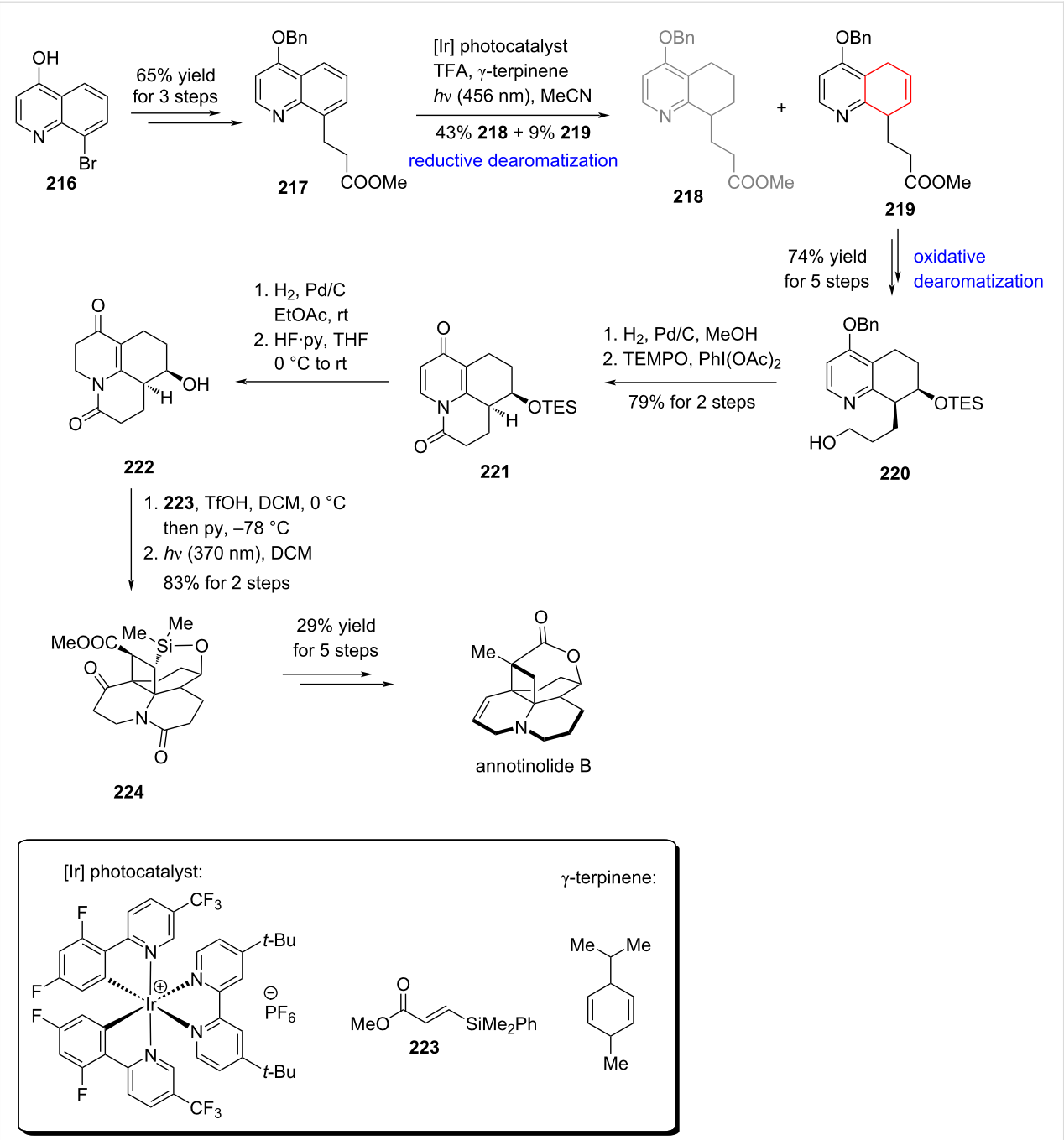

Scheme 32: Total synthesis of annotinolide B by Smith and co-workers.

peutic agents. In this sense, the next decade holds the promise not merely of incremental improvements, but of a paradigm shift in how chemists harness arene hydrogenation in complex molecule synthesis.

Funding

This work was supported by the National Natural Science Foundation of China (grant no. 82225041, X.Q.) and Beijing Natural Science Foundation (grant no. Z230020, X.Q.). The authors gratefully acknowledge the Beijing Municipal Government and Tsinghua University for their financial support.

Author Contributions

Haoxiang Wu: writing – original draft. Xiangbing Qi: conceptualization; funding acquisition; investigation; project administration; supervision; writing – review & editing.

ORCID® iDs

Haoxiang Wu - https://orcid.org/0009-0002-9588-2431
Xiangbing Qi - https://orcid.org/0000-0002-7139-5164

Data Availability Statement

Data sharing is not applicable as no new data was generated or analyzed in this study.

References

1. Nicolaou, K. C.; Vourloumis, D.; Winssinger, N.; Baran, P. S. *Angew. Chem., Int. Ed.* **2000,** *39,* 44–122. doi:10.1002/(sici)1521-3773(20000103)39:1<44::aid-anie44>3.0.co;2-l
2. Min, L.; Han, J.-C.; Zhang, W.; Gu, C.-C.; Zou, Y.-P.; Li, C.-C. *Chem. Rev.* **2023,** *123,* 4934–4971. doi:10.1021/acs.chemrev.2c00763
3. He, W.; Wang, P.; Chen, J.; Xie, W. *Org. Biomol. Chem.* **2020,** *18,* 1046–1056. doi:10.1039/c9ob02627d
4. Cannon, J. S.; Overman, L. E. *Angew. Chem., Int. Ed.* **2012,** *51,* 4288–4311. doi:10.1002/anie.201107385
5. Bonjoch, J.; Solé, D. *Chem. Rev.* **2000,** *100,* 3455–3482. doi:10.1021/cr9902547
6. Makarova, M.; Rycek, L.; Hajicek, J.; Baidilov, D.; Hudlicky, T. *Angew. Chem., Int. Ed.* **2019,** *58,* 18338–18387. doi:10.1002/anie.201901564
7. Nißl, B.; Mülbaier, M.; Grisoni, F.; Trauner, D.; Bermúdez, M.; Dialer, C.; Konrad, D. B. *Angew. Chem., Int. Ed.* **2025,** *64,* e202502404. doi:10.1002/anie.202502404
8. Chen, P.; Wang, J.; Zhang, S.; Wang, Y.; Sun, Y.; Bai, S.; Wu, Q.; Cheng, X.; Cao, P.; Qi, X. *Nat. Commun.* **2024,** *15,* 679. doi:10.1038/s41467-024-45037-0
9. Corey, E. J. *Chem. Soc. Rev.* **1988,** *17,* 111–133. doi:10.1039/cs9881700111
10. Kawamura, S.; Chu, H.; Felding, J.; Baran, P. S. *Nature* **2016,** *532,* 90–93. doi:10.1038/nature17153
11. Bao, R.; Zhang, H.; Tang, Y. *Acc. Chem. Res.* **2021,** *54,* 3720–3733. doi:10.1021/acs.accounts.1c00459
12. Young, I. S.; Baran, P. S. *Nat. Chem.* **2009,** *1,* 193–205. doi:10.1038/nchem.216
13. Kärkäs, M. D.; Porco, J. A., Jr.; Stephenson, C. R. J. *Chem. Rev.* **2016,** *116,* 9683–9747. doi:10.1021/acs.chemrev.5b00760
14. Munda, M.; Niyogi, S.; Shaw, K.; Kundu, S.; Nandi, R.; Bisai, A. *Org. Biomol. Chem.* **2022,** *20,* 727–748. doi:10.1039/d1ob02115j
15. Schreiber, S. L. *Science* **2000,** *287,* 1964–1969. doi:10.1126/science.287.5460.1964
16. Nicolaou, K. C.; Edmonds, D. J.; Bulger, P. G. *Angew. Chem., Int. Ed.* **2006,** *45,* 7134–7186. doi:10.1002/anie.200601872
17. Li, L.; Chen, Z.; Zhang, X.; Jia, Y. *Chem. Rev.* **2018,** *118,* 3752–3832. doi:10.1021/acs.chemrev.7b00653
18. Taylor, R. D.; MacCoss, M.; Lawson, A. D. G. *J. Med. Chem.* **2014,** *57,* 5845–5859. doi:10.1021/jm4017625
19. Scott, K. A.; Cox, P. B.; Njardarson, J. T. *J. Med. Chem.* **2022,** *65,* 7044–7072. doi:10.1021/acs.jmedchem.2c00223
20. Vitaku, E.; Smith, D. T.; Njardarson, J. T. *J. Med. Chem.* **2014,** *57,* 10257–10274. doi:10.1021/jm501100b
21. Wertjes, W. C.; Southgate, E. H.; Sarlah, D. *Chem. Soc. Rev.* **2018,** *47,* 7996–8017. doi:10.1039/c8cs00389k
22. Zhuo, C.-X.; Zhang, W.; You, S.-L. *Angew. Chem., Int. Ed.* **2012,** *51,* 12662–12686. doi:10.1002/anie.201204822
23. Roche, S. P.; Porco, J. A., Jr. *Angew. Chem., Int. Ed.* **2011,** *50,* 4068–4093. doi:10.1002/anie.201006017
24. Walters, W. P.; Green, J.; Weiss, J. R.; Murcko, M. A. *J. Med. Chem.* **2011,** *54,* 6405–6416. doi:10.1021/jm200504p
25. Lovering, F.; Bikker, J.; Humblet, C. *J. Med. Chem.* **2009,** *52,* 6752–6756. doi:10.1021/jm901241e
26. Quideau, S.; Pouységu, L.; Deffieux, D. *Synlett* **2008,** 467–495. doi:10.1055/s-2008-1032094
27. Yu, L.-M.; Chen, H.; Fang, W.; Cai, R.; Tao, Y.; Li, Y.; Dong, H. *Org. Biomol. Chem.* **2024,** *22,* 7074–7091. doi:10.1039/d4ob00766b
28. Huck, C. J.; Boyko, Y. D.; Sarlah, D. *Nat. Prod. Rep.* **2022,** *39,* 2231–2291. doi:10.1039/d2np00042c
29. Wiesenfeldt, M. P.; Nairoukh, Z.; Dalton, T.; Glorius, F. *Angew. Chem., Int. Ed.* **2019,** *58,* 10460–10476. doi:10.1002/anie.201814471
30. Wang, D.-S.; Chen, Q.-A.; Lu, S.-M.; Zhou, Y.-G. *Chem. Rev.* **2012,** *112,* 2557–2590. doi:10.1021/cr200328h
31. Kita, Y.; Yamaji, K.; Higashida, K.; Sathaiah, K.; Iimuro, A.; Mashima, K. *Chem. – Eur. J.* **2015,** *21,* 1915–1927. doi:10.1002/chem.201405408
32. Kim, A. N.; Stoltz, B. M. *ACS Catal.* **2020,** *10,* 13834–13851. doi:10.1021/acscatal.0c03958
33. Kuwano, R.; Kameyama, N.; Ikeda, R. *J. Am. Chem. Soc.* **2011,** *133,* 7312–7315. doi:10.1021/ja201543h
34. Lückemeier, L.; Pierau, M.; Glorius, F. *Chem. Soc. Rev.* **2023,** *52,* 4996–5012. doi:10.1039/d3cs00329a
35. Faísca Phillips, A. M.; Pombeiro, A. J. L. *Org. Biomol. Chem.* **2017,** *15,* 2307–2340. doi:10.1039/c7ob00113d
36. Gunasekar, R.; Goodyear, R. L.; Proietti Silvestri, I.; Xiao, J. *Org. Biomol. Chem.* **2022,** *20,* 1794–1827. doi:10.1039/d1ob02331d
37. Dyson, P. J. *Dalton Trans.* **2003,** 2964–2974. doi:10.1039/b303250g
38. Moock, D.; Wiesenfeldt, M. P.; Freitag, M.; Muratsugu, S.; Ikemoto, S.; Knitsch, R.; Schneidewind, J.; Baumann, W.; Schäfer, A. H.; Timmer, A.; Tada, M.; Hansen, M. R.; Glorius, F. *ACS Catal.* **2020,** *10,* 6309–6317. doi:10.1021/acscatal.0c01074
39. Zheng, L.-S.; Wang, F.; Ye, X.-Y.; Chen, G.-Q.; Zhang, X. *Org. Lett.* **2020,** *22,* 8882–8887. doi:10.1021/acs.orglett.0c03261
40. Li, W.; Zhang, S.; Yu, X.; Feng, X.; Yamamoto, Y.; Bao, M. *J. Org. Chem.* **2021,** *86,* 10773–10781. doi:10.1021/acs.joc.1c00958
41. Feng, G.-S.; Zhao, Z.-B.; Shi, L.; Zhou, Y.-G. *Org. Chem. Front.* **2021,** *8,* 6273–6278. doi:10.1039/d1qo01144h
42. Wagener, T.; Lückemeier, L.; Daniliuc, C. G.; Glorius, F. *Angew. Chem., Int. Ed.* **2021,** *60,* 6425–6429. doi:10.1002/anie.202016771
43. Yang, Z.-Y.; Luo, H.; Zhang, M.; Wang, X.-C. *ACS Catal.* **2021,** *11,* 10824–10829. doi:10.1021/acscatal.1c02876
44. Liu, Z.; He, J.-H.; Zhang, M.; Shi, Z.-J.; Tang, H.; Zhou, X.-Y.; Tian, J.-J.; Wang, X.-C. *J. Am. Chem. Soc.* **2022,** *144,* 4810–4818. doi:10.1021/jacs.2c00962
45. Wu, J.; Chen, Z.; Barnard, J. H.; Gunasekar, R.; Pu, C.; Wu, X.; Zhang, S.; Ruan, J.; Xiao, J. *Nat. Catal.* **2022,** *5,* 982–992. doi:10.1038/s41929-022-00857-5
46. Wu, H.; Yang, J.; Peters, B. B. C.; Massaro, L.; Zheng, J.; Andersson, P. G. *J. Am. Chem. Soc.* **2021,** *143,* 20377–20383. doi:10.1021/jacs.1c09975
47. Zhang, F.; Sasmal, H. S.; Rana, D.; Glorius, F. *J. Am. Chem. Soc.* **2024,** *146,* 18682–18688. doi:10.1021/jacs.4c05883
48. Li, H.-X.; Yu, Z.-X. *Org. Lett.* **2024,** *26,* 3458–3462. doi:10.1021/acs.orglett.4c01029

49. Kuwano, R.; Ikeda, R.; Hirasada, K. *Chem. Commun.* **2015,** *51,* 7558–7561. doi:10.1039/c5cc01971k
50. Li, C.; Pan, Y.; Feng, Y.; He, Y.-M.; Liu, Y.; Fan, Q.-H. *Org. Lett.* **2020,** *22,* 6452–6457. doi:10.1021/acs.orglett.0c02268
51. Papa, V.; Cao, Y.; Spannenberg, A.; Junge, K.; Beller, M. *Nat. Catal.* **2020,** *3,* 135–142. doi:10.1038/s41929-019-0404-6
52. Wang, L.; Lin, J.; Xia, C.; Sun, W. *J. Org. Chem.* **2021,** *86,* 16641–16651. doi:10.1021/acs.joc.1c01925
53. Han, Z.; Liu, G.; Yang, X.; Dong, X.-Q.; Zhang, X. *ACS Catal.* **2021,** *11,* 7281–7291. doi:10.1021/acscatal.1c01353
54. Liu, C.; Wang, M.; Liu, S.; Wang, Y.; Peng, Y.; Lan, Y.; Liu, Q. *Angew. Chem., Int. Ed.* **2021,** *60,* 5108–5113. doi:10.1002/anie.202013540
55. Wang, Y.; Li, H.; Yang, H.; Fan, M.; Liu, Q. *CCS Chem.* **2024,** *6,* 1535–1546. doi:10.31635/ccschem.023.202303289
56. Kim, A. N.; Ngamnithiporn, A.; Bartberger, M. D.; Stoltz, B. M. *Chem. Sci.* **2022,** *13,* 3227–3232. doi:10.1039/d1sc06729j
57. Xu, A.; Li, C.; Huang, J.; Pang, H.; Zhao, C.; Song, L.; You, H.; Zhang, X.; Chen, F.-E. *Chem. Sci.* **2023,** *14,* 9024–9032. doi:10.1039/d3sc00803g
58. Han, Z.; Feng, X.; Du, H. *J. Org. Chem.* **2024,** *89,* 3666–3671. doi:10.1021/acs.joc.3c02954
59. Ge, Y.; Wang, Z.; Han, Z.; Ding, K. *Chem. – Eur. J.* **2020,** *26,* 15482–15486. doi:10.1002/chem.202002532
60. Rong, N.; Zhou, A.; Liang, M.; Wang, S.-G.; Yin, Q. *J. Am. Chem. Soc.* **2024,** *146,* 5081–5087. doi:10.1021/jacs.4c00298
61. Liu, Z.; Yu, Y.-J.; Wang, G.-W.; Lu, S.-M.; Zhou, Y.-G.; Chen, M.-W. *Org. Lett.* **2025,** *27,* 9890–9895. doi:10.1021/acs.orglett.5c02777
62. Moock, D.; Wagener, T.; Hu, T.; Gallagher, T.; Glorius, F. *Angew. Chem., Int. Ed.* **2021,** *60,* 13677–13681. doi:10.1002/anie.202103910
63. Schiwek, C. H.; Jandl, C.; Bach, T. *ACS Catal.* **2022,** *12,* 3628–3633. doi:10.1021/acscatal.2c00400
64. Ding, Y.-X.; Zhu, Z.-H.; Chen, M.-W.; Yu, C.-B.; Zhou, Y.-G. *Angew. Chem., Int. Ed.* **2022,** *61,* e202205623. doi:10.1002/anie.202205623
65. Viereck, P.; Hierlmeier, G.; Tosatti, P.; Pabst, T. P.; Puentener, K.; Chirik, P. J. *J. Am. Chem. Soc.* **2022,** *144,* 11203–11214. doi:10.1021/jacs.2c02007
66. Gupta, P.; Hierlmeier, G.; Baete, C.; Pecoraro, M. V.; Tosatti, P.; Puentener, K.; Chirik, P. J. *ACS Catal.* **2024,** *14,* 15545–15552. doi:10.1021/acscatal.4c04620
67. Luo, C.; Wu, C.; Wang, X.; Han, Z.; Wang, Z.; Ding, K. *J. Am. Chem. Soc.* **2024,** *146,* 35043–35056. doi:10.1021/jacs.4c05365
68. Hook, J. M.; Mander, L. N. *Nat. Prod. Rep.* **1986,** *3,* 35–85. doi:10.1039/np9860300035
69. Donohoe, T. J.; Garg, R.; Stevenson, C. A. *Tetrahedron: Asymmetry* **1996,** *7,* 317–344. doi:10.1016/0957-4166(96)00001-8
70. Liu, D.-H.; Ma, J. *Angew. Chem., Int. Ed.* **2024,** *63,* e202402819. doi:10.1002/anie.202402819
71. Baldwin, J. E.; Claridge, T. D. W.; Culshaw, A. J.; Heupel, F. A.; Smrcková, S.; Whitehead, R. C. *Tetrahedron Lett.* **1996,** *37,* 6919–6922. doi:10.1016/0040-4039(96)01516-x
72. Baldwin, J. E.; Claridge, T. D. W.; Culshaw, A. J.; Heupel, F. A.; Lee, V.; Spring, D. R.; Whitehead, R. C.; Boughtflower, R. J.; Mutton, I. M.; Upton, R. J. *Angew. Chem., Int. Ed.* **1998,** *37,* 2661–2663. doi:10.1002/(sici)1521-3773(19981016)37:19<2661::aid-anie2661>3.0.co;2-d
73. Liu, H.; Jia, Y. *Nat. Prod. Rep.* **2017,** *34,* 411–432. doi:10.1039/c6np00110f
74. Saá, C.; Crotts, D. D.; Hsu, G.; Vollhardt, K. P. C. *Synlett* **1994,** 487–489. doi:10.1055/s-1994-22898
75. Nichols, D. E. *ACS Chem. Neurosci.* **2018,** *9,* 2331–2343. doi:10.1021/acschemneuro.8b00043
76. Lee, K.; Poudel, Y. B.; Glinkerman, C. M.; Boger, D. L. *Tetrahedron* **2015,** *71,* 5897–5905. doi:10.1016/j.tet.2015.05.093
77. Knight, B. J.; Harbit, R. C.; Smith, J. M. *J. Org. Chem.* **2023,** *88,* 2158–2165. doi:10.1021/acs.joc.2c02564
78. Fukuyama, T.; Inoue, T.; Yokoshima, S. *Heterocycles* **2009,** *79,* 373–378. doi:10.3987/com-08-s(d)42
79. Lewin, G.; Schaeffer, C.; Dacquet, C. *J. Nat. Prod.* **1997,** *60,* 419–420. doi:10.1021/np960482l
80. Doering, N. A.; Sarpong, R.; Hoffmann, R. W. *Angew. Chem., Int. Ed.* **2020,** *59,* 10722–10731. doi:10.1002/anie.201909656
81. Muratake, H.; Natsume, M. *Angew. Chem., Int. Ed.* **2004,** *43,* 4646–4649. doi:10.1002/anie.200460332
82. Muratake, H.; Natsume, M. *Tetrahedron Lett.* **2002,** *43,* 2913–2917. doi:10.1016/s0040-4039(02)00453-7
83. Peese, K. M.; Gin, D. Y. *J. Am. Chem. Soc.* **2006,** *128,* 8734–8735. doi:10.1021/ja0625430
84. Scott, J. D.; Williams, R. M. *Chem. Rev.* **2002,** *102,* 1669–1730. doi:10.1021/cr010212u
85. Magnus, P.; Matthews, K. S. *J. Am. Chem. Soc.* **2005,** *127,* 12476–12477. doi:10.1021/ja0535817
86. Mander, L. N.; McLachlan, M. M. *J. Am. Chem. Soc.* **2003,** *125,* 2400–2401. doi:10.1021/ja029725o
87. Larson, K. K.; Sarpong, R. *J. Am. Chem. Soc.* **2009,** *131,* 13244–13245. doi:10.1021/ja9063487
88. Landwehr, E. M.; Baker, M. A.; Oguma, T.; Burdge, H. E.; Kawajiri, T.; Shenvi, R. A. *Science* **2022,** *375,* 1270–1274. doi:10.1126/science.abn8343
89. Xu, J.; Shao, L.-D.; Li, D.; Deng, X.; Liu, Y.-C.; Zhao, Q.-S.; Xia, C. *J. Am. Chem. Soc.* **2014,** *136,* 17962–17965. doi:10.1021/ja5121343
90. Bosch, C.; Fiser, B.; Gómez-Bengoa, E.; Bradshaw, B.; Bonjoch, J. *Org. Lett.* **2015,** *17,* 5084–5087. doi:10.1021/acs.orglett.5b02581
91. Saborit, G. V.; Bosch, C.; Parella, T.; Bradshaw, B.; Bonjoch, J. *J. Org. Chem.* **2016,** *81,* 2629–2634. doi:10.1021/acs.joc.6b00025
92. Wei, X.; Qu, B.; Zeng, X.; Savoie, J.; Fandrick, K. R.; Desrosiers, J.-N.; Tcyrulnikov, S.; Marsini, M. A.; Buono, F. G.; Li, Z.; Yang, B.-S.; Tang, W.; Haddad, N.; Gutierrez, O.; Wang, J.; Lee, H.; Ma, S.; Campbell, S.; Lorenz, J. C.; Eckhardt, M.; Himmelsbach, F.; Peters, S.; Patel, N. D.; Tan, Z.; Yee, N. K.; Song, J. J.; Roschangar, F.; Kozlowski, M. C.; Senanayake, C. H. *J. Am. Chem. Soc.* **2016,** *138,* 15473–15481. doi:10.1021/jacs.6b09764
93. Welin, E. R.; Ngamnithiporn, A.; Klatte, M.; Lapointe, G.; Pototschnig, G. M.; McDermott, M. S. J.; Conklin, D.; Gilmore, C. D.; Tadross, P. M.; Haley, C. K.; Negoro, K.; Glibstrup, E.; Grünanger, C. U.; Allan, K. M.; Virgil, S. C.; Slamon, D. J.; Stoltz, B. M. *Science* **2019,** *363,* 270–275. doi:10.1126/science.aav3421
94. Lerchen, A.; Gandhamsetty, N.; Farrar, E. H. E.; Winter, N.; Platzek, J.; Grayson, M. N.; Aggarwal, V. K. *Angew. Chem., Int. Ed.* **2020,** *59,* 23107–23111. doi:10.1002/anie.202011256
95. Grigolo, T. A.; Smith, J. M. *Chem. – Eur. J.* **2022,** *28,* e202202813. doi:10.1002/chem.202202813
96. Grigolo, T. A.; Subhit, A. R.; Smith, J. M. *Org. Lett.* **2021,** *23,* 6703–6708. doi:10.1021/acs.orglett.1c02276

97. Knight, B. J.; Tolchin, Z. A.; Smith, J. M. *Chem. Commun.* **2021,** *57,* 2693–2696. doi:10.1039/d1cc00056j
98. Kerkovius, J. K.; Stegner, A.; Turlik, A.; Lam, P. H.; Houk, K. N.; Reisman, S. E. *J. Am. Chem. Soc.* **2022,** *144,* 15938–15943. doi:10.1021/jacs.2c06584
99. Magann, N. L.; Westley, E.; Sowden, M. J.; Gardiner, M. G.; Sherburn, M. S. *J. Am. Chem. Soc.* **2022,** *144,* 19695–19699. doi:10.1021/jacs.2c09804
100. Nakashima, Y.; Inoshita, T.; Kitajima, M.; Ishikawa, H. *Org. Lett.* **2023,** *25,* 1151–1155. doi:10.1021/acs.orglett.3c00133
101. Qi, X.; Han, S.; Lou, M. *Synlett* **2024,** *35,* 586–592. doi:10.1055/a-2021-7944
102. Wang, X.; Zhang, M.; Liu, X.; Lou, M.; Li, G.; Qi, X. *Org. Lett.* **2024,** *26,* 824–828. doi:10.1021/acs.orglett.3c03938
103. Duvvuru, B.; Smith, M. W. *J. Am. Chem. Soc.* **2025,** *147,* 39042–39046. doi:10.1021/jacs.5c14142
104. Liu, D.-H.; Nagashima, K.; Liang, H.; Yue, X.-L.; Chu, Y.-P.; Chen, S.; Ma, J. *Angew. Chem., Int. Ed.* **2023,** *62,* e202312203. doi:10.1002/anie.202312203

License and Terms